Broder J. Merkel
Andrea Hasche-Berger

Editors

Uranium in the Environment

Mining Impact
and Consequences

Springer

BERGAKADEMIE
TECHNISCHE
UNIVERSITÄT
FREIBERG

Broder J. Merkel
Andrea Hasche-Berger
Uranium in the Environment
Mining Impact and Consequences

Broder J. Merkel
Andrea Hasche-Berger
(Editors)

Uranium in
the Environment

Mining Impact and Consequences

With 376 Figures and a CD-ROM

Springer

EDITORS:

PROF. DR. BRODER J. MERKEL
DIPL. -GEOL. ANDREA HASCHE-BERGER
TU BERGAKADEMIE FREIBERG
INSTITUT FÜR GEOLOGIE
GUSTAV-ZEUNER-STRAßE 12
09596 FREIBERG
GERMANY

E-MAIL: MERKEL@GEO.TU-FREIBERG.DE
         ANDREA.HASCHE@GEO.TU-FREIBERG.DE

Contents

Preface

Uranium is an element to be found ubiquitous in rock, soil, and water. Uranium concentrations in natural ground water can be more than several hundreds µg/l without impact from mining, nuclear industry, and fertilizers. Considering the WHO recommendation for drinking water of 15 µg/l (has been as low as 2 µg/l before) due to the chemical toxicity of uranium the element uranium has become an important issue in environmental research.

Besides natural enrichment of uranium in aquifers uranium mining and milling activities, further uranium processing to nuclear fuel, emissions form burning coal and oil, and the application of uranium containing phosphate fertilizers may enrich the natural uranium concentrations in soil and water by far.

In October 1995 the first international conference on Uranium Mining and Hydrogeology (UMH I) was held in Freiberg being organized by the Department of Geology at the Technical University Bergakademie Freiberg by the support of the Saxon State Ministry of Geology and Environment. Due to the large scientific interest in the topic of uranium a second conference (UMH II) took place in Freiberg in September 1998. Furthermore, in September 2002 scientists working on the topic of uranium mining and hydrogeology attended the third conference (UMH III) which was jointly held together with the International Mine Water Association (IMWA) Symposium 2002. The reviewed papers and posters of the 2002 conference have been published by Springer entitled Uranium in the aquatic environment (edited by Merkel, Planer-Friedrich and Wolkersdorfer).

The immense interest in the third conference showed the still existing high significance of international exchange and interdisciplinary discussion of scientists in the field of uranium mining and remediation issues. In consequence of this, in September 2005 the fourth consecutive conference (UMH IV) was held in Freiberg. The conference addressed scientists and engineers working in the mining and rehabilitation business. The focus of the book is on uranium mining and milling sites, mining sites with considerable amount of uranium and radionuclides as by-products e.g. phosphate production for fertilizers, abandoned mines, clean up measures, natural attenuation, monitoring measures, modeling techniques, and risk assessment studies. Furthermore the book addresses scientist interested in Uranium in groundwater in general as well as water work managers and political decisions makers.

Freiberg, September 2005

Broder J. Merkel   Andrea Hasche-Berger
Technische Universität Bergakademie Freiberg (TU BAF)

Long-term Aspects of Uranium Mining Remediation

Hartmut Biele, Stephanie Hurst

Saxon State Agency of Environment and Geology, Postfach 80 01 32, 01101 Dresden, Germany, E-mail: Stephanie.Hurst@lfug.smul.sachsen.de

Abstract. After completion of the remediation of the legacy of uranium mining and milling for most of these objects and sites a continued monitoring will be necessary and some of these objects may require maintenance.

The main remediation objects in Saxony are waste rock piles, tailings ponds/deposits and underground mines. The monitoring and maintenance needs of the individual objects differ substantially and consequently the regulatory requirements (both type and extent of monitoring) placed on the individual objects will vary following an object-/site specific approach. Among the most sensitive monitoring parameters are the qualities of seepage and ground water. Another essential parameter is the monitoring of performance and maintenance of functionality of the covers placed on the waste rock piles and tailings to control radon exhalation and contaminated seepage. Unfortunately, there is no reliable database available for the long-term performance of the remediation measures and there has been no effort yet to develop such a database. To obtain a reliable estimate of the period of time needed for the active post remedial care, it is recommended to carry out studies on natural analogues. At present, the Saxon regulatory authorities demand a monitoring and maintenance period of 25 (radiation protection) rsp. 30 years (conventional waste regulations).

Provided the remedial measures taken prove to perform well, the monitoring effort will decrease with time. Considering the fact that the remediation measures implemented were designed for a 200 to 1000 years long stabile performance it is

expected that little maintenance will be needed. However, singular cases of disruption, such as damages of cover cannot be excluded.

A most relevant issue in this respect is the funding of the long-term post remedial tasks. The owner responsible for the uranium sites and objects that were in legal possession of Wismut on June 30, 1990 is and will remain the Federal Government of Germany. For the former Wismut sites, which are legally owned by other parties, the responsibility for funding of long term monitoring and maintenance is in the hands of the actual owners.

Introduction

Long-term stewardship is the only surety for a safe and healthy environment around uranium mining residues. Effective public institutions, the long-term preservation of knowledge and the provision of funds provide the main basis for a successful long-term stewardship. The lack of one of these issues may cause a failure of the stewardship and consequently also of the safety of the environment.

An international consensus regarding the necessity of long-term stewardship can be deduced from IAEA Report (2005) and similar publications.

In the following text the main objectives regarding long-term stewardship are discussed and the current status of the discussion in Saxony is presented.

Sites and Objects

Uranium mining in Saxony took place from 1945 to 1990 by the SAG/SDAG Wismut.

Exploration for uranium ore was performed more or less in the whole area of the former GDR. Nevertheless, the main focus was located in the south. Mineable deposits were found in Saxony and Thuringia. In Saxony three major sites were mined:

- Aue (Ore mountains) hydrothermal vein deposit
- Königstein creataceous sandstone deposit (uranium fixed at organic compounds)
- Gittersee Permian coal deposits (uranium enriched coal seams)

The ore was milled in Crossen, where one of the worlds biggest uranium tailings site

- Helmsdorf/Dänkritz

was constructed (ca. 50 ha, i.e. ca. 125 acre; ca. 50 million m³).

Beside these sites uranium was mined and milled also at some smaller sites in the ore mountain area in the first two decades (until 1962). Wismut produced in total 251 000 t of ore.

The residues from conventional underground mining are
- waste rock piles,
- tailings ponds,
- open mine shafts and drifts and
- contaminated mine water.

From in – situ – leach mining
- acidic solutions (sulphuric acid; pH 1.5 – 3)

remained in the pores and fissures of the host rock and in the mine shafts and drifts.

Additionally
- soil and building material

contaminations existed at former mining and milling areas.

Remediation measures

Waste rock

Waste rock piles commonly are shaped in a way to provide for surface water drainage from the tops and stability of the slope areas. Subsequently they are covered with one meter of soil. The soil properties are optimized resp. low permeability for precipitation and radon emission (Leitfaden Uranbergbausanierung 2000; Forschungsinstitut für Bergbaufolgelandschaften e.V. and G.U.B 1987; Freistaat Sachsen 1997).

Tailings

For tailings ponds a similar procedure is needed. After pumping and treating the pond water from the surface, an intermediate cover to stabilize the surface for further steps is applied.

Following this, the slopes and surface area are shaped and covered (Palme and Wittig 2003; Palme 2003a, 2003b). The minimum cover thickness is 1.5 m.

Underground mines

The stabilization of open mine shafts and drifts is subject matter of the mining authorities only.

The flooding water on he other hand has to be treated in a way to guarantee low emissions of radionuclides and heavy metals (Merkel 2002; Meyer et al. 2002). Experiences from old mines show that after a maximum of two decades following the flooding of the mine natural attenuation processes will bring the water quality to original background values.

Steps

The chronological procedure from the end of uranium mining to the long-term phase is shown in a simplified way in Fig. 1.

After remediation of the objects described above a warrantee phase of 5 years is following. During this phase the remediation measures are undergoing a practical test. The monitoring program of the remediation phase may be reduced. The plant cover is developing which has to stabilize the cover geotechnically.

In the eventually following long-term phase the base monitoring program is replacing the monitoring of the remediation phase. Maintenance, i.e. repair activities, may be needed and must be institutionally fixed and technically installed.

Remediation is the step where the highest effort and costs are needed, while the warranty phase and the long term phase are comparably inexpensive.

In the last few years many comments on the length of time needed for the long term phase were made. They showed that society cannot come away from the responsibility for the uranium mining legacy. To take this responsibility does not necessarily mean high burden.

Funding

A basic legal fact is the responsibility of the owner for the funding of long-term measures.

In the case of the Wismut legacy the federal government has to provide the financial means. It has been discussed also to entrust the State of Saxony with the ownership and consequently with the funding and with the responsibility for long term stewardship. In such a case the former owner has to provide the new owner with the respective financial means.

If ownership changes responsibility for the funding of long term measures is also changing.

The new owner has to take care for all issues associated with long term stewardship.
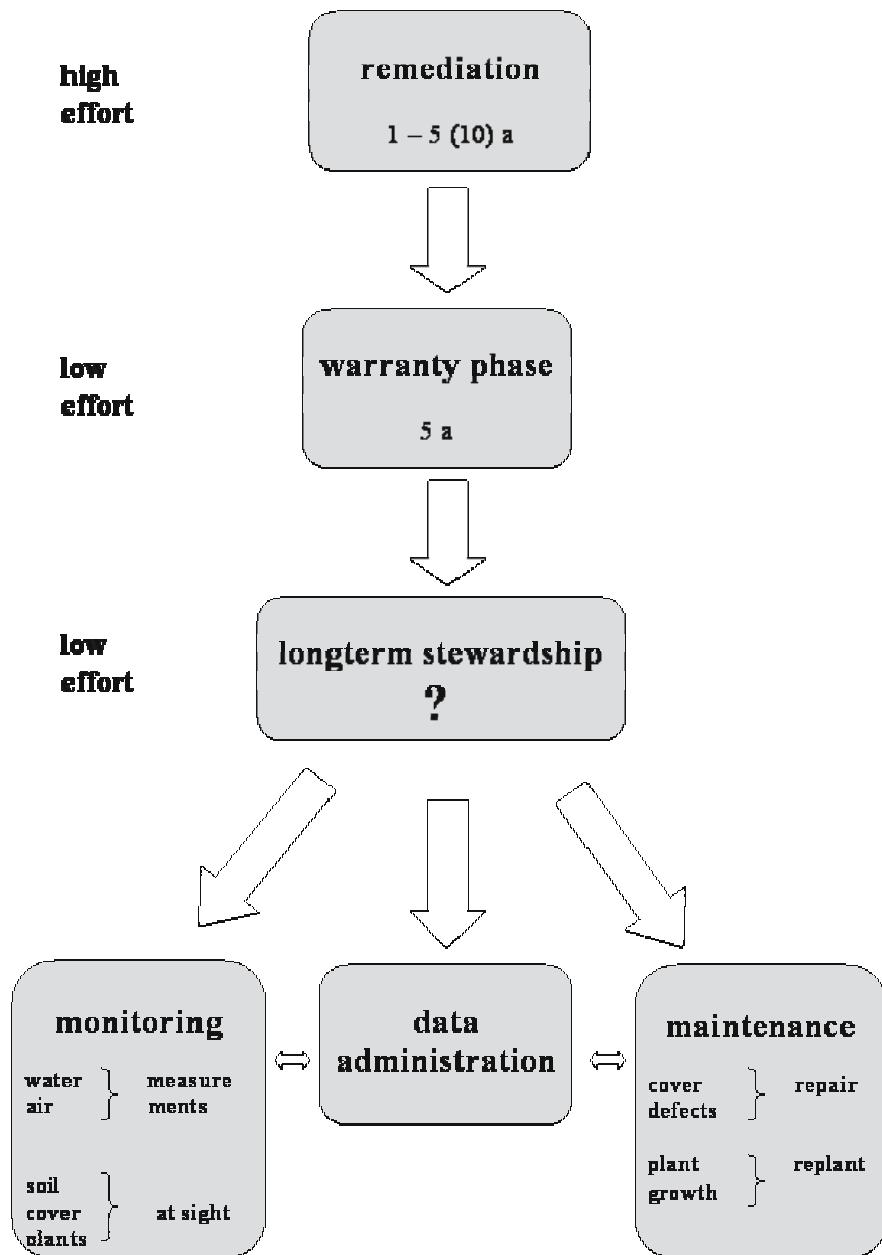
Fig. 1.   Chronological procedure from the end of uranium mining to the long-term phase.

The planning of the dimensions of the financial means needed for long term measures has to take into consideration possible future interest rates. Conservative calculations should base on not more than one percent. This is the result of considerations on the development of the interest rates between the year 1950 and the year 2000 in the USA.

Knowledge

To ensure that information is kept over generations two main factors have to be taken into account:
- Willingness of the communities to take over responsibility for information transfer.
  The main issue is to make information about the restricted use of the objects long term stable. The communities are those concerned by the restricted use of objects situated on the community area. They are making decisions on the future use of their municipal land. To feel responsible for the remediated objects is prerequisite for the functioning of their long-term stability. For this reason permanent contact and exchange with the communities from the beginning of remediation is needed. The discussions already during the remediation process are a helpful base for the acceptance of the remediated objects. The objects must become harmonically and aesthetic fitting components of the natural scenery. On such a base the communities will take care and make wise use of their objects and make sure money for remediation measures is well spent.

Fig. 2.   Surface water runoff facility at waste rock pile 366 in Schlema.

- Optimized information/data management
  Generally two types of data have to be managed: Object data (properties of objects) and monitoring data (field and lab measurements, visual inspection results). Monitoring data are representing the "living" part of the data store while the object data are representing the "dead" part. Monitoring data are the base of all future technical decisions about e.g. ongoing water treatment, need of cover repair, need of monitoring frequencies or change of use restrictions.
  The data bank systems for the monitoring data should contain tools to evaluate the data (developments, statistics etc.) and to represent the state of the information (graphs, outlines etc.). There should be tools to connect the monitoring data with the object data and to export informations for the public to fulfil the conditions of the environmental information law. The German Environmental Information Law of February 2005 was made on the base of the European Directive on Public Access to Environmental Information (2003/4/EC).

In Saxony the data bank KANARAS (<u>ca</u>taster for <u>na</u>tural <u>ra</u>dioactivity in <u>S</u>axony) is in construction. It is consisting of

- ➢ Wismut data bank (Wismut sites, produced by Wismut ltd)
- ➢ A.LAS.KA (radiological data of old sites, federal)
- ➢ FbU (radiological and geographical data of old sites, federal prod.)
- ➢ DURAS (radiological analyses of saxon state lab UBG)

There are no experiences at all on the long-term safety of digital data. On the other hand the longevity of paper written information was prooved in many cases. Under these circumstances there is still a need to keep as much paper documents as possible.

Additionally there will be a need for long-term conservation of some important object informations in the Saxonian state archive. The legal and material conditions for this step are not yet compiled.

Institutional Control

Institutional control in the long-term stewardship phase will – as in the remediation phase - be an issue for different state authorities.

But the framework for these authorities will be different. While during remediation an active constructive development of the best resp. optimized measures was needed, in the long-term phase the institutions play a relatively passive observative role.

For radiation protection institutions Radon behavior is the radiologically most important factor. Therefor they will - as well as ground- and surface water authorities - be interested in the visual control of the covers and the monitoring data for the water path. The quality development of seepage water will be an issue for many decades. As long as active water treatment will be needed, good technical performance of the treatment plants has to be guaranteed and it has to be taken

care that the residues of the treatment are minimized and deposed in a radiologically safe way.

Secondarily radiation protection authrities will controll plant growth by vision. This item will be the main issue for the forestry authorities.

Cover and slope stability will be monitored under the responsibility of the mining authority. Anyway also the water and radiation protection authorities have the duty to take care for the protective function of the covers. From the radiation protection point of view an opening in the cover may work as a chimney for radon and is defintely a case for immidiate repair activities.

Further on all institution for public concerns must be provided after remediation with updated maps of the remediation areas. They have to take care that restrictions for use are kept when the communities are planning new projects.

Maintenance

All remediation measures are planned and performed in a way to minimize future activities.

Nevertheless it may be the case that mending of covers or other subjects is needed. E.g. after storms uprooting of trees may happen and covers of waste rock piles or tailings ponds may be perforated or – in the worst case - completely destroyed.

Surface water runoff facilities like the one shown in the Fig. 2., may be other important subjects of maintenance especially in the first years of long-term stewardship. Experience has already shown, that leavefall in autumn may fill the facilities. As a consequence mixtures of leaves and earth may create blockades for the runoff (Ohlendorf 2004).

Consequences and work to be done

The Saxon state agency of environment and geology as the responsible licensing authority has developed a task schedule for all open questions regarding long-term stewardship. It contains the following issues:

- Financial arrangements of the federal government
- Longterm responsibility for the stewardship /Change of ownership
- Long-term stewardship measures
- Documentation and data management
- Authorities – controlling
- Communities – Bearer of information and project planners

For the tasks which are in the responsibility of the State of Saxony a time schedule was made.

References

Long-term …   IAEA Report (2005)

Leitfaden Uranbergbausanierung (2000) Wegweiser für den Umgang mit radioaktiv kontaminierten Materialien, Flächen, Bergehalden und Absetzanlagen aus dem Uranbergbau. Freistaat Sachsen. Staatsministerium für Umwelt und Landwirtschaft.

Forschungsinstitut für Bergbaufolgelandschaften e.V., G.U.B., Ingenieurgesellschaft Lausitz GmbH Bernsdorf, Finsterwalde, 15.08.1997: Grundsätzliche Darstellung und Prognostizierung der möglichen zeitlichen Veränderlichkeit von relevanten bodenphysikalisch-mechanischen Kennwerten in Bezug auf das Langzeitverhalten von Abdeckungen auf Halden der Wismut GmbH am Beispiel der Halde 366 am Standort Aue-Alberoda und Einschätzung zum System Boden-Pflanze.

Workshop Sanierung der Hinterlassenschaften des Uranbergbaus. Teil II: Abdeckung von Halden des Uranbergbaus, Tagungsband der Veranstaltung am 10. April 1997, Dresden. Hrsg. Freistaat Sachsen, Materialien zu Strahlenschutz/Umweltradioaktivität

Palme Hans, Wittig Manfred (2003) The sustainable management of industrial uranium tailing ponds - a geotechnical challenge. A case study of the Helmsdorf site. - Bauhaus-Universität Weimar, Schriftenreihe Geotechnik, Heft 10, Weimar 2003

Palme Hans (2003a): Geotechnische Probleme bei der Verwahrung von industriellen Absetzanlagen des Uranbergbaus am Beispiel der IAA Helmsdorf. - Veröff. Des Institutes für Geotechnik der TU BA Freiberg, 1. Heft

Palme Hans (2003b): Sanierung von Hinterlassenschaften des Uranerzbergbaus am Beispiel der IAA Helmsdorf. - Zeitschrift Kompakt, Jahrgang 4, Nr. 1

Merkel Broder J. (2002): Flooding of the Königstein Uranium Mine – Aquifer Reactivity Versus Dilution. Uranium in the Aquatic Environment. Proceedings of the International Conference Uranium Mining and Hydrogeology III and the International Mine Water Association Symposium, Freiberg, Germany; Springer Berlin, Heidelberg.

Meyer, Jürgen; Jenk, Ulf; Göhrs, Andrea; Schuppan, Werner (2002): Characterisation of Final Mine Flooding at the Schlema-Alberoda Site of Wismut GmbH with Particular Emphasis on Flooding Water Quality Evolution - Uranium in the Aquatic Environment. Proceedings of the International Conference Uranium Mining and Hydrogeology III and the International Mine Water Association Symposium, Freiberg, Germany; Springer Berlin, Heidelberg.

Ohlendorf, Frank (2004): Failure of Surface Water runoff facilities. – personal communication

Returning the WISMUT Legacy to Productive Use

Manfred Hagen , Alexander Thomas Jakubick

WISMUT GmbH, Jagdschänkenstraße 29, 09117 Chemnitz, Germany,
E-mail: a.jakubick@wismut.de

> …- Cela est bien dit, répondit Candide, mais il faut cultiver notre jardin »
> Voltaire, Candide

Abstract. The prime goal of the Wismut environmental remediation (ER) project follows from the legal requirement to abate health risks, mitigate existing environmental damages and prevent future hazards.

The extent of remedial measures is derived by investigation of the object-specific remediation feasibility rather than by application of uniform standards. The ER workflow, unlike common civil engineering projects that are a linear succession of tasks, is an iterative process. Within the ER workflow, Conceptual Site Models (CSM) guide the optimization of designs and investigations while both operational works and environmental base line are monitored. The acquired data are collected and analyzed on a corporate wide level to provide decision-making support for senior management.

In the present, advanced stage of the Wismut remediation the reutilization of the reclaimed areas and objects is receiving an increased attention. There are no legal restrictions on utilization of areas, which received a complete clean up. Utilization of areas, waste rock piles and tailings ponds reclaimed for restricted use allows only settlement of industry and trades or forestation, however, exemptions are possible if the responsibility for long term monitoring and maintenance are satisfactorily ensured. A mutually beneficial integration of reclamation plans with the communal/regional development has been successfully practiced in two former

mining towns, the first leading to rebirth of the health spa in Schlema and the second helping the preparation of the Federal Garden and Landscape Exhibition in 2007 (BUGA 2007) hosted by the towns of Ronneburg and Gera.

Background
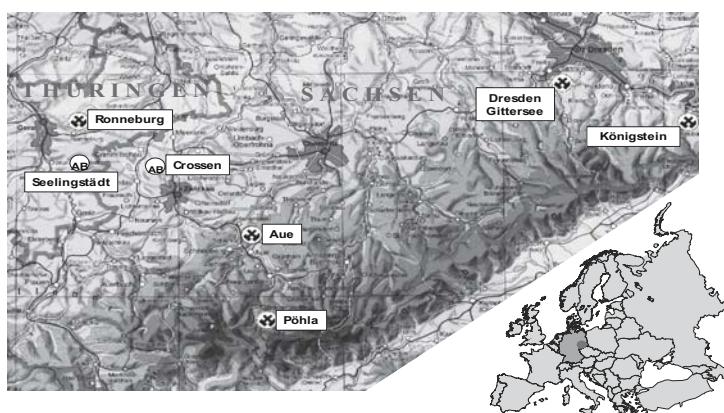
Between 1945 and reunification of Germany (1989) more than 231 000 t of U_3O_8 have been produced in Saxony and Thuringia, East Germany. The mining and milling sites are in Fig. 1.

The mining and milling operations affected an area of approximately 100 km^2 and left behind probably the "worst" uranium-mining legacy in the world. The inventory and range of liabilities left behind at the time of production closure in December 1990 was as follows:

Operations areas (37 km^2), five (5) large underground mines, an open pit mine (84 M m^3), waste rock dumps (311 M m^3) and tailings (160 M m^3). The specific activity of the waste rock is 0.5 to 1 Bq/g and of the tailings up to 10 Bq/g.

To proceed with the Environmental Remediation (ER) of this legacy, a special "Wismut Act" has been passed in the Federal Parliament, December 1991. Based on this Act the Federal Government committed DM 13 billion (€ 6.6 billion) to the ER Program (the sum was later revised to € 6.2 billion) and for purposes of reclamation the national corporation Wismut GmbH was established.

Initially there was no sufficient and proven uranium mine closure experience available in Germany and, in order to commence work without delay, extensive use has been made of the experience available internationally. Cooperation was sought with the US Department of Energy's UMTRA Project and the relevant institutions and companies in Canada. Yearly international topical workshops were

Fig. 1.   Mining and milling sites of Wismut.

organized at Wismut to foster know how acquisition and identify suitable technologies to be adopted; Regular meetings of the Uranium Mine Remediation and Exchange Group, UMREG served as a platform for international peer review of the envisaged concepts, methodologies and regulatory approaches.

Objectives and scope of the Wismut Remediation Program follow from the legal requirements of the "Federal Mining Law" (*BbergG*) stipulating the owner's obligation to abate public hazards and mitigate damages caused by mining as well as prevent future hazards after mine closure, "Ordinance for provision of radiation protection for waste rock dumps and industrial settlement ponds and for use of materials deposited therein" (*HaldAO*) regulating the radioactive aspects of remediation and "Water Resources Management Act" protecting surface and ground water from contamination.

The paper views the reclamation of the Wismut legacy as an opportunity to return the affected land, mining and milling waste sites to productive use, thus enhancing the revitalization of the former mining areas in Saxony and Thuringia.

Reclamation Management Framework

The remediation process

Prior to commencement of remedial measures, the pre-existing status of the area deemed to have been affected by mining/milling activities (approximately 100 km^2) was appraised in an initial gamma radiation survey in 1990. The initial characterization survey showed that approximately 85 % of the "affected" area had near background levels of radiation and could be released for unrestricted use.

Following initial survey, the reclamation focused on five mining sites (Ronneburg, Aue/Schlema, Poehla, Koenigstein, Gittersee) and two mill sites (Seelingstadt and Crossen). Conceptual remedial designs and closure plans were developed for each site, often concurrently with preparation of detailed designs and plans. The basic remediation goal (*s. s.*) follows from legal requirements of the Federal Mining Law, Radiation Protection Ordinance and Water Resources Management Act. Compliance with legal requirements can be achieved by straightforward technical measures such as, (a) excavation and relocation of contaminated materials, (b) reshaping of the affected areas, waste rock piles and tailings deposits to stabile landforms having slopes resisting erosion and providing good surface runoff, (c) covering of contaminated areas and objects to contain the health and environmental hazards and support vegetation, and (d) treatment of seepages and discharges.
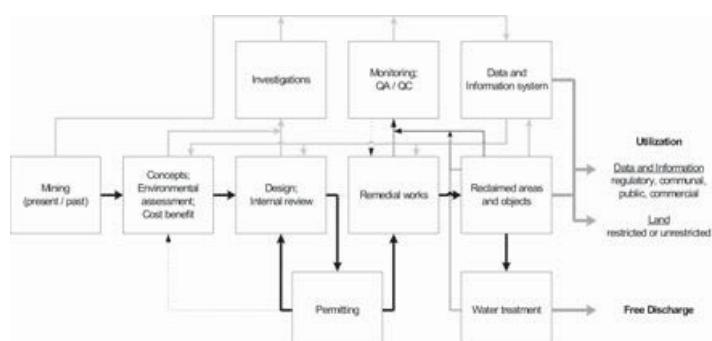
At the present stage of the Wismut project, the implementation of the remedial measures is done in 14 projects coordinated from 3 Site Management Units (Ronneburg, Aue and Königstein). Strategic direction, feedback, optimization and specialists support is provided from the Head Office in Chemnitz.

Remedial work at Wismut begins with preparation of an object-specific Environmental Impact Assessment (EIA) specifying the type and extent of physical measures to be taken. Although the preparation of EIA sometimes necessitates the acquisition of additional data and performance of investigations, it has the advantage of a transparent and traceable justification of the extent of remediation. The object-/ site-specific EIA approach has been selected over the use of prescriptive environmental limits because the EIA directly relates the extent of remediation to the actual level of risk presented by the contaminated area or object. Thanks to this approach a better remediation economics has been achieved than by use of a prescriptive generic "one solution fits all remedial problems" approach, which in most cases leads to over-engineering and consequently to excessive costs.

The radiological impact is measured by the effective individual dose, calculated for realistic release and uptake scenarios. If the calculated dose in excess of the background level exceeds the 1 mSv per year –a limit recommended by the International Commission for Radiation Protection, ICRP- the required remedial measure is specified such to achieve compliance with the 1 mSv per year criterion. Along with the radiological impact assessment, the regulated limits for conventional contamination are observed as well (e.g., As is a commonly occurring contaminant, which may take precedence over radiological impact). Following impact assessment, the feasibility of remedial design options is evaluated based on cost/benefit analysis.

Unlike in regular civil engineering projects, the implementation of the remedial measures is an iterative process rather than a linear succession of tasks, Fig. 2 (WISMUT 1995).

Although most of the delays in the remedial workflow occur due to the feedback loop created by the regulatory process, sometimes they are caused by inadequate knowledge, need of additional data and investigations. This is particularly the case for contaminants sources collocated at the same site. For optimization of the engineering solution and additional data requirements as well as prioritization of the additional remedial investigations and measures in such cases the use of a Conceptual Site Model (CSM) proved to be very helpful (Jakubick, Kahnt, 2002).
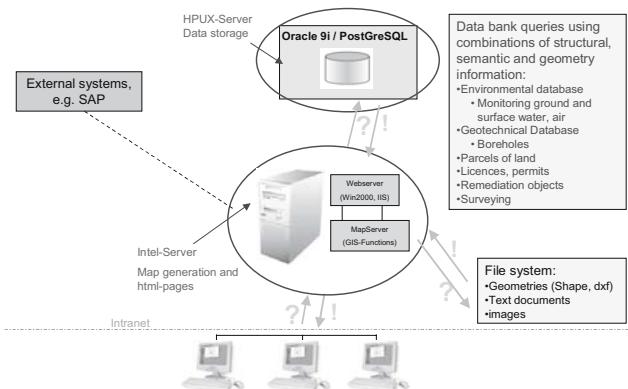
Fig. 2.   Remediation process flow, products of remediation and subsequent utilization.

Data Management

The reclamation workflow is managed by an SAP based interactive, process oriented system equipped with applications and tools sufficiently flexible to adjust to the changes occurring in course of the reclamation progress.

For data and information management an interactive, object oriented system has been created that makes the heterogeneous databases accessible on a corporate wide basis, while leaving maintenance and updating responsibilities at the data source level. The typical data/information content of the database comprises documents, photographs, object-related data, monitoring data, measurements and digital maps, geo-referenced aerial survey photographs.

Data transfer is realized through a web-based access to the "source" databanks with subsequent placement of the requested data in an object related (holding) databank on a central ORACLE server (Fig. 3). This allows fast overviews, rapid applications, specific data quires to answer multifaceted questions that require overlaying of different types of data and information. Tasks, using locator and intersection functions for geometry-based data (polygons of objects, locations of measurement points), handled otherwise by GIS can be easily accomplished using the capabilities of the databank. Users access to a continuously updated GIS supported information system is provided at all times and the only requirement on the user side is an internet explorer and fast internet access (DSL). Data safety is secured by applying very stringent conditions to the inter-/intranet access.

Fig. 3.   Technical Data and Information management system used to integrate detached heterogeneous databases.

Implementation of Remedial Measures

Contaminated areas
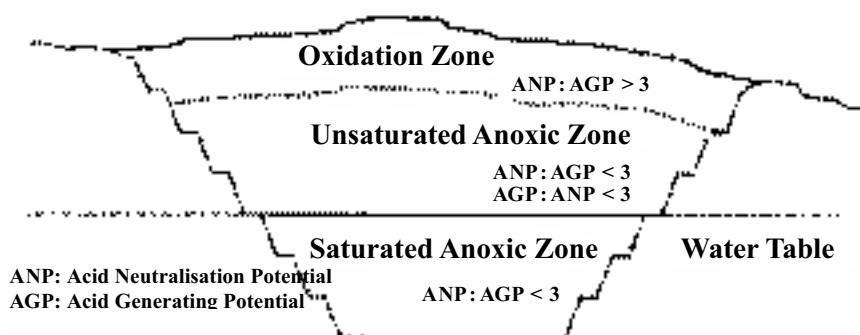
The reclamation goal for contaminated areas is (whenever feasible) to maximize the number and size of areas reclaimed for unrestricted use, which usually requires a complete area clean up.

Waste rock

Reclamation of waste rock piles is by reshaping/stabilization and covering *in situ* or by relocation to a central pile or into the open pit mine.

At Ronneburg, the waste rock piles located near the surface mine were relocated into the open pit thus resolving both the remediation of the waste rock piles and the stabilization of the open pit. The backfilling procedure follows the strategy of placing the waste rock with the highest acid generating potential (i.e. with high pyrite content) on the bottom of the pit into a zone below the groundwater level anticipated after flooding of the underground and surface mines, thus preventing oxidation of the acid generating minerals and development of acidic seepage (Jakubick, Gatzweiler, Mager, Robertson, 1997). Waste rock containing an overabundance of alkaline minerals is placed in the upper part (zone) of the pit, Fig. 4.

Following the described procedure, approximately 40,000 m^3 of waste rock per day are relocated into the pit.

Oxidation Zone

ANP : AGP > 3

Unsaturated Anoxic Zone

ANP : AGP < 3
AGP : ANP < 3

Saturated Anoxic Zone   **Water Table**

ANP: Acid Neutralisation Potential
AGP: Acid Generating Potential   ANP : AGP < 3
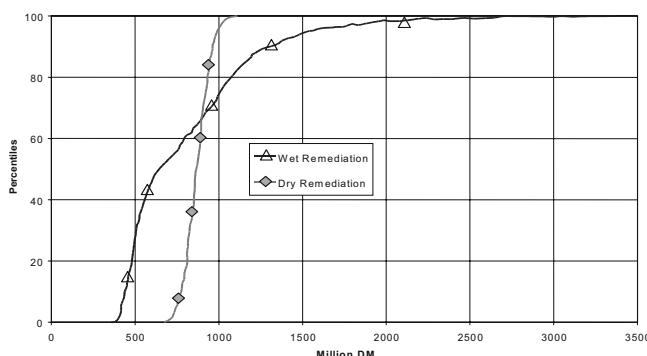
Fig. 4.   Backfilling strategy of the open pit mine at Ronneburg. Acid generating waste rock is placed in the saturated anoxic zone, neutral waste rock in the unsaturated anoxic zone and alkaline waste rock into the oxidation zone.

Tailings ponds

The objectives of remediation are stabilization of the tailings mass, provision of erosion stability and prevention of environmental contamination (WISMUT 1999). The tailings ponds at Wismut are reclaimed as "dry landforms". The "dry" reclamation strategy was justified by using a probabilistic risk assessment under consideration of the remedial costs, health and environmental benefits as well as socio-economic factors with the aim to develop a site-specific remedial solution sustainable in the long term.

The results of the risk analysis for the Helmsdorf tailings pond are presented in Fig. 5 in terms of cumulative probability of equivalent costs (sum of reclamation costs and environmental benefits -including costs of post reclamation maintenance and repairs) over the lifetime of the reclaimed tailings object. The comparison of the "dry" and water capped remedial solutions in Fig. 5 shows a better performances for the dry reclamation above 65 % of cumulative probability, i.e. in the long term, when less probable events of severe consequence (such as dam failure) enter consideration (Roberds, Voss, Jakubick, Kunze, Pelz, 1996). In the short and mid term (up to a cumulative probability level of approximately 65 %), the remedial solution using a water cap (similar to the solution implemented at Elliot Lake) promises a better economic performance. Whether decision-making should consider low probability, high consequence events or not depends on the socio-economic factors relevant for the site. In case of the Helmsdorf site, the seismic zoning of the area and the fact that the main tailings dam is located only 150 m upstream from the community of Oberrothenbach made it necessary to include the possibility of an earthquake in the analysis and consider consequences of a dam failure. The obvious result was the preference of a dry remediation, which precludes any liquefaction of tailings.

On a more general level, Fig. 5 demonstrates that ultimately, beyond cost/benefit

Fig. 5.   Equivalent Costs (remedial costs minus environmental gains) for the Wet and Dry Tailings Reclamation Options for the Helmsdorf tailings pond.

Plenary
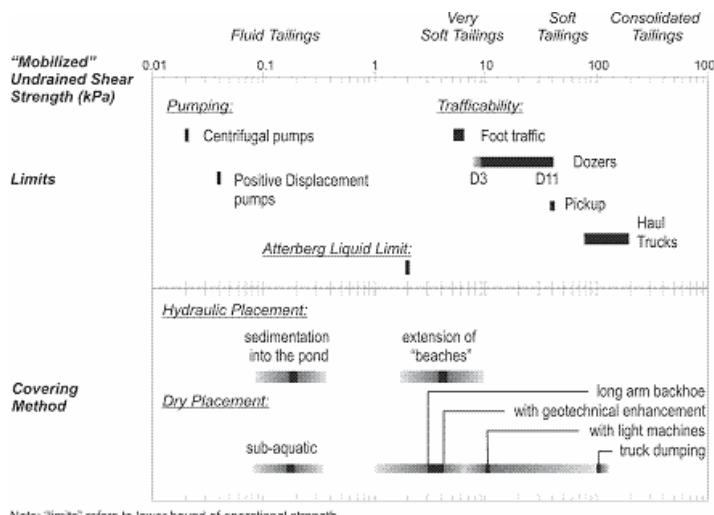
considerations, decision-making in reclamation is controlled by stakeholder's related socio-economic factors.

An overview of the most common technologies, used (worldwide) for stabilization of tailings and limits of their applicability are summarized in Fig. 6 (Jakubick, McKenna, Robertson, 2003). The suitable ranges of application of a particular technology depend primarily on the state of consolidation of the tailings, which is expressed in Fig. 6 in terms of the *in situ* shear strength of the tailings/slimes.
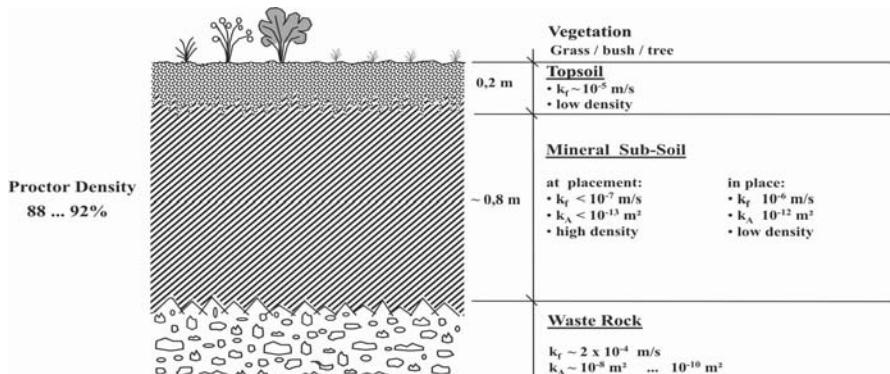
Final Covering

All landforms created out of reclaimed tailings deposits, waste rock piles (remediated *in situ* or relocated into the open pit) receive a final cover designed to reduce radiation, radon exhalation, and limit infiltration and support vegetation of the surface. An exhaustive overview and international comparison of various cover types has been presented at UMREG 2002 (Hagen, Jakubick, Lush, Metzler, 2003).

For steep waste rock pile slopes (1: 2 to 1: 2.5), Wismut experience shows that using cover designs resembling soil profiles indigenous to the area and avoiding any unnecessary interlayering that could act as a sliding plane provides usually the most stabile cover design. The relatively simple, 1 m thick, two-layer cover system (Fig. 7) used for the waste rock piles in the Ore Mountains (Erzgebirge) showed an excellent performance during the period of extreme rainstorms and inundations in August 2002. The weather event brought a multiple of the hundred years precipitation to the region and was rated as the highest rainfall expected in thousand years. Wherever the cover had been completed and the vegetation estab-

Fig. 6.   Limits and ranges of safe trafficability of the tailings surface and feasibility of various tailings stabilization technologies in dependences to the *in situ* shear strength of the tailings.

Fig. 7. A two-layer cover system emulating natural soils used at Schlema.

lished, no damage to the cover occurred. Based on the evaluation of the state of the cover after this unexpected natural test it could be concluded that the long term resilience and functionality of the described cover has been effectively proven.

One of the key performance objectives of final covers placed on uranium mining waste rock and mill tailings are, beyond physical protection of the contained contamination, radon attenuation. A novel type of assessment of long-term radon attenuation of covers has been demonstrated at Wismut (IAF Radioökologie GmbH, 2002). The method is based on measuring traces of lead (Pb-210) in the remediated object and in the cover placed on the object.

The lead traces Pb (z) are estimated as the depth-dependent differences of the specific activities of Pb-210 and Ra-226 in a cover layer:

$$Pb\ (z) = A_{Pb-210}(z)\ -\ A_{Ra-226}(z)$$

The method is primarily suitable for testing of covers older than 30 years and is based on growth of Pb-210
($t_{1/2}$ = 22 a) from Rn-222 ($t_{1/2}$ = 3,8 d), a daughter product of Ra-226 ($t_{1/2}$ = 1590 a), which is usually the main contaminant in uranium tailings.

In covers providing adequate sealing, most of the radon decays into Pb-210 after a penetration depth of 1 to 5 cm. The lead traces show discernibly positive values and the sum of the specific activities of the lead traces below and above the cover-object interface is positive.

In inadequate covers, the positive lead traces above the cover-object interface are weak (little accumulation of Pb-210) and the lead traces in the tailings or waste rock are strongly negative due to weak attenuation of radon transported toward the cover. The sum of the specific activities below and above the interface is negative.

Fig. 8 shows the performance of an inadequate tailings cover constructed more than 30 years ago. The thickness of the cover is 50 cm and consists of a single layer of mineral soil (mostly sand). The lead traces measured are clearly negative, evidencing that a 50 cm cover layer of the sandy material used is insufficient to provide adequate radon attenuation.

Flooding of mines
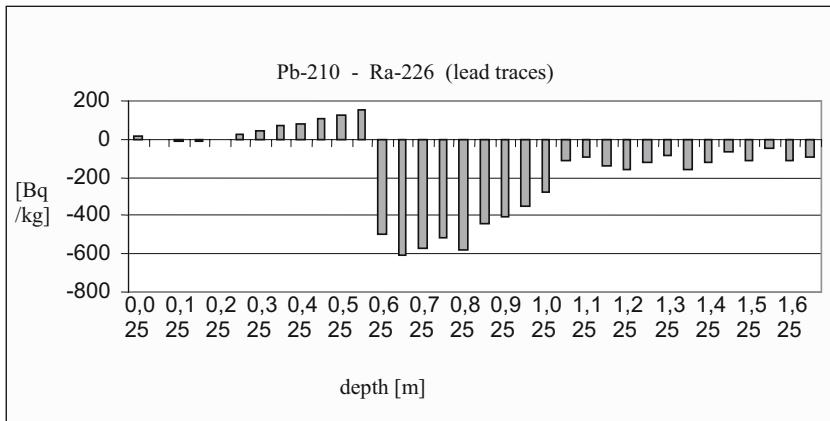
The mine flooding is done in a controlled way to prevent contamination of surface water bodies and of aquifers serving as water supply (Jakubick, Jenk, Kahnt, 2003). Mine water discharges are in order of 50 to >1000 m^3/h, depending on the characteristics of the mine. Other discharges in need of treatment arise from dewatering of tailings ponds (several hundreds m^3/h) and from waste rock dump seepages (1 to 30 m^3/h). The water treatment residues (containing approximately 500Bq/g) are disposed of into waste rock piles and tailings.

Observations of mine discharges, which present the largest long-term source of contaminated water, indicate that the initial peak load of contaminants decreases within several years more or less exponentially (WISMUT 1997). After the peak load is over, it is to be expected that treatment requirements decrease as well, allowing the introduction of alternative, more cost-efficient methods.
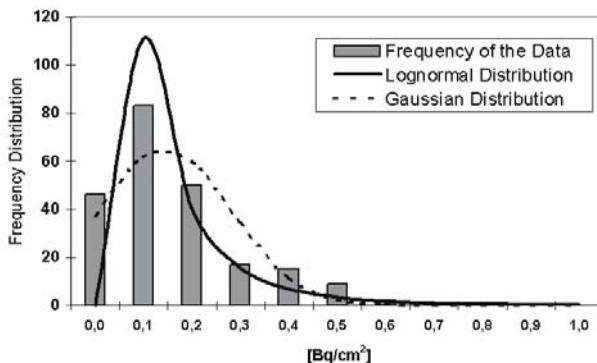
Scrap metal

During remediation, considerable amounts of contaminated debris and scrap metals arise from demolition of structures. The contaminated metal components have a total alpha surface activity (TAA) in the range of mBq/cm^2 to Bq/cm^2 (of U-238 and daughters). After demolition, contaminated and non-contaminated scrap metal usually ends up intermixed in unsorted heaps, showing typically a contamination distribution as presented in Fig. 9.

The separation of non-contaminated metal for recycling requires a reliable discrimination from contaminated material. To improve selectivity without giving up using standard portable, large surface (beta) contamination monitors in the field, a sophisticated method of calibration and measurement has been introduced. Based

Fig. 8.   Distribution of lead traces in a cover- tailings system at Lengenfeld. The cover was built in 1970s .

Fig. 9.   Typical contamination frequency distribution of TAA values in a scrap metal heap at WISMUT.

on the operational history of the particular facility and/or equipment dismantled, the level of contamination is pre-categorized and the anticipated nuclide vector and index nuclide established in the laboratory. Prior to the field campaign, the field instruments are calibrated against laboratory measurements of the specific waste type. Following this procedure, the estimation of TAA from the measured beta-count rates proved to be feasible with the required accuracy.

The decision whether to release or disposal of the scrap metal is based on the comparison of the TAA reference value (0.5 Bq/cm^2) with the upper limit of the confidence interval (95 % confidence value) applicable to the particular contaminated scrap metal heap.

The contaminated metal, which cannot be released, is disposed of into tailings, open pit backfill or waste rock piles. Investigations demonstrated that the risk potential of these objects increases only marginally due to the added scrap metal.

Monitoring

Operational monitoring

Operational monitoring of the ongoing remedial works is part of the radiation safety plan for protection of workers, general public and environment exposed to the contaminants handled in course of remedial works.

The monitoring is done at the working site where the emissions arise and at places where impacts may be expected. The purpose of operational monitoring is to observe whether in course of handling of environmental, radiological or chemical contamination the regulated standards are kept and the contaminants release does not lead to unacceptable radiological or chemical exposure. In addition to measurements of direct gamma radiation, critical radionuclides and chemical con-

taminants, great emphasis is placed on measurement of dust emission (that may contain long lived alpha emitters and toxic elements). Sprinkling (water trucks) is applied routinely to prevent dusting at working places and construction roads during dry periods. Commonly, water arising on the site is used for sprinkling, which is then recycled within the site.

Monitoring of the environmental baseline

The monitoring program was designed with consideration of the fact that the remediation is carried out as an intervention measure mitigating a pre-existing situation. Because pre-mining baseline measurements were unavailable for the remediation sites, the monitoring program was developed on the basis of the initial characterization survey (see "The remediation process" section) and predictive analysis of the exposure pathways.

The baseline monitoring network is used to measure the level of contaminants typical for Wismut sources and related parameters in surface and ground water, seepage, air (particulates and radon), gamma radiation levels, soil and, in some instances in the human food chain. Good overviews of the Wismut approach to monitoring and of other international monitoring programs are provided in (UMREG'03).

The monitoring of liquid discharges demonstrates very well the effectiveness of the first remedial measures: Beginning of 1990 the Wismut discharges carried a uranium load of approximately 28 tons, which already 1998 decreased to less than 4 tons of uranium per year. The decrease since 1998 was less spectacular but continual and the Uranium load presently amounts to approximately 3t per year. A similar decrease pattern has been recorded for Ra-226: Early 1990 the discharges contained more than 23 000 MBq Ra-226, which decreased to less than 300 MBq by early 2004.

Completion of reclamation, release from regulatory supervision and long-term stewardship

Upon completion of remediation of an area or object, a final certificate is issued, which presents the basis for application for release from regulatory supervision. Presently, with more complex objects nearing completion the need arises to submit the reclaimed areas and objects to final assessments and, based on the results, adjust the extent of monitoring the future needs.

Concerning data management it follows that for purposes of long-term stewardship it is necessary to retain (WISMUT'05):
- Key data on the inventory and on the "as-remediated" status of the reclaimed areas and objects
- Environmental monitoring data
- Predictions re long term performance along with supporting documentation, such as CSM

The Wismut data system is to serve as an evidence of proficiency of the remedial measures and provide support for:

- Management of the "Wismut real estate",
- Handling of claims and liability issues,
- Handling of information requests of investors, regional and communal developers,
- Handling of public inquiries,
- Continual adjustment/optimization of water treatment to the development of mine and seepage water characteristics.

In addition, the Wismut data bank system is to serve as a remediation knowledge base and help answering questions in case of potential repairs.

In agreement with the regulator a post-remediation period of five years has been foreseen by Wismut as a "remediation warranty" period during which the performance of the reclaimed objects regarding erosion, geomechanical failure, direct gamma radiation, radon emission and seepage control will be monitored.

After conclusion of physical remedial works and establishment of stable conditions, the number of monitoring points and frequency of measurements will be adjusted and reduced to the slower rate of changes typical for natural processes.

The duration of the post-warranty phase monitoring is currently a matter of dispute with the regulator.

Utilisation of reclaimed areas and objects

The most tangible results of remediation are the reclaimed land, rehabilitated waste rock piles and tailings. Observing the experience made by external projects led us to conclude that both sustainability of the remediation results and post remedial stewardship is best guaranteed if the reclaimed land and objects are put to productive use (irrespective whether unrestricted or restricted). To achieve this goal,

a) in addition to containment of the health and environmental risks, the socio-economic effect of environmental reclamation, particularly its contribution to the regional revitalization and development must be given due (sometimes even decisive) consideration, and

b) the future use of the reclaimed areas/objects should be specified prior to reclamation.

We believe that value added results can be achieved at no additional (or at reimbursable) costs, if reclamation is done with a well-defined utilization in mind (WISMUT 2004). *Vice versa*, successful utilization goals can only be developed in cooperation with the future user (i.e. municipality or developer), community and regulatory authorities. If consensus is achieved with the stakeholders prior to remedial works, a "reclamation by objectives" becomes practicable, i.e. the objectives for the individual remedial steps can be set consistent with the ultimate utilisation goal.

Concerning utilization, there are no legal restrictions placed on areas completely cleaned up of contamination. Considering the population density of Thuringia (154 inhabitants per km^2) and Saxony (247 inhabitants per km^2), there are usually no problems finding interested parties for the land, which had been completely cleaned-up.

However, given the high costs of a complete clean up and the relatively small risk presented by slightly contaminated areas, a remediation aiming for unrestricted utilisation cannot be justified in many cases. In line with the recommendations of the German Commission on Radiological Protection (SSK-92, volume 23) a partial reclamation can be performed in such cases; the restricted utilisation usually implies that only settlement of industry and trade is recommended.

The utilization of waste rock piles and tailings ponds is regulated by the "Ordinance for provision of radiation protection for waste rock dumps and industrial settlement ponds and for use of materials deposited therein, (HaldAO)", which specifies forestation as the eligible utilization. Although the type of utilisation in the above cases is restricted, exemptions to the recommended utilisation are possible, if the obligations for long-term stewardship can be satisfactorily settled. The economic objective under the exemption rule is to find a potential utilization, which could at least partly cover the costs of the long-term monitoring and maintenance.

Reclamation with the objective of implementation of a specific utilization often requires an extensive soil conditioning in addition to the "regular" remediation (following strictly legalistic sense). We are of opinion that soil conditioning in such cases is not "additional costs" but present the price for avoiding maintenance costs at a later point; Indeed, a value added upgrading of a remediated area/object should be viewed as an investment into making future utilization possible.

The most common utilizations of reclaimed areas/objects are forestation or establishment of green fields. Forestation has the advantage of being a low maintenance utilization option, sustainable in the long run.

The rationale for implementation of more "creative" types of utilization such as establishment of a golf course, ground for model plane practice, erection of solar panels, etc. is that these uses act as seeds for further regional/communal development.

A good example of successful integration of reclamation and town (re-) development is provided by the city of Schlema, where recreational facilities, such as the health spa, parks, promenade, golf course, etc. were established on a backfilled and rehabilitated mine subsidence area and on rehabilitated waste rock piles.

Major impulses for the development of the former mining towns of Ronneburg and Gera are expected to come from the Federal Garden and Landscape Exhibition in 2007 (BUGA 2007), the planning of which is closely related to the progress of reclamation works in the open pit mine located near the town of Ronneburg.

Furthermore, even if not always fully realized by the stakeholders, the mine and seepage waters discharged after treatment often present an important contribution to maintaining a steady flow in the streams managed by the regional authorities usually affecting a substantial improvement of the environmental quality of the water as well.

Lastly, it must be clearly stated that the know how acquired in course of Wismut remediation presents a unique commercial asset, which is to be utilized as broadly as possible both locally and for the benefit of the numerous areas in need of post mining reclamation.

Technology transfer

In course of remediation a considerable degree of work standardization has been achieved and since 1995 the Wismut remediation technology has been applied in a number of external projects, mainly in Central and Eastern European countries, Russia and Central Asia. The external activities mainly focused on (1) assistance with concept development, planning, engineering and procurement of works, (2) specialized training and education and (3) auditing and project monitoring (STETE European Security, 1/2004). Since 2002, the responsibility for external activities lays primarily with WISUTEC GmbH, a commercial daughter of WISMUT GmbH.

References

WISMUT' 95, Proceedings of International Workshop on Environmental Remediation in Waste Rock Piles, November 6-8, 1995, Chemnitz, Germany.

Jakubick, A.T., R. Kahnt, „Remediation oriented use of conceptual site models at WISMUT GmbH: Rehabilitation of the Trünzig tailings management area" in Merkel, B. J. et al. (Eds.) Uranium in the Aquatic Environment. Proceedings of the International Conference Uranium Mining and Hydrogeology III and the International Mine Water Association Symposium, Freiberg, Germany, 15-21 September 2002. Springer-Verlag 2002.

Jakubick, A.T., R. Gatzweiler, D. Mager, A. Robertson, „The Wismut Waste Rock Pile Remediation Program at the Ronneburg Mining District", Proceedings of 4th International Conference on Acid Rock Drainage, Vancouver, B.C. Canada, May 31-June 6, 1997

WISMUT'99, Proceedings of International Workshop on Stabilization of Fine Tailings, Part 1: The Scientific Basis, Edmonton, Canada, May 26-27, 1999, Syncrude Canada Ltd. and Part 2: Practice and Experience, Chemnitz; Germany, June 23-25, 1999, Wismut GmbH.

Roberds, W., C.Voss and Jakubick, A.T., C. Kunze, F.Pelz „Multi-Attribute Decision Analysis of Remediation Options for Uranium Mill Tailings Impoundment in Eastern Germany", Inter. Topical Meeting on Probabilistic Safety Assessment: Moving toward Risk-Based Regulation, ANS Meeting, Park City, Utah, September 29 -October 3, 1996

Jakubick, A.T., G. McKenna, A.M. Robertson, „Stabilization of Tailings Deposits: International Experience, Mining and the Environment III, 25-28 May 2003, Sudbury, Ontario, Canada

Hagen, M., A.T. Jakubick, D. Lush, D. Metzler, „Integrating Technical and Non-technical Factors in Environmental Remediation", Proceedings of UMREG'02, 2003, Wismut GmbH and ICEM 2003.

WISMUT Report, "Retrospektive Untersuchung des Langzeitverhaltens der Radon-Dämmwirkung von einfachen mineralischen Abdeckungen auf Dammböschungen industrieller Absetzanlagen und auf der Nordhalde am Standort Ronneburg mittels Bleispurmethode"; IAF Radioökologie GmbH, Chemnitz, Mai 2002.

Jakubick, A.T., U. Jenk, R. Kahnt, "Modeling of Mine Flooding and Consequences in the Mine Hydrogeological Environment: Flooding of the Koenigstein Mine, Germany", Environmental Geology, Springer, 2002.

WISMUT'97, Proceedings of International Workshop on Water Treatment and Residues Management – Conventional and Innovative Solutions, September 24. –26, 1997, Chemnitz.

STETE, "Cleaning up Radioactive Environments: Undoing a Wasteland", OSCE Review, Vol. 11, 1/2004, Published by the Finnish Committee for European Security, Helsinki

UMREG'03, Proceedings of the Uranium Mine Remediation Exchange Group Meeting at Oxford, September 24, 2003.

WISMUT'05, "Das Datenmanagement in der WISMUT GmbH – Stand und Perspektiven", March 16, 2004, Chemnitz

WISMUT'04, Proceedings of the Workshop on Utilisation of Areas, Waste Rock Piles and Tailings Ponds, May 11. – 12, 2004, Chemnitz

The Effects of Weathering and Diagenetic Processes on the Geochemical Stability of Uranium Mill Tailings

Greg Sinclair[1], Graham Taylor[2], Paul Brown[3]

[1]Rio Tinto Technical Services, 1 Research Avenue, Bundoora, VIC 3083, Australia
[2]PO Box 43, Stirling, SA 5152, Australia
[3]Australian Sustainable Industry Research Centre, Building 4W, Gippsland Campus, Monash University, Churchill, VIC 3842, Australia, Email:
paul.brown@asirc.org.au

Abstract. In the present study, a detailed examination of tailings cores and pore waters, kinetic column test work and geochemical modelling was combined with results from earlier studies to examine the key processes governing the geochemical stability of the Ranger tailings. Conclusions drawn from the work clearly demonstrates that the solid state speciation and mobility of metals and radionuclides in the tailings pile are governed by the processes of oxidative dissolution of sulfide minerals, weathering of phyllosilicates and organic matter diagenesis.

Introduction

In response to growing community concerns and increasing government regulation, mining companies are placing a greater emphasis on mine waste management to ensure that potentially harmful substances are safely stored in a manner that permits the restoration of post mining land uses. These wastes principally comprise waste rock arising from mining operations and tailings produced from the milling process. The milling process is designed to separate the ore (economic mineralisation) from gangue minerals, the latter often comprising of acid forming sulfides, radionuclides and toxic metals/metalloids such as lead, copper, mercury, cadmium, arsenic and selenium.

In the generation of tailings, the physicochemical properties (particle size, moisture content, chemical composition) of the host rock are altered by the action of comminution (mechanical crushing and grinding) and concentration which invariably requires lixiviants (such as acid, cyanide or oxidants) and other process chemicals. As a consequence the gangue minerals that comprise the tailings are much more susceptible to erosion and chemical weathering which, if not controlled, can lead to the release of harmful quantities of contaminants (far in excess of those released from the original ore body) into the environment. Therefore, the security of tailings disposal, particularly in the long-term and effective rehabilitation of tailings repositories are vital attributes of mine planning.

The principal objectives of decommissioning and rehabilitation of tailings storage facilities (TSFs), particularly above ground TSFs, are well known and according to the International Commission on Large Dams (ICOLD, 1996), include:

- Stabilisation of the impoundment - involving consideration of long-term stability, seismology, erosion protection and drainage systems;
- Hydrology - long-term assessment of catchment runoff, diversion arrangements and   risk of breaching during heavy rainfall events;
- Contamination - leachate control or containment, surface and seepage water quality;
- Aesthetic or visual impact;
- After use or final land-use considerations; and
- Safety - public accessibility and inherent dangers, long-term surveillance and monitoring.

However, despite national and international standards/guidelines on tailings management there are still disastrous failures and long-term or chronic environmental impacts arising from TSFs. The most recent and notable catastrophic dam failures include Marcopper in the Philippines (1996), Merrienpruitt in South Africa (Wagener, 1997), the Las Frailes incident in Spain (1998) and Baia Mare in Romania (2000). All of these incidents involved a failure that resulted in the immediate release of large quantities of tailings and/or effluent into local rivers and nearby communities.

To allay community concerns prudent design, planning and management of TSFs for both operation and closure require a systematic risk-based approach to identify potential hazards, controls and mitigating measures. Fundamental to this assessment and planning process is a detailed understanding of the mineralogical characteristics and geochemical mechanisms that control the long-term evolution of the tailings and possible transfer of contaminants from the storage facility to the environment. Only through a thorough understanding of these mechanisms will it be possible to improve the certainty of environmental impact assessment and, in so doing, better define the requirements for the safe operation and ultimate long-term closure of TSFs.

Australia, like many other developed countries, has a history of rehabilitation of uranium mill tailings that shows an evolutionary approach in techniques and standards from the minimalistic strategies of the 1950's, through the post closure

planning era of the 1980's, to the holistic life of mine planning of the present time (Waggitt, 1994).

Cost effective design and safe management of uranium mill tailings can only be achieved if the risks to human health and the environment are recognised and understood at the time of mine planning. The application of environmental geochemistry is essential in the early phase of mine planning as it provides a systematic means of understanding the interactions at the tailings solid-water interface. These reactions are fundamental to the evolution of tailings pore waters and the rate of re-distribution and hence fate of contaminants within the tailings pile. At the macro level, this information is required to assess the long-term integrity of the proposed or existing TSF and its ability to prevent impacts on the beneficial values (ecological, human health) of surface and ground waters.

The paucity of integrated geotechnical/geochemical assessment protocols combined with the community's demand for greater environmental stewardship and conservation, provides a unique research opportunity to study the role of environmental geochemistry in the initial impact assessment of uranium mill tailings and for their subsequent long-term management and disposal.
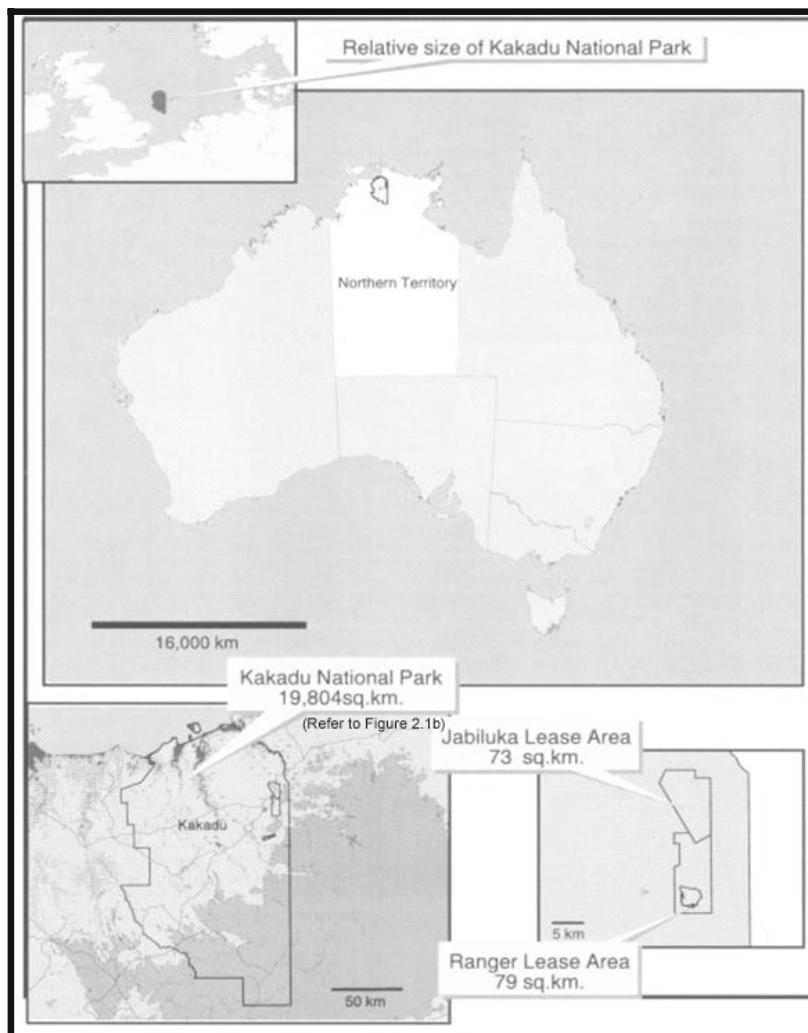
For these reasons, the Ranger uranium mine was chosen as an ideal site for researching the effects of weathering and diagenesis on the long-term geochemical stability of uranium mill tailings. More specifically, we set out to demonstrate that the solid state speciation and mobility of metals and radionuclides in the tailings pile are governed by the processes of oxidative dissolution of sulfide minerals, weathering of phyllosilicates and organic matter diagenesis. Combined, these processes lead to the formation of authigenic minerals which control the solubility of pore water constituents and the long-term geochemical evolution of the tailings pile.

The Ranger Mine Project

Energy Resources of Australia Limited (ERA) owns and operates the Ranger Mine. The Ranger Mine and associated leases (Fig. 1) occupy a combined project area of approximately 79 km^2 enclosing some nine radiometric anomalies. Although the project area is excluded from Kakadu National Park, it does lie on Aboriginal land and hence is leased from the local Traditional Owners. To the north and adjoining the Ranger Project Area (RPA), is the 73 km^2 Jabiluka Project Area which is also leased by ERA. Fig. 2 shows the areal extent of both the Jabiluka and Ranger mine sites.

The Ranger operations consist of two ore bodies, Ranger #1 and #3 that are mined by open pit methods. Total reserves were estimated at 166 300 tonnes of U_3O_8 (Savory, 1994). Processing of ore from Ranger #1 commenced in October 1981 and was continuously mined until 1994 when the economic ore was depleted. Ore is currently sourced from the Ranger #3 pit which has a projected mine life of 13 years that will end in 2008.

Fordham (1993) after Eupene et al. (1975) succinctly summarized the mine geology as being dominated by intense chloritisation with variable lithology. Rock types within the ore body include mica-quartz-feldspar schists subjected to varying degrees of chloritisation, magnesium or dolomitic carbonates, carbonaceous schists, gneisses, dolerites and pegmatites. The primary ore mineral in Ranger #1 is uraninite ($UO_2(s)$). Secondary uranium minerals such as torbenite ($Cu(UO_2)_2(PO_4)_2 \cdot 8\text{-}12H_2O$) and saleeite ($Mg(UO_2)_2(PO_4)_2 \cdot 8H_2O$) are enriched in a 20 m thick lateritic ore zone (Savory, 1994).

Fig. 1.   Relative sizes and location of Kakadu National Park, Jabiluka and Ranger Mine leases.
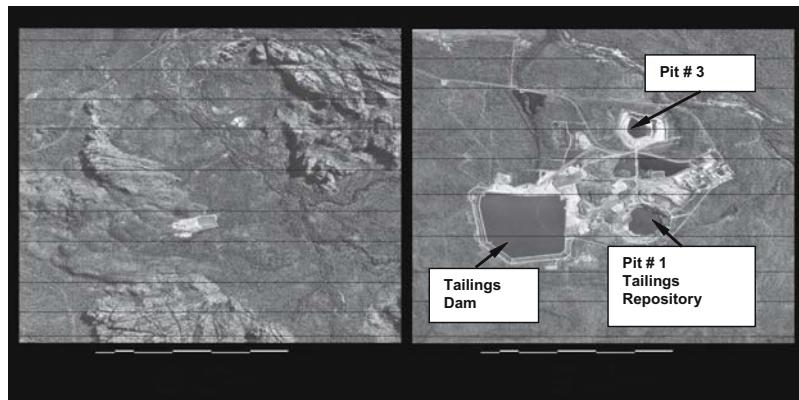
Almost 50% of the gangue is magnesium chlorite, with an additional 40% comprising quartz and sericite. Petrographic analyses (Savory, 1994) show that ore minerals invariably occur within a matrix of fine compact chlorite. The primary ore also contains galena, localized pyrite, smaller quantities of finer chalcopyrite, dolomite, apatite, rutile and hematite.

Tailings management incorporates a 107 ha tailings dam and the Ranger #1 (or Pit #1) void (Fig. 2). The tailings dam has a capacity of 15 Mm^3 and currently stores approximately 13 Mm^3 of Ranger #1 tailings at an overall density of 1.09 t/m^3. Tailings are no longer pumped to the dam, as it is used to evaporate excess process water. Since December 1996, tailings from the milling of Ranger #3 ore and the remaining stockpiled Ranger #1 ore have been deposited into the Pit #1 void. At the end of mine life, the closure plan requires that all tailings be transferred to the Pit #1 and #3 voids for final storage. Thus, the site of the existing tailings dam will be rehabilitated and restored such that the land can be incorporated back into Kakadu National Park. Careful design of the pit repositories and isolation of the tailings from surface and ground waters will be essential for the long-term protection of Kakadu's World Heritage values.

The tailings dam is a 1 km^2 ring dyke or turkey's nest impoundment located 500 m due west of the Ranger #1 pit. It lies across the head of a shallow valley which once formed the headwaters of Coonjimba Creek as shown in Fig. 2 (Sinclair, 1992).

The main minerals in the solid phase of the tailings at Ranger are quartz, chlorite, muscovite and gypsum. Large particles of hematite have been observed by SEM, and other minerals found in minor amounts are pyrite, chalcopyrite, galena, uraninite and brannerite (Fordham, 1993). Sulfur speciation is predominated by acid-soluble sulfates (Fordham, 1993).

Lime was used to neutralise acid tailings, usually to a pH just above neutral. Magnesite was also used as an alternative to lime (Fordham and Beech, 1989). The deposition of acid tailings was also trialled to improve settled density (Fordham and Beech, 1989; Richards and Peter, 1990; Fordham et al., 1992; Fordham, 1993; Fordham et al., 1993).

Fig. 2.   Aerial view of Jabiluka (left) and Ranger (right) Mine sites.

Integrated Study Program

Within the present study, an integrated research program was developed to characterise the key equilibrium and kinetic processes that control the long-term geochemical evolution and fate of contaminants such as evaporites (Mg/Ca sulfate salts), radionuclides (uranium and radium-226) and trace metals (Cu, Pb, Cd, Ni and Co) within the Ranger tailings pile.

Specific activities undertaken within the study included:

- A critique of contemporary international research on the application of environmental geochemistry for assessing the risks and long-term closure requirements of tailings storage facility;
- Mineralogical and geochemical characterisation of fresh (run of mill) and aged (permanently stored) uranium mill tailings;
- Establishment of tailings depth profiles within the tailings storage facility for the *in situ* measurement of pore water chemistry;
- An assessment of the solid state speciation or partitioning of radionuclides within the tailings solids;
- Establishment of large scale laboratory kinetic leach columns to simulate the long-term geochemical evolution of the tailings pile and to identify mechanisms responsible for the solubility and release of radionuclides and accessory minerals into the receiving environment; and
- Development of a geochemical model that combines both equilibrium and kinetic processes to predict the chemical mass balance and long-term evolution of tailings pore waters.

The study attempted to highlight the important geochemical features of uranium mill tailings that either have positive and/or detrimental implications for their long-term management. Acquisition of such knowledge will assist in the development of appropriate controls and contingency measures to ensure that problematic drainage or seepage losses do not impact on the beneficial uses (human health and ecological) of regional surface and ground waters.

Field Investigations

Two sampling campaigns were conducted in the tailings dam, one in January 1998 to collect undisturbed tailings cores and the second in June 1999 to install and collect in-situ porewater samples. Data obtained from these campaigns allowed for a detailed evaluation of vertical and lateral hydrogeological and hydrochemical profiles within the tailings impoundment. Sample locations for both campaigns are shown in Fig. 3. Vertical cross-sections of core profiles are shown in Fig. 4.
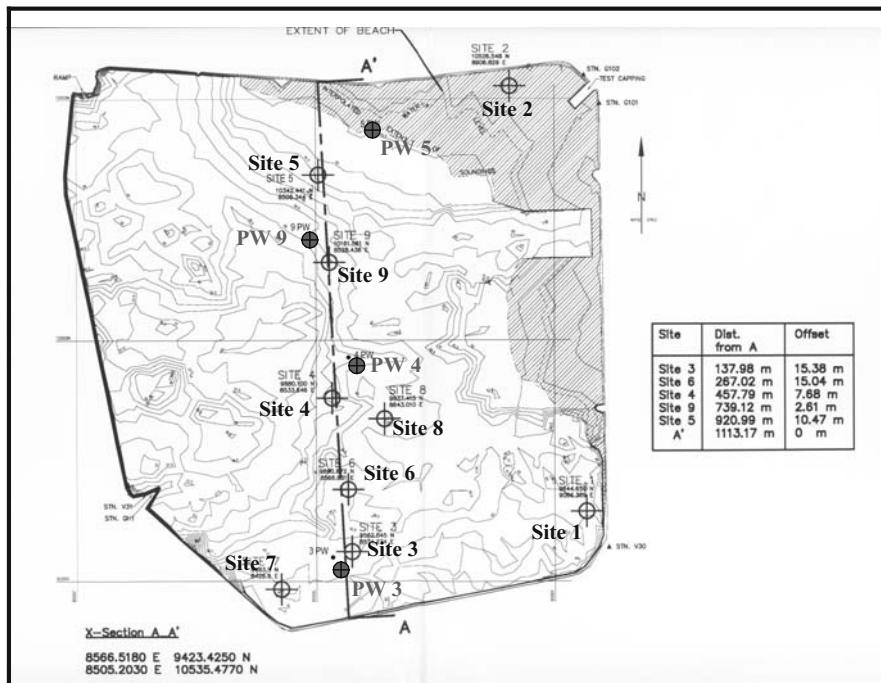
Fig. 3.   Tailings dam sample profile locations.
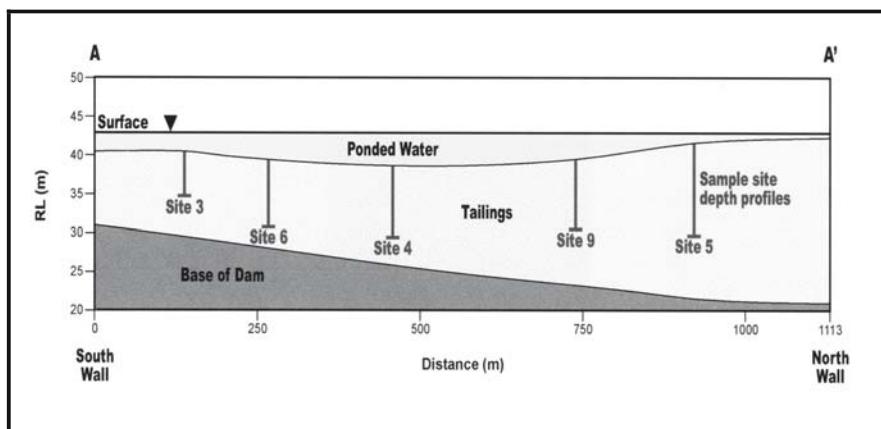
Fig. 4.   Cross section A-A' tailings core profiles (January, 1998).

Tailings and Mill Chemistry

Markos (1979) has described the geochemical reactions that occur in a typical sulfuric acid-leach/tailings neutralisation uranium mill, resulting from the interaction of the acid-lixiviant and the uraniferous ore. Importantly, ferric ion (Fe^{3+}) is required in the leach solution to achieve rapid and complete oxidation of tetravalent uranium. Uraninite ($UO_2(s)$) is the principal uranium mineral:

$$UO_2(s) + 2Fe^{3+} \leftrightarrow UO_2^{2+} + 2Fe^{2+} \tag{1}$$

The addition of an oxidant, such as pyrolusite (MnO_2) or sodium chlorate ($NaClO_3$), in sufficient quantity ensures that iron is present predominantly as Fe^{3+}. The second part of the leaching oxidation process is the addition of dilute sulfuric acid to control the pH at around 1.8. At this pH, the sulfuric acid ionizes to sulfate, bisulfate and hydrogen ion. Acid is not consumed directly by dissolution of UO_2 but is required to oxidise iron from the ferrous to ferric valency state. In addition to uranium, the oxidation process also causes the dissolution of gangue minerals (carbonates and aluminosilicates) and accessory metal/metalloid sulfides.

Because acidic (pH 2) uranium tailings water is high in aqueous sulfate and near gypsum saturation, the addition of slaked lime ($Ca(OH)_2$) to neutralise the tailings to pH 7 to 8 initiates gypsum precipitation. The addition of lime also initiates the precipitation of a number of other secondary minerals as described by Morin (1983): ferrihydrite ($Fe(OH)_3$), gibbsite ($Al(OH)_3$), aluminosilicates ($Al_2Si_2O_5(OH)_4$) and amorphous silica ($SiO_2(am)$). The formation of these secondary minerals creates a highly reactive geochemical environment that affects the solubility of radionuclides and metals via direct precipitation-dissolution, coprecipitation and sorption processes.

The tailings also contain significant quantities of microbiologically reactive organic and nitrogen compounds. The presence of organic matter in the tailings is significant as several studies (Sholkovitz, 1973; Froelich et al. 1979; Van der Weijden, 1992; Postma and Jakobsen, 1996) on natural sediments show that post-depositional reactions are primarily fuelled by the microbially-mediated decomposition of organic matter.

Organic matter is the key to any biogeochemical consideration of sediment diagenesis, not only because it represents chemical potential energy capable of driving diagenetic reactions but also because it plays a critical role in cycling radionuclides and trace metals. This metal cycling occurs as a result of the redox couple that forms between the electron donor (organic matter) and an in-situ oxidant that accepts electrons from organic matter (Stumm and Morgan, 1996). The oxidation of organic matter proceeds via the reduction of various oxidants in their decreasing free energy yield per mole of organic carbon oxidised. Reactions releasing the highest free energy yield ($-\Delta G^{\circ}_r$) also produce the greatest available energy for bacterial utilisation.

The order of oxidation proceeds with the initial removal of dissolved oxygen followed by the reduction of nitrate, manganese(IV), uranium(VI), iron(III), molybdenum(VI) and sulfate, as is summarised in Table 1. These reactions best rep-

resent the key redox couples within the tailings pile and are well documented as being mediated by heterotrophic bacteria.

Of the 45 cores recovered from the tailings impoundment, six were selected as best representing the various lithogenic and authigenic phases observed along the 1 km long N-S sampling transect (see Figs. 3 and 4). These cores were subjected to a detailed physical, mineralogical, geochemical and analytical program, the results of which are only partially described in the following sections to demonstrate how organic matter diagenesis and authigenisis control the long-term geochemical stability of the tailings pile.
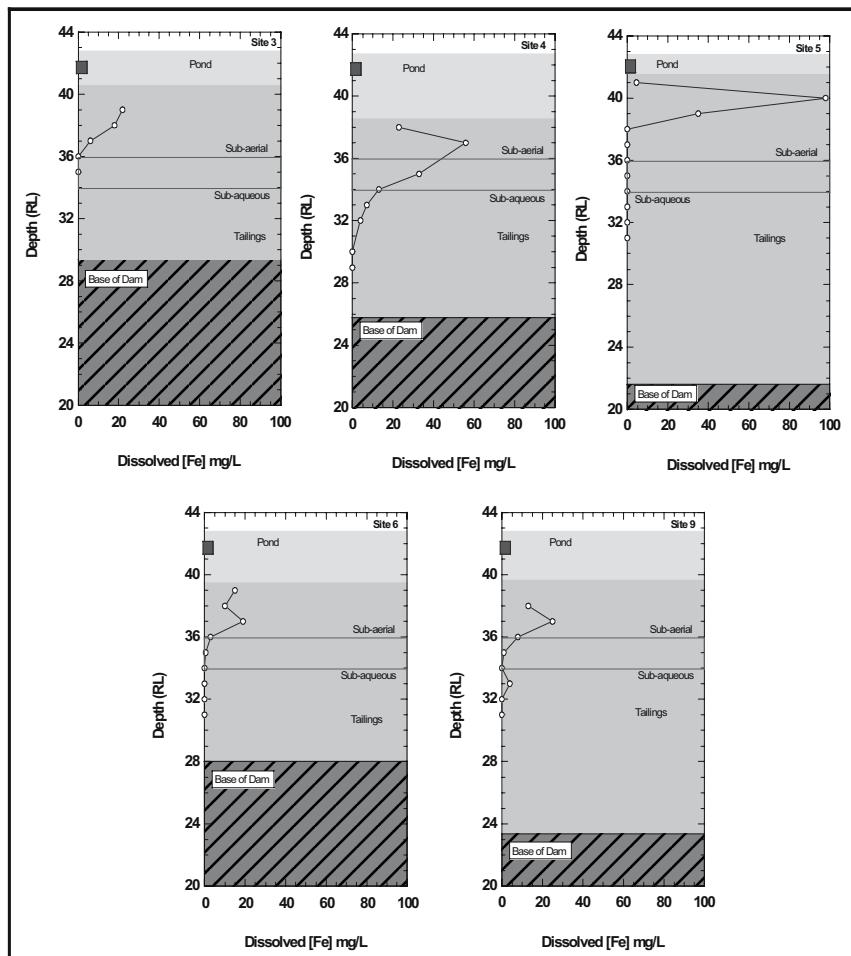
Table 1. Half cell reactions of oxidants present in the tailings pile and their associated free energies and electron activities.

Half Cell Reaction*	ΔGr	$p\varepsilon$
	kJ mol^{-1}	
Oxidation Reaction		
$CH_2O + H_2O \leftrightarrow HCO_3^- + 5H^+ + 4e^-$		
Reduction Reactions		
$O_2 + 4H^+ + 4e^- \leftrightarrow 2H_2O$	-474	13.76
$0.8NO_3^- + 4.8H^+ + 4e^- \leftrightarrow 0.4N_2 + 2.4H_2O$	-480	12.00
$2MnO_2 + 2HCO_3^- + 6H^+ + 4e^- \leftrightarrow 2MnCO_3 + 4H_2O$	-478	8.60
$4Fe(OH)_3 + 4HCO_3^- + 8H^+ + 4e^- \leftrightarrow 4FeCO_3 + 12H_2O$	-376	0.70
$2UO_2(SO_4)_2^{2-} + 4e^- \leftrightarrow 2UO_2(am) + 4SO_4^{2-}$	-56	0.17
$2UO_2(CO_3)_2^{2-} + 4H^+ + 4e^- \leftrightarrow 2UO_2(am) + 4HCO_3^-$	-146	0.11
$2MoO_4^{2-} + 8H^+ + 4e^- \leftrightarrow 2MoO_2 + 4H_2O$	-342	-1.86
$0.5SO_4^{2-} + 4.5H^+ + 4e^- \leftrightarrow 0.5HS^- + 2H_2O$	-96	-3.76

* Equations are representative of the following average porewater concentrations and conditions: [U] = 1.7×10^{-6} mol L^{-1}; [NO$_3^-$] = 1.1×10^{-3} mol L^{-1}; [SO$_4^{2-}$] = 0.25 mol L^{-1}; pH = 7; [Mo] = 2.0×10^{-6} mol L^{-1}; [HCO$_3^-$]= 2.5×10^{-4} mol L^{-1}; 25˚C; 1 bar. ΔG_r and $p\varepsilon$ were calculated from thermodynamic data reported by Stumm and Morgan (1996) and Grenthe et al. (1992). CH$_2$O is used to represent organic matter.

Tailings Porewater Geochemistry
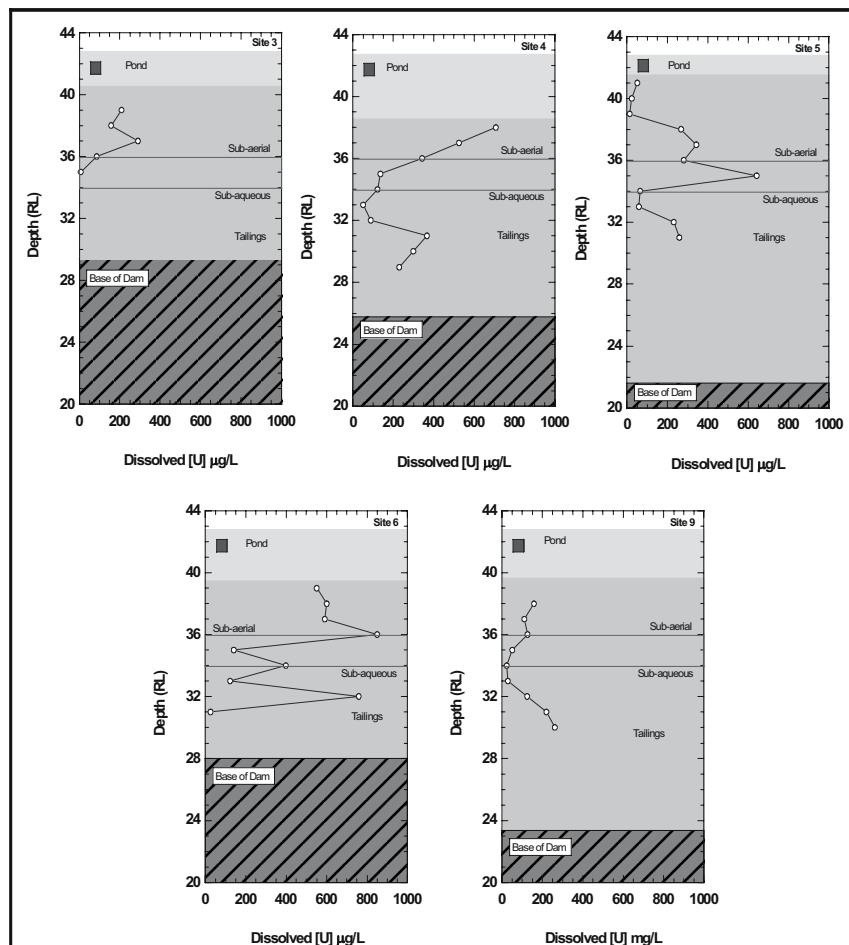
The major ion porewater profiles are vertically stratified in two distinctive geo-chemical zones: (a) an upper zone which extends from the surface of the tailings down to RL 35 m. This zone is characterised by high conductivity (> 25 mS/cm) and near neutral to slightly acidic pH water and (b) a lower zone which extends from the inflection point at RL 35 to the base of the dam. This zone is characterised by a 50% decrease in conductivity within a few metres of the in-flection point and slightly basic pH water. Like the overlying tailings pond water, the major ion chemistry is characterised by magnesium, sulfate, calcium, manganese, and ammonia.

Fig. 5a. Porewater profiles for dissolved iron.

Porewater iron is a well known redox indicator and within the tailings pile, dissolved concentrations increase in the near surface sediments (1 m) up to about 100 mg/L (Fig. 5a). These elevated values are considerably higher than the water column value of 0.44 mg/L, and suggests that the high porewater inventory does not stem from the overlying pond water. Rather, these data suggest that the high dissolved Fe values are derived from reductive dissolution of Fe(III) oxides. Below the zone of Fe reduction (RL 35 m), Fe is removed from solution as authigenic sulfides in accordance with the redox zonation principles described by Froelich et al. (1979).

Porewater profiles for dissolved U (Fig. 5b) are variable and as such it is difficult to draw firm conclusions from the observed trends. In general, however, the U porewater profiles show a concentration minima coincident with Fe maxima (see Fig. 5a) in the near surface sediments (> RL 39 m). Below this horizon, U levels at

Fig. 5b. Porewater profiles for dissolved uranium.

most sites exhibit a concentration maximum (between RL 37 to 36 m) with values ranging from 180 to 800 µg/L. Within the constraints of available data, a second concentration peak is observed at RL 33 below which U levels significantly decrease (Sites 3 and 6) to around 1 µg/L. Such observations imply that U is associated with Fe(III) oxides and is redistributed following the reductive dissolution of Fe. The overlying pond water U concentrations were on the order of 50 µg/L (see Fig. 5b), which is well below the observed porewater maxima of around 800 µg/L. This suggests that U is being mobilised within the tailings pile via diagenetic processes rather than being supplied from the inventory of overlying pond water. Furthermore, the results of the solid state speciation test work confirm that 35 to 40% of the total U contained in the gel and fine grain tailings is associated with readily reducible phases such as amorphous Fe oxyhydroxides.

Profiles of other trace metals (Co, Ni, Cu and Mo) which form insoluble metal sulfide minerals were also examined. The profiles of Co and Ni mirror the Fe profile (see Fig. 5a) and are consistent with the notion of sulfide formation below RL 37 m. Below this RL, the concentrations of Ni and Co decrease by an order of magnitude compared with their concentrations of > 100 µg/L in the upper oxic zone. The dissolved Cu distribution does not follow the same pattern. However, elevated levels of dissolved Cu can persist in sulfidic porewaters due to the formation of strong Cu-organic or polysulfide complexes which can maintain Cu in solution. Under conditions of low redox potential, Mo is believed to be reduced to the tetravalent state and then is coprecipitated with mackinawite ($FeS_{0.9}$) (Bertine, 1972).

Radium porewater profiles do not correlate well with either Sr or the expected geochemical analogue Ba. Such trends while inconsistent with other studies can perhaps be attributed to the presence of a non-barite host phase for Ra. Indeed, porewater concentrations of Ba are exceedingly low, with most values at or near the detection limit of 0.005 mg/L. The reductive dissolution of Ra-bearing barite or radiobarite, can result in the addition of substantial Ra to porewaters. In a uranium tailings impoundment in Canada, for example, the dissolution of radiobarite in reducing horizons resulted in elevated levels in porewaters of ca. 80 Bq/L (Martin et al. 2003). The relatively low Ra and Ba values measured in the porewaters at Ranger suggest that such processes are not occurring to any appreciable extent and that other mechanisms are controlling the mobility of Ra under the predicted reducing environment.

Kinetic Column Leach Studies

To evaluate the long-term geochemical stability of the tailings, it is necessary to understand the mechanisms responsible for controlling the release and subsequent transport of radionuclides and accessory metals/salts (collectively described as contaminants) into the environment. Laboratory scale leach columns were established as a means of assessing the leachability and kinetic behaviour of tailings under simulated weathering conditions.

Two parallel column experiments were conducted. The first column assessed the leaching characteristics of fresh tailings ("fresh tailings") exposed to simulated rainfall events. These tailings are direct from the plant and representative of those that are currently being deposited into Pit #1. They are of a coarse grind and are neutralised to a pH of around 6. The second column was loaded with tailings ("aged tailings") that were dredged from the tailings dam at a depth of 4 m below the tailings–pond water interface. These tailings are aged > 5 years, are fine grained and were deposited at a higher pH (6 to 8). They are representative of tailings that were originally deposited sub-aerially but from 1994 onwards were subsequently covered by water.
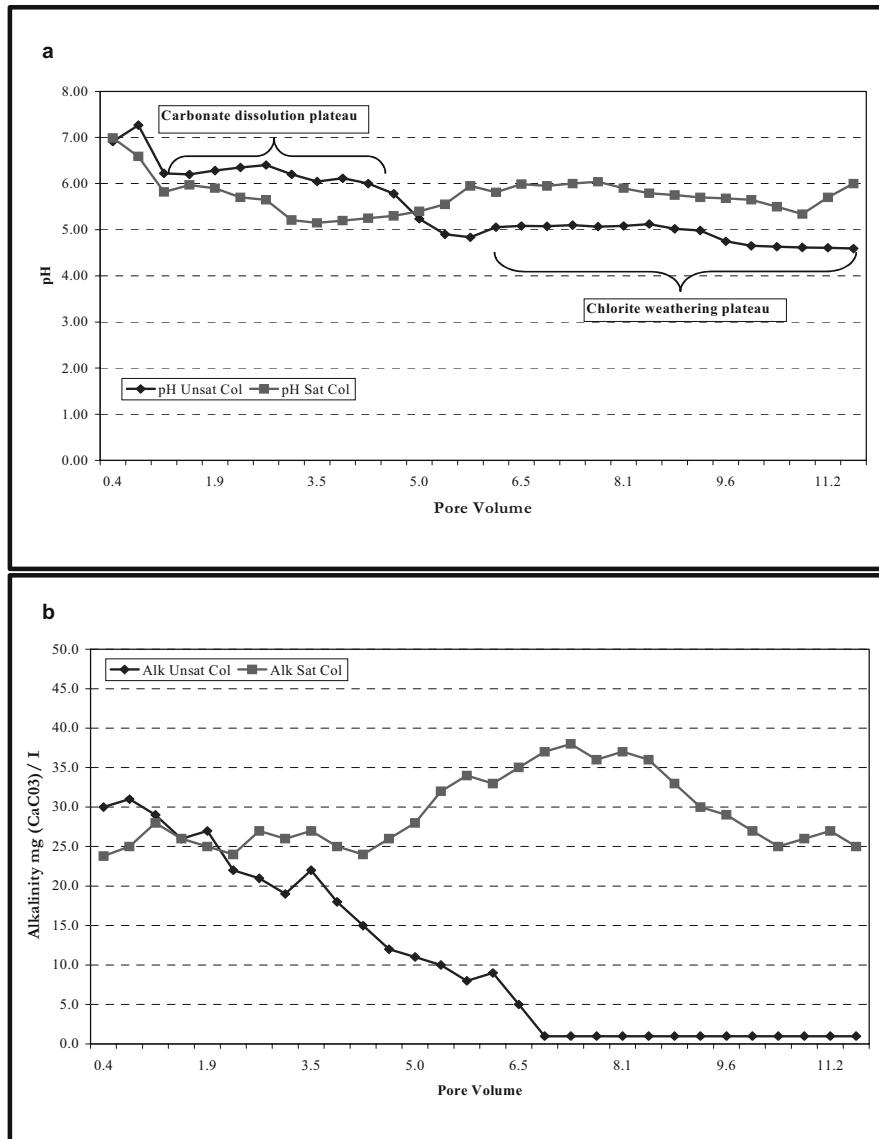
The design of the kinetic column study has attempted to account for climatic, hydrological, chemical and depositional parameters that have a significant influence on the in-situ weathering processes in the tailings. To achieve the desired design outcome, two columns were constructed for both the fresh and aged column studies. The upper column is designed with a high surface area per unit mass of tailings solids to ensure unsaturated leach conditions. The purpose of this column is to simulate leaching and exposure conditions similar to those that occur in the upper unsaturated zone (beaches) of the tailings dam. An understanding of unsaturated geochemical processes is necessary as the tailings were deposited sub-aerially over a ten year period (1986 to 1994). In the longer term, it is also conceivable that unsaturated zones may develop in the tailings repositories following final decommissioning and close-out. The lower column is completely encapsulated to maintain a constant state of water saturation and to prevent atmospheric contact. The purpose of this column is to simulate leaching conditions deep within the tailings dam and Pit #1 repositories where the tailings are stored below the water table and isolated from the atmosphere.

The columns were leached for a period of 520 days. During this period, there were 30 discrete leaching events in which 14.4 L of simulated rainwater was introduced into the upper unsaturated column via spray irrigation every 2.5 weeks (5.76 L/week).

Fig. 6a shows the pH elution trends for the aged unsaturated tailings over the 520 day (or 11.54 pore volumes) leaching period (the fresh tailings profile is similar). At the commencement of the leaching trial the pH of the fresh and aged tailings was 6.5 and 7, respectively. Within 1.12 pore volumes (≈ 2.8 months); the pH in each of the unsaturated columns had decreased by around 1 unit. Following this initial decline, the pH in the fresh unsaturated tailings formed two plateaus, one at 5 and another at 4.5 before declining to a final pH of 4 by the end of the leaching period. These successive pH plateaus are a likely indicator of the magnitude and reactivity of acid neutralising minerals such as aragonite and chlorite. Given that aragonite will react more rapidly than chlorite, it is conceivable that the first pH plateau, from pore volumes 1.12 to 5, represents the buffering associated with carbonate dissolution. This tenet is supported by the alkalinity trends, which show complete consumption of alkalinity in both the fresh and aged columns over the same elution period. Following the depletion of available aragonite/alkalinity, chlorite weathering reactions neutralise the acid generated from sulfide oxidation

via the release of interlayer hydroxyl groups (brucite) as chlorite is altered to kaolinite.

In the saturated columns as a consequence of the various reduction reactions, alkalinity is generated by the oxidation of organic matter and, as such, tends to increase as successive oxidants are utilised by bacteria (Stumm and Morgan 1996). This trend is observed in Fig. 6b, where alkalinity increased in accord with the

Fig. 6.   Trends in (a) pH and (b) alkalinity for the aged tailings.
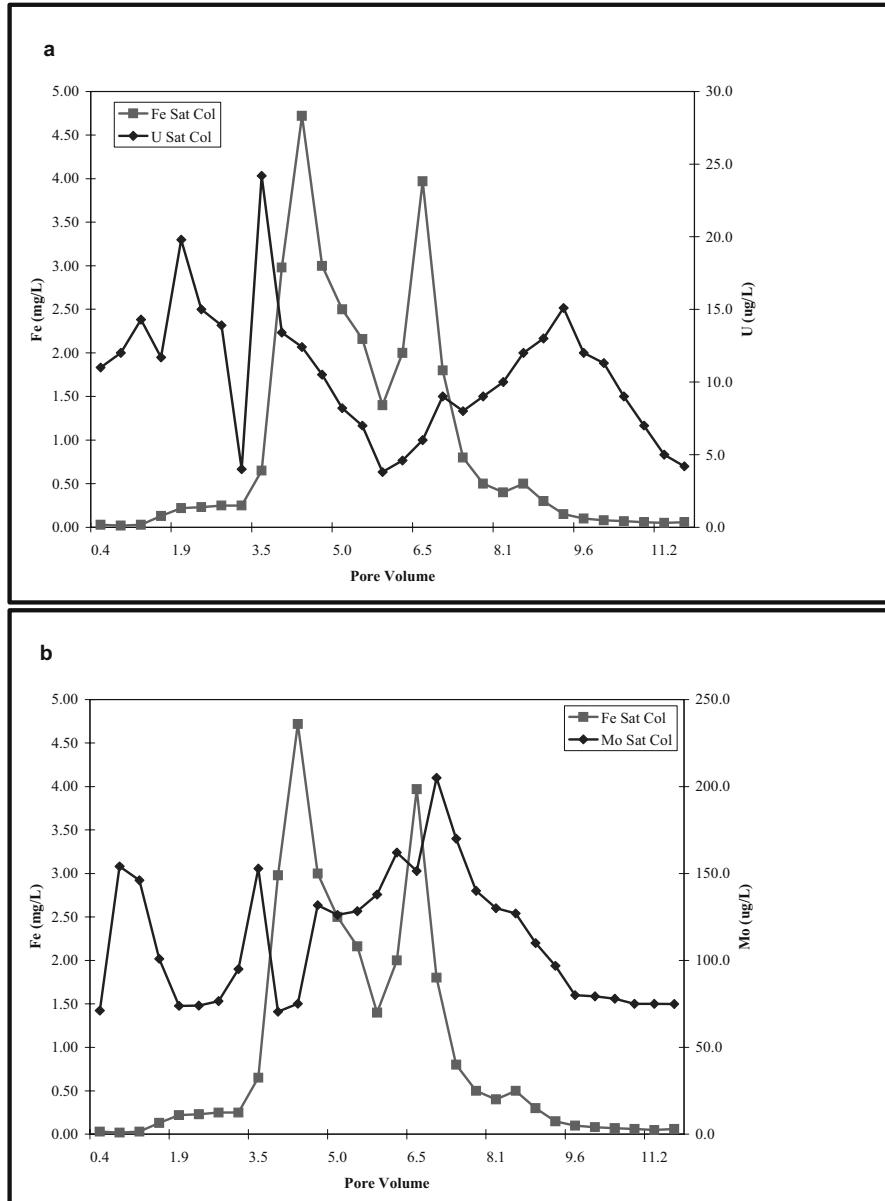
progression of the expected redox reaction sequence. More specifically, there was a noticeable increase in alkalinity (pore volume 6.5) at around the same time as Fe(III) reduction was at its peak.

A measure of the electrical conductivity (EC) of the column discharge provides an indication of the leaching of soluble salts from the unsaturated tailings. The initial leachate was highly saline with ECs of 24 and 17 mS/cm being measured for the fresh and aged unsaturated tailings, respectively. This salinity was mainly due to high concentrations of the major ions: SO_4^{2-}, Mg^{2+}, Mn^{2+}, Ca^{2+} and NH_4^+. After approximately 5 pore volumes of leachate had passed from both the fresh and aged columns, the EC had significantly decreased to around 5 mS/cm. A corresponding decrease was also observed in the concentrations of the major ions with the exception of calcium which remained relatively steady, ranging between 350–380 mg/L in the fresh unsaturated tailings and 450 mg/L in the aged unsaturated tailings (both being controlled by the solubility of gypsum).

The weathering of chlorite in acidic environments (unsaturated columns) will form secondary aluminosilicates such as kaolinite, amorphous SiO_2 phases and various Al-bearing secondary minerals. As a consequence, Al and SiO_2(aq) are mobilised and their respective solubility governed by the newly formed secondary minerals. The dissolution of Al is coincident with a pH of ≤ 6 and closely follows the trend reported by Nordstrom (1982), in which Al-sulfate minerals such as basaluminite ($Al_4(OH)_{10}SO_4$), jurbanite (AlOHSO$_4$) and alunite ($KAl_3(SO_4)_2(OH)_6$) control the solubility of Al in acidic sulfate-rich waters. Dissolved silica is an important indicator for determining the solubility and equilibrium conditions pertaining to the formation of secondary silicate minerals. Silicon leachate concentrations (an indicator of SiO_2(aq)) remained relatively steady at 10 mg/L, then rapidly increased at the same juncture as alkalinity was exhausted and the pH decreased to around 4.8 (see Fig. 6).

Lead, Cu and Cd leachate concentrations for the unsaturated tailings were significantly higher than those observed for the saturated tailings. The elevated levels of Pb, Cu and Cd are clearly related to the oxidative dissolution of sulfide minerals.

The coincidence of U concentration minima and Fe maxima (Fig. 7a) in the saturated column reflects the onset of U reduction and removal from solution as a U(IV) authigenic mineral, presumably uraninite. These trends are consistent with studies by Lovely et al. (1991) and Gorby and Lovely (1992) who proposed that

Fig. 7.   Trends in (a) Fe and U and (b) Fe and Mo in aged tailings leachates.

dissimilatory Fe(III) reducing bacteria can also utilise U(VI) as an electron accep-tor to derive energy for growth. As a consequence, U(VI) is reduced to U(IV) and subsequently precipitated as uraninite. The presence of dissimilatory bacteria in the columns explains the simultaneous reduction of U(VI) with Fe(III) as accord-ing to the predicted sequence of redox reactions described in Table 1, U(VI) re-duction (pε 0.11-0.17) and subsequent precipitation as amorphous UO_2 was ex-pected to occur after Fe(III) reduction at pε 0.7. The leachate concentrations of molybdenum (Fig. 7b) also closely approximate the reductive dissolution of Fe(III) oxides. The decrease in Mo concentrations from 9.6 pore volumes may suggest the onset of reducing conditions sufficient to remove Mo as insoluble mo-lybdenite (MoS_2) or more likely as a co-precipitate with mackinawite (Bertine, 1972). Legeleux et al. (1994) reported that the reduction of Mo requires a strong reductant such as H_2S to precipitate molybdenite. This finding is also consistent with the redox sequence described in Table 1 in which Mo(VI) reduction (pε -1.86) is predicted to occur under strongly reducing conditions.

Geochemical Modelling

Geochemical models were used to simulate and confirm the hypothesised mecha-nisms described above. Models are a simplification of a much more complex natu-ral system and as such, they can only be used to augment actual field and experi-mental data. This integrated approach provided valuable insight into the key equilibrium and quasi-steady-state reactions governing the long-term evolution of the tailings porewaters.

The kinetic model STEADYQL (Furrer et al., 1989, 1990) was used to predict the final leachate pH and solute concentrations for Fe, Al, Si and Cu following weathering of the two dominate phyllosilicate minerals (chlorite and muscovite) and the oxidative dissolution of pyrite and chalcopyrite in the unsaturated col-umns. The soluble reaction by-products from these kinetically controlled reactions were then allowed to equilibrate with respect the formation of authigenic phases such as kaolinite, ferrihydrite and chalcedony. The predicted values are compared with actual measurements to confirm the key geochemical processes governing the leachate/porewater chemistry of the unsaturated tailings. The predicted leachate pH and Fe, Al, Si and Cu concentrations are shown in Table 2 along with actual experimental data collected at the cessation of the 520-day leaching period. As a general statement, the predicted leachate values for pH, Fe, Al and Cu are in good agreement with the experimental data and in so doing, attest to the oxidative disso-lution of metal sulfides and weathering of phyllosilicate minerals in the undersatu-rated tailings. Predicted silica concentrations are lower than actual leachate values but are of the correct magnitude expected for chlorite dissolution (Lowson et al., 2005). More specifically, the results presented in Table 2 confirm that leachates from the undersaturated tailings have a propensity to generate acid via the prefer-ential oxidation of pyrite and chalcopyrite. In addition to the generation of acid,

these reactions also result in the precipitation of Fe oxyhydroxides, presumably ferrihydrite, and the release of soluble Cu.

Equilibrium modelling, using the HARPHRQ code (Brown et al., 1991), indicated that elemental porewater concentrations were governed by various mineral phases. Alunite appears to be controlling the observed Al porewater concentrations. Barium is controlled by a poorly ordered micro-crystalline form of barite, as has previously been reported by Martin et al. (2003). The presence of such a phase was confirmed by SEM-EDX. Strontium, however, was found to be controlled by the solubility of strontianite ($SrCO_3$) rather than celestite ($SrSO_4$). Calcium and sulfate are clearly controlled by the solubility of gypsum, whereas iron is controlled by iron oxyhydroxide precipitation at shallow depths and mackinawite at lower depths. In the regions of the porewaters where alkalinity increases (see Fig. 6b), the solubility of Mn is controlled by rhodochrosite. Modelling of the saturated column leachates confirmed these findings.

Conclusions

Run of mill uranium tailings are a complex heterogeneous mixture of lithogenic (primary gangue minerals and weathering products) and secondary (components that form during milling) minerals, residual process chemicals and biogenic (products of biological activity) phases. Following transfer to the tailings storage facility, post depositional reactions alter the mineralogical and hydrochemical characteristics of the tailings solids and porewaters in accordance with weathering and diagenetic processes. These mechanisms will have a profound impact on the long-term geochemical stability of the tailings pile and as such will need to be taken into account in the design, management and closure of the final tailings repositories at the Ranger mine (Pits #1 and 3).

Table 2. Summary of predicted and actual leachate chemistry for unsaturated tailings.

Parameter	Predicted	Measured (fresh)	Measured (aged)
pH	4.3	4.02	4.6
Fe [3]	0.03	0.02	0.02
Al	0.32	3.00	0.29
Si [2]	8.45	30.00	19
Cu	0.40	0.80	0.05

(1) With the exception of pH, all concentrations are in mg/L
(2) Si solubility in the model is assumed to be controlled by kaolinite and chalcedony
(3) Fe is controlled by ferrihydrite

References

Bertine, K.K., Mar. Chem., **1**, 43-53, 1972.

Brown, P.L., Haworth, A., Sharland, S.M. and Tweed, C.J., HARPHRQ: A geochemical speciation program based on PHREEQE. Nirex Safety Studies Report NSS/R18, 1991.

Eupene, G.S, Fee, P.H. and Coville, R.G., Ranger ore uranium deposits. In Knight, C.L., ed, Economic Geology of Australia and Papua New Guinea. 1. Metals. Parkville, Australian Institute Mining and Metallurgy Monograph 5, 308-317, 1975.

Fordham, A.W., Aust J. Soil Res., **31**, 365-90, 1993.

Fordham, A.W., and Beech, T.A., Chemical changes in variously treated tailings with time. Report 1: Chemical compositions of the solution phase in acid and neutralised tailings, CSIRO Minesite Rehabilitation Research Group, 1989.

Fordham, A.W., Peter, P. and Milnes, A.R., Review of information relating to densification of tailings and deposition of acidic tailings in the tailings dam, plus recommendations for further investigations. CSIRO Minesite Rehabilitation Research Group, 1992.

Fordham, A.W., Riley, G.G., Nefiodovas, A. and Martin, R., Examination of tailings from Ranger tailings dam. CSIRO Minesite Rehabilitation Research Program, 1993.

Froelich, P. N., Klinkhammer, G. P., Bender, M. L., Luedtke, N. A., Heath, G. R., Cullen, D., Dauphin, P., Hammond, D., and Hartman, B., Geochim. Cosmochim. Acta, **43**, 1075-1090, 1979.

Furrer, G., Westall, J. and Sollins, P., Geochim. Cosmochim. Acta, **53**, 595-601, 1989.

Furrer, G., Westall, J. and Sollins, P., Geochim. Cosmochim. Acta, **54**, 2363-2374, 1990.

Gorby, Y.A. and Lovely, D.R., Environ. Sci. Technol., **26**, 205-207, 1992.

Grenthe, I., Fuger, J., Konings, R.J.M., Lemire, R.J., Muller, A.B., Nguwen-Trung, C. and Wanner, H., Chemical thermodynamics of uranium. North-Holland, 1992.

ICOLD - International Commission on Large Dams, A Guide to tailings dams and impoundment. Design, construction, use and rehabilitation. Bulletin No. 106, 239 pp. Commission Internationale des Grandes Barrages, Paris. 1996.

Legeleux, F., Reyss, J.L., Bonte, P. and Organo, C., Oceanologica Acta, **17**, 1994.

Lovely, D. R., Phillips, E. J. P., Gorby, Y. A., and Landa, E. R., Nature, **350**, 413-416, 1991.

Lowson, R. T., Comarmond, J. M., Rajaratnam, G. and Brown, P. L., Geochim. Cosmochim. Acta, **69**, 1687-1699, 2005.

Markos, G., Geochemical mobility and transfer of contaminants in uranium mill tailings. Symposium on Uranium Mill Tailings Management. p. 55-63. Proceedings at a Symposium Colorado State University, Fort Collins, Colorado. 1979.

Martin, A. J., Crusius, J., Mcnee, J. J. and Yanful, E. K., Appl. Geochem., **18**, 1095-1110, 2003.

Morin, K. A., Prediction of subsurface contaminant transport in acidic seepage from uranium tailings impoundments, Vol. I and II. Ph.D. dissertation, Department of Earth Sciences, University of Waterloo, Waterloo, Ont., 1983, 713 pp.

Nordstrom, D.K., Geochim. Cosmochim. Acta, **46**, 681-692, 1982.

Postma, D. and Jakobsen, R., Geochim. Cosmochim. Acta, **48**, 903-910, 1996.

Richards, B.G. and Peter, P., Sedimentation and consolidation of acid tailings: Summary of progress. CSIRO Minesite Rehabilitation Research Group, 1990.

Savory, P. J., Geology and grade control at ERA – Ranger Mine, Northern Territory, Australia. In: Proceedings Australasian Institute for Mining and Metallurgy Annual Conference, Darwin, p. 97-101, 1994.

Sholkovitz, E.R., Geochim. Cosmochim. Acta, **37**, 2043-2073.

Sinclair, G., Hydrological and geochemical assessment of the tailings dam seepage collector system. Energy Resources of Australia, 1992.

Stumm W. and Morgan J.J., Aquatic Chemistry, Third Ed. Wiley-Interscience, 1996.

Van der Weijden, C. H., Early diagenesis and marine pore water. In: Diagenesis IIII, G.V. Wolf K.H. and Chilingarian (Eds), Elsevier, p. 13-133, 1992.

Wagener, F., Strydom, K., Craig, H. and Blight, G., The tailings dam flow failure at Merriespruit, South Africa: causes and consequences. In: Proceedings of the Fourth International Conference on Tailings and Mine Waste, Fort Collins, Colorado, USA, p. 657-666, 1997

Long term fate of uranium tailings in mountain areas

Broder J. Merkel

TU Bergakademie Freiberg, Lehrstuhl für Hydrogeologie, Gustav-Zeuner-Straße 12, 09596 Freiberg, Germany, E-mail: merkel@geo.tu-freiberg.de

Abstract. Common passive controls for uranium tailings include constructing thick earthen covers, protected by rock, over the waste. Earthen covers effectively limit dust and radon emissions and gamma radiation and, in conjunction with the rock covers, help stabilizing the tailings to prevent dispersion of the tailings through erosion or intrusion. In some cases, piles may be moved to safer locations (e.g. deep mines). However, the long term fate of uranium tailings in mountain areas is different from tailings in flat landscapes. Especially under humid climatic conditions the amount of rainfall is high as is the leaching and erosion potential. The uranium tailing Schneckenstein in the eastern part of Germany was chosen for a case study. The deposited uranium and other toxic elements will contaminate the downstream aquatic environment for thousands to more than ten thousand years depending on the scenarios chosen. Safeguarding the Schneckenstein tailing can be done over a few decades but gets much more difficult in the long term perspective. Because natural attenuation is unlikely to happen, enhanced natural attenuation or active measures have to be taken. Advantages and disadvantages of several options are discussed.

Introduction
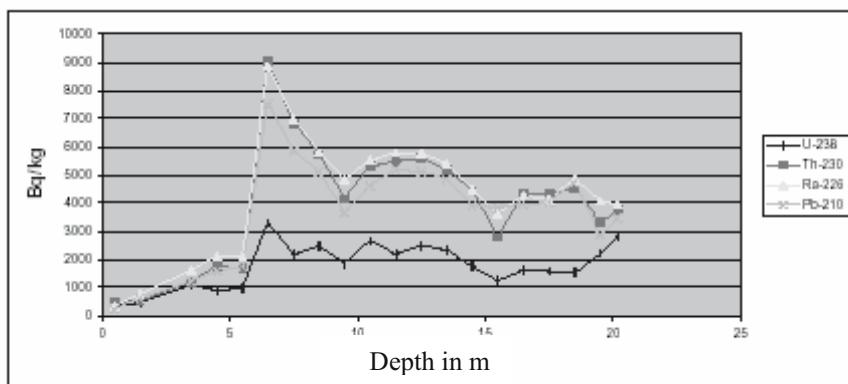
Uranium tailings may contain radioactive elements in considerable amounts depending on the extraction technique applied. After milling of the mined ore either gravimetrical flotation or chemical leaching was commonly applied. If in the case of gravimetrically separation no further enrichment steps have been applied a tailing will contain only low amounts of radioactive elements. However, if chemical

leaching either acidic or caustic is applied only uranium is extracted from the ore and radium (mainly [226]Ra, half life 1600 years) and thorium (mainly [230]Th, half life 80,000 years) may remain in the tailings. Radium will remain in the tailings only if e.g. BaCl is added and radium is thus coprecipitated with Bariumsulfate.

Wismut SDAG, the Soviet-German mining enterprise at those times applied flotation and chemical leaching in terms of separation techniques. Chemical leaching was done with sulfuric acid, $NaClO_3$ and Na_2CO_3. While flotation will produce sandy tailings chemical leaching generates silt and clay tailings due to dissolution of feldspars and subsequent clay mineral formation. All other radioactive daughters of the three radioactive decay chains from [235]U, [238]U, and [232]Th remain in the tailings. Depending on the performance of the leaching and separation technique only a certain amount of the uranium is extracted while the non-leached uranium remains in the tailings as well. Fig 1 shows that uranium is contained in the tailings in an average concentration of 2 KBq/kg, which is considerably high. Thorium, radium, and lead are not in radioactive equilibrium but enriched 3 to 4 fold. Close to equilibrium concentrations can be seen in the waste rock cover (0-5 m) and at the bottom of the tailing pond.

Description of the tailing site Schneckenstein

The Schneckenstein tailing is one of several uranium mining and milling sites in eastern Germany which has been opened up by the Soviet Union forces immediately after Second World War when a first rush for uranium happened to take place. 15 year later the Wismut SDAG closed down several of these small facilities and focused on a few big mines and two milling and separation sites. Table1 gives an overview on former mining and milling sites in Saxony.

Fig.1.   Distribution of [238]U, [230]Th, [226]Ra, and ^{210}Pb in the Schneckenstein uranium tailing.

Table 1. Uranium mining and milling sites in Saxony (Wismut GmbH 1991).
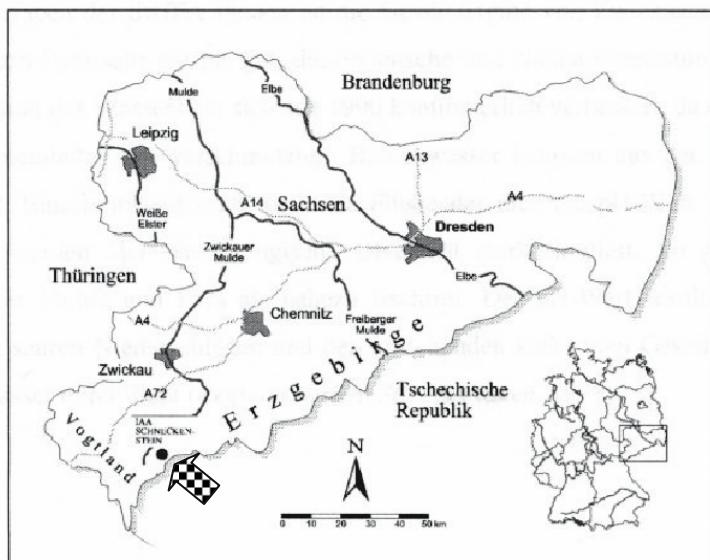
Site name / city	Tons (uranium)	%
1. Western part of Erzgebirge (total)	*95,140*	*92.4*
Niederschlema-Albernroda	80,943	78.6
Oberschlema	7,407	7.2
Johanngeorgenstadt	4,155	4.0
Tellerhäuser	1,180	1.2
Antonsthal	667	0.7
Seiffenbach	288	0.3
Schneeberg	212	0.2
Others	288	0.3
2. Middle and East Erzgebirge (total)	*1,411*	*1.4*
Annaberg	923	0.9
Bärenstein	222	0.2
Marienberg	166	0.2
Others	100	0.1
3. Vogtland (total)	*6,406*	*6.2*
Zobes	5,672	5.5
Schneckenstein	**660**	**0.6**
Others	74	0.1
Sum: Erzgebirge and Vogtland	*102,957*	*100.0*

The Schneckenstein tailing is located in the south western part of Saxony (Fig. 2) in the Boda valley at an altitude between 740 and 815 m as l. Mining activities within the Schneckenstein area date back to the year 1506 with tin, arsenic, and pyrite being mined. From 1938 on processing residues were deposited in a small tailing, that still was in use when Wismut SDAG took over the processing plant in 1947 and established their Wismut object No. 32. The Schneckenstein mine itself was never mined for uranium but Wismut SDAG processed uranium ores from several small uranium mines in the vicinity (e.g. Gottesberg) and from other mines in Saxony and Thuringia. Uranium contents in these ores were considerably low with 200 to 1200 g U/t on average. In May 1948 the dam for a first settling pond (IAA II) was built, in 1951 a new dam for a second settling pond followed (IAA I). The surface area and the volume of the two tailings comprise 105.000 m^2 and 700,000 m^3 respectively. Due to a general change in the policy of WISMU SDAG the Scheckenstein milling site was shut down in 1957 and handed over to VEB Wolfram-Zinnerz Pechtelsgrün without remarkable reclamation work done. Severe erosion problems occurred in the following years causing as well instability of the northern dam site. Sediments from the tailings were spilled into the Bodabach. The tailings sediments were deposited downstream in numerous small basins and lakes. In order to solve this situation in the early sixties the tailings surface was covered with waste rock material. This capping reached a thickness between 1 and 5 m. Additionally, surface water was diverted by hanging ditches, the northern dam´s inclination was reduced from 1:1 to 1:2.5 and eight existing drainage pipes were lengthened. The drainage water was merged with the water from

the eastern hanging ditch and then discharged to the Bodabach creek. Reforestation with spruce and birch followed, and lupine was planted for soil amelioration. No further rehabilitation work or monitoring was done until nowadays.

Rainfall data are available from a station in Morgenröthe-Rautenkranz from 1951 on. The average rainfall was 1053 mm, with a minimum of 752 mm and a maximum of 1438 mm. The catchment area of the tailing is about 0.95 km^2 with a surface discharge of 18 to 19 L/s on average. The water saturation of the tailing material is nowadays between 0.6 and 0.9 with an average water content of 0.3 (Merkel et al. 1998). At the foot line of the tailing dam a total average discharge of about 10 L/s can be monitored containing varying increased concentrations of uranium (11 to 1600 µg/l) and arsenic (2 to 73 µg/l). Roughly 50% of the water is flowing from a pipe which is draining a spring buried by the tailing. However, even this "spring"-water exhibits elevated concentrations with respect to uranium and arsenic, which is an indication for leakage of tailing water into the pipe. Assuming a vertical seepage rate of 20 mm per year through the unsaturated tailings and taking into account the area of 105,000 m^2 this will sum up to 2000 m^3/y. In comparison to 315,360 m^3/y draining from the tailings dam (157,680 m^3/y from the tapped spring and 157,680 m^3/y from other sources) the seepage through the tailing is 0.6 respectively 0.3 percent of the total drainage.

Fig. 3 gives an idea of the hydrogeological setting of the tailing. The thin groundwater layer built by weathered granite receives some contaminants from the vertical seepage. Based on a width of the valley of 250 m, an average thickness of the weathered granite of 1 m, a slope of 0.1 and a conductance of $1 \cdot 10^{-5}$ m/s this yields to a flow of 7900 m^3/y. Thus, there should be a significant increase in the
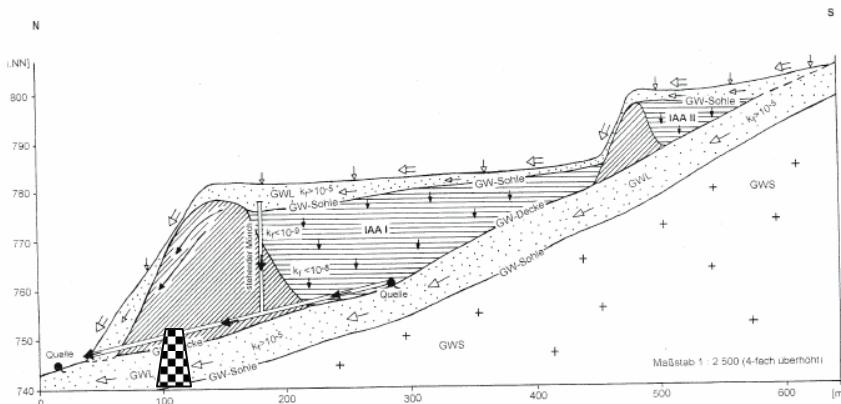
Fig. 2.   Map of the Federal State of Saxony in Germany showing the location of the Schneckenstein Uranium milling site.

concentrations of uranium and arsenic on the groundwater downstream of the tailing based on average seepage water concentrations of 1,100 µg/l for uranium and 2,000 µg/l for arsenic. However, no elevated concentrations were found in the downstream ground water monitoring well. (Merkel et al. 1998). This is an indication that during the construction of the dam in 1951 which was done by means of a solid wall based on non-weathered granite the natural ground water stream was blocked off and the groundwater forced to enter the drainage system. Obviously this foundation of the latter tailing dam is still tight and maintaining groundwater protecting (Fig. 3).

Besides the vertical seepage through the tailings, seepage towards the more permeable tailing dam might occur and since the tailing dam itself is built from coarse tailing material this explains as well the elevated concentrations with respect to arsenic and uranium in the dam drainage. Furthermore, water from the shallow groundwater on top of the tailings flowing in the waste rock cover material might migrate as well into the dam increasing the load of arsenic, uranium, and other metals.

While the radioactive material content of the tailing is well recognized, the immense volume of toxic metals is less well known in many uranium tailings. However, this is not true for the Schneckenstein tailing as can be seen from Table 2.

Fig. 3. Cross section north-south of the Schneckenstein tailing. Vertical exaggeration is 1:4. Length of the tailing in maximum 800 m, width 250 m, average depths 7 m, dam height about 40 m. Aquifer at bottom of tailing not to scale.
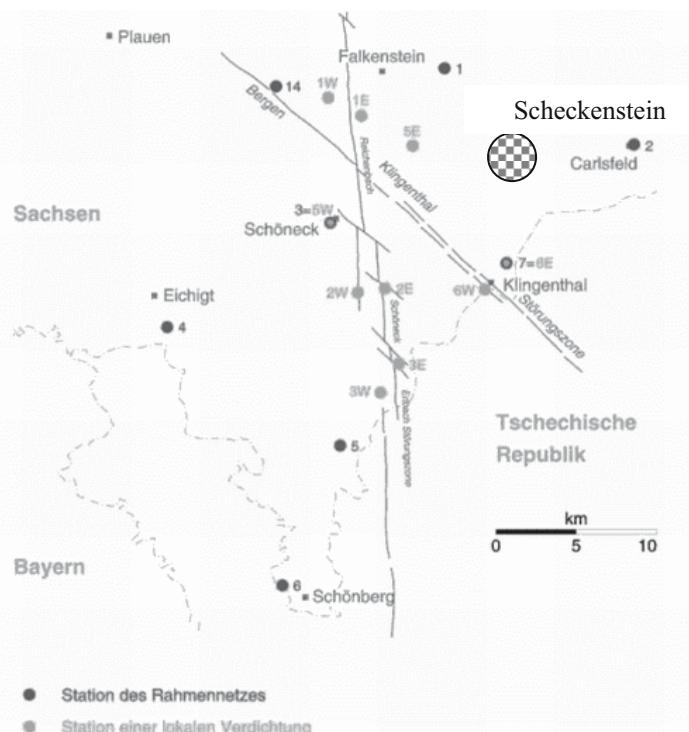
Table 2. Concentrations and mass of elements in the Schneckenstein tailing (from unpublished data of Wismut GmbH).

Element	IAA I in mg/kg	Tons	IAA II in mg/kg	Tons	Total mass in Tons
Titanium	10000	8100	8300	1179	9279
Vanadium	667	540	373	53	593
Chromium	607	491	431	61	552
Manganese	3233	2619	1683	239	2858
Cobalt	533	432	215	30	462
Nickel	6000	4860	4210	598	5458
Copper	1667	1350	1044	148	1498
Zink	5867	2322	542	77	2399
Arsenic	300	243	3300	469	712
Strontium	733	594	637	90	684
Yttrium	550	445	309	44	489
Molybdenum	21	17	11	2	19
Cadmium	7	6	-	-	6
Tin	30	24	382	54	78
Antimony	9	7	10	1	8
Cesium	70	57	23	3	60
Wolfram	53	43	71	10	53
Lead	500	405	298	42	447
Bismuth	21	17	67	9	26
Uranium	193	157	253	36	193
Sum	-	22730	-	3145	25874

Processes controlling the system

Several processing are controlling the processes in and around a tailing environment. They can be distinguished between climatic, tectono-physical, erosion, and hydrochemical processes. With respect to climate one has to consider climate change in the long term, which could lead to a change in the pattern of rainfall (e.g. more severe rainfall events with high intensity and thus more potential for surface erosion processes), an increase or decrease of the yearly rainfall and subsequently changes in the vegetation in the area of interest. A very likely and very severe stress on tailings sites is glaciation. This is exclusively a long-term concern and not to be considered in the case of the Erzgebirge. With respect to tectono-physical activities neo-tectonics and seismic loadings have to be discussed. No neo-tectonic movements are to be expected in the area of Schneckenstein, however, very frequent micro seismic activities of low magnitude are observed. Seismic events with a bigger magnitude can not be excluded and have to be considered as likely with frequencies of several hundred years (Leydecker 1999). As can be seen from Fig.4 the Schneckenstein tailing is situated close to the active fault zone of the Vogtland seismicity center.

One major problem is erosion. The dam stability is technically proved since the slope is about 1:2.5, however, this does not say anything with respect to the long term erosion behavior of the tailing impoundment. Just 40 years after capping the tailings with waste rock several spots can be found where the waste rock cover is eroded and the tailings exhibited to the surface. In terms of hundreds and thousands of years, erosion and surface channeling will occur. Furthermore, it is likely that internal erosion (piping) happens within the tailings and the dam. This might cause sinkholes and further surface erosion. Internal erosion will preferably occur after failure of the draining pipes. This is already the case since from the former eight drainage pipes which were lengthened during the reclamation work in the 60´s, only two seem to work properly. Form the other six drainage pipes no or very little flow is seen anymore. In particular, that pipe is important, which is tapping water from a former spring buried by the tailing with an average yield of about 5 L/s. This pipe is in still operation and is working fine, however, the question is how long will this be? If the pipe collapses then the pressure head in the tailing will rise and part of the tailing will get water saturated again. This will increase the leaching and thus increase the contaminant load from the tailing. This

Fig. 4.   Center   of   Vogtland   micro   seismic   activity http://www.umwelt.sachsen.de/de/wu/umwelt/lfug/   according   to   Berger 1997.

might as well increase the risk of internal erosion (piping). Independent from potential climate changes in the long term surface erosion and internal erosion will take place. Gullies will form and increasing amounts of tailing material will be carried to the downstream vicinity if no action is taken. However this has to seen on a time scale of hundreds and thousands of years and thus an institutional control and a continuous maintenance can hardly be imagined.

The final subject to address are chemical processes. They may alter the situation to the better or worse. In the very beginning of a tailing´s history oxidizing conditions are controlling the system. This might change over time and depends on reducing processes and diffusion controlled processes. Oxygen may enter the tailings either by dissolved oxygen in seepage water or by diffusion. Both pathways can be estimated by means of models. However, simple boundary conditions have to be assumed. The concept of acid generation and contaminant transport in decommissioned sulfide-bearing mine-tailings impoundments was presented by Blowes (1995). But deep root penetration, internal erosion and its affects on oxygen availability below the surface are of concern at sites with acid generation potential and as well uranium tailings since uranium will be highly mobile as long as oxidizing condition prevails.

Another aspect is the impact of hard pan formation in mine waste environments. Hard pan formation has been observed in waste rock piles in several parts of the world (Blowes et al. 199, Rammlmair 2002). Little information is available about hard pan formation in tailings. Rammlmair (2002) is assuming encapsulated cells with little alteration by the formation of hard pans. This may happen as long as the assumption is true that hard pans have a lower permeability than the waste rock. However, hard pans might form cracks under shear stress and will then be even more permeable than the unconsolidated material.

Remediation measures

From these results it is unlikely that natural attenuation will be a potential way to solve the problem. So what are the choices? Transferring and burying the tailings in a subsurface repository (e.g. an abundant mine) would be one choice. This could be combined with a reprocessing of the tailings and extraction of elements contained which might be of commercial interest nowadays. Another option could be an in situ stabilization of the tailings, which has to account for transferring uranium from the oxidation state six to four, coating the precipitated uranium-oxide to prevent re-oxidation, and prevent mechanical erosion.

Coating

Coating of minerals in waste rock piles and tailings has been suggested by several scientists using phosphate or other minerals. Natural forming crusts have already been discussed in chapter 2 since hard pan formation starts with the formation of

coatings on minerals. The formation of carbonates depends on the ratio metal to alkalinity (mainly inorganic carbon). Adding reactive chemicals to tailings is very difficult due to the low permeability of the fine grained material. Thus gases seem to be an option worth thinking about. By injection of CO_2 into tailings via gas wells alkalinity could be controlled. An additional adjustment of the pH adding gases or nano-particles could be reasonable at least in cases, where sufficient amounts of calcium are present in the tailings. Thermodynamic models and laboratory experiments show promising results, but have to be confirmed by kinetic models and field tests.

Capping with reactive material

Any common constructed cap for uranium tailings is in some way reactive, because radon is given enough time in the radon barrier to decay to metals and thus being not longer volatile and highly mobile. However, Schneider et al. (2001) was the first to suggest a capping of uranium tailings containing chemical reactive material. On contrary to reactive barriers the idea of this type of capping is to add substrate to the capping which will be dissolved over time and migrate slowly into the underlying tailings performing reactions with the contaminants in the tailings. Another option of a reactive capping system is a system maintaining certain pH or consuming oxygen from the percolating seepage water in order to maintain reducing conditions in the tailings. However, both coating and capping have always to be seen as possible options in combination with the risk of severe erosion. If the latter happens, neither coating nor a reactive barrier will solve the long term risk of a uranium tailing.

Conclusions and suggestions

The Schneckenstein Tailing has to be considered as an environmental problem for an indefinite time, since the amount of uranium in the tailing is considerably high (193 tons) due to the leaching technology applied. Radium and thorium have not been quantified so far. Other toxic elements are contained and have to be taken into account as well. Nowadays leaching of arsenic and uranium in particular happens. Due to the relief energy in mountain areas in particular erosion will be a severe problem in the long term which would require an institutional monitoring and maintenance over centuries and more. Future scenarios are likely where increasing erosion (interior piping and surface erosion) may happen. In that case the downstream environment will suffer from radioactive and toxic elements. Thus the Schneckenstein tailings should be assessed within the framework of existing development of tailings decommissioning technologies. Active controls are necessary including building fences, putting up warning signs, and establishing land use restrictions. The only safe option so far seems to be either reprocessing of the tail-

ings, insitu treatment which has to be developed, or shifting the entire tailing into a safe deep mine in order to isolate it from the environment.

References

Berger H.-J. (1997): Tektonische Strukturkarte 1:200 000. - Auszug nach Geologischer Übersichtskarte der BRD, Blatt Zwickau, unpuplished Report of LfUG.

Blowes (1995) Acid Generation and Contaminant Transport in Decommissioned Sulfide-Bearing Mine-Tailings Impoundments. In: Merkel B, Hurst St, Löhnert EP, Struckmeier W (Eds.) Uranium Mining and Hydrogeology I, Verlag Sven von Loga, Köln

Blowes DW, Reardon EJ, Jambor JL, Cherry JA (1991): The formation and potential importance of cemented layers in inactive sulfide mine tailings. Geochim. Cosmochim. Acta, 55, 965-978

Landgraf A., Planer-Friedrich B., Merkel B. (2002): Natural attenuation in a wetland under unfavorable conditions - Uranium tailing Schneckenstein / Germany. In: Uranium in the aquatic environment; Springer

Leydecker, G. (1999): Earthquake Catalogue for the Federal Republic of Germany and Adjacent Areas for the Years 800 - 1994 (for Damaging Earthquakes till 1998). - Bundesanstalt für Geowissenschaften und Rohstoffe, Hannover

Merkel B, Preußer R, Namount T, Gottschalk S, Kutschke S (1998) Natural Leaching of Uranium from the Schneckenstein Uranium Mine Tailing. In: Uranium Mining and Hydrogeology II, Verlag Sven von Loga, Köln

Morrison SJ, Metzler DR, Carpenter CE (2001) "Uranium Precipitation in a Permeable Reactive Barrier by Progressive Irreversible Dissolution of Zerovalent Iron", Environmental Science & Technology, 35(2) 385-390.

Rammlmair D, (2002) Hard pan formation on mining residuals. In: Uranium in the aquatic environment; Springer

Schneider P, Neitzel PL, Osenbrück K, Noubacteb C, Merkel B, Hurst St (2001) In-situ Treatment of Radioactiove Mine Water using Reactive Materials – Results of Laboratory and Field Experiments in Uranium Ore Mines in Germany. Acta hydrochim. hydrobiol, 29(2-3) 129-138

WISMUT GMBH (1991): Beitrag zu Uranium Resources, Production and Demand 1991 der NEA/IAEA; Chemnitz.

Rock phosphates and P fertilizers as sources of U contamination in agricultural soils

Sylvia Kratz, Ewald Schnug

Institute of Plant Nutrition and Soil Science, Federal Agricultural Research Center, Bundesallee 50, D-38116 Braunschweig, Germany,
E-mail: sylvia.kratz@fal.de

Abstract. U concentrations were analyzed in a set of mineral fertilizers with and without P and compared to U concentrations in various organic fertilizers. Mean concentrations between 6 and 149 mg/kg U were found in P containing mineral fertilizers, while mean concentrations in mineral fertilizers without P were below 1.3 mg/kg U. Mean U concentrations in farmyard manures did not exceed 2.6 mg/kg U. As a consequence, an average P dressing of 22 kg/ha P would charge the soil with up to 17-61 g/ha U when added as mineral fertilizer but less than 10 g/ha when given as farmyard manure or slurry. Expected U uptake by crops is less than 1 g/ha U.

Introduction

Phosphate fertilizers are used in agriculture worldwide to supply crops with adequate amounts of P for growth and development. In 2002/2003, 1.46 million tons of P were used for agriculture in the European OECD countries, 142746 t of which in Germany (Statistisches Bundesamt 2004). P fertilizers may contain considerable amounts of U, data on U concentrations from the international literature range from less than 10 to more than 360 mg/kg (Hamamo et al. 1995; Makweba and Holm 1993). Little data exists on U accumulation in soils and U plant uptake from P fertilization. According to Mortvedt and Beaton (1995), no increase in soil and plant U was detected in a long term experiment with triple superphosphate fertilization. Similar results were published by Hamamo et al. (1995). However, as these authors stated, considering the mobility of U^{6+} (uranyl ion), it is hardly surprising that no soil accumulation was found, rather, these results imply that the U applied with the P fertilizer had leached into the groundwater that drained from the experimental fields. Increased U concentrations in surface and ground water

and water from drainage channels after long term mineral P fertilization have been reported for the Kanovci Area, Croatia (Barisic et al. 1992), as well as for wetlands in the Florida Everglades (Zielinski et al. 2000) and for the river waters of the Corumbatai River Basin, Brazil by Conceicao and Bonotto (2000, 2003).

Considerable research efforts on U extraction from phosphoric acid, which is the basic component of P fertilizer production, were already made in the 1960s (Romero Guzman et al. 1995a), however, the problem of U in mineral fertilizers has not been addressed in Germany until very recently.

In this paper, results from a screening of U concentrations in a set of various mineral and organic fertilizers are presented and compared to data from the international literature. U loads from P fertilization with various types of fertilizers are calculated and options for the reduction of uranium inputs into agricultural soils with fertilization are discussed.

Uranium in rock phosphates

The basic raw material for the production of P containing mineral fertilizers are rock phosphates. About 87% of the rock phosphates used for fertilizer production are of marine-sedimentary origin (Van Kauwenbergh 1997). During deposition and diagenesis, U and other heavy metals or trace elements from the seawater are enriched in marine-sedimentary phosphates (Aly and Mohammed 1999; Karhunen and Vermeulen 2000), therefore they are often characterized by high concentrations of these elements (El-Arabi and Khalifa 2002; Makweba and Holm 1993). In the apatite structure, U may occur mainly in two forms (El-Arabi and Khalifa 2002):

- as U^{4+}, it substitutes for Ca^{2+} in the apatite crystal
- as U^{6+}, or more precisely, as uranyl ion $(UO_2)^{2+}$, it is either adsorbed to a phosphate mineral, or fixed to the phosphate ion to form a secondary phosphate mineral.

Table 1 shows how U concentrations vary depending on the origin of the rock phosphate for the 10 largest producers worldwide.

Production processes of P fertilizers
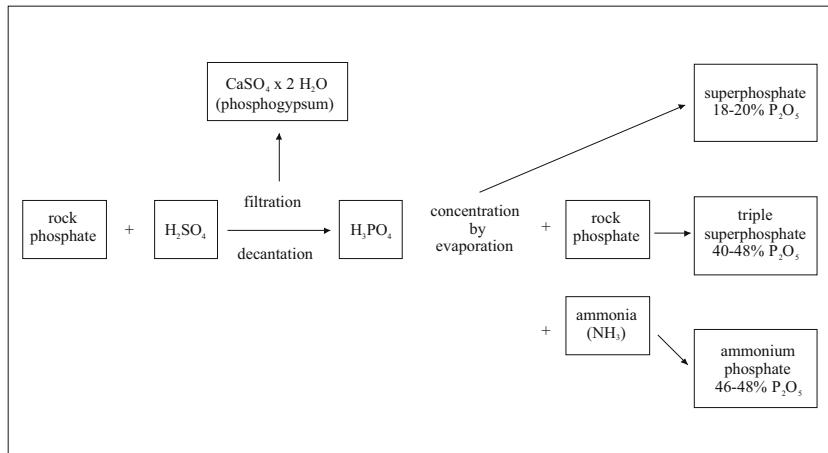
There are two common types of production for P containing fertilizers, which differ in the type of acid used to dissolve the rock phosphate and the type of fertilizer resulting from the process.

Wet process phosphoric acid
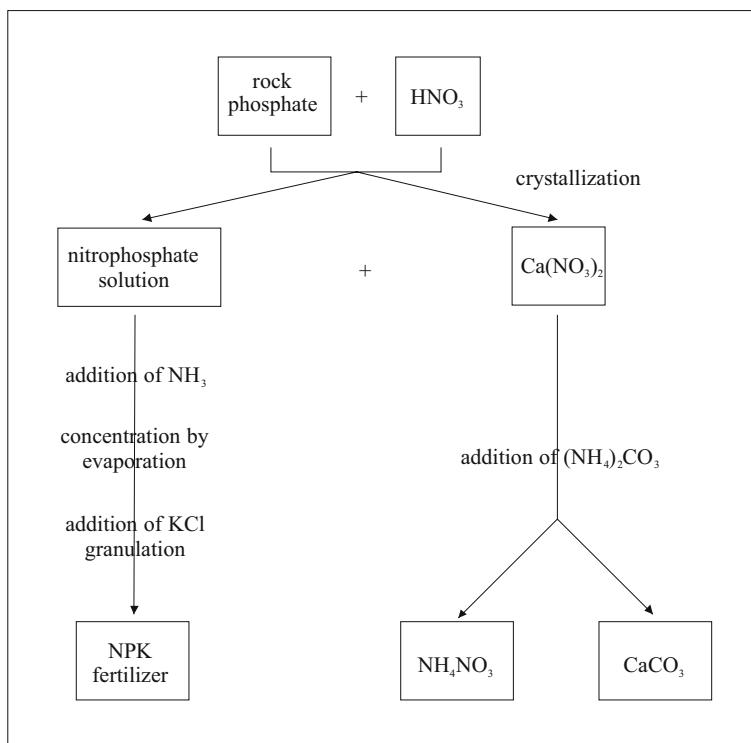
Wet process phosphoric acid is produced by attacking the rock phosphate with concentrated sulphuric acid (H_2SO_4) (Fig. 1). In this process, phosphogypsum is formed as a by-product. After filtration and decantation, the phosphoric acid is concentrated in an evaporation process and can then be granulated into superphosphate. By adding more rock phosphate to the H_3PO_4, triple-superphosphate can be manufactured, while the addition of ammonia (NH_3) allows for the production of ammonium phosphate (Pantelica et al. 1997; Erdem et al. 1996; Romero Guzman et al. 1995b).

Table 1. Uranium concentrations in rock phosphates of different origin, sorted by amount of production (mine production data from Jasinski 2003; uranium data from Hayumbu et al. 1995; Pantelica et al. 1997; Raven and Loeppert 1997; Romero Guzman et al. 1995a; Van Kauwenbergh 1997).

Origin (s = sedimentary, i = igneous)	Mine Production in 2002 (gross weight, in 1000 t)	U concentrations, range (in mg/kg)
United States (s)	35800	65 - 141
Morocco + Western Sahara (s)	24000	75 - 130
China (s)	21000	23 - 31
Russia (i)	10500	27 - 85
Tunisia (s)	7500	32 - 48
Jordan (s)	7000	46 - 129
Brazil (i)	4700	182 - 220
Israel (s)	3500	99 - 150
South Africa (i)	2800	23
Syria (s)	2400	75 - 106

Fig. 1. Flow chart for phosphate fertilizer production by sulphuric acid attack (modified after Romero Guzman et al. 1995b; Pantelica et al. 1997).

Fig. 2.   Flow chart for phosphate fertilizer production by nitric acid attack (modified after Pantelica et al. 1997; Gupta and Singh 2003).

Plenary

Nitrophosphate process

By attacking rock phosphate with nitric acid (HNO_3), fertilizers of the nitrophosphate type (NP, NPK) are obtained (Fig. 2). In the first step, a nitrophosphate solution is produced. This solution is further enriched with N by adding NH_3, and is then concentrated by evaporation. Now, an NP fertilizer can be manufactured, while the addition of KCl results in an NPK fertilizer.

As is shown in Figs. 1 and 2, in both processes a P containing acid solution is produced from the rock phosphate, which is then concentrated by evaporation. Due to this evaporation step, U is enriched in the final product compared to the raw material (Erdem et al. 1996; Uyanik et al. 1999).

U concentrations and loads in fertilizers

A literature review was made to collect information on U concentrations in mineral and organic fertilizers in a database on unwanted substances in fertilizers (FAL database). In addition to this, a set of 65 mineral and organo-mineral fertilizers as well as a collection of 500 manures and slurries from organic farms were analyzed for their U concentration. The results are presented in Tables 2-4.

Table 2. Uranium concentrations (mg/kg) in mineral fertilizers without and with P, from different sources (DB-NE = FAL database, non-european sources, DB-E = FAL database, European sources, FAL = FAL sample collection)

Fertilizer type	Data source	n	min	max	mean	s
Mineral fertilizers without P						
N fertilizer	DB-NE	1			0.26	
N fertilizer	FAL	7	0.02	1.39	0.35	0.48
K fertilizer	DB-NE	2	0.23	0.49	0.36	0.18
K fertilizer	FAL	3	0.03	0.62	0.23	0.34
Lime	DB-NE	1			1.31	
Secondary nutrient fertilizer	FAL	4	0.04	2.24	0.99	0.95
Mineral fertilizer with P						
P fertilizer	DB-NE	18	8.7	362	149	101
P fertilizer	FAL	12	1.8	160	35	47
NP fertilizer	DB-NE	4	2.9	198	131	90
NP fertilizer	DB-E	4	3.5	149	59	70
NP fertilizer	FAL	5	0.62	61	17	25
PK fertilizer	DB-NE	1			99	
PK fertilizer	FAL	3	31	163	82	71
NPK fertilizer	DB-NE	1			46	
NPK fertilizer	DB-E	3	24	62	43	19
NPK fertilizer	FAL	22	0.04	28	6.3	8.1
organo-mineral NPK	FAL	5	7.4	28	19	8.1

Table 3. Uranium concentrations (mg/kg) in different types of P fertilizers, from different sources (DB-NE = FAL database, non-european sources, FAL = FAL sample collection).

Fertilizer type	Data source	n	min	max	mean	s
Superphosphate	DB-NE	7	80	325	134	90
Superphosphate	FAL	6	1.8	2.0	1.9	0.09
Triple superphosphate	DB-NE	7	186	362	225	62
Triple superphosphate	FAL	2	52	160	106	76
Soft rock phosphate	DB-NE	4	8.7	144	43	67
Soft rock phosphate	FAL	2	57	73	65	11

U concentrations in mineral fertilizers

As is shown in Table 2, mean U concentrations in mineral fertilizers without P are below 1.4 mg/kg, while mean U concentrations in P containing mineral fertilizers range from 6 to 149 mg/kg. In the literature, maximum concentrations up to more than 362 mg/kg are found. The highest concentrations are found in pure P and in NP fertilizers, which also have the highest P concentrations.

Looking at different types of P fertilizers, it can be seen that even within a particular type, large variations of U concentrations may occur (Table 3). This is probably due to the different origins of the rock phosphates used for production, as they vary strongly in their U concentrations, too (see Table 1). For example, the 6 superphosphates analyzed by FAL were all produced from Kola phosphates, which are very low in U concentration. The highest U concentrations are found in triple superphosphate, which is also the P fertilizer with the highest P concentration.

U concentrations in organic fertilizers

Organic fertilizers like manures and slurries are generally low in U concentrations, no matter whether they come from organic or conventional farms. Mean U concentrations do not exceed 2.6 mg/kg dry weight, while maximum concentrations may reach up to 11.6 mg/kg dry weight in individual cases (Table 4). For sewage sludge, only one reference was found, which reports a mean U concentration of 8 mg/kg dry weight for unstabilized wet sludge, and 31 mg/kg dry weight for sludge stabilized with lime.

Table 4. Uranium concentrations (mg/kg dry weight) in different types of organic fertilizer, from different sources (DB-NE = FAL database, non-european sources, DB-E = FAL database, European sources, FAL = FAL sample collection).

Type of fertilizer	Data source	n	min	max	mean	s
Manure and slurry from organic farming						
Organic cattle manure	FAL	197	0.05	3.7	0.75	1.2
Organic pig manure	FAL	57	0.03	1.4	0.24	0.24
Organic poultry manure	FAL	43	0.05	4.6	1.1	1.2
Organic sheep manure	FAL	22	0.07	11.6	2.6	2.6
Organic goat manure	FAL	3	0.05	1.14	0.28	0.27
Organic cattle slurry	FAL	46	0.09	0.37	0.23	0.13
Organic pig slurry	FAL	1	0.05	0.05	0.05	.
Manure and slurry from conventional farming						
Conventional broiler manure	FAL	10	0.33	5	0.97	1.42
Conventional cattle slurry	DB-NE	20	0.1	3.5	1.4	
Sewage sludge						
Germany	DB-E	204			3.5	
Lower Saxony, Germany	DB-E	10			0.91	

U loads with P fertilization

Under good agricultural practice, P fertilization is usually done according to the P demand of the crop. Therefore it is interesting to know which U loads are put onto agricultural soils with typical rates of P fertilization. In Table 5, U loads are calculated for a number of different mineral and organic P fertilizers when a P rate of 22 kg/ha P is applied. For comparison, expected U uptake of plants is also shown. With only very few exemptions at the lower end of the given ranges, U uptake by plants, which can be expected to be less than 1 g/ha*a, will be exceeded no matter which type of fertilizer is used, however, the "excess supply" is much higher for mineral fertilizers than for farmyard manures or slurries. U loads applied with sewage sludge, are also comparatively low.

Strategies for reduction of U inputs into agricultural soils from fertilization

Looking at the potential U loads to be expected from P fertilization it is clear that some measures should be taken to prevent the accumulation of U in agricultural soils and its discharge into the environment by leaching in the long term. In theory, there are two ways to tackle this problem: One is for the fertilizer industry to

Table 5. U loads for different types of P fertilization and expected U uptake by plants (based on data on U concentrations from Mortvedt and Beaton 1995; data on DM yield after Hydro Agri Dülmen 1993).

Type of fertilizer	P concentration (% P)			U load (g/ha*a) at a P rate of 22 kg/ha P (=50 kg/ha P_2O_5)		
Triple superphosphate[1]		18.5		6.2	-	19
NP[1]	5.3	-	21.6	0.13	-	17
PK[1]	5.8	-	8.4	11	-	61
NPK[1]	1.5	-	13.2	<0.01	-	20
Organic cattle slurry[1]	0.14	-	2.5	0.31	-	5
Conventional cattle slurry[2]		0.8			3.8	
Organic pig manure[1]	0.23	-	2	0.1	-	9.4
Conventional broiler manure[1]	1.2	-	1.5	0.57	-	9
Sewage sludge[2]	2.1	-	2.2	0.9	-	3.3
Type of crop	DM yield (dt/ha)			U uptake by plants (g/ha*a)		
Corn grain and leaves	75+75			0.15		
Wheat grain and straw	70+70			0.28		
Timothy forage	130			0.78		

[1]data from FAL samples,
[2]data from literature; note: ranges are given where raw data sets were available, otherwise, a mean value is given)

produce U free mineral fertilizers, the other is for farmers to select fertilizers which are low in U concentration for P fertilization.

Options for the fertilizer industry: U extraction from phosphoric acid

Several methods have been developed to extract U from phosphoric acid. The scope of this paper only allows a short description, for more technical details on this topic the reader is referred to Gupta and Singh (2003).

1. <u>Precipitation</u> of U from phosphoric acid, using an organic reagent (e.g. acetone) as dispersant and ammonium fluoride (NH_4F) as precipitant. Reduction of U^{6+} to U^{4+} by addition of Fe powder. In order to produce "yellow cake", U needs to be recovered from the precipitate by dissolution in diluted H_2SO_4 or HNO_3 and subsequent purification by ion exchange or solvent extraction.
2. <u>Ion exchange separation with a chelating resin</u> (with subsequent elution and precipitation of U in order to produce yellow cake).
3. <u>Membrane separation</u> of U, using liquid membranes with a strong affinity for U (as yet still in experimental development stage).
4. <u>Froth flotation</u>: complexing U with a surface active agent of hydrophobic nature (froth needs to be purified to produce high grade yellow cake).
5. <u>Solvent extraction</u> of U, using various synergistic mixtures of organic solvents such as DNPPA (di nonyl phenyl phosphoric acid) + TOPO (tri n octyl

phosphine oxide) (Singh et al. 2001), followed by purification and precipitation. In this process, U extraction rates of >90% can be realized.

Of the methods listed here, solvent extraction appears to be the most successful one, which is well capable to be practiced by the uranium industry on a large commercial scale (Gupta and Singh 2003). However, according to WISE (2002), operating costs for the uranium recovery plants which had been built in the United States, Canada, Spain, Belgium, Israel and Taiwan from the 1970s onwards were by far higher than the current uranium market price, which is why most of them have been closed again by now. Therefore, as yet U extraction from phosphoric acid remains more of scientific than of commercial interest (Romero Guzman et al. 1995b).

Options for farmers: Selection of adequate fertilizers

As long as no U free fertilizers are produced, the only option for farmers to reduce the U input into soils and the environment by fertilization is to select fertilizers which are low in U concentrations. The use of rock phosphates from deposits which are low in U concentration still allows to produce such mineral fertilizers. Prerequisite for an informed choice by farmers is that U concentrations in commercial fertilizers are openly declared. As the above calculations imply, farmyard manures and slurries appear to hold quite some attraction, since they – when applied according to the rules of good agricultural practice - allow to supply the crops with the required amount of P by keeping uranium loads at a relatively low level.

Conclusion

According to WISE (2002), the potential uranium concentration of known phosphate rock world reserves is in the range of 5 to 15 million t U. Thus, at the current global rate of consumption, phosphatic uranium could meet the global demand for about 440 years, while known uranium resources will only last for about 86 years (OECD 1999, cited in Singh et al. 2001).

In the context of the ongoing discussion on sustainable farming, the conservation of resources and the precaution principle, we suggest that more emphasis should be placed on further development of economically feasible methods for the extraction of uranium from phosphoric acid. In addition to this, the efficient use of farmyard manures as a P source which is very low in uranium should be given increased consideration.

References

Aly M M, Mohammed N A (1999) Recovery of lanthanides from Abu Tartur phosphate rock, Egypt. Hydrometallurgy 52: 199-206.

Barisic D, Lulic S, Miletic P (1992) Radium and uranium in phosphate fertilizers and their impact on the radioactivity of waters. Water Research 26(5) 607-611

Conceicao F T, Bonotto D M (2000) Anthropogenic influences on the uranium concentration in waters of the corumbatai river basin (SP), Brazil. Revista Brasileira de Geociencias 30(3): 555-557

Conceicao F T, Bonotto D M (2003) Use of U-isotope disequilibrium to evaluate the weathering rate and fertilizer-derived uranium in Sao Paulo state, Brazil. Environmental Geology 44: 408-418.

El-Arabi A E, Khalifa I H (2002) Application of multivariate statistical analyses in the interpretation of geochemical behaviour of uranium in phosphatic rocks in the Red Sea, Nile Valley and Western Desert, Egypt. Journal of Environmental Radioactivity 61: 169-190

Erdem E, Tinkilic N, Yilmaz V T, Uyani A, Ölmez H (1996) Distribution of uranium in the production of triple superphosphate (TSP) fertilizer and phosphoric acid. Fertilizer Research 44: 129-131

Gupta C K, Singh H (2003) Uranium resource processing. Secondary resources. Berlin / Heidelberg. ISBN 3-540-67966-9

Hamamo H, Landsberger S, Harbottle G, Panno S (1995) Studies of radioactivity and heavy metals in phosphate fertilizer. Journal of Radioanalytical and Nuclear Chemistry 194 (2): 331-336

Hayumbu P, Haselberger N, Markowicz A, Valkovic V (1995) Analysis of rock phosphates by x-ray fluorescence spectrometry. Applied Radiation and Isotopes 46 (10): 1003-1005

Hydro Agri Dülmen (1993) (ed) Faustzahlen für Landwirtschaft und Gartenbau. Münster-Hiltrup. ISBN 3-7843-2512-2

Jasinski S M (2003) Phosphate Rock. U.S. Geological Survey, Mineral Commodities Summary, January 2003.
http://minerals.usgs.gov/minerals/pubs/commodity/phosphate_rock/phosmyb03.pdf

Karhunen J, Vermeulen S (2000) Natural radioactivity of phosphates and phosphogypsum. Fertilizer International 378: 75-81

Makweba M M, Holm E (1993) The natural radioactivity of the rock phosphates, phosphatic products and their environmental implications. The Science of the Total Environment 133: 99-110

Mortvedt J J, Beaton J D (1995) Heavy metal and radionuclide contaminants in phosphate fertilizers. In: Tiessen H (ed) SCOPE 54 – Phosphorus in the global environment – transfers, cycles and management, chapter 6. http://www.icsu-scope.org/downloadpubs/scope54/6mortvedt.htm

OECD (1999) Environmental activities in uranium mining and milling. Report by OECD-Nuclear Energy Agency and IAEA.

Pantelica A I, Salagean M N, Georgescu I I, Pincovschi E T (1997) INAA of some phosphates used in fertilizer industries. Journal of Radioanalytical and Nuclear Chemistry 216 (2): 261-264

Raven K P, Loeppert R H (1997) Trace element composition of fertilizers and soil amendments. Journal of Environmental Quality 26: 551-557

Romero Guzman E T, Ordonez Regil E, Pacheco-Malagón G (1995a) Uranium leaching from phosphate rock. Journal of Radioanalytical and Nuclear Chemistry – Letters 201(4): 313-320

Romero Guzman E T, Solache Rios M, Iturbe Garcia J L, Ordonez Regil E (1995b) Uranium in phosphate rock and derivates. Journal of Radioanalytical and Nuclear Chemistry 189 (2): 301-306

Singh H, Vijayalakshmi R, Mishra S L, Gupta C K (2001) Studies on uranium extraction from phosphoric acid using di-nonyl phenyl phosphoric acid based synergistic mixtures. Hydrometallurgy 59: 69-76

Statistisches Bundesamt (2004) Fachserie 4 / Reihe 8.2 Produzierendes Gewerbe - Düngemittelversorgung, Wirtschaftsjahr 2003/2004. Wiesbaden.

Uyanik A, Tinkilic N, Odabasoglu M, Karaca H (1999) Spectrophotometric determination of uranium in waste water of phosphoric acid and fertilizer manufacturing process. Turkish Journal of Chemistry 23: 275-284

Van Kauwenbergh S J (1997) Cadmium and other minor elements in world resources of phosphate rock. Proceedings of the Fertilizer Society No. 400, London.

Monitoring of natural radionuclides in soils as a tool for precision farming - methodical aspects

Michael Tauchnitz[1], Detlev Degering[2], Carsten Pretzschner[1], Thomas Wonik[3], Juergen Boess[4]

[1] TU Bergakademie Freiberg, Institute of Applied Geophysics, Gustav-Zeuner-Straße 12, D-09599 Freiberg/Sa., Germany
[2] Saxon Academy of Sciences at Leipzig, Quaternary Geochronology section at the TU Bergakademie Freiberg, B.-v.-Cotta-Str. 4, D-09599 Freiberg/ Sa., Germany, E-mail: degering@physik.tu-freiberg.de
[3] Leibniz Institute for Applied Geosciences (GGA), Germany
[4] Geological Survey of Lower Saxony (NLfB), Germany

Abstract. The use of natural radionuclide contents for the evaluation of soil quality data was tested by field logs and additional laboratory analyses on vertical profiles. The latter proved a well mixing of soil material in the uppermost 30 cm by ploughing. A mathematical procedure for the consideration of soil moisture and the determination of the "information depth" is presented and lead to good agreement between field and laboratory data.

Introduction

The future environmental requirements as well as the development of the business environment force the trend to an economical use of fertilisers, sowings, plant protectants etc. in agriculture. Highly resolved soil data are an important prerequisite for sustainable cultivation. The soil texture determines the basic fertilisation with K, P, Mg as well as the depth of ploughing (Voßhenrich 2003). Therefore, GPS controlled farming, often referred to as *precision farming,* will play a growing role in modern agriculture.

Techniques used for the collection of soil data must correspond to the needs for high resolution, reliability and inexpensive realisation. Based on the close relationship to the clay content, radiometric measurements provide the opportunity to draw a relation between the content of natural radionuclides and the different soil types.

In the present paper we report first results of radiometric logging on farmland conducted by gammaspectrometric investigations on the vertical distribution of
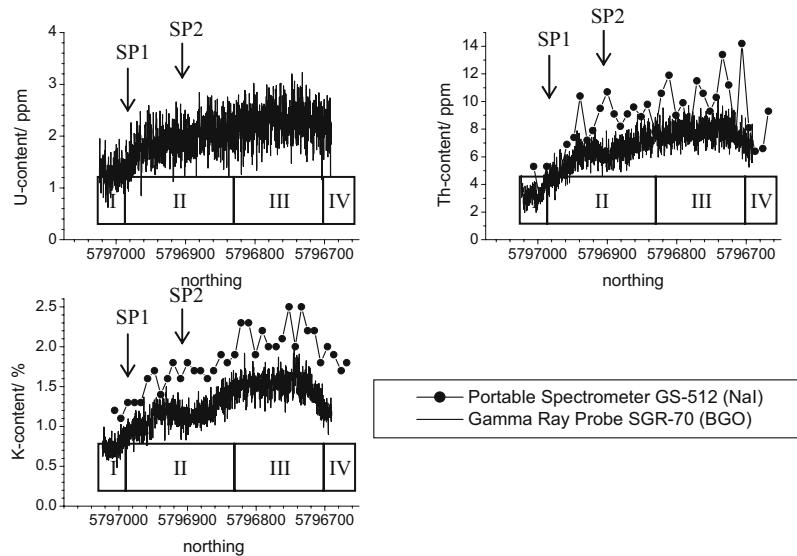
radionuclides and by methodical considerations on the relation between radionuclide analysis in the laboratory and field data.

Experimental

All measurements displayed here were made at an investigation area near Hörsingen, Saxony-Anhalt. The local soil is characterised by underlying variegated sandstone and in the upper parts by glacial material.

Field logging was carried out in two different ways at the surface of the acre: by measurements on a regular grid using a portable Gamma ray spectrometer and by continuous tracking of a borehole probe along defined profiles.
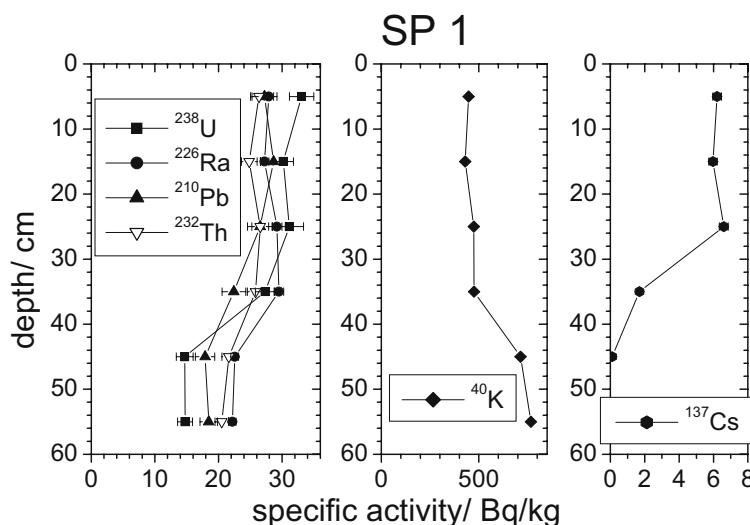
The portable spectrometer GS-512 (Geofyzika 1998) contains a 3'' x 3'' NaI(Tl) scintillation detector. For the determination of the radionuclide contents three energy ranges of the gamma rays were used: around 1461 keV (^{40}K) for Potassium, around 1764 keV (^{214}Bi) for Uranium and around 2614 keV (^{208}Tl) for Thorium. The integration time amounted to 25 s, the grid spacing was 10 m. The correlations between the pulse rates and radionuclide concentrations were determined by calibration pads of known K, U and Th content (IAEA 2003).

Fig. 1.   Contents of Uranium (top left), Thorium (top right) and Potassium (down left) at a section on area Hörsingen as measured by different equipments. The Roman numerals in the boxes denote different soil types: I - moist similigley, II - pelosol soil, III - pelosol-braunerde, IV - gley colluvium. SP 1 and SP 2 give the positions of the two sampling points for laboratory γ-spectrometry.

The borehole probe SGR-70 (ANTARES, Stuhr) is equipped with a BGO crystal in a robust housing. At a logging velocity of 3 m/ min every 5 cm a 512 channel γ-spectrum was recorded. The evaluation software allows the analysis of the K, U and Th concentrations using the same γ-lines as indicated above. Calibration was performed in borehole geometry.

Samples for gammaspectrometric investigations were taken at two vertical profiles on this area. Each sample represents a range of 10 cm in depth. At position SP 1 the maximum depth was 60 cm, at position SP 2 only 40 cm. We used a high resolution low level gammaspectrometer equipped with a 38 % n-type HPGe detector. The dried sample material was filled into gas-proof so called Marinelli beakers which cover the cylindrical detector on each side. Measuring times up to 24 h were necessary in most cases. The effect of self attenuation was taken into account for the activity calculation. Generally, the following long living natural radionuclides could be determined (in some cases by using gamma emitting short living daughter nuclides): ^{238}U, ^{226}Ra, ^{210}Pb from ^{238}U decay series, ^{228}Ra, ^{228}Th from ^{232}Th series and ^{40}K. ^{137}Cs from the atmospheric nuclear weapons tests and the Chernobyl accident was detected down to 50 cm depth.
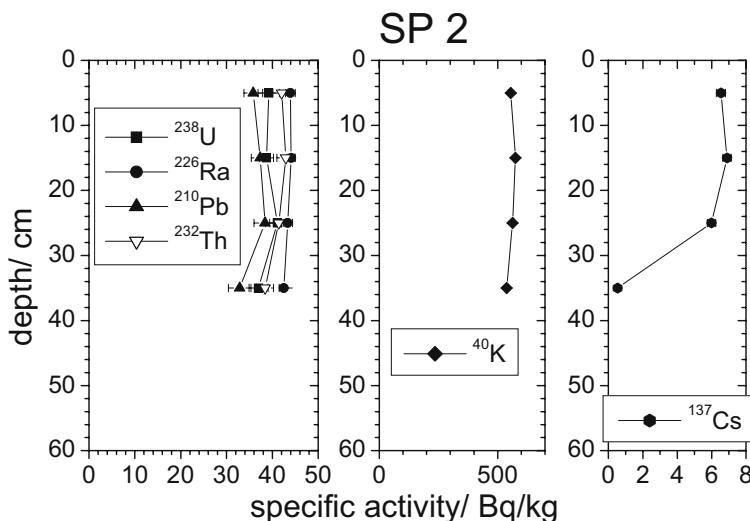
Fig. 2.   Depth profile of the specific activities of members of the ^{238}U decay series and the ^{232}Th series (left), ^{40}K (middle) and ^{137}Cs (right) at sampling point SP 1.

Results

Fig.1 shows the field logs. Along the section the soil type varies in a definite way: Part I is sandy to loamy moist similigley, part II contains a loamy to sandy pelosol whereas in part III slightly loamy, partly clayey pelosol-braunerde was found. The last segment IV is a sandy colluvium with gley properties.

Due to a technical defect no Uranium values were recorded by the GS-512 spectrometer. For Thorium and Potassium the trends of the concentrations correlate between the two equipments but their total values differ by a factor of 1.2 to 1.5. Note the position of the two sampled profiles SP1 and SP2 which are situated in areas of different radionuclide concentrations and soil types.

The laboratory gammaspectrometric measurements of the samples from SP 1 (Fig. 2) and SP 2 (Fig. 3) show almost constant values of the geogenic activities (^{238}U and ^{232}Th series as well as ^{40}K) in the uppermost 40 cm. No disequilibrium between ^{228}Ra and ^{228}Th was found in both profiles. Therefore, their mean value is quoted as ^{232}Th in all diagrams. A distinct change of the contents appears beneath the upper layer (investigated just at sampling point SP 1). The Potassium concentration increases whereas Uranium and Thorium are reduced. Similar effects were found at SP 1 for the ratios between the nuclides: ^{238}U/^{226}Ra varies between 1.1 and 1.2 in the upper part and lies at 0.7 at the lower one, ^{238}U/^{232}Th falls from about 1.2 to 0.7 whereas ^{226}Ra/^{232}Th remains nearly constant at 1.1 over the whole profile.
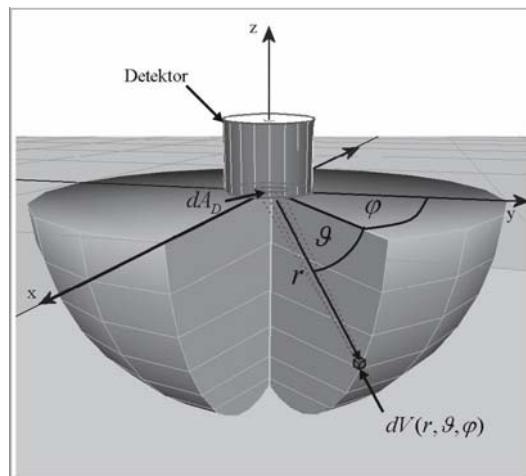
Fig. 3.   Depth profile of the specific activities of members of the ^{238}U decay series and the ^{232}Th series (left), ^{40}K (middle) and ^{137}Cs (right) at sampling point SP 2.

Sensors for in-situ monitoring of uranium and related elements

Unlike this, ^{137}Cs activities show a sharp decrease below 30 cm depth at both sections. This step parallels to an increase of the [226]Ra/^{210}Pb ratio from about 1.0 to 1.3.

Discussions

The most evident conclusion of the laboratory analyses is the determination of the ploughing depth to about 30 cm. The contents of the geogenic nuclides as well as that of the airborne ^{137}Cs are homogenous in this region which indicates a well mixed soil. The further run of the ^{137}Cs curve indicates the downward migration with time. For the nuclear weapons fraction, the European Comission (1998) estimates the ^{137}Cs contamination for 1986 in the region of Hörsingen of about 2 kBq/m². For the Chernobyl fraction, BGA (1991) gives values of 2.0 -3.5 kBq/m². From the measured ^{137}Cs profile we estimate an actual total amount of about 3.1 kBq/m² which corresponds to 4.8 kBq/m² in 1986. This result points at a nonessential ^{137}Cs loss by migration or plant uptake.

The step in the radionuclide composition at 40 cm depth is thus not linked to the ploughing depth but rather to a change in the parent material of the soil from glacial sediments to variegated sandstone. In this context the decrease of the [238]U/[226]Ra ratio suggests an enrichment of the alcaline earth element Radium in the lower soil probably caused by a displacement from the upper part. The constant [226]Ra/[232]Th ratio is then astonishing but may be explained by the fact that [232]Th is analyzed via its daughter nuclides [228]Ra (half life 5.75 a) and [228]Th (1.91 a). So the [232]Th profile is rather that of [228]Ra which behaves chemically like [226]Ra.

Fig. 4.   Sketch of the geometrical relations and the variables used for the calculation of the moisture correction of the count rates.

Sensors for in-situ monitoring of uranium and related elements

For a correlation of the laboratory and the field measurements two items must be considered: (i) the connection between count rate and soil moisture and (ii) the thickness of the soil layer that governs the measured count rate in the field logs.

The mathematical treatment uses the geometric relations shown in Fig. 4. The gamma ray detector is put directly onto the soil surface. Spherical coordinates are chosen for symmetry reasons.

A volume element dV at the surface of a hemisphere with radius r has the activity

$$dA = A_{sp} \cdot \frac{\rho_m}{(1-M)} \cdot dV$$

with

A_{sp} - specific activity, determined on a dry sample
ρ_m - density of moist soil
M - moisture, ratio of mass of water to dry mass

The total gamma quanta rate emitted by the hemisphere is then

$$d\dot{n}_{H\gamma}(r) = \int_0^{\pi/2} \int_0^{2\pi} A_{sp} \cdot p \cdot \frac{\rho_m}{(1-M)} \cdot r^2 \cdot \sin\vartheta \, d\vartheta \cdot d\varphi \cdot dr$$

$$= A_{sp} \cdot p \cdot \frac{\rho_m}{(1-M)} \cdot r^2 \cdot 2\pi \cdot dr$$

with

p - number of quanta of a certain gamma energy emitted per decay

The fraction of the gamma rate emitted into the direction of a detector cross section element dA_D including the gamma ray attenuation in the soil is
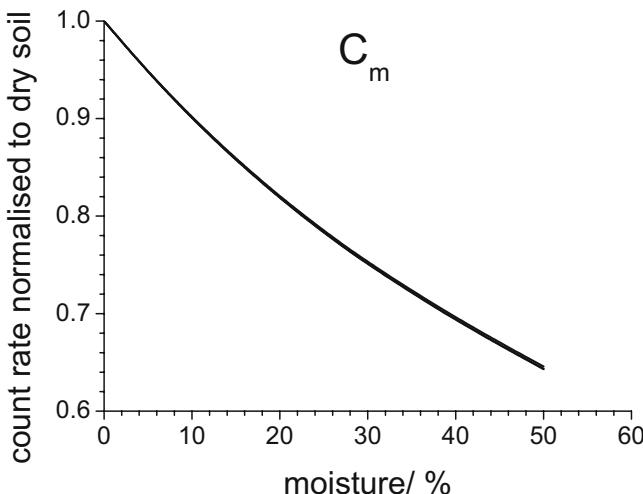
$$d\dot{n}_H(r) = A_{sp} \cdot p \cdot \frac{\rho_m}{(1-M)} \cdot \frac{1}{2} \cdot e^{-\mu_M \cdot \rho_m \cdot r} \cdot dA_D \cdot dr$$

where μ_M is the mass attenuation coefficient of the moist soil for the observed gamma energy. The coefficient is defined only for narrow parallel beams without any scattering. Since scattering leads to an energy loss and the detector shall count only quanta of the full gamma energy, the condition is fulfilled.

Integration over the half space ($r = 0 \ldots \infty$) and normalisation to the rate of a dry soil gives the ratio of "moist count rate" to "dry count rate", the correction factor C_m:

$$C_m = \frac{d\dot{n}}{d\dot{n}_D} = \frac{1}{(1-M)} \cdot \left(\frac{\mu_{MD}}{\mu_M} \right)$$

where $d\dot{n}_D$, μ_{MD} and $d\dot{n}$, μ_M denotes count rate and mass attenuation coefficient for the dry and the moist soil, respectively.

Fig. 5.   Calculated ratio C_m of the gamma count rate received from a moist soil to the count rate of a dry soil. The curves for the three γ-peaks at 1461 keV, 1764 keV and 2614 keV, respectively, coincide within the width of the drawn lines.
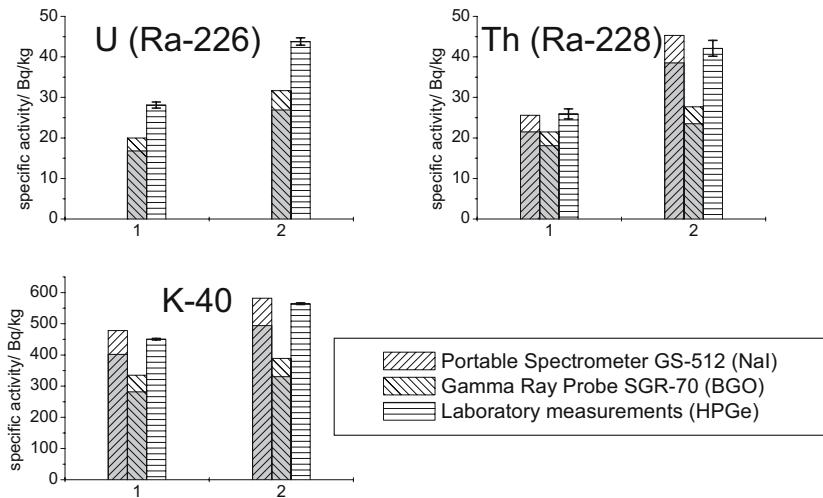
Values of the mass attenuation coefficient were calculated using the software PHOTCOEF (Buecherl 1994) for the simplified system SiO_2 (soil) plus H_2O and different moisture contents at the gamma energies used in the field measurements. The derived moist-to-dry count rate ratio C_m presented in Fig. 5 shows negligible differences between the three gamma energies. The necessity of correcting the count rates for moisture effects is obvious: e.g. a moisture M = 17 % as found in the above 30 cm of the vertical profiles leads to a reduction of the count rate compared to a dry soil of 16 %.

With the deduced formulae it is also possible to estimate the radius of a hemisphere which contributes a certain fraction to the total gamma count rate. In Table 1 the radius are listed which account for 90 % of the count rate.

This "information radius" exceeds in moist soils only for Th slightly the depth over which homogenously mixed soil material was found. Radionuclide concentrations determined from count rates corrected to dry soil should therefore agree

Table 1. Radius of the soil hemisphere which contributes to 90 % of the detected count rate at the given energies and moistures. A dry soil density of 1.4 g/cm³ was used for the calculation.

moisture/ %	radius responsible for 90 % of the count rate/ cm		
	U (1764 keV)	Th (2614 keV)	K (1461 keV)
0	34.5	42.2	31.3
20	28.2	34.6	25.6

Fig. 6. Comparison of the specific activities of Uranium (top left), Thorium (top right) and Potassium (down left) at the two sampling points on area Hörsingen as measured by different equipments. The laboratory measurements were carried out on dried samples; the values for GS-512 and SGR-70 are corrected to dry soil. Uncorrected contents are marked by grey bars.

with the mean value of the specific activities in the uppermost 30 cm from laboratory measurements.

Radionuclide contents analysed by different equipments at the two vertically sampled points are summarised in Fig. 6. A fairly good agreement with the laboratory results is achieved for the GS-512 values. The lower concentrations of the borehole probe are a consequence of the unequal geometries used in calibration and field log, respectively.

The figure furthermore illustrates the must of a moisture consideration in the field data evaluation. Since the moisture distribution is currently unknown for the whole investigation area, the curves in Fig.1 are only a rough estimation of the true values. Nevertheless a relation between radionuclide and clay content is visible. Clay contents deduced from the soil classes at 15 positions on the area allow an estimation of this quantity along the logged profile. According to this, region I (cf. Fig.1) contains 8 - 12 % clay, region II 17 - 30 %, region III 45 - 65 % and region IV 8 - 12 %. These variations are mirrored in the radionuclide contents even though accurate correlations require moisture data for the whole area.

Conclusions

Field logs of the gamma radiation are suitable for a correct determination of natural radionuclide contents in agriculturally used soils. The radiation originates mainly from the well mixed ploughing depth. Only slight radioactive disequilibria were found at the investigated area in this layer but more explicitly in the bottom soil.

To achieve reliable results the count rates must be corrected for the appearing moisture content. This requires the logging of the water content for the whole area in future investigations.

References

BGA (1991) Bodenkontamination mit Cs137 im Jahr 1986, Karten erstellt auf der Grundlage von Daten des Bundesamtes für Strahlenschutz, Bundesgesundheitsamt, Institut für WaBoLu

Bücherl Th. (1994) Software PHOTCOEF, München

European Comission (1998) Atlas of caesium deposition on Europe after the Chernobyl accident, Comission of the European Communities, Luxemburg

Geofyzika (1998) Gamma Ray Spectrometer-Instruction Manual, Version 2.0. Brno

IAEA (2003) Guidelines for radioelement mapping using gamma ray spectrometry data. International Atomic Energy Agency

Electrophoretic characterization of thorium species in very dilute solutions containing humic acid

Petr Benes

Czech Technical University in Prague, Department of Nuclear Chemistry, Brehova 7, 115 19 Praha 1, Czech Republic, Email: Benes@fjfi.cvut.cz

Abstract. Electrophoretic mobility of thorium was measured in aqueous solutions (HClO4+ NaClO4, I = 0.01) as a function of thorium concentration (<< 10-7 – 10-5 M), pH (2 – 10) and solution composition (Aldrich humic acid, NaHCO3) using free-liquid electrophoresis. Results have shown that negatively charged thorium humate complexes can prevail at pH 2 – 10 even in solutions containing very low concentration of humic acid (0.1 – 1 mg/L) and medium concentration of carbonates (0.001 M). The mobilities determined can serve for analysis of formation of the humate complexes in aqueous solutions and natural or wastewaters.

Introduction

Complexation of natural radionuclides with humic substances present in surface and ground waters can strongly affect speciation and migration of the radionuclides. Although the strong interaction of humic substances with thorium in natural waters has been documented (Wahlgren and Orlandini 1982, Miekeley and Kuechler 1987, Zeh et al. 1995, Kim and Marquardt 1999), formation and properties of humic complexes of tetravalent thorium and uranium are not well known (Reiller 2005). It is due to the strong hydrolysis and other complexation reactions of the tetravalent metals as well as easy precipitation of their hydroxides, extensive sorption on surfaces and, in the case of uranium, also to redox reactions. Most of the data on the complexation on of thorium with various humic and fulvic acids were obtained at pH 3.95-6.5. Only recently was formation of thorium humate studied in the neutral pH region (6.75-7.9, Reiller et al. 2003). No experimental data on the formation of similar complexes of tetravalent uranium are available.

Thorium can be used as model for other tetravalent actinides (Choppin 1999), therefore basic knowledge on its complexation with humic substances is also ap-

plicable for uranium (Reiller 2005). In this paper, thorium complexation with well characterized Aldrich humic acid is studied in a broad range of experimental conditions using free-liquid electrophoresis. Among principal advantages of the method (Benes and Majer 1980) belongs that it can be applied for very low concentrations of thorium and thus precipitation of thorium hydroxide can be avoided. Furthermore, electrophoretic mobilities measured by the method characterize the charge of the complexes formed and can serve for analysis of the effects of saturation of humic acid with the metal. The electrophoresis can also be used for analysis of speciation of thorium in natural waters, if mobilities of typical thorium species are known. Determination of such mobilities is one of the aims of the paper.

Experimental

Ultrapure water (Millipore Milli-Q 50 system) and A.R. reagents were used for preparation of all solutions in this work. Stock solution of carrier-free [234]Th in 1 M $HClO_4$ was prepared by separation of [234]Th from $UO_2(NO_3)_2.6H_2O$ (Benes 2005). Purification, characterization and preparation of stock solutions (500 mg/L) of Aldrich humic acid were described in detail previously (Mizera et al. 2003).

Experimental solutions were prepared by mixing stock solution of [234]Th with water and stock solutions of NaOH or NH_4OH, $NaHCO_3$ and humic acid so as to obtain the desired pH and composition of the solution. Other concentrations of thorium than "carrier-free" ($<< 10^{-7}$ M) were obtained by addition of [232]Th. The ionic strength of the solutions was maintained close to 0.01 mol/L. The solutions were used for experiments 24 hours after their preparation. Before the use, pH of each solution was measured and, if necessary, readjusted.

The apparatus and procedure for free-liquid electrophoresis used in this work were described in detail earlier (Benes and Majer 1980). The electrophoretic cell consisted of three parts made of plastic tubings connected with two three-way Teflon stopcocks. The central part of the cell was filled with working solution labelled with [234]Th, the side arms contained a working solution of the same pH and composition except for the label. The electrophoretic experiments were carried out at a constant current (around 1 mA, with potential difference at the electrodes 230-240 V) at 22 ± 3 °C, mostly for 60 min. The electrophoretic mobilities of thorium towards anode ($_-u$) and cathode ($_+u$) were calculated from the distribution of activity ([234]Th) between the side arms and central part of the cell, while adsorption on the walls of the cell was taken into account.

All activity measurements were made by liquid scintillation counting in glass vials using Triathler Multilaber Tester and Rotiszint eco plus scintillation cocktail. Specific conductivity of the solutions was determined with a conductometer OK 102/1 equipped with a bell electrode OK-9023 (Radelkis, Budapest), pH was measured with combined glass electrode and Orion 525A pH meter. Further experimental details can be found elsewhere (Benes 2005).

Results and discussion

Electrophoretic mobilities presented in this paper are the mean values obtained by two to six experiments carried out with one (two experiments) or more thorium solutions. Their accuracy depends on the concentration of thorium used and on the adsorption of thorium in the electrophoretic cell. Possible errors in measurement of mobilities by this method were discussed in detail recently (Mizera et al. 2003, Benes 2005). Variation of the mobilities given in Table 1 is characterized by attached error, representing span of the data measured (for two experiments) or standard deviation of the mean (for more experiments).

Table 1 contains the mobilities determined in solutions of pH 2-4, where no polynuclear hydrolysed species or precipitate of thorium oxide/hydroxide are formed at $\leq 10^{-5}$ M thorium concentration (Neck and Kim 2001). The data represent the mean mobility $_{+}u$ or $_{-}u$ of all thorium species present in solution:

$$_{+(-)}u = \Sigma \ _{+(-)}u_i \cdot \delta_i \tag{1}$$

Here u_i and δ_i are the mobility and abundance of species i, respectively.

The data obtained in the absence of humic acid characterize the mobility of dissolved inorganic thorium species. As can be seen such species migrate predominantly to cathode. Their mobility towards anode is small and, with the exception of a few results (only for carrier-free ^{234}Th), it may be within a background mobility caused by experimental errors ($0 \pm 0.30 \times 10^{-4}$ $cm^2s^{-1}V^{-1}$, Benes 2005). The positive mobility decreases with increasing pH and with decreasing concentration of thorium, mainly due to the progressive hydrolysis of thorium and formation of pseudocolloids (at $\leq 10^{-6}$ M Th concentration) by adsorption of $Th(OH)_n^{(4-n)+}$ cations (n = 0 - 3) on colloidal impurities ever present in solution. Existence of pseudocolloids can explain the negative mobilities found and the dependence of $_{+}u$ on the concentration of thorium: abundance of pseudocolloids is known to decrease with increasing metal concentration and their predominantly negative charge can be reversed by adsorption of polyvalent ions (Benes and Majer 1980).

Addition of humic acid brings about decrease in $_{+}u$ and increase in $_{-}u$ of thorium that depend on the concentration of humic acid and thorium. The changes are due to the formation of negatively charged or neutral ThHA complexes (no indication of positively charged complexes has been obtained) and can be used for calculation of the abundance and mobility of the complexes. If no other forms of thorium than $Th(OH)_n^{(4-n)+}$ (n = 0 - 4) and ThHA are present, abundance of ThHA can be calculated as

$$\%ThHA = 100 \ \delta_{ThHA} = 100 \ (1 - _{+}u \ / \ _{+}u_{\ Th(0H)}) \tag{2}$$

where $_+u_{Th(OH)}$ is the mean mobility of $Th(OH)_n^{(4-n)+}$ measured under the same conditions (ionic strength and pH). It has been shown recently that $_+u_{Th(OH)}$ can be well represented by the $_+u$ values determined for 10^{-5} M Th in the absence of humic acid (Benes 2005, the bold figures in Table 1). Other data of Table 1 are not suitable for this purpose as they are affected by the presence of pseudocolloids, whose ratio to the dissolved inorganic thorium species can change upon the addition of humic acid.

Table 1. Electrophoretic mobility of thorium (in 10^{-4} cm^{2}s^{-1}V^{-1}) in solutions of 0.01M (HClO$_4$ + NaClO$_4$) as a function of pH and initial concentration of thorium [Th] and Aldrich humic acid [HA].

Mobility	[Th], M[a]	[HA], mg/l	pH 2	pH 3	pH 4
$_+u$	c.f.	0	0.59±0.15	0.69±0.28	0.36±0.22
$_+u$	c.f.	0.1	0.19±0.07	0.23±0.16	0.11±0.10
$_+u$	c.f.	1.0	0.14±0.07	0.17±0.08	0.10±0.04
$_+u$	c.f.	10	0.12±0.05	0.12±0.07	0.09±0.03
$_+u$	1×10^{-7}	0	2.52±0.20	0.69±0.07	0.39±0.01
$_+u$	1×10^{-7}	0.1	2.08±0.42	0.28±0.17	0.19±0.05
$_+u$	1×10^{-7}	1.0	0.36±0.09	0.30±0.13	0.19±0.07
$_+u$	1×10^{-7}	10	0.29±0.13	0.14±0.07	0.13±0.01
$_+u$	1×10^{-6}	0	4.19±0.01	1.62±0.22	0.86±0.04
$_+u$	1×10^{-6}	10	0.10±0.15	0.10±0.04	0.07±0.06
$_+u$	1×10^{-5}	0	**4.52±0.07**	**3.93±0.27**	**2.57±0.05**
$_+u$	1×10^{-5}	10	2.05±0.08	0.42±0.02	0.07±0.03
$_-u$	c.f.	0	0.42±0.23	0.58±0.13	0.53±0.09
$_-u$	c.f.	0.1	0.54±0.13	1.65±0.27	1.58±0.20
$_-u$	c.f.	1.0	1.61±0.33	1.96±0.17	2.12±0.17
$_-u$	c.f.	10	1.98±0.30	3.00±0.23	2.95±0.20
$_-u$	1×10^{-7}	0	0.15±0.12	0.29±0.03	0.15±0.05
$_-u$	1×10^{-7}	0.1	0.21±0.13	1.25±0.08	2.04±0.09
$_-u$	1×10^{-7}	1.0	1.25±0.10	2.25±0.15	2.21±0.18
$_-u$	1×10^{-7}	10	1.78±0.27	2.98±0.08	2.80±0.19
$_-u$	1×10^{-6}	0	0.11±0.03	0.05±0.05	0.16±0.07
$_-u$	1×10^{-6}	10	1.25±0.26	1.77±0.04	2.64±0.13
$_-u$	1×10^{-5}	0	0.13±0.13	0.17±0.05	0.25±0.02
$_-u$	1×10^{-5}	10	0.47±0.12	0.49±0.07	0.66±0.31

[a] c.f. denotes that carrier free ^{234}Th was used. Total thorium concentration was probably lower than 10^{-9} M in this case.

Results of the calculation are shown in Table 2 and represent means of values *%ThHA* obtained by combination of all measured values of $_+u$ and $_+u_{Th(OH)}$ for the given conditions. Limits attached are the ranges of variability of the values. The data clearly indicate that thorium is extensively complexed even at very low concentrations of humic acid and low pH values. The abundance *%ThHA* little depends on pH and [HA] except for conditions when the concentration of thorium approaches saturation of the complexing capacity of humic acid present in solution. Practically complete complexation is observed at 10 mg/L HA for 10^{-6} M Th and also at pH 4 for 10^{-5} M Th. *%ThHA* values for the lower thorium concentrations are lower. This can be explained by a higher formation of pseudocolloids or, more probably, by error in determination of $_+u$ (Benes 2005). Most of the mobilities $_+u$ used in the calculation of *%ThHA* lay within the possible backround range $(0 – 0.30 \times 10^{-4}$ cm^{2}s^{-1}V$^{-1})$.

Of special interest is the saturation of complexing capacity of humic acid with thorium, indicated by the data in Table 2 for $10^{-7}(10^{-5})$ M Th and 0.1(10) mg/L HA. The general complexation capacity of humic acid can be expressed using concentration of humic acid ([HA], in mg/L), its proton exchange capacity (PEC, in mol/kg) and the degree of dissociation of complexing (here carboxyl) sites of the acid (α), determined by acidobasic titration of the acid:

$$CC_{HA} = 10^{-6} \text{ [HA]. PEC. } \alpha \tag{3}$$

In Table 3, complexing capacities calculated using Eq. (3) and data on PEC and α taken from Mizera et al. (2003) are compared with the concentrations of ThHA, calculated from [Th] and *%ThHA* values given in Table 2. As can be seen, concentrations of ThHA formed in the solution exceed complexation capacities of humic acid for bonding of monovalent cations, represented by the concentration of available dissociated sites (COO$^-$) of the acid. The effect increases with decreasing pH. Considering that thorium cations participating in the complexation under studied conditions carry higher charge than 1 (up to 4+), the exceeding of CC_{HA} is still more pronounced and means that either the complexation proceeds at least partially by displacement of H$^+$ from non-dissociated COOH groups of humic acid or positively charged ThHA complexes are formed. The latter possibility is not supported by the data on the negative mobility of ThHA complexes (see below).

Assuming that no other negatively charged form of thorium is present in solution the mean mobility of ThHA complexes is equal to
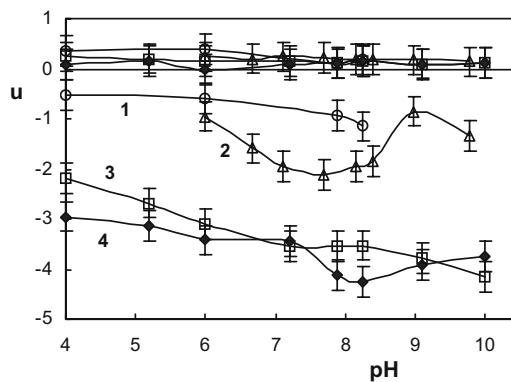
$$_-u_{ThHA} = {_-u} / \delta_{ThHA}. \tag{4}$$

Mobilities calculated from Eq. (4) and data taken from Tables 1 and 2 are shown in Table 4, together with the ranges of their variability calculated from the corresponding variabilities of the values of $_-u$ and *%ThHA* used. No background mobilities ($_-u$ found in absence of HA) were subtracted in the calculation.

Data in Table 4 show the tendency of $_-u_{ThHA}$ to increase with pH and to decrease with increasing [Th]/[HA] ratio. The first effect is due to the increase in dissociation of COOH groups of humic acid with increasing pH and was not found

in solutions of 10^{-5} M thorium, where precipitation of thorium humate was observed at all pH values. The effect of [Th]/[HA] ratio on u_{ThHA} in $10^{-7} – 10^{-6}$ M Th solutions can be at least partially explained by the neutralization of negative charge of humic acid molecules with thorium cations bound in ThHA complex. Detailed analysis of the effects is in progress.

At pH values larger than 4, electrophoretic mobilities were determined only for carrier-free ^{234}Th, in order to avoid precipitation of thorium hydroxide (Neck and Kim 2001). The effects of pH, concentration of humic acid and addition of 0.001 M NaHCO$_3$ were studied. Results are shown in Fig.1, the error bars represent the maximum probable error ($\pm 0.30 \times 10^{-4}$ cm^{2}s^{-1}V^{-1}).

Fig. 1. Electrophoretic mobility of carrier-free ^{234}Th (in 10^{-4} cm^{2}s^{-1}V^{-1}) as a function of pH and composition of solution: **1** – 0.01 M NaClO$_4$ + NaOH or NH$_4$OH, **2** – as in **1** + 0.001 M NaHCO$_3$, **3** – as in **1** + 1 mg/L humic acid, **4** – as in **1** + 10 mg/L humic acid.

Table 2. Abundances of ThHA complexes (*%ThHA*) calculated using Eq.(2) and data of Table 1 as a function of pH and initial concentration of thorium [Th] and Aldrich humic acid [HA].

[Th], M[a]	[HA], mg/L	pH 2	pH 3	pH 4
c.f.	0.1	95.6±0.3	93.8±4.5	95.6±4.0
c.f.	1.0	96.8±1.6	95.5±2.3	96.1±1.6
c.f.	10.0	97.3±1.2	96.8±2.0	96.6±1.4
1×10^{-7}	0.1	69.4±4.2	92.4±5.0	92.4±1.9
1×10^{-7}	1.0	92.0±2.1	92.1±3.9	91.8±3.6
1×10^{-7}	10.0	93.6±3.0	96.1±2.1	94.9±0.1
1×10^{-6}	10.0	99.4±0.6	97.4±1.2	97.2±2.4
1×10^{-5}	10.0	54.6±2.5	89.4±1.1	97.3±1.2

[a] c.f. denotes that carrier free 234Th was used.

It can be seen that thorium migrates at pH > 4 predominantly to anode, its positive mobility is generally within background values. The negative mobility in the absence of added carbonates and humic acid is due to formation of pseudocolloids and/or carbonate complexes (absorption of CO_2 from the air). Addition of carbonates brings about increase of the mobility in the range of pH 6-8.5 where $Th(OH)_3CO_3^-$ and $Th(OH)_2(CO_3)_2^{2-}$ ions are formed (Altmaier et al. 2005). The high negative migration in solutions containing humic acid reflects predominance of negatively charged humates, whose mobility increases with pH up to about pH 8. This increase is caused by the increasing dissociation of COOH groups of the humic acid (up to pH 6, Mizera et al. 2003) and decreasing neutralization of negative charge of humic acid as the average positive charge of thorium hydroxocomplexes decreases with pH (up to pH 8, Neck and Kim 2001). The differences between the mobility at different concentrations of humic acid are due either to different abundance of the humic complexes or to different neutralization of the charge.

The difference between the mobility of thorium in solutions containing carbonates and humic acid can be used for determination of proportion of carbonate and humate complexes of thorium in waters containing both the ligands.

Preliminary experiments have shown that humate complexes predominate at pH 8-9 and $\geq$ 1 mg/L Aldrich humic acid even in solutions 0.001 M in HCO_3^-. Further study of thorium complexation with free-liquid electrophoresis is in progress.

Table 3. Comparison of complexation capacities CC_{HA} and [ThHA] concentrations (both in mol/L) in solutions of 0.01M ($HClO_4$ + $NaClO_4$) containing 10^{-7} M Th + 0.1 mg/L HA or 10^{-5} M Th + 10 mg/L HA.

Compared values	pH 2	pH 3	pH 4
[ThHA] $\times 10^7$	0.694	0.924	0.924
[ThHA] $\times 10^5$	0.546	0.894	0.973
$CC_{HA} \times 10^7$ or 10^5	0.14	0.84	2.17

Table 4. Electrophoretic mobilities of ThHA complexes ($\_u_{ThHA}$, in 10^{-4} cm²s⁻¹V⁻¹) in solutions of 0.01M ($HClO_4$ + $NaClO_4$) calculated using Eq.(4) and data of Tables 1 and 2 as a function of pH and initial concentration of thorium [Th] and Aldrich humic acid [HA].

[Th], Mᵃ	[HA], mg/l	pH 2	pH 3	pH 4
c.f.	0.1	0.57±0.15	1.78±0.37	1.66±0.27
c.f.	1.0	1.67±0.37	2.06±0.23	2.21±0.22
c.f.	10.0	2.04±0.33	3.11±0.30	3.06±0.26
1×10^{-7}	0.1	0.31±0.20	1.36±0.16	2.21±0.14
1×10^{-7}	1.0	1.36±0.14	2.45±0.27	2.42±0.29
1×10^{-7}	10.0	1.91±0.35	3.11±0.16	2.96±0.22
1×10^{-6}	10.0	1.26±0.27	1.83±0.07	2.72±0.20
1×10^{-5}	10.0	0.87±0.26	0.55±0.08	0.69±0.34

ᵃ c.f. denotes that carrier free 234Th was used.

Acknowledgement

References

Altmaier M, Neck V, Mueller R, Fanghaenel Th (2005) Solubility of ThO2·xH2O (am) in carbonate solution and the formation of ternary Th(IV) hydroxide-carbonate complexes. Radiochim. Acta 93: 83-92

Benes P, Majer V (1980) Trace Chemistry of Aqueous Solutions. Elsevier, Amsterdam, 43,110

Benes P (2005) Use of free-liquid electrophoresis for analysis of thorium complexation with humic acids. In: Buckau G (Ed) Humic Substances in Performance Assessment of Nuclear Waste Disposal: Actinide and Iodine Migration in the Far-Field. Report FZKA 7070, Research Center Karlsruhe, 125-141

Kim JI, Marquardt CM (1999) Chemical reaction of Np(V) with humic colloids in groundwater: influence of purification on the complexation behaviour. Radiochim Acta 87: 105-108

Miekeley N, Kuechler IL (1987) Interactions between thorium and humic compounds in surface waters. Inorg Chim Acta 140: 315-319

Mizera J, Benes P, Masnerova G (2003) Electrophoretic determination of the degree of Eu complexation by humic acid: analysis and assessment of experimental error. In: Buckau G (Ed) Humic Substances in Performance Assessment of Nuclear Waste Disposal: Actinide and Iodine Migration in the Far-Field. Report FZKA 6800, Research Center Karlsruhe, 191-202

Neck V, Kim JI (2001) Solubility and hydrolysis of tetravalent actinides. Radiochim. Acta 89: 1-16

Reiller P, Moulin V, Casanova F, Dautel Ch (2003) On the study of Th(IV)-humic acid interactions by competition sorption studies with silica and determination of global interaction constants. Radiochim Acta 91: 513-524

Reiller P (2005) Prognosticating the humic complexation for redox sensitive actinides through analogy, using the charge neutralization model. Radiochim. Acta 93: 43-55

Wahlgren MA, Orlandini KA (1982) Comparison of the geochemical behaviour of plutonium, thorium and uranium in selected North American lakes. In: Environmental Migration of Long-Lived Radionuclides, IAEA Vienna, 757-774

Zeh P, Kim JI, Buckau G (1995) Aquatic colloids composed of humic substances. In: Binding Models Concerning Natural Organic Substances in Performance Assessment. Proceedings of NEA Workshop, OECD NEA, 81-90

Field Portable and Autonomous Immunosensors for the Detection of Environmental Contaminants

Diane A. Blake[1], Haini Yu[1], Elizabeth A. James[1], Xia Li[1], Robert C. Blake[2]

[1]Department of Biochemistry, Tulane University Health Sciences Center, 1430 Tulane Avenue SL-43, New Orleans, LA, 70112, USA, E-mail: blake@tulane.edu
[2]School of Pharmacy, Xavier University of Louisiana, 1 Drexel Drive, New Orleans, LA 70125, USA

Abstract. A monoclonal antibody that binds with high affinity to UO22+ complexed with the chelator 2,9-dicarboxyl-1,10-phenanthroline was used to develop a sensor-based assay for UO22+. The assay range for UO22+ was 0.5 to 25 nM (0.12 to 6 ppb). The average coefficients of variation in the assay was 2.2%. The immunoassay results were comparable to those obtained using the Kinetic Phosphorescence Assay. The versatility of this sensor platform was further demonstrated by the development of an immunoassay for caffeine.

Introduction

Antibody-based techniques are alternative approaches for environmental analyses. These approaches are attractive to local and governmental agencies because they have significant advantages over the traditional analytical methods. Immunoassays are remarkably quick, reasonably portable to the analysis site, and simple to perform. Because most of the technology of an immunoassay is "built" into the antibody that is at the core of this detection system, sample pretreatment is usually minimal and the instrumentation designed to transduce the antibody binding event to a measurable signal can be relatively small and inexpensive. The immunoassay and instrument can also be formatted for high throughput analysis. In addition, studies have shown that the use of immunoassays during remediation processes can reduce analysis costs by 50% or more (Szurdoki et al. 1996). Although most environmental immunoassays are directed toward complex organic chemicals, (Giraudi and Baggiani 1994; Van Emon et al. 1998; Abad et al. 1999) this technique is theoretically applicable to any analyte, including a metal ion, if a suitable antibody can be generated.

In this study, we describe a new approach for uranium analysis, based on an immunosensor and an antibody with specificity for chelated UO_2^{2+} (Blake et al 2004). The immunosensor described herein is a flow fluorimeter with broad applications for the assay of low molecular weight analytes. In the present study, we show how this sensor can be employed to measure two different environmentally relevant analytes, UO_2^{2+} and caffeine.

Methods

The uranium-selective chelator 2,9-dicarboxyl-1,10-phenanthroline (DCP) was obtained from Alfa Aesar (Ward Hill, MA). A Cy5-labeled Fab fragment of goat anti-mouse IgG was a product of Jackson ImmunoResearch Laboratories (West Grove, PA). Poly(methylmethacrylate) and azlactone beads (98 ± 8 μm diameter) were obtained from Sapidyne Instruments Inc (Boise, ID). A UO_2^{2+} standard was obtained from the National Institute of Standards and Technology (Gaithersburg, MD). The 12F6 monoclonal antibody, which binds to UO_2^{2+}- DCP complexes, and UO_2^{2+}-DCP-BSA conjugate were available from a previous study (Blake et al. 2004). Reaction mixtures for UO_2^{2+} were prepared in HBS buffer (137 mM NaCl, 3 mM KCl, 10 mM HEPES, pH 7.4). The inline immunosensor timing files used for the analysis were described in detail in (Yu et al. 2005).

A sensor assay for caffeine was also developed using commercially available reagents. A caffeine-bovine serum albumin conjugate (caffeine-BSA) and a monoclonal antibody to caffeine were obtained from YJ BioProducts (Rancho Cordova, CA). Additional monoclonal antibodies to caffeine (clones 9410, 8.F.28, and 1.BB.877) were obtained from Biodesign (Saco, ME) and U.S. Biologicals (Swampscott, MA). A standard solution of caffeine (1 mg/ml) was purchased from Sigma-Aldrich (St. Louis, MO). Equilibrium dissociation constants for the interaction of these antibodies with caffeine were determined as described by (Blake and Blake 2003) in PBS (137 mM NaCl, 3 mM KCl, 10 mM phosphate, pH 7.4).
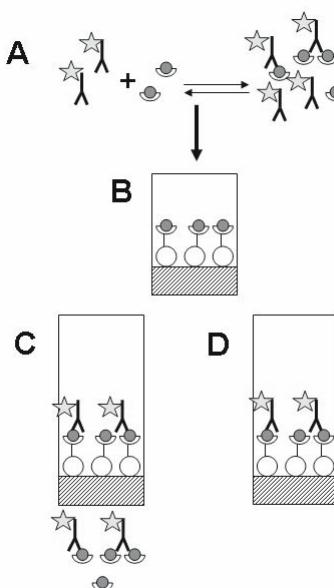
Results

Immunosensor-based assay for uranium

The method employed for the analysis UO_2^{2+} is diagrammed in Fig. 1. The sensor consisted of a capillary flow/observation cell containing microbeads coated with an immobilized version of the metal-chelate complex. The fluorescently labeled antibody was mixed with soluble metal-chelate complex derived from the environmental sample, and the assay components were allowed to come to equilibrium. This mixture was then passed rapidly through the observation cell. Only those antibody molecules with unoccupied binding sites were available to bind to
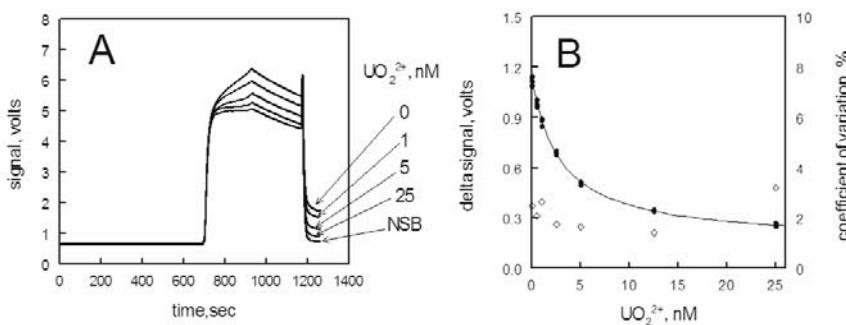
the immobilized ligand on the surface of the beads; antibodies whose binding sites were already occupied with ligand were not. An LED was used to excite the fluorescently labeled antibody bound to the microbeads and a photodiode measured the amount of fluorescence emanating from the observation cell. The amount of antibody bound to the microbeads was inversely proportional to the amount of metal-chelate complex in the sample, because the binding of the antibody to the complex reduced the free antibody concentration in a dose-dependent fashion.

Primary data for the analysis of UO22+ by a prototype in-line immunosensor that had the ability to autonomously prepare and run a standard curve from reagents stocks is shown in Fig 2A. For clarity, not all instrument traces are shown. The period between 0 and 700 seconds in the trace represents the time of automated reagent mixing, the period between 700-1120 seconds corresponds to the application of the reaction mixture to the microcolumn/observation cell, and the period between 1120 and 1260 seconds represents a buffer wash that removed unbound antibody from the microbead column. Individual instrument traces for assay mixtures containing 0, 1, 5, and 25 nM UO_2^{2+} are shown, as is a control for

Fig. 1. A. Fluorescently labeled antibody (**Y★**) is mixed with environmental sample containing the analyte (the metal-chelate complex) and the mixture is allowed to come to equilibrium. **B.** The equilibrated sample is passed rapidly through an observation cell that contains an immobilized version of the metal-chelate complex. **C.** Antibodies whose binding sites are already occupied with the metal-chelate complex are not retained by the column. **D**. After a buffer wash, only those antibodies with open binding sites contribute to the final signal, which is inversely proportional to the amount of metal-chelate complex in the environmental sample.

non-specific binding (NSB) in reaction mixture that omitted the uranium-specific 12F6 antibody. The instrument automatically calculated the response to varying concentrations of uranium by subtracting a baseline reading from the reading after the unbound antibody had been washed from the column (the average instrument response from 1250-1255 seconds minus the average instrument response during the first 5-10 seconds of the trace). This instrument response (delta signal) was plotted versus UO_2^{2+} concentration to generate the uranium dose-response curve shown in Fig. 2B. For this demonstration, the instrument responses generated by 3 replicate analyses of each UO_2^{2+} concentration were plotted as individual points. The coefficients of variation in this experiment ranged from 1.4 to 3.9%. This assay accurately measured UO_2^{2+} at concentrations from 0.5 to 25 nM (0.12 to 6 ppb) and the results were comparable to KPA assays run at the same time (data not shown). The drinking water limit for uranium set by the United States Environmental Protection Agency is 30 ppb (US EPA 2000). Thus, this sensor-based assay has sufficient sensitivity to monitor UO_2^{2+} at environmentally relevant concentrations.

Fig. 2. A, Individual instrumental traces when 12F6 monoclonal antibody (0.33 nM), Cy5-Fab fragment of goat anti-mouse IgG (6.5 nM), DCP (100 nM), bovine serum albumin (12.5 μg/ml) and varying concentrations of UO_2^{2+} (as indicated) were mixed by the immunosensor and applied to a microcolumn of beads containing immobilized UO_2^{2+}-DCP. NSB reaction mixture contained Cy5-Fab fragment (6.5 nM), DCP (100 nM), and bovine serum albumin (12.5 μg/ml). **B,** (●) Instrument response (delta signal) plotted versus UO_2^{2+} concentration. Triplicates were run at each UO_2^{2+} concentration; the data are plotted as individual points. (◇), Coefficient of variation (% CV) at various UO_2^{2+} concentrations.

Table 1. Binding affinities of commercially available antibodies for caffeine.

Vendor	Clone Number	K_d, nM[a]
YJ BioProducts	not applicable	1.21
Biodesign International	9401	0.89
United States Biological	1.BB.877	1.20
United States Biological	8.F.28	1.47

[a] Equilibrium dissociation constants were determined using KinExA 3000[TM] as described in (Blake and Blake, 2003; Blake et al. 1999) using poly(methylmethacrylate) microbeads adsorption-coated with a caffeine-bovine serum albumin conjugate.

Immunosensor-based assay for caffeine

The handheld and autonomous immunosensors under development in our laboratory have sufficient flexibility to accommodate the analysis of a wide variety of analytes. An example of this functionality is an immunosensor-based assay for caffeine that utilized commercially available reagents. Assays for caffeine are relevant in environmental monitoring and for quality control in the food industry.

The method of analysis employed by the handheld and in-line sensors under development in our laboratories (as outlined in Fig. 1) makes it relatively straightforward to develop new applications. Antibodies must be identified that bind to the analyte at a relevant concentration range, and a microbead column must be developed that contains an immobilized version of the analyte. Once these reagents have been identified, the software associated with these sensors can be easily modified to accommodate the requirements of specific antibodies and/or analytes. Four different commercially available antibodies to caffeine were evaluated for use in this assay, as shown in Table 1.

In our experience, the immunosensors under development in our laboratories have the ability to detect analyte concentrations that are $\geq 10\%$ of the K_d value, so

any of the four antibodies surveyed in Table 1 could theoretically provide sufficient sensitivity for analysis of environmental water samples.

Another important variable in the development of immunoassays for environmental analyses is the effect of sample matrix on the immunoassay. In this model study for caffeine, we evaluated the ability of the four commercially available monoclonal antibodies to correctly measure caffeine levels in Diet Coke[TM]. Spike and recovery data for two of these antibodies are given in Table 2, below. It is clear that the 2 antibodies tested are influenced to different extents by other components in the Diet Coke[TM] sample. For this particular application, antibody 1.BB.877 appears most suitable for subsequent assay development.

Discussion

A practical focus of our laboratories is the development of both autonomous, in-line and portable, hand-held immunosensors that operate on the same principle as that of a commercial flow fluorimeter designed to study antibody-antigen binding interactions (Blake and Blake, 2003). The experiments summarized above represent preliminary data collected to illustrate the versatility of the immunosensor devices currently under development in our laboratories. Perhaps the most challenging analyte for any immunoassay is a heavy metal ion such as UO_2^{2+}. Since the uranyl ion is not sufficiently large to elicit an immune response by itself, it must be tightly complexed with a larger molecule, in this case a uranium chelator covalently conjugated to a protein, in order to be rendered as a target for the im-

Table 2. Spike and recovery data for caffeine in Diet Coke[TM] using 2 different monoclonal antibodies[a]

1.BB.877			YJ BioProducts		
Added (nM)	Found (nM)	% Recovery	Added (nM)	Found (nM)	% Recovery
0.1	.0788	79.9	0.2	0.29	145.3
0.3	0.326	108.7	0.6	0.096	160.8
0.6	0.750	121.8	1.0	1.43	143.5
1	1.073	107.3	4	5.34	133.4
5	5.825	116.5	8	9.63	120.4
10	12.628	126.3	50	71.61	143.2
Average		110.1	Average		141.1

[a]Standard curves for caffeine were constructed as described for the uranium immunoassay, using a commercially available caffeine standard. The caffeine in Diet Coke[TM] samples (www2.coca-cola.com/mail/goodanswer/soft_drink_nutrition.pdf) was diluted into PBS to the indicated concentrations, and the delta signal was used to determine caffeine concentration from the standard curve.

Analytical speciation techniques for uranium and related elements

mune response. Thus any immunoassay for chelated UO_2^{2+} must include at least one additional equilibrium between the metal ion and the chelator in addition to the necessary antibody-antigen recognition event. The highly precise and reproducible antigen inhibition data shown for UO_2^{2+} in Fig. 2B indicates that the autonomous in-line sensor is quite capable of identifying and quantifying UO_2^{2+} in a mixture of antibody and antigen where the 'antigen' is itself the product of an independent metal-chelator binding equilibrium.

The preliminary data developed with caffeine and antibodies directed against caffeine illustrate that the same device and assay principles can just as readily be applied to identify and quantify a simple organic contaminant. A prototype immunoassay for caffeine is more than a simple model chosen to contrast with the more complex immunoanalysis of UO_2^{2+}. Caffeine is one of the more abundant contaminants in surface waters in the United States and Europe (Kolpin et al, 2002; Weigel et al, 2002). The only source of caffeine in the environment is man, and caffeine has been proposed as a chemical surrogate for fecal coliform bacteria of human origin (Standley et al, 2000; Glassmeyer et al, 2003). In the United States, caffeine concentrations in surface waters ranged from non-detect to 31 nM (6 ppb) with a median value of approximately 0.5 nM (0.1 ppb) (Kolpin et al, 2002).

Regardless of the identity of the analyte or the existence of multiple equilibria in the formation of the actual antigen recognized by the antibody, it is important to realize and acknowledge that the performance characteristics of any immunoassay depends on the binding properties of the antibody. Given an acceptable level of reproducibility and uniformity in reagent preparation and handling, it is evident that the sensitivity and precision of an antibody-based assay is critically dependent on the thermodynamics and kinetics of the antibody-antigen binding interaction. The sensitivity and limit of detection of any immunoassay, regardless of format, depends primarily upon the affinity of the antibody for the environmental contaminant; the tighter the binding, the more sensitive the final assay. Similarly, the precision of any immunoassay that is designed to provide a rapid response depends upon the rate of binding between the antibody and the antigen. Most immunosensor formats include an initial incubation step, where a limiting quantity of the antibody is exposed to a molar excess of the analyte, prior to signal generation. If the binding reaction between the antibody and the analyte is not very close to or at equilibrium before the next step in the assay is executed, then the duration of the incubation step must be precisely and reproducibly controlled or the overall precision of the assay will suffer.

When the concentration of the analyte is in a 4-fold or greater molar excess to that of the antibody, the bimolecular association of the limiting antibody with the excess antigen is approximately a first order process (pseudo-first order kinetics), and the approach to the binding equilibrium can be described as a single exponential function of time. The apparent rate constant, k, for this exponential function of time is approximately equal to k_{on}[analyte]+k_{off}, where k_{on} and k_{off} are the association and dissociation rate constants, respectively, for the reversible binding reaction (Moore and Pearson, 1981). The rate equation can be manipulated to determine the half-life of the binding reaction: $t_{1/2}$= ln 2/k (Moore and Pearson,

1981) and this $t_{1/2}$ value can then be used to estimate whether a binding reaction is close to equilibrium. As a practical example, the k_{on} and k_{off} for the association and dissociation of the 12Fb antibody and UO_2^{2+}-DCP complex used in this study are 2.0 x 10^7 M^{-1} s^{-1}, and 1.8 x 10^{-2} s^{-1}, respectively (Blake et al, 2004). The $t_{1/2}$ at the lowest analyte concentration in the uranium standard curve (0.5 x 10^{-9} M) can be calculated to be 24.75 s by substitution into the equations above. After 5 half-lives, the binding reaction has achieved 96.875% of its equilibrium value. Therefore, this particular antibody-analyte binding reaction has essentially achieved equilibrium in 5 x 24.75 s, or 2 minutes.

For highly sensitive assays where the k_{on}[analyte] term is very small because [analyte] is a vanishingly small number, the term that defines both k and the $t_{1/2}$ is the dissociation rate constant. Any highly sensitive immunoassay (measurements at the picomolar level or below) will require a very high affinity antibody, and this antibody must necessarily have a slow dissociation rate constant. Consequently, there will always be a practical trade-off between sensitivity and rapidity in any immunoassay; the greater the desired sensitivity, the longer one must wait to achieve effective equilibrium in the initial binding reaction.

Acknowledgements

References

Abad A et al. (1999) Determination of carbaryl, carbofuran and methiocarb in cucumbers and strawberries by monoclonal enzyme immunoassays and high-performance liquid chromatography with fluorescence detection. An analytical comparison., J. Chromatog. A. 833: 3-12.

Blake RC 2nd, Blake DA (2003) Kinetic exclusion assay to study high-affinity binding interactions in homogeneous solutions in *Methods in Molecular Biology: Antibody Engineering - Methods and Protocols* (Lo, B. K. C., ed) pp. 417-430, Humana Press, Towata, NJ.

Blake RC 2nd et al. (2004) Novel monoclonal antibodies with specificity for chelated uranium(VI): isolation and binding properties. Bioconjugate Chemistry. 15: 1125-1136.

Giraudi G, Baggiani C (1994) Immunochemical methods for environmental monitoring, Nucl. Med. Biol. 21: 557-572.

Glassmeyer, SI et al. (2003) Transport of chemical and microbiological contaminants from known wastewater discharges: Potential chemical indicators of human fecal contami-

nation. Presented at U.S. EPA's Research on Microorganisms in Drinking Water Workshop, Cincinnati, OH, August 5-7.

Kolpin DW et al. (2002) Pharmaceuticals, hormones, and other organic wastewater contaminants in U.S. streams, 1999-2000: a national reconnaissance. Environmental Science & Technology. 36:1202-1211.

Moore JW and Pearson RG (1981) *Kinetics and Mechanism*, John Wiley and Sons, Inc., New York, pp 60-70.

Standley, LG et al. (2000) Molecular traces of organic matter sources to surface water resources. Environ. Sci. Technol. 34:3124-3130.

Szurdoki F et al. (1996) Rapid assays for environmental and biological monitoring, J. Environ. Sci. & Health - Part B: Pesticides, Food Contaminants, & Agricultural Wastes. 31: 451-458.

U. S. Environmental Protection Agency (2000) National Primary Drinking Water Regulations: Radionuclides; Final Rule, *Fed. Reg.* Vol. 65, No. 236, Washington D. C. pp 76707-76814.

Van Emon JM et al. (1998) Bioseparation and bioanalytical techniques in environmental monitoring. J. Chromatog. B, Biomedical Sciences & Applications. 715:211-228.

Weigel S, Kuhlmann J, and Huhnerfuss H (2002) Drugs and personal care products as ubiquitous pollutants: occurrence and distribution of clofibric acid, caffeine and DEET in the North Sea, Science of the Total Environment. 295:131-141.

Yu H, Jones RM, Blake DA (2005) An immunosensor for autonomous in-line detection of heavy metals: validation for hexavalent uranium. Int. J. Env. Anal. Chem., in press.

A method to measure arsenic readily released to pore waters from uranium mill tailings

John Mahoney[1], Donald Langmuir[2], John Rowson[3]

[1]Hydrologic Consultants, Inc., 143 Union Blvd., Suite 525, Lakewood, Colorado,
E-mail: jmahoney@hcico.com
[2]Hydrochem Systems Corp., Denver, Colorado
[3]COGEMA Resources, Inc., PO Box 9204, Saskatoon, SK, Canada

Abstract. A method to quantify the amount of readily released arsenic in uranium mill tailings was developed using a technique known as <u>E</u>quilibrium <u>P</u>artitioning <u>I</u>n <u>C</u>losed <u>S</u>ystems (EPICS). The method employs a gentle leaching solution that, except for its arsenic (As) concentration, is identical to the neutralized raffinate that contacts the tailings. Prior to implementation, the experimental design and mathematical approach were verified in geochemical models using PHREEQC. Laboratory experiments using tailings from the Athabasca Basin of Northern Saskatchewan demonstrated that As that could be readily released to pore waters is about 0.2 % of the total As in the tailings.

Introduction

Predicting the mobility of contaminants such as arsenic (As) in ground water has become increasingly important as risk assessment plays a greater role in the licensing of waste disposal facilities. In the Athabasca Basin of northern Saskatchewan, elevated concentrations of As in uranium ore (up to 10% by weight) have required that studies be conducted to assist in designing methods to reduce pore water concentrations of As in the neutralized tailings that are disposed in a tailings management facility (TMF).

At the JEB mill at McClean Lake, uranium is extracted from the ore using sulfuric acid. The leach residue from the ore consists chiefly of unreacted quartz and illite, with lesser amounts of kaolinite and chlorite. After uranium extraction, the leach residue solids are mixed with the barren leach solution (raffinate), which commonly has a pH below 2.0. To reduce dissolved As concentrations, which often reach 700 mg/L in the acid raffinate, the raffinate has its molar Fe/As ratio in-

creased to 3/1, if necessary, by the addition of ferric sulfate (Langmuir et al. 1999). The raffinate and leach residue slurry is then neutralized by lime addition to pH 4 and subsequently to pH 7-8. After neutralization, concentrations of As in slurry pore waters from the mill are typically less than 1 mg/L. Precipitated phases that contain important amounts of As include the arsenate mineral scorodite ($FeAsO_4 \cdot 2H_2O$) in a poorly crystalline matrix, a possible oxyhydroxide coprecipitate with a variable Fe/As ratio, and As that may be surface precipitated or adsorbed onto ferrihydrite and other mineral surfaces. Solids in the neutralized tailings are typically comprised of 50-70% leach residue minerals with the remainder as precipitated solids. The slurry is pumped into the JEB TMF for disposal using subaqueous emplacement. Underdrains allow for removal of pore water expelled by settling and compaction in the TMF. The pore water is pumped to a water treatment facility. Canadian regulatory agencies have expressed concern that significant concentrations of adsorbed As might be released over time from the tailings. This study was performed to determine the amount of readily releasable As.

EPICS method and model

Fuller et al. (1988) and Darland and Inskeep (1997) among others, suggest that readily desorbable As is a small fraction of total adsorbed As, and that most adsorbed As is strongly bound to mineral surfaces. In our study, readily desorbed As has been measured using a method that involves the successive addition, to the neutralized raffinate and tailings, of aliquots of the same raffinate, but free of As, and measuring the As released to solution following each addition. This method is less aggressive than others (c.f. Shiowatawa et al. 2003, Kim et al. 2003), and avoids dissolution of amorphous arsenate phases. In this study it is assumed that desorbable As does not include As from dissolution of arsenate minerals, Fe/As oxyhydroxides precipitates or surface precipitates.

Mathematical derivation

To quantify the readily desorbable As in the tailings, a series of laboratory measurements were performed using a procedure based upon a methodology described by Gossett (1987), which he called Equilibrium Partitioning in a Closed System (EPICS). Conceptually, the method is simple. By changing the liquid to solid ratio in a slurry, while keeping the amount of desorbable As plus dissolved As and the mass of solids constant, the amount of desorbable As can be calculated based upon changes in the dissolved As concentration.

   The following example explains the method. A sample of 1 L of solution with a concentration of 1.0 mg/L of dissolved As is diluted to 2 L. The As concentration is thus reduced to 0.5 mg/L. If releasable As is available to the solution, some of it will be released and As concentrations will exceed 0.5 mg/L. When the system undergoes further dilution, As concentrations will not decrease in accordance with

a simple dilution process, but rather additional releasable As will transfer from the solids to the solution. As infinite dilution is approached, the amount of potentially releasable As approaches zero. All of the As is in solution but, the concentration becomes too low to measure. In this study we extrapolate from measured As concentrations to calculate the releasable amount.

In the neutralized tailings slurry, the precipitated forms of As, which are defined as $As_{(ppt\_form)}$, include arsenate minerals such as scorodite, Fe/As oxyhydroxide coprecipitates or surface precipitates. Adsorbed As that is not readily desorbed is also considered part of $As_{(ppt\_form)}$. Desorbable As is termed $As_{(desorb\_form)}$. Possible sorbent phases may include ferrihydrite, hydroxysulfate minerals, clays and gypsum. The third form of As is dissolved in solution ($As_{(aq\_form)}$). These forms make up the total As ($As_{(total)}$).

$$As(\ total\ ) = As(\ ppt\_form\ ) + As(\ desorb\_form\ ) + As(\ aq\_form\ ) \qquad (1)$$

The term "form" provides a conceptual description of the different types of arsenic in the system. Equations 1 and 2 do not explicitly describe concentrations. Total and aqueous As concentrations can be readily determined using standard analytical methods. The desorbable As plus dissolved As in equation (1) may be defined as the readily released As ($As_{(rr)}$),

$$As(\ rr\ ) = As(\ desorb\_form\ ) + As(\ aq\_form\ ) \qquad (2)$$

Desorbable As responds rapidly to changes in conditions such as temperature, pH or liquid to solid ratio. Arsenic in precipitated form, or irreversibly bound to surfaces, will respond to such changes at a much slower rate or not at all.

There are several mathematically equivalent approaches to estimate the amount of readily released As in the tailings. The most straightforward is based upon the EPICS method (Gossett, 1987). In Gossett's work, the EPICS methodology was used to measure Henry's Law Constants for volatile organic compounds. We use a similar approach here to measure the distribution coefficient for readily released As (K_d^{rr}).

For a fixed mass of slurry ($M_{(solid)}$), the readily released As ($As_{(rr)}$) is operationally defined by Equation 3:

$$As(\ rr\ ) = As(\ desorb\ )M(\ solid\ ) + As(\ aq\ )V(\ aq\ ) \qquad (3)$$

Where $As_{(desorb)}$ is the desorbable As concentration associated with slurry solids, and $As_{(aq)}$ and $V_{(aq)}$ are the aqueous As concentration and volume of the aqueous phase.

The distribution coefficient for readily released As is defined as:

$$K_d^{rr} = \frac{As_{(desorb)}}{As_{(aq)}} \qquad (4)$$

The superscript rr distinguishes this distribution coefficient from the total distribution coefficient, K_d^{total}, which is defined by

$$K_d^{total} = [As_{(ppt)} + As_{(desorb)}]\ /As_{(aq)}. \qquad (5)$$

Substituting Equation 4 into Equation 3, we obtain:

$$As\,(\,rr\,) = As\,(\,aq\,)\,[V\,(\,aq\,) + Kd^{\,rr}\,M\,(\,solid\,\,)]\tag{6}$$

If samples 1 and 2, prepared with different volumes of liquid, both contain the same total amount of readily releasable As and mass of solid, then

$$As(aq1)[V(aq1)+Kd^{rr}M(solid)] = As(aq2)[V(aq2)+Kd^{rr}M(solid)] = As(rr)\tag{7}$$

Where the subscripts 1 and 2 represent the As concentrations and volumes at specified steps. Solving for $K_d^{\,rr}$ gives:

$$Kd^{\,rr} = \frac{As\,(\,aq\,1\,)V\,(\,aq\,1\,) - As\,(\,aq\,2\,)V\,(\,aq\,2\,)}{[\,As\,(\,aq\,2\,) - As\,(\,aq\,1\,)]\,M\,(\,solid\,)}\tag{8}$$

This equation shows that $K_d^{\,rr}$ can be determined by experimentally changing the proportions of water to solid in a system in which $As(rr)$ and $M_{(solid)}$ are fixed.

The simplest method of computing $K_d^{\,rr}$ from such experimental data, is to plot the inverse of the As concentrations ($1/As_{(aq)}$) versus the volume of solution for two or more measurements. It can be demonstrated (Mahoney et al. 2005) that $K_d^{\,rr}$ then equals the intercept (b) of the line, divided by the slope (m) of that line times the mass of solid, or

$$K_d^{\,rr} = b\,/\left[mM_{(solid)}\right].\tag{9}$$

Because all of the concentrations used in these calculations are derived from solution analyses, the proportion of liquid to solid is not explicitly required, so a dimesionless $K_d^{\,rr}$ is commonly obtained. This can be converted to a true distribution coefficient (in units of V/M) when the mass of solids and initial volume of solution are known.

One method to estimate the amount of readily released As is to calculate $F_{(desorb)}$, the fraction of As that is readily desorbed:

$$F\,(\,desorb\,) = \frac{As(\,desorb\,)M\,(\,solid\,)}{As(\,desorb\,)M\,(\,solid\,) + As(\,aq\,)V\,(\,aq\,)}\tag{10}$$

The readily released As is then calculated:

$$As\,(\,rr\,) = \frac{[\,As\,(\,aq\,)V\,(\,aq\,)]}{[\,1 - F\,(\,desorb\,)]}\tag{11}$$

Model simulations

A series of model simulations were performed to verify that the assumptions and the computational method could be applied to the more complicated system of As desorption from ferrihydrite. Desorption reactions were modeled using PHREEQC (Parkhurst and Appelo, 1999), and the diffuse layer model (Dzombak and Morel, 1990). PHREEQC was used because the distribution of the different forms of As

can be determined at each modeling step. Therefore, the amount of readily re-leased As measured using the EPICS calculation could be directly compared to the amount estimated using PHREEQC.

For the primary leaching solution, which was arsenic-free, the assumed major ion concentrations were 400 mg/L Ca, 230 mg/L Na, 243 mg/L Mg and 2400 mg/L SO_4. Arsenic, at 0.1, 1.0 and 10.0 mg/L, was added to the primary solution to produce the starting solutions. Diffuse layer model weak sites (Hfo_wOH) at 0.001 mol/L were used. For each step, the 1 L of As bearing solution was mixed with a volume of the "As-free" leaching solution, and the mixture equilibrated with the adsorption sites.

To obtain the data required for the EPICS calculation, leaching solution was added to the initial 1-L system, changing the solution/sorbent ratio. In these simu-lations the final volumes were 1.2, 1.4, 1.6, 1.8, 2.0, 3.0, 4.0 and 5.0 L. In the PHREEQC models, the leaching solution is added using the MIX keyword, which calculates the changes in volume as solutions are added together. This makes the PHREEQC program ideally suited to verifying the EPICS method.
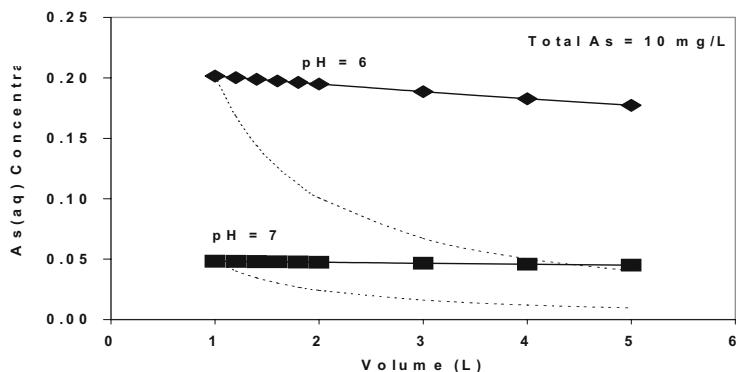
Table 1 lists some of the verification calculations and provides a comparison of EPICS and PHREEQC site concentrations. Readily released As concentrations, using the EPICS methodology, and the initial values used in PHREEQC are in close agreement. The simulations show that the method is computationally sound.

Fig. 1 shows As concentrations for two simulations. The theoretical dilution lines show As concentrations if simple dilution is the only process. Departures of model-simulated lines from the dilution lines indicate that a significant reservoir of As buffers dissolved As concentrations. The data are replotted as inverse con-centrations, which linearizes both the data and the dilution lines (Fig.2). By defini-tion, the dilution lines correspond to a K_d^{rr} of 0.0. These lines have an intercept of zero, and a slope equal to the inverse concentration of the first data point.
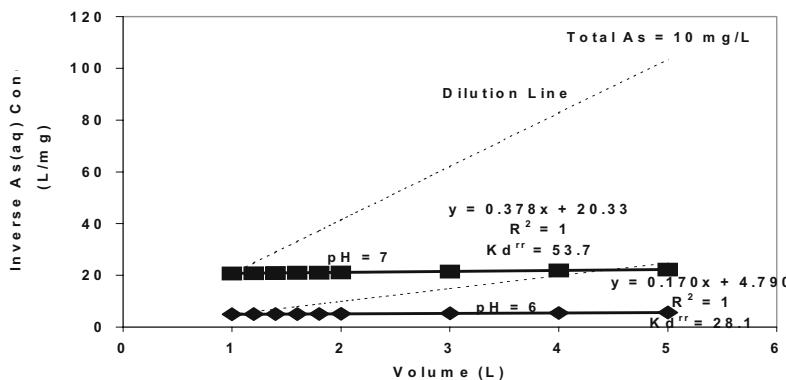
Table 1. EPICS procedure verification by comparison with PHREEQC results.

Initial As (mg/L)	pH	As(aq) (moles/L)	K_d^{rr}	$F_{(desorb)}$	Readily Released As (moles/L)		Agreement % EPICS vs PHREEQC
					EPICS	PHREEQC	
0.1	7	9.14×10^{-10}	5725	1.00	1.34×10^{-6}	1.34×10^{-6}	100
1	7	1.03×10^{-8}	123	0.99	1.34×10^{-5}	1.34×10^{-5}	100
10	6	2.69×10^{-6}	28.4	0.93	1.30×10^{-4}	1.34×10^{-4}	97.3
10	7	6.45×10^{-7}	53.5	0.96	1.30×10^{-4}	1.34×10^{-4}	97.4

For the pH 7.0 data, the K_d^{rr} was 54, for the pH 6.0 data the K_d^{rr} was 28. In simple systems the K_d^{rr} for As should decrease as pH increases. The apparently unusual behavior is because of the large sulfate concentrations. Desorption of sulfate with increasing pH increases the number of sites available for As adsorption, which increases K_d^{rr}.

Fig. 1.   PHREEQC model derived concentrations of EPICS procedure assuming As adsorption on hydrous ferric oxide. Dilution lines are dashed.

Fig. 2.   Inverse concentrations of PHREEQC modeled EPICS process, showing regression fit and calculation of Kdrr.

Experimental methods and measurements with tailings

A pre-weighed container (approximately 7-L size, wide-mouth plastic bucket) was partially filled with approximately 1 L of neutralized tailings slurry. The pH and mass of the slurry were measured. The initial volume was defined as V1. The slurries typically contained 400-600 g of solids. The remainder of the slurry was neutralized raffinate. Solids were allowed to settle and an aliquot of supernatant solution was carefully drawn off. This and subsequent aliquots were kept as small as possible, and were always less than 25 mL. The large initial volumes and small aliquots was necessary to keep the system 'closed' with respect to total As. The aliquot was filtered (0.45µm) and analyzed for total As. After each aliquot was drawn off, the container was reweighed to estimate the mass of solution removed.

The starting solution was the neutralized and unmodified raffinate, which typically has an As concentration of <1 mg/L. The second water was the "As-free" leaching solution, which retained the pH and major ion composition of the neutralized raffinate. In the leaching solution, arsenic concentrations were required to be less than 0.01 mg/L.

Because of the large volumes required by the procedure, the amounts of solution and masses of solids in the mixtures were measured gravimetrically. To start the experimental procedure, approximately 1 L of "As-free" leaching solution was added to a liter of the tailings slurry. The new volume was defined as V2. The slurry was mixed, and the pH was measured. The slurry was mixed again and the solids allowed to settle. In most experiments settling times were limited to 1 hr. The pH was rechecked, and a sample was withdrawn for analysis. Because dissolved As concentrations are a strong function of pH, the pH was kept constant throughout the process.
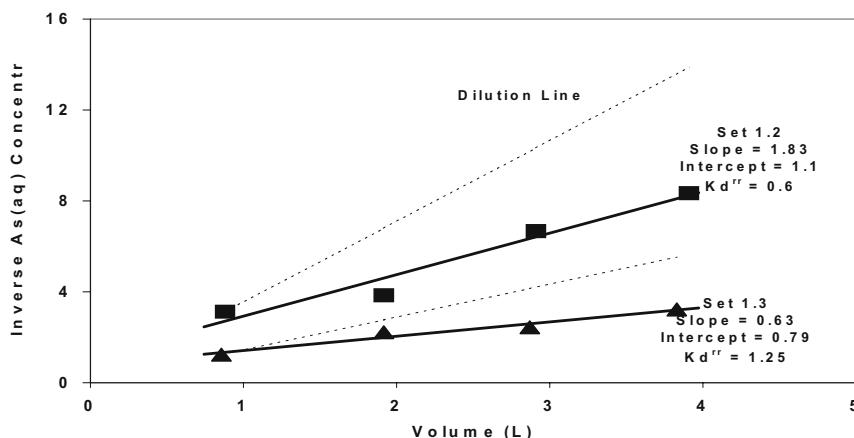
The process of adding leach solution, measuring the weight and volume of the new mixtures, and extracting aliquots for analysis was repeated two more times (V3 and V4). Finally, the water in the slurry was removed by filtration. The solids were weighed and analyzed for As.

Results and discussion
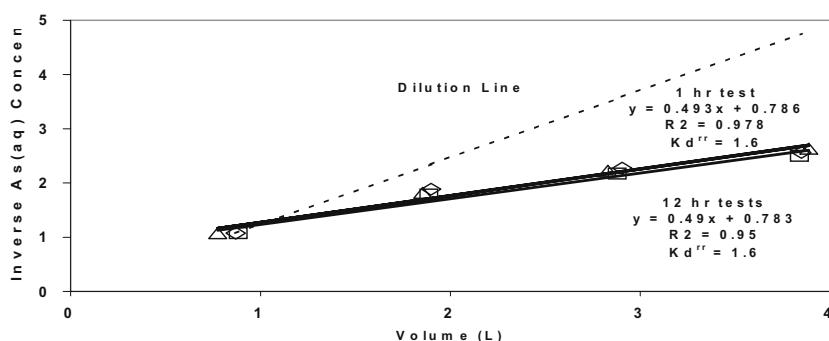
Initial desorption experiments were run with one hour between extractions. Some examples are shown on Fig. 3. Values for K_d^{rr} were estimated using the regression derived slopes and intercepts from the inverse concentration data. Compared to the dimensionless K_d^{total} values, which range from 600 to 1400 for the experiments, the values for K_d^{rr} are small and range from 0.44 to 2.77. In spite of an up to five-fold dilution in some experiments, only slight changes in pH were noted and corrections to the pH of the slurries were not required.

The results of the first series of tests indicated that little As was released from the solids when extraction times were limited to approximately 1 hr, and the complete procedure took less than 4 hrs. A short time for the extractions was used because of concerns that other processes such as mineral dissolution could release additional As. The low amounts of readily released As demonstrated that dissolution from other phases was not an issue. Additional tests were run using longer times between dilutions. Two tests were run with 12 hrs between measurements, with samples gently mixed every two hours. One test was run as a control, with one hour between measurements.

Fig. 4 shows that there was no difference in the results between the 12-hr leaching/sampling times and the one-hour steps. The fact that additional As was

Fig. 3.   Inverse concentrations for EPICS experiments using 1 hour between extractions.

Fig. 4.   Results of EPICS method comparing 1 hour (triangles) and 12 hour extraction times. The figure includes two sets of 12 hour-measurements (diamonds and squares).

Analytical speciation techniques for uranium and related elements

Table 2. Calculation of readily released arsenic using the EPICS method.

Test	K_d^{rr}	$F_{(desorb)}$	Initial $As(aq)$ (mg/L)	As desorbed (mg/L)	Readily Released As (mg/L)
1.2 (1hr)	0.6	0.38	0.32	0.19	0.51
1.3 (1 hr)	1.25	0.56	0.81	1.01	1.82
2.1 (1 hr)	1.6	0.62	0.93	1.49	2.42
2.2 (12 hr)	1.6	0.62	0.93	1.49	2.42

not released over time demonstrates that the As associated with the solid phases is practically immobile.

The amount of readily released arsenic is calculated based upon the K_d^{rr} and $F_{(desorb)}$. Table 2 compares initial $As(aq)$ concentrations to the concentration of desorbed As, and to the total amount of readily released As. Among the eight sets of measurements (not all included in Table 2), initial $As(aq)$ concentrations constitute from 38 to 70% of the total readily released As in the slurry.

Upon completion of the leaching process, the solids were weighed and analyzed for As. When compared to the total As content in the tailings, only a very small percent of the total As is dissolved in solution or readily desorbed from the solids. Based upon an average of eight measurements, only 0.21±0.08% of the total As is considered readily releasable. The low percentage of readily releasable As, demonstrates that processing of the tailings in the JEB mill to immobilize As has been optimized.

Conclusions

A method for measuring As desorption from mill tailings (or other solids) was developed based on the EPICS model of Gossett, (1987) The method: (1) is relatively gentle and avoids leaching the As from poorly crystalline arsenate solids and the strongly adsorbed As, and (2) simulates the composition of pore waters in the JEB TMF.

Prior to performing the desorption experiments, the mathematical derivation of the EPICS method was checked by comparing EPICS-predicted desorption results to the same results predicted using an adsorption model in the geochemical code PHREEQC. The comparison showed the EPICS method to be computationally sound.

The results indicate that the amount of As readily released from the tailings was small and was similar in magnitude to the concentration of As in the initial tailings solution. In all cases, the As desorbed by dilution was less than 3 mg/L. Previous work (Langmuir et al., 1999) indicated that the vast majority of the As in the tailings is strongly bound in solids, either as arsenate minerals or as specifically adsorbed arsenate on ferrihydrite. Of this total amount, the readily releasable As averaged only 0.21±0.08%. That 99.8% of the total As in the tailings is fixed and

not readily desorbed supports the efficacy of the procedures used for As immobilization in the JEB mill.

The method is applicable to desorption measurements not only from tailings, but also from other complex solids including soils and sediments. Additional details related to this work are given in Mahoney et al. (2005).

References

Darland, J.E., and Inskeep, W.P., 1997. Effects of pore water velocity on the transport of arsenate. Envir. Sci. & Technol. 31, 704-709.

Dzombak, D.A., and Morel, F.M.M., 1990. Surface Complexation Modeling - Hydrous Ferric Oxide: New York, John Wiley and Sons, 393 p.

Gossett, J.M., 1987. Measurement of Henry's Law constants for C_1 and C_2 chlorinated hydrocarbons. Envir. Sci. & Technol., 21, 202 – 208.

Kim, J-Y., Davis, A.P., and Kim. K-W., 2003. Stabilization of available arsenic in highly contaminated mine tailings using iron. Envir. Sci. & Technol. 37, 189-195.

Langmuir, D., Mahoney, J., MacDonald, A., and Rowson, J., 1999. Predicting arsenic concentrations in the porewaters of buried uranium mill tailings. Geochim. et Cosmochim. Acta, 63, 3379-3394.

Mahoney, J., Langmuir, D., Gosselin, N., and Rowson, J., 2005. Arsenic readily released to pore waters from buried mill tailings. Applied Geochem. 20, 947-959.

Parkhurst, D.L., and Appelo, C.A.J., 1999. User's guide to PHREEQC (Version 2), A computer program for speciation, batch-reaction, one-dimensional transport, and inverse geochemical calculations: U.S.G.S. Water-Resources Invest. Report 99-4259, 312 p.

Shiowatana, J., McLaren, R.G., Chanmekha, N., and Samphao, A., 2001. Fractionation of As in soil by a continuous-flow sequential extraction method. J. Envir. Qual. 30, 1940-1949

Impact of humic acid on the uranium migration in the environment

Susanne Sachs, Gerhard Geipel, Jens Mibus, Gert Bernhard

Forschungszentrum Rossendorf e.V., Institute of Radiochemistry, P.O. Box 510 119, D-01314 Dresden, Germany, E-mail: s.sachs@fz-rossendorf.de

Abstract. Redox properties of different humic acids (HA) were determined and the stability of the oxidation state of U(VI) in presence of humic acid was studied. Applying laser-induced photoacoustic spectroscopy a qualitative spectroscopic proof for the reduction of U(VI) to U(IV) by humic acid was obtained. By column experiments it was found that humic acid influences the transport of both, U(IV) and U(VI). In presence of humic acid both redox species migrate nearly as fast as the groundwater flow. In case of U(VI) humic acid exhibits a clear mobilizing effect. There are strong indications for a similar impact on the U(IV) migration.

Introduction

The remediation of contaminated areas and facilities of the former uranium mining and milling in Saxony and Thuringia (Germany) requires profound knowledge on interaction processes of uranium in natural aquifer systems. Humic acids, ubiquitous, polyelectrolytic, organic macromolecules, are of high importance for these processes. Due to their pronounced ability for complex formation they can impact the speciation and therefore the transport of radiotoxic and toxic metal ions in the environment. In addition to that, humic acids can affect the oxidation state of metal ions because of their redox properties (e.g., Choppin 1999, Zeh et al. 1999, Schmeide and Bernhard 2005). The oxidation state stability of U(VI) in presence of lignin, wood degradation products, and humic acid was studied by Abraham (2002). It was observed, that U(VI) is reduced to U(IV) by these materials. A further characteristic of humic acids is their colloidal behavior in solution. Results of column experiments with natural sandy aquifer material and groundwater rich in humic substances demonstrated that a certain fraction of load metal ions, e.g., U(VI) (Artinger et al. 2002), migrate humic colloid-borne, controlled by kinetic processes, as fast as the groundwater flow.

Reducing conditions can occur in deep underground environments. They are expected in deep water of flooded timbered underground mines (Abraham et al. 2004). Under such conditions, redox processes mediated by wood degradation products and humic substances can induce, among other processes, the reduction of U(VI) to U(IV). Consequently, the tetravalent oxidation state can dominate the speciation and migration of uranium. Profound knowledge on the influence of humic substances on the redox speciation of uranium and on the transport of U(IV)/U(VI) is a pre-requisite for the trustworthy modeling of the uranium migration in the environment. However, the existing understanding and data base for these processes is insufficient up to now.

In order to improve the knowledge on the interaction between humic acids and uranium the redox properties of different humic acids were studied (Sachs et al. 2004 and 2005). Investigations were performed to characterize the oxidation state stability of U(VI) in presence of different humic acids on a time-scale of several weeks (Sachs 2005). In addition to that, the transport behavior of the redox couple U(IV)/U(VI) in quartz sand in presence of humic acid was studied by column experiments and compared to that of U(VI) in absence of humic acid (Mibus et al. 2005).

Experimental

Humic material

The present studies were performed using synthetic humic acid M42 (condensation product of xylose and glutamic acid) and Cat-Gly (oxidation product of catechol synthesized in presence of glycine). Synthesis and characterization of these model substances are described in detail in Sachs et al. (2004). For comparison natural humic acid from Aldrich (AHA) was applied after purification (Kim and Buckau 1988). Table 1 shows some elemental and functional properties of the humic acids used in these study in comparison to natural humic acids (Stevenson 1994). From Table 1 it becomes clear that synthetic humic acid M42 an Cat-Gly show elemental compositions close to those of AHA and other natural humic acids. Due to the use of nitrogen-containing precursors, both model substances show higher nitrogen contents than AHA. The carboxyl group content of M42 and Cat-Gly are similar to those of natural humic acids. However, due to the use of catechol as starting material, Cat-Gly show a significant higher phenolic/acidic OH group content than M42 and AHA.

Table 1. Characterization of the humic acids applied in this study.

	Humic acid			
	M42	Cat-Gly	AHA	Natural humic acid (Stevenson 1994)
	Elemental composition			
C (%)	56.1 ± 0.3	48.8 ± 0.1	58.6 ± 0.1	53.8 - 58.7
H (%) [a]	4.1 ± 0.1	2.8 ± 0.2	3.0 ± 0.1	3.2 - 6.2
N (%)	4.4 ± 0.1	5.1 ± 0.1	0.8 ± 0.1	0.8 - 4.3
S (%)	-	0.9 ± 0.1	3.8 ± 0.1	0.1 - 1.5
O (%) [b]	26.8 ± 0.3	31.1 ± 0.2	23.5 ± 0.1	32.8 - 38.3
Ash (%)	0.1	1.7	2.4	
Moisture (%)	8.4	9.5	7.9	
	Functional groups			
COOH (meq/g) [c]	3.76 ± 0.09	4.16 ± 0.04	4.49 ± 0.14	1.5 - 5.7
Phenolic/acidic OH groups (meq/g) [d]	2.0 ± 0.2	6.6 ± 0.7	3.1 ± 0.1	2.1 - 5.7

[a]Corrected for the water content of the humic acid. b The oxygen content was calculated from the difference to 100% under consideration of the ash and moisture content. c Determined by calcium acetate exchange (Schnitzer and Khan 1972). d Radiometrically determined (Bubner and Heise 1994).

Redox studies

The humic acids were characterized with regard to their redox properties (Sachs et al. 2004 and 2005). For that, the formal redox potentials of the humic acids were measured according to Österberg and Shirshova (1997). The Fe(III) redox capacities of the humic materials were determined at pH 3.0 and pH 9.2 according to Mack (2002) and Matthiessen (1995), respectively.

The redox stability of U(VI) in presence of synthetic humic acid Cat-Gly and natural humic acid AHA was studied at pH 6, 8, and 9 in 0.1 M $NaClO_4$ (Sachs et al. 2005). According to Abraham (2002), U(VI) solutions with humic acid were prepared with initial concentrations of $1 \cdot 10^{-4}$ M and 0.4 g/L, respectively. The sample preparation was performed applying CO_2-free solutions under nitrogen atmosphere and exclusion of light. The pH values of the solutions were adjusted with NaOH and $HClO_4$ and periodically checked in order to keep the pH conditions constant. Laser-induced photoacoustic spectroscopy (LIPAS) was applied for the direct spectroscopic detection of U(IV). For that, a tunable laser system (Geipel et al. 1998) was used. The wavelength range between 600 and 675 nm was studied. In contrast to U(VI), U(IV) shows characteristic absorption bands in this range. For sample preparation, an aliquot of the sample solution was acidified with 6 M H_2SO_4 in order to precipitate the humic acid, to decompose U(IV) humate complexes, and to stabilize U(IV) in form of the sulfate complex. The humic acid precipitate was separated and the supernatant was spectroscopically studied by LIPAS.

Column experiments

Migration experiments were performed in a glove box under nitrogen atmosphere, at room temperature and exclusion of light. Columns, 250 mm in length and 50 mm in diameter, packed with quartz sand (marine fine sand from Heerlen, Netherlands, mean grain diameter 153 μm) were used.

The experiments were performed using synthetic humic acid M42. In order to allow a very precise humic acid detection in environmentally relevant concentrations, the humic acid solutions were spiked with ^{14}C-labeled synthetic humic acid M42 (Sachs et al. 2004). Both, the unlabeled and ^{14}C-labeled synthetic humic acid show comparable properties.

The transport properties of the conservative tracer were determined by tritiated water (HTO). For the study of the U(IV) migration in presence of humic acid, U(IV) was prepared by electrochemical reduction of an uranyl ([234]U) nitrate solution. The [234]U(IV) solution was added to the ^{14}C-labeled humic acid solution. The final concentrations of uranium and humic acid in solution amounted to 50 mg/L ([14]C: 70 kBq/L) and $1 \cdot 10^{-6}$ M [234]U (64 kBq/L), respectively. The pH value was adjusted to pH 7.5 and the ionic strength was set to 0.1 M $NaClO_4$. This solution was equilibrated for two hours prior to start of the experiment. A continuous pulse was applied to inject the tracer. The tracer impulse was followed by a multiple elution of the column with 0.1 M $NaClO_4$ (pH 7.5). Breakthrough curves of humic acid and uranium were measured by fraction analysis using liquid scintillation counting (LSC; Wallac, Perkin Elmer with α-β separation).

In order to differentiate between U(IV) and U(VI) in the initial solution and in the effluent fractions the redox speciation was determined by liquid-liquid extraction with TTA (thenoyltrifluoracetone; Bertrand and Choppin 1982). A detailed

Table 2. Formal redox potentials (E^{0*}) and Fe(III) redox capacities determined for the studied humic materials.

Humic acid	E^{0*} (mV)	$\Delta E/\Delta pH$ (mV/pH)	Fe(III) Redox capacity (meq/g) [a]	
			pH 3.0	pH 9.2
M42	548 ± 19	-67 ± 10	6.1 ± 0.1	18.1 ± 0.6
Cat-Gly	517 ± 12	-57 ± 12	14.5 ± 1.6	36.9 ± 0.2
AHA	570 ± 9	-65 ± 1	1.2 ± 0.1	7.2 ± 1.9

[a] Reaction time: ~3 weeks.

Table 3. Redox potentials (E_h) of U(VI)/U(IV) and formal redox potentials (E^{0*}) of humic acid Cat-Gly and AHA at pH 0 and pH 8.

		pH 0	pH 8
U(VI)/U(IV) (Choppin 1983)	E_h (mV)	338	-70 ± 80
Cat-Gly	E^{0*} (mV)	517 ± 12	61 [a]
AHA	E^{0*} (mV)	570 ± 9	50 [a]

[a] Calculated from the pH dependence of the formal redox potential.

description of the experimental set-up and of all experimental conditions is given in (Mibus et al. 2005).

Results and discussion

Redox properties of the studied humic acids

The results of the humic acid characterization with regard to their redox properties are summarized in Table 2.

The formal redox potential of AHA agrees with those of Aldrich humic acid (578 ± 16 mV, -(57 ± 10) mV/pH) and lignin (579 ± 6 mV, -(54 ± 1) mV/pH) determined by Mack (2002). Compared to AHA, slightly lower formal redox potentials were measured for M42 and Cat-Gly.

The comparison of the Fe(III) redox capacities shows that both humic acid alike products, especially synthetic humic acid Cat-Gly, exhibit a more pronounced redox behavior towards Fe(III) ions than AHA. In previous studies it was observed that phenolic/acidic OH groups dominate the redox properties of humic acids (Sachs et al. 2004). Thus, the significant increase of the Fe(III) redox capacities of Cat-Gly compared to M42 and AHA basically can be ascribed to its higher phenolic/acidic OH group content.

Redox stability of U(VI) in presence of humic acids

The ability of humic acid to influence the oxidation state of metal ions is determined by their redox potentials. Comparing the redox potentials of U(VI)/U(IV) with the formal redox potentials of AHA and Cat-Gly (Table 3) it becomes clear that these are close together in the studied pH range. Therefore, it can be concluded that a humic acid-mediated reduction of U(VI) to U(IV) is possible.
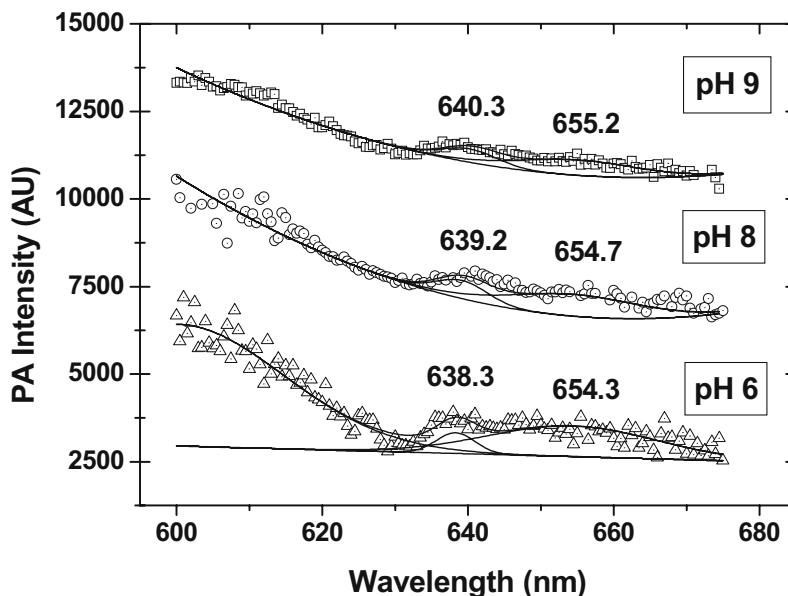
Fig. 1 depicts the LIPAS spectra of the uranium solutions equilibrated with synthetic humic acid Cat-Gly for 52 days. The Cat-Gly samples show in their LIPAS spectra two absorption bands at about 640 and 655 nm. In contrast to that, no absorption signals were found in the spectra of the AHA solutions (not shown, Sachs 2005). Thus, it was concluded that no detectable U(IV) concentration (limit of detection 10^{-6} mol/L; Abraham 2002) was formed by an AHA-mediated U(VI) reduction.

The U(IV) aquo ion shows characteristic absorption maxima at 629.5, 649.1, and 671.7 nm (Geipel et al. 2002). These are close to those observed in the uranium solutions of the Cat-Gly samples. This is an indication for the occurrence of U(IV) in the uranium solutions of the synthetic product. Further, the spectra of the synthetic humic acid test solutions are similar to that which was obtained after equilibration of a U(VI) solution with wood degradation products. In this study the

spectroscopic evidence for the reduction of U(VI) to U(IV) by these substances was given (Abraham, 2002).

In the measured LIPAS spectra the absorption bands are shifted compared to those of the solvated U(IV) ion. Similar peak shifts were already identified for the U(IV) complexation by arsenate (645.1, 662.9 nm; Geipel et al. 2002), phosphate (645.0, 656.6, 667.0 nm; Geipel et al. 2002) and sulfate (634.6, 652.8, 670.0 nm; Sachs et al. 2005). The observed shifts of the absorption maxima can be attributed to the formation of U(IV) sulfate complexes after adding sulfuric acid for sample preparation. The deviations of the peak maxima compared to those of U(IV) in 1.2 M H_2SO_4 (Sachs et al. 2005) could be explained by an additional interaction of U(IV) by incompletely removed humic acid molecules.

It can be concluded that humic acid Cat-Gly with pronounced redox properties is able to reduce a part of the added U(VI) to U(IV). The higher Fe(III) and U(VI) redox capacities of Cat-Gly compared to AHA can be attributed to its higher phenolic/acidic OH group content. Studies are in progress in order to quantify the U(VI) redox capacities of Cat-Gly. Similar results were already obtained for the reduction of Np(V) to Np(IV) (Schmeide and Bernhard 2005) and can be expected for other actinide and metal ions.

Fig. 1. LIPAS spectra of uranium solutions equilibrated with humic acid Cat-Gly at pH 6, 8, and 9. The humic acid was separated before the LIPAS measurements. The spectra are shifted along the y-axis for clarity.
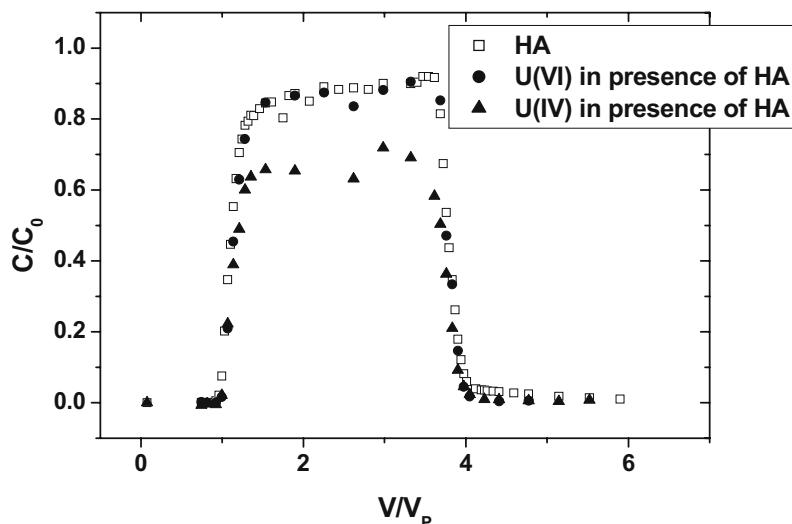
Migration of U(IV)/U(VI) in presence of humic acid

The distribution of U(IV) and U(VI) in the starting solution amounts to 13 % and 84 %, respectively. The measured redox speciation was stable over the entire experiment. It was also determined in the effluent fractions. Therefore, it can be concluded that no redox processes occurred in the column.

Fig. 2 shows breakthrough curves for humic acid, U(IV) and U(VI). Retardation factors, R_f, representing the quotient of the effluent volume and the effective pore volume, as well as total recoveries of all studied species were determined. These are summarized in Table 4 in comparison to those of U(VI) in absence of humic acid (Mibus et al. 2005).

The R_f values of humic acid, U(IV), and U(VI) agree within their experimental errors. They are only somewhat higher than that of the conservative tracer HTO ($R_f = 1$). This indicates a slightly retarded transport of the studied species compared to the water flow.

Comparing the transport parameters of U(VI) in absence and presence of humic acid (Table 4) it becomes clear that the presence of humic acid significantly decreases the R_f value of U(VI). This points to an accelerated U(VI) transport in presence of humic colloids. Furthermore, the U(VI) recovery is increased in presence of humic acid, which is attributed to the formation of soluble U(VI) humate complexes. From these results it can be deduced, that the U(VI) migration in presence of humic acid is governed by a humic colloid-borne transport.

Fig. 2.   Breakthrough curves of HA, U(IV), and U(VI) in the laboratory system quartz sand/0.1 M NaClO$_4$ at pH 7.5 ([HA]: 50 mg/L, [U]$_{tot}$: 1·10^{-6} mol/L). C: measured and C$_0$: initial concentration; V: effluent volume; V$_P$: effective pore volume.

Table 4. Retardation factors (R_f) and total eluate recoveries (R_{eluate}) of humic acid, U(IV) and U(VI) (Mibus et al. 2005).

Species	R_f	R_{eluate}
Humic acid	1.09 ± 0.02	0.90 ± 0.02
U(IV) + humic acid	1.11 ± 0.02	0.66 ± 0.05
U(VI) + humic acid	1.13 ± 0.02	0.90 ± 0.06
U(VI)	2.22 ± 0.11	0.43 ± 0.02

Although U(IV) and U(VI) are characterized by different thermodynamic properties (Choppin 1983) no significant differences were observed in their R_f values under the applied experimental conditions. However, the eluate recoveries of the studied species differ. These effects are caused by association/dissociation processes in the system U(IV)/U(VI)-humic acid-quartz sand. In spite of the higher uncertainty of the extraction data, the U(IV) recovery is lower than that of U(VI). This points to a stronger interaction of U(IV) with the quartz sand surface and thus to a more distinct immobilization. Nevertheless, there are strong indications that humic acid has not only a mobilizing effect on the U(VI) transport in the investigated system but also on the U(IV) migration due to its complexing ability.

Conclusions

The redox properties of humic acids with different functionalities were determined. Among the studied materials synthetic humic acid Cat-Gly, that is characterized by a high phenolic/acidic OH group content compared to the other humic acids used in this work, shows the most pronounced redox properties. Applying this synthetic humic acid a qualitative spectroscopic proof for the reduction of U(VI) to U(IV) by humic acid with distinct redox properties was obtained. By means of column experiments it was observed that humic acid affects the migration behavior of both U(IV) and U(VI). The column experiment shows that U(IV) and U(VI) can be transported by humic colloids. In case of U(VI) a strong transport accelerating effect of humic acid was observed.

Although the systems under investigation represent a considerable simplification of natural aquifers they are suitable to identify processes that impact the migration of uranium in the environment. The performed studies demonstrate the relevance of humic materials for the migration of uranium under oxic as well as under reducing conditions. From that, it follows the requirement to involve interaction processes between humic acids and uranium in the geochemical modeling of the migration behavior of uranium in the environment.

Acknowledgements

References

Abraham A (2002) Einfluss von Huminstoffen und Holzabbauprodukten auf den Valenzzustand von Uran. PhD Thesis, TU Dresden

Abraham A, Baraniak L, Bernhard G (2004) Bog Ground Aquifer Systems as a Natural Analogue for Future Redox Conditions in Flooded Underground Mines. J. Radioanal. Nucl. Chem. 261: 597-604

Artinger R, Rabung, T, Kim JI, Sachs, S, Schmeide K, Heise KH, Bernhard G, Nitsche H (2002) Humic Colloid-Borne Migration of Uranium in Sand Columns. J. Contam. Hydr. 58: 1-12

Bertrand PA, Choppin GR (1982) Separation of Actinides in Different Oxidation States by Solvent Extraction. Radiochim. Acta 31: 137-137

Bubner M, Heise KH (1994) Characterization of Humic Acids. II. Characterization by Radioreagent-Derivatization with [^{14}C]Diazomethane. In: FZR-43, Annual Report 1993 (Nitsche H, Bernhard G, eds.), Forschungszentrum Rossendorf, Institute of Radiochemistry, Rossendorf, Germany: 22

Choppin GR (1983) Solution Chemistry of the Actinides. Radiochim. Acta 32: 43-53

Choppin GR (1999) Role of Humics in Actinide Behavior in Ecosystems. In: Chemical Separation Technologies and Related Methods for Nuclear Waste Management (Choppin GR, Khankhasayev MKh, eds.), Kluwer Academic Press: 247-260

Geipel G, Bernhard G, Brendler V, Nitsche H (1998) Complex Formation between UO_2^{2+} and CO_3^{2-}: Studied by Laser-Induced Photoacoustic Spectroscopy (LIPAS). Radiochim. Acta 82: 59-62

Geipel G, Bernhard G, Brendler V (2002) Complex Formation of Uranium(IV) with Phosphate and Arsenate. In: Uranium in the Aquatic Environment (Merkel BJ, Planer-Friedrich B, Wolkersdorfer C, eds.), Springer Verlag, Berlin: 373-380.

Kim JI, Buckau G (1988) Characterization of Reference and Site Specific Humic Acids. RCM-Report 02188, TU München

Mack B (2002) Redoxeigenschaften von Lignin und Huminsäuren und deren Wechselwirkung mit Eisen. PhD Thesis, TU Dresden

Matthiessen A (1995) Determining the Redox Capacity of Humic Substances as a Function of pH. Vom Wasser 84: 229-235

Mibus J, Sachs S, Nebelung C, Bernhard G (2005) Migration of Uranium(IV)/(VI) in the Presence of Humic Acids in Quartz Sand: A Laboratory Column Study. J. Contam. Hydr., submitted

Österberg R, Shirshova L (1997) Nonequilibrium Redox Properties of Humic Acids. Geoch. Cosmoch. Acta 61: 4599-4604

Sachs S, Schmeide K, Brendler V, Křepelová A, Mibus J, Geipel G, Heise KH, Bernhard G
(2004) Investigation of the Complexation and the Migration of Actinides and Non-
radioactive Substances with Humic Acids under Geogenic Conditions. Wissen-
schaftlich-Technische Berichte, FZR-399, Forschungszentrum Rossendorf, Rossendorf

Sachs S, Geipel G, Bernhard G (2005), Study of the Redox Stability of Uranium(VI) in
Presence of Humic Substances. In: FZKA 7070, Wissenschaftliche Berichte (Buckau
G, ed.), Forschungszentrum Karlsruhe, Karlsruhe, in press

Schmeide K, Bernhard G (2005) Study of the Neptunium(V) Reduction by Various Natural
and Synthetic Substances. In: FZKA 7070, Wissenschaftliche Berichte (Buckau G,
ed.), Forschungszentrum Karlsruhe, Karlsruhe, in press

Schnitzer M, Khan SU (1972) Humic Substances in the Environment (McLaren AD, ed.),
Marcel Dekker, Inc., New York

Stevenson FJ (1994) Humus Chemistry, 2nd ed., John Wiley&Sons, New York

Analytical speciation techniques for uranium and related elements

Uranium speciation in two Freital mine tailing samples: EXAFS, μ-XRD, and μ-XRF results

Andreas C. Scheinost[1,2], Christoph Hennig[1,2], Andrea Somogyi[3], Gemma Martinez-Criado[4], Reinhard Knappik[5]

[1]Institute of Radiochemistry, FZR, Dresden, Germany,
[2]The Rossendorf Beamline at ESRF, Grenoble, France, E-mail: scheinost@esrf.fr
[3]Synchrotron Soleil, Gif-sur-Yvette, France
[4]ESRF, ID-22, Grenoble, France
[5]VKTA Rossendorf, Dresden, Germany

Abstract. We investigated the uranium speciation in a former WISMUT mine tailing, which was buried for 30 years under mine and construction debris. Chemical extractions, EXAFS, μ-XRD, and μ-XRF reveal two major U pools. The first with a relatively high potential mobility was identified as U(VI) sorbed to layer silicates by inner-sphere complexation; the second pool is represented by the relatively insoluble U(IV) minerals pitchblende and coffinite, and by the U(VI) solids uranyl hydroxide and vanuralite. Distribution between the two pools seems to be controlled by pH. Evidence for reductive precipitation of uraninite was found.
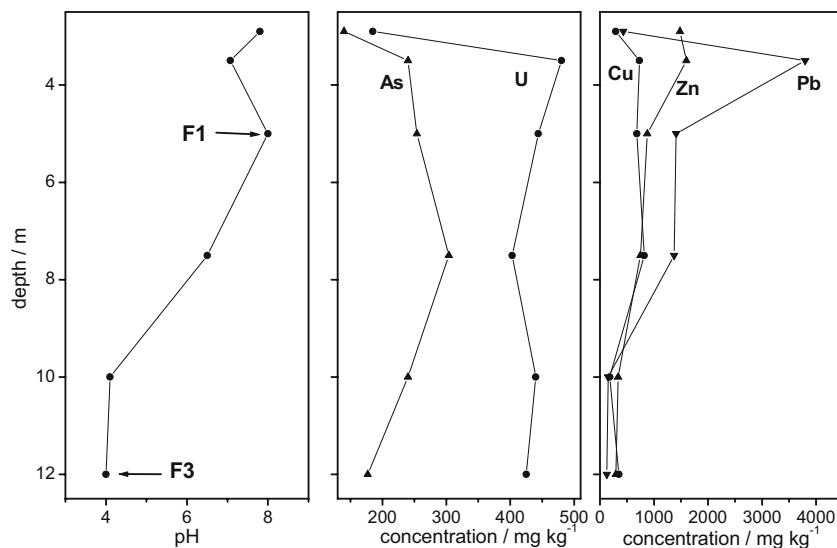
Introduction

During uranium ore extraction, uranium is converted from relatively insoluble U(IV) and U(VI) minerals to highly soluble U(VI) species. Contaminated mine waste piles, tailings and surrounding soils are usually covered by soil material to reduce the Rn emission and radionuclide spreading by wind and water erosion. Under these conditions, microbial and surface-catalytic reduction may transform uranium back to more immobile, tetravalent or hexavalent species. The mechanisms and kinetics of such processes are largely unknown, but are crucial to predict the long-term risks associated with mining sites, nuclear waste repositories and other contaminated sites.

In spite of their environmental relevance, only few studies succeeded to reliably identify uranium species in contaminated soils and sediments. Hunter and Bertsch (1998) found uranyl hydroxide phases and U(VI) associated with organic matter

and amorphous Fe oxides in soils at the Savannah River DOE site. Morris et al. (1996) found autunite- and schoepite-like phases in soils of at Fernald (Ohio). Roh et al. (2000) found schoepite, uranophane, coffinite, U-Ca-oxide and U-Ca-phosphates at Oak Ridge (Tennessee). Catalano et al. (2004) found boltwoodite in sediments at Hanford (Washington). Here we present the first study on U speciation at a former WISMUT (Germany) uranium mining and extraction site, which had been covered for 30 years.

Metal speciation in soils and sediments is a difficult task, since commonly several aqueous, sorbed and mineral species coexist (Manceau et al. 1996; Scheinost et al. 2002). This may be especially true for uranium mining sites, which reflect the rich mineralogy of the Saxonian Erzgebirge. Therefore, we had to combine synchrotron microfocus techniques (μ-XRF and μ-XRD) with bulk X-ray absorption spectroscopy (XAS) and chemical extraction techniques to decipher uranium speciation along a depth profile of a former mine tailings.

Fig. 1.   Depth profiles of pH, U, As, Cu, Zn and Pb concentrations at Freital Tailings 1. The sampling depth of samples F1 and F2 is indicated by arrows.

Samples

Sediment cores were collected in 1992 at tailings 1 of the former Wismut operation site Freital near Dresden, Germany (Knappik et al. 1996). The mine tailings were used from 1949 to 1960 for ore-extraction wastes, and were covered from 1968 on by communal waste (mostly construction debris) and soil, followed by a second cover of mine debris. Samples F1 and F3 were collected at 5 and 12 m depth, respectively (Fig.1). The low pH of 4 at depths below 10 m reflects the former hydrochloric-acid ore-extraction procedure as well as pyrite oxidation and concomitant sulfuric acid release. At smaller depth, the construction debris and tin mine waste used for covering the tailings have created a neutralizing infiltration front with pH values as high as 8. The high pH is associated with high calcium contents, resulting from construction debris, and with high sulfur contents from pyrite oxidation. The cover by mine debris is most likely responsible for the peak concentrations of copper, zinc and lead at 4 m depth, which then decrease with increasing depth. Uranium concentrations vary between 400 and 500 mg/kg at selected sampling depths, while arsenic concentrations are roughly half of uranium concentrations.
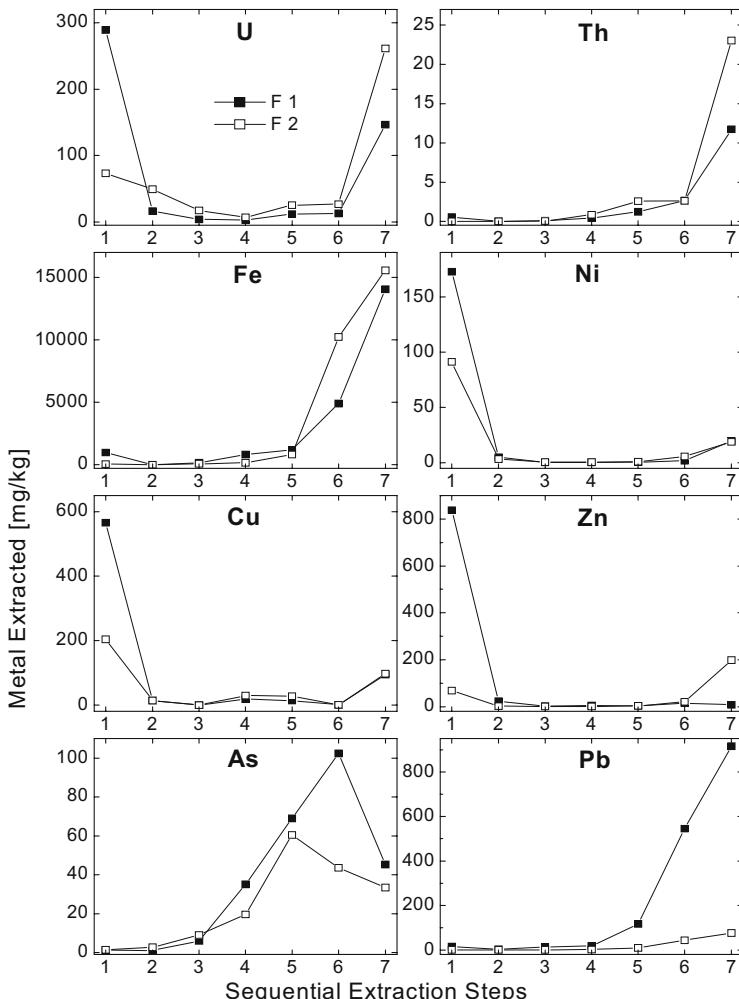
Selective sequential extractions

Selective sequential extractions (SSE) were performed with a 7 step procedure (Zeien and Brümmer 1989): **1.** Water soluble salts and exchangeable ions: 1 M NH_4NO_3. **2.** Weakly complexed ions (often specific sorption): 1 M NH_4OAc at pH 6.0. **3.** Metals bound by Mn hydroxides: 0.1 M $NH_2OH-HCl$ + 1 M NH_4OAc at pH 6.0 and 5.5, resp. **4.** Strongly complexed metals (bound to organic matter): 0.025 M NH_4-EDTA at pH 4.6. **5.** Metals bound by easily reducible Fe(III) minerals: 0.2 M NH_4-oxalate at pH 3.25. **6.** Metals bound by other reducible Fe(III) minerals: 0.1 M ascorbic acid + 0.2 oxalate at pH 3.25. **7.** Recalcitrant minerals: microwave digestion. Total elemental concentrations were determined by ICP-MS, and complemented by graphite furnace AAS and energy-dispersive XRF analysis (Spectro XLab 2000).
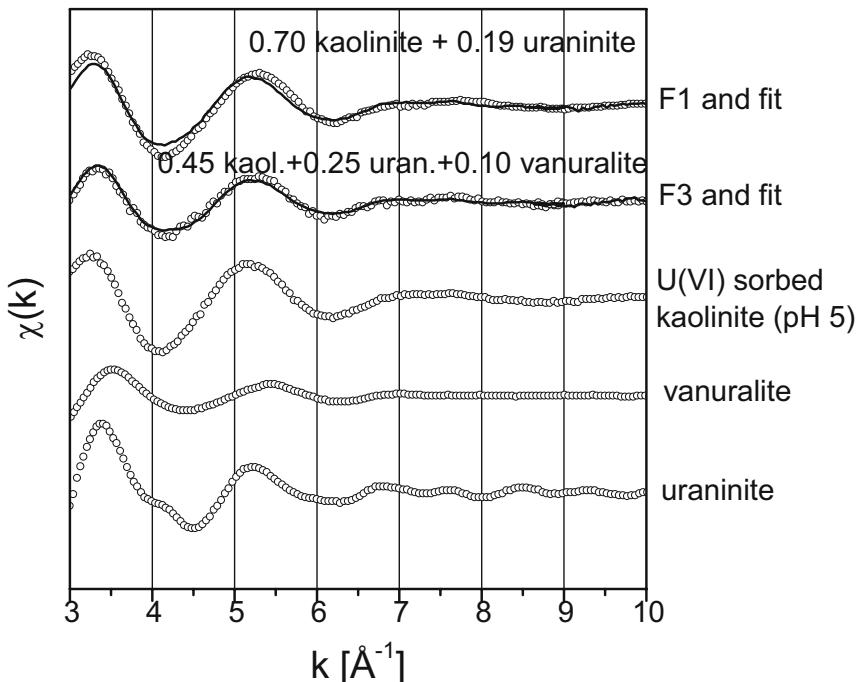
The selective sequential extraction results suggest that in sample F1 (pH 8) the predominant part of U is highly mobile, while in F3 (pH) most U is strongly bound by recalcitrant mineral phases (Fig.2). Other mobile metals include Ni, Cu and Zn, while Th and Pb are bound by recalcitrant mineral phases. Therefore, U, Ni, Cu and Zn are susceptible to leaching from these tailings.

EXAFS spectroscopy

Bulk U L_{III}-edge X-ray absorption fine structure (EXAFS) spectra were collected at the Rossendorf Beamline (BM20, ESRF) at room temperature using a 13-element Ge fluorescence detector (Canberra) with digital signal processing (XIA). In spite of the enhanced energy resolution of this detector, the U-L_{III} line was partly hidden behind the strong K-lines of Rb and Sr, preventing collection of high quality spectra (Fig.3). Hence unweighted U L_{III}-edge EXAFS spectra of F1 and F3 were analyzed by linear combination fits using an EXAFS data base of 60 references encompassing aqueous, sorbed and mineral species. The best fit results

Fig. 2.   Selective sequential extraction results of samples F1 and F3.

Analytical speciation techniques for uranium and related elements

Fig. 3.   Uranium L_{III}-edge EXAFS spectra of F1 and F3, their best linear combination fits, and the EXAFS spectra of selected uranium references.

suggest that F1 contains 70 % of total U sorbed as U(VI) innersphere sorption complexes on kaolinite or clay minerals with similar edge sites, and 20 % bound by uraninite. The fit results of F3 suggest a smaller amount of sorbed U(VI) and more uraninite as in F1, and an additional mineral phase, vanuralite (Fig.3).

Synchrotron μ-XRF and μ-XRD
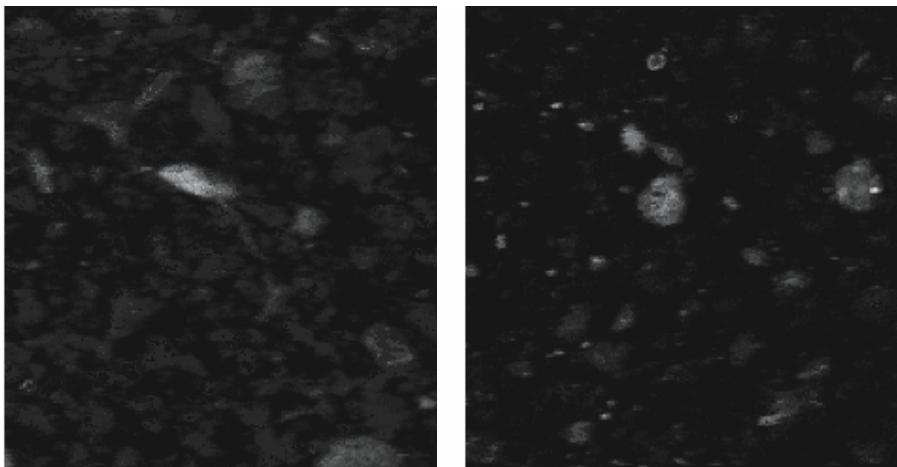
Micro-XRF and μ-XRD was performed on beamline ID-22 (ESRF), using KB-mirrors to focus the beam size to 2 x 6.7 μm². Micro-XRF spectra were collected with a SiLi detector. Clay-sized samples were sprinkled on Kapton tape. Elemental maps were produced from 2-dimensional micro-XRF arrays by deconvolution of the fluorescence lines with AXIL (University of Antwerp). Micro-XRD Laue patterns were collected with a CCD camera positioned 60 mm behind the sample and normal to the incident beam. An incident energy of 18 keV, corresponding to a wavelength of 0.6887 Å was used. The camera 2-d images were converted to powder patterns with Fit2D (A. Hammersley, ESRF) and then analyzed by the search software EVA (Siemens).

Fig.4 shows elemental distribution and elemental associations as tricolor maps, i.e. the concentration of selected elements is coded by one of the colors red, green

and blue. In sample F1, closely associated U and Cu (U/Cu, r=0.84) occur predominately in K-rich aggregates with diameters of tens to hundreds of μm, creating purplish hues (Fig.4 left). Uranium concentrations in these regions are in the mg/kg range, suggesting either minerals where U is not a substantial component or U sorption complexes. In addition, U occurs as small crystals without any other heavier (≥Si) elements (red dots), presumably uranium oxides.

Elongated areas with close association of Ca and S suggest gypsum (green), blue regions indicate feldspar minerals. In sample F3, U does not show strong correlations with other elements across the whole map (Fig.4 right), indicating a varied U mineralogy or sorption to various minerals. In two larger aggregates, U (and Cu, Z, Ni) are associated with K as in F1. However, other U-rich areas are associated with V (purplish regions), Cu (yellow) or Ca (not shown). Again, in some small spots U is not associated with other elements ≥ Si. Uranium concentrations are often in the g/kg range suggesting the presence of U minerals.
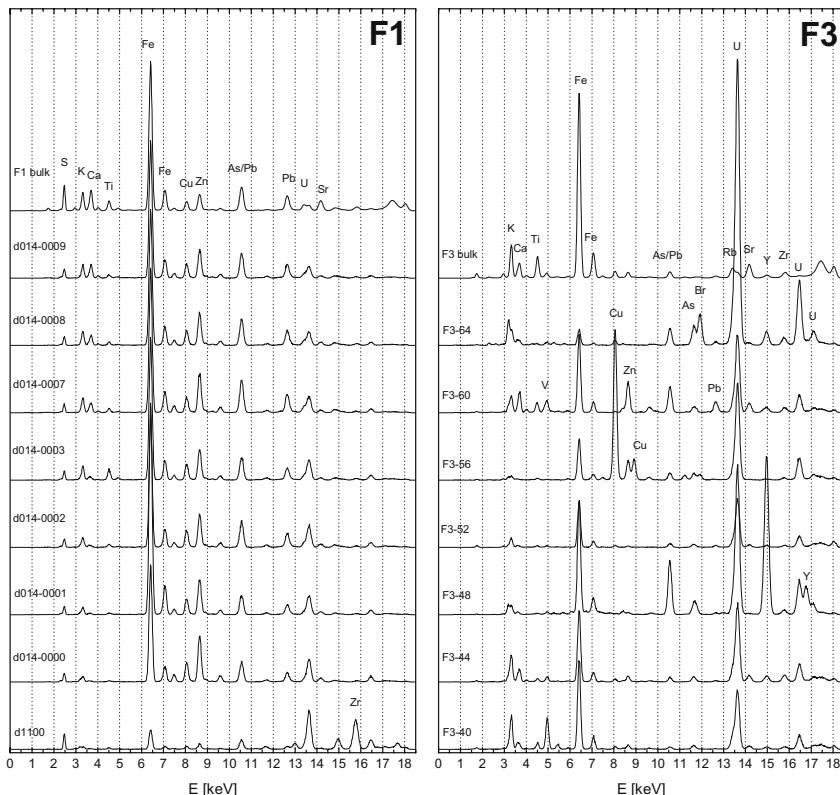
Based on this elemental mapping, single spots containing U were selected for μ-XRD. The μ-XRF spectra of these spots are shown in Fig.5, the corresponding mineral composition as derived from μ-XRD patterns is given in Table 1. The μ-XRF spectra demonstrate the relatively homogenous elemental composition of spots in F1, while spots in F3 have differing elemental compositions. The μ-XRD Laue patterns of F1 show predominately ring patterns suggesting an assembly of particles within the probed spot size, while those of F3 show both powder and single-crystal patterns (data not given). Hence μ-XRF and μ-XRD both confirm that U in F1 is associated with mineral aggregates with diameters of tens of micrometers, while U in F3 is associated with both single crystals and with mineral aggregates.

Fig. 4.   Synchrotron μ-XRF maps (400x400 μm^2) of samples F1 (left) and F3 (right). The color encoding for F1 is U (red), K (blue), S (green). The color encoding for F3 is U (red), Cu (green), V (blue).

The bulk mineral composition of both samples consists of quartz and phyllosilicates; F1 shows in addition gypsum, and F2 in addition feldspar (Table 1). In F1, μ-XRD revealed in addition to the bulk minerals jarosite, but no U minerals. Together with the large amount of exchangeable U (Fig.2) and its diffuse distribution within K-rich aggregates (Fig.4), this suggests that most U is sorbed onto the edge sites of phyllosilicates in F1. This is in line with bulk-EXAFS suggesting formation of inner-sphere sorption complexes on kaolinite. At pH 8, high [HCO_3^-] could prevent U(VI) sorption due to formation of neutral aqueous carbonato complexes, but since [HCO_3^-] is low (<0.5 mg/L) (Knappik et al. 1996) sorption takes place. Both μ-XRF and EXAFS suggest also a smaller amount of U oxide/uraninite, which was not detected by μ-XRD. The large secondary gypsum precipitates found in this sample contain only a very minor amount of U, hence do not constitute a relevant sink for U.

In F3, the U(IV) minerals coffinite and uraninite, and the U(VI) minerals uranyl hydroxide and vanuralite were identified. In addition, a smaller part of U is

Fig. 5.   Bulk XRF and synchrotron μ-XRF spectra of selected spots of samples F1 and F3. The corresponding mineral composition as derived from μ-XRD is given in Table 1.

Analytical speciation techniques for uranium and related elements

again associated with phyllosilicate minerals suggesting sorption (Table 1).

While we found four U minerals with μ-XRD, we could confirm only two minerals, uraninite and vanuralite, by linear combination fit of EXAFS spectra (Fig.3), although reference spectra for the other phases were available and were tested as targets. While this could be due to the limited EXAFS data quality achievable with such difficult samples, it may also suggest that the total amount of U in coffinite and uranyl hydroxide is below the detection limit of the bulk EXAFS method.

At the low pH of 4, specific sorption of uranyl ions to the variable-charge edge sites of phyllosilicates is reduced due to competition with protons. Hence we considered non-specific sorption to permanent-charge phyllosilicates like montmorillonite as an alternative. Such minerals were not identified by XRD and μ-XRD (Table 1). Furthermore, linear combination fits of the EXAFS spectra revealed the presence of U-sorbed kaolinite (Fig.2), while U-sorbed montmorillonite gave a significantly poorer fit. Hence in spite of the relatively low pH, formation of inner-sphere sorption complexes seems to be the prevalent sorption process because of the lack of permanent-charge phyllosilicates.

While the limited number of spots investigated by μ-XRF may not provide a statistically reliable U speciation in F3, the prevalence of U in recalcitrant mineral phases is confirmed by the two bulk methods, SSE and EXAFS. The small amount of U minerals is far below the detection limit of bulk XRD.

In terms of remediation strategies and the geochemical kinetics of U cycles, it would be important to know, if the identified U minerals are primary phases left behind by an incomplete extraction of the ore, or if they are secondary minerals formed from soluble U(VI) by precipitation and reduction-precipitation. The main U ore extracted at the Freital site was pitchblende associated with local coal deposits, but also pitchblende from other Saxonian and Thuringian mining locations, hence the identified uraninite could have been inherited from the ore. However, EXAFS spectra of seven natural pitchblende samples from Erzgebirge and worldwide sources revealed significant fractions of U(VI) due to oxidation (not shown), and did not fit the EXAFS spectra of F1 and F3. In contrast, a synthetic uraninite sample with a composition close to UO_2 gave a reasonable fit of the sample spectra (Fig.3). This suggests that the observed uraninite could be in fact a recent secondary precipitate, formed most likely after microbial reduction of soluble U(VI).

As minor fractions, coffinite and vanuralite were also minerals of the U ore. Both may have resisted the acidic ore extraction procedure, hence are most likely inherited. At one spot in F3, the synthetic phase uranyl hydroxide was identified (card 70-1520), which is most likely a secondary precipitate, but of only minor importance for the U mineralogy due to its small abundance.

Table 1. Mineral phases identified in bulk samples and in selected spots by μ-XRD.

Sample	main elements	identified phases
F1-bulk		Qz, muscovite, (illite), kaolinite, gypsum
F1-d1100	S, Fe, As, Pb, Bi, U, Y/Rb, Zr	(Qz), muscovite, (jarosite)
F1-d014-00	S, K, Fe, Ni, Cu, Zn, Pb, U	(Qz), kaolinite, muscovite, jarosite
F1-d014-01	d014-00	(Qz), kaolinite, muscovite, jarosite
F1-d014-02	d014-00 +Ti	kaolinite, muscovite, (illite), jarosite
F1-d014-03	d014-00 +Ti	(Qz), kaolinite, muscovite, jarosite
F1-d014-07	d014-00 +Ca +Ti	(Qz), kaolinite, muscovite, (illite) , gypsum, jarosite
F1-d014-08	d014-00 +Ca +Ti	(Qz), kaolinite, muscovite, (illite) , gypsum, jarosite
F1-d014-09	d014-00 +Ca +Ti	(Qz), kaolinite, muscovite, gypsum, jarosite
F3-bulk		Qz, microcline, kaolinite, muscovite, (illite)
F3-d040	K, V, Fe, U	Qz, muscovite, (illite), hematite, **vanuralite** $(Al(UO_2)_2V_2O_8(OH) \times 11H_2O)$
F3-d044	K, Ca, Fe, U	Qz, muscovite , (**uraninite**), (**uranyl hydroxide**)
F3-d048	K, Fe, As, U, Y	(Qz), hematite, **uraninite**, xenotime
F3-d052	K, Fe, U	muscovite, (illite), **uraninite, uranyl hydroxide**
F3-d056	Fe, Cu, Cr, U	(Qz), muscovite, (illite)
F3-d060	K, Ca, Ti, V, Fe, Zn, As, Pb, U	(Qz), muscovite, (illite)
F3-d064	K, Ca, Fe, Br, U	Qz, **coffinite**

Conclusions

At smaller depth (F1, 5 m), hydrochloric acid from the ore extraction and sulfuric acid from pyrite oxidation was completely neutralized by the construction debris used as cover material, resulting in precipitation of jarosite and gypsum. The predominant uranium species at this depth is U(VI) sorbed to variable-charge sites of clay minerals. At greater depth (F3, 12 m), the low pH from ore extraction was conserved. The predominant part of U is hosted by U(IV) and U(VI) minerals. While coffinite and vanuralite are most likely inherited from the U ore, evidence of uraninite with a formal U oxidation state close to 4 suggests a reduction and precipitation process in the tailings sediments. The U minerals were recalcitrant during chemical extractions, indicating low uranium solubility even at oxic redox conditions. Hence the results demonstrate a potentially high mobility of U at lower depth and high pH, while U at greater depth and low pH is hosted by low-soluble minerals, which in part may have formed by a natural (microbial) attenuation mechanism within the 50 to 30 years since the deposition of the mine tailings. The high spatial variability of geochemical parameters in such tailings, the related variability of uranium speciation, and finally the kinetic aspects of mineral disso-

lution/precipitation have to be considered by coupled kinetic geochemical and transport models, posing a substantial challenge for reliable risk assessments.

Acknowledgements

References

Catalano J G, Heald S M, Zachara J M, Brown G E (2004) Spectroscopic and diffraction study of uranium speciation in contaminated vadose zone sediments from the Hanford site, Washington state. Environmental Science & Technology 38(10): 2822-2828.

Hunter D B, Bertsch P M (1998) In situ examination of uranium contaminated soil particles by micro-X-ray absorption and micro-fluorescence spectrocopies. Journal of Radioanalytical and Nuclear Research 234(1-2): 237-242.

Knappik R, Mocker D, Friedrich H-J. (1996) Migrationsverhalten von Radionukliden in Tailings unter besonderer Berücksichtigung des Oxidationspotentials in alten Tailingsablagerungen. VKTA Rossendorf.

Manceau A, Boisset M C, Sarret G, Hazemann J L, Mench M, Cambier P, Prost R (1996) Direct determination of lead speciation in contaminated soils by EXAFS spectroscopy. Environmental Science & Technology 30: 1540-1552.

Morris D E, Allen P G, Berg J M, ChisholmBrause C J, Conradson S D, Donohoe R J, Hess N J, Musgrave J A, Tait C D (1996) Speciation of uranium in Fernald soils by molecular spectroscopic methods: Characterization of untreated soils. Environmental Science & Technology 30(7): 2322-2331.

Roh Y, Lee S R, Choi S K, Elless M P, Lee S Y (2000) Physicochemical and mineralogical characterization of uranium-contaminated soils. Soil & Sediment Contamination 9(5): 463-486.

Scheinost A C, Kretzschmar R, Pfister S, Roberts D R (2002) Combining selective sequential extractions, X-ray absorption spectroscopy and principal component analysis for quantitative zinc speciation in soil. Environmental Science & Technology 36(23): 5021-5028.

Zeien H, Brümmer G W (1989) Chemische Extraktion zur Bestimmung von Schwermetallbindungsformen in Böden. Mitteilungen der Deutschen Bodenkundlichen Gesellschaft 59(1): 505-510.

Site characterisation of the potential Natural Analogue Site Heselbach in Bavaria/Germany

Dagmar Schönwiese[1], Thomas Brasser[2], Ulrich Noseck[2]

[1] Institut für Umweltgeologie, TU, 38106 Braunschweig, Germany,
E-mail: ch5@grs.de
[2] Gesellschaft für Anlagen- und Reaktorsicherheit (GRS) mbH, 38122 Braunschweig, Germany

Abstract. The U-enrichment at Heselbach/Bavaria was checked to be a suitable Natural Analogue for transport processes in the far field of an underground repository. For that reason investigations at Heselbach were carried out to identify mobilization and immobilization processes of uranium and thorium in lignite and clay sediments. Geology, hydrology and radiochemistry were studied in order to get detailed information on these topics. Subsequent to the experimental investigations a uranium transport model has been developed.

Introduction

With regard to long-term performance assessment (PA) for radioactive waste repositories Natural Analogues (NA) have been investigated for several decades to improve the understanding of the behaviour of radioactive elements in the natural environment. In NA-studies the potential mobility of radionuclides could be obtained by studying the natural occurrence of these critical elements on time scales which are relevant for underground repositories (~ 1 Ma). Next to the quantification of relevant transport processes NA-studies could be further used to identify natural immobilization processes.

U-enrichments are often formed where oxygenated or carbonate-enriched ground- or surface waters with highly soluble uranyl-carbonate complexes encounter organic-rich sediments (Culbert and Leighton 1978). Main mechanisms which could induce immobilization of uranium in such an environment are adsorption, ion exchange, reduction and/or (co)-precipitation processes. Negatively charged substances like humic acids or clay minerals do have a strong affinity for the positively charged uranyl-ion (Shanbhag and Choppin 1981) and may appear as adsorbents. In environments with high rates of evaporation U(VI)-minerals like
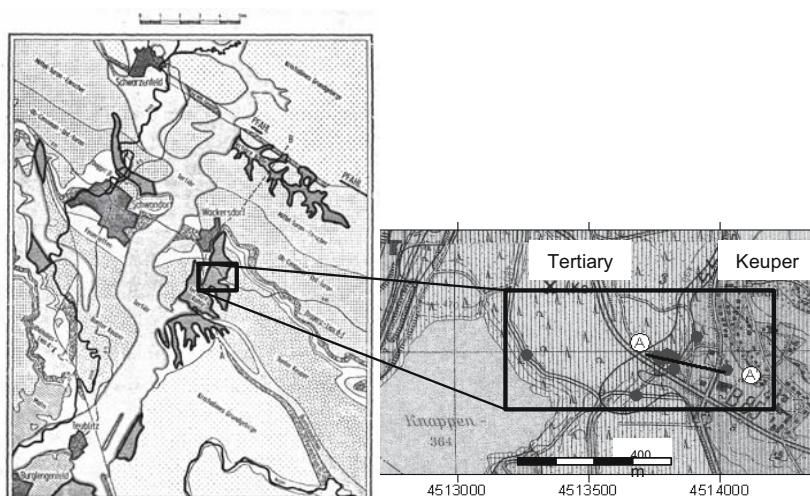
autunite $[Ca(UO_2)_2(PO_4)_2]$ or carnotite $[K_2(UO_2)(VO_4)_2]$ may precipitate. The embedding of uranium in new mineral formations like Fe-(Mn)-oxyhydroxides could be a further possibility to generate a natural uranium accumulation (Payne et al. 1996). Reduction of U(VI) to U(IV) by organic matter, Fe^{2+} minerals like pyrite or Markasit, H_2S, CH_4 and/or sulfate reducing bacteria are another common enrichment process which produces insoluble U(IV)-minerals such as uraninite $[UO_2]$ or coffinite $[UO_2SiO_4]$.

To find out what are the dominating immobilization processes at Heselbach site a sequential extraction procedure, EXAFS-analyses, and U(VI)/U(IV) separation were performed. Hydrological investigations including aqueous chemistry and flow regime studies as well as radiometric analyses complete the site characterization and enable the development of a U-transport model for this location.
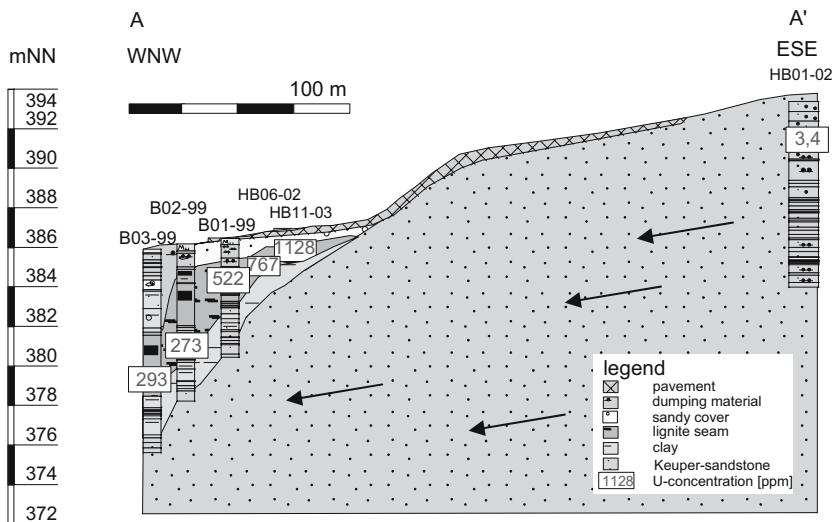
Site location and description

The Heselbach U-enrichment in Bavaria, Germany is located 30 km N from Regensburg and 30 km S from Weiden. The research area comprises 0.3 km^2 and is located at the E-margin of the former Wackersdorfer lignite-mining district. In Fig. 1 the geology of the tertiary river system with research area and drilling locations is plotted.

At the outer rim of the basin structure, relics of the tertiary (miocene) lignite

Fig. 1. Geological situation of the tertiary Ur-Naab basin with research area (a) and location of exploration drillings and cross section A-A' at the rim of the tertiary side bay (b).

Fig. 2.   Cross section A-A' of the tertiary rim with specification of the uranium content in sediment samples. The main groundwater flow is oriented from east to west.

seams remained in which uranium is distributed up to 1200 ppm over a distance of approximately 150 m.

The Keuper sandstone (km, Burgsandstein) does build the eastern limitation and the underlying strata of the tertiary basin. The sediments of the basin itself are composed of a clay horizon at the basis, followed by a clayey lignite seam which is covered by a sand-silt layer on top. The spatial distribution of the sediments at the rim of the basin structure is demonstrated in the cross section A-A' (Fig. 2).
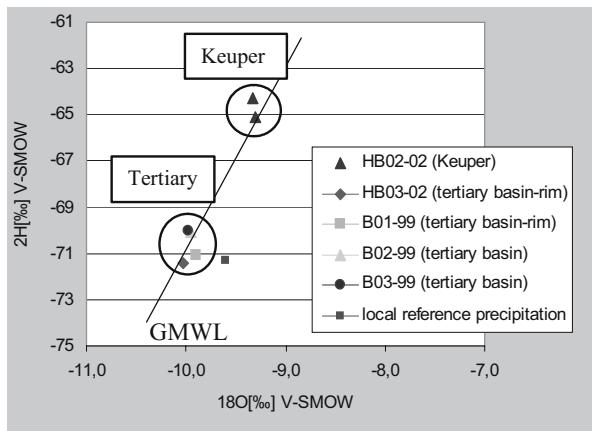
Field and laboratory methods

Hydrology and Hydrochemistry

To characterize the flow regime at Heselbach site hydraulic conductivities of the important hydrostratigraphic units were measured in situ by slug & bail and back-fill tests using the Bower and Rice method calculation.

The determination of the flow velocity in the lignite layer was performed with a tracer test which took place from January to July 2004. A saturated NaCl solution was poured into the injection borehole and detected every 15 min. as electrical conductivity in the nearby observation borehole.

Parameters measured in the field include pH, temperature and electrical conductivity as well as the spectrophotometric determination of $Fe^{2+}/Fe_{(tot)}$ and $SO_4^{2-}/$

Fig. 3. Stabile isotope composition of groundwater and lo-
cal reference samples (database ISOHIS, IAEA).

S^{2-} concentrations. Redox values of the groundwater in the lignite layer were de-
tected with an in situ data logger.

For groundwater chemistry investigations several sets of water samples were
taken into the lab. Samples for natural isotope analyses (^{18}O, ^2H and ^3H) allow the
estimation of groundwater ages and the identification of seasonal mixture proc-
esses. Samples for analyzing major anions and cations as well as U and Th were
filtered < 0.45 µm, acidified with nitric acid and refrigerated. These elements were
measured by ICP-OES or ICP-MS. Dissolved carbon concentrations (TC, TIC)
were analyzed by IR-spectroscopy from a sealed original sample. DOC-samples
were filtered < 0.1 µm and acidified with phosphoric acid (50%). A further sample
set was stabilized with chloroform to inhibit bacterial growth during transportation
and used for detection of ammonium and phosphate by spectral photometry.

Sediment Analyses

All redox sensitive sediment samples were stored in sealed tins under anaerobic
conditions until further processing took place in a glove box. A five step sequen-
tial extraction procedure after Percival 1990 has been carried out to get informa-
tion about the distribution of the uranium phases in the sediments.

Selected uranium decay chain isotopes of sediment samples with elevated U-
concentrations were determined by alpha-spectrometry. EXAFS-analyses from
two selected samples and U(IV)/U(VI))-separation using ion exchange columns
(Ervanne and Suksi 1996) provide information of the uranium-valence-state.

Table 1. Tritium concentrations of groundwater (2003)- and local reference (2000) samples.

sediment stratigraphy		Keuper	Tertiary	Tertiary	Tertiary	Tertiary
location/ drilling	local reference	HB02-02	HB03-02	B01-99	B02-99	B03-99
^{3}H [TU]	9.1 ± 1.6	9.5 ± 0.5	21.7± 1.0	19.8± 0.9	19.3±0.9	21.9±1.0

[a] database ISOHIS (IAEA)

Results and discussion

Groundwater flow regime

Measurements of the hydrological parameters identified a horizontal hydraulic conductivity of $1.54 \cdot 10^{-5}$ m/s for the Keuper sandstone and $2.90 \cdot 10^{-9}$ m/s for the clayey lignite. The very low calculated flow velocity of just 0.01-0.40 m/a in the clayey lignite seam could be confirmed by a tracer test. Even after 6 months the tracer was not detectable in just a distance of 1.1 m from the input borehole indicating nearly stagnant conditions in the tertiary basin.
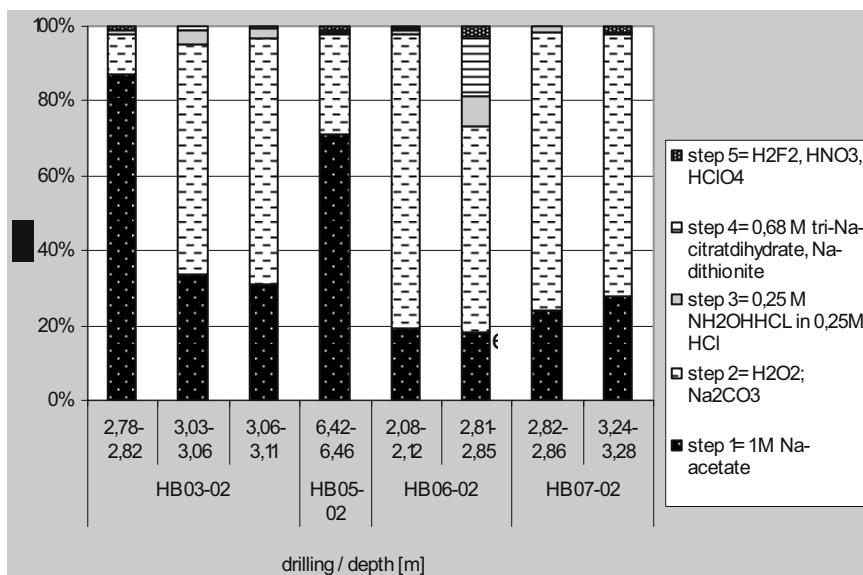
Correspondingly to those findings two different groups of groundwater could be identified by natural isotope analyses (Fig. 3). Drillings at the rim of the tertiary basin show a near-surface influence, evident by mixture processes with actual rain water.

The ^{3}H-concentrations of about 20 TU in groundwater samples of the tertiary basin (table 1) indicate a groundwater age of more than 25 years and a rather long groundwater retention time within these layers.

Groundwater chemistry

On-site measurements of Heselbach groundwater show a pH-value around 5 and an Eh-value of 0.1V in the lignite seam. The Fe^{2+}-concentrations vary between 0.02-0.64 mg/l in the tertiary basin groundwater and do increase with the distance of the basin rim and filter depth. This effect demonstrates the susceptibility of the chemical milieu at Heselbach and manifests the oxygen influence in subsurface drillings at the basin rim.

In general groundwater samples from the tertiary basin are from $Ca-SO_4-Cl$-type. U-concentrations vary from 1 to 10 µg/l, DOC-values are < 10 mg/l.

Fig. 4.   Uranium distribution [%] of sequential extracted sediment samples
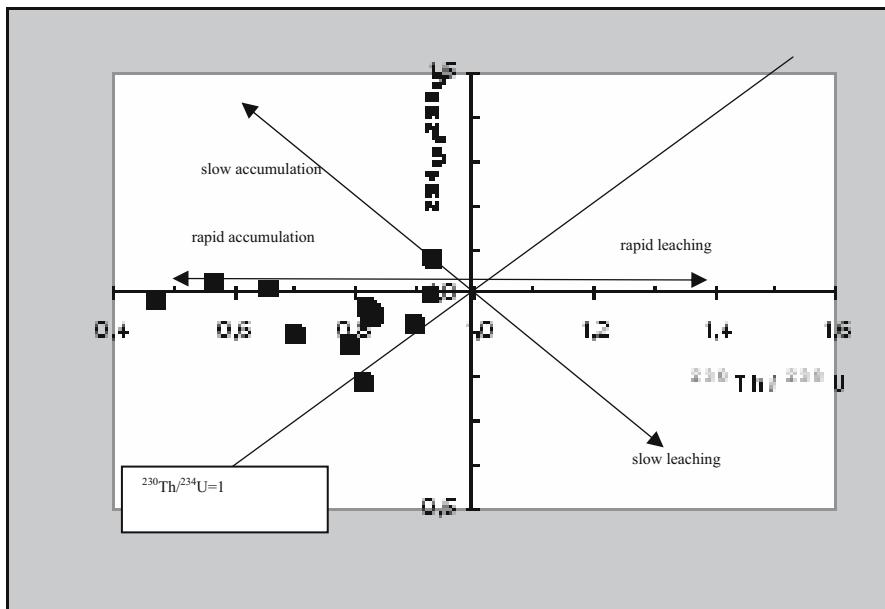
Uranium fixation and remobilization

Sequential extraction examinations determine that > 90 % of the U is bound to the adsorbed (1 M Na-acetat) and the organic (H_2O_2, Na_2CO_3) fraction (Fig. 4).

Furthermore EXAFS-measurements demonstrate that uranium does occur in the U(VI)-valence-state with covalent bonds to oxygen atoms, most likely as UO_2^{2-} (Dardenne and Denecke 2004). This result corresponds to the U(IV)/U(VI)) separation analysis, which identified 99 % of the present U as U(VI) (Suksi 2004).

In addition to the experimental investigations saturation indices were calculated using the PHREEQC-code. The WATEQ4F database was used without the contested uranium-phosphate complexes $UO_2(HPO_4)_{aq}$ and $UO_2(HPO_4)_2^{2-}$ (Duerden 1992). Organic compounds and colloids have not been taken into account. The calculations indicate that U(IV)-minerals like uraninite [$UO_2(c)$] and coffinite [$USiO_4$] as well as the U(IV)/U(VI)-mineral U_4O_9 could be theoretically originate at Eh-values $\leq 0.1V$. U(VI)-minerals are not existent at any redox-value.

Altogether the uranium fixation at Heselbach site could be interpreted as an U(VI)-organic phase like Uranylhumate and/or as an Uranyl-sorption process on Fe-(Mn)-oxyhydroxides or clay minerals. Top concentrations of 130 µg/l uranium in groundwater samples of borehole HB03-02 are due to the increased hydrogen carbonate concentration, which is caused by recent paving work (calcareous gravel). The observed actual remobilisation of part of the uranium is a further hint that rather fast adsorption processes play an important role at Heselbach site.

Fig. 5. Activity Ratios from sediments of the clayey lignite seam plotted in a Thiel-diagram

Radiometry

^{234}U/^{238}U versus ^{230}Th/^{238}U activity ratios of sediment samples of the clayey lignite seam are plotted in Fig.5. Nearly all samples are accumulated in the lower left quadrant and show a significant disequilibrium state indicating a rather rapid uranium accumulation process.

In the Keuper sediments ^{234}U/^{238}U activity ratios vary between 0.75-0.89. These low activity ratios lead to the assumption that α-recoil processes worked over a long time period inducing the observed ^{234}U-depletion before sudden changes of the chemical milieu caused oxidation and U-transportation. Age calculations of the U-enrichment with the ^{234}U/^{230}Th dating method indicate at least a uranium input during the last 200,000 y.

Conclusions and Uranium transport model

The site characterization of Heselbach/Bavaria, Germany can be summarized by following conclusions:
1. U is accumulated up to 1200 ppm in a depth of 0.5-8 m in the tertiary clayey lignite seam and the underlying clay sediment.
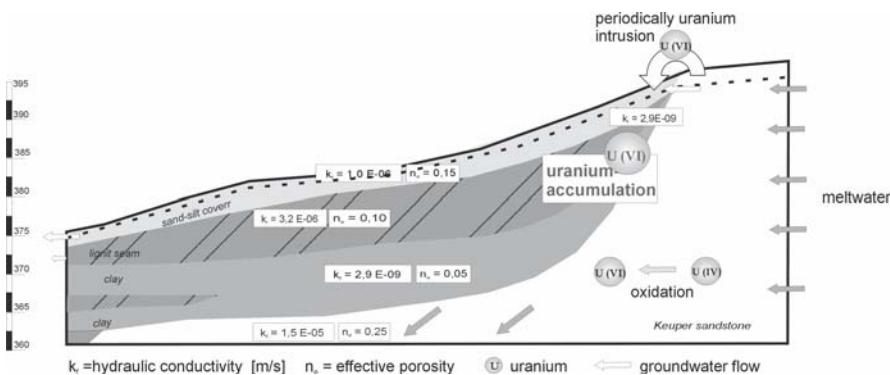
2. Hydraulic investigations ascertained nearly stagnating groundwater with a very low flow velocity in the U-bearing sediments of the tertiary basin.
3. U exists as U(VI); the formation of Uranylhumate, adsorption of uranyl on Fe-(Mn)-oxyhydoxids and clay minerals or embedding are the dominating U-immobilization processes at Heselbach site.
4. U-series-disequilibrium analyses of tertiary lignite samples show rapid accumulation processes during the last 200,000 y.
5. Recent U-remobilization caused by anthropogenic elevation of the hydrogen carbonate concentration demonstrates the disposability of part of U.

Based on the presented results the sketched U-transport model was developed (Fig. 6). Meltwater intrusions during the Quaternary might have changed the chemical milieu and induced a sudden U-oxidation and remobilization from the Keuper sandstone. Increased water levels during that period filled the tertiary basin structure periodically and generated the U-enrichment in the tertiary sediments.

Acknowledgement

Fig. 6. Geological-hydrological U-transport model for Heselbach site

References

Culbert RP, Leighton DG (1978) Uranium in alkaline waters-Okanagan area, British Columbia. CIM Bull May: 103-110

Dardenne K, Denecke MA (2004) Speciation of uranium in samples originating from uranium-rich horizons near Ruprechtov and Heselbach. ANKA Annual report 2004: 45-46

Duerden P et al. (1992) Alligator Rivers Analogue Project.-Final Report. Volume 1

Ervanne H, Suksi J (1996) Comparison of Ion-Exchange and Coprecipitation Methods in Determining Uranium Oxidation States in Solid Phases. Radiochem 38 (4): 306-309

IAEA (2004): Isotope Hydrology Information System, accessible at http://isohis.iaea.org

Noseck U et al (2002) Tertiäre Sedimente als Barriere für die U/Th-Migration im Fernfeld von Endlagern. GRS-176: 284 pp

Payne TE, Davis JA, Waite TD (1996) Uranium Adsorption on Ferryhydrite - Effects of Phosphate and Humic Acid. Radiochim. Acta 74: 239-243

Percival JB (1990) Clay mineralogy, geochemistry and partitioning of uranium within the alteration halo of the Cigar Lake Uranium Deposit, Saskatchewan, Diss. Carleton University, Ottawa

Shanbhag PM, Choppin G (1981) Binding of uranyl by humic acid. J Inorg Nuclear Chem 43: 3369-3372

Suksi J (2004) personal communication

Speciation of Colloid-borne Uranium by EXAFS and ATR-FTIR spectroscopy

Kai-Uwe Ulrich[1], André Rossberg[1,2], Andreas C. Scheinost[1,2], Harald Foerstendorf[1], Harald Zänker[1], Ulf Jenk[3]

[1]Institute of Radiochemistry, FZ Rossendorf e.V., PF 510119, D-01314 Dresden, E-mail: k.ulrich@fz-rossendorf.de
[2]Rossendorf Beamline at ESRF, B.P. 220, F-38043 Grenoble
[3]Wismut GmbH, Jagdschänkenstrasse 29, D-09117 Chemnitz
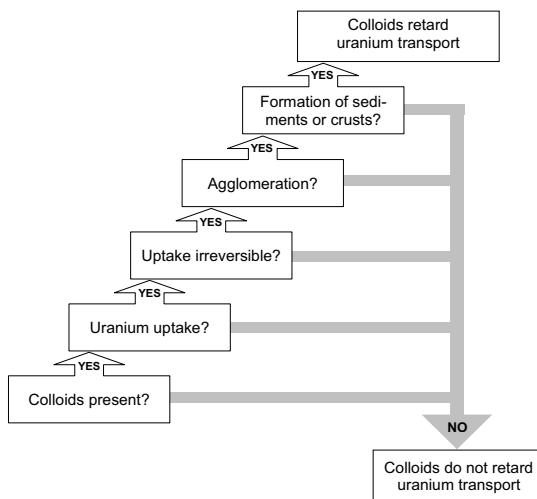
Abstract. De-acidification of acid mine waters transfers dissolved uranium into a colloidal form. Spectroscopic studies on colloid-borne uranium obtained by simulation of mine flooding in the laboratory showed that matrix ions such as sulfate and silicate are not involved in inner-sphere surface sorption complexes of UO_2^{2+} on ferrihydrite. At ambient air atmosphere, the data suggest the formation of ternary U(VI) carbonato surface complexes with either monodentate or bidentate coordination of carbonate and uranyl even at moderately acidic conditions. A revised model is proposed for UO_2^{2+} sorption on ferrihydrite in the absence of carbonate.

Introduction

Flooding of abandoned uranium mines entails the risk of distributing contaminated water into adjacent groundwater aquifers and surface waters. Uranium in its oxidized state is highly soluble at both acidic and alkaline conditions, the latter being due to the formation of U(VI) carbonato complexes. However, moderately acidic conditions favor the sorption of uranyl onto colloids and mineral surfaces (e.g., Hsi and Langmuir 1985, Waite et al. 1994), and this process may retard the transport of the highly mobile uranium(VI) and even immobilize it (Fig. 1). Sulfide oxidation and hydrolysis reactions result in strongly acidic and highly mineralized pore waters in many mines. Similar waters result from in situ leaching of uranium with sulfuric acid as was applied in the Königstein mine (Saxony, Germany) from 1984-1991. Flooding this type of mines by near-neutral water will elevate the acidic pH up to the range where changing speciation of uranium may affect its migration *via* the water path.

Fig. 1.   Flow diagram that indicates when colloids become significant for the retardation of uranium(VI) transport in flooded mines.

This study aims at (i) simulating mine flooding in a mesocosm experiment, (ii) characterizing the freshly formed colloids, their stability and U uptake, and (iii) investigating the structure and stability of sorbent and sorbate binding on the molecular level by Extended X-ray Absorption Fine Structure (EXAFS) and Attenuated Total Reflection Fourier-Transform Infrared (ATR-FTIR) spectroscopy.

Mine flooding simulation experiment

Floodwater from the Königstein mine (pH 2.85, elevated concentrations of sulfate, iron, aluminum and uranium) and near-neutral, suboxic groundwater from an aquifer above the mine, served as the reaction partners (Table 1). A defined volume of floodwater (5-6 L) was mixed with up to 100 L of groundwater by stepwise addition of 10-20 L aliquots within five days. Bubbling of oxygen provided turbulence, accelerated the process of iron(II) oxidation, and removed most of the CO_2.

The pH increased as a function of the mixing ratio, i.e. the volume of the mixture divided by the initial floodwater volume (Fig. 2). The proportion of colloidal Fe rose with progressive iron oxidation (shown by falling $[Fe(II)]/[Fe_{tot}]$ ratio) and pH increase and was thus a function of both mixing ratio and time. At pH >4.5 colloidal Al and U emerged, reaching a proportion of ~60% at pH 5 and of 95-99% at pH 6 (Fig. 2). The colloid concentration raised up to 40 mg/L. After filtration, scanning electron microscopy on the Nucleopore membrane visualized particles of 70-100 nm in both isolated and aggregated forms. The tendency of aggregation was caused by a low electrostatic stability. Below the point of zero charge at pH~6, a low Zeta potential of 5-10 mV was measured. X-ray diffraction of the dried and pulverized colloid samples showed two weak, broad peaks which are

typical of two-line ferrihydrite (Fh) (Schwertmann et al. 1999). ICP-MS analysis of the digested sample MW2 verified the dominance of Fe (373 mg/g), besides Al (56 mg/g), S (24 mg/g), U (21 mg/g), Si (14 mg/g), and C (6.5 mg/g).

The U-L_{III} EXAFS spectrum of the colloid sample MW2, concentrated to a wet paste, closely resembled spectra published before, but the interpretations given in the literature are inconsistent. For instance, Waite et al. (1994) described the uranyl sorption onto Fh by an inner-sphere surface complex. Whereas Allard et al. (1999) failed to identify this complex in case of a natural Fe-rich gel which had trapped uranium, Bargar et al. (1999) explained their spectra by ternary U(VI) carbonato complexes adsorbed onto hematite over a wide pH range. Owing to the sample composition, ternary complexes with sulfate and silicate came into consideration as well. In order to elucidate the molecular uranium binding structure in the colloid sample in detail, a set of simplified sorption experiments has been carried out to synthesize samples for comparative EXAFS and ATR-FTIR studies.

Uranium sorption experiment
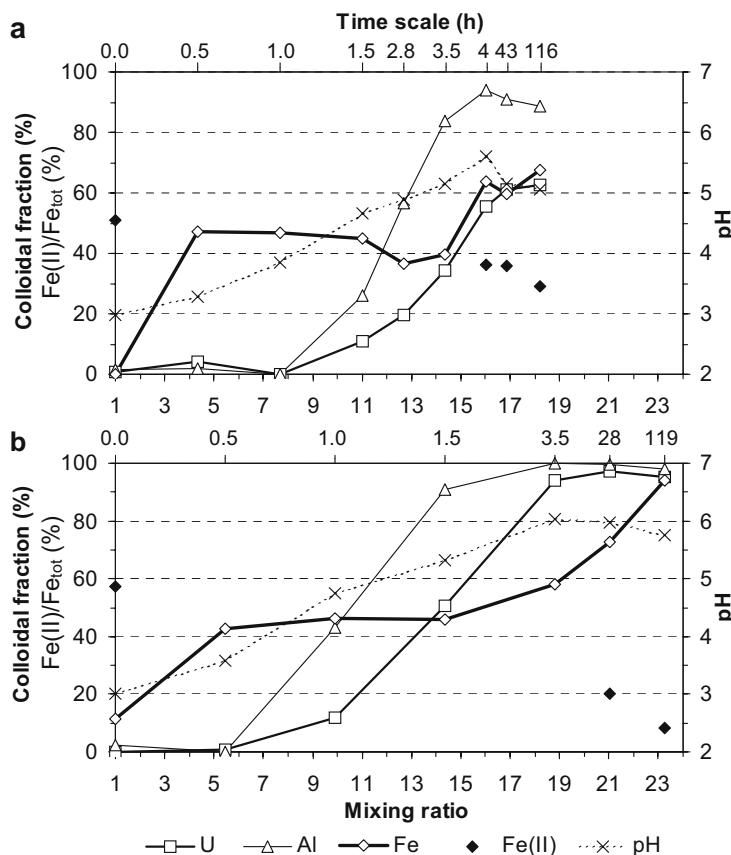
The first series of experiments checked the influence of sulfate and silicate on

Table 1. Analysis of floodwater (Königstein mine, Nov. 2003) and groundwater from an adjacent aquifer (E_H in mV, electrical conductivity in mS cm^{-1}, concentrations in mg L^{-1}).

Parameter	Floodwater	Groundwater	Parameter	Floodwater	Groundwater
pH	2.85	6.50	[Fe(II)]	192	2.4
E_H	480	290	[Fe(III)]	84.0	0.8
EC	2.09	0.255	[K]	3.8	1.6
[O_2]	0.4	6.6	[Mg]	17.2	3.1
[TIC]	10.5	15.1	[Mn]	12.4	0.012
[TOC]	1.3	0.33	[Na]	25.2	4.9
[SO_4^{2-}]	1260	64.8	[Si]	5.4	1.7
[Al]	41.8	0.50	[U]	16.3	0.005
[Ca]	122	35.5	[Zn]	13.0	0.116

U(VI) sorption. Precipitates of colloidal ferrihydrite (Fh) were prepared from solutions of 1 mM Fe(NO$_3$)$_3$·9H$_2$O, 10 mM NaNO$_3$ (background electrolyte), and 12 µM UO$_2$(NO$_3$)$_2$ in the presence of either sulfate or silicate or both anions at ambient air atmosphere (pCO$_2$=10$^{-3.8}$ atm). Table 2 gives the initial concentrations and the ion uptake by the colloids.

A second series of experiments checked the contribution of carbonate to U(VI) sorption. Fh was prepared from solutions of 1 mM $FeCl_3 \cdot 6H_2O$, 15 mM NaCl as background electrolyte, and varied concentrations of UO_2Cl_2 added both at ambient air atmosphere ([U] = 0, 6, 12, 30, 50, 75, 100 µM) and in a N_2-purged glove box ([U] = 0, 12, 100 µM) with [CO_2] <2 ppm. To initiate the formation and aggregation of Fh colloids, 1 M or 0.1 M NaOH solution was added under vigorous stirring until pH 5.5 or pH 8.0 was reached. Control and re-adjustment of the pH were done after 6, 12, and 24 hours. After having reached equilibrium within 24 h, the aggregated colloids were allowed to settle for 65-70 h and then concentrated to a wet paste by ultra-centrifugation (285,000 g; 30 min). This paste was transferred into a polyethylene vial designed for use on a cryostat sample holder and stored in liquid N_2 until the measurement to avoid sample alteration.

Fig. 2. Percentage of colloidal U, Al, Fe (based on 3 kD ultrafiltration), $Fe(II)/Fe_{tot}$ fraction (left ordinate) and pH (right ordinate) as functions of mixing ratio (lower abscissa) and time (upper nonlinear abscissa) in two flooding simulation experiments MW1 (a) and MW2 (b).

Analytical speciation techniques for uranium and related elements

Table 2. Initial concentration and uptake (based on 3 kD ultrafiltration) of sulfate, silicate, and uranyl by colloidal ferrihydrite in the sorption experiments at final pH 5.5.

Sample	Initial concentration (mM)			Uptake (%)		
	$[SO_4^{2-}]$	$[Si(OH)_4]$	$[UO_2^{2+}]$	SO_4^{2-}	$Si(OH)_4$	UO_2^{2+}
A	1.2	-		7.6	-	98.2
B	4.8	-	0.012	3.5	-	95.6
C	-	0.075	0.012	-	66.5	99.4
D	-	0.3	0.012	-	63.2	98.9
E	-	1.2	0.012	-	32.4	98.3
F	1.2	1.2	0.012	5.2	34.2	99.2
G	4.8	0.3	0.012	4.8	31.8	96.3

EXAFS study
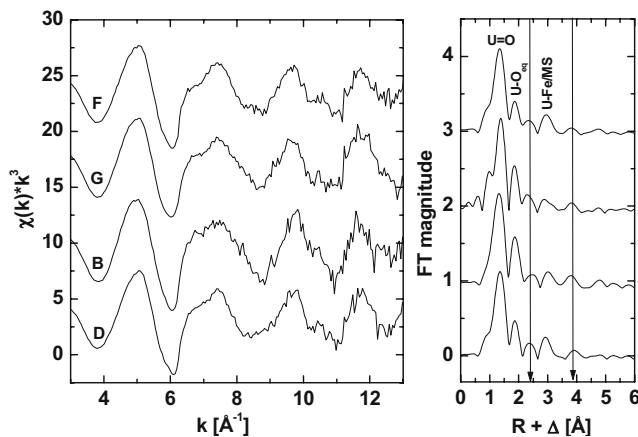
EXAFS spectroscopy at the U-L$_{III}$ absorption edge (E$_0$=17185 eV) enables an element-specific detection of the type, number, and distance of atoms surrounding the U atom up to a radius of ~6 Å (Teo 1986). The measurements were carried out at the Rossendorf Beamline (BM20) located at the European Synchrotron Radiation Facility in Grenoble using a He cryostat (~30 K). Since the relaxation of an excited core electron produces X-ray fluorescence which can be detected more sensitively at low U concentrations, a solid-state 13-element germanium fluorescence detector was used. Energy calibration was based on the X-ray absorption of an yttrium foil. For statistical reasons 6-8 spectra of each sample were averaged. The codes EXAFSPAK, WINXAS 3.0, and FEFF 7.02 were applied for data processing including dead-time correction of the fluorescence signal, shell fitting, and *ab initio* calculation of backscattering phase and amplitude functions. Further data refinement was achieved by a Monte-Carlo approach (Rossberg and Scheinost 2005).

The first approach of shell fitting explained the two highest peaks of the Fourier transforms (FTs) in Figs. 3 and 4 (right) and Fig. 5 (left) by two axial O atoms (U=O) of the UO_2^{2+} cation as nearest neighbors of the U atom, and by 5±1 O atoms of the -OH/H$_2$O hydrate shell in the equatorial plane (U-O$_{eq}$). Another prominent peak at R+Δ~2.9 Å is mainly explained by the backscattering contribution of one Fe atom, including also a small contribution of the U=O multiple scattering (MS) amplitude. This result strongly suggests the binding of the UO_2^{2+} cation to the Fe hydroxide surface by a bidentate inner-sphere complex. Two minor peaks at R+Δ~2.4 Å and ~3.8 Å (indicated by arrows in Fig. 3, right) remained unexplained. Since these FT peaks were visible in all spectra of the first series of sorption experiments, and also appeared in the absence of sulfate and silicate (Fig. 4A), S and Si could be excluded as backscattering atoms. Hence sulfate and silicate are not involved in the inner-sphere surface sorption complex of uranyl.

In the second series of sorption experiments the contribution of carbonate to the U sorption on Fh at pH 5.5 and 8.0 was examined. The EXAFS spectra of the

samples prepared in presence and in absence of CO_2 were fairly alike (Fig. 4). However, in the case of pH 8.0, the FT of the calculated difference spectrum showed a noticeable backscattering contribution to the peaks at R+Δ~2.4 Å and ~3.8 Å. The first peak is explained by a carbon shell and the second by the backscattering of a distal carbonate O atom, supporting bidentate coordination of carbonate in the equatorial plane of UO_2^{2+}. This result at pH 8.0 suggests sorption of a ternary U(VI) carbonato complex on Fh. At pH 5.5 the backscattering contributions of bidentately coordinated carbonate are not visible in the difference spectrum, possibly because the concentration of these ternary complexes is below the limit of detection. It cannot be ruled out that substantial portions of monodentately bound carbonate are present at the lower pH, because the detection limit of such backscattering contributions is higher than for bidentately coordinated carbonate.
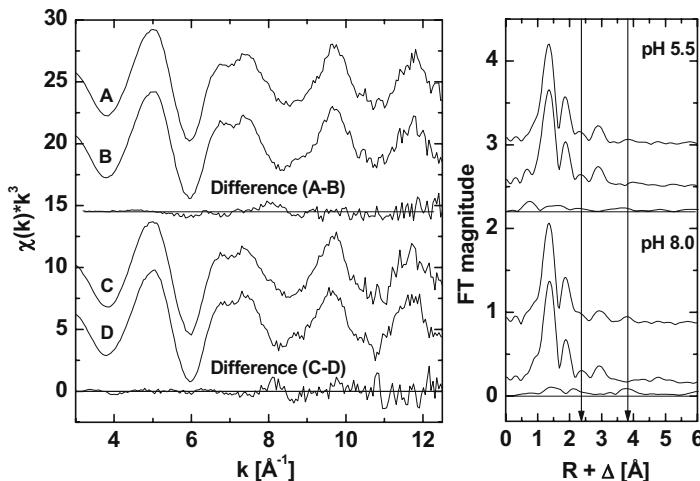
Since the FT peak at R+Δ~2.4 Å was also observed for samples where great care had been taken to keep the system carbonate-free, the Monte-Carlo approach (Rossberg and Scheinost 2005) was used to test whether the experimental EXAFS spectra could be explained by uranyl adsorption on crystallites of hematite. The local hematite structure was chosen because EXAFS data from the Fe-K absorption edge supported the existence of face-sharing linkages between Fe octahedra which are characteristic of hematite and also occur in 2-line ferrihydrite (Janney et al. 2000). The resulting structural model (Fig. 5 right) indicates UO_2^{2+} bidentately bound to a FeO_6 octahedron with atomic distances of $R_{(U-O)}$~2.30 Å and $R_{(Fe-O)}$ ~2.21 Å, yielding a distance of 2.88 Å to an edge-shared O atom of an adjacent FeO_6 octahedron. This model includes the first Fe shell at a distance of 3.46 Å and predicts a second Fe shell at a distance of 4.35 Å which tightly fits the experimental data and is represented by the small FT peak at R+Δ~3.8 Å (Fig. 5 left).
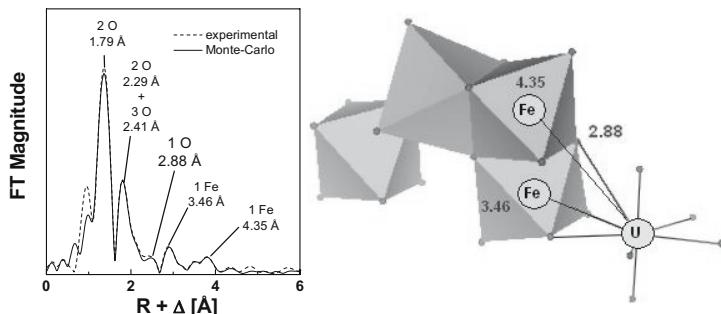
Fig. 3. U-L_{III} EXAFS spectra and FTs of four selected colloid samples (pH 5.5; cf. Table 2).

ATR-FTIR spectroscopy

The ATR technique provides direct acquisition of FTIR spectra of freshly ultra-centrifuged colloid pastes without further treatment. The respective supernatants of the concentrated colloid samples were used to record spectra for background correction. For each spectrum shown in Fig. 6, 128 scans were accumulated at a spectral resolution of 4 cm^{-1}.

Fig. 4. U-L$_{III}$ EXAFS spectra and FTs of precipitated Fh colloids on which 12 μM UO$_2^{2+}$ adsorbed at pH 5.5 (A+B) and pH 8.0 (C+D) at ambient air (A+C) and N$_2$ atmosphere (B+D). Calculated difference spectra (A-B) and (C-D) and their FT magnitudes also shown.

Fig. 5. U-L$_{III}$ EXAFS-FT of a colloid sample from the mesocosm experiment (Fig. 2b) where carbonate was not detectable in solution at pH 5.5. The values in Angstrom above the peaks indicate the interatomic distances after phase shift correction, fitted by the Monte-Carlo approach (Rossberg and Scheinost 2005). A tentative structural model is shown on the right.

The spectrum of pure Fh prepared at pH 5.5 in NaCl matrix and N_2 atmosphere shows a broad absorption band around 937 cm^{-1} representing the $\delta(OH)$ bending vibration of the Fh phase (Fig. 6A middle). The spectra of samples containing uranyl ions exhibit an additional band around 903 cm^{-1}, the intensity of which correlates with increasing UO_2^{2+} concentration (Fig. 6C-E middle). This band represents the antisymmetric (ν_{as}) stretching vibration of UO_2^{2+} adsorbed to the Fe hydroxide phase. The assignment to dissolved UO_2^{2+}-carbonato or -hydroxo complexes can be ruled out since these compounds are known to excite bands at substantially higher wavenumbers (> 920 cm^{-1}).
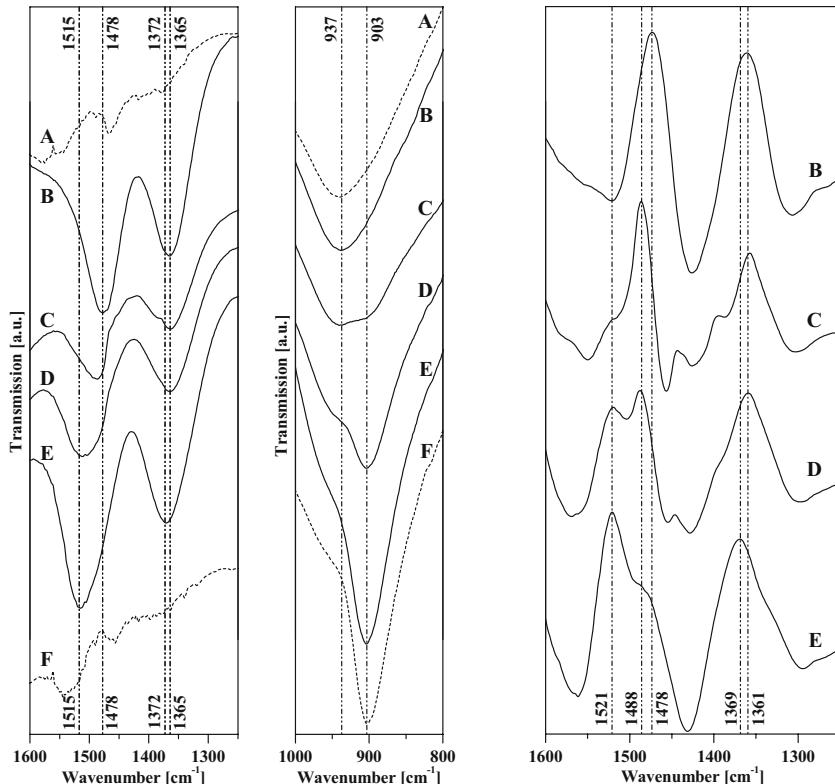
The spectra of the samples prepared at ambient air atmosphere show additional bands around 1365 and 1500 cm^{-1} (Fig. 6B–D left) which are due to the symmetric (ν_s) and antisymmetric (ν_{as}) stretching vibration of carbonate (CO_3^{2-}) anions bound to the colloidal phase, respectively. These bands show a continuous shift to higher wavenumbers with increasing UO_2^{2+} concentration. In particular the frequency of the $\nu_{as}(CO_3^{2-})$ vibration shifts from 1478 to 1515 cm^{-1}, the latter being reached by the sample with initially 100 µM UO_2^{2+}. A similar, but smaller effect is observed for the $\nu_s(CO_3^{2-})$ vibration ($\Delta\nu \sim 7$ cm^{-1}; Fig. 6E left).

To elucidate the peak positions of overlapping carbonate bands, the second derivatives (SD) of the transmission spectra were calculated in the spectral region of 1600-1250 cm^{-1} (Fig. 6 right). SD maxima indicate the peak positions of components underlying the transmission bands. A comparison of the SD spectra of pure Fh (Fig. 6B right) and of Fh prepared in presence of 100 µM UO_2^{2+} (Fig. 6E right) again shows a clear difference in the spectral position of the $\nu_{as}(CO_3^{2-})$ mode. Another maximum appears at 1488 cm^{-1} in the SD spectrum of Fh prepared in presence of 50 µM UO_2^{2+} (Fig. 6D right), and forms the dominant maximum in the SD spectrum of the sample prepared in presence of 12 µM UO_2^{2+} (Fig. 6C right).

The FTIR results show that the axial O atoms of the UO_2^{2+} sorption complex on Fh are not affected by the presence of CO_2 or HCO_3^- in the system, since the frequency of the $\nu_{as}(UO_2^{2+})$ mode is unaltered compared to the spectra recorded in absence of CO_2. A coupling of carbonate *via* the axial O atoms is expected to induce a shifting of the $\nu_{as}(UO_2^{2+})$ band (Čejka 1999).

In contrast, the Fh-carbonate interactions were strongly influenced by the presence of UO_2^{2+}. Mono- or bidentate binding of carbonates to metal complexes can be distinguished by the degree of splitting of the ν_{as} and $\nu_s(CO_3^{2-})$ modes (Lefèvre 2004). The spectra of pure Fh show a splitting of ~115 cm^{-1} (Fig. 6B left) which can be interpreted as monodentate binding of the CO_3^{2-} anions to the mineral phase (Lefèvre 2004, Bargar et al. 2005). In the presence of uranium this splitting expanded to 150 cm^{-1} at pH 5.5 (Fig. 6D, E) and 160 cm^{-1} at pH 8.0 (data not shown). For instance, a band splitting of ~190 cm^{-1} was found for the bidentate binding of CO_3^{2-} to the equatorial hydrate shell of UO_2^{2+} in the mineral Andersonite, $Na_2Ca[UO_2(CO_3)_3]\cdot6H_2O$ (Amayri et al. 2004). Since solutions in equilibrium with air exhibit substantially higher HCO_3^- concentrations at pH 8.0 than at pH 5.5, and since the EXAFS data support bidentate sorption of carbonate to uranyl at pH 8.0, the band splitting of ~160 cm^{-1} may reflect a dominance of surface complexes with bidentate coordination of carbonate and uranyl. In contrast, the band splitting of ~125 cm^{-1} (Fig. 6C right) suggests another surface complex,

most likely with monodentate coordination of carbonate and uranyl. Nevertheless, the shifting of the carbonate band positions already at low UO_2^{2+} concentrations shows that ternary carbonato complexes contribute to the sorption of uranium on Fh at pH 5.5.

Fig. 6.   ATR-FTIR spectra of the Fh-UO_2^{2+} samples prepared at pH 5.5. The samples were prepared in N_2 atmosphere (A, F) and in air atmosphere (B–E). Left panel: region of the carbonate stretching vibrations. Middle panel: region of the uranyl stretching vibration. Right panel: second derivative spectra of the carbonate stretching region. The initial UO_2^{2+} concentrations were as follows: 0 μM (A,B); 12 μM (C); 50 μm (D); 100 μM (E, F).

Conclusion

Two spectroscopic approaches (EXAFS and ATR-FTIR) were applied on samples to identify the binding of uranyl on colloids formed during the experiment of simulated mine flooding. The experiments yielded the following results:

- Even though matrix anions such as sulfate or silicate were present in significant concentrations, these ions were not involved in the UO_2^{2+} adsorption on colloidal ferrihydrite at moderately acidic conditions.
- In absence of carbonate, the EXAFS data require a modification of the common structure of the binary, edge-shared inner-sphere surface complex of UO_2^{2+} and ferrihydrite in that the U atom has a neighbored oxygen atom at a distance of ~2.9 Å, provided by two edge-shared FeO_6 octahedra.
- At pH 5.5, low uranyl and air-equilibrated carbonate concentrations favor the sorption of ternary mononuclear complexes on Fh, most likely with monodentate coordination of carbonate and uranyl, as shown by the ATR-FTIR results.
- At pH 8.0, the same experimental conditions suggest a contribution of ternary mononuclear sorption species with bidentate coordination of carbonate and uranyl as derived from EXAFS measurements.
- At both pHs, FTIR spectra of samples with initially higher U concentrations (0.1 mM) and air-equilibrated carbonate concentration suggest a dominance of ternary sorption species with bidentate coordination of carbonate and uranyl.

Our next research step will focus on the stability of uranium binding during the transformation of colloids into sediments and crusts and during the aging of the metastable ferrihydrite into more crystalline iron minerals. The question of binding stability (reversibility *vs* irreversibility) is crucial for the role of colloids in uranium(VI) transport (cf. Fig. 1).

Acknowledgements

References

Allard T, Ildefonse P, Beaucaire C, Calas G (1999) Structural chemistry of uranium associated with Si, Al, Fe gels in a granitic uranium mine. Chem Geol 158: 81-103

Amayri S, Arnold T, Reich T, Foerstendorf H, Geipel G, Bernhard B, Massanek A (2004) Spectroscopic characterization of the uranium carbonate andersonite $Na_2Ca[UO_2(CO_3)_3]\cdot6H_2O$. Environ Sci Technol 38: 6032-6036

Bargar JR, Reitmeyer R, Davis JA (1999) Spectroscopic confirmation of uranium(VI)-carbonato adsorption complexes on hematite. Environ Sci Technol 33: 2481-2484

Bargar JR, Kubicki JD, Reitmeyer R, Davis JA (2005) ATR-FTIR spectroscopic characterization of coexisting carbonate surface complexes on hematite. Geochim Cosmochim Acta 69: 1527-1542

Čejka J (1999) Infrared Spectroscopy and Thermal Analysis of the Uranyl Minerals. In Uranium: Mineralogy, Geochemistry and the Environment. The Mineralogical Society of America, Washington

Hsi CKD, Langmuir, D (1985) Adsorption of uranyl onto ferric oxyhydroxides: Application of the surface complexation site-binding model. Geochim Cosmochim Acta 49: 1931-1941

Janney DE, Cowley JM, Buseck PR (2000) Structure of synthetic 2-line ferrihydrite by electron nanodiffraction. Amer Mineralogist 85: 1180-1187

Lefèvre G (2004) In situ Fourier-transform infrared spectroscopy studies of inorganic ions adsorption on metal oxides and hydroxides. Adv Colloid Interface Sci 107: 109-123

Rossberg A, Scheinost AC (2005) Linking Monte Carlo simulation and Target Transformation Factor Analysis: A novel tool for the EXAFS analysis of mixtures. Physica Scripta T115: 912-914

Schwertmann U, Friedl J, Stanjek H (1999) From Fe(III) ions to ferrihydrite and then to hematite. J Colloid Interface Sci 209: 215-223

Teo BK (1986) EXAFS: Basic principles and data analysis. Inorganic Chemistry Concepts 9, Springer Berlin

Waite TD, Davis JA, Payne TE, Waychunas GA, Xu N (1994) Uranium(VI) adsorption to ferrihydrite: Application of a surface complexation model. Geochim Cosmochim Acta 58: 5465-5478

Influence of allochthonous plant litter on the fixation of Uranium in sediments

Holger Dienemann, Claudia Dienemann, E. Gert Dudel

Technische Universität Dresden, Institut für Allgemeine Ökologie und Umweltschutz, Pienner Straße 8, 01737 Tharandt, Germany,
E-mail: h_dienemann@yahoo.de

Abstract. Plant litter of *Alnus glutinosa* (L.) GAERTNER (alder) and *Quercus spec.* (oak) was investigated downstream an abandoned uranium mine tailing. Uranium concentrations in unwashed samples varied between 20 – 2000 $\mu g*g^{-1}*DM^{-1}$ with differences between plant compartments: wood (app. 50 $\mu g*g^{-1}*DM^{-1}$), leaves (app. 200 – 400 $\mu g*g^{-1}*DM^{-1}$) and alder cones (app. 700 $\mu g*g^{-1}*DM^{-1}$). Compared to leaves from oak alder leaves contain significantly more uranium. Washing partially removes attached particles from the leaf surface. Uranium concentrations in unwashed alder leaves were usually smaller than in washed samples (<2000$\mu g*g^{-.1}*DM^{-1}$).

Introduction

After World War II various dumps and tailings were formed in Saxony and Thuringia as a result of uranium mining activities. Contaminated mining- and seepagewateremerge up until today (Merkel et al., 1998) from many of those. In some cases this leads to the development of natural wetlands (in East Germany e.g. in Schneckenstein, Lengenfeld, Johanngeorgenstadt, Neuensalz).

It is known that uranium may precipitate in the course ofreduction processes e.g. mediated by sulfur reducing bacteria (Dybeck, 1962). But it has to be considered that the decay of organic matter releases carbon dioxide.Especially in the form of carbonate in a neutral to alkaline milieu this is able to form complexes with uranium and thus transfer it into solution. In the past numerous experimentson biosorption of uranium onto various materials like yeast etc. were carried out (Golab et al., 1991; Bustard et al., 1997). However, in natural wetlands permanent decay causes continuous change of surfaces, hencelab results are not applicable.

Therefore the question of uranium fixation on plant litter in natural systems still remains.

Material and methods

Sampling sites in Saxony (Neuensalz Tailing Mechelgrün/Vogtland) were chosen based on the German "Altlastenkataster (A.LAS.KA; Altlastenkataster = Register of old neglected deposits of toxic waste)" as well as on hydrological and geological maps. The selected sites have local activity concentrations higher than 1 Bq*g^{-1} *DM^{-1} in sediments and uranium concentrations in seepage-water higher than 20 µg L^{-1}.
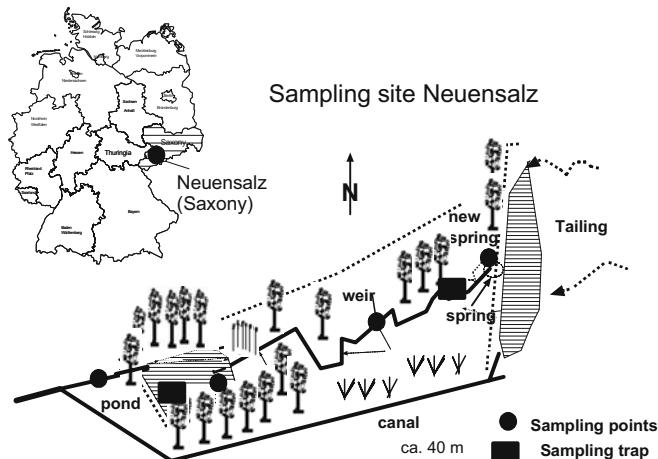
Two sampling points are located in a pond called "Forellenteich" (app. 1000m²), the more western point being a sediment trap (size 750x250x100mm, exposition time: June-August 2003). By the trap mainly leaves of alder s.a. were collected along with some few oak leaves.

Leaves and cones or acorns respectively of oak and alder were gathered at the sampling points. Unwashed leaf samples were carefully removed from the trap using plastic tweezers. Some samples had to be cleared of invertebrates, snails and algae.

Leaf-surfaces of washed samples were thoroughly rinsed 5 times with aqua dest. Acorns (were cut in halves, one half being the unwashed part. The other half was cleaned carefully with a toothbrush.

All samples were air-dried to constant weight (dry matter). Litter samples were mineralised using HNO3/H2O2, sediment samples using HNO3/HCl in a pressure- and temperature-controlled microwave system (Mars 5, CEM, U.S.A.).

PH-values were measured directly in the field (TM 39, Meinsberg). All water

Fig. 1.   Sampling site Neuensalz (schematic) with sampling points (weir: gauge station)

Analytical speciation techniques for uranium and related elements

samples were filtered within 24 hours through 0.45 μm membrane filters (cellulose nitrate, Sartorius, Göttingen) and acidified with HNO3. Uranium, lead and arsenic were analysed by ICP-MS (PQ2+, TJA, U.K). Anions were measured ursing ion-chromatography (DX-500, AS 14).
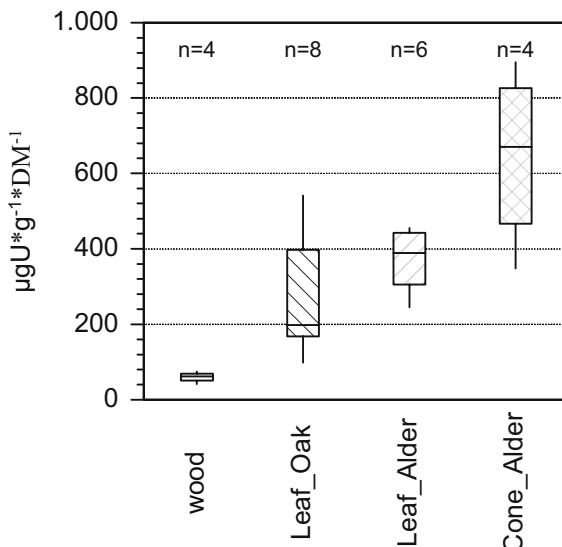
Results

Based on pH-values water within the sampling site can be classified as neutral to slightly alkaline (pH 7.5-8.5) with a conductivity of about 1000 $\mu S*cm^{-2}$. Nitrate concentrations in the pond range between $15 - 30$ mgL^{-1}, uranium concentrations below the tailing between 150-250 μg L^{-1}.

A temperature gradient between (sampling points) "new spring" (11.5 °C) and "weir" (6,9 °C) can be seen in December 2003. This is caused by mine waters leaving the ground at a relatively constant temperature of app. 12 °C cooling down as it flows.

Uranium in litter from different plant species and plant compartments

Uranium concentrations in the litter differ nearly one order of magnitude between different plant compartments selected form the sediment (see Fig 2) where at the same time variation within each compartment is high. The concentration between leaf from oak and alder is not very, but the median of all alder leaf samples is a little higher than the median of oak leaves.

Fig. 2.   Uranium content in unwashed plant samples the Forellenteich (July 2003).

Analytical speciation techniques for uranium and related elements

A comparison between cones (alder) and acorn shells is difficult, because they both fall at different times. Unwashed acorn shells in April (after an exposition time of 5 ½ months, similar to the alder cones) contain less uranium (Acorns: median 100 $\mu g*g^{-1} *DW^{-1}$).
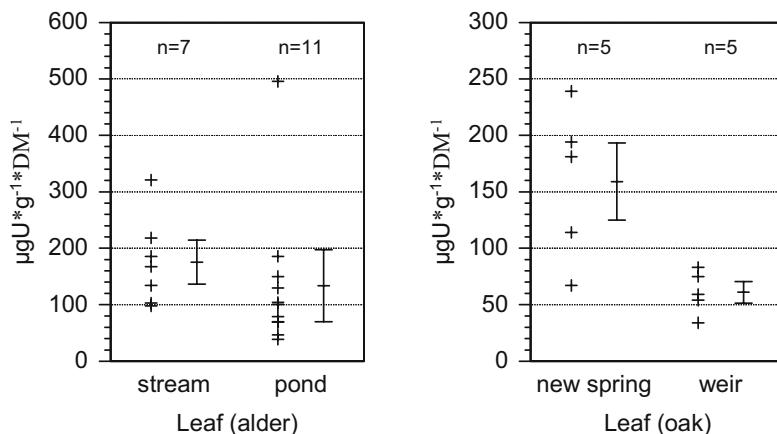
Distribution of uranium in the sampling aera

Geochemistry uses catena for proving emissions of uranium from dumps or along seepage-water paths as well as the elimination potential for e.g. nitrate. Uranium concentration in leaves from alder and oak of different sampling points are shown in Fig. 3. The distance between the point in the stream and the pond is app. 160 m, (a) between new spring and weir app. 150 m (b).
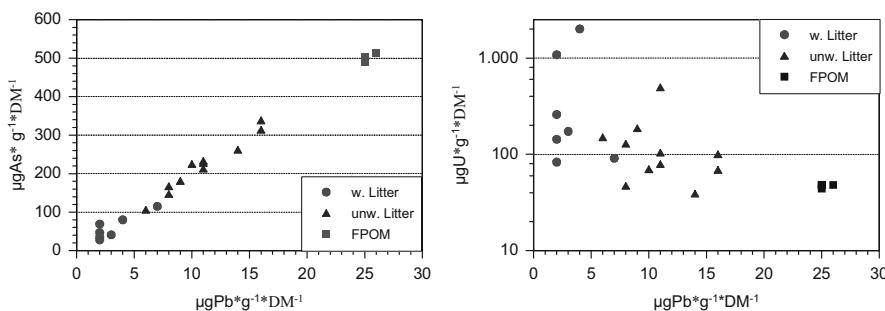
Fig. 3 suggests a otherwise: there seems to be a coherence/connection between between the distance from the source and the uranium concentration in the plant litter. This correlation seems stronger for oak leaves (Fig.3b) from spring and weir than for alder leaves from stream and pond.

Distribution of uranium in and on plant litter

Uranium and arsenic both can be precipitated by HFO (HydroFerricOxide). Hydrochemically arsenic and uranium often react antagonistically. Due to high iron content with great variations in leaves it is difficult to find a reference for this micro nutrient. In opposition to iron lead is only scarcely transported into wood and leaves by the investigated plants. Lead is known to have a high affinity to organic

Fig. 3.   a) Uranium concentrations in unwashed alder leaves from traps in the stream and in the pond "Forellenteich", exposition time tree months: June – August 2003) and b) in unwashed oak leaves from new spring and weir (December 2003).

Analytical speciation techniques for uranium and related elements
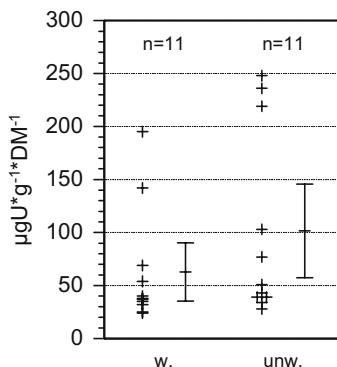
Fig. 4.   Contents of uranium and arsenic in unwashed and washed alder leaves (dry matter) and in FPOM (fine particular organic material) (trap in "Forellenteich", summer 2003).

substance, hence it is enriched in organic layers. So a removal of lead by washing processes would hint the existence of attached particles and. biofilms. Fig. 4 shows the concentrations of As and Pb as well as Pb and U for washed and unwashed samples as well as in the FPOM (fine particular organic matter). Arsenic and lead display a clear correlation.

Uranium shows a different behaviour. Highest uranium concentrations were found in washed leaves (2000 $\mu gU*g^{-1}$) and there is no positive correlation between lead and uranium. Uranium contents in FPOM are even smaller than in the leaves.

A comparison of washed and unwashed acorns is shown in Fig. 5. In difference to leaves acorns have a "closed " surface, their structure can rather be compared with wood (see Fig. 2).

Acorn shells displayed in Fig. 5 contain significantly more uranium than wood. The uranium concentration in washed (cleaned) samples is distinctly lower than in unwashed samples.

Fig. 5.   Uranium concentrations in washed and unwashed acorn shells (April 2004).

Analytical speciation techniques for uranium and related elements

Discussion

Aboveground parts of trees scarcely take up uranium (Stoklasa 1932, Thomas 2000, Brackhage and Dudel 2002). For alder this was confirmed by Brackhage et al. (2004) in the same site. Compared to plant litter on dumps (Schlema; Diene-mann et al. 2002) the here found plant litter samples had a 10power higher ura-nium content, which leads to the conclusion that uranium contamination is based on contact with water or sediment.

   Selected processes which may lead to an enrichment of uranium in plant litter are discussed in the following:

(1) If contact with sediment and thus the sorption of ore particles were the main process washed samples should generally contain less uranium than unwashed samples. This is definitely not true for the trap-samples from the pond. In op-position to uranium lead and arsenic show a distribution as expected. How-ever, this might be caused by an loosely attached biofilm which was removed by the washing process.

(2) Arsenic and uranium both could be bound onto iron hydroxides by co-precipitation. Here arsenic shows a higher affinity to HFO. However, since arsenic concentrations in alder leaves could obviously be reduced by washing processes (Fig. 4) while uranium concentrations were not influenced, this fixation can be excluded.

(3) On the surface of a biofilm there might be an oxidative milieu which could arsenic cause to be fixed. Within the biofilm conditions are reducing (Smith 2001). Thus U(VI) might be reduced to U(IV), which might precipitate (Brooks et al. 2003, Bender et al. 2000). But even this does not provide a sat-isfying explanation for the differences between washed and unwashed sam-ples.

(4) Possibly all results could be caused by sorption (see Kalin et al., 2005). How-ever, during decay surfaces constantly change so the sorption conditions un-dergo a constant change and it seems unlikely for uranium to stay attached all the time under changing conditions. Maximum uranium concentrations of al-most 2 mgU*g^{-1} and extremely high standard deviation in the washed as well as in the unwashed samples from the trap in the pond supports the assumption of uranium precipitation.

(5) The reducing effects of tannic acids have been used for centuries in leather treatment. According to the Japanese patent JP2001235593 uranium com-pounds may be reduced by tannic acid. According to another Japanese patent (JP2038316) uranium can be won using acorns (in neutral to alkaline milieu).

      Unwashed acorn contain more uranium than washed acorns (in opposition to alder leaves) Since oak leaves contain more tannic acid than alder leaves, the influence of tannic acid cannot be the main process responsi-ble for uranium fixation in neutral to basic milieu. Uranium concentra-tions in oak leaves were significantly smaller than in alder leaves just as acorn shells contained less uranium than alder leaf litter.

(6) An explanation for higher uranium contents in alder leaves compared to oak leaves could be the different surface. Another distinction between the leaves is the decay rate. Several scientists show alder leaves to decompose relatively fast (Gessner 1991, Sridhar et al. 2001). One possible explanation could be the C/N-ratio as discussed in Schönbrunn (1992). Among others, temperature has a major impact on the decay rate. Measurements showed temperature at the spring to be always distinctly higher than at the weir. This may accelerate microbial turnover processes. Hence the smaller uranium concentrations in oak leaves found at the weir could be caused by differing microbial community. Altogether this process offers the opportunity to discuss the order of uranium concentrations between unwashed samples like wood, oak leaves and alder leaves.

(7) This order could also be explained by direct microbial reduction of uranium in plant litter. For this process, different surfaces of leaves and wood are important. But then, the inhibition of microbial decay of oak litter and pine litter by organic substances is known for years.

Different authors prove a massive uranium enrichment by *Pseudomonades* - (Tawfik et al. 2005; Fritsche 1985). Their appearance in plant litter as well as in sediment has been described by Fritsche (1985). Other bacteria like *Geobacter metallireducens, Desulfovibrio desulfuricans, Shewanella putrefaciens* and *Clostridium sp.* are known for the ability to reduce and precipitate uranium(VI)compounds (Lovley et al., 1991, 1992, 1993a, 1993b; Francis et al. 1991, 1994; Payne et al., 2004). Suzuki and Banfield (1999) show many fungi to contain even more uranium than bacteria. This might also be applicable for aquatic hyphomycetes. Gessner and Chauvet (1993) and Schönborn (1992) proved aquatic hyphomycetes to play a key role at decomposition processes.

(8) Alder cones consist of a relatively nutrient rich seed and a relatively stable cone. It is possible that the seed itself is faster decayed in permanent ponds or streams. There is an obvious pH-gradient due to decay. (Furthermore, decay sets free fulvic and humic acids, which precipitate with uranium to fulvates and humates. Borstel (1984) assumes this may be a way of enriching uranium in coals.

Conclusion

It is essential for radiological measurements of subhydric humus layers to investigate them separated from the sediment below, where extremely high activities (> 10 Bqg^{-1}) may occur.

Besides restrictions for use and access of concerned water-bodies it is necessary to create rules for sediment clearing regarding the radiological aspects. An application of these results could lead to more effective passive water treatment facilities.

Acknowledgement

References

Bender J., Duff M.C., Phillips P., Hill M. (2000). "Bioremediation and bioreduction of dissolved U(VI) by microbial mat consortium supported on silica gel particles." Environmental Science & Technology 34(15): 3235-3241.

Borstel v. D. (1984) Bindungsformen vvon Uran in kohligen Ablagerungen von Sedimenten unterschiedlichen Diagenesegrades. Disseration TU Clausthal

Brackhage C., Dudel E.G. (2002) Long-term differences in transfer and accumulation of potentially toxic trace elements and radionuclides in trees on uranium mining dumps (Erzgebirge, Germany). In: Merkel B.J., Planer-Friedrich B., Wolkersdorfer C. (Ed.): Uranium Mining and Hydrogeology III including the International Mine Water Association Symposium 15.09.-21.09.2002 Freiberg / Germany 471-479

Brackhage C., Scholz O. Dudel E.G. (2004) The role of rhizofiltration and compartimentation in the removal of uranium and heavy metals from mining leachates using wetlands. 7th Intecol International Wetlands Conference, Utrecht. S.41

Brooks S.C., Fredrickson J.K., Carroll S.L., Kennedy D.W., Zachara J.M., Plymale A.E., Kelly S.D., Kemner K.M., Fendorf S. (2003). Inhihition of bacterial U(VI) reduction by calcium. Environmental Science & Technology 37(9): 1850-1858

Bustard M., McHale P.M. (1997) Biosorption of uranium by cross-linked and alginate immobilized residual biomass from distillery spent wash. Bioprocess Eng 17: 127-130

Dienemann H., Brackhage C., Dannecker A., Dudel E.G., Rotsche, J. (2002) Soil formation and quality on uranium mining dumos depending on different tree species under special consideration of seleted radionuclide contamination. In: Merkel B.J., Planer-Friedrich B., Wolkersdorfer C. (Ed.): Uranium Mining and Hydrogeology III including the International Mine Water Association Symposium 15.09.-21.09.2002 Freiberg / Germany 489-494

Dybek J. (1962) Zur Geochemie des Urans. Claustaler Hefte zur Lagerstättenkunde und Geochemie der mineralischen Rohstoffe. Heft 1

Francis A.J., Dodge C.J., Gillow J.B., Cline C.E. (1991) Microbial transformation of uranium in wastes. Radiochimica Acta 52-3: 311-316

Francis A.J., Dodge C.J., Lu F, Halada G.P., Clayton C.R. (1994) XPS and XANES studies of uranium reduction by Clostridium sp. Environ. Science Technol. 228: 636-639

Frritsche W. (1985) Umweltbiologie. Akademie-Verlag Berlin

Gessner M.O. (1991) Fallaubabbau im Fließgewässer: Dynamik aquatischer Hyphomyzeten und chemische Blattveränderungen. Dissertation. Albert-Ludwigs-Universität Freiburg

Gessner M.O., Chauvet E. (1993). Ergosterol-to-Biomass Conversion Factors for Aquatic Hyphomycetes. Applied and Environmental Microbiology 59(2): 502-507

Golab D.R., Orlowska B., Smith R.W. (1991) Biosorption of Lead and Uranium by Streptomyces Sp.. Water Air Soil Pollut 60: 99-10

Kalin M., Wheeler W.N., Meinrath G. (2005) The removal of uranium from mining waste water using algal/microbial biomass. J. Environ. Radioactivity 78: 151-177

Loveley D.R., Phlilips E.J.P., Gorby Y.A., Landa E.R. (1991) Microbialreduction of uranium. Nature 350: 413-416

Loveley D.R., Widman P.K., Woodward J.C., Phillips E.J.P. (1993). Reduction of uranium by cytochrome c3 of Desulfofibrio vulgaris. Applied Environ. Microbiol. 59: 3572-3576

Loveley D.R., Rden E.E., Phillips E.J.P., Woodward J.C. (1993b) Enzymatic iron an uranium reduction by sulfate-reducing bacteria. Marine Geol. 113: 41-53

Loveley D.R. and Phillips E.J.P. (1992) Reduction of uranium by Desulfofibrio desulfuricans. Environ.Science Technol. 26: 2228-2234.

Lutze W., Gong W. and Nuttall H.E. (2002) Microbially mediated reduction and immobilization of uranium in groundwater. In: Merkel B.J., Planer-Friedrich B., Wolkersdorfer C. (Ed.): Uranium Mining and Hydrogeology III including the International Mine Water Association Symposium 15.09.-21.09.2002 Freiberg / Germany 471-479

Macaskie L.E., Blackmore J.D., Empson R.M. (1988) Phosphatase overproduction and enhanced uranium accumulation by a stable mutant of a *Citrobacter sp*. isolated by a novel method. FEMS Microbiology Letters 55: 157-162

Merkel B.J., Preußer R., Namoun T., Gottschalk S., Kutschke S. (1998) Natural Leaching of Uranium from the Schneckenstein Uranium Mine Tailing. In: Merkel B.J. & Hellig C. (Eds) (1998): Uranium Mining and Hydrogeology II. Proc. of the Intern. Conference and Workshop, Freiberg, Germany, Verlag Sven von Loga, Köln

Payne T.E., Hatje V., Itakura T., McOrist G.D., Russell R. (2004). Radionuclide applications in laboratory studies of environmental surface reactions. Journal of Environmental Radioactivity 76(1-2): 237-251.

Smith W.-L. (2001) Hexavalent chromium reduktion and precipitation by sulfate-reducing bacterial biofilms. Enviromental Geochemistry and Health 23: 297-300

Schönborn W. (1992) Fließgewässerbiologie. Gustav Fischer Verlag Jena Stuttgart

Sridhar K.R., Krauss G., Barlocher F., Raviraja N.S., Wennrich R., Baumbach R., Krauss G.J. (2001) Decomposition of alder leaves in two heavy metal-polluted streams in central Germany. Aquatic Microbial Ecology 26(1): 73-80.

Stoklasa J., Penkava J. (1932) Biologie des Radiums und Uraniums. Berlin, Paul Parey Verlag.

Suzuki Y. and Banfield J.F. (1999). Geomicromicrobiology of uranium. In: Reviews in Mineralogy 38: 393-432. Uranium: Mineralogy, Geochemistry and the Environment; eds. P.C. Burns and R. Finch; Mineralogical Society of America

Tawfik Z. Abu-Shady M., Haytham M. (2005) Uranium uptake by some locally isolated and some reference bacterial species. Acta Pharm. 55 93-105

Thomas P.A. (2000) Radionuclides in the terrestrial ecosystem near a Canadian uranium mill - Part I: Distribution and doses. Health Phys 78(6): 614-624

Tanaka Y. (1993) Aerobic cellulolytic bacterial flora associated with decomposing *Phragmits communis* in a seawater lake. Hydrobiologia 263 145 – 154

Analytical speciation techniques for uranium and related elements

Advanced Investigations of Unconventional Uranium and Thorium Deposits by *In-Situ μ-*EDXRF Analysis

Antje Wittenberg, Ulrich Schwarz-Schampera

Bundesanstalt für Geowissenschaften und Rohstoffe, Stilleweg 2, D-30655 Hannover, E-mail: A.Wittenberg@bgr.de

Abstract. Exploration and identification of primary and secondary uranium and thorium enrichments can be facilitated by the μ-energy dispersive X-ray fluorescence (EDXRF) technique that allows the high resolution, *in-situ*, multi-element determination at the microscopic scale (10 to 100μm). EDXRF analysis is fast and useful for the identification of unconventional uranium and thorium deposits, the localisation of primary uranium and thorium minerals as well as secondary uranium- and thorium-bearing phases. A current project aims at the siting of uranium and thorium mineralisation in ores from the Witwatersrand Au (uraninite), Vergenoeg Fe-F (uraniferous monazite), and Palabora Cu (uranothorite) deposits.

Resource situation

Uranium deposits associated with unconformities at the base of Proterozoic sedimentary basins represent the most important type of uranium deposits of the world. Other uranium (and thorium) sources include sandstone deposits, hematite breccia complex deposits, quartz-pebble conglomerate deposits, vein-type deposits, intrusive deposits, volcanic and caldera-related deposits, metasomatite deposits, collapse breccia pipe deposits, and phosphorite deposits. Uranium is also produced as a by-product in other deposit-types, and elevated uranium contents in country rocks may be regarded prospective in the near future. At present, primary uranium production accounts for only about 50% of the annual consumption in the nuclear fuel cycle. Uranium prices have more than doubled since 2004, and worldwide demand and exploration activities are strongly growing. It has been estimated that 2004 uranium exploration expenditures in the Athabasca basin, which hosts world's most important uranium reserves, will be total more than 25 M$, almost double the year 2003 spending. Other countries renewed the interest in the

use of thorium in the nuclear fuel cycle. As a consequence, the increasing demand for uranium results in new exploration activities also on alternative uranium and thorium resources in many countries (e.g., China, India, Brazil). There is large potential for unconventional low grade but moderate to large scale uranium deposits. Low grade uranium deposits are quite often dominated by uraniferous thorianite that was regarded largely uneconomic in the past. Highly elevated uranium and thorium concentrations are associated with alkaline magmatic systems and hosted by uraniferous rare earth phosphates. The unaltered basement country rocks underneath the largest uranium deposits and elsewhere account for up to 60% of the uranium in these systems and uranium might be developed as a significant by-product from deposits of other commodities.

Methodology

The acquisition of solid phase geochemical data is time-consuming, requires challenging sample preparation techniques and results in loss of sample material. The development of non-destructive energy differentiated µ-X-ray fluorescence analysis (µ-EDXRF) provides the capability of acquiring high-resolution geochemical analyses from different types of geological materials. The sample preparation is minimized since no coating is necessary. Depending on the application, the effect of surface roughness can be neglected. The µ-EDXRF instruments allow relatively fast, continuous, and reliable spot analysis, line or area scans (mapping) of samples such as thin sections, flat hand specimens, as well as split cores, providing records of variations in the geochemical composition. The latter can be used in order to study element distributions even over wider structures and core length. The µ-EDXRF technique provides non-destructive, multi-element, µ-scale analysis of elements down to the trace concentration level.

Facilities

Two µ-EDXRF facilities by COX Analytical Instruments / Sweden based on X-ray fluorescence are in use at the BGR, the ITRAX™ X-ray microscope and the ITRAX™ geoscanner (Rammlmair et al. in press and therein). Both systems operate under normal air conditions using a 3 kW long fine focus Mo side-window tube. This allows for optimized analyses of different element groups.

- The ITRAX™ X-ray microscope using X-rays for element analysis, using an energy-dispersive Roentec™ UHV Dewar Si(Li)-detector. The element range includes all elements from Mg and heavier (Z > 12), with detection limits at the µg/g level. For most applications the tube runs with 45 kV and 30 mA having the capacity for the simultaneous detection of light and heavy elements. High sensitivity is obtained by the mounted Cox™ mono capillary X-ray optical unit of 100µm beam size. Typically, the step size equals the spot size of the capillary and a counting time of 500 or 1000 µs/spot are used. The data can be per-

Analytical speciation techniques for uranium and related elements

formed as point, line or accumulated spectra of an area. The measuring spot, and thereby the lateral analytical resolution, can be varied in the 10 – 100 µm range. The sample stage is designed to enable precise movement of the sample at steps of 10 µm. Based on analytical parameters, these spectra will be processed to present information on the semi-quantitative concentrations of the achieved elements at a single spot or resulting in element maps. The pixel size of the resulting map equals the spot size of the measurement. Almost any type of sample can be mounted on an x-y-z-stage allowing weight of several kilograms and an element mapping of sample sizes up to 250 x 300 mm.

- The ITRAX™ geoscanner allows for the characterization of the chemical composition along samples up to 750 mm in length. The X-ray beam focuses through a Cox™ flat-beam capillary optic of a rectangular cross-section of 250 µm x 22 mm. Because of the relative large beam size and high counting times (up to 120 seconds) and step sizes of 10 to 250 µm, the geoscanner is more sensitive than the ITRAX™ microscope. The X-ray fluorescence signal is detected by a Roentec XFlash® 2001 Detector. An X-ray line-scanning camera provides optical images of X-ray absorption by the sample at a defined thickness at a microscopic scale. The transmitted X-rays are recorded with an array of 1024 diodes, each 25 µm wide. The optical line camera system consists of a CCD color camera operating in line mode, synchronized with the stepper motor movement. The camera has 640 pixels/line and is equipped with a Schneider CM 120 BK COMPACT XENOPLAN lens system giving a field view of about 8 mm (depending on the chosen spacing) perpendicular to the scanning direction corresponding to 0.0125 mm/pixel (Cox Analytical Systems, pers. com).
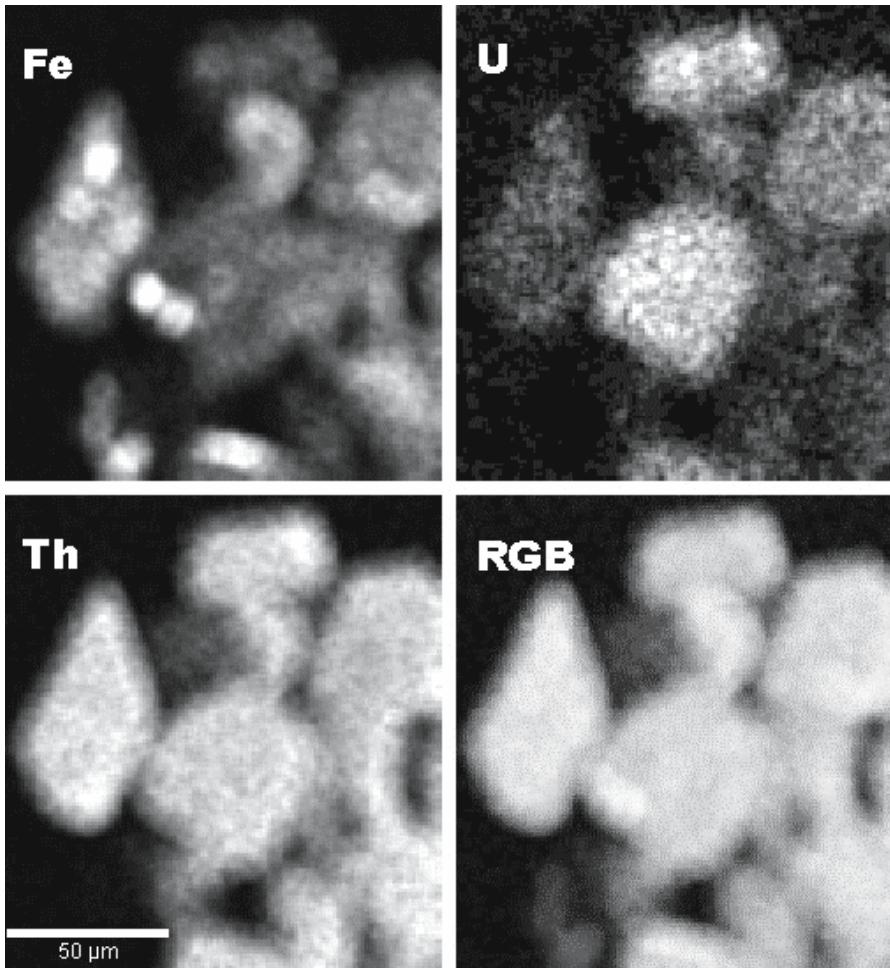
Measurements

Exploration and identification of primary and secondary uranium and thorium enrichments is greatly facilitated by the µ-EDXRF technique that allows the high resolution in-situ and simultaneous determination of a number of elements, combined with minimal sample preparation efforts (i.e., plain surface). Thus, ordinary thin or thick sections, as well as flat hand specimens can be used. This method is fast and optimized for the localization of primary and secondary uranium and thorium minerals and uraniferous mineral phases at concentrations of about 500µg/g to several weight percent of uranium and thorium.

A current project aims at the localization of uranium mineralization and the mineralogical siting in ores from the Witwatersrand Au (uraninite), Vergenoeg Fe-F (uraniferous monazite), and Palabora Cu (uranothorite) deposits.

Results

In order to optimize the technique for current research activities, electron microprobe mineral standards as well as a sample collection, studied in greater detail by electron microprobe (EMP) measurements, were used. The X-ray microscope measurements were performed at 45 kV and 30 mA with 500, 1000 and 2000 ms/spot and step sizes of 10, 50 and 100 µm. A thorite EMP-standard shows dis-

Fig. 1. Element maps of an EMP thorite standard (standard # 215-15 by Micro-Analysis Consultans™). Measurement was performed with a step size of 10µm. The intensity corresponds to the amount of the studied element at that particular point. The RGB color model was used in order to combine the single element maps. Color key: Fe – red; Th – green; U – blue; Fe + Th – yellow; Fe + U – violet; Th + U – turquoise; Fe + Th + U white.

Analytical speciation techniques for uranium and related elements

tinct inhomogeneous chemical distributions of uranium and thorium (Fig. 1), which are not specified within the recommended values. However, since the recommended values are specified only by EMP analysis, the observed mineralogical heterogeneity is very unlikely to be recorded. Additional measurements with a step size of 10 µm resulted in very detailed image resolution and allows for the study of the mineralogical distribution and siting.

Besides uranium and thorium mineral samples, a collection of samples from different ore deposits which hosts elevated to significant uranium and thorium concentrations of unknown distribution was investigated (Fig. 2). As an example, the distribution and compositional variability of uranothorianite from the Palabora carbonatite, South Africa, was studied (Neff 2003). The distribution of thorianite and its close association with the world-class copper and significant gold mineralization was clearly established. The distribution of uranium within the thorianite is heterogeneous and rather confined to distinct zones of secondary remobilization.

Concluding remarks

The *in situ* µ-EDXRF analysis is a suitable, fast and valid technique that can be used to localize uranium and thorium mineralization and low-grade uranium- and thorium-bearing phases over a large sample volume. The significant advantage of this technique is the avoidance of any contamination due to sample preparation like grinding. Instead, measurements already on plain surfaces result in good-quality data that allows the definition of uranium- and thorium-bearing, mineralized zones. In cases of strong uranium and thorium enrichments and the formation of uraninite and thorianite as ore-forming minerals, high quality and reproducible measurements can be performed at simple analytical conditions (100 µm step size by 500 µs counting time). In contrast a higher resolution is needed (down to 10 µm) in cases of uranium and thorium concentrations at the trace element level and very finely dispersed distributions of uranium- and thorium-bearing minerals. The higher resolution, however, leads to precise and reliable detection limits.

In contrast to already existing techniques to identify uranium this method allows the fast localization of uranium simultaneously to the recording of other elements. Due to the intensity of a signal (count rate) the relative distribution of the detected elements corresponding to its concentration can be visualized. Hence, besides the localization the measurements allow a quick identification of the mineralogical composition of the host.

References

Neff J (2003) Mineralogical and geological characterisation of carbonatite with focus on fault zone samples, Palabora copper orebody, South Africa. Diplomkartierung und Diplomarbeit TU Freiberg, pp. 92

Analytical speciation techniques for uranium and related elements

Depleted Uranium (DU) – Chemo- and Radiotoxicity

Albrecht Schott[1], Richard A. Brand[2], Joachim Kaiser[3], Dietmar Schmidt[4]

[1]World Depleted Uranium Centre, WODUC e.V., Harnackstr. 18, 14195 Berlin, Germany, E-mail: albrecht_schott@arcor.de
[2]World Depleted Uranium Centre, WODUC e.V., Institute of Physics, Universität Duisburg-Essen, 47048 Duisburg, Germany
[3]World Depleted Uranium Centre, WODUC e.V., Westendstr. 30, 63303 Dreieich, Germany
[4]World Depleted Uranium Centre, WODUC e.V., Karl-Marx-Allee 84, 10243 Berlin, Germany

Abstract. DU metal used for civil or military purpose reacts with water, undergoes radiolysis, dissolves and contaminates soil and ground water. DU is pyrophoric and burns on impact (3000ºC). DU oxide particles (mainly U^{6+}!) have a diameter of about 1.5 µm to 10 Å; 10 Å particles behave like a gas, carried by the air and travel long distances before they come down. DU is taken up by living organisms. Its α-radiation causes chromosome brakes (CB). A pilot study performed with Gulf War Veterans, originated by one of the authors (AS), did find 5.2 times more CBs on the average, with a maximum of 14 times higher. DU reaches all parts of an organism and leads to chemical and radiological damage.

Introduction

First of all I have to thank the organisers of this International Meeting, especially Prof. Dr. B. J. Merkel, to have given us the opportunity to participate and to make a contribution.

To introduce myself: I am a chemist. I am Founder and Head of the World Depleted Uranium Centre, WODUC e.V., based in Berlin. WODUC is an outcome of the Antidiscrimination Network MSD e.V. headed by me. We are a strictly independent scientific NGO. We work on the consequences of the civil and military use of Depleted Uranium (DU). DU is the byproduct – 4 million metric tons world wide – of 235 U enrichment of natural uranium: DU is 99,8% 238U, it still

contains 0,2 % 235 U. DU shells sometimes contain 236 U from recycled fuel cells from atomic power plants accompanied by small amounts of plutonium.

We work on the following subjects:

1. Remediation of DU contaminated soil and water.
2. Chemical, physical and biological analysis of water, soil, plants and animals.
3. Diagnosis of DU poisoning of civilians and war veterans. Urine/Uranium test, Chromosome-Aberration Analysis, analysis of biopsy and autopsy materials.
4. Development of health treatment procedures.
5. Documentation
6. Information of the general public: DU brochure, lectures, articles, independent inquiries (Lloyd-Inquiry London 2004) etc.
7. Resolution on the Banning of DU (April 2000).
8. Sometimes we do what others talk about. We do what has to be done for humanitarian and scientific reasons irrespective of any political constellations.

Why do I attend this meeting? Your experiences can be helpful for us and vice versa. The uranium mining waste is recycled to a large extent. In nearly all countries you find DU contaminated soil from civilian and military use. In Germany about 18 sites are known, worldwide over 600. Procedures to remediate environment especially agricultural soil have to be developed. Only the very first steps in this direction have been carried out.

I want to sensibilise you to this new uranium waste problem, to draw your attention to this subject. DU remediation is not only a great scientific challenge but it is also a great market in future. Our goal is constructive cooperation.

Basics on DU

Toxicologically, uranium is a multi-talent! What are the atomic and molecular mechanisms of this dangerous talent?

Three basic aspects of this toxicity:

1. It is chemically poisonous, a characteristic of its atomic shell.
2. It is radiologically poisonous as an alpha-emitter. The spontaneous decay is a characteristic of the atomic nucleus.
3. We have to consider the experimental observation that **mutuality can strengthen chemical and radiological toxicity**, in particular at low uranium concentrations (Miller et al. 2002, 2002). A new and basic understanding of heavy metal toxicity mechanisms is being developed in keen and ingenious steps.

Chemical toxicity of uranium

Chemo- and Radiotoxicity

General Remarks

DU metal reacts with water, undergoes radiolysis, dissolves and contaminates soil and groundwater. DU is very pyrophoric and burns on impact (3000°C). DU oxide particles consist of water soluble U^{6+} (in addition to ceramic DU). Uranium minerals mainly consist of water insoluble U^{4+}.

The chemo-toxicities of natural and depleted uranium are the same of course. The uranium isotopes are α-emitters. Only the decay rates differ. The α-toxic potential depends on the decay rate **and** the concentration of the uranium isotope. This fact sometimes is not mentioned, so the DU concentration is a basic parameter differentiated by the speciation (see below).

The DU oxide particles have a diameter of about 1.5 μm to 0.001μm (10 Angstrom). 10 Angstrom particles behave like a gas, enter the atmosphere, are carried by the wind and travel long distances before they come down.

Particle filters for this size particle do not exist. DU is taken up by plants, animals and humans. Inhalation of DU dust plays a major role in this contamination. DU reaches all parts/organs of an organism. It passes the blood-brain barrier and the placental barrier.

DU is chemically very toxic (T+). As α-emitter it leads to chromosome breaks (CB). I (AS) am originator of the first peer reviewed pilot study with British Gulf War Veterans. Their lymphocytes had five times more CBs than a comparative population, and fourteen times more maximum.

Uranium Speciation

Chemically malicious is uranium always, radiologically malicious only once: at the moment of its decay. Afterwards however its chemotoxic and radiotoxic decay products continue to be effective. The chemical characteristics, thus the toxicity, are a result of the electronic structure, the importance of the external electron shells. We compare sodium and uranium.

Singly ionized sodium has a noble gas configuration. Only Na^+ is present in the organism.

With uranium the behaviour is completely different. Several electron shells are only partly filled! Only after loss of six electrons does uranium achieve a stable noble gas configuration and becomes thereby U^{6+}, the most stable form in the organism. However by loss of 2, 3, 4 or 5 electrons, i.e. on the way to the most stable form, U^{2+}, U^{3+}, U^{4+} are formed, which are also stable, and U^{5+}. All these oxidation states are well-known. They could all be involved in metabolic processes.

Chemical toxicity of uranium

Table 1.

Atomic Nr.	Element	Electronic shell							
		K 1.	L 2.	M 3.	N 4.	O 5.	P 6.	Q 7.	
10	Ne	2	8						
11	**Na**	**2**	**8**	**1**					-1e~Na$^+$ („Neon")
86	Rn	2	8	18	32	18	8		
92	**U**	**2**	**8**	**18**	**32**	**21**	**9**	**2**	-2e~U^{2+}
									-3e~U^{3+}
									-4e~U^{4+}
									-5e~U^{5+}
									-6e~U^{6+} („Radon")

We now consider U^{6+}. t can be present in two forms – as the uranyl cation UO$_2^{2+}$ or as the uranat anion UO$_4^{2-}$. The characteristics of the uranium molecule are strongly pH dependent.

The variety of the molecular forms in which uranium can be present extends again by the ability of the uranium atom to form complex connections. Uranium in the uranyl form can be absorbed in the organism for example with phosphate or carbonate complex connections. Here we refer to the fundamental work of Professor Bernhard and his co workers (Guenther 2004).

All these different forms have different biological activities and thus also different toxicities. Hereby it is clear that the toxicity can be directly set by the uranium ionization; this is not the case with lead, which has been claimed.

Toxicity develops on the level of molecular mechanisms, in particular the intermediary metabolism, diaphragm transportation, genetic, and in particular reproductive procedures. Here uranium intervenes.

Redox procedures play thereby a substantial role. Think for example of the mitochondrial energy metabolism. By its ability to take on different oxidation levels, uranium could intervene also in this connection on molecular level in metabolism.

The elucidation of the functions of uranium, the way uranium intervenes in life procedures, is a crucial step for treatment and eventual therapy of uranium intoxication with humans and animals, but the same holds for the bioremediation and biogeochemistry of the uranium.

Depleted Uranium (DU) and Natural Uranium (NU)

As mentioned the chemical toxicities of NU and DU are basically the same. What are the differences? What would be possible guidelines? A main point is the origin of the uranium. As long as we deal with uranium minerals we in most cases have to do with U^{4+}-based compounds. They are not water-soluble and their toxicity depends on the chemical "assimilation" they undergo in an organism, that means the oxidation/solubilisation etc.

The toxicity, i.e. the damage to the molecular mechanisms of intermediary metabolism depends on the uranium speciation, on the building of chemical complexes, on the redox-state of the molecular reaction mechanisms, on the pH value of the system. This is an extremely complex situation.

DU in contrast to NU is found in the environment in metallic form. 99% of the machine gun bullets fail their target and penetrate the ground. Technical machinery using DU for example as counterweights or as radiation protection goes to the trash when they are no longer used. This metallic uranium undergoes radiolysis and results in U^{6+}.

On impact, pyrophoric DU shells burn at about 3000°C forming uranium oxide (U^{6+}). The higher the burning temperature, the less water-soluble oxide is formed. This also depends on the conditions of impact resulting in varying percentages of soluble and water-insoluble "ceramic" DU oxide (with a particle size from 10 Å to 1,5 μm). This mixture enters the atmosphere and reaches the ground water. Possible proliferation is discussed below.

Uranium is taken up by plants. The mechanisms are not fully understood. It interferes with plant metabolism. Basic research in this field has been done by Guenther (2003) and Kothe (2005, in press) and Merten (2004).

The DU dust is inhaled by animals and humans. The water soluble DU oxide immediately enters metabolism, the ceramic DU is stored mainly in lymph nodes and released over years.

The mainly affected organs are: blood, kidney, lung tissue, CNS, liver, reproductive system, muscle and bone marrow. Every organ has his specific metabolism and in consequence develops specific toxicity.

Technical Aspects of Uranium Contamination

I go now to the technical aspects of uranium contamination. Some mechanisms are known already. There is immense need of basic and applied research in this area.

Which are the different sources of uranium contamination above natural levels in the environment? The most important source is the uranium mining industry, refining uranium ore up to the stage of yellow cake (including fine dust formation, also from the slag). Sources not related to the uranium industry include mining of phosphate minerals including the production and processing of the phosphate fertilizers. In this way infiltration takes place into the food chain. The burning of coal also leads to uranium in the environment. Most importantly, the production of reactor core fuel elements, atom bombs, mini atom bombs and DU weapons as well as civilian DU products leads additionally to uranium contamination. Here also testing and accidents must be considered, in particular in the military range.

Clinical Aspects of Uranium Intoxication

Uranium enters the organism by respiration, through the food chain and through injuries. It arrives at every part of the body. The particles, down to 10 Å in size,

dissolve and reach all, we emphasize all organs of the body, even those normally protected. Brain and placental blood barriers are penetrated. During pregnancy, the foetus will be contaminated. Presumably, this is also true for the blood testicle barrier. Insoluble, ceramic DU is stored in lymph nodes of the lung and transferred over time to the whole organism.

In the course of evolution many toxic heavy metals have found entrance into metabolism in the form of trace elements, usually as active substances. In the case of uranium to my knowledge no such example has been found.

Uranium compounds have different valences and can be deposited preferentially on blood proteins or to diaphragm proteins of blood cells (Erythrocytes and Leukocytes). This also ensures its complete distribution in organisms.

Irradiation by uranium alpha-radiation can be demonstrated and reliably quantified by measuring the chromosome breaks in the Lymphocytes. A pilot study with 16 British Gulf War veterans demonstrated an average 5-fold increase of Chromosome breaks, with a maximum of 14-fold increase (Schroeder 2003).

A substantial part of our toxicological knowledge is due to systematic toxicological research as well as laboratory and industrial accidents connected with the development and building of the atom bomb. (Voegtlin, Hodge 1949, Toxicological Profile for Uranium 1990, Toxicological Profile for Uranium (Update) 1999) Unfortunately many documents and research results have never been made public.

Kidney damage has been demonstrated from experiments on animals. The classical way to produce kidney damage for the examination and testing of medical treatment procedures is by administrating Uranylacetat. This leads to a reduction of the glomerular ultrafiltration coefficient Kf. Electron microscopic studies have shown a decrease in the density and diameter of the endothelial window, which leads to a decrease in K_f and the glomerular filtration rate GFR because of a decrease in the filter area Here as well there is evidence of the formation of complexes of uranyl with phosphoryl- carboxyl- and sulfhydryl-groups on the surface of the cell membrane. Since the proximal tubulus of the kidney is very much dependent on the oxidative generation of high-energy phosphate, ATP, an effect from uranium is to be examined here too.

In the uranium mining industry, illnesses of the gastrointestinal tracts have led to an increase in deaths. Haematological effects, in particular a decrease of the haemoglobin concentration, have been observed. An increase in lymphatic leukaemia has also been observed. Reproductive effects: because the y-y-chromosome (few genes) is more resistant to radiation than the x-x-chromosome, an increase in the ratio in births of boys to girls was found. Gene-toxic effects: With mountain workers an increased number of chromosome breaks was determined.

Chemical toxicity of uranium

Migration Paths of the Depleted Uranium (DU) and their Research in Iraq

During the Gulf wars of 1991 and 2003, the southern and central regions of Iraq were affected by the use of armour- and bunker-piercing weapons containing DU. The amount of the released DU is estimated as probably 340 metric tons in 1991 and probably 1200 metric tons in 2003. Two migration paths with different extents must be discussed: **water / soil** and **wind**.

Migration Path Water / Soil

The majority of the fired ammunition (more than 90%) missed their targets (tanks, fighting vehicles, buildings, bunker etc.) and finished in the ground penetrating to different depths. Consequently the solid DU- rounds are affected by percolating water. There is the chance of contacts with the ground water in the area of the alluvial plain of the Euphrates and Tigris. The United Nations Enviromental Program (UNEP) has determined that DU-penetrators buried near the ground surface in Bosnia Herzegovina had decreased in mass by approximately 25% over 7 years (UNEP 2003).

The oxidation and corrosion depend on the rainfall. The dry southern and middle regions of Iraq have low annual precipitation, not more than 200 mm (Baghdad: 154 mm, Basra: 172 mm). Nevertheless, short and havy thundery shower sometimes occur and thus the annual rainfall varies.

The DU ammunition in the ground are often surrounded by a salty milieu, especialy in irrigated fields of the Euphrates and Tigris lowland plain. The Food and Agriculture Organisation (FAO) estimated in 1998 that 5.5 million out of a total of 11.48 million hectare are agriculturally useless because of salination and the trade embargo imposed during that period. The highest water-bearing aquifers can have a content of salt of 5000 ppm – 60000 ppm (DIA 1991) classified as brackish or saline.

Migration Path Wind

When a DU-containing shell impacts a target DU-dust is produced (size of the particles vary between 1.5 μm to 10 Å) and will be transported by the wind. The wind direction, its strength and frequency fluctuate seasonally and regionally (Wilkerson 1991).

The main wind is the summer "shamal" from June to September: the wind of the 120 days, coming out of the south and southeast, with average speeds up to 50 KmH and dust plumes and walls up to some thousands meter high. It meets a dry ground nearly free of vegetation. The thermal radiation at night (loss of temperature) and the violent heating during the day lead to horizontal air movements and turbulences over the ground as well. The velocity of the winds and of the tur-

bulences is sufficient to carry the dust over longer distances. Decreased speeds lead to a fall-out over a larger area and wind-protected sites will receive a local sedimentation.

Research

Here we make some recommendations for investigations which will be brought under discussion. A multistage approach which takes into account the current security situation would be favourable. For a successful implementation, the Iraqi administration and companies would have to be more and more involved and under better security conditions.

The first step would not include field work. The affected sites, the battle areas and the areas of DU use will be registered by date including details. Necessary data for follow-up investigations will also be collected and a first risk assessment will be undertaken.

The second step, based on the first one and branching out into local, regional and national research, corresponds to determining the extent of the two migration paths.

For a start, remote sensing can be used to determine the main investigation sites for follow-up geoscientific studies (including geophysical, geochemical, hydrological, geological, meteorological and other methods). Remote sensing allows a carefully targeted and cost cutting project.

Step 1: Acquiring Data and Registering Sites

1. Collecting situation and battle reports (Pentagon, Department of Defense, internet, privat reports) and registration of the sites of battles and use of DU.
2. Acquiring data concerning the sites:
   - Data from satellites (ASTER, IKONOS, OrbView, Quickbird etc.) and aerial photos.
   - Geological, hydrogeological, geochemical, geophysical and other data, information on restricted zones.
   - Meteorological data for the whole of Iraq and Kuwait.
3. Establishing a registry of battle sites and sites where DU was used.
4. Assessment of the length of potential migration paths of DU- particles, first assessment of risk

Step 2: Local, Regional and National Investigation by Integrated Methods

1. Local investigation using remote sensing:
   - Detailed mapping of battle sites and sites of use of DU: emplacement, tanks, military vehicles, impacts of duds, damaged buildings and grounds etc.
   - Establishing of Digital Elevation Models (DEM).
   - Fixing of wind-protected sites as potential accumulation sites.

Chemical toxicity of uranium

- Recommendations for geoscientific site investigations
2. Local geoscientific integrated investigation of selected pilot sites:
   - Geophysical survey: radiometry, electromagnetic, magnetic, conductivity.
   - Search for munitions and shells in the ground.
   - Analyses of wind-protected sites.
   - Analyses of the soil and the ground water system.
   - Modelling of ground water flow.
   - Modelling of the spreading of the DU-dust by the wind.
   - Forecast of the risks involved.
3. Regional and national investigations:
   - Setting up of a stationary air measurement system (air samplers) for Iraq and Kuwait.
   - Analyses of agricultural areas und standing water.
   - Analyses of agricultural products and drinking water.
   - Analyses of humans and animals.

Techniques for DU Remediation

In 1996 a patent was obtained on DU remediation (Ma 1996). It is based on the classical leaching procedures combined with mechanical separation steps. Bioremediation procedures are developed by Guenther (2003), Kothe (2005 in press) and Merten (2004).

With respect to the current situation this contribution shows different aspects of DU toxicity. We just seek one thing: constructive cooperation.

References

DIA (1991) Iraq Water Treatment Vulnerabilities. Short report of the DIA Washington for the CENTAF UK Strike Command.
URL: www.gulflink.osd.mil/declassdocs/dia/19950901/950901 511rept 91.html

Guenther et al. (2003) Uranium Speciation in Plants. Radiochimica Acta 91: 319-328 (2003)

Kothe et al. (2005 in press)

Merten et al. (2004) Studies on Microbial Heavy metal Retention from Uranium Mine Drainage Water with Special Emphasise on Rare Earth Elements. Mine Water and the Enviroment (2004) 23: 34-43

Miller et al. (2002) Genomic Instability in Human Osteoblast Cells after Exposure to Depleted Uranium: delayed Lethality and Micronuclei Formation. Journal of Environmental Radioactivity 64: (2003) 247-259

Miller et al. (2002) Potential Late Health Effects of Depleted Uranium and Tungsten Used in Armor-Piercing Munitions: Comparison of Neoplastic Transformation and Genotoxicity with the Known Carcinogen Nickel. Military Medecine, 167, Suppl. 1:120, 2002

Schroeder et al. (2003) Chromosome Aberration Analysis in Peripheral Lymphocytes of
    Gulf and Balkans War Veterans. Rad. Prot. Dos., 103:211-219 (2003)

Toxicological Profile for Uranium (1990). Agency for Toxic Substances and Disease Reg-
    istry, U.S. Public Health Service, December 1990

Toxicological Profile for Uranium (Update) (1999).

UNEP (2003) Depleted Uranium in Bosnia and Herzegovina. Post Conflict Environmental
    Assessment. URL: http://postconflict.unep.ch/publications/BiH_DU_report.pdf

Voegtlin, Hodge (1949) Pharmacology and Toxicology of Uranium Compounds. McGraw-
    Hill Book Company, Inc. 1949

Wilkerson (1991) Dust and Sand Forecasting in Iraq and Adjoining Countries. Air Weather
    Service, Scott Air Force Base, Illinois. 62225-5008

Effect of uranium and cadmium uptake on oxidative stress reactions for *Phaseolus vulgaris*

Hildegarde Vandenhove[1], Ann Cuypers[2], May van Hees[1], Jean Wannijn[1]

[1]Belgian Nuclear Research Centre, Mol, Belgium
[2]Limburg University Centre, Diepenbeek, Belgium

Abstract. Bean seedlings were grown under controlled conditions on a Hoagland solution. Ten-day-old seedlings were exposed to 0, 0.1, 1, 10, 100 and 1000 µM U or 0.5 and 1 µM Cd. Following 7 days' exposure, plants were sampled for determination of contaminant uptake, biometric parameters (shoot and root length, area of primary leaves, weight of shoot, root and primary leaves) and activity of enzymes involved in the plant's anti-oxidative defense mechanisms. Generally we did not observe a significant difference in plant development between control and treated plants based on biometric parameters. Enzyme activities in roots were stimulated with increasing contaminant concentrations (though generally not significantly). However, for roots exposed to 1000 µM U, enzyme activity was generally significantly reduced. In shoots no significant difference in the defense mechanism between the treatments was observed.

Introduction

Large areas of land have been contaminated by radionuclides and fission-by products including uranium from nuclear weapons facilities, above ground nuclear testing, nuclear reactor operations, improper waste storage practices and nuclear accidents. Radioactive contamination of the environment surrounding facilities where uranium or uranium bearing minerals have been mined and processed has occurred in many countries. Uranium is reported to be the most frequent radionuclide contaminant in ground and surface water soils of the United States Department of Energy facilities (Entry et al. 1996). Uranium is both radiotoxic and chemotoxic, yet the mechanisms of toxicity has been predominantly studied for man and for some animal species (Ribera et al. 1996). On the other hand, little information on uranium toxicity at the cellular level is available for plants. Chemical

toxicity would be predominantly caused by the aqueous hexavalent ion UO_2^{+2}. General physiological phenomena occurring at the cellular level following radiation are direct effects on molecules or indirectly through a water radiolytic reaction resulting in the production of highly reactive oxygen species (ROS).

In plants, environmental adversity often leads to the increase in formation of ROS. Under natural (non-stress) conditions ROS occur in the plant cell and therefore plants possess several anti-oxidative defense mechanisms to control the redox state of the cell which is essential for normal physiological and biochemical functioning. The defense systems comprise anti-oxidative enzymes (superoxide dismutases, peroxidases, catalases, glutathione reductase) and antioxidants (e.g. glutathione, ascorbate,…). Heavy metal toxicity results in an enhancement of the anti-oxidative defense system (Clijsters et al. 1999, Cuypers et al. 2002). Resistance to such conditions may be correlated with enzymes in oxygen detoxification (Bowler et al. 1991).

The present study aims to analyze the biological effects induced by bioaccumulation of uranium by *Phaseolus vulgaris.* Following a 1 week exposure, plant development and the capacity of enzymes involved in the anti-oxidative defense mechanism of the plant were analyzed. The enzymes studied cover enzymes for the acorbate-gluthatione cycle (Gluthatione reductase), some enzymes capable of quenching reactive oxygen species (Guaiacol and syringaldazine peroxidase, superoxide dismutase), and enzymes which catalyze reactions leading to the reduction of $NAD(P)^+$.

Materials and methods

Bean seedlings were grown in plastic bowls containing 3 L of a modified Hoagland nutrient solution (fourth strength for macronutrients and full strength of micronutrients) which was adjusted to pH 5.0 by addition of KOH. Dwarf beans, *Phaseolus vulgaris* L. cv. Limburgse vroege, were grown under controlled conditions. Bean seeds received a cold treatment (+4°C) for 3 days to break dormancy and to synchronize germination. They were transferred to the growth chamber to germinate for 4 days between water-soaked rock wool. Subsequently the seed coats were removed and the seeds were placed on perforated polystyrene floats in an aerated modified Hoagland's nutrient solution, which was renewed every other day. The conditions in the growth chamber were a 10 h photoperiod at 65 % relative humidity and day/night temperatures of 22°C. Light was supplied by cool white fluorescent lamps at a photosynthetic photon flux density of 165 $\mu molm^{-2}s^{-1}$ at the leaf level. Ten days old bean seedlings were treated with different concentrations of ^{238}U, supplied as uranylnitrate (0, 0.1, 1, 10, 100 and 1000 μM), or Cd, supplied as 0.5 or 1 μM $CdSO_4$. Per treatment, 2 containers were prepared containing each 10 plants. After application of the metals to the nutrient solution, plants were harvested after 1, 2, 4 and 7 days, processed and stored prior to the measurements. The solution was changed after every sampling. Only the results after 7 days exposure will be presented here. Plants were analyzed for shoot and

root length, leaf area, weight of roots, primary leaves and the rest of the plant. The roots from the control and metal treated plants were rinsed in 10 mM CaCl$_2$ to remove the adhering uranium or cadmium. For the determination of the tissue metal content, roots and primary leaves were dried at 100°C. The metal content was determined by ICP-MS after wet digestion of the dried material in concentrated HCl. Prior to the measurements of enzyme activities, samples of ~0.5 g were frozen in liquid nitrogen and stored at -70°C.

Plant tissue was homogenised (Smeets et al. 2005) and enzymes were measured spectrophotometrically. Guaiacol or syringaldazine peroxidase capacities (GPOD, SPOD, EC.11.1.7.) was measured according to Bergmeyer (1974) and Imberty et al. (1984), respectively. Superoxide dismutase (SOD, EC 1.15.1.1) catalyses the conversion of superoxide radicals into dioxygen and hydrogen peroxide and is measured according to McCord and Fridovich (1969). Analysis of the glutathione reductase (GR, EC 1.6.4.2) capacity was based on the reduction of GSSG, using NADPH (Bergmeyer 1974). Measurement of the capacities of glucose-6-phosphate dehydrogenase (G6PDH; EC 1.1.1.49) and isocitrate dehydrogenase (ICDH; EC 1.1.1.42) was performed as described by Bergmeyer (1974).

Statistical analysis of data was performed with the statistical software *Statistica for Windows* (Statsoft, 2003). Significant differences were considered at *P*= 0.05, and mean values were ranked by Tukey's multiple range tests when more than two groups were compared with ANOVA. All data are represented as mean±stdev, unless explicitly mentioned.
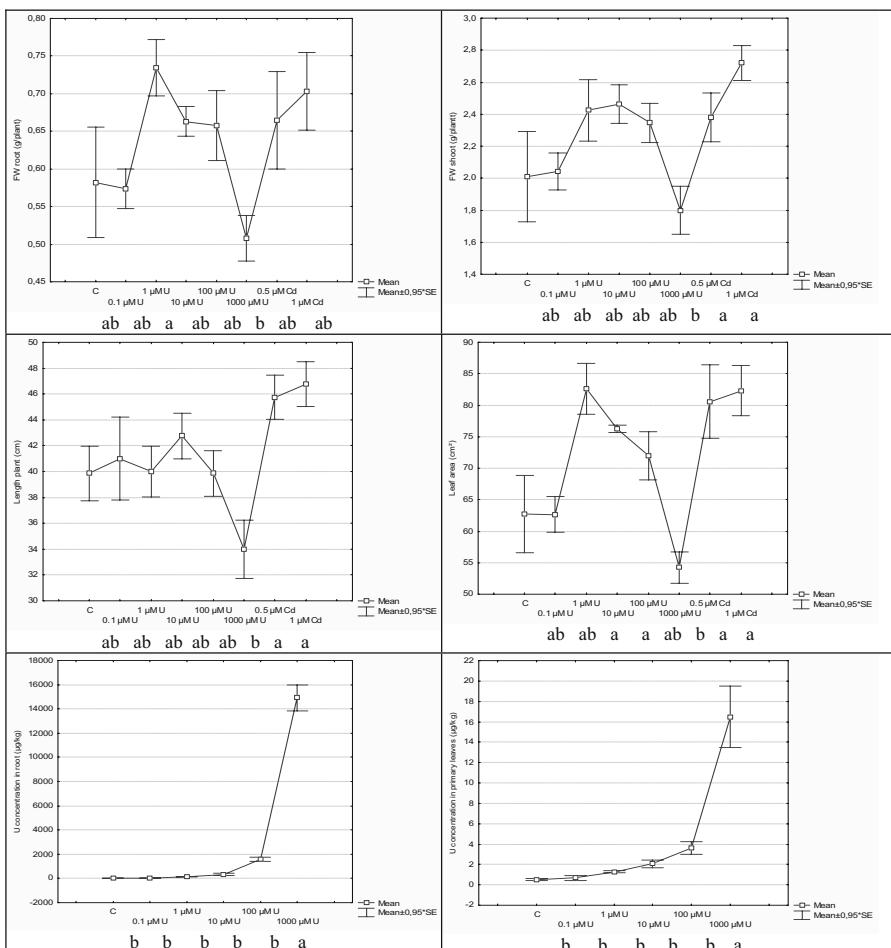
Results

For all growth parameters studied the same tendency with treatment is observed (Fig. 1): the values reached a peak at a uranium concentration in the nutrient solution of 1 or 10 µM and then steadily declined with a steep decrease between 100 and 1000 µM uranium in the solution. However, there was no significant difference in plant development observed between treatments and control. The hormesis-like response up to a 1-10 µM uranium concentration, could perhaps be explained by the use of uranylnitrate and the response of the plant to nitrate. The presence of Cd in the nutrient solution at concentrations of 0.5 and 1 µM tended to promote plant growth though not significantly.

The bottom pictures of Fig. 1 represent the uranium concentrations in the roots and primary leaves. The uranium concentration (FW) in roots ranged from 31 ± 4 ppm to 14916 ± 2208 ppm at a 0.1 µM and 1000 µM solution concentration, respectively. A significant difference is only observed between the root uranium concentration at 1000 µM and the other treatments. Concentrations in primary leaves range from 0.7±0.5 ppm to 16.5±6.3 ppm at a 0.1 µM and 1000 µM solution concentration, respectively, or a factor 40 to 900 lower than the concentrations observed in the roots. The observed root/shoot ratios agree with those reported in literature (Dushenkov et al. 1997; Shahandeh and Hossner 2002). The Cd concentrations (FW) were 27.2±7.1 ppm and 19.6±7.2 ppm for the roots and

3.5±2.6 ppm and 2.0±1.4 ppm for the leaves, for an external Cd concentration of 0.5 and 1 ppm Cd, respectively. The 10-fold higher Cd content in the roots as compared to the leaves has been extensively reported and is in accordance to the literature (Nan et al. 2002).
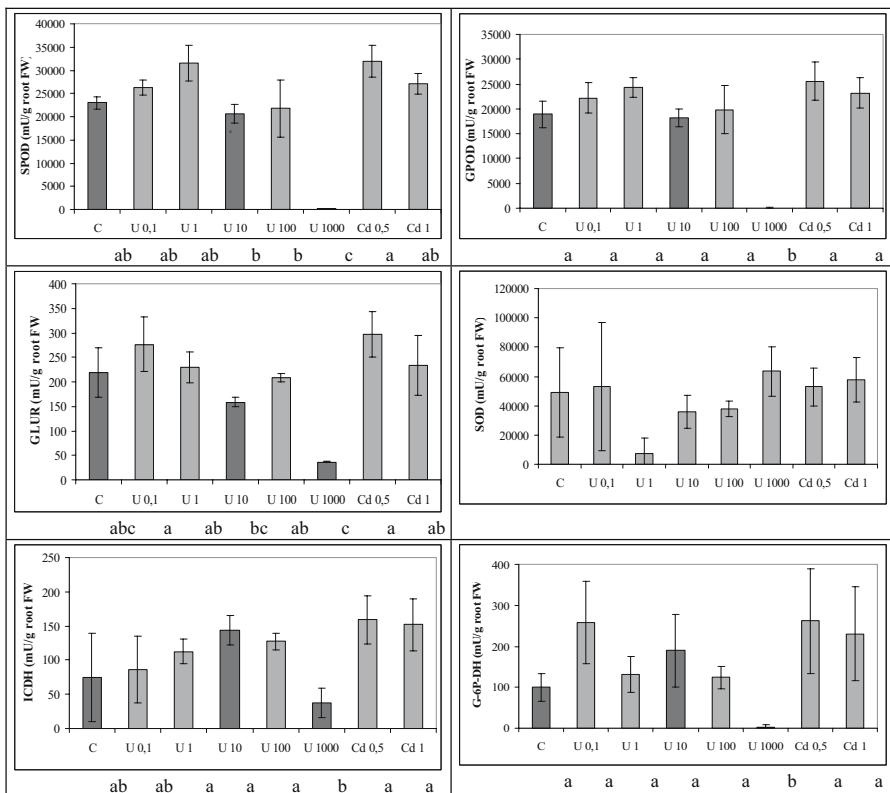
The capacity of some enzymes involved in the antioxidative defense mechanism in bean roots and primary leaves were analyzed. Between treatments, there were no significant differences or consistent patterns in enzyme capacity observed for the leaves. Therefore, enzyme capacity is only discussed at the root level (Fig. 2). In the roots, uranium seems to have an effect on the biochemical parameters studied: up to an ambient concentration of 1 or 10 µM uranium, the capacities of

Fig. 1.   Effect of exposure of beans (*Phaseolus vulgaris*) to different uranium and cadmium concentrations on shoot and root fresh weight, plant length and surface area of primary leaves and uranium concentrations in roots and primary leaves. Treatments with different letter annotations are significantly different.

Chemical toxicity of uranium

guaiacol and syringaldazine peroxidase (GPOD, SPOD), gluthatione reductase (GLUR) and the NADP$^+$-reducing enzymes isocitrate dehydrogenase (ICDH) and glucose-6P-dehydrogenase (G-6P-DH) increase. This tendency is, however not significant. The capacity of superoxide dismutase (SOD) showed an irregular pattern with treatment and no significant differences were observed. For all enzymes but SOD, the capacity almost ceased at 1000 µM uranium.

Exposing the roots to 0.5 or 1 µM Cd resulted in a non-significant increase in enzyme capacity compared to the control.

Fig. 2. Effect of exposure of beans (*Phaseolus vulgaris*) to different uranium and Cd concentrations on enzyme capacity of syringaldazine peroxidase (SPOD), guaiacol peroxidase (GPOD), glutathione reductase (GLUR), superoxide dismutase (SOD), isocitrate dehydrogenase (ICDH) and glucose-6-phosphate dehydrogenase (G-6P-DH),. Treatments with different letter annotations are significantly different. No significant differences observed for SOD capacity.

Chemical toxicity of uranium

Discussion

Most of the effects observed following plant exposure to uranium are not significant, except for the significant reduction in capacity of enzymes involved in the plant's oxidative defense mechanism when exposed to 1000 μM uranium in the external solution. Plant development seemed also hampered at 1000 μM. The exposure of the plants (external exposure from uranium in the nutrient medium and internal exposure following uptake) was calculated using the dose conversion coefficients for external exposure from ^{238}U in water [1.3 X 10^{-7} (μG/h)/(Bq/kg)] and for internal exposure following uptake in vegetation [2.4 X 10^{-2} (μG/h)/(Bq/kg)] by Amiro (1996) and taken up by Taranenko et al. (2004). External exposure from uranium is negligible even with an external solution concentration of 1000 μM (3.85 x 10^{-4} μGy/h). The dose proposed at which no significant effects are expected at the level of the population as proposed in IAEA (2001) and reiterated in UNSCEAR (1996) are 10 mGy/d (or 416 μGy/h). This benchmark of ~400 μGy/h was not reached in the leaves, not even when exposed to 1000 μM U given the limited transfer to the leaves (concentration < 16 mg U/kg FW). For roots exposed to 100 μM U (root concentration ~1600 mg U/kg FW just exceeded the benchmark (477 μG/h). For roots exposed to 1000 μM U (root concentration ~14900 mg U/kg FW), the benchmark was exceeded 10-fold. Hence, only when the benchmark of 400 μGy/h is exceeded, effects are observed for the biometric and biochemical parameters investigated.

To the authors knowledge, no research has been performed so far on the effect of uranium uptake on the capacity of enzymes involved in the antioxidant defense system of plants. Zaka et al. (2002) studied the effects of low chronic doses of ionizing radiation on antioxidant enzymes in *Stipa capillata*. External gamma-radiation at a dose rate of 65 μSv/h induced an enhancement of the peroxidase (not specified), GLUR, SOD and G-6P-DH activities in plants originating from contaminated areas (Semipalatinsk) but not for control plants. This was interpreted by the authors that half a century of residence in led to a natural selection of the most adapted genotypes characterized by an efficient induction of the anti-oxidant enzyme activities.

The literature offers conflicting information on the phytotoxicity of uranium. For soils, levels as low as 5 mg/kg have been cited as toxic, whereas many studies reported no toxicity symptoms at levels 100-1000-fold higher (Sheppard et al. (1992). Sheppard et al. (2004) reported on ecotoxicity thresholds for uranium for freshwater plants (studies with algae). The effective concentrations at which a 25 % reduction of growth was observed ranged between 0.01 and 0.12 mg/L (0.05 and 0.5 μM), concentrations at which we did not observe any effects. From the study by Sheppard et al. (1992) beans were reported as being most resistant to high U levels, showing no effect in germination tests at 1000 mg/kg when germination rate for other crops was clearly reduced. Geometric means of uranium solid-liquid distribution coefficients (Kd) vary from 15 to 1600 ml/g for different textured soil (Thibault et al. 1990), resulting in soil solution uranium concentrations of respectively 3 and 300 μM. If we would apply this highest figure, no ef-

Chemical toxicity of uranium

fects would be observed up to a uranium concentration in the solution of 300 µM, which is in agreement with our results.

Low Cd concentrations were used in our study, since this is similar to what is measured in the soil pore water of a slightly polluted sandy soil in the vicinity of an old Zn smelter in Belgium. Despite of the low concentrations, exposure of 10-day-old bean seedlings to 2 µM Cd resulted in a 20-40 ppm Cd concentration in the primary leaves after 24 h respectively 72 h (Smeets et al. 2005). Although in our experimental set-up, bean seedlings were exposed for 7 days to similar Cd concentrations, the uptake seems to be less pronounced. Probably the bioavailability of Cd in the nutrient solution is decreased and might be too low to impose a strong difference between control and treated plants.

Except for the SOD activities, the capacities of the enzymes studied showed an increased trend, although not significant. Elevation of environmental Cd concentrations has been reported to impose oxidative stress in plant cells (Chaoui et al. 1997, Smeets et al. 2005). An enhancement of the antioxidative defense mechanism can therefore be expected, while no visible damage nor changes in the biometric parameters will be observed.

Conclusions

Activity of stress enzymes was only significantly affected (decreased) at uranium concentrations of 1000 µM. Only at this soil solution concentration, the root uranium concentrations resulted in a dose clearly exceeding the set no-effect benchmark at population level. The reduction in enzyme activity is clearly a marker for prospected significant reductions in plant development at the highest uranium concentrations. Although the cadmium concentrations applied did not significantly affect the plant development nor the antioxidant enzyme capacities, the latter was slightly enhanced.

References

Amiro BD (1996) Radiological dose conversion factors for generic non-human biota used for screening potential ecological impacts J. Environ. Radioact. 35(1) 37-51.

Bergmeyer HU, Gawehn K, Grassl M (1974) Enzymes as biochemiucal reagents. In: Methods in enzymatic analysis. Ed.: Bergmeyer HU. Academic press, New York.

Bowler C, Slooten L, Vandenbranden S, De Rycke R, Botterman J, Sybesma C, van Montagu M, Inzé D (1991) Manganese superoxide dismutase can reduce cellular damage mediated by oxygen radicals in trasngenic plants. The EMBO Journal 10(7): 1723-1732

Chaoui A, Mazhoudi S, Ghorbal MH, El Ferjani E (1997) Cadmium and zinc induction of lipid peroxidation and effects on antioxidant enzyme activities in bean (Phaseolus vulgaris L.). Plant Sc. 127: 139-147.

Clijsters H, Cuypers A, Vangronsveld J (1999) Physiological responses to heavy metals in higher plants; defense against oxidative stress. Zeitschrift für Naturforschung 54c, 730-734

Cuypers A, Vangronsveld J, Clijsters H (2002) Peroxidases in roots and primary leaves of Phaseolus vulgaris, copper and zinc phytotoxicity: a comparison. J. Plant Physiol. 159: 869-876

Dushenkov S, Vasudev D, Kapulnik Y, Gleba D, Fleisher D, Ting KC, Ensley B (1997) Removal of uranium from water using terrestrial plants. Environm. Sci. Technol. 31: 3468-3474

Entry JA, Vance NC, Hamilton MA, Zabowski D, Watrud LS, Adriano DC (1996) Phytoremediation of soil contaminated with low concentrations of radionuclides. Water Air Soil Pollut. 88: 167-176

IAEA, International Atomic Energy Agency (1992) Effects of ionising radiation on plants and animals at levels implied by current radiation protection standards. Technical Report Series N° 332, International Atomic Energy Agency, Vienna, Austria.

Imberty A, Goldberg R, Catesson AM (1984) Tertamethylbenzidine and p-phenylenediamine-pyrocatechol for peroxidase histochemistry and biochemistry: two new, non-carcinogenic chromogens for investigating lignification processes. Plant Sci. Letters 35: 103-108

McCord JM, Fridovich I (1996) Superoxide dismutase: an enzymatic function for erythrocuperein (hemocuperein). J. Biolog. Chem. 244(22): 6049-6055

Nan Z, Li J, Chang G (2002) Cadmium and zinc interactions and their transfer in soil-crop system under actual field conditions. Sc.Tot. Environ. 285: 187-195.

Ribera D, Labrot F, Tisnerat G, Narbonne JF (1996) Uranium in the environment: Occurrence, transfer and biological effects. Reviews Environ. Contamin. Toxicol. 146: 53-89

Shahandeh H, Hossner LR (2002) Role of soil properties in phytoaccumulation of uranium. Water, Soil, Air Pollut. 141: 165-180

Sheppard SC, Evenden WG, Anderson AJ (1992) Multiple assay of uranium toxicity in soil. Environ. Toxicol. Water Qual. 7: 275-294.

Sheppard SC, Sheppard MI, Gallerand MO, Sanipelli B (2005) Derivation of ecotoxicity tresholds for uranium. J. Environ. Rad. 79(1): 55-83.

Smeets K, Cuypers A, Lambrechts A, Semane B, Hoet P, Van Laer A, Vangronsveld J (2005) Induction of oxidative stress and antioxidative mechanisms in Phaseolus vulgaris after Cd application. Plant Physiol. Biochem.: in press.

Taranenko V, Pröhl G, Gómez-Ros JM (2004) Absorbed dose rate conversion coefficients for reference biota for external exposures. J. Radiol. Protec. 24: A35-A62

Thibault DH, Sheppard MI, Smith PA (1990) A critical complialtion and review of default soil solid/liquid partitioning coefficients, Kd, for use in environmental assessments. AECL-10125, Whiteshell Nuclear Research Establishment, Atomic Energy of Canada, Pinawa, Canada.

UNSCEAR, United Nations Scientific Committee on the Effects of Atomic Radiation (1996) Effects of radiation on the Environment. A/AC.82/R.549, United Nations, Vienna, Austria

Zaka, R., Vandecasteele, C.M. and Misset, M.T. 2002b. Effect of low chronic doses of ionizing radiation on antioxidant enzymes and G6PDH activities in Stipa capillata (Poaceae). J. Exper. Bot., 53(376): 1979-1987

Coupled Microbial and Chemical Reactions in Uranium Bioremediation

Linda A. Figueroa, Bruce D. Honeyman, James F. Ranville

Colorado School of Mines, Golden, Colorado, 80401, USA,
E-mail: lfiguero@mines.edu

Abstract. The chemical composition of the water and sediment affects the extent that uranium is immobilized in a microbially active environment. This paper summarizes an integrated framework of coupled microbial and chemical reactions in uranium bioremediation. The research is aimed at improving selection, design and operation of uranium biotreatment systems that use natural organic material to support the microbial consortium. Highlights of experimental and modeling efforts are presented.

Introduction

An estimated 350,000 tons of uranium (U) were produced in the United States (US) by 1998. A high proportion of the uranium ore in the US is located in the Rocky Mountain region. There are hundreds of small uranium mine sites that are not currently addressed by existing federal remediation programs. Over 1300 abandoned uranium mines have been identified on Navajo Tribal lands in Arizona and New Mexico alone. The cost of effective mitigation of numerous small and remote abandoned uranium-mining sites lends itself to passive treatment technologies. There is a need for relatively low cost and low maintenance control and treatment systems to mitigate critical and numerous sites.

Wetlands have been shown to effectively remove uranium from mining influenced water. However, the long-term stability has been variable. In some wetlands uranium retention tends to be associated with reversible sorption of U(VI). Uranium is very stable in other wetlands and requires leaching with sulfuric acid to mobilize. It is difficult to control reducing conditions in wetlands as the intrusion of the plant roots into sediments provides a pathway for oxygen to enter the sediment. Even if the lower portion of the sediment is anaerobic, a fraction of the sediment is not and thus the fraction of flow that bypasses the anaerobic environment does not allow for the reduction of uranium.

In-situ biosystems can be used to ensure anaerobic conditions are maintained in a passive remediation scheme. Permeable reactive barriers and in-situ sulfate reducing bioreactors are two biosystems that minimize oxygen intrusion and are thus able to maintain the requisite anaerobic environment needed for uranium reduction. However, ensuring anaerobic conditions is only one part of promoting successful uranium reduction and precipitation. Ultimately, the microbial functions expressed coupled with the aqueous chemistry will control the extent of uranium reduction and immobilization. Uranium fate and treatment has been a focus area since the early 1990's at the Colorado School of Mines (CSM). The efforts have centered on a theme of integration of chemical, microbial and physical processes on uranium fate, transport and remediation. Unanswered questions critical to design of successful passive remediation include understanding how solid and solution phase chemistry affects the microbial distribution, the microbial interactions with uranium, and the availability of uranium for immobilization. Understanding these effects will allow for more effective design and operation of passive biosystems.

Microbial ecology of uranium reducing biosystems

The microbial community composition in anaerobic environments is controlled by the type of biopolymer present (e.g. cellulose or protein) and the subsequent products formed by hydrolysis and fermentation. Selected bacteria from different substrate niches (e.g. glucose vs. lactate vs. acetate) are capable of uranium reduction. Most do not grow on the energy released from the uranium/organic carbon redox couple. Thus, reduction of uranium represents a competitive use of organic carbon as an electron donor for the uranium-reducing microorganism. The microorganism must also use additional organic carbon with its energy producing electron acceptor to grow and remain active. At the same substrate level there are microorganisms that do not reduce uranium and also compete for the same organic compounds. Carbon flow through non-uranium reducing microorganisms at all substrate levels could result in no uranium reduction in an apparently appropriate anaerobic environment. The structure of the active microbial ecology is also sensitive to the solution phase chemical composition of the water. For example, salinity or concentration of specific inorganic ions can affect the community structure. In addition, the solid phase organic material, microorganisms, and microbial byproducts serve as ligands or bind sites for uranium sorption and complexation that further complicate uranium reduction. Thus predicting the overall uranium reduction requires understanding the contribution of multiple microbial functions, the microbial competition at each substrate, and uranium bioavailability. Approaches available to study microbial processes in these complex biosystems include molecular methods (e.g., DNA extraction, PCR, Cloning, and DNA sequencing) to elucidate community structure, bioassays to examine inherent microbial functions, measurement of changes in microbial substrates (sequential extraction protocols and High Pressure Liquid Chromatography, HPLC) and products (Gas Chroma-

tography and HPLC), and coupled modeling of microbial and chemical kinetics with reactive transport.

Chemistry of uranium immobilization

Uranium immobilization in anaerobic environments occurs for uranium species in both the U(VI) and U(IV) oxidation state. U(VI) species are typically immobilized by sorption processes while U(IV) immobilization is as insoluble $UO_{2(S)}$. The reduction of U(VI) to U(IV) and subsequent precipitation as $UO_{2(S)}$ is the goal of anaerobic passive treatment schemes. However, the presence of ligands or solids tends to reduce uranium reduction and the formation of $UO_{2(S)}$ in the presence of U(IV). While the inorganic solution phase chemical reactions for uranium are relatively well understood, the interactions with organic ligands, colloids and particles are not well understood. Part of the difficulty with colloids and particles is the broad range of chemical characteristics exhibited. Colloids may be made up of extracelluar polysaccharides, enzymes, and other functional exudates from microbial growth or a broad range of humic materials resulting from the microbial degradation of lignocellulose materials. Therefore, it is important to understand the additional effect of microbially related organic compounds on uranium bioavailability and precipitation availability. Approaches to elucidate the chemical dependent aspects of these complex uranium biosystems include characterization of uranium partitioning between solution and solid phase complexes by field flow fractionation (FFF) coupled with size exclusion (SEC), ultraviolet absorbance (UVA) or inductively coupled plasma - mass spectrometry (ICP-MS), measurement of uranium oxidation state and surface complexes using Extended X-ray Absorption Fine Structure (EXAFS) and X-ray Absorption Near-Edge Spectroscopy (XANES), quantification of surface chemical characteristics and surface complexation modeling, and integration of surface complex modeling into a reactive transport model.
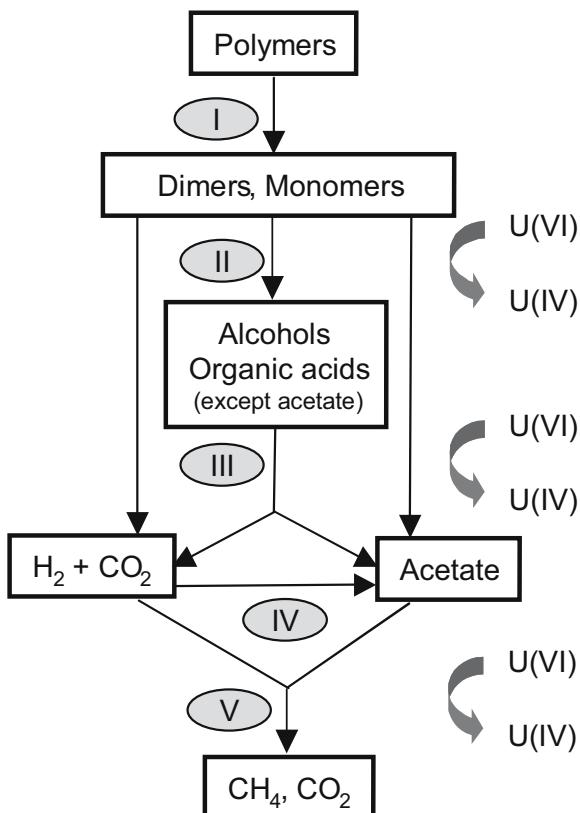
CSM uranium bioremediation

Microbial ecology efforts

There are many elements of the microbial ecology of uranium bioremediation that require more research to improve design and operation of biotreatment systems. A conceptual model of the microbial ecology of uranium reduction is presented in Figure 1. This conceptual model provides a useful framework to direct needed research efforts to improve uranium bioremediation. One element is the direction of the carbon flow to the desired substrates and microbial functions. Sulfate reduction and fermentation are model microbial functions that also facilitate uranium

reduction. Examples of CSM work in this area include the effect of initial solid phase organic matter composition on sulfate reduction (Figueroa et al. 2004); monitoring changes in solid phase organic substrates over time (Place et al. 2005); examining metal toxicity on cellulose degradation and thus on overall sulfate reduction (Logan 2003); modeling concurrent kinetics of uranium and sulfate reduction (Spear 2000); and modeling decomposition of biopolymers coupled to sulfate reduction (Hemsi et al. 2005).

The microbial community structure and long-term sustainability of anaerobic biozones can be directed by the types of organic matters used for construction of wetlands and bioreactors. However, there has not been an effective correlation developed between microbial community structure/function and initial solid phase substrate composition particularly temporally. Initial reactivity of treatment sys-

Fig.1. Conceptual model of the microbial ecology of uranium reduction. I=extracellular hydrolysis; II=primary fermenters, and acidogens; III=secondary fermenters, acidogens, iron- and sulfate -reducers; IV=acidogens, V=acetate or hydrogen consumption by methanogens, and iron- or sulfate-reducers.
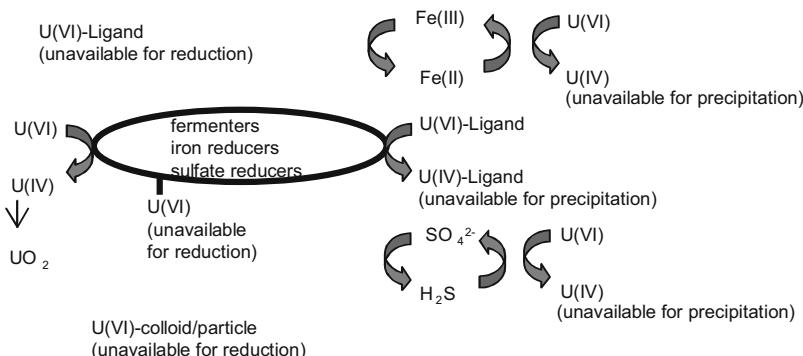
tems tends to be high but after one year rates of sulfate reduction are significantly lower than initial rates. In some systems these rates are sustained for at least 5 years, in other systems significant activity may cease in less than a year. More information is needed on both the microbial community structure and function in conjunction with initial organic matter composition and changes in both with time. The elucidation of the microbial community structure of anaerobic treatment zones is only recently being monitored (e.g., Pruden et al. 2005). Similarly, quantification of the composition of the solid phase organic substrates is a relatively recent effort (Figueroa et al. 2004, Place et al. 2005). The nutritional composition of organic substrates can be characterized by applying sequential extractions methods commonly used in food science, forestry and agriculture fields. Sustainability of sulfate reduction as a function of initial substrate composition was evaluated for oak wood, pine wood, alfalfa and corn stover. A high percentage of cellulose in conjunction with a high cellulose-to-lignin ratio was related to substrate sustainability. Organic substrate composition and microbial community structure and activity over time are currently being assessed in several field-scale sulfate-reducing bioreactors. The expectation is to gain greater insight into how substrate composition affects sulfate reduction and how to design substrate mixtures to optimize desired microbial function. A biomodule for modeling sulfate reduction controlled by decomposing organic solids (Hemsi et al. 2005) was also developed. The module is design to integrate into reactor models and reactive transport codes such as MODFLOW. The field data collected will be used to validate the coupled microbial process and transport model.

Uranium availability efforts

Understanding the effect of solid and solution phase composition on availability of uranium for reduction and precipitation reactions is critical to designing successful uranium bioremediation systems. A conceptual model for uranium availability is presented in Figure 2. The organic ligands and particles in bioremediation systems are complex as natural organic materials and degradation products are represented by a distribution of sizes and chemical characteristics. Examples of CSM efforts in uranium availability include the characterization of particle size distributions and composition coupled to uranium binding and mobility (Jackson et al. 2005a & 2005b, Hendry et al. submitted, Honeyman and Ranville 2002); the effect of exobiopolymers on thorium complexation (Quigley et al. 2002); surface complexation modeling of uranium sorption to bacterial surfaces (Landkamer 2003); and surface complexation modeling coupled to reactive transport of uranium (Kantar 2001).

Microbiology of uranium

The effects of solid and solution phase chemical constituents on uranium availability are important to developing predictive models for uranium bioremediation. Besides inorganic constituents, microorganism and their by-products provide surfaces and compounds that interact with uranium. Landkamer (2003) examined the sorption of uranium onto a gram-negative bacterium Desulfovibrio vulgaris. There were many artifacts to overcome in understanding sorption to bacteria and an experimental and modeling framework was developed. For example, the preparation protocol required the removal of a suspected iron sulfide layer precipitation on the bacterial surface during growth conditions. This layer caused difficulties in reproducibility of sorption data and interfered with uranium binding to bacterial surface function groups until it was removed. Also, the three dimensional nature of the bacterial surface required the inclusion of a three dimensional volume (using the Donnan model) in the surface complexation modeling to account for the porous nature of the bacterial surface. The model calibration included the examination of uranium sorbed onto bacterial surfaces by X-ray absorption spectroscopy to determine the distribution of function groups binding uranium to the bacterial surface and the oxidation state of the uranium. Sorption of U(VI) to bacterial surfaces may reduce its availability for uranium reduction and subsequent $UO_{2(S)}$ precipitation.

The characterization of natural organic matter coupled with uranium binding capabilities was studied using coupled analytical methods. Jackson et al. (2005a) reported cell suspension separation using FFF into two separate peaks that represent different particle sizes and distributions. One peak eluted in a time frame that suggests it was the nominally 1 micron sized bacterium. The other peak eluted earlier and is hypothesized to be bacterial exopolymer. Uranium sorption to these two size fractions significantly varied in extent as a function of pH. At pH 8 and 1 micromole uranium, the percent uranium sorption was about equal between the two fractions. However, at pH 6, 80% of the uranium was associated with the cell fraction and only 20% with the extracellular fraction. Jackson et al. (2005b) also measured uranium and nickel distribution in the dissolved fraction of contami-

Fig. 2.   Conceptual model of uranium availability for reduction and precipitation in the presence of complexing ligands and particles.

Microbiology of uranium

nated sediment extracts by FFF, SEC coupled to UVA and ICP-MS. Uranium was found complexed to dissolved organic matter (DOM) and a colloidal fraction. This will tend to make the uranium unavailable for bioreduction or removal by sorption. In addition, the nickel was predominately present as a free ion or labile complex that is more bioavailable. Nickel in particular has demonstrated differential toxicity to fermenters over acidogens and sulfate reducers. Thus, the uranium bioreduction ability of a microbial community could be impaired by the presence of a toxic metal such as nickel.

Summary

The complex microbial, chemical and physical interactions within anaerobic biozones require a systems approach to understanding the complex interrelationships. The framework for microbial ecology of uranium reduction coupled with the availability of uranium provides a useful way to conceptualize the key processes. Elucidation of the interactions will allow for improvements in design and operation of passive biotreatment systems such as wetlands, permeable reactive barriers and sulfate-reducing bioreactors.

References

Figueroa L, Seyler J, Wildeman T (2004) Characterization of organic substrates used for anaerobic bioremediation of mining impacted waters. Proceedings of the 2004 International Mine Water Association Conference Sept. 20-24, 2004, Jarvis, A editor, Newcastle, England, 43-52.

Hemsi P, Shackelford C, Figueroa L (2005) Modeling the influence of decomposing organic solids on sulfate reduction rates for iron precipitation. Environ Sci Technol 39: 3215-3225.

Hendry J, Ranville , Reszat T, Xie Q, Honeyman B (submitted) Quantifying uranium complexation by groundwater dissolved organic carbon using asymmetrical flow field flow fractionation. J. Contam. Hydrol.

Honeyman B, Ranville J (2002) Colloid properties and their effects on radionuclide transport through soil and groundwaters. Soil Geochemical Process of Radionuclides. Chapter 7. Soil Science Society of America Special Publication. p. 131 – 163.

Jackson B, Ranville J, Bertsch P, Sowder A (2005a) Characterization of colloidal and humic-bound Ni and U in the 'dissolved' fraction of contaminated sediment pore waters. Environ. Sci. Technol. 39 (8): 2478-2485

Jackson B, Ranville J, Neal A (2005b) Application of flow field flow fractionation-ICP-MS for the study of uranium binding in bacterial cell suspensions, Anal. Chem. 77 (5): 1393-1397.

Kantar, C. (2001). The Role of Citric Acid in the Transport of U(VI) Through Saturated Porous Media: The Application of Surface Chemical Models to Transport Simulations of

Bench-Scale Experiments. Doctoral Thesis Colorado School of Mines, Golden, Colorado, USA.

Landkamer L (2003) Sorption of U(VI) to Desulfovibrio vulgaris at gram-negative bacterium development of an experimental and modeling framework for the characterization and prediction of metal sorption to bacteria. Doctoral Thesis T5732, Colorado School of Mines, Golden, Colorado, USA.

Logan M (2003) Microbial activity and the rate-limiting step in degradation of cellulose-based organic material to support sulfate reduction in anaerobic columns treating synthetic mine drainage. Masters of Science Thesis T5797, Colorado School of Mines, Golden, Colorado, USA.

Place D, Claveau E, Figueroa L (2005) Tracking organic substrate alterations in passive reactive zones for planning and monitoring. Proceedings of the 2005 National Meeting of the American Society of Mining and Reclamation (ASMR), June 19-23, 2005. Barnhiesel, R editor, Lexington, Kentucky, USA, 921-934.

Pruden A, Hong H-S, Inman L, Logan M, Sans C, Ahmann D, Figueroa L, Reardon K (2005) Microbial characterization of sulfate reducing columns remediating acid mine drainage, Proceedings of the 2005 National Meeting of the American Society of Mining and Reclamation (ASMR), June 19-23, 2005. Barnhiesel, R editor, Lexington, Kentucky, USA, 935-944.

Quigley M, Santschi P, Huang C-C, Guo L, Honeyman B (2002). Role of polysaccharides for 234Th complexations by natural organic matter. Limnol. Oceanogr. 47:367-377.

Spear J, Figueroa L, Honeyman B (2000) Modeling reduction of U(VI) under variable sulfate concentrations by sulfate-reducing bacteria. Appl. Environ. Microbiol. 66:3711-3721.

Biotransformation of uranium complexed with organic ligands

Arokiasamy J Francis

Environmental Sciences Department, Brookhaven National Laboratory, Upton, New York 11973, USA, E.mail: ajfrancis@bnl.gov

Abstract. Natural ligands can affect the bacterial metabolism and reductive precipitation of uranium. The metabolism of metal-organic complexes by bacteria depends upon the type of complex formed between the metal and organic ligand. For example, Fe(III) forms a bidentate complex with citric acid, and was readily metabolized by *Pseudomonas fluorescens* under aerobic conditions, whereas the binuclear complex formed between U and citric acid was recalcitrant. When supplied with an electron donor, anaerobic bacteria reduced U(VI)-citrate to U(IV)-citrate with little precipitation of uranium. X-ray absorption near-edge structure (XANES) and extended X-ray absorption fine structure (EXAFS) spectroscopy analysis showed that the reduced uranium was present in solution as mononuclear U(IV)-citrate complex. These results suggest that when reduced uranium is complexed with organic ligands, it can be mobile.

Introduction
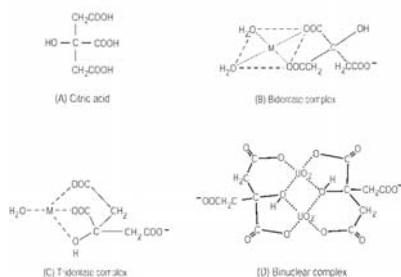
Uranium exists in the environment predominantly as U(VI)- and U(IV)-oxidation states. Natural organic complexing agents present at the contaminated sites may not only affect the mobility of uranium, but also its microbial transformation and reductive precipitation. Biotransformation of the complexed radionuclides should precipitate the radionuclides and retard their migration. The mechanisms of microbial reduction and the precipitation of uranyl nitrate and uranyl carbonate are well understood. However, there is a paucity of comparable information on transformation of uranium complexed with natural low-molecular-weight soluble organic ligands.

We investigated the mechanisms of complexation of, and biotransformation of uranium with natural organic ligands, such as ketogluconic, oxalic, malic, citric,

protocatechuic, salicylic, phthalic, and fulvic acids, and catechol. Potentiometric titrations of uranium with the organic ligands confirmed that complexes were formed; EXAF analyses characterized their structures. Ketogluconic acid formed a mononuclear complex with uranium involving the carboxylate group, while malic acid, citric acid, and catechol formed binuclear complexes. Phthalic acid formed a bidentate complex involving the carboxylate group, while catechol bonded to uranium through the two hydroxyl groups. The hydroxycarboxylic acids were bound in a tridentate fashion to uranium through two carboxylate and the hydroxyl groups. In this paper, I examine the biotransformation of uranium complexed with citric acid in aerobic and anaerobic such as denitrifying, iron-reducing, fermentative, and sulfate-reducing environments.

Citric acid and metal complexes

Citric acid, a naturally occurring compound, is a multidentate ligand that forms stable complexes with various metal ions. It forms different types of complexes with transition metals and actinides including bidentate, tridentate, binuclear, or polynuclear complex species (Fig. 1).

Fig. 1.   Metal citrate complexes.
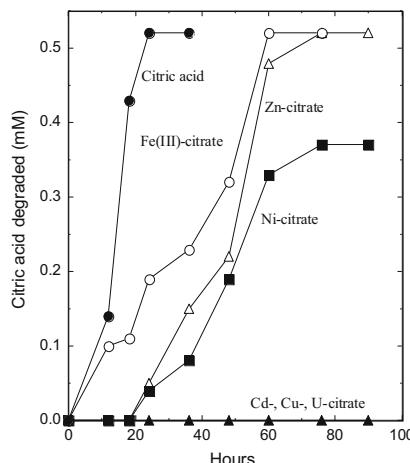
Biotransformation of binary uranyl-citrate complexes under aerobic conditions.

Biodegradation of metal citrate complexes depends upon the type of complex formed between the metal and citric acid; bidentate complexes are readily biodegraded, whereas tridentate complexes are recalcitrant (Francis et al 1992). Pseudomonas fluorescens under aerobic conditions readily broke down the bidentate complexes of Fe(III)-, Ni-, and Zn-citrate, but not tridentate Al-, Cd- and Cu-citrate, nor the binuclear U-citrate complexes, which include the hydroxyl group
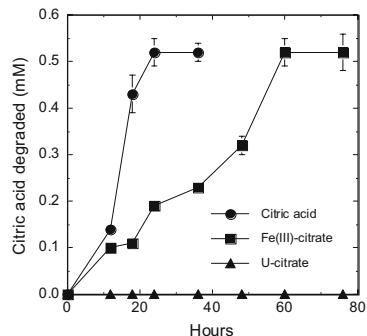
of citric acid (Fig. 2). The lack of degradation was not due to metal toxicity; rather, limited by the transport and/or metabolism of the complex by the bacteria (Joshi-Tope and Francis, 1993). No relationship was observed between the biodegradability and the stability of the complexes. The tridentate Fe(II)-citrate complex, although recalcitrant, was readily biodegraded after oxidation and hydrolysis to the bidentate Fe(III)-citrate form, denoting a structure-function relationship in the metabolism of the complex (Francis and Dodge 1993). The presence of the free hydroxyl group of citric acid is the key determinant affecting this process. Thus, adding excess citric acid to equimolar (0.52mM) uranyl citrate resulted in the metabolism of the excess citric acid; the uranyl-citrate complex was not toxic to the bacterium. In the presence of 1-, 2-, and 3-fold excess citric acid, the citric acid remaining in each complex after biodegradation was 0.75, 0.80, and 0.83 mM, respectively. The final stoichiometry of U-citric acid in all three treatments was approximately 2:3, indicating the formation of 2:3 U-citric acid complex.

Biotransformation of uranyl-citrate by *Pseudomonas fluorescens* under denitrifying conditions.
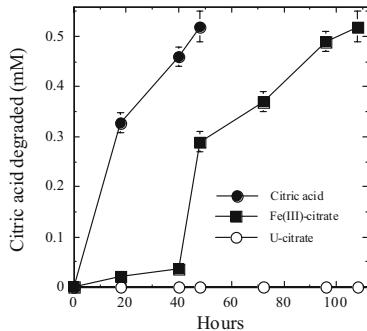
Citrate metabolism by *Pseudomonas fluorescens* under denitrifying conditions is facilitated by the enzyme aconitase, as in aerobic metabolism. Breakdown of the various metal-citrate complexes by *P. fluorescens* under denitrifying conditions was similar to that observed aerobically, but the rates were much lower (Figs 3A and B). The bacterium completely degraded bidentate complexes, but did not metabolize the tridentate complexes, and the binuclear U-citrate complex (Joshi-Tope and Francis, unpublished results).

Fig. 2. Biodegradation of metal citrate complexes by *P. fluorescens* under aerobic conditions (Joshi-Tope and Francis, 1993).

Microbiology of uranium

Fig. 3A. Biotransformation of uranyl-citrate by *P. fluorescens* under aerobic conditions.

Fig. 3B. Biotransfromation of uranyl-citrate by *P. fluorescens* under denitrifying conditions.
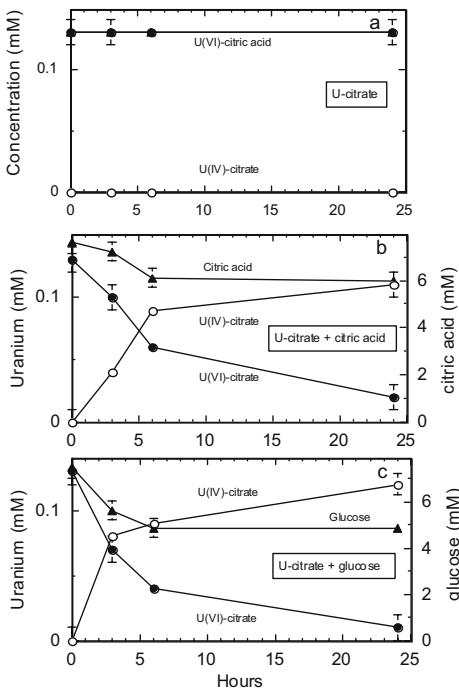
Biotransformation of metal-citrates by *Clostridia* under anaerobic conditions

Clostridium sphenoides metabolized the bidentate Fe(III)-, Ni-, and Zn-citrate complexes, converting citric acid to acetic- and butyric- acids, CO_2, and H_2. The metals released from the complexes were present in solution. Fe(III)-citrate was readily metabolized by *C. sphenoides* with the reduction of the ferric to the ferrous form; the latter remained in solution. The tridentate Cd-, Cu-, and U-citrate complexes were not metabolized by the bacterium (Francis et al 2002). In the presence of excess citric acid or glucose, U(VI)-citrate was reduced to U(IV)-citrate that remained in solution (Fig. 4A). These results agree well with observations of the metabolism of metal-citrate complexes by *P. fluorescens* in aerobic and denitrifying environments.
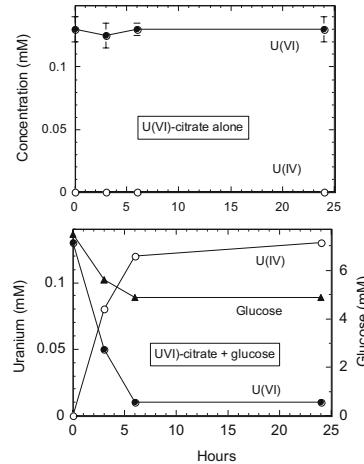
In contrast, *Clostridium* sp. did not metabolize citric acid nor reduce the Fe(III) or U(VI) bound to the acid (Fig. 4B). However, on adding glucose, Fe(III)-citrate was reduced to Fe(II)-citrate, and U(VI)-citrate was reduced to U(IV), which then remained in solution as the U(IV)-citrate complex (Fig. 4B). Glucose was metabolized to acetic- and butyric-acids, CO_2, and H_2

Sulfate-reducing *Desulfovibrio desulfuricans* and the facultative iron-reducing bacterium *Shewanella halotolerans* anaerobically reduced U(VI) complexed with oxalate or citrate to U(IV) , but little uranium was precipitated. The reduced U(IV) remained in solution complexed with oxalate or citrate (Ganesh et al 1997; 1999).

These results show that complexed uranium is readily accessible for the microorganisms as an electron acceptor, despite the bacteria's inability to metabolize the organic ligand complexed to the actinide.
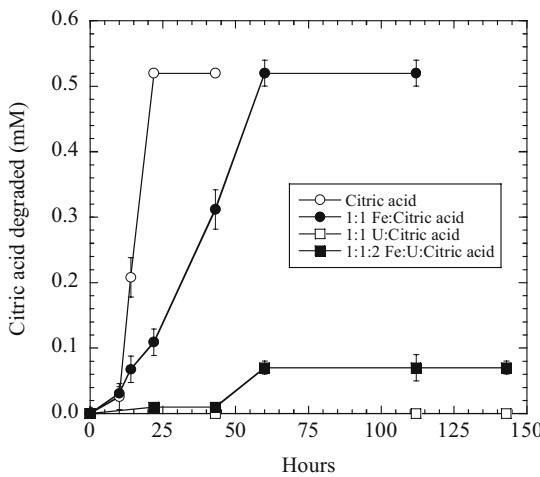
Fig. 4A. Biotransformation of uranyl citrate by *C. sph*enoides.
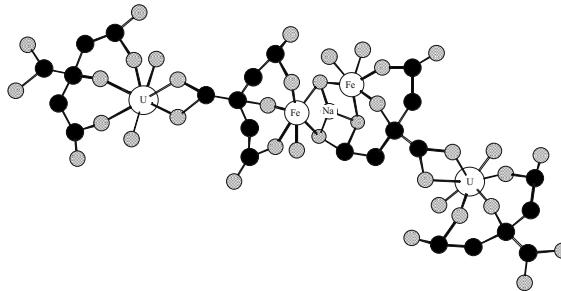
Fig. 4B. Biotransformation of uranyl citrate by *Clostridium* sp.

Biotransformation of Ternary Fe(III)-U(VI)-citrate complexes.

Citric acid forms ternary mixed-metal complexes with various metal ions involving the hydroxyl and carboxyl groups of citric acid. The presence of 1:1:2 Fe:U:citric acid in solution was confirmed by potentiometric titration, UV-vis spectrophotometry, gel-filtration chromatography, and extended x-ray absorption fine structure (EXAFS) (Fig. 5) analysis (Dodge and Francis, 1997; 2003). Biotransformation studies of Fe-U-citrate complex by *P. fluorescens* showed that the ternary 1:1:2 Fe:U:citric acid complex was resistant. When a one-fold excess of citric acid was added to this complex, it was completely degraded with no change in its stoichiometry. However, with a two-fold excess, a 1:1:1 Fe:U:citric acid complex remained in solution after all the citric acid was biodegraded. Thus, similar to the U-citrate complex, the Fe-U-citrate complex appears to resist biodegradation (Dodge and Francis, 1997). With the persistence of mixed-metal-citrate complexes in wastes and contaminated environments, uranium may thus be mobi-

Fig, 5. Biotransformation of 0.52 mM citric acid, 1:1 Fe-citrate, 1:1 U-citric acid, and 1:1:2 Fe-U-citric acid complexes (Dodge and Francis 1997).

Fig. 6. Proposed structure of the ternary 2:2:4 Fe:U:citric acid complex (Dodge and Francis 2003).

lized. Although a wide variety of microorganisms are present in uranium mining wastes and in natural radioactive mineral deposits, there has been no full evaluation of the extent to which they regulate the mobility of uranium complexed with organic and inorganic ligands. Undoubtedly, a fundamental understanding of the molecular-level mechanisms of interactions of microorganisms with radionuclides associated with natural organic and inorganic ligands and colloids under various microbial- process conditions will aid in developing appropriate strategies for the remediation and long-term stewardship of contaminated sites.

Acknowledgements

References

Dodge, C.J. and A.J. Francis. 2003. Structural characterization of a ternary Fe(III)-U(IV)-citrate complex. Radiochim. Acta 91: 525-532.

Dodge, C.J. and Francis, A.J. 1997. Biotransformation of binary and ternary citric acid complexes of iron and uranium. Environ. Sci. Technol. 31: 3062-3067.

Dodge, C.J. and Francis, A.J. 2003. Structural characterization of a ternary Fe(III)-U(VI)-citrate complex. Radiochim.Acta 91: 525-532.

Francis, A.J. and C.J. Dodge. 1993. Influence of complex structure on the biodegradation of iron citrate complexes. Appl. Environ. Microbiol. 59:109-113.

Francis, A.J. G.A. Joshi-tope, C.J. Dodge, and J.B. Gillow. 2002. Biotransformation of uranium and transition metal citrate complexes by *Clostridia.* J. Nuc. Sci. Technol. Supplement 3, 935-938.

Francis, A.J., C.J. Dodge, and J.B. Gillow. 1992. Biodegradation of metal citrate complexes and implications for toxic-metal mobility. Nature 356:140-142.

Ganesh R., K.G. Robinson, G.R. Reed, and G. S. Saylor. 1997. Reduction of hexavalent uranium from organic complexes by iron and sulfate reducing bacteria. Appl. Environ. Microbiol. 63:4385-4391.

Ganesh R., K.G. Robinson, L. Chu, D. Kucsmas, and G.R. Reed. 1999. Reductive precipitation of uranium by *Desulfovibrio desulfuricans*: Evaluation of cocontaminant effects and selective removal. Wat. Res. 33: 3447-3458.

Joshi-Tope, G. and Francis, A. J. 1995. Mechanisms of biodegradation of metal-citrate complexes by *Pseudomonas fluorescens*. J. Bacteriol. 177:1989-1993.

Changes of bacterial community structure of a uranium mining waste pile sample induced by addition of U(VI)

Andrea Geissler, Andreas C. Scheinost , Sonja Selenska-Pobell

Institute of Radiochemistry, Forschungszentrum Rossendorf, D-01314 Dresden, Germany, E-mail: a.geissler@fz-rossendorf.de

Abstract. Several portions of a uranium mining waste pile sample were supplemented with different amounts of U(VI) in form of uranyl nitrate to investigate the interactions between the indigenous bacterial populations and U(VI). Selective sequential extractions showed that most of the supplemented U(VI) remained predominantly in weak complexes and hence bioavailable. Analysis of 16S rDNA clone libraries from untreated and U(VI)-supplemented samples revealed changes in the structure of the bacterial community.

Introduction

Bacteria have developed different mechanisms to tolerate and to interact with uranium. Some of them are able to oxidize insoluble U(IV) minerals and hence make uranium more mobile. Other can immobilize uranium by reducing U(VI) to U(IV) or by biosorption and biomineralization (Selenska-Pobell 2002). Because of these abilities bacteria play a major role in the natural as well as anthropogenically influenced biogeochemical cycling of uranium (Lovley 2002). They were also used for development of bioremediation approaches of uranium-contaminated sites (North et al. 2004; Raff et al. 2003; Suzuki et al. 2003). In this study we attempted to understand better how U(VI) influences and interacts with the indigenous bacterial community of a uranium mining waste pile by combining geochemical and molecular biological techniques. Several portions of a soil sample collected from a uranium mining waste pile were supplemented with different amounts of U(VI) in form of uranyl nitrate. Selective sequential extractions were performed to quantify bioavailable uranium pools in the untreated and U(VI)-supplemented samples. Bacterial communities were analyzed before and after supplementation with U(VI) by means of culture-independent molecular 16S rDNA retrieval.

Materials and Methods

Experimental design

The soil sample studied JG35 was collected under sterile conditions in July 1997 at 2m depths from the uranium mining waste pile Haberland near the town of Johanngeorgenstadt, Germany. It was stored frozen at –20°C. The sample labeled JG35+U1 was prepared by adding a 1 mM uranyl nitrate solution (pH 4.0) in one step to 15 grams of the JG35 sample to achieve a final concentration of 100 mg/kg U(VI). The sample was then incubated for four weeks in the dark at 10 °C. The sample labeled JG35+U2 was prepared in a similar way, but this time the amount of uranium was increased up to 300 mg/kg supplementing it in several steps in order to achieve an optimal distribution of the metal in the soil material. This sample was incubated on the whole for 14 weeks in the dark at 10 °C. After 14 weeks, the sample JG35+U2 was split in two parts. Sample JG35+U2A was used for DNA extraction and selective sequential extractions as described below. The other part (JG35+U2B) was incubated under anaerobic conditions in an anaerobic jar with Anaerocult$^{®}$ (Merck, Germany) for another 14 weeks.

Selective sequential extractions

Selective sequential extractions (SSE) were performed using a seven-step procedure (Zeien and Brümmer, 1991). The targeted species and the extracting procedure of each step are as follows: **1.** Water soluble salts and exchangeable ions: 1 M NH_4NO_3. **2.** Weakly complexed ions (often specific sorption) or bound by calcium carbonate: 1 M NH_4OAc at pH 6.0**. 3.** Metals bound by Mn hydroxides: 0.1 M NH_2OH-HCl + 1 M NH_4OAc at pH 6.0 and 5.5, resp. **4.** Strongly complexed metals (bound to organic matter): 0.025 M NH_4-EDTA at pH 4.6. **5.** Metals bound by easily reducible Fe(III) minerals: 0.2 M NH_4-oxalate at pH 3.25. **6.** Metals bound by other reducible Fe(III) minerals: 0.1 M ascorbic acid + 0.2 oxalate at pH 3.25. **7.** Recalcitrant minerals: two-step microwave digestion. Extracted uranium was measured by inductively coupled plasma mass spectrometry (ICP-MS).

DNA extractions and 16S rRNA gene analysis

Total DNA was extracted from untreated and U(VI)-supplemented soil samples according to Selenska-Pobell (1995). The final purification of the DNA extracted from the samples JG35+U1, JG35+U2A and JG35+U2B was done with Nucleobond® cartridges AXG-100 (Marcherey-Nagel, Germany). Partial bacterial 16S rRNA genes were amplified from total DNA with the degenerated primer 43F (5'-(ACT)(AG)(GT)GC(GCT)T(AT)A(GCT)(AG)CATGCAAGTC) and primer 1404R (5'-GGGCGGWGTGTACAAGGC-3') (Marchesi et al. 1998). The construction of the clone libraries and their analysis were performed as described in Selenska-Pobell et al. (2001).

Results and Discussion

Selective sequential extractions
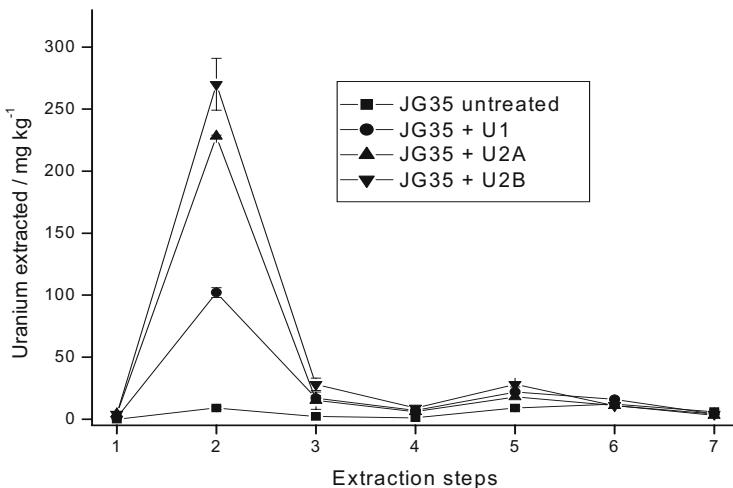
The untreated sample had a natural U content of 40 mg kg-1, which was distributed among SSE steps 2,5,6 and 7, hence indicating a wide variety of uranium species (Fig. 1). All three treatments increased almost exclusively SSE step 2, indicating that the added uranium was either weakly complexed or bound by carbonate phases. The analyses were done at pH 4.0, precluding the formation of U(VI)-carbonate complexes. There is no qualitative difference between the aerobic and the anaerobic treatments, suggesting that independent of treatment no reduction of U(VI) took place. This result was further supported by U L_{III}-EXAFS spectroscopy, which revealed only U(VI) species.

Analysis of 16S rDNA clone libraries from untreated and U(VI)-supplemented soil samples
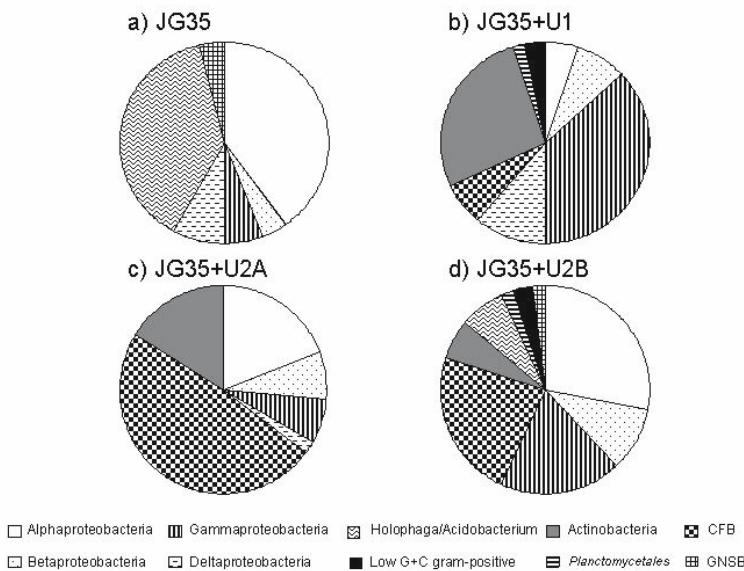
The results from the 16S rDNA retrievals of the untreated and U(VI)-supplemented soil samples are summarized in Fig. 2. As shown in Fig. 2a the bacterial community of the untreated sample JG35 was predominated by representatives of Alphaproteobacteria and the *Holophaga*/*Acidobacterium* phylum.

   Similar results were obtained in our previous studies on bacterial diversity of other equally polluted samples collected from the same site (Selenska-Pobell 2005). By increasing the uranium content to approximately 100 mg/kg (sample JG35+U1) only a few Alphaproteobacteria and no *Holophaga*/ *Acidobacterium* were found (Fig. 2b). Instead, the most predominant 16S rRNA gene sequences belonged to Gammaproteobacteria, Actinobacteria and Deltaproteobacteria. Almost 40 percent of the retrieved sequences were closely related to Gamma-*Pseudomonas* species which are known for accumulating (Francis et al. 2004, Merroun et al. 2002) and/or for reducing U(VI) (McLean and Breveridge 2001). The investigation of the bacterial community from the most contaminated soil sample from the same site, which was collected from different depth, also revealed enrichment with Gamma-*Pseudomonas* (Selenska-Pobell 2005). Within the Actinobacteria sequences closely related to *Arthrobacter* spp. were detected. *Arthrobacter* spp. have been frequently observed in different extreme, heavy-metal-contaminated environments (Hanbo et al. 2004) and also in high level nuclear waste-contaminated vadose sediments (Fredrickson et al. 2004). This suggests a potential to resist heavy metals and radionuclides. Members of the metal-reducing *Geobacteraceae* family within the Deltaproteobacteria subdivision were also identified in this sample. Its cultivated members are able to reduce U(VI), Fe(III), and elemental sulfur (Straub and Buchholz-Cleven 2001, Lovley et al. 1993). A propagation of members of the Deltaproteobacteria was also observed after biostimulation in a subsurface sediment cocontaminated with uranium and nitrate

(North et al. 2004). Interestingly, one sequence representing three clones was strongly clustered with low G+C gram-positive sulfate-reducing bacteria, *Desulfosporosinus* spp. It was demonstrated that organisms closely related to *Desulfosporosinus* spp. posses a potential for enzymatic reduction of U(VI) (Suzuki et al. 2002, 2003). As shown in Fig. 2c, the bacterial community structure of the sample JG35+U2A differed significantly from the two samples described above. Most of the retrieved sequences were closely related to representatives of the *Cytophaga*/*Flavobacterium*/*Bacteroides* (CFB) group. Also, *Arthrobacter* spp. were identified, but not as strongly predominant. After the incubation of a part of the sample JG35+U2 under anaerobic conditions, the bacterial community was equally predominated by representatives of *Cytophaga*/ *Flavobacterium*/*Bacteroides*, Alpha-, and Gammaproteobacteria (Fig. 2d). The proliferation of Alpha- and Gammaproteobacteria through the incubation under anaerobic conditions could be promoted by cocontamination with nitrate, because members of these groups have the ability to reduce nitrate. The latter is an energetically more favorable electron acceptor than U(VI) and Fe(III). In the JG35+U2B sample 16S rDNA sequences were additionally found which belong to *Holophaga*/*Acidobacterium* phylum*, Planctomycetales,* low-G+C Gram-positive and green non-sulfur bacteria (GNSB). Interesting but not surprising was the detection of *Desulfosporosinus* spp. in the sample JG35+U2B (see above). However, no reduction of U(VI) to U(IV) was observed by the anaerobic treatment (data not shown). Our results demonstrate that in dependence of the uranium content and the redox conditions, the addition of U(VI) in form of uranyl nitrate to a low contaminated uranium mining waste pile sample leads to changes in the bacterial community structure. The analysis of the 16S rDNA clone libraries shows that, through addition of uranyl nitrate, *Pseudomonas* spp., *Arthrobacter* spp. and *Geobacter* spp. as well as members of *Cytophaga*/*Flavobacterium*/ *Bacteroides* group were stimulated which suggests that they have a potential to resist uranium. Such experiments may help to improve our knowledge about the role of certain bacteria in the geochemical cycle of uranium. Future studies will be focused on changes in bacterial community structure and formation of different U complexes after longer incubation under anaerobic conditions.

Fig. 1. Selective sequential extraction results (mean and standard deviation of 3 replicates).

Fig. 2. Bacterial diversity of the untreated soil sample JG35 (a) and the samples with added U(VI) JG35+U1 (b), JG35+U2A (c) and JG35+U2B (d).

Acknowledgements

References

Francis AJ, Gillow JB, Dodge CJ, Harris R, Beveridge TJ, and Papenguth HW (2004) Uranium association with halophilic and non-halophilic bacteria and archaea. Radiochim. Acta 92: 481-488

Frederickson JK, Zachara JM, Balkwill DL, Kennedy D, Li SW, Konstandarithes HM, Daly MJ, Romine MF, and Brockman FJ (2004) Geomicrobiology of high-level nuclear waste-contaminated vadose sediments at the Hanford Site, Washington State. Appl. Environ. Microbiol. 70: 4230-4241

Hanbo Z, Changqun D, Qiyong S, Weimin R, Tao S, Lizhong C, Zhiwei Z, and Bin H (2004) Genetic and physiological diversity of phylogenetically and geographically distinct groups of *Arthrobacter* isolated from lead-zinc mine tailings. FEMS Microbiol. Ecol. 49: 333-341

Lovley DR, Giovannoni SJ, White DC, Champine JE, Phillips EJP, Gorby YA, and Goodwin S (1993) *Geobacter metallireducens* gen. nov. sp. nov., a microorganism capable of coupling the complete oxidation of organic compounds to the reduction of iron and other metals. Archiv. Microbiol. 159: 336-344

Lovley DR (2002) Dissimilatory metal reduction: from early life to bioremediation. ASM News 68: 231-237

Marchesi JR, Sato T, Weightman AJ, Martin TA, Fry JC, Hiom SJ, and Wade WG (1998) Design and evaluation of useful bacterium-specific PCR primers that amplify genes coding for bacterial 16S rRNA. Appl. Environ. Microbiol. 64: 795-799

McLean J, and Breveridge TJ (2001) Chromate reduction by a pseudomonad isolated from a site contaminated with chromated copper arsenate. Appl. Environ. Microbiol. 67: 1076-1084

Merroun M, Henning C, Rossberg A, Reich T, Nicolai R, Heise KH, Selenska-Pobell S (2002) Characterization of uranium (VI) complexes formed by different bacteria relevant to uranium mining waste piles. In: Merkel B, Planer-Friedrich B, and Wolkersdorfer C ed. Uranium in the aquatic environment. Berlin, Heidelberg, Springer-Verlag; 505-511

North NN, Dollhopf SL, Petrie L, Istok JD, Balkwill DL, and Kostka JE (2004) Change in bacterial community structure during in situ biostimulation of subsurface sediment co-contaminated with uranium and nitrate. Appl. Environ. Microbiol. 70: 4911-4920

Raff J, Soltmann U, Matys S, Selenska-Pobell S, Böttcher H, and Pompe W (2003) Biosorption of uranium and copper by biocers. Chem. Mater. 15 (1): 240-244

Selenska-Pobell S (1995) Direct and simultaneous extraction of DNA and RNA from soil. In: Akkermans ADL, van Elsas JD, De Bruijn FJ, eds Molecular Microbial Ecology Manual 1.5.1. Dordrecht, Netherlands: Kluwer Academic Publishers: 1-17

Selenska-Pobell S, Flemming K, Kampf G, Radeva G, Satchanska G (2001) Bacterial diversity in soil samples from two uranium mining waste piles as determined by rep-APD, RISA and the 16S rDNA retrieval. Antonie van Leeuwenhuek 79: 149-161

Selenska-Pobell S, (2002) Diversity and activity of bacteria in uranium waste piles. In Keith-Roach M & Livens F ed. Interactions of Microorganisms with Radionuclides. Oxford, UK, Elsevier Sciences: 225-253

Selenska-Pobell S (2005) Uranium contaminated environments as a reservoir of unusual bacteria prospective for bioremediation and nanotechnology. Perspectives in Environmental Microbiology. Oxford, UK; Elsevier Sciences; in press

Straub KL, and Buchholz-Cleven BEE (2001) *Geobacter bremensis* sp. nov. and *Geobacter pelophilus* sp. nov., two dissimilatory ferric-iron-reducing bacteria. Int. J. Syst. Evol. Microbiol. 51: 1805-1808

Suzuki Y, Kelly SD, Kemner KM, and Banfield JF (2002) Nanometre-size products of uranium bioreduction. Nature 419: 134

Suzuki Y, Kelly SD, Kemner KM, and Banfield JF (2003) Microbial populations stimulated for hexavalent uranium reduction in uranium mine sediment. Appl. Environ. Microbiol. 69: 1337-1346

Zeien H, Brümmer GW (1991) Ermittlung der Mobilität und Bindungsformen von Schwermetallen in Böden mittels sequentieller Extraktionen. Mitteilungen der Deutschen Bodenkundlichen Gesellschaft 66: 439-442

Sorption mechanisms and models. Their influence on transport calculation

Michel Fédoroff, Grégory Lefèvre

Centre National de la Recherche Scientifique, Ecole Nationale de Chimie de Paris, Laboratoire d'Electrochimie et de Chimie Analytique, 11, rue Pierre et Marie Curie, 75231 Paris cedex 05, France, Email : michel-fedoroff@enscp.fr

Abstract. Approaches for the prediction of transport of radioactive species in underground and surface water based on experimentally determined distribution coefficients (Kd) and sorption isotherms have a limited predictive capability, due to their sensitivity to many parameters. Models based on thermodynamic equilibrium can account for the influence of multiple parameters, but show important theoretical and experimental limitations, which restrict their predictive character for transport calculation.

Introduction

Sorption and desorption at the solid-liquid interfaces play a major role in many phenomena and technologies: catalysis, chemical separations, decontamination of liquid wastes, transport of toxic and radioactive species in surface and underground waters, prediction of the future evolution of waste depositories. Use of sorption data and modeling to transport prediction must be based on a very good knowledge of sorption mechanisms, otherwise the prediction, especially at long term, may be hazardous. In accordance with the length of this short review, we shall examine the main approaches and models used to quantify sorption processes. We shall emphasize the main theoretical and experimental problems connected to the acquisition and modeling of sorption data. We shall compare sorption models and examine their adequacy with sorption mechanisms. The cited references are only a few examples of numerous articles.

Distribution coefficients

In transport models, the contribution of sorption is generally represented by the "distribution coefficient", noted Kd or Rd, which is the ratio of the concentration of the element in the solid phase to its concentration in the aqueous phase. Kd is generally used in the calculation of the migration of an element through the retardation factor R, which is the ratio of the velocity of water to the velocity of the element through the same volume. As an example, the most simple relation between the retardation factor R and Kd is (Serne 1987):

$$R = 1 + Kd \, \rho \, (1 - \varepsilon) \, / \varepsilon$$

where, ρ and ε are the volumic mass (in kg/L) and the porosity of the solid phase respectively, and Kd is expressed in L/kg. This expression is valid for a monodirectional flow in a homogeneous porous medium, with a constant Kd. Several models and computer codes have been developed (Jauzein 1989, Van der Lee 2002) for more complicated situations, close to natural systems.

Kd values come either from experiments which are often gathered in data banks (Stenhouse 1994), or are calculated from models. Experimental Kd values depend on the experimental conditions and often do not represent an equilibrium value. They depend on many factors: temperature, concentration of the element, pH, influence of complexing agents and competing elements, kinetics. Therefore, extrapolation of Kd values to scales larger than those of laboratory experiments, especially to natural systems, is hazardous.

Empirical linear or non linear expressions of the concentration of competing elements have been proposed for the calculation of Kd (Holstetler 1980). However, these expressions are valid only for certain experimental conditions and are generally not based on real physico-chemical processes.

Sorption isotherms

An isotherm represents the variation of the concentration of the element in the solid phase, or the variation of Kd, versus the equilibrium concentration of the element in the aqueous solution, at a constant temperature. An equilibrium of sorption is supposed to be achieved, but apparent isotherms are often used. Isotherms are fitted by several mathematical models, which have some theoretical bases, but are often used as empirical ones. We shall not detail them, but just indicate the more often used: the Langmuir (1918), derived from the sorption of gas molecules on a solid, whose sites have equal sorption energy, but often applied to a solid in aqueous solution, the Dubinin-Radushkevitch (1947) isotherm and the Freundlich (1926) isotherm, with non homogeneous sorption sites

Although sorption isotherms include the influence of the element concentration, they depend on many other parameters and are generally used as empirical models in transport calculation.

Sorption models

Sorption models assume a certain number of sorption equilibriums able to calculate the concentrations of all species of an element in the solution and on the surface of the solid. They suppose that equilibrium is achieved. Theoretically, they are able to calculate the Kd values of an element, taking in account all factors such as pH, competing elements, complexing agents. Two main models of that kind have been developed.

Ion exchange model

This model is based on the mass-action law, quantifying the exchange of ions between the solid and the solution, through a thermodynamic equilibrium constant K. No hypotheses have to be done on the real mechanisms at the atomic scale. However, calculation of the thermodynamic constant from concentrations needs activity coefficients. Generally, the activity coefficients in the liquid phase can be calculated, especially in dilute solutions. On the other hand, the activity coefficients in the solid phase cannot be calculated a priori. Therefore, K is replaced by a "corrected selectivity coefficient" K_c, from which the activity coefficients in the solid are excluded.

K_c is generally not constant as the concentration of the element sorbed in the solid increases, but it may be almost constant, when the sorbed element is at trace level or when the interactions between adjacent sorption sites are negligible. However, the thermodynamic constant can be calculated from the Gaines-Thomas (1952) equation:

$$\ln(K) = (Z_A - Z_B) + \int_{X_B=0}^{X_B=1} \ln(K_C)dX_B \text{ and } \Delta G^0 = -\frac{RT}{Z_A Z_B}\ln(K)$$

where X_B is the ionic fraction of the element B in the solid after exchange with the element A, Z_A and Z_B, the ionic charges and ΔG° the Gibbs free energy.

It is possible to interpret the variation of K_c with the concentration in the solid, by considering the partition function Q (Barrer 1956):

$$Q = \sum_j \exp(\frac{-E_j}{kT}) \text{ connected to K and Kc by } \Delta G^\circ = \text{-RT lnQ}$$

where E_j is the energy of each level in the solid. Often, the calculation can be simplified by limiting to the additional energy change in the solid when two adjacent sorption sites are occupied.
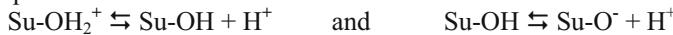
The ion exchange model is particularly useful for solids in which the sorption process is not superficial, but results from a penetration of the sorbed element into the bulk of the solid. As an example, the variation of $\ln(K_c)$ with the Sr^{2+} concentration in poly-antimonic acid $H_2Sb_2O_6$, confirmed by X-ray diffraction, showed

that sorption proceeds through the successive substitution of two sites of the crystal framework (Zouad 1992).

Surface complexation models

These models were developed for oxyhydroxides. They are based on the acid-base properties of superficial hydroxide groups of these solids. Several types of such models were developed: the monosite 2-pK and 1-pM models, the multisite 1-pK model, the pK-distribution model.

The "**monosite 2-pK model**" (Stumm 1992) assumes that the surface is covered by one type of hydroxide groups with amphoteric properties, leading to the following equilibria:

$$Su\text{-}OH_2^+ \leftrightarrows Su\text{-}OH + H^+ \qquad \text{and} \qquad Su\text{-}OH \leftrightarrows Su\text{-}O^- + H^+$$

where Su represents the surface. The corresponding thermodynamic constants are:

$$K^+ = \frac{(SuOH)(H^+)}{(SuOH_2^+)} \qquad \text{and} \qquad K^- = \frac{(SuO^-)(H^+)}{(SuOH)}$$

Without other sorbed species leading to charged complexes, the "surface charge" is defined as:

$$Q = [Su\text{-}OH_2^+] - [Su\text{-}O^-]$$
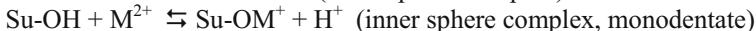
Another important parameter is the superficial density of sites Q_{max}, which is the maximum concentration of –OH surface sites able to react with protons.

The point of zero charge (pzc) is the pH value for which the surface charge is equal to zero. The variation of surface charge with pH is generally determined by acid or base titration of a suspension of the solid. The surface charge can also be measured by electro-kinetic methods.

The main theoretical difficulty results from electrostatic interactions in the vicinity of the surface. The activity (H^+) measured in the bulk of the solution is different from the activity in the vicinity of the surface and the apparent constants vary with the surface charge. For ions present in the electrical field of surface charge, is it necessary to consider an electrostatic free energy: $\Delta G_{elec} = z\, F\, \Psi(x)$, where z is the charge of the ion, F the Faraday constant and $\Psi(x)$ the electric potential at a distance x to the surface. This potential cannot be calculated a priori. Several models, based on the distribution of ions near to the surface have been proposed in order to connect the potential to the surface charge (constant capacitance model, diffuse layer model, basic Stern model, triple layer model,..). These models use a certain number of parameters, which are fitted from experimental sorption data together with sorption constants. Through these models, it is theoretically possible to calculate the "intrinsic" thermodynamic constants K^+ and K^-.

The sorption of ions depends on the nature and sign of the ion, together with the sign and charge of the surface, and, hence on pH. Two types of interactions are considered. Pure electrostatic interactions lead to "outer sphere" surface com-

plexes. Formation of covalent bindings with surface groups leads to "inner sphere complexes". Beneath are some examples of surface complexes:

$$Su\text{-}O^- + M^+ \leftrightarrows Su\text{-}O^- M^+ \quad \text{(outer sphere complex)}$$
$$Su\text{-}OH + M^{2+} \leftrightarrows Su\text{-}OM^+ + H^+ \quad \text{(inner sphere complex, monodentate)}$$
$$2Su\text{-}OH + M^{2+} \leftrightarrows (Su\text{-}O)_2M + 2H^+ \quad \text{(inner sphere complex, bidentate)}$$

As an example, the surface charge for the monodentate is:

$$Q = [Su\text{-}OH_2^+] - [Su\text{-}O^-] + [Su\text{-}OM^+]$$

Thermodynamic sorption constants can be calculated from these models together with Kd values, and their variation with pH and concentrations of other species in solution.

   Another surface complexation model is the **1-pK "Multisite complexation model"** or "Music" (Hiemstra 1989). It considers that the surface presents several families of oxide and hydroxide sites, each one with a specific acidity constant pK. However, each type of sites **cannot** be amphoteric (1-pK model), but the occurrence of several families of sites may confer an amphoteric property to the surface. Another feature of this model is the fact that the charge of a site may be fractional, this charge depending on the coordinance of the surface site. An example is:

$$Su\text{-}OH^{1/2-} + H^+ \leftrightarrows Su\text{-}OH_2^{1/2+}$$

Contrary to the 2-pK model, the acidity constants are calculated here a priori, from atomic geometrical and electrostatic considerations and by comparison to the monomeres of the same oxides. This model is more realistic than the monosite 2-pK model, but it requires a good knowledge of the crystal structure and surface orientations of the solid.

Evaluation of sorption models

Sorption mechanisms

The question is: do models represent the true sorption mechanisms? If not, what is the validity of such models when using them far from laboratory conditions, especially for radioactive waste, where prediction must be valid for more than thousands of years and applied to natural systems? To insure a safe extrapolation of models, it is necessary to know as better as possible the real sorption mechanisms. We must use methods able to localize the sorbed elements, determine the nature of their species and types of bindings. This goal can only be achieved by using a multidisciplinary approach, with several different methods (microscopic methods, bulk and surface spectroscopic methods) which bring complementary results.

   As an example, we indicate in Table 1 the main sorption mechanisms for some elements on hydroxyapatites (Fedoroff 1999, Monteil-Rivera 2000). The main feature is that the sorption mechanisms depend strongly on the element and that tradi-

Table 1. Main sorption mechanisms of some elements on hydroxyapatites.

Element	Sorption mechanisms
Cd^{2+}	Exchange with Ca^{2+} in the crystal framework in 2 sites, with diffusion in ≈ 3 superficial unit cells. Equilibrium not achieved within 10 d at 75°C
Pb^{2+}	Formation of new solid phases + slight incorporation into apatite framework
UO_2^{2+}	Formation of new amorphous solid phase
Eu^{3+}	Superficial sorption (site 1) + Incorporation in the apatite framework (site 2)
SeO_3^{2-}	Exchange with PO_4 groups of 1 superficial unit cell

tional models, described above, cannot be applied. Equilibrium is not achieved in many cases.

In the case of oxy-hydroxides, the general principles of surface complexation can be applied, but the determination of the real sorption sites and complexes, and of the true thermodynamic constants present many theoretical and experimental difficulties. We shall examine only several of these problems.

Choice among surface complexation and electrostatic models

The problem is the choice between the monosite or multisite models and among the different electrostatic models of the double layer. The same experimental system can often be fitted with different models, sometimes with different types of surface complexes. An important point is that calculated sorption constants for sorbed ions other than protons depend on the K^+ and K^- constants for protons, which in turn depend on the electrostatic model chosen.

In Table 2, we show some examples of parameters found by fitting one titration curve of goethite by different models using a least squares method. Considering the sum of squares is not of good help to choose the "best" model. The parameters obtained for the monosite 2-pK model depend on the electrostatic model and on the way how the least square fitting was run. It should be noted that, while one could consider that the variation on pK's is not so high, the variation of the fitted site density is very important. In the given example, we have considered only one site for the 1-pK model. The ion exchange model gives also a good fit, but the values of pK's are different since this model does not consider any electrostatic effect.

Table 2. Examples of comparison of models used to fit a set of titration data for goethite: calculated intrinsic constants pK$^+$ and pK$^-$, surface site density, capacitance and pzc.

Models and methods	pK$^+$	pK$^-$	Sites at/nm^2	Cap. C/m^2	PZC
Ion exchange	9.1	11.8	1.8		
2-pK monosite					
CCM, NWLS on H$^+$	6.9	9.2	3.9	1.2	8.1
CCM, WLS on pH	6.9	8.7	1.5	1.7	7.8
DLM, WLS on pH	7.4	8.1	0.3		7.8
1-pK multisite -OH$^{1/2-}$/OH$_2^{1/2+}$					
CCM, WLS on H$^+$	7.8		6.6	1.1	
CCM, NWLS on H$^+$	7.8		13	1.1	

CCM: constant capacitance model, DLM: diffuse layer model
WLS: weighted least squares, NWLS: not weighted least squares

Finally, at present time, it is difficult to make a choice. The main problem is that the electrostatic parameters are presently fitted from titration data. To our point of view, we should avoid using models with a large number of free parameters. One of the simplest but rather complete model is BSM (basic Stern model), which considers a layer with a constant capacitance, followed by a diffuse layer.
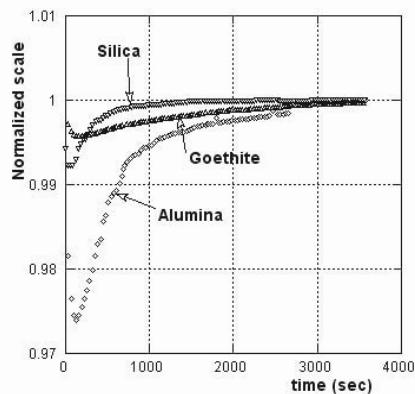
More and more examples show that the orientation of faces has an influence on the sorption properties. As an example, Rabung et al (2004) showed that Cm(III) is preferentially sorbed on (001) faces of sapphire by a factor of $\approx$7 compared to (110) planes and $\approx$25 compared to (018) planes at pH 4.5. So, for solids whose structure and crystal habits is known, it is likely to use the multisite model, rather than a monosite one.

For the sorption of ions other than protons and hydroxyls, the problem is the same, since it is also possible to fit the sorption isotherms with different types of surface complexes (monodentate, bidentates…). Spectroscopic methods have to be used to differentiate between complexes.

Another theoretical limitation is that, contrary to an equilibrium in a homogeneous liquid phase, there is no uniform definitions of standard and reference states for reactions at solid-liquid interfaces. The introduction of a reference site density has been proposed (Kulik 2002).

Kinetics

Models shown above suppose that equilibrium is achieved. In fact, kinetic effects play an important role in sorption chemistry. Kinetics may be a critical factor which will limit the sorption process in column operation and for transport, even

Fig. 1.   Kinetics of proton sorption during titration of
alumina, silica and goethite.
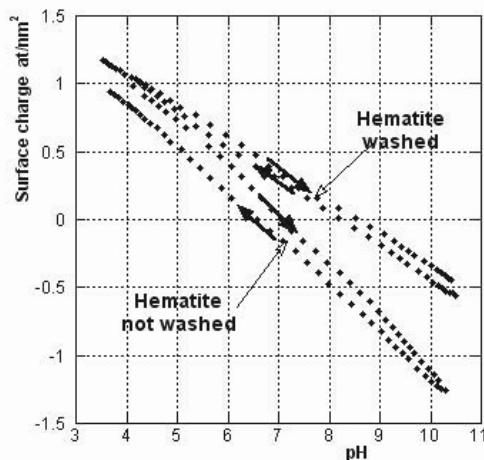
when equilibrium Kd values are very high. It may be also a factor which disturbs
the measurement of equilibrium thermodynamic constants.

   As an example, we show the variation of pH after an addition of acid during ti-
tration of a suspension of alumina, silica or goethite, in order to determine the sur-
face charge versus pH curve (Fig. 1). The delay to obtain an equilibrium value de-
pends on the solid and is connected to several factors such as its porosity. For this
type of alumina, a delay of 1 hour is needed after each addition, otherwise the pH
and calculated surface charge do not correspond to equilibrium values.

   Apart from the sorption of protons, kinetics limits also more or less the sorp-
tion of many ions. Kinetics and reversibility should be measured systematically,
since they may be the main factors controlling the transport of ions. They can also
indicate the nature of the sorption process.

Some factors affecting surface charge measurement, sorption and transport

It is evident that it is important to consider the different species of the elements
present in the solution. Several computer codes and data banks such as the code
developed by Van der Lee (2001) can be used to predict speciation. In certain
cases, precipitation, either in the bulk of the solution, either on the surface of the
solid may occur. Dissolution of the solid has also to be taken into account, since it
has an effect on the pH during titration experiments and, hence, on the calculated
surface charge. A correction for dissolution must be applied. In the case of the ti-
tration of γ-alumina (Lefevre 2004), the surface charge not corrected for dissolu-
tion seems to increase continuously with increasing H^+ concentration in solution,

Fig. 2.   Influence of washing treatment on forward
and backward titration curves of hematite

in contradiction with a defined surface site density. After correction for dissolution, the real charge achieves a maximum, which corresponds to the surface density of active sites.

It is well known from geological processes, that mineral species are subject to alteration, dissolution, recrystallization. However, the quantitative impact of such processes on the long term is difficult to be estimated, although some information can be deduced from thermodynamic data on the stability of minerals and through exchange of knowledge between chemists and geologists. An example is the large decrease of the density of active sites when γ–alumina is kept in water (Lefevre 2002). Investigation by X-ray diffraction, scanning electron microscopy (SEM), TGA and DTA showed that this modification of surface reactivity is induced by a transformation of γ–alumina into bayerite ($Al(OH)_3$).

Impurities and, especially, surface contaminations, can hide the "intrinsic" surface reactivity of a solid. We show on Fig. 2 the influence of a washing procedure, including treatments by acid and basic solutions, on the titration curves of hematite. This procedure removes species such as carbonates and sulfates, shifts the titration curves and, hence, the calculated surface charge and the pzc.

The majority of laboratory sorption experiments are supposed to be done in clean and abiotic conditions. This is certainly not the case in many of them, but the problem is quite more important in natural media. Presence of colloids in underground water can drastically accelerate the mobility of elements, if these elements are preferentially sorbed on colloids and if the porosity of the media allows the motion of colloids. In other conditions, sorption on colloids can reduce the mobility of radionuclides. Bacteria, by the possibilities of specific interactions with dissolved elements, can also have an important effect on the transport.

Thermodynamic and kinetical modeling

Conclusion

This short review could not describe all aspects of sorption processes and their impact on transport. We hope that we could, however, show the progress obtained in the knowledge and modeling of sorption processes and, in the same time, the new problems that this progress has induced. Among the next steps for future progress, we may quote: use of high-purity solids with known surface orientations, use of better electrostatic models with parameters determined independently from sorption measurements, models with realistic surface electron density taking into account surface reconstruction. Experimental and theoretical work has to be done to transpose knowledge on simple solid phases to complex systems, with choice of the pertinent major parameters for transport prediction.

References

Barrer R. M., Falconer J. D. (1956) Proc. Roy. Soc. 236A: 227

Dubinin M. M., Radushkevich L. V. (1947), Proc. Acad. Sci, Phys. Chem. USSR, 55: 331

Fedoroff M., Jeanjean J., Rouchaud J. C., Mazerolles L., Trocellier P., Maireles-Torres P., D. J. Jones D. J. (1999), Solid State Sciences, 1: 7

Freundlich H. (1926), "Colloid and Capillary Chemistry", Methuen, London, England

Gaines G. L., Thomas H. (1953), J. Chem. Phys. 21: 214

Hiemstra T.,Van Riemsdjik W. H., Bolt G. H. (1989) J. Colloid Interface Sci. 133: 91

Holstetler D. D., Serne R. J., Baldwin A. J., Petrie G. M. (1980), "Status report on sorption information retrieval systems", PNL-3528, Pacific Northwest Lab. Richland, Washington, USA

Jauzein M., André C., Margrita R. , Sardin M., Schweich D. (1989), Geoderma, 44: 95

Kulik D. A. (2002) Radiochim. Acta 90: 815

Langmuir D. (1918), J. Am. Chem. Soc., 40: 1361

Lefevre G., Duc M., Lepeut P., Caplain R., Fedoroff M. (2002), Langmuir, 18: 7530

Lefevre G., M. Duc M., Fedoroff M. (2004) J. Colloid Interface Sci., 269: 274

Monteil-Rivera F., Fedoroff M., Jeanjean J., Minel L., Barthes M. G., Dumonceau J. (2000), J. Colloid and Interface Sci., 221(2): 291

Rabung T. ,Schild D., Geckeys H., Klenze R., Fanghänel T. (2004) J. Phys. Chem. B 108: 17160

Serne R. J., Muller A. B. (1987), "A perspective on adsorption of radionuclides onto geologic media", in "the geological disposal of high level radioactive wastes", Brookins, D. G. Edit., Theophrastus Pub., Athens

Stenhouse M., Pöttinger J. (1994), Radiochim.Acta 66/67: 267

Stumm W. (1992), "Chemistry of the Solid-Water Interface", Wiley-Interscience

Van der Lee J. (2001) Chess: Software for Geochemistry, Hydrology and Environmental Science, Ecole des Mines, Fontainebleau, France

Van der Lee J., de Windt L., Lagneau V., Goblet P. (2002) Hypec: Module-oriented modelling of reactive transport, Ecole des Mines, Fontainebleau, France

Zouad S., Jeanjean J., Loos-Neskovic C., Fedoroff M. (1992), J. Solid State Chem. 98: 1

Simulation of propagation of leachate after the ISL mining closure

Alexander Roshal, Dan Kuznetsov

Geolink Consulting, Warshavskoe shosse 39a, 117105 Moscow, Russia,
E-mail: dkuznetsov@geolink-group.com

Abstract. The solution formed in the process of uranium in-situ leaching propagates after the mining closure with the regional groundwater flow. Forecasting the migration of solution requires account of chemical reactions in the system of the acid solution and subsurface medium. The process of propagation of solution, and methods for this process modeling are considered in the paper. The Eulerian approach to calculation of reactions leads in the present case to significant numeral dispersion. In order to avoid this numerical effect, we have solved two independent passive mass transport problems. The final solution is a geometrical intersection of passive solutions.

Introduction

The forecast of propagation of leaching solutions is the important part of assessment of potential impacts of uranium in-situ leaching. This paper presents the model results of migration of leachate for one of the uranium in-situ leaching sites. The goal includes forecasting the migration of leachate, and assessing risks of pollution of groundwater used for water supply. An aquifer system within the study area consists of several layers. Uranium ore is deposited in the lower aquifers at a depth of near $500m$ from the land surface. The upper aquifers are used for groundwater supply. The ISL operational scheme of studied mining plant consists of injecting and pumping well rows, and sulfuric acid is used as a leaching liquid.

The territory has an area of about 150 square kilometers. Size of a model grid cell used for the forecasting simulation is $50x50m$. The aquifer system was divided into 9 model layers. Taking into account hydrodynamic dispersion for the mass transport modeling brings insignificant corrections to the resulting area of solution distribution in the present case. So dispersion was not accounted for.

Sulfuric acid not only provides chemical conditions for uranium dissolution, but also reacts with the subsurface medium, mostly with the carbonate minerals. Products of these reactions that appear in the solution are mainly calcium, magnesium, and sodium sulfates. A domain of high acid and sulfate concentration is formed in the process of leaching, and its size is close to the size of uranium ore deposit. A domain filled with sulfates has larger size than the domain filled with acid. Besides that, the total sorption of sulfates requires more time than the total acid neutralization. As an example, we consider only the propagation of acid solution.

Description of the process

It is supposed that all reactions proceed relatively fast compared to the groundwater flow, and the local equilibrium assumption is valid. The neutralization of acid provided by reactions with the medium results in a transition of uranium and other elements from the solution to solid phase. Thus the process of acid neutralization results in retardation of propagation of acid front in relation to the propagation of "clear" water.

Let determine a retardation factor for the leachate. Suppose that capacity of sorption E is a constant, which depends on the content of acid sorbing minerals in the subsurface medium. Balance equation for an elementary element dl, containing acid in the porous space, and acid spent for the reaction over dt time interval, can be written as follows:

$$(n\, C + \rho\, E)\, F\, dl = Q\, dt\, C, \qquad Q = v\, F, \tag{1}$$

where the variables are defined as follows: C, concentration of acid in solution [ML-3]; n, porosity [-]; E, capacity of sorption [MM-1]; ρ, bulk density of subsurface medium [ML-3]; F, cross section of the element; Q, Darcy flow rate [L3T-1]; v/n, seepage velocity.

Velocity of the acid front can be obtained from (1) as follows:

$$\frac{dl}{dt} = \frac{v}{(n + \rho\, E / C)} \tag{2}$$

Hence the retardation factor is

$$R = 1 + \frac{\rho\, E}{n\, C} \tag{3}$$

As a result of field and numerous laboratory tests and simulation of pilot leaching, the average retardation factor for the territory had been taken equal to $R_0 = 10$.

The acid solution extends in all directions from the system of technological wells, while the mining is proceeding. This is provided by pumping wells, which lift the leachate on the surface for further processing, and is not an assumption in our case. Modeling results show that presence of the natural regional groundwater

flow practically has not an influence on directions of transport of leachate, and that we deal with a single front between natural water and the leachate.

The situation after the mining closure is another one. When technological injecting and pumping wells are stopped, the propagation of leachate's remainder is completely determined by the regional groundwater flow. Thus two fronts appear. A forward front is a front where the solution reacts with the medium. A back front is a front where the leachate is displaced by natural water. Velocities of these fronts are different.

We suppose that processes of neutralization are irreversible. This means that neutralization processes proceed only at the forward front. Therefore the forward front of the solution propagates with the velocity, which is determined by the appropriate retardation factor. The back front of the solution propagates with the same velocity as "clear" natural water. The retardation factor for the back front is equal to 1.0 for all components. So we need to model two liquids together, the only one interacting with the subsurface medium.

Test of the Eulerian approach to reaction calculating

There are numerous different Eulerian-Lagrangian methods that made it possible to model mass transport and chemical reactions in groundwater systems (Zheng and Wang (1999); Clement (1997); Prommer et al. (2003)). It is noteworthy that the Eulerian approach involved the use of the concentration averaged over the whole cell of the model grid, rather than the "natural" concentration in some concrete point of the space. A particular method for calculation of concentration may vary, but values obtained as a result of calculation approximately correspond to the relative volume of component in the grid cell.

Consider 1D groundwater flow where one liquid, with relative concentration $C_0 = 1.0$, displaces another liquid with zero concentration. The first liquid reacts with the medium. The reaction mechanism, for example, is the same as for the acid-medium reaction in our leachate, when the retardation factor is in inverse proportion to the concentration of solution:

$$R = 1 + \frac{A}{C} , \tag{4}$$

where C is a relative concentration of displacing solution, A is a time independent constant.

The distance of propagation of displacing front at the time moment ΔT equals to

$$\Delta L = \frac{v \, \Delta T}{n \, R_0} \tag{5}$$

Let ΔL be a spatial step of 1D model grid. Then we will simulate the propagation of solution by using equations (3) and (5). Divide a time interval ΔT onto m

equal time steps Δt :
$$\Delta T = m\, \Delta t$$

The distance, which is passed by the solution during the one time step, equals to:

$$\Delta x_i = \frac{v\, \Delta t}{n\, R_{i-1}} \quad,$$

where R_{i-1} is a current value of the retardation factor calculated by equation (4), by using the value of "concentration" from the previous time step.

After the i-th time step, the calculated "concentration" of displacing solution equals to:

$$C_i = \frac{\sum\limits_{i=1}^{m} \Delta x_i}{\Delta L} = \left[\sum\limits_{i=1}^{m} \frac{1}{R_{i-1}} \right] \frac{R^0}{m} \tag{6}$$

Thus we obtain an absurd result: the distance passed by the displacing solution depends on the modeling time discretization.

Check the result of modeling using equations (4) and (6). When $m = 1$, the result is exact. However, when m equals to any other value, the situation is changing. Let, for example, $m = 2$ and $A = 9$, where A is the constant from equation (4). Suppose that before the first time step displacing solution locates in the previous model cell, and the retardation factor for displacing solution initially equals to $R_0 = 10$. The results of this numerical "modeling" are presented in the table (Table 1). We have obtained the wrong result. Displacing solution has left the model cell in 3rd time step instead of 2nd time step as it follows from equation (5).

Test these numerical effect ones more. The results of calculation, when $m = 5$, are presented in the table (Table 2). The result is wrong again. Displacing solution has left the model cell in the 10th time step instead of the 5th time step as it follows from equation (5).

It is not difficult to show that numerical errors don't reduce, when time steps decrease, and even become increasing and accumulating. The solution propagates with variable velocities since the model "concentration" is calculated in each time step, and different in each time step. The retardation factor, in this case, equals to its real value only in the first time step, and greater in any further steps. Thus the time of solution leaving from the cell is determined by some average value, which is always greater than the real value of the retardation factor. Note that the considered example can be extended for any other reaction process described by concentrations, and numerical effects have also the same nature for other processes.
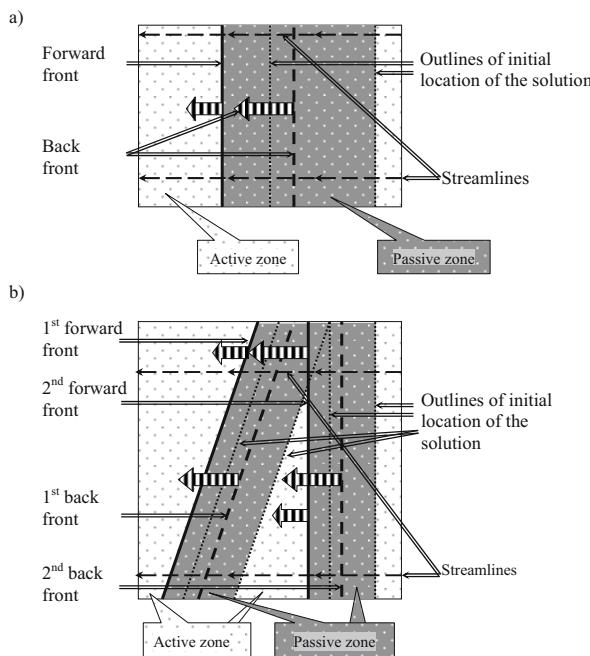
Thus the Eulerian approach can cause significant numerical errors that increase when time steps decrease. The alternative for the Eulerian approach is a pure Lagrangian approach to mass transport modeling, for example, similar to one of the methods described in Batycky (1997), Thiele et al. (1995), Thiele (2001). We used another method proceeding from requirements of the following expertise. The method uses the only advection part of widely distributed MT3DMS code described in the next section.

Solution method

Since the reaction process is irreversible, it proceeds only at the forward front. The solution doesn't interact with the medium upstream from the forward front, since the solution and medium are in the equilibrium there. Thus the medium, where the solution propagates, can be divided into two zones by the forward front of the solution (Fig.1a):

1) The active medium zone located downstream from the forward front of the solution
2) The passive medium zone located upstream from the forward front of the solution

For simulation of migration of this solution, the following approach can be used. Two mass transport problems are solved. Transport parameters of the subsurface medium are uniform in both problems. In the first problem, the transport of the active solution is modeled. The retardation factor is identical for the whole space, and equals to the retardation factor for the studied component of the solution. In the second problem, the propagation of the passive tracer is modeled. The retardation factor in this case is also identical for the whole space, and equals to 1.0. Thus

Fig. 1. Scheme of propagation of the active solution in groundwater flow. a) – simple configuration of the area filled with the solution. b) – curved area filled with the solution.

Thermodynamic and kinetical modeling

we have two areas filled with the solution:
1) Area of spreading of the active solution, which interacts with the medium
2) Area of spreading of the passive solution, which doesn't interact with the medium
3) The final solution is found by intersection of the two areas (shared part of the areas 1. and 2.).

The considered technique is correct, if and only if any streamline traverses the solution area only once. This assumption is valid for many cases, but a part of orebodies of the studied deposit is curved, and some streamlines traverse the area of the solution twice. This means that while the solution is propagating, two forward and two back fronts are formed, and the active medium zone locates not only upstream, but also downstream from one of the forward fronts (Fig.1b).

The second forward front initially propagates in the active medium zone, but in some time it will locate in the passive medium zone, which has been formed by the first forward front (Fig.1b). Since the active solution has already reacted with the medium in this zone, a new front doesn't react there. Hence the second forward front of the solution propagates in this zone with the same velocity as a passive tracer. So our scheme requires correction to this situation.

The way out of the situation is simple, but requires manual intervention. The passive medium zone can be periodically extended according as the forward front of the solution is propagating. It should be done when the back front has come near the previous boundary between the active and passive media. In our case study, we had to correct the passive and active zone boundaries only twice.

Table 1. Results of test mass transport calculation, when m=2.

Step	R_i	C_i
1	10.00	0.500
2	19.00	0.763
3	12.79	<1.0

Table 2. Results of test mass transport calculation, when m=5.
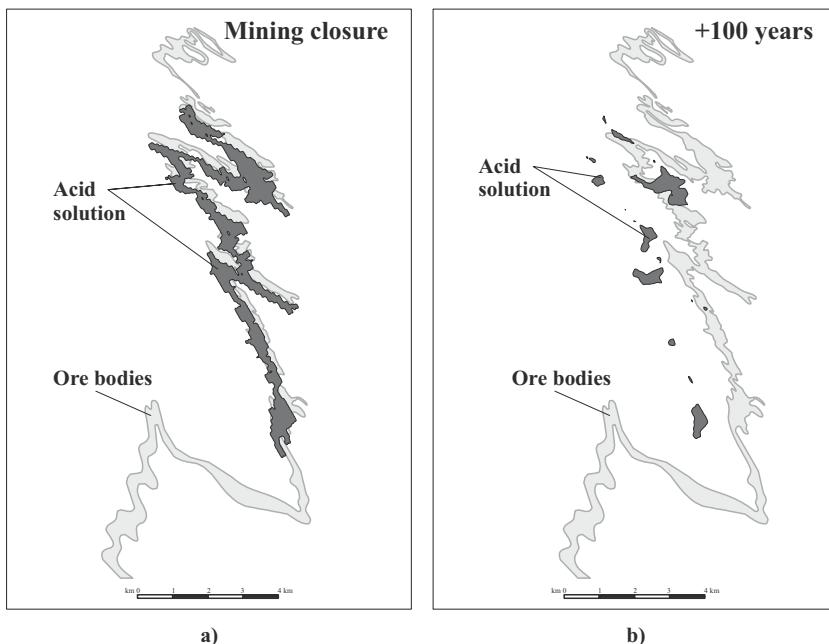
Step	R_i	C_i
1	10.00	0.200
2	46.00	0.243
3	37.96	0.296
4.	31.39	0.360
5	26.01	0.437
6	21.60	0.529
7	18.00	0.640
8	15.05	0.773
9	12.64	0.932
10	10.66	> 1.0

Results

By having used the method described, the model forecast of propagation of leachate was done for mining and after mining time. The flow problem was solved by Chebyshev's chess algorithm from the ModTech suite, and the MT3DMS code was used for the mass transport modeling.

Outlines of uranium ore bodies and zones filled with the leachate are shown in Fig.2 for one of the model layers. Fig.2a contains the spreading area of the leachate at the moment of mining closure. Configuration of the leachate area is close to configuration of the ore bodies. An area of the solution, which would have spread in 100 years from the moment of the mining closure, is shown in Fig.2b. Area filled with the solution is significantly smaller in this case.

Model results show that time required for the total neutralization of the acid is near of 370 years. The maximum distance of propagation of solutions is near of 700-800m. In spite of relatively significant time required for acid neutralization at the considered deposit, practically there is no risk of contamination of groundwater used for water supply by the leachate. Only the upper layers are used for water supply at the territory, and uranium ore bodies locate significantly deeper. Even at the moment of maximum size of areas filled with the solution, solution locates deeper than groundwater used for water supply, and doesn't affect the upper aquifers.

Fig. 2.   Spreading of the leachate at the moment of mining closure a) and 100 years after mining closure b).

Thermodynamic and kinetical modeling

Conclusion

Simulation of propagation of leachate during and after the uranium in-situ leaching is considered in the paper. During the mining, the leachate extends in all directions from the system of technological wells. Regional groundwater flows have low influence on the initial zone filled with the leachate. After the mining closure, when all technological wells are stopped, a zone filled with the leachate propagates with the regional groundwater flow. The size of the zone decreases by interaction of the active components with the subsurface medium.

There are various numerical methods that made it possible to model propagation of the reactive solution in the groundwater flow. Some of the methods use the Eulerian approach to reaction calculating. In the considered case, the Eulerian approach leads to significant numerical dispersion. Conjugation of solutions of two passive mass transport problems was used in order to reduce errors caused by numerical dispersion. Propagation of an active solution is modeled in the first problem. The second problem considers the propagation of a passive tracer that doesn't interact with the medium. Parameters of the transport are the same for two problems, except for the retardation factor. So two areas filled with the active and passive solution are formed. The final solution is found as intersection of these two areas.

The model forecast shows that the maximum distance of propagation of leachate does not exceed 700-800m. The total time of the forecast is 400 years. Results show that the total neutralization of acid should occur during this time. In spite of relatively significant time required for the neutralization of acid, there is no risk of contamination of groundwater used for water supply. This is conditioned by deep occurrence of the uranium ores deposit.

References

Batycky RP (1997) A Three-Dimensional Two-Phase Field Scale Streamline Simulator, PhDThesis, Stanford University, Dept. of Petroleum Engineering, Stanford, CA.

Clement TP (1997) A Modular Computer Code for Simulating Reactive Multispecies Transport in 3-Dimensional Groundwater Systems. Technical Report PNNL-SA-11720, Pacific Nortwest National Laboratory, Richland, Washington.

Prommer H, Barry DA, Zheng C (2003) MODFLOW/MT3DMS-based reactive multicomponent transport model. Groundwater 41: 247-257

Thiele MR, Blunt MJ, Orr FM (1995) Modeling Flow in Heterogenous Media Using Streamtubes - I. Miscible and immiscible displacements," InSitu 19 (3), 229-339.

Thiele MR (2001) Streamline Simulation. 6th International Forum on Reservoir Simulation

Raffinate Neutralization Experiments at the McClean Lake Mill – Removal of Arsenic and Nickel

John Mahoney[1], Donald Langmuir[2], Maynard Slaughter[3], John Rowson[4]

[1]Hydrologic Consultants, Inc. Lakewood, Colorado, USA,
E-mail: jmahoney@hcico.com
[2]Hydrochem Systems Corp., Silverthorne, Colorado, USA
[3]Crystal Research Laboratories, Greeley, Colorado, USA
[4]COGEMA Resources, Inc., Saskatoon, Saskatchewan, Canada

Abstract. Uranium ores at the McClean Lake Operation in the Athabasca Basin of Northern Saskatchewan can produce elevated levels of arsenic (up to 700 mg/L) and nickel (up to 500 mg/L) in acidic (pH<1.5) spent leaching solutions (raffinates). Prior to neutralization, if necessary, ferric sulfate is added to tailings slurries to increase their Fe/As (molar) ratio to greater than 3. The slurries are then neutralized with lime to pH 4, and subsequently to pH 7-8. After neutralization, As and Ni concentrations average less than 1 mg/L. Solids from bench scale experiments demonstrate that As is associated primarily with scorodite and annabergite, with small amounts adsorbed onto or co-precipitated with ferrihydrite.

Introduction
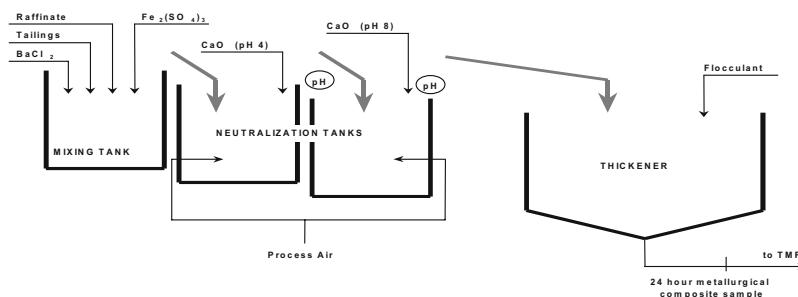
Predicting the mobility of contaminants such as arsenic in ground water has become increasingly important as risk assessment plays a greater role in the licensing of waste disposal facilities. In the Athabasca Basin of northern Saskatchewan, elevated concentrations of arsenic (up to 10% by weight) and nickel (approximately 5 %) in uranium ores have required that detailed studies be conducted to assist in designing methods to reduce pore water concentrations of As and Ni in the tailings (Langmuir et al. 1999).

At the JEB Mill at McClean Lake, uranium is extracted from ore using sulfuric acid. The leach residue consists chiefly of unreacted quartz and illite, with lesser amounts of kaolinite and chlorite. After extraction, the leach residue solids are mixed with the barren leach solution (raffinate), which commonly has a pH below

2.0. To control dissolved As concentrations, which often reach 700 mg/L in the acid raffinate, a tailings neutralization circuit was included in the mill (Fig. 1). Prior to neutralization, the raffinate has its molar Fe/As ratio increased to a minimum of 3 by the addition of ferric sulfate. The raffinate and leach residue slurry is then neutralized by lime addition in the first neutralization tank to pH 4, and subsequently to pH 7-8, in a second neutralization tank. Residence times in each neutralization tank are approximately 90 minutes. After neutralization, As and Ni concentrations in slurry pore waters are typically less than 1 mg/L. Extensive laboratory work has demonstrated that a pH of approximately 7 is optimum to minimize both Ni and As concentrations. This pH was selected because, as an oxyanion As is least soluble under low pH conditions, whereas cationic Ni is least soluble at alkaline pH values (Jones et al., 1997). Neutralization also causes the precipitation of gypsum [$CaSO_4 \cdot 2H_2O$], hydrobasaluminite [$Al_4SO_4(OH)_{10} \cdot nH_2O$, n = 2–3], ferrihydrite [an Fe(III) hydroxide] and theophrastite [$Ni(OH)_2$]. Precipitated phases that contain important amounts of As include the poorly crystalline arsenate minerals scorodite or ferric arsenate [$FeAsO_4 \cdot 2H_2O$], and annabergite [$Ni_3(AsO_4)_2 \cdot 8H_2O$], a possible oxyhydroxide coprecipitate with a variable Fe/As ratio, and surface precipitated or adsorbed As (cf. Mahoney et al., 2005).

Solids in the neutralized slurry are typically comprised of 50-70% leach residue with the remainder as precipitated (secondary) solids. The slurry is pumped into the JEB Tailings Management Facility (TMF) for final disposal using a subaqueous emplacement process. Underdrains in the TMF allow for the removal of the pore water expelled by settling and compaction. The drain water is pumped to a water treatment facility for final processing before being released to the surface environment.

Neutralization tests using mill-produced raffinate were performed to: 1) study changes in solution composition as a function of pH; 2) evaluate the influence of different neutralizing agents on dissolved arsenic concentrations; 3) produce arse-

Fig. 1.   Diagram of Tailings Neutralization Circuit – JEB Mill.

Thermodynamic and kinetical modeling

nic and nickel-rich solids for quantitative mineralogical analysis, including x-ray diffraction and spectroscopic analyses using x-ray absorption fine structure (XAFS) techniques; and 4) develop a geochemical model of the neutralization process.

Experimental Methods

The testing program was designed to evaluate the influence of factors including pH, selection of neutralizing agent, and the presence or absence of leach residue on the concentration of arsenic in the solution and the mineralogy of the precipitated phases.   To perform the first experiments, approximately 60 liters of raffinate (Raffinate 1) were collected and spiked with As, Ni and Fe(III) (Table 1). Additional experiments, which consumed approximately 20 liters of raffinate (Raffinate 2), were performed primarily to assess redox reactions. Both raffinates were spiked with anhydrous As_2O_5 and $NiSO_4:5H_2O$. Ferric sulfate (Triron® solution) was added to increase the Fe/As ratio.

   The experiments were designed to evaluate the behavior of As and Ni over the pH range of 2.0 to 8.0. Various neutralizing agents were used including dry $Ca(OH)_2$, NaOH pellets, and slaked lime (CaO) slurry. The procedure involved adding a neutralizing agent (base) to all of the beakers while continuously stirring. The pH was monitored and more base was added to successive beakers. After reaching their target pH values, the slurries were filtered and the solutions analyzed.

Table 1. Raffinate compositions, concentrations in mg/L.

Parameter	Raffinate 1 Unspiked	Raffinate 1	Raffinate 2 Unspiked	Raffinate 2
pH		1.5		1.1
Total As	362	732 (920)		693 (729)
Sum of As (III+V)			351	668
As(III)			100	447
As (V)			251	221
Fe Total	629	2,400 (2,700)	808	1,854 (2,400)
Fe (II)			640	685
Al		420		200
Ca		760		589
Cl		14		13
K		210		357
Mg		260		229
Na		48		23
Si		260		190
Sulfate		14,100		21,430
Ni	203	560 (550)	230	515 (529)
Eh (mv)				668
Fe/As(molar)	NA	4.4	NA	3.6
Fe/Ni(molar)	NA	4.5	NA	3.8

Concentrations in ( ) represent rapid turnaround time semi-quantitative analyses
NA – Fe/As and Fe/Ni ratio are not calculated for unspiked raffinate

Thermodynamic and kinetical modeling
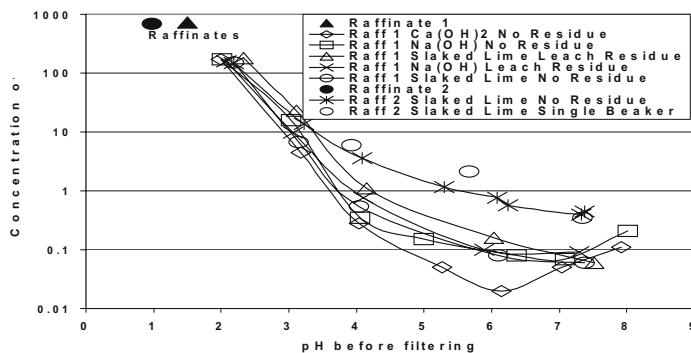
The Raffinate 2 experiments placed particular emphasis on redox measurements including nearly continuous readings with a platinum electrode as the neutralizations proceeded. Laboratory analyses included total As, and analyses for As(III) and As(V). Iron measurements included total Fe and Fe(II), with Fe(III) estimated by difference.

To further concentrate As-bearing phases, one set of experiments was performed using approximately 5 liters of spiked raffinate (Raffinate 2) and a single "beaker". The neutralization procedure was similar to the batch experiments except that when the neutralized raffinate was filtered, the solution, less an aliquot for analysis, was returned to the "beaker" for additional neutralization and filtration. These experiments removed previously precipitated solids, thus separating the different solids as the pH increased.

Results and Discussion

Fig. 2 shows the concentration of total arsenic as function of pH during the tests. Results for the different experimental conditions are generally similar. The experiments that used Raffinate 2 show higher arsenic concentrations in the higher pH ranges. This is caused by the smaller Fe/As ratio in Raffinate 2 than in Raffinate 1. The figure includes data sets that used slaked lime or sodium hydroxide as neutralizing agents. Arsenic concentrations do not significantly differ, regardless of which base is used. The overall similarity of the As concentrations for the Raffinate 2 experiments, which contained accumulated solids, and the single beaker experiments, in which solids were removed, suggests that, at least for arsenic, the precipitated solids do not continue to react with the solution.

Fig. 3 shows the concentration of Ni as a function of pH during the neutralization experiments. As was observed for arsenic, the different neutralizing agents do not influence dissolved Ni concentrations. Separately, at similar pH values, concentrations of Ni in the three samples from the single beaker experiment were

Fig. 2.   Arsenic concentrations during raffinate neutralization experiments.

Thermodynamic and kinetical modeling

greater than in samples from the batch tests. The differences are most significant at higher pH values. This suggests that Ni concentrations may be influenced by the presence of previously precipitated solids.

Fig. 4 shows major component concentrations during the neutralization of Raffinate 2, including the three single beaker samples. As just noted, concentrations of As and Fe both decrease with rising pH at low pH values. Ni concentrations also consistently show small decreases from pH 2 to approximately 5. Aluminum begins to precipitate near pH 4.

Fig. 5 shows the number of moles precipitated for As, total Fe, Ni and Fe(II) at each neutralization step. The figure demonstrates that Fe and As are removed at a one to one proportion at pH of 2.18, which provides strong evidence that scorodite is formed under these conditions. As the pH increases to 3.22 much of the remaining As is removed as scorodite. Approximately 98 percent of the total As is removed from solution by a pH of 3.22. A significant amount of additional Fe is also removed in this pH range.

Small amounts of Ni are also removed even under low pH conditions. It is believed that strong pH gradients are formed during the addition of slaked lime, and that these gradients, coupled with the abundance of As and Ni, allow for the formation of annabergite $[Ni_3(AsO_4)_2 \cdot 8H_2O]$. Saturation index calculations demonstrate that annabergite is not in equilibrium with the solution at any pH of the bulk solution during neutralization. However mineralogical studies indicate that the phase is present. With increasing pH (greater than 5) significant amounts of Ni are removed.
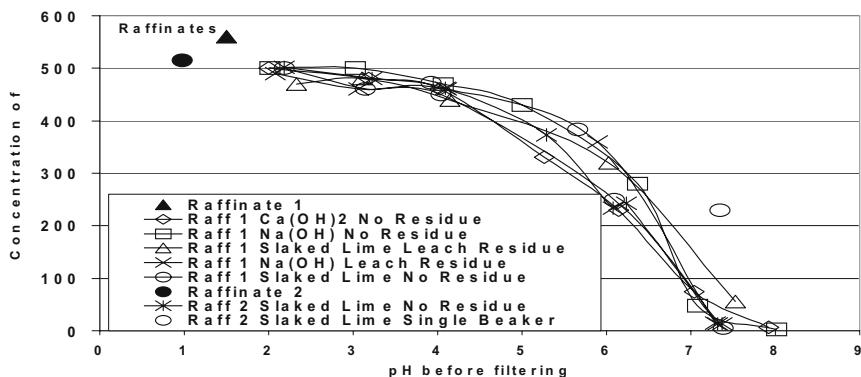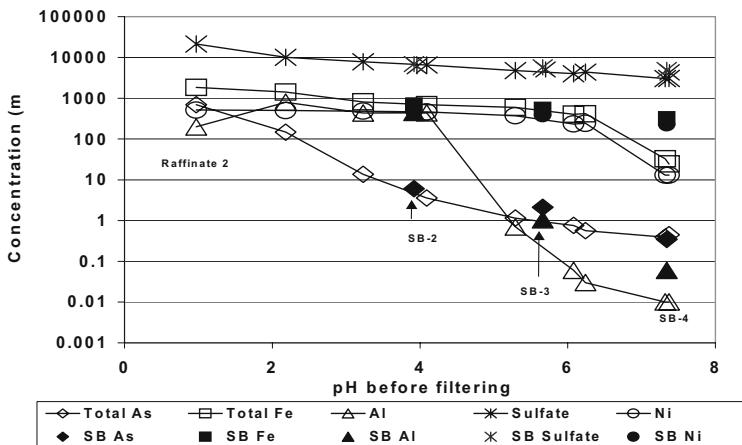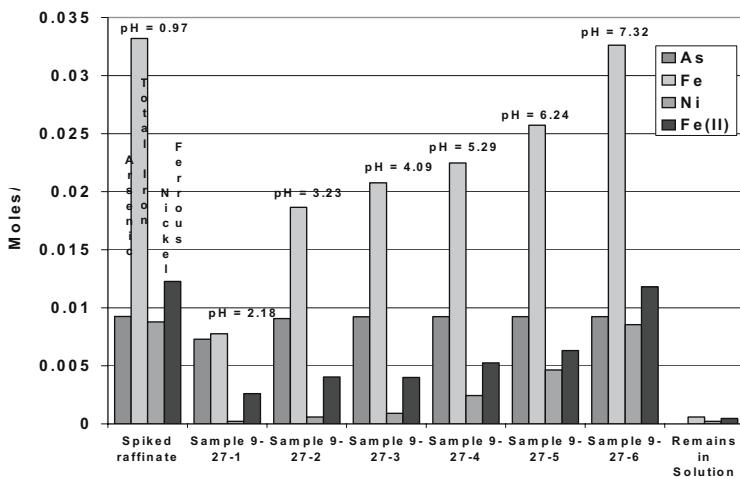
Fig. 3.   Nickel concentrations during raffinate neutralization experiments.

Thermodynamic and kinetical modeling

Fig. 4.   Changes in major components during slaked lime neutralization of Raffinate 2.

Fig. 5.   Cumulative molar concentrations removed from neutralized raffinate. The spiked raffinate sample shows initial concentrations in solution.

Thermodynamic and kinetical modeling

Saturation Index Calculations
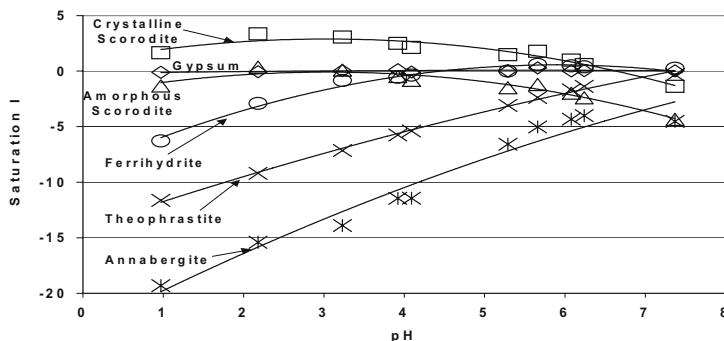
The geochemical modeling program PHREEQC (Parkhurst and Appelo, 1999) was used to calculate saturation indices for these samples. Saturation indices (SI) are defined as

$$SI \ = \ log\frac{(IAP)}{(Ksp)} \tag{1}$$

Where, IAP is the ion activity product of the mineral. At a saturation index of 0.0, the IAP equals the Ksp and the mineral is at equilibrium with the solution. Positive values mean that the IAP is greater than the Ksp and the solution is super-saturated with respect to the mineral. Baring kinetic constraints, the mineral should precipitate and concentrations in solution should decrease. Negative SI values mean that the solution is undersaturated and the mineral, if present, should dissolve.

Fig. 6 show saturation indices for gypsum, crystalline and amorphous scorodite, annabergite, ferrihydrite and theophrastite [Ni(OH)$_2$]. The raffinate is undersaturated with respect to amorphous scorodite, but oversaturated with respect to the crystalline form. The results from pH 3.0 to about pH 5.0 are particularly noteworthy; the solutions are at saturation with respect to amorphous scorodite. The crystalline form remains oversaturated. The bracketing of SI values between amorphous and crystalline scorodite suggests that scorodite of intermediate crystallinity limits As concentrations in these solutions.

For the other phases, the calculations demonstrate that gypsum is at saturation under all pH conditions. Ferrihydrite reaches saturation at a pH of approximately four. Theophrastite remains undersaturated until a pH of approximately seven is reached. Annabergite is always undersaturated.

Fig. 6. Saturation indices for selected phases from Raffinate 2 measurements, speciated iron and arsenic activities based upon measured pe and total concentrations.

Table 2. Parameters used in geochemical model.

pH	-Log Ksp Al_Scorodite	Proportions	Measured As (mg/kg)	Modeled As (mg/kg)	Measured Ni (mg/kg)	Modeled Ni (mg/kg)
0.97			686		529	
2.18	22.31	0.96/0.04	150	181	510	510
3.23	22.66	0.87/0.13	13.6	13.1	487	486
4.09	23.16	0.82/.018	3.5	3	467	467
5.29	24.00	0.6/0.4	1.1	1	376	390
6.24	25.11	No Mix	0.56	0.55	245	390
7.32	25.11	No Mix	0.37	0.55	13.2	29

Geochemical Modeling Simulations

To understand the precipitation of minerals during the raffinate neutralization experiments, a geochemical model was developed using PHREEQC (Parkhurst and Appelo, 1999). The model was primarily designed to describe the changes in As, Ni and Fe concentrations.

The results in Fig. 5 demonstrate that a scorodite-like phase is removed as the raffinate is first neutralized. Saturation index calculations provide supporting evidence that the phase is initially amorphous. Mineralogical analysis suggests that the scorodite has an approximate composition of: $Fe_{0.9}Al_{0.1}AsO_4 \cdot 2H_2O$. Accordingly, the model included precipitation of an initially amorphous Al-bearing scorodite. To improve the fit between measured and modeled arsenic concentrations, increasingly negative log K_{sp} values for amorphous Al scorodite were assumed with increasing pH. With slight adjustments to the K_{sp} for Al scorodite (Table 2), the simple equilibrium model did an excellent job of matching measured As and Fe concentrations.

To match nickel concentrations, a non-equilibrium sub-step was added to the model. In this sub-step a portion of the raffinate is neutralized to pH 7, which removes nickel either as annabergite or $Ni(OH)_2$. The pH 7 solution, less the precipitated solids, is then mixed back with the solution obtained from the previous step and equilibrated to produce a final concentration for the model defined pH. The sub-step reflects the disequilibrium, high pH conditions that must surround particles of incompletely reacted base. Such locally elevated pH values will cause minerals to precipitate that are not stable at the lower pH of the bulk solution.

The proportions of raffinate and pH 7.0 solution were estimated from measured changes in nickel concentrations in the bulk solution with increasing pH. For example, Raffinate 2 (pH 0.97) had an initial nickel concentration of 529 mg/kg (PHREEQC uses molalities, which are then converted to mg/kg of water). At pH 2.18, the nickel concentration was 510 mg/kg, indicating a loss of approximately 4 percent of the nickel between pH 0.97 and 2.18. A mixture of 96 percent raffinate and 4 percent neutralized raffinate (pH 7.0) produced a nickel concentration of approximately 510 mg/kg, an acceptable model fit. Proportions were increased
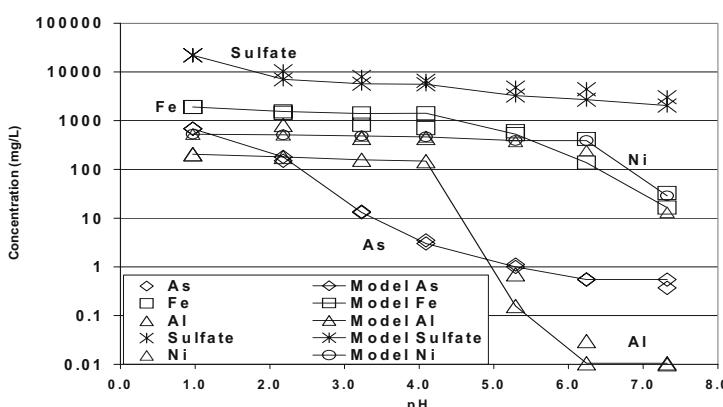
with increasing pH (Table 2). Subsequent model steps used the previous equili-
brated solution as the starting composition. Thus, in the first sub-step annabergite
was removed, but with decreased As concentrations, annabergite became under-
saturated and $Ni(OH)_2$ precipitated in the later steps.

The pH 5.29 solution was the starting solution for pH 6.09 and 7.38 steps. To
model the pH 6.09 sample, the pH 5.29 solution was neutralized to a pH of 6.09.
Only gypsum, hydrobasaluminite and ferrihydrite precipitated at this pH. At pH
7.32, the model predicted that gypsum, theophrastite and ferrihydrite would pre-
cipitate. The predicted concentrations for the Raffinate 2 experiments using this
conceptual geochemical model for the raffinate neutralization process are pro-
vided in Fig. 7.

The complexity of the model reflects the fact that neutralization of the raffinate
is a complicated process in which both equilibrium and nonequilibrium reactions
take place. The model presented in this paper is obviously not unique. Numerous
aspects, which have been arbitrarily defined, could be redefined and would still
provide excellent fits to the data.

The equilibrium portions of the model suggest that precipitation of a scorodite
phase of increasing crystallinity (smaller solubility product constant) with increas-
ing pH, limits maximum arsenic concentrations up to pH 6-7. Adsorption reac-
tions are not required to explain arsenic behavior. Mahoney et al. (2005) showed
that reversible adsorption reactions have little impact on the concentration of arse-
nic.

The change in nickel concentrations with rising pH is explained by the precipi-
tation of annabergite or theophrastite in local environments under the high pH
conditions associated with unreacted base. Interaction with secondary solids may
also play a role in the behavior of nickel. Nickel concentrations are lower than a
mineral precipitation equilibrium model alone would predict, except at the highest
pH values, when theophrastite $[Ni(OH)_2]$ approaches saturation (Fig. 6).

Fig. 7. Comparison of measured and modeled concentrations of some major species dur-
ing the neutralization of Raffinate 2 using slaked lime.

Thermodynamic and kinetical modeling

References

Jones, C.A., Inskeep, W.P., and Neuman, D.R., 1997. Arsenic transport in contaminated mine tailings following liming. J. Envir. Qual. 26, 433-439.

Langmuir, D., Mahoney, J., MacDonald, A., and Rowson, J., 1999. Predicting arsenic concentrations in the porewaters of buried uranium mill tailings. Geochim. et Cosmochim. Acta, 63, 3379-3394.

Mahoney, J., Langmuir, D., Gosselin, N., and Rowson, J., 2005. Arsenic readily released to pore waters from buried mill tailings. Applied Geochem. 20, 947-959.

Parkhurst, D.L., and Appelo, C.A.J., 1999. User's guide to PHREEQC (Version 2), A computer program for speciation, batch-reaction, one-dimensional transport, and inverse geochemical calculations: U.S.G.S. Water-Resources Invest. Report 99-4259, 312 p.

Dynamical Models for Uranium Leaching – Production and Remediation Cases

Harald Kalka[1], Horst Märten[1,2], Rene Kahnt[3]

[1]Umwelt- und Ingenieurtechnik GmbH Dresden, Germany
E-mail: h.kalka@uit-gmbh.de
[2]Heathgate Resources Pty. Ltd., Australia, E-mail: h.maerten@uit-gmbh.de
[3]WISMUT GmbH, Chemnitz, Germany

Abstract. Leaching is a process of mass transfer between immobile mineral aggregate phases and mobile phases (reactive fluid). For such reactive transport phenomena a dynamical compartment model was developed. It combines solute transport in double porosity media with geochemistry (kinetics as well as thermodynamics described by PHREEQC). Besides several other applications, the model has been used to simulate quite different real-world scenarios related to uranium mining: (i) production case at Beverley mine and (ii) remediation case at Königstein mine.

Introduction: General Model Concept

Geochemical and hydrogeological modeling related to uranium mining cases is the scientific background for forecasts including optimization of plant operation and remediation. This paper describes model simulations of two quite different real-world scenarios:

- Production case: In-situ leaching (ISL) of uranium at Beverly mine, South-Australia $\Rightarrow$ focused on optimum leaching chemistry and hydrology, interfering leaching effects as well as groundwater restoration after mining
- Remediation case: Flooding of Königstein mine, where ISL has been performed in underground mine works in the past $\Rightarrow$ focused on most efficient flooding and minimum impact on the environment (adjacent aquifers)

In both examples, *geochemical* and *technological* processes are combined in an intricate manner. Code families for reactive transport alone (Domenico and

Schwartz 1998; PHAST, TACK and other programs) are not adequate to describe such complex systems.

Main Principles

To solve the problem numerically with adequate resolution the system is decomposed in suitable compartments (or boxes). The compartments are coupled by hydraulic and mass flows: *internal* couplings between compartments and *external* couplings to the environment. The structure of the box-system depends on the local conditions incl. availability of relevant data (cf. Fig.1 and Fig.5).

In addition to this global design and flow pattern each compartment can be "equipped" with (i) proper mechanisms of mass transformation (geochemistry) and (ii) technological devices like pumps, pipelines, plant components (like ion-exchange columns for U capture) and reactive materials.

Mathematically, the governing set of differential equations for each compartment i is derived from the principle of material balance:

$$\frac{dm_i}{dt} = \left(\frac{dm_i}{dt}\right)_{trans} + \left(\frac{dm_i}{dt}\right)_{reac} \tag{1}$$

This equation holds for any chemical element/species with mass $m = cV$, where both concentration $c(t)$ and water volume $V(t)$ are time-dependent. The transport term describes the hydraulic processes (without reactions) and is given by

$$\left(\frac{dm_i}{dt}\right)_{trans} = \sum_j \left(Q_{j \to i} c_j - Q_{i \to j} c_i\right) + Q_i^{in} c^{in} - Q_i^{out} c_i \tag{2}$$

Here, $Q_{i \to j}(t)$ denotes the internal flow from box i to box j; $Q_i^{in}(t)$ and $Q_i^{out}(t)$ represent the external flow *from* or *to* the environment, respectively. Whereas $Q_{i \to j}(t)$ is calculated from hydraulic conditions at time t (using Darcy's Law), the quantities $Q_i^{in}(t)$ and $Q_i^{out}(t)$ are input data ("boundary conditions" taken from the regional model). The water balance equation is a special case of Eq. (2) with $c = const$ as the "concentration" of H_2O molecules:

$$\frac{dV_i}{dt} = \sum_j \left(Q_{j \to i} - Q_{i \to j}\right) + Q_i^{in} - Q_i^{out} \tag{3}$$

In case of flooding scenarios, the water amount in a compartment is not constant, but instead changes with time: $dV/dt > 0$ (cf. remediation case Königstein mine).

The reaction term in Eq. (1) is the key quantity of the model. Its proper specification defines the mass transformations between solid and aqueous phases, i.e., the leaching process inside the compartment i. In this way, this term operates as a source/sink term. If N_{phas} denotes the number of aqueous and solid phases, Eq. (1) splits into N_{phas} differential equations. Examples are given below: First, Eq. (4) and (5) for a single compartment (without transport term), and second, Eq. (11) and (12) for a modified double-porosity model.

Geochemistry

The specific chemical simulations inside each compartment – represented by the second term in Eq. (1) – are carried out by using the well-known U.S.G.S.-code PHREEQC (Parkhurst and Appelo 1999), which is implemented as a subroutine. In this way, the model includes the standard procedures:

- aqueous speciation and complexation
- mixing of water flows
- mineral dissolution and precipitation
- acid-base reactions (H^+-transfer)
- oxidation-reduction reactions (e^--transfer)
- reactions due-to addition and dosage of chemicals
- ion exchange

Reactions that are not in thermodynamic equilibrium are represented by kinetic concepts. The latter are defined by the *order* and *rate* of the reaction.

Production Case: In-situ Leach at Beverley Mine
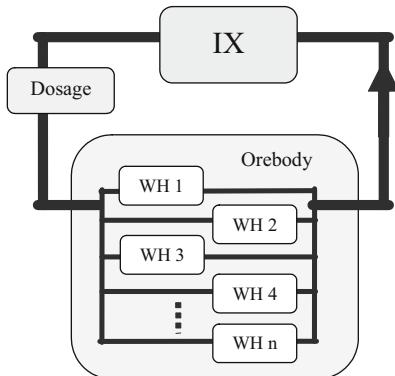
Heathgate Resources Pty Ltd operates the uranium in-situ leaching mine in Beverley, South Australia. It is Australia's first commercial acid ISL mine commissioned in late 2000.

The above dynamic compartment model has been adapted to ISL processing for optimizing wellfield operation and uranium processing under various orebody conditions (minimizing both operational costs and environmental impacts). The simulation includes underground leaching dynamics in conjunction with U recovery and further technological stages in the processing plant (total water/material balance for ISL production cycle).
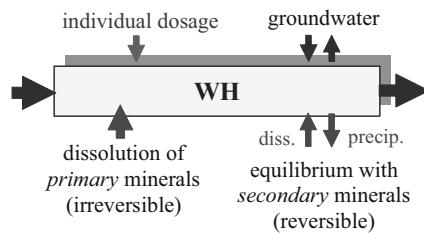
ISL Production Circuit – Compartment Structure

To describe the leaching dynamics and the corresponding mass transformations for U and other important species like SO_4, Fe, Cl, Ca, Si etc., the technological scheme "ISL cycle" is mapped onto a system of several interconnected compartments as schematically shown in Fig.1.

The acid solution (barren lixiviant) is injected into the underground via a sophisticated system of wells. Uranium is mobilized in the permeable ore body, together with interfering leaching effects and acid consumption. Submersible pumps in extractors pump the uranium-rich solution (pregnant lixiviant) to the surface for processing in the plant abbreviated by "IX" (IX stands for ion exchange applied to capture the U from the lixiviant circulating in a closed loop). The barren lixiviant is refreshed by adding sulfuric acid and oxidizing reagents. The loaded IX resin is further processed to recover U and to produce yellow cake finally.

Thermodynamic and kinetical modeling

Fig. 1. Simplified compartment struc-
ture of the closed ISL cycle.

Fig. 2. Mass transfer within a single wellfield
(diss. – dissolution, prec. – precipitation).

The subsystem "orebody" simulates the in-situ leaching process in several well-fields (wellhouses WH# with distribution to injection wells and collectors to combine pregnant lixiviant flows from the extractors). As shown in Fig.2, each well-field represents a separate compartment to calculate the leaching processes involving reactions between minerals and the moving aqueous solution, but also including such effects like groundwater exchange within the aquifer. The dissolution of *primary* minerals is controlled by pH, ORP and salinity of the lixiviant. At the same time, the solution is assumed to be in chemical equilibrium with *secondary* minerals (as the reason for precipitation effects).

Finally, the compartment "IX" represents a network of ion-exchange columns for the sorption of Uranium from the lixiviant (Kalka 2004).

Analytical Approach for a Single Wellfield

At a first stage of modeling, the leaching dynamics is studied within a simple analytical model for a single wellfield. A wellfield consists of a network of 28 injection and 14 extraction wells with a complex flow pattern. Just this complexity gives rise to an effective description (averaging over different ore grades and hydraulic parameters within an ideally mixed reservoir). The uranium leaching process is understood as a combination of dissolution and flushing. Mathematically, it can be described by

$$\frac{dm_{ore}}{dt} = -\lambda m_{ore} \qquad \text{with} \qquad m_{ore}(0) = m_0 \qquad (4)$$

$$\frac{dm}{dt} = \lambda m_{ore} - qm \qquad \text{with} \qquad m(0) = 0 \qquad (5)$$

where m_{ore} and $m(t) = c(t)V_P$ refer to the uranium in the orebody and in the aqueous phase, respectively; V_P is the pore water volume. The "initial mass" $m_0 = c_0 V_P$

Thermodynamic and kinetical modeling

at $t = 0$ represents the available pre-mining reserve in the orebody. λ symbolizes the dissolution rate, whereas q is the flushing rate (inverse residence time or pore-volume exchange rate). Integrating both equations one gets the uranium concentration in the lixiviant

$$c(t) = c_0 \frac{\lambda}{\lambda - q} \left[e^{-qt} - e^{-\lambda t} \right] \tag{6}$$

Finally, leaching at a flow rate Q per wellfield yields the time dependent mass flow $j(t) = Q \cdot c(t)$ as

$$j(t) = m_0 \frac{\lambda q}{\lambda - q} \left[e^{-qt} - e^{-\lambda t} \right] \qquad \text{with} \quad \int_0^\infty j(t)dt = m_0 \tag{7}$$

This model includes 3 parameters

"Initial" concentration: $c_0 = m_0 / V_P$ (8)

Flushing rate: $q = Q / V_P$ (9)

Dissolution rate: $\lambda = a \cdot e^{b\,(2-pH)}$ (10)

Here, the dissolution rate of the main uranium-silicate mineral *coffinite* is assumed to be pH-dependent with $a \approx 0.5 \cdot 10^{-7}\ \text{s}^{-1}$ and $b \approx 3.2$.

For example, the wellfields WH8 and WH9 are characterized by an area of about 10 000 m² at an effective aquifer thickness of about 10 m; the porosity is $n \approx 0.3$. Accordingly, the estimate yields:
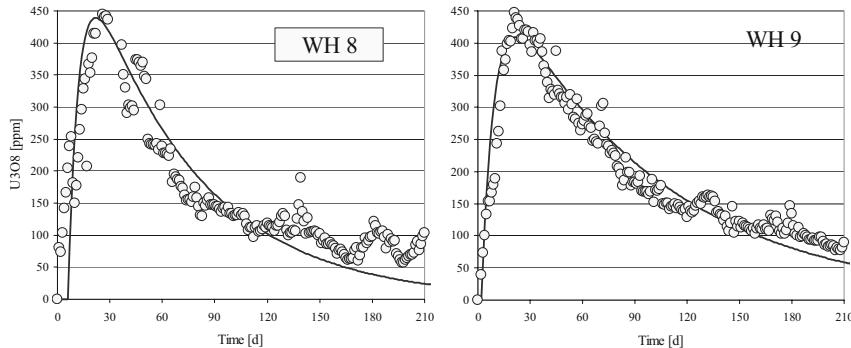
WH8: $V_P = 30\ 000\ \text{m}^3$ $m_0 \approx 170\ \text{t U}_3\text{O}_8$
WH9: $V_P = 35\ 000\ \text{m}^3$ $m_0 \approx 225\ \text{t U}_3\text{O}_8$

The initial mass m_0 was taken from geologic exploration data that show higher ore grade in WH9. The leaching was performed at an average flow rate of $Q = 200\ \text{m}^3/\text{h}$, whereas the leaching pH was 1.6 and 1.7, respectively. Using these data one gets the two parameter sets

WH8: $c_0 = 5.7\ \text{g/L}$ $q = 0.160\ \text{d}^{-1}$ $\lambda = 0.016\ \text{d}^{-1}$
WH9: $c_0 = 6.4\ \text{g/L}$ $q = 0.136\ \text{d}^{-1}$ $\lambda = 0.011\ \text{d}^{-1}$

Fig. 3.   Measured and calculated uranium concentration in the lixiviant for two wellfields.
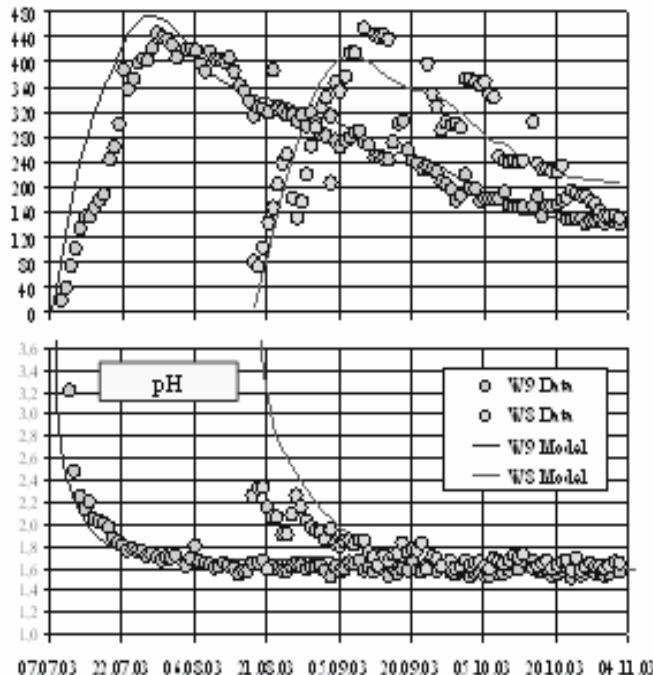
The uranium extraction curves based on Eq. (6) are shown in Fig. 3. Despite the simplicity of the analytical model there is a good agreement with the observed data. Deviations from the measured data after more than 6 months are due to additional technological measures (like shut-off's of wells and addition of infill wells) to optimize leaching performance for maximum recovery.

Numerical Model Calculations for ISL Cycle Operation

The compartment model for the ISL cycle shown in Fig.1 combines the geochemistry (leaching) with the process chemistry (U-removal in ion-exchange columns) in a consistent way. The dynamics is simulated by discretization of the process into small time steps in the order of $\Delta t \approx 10$ h and assuming a quasi-equilibrium (calculated with PHREEQC) at each time step.

The dissolution kinetics for coffinite $USiO_4$ and other *primary* silicate minerals was assumed as first-order with a pH-dependent rate similar to Eq. (10). The dissolution of silicate minerals leads to interfering leaching, which influence the concentration of Si, Al, Fe, K, Mg, Ca etc. in the lixiviant, superposed by dilution effects due to wellfield start-up's (thus, keeping those concentrations quite constant). Additionally, chemical equilibrium with *secondary* minerals like gypsum, hydroxides, amorphous silica was taken into account. For example, adsorptive capacities of precipitated amorphous/colloidal silica SiO_2 are important for U(VI)-compounds.

In conclusion, the model calculations yield the time dependent dependence of pH, ORP and major ion concentrations (U, SO_4, Cl, Fe, Ca, Na, Al, Mg, K, Si). Fig. 4 shows the results for WH8 and WH9 as an example.

Thermodynamic and kinetical modeling

Fig. 4.   Time-dependence of U_3O_8 and pH in the lixiviant of WH8 and WH9 – prediction and reality

Remediation Case: Flooding of Königstein Uranium Mine

The sedimentary uranium deposit of Königstein is located in the south-east of Saxony. Mining commenced in 1967. In 1984, ISL in the mineworks replaced conventional mining entirely. After an intermediate phase between 1991 and 2000, mainly for remediation works in the underground, flooding started in January 2001 (Schreyer et al. 2002).
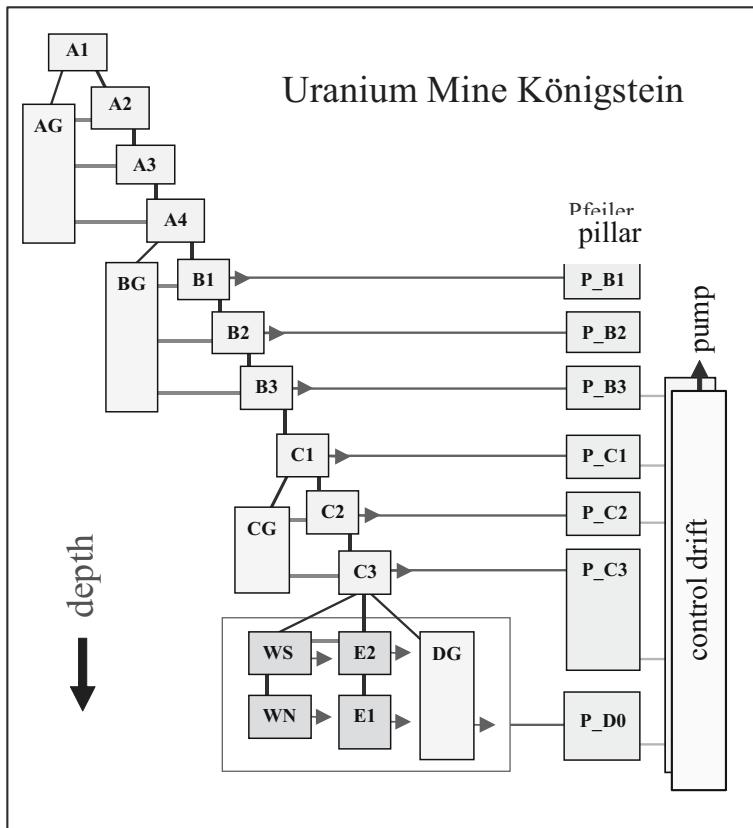
Simulations of deep-mine flooding is a special task quite different from common hydrogeologic modeling because: (i) there are open mine voids in combination with porous media and fracture networks, (ii) the system is extremely dynamic (several cm per day rise of flooding level), (iii) the hydraulic changes cause drastic changes in geochemistry due to increased rock-water contact, and (iv) technological operations are included (pumping from a control tunnel system).

In conclusion: The description of flooding dynamics calls for a special site-specific compartment model (Kalka et al. 2002).

Thermodynamic and kinetical modeling
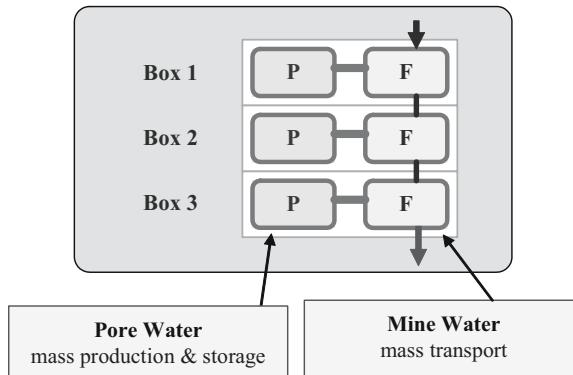
Compartment Structure

The compartment structure of the Königstein mine is schematically shown in Fig. 5. It consists of 18 mine-works compartments and 7 compartments of sandstone pillar between former mine-works and control tunnel, where flooding water is collected via a drainage system and pumped to the surface for treatment.

To describe the geochemical mass transformations (leaching and flushing) each compartment is decomposed into two subspaces: (i) "pore space" P containing the highly contaminated pore fluid and (ii) a "free space" F of water in mine voids. As shown in Fig. 6 the boxes are connected only via the percolating mine water in the open voids of space F. On the other hand, the production (and storage) of mass occurs in the pore space, whereas the stagnant water is in contact with the rock and secondary minerals. P and F are coupled by density driven forces.

Fig. 5.   Compartment structure of the Königstein mine.

Thermodynamic and kinetical modeling

Fig. 6.   Interplay between stagnant pore water and mobile mine water (leaching process).

Model Calculations

The model is based on a set of differential equations for the mass changes in both P and F in a given compartment i:

$$\frac{dm_i^F}{dt} = \left(\frac{dm_i}{dt}\right)_{trans} + \left|Q_i^{exch}\right|(c_i^P - c_i^F) + m_i^{sekm}\,\delta\,(t - t_i) \qquad (11)$$
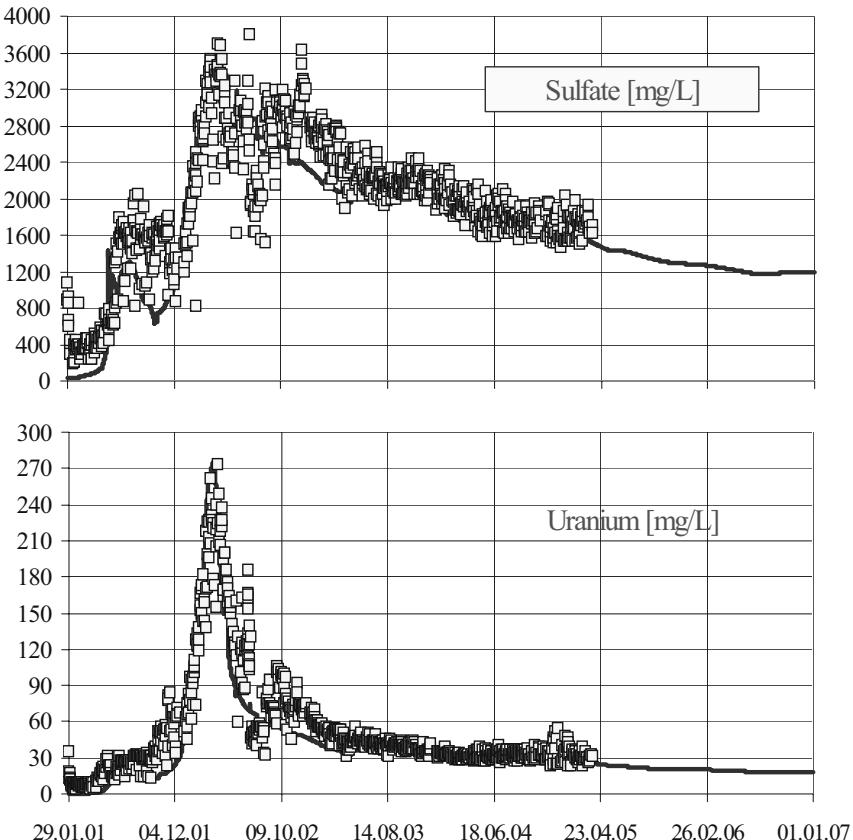
$$\frac{dm_i^P}{dt} = -\left|Q_i^{exch}\right|(c_i^P - c_i^F) \qquad (12)$$

Here, the contaminant source consists of two parts: a *long-term* source which describes the transport of contaminants from P to F (leaching process) and a *short-term* source which describes the dissolution of secondary minerals/salts once the open voids get contact with flooding water. The leaching is density-driven with

$$Q_i^{exch} = \Lambda\,(\rho_i^P - \rho_i^F)/\rho_0 \qquad (13)$$

and $\rho_0 = 10^3$ kg/m^3. The value of the exchange parameter $\Lambda \approx 1\,500$ m^3/h was adjusted to previous flooding history. The high contamination in the sandstone pores is a relic of the former block-leaching mining with sulphuric acid.

The model predicts the hydraulic processes (rise of water level and pillar drainage) as well as the time dependence of geochemistry and water composition (pH and 13 elements) at different locations in the mine. For example, Fig.7 shows the sulfate and uranium concentrations in the drainage water behind the pillar. For illustration, on a 1.5 GHz PC the running time is 8 h for a total time span of 8 years; the "subroutine" PHREEQC is called about half million times.

Thermodynamic and kinetical modeling

Fig. 7.   Sulfate and uranium concentration in the drainage water behind the pillar (available data and forecast).

Conclusions

Modeling of uranium chemistry in heterogeneous aquatic systems including technological processes (drainage, pumping, treatment, reactive materials) requires the adequate combination of hydrogeology, geochemistry, reaction kinetics as well as process chemistry. To solve the non-standard task for the two application cases discussed in this paper, individual models with a quite different (multi-dimensional) compartment structure were developed. The compartment model describes mass transport *within* and *between* the compartments as well as chemical equilibrium and nonequilibrium processes (e.g. dissolution kinetics) performed by the use

of PHREEQC. In particular, the dual-porosity model has been implemented into model compartments.

After model construction and calibration, the software tools are extensively used for forecast and simulation of various production (ISL) and flooding scenarios. In this way, models of such type are useful to

- Evaluate the dynamics of mine water / flood water chemistry in complex environments
- Select optimized strategies for leaching (ISL) and remediation (flooding)
- Interpret laboratory and pilot experiments
- Systemize chemical and hydraulic field data
- Derive a guidance for process monitoring

References

Domenico P.A., Schwartz F.W. (1998) Physical and Chemical Hydrogeology. John Wiley & Sons, New York

Kalka H. (2004) Ion Exchange Model for the Removal of Uranium from In-situ Leaching Lixiviants at Beverley Mine, Final Report to Heathgate Resources Pty Ltd, UIT GmbH Dresden

Kalka H., Märten H., Münze R. (2002) Flooding and Post-flooding Scenarios – Dynamics and Geochemistry. In "Uranium in the Aquatic Environment" (B.J. Merkel et al. Eds.), Springer-Verlag Berlin Heidelberg 2002, 1021-1028

Parkhurst D.L., Appelo C.A.J. (1999) User's guide to PHREEQC (version 2). Water-Resources Investigation Report 99-4259, Denver Colorado

Development of a 2-D modeling system for reactive transport in variable saturated porous media

Olaf Nitzsche, Guido Deissmann, T. Cramer

Brenk Systemplanung GmbH, Heider-Hof-Weg 23, 52080 Aachen, Germany,
E-mail: o.nitzsche@brenk.com

Abstract. In this paper we present a modeling approach developed for multicomponent reactive transport in partly or fully saturated media. The processes included in this modeling system comprise water flow and advective and/or diffusive transport of dissolved species, stationary and instationary gas phase diffusion, exchange between solutes and gaseous components, complexation and oxidation-reduction reactions in the aqueous phase, dissolution/precipitation reactions including sulfide mineral oxidation, buffering reactions, chemical weathering, and retardation processes (e.g. sorption).

Introduction

Reactive fluid flow and geochemical transport in partly saturated porous media have been of increasing interest to investigators in the areas of geo- and environmental sciences such as contaminant transport, groundwater quality, waste disposal, and acid mine drainage remediation.

Reactive transport modeling may be helpful for predicting seepage and groundwater pollution at as given system. A realistic prediction of the transport and fate of heavy metals and radionuclides is critical e.g. for the assessment of the future environmental impact of mines (e.g. Bain et al. 2000, 2001), waste dumps (e.g. Pruess et al. 2002), mill tailing sites (e.g. Zhu et al. 2000; Salmon and Malmström 2000). Reactive transport modeling can also be used to analyze and optimize the performance of reactive barriers and cover systems and to develop effective remediation strategies (e.g. Bozkurt et al. 2000; Romano et al. 2002).

Reactive transport modeling is a challenging issue because of the complexity of multiphase fluid flow, water-gas-rock interaction mechanisms, and difficulties

dealing with physical and chemical heterogeneities and the strong non-linearities in the governing equations.

In this paper we present a modeling approach developed for multicomponent reactive transport in partly saturated or saturated geochemical systems that has been used inter alia for the prediction of seepage, ground and surface water qualities at uranium mining and milling sites.

Conceptual model approaches

In reactive transport models the water and gas flow equations, the advective-dispersive transport equation and the mass action and mass balance equations for chemical reactions have to be solved together, either simultaneously or sequentially. A basic theoretical discussion of that problem can be found in Rubin (1983). Many reactive transport models have been developed in the past (c.f. Lichtner 1984; Steefel and Lasaga 1994; Walther et al. 1994; Mayer et al. 1999).

A simultaneous solution of the whole system is necessary for density depending flow problems e.g. in ground water or mine water with very high salinity. In our model, density effects are neglected at present. Therefor we can divide the problem into two phase flow on the one hand and in the advective-dispersive solute transport in the water phase and a diffusive transport in the gas phase.

For the remaining transport and reaction equations both simultaneous or sequential solutions are possible. A detailed description of both approaches is given in Saaltink (2000). The sequential approach (sequential non iteration approach SNIA or sequential iteration approach SIA) produces a smaller set of equations which have to be solved simultaneously. However, this advantage must be payed often by a high number of iterations (SIA) or a very small time step (SNIA). In our model, we use a simultaneous solution with the so called direct substitution approach (DSA), see e.g. (Lichtner 1984, 1996).

Mathematical description

Water flow

The water flow is considered as an instationary constant density flow in partly or fully saturated porous media. This allows to study effects of strong variations of the moisture content e.g. in the vadose zone. As mathematical formulation the Richards equation is used:

$$\frac{\partial \theta}{\partial t} = \frac{\partial}{\partial x_i}(K(\theta) * (\frac{\partial h}{\partial x_i} + e_z)) - Q$$

with:

x_i spatial coordinates,
t time,
θ volumetric water content,
h pressure head,
$K(\theta)$ unsaturated hydraulic conductivity
e_z gravity direction vector
Q external source/sink term or root water extraction term.

The water retention function and the unsaturated hydraulic conductivity are described by the Mualem-van Genuchten equations (Mualem, 1976, van Genuchten, 1980):

$$\theta(h) = \begin{cases} \theta_r + \dfrac{\theta_s - \theta_r}{(1 + |\alpha * h|^n)^m} & h < 0 \\ \theta_s & h \geq 0 \end{cases}$$

$$K(\theta) = \begin{cases} K_s * S_e^{1/2} * \left[1 - (1 - S_e^{1/m})^m\right]^2 & h < 0 \\ K_s & h \geq 0 \end{cases}$$

$$S_e = \frac{\theta - \theta_r}{\theta_s - \theta_r}, \quad m = 1 - \frac{1}{n}$$

with
θ_r residual water content,
θ_s saturated water content,
K_s saturated hydraulic conductivity,
n pore space distribution parameter [-]
α the air entrance parameter

The Darcy velocity, which is a input parameter for the transport equation is calculated by the Darcy law:

$$q_i = -K(\theta) * \left(\frac{\partial h}{\partial x_i} + e_z\right)$$

Advectiv-dispersive solute transport

The equation for advectiv-dispersiv solute transport has the following form:

$$\frac{\partial \theta_w * c_{w,k}}{\partial t} + \frac{\partial c_{s,k}}{\partial t} = \frac{\partial}{\partial x_i}\left(\theta_w * D_{i,j} * \frac{\partial c_{w,k}}{\partial x_j}\right) - \frac{\partial q_i * c_{w,k}}{\partial x_i} + R_k + Q * f(c_{w,k})$$

with
θ_w volumetric water content,

$c_{w,k}$ disolved concentration of component k,
$c_{s,k}$ sorbed concentration of component k,
$D_{i,j}$ dispersions-diffusion tensor,
q_i DARCY-velocity,
Q external source/sink
R_k reaction term (see section chemical reactions).

Gas transport

In our model gas transport is addressed as a diffusional transport of different gaseous components only. Gas advection effects are neglected. The diffusion is described by Ficks law. Relevant chemical species for diffusive gas transport can be e.g. O_2, CO_2, H_2, H_2S. Considering the mass balance equation for gases, the gas transport is calculated as:

$$\frac{\partial \theta_g * c_{g,k}}{\partial t} = \frac{\partial}{\partial x_i} (\theta_g * D_g (\theta_g) * \frac{\partial c_{g,k}}{\partial x_i})$$

with

θ_g volumetric gas content,
$c_{g,k}$ concentration in gas of the component k, and
D_g gas diffusion coefficient.

For the estimation of the effective gas diffusion coefficient

$$D_{eff}(\theta_g) = \theta_g * D_g(\theta_g)$$

various empirical models for calculation of the moisture dependent gas diffusion coefficients can be applied. A good review of such models can be found in (Rogers and Nielson 1991). Theses models give results for the diffusion coefficient with a variation of more then one order of magnitude. For using in field case studies, relevant diffusion coefficient models should be selected with care. Ongoing studies on cases with highly variations in soil moisture (using precipitation and evaporation date on a daily base) show some effects of instationarity on the average oxygen flux through the soil.

Chemical reactions

The chemical reactions included in the presented model comprise:
- complexation and oxidation-reduction reactions in the aqueous phase,
- exchange between solutes and gaseous components,
- dissolution/precipitation reactions including sulfide mineral oxidation, buffering reactions, chemical weathering,
- retardation processes (e.g. sorption), and
- chemical reactions in the gas phase
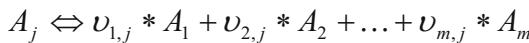
Aqueous complexation in solution is modeled as an equilibrium process. Oxidation-reduction processes in solution and mineral precipitation/dissolution reactions can be considered as equilibrium or kinetic processes.

The exchanges of species between aqueous and gas phase is described by Henry's law.

Sorption is described either as ion exchange process (Appelo and Postma 1994) or with surface complexation models (Dzombak and Morel 1990). The number of sorption sites is variable and can be linked to different mineral phases (e.g. clay minerals or $Fe(OH)_3$). The concentration of the sorbing phases may vary with time according to the respective environmental conditions. Therefore precipitation of minerals with sorption sites increases the sorption capacity. Dissolution of such minerals leads to a decrease in sorption capacity and release sorbed chemical species.

With the mass action law for a reaction (aqueous complexation, fast aqueous oxidation-reduction reaction, gas water exchange, ion exchange and surface complexation):

$$A_j \Leftrightarrow \upsilon_{1,j} * A_1 + \upsilon_{2,j} * A_2 + \ldots + \upsilon_{m,j} * A_m$$

the describing equation for an equilibrium process is written as

$$c_j = \frac{1}{\gamma_j * K_j} * \prod_{i=1}^{m} (\gamma_i * c_i)^{\upsilon_{i,j}}$$

with

A_j secondary species j,
$A_{(1..m)}$ master species i,
$v_{i,j}$ stoechiometric coefficient ,
c_j concentration of secondary species ,
c_i concentration of master species ,
γ_j activity coefficient of secondary species,
γ_i activity coefficient of secondary species
K_j equilibrium/selectivity constant.

Kinetic reaction (slow aqueous oxidation-reduction reaction and mineral reactions) are described by several different functions with the general form:

$$R_{eff} = f_k * k_r * f(c_1, c_2, \ldots, c_n) * (1 - \frac{IAP}{K_{equ}}) * \frac{A}{V}(t)$$

with:

R_{eff} effective reaction rate
f_k calibration factor
k_r intrinsic rate constant
IAP ion activity product
K_{equ} equilibrium constant
A/V specific reaction surface
c_i concentration of involved master species

Activity corrections for species are done with the Davies equation. Temperature corrections are done with the vant Hoff equation for complexation reactions and with the Arrhenius equation for kinetic rate constants.

In the gas phase, soil respiration processes and their seasonal variation are considered for O_2 and CO_2. Although a first order or Michaelis-Menten kinetic describes such the oxygen consumption process better then a zero order kinetics, the latter approach is used here (see Rappoldt and Crawford 1998). Often, the available data comprise seasonal variations of CO_2 respiration rates at the soil surface together with the depth of the active microbiological and root zone (e.g. Ewel et al. 1987; Buchmann 2000). From these values, a time dependent volumetric zero order rate can be calculated. In the presented model we assume a linearly decreasing rate with depth, i.e. the maximum rate is near the surface and zero at the maximum root depth. Test case studies with the model using soil respiration data from (Buchmann 2000) gave reductions of the oxygen flux of appr. 20 %.

The substitution of the concentration terms by their mass balance action equations and the coupling with the reaction term leads to the final set of equations in the DSA approach:

$$\frac{\partial \theta_w T_i^w}{\partial t} + \frac{\partial \theta_g T_i^g}{\partial t} + \frac{\partial T_i^s}{\partial t} = \frac{\partial}{\partial x_i}(\theta_w * D_{i,j} * \frac{\partial T_j^w}{\partial x_j}) + \frac{\partial}{\partial x_i}(\theta_g * D_g * \frac{\partial T_i^g}{\partial t}) - \frac{\partial q_i * T_i^w}{\partial x_i} + R_i, \quad i = 1 \ldots k$$

with

$$T_i = c_i^{master} + \sum_{j=1}^{m} c_{i,j}$$

T_i total concentration of a chemical species in gas, water and sorbed phase
c_i^{Master} concentration of the master species,
c_{ij} concentration of the secondary species
m number of relevant secondary species for a master species

The mass of solid phase kinetic reactants is calculated explicit after each time step by the equation

$$\frac{\partial M_k}{\partial t} = -\sum R_i$$

Numerical solution

The resulting equations are solved for both cases by the finite element method. In the presented version, 1 D and 2 D cases can be considered. Spatial discretisation in 2 D is done with irregularly tetragons or triangles. For both, water flow and solute transport the same spatial discretisation is used.

Water flow

The water flow equations are solved with the freely available code from SWMS-2D (Simunek et al. 1994). Some changes have been made with respect to the coupling with the reactive transport part. Especially the gas diffusion coefficient calculation was added to the code. Parameters for water flow are set in standard SWMS-2D input files. Due to the use of a mixed (water content and pressure head) formulation within the SWMS-2D code, unsaturated and saturated zones within one case are possible. From the water flow code, the darcy velocities, water and gas filled porosities and the calculated gas diffusion coefficients are transferred to the transport calculation code at each time step. The automatic time step control must fulfill the criteria of both parts. Otherwise both steps will be reseted.

Transport and Reaction

The used finite element method gives a discretisation of the overall transport equations. The result is a set of algebraic nonlinear equations. The number of unknowns is the number of nodes times the number of master species. This system of equations is linearised by a Newton Raphson method and solved with an iterative method. Thermodynamic parameters can be read from PHREEQC (Parkhurst, and Appelo 1999) input files. Parameters for gas diffusion coefficient calculation are given in a separate file.

References

Appelo, C.A.J., Postma, D. (1994) Geochemistry, groundwater and pollution. A.A. Balkema, Rotterdam, 536p.

Bain, J.G., Blowes, D.W., Robertson, W.D., Frint, E.O. (2000) Modelling of sulfite oxidation with reactive transport at a mine drainage site. Journal of Contaminant Hydrology 41: 23-47.

Bain, J.G., Mayer, K.U., Blowes, D.W., Frint, E.O., Molson, J.W.H., Kahnt, R., Jenk, U. (2001) Modelling the closure-related geochemical evolution of groundwater at a former uranium mine. Journal of Contaminant Hydrology 52: 109-135.

Bozkurt, S., Sifvert, M., Moreno,L., Neretnieks, I. (2001) The long term evolution of and transport in a self-sustained final cover on waste deposits The Science of the Total Environment 271: 145-168.

Buchmann, N. (2000) Biotic and abiotic factors controlling soil respiration rates in Picea abies stands. Soil Biology & Biochemistry 32: 1625-1635.

Dzombak, D.A., Morel, F.M.M. (1990) Surface complexation modeling - Hydrous ferric oxide. John Wiley, New York, 393p.

Ewel, K.C., Cropper Jr., W.P., Gholz, H.L. (1987) Soil CO_2 evolution in Florida slash pine plantations II: Importance of root respiration. Can. Jour. Forest Res. 17: 330-333, 1987

van Genuchten, M.Th. (1980) A closed-form equation for predicting the hydraulic conductivity of unsaturated soils. Soil Sci. Soc. Am. J., 44: 892-898.

Lichtner, P.C. (1984) Continuum model for simultaneous chemical reactions and mass transport in hydrothermal systems. Geochimica et Cosmochimica Acta 49: 779-800.

Lichtner, P.C. (1996) Continuum Formulation of Multicomponent-Multiphase Reactive Transport. In: Lichtner. P.C., Steefel, C.I., Oelkers, E.H. (ed.) Reactive Transport in Porous Media. Reviews in Mineralogy Vol. 34, Mineralogical Society of America, Washington, 1-81.

Mayer, K.U., Benner, S.G., Blowes, D.W. (1999) The reactive transport model MIN3P: application to acid mine drainage generation and treatment - nickel rim mine site, Sudbury, Ontario. in: Mining and Environment, Conference Proceedings Volume 1, September 13-17, Sudbury, Ontario, 145-154.

Mualem, Y. (1976) A new model for predicting the hydraulic conductivity of unsaturated porous media. Water Resources Research 12, 513-522.

Parkhurst, D.L. Appelo, C.A.J. (1999) User's Guide to PHREEQC (version 2)- a computer program for speciation, reaction path, advective-transport, and inverse geochemical calculations. Water-Resources Investigations Report 99-4259. U.S. Department of the Interior, U.S. Geological Survey, Denver.

Pruess, K., Yabusaki, S., Steefel, C., Lichtner, P. (2002)   Fluid Flow, Heat Transfer, and Solute Transport at Nuclear Waste Storage Tanks, in the Handford Vadose Zone. Vadose Zone Journal 1:68:88.

Rappoldt, C, Crawford, J.W. (1998) The distribution of anoxic volume in a fractal model of soil. Geoderma 88: 329-347.

Rogers, V.C., Nielson, K.K. (1991) Correlations for predicting air permeabilities and 222Rn diffusion coefficients of soils. Health Physics 61: 225-230.

Romano, C.G., Mayer, K.U., Jones, D.R., Ellerbroek, D.A., Blowes, D. (2003) Effectiveness of various cover scenarios on the rate of sulfide oxidation on mine tailings. Journal of Hydrology 271: 171-187.

Rubin, J. (1983) Transport of Reactive Solutes in Porous Media: Relation Between mathematical Nature of Problem Formulation and Chemical Nature of Reactions. Water Resources Research 19: 1231-1252.

Saaltink, M., Carrera, J., Ayora, C. (2001) On the behavior of approaches to simulate reactive transport. Journal of Contaminant Hydrology 48: 213-235.

Salmon, S.U., Malmström, M. (2000) Steady stade, geochemical box model of tailings impoundment: Application to Impoundment 1, Kristineberg, Sweden, and prediction of effect of remidiation. Mitigation of the environmental impact from mining waste (project report).

Simunek, J.; Vogel, T.; van Genuchten, M.Th. (1994) The SWMS-2D code for simulating water flow and solute transport in two-dimensional variably saturated media (Version 1.21).US Salinity Laboratory, Research Report 132.

Steefel, C., Lasaga, A. (1994) A coupled model for transport of multiple chemical species and kinetic precipitation / dissolution reactions with applications to reactive flow in single phase hydrothermal systems. American Journal of Science 294, 529-592.

Walther, A.L., Frind, E.O., Blowes, D.W., Ptacek, C.J., Molson, J.W., (1994) Modeling of multicomponent reactive transport in groundwater: 1. Model development and evaluation. Water Resources Research 30, 3137-3148.

Zhu, C., Fang, Q.H., Burden, D.S. (2001) Multi-component reactive transport modeling of natural attenuation of an acid groundwater plume at a uranium mill tailings site. Journal of Contaminant Hydrology 52 85-108.

Modelling of uranium release from waste rock pile

Dusan Vopalka, Petr Benes, Klara Doubravova

Czech Technical University, Department of Nuclear Chemistry, Brehova 7, 115 19 Praha 1, Czech Republic, E-mail: vopalka@fjfi.cvut.cz

Abstract. Uranium release/uptake on material of waste rock pile No. 66 at Schlema-Alberoda (Saxony, Germany) was studied by both static (batch) and dynamic (column) experiments with the aim to obtain input data for modelling of uranium migration in the pile. Most of the experiments were carried out by radiotracer method using [233]U as the label. An ambiguous influence of humic acid (concentration 10 and 50 mg/L) on the migration of uranium was observed. The column elution experiments were modelled using PHREEQC that enabled to respect the kinetic character of the desorption process.

Introduction

The study of environmental impact of uranium mining waste rock piles has a large importance as the piles are often situated, e.g. in Germany or in Czech Republic, in urbanized environment. These wastes can also serve as a geological analogue of other kinds of nuclear waste repositories. Understanding of contaminant migration processes at the basic level in a laboratory study can help to develop models, which may be used in transport codes to predict the fate of pollutants on the field scale. An extensive environmental study was performed in the waste rock piles region at Schlema-Alberoda (Saxony, Germany) mainly between 1990-2000 (e.g., Schmeide et al. 2003). Our work performed with waste materials from uranium mining was aimed at better understanding of uranium release/uptake processes and at obtaining suitable input data for modelling of uranium migration.

Waste material from rock pile No. 66 at Schlema-Alberoda was selected for the study. Sampling of the rock material, which included sieving under 1 mm of particle size, and its characterization that comprised mineralogy, granulometric analysis, elemental composition, determination of total carbon, inorganic carbon, specific surface area, and exchangeable uranium was performed (Sachs et al. 2004). Most of sorption/desorption studies by batch and column experiments accom-

plished in our laboratory were carried out by radiotracer method using [233]U as the tracer. Distribution of [233]U was measured with liquid scintillation counting. Some evaluations were based on determination of [238]U and [233]U by means of ICP-MS.

Batch experiments
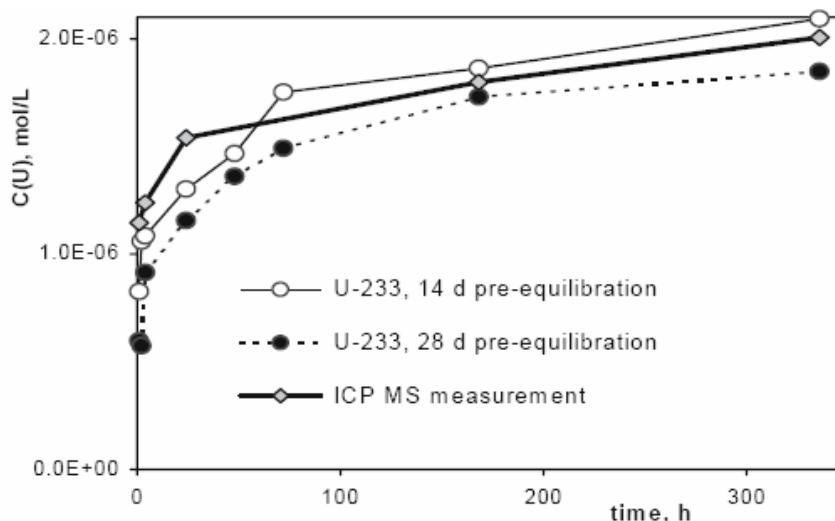
Determination of exchangeable uranium

The experiments, results of which are presented in this contribution, were performed with the simulated seepage water from the pile No. 66 (0.0175 M $MgSO_4$, 0.0091 M $CaSO_4$, 0.00258 M $NaHCO_3$) aiming to obtain data that could be used in subsequent modelling of uranium migration in near to real conditions.

First experiments aimed at determination of uranium in the rock sample accessible to leaching with natural water and exchangeable with ions in the water. This so called exchangeable or "labile" (Davis and Curtis, 2003) uranium U_{ex} was determined by isotope exchange with [233]U in simulated seepage water. In this medium neither changes in concentration in total uranium and [233]U nor the change of phase ratio V/m from 20 to 100 mL/g significantly affected the U_{ex} value (20 µg/g, 8.4×10^{-5} mol/kg) that represented approx. 34 % of total uranium in the sample (Sachs et al., 2004). The absence of significant effect was probably due to relative stability of composition of the liquid phase even in changing the phase ratio, as the use of simulated seepage water hindered further leaching of waste rock material.

Sorption/desorption equilibrium and kinetics

Batch experiments carried out with simulated seepage water (pH 8) examined effects of concentration of added uranium and humic acid on uranium distribution and kinetics of uranium sorption and desorption. The near-to-equilibrium distribution data of total uranium (labile + added) corresponded to approximately linear sorption isotherm, K_d = 17 mL/g (Vopalka et al. 2005), with a slight dependence on the volume to mass ratio V/m. Significant increase of equilibrium concentration on the solid phase with the increase of V/m could be explained by the dependence of the exchange between both portions of uranium (added and labile) on the mass ratio. The effect of added Aldrich humic acid (HA, 10 and 50 mg/L) was almost negligible with exception of experiments at higher concentrations of added uranium that caused the increase of sorbed uranium significantly over U_{ex}, in those cases the addition of HA caused an increase of K_d to 25-30 mL/g. The small effect of HA could be explained by saturation of added HA by Ca and Mg present in the simulated seepage water.

Fig. 1. Kinetics of uranium release from the rock material with simulated natural water at room temperature and $V/m = 20$ mL/g – concentration of uranium in water measured by ICP MS or calculated from ^{233}U activity.

Slow kinetics of ^{233}U uptake was found with about two weeks required to obtain a steady-state distribution at $V/m = 10\text{-}100$ mL/g (Bryan et al., 2004). Rather complicated effects of experimental conditions (total uranium added, V/m, concentration of HA, the pre-equilibration of phases preceding addition of the spike) on the kinetics were observed. Measured kinetics of ^{233}U uptake always partly represents also isotope exchange ^{233}U–U$_{nat}$, which dominates if the initial concentration of total uranium in liquid phase is near to that in equilibrium with U_{ex}. In the case when the exchangeable amount of the studied contaminant is comparable with the added amount, which is spiked by radioactive tracer, the parameters of the sorption kinetics obtained by evaluation of the uptake of the spike do not describe the kinetic behaviour of the contaminant.
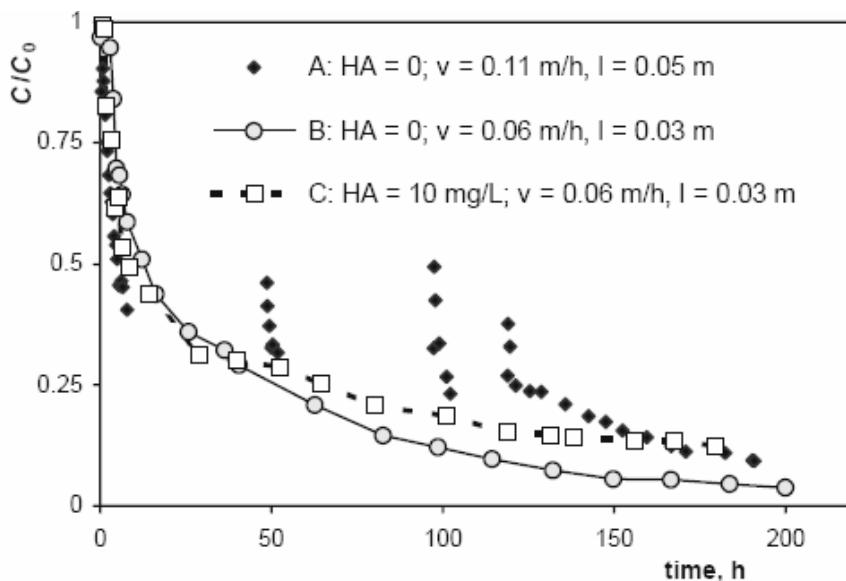
Kinetics of uranium release from the rock material was studied both by radiotracer method and by direct (ICP-MS) measurement of released uranium. In the first case, the material was pre-equilibrated with ^{233}U. In order to avoid premature release of uranium, the pre-equilibration was made with 5.6×10^{-6} M solution of uranium labelled with ^{233}U. This concentration is near to that in equilibrium with U_{ex}. For comparison was the kinetics of uranium release studied also in an experiment, in which no pre-equilibration with ^{233}U was used, and the release of natural uranium was measured (Vopalka et al. 2004). Results of the experiments at $V/m = 20$ mL/g are presented in Fig.1. A good agreement between the results of the direct U measurement and of the radiotracer method suggests that the radiotracer method used is suitable for the physical modelling of uranium release from the studied material and for the determination of input data for modelling of uranium release from the pile.

Thermodynamic and kinetical modeling

Column experiments
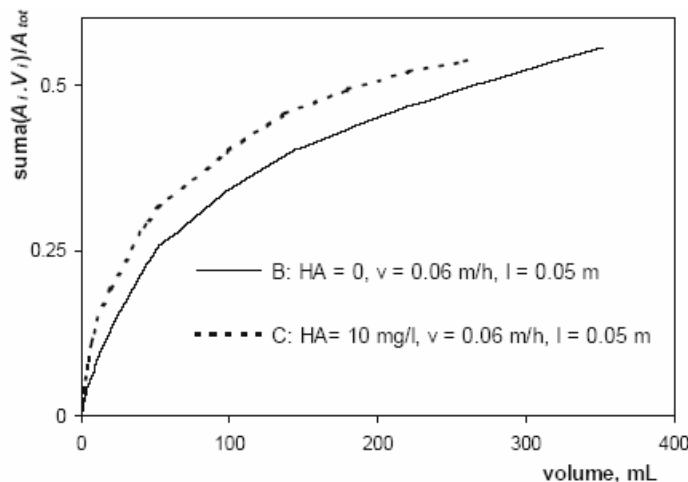
Humic colloid-mediated uranium migration can be studied by column experiments that together with batch experiments might provide an insight into U migration in aquifers. Presence of colloids mostly lowers the retardation quality of porous rock layer (Roy and Dzombak 1998; Warwick et al. 2000) and the kinetic character of interaction of contaminant with natural colloids requires more complicated techniques of migration modelling (e.g., Zurmühl 1998). Preparation and accomplishment of our dynamic experiments aimed at simple modelling of dynamic conditions of uranium leaching and migration in waste rock pile using the method developed with the use of results of batch experiments.

   Dynamic experiments were carried out with small columns (inner diameter 0.9 cm, height of rock layer 3 and 5 cm) and linear flow-through velocities between 0.02 and 0.11 m/h. The elution experiments using simulated seepage water that did not contain uranium were preceded by equilibration of the rock sample with uranium solution spiked by ^{233}U directly in the assembled circuit (column and tubings) unless a steady state, characterized by approx. the same values of input and output activities of the spike, was attained (7-10 days). This procedure was based on the results of batch kinetic elution experiments that proved feasibility of this approach. Also here, parallel experiments were run with the non-spiked and non-equilibrated rock and the comparison of results was satisfactory.

   The experiments using flow-interruption technique (e.g. Kookana et al. 1994)

Fig. 2.   Dynamics of uranium release from the layer of rock material eluted by simulated seepage water (*l* - height of the sediment layer, *v* - linear flow velocity).

Fig. 3.   Influence of the humic acid presence in the water phase on the relative cumulative outflow of uranium from the apparatus (l - height of the sediment layer, v - linear flow velocity).

showed that non-equilibrium conditions existed during the experiments (Fig.2, curve A). Some of the column experiments confirmed the results of batch experiments that showed only small influence of the presence of HA, e.g. demonstrated by the agreement of the beginning of curves B and C at Fig.2. In contrast to these results, a significant influence of humic acid on U release was observed in other dynamic experiments (see curves B and C on Fig.3). These results, which are presented in the form of relative cumulative activity that is more demonstrative with respect to balance considerations and is also convenient for the calibration of transport models, proved the expected enhancement of uranium transport by complexation with HA. The discrepancy found between the different effects of HA presence was not explained. Large retention of humic acid in the waste rock layer was observed, probably aided by the high content of small particles in the sample (33 wt. % of particles with size under 0.1 mm).
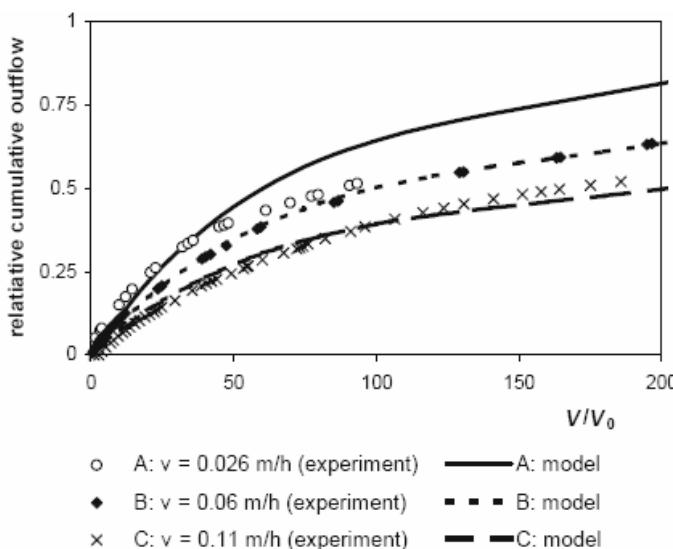
Mathematical modelling

Knowledge of the transport behaviour of uranium in groundwaters is needed for remediation of abandoned milling sites. Parameters necessary for the simulation of uranium migration in real sites could be obtained from evaluation of laboratory experiments that respect the main characteristics of the real system studied. Such laboratory small-scale experiments serve for the development of transport models describing the real situation. The experimental procedure described above represents a physical model of uranium leaching from material coming from waste rock

pile near Schlema-Alberoda. The description of experiments aimed at the future extension of the model for field conditions.

The speciation in real water phase, which was modelled using simulated seepage water, is simple: in pH range about 8 predominates a soluble aquo-complex of di-calcium uranyl carbonate $Ca_2[UO_2 (CO_3)_3]_{aq.}$ (Schmeide et al. 2003). According to this simplicity only one uranium species was used for modelling of uranium interaction with the rock surface. The interaction and transport modelling was accomplished in the environment of computer code PHREEQC (Parkhurst and Appelo 1999; Nitzsche and Merkel 1999). The interaction of uranium with the surface was modelled via a formal exchange site, and kinetic character of uranium release recognized in experiments was taken into account.

The model was calibrated by results of one leaching experiment with the simulated seepage water not containing humic acid (see Fig.4. curve B). Validation of the model on results of other experiments was partially successful, in that satisfactory description of the influence of linear flow velocity, which is very important from the point of view of possible spread of uranium in the environment, was achieved (Fig.4).

Fig. 4.   Influence of the linear flow velocity on the release of uranium from the layer of waste rock material (height 0.05 m, porosity 0.35): comparison of experimental and model results.

Conclusions

The results of batch experiments, which comprised the determination of exchangeable uranium U_{ex} (about 20 µg/g) and of uranium concentration in solution in equilibrium with U_{ex}, enabled the preparation of column experiments using [233]U as a tracer that can model real conditions in the waste rock pile. It was found that measured kinetics of [233]U uptake does not correspond to kinetics of release/uptake of total uranium (labile + added) due to complications caused by the isotope exchange.

   The results of dynamic elution experiments proved the kinetic character of uranium release for experimental conditions used. Substantial release of uranium from the layer of rock pile material in near natural conditions was found: 10 days leaching by simulated seepage water that did not contain uranium released about 50% of accessible uranium. Variable and ambiguous effect of the HA presence on the release rate of uranium from the layer of rock pile material was observed.

   Mathematical modelling of the leaching of uranium from the layer of waste rock material was performed by PHREEQC that also enables transport modelling. Satisfactory description of the influence of the flow rate on the uranium release was achieved using model calibrated on one set of experimental data. The model can be recommended for a general modelling of uranium migration in real conditions.

Acknowledgement

References

Bryan N, Vopalka D, Benes P, Stamberg K, Doubravova K (2004) Determination of chemical parameters for the Schlema-Alberoda uranium tailings pile migration case study. In: FZKA 6969, Wissenschaftliche Berichte (Buckau G., ed.), Forschungszentrum Karlsruhe, Karlsruhe, Germany, 215-224

Davis JA, Curtis GP (2003) Application of Surface Complexation Modeling to Describe Uranium (VI) Adsorption and Retardation at the Uranium Mill Tailings Site at Naturita, Colorado. Report NUREG/CR-6820, U.S. Geological Survey, Menlo Park, CA, p. 29

Kookana RS, Najdu R, Tiller KG (1994) Sorption non-equilibrium during cadmium transport through soils. Austral J Soil Res 32:235-248

Nitzsche O, Merkel B (1999) Reactive transport modeling of uranium 238 and radium 226 in groundwater of the Königstein uranium mine, Germany. Hydrogeology Journal 7:423-430

Parkhurst DL, Appelo CAJ (1999) User's guide to PHREEQC (version 2) – a computer program for speciation, batch-reaction, one-dimensional transport and inverse geo-chemical calculations. Water Resour Invest Rep 99–4259, Denver, Colorado

Roy SB, Dzombak DA (1998) Sorption nonequilibrium effects on colloid-enhanced transport of hydrophobic organic compounds in porous media. J Contam Hydrol 30:179-200

Sachs S, Benes P, Vopalka D, Stamberg K, Mibus J, Bernhard G, Bauer A (2004) Sampling and Characterization of Rock Material from Uranium Mining Waste Rocks for Study and Modeling of Release and Migration of Uranium. In: FZKA 6969, Wissenschaftliche Berichte (Buckau G., ed.), Forschungszentrum Karlsruhe, Karlsruhe, Germany, 75-84

Schmeide K, Geipel G, Heise KH, Bernhard G (2003) Uranium Mining Waste Rock Pile No. 250 in the Region Schlema/Alberoda (Saxony, Germany). In: FZKA 6800, Wissenschaftliche Berichte (Buckau G., ed.), Forschungszentrum Karlsruhe, Karlsruhe, Germany, 79-98

Vopalka D, Benes P, Prochazkova S (2004) Release and sorption of uranium in the system waste rock from uranium mining – natural water. In: Advances in Nuclear and Radiochemistry – Extended Abstracts of Papers presented at NRC-6 (Qaim SM, Coenen HH, eds.), Schriften des Forschungszentrum Jülich, General and Interdisciplinary, Band 3, 696-698

Vopalka D, Doubravova K, Benes P. (2005) Study of uranium waste release from waste rock pile material : Column experiments. In: FZKA 7070, Wissenschaftliche Berichte (Buckau G., ed.), Forschungszentrum Karlsruhe, Karlsruhe, Germany, 115-123

Warwick P, Hall A, Pashley V, Bryan ND, Griffin D (2000) Modelling the effect of humic substances on the transport of europium through porous media: A comparison of equilibrium and equilibrium/kinetic models. J Contam Hydrol 42:19-34

Zurmühl T (1998) Capability of convection–dispersion transport models to predict transient water and solute movement in undisturbed soil columns, J Contam Hydrol 30:101-128

The Role of Groundwater-Stream Interactions for Uranium Fluxes in Fluvial Systems

Frank Winde

North West University, School of Environmental Sciences and Development, Private Bag X6100, Potchefstroom, 2520, Republic of South Africa,
E-mail: frank.winde@gmx.de

Abstract. Based on results from the Wismut region (Germany), this paper concentrates on hydrodynamic aspects of contaminant transport from uranium mining tailings deposits via alluvial groundwater into a receiving stream. The focus is on event-related hydraulic interactions between groundwater and surface water in the hyporheic zone, observed by long-term, quasi- continuous *in situ* measurements with electronic probes. Analyses of time series suggest that interactions between contaminated groundwater, porewater in channel sediments and stream water are highly dynamic, impacting on U-fluxes and mobility. Processes observed during flood events also question established views on run-off generation in streams.

Introduction

Highly contaminated seepage from uranium mining tailings deposits frequently not only pollutes underlying aquifers but also affects adjacent streams into which contaminated groundwater feeds as baseflow. This route of waterborne contaminant migration is referred to as 'aqueous pathway'.

Contaminant transport along the aqueous pathway depends not only on the contaminant's concentration in the polluted water body but also on the rate (volume per time unit) at which the polluted water moves through the aquifer and discharges into the stream. While movement of water within different types of aquifers and stream channels is relatively well understood, the same is not true for trans-compartmental transport of U across the groundwater-surface water interface including ground- and surface water interactions (Maddock et al. 1995).

Apart from controlling the extent of associated diffuse stream pollution, hydraulic stream-groundwater interactions also impact on chemical processes, particular in stream sediments, which are known to act as a long-term sink for heavy

metals. However, under certain physico-chemical conditions contaminated sediments may also act as (secondary) sources of pollution by temporarily releasing accumulated heavy metals back into the water column (Jenne 1995, Evans et al. 1997). For this reason and because of the important role sediments and the zone below the running water (hyporheic zone) play as ecological habitats, research into processes at the interface of ground- and surface water became an international research focus in recent years, which is well summarised by Sophocleous (2002).
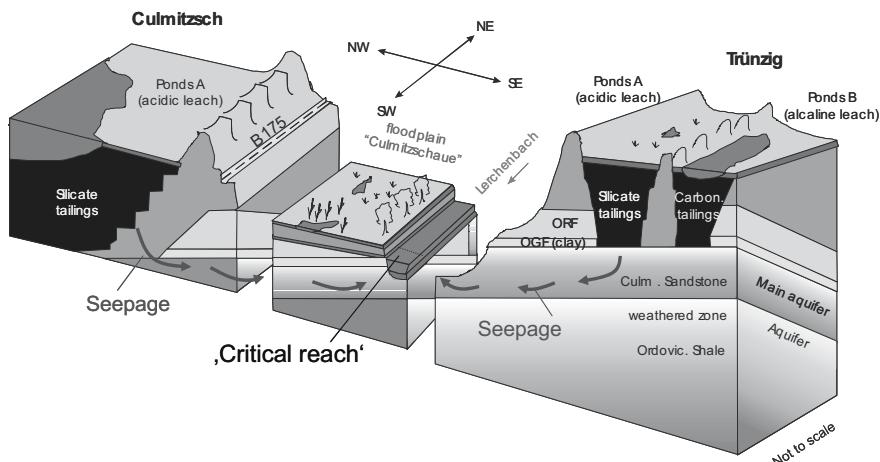
This paper focuses on results from a mining affected stream in the Wismut region in the south of East Germany. The emphasis is placed on hydrodynamic interactions between contaminated alluvial groundwater and stream water, including short-term processes, which with previous methods, were not detectable.

The method applied in this study is based on *in-situ* measurements by datalogger-controlled probes measuring water levels and electrical conductivity at ten-minute intervals. These probes were installed within, adjacent to and below the stream channel, using mining-induced elevation of the groundwater EC (mainly sulphate and chloride) to identify and trace the origin of different types of water fluxes at the ground–surface water interface.

Hydrological and geohydrological conditions in the study area

The Wismut region is a former uranium mining area in the south of East Germany comprising a number of different sites and facilities. This study focuses on an area around the town of Seelingenstädt where two large tailings storage facilities (Trünzig and Culmitzsch) impact on a small perennial water courses ('Lerchenbach'). The Lerchenbach is a roughly E-W running tributary to the Weiße Elster river and drains a mainly agricultural area in which, between 1947 and 1967, uranium was mined by the Soviet-owned SAG Wismut. Two shallow, low-grade ore bodies with an average U-concentration of some 660ppm were mined in open pit operations. After being mined out during the 1960's these open pits were transformed into four large, unlined tailings ponds – two on either side of the Lerchenbach (left: Culmitzsch A and B, right: Trünzig A and B). These ponds are separated by the 1.5km long and some 400m-wide floodplain of the Lerchenbach ('Culmitzschaue'). All four ponds contain tailings from the nearby U recovery plant that was operating in Seelingenstädt between 1960 and 1991.

Being placed on unlined highly permeable sandstone (Culmitzsch sandstone, CuS) which acts as main aquifer stretching across the floodplain, large volumes of tailings seepage migrate out of the ponds towards the stream (Fig. 1).
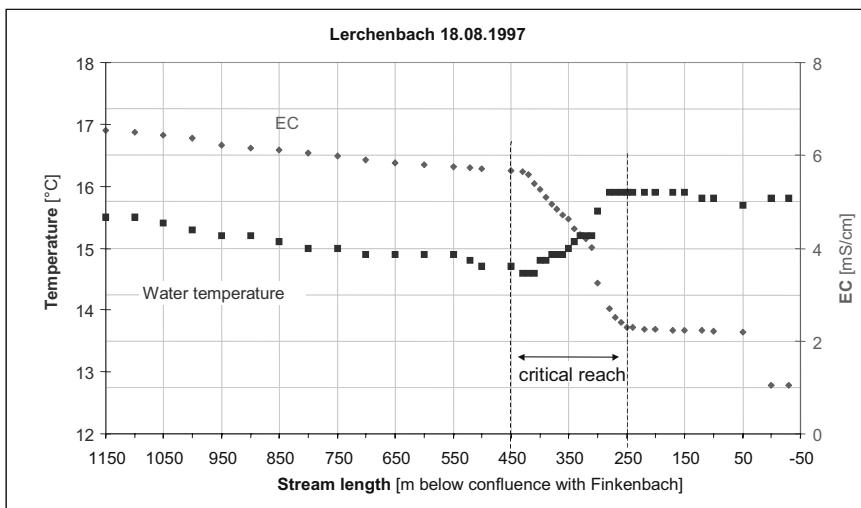
Fig. 1: Simplified geology of the study area depicting the location of the 'critical reach' in the Lerchenbach where Culmitzsch sandstone hydraulically links the geological base of the tailings ponds on both sides of the stream with the stream channel. Tailings pond 'Culmitzsch B' is not shown since it drains into an adjacent catchment (Fuchsbach).

EC-values exceeding 20mS/cm measured in alluvial groundwater indicate that inflow of contaminated tailings seepage is the main cause of rising levels of the alluvial groundwater, which now submerges large parts of a formerly dry floodplain.

Since the start of rehabilitation in the early 1990's outflow of tailings seepage is increasingly intercepted by drainage systems. In 1995 a total volume of some 1.26 million m³ of seepage was intercepted containing on average 1.61mg/l uranium (U_{nat}), 9200mg/l sulphate and 1400mg/l chloride (Wismut GmbH 1997). After removing uranium and radium but leaving the salt concentration nearly unchanged the treated seepage is discharged via the Finkenbach into the Lerchenbach and further into the Weiße Elster River. Owing to decreased assimilation capacity discharge is not allowed during low-flow conditions frequently occurring in summer.

Longitudinal EC-profiles of the Lerchenbach taken during discharge-free periods indicate a pronounced EC-increase over a 200m-long stretch, which therefore was termed 'critical reach'. Closer investigations revealed that this EC increase is caused by an outcrop of Culmitzsch Sandstone forming the geological base of the stream channel in critical reach. Hydraulically linking the stream to the base of the unlined tailings ponds nearby the sandstone allows for tailings seepage to mix with alluvial groundwater and migrate into the stream. With EC levels an order of magnitude above natural stream water, inflow of seepage contaminated groundwater largely explains the observed leap in longitudinal profiles. The fact that water temperature in the critical stream drops parallel to the rise of EC further supports the assumption that most of the stream pollution is caused by contaminated groundwater which, in summer, is significantly cooler than stream water (Winde 2000; Fig. 2).

Thermodynamic and kinetical modeling
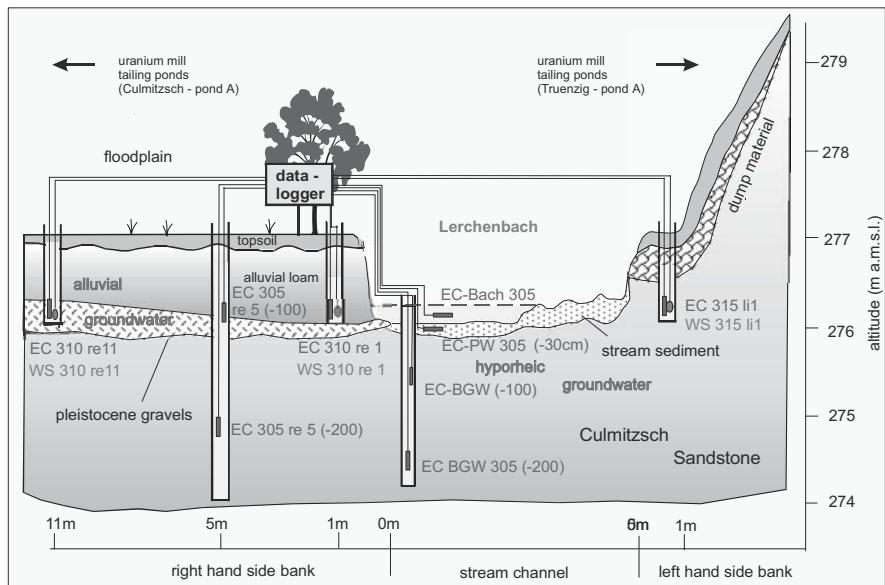
Fig. 2.   Longitudinal profile of EC and temperature of stream water in the Lerchenbach under discharge-free conditions (18/08/1997).

Using a volume-concentration approach based on EC and flow rate measurements, the volume of seepage-contaminated water needed to cause the observed leaps of EC was calculated for the different profiles. With rates ranging from 13.9l/s to 16.3l/s the diffuse inflow of contaminated water accounts for approximately 15% of the total run-off at this point of the stream (0.44 - 0.51 million m³/a). Based on a strong correlation between EC and U concentration found for stream water downstream of the critical reach (R= 0.967; n=41; 95% confidence interval) a load of approximately 800kg U/a was calculated entering the stream via contaminated groundwater (Winde 2000).

Methodology

In order to track the dynamics of the contaminated groundwater seeping into the stream channel and its hydraulic interactions with stream water, datalogger-controlled *in-situ* probes measuring EC and water level were placed in boreholes along a cross-section right within the critical reach. With EC-levels of the contaminated groundwater being more than an order of magnitude higher than those of the uncontaminated stream water, measuring the EC in all involved water bodies allowed for tracing the origin of observed fluxes. Piezometric sensors recorded changes of water levels. Flow rate and stream level as well as meteorological parameters were measured at ten-minute intervals at a second datalogger station located some 800m downstream of the critical reach. The structure of the datalogger station installed at the critical reach of the Lerchenbach is shown in Fig. 3.

Fig. 3.   Position und type of sensors of the measuring station located in the critical reach of the Lerchenbach (EC: probes for measuring electrical conductivity; WS: probes for measuring water level).

All probes were controlled by a heavy-duty battery powered datalogger (DL 2e, Delta T, UK) recording data at ten-minute intervals over periods ranging from 0.5 to 2.5 years depending on the location of the probe. In order to avoid electrical interferences between the different EC-probes their respective power circuits were electrically separated from each other. All EC probes were repeatedly calibrated against a lab-calibrated field meter.

Observed interactions between groundwater and stream
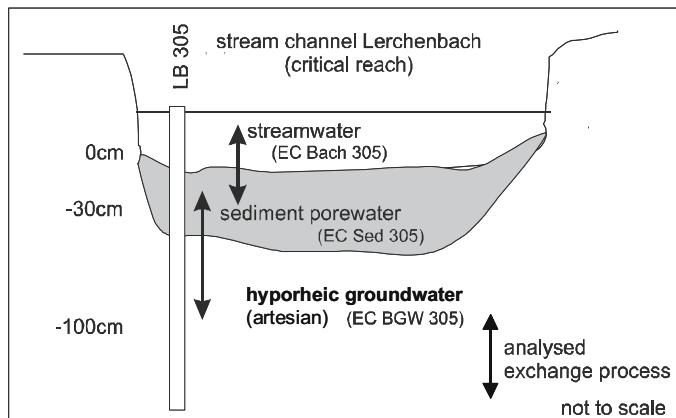
Processes investigated are schematically depicted in Fig. 4.

Examples of time series for all three EC-probes placed in the different compartments of the fluvial system in relation to each other and to the water level in the stream channel are displayed in Fig. 5.
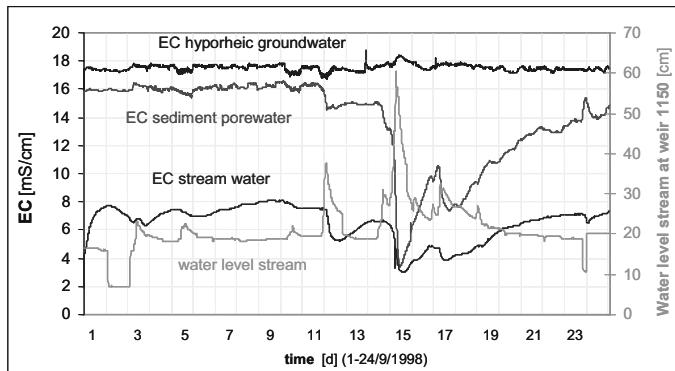
During the selected period late summer low-flow conditions prevail, interrupted only by three rain-triggered flood events on days 12, 15 and 17 of which the event on day 15 is the strongest. A high degree of similarity between EC-chart and level of both hyporheic groundwater and porewater before the first flood event (days 1-10) suggests that under these conditions porewater mainly consists of artesian groundwater pushing from the Culmitzsch Sandstone as major local aquifer into overlying coarse stream sediments. Migrating further through the sediment col-

umn into the above stream results in steep increases of the stream water EC observed in the critical reach of the Lerchenbach (Fig. 2). The fact that the EC level of porewater is slightly lower than that of the groundwater it mainly consists of, suggests that stream water (of significantly lower EC) also infiltrates into the sediment somewhat diluting the groundwater proportion. Thus, porewater in stream sediments is made up of surface- and groundwater with the latter dominating under normal and low-flow conditions.
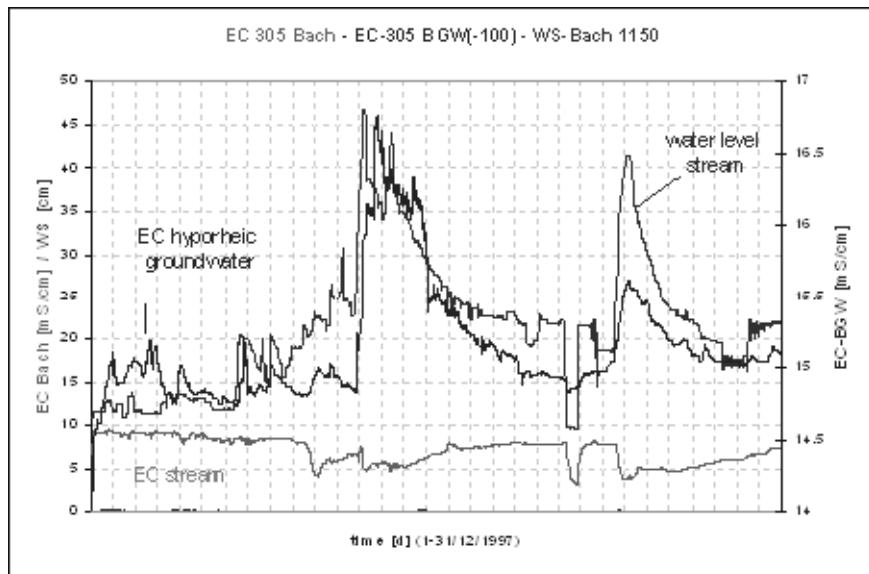
The mixing ratio between surface and groundwater, however, changes pro-

Fig. 4.   Hydraulic interactions between near-stream (hyporheic) groundwater, porewater in coarse bottom sediment of the stream channel and running stream water. The bottom sediments of the stream channel mainly consist of fine-coarse sand fraction particles and gravel and is, therefore, in general highly penetrable.
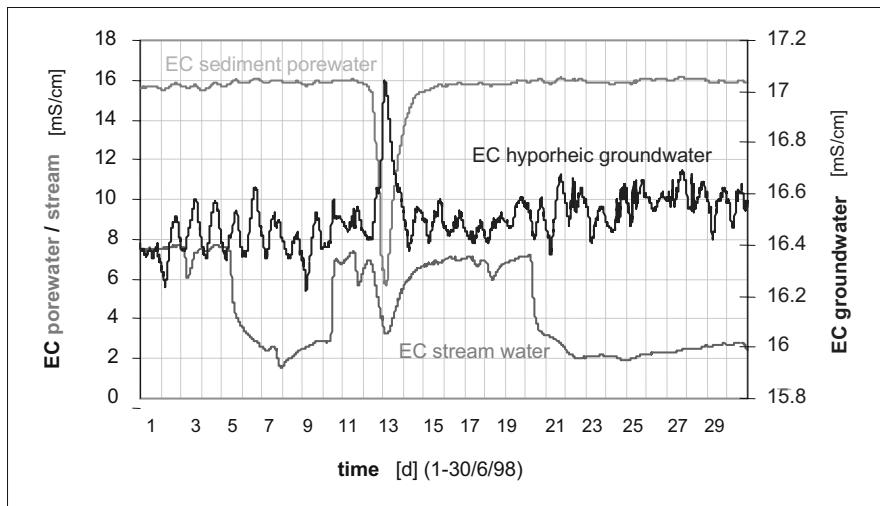
Fig. 5.   EC-time series of the hyporheic groundwater, stream water and sediment porewater in relation to stream flow for late summer period in 1998 showing an example for the replacement of sediment porewater by stream water during a flood event on day 15.

Thermodynamic and kinetical modeling

Fig. 6.   Two examples for a 'dam-up effect' of contaminated groundwater in the hyporheic zone as observed during two flood events in winter (December) 1997.

foundly during flood events. At the event on day 15 the porewater EC drops steeply until - at peak flow - it finally reaches the level of the stream water EC (Fig. 5). This suggests that pre-event porewater is displaced by stream water infiltrating deeper into the sediment, subsequently filling all pores at least to the depth at which the EC sediment probe is installed. This is most likely caused by increasing hydraulic pressure the rising stream water column exerts on the sediment (at peak flow the height of the water column tripled compared to pre-event level). With artesian groundwater underneath the stream channel counteracting the increasing pressure by stream water, the 'sandwiched' porewater can only be displaced by being 'squeezed' out from the sediment into the stream *ahead* of the flood wave rolling downstream (Indications that this indeed occurs and highly contaminated porewater is mixing with stream water during the rising limb of the hydrograph are presented in chapter 'Consequences for stream pollution and U mobility' (Fig. 9)). In addition to this the rising pressure by stream water increasingly prevents further ingress of contaminated, artesian groundwater into the stream channel. Consequently the artesian groundwater dams up underneath the bottom of the stream channel coinciding with sharply rising EC-levels that mirror the hydrograph (Fig. 6).

Why exactly the groundwater EC rises when the artesian pressure builds up is not yet clear. A possible explanation is that under normal flow conditions less contaminated stream water is able to penetrate the channel bottom slightly lowering the EC of the receiving hyporheic groundwater in the bedrock. During flood events however, this infiltration stops despite the increasing pressure from a rising

Fig. 7. Example of an incomplete displacement of porewater in stream channel sediments as observed on 13/06/1998. (EC-peaks of stream water indicate discharge of waste water.).

stream water column. This, in turn, might be caused by mounting pressure from both sides –above from the stream water column and below from dammed-up artesian groundwater – that results in some kind of stable hydraulic condition at the interface of the two water bodies. Increasingly preventing further mixing and associated dilution by stream water the EC of the hyporheic groundwater rises. The amount of surface water ingress into the bedrock seems to be indirect proportional to the height of the stream water column. Further indications that stream water under low-flow conditions indeed interacts to a depth of at least 1m below channel bottom with hyporheic groundwater are presented and discussed in Winde (2003).
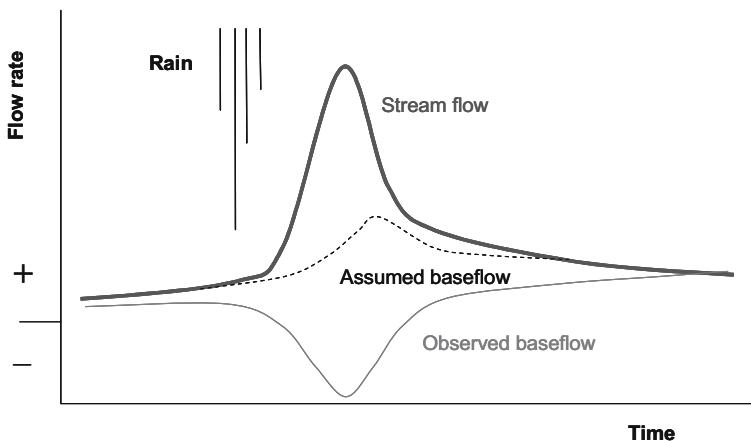
An evaluation of all 21 flood events in which porewater exchange was observed during 27 November 1997 and 6 November 1998 revealed that not all events led to a complete replacement of porewater by stream water. This is the case when the EC level of porewater drops but does quite reach the EC level of the stream water. The EC difference between the two water types at peak flow of flood events was used to calculate the proportion of the total pre-event porewater volume replaced by stream water. On average 51% of the total porewater volume was replaced, ranging from 2% to 100%. Fig. 7 shows an event during which 79% of the porewater was replaced.

Despite the fact that increasing hydraulic pressure of a rising stream water column seems to be the major force behind the porewater exchange, only a weak statistical relationship between the amount of water level increase during a flood event (measured in cm) and the degree to which porewater is replaced (measured in % of total porewater volume) was found (R = 0.45; n=20). This suggests that other factors also impact on the process, including:

- seasonal changes in groundwater levels impacting on the amount of artesian pressure of the hyporheic groundwater;
- pre-event EC-levels of stream water impacting on density and ability to displace the more dense contaminated porewater;
- temperature differences between stream and groundwater impact on density and viscosity of the latter and therefore on its ability to displace the thermally more constant groundwater,
- dynamic of flood events (e.g. flash floods vs. slowly rising water levels, levels of turbulence etc.).

Consequences for run-off generation in streams

During flood events, stream flow consists of three major components with their relative contributions to run-off changing during the event. While direct surface run-off of rainwater (including overland flow and channel precipitation) as well as interflow (subsurface flow in the unsaturated zone of slopes) are relatively quick responses to rainfall-controlled stream flow generation in the initial phase of flood events, the contribution of baseflow is generally thought to steadily increase during the event driven by higher recharge rates and the resulting rise of groundwater levels (Baumgartner & Liebscher 1990: 481). This, however, could not be confirmed by this study. Instead, the contrary was observed, i.e. baseflow was increasingly reduced during the rising limb of the hydrograph thus not contributing

Fig. 8.   Schematic depiction of groundwater contributions (baseflow) to stream flow during flood events as assumed by conventional hydrograph analyses (Baumgartner & Liebscher 1990:481; 'Assumed baseflow' - dashed line) versus (an idealised model of) observed baseflow as found by real-time *in-situ* measurement in the Lerchenbach.

Thermodynamic and kinetical modeling
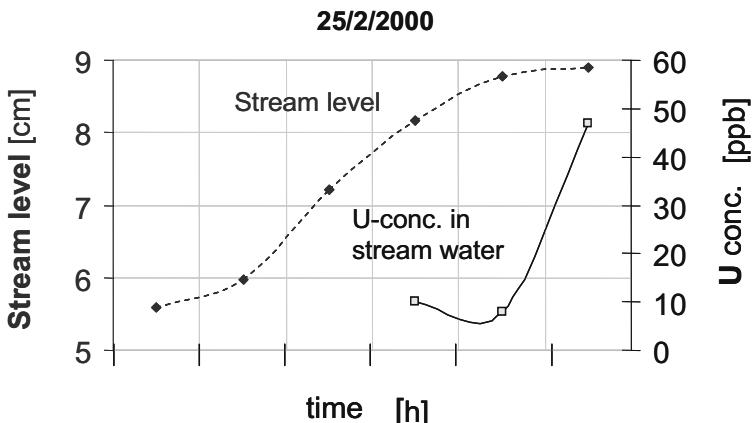
to run-off during peak flow at all. The fact that the recovery of porewater-EC to pre-event levels took up to two weeks after flow peaks (Fig. 5) further suggests that baseflow contributions to stream run-off at the falling limb of the hydrograph are also relatively small, if existent at all. A simplified schematic comparison of the contributions of groundwater to flood events according to the current under-standing and the actual contribution as reflected in the *in-situ* measurements is displayed in Fig. 8.

Being in contradiction to a well-established hydrological concept the presented results must be interpreted with utmost caution and should ideally be confirmed at other sites. However, the fact that baseflow was suppressed in a reach where groundwater discharges under artesian pressure suggests that event-related sup-pression of baseflow under non-artesian conditions, as prevalent in the vast major-ity of streams, readily occurs as well – possibly even earlier during the event and lasting longer after the event. It is, therefore, assumed that suppression of base-flow as observed in 21 flood events is not only a local peculiarity confined to the Lerchenbach but a phenomenon of general significance applicable to many other streams.

Hydrological models based on the conventional understanding that groundwa-ter increasingly contributes to stream flow during flood events may systematically underestimate the contribution of direct surface run-off and interflow to flood events. This, in turn, could result in underestimates of possible benefits from measures aimed at the reduction of surface run off e.g. from sealed areas such as settlements and industrial areas.

Consequences for stream pollution and uranium mobility

The observed displacement of porewater from channel sediments during flood events and the simultaneous suppression of contaminated groundwater seepage into the stream channel not only impacts directly on the extent of associated stream pollution and the resulting U-concentration in the receiving stream but also on the chemical mobility of dissolved uranium and other heavy metals within the aqueous system. While the suppression of inflow of uranium-polluted groundwa-ter in general lowers U-concentrations in the stream during flood events this is not necessarily the case during the rising limb of the hydrograph. Analyses of stream water samples taken from the Lerchenbach downstream of the critical reach dur-ing a flood event in February 2000 suggest that despite dilution by uncontami-nated rainwater the concentration of dissolved U in the stream increased (Fig. 9).

Thermodynamic and kinetical modeling

Fig. 9.   Stream level (dashed line) vs. concentration of dissolved U in stream water during a flood event in the Lerchenbach on 25 February 2000 (raw data: Schippel 2001). Despite dilution by uncontaminated rainwater causing the stream level to rise, the concentration of dissolved U also increases due to the 'squeezing effect'.

This somewhat paradoxical observation might be explained by the described displacement of highly U-contaminated porewater from stream channel sediments ahead of the flood wave ('squeezing effect') – causing a short-term peak of the U-concentration in stream water (Winde 2003).

In addition to such direct impacts the observed exchange of porewater may also affect U-levels in the stream indirectly by impacting on the chemical mobility of dissolved uranium. This refers mainly to the drastic change of chemical conditions inside the pores of the stream sediments. Constituting an interface between reducing groundwater conditions and oxidised stream water, such sediments frequently act as geochemical barriers in which dissolved U and other heavy metals are immobilised and accumulated. The profound change in the chemical composition and physical properties of water within the sediment pores is likely to impact on its ability to further act as sink for dissolved metals. It may, in fact, even cause a temporary release of accumulated contaminants back into the water column. This, however, depends on the kinetics of chemical immobilisation (e.g. adsorption, precipitation, co-precipitation etc.) and remobilisation (e.g. de-sorption, dissolution etc.) of uranium species. Relating such kinetics to observed dynamics of the porewater replacement (e.g. time needed to replace reduced groundwater by uncontaminated and well-oxygenised stream water vs. the inverse process) might allow for a more accurate estimate of possibly re-mobilisation of contaminants from polluted stream sediments.

For pristine reaches with non-artesian conditions downstream of the point of contamination, the possible infiltration of polluted stream water deep into the hyporheic zone during flood events should be considered as a possible mechanism of groundwater pollution and therefore be assessed in monitoring programmes.

Acknowledgement

References

Baumgartner H, Liebscher L (1990): Lehrbuch der Hydrologie.- Bd. 1, Allgemeine Hydrologie- Berlin, Stuttgart.

Evans RD, Provini A, Mattice J, Hart B, Wisniewski J (1997): Interactions between Sediments and Water. Summary of the 7th International Symposium. Water, Air, and Soil Pollution 99 (1/4): 1-7

Jenne EA (1995): Metal adsorption onto and desorption from sediments: I. rates. Allen HE (Ed.) (1995): Metal contaminated aquatic sediments. Michigan.81-105.

Maddock IP, Petts GE, Evans EC, Greenwood MT (1995): Assessing river-aquifer interactions within the hyporheic zone. In: Brown AG [Ed.] (1995): Geomorphology and Groundwater. Wiltshire 53-74.

Schippel N (2001): Lösungs- und Schwebstofftransport in einer Uranbergbaufolgelandschaft – eine Jahresbilanzierung für den Lerchenbach. Diplomthesis at the Institute for Geography, University of Jena, 128 pp., unpublished.

Sophocleous MA (2002): Interactions between groundwater and surface water: the state of the science. Hydrogeology Journal vol. 10, no. 1, 52-67.

Winde F (2000): Gelöster Stofftransfer und fluviale Prozessdynamik in Vorflutern des ostthüringischen Uranbergbaugebiets. Jenaer Geographische Schriften 9, 111-127.

Winde F (2003): Urankontamination von Fließgewässern – Prozessdynamik, Mechanismen und Steuerfaktoren. Untersuchungen zum Transport von gelöstem Uran in bergbaulich gestörten Landschaften unterschiedlicher Klimate. Habilitationsschrift, University of Jena, 377pp.

Wismut GmbH (1997): Ergebnisse der chemischen Vollanalyse von Wasserproben des Lerchenbaches am MP 310. Tageswerte Juni, Juli, August 1997. unpublished.

Thermodynamic and kinetical modeling

Long-term performance of reactive materials in PRBs for uranium remediation

Vera Biermann[1], Franz-Georg Simon[1], Mihály Csővári[2], József Csicsák[3], Gábor Földing[2], Gábor Simoncsics[3]

[1]Federal Institute for Materials Research and Testing, 12200 Berlin, Germany, E-mail: vera.biermann@gmx.de
[2]Mecsek-ÖKO Rt Ore Environment Corp., Esztergár Lajos u. 19, 7614 Pécs, Hungary
[3]MECSEKERC, Rt Esztergár Lajos u. 19, 7614 Pécs, Hungary

Abstract. Elemental iron (Fe^0) and hydroxyapatite (HAP) were evaluated as reactive materials in PRBs for uranium remediation. Laboratory experiments were carried out and a pilot-scale reactive barrier with Fe^0 was installed in Pécs (Southern Hungary). Results of 2.5 years of operation are reported. The PRB has a considerable influence on groundwater composition: uranium concentrations decrease from 900 µg/l to <10 µg/l, TDS drop from 1,000 mg/l to 500 mg/l.

Introduction

Long-term performance of permeable reactive barriers (PRBs) was investigated by a consortium of eight partners within the FP 5 project PEREBAR funded by the European Union (Roehl et al. 2005). The main part of the research was focused on the remediation of groundwater contaminated with uranium. Laboratory and field experiments were carried out with a variety of reactive materials suitable for groundwater remediation.

Furthermore a case study was performed for the former Hungarian uranium ore mining and processing site near the city of Pécs in Southern Hungary, where mining started in 1958 followed by milling in 1962. About 46 million tons of rock were mined and the ore processing resulted in the accumulation of 27.5 Mt of tailings and approximately 19.3 Mt of waste rocks on the site, containing 2.3 Kt of uranium in total (Csövári 1998). As part of ongoing remediation activities a pilot-scale PRB was installed to investigate the long-term performance of PRBs for groundwater protection against uranium pollution.

This paper presents results of laboratory tests with elemental iron (Fe^0) and hydroxyapatite (HAP) as reactive materials as well as performance data of the pilot-scale PRB in Pécs.

Laboratory tests

Two long-term column studies were performed using artificial groundwater (AGW) for test periods of up to 30 months. The tested materials were shredded cast iron (granulated grey cast iron, 0.3 - 1.3 mm) supplied by Gotthard Mayer, Rheinfelden, Germany, and food quality grade hydroxyapatite ($Ca_5(PO_4)_3OH$, 99 % < 0.4 mm) supplied by Chemische Fabrik Budenheim CFB, Germany.

Experimental

In both experiments the reactive material was mixed with filter sand (0.25 - 1.0 mm) and placed into columns of 50 cm height and 5.9 cm inner diameter with a layer of filter sand at either end to achieve uniform flow conditions within the reactive material. Table 1 lists the specifications of the individual columns.

The columns were operated in up-flow mode using a peristaltic pump set to a flow rate of 1.6 ml/min. Average flow rates ranged between 1.0 and 1.4 ml/min due to wear of pump tubes. The composition of the AGW was based on groundwater chemistry data at the site of the experimental PRB in Pécs (Table 2).

The groundwater is characterized by high uranium, bicarbonate, and sulfate concentrations. At room temperature AGW A was supersaturated with respect to calcite and precipitates caused blockages of the recharge tubing. Therefore the AGW composition was modified in experiment B.

In the second experiment the columns contained less reactive material and the uranium concentration of the AGW was increased by a factor of 20. Furthermore,

Table 1. Specification of the columns used in long-term experiment A and B.

Column	Reactive material (RM)	Mass ratio RM/sand	Mass of RM g	Height of reactive zone cm	Reactive pore volume l
A2	HAP	0.20	306	40	0.45
A3	HAP	0.10	158	40	0.45
A4	Fe^0	0.70	1795	40	0.47
A5	Fe^0	0.50	1160	40	0.47
A6	Fe^0	0.30	587	40	0.42
B1	HAP	0.10	90	20	0.23
B2	HAP	0.10	90	20	0.23
B3	Fe^0	0.05 / 0.15	174	10 / 20	0.35
B4	Fe^0	0.05 / 0.15	173	10 / 20	0.34

Table 2. AGW composition in comparison to the groundwater at the field site in Pécs.

	pH	EC[a]	U(VI)	TDS[b]	Ca	Mg	Na	K	SO$_4$	TIC[c]	Cl
		µS/cm	mg/l	mg/l	mg/l	mg/l	mg/l	mg/l	mg/l	mg/l	mg/L
AGW A	7.0	910	0.49		80	41	60	14	300	250	50
AGW B	7.5	1082	9.6		17	61	95	21	382	114	43
Pe-4[d]	7.22	1671	1.14	1197	166	63	105	20	381	591	
Hb01/1[e]	7.10	1496	0.72	1030	168	53	86	20	361	474	

[a] Electrical conductivity
[b] Total dissolved solids
[c] Total inorganic carbon calculated as HCO$_3^-$
[d] Monitoring well located approximately 15 m upstream of the PRB in Pécs, average values for the monitoring period 13.03.-11.11.2002
[e] Monitoring well located approximately 15 m downstream of the PRB in Pécs, average values for the monitoring period 2000-2002 prior to the installation of the PRB

the Fe^0-columns B3 and B4 were set up similar to the pilot-scale PRB in Pécs, with a zone of low iron concentration (5 %) at the entrance followed by a larger zone of higher iron content (15 %), in order to improve the long-term hydraulic conductivity of the Fe^0-columns.

Results

In both column experiments Fe^0 and HAP exhibited an uranium retention of more than 99 %. Effluent uranium concentrations were below the limit of detection (13 to 87 µg/l and 2 to 11 µg/l in experiment A and B respectively) of the spectro-photometric method employed for routine uranium analysis. Measurements with ICP-MS yielded maximum effluent uranium concentrations of 1.3 µg/l corresponding to an uranium retention of at least 99.7 % for all columns.

In experiment A no breakthrough was observed during 19 to 30 months of column operation, which corresponds to the treatment of 0.35 l to more than 8.7 l of AGW A per g of reactive material. In experiment B, however, a breakthrough occurred in both HAP-columns with effluent uranium concentrations exceeding the proposed limit of 20 µg/l in drinking water (Merkel and Sperling 1998) after the treatment of 3.2 l of AGW B per g HAP (Fig. 1, data for column B1 not shown).
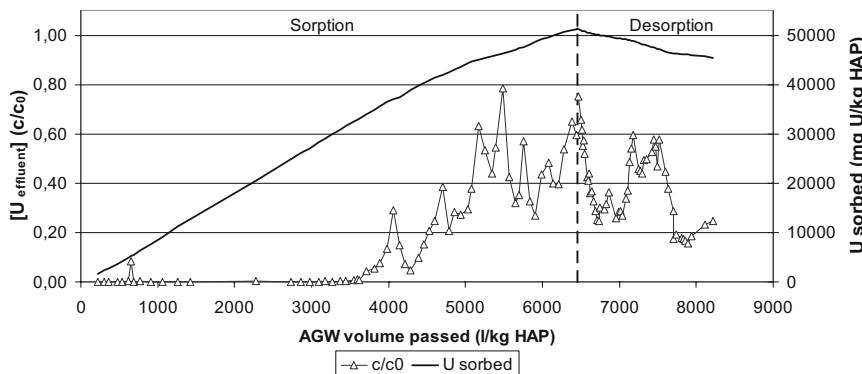
When 5.4 l/g had passed through the columns B1 and B2, more than 75 % of the influent uranium concentration was measured in the effluents. Column B1 was dismantled for analysis after treating a total of 6.0 l/g and sorbing 48.7 mg U/g HAP. The operation of column B2 was continued substituting AGW B with uranium-free AGW. Effluent uranium concentrations of B2 remained in the range of several mg/l, i.e. between 15 % and 60 % of the uranium concentration of AGW B.

The Fe^0-columns in experiment A suffered from loss of permeability. After one year of operation the columns with 70 % and 50 % Fe^0 became basically impermeable, with coefficients of hydraulic conductivity k as low as 1.5×10^{-8} and 1.8×10^{-8} m/s, and had to be dismantled. In contrast the HAP-columns maintained a
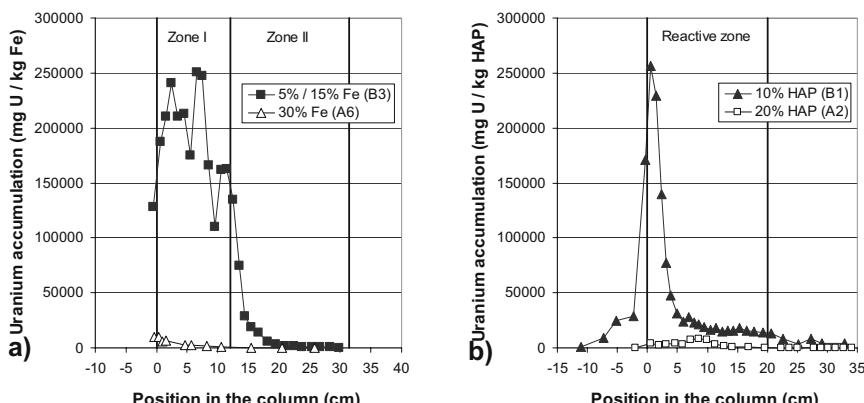
good hydraulic conductivity for 30 months (k-values decreased by about two orders of magnitude to 3×10^{-6} m/s). In experiment B neither Fe^0- nor HAP- columns showed problems with respect to hydraulic conductivity. Column B3 was dismantled after treating 4.0 l/g Fe^0 though no breakthrough had occurred but a total of 38 mg U/g Fe^0 (3.8 %) had been sorbed.

After the experiments the column material was analyzed and the uranium distribution within the columns was determined. The results are displayed in Fig. 2 with uranium accumulation calculated as ppm, i.e. mg U / kg reactive material in each sample.

In all Fe^0-columns highest uranium concentrations were found within the first 10 cm of the reactive zone with a maximum load of 250,000 ppm U on Fe^0 (25 %) in column B3, 7.5 cm above the filter layer of sand (Zone I). Hardly any uranium

Fig. 1. Breakthrough curve and subsequent desorption of uranium from column B2. At the vertical dashed line AGW B was substituted by AGW without uranium. c/c_0 is the ratio of effluent uranium concentration to influent uranium concentration during the sorption phase. The solid line indicates the cumulative sorption of uranium onto the column.

Fig. 2. Uranium distribution within Fe^0-columns (a) and within HAP-columns (b).

Active and passive water treatment techniques

was found above 20 cm height. In the HAP-columns, however, the uranium distribution was different. In experiment A the load reached its maximum with 8,000 ppm U on HAP at a height of 9 to 10 cm while about 3,000 ppm were found at the beginning of the reactive zone. In experiment B the maximum load was 250,000 ppm U on HAP at the entrance of the reactive zone. Uranium concentrations leveled off at 15,000 ppm above a height of 5 cm (Fig. 2).

Field tests: experimental permeable reactive barrier

An extensive site selection procedure including geophysical screening methods, core drilling, and hydrogeological characterization of several sites was performed. Based on these investigations the Zsid-valley, which links the waste rock piles with a shallow aquifer that serves as a source for drinking water, was found suitable for the construction of a pilot-scale PRB (Csövári et al. 2005a).

The geology of the valley is characterized by sediments. The upper 1-2 m layer consists of clay and clayey sand ($k\sim2x10^{-7}$ m/s), under which mainly sand and patches of clayey sand are present (3-4 m, $k\sim1x10^{-5}$ m/s). At a depth of 6-7 m a thick sandstone formation can be found (>10 m, $k\sim1x10^{-13}$ m/s) on top of which a thinner cracked zone is situated ($k\sim1-2x10^{-6}$ m/s). The groundwater composition in the valley exhibited elevated uranium as well as high bicarbonate and sulfate concentrations (Table 2).

Design and construction of the PRB

In August 2002 a continuous PRB with a length of 6.8 m, a depth of 3.9 m, and a width of 2.5 m was installed into the aquifer using open trench excavation, 38 tons of shredded cast iron as reactive material, and approximately 60 m³ of sand. The reactive zone consists of two sections: the first section is 0.5 m wide and contains 0.39 t/m³ Fe^0 with a particle size of 1-4 mm while the second section is 1.0 m wide and contains 1.28 t/m³ Fe^0 with a particle size of 0.2-1.2 mm.
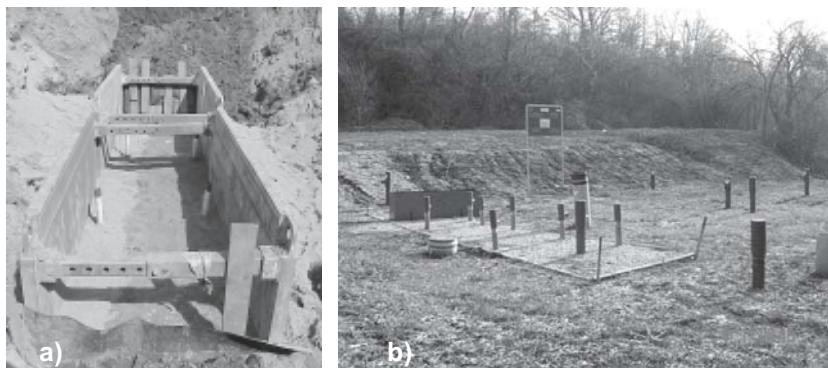
To achieve good flow conditions the Fe^0 was mixed with sand and on both sides of the reactive zone a 0.5 m wide drain was built of sand. The bottom, sides, and top of the PRB are separated from the host soil with HDPE for directing the inflow. Fig. 3 shows the PRB during and after construction. A monitoring system consisting of 28 monitoring wells in and around the PRB was also installed (Fig. 4). The PRB does not need any maintenance.

Performance of the PRB
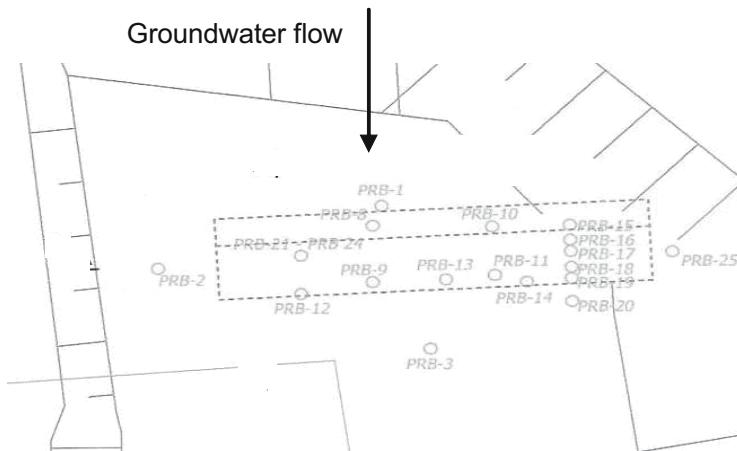
The PRB has been in operation for two and a half years. Up to now there have been no problems and the PRB performs well. Monitoring data for 2005 are presented in Table 3. Uranium was measured using a fluorimetric method with a detection limit of some µg/l.

In the first reactive zone a slight increase in pH was observed and most of the uranium (>96 %) and part of the total dissolved solids (7 % TDS), especially calcium and bicarbonate, were removed from the inflowing groundwater. At the same time elevated iron concentrations of more than 5 mg/l were observed.

In the second reactive zone pH values increased further while uranium was re-

Fig. 3. Pilot-scale PRB and monitoring wells in Pécs during (a) and after (b) construction.

Fig. 4. Location of the monitoring system within and around the PRB. The monitoring wells Pe-4, located approximately 15 m upstream, and Hb01/1, located approximately 15 m downstream of the PRB, are not displayed.

Active and passive water treatment techniques

moved to effluent concentration levels of 10 µg/l. In comparison to the inflowing water TDS, sulfate, and bicarbonate concentrations decreased by 50 % and calcium concentration was reduced by 93 %. Iron concentration dropped to 30 µg/l.

Effect of PRB on water chemistry of the test site

The PRB was built as a continuous wall intersecting only part of the valley's groundwater flow. Nevertheless the PRB has a remarkable effect on the water chemistry of the valley. This effect can be evaluated by the data of well Hb01/1 downstream of the PRB, which monitors the water passing the valley. Table 4 presents data for a five year period prior to and after the construction of the PRB in August 2002.

It can be seen that water chemistry in monitoring well Hb01/1 changed significantly: uranium concentration dropped from 718 µg/l to below 50 µg/l. TDS also decreased together with calcium, magnesium, and bicarbonate. At the same time water quality upstream of the PRB only changed to a minor extent (data not given). Therefore the observed changes in the water quality of monitoring well Hb01/1 can be attributed to the performance of the pilot-scale PRB.

The overall effect of the PRB on uranium concentration in the valley is illustrated by the isolines in Fig. 5 based on monitoring data not given in the tables above. The figure shows that uranium is removed with high efficiency. Because of the limited dimensions of the PRB lateral flow of contaminated water is bypassing
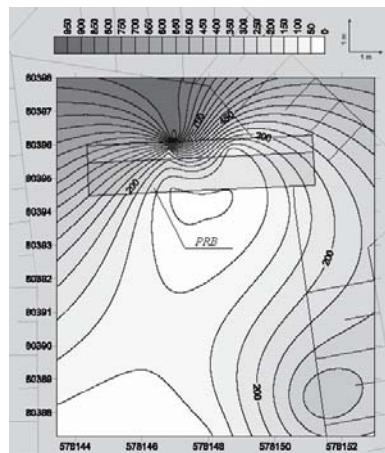
Table 3. Monitoring data of the PRB as of March 22nd 2005 after 31 months of operation.

Well	Location	pH	EC µS/cm	U(VI) µg/l	TDS mg/l	Ca mg/l	SO$_4$ mg/l	HCO$_3$ mg/l	Fe mg/l
PRB-1	Inflow	6.9	1400	940	1010	150	320	525	0.002
PRB-10	Zone I	7.3	1330	37	937	125	300	275	5.5
PRB-11	Zone II	8.7	865	10	550	10	185	299	0.03
PRB-14	Outflow	8.7	780	2	540	14	170	268	0.03
PRB-3[a]	Downstream	8.5	420	56	240	5	95	116	0.017
PRB-25	Side (left)	8.7	1380	290	1020	180	280	641	5.03
PRB-2	Side (right)	7.4	930	190	640	37	190	317	0.099

[a] Water is probably diluted by lateral water flow

Table 4. Effect of the pilot-scale PRB on water chemistry of the Zsid valley, measured at well Hb01/1 approximately 15 m downstream of the PRB.

Monitoring date/period	pH	EC µS/cm	U(VI) µg/l	TDS mg/l	Ca mg/l	Mg mg/l	SO$_4$ mg/l	HCO$_3$ mg/l	Fe mg/l
2000-2002	7.1	1496	718	1030	168	53	361	474	<0.01
08/2002-03/2003	7.7	923	70	540	54	33	170	299	<0.01
06.07.2004	7.8	780	40	465	28	26	150	305	0.18
22.03.2005	7.7	740	42	500	28	30	186	226	0.064

Fig. 5.   Isolines of uranium concentrations in and around the pilot-scale PRB.

the barrier and results in gradually increasing uranium concentrations further downstream. If the PRB were a full-scale barrier it would cross the whole valley and stop the migration of uranium with the groundwater flow entirely.
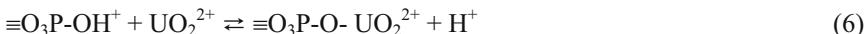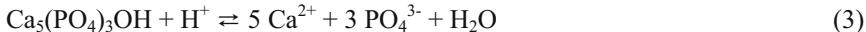
Discussion

The results of the column experiments demonstrate that Fe^0 is well suited for uranium remediation. Uranium loads of up to 25 % can be achieved provided that hydraulic conductivity is maintained. Loss of permeability in Fe^0-columns can be attributed to the formation of secondary minerals. Reduction of dissolved oxygen to ferric oxyhydroxides causes clogging in the lower part of Fe^0-columns (Mackenzie et al. 1999). Under anaerobic conditions $Fe(OH)_2$, $FeCO_3$, and $CaCO_3$ precipitates can be found as mineral solubility decreases with increasing pH due to iron corrosion, especially in the presence of elevated carbonate concentrations.

As most of the uranium was found in the lower part of the Fe^0-columns where most of the precipitation processes occur, both reductive precipitation (Reaction 1) and adsorption onto corrosion products (Reaction 2 (Bargar et al. 2000)) are feasible (Cantrell et al. 1995).

$$Fe^0 + UO_2(CO_3)_2^{2-} + 2\ H^+ \rightleftarrows Fe^{2+} + 2\ HCO_3^- + UO_2(s) \tag{1}$$

$$\equiv Fe(OH)_2 + UO_2^{2+} + CO_3^{2-} \rightleftarrows \equiv FeO_2\text{-}UO_2CO_3^{2-} + 2\ H^+ \tag{2}$$

Possible reaction mechanisms of HAP with uranium include the dissolution of HAP (Reaction 3) with subsequent precipitation of uranium phosphate minerals like autunite (Reaction 4 (Arey et al. 1999)) as well as surface complexation (Reaction 5 and 6 (Fuller et al. 2002)).

$$Ca_5(PO_4)_3OH + H^+ \rightleftarrows 5\ Ca^{2+} + 3\ PO_4^{3-} + H_2O \tag{3}$$
$$2\ UO_2^{2+} + Ca^{2+} + 2\ PO_4^{3-} \rightleftarrows Ca(UO_2)_2(PO_4)_2 \tag{4}$$
$$\equiv OH + UO_2^{2+} \rightleftarrows \equiv O\text{-}UO_2^+ + H^+ \tag{5}$$
$$\equiv O_3P\text{-}OH^+ + UO_2^{2+} \rightleftarrows \equiv O_3P\text{-}O\text{-}\ UO_2^{2+} + H^+ \tag{6}$$

As these processes do not involve redox reactions, no change of pH and therefore no significant precipitation and clogging of pore space occurs. The observed uranium distribution within the HAP-columns as well as kinetic experiments indicate two different retention mechanisms: fast but reversible sorption of up to 15,000 ppm of uranium onto surface sites and a slow, possibly irreversible, process that accounts for uranium loads up to 25 % if residence time is sufficient. However, no solid uranium phase such as meta-autunite could be identified via x-ray diffraction analysis of HAP column material. Therefore further efforts are necessary to clarify the reaction mechanism especially with respect to uranium desorption that was observed in Experiment B.

The monitoring data of the field experiment show that the PRB performs well. Considering the high sorption capacity of Fe^0 for uranium that was demonstrated in the column experiments, loss of permeability due to clogging with precipitates has to be regarded as the limiting factor for PRB performance. The decrease in TDS indicates that precipitation takes place. In zone I Fe^0 corrodes readily causing an increase in pH and dissolved iron, as well as a decrease in redox potential and uranium, the latter via reductive precipitation or co-precipitation with $Fe(OH)_2$.

With increasing pH minerals such as calcite and siderite precipitate as their solubility is reduced. This effect is more pronounced in zone II due to its higher Fe^0 content. It is supposed that sulfate reduction and subsequent formation of FeS also take place in zone II. Based on TDS monitoring data for the past 2.5 years approximately 0.5 kg/m^3 of solids precipitate from the passing water within the PRB. The accumulation of these compounds may lead to decreasing permeability within the PRB body. So far no adverse effects have been observed but the hydraulic performance of the PRB will be investigated in future work.

Decreasing pH-values within the barrier might be an indicator for decreasing efficiency of the PRB. In 2002 pH in zone II was 9.43 (Csövári et al. 2005b) compared to 9.5 and 8.7 in 2004 and 2005 respectively. For column experiments such a decrease in pH was explained by the development of preferential flow paths due to clogging (Kamolpornwijit et al. 2003; Simon and Biermann 2005). However, in PRBs a change in flow pattern or a reduced iron corrosion rate due to coating of Fe^0 surfaces seem more likely, especially as iron concentrations in zone I decreased from 17 mg/l in 2002 to 5.5 mg/l in 2005. Nevertheless the PRB is still very effective for removing of uranium from ground water.

Conclusions

The purpose of the column experiments was to perform accelerated testing of the processes within PRBs so that ageing effects become visible earlier than in natural systems. Therefore higher flow rates and higher uranium concentrations were used. In experiment B 4000 l/kg Fe^0 were treated with the Fe^0-columns compared to about 50 l/kg Fe^0 that passed the PRB so far. Uranium sorption was simulated and the importance of water composition (TDS, Ca, TIC) and Fe^0 content for the overall performance became apparent. However, barrier life-time calculations based on column tests can only give a rough estimate as complex groundwater conditions and geological processes cannot easily be simulated in the laboratory.

The pilot-scale PRB in Pécs demonstrates the high efficiency of Fe^0 for uranium remediation. A small decrease in the reactivity of the PRB is observed, which manifests itself in the decreasing pH of the water in the second zone of the barrier.

References

Arey S J, Seaman J C, Bertsch P M (1999) Immobilization of Uranium in Contaminated Sediments by Hydroxyapatite Additon. Environ Sci Technol 33: 337-342

Bargar J R, Reitmeyer R, Lenhart J J, Davis J A (2000) Characterization of U(VI)-carbonato ternary complexes on hematite: EXAFS and electrophoretic mobility measurements. Geochim Cosmochim Acta 64: 2737-2749

Cantrell K J, Kaplan D I, Wietsma T W (1995) Zero-Valent Iron for the in situ remediation of selected metals in groundwater. J Hazard Mat 42: 201-212

Csövári M (1998) The most important material balance data for Mecsek uranium ore mining and processing. Hung J Mining Metall 136: 571-575

Csövári M, Berta Z, Csicsák J, Földing G, Simoncsics G (2005a) Mecsek Ore, Pécs, Hungary case study, in: Roehl K E, Meggyes T, Simon F G, Stewart D I (Ed.), Long-term performance of permeable reactive barriers. Trace metals and other contaminants in the environment, Nriagu J (Series Ed.), Vol. 7: 211-245, Elsevier, Amsterdam

Csövári M, Csicsák J, Földing G, Simoncsics G (2005b) Experimental iron barrier in Pécs, Hungary case study, in: Roehl K E, Meggyes T, Simon F G, Stewart D I (Ed.), Long-term performance of permeable reactive barriers. Trace metals and other contaminants in the environment, Nriagu J (Series Ed.), Vol. 7: 265-283, Elsevier, Amsterdam

Fuller C C, Bargar J R, Davis J A, Piana M J (2002) Mechanisms of Uranium Interactions with Hydroxyapatite: Implications for Groundwater Remediation. Environ Sci Technol 36: 158-165

Kamolpornwijit W, Liang L, West O R, Moline G R, Sullivan A B (2003) Preferential flow path development and its influence on long-term PRB performance: column study. J Contam Hydrol 66: 161-178

Mackenzie P D, Horney D P, Sivavec T M (1999) Mineral precipitation and porosity losses in granular iron columns. J Hazard Mat 68: 1-17

Merkel B, Sperling B (1998) Hydrogeochemische Stoffsysteme II. Schriftenreihe des Deutschen Verbandes für Wasserwirtschaft und Kulturbau e.V. (DVWK); 117, Deutscher Verband für Wasserwirtschaft und Kulturbau e. V. (DVWK), Bonn

Roehl K E, Meggyes T, Simon F G, Stewart D I (2005) Long-term performance of permeable reactive barriers. Trace metals and other contaminants in the environment, Nriagu J (Series Ed.), Vol. 7, Elsevier, Amsterdam

Simon F G, Biermann V (2005) Behaviour of uranium in elemental iron and hydroxyapatite reactive barriers: column experiments, in: Roehl K E, Meggyes T, Simon F G, Stewart D I (Ed.), Long-term performance of permeable reactive barriers. Trace metals and other contaminants in the environment, Nriagu J (Series Ed.), Vol. 7: 77-109, Elsevier, Amsterdam

Uranium leaching during short term application of pit-water on a carbonate containing soil in the Mendoza province of Argentina

Juan Pablo Bonetto[1], Silvia López[1], Silvia Ratto[2], Valeria Schindler[3], Ewald Schnug[4]

[1]Agronomic Group, Ezeiza Atomic Center, National Atomic Energy Comision. Presbítero Juan Gonzalez y Aragón 15. Ezeiza, Buenos Aires Province, Argentina, E-mail: jpbonett@cae.cnea.gov.ar
[2]Edaphology, Agronomic School, Buenos Aires University. Av. San Martín 4453, 1417, Buenos Aires City, Argentina.
[3]Animal Production, Agronomic School, Buenos Aires University. Av. San Martín 4453, 1417, Buenos Aires City, Argentina.
[4]Institute of Plant Nutrition and Soil Science, Federal Agricultural Research Center, Bundesallee 50, D-38116 Braunschweig, Germany, E-mail: pb@fal.de

Abstract. Pit-water from an Uranium (U) mine in San Rafael, Argentina, was applied to soil columns in a short-term experiment to evaluate retention of U. The mine soil was coarse-textured, with $pH_{(KCl)}$ 7.7 and a carbonate content of 6%, which may favour the formation of uranyl-carbonates. Triple superphosphate (TSP) and ground plant material were added as amendments to reduce U mobility in soil. Plants were sown to study their effect on U leaching. > 99 % of the U applied was retained by the soil. Plant growth increased U mobility but also reduced leachate volumes through evapotranspiration. TSP increased plant biomass, reducing the mass of U leached, while ground plant material enhanced leaching of U.

Introduction

The San Rafael open pit Uranium Mine and Processing Facility (CMFSR) is an 800 ha site lying in the Sierra Pintada, 30 km SE of the city of San Rafael (34.6°S, 68.4°W, elevation 227 m) in the province of Mendoza, Argentina.

After an almost 10 year relapse in the mining activities, its open-air pits have become flooded through groundwater inflow and surface water run-off initially used in the facility processes. Added to the risk of overflowing, since water bal-

ance favors water accumulation in spite of being a semi-arid region, a restarting of the activities is currently in study, and the pits would need to be emptied to allow the continuation of mining processes.

The pit water cannot be disposed in the surrounding water courses due to its U content of 3500 µg l^{-1}. Among the different treatment and disposal alternatives, also application of the water to the soil is under consideration, based on the proposition that the soil will retain the contaminants, minimizing their movement to the grounwater. Uranium (VI) mobility in soils may be limited by formation of low solubility complexes, and by adsorption, preferably to Fe and Mn oxyhydroxides, organic matter (OM) and clays (Langmuir 1978; Ribera et al. 1996).

Field irrigation with U containing waters has been studied and put to practice in Australia with varying results (Riley 1992; Noller and Zhou 1992). Willet and Bond (1992) determined that the amount of U involved in land application of effluent water from Ranger Uranium Mine (Australia), could be immobilized by low OM, poor sorption capacity, highly weathered soils, even though the equally applied major ions were expected to be readily mobile in the soil profile (Bond and Willet 1992). The CMFSR soils, however, though also coarse-textured, present a slightly alkaline pH and a higher carbonate content than those of Ranger.

In solutions of neutral to alkaline pH, presence of carbonate ions induces the formation of stable uranyl-carbonate complexes (Finch and Murakami 1999). These highly soluble complexes are mainly neutral or negatively charged, minimizing adsorption to soil particles and enhancing U mobility (Elless and Lee 1998; Finch and Murakami 1999). In contrast, the presence of phosphates, may induce precipitation of highly insoluble uranyl-phosphate complexes (Finch and Murakami 1999). The low solubility and high stability of these complexes have led to several studies on the remediation of contaminated water and soils by U immobilization with phosphates, mainly apatites (Seaman et al. 2001; Knox et al. 2003).

Sorption to inactivated plant biomass such as that of *Larrea Tidentata* has also been studied as a means for heavy metal immobilization and extraction from contaminated solutions (Gardea-Torresdey et al. 1997). This plant species has been found growing in heavy metal contaminated areas in the arid southwest region of the United States, and subsequently studied and recognized as a heavy metal accumulator (Gardea-Torresdey et al. 1996). *Larrea spp*. (mainly *L. nitida* and *L. divaricata)* thrive in most of the CMFSR and its surroundings. Its use in the form of processed tissue, as fresh OM amendment, could prove a means of increasing U sorption capacity of the soil.

Presence of vegetation can reduce water percolation due to an increase in water demand through evapotranspiration (hydraulic control), thus limiting heavy metal leaching. Plants have also the potentiality of reducing U contamination in soils by extraction through roots (phytoextraction) (Dushenkov 2003). However, plants may also increase the risk of trace metal leaching through the soil. Root growth and exploration create macropores in the soil that may enhance solute transport through preferential flow (Gabet et al 2003). Furthermore, it is recognized that plant presence may favor contaminants leaching through organic acid roots exu-

dates that complex metals and enhance their solubility, also by enhanced microbial activity in the rhizosphere (INEEL 2000).

A column experiment was carried out to determine U leaching during a short term application of pit water to a coarse textured, low OM, high-carbonate soil. Treatments included plant presence, and addition of soil amendments such as triple superphosphate fertilizer and processed *Larrea spp.* tissue to evaluate their effect on U leaching.

Materials and methods

Experimental design and statistical analyses

The experimental design was 2x3 factorial completely randomized with 5 replicates. The factors were *plant* (two levels: plants and no plants), *amendment* (three levels: no amendment, *Larrea spp.* tissue (Lr) and triple superphosphate fertilizer (TSP)). The resultant 6 treatments and their abbreviations were: No plants, no amendment (NN); no plants, Lr (NL); no plants, TSP (NP); plants, no amendment (PN); plants, Lr (PL) and plants, TSP (PP). Statistical analysis of the data involved analysis of variance (ANOVA) using the General Lineal Model (GLM) and analysis of regression using the Regression Procedure (REG) of the Statistical Analysis System (SAS Vs. 8).

Soil and amendments

The soils in the area surrounding the CMFSR are classified as an association of Typic Paleorthids (70%) and Typic Torrifluvents (30%) (Hudson et al., 1990). The upper 20 cm layer of soil was sampled from an unaltered area of the mine, of which some properties are presented in Table 1.

The soil was air dried, passed through a 2 mm sieve, and homogenized prior to packing the columns. Commercial TSP was finely ground and applied as amend-

Table 1. Selected properties of soil, amendments and pit water used in the experiment.

	Soil	TSP	Lr	Pit-water
U ($\mu g\ g^{-1}$)	2.4 †	84.0	0.1	3500 ($\mu g\ L^{-1}$)
Total Phosphorus ($\mu g\ g^{-1}$)	641	$2\ 10^5$		
Phosphorus $_{available}$ ($\mu g\ g^{-1}$)	0.98	$2\ 10^5$		
PH $_{(KCl)}$	7.7			7.2
C$_{organic}$ (%)	0.36			
Carbonates (%)	6			
Texture	Loamy sand			

† Within baseline values for soils in San Rafael.

Active and passive water treatment techniques

ment. Twigs with leaves were cut from *Larrea spp*. plants from uncontaminated areas around the CMFSR. They were oven dried, finely ground and homogenized before use as amendment. Water sampled from the pit was used for irrigation. Some properties of the pit-water and the amendments are also presented in Table 1.

Column preparation

30 soil columns were built out of 10 cm diameter polyvinylchloride pipes, and cut to 33 cm length. Each pipe was fitted with a bored end-cap to allow for the liquids to leach. A voile cloth filter was placed at the bottom to prevent loss of fines. 318 g of acid-washed sand were added to each column as a filtering bed, covering the bottom 2 cm of the columns. Over the sand, an initial 3311 g of soil were packed, equivalent to a depth of 27 cm. The soil was added in various steps, slightly tapping the columns and humidifying. The columns were then randomly selected to receive each of the 6 treatments. A final 376 g of soil, equivalent to a 3 cm layer, were thoroughly mixed with 88.2 mg TSP, 1000 mg Lr, or shaken without amendment, and added to each column, giving concentrations of 47 mg kg soil^{-1} P and 2660 mg kg soil^{-1} Lr for the last 3 cm layers. *Agropyron elongatum* seeds were planted in separate trays with acid-washed sand. After 16 days cultivation on Hoagland solution, 30 seedlings were transplanted to the corresponding packed columns. The finished columns were placed in wooden supports specially built for the purpose. Each leachate was collected in a plastic 0.5 L bottle through a plastic funnel. The experiment was carried out in a growth chamber providing a 12 hour light period and a controlled temperature.

Irrigation and U analyses

Before initiating pit-water irrigation, distilled water was applied to all columns until field the first drops of gravitational water started to leach. The experiment commenced on first application of pit-water. Irrigation was manually applied employing controlled slow flow from a burette, ensuring that all columns received the same daily volume of water. It was applied in an amount enough to keep all columns slightly over field capacity, obtaining a minimum of leachate every day. At the end of every week, leachates were collected, their volumes measured and compared against the amount of pit-water applied. Aliquots were taken and acidified with nitric acid prior to total U measurement by means of laser fluorescence employing a Scintrex UA-3 analyzer.

Results and discussion

Leachate volumes

Irrigation volumes were increased weekly (Table 2) to compensate for increasing water use due to plant growth, and to receive a minimum amount of leachates. For the first half of the experiment, vegetated columns leached less volume than unvegetated ones, but there was no difference in leachate volumes due to amendment effect (Table 2).

   The results for the second half (Table 2) revealed interactions between factors *plant* and *amendment* for leachate volumes, so comparisons of the three amending levels were performed within each of the two plant levels. No differences were found among the amendments applied to the unvegetated columns. Where plants were growing, the PP treatment leached less volume than PN and PL. This had also been observed in week three, but the difference had failed to be statistically significant. Within each of the amendment levels, *A. elongatum* considerably re-

Table 2. Weekly irrigated and leached volumes and ANOVA for leachate volume.

	Week 1	Week 2	Week 3	Week 4	Week 5	Week 6
	Irrigated volume (ml week^{-1})					
All treatments	300	400	425	550	650	830
	Leachate volume (ml week^{-1})					
Treatment[1]	Week 1	Week 2	Week 3	Week 4	Week 5	Week 6
NN	139	138	172	270	405	587
NL	123	109	167	257	386	570
NP	132	135	174	271	404	586
PN	96	67	105	116	193	315
PL	94	76	100	121	197	317
PP	93	65	81	45	59	96
	Average					
No plants	131 a	127 a	171 a	266	398	581
Plants	94 b	69 b	95 b	94	150	243
No amendment	117	102	138	193	299	451
Lr	108	92	133	189	291	443
TSP	112	100	127	158	154	341
	Probability of F^{2}					
Plant	***	***	***	***	***	***
Amendment	-	-	-	**	***	***
Plant x Amend.	-	-	-	***	***	***
CV (%)	10.2	19.3	11.0	10.4	9.4	6.9

[1]NN = no plants, no amendment; NL = no plants, processed *Larrea spp.* tissue; NP = no plants, triple superphosphate; PN = plants, no amendment; PL = plants, processed *Larrea spp.* tissue and PP = plants, triple superphosphate.
[2]Probability of F (- = $p > 0.05$; * = $p < 0.05$; ** = $p < 0.01$; *** = $p < 0.001$). Means in columns followed by the same letter are not significantly different at $p \leq 0.05$ level (Fisher´s LSD test)

Table 3. Regression equations for the relationship between irrigated volume (X) and leachate volume (Y) .

Treatment[1]	Regression	Probability of F[2]	R^2 (%)
NN	Y = 0.913 X - 195	***	95.6
NL	Y = 0.912 X - 211	***	95.4
NP	Y = 0.920 X - 200	***	96.2
PN	Y = 0.441 X - 83.4	**	86.0
PL	Y = 0.447 X - 84.2	**	88.2
PP	Y = 0.001 X + 72.4	-	0.0

[1]NN = no plants, no amendment; NL = no plants, processed *Larrea spp.* tissue; NP = no plants, triple superphosphate; PN = plants, no amendment; PL = plants, processed *Larrea spp.* tissue and PP = plants, triple superphosphate.
[2]Probability of F (- = $p > 0.05$; * = $p < 0.05$; ** = $p < 0.01$; *** = $p < 0.001$).

duced leachate volumes. The volume of water evapotranspired from vegetated columns resulted higher than that evaporated from unvegetated ones. Plant growth increased evapotranspiration. Dry matter yields, weighed at the end of the experiment, resulted higher both in roots (Pr < 0.0001) and in shoot (Pr < 0.0007) for PP plants than for PN and PL plants. The soil had a very low plant available Phosphorus (P) content, therefore the plants in the PP treatment benefited from the additional P supplied by the TSP to produce higher biomass, so leachate volume was lowest. Additionally, reduced plant growth may have occurred in treatments PS and PL due to U toxicity. U present in calcareous soils is expected to be not only mobile but also highly available to plants, favoring U phytotoxicity in greenhouse experiments (Shahandeh and Hossner 2002; Meyer et al. 2004; Lamas 2005). P addition has been found to alleviate toxic effects of U, probably due to complexation, reduced solubility and consequently a decrease in U availability to plants (Ebbs et al. 1998). The addition of TSP in the PP treatment may have prevented, or at least reduced, this.

Results of linear regression analyses revealed a close significant positive linear relationship between leachate volumes and irrigated volumes for all treatments except for PP (Table 3). This indicates that virtually all increase in leachate volume can be explained by increasing volumes irrigated. Treatments NN, NL and NP had very similar regression models, suggesting that there was no specific amendment effect. The models for PN and PL were also very similar to each other, and the resulting R^2 was only slightly lower than those in the no-plant treatments. This suggests that part of the irrigated water was used by plants, and that every weekly increase in irrigation volume exceeded any increasing need of the plants for water. The leachate volume in PP showed no relationship to the irrigated volumes. Being the treatment with highest plant growth, this suggests that the weekly increases in irrigation were almost completely used by the plants.

Uranium concentration in leachates

For all of the treatments U concentration in the leachates was much lower than in the applied pit water (Table 4). Since week 2, leachates from columns with plant growth had higher U concentrations than those from unvegetated columns. Week 5 showed an interaction between plant presence and amendment, but plant presence again increased U concentration in all three amendment levels. Apart from the probability of preferential flow generated by the roots (Gabet et al. 2003), rhizosphere exudates might also be at least partly responsible for the increased U concentrations. Higher metal mobility in soils due to plant presence has been reported by Banks et al. (1994) for Zn in a short-term greenhouse experiment, and by Zhu et al. (1999) for Cd and Zn in leachates from a 1 year duration column experiment, attributing this to an increase in metal solubility due to complexation with organic compounds exuded by roots and rhizosphere microorganisms.

Amendment effect was significant only for weeks 1 and 2, where Lr increased U concentrations compared to TSP and no amendment (Table 4). Lr also produced higher U concentrations in the following four weeks in unvegetated columns. Though these differences failed to be statistically significant, they clearly indicate an effect of Lr amendment not produced by TSP amendment. In vegetated col-

Table 4. U concentration in leachates and ANOVA results for   U concentration in leachates.

Treatment[1]	U concentration in leachates (μg U L^{-1})					
	Week 1	Week 2	Week 3	Week 4	Week 5	Week 6
NN	46	83	68	47	28	25
NL	84	132	88	77	43	30
NP	53	82	76	53	24	21
PN	59	116	140	140	102	101
PL	98	165	157	156	122	155
PP	53	134	146	186	188	149
Average						
No plants	61	99 b	77 b	59 b	32	25 b
Plants	70	207 a	148 a	161 a	137	135 a
No amendment	52 b	99 b	104	93	65	63
Lr	91 a	148 a	122	116	82	92
TSP	53 b	108 b	111	119	106	85
	Probability of F[2]					
Plant	-	*	***	***	***	***
Amendment	***	*	-	-	-	-
Plant x Amend.	-	-	-	-	**	-
CV (%)	21	27	37	27	33	40

[1]NN = no plants, no amendment; NL = no plants, processed *Larrea spp*. tissue; NP = no plants, triple superphosphate; PN = plants, no amendment; PL = plants, processed *Larrea spp*. tissue and PP = plants, triple superphosphate.
[2]Probability of F (- = p > 0.05; * = p < 0.05; ** = p < 0.01; *** = p < 0.001). Means in columns followed by the same letter are not significantly different at p $\leq$ 0.05 level (Fisher´s LSD test).

umns, from week 3 onwards, both amendments alternately increased U concentration as compared with unamended columns, though again without statistical significance. Similarly to the discussed effect of root exudates, Lr mixing with the soil may have enhanced U mobilization due to the organic source of the amendment. As discussed by Kim (1991), trace elements, including U, are proportionally higher in groundwaters whose colloids have higher dissolved organic carbon contents, implying bondage and transport of trace elements on humic substances. In this experiment TSP also appears to be responsible for increased U concentrations, but more likely by enhancing the plant (root) effects due to the increased plant biomass, since no incidence of TSP in U concentrations of unvegetated columns was found.

Results of linear regression analyses (Table 5) showed a significant negative linear relationship between U concentration in leachates and irrigated volumes only for the unvegetated treatments. No linear relationship was found in the vegetated ones. For these analyses, values from week 1 were not included, since the distilled water applied to the columns before irrigation with pit water may have reduced U concentration of the first leachates collected.

Weekly increases of irrigated volume meant weekly increases in mass of applied U to the columns, since U concentration in the applied pit-water was constant. Therefore, for the unvegetated columns, decreasing U concentration with increasing leachate volumes indicated that the U retention capability of the soil was not exceeded during this experiment. Since vegetated columns packed the same soil, the lack of a linear relationship revealed U mobilization and leaching due to plant growth.

Table 5. Regression equations for the relationship between irrigated volume (X) and U concentration in the leachate (Y).

Treatment	Regression	Probability of F	R^2 (%)
NN	Y = - 0.132 X + 126	*	85.7
NL	Y = - 0.208 X + 193	*	83.3
NP	Y = - 0.152 X + 138	*	89.2
PN	Y = - 0.072 X + 161	-	43.4
PL	Y = - 0.037 X + 172	-	15.5
PP	Y = - 0.042 X + 136	-	9.0

[1]NN = no plants, no amendment; NL = no plants, processed *Larrea spp*. tissue; NP = no plants, triple superphosphate; PN = plants, no amendment; PL = plants, processed *Larrea spp*. tissue and PP = plants, triple superphosphate.
[2]Probability of F (- = p > 0.05; * = p < 0.05; ** = p < 0.01; *** = p < 0.001)

Mass of Uranium leached

Though only in a very small proportion of the total mass applied, pit-water U leached from the soil columns from the beginning of the experiment on (Table 6). Plant growth increased the amount of U leached in week 5, though this effect was not so important in TSP amended columns. An interaction between factors *plant* and *amendment* was produced in week 6 only, where the same effect of plant growth was observed in treatments without amendment and with Lr addition, but, again, not within TSP.

For both vegetated and unvegetated columns, Lr amendment increased the mass of U leached in comparison with TSP amendment and unamended soil. Statistical significance of this effect, however, was observed only for the three last weeks. Also in week 5 and 6, leached U was even lower in TSP amended treatments than in unamended ones. The mass of U leached was obtained as the product of leachate volume and U concentration in the leachates. As discussed before, higher mobility of U produced by Lr amendment increased U concentration in leachates, thus increasing the mass of U leached from the columns, since leachate volume was not affected by this amendment.

Likewise, higher U concentration in leachates of vegetated treatments was a re-

Table 6. Weekly applied mass of U. Amount and ANOVA for mass of uranium leached weekly.

	Week 1	Week 2	Week 3	Week 4	Week 5	Week 6
	Applied U mass (μg week^{-1})					
All treatments	1050	1400	1487	1925	2275	2905
	Mass of U leached (μg week^{-1})					
Treatment[1]	Week 1	Week 2	Week 3	Week 4	Week 5	Week 6
NN	6	11	12	13	11	15
NL	10	14	15	20	16	17
NP	7	11	13	14	10	12
PN	6	8	15	16	19	31
PL	9	13	17	18	23	48
PP	5	8	12	8	11	14
	Average					
No plants	8	12	13	16	12 **b**	15
Plants	7	10	15	14	18 **a**	31
No amendment	6 **b**	9	13	14 **b**	15 **b**	23
Lr	9 **a**	13	16	19 **a**	19 **a**	32
TSP	6 **b**	9	12	11 **b**	10 **c**	13
	Probability of F^2					
Plant	-	-	-	-	**	***
Amendment	***	-	-	**	***	***
Plant x Amend.	-	-	-	-	-	***
CV (%)	22	35	40	29	28	32

[1]NN = no plants, no amendment; NL = no plants, processed *Larrea spp.* tissue; NP = no plants, triple superphosphate; PN = plants, no amendment; PL = plants, processed *Larrea spp.* tissue and PP = plants, triple superphosphate.
[2] Probability of F ($- = p > 0.05$; $* = p < 0.05$; $** = p < 0.01$; $*** = p < 0.001$). Means in columns followed by the same letter are not significantly different at $p \leq 0.05$ level (Fisher´s LSD test).

sult of enhanced U mobility caused by plant growth. Thus, the combination of plant growth and Lr amending produced the highest mass of U leached. But plant growth also reduced leachate volumes, so that only by weeks 5 and 6 were the leachate volumes of PN and PL high enough, and the U concentration in NN and NL low enough, to yield significant differences due to plant presence. The higher biomass obtained with the application of TSP in PP columns produced such lower leachate volumes that, in spite of the resultant increase in U concentration, the mass of U leached resulted lower than in PN and PL.

Conclusions

A 6 week irrigation experiment with U containing pit-water was carried out on soil columns. The coarse textured, low organic-matter soil containing 6 % carbonates, retained > 99 % of the 11042 µg U applied during the irrigation. Plant presence in some of the columns enhanced U mobility, increasing U concentration in the leachates and the mass of U leached. Plant growth also reduced the leachate volume between 30 – 65 % through evapotranspiration. Thus, upon reaching enough biomass the mass of U leached could be reduced in comparison to unamended unvegetated soil. TSP amending produced an increment in plant biomass due to the soluble P addition to a soil with low plant available P, so that vegetated, TSP amended columns discharged the lowest mass of U. However, the amount of P thus applied resulted too low to produce any effect on U leaching from unvegetated columns. Lr amending also enhanced U mobility, increasing U concentration in leachates and also the mass of U leached, since it did not affect the leachate volume.

   Application of U containing pit-water to this soil allows most of the contamination to be retained by the soil, preventing it to reach groundwater. However, the U concentration in most of the leachates, specially with plant presence, were above recommended critical values for drinking water of 15 - 30 µg l^{-1} (WHO 2004), and also the mass of U charged to the soil would remain a persisting thread for the food chain or other compartments of the natural environment. Therefore, only previous treatment of the pit water to lower U concentration below critical values would make irrigation acceptable in open systems, allowing for lower concentration in leachates with minimal charge to the soil.

References

Banks MK, Schwab AB, Fleming GR, Hetrick BA (1994) Effects of plants and soil microflora on leaching of Zn from mine tailings. Chemosphere 29: 1691-1699

Bond WJ, Willet IR (1992) Movement of water and major ions in the Jabiru land application experiment. *In:* Akber RA (ed) Proceedings of the Workshop on Land Application of Effluent Water from Uranium Mines in the Alligator Rivers Region. Canberra: Su-

pervising Scientist for the Alligator Rivers Region, Australian Government Publishing Service, pp. 79-104

Dushenkov S (2003) Trends in phytoremediation of radionuclides. Plant Soil 249: 167-175

Ebbs SD, Brady DJ, Kochian LB (1998) Role of uranium speciation in the uptake and translocation of uranium by plants. J Exp Bot 49: 1183-1190

Elless MP, Lee SY (1998) Uranium solubility of carbonate-rich uranium-contaminated soils. Water Air Soil Pollut 107: 147-162

Finch R, Murakami T (1999) Systematics and paragenesis of uranium minerals. *In:* Burns PC, Finch R (eds) Uranium: Mineralogy, geochemistry and the environment. Reviews in mineralogy 38. Washington DC : Mineralogical Society of America, pp. 91-180

Hudson RR, Aleska A, Masotta HT, Muro E (1990) Provincia de Mendoza, Escala 1:1000000. In: Moscatelli G (ed) Atlas de suelos de la República Argentina. Proyecto PNUD ARG 85/019. Buenos Aires : SAGyP – INTA, Tomo II, pp. 75-106

Gardea-Torresdey JL, Polette L, Arteaga S, Tiemann KJ, Bibb J, Gonzalez JH (1996) Determination of the content of hazardous heavy metals on *Larrea tridentata* grown around a contaminated area http://www.engg.ksu.edu/HSRC/96Proceed/

Gardea-Torresdey JL, Hernandez A, Tiemann KJ, Bibb J, Rodriguez O (1997) Uptake and removal of toxic metal ions from solution by inactivated cells of *Larrea tridentata* (creosote bush). http://www.engg.ksu.edu/HSRC/97Proceed/Proc97.html

Gabet EJ, Reichman OJ, Seabloom EW (2003) The effect of bioturbation on soil processes and sediment transport. Ann. Rev. Earth Planet Sci 31:249-273

INEEL - Idaho National Engineering and Environmental Laboratory (2000) Proceedings from the workshop on phytoremediation of inorganic contaminants. November 30 – December 2, 1999. Argonne National Laboratory, Chicago, Illinois. INEEL/EXT-2000-00207. U. S. Department of Energy.
www.osti.gov/energycitations/servlets/purl/761921-Z01spc/native/761921.pdf

Kim JI (1991) Actinide colloid generation in groundwater. Radiochim Acta 52/53: 71-83

Knox AS, Kaplan DI, Adriano DC, Hinton TG, Wilson MD (2003) Apatite and phillipsite as sequestering agents for metals and radionuclides. J Environ Qual 32: 515-525.

Lamas, MC (2005) Factors affecting the availability of uranium in soils. FAL - Agricultural Research, Special Issue (in print).

Langmuir D (1978) Uranium solution-mineral equilibria at low temperatures with applications to sedimentary ore deposits. Geochim Cosmochim Acta 42: 547-569.

Meyer MC, Schnug E, Fleckenstein J, McLendon T, Price D (2004) Uptake of munitions-derived depleted uranium by three grass species. J Plant Nutr 27: 1415-1429

Noller BN, Zhou JX (1992) Land application at Ranger Uranium Mine, Northern Australia: Six years review. *In:* Akber RA (ed) Proceedings of the Workshop on Land Application of Effluent Water from Uranium Mines in the Alligator Rivers Region. Canberra : Supervising Scientist for the Alligator Rivers Region, Australian Government Publishing Service, pp. 25-42

Ribera D, Labrot F, Tisnerat G, Narbonne J-F (1996) Uranium in the environment: Occurrence, transfer, and biological effects. Rev Environ Contam Toxicol 146: 56-89

Riley GH (1992) Land application for disposal of excess water: An overview. *In:* Akber RA (ed) Proceedings of the Workshop on Land Application of Effluent Water from Uranium Mines in the Alligator Rivers Region. Canberra : Supervising Scientist for the Alligator Rivers Region, Australian Government Publishing Service, pp. 14-22

Active and passive water treatment techniques

Seaman JC, Arey JS, Bertsch PM (2001) Immobilization of nickel and other metals in contaminated sediments by hydroxyapatite addition. J Environ Qual 30: 460-469

Shahandeh H, Hossner L (2002) Role of soil properties in phytoaccumulation of uranium. Water Air Soil Pollut 141: 165-180

WHO (2004) http://www.who.int/water_sanitation_health/dwq/chemicals /en/uranium.pdf

Willet IR, Bond WJ (1992) Adsorption properties of the soils of the Ranger uranium mine land application area for solutes in water from retention pond 2. *In:* Akber RA (ed) Proceedings of the Workshop on Land Application of Effluent Water from Uranium Mines in the Alligator Rivers Region. Canberra : Supervising Scientist for the Alligator Rivers Region, Australian Government Publishing Service, pp. 113-138

Zhu D, Schwab AP, Banks MK (1999) Heavy metal leaching from mine tailings as affected by plants. J Environ Qual 28: 1727-1732

Simultaneous In-Situ Immobilisation of Uranium and Arsenic by Injectible Iron and Stimulated Autotrophic Sulphate Reduction

Diana Burghardt[1], Elisabeth Stiebitz[1], Kai Knöller[2], Andrea Kassahun[1]

[1]Dresden Groundwater Research Centre, Meraner Str. 10, 01217 Dresden, Germany, E-mail: dburghardt@dgfz.de
[2]UFZ Centre for Environmental Research Leipzig - Halle, Theodor-Lieser Str. 2, 06120 Halle, Germany

Abstract. The combination of injectible grey cast iron (gcFe) and nano-scale iron (naFe) corrosion with autotrophic sulphate reduction (aSR) for simultaneous U and As immobilisation was investigated in column experiments. NaFe resulted in an intensive corrosion, the formation of a homogenous reactive zone, a distinct aSR and complete U and As immobilisation. At the gcFe column, a particle displacement resulted in the formation of reactive gcFe clusters, which were partly bypassed by the influent groundwater. Nevertheless, the lasting gcFe corrosion caused a complete As, but only partial U immobilization.

Introduction

The intensive uranium ore mining which took place until the mid-seventies has devised many abandoned mine processing sites in Eastern Germany. Hydraulic connections to aquifers, which are present at many sites, resulted in numerous, smaller and decentralised groundwater run-offs contaminated with heavy metals, arsenic (As) and radionuclides including uranium (U). Their concentrations frequently exceed groundwater standards for remedial actions at inactive U processing sites (Schneider et al. 2001). For Germany, this standards are recommended with 0,3 mg U/L (SSK 1992) and 0,02-0,06 mg As/L (LAWA 2000)
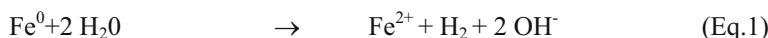
In order to prevent an ongoing contamination of ground- and surface water, many abandoned mine processing sites need restoration. In Germany, classical pump-and-treat technologies and conventional water treatment methods are common remediation practice. This is a cost intensive approach which leaves in addition concentrated residues for disposal (Neitzel et al. 2000) Therefore, the devel-

opment of long term active and inexpensive in-situ treatment methods has become a research topic of major importance and interest.

The use of zero valent iron (ZVI) for in-situ containment of uranium within permeable reactive barriers (PRB) is already almost standard approach in the US. The activity of sulphate reducing bacteria within ZVI-PRB is well known (Gu et al.1999). It is considered much than a problem instead a chance to improve clean-up efficiency especially for contaminant mixtures by providing additional immo-bilisation reactions. Those reactions can be of major concern for remediation of contaminant mixtures such as groundwater runoffs from uranium mine processing sites. Moreover, the application of PRB requires excavation and is still limited to shallow aquifers (Simpkin 2003), whereby this method is often ineffective for smaller, decentralised groundwater run-offs.

A potential alternative to PRB are reactive zones (RZ). They are created by in-stalling a line of overlapping injection points perpendicular to the groundwater flow direction. For this purpose, metallic iron to be injected is necessary in rela-tive small quantities ($\leq$ 1wt% of aquifer material) (Simpkin 2003) and very small size (usually $<<100$ μm in diameter, depending on aquifer's pore channel size). Because of small quantities of metallic iron, reducing conditions and contaminant removal capacity of RZ are not as high as PRB, whose iron content is usually greater than 20 wt% of aquifer material. However, due to the use of injection lances, the RZ technology is more flexible and is only limited by achievable depth of drilling equipment used. Therefore, this innovative technology seems to be more economic to sites with smaller, decentralised run-offs and was focused in this study.

The combination of anaerobic iron corrosion and biological sulphate reduction for an in-situ immobilisation of arsenic and uranium has some further advantages in reactive treatment zone applications of metallic iron. Hydrogen, generated by the anaerobic iron corrosion (Equation 1), accumulates at the iron surfaces and causes their passivation. Autotrophic sulphate reducing bacteria may consume this hydrogen (Equation 2), thereby promoting a continuation of the corrosion process. The produced sulfide precipitates with ferrous iron as patches of iron sulphide at anodic areas of the iron surfaces (Equation 3). This process also promotes corro-sion, since iron sulphide does not precipitate on the iron surface as a uniform, pas-sivating film (Ehrlich 1997). Finally, the stimulation of sulphate reduction by gaseous H_2 and CO_2 seems very attractive for in-situ treatment methods because of the more evenly and efficiently in-situ storage of gases compared to liquid and solid carbon source. Therefore, an anerobic corrosion of injectible iron materials combined with an autotrophic sulphate reduction was favoured in this study.

$$Fe^0 + 2\ H_2O \qquad \rightarrow \qquad Fe^{2+} + H_2 + 2\ OH^- \qquad (Eq.1)$$

$$SO_4^{2-} + H^+ + 4\ H_2 \qquad \rightarrow \qquad HS^- + 4\ H_2O \qquad (Eq.2)$$

$$Fe^{2+} + HS^- \qquad \rightarrow \qquad FeS(s) + H^+ \qquad (Eq.3)$$

Materials and Methods

Zero valent iron materials (ZVI), which were often used in PRB technologies (US-EPA 1998), tend to surface passivation by formation of precipitates due to their high purity (Friedrich and Knappik 2001). Therefore, a particulate, impure grey cast iron (gcFe) was selected for the column tests. Impurities like carbides counteract an early passivation of the iron surface and promote iron corrosion. The gcFe was obtained from Maier Metallpulver GmbH, Rheinfelden (Germany). The particles were gas classified < 30 µm before use. Nano-scale iron (naFe) was selected as alternative iron material. Injectible naFe is a promising new material for groundwater remediation. A markedly improved reactivity due to much greater surface area for reductive dehalogenation was described by (Vance 2003). NaFe (colloid size 0,1 µm) was obtained from the Toda Kogyo Europe GmbH, Japan.

The influent groundwater (Table 1) was collected at the abandoned mine processing site in Lengenfeld (Eastern Germany). Originally, it contained about 0,14 mg U/L and 0,09 mg As/L. Oxygen, possibly diffusing into the groundwater during storage, was removed by vacuum degasification. Subsequently, the groundwater was transferred into gas-tight bags (PP/Al/PE, Tesseraux GmbH, Germany) and enriched with about 15 mg U/L (as $UO_2(NO_3)_2 \cdot 6H_2O$) and 5 mg As/L (as $NaAsO_2$) for a better quantification of the pollutant immobilisation. To maintain CO_2 partial pressure at groundwater conditions, a defined CO_2/ N_2 atmosphere (30 ml CO_2 and 470 ml N_2 according Henry's law) was kept within the influent bags.

For the flow experiments, three columns (length: 50 cm, diameter 10cm) were operated for 112 days at 12°C. Preceding to the column tests, injection tests in 60 L -test barrels as well as hydraulic conductivity-tests were performed to determine optimal amounts of injectible iron application. About 2 g/kg (0,2 wt%) gcFe or naFe could be injected without hydraulic conductivities within the reactive zones, which is well below 1 wt% denoted for RZ by (Simpkin, 2003). According to injection test results, in two columns 0,2 wt% gcFe, in the third column 0,2 wt% were used. Autotrophic sulphate reducing bacteria, raised in separate microcosms from the native groundwater, were added to a gcFe column (column 1) and a naFe column (column 2). The second gcFe column (column 3) remained abiotic, providing a reference. The gas saturation of the pore volume was estimated to about 3 % for H2 and about 0.6 % for CO_2 in gas storage tests under flow conditions. To keep gas content close to saturation, the two biotic columns 1 and 2 were supplied with 20 ml H2 and 10 ml CO_2 two times a week. After 56 days, H2 injection was performed three times a week. The abiotic column 3 received 10 ml CO_2 two times a week.

Table 1. Average composition of influent groundwater used for the column tests.

pH	E_h	O_2	TOC	TIC	As	U	SO_4
[-]	[mV]				[mg/L]		
6,6	309	1,3	5,4	69	5,0	15,0	236

Active and passive water treatment techniques

To estimate effective porosities, tracer tests with 1 g NaCl/L groundwater were carried out preceding the flow experiments. According to the determined effective porosity, the influent flow rate was set to about 0,2 L/d using a peristaltic pump (ISMATEC IPC-N) in order to ensure a residence time of 7 days. Thereby, the reaction time for autotrophic sulphate reduction was optimised and every replaced pore volume could be sampled. To avoid O_2 uptake, influent tubes were equipped with PP mantles flushed continuously with N_2.

The column effluent was passed through 100-mL glas vials, which were replaced for sampling. Every replaced pore volume was analysed for pH, redox, major and trace elements (ICP-OES, Spectro), sulphate (IC, Dionex), ferrous iron (photometer), inorganic carbon (TOC/TIC -Analyzer, Shimadzu) as well as for the isotopic composition of sulphate ($^{18}O/^{16}O$ and $^{34}S/^{32}S$). Isotope measurements (IRMS) were carried out at the UFZ Centre for Environmental Research Leipzig-Halle, department of isotope hydrology. The influent groundwater was analysed for the same parameters. A change of the hydraulic head due to mineral precipitation or bioclogging was continuously monitored at the column influent by piezometer tubes. According to Darcy' Law, hydraulic heads were used for calculation of hydraulic conductivities.

Subsequent to column tests, pore water and sediment samples were collected from the sediment columns along the flow path in distance of 5, 15, 25, 35, 45 cm from the influent inlet. Thereby, a nitrogen-pressure filtration of sediment samples was used to collect pore waters in gas-tight plastic syringes. To protect sulphate reducing bacteria and reduced mineral phases, the biotic columns 1 and 2 were dismantled under nitrogen atmosphere. Pore waters were analysed for pH, redox and major and trace elements (ICP-OES) as well as microbial counts of sulphate reducing bacteria (MPN-method). MPN counts were performed by the G.E.O.S mbH Freiberg. After pore water extractions sediment samples were used for acid volatile sulphur digestions and sequential extractions in order to identify uranium and arsenic binding forms. Sequential extractions were carried out according the method of (Zeien 1995).

Results and Discussion

At column 1 (biotic, grey cast iron), a particle displacement was observed after the fifth replaced pore volume (Fig. 1a). This process was accompanied by an increase of hydraulic conductivity. In contrast, the homogenous blackening of the biotic nano scale iron column remained till the end of the test period (Fig.1b). This observation is explained by different particle retention mechanisms. Whereas grey cast iron (particle size ≤ 30 μm) was deposited in the pore space by sedimentation, nano scale iron (colloid size ≈ 0,1 μm) and its transformation products were retained by adsorption to the sediment surface.

Grey cast iron showed a lasting and constant corrosion, which resulted in an increase of effluent pH (from pH 6,5 to maximal pH 8) and a decrease in redox potential (from 480 mV to about 80 mV) in column 1 (biotic, grey cast iron).

Because of iron hydroxide formation and the lack of sulphate reducing bacteria, only a slight environmental change was observed in column 3 (abiotic, grey cast iron) until the seventh replaced pore volume. The redox potential decreased about 100 mV, pH increased from pH 6.5 to maximal pH 7.4. In contrast, naFe showed a temporary and intensive corrosion. Until the third replaced pore volume, the effluent pH was above 9. To the end of the test, the pH remained between 8 and 8.5 and the redox potential decreased from 480 to about 100 mV.

During the whole test time, U and As were completely immobilised in column 2 (biotic, nano scale iron). In both grey cast iron columns (1 and 3) arsenic was also completely immobilised, while uranium retention was incomplete (Fig. 2). The U peak after seven replaced pore volumes correlated with a temporary redox reduction in the influent groundwater. Due to those redox fluctuations, no iron hydroxide formation and the subsequent uranium sorption was possible. However, uranium retention in the reduced column 1 (biotic, grey cast iron) was clearly better than in column 3 (abiotic, grey cast iron).

Significant amounts of ferrous iron were discharged from the reduced column 1 (biotic, grey cast iron). Despite a reducing redox potential, no ferrous iron was detected in the effluent of column 2 (bio-naFe). Due to iron hydroxide formation, no ferrous iron was measured in the effluent of column 3 (abiotic, grey cast iron). (Fig. 3). During the test period, the effluents of both grey cast iron columns (1 and 3) showed no decrease in sulphate concentrations. A significant sulphate reduction (5 to 8,5 mg/L*d) was observed at column 2 (bio- naFe). Performing a balance between H_2 required for measured sulphate decrease (see Equation 2) and injected H_2, it could be evidenced that autotrophic sulphate reduction was limited by available (injectible) H_2 amounts.

One line of evidence for the occurrence of bacterial sulphate reduction was the enrichment of ^{34}S isotope in the dissolved sulphate during its passage through column 2 (biotic, nano scale iron). The preferential utilization of ^{32}S by bacteria leads to increasing $\delta^{34}S$ values in the residual sulphate and very low $\delta^{34}S$ values in the produced sulphide. Assuming piston-flow conditions with no preferential flow occurring in the columns, the enrichment of ^{34}S follows a Rayleigh type fraction-

a)   b)
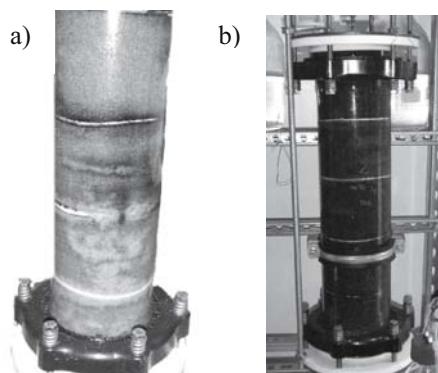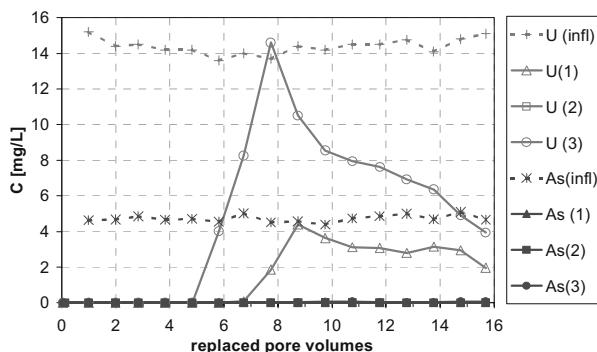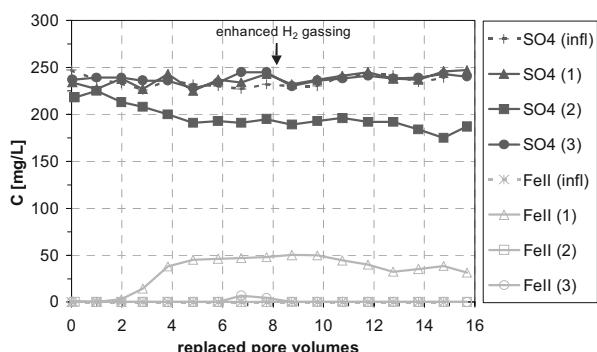
Fig. 1. Column tests: a) Column 1, b) Column 2

Active and passive water treatment techniques

ation model. Applying this model, an enrichment factor ($^{34}\varepsilon$) of -30 ‰ (between residual aquatic sulphate in the column effluent an freshly formed sulphide) was determined for column 2 (Fig. 5). This value is in the medium range of natural, heterotrophic sulphate reduction (Knöller and Trettin 2003). However, no data are known for autotrophic sulphate reduction so far. Although no significant decrease of the sulphate concentration was measured in the effluent of column 1 (biotic grey cast iron), a slightly negative correlation between $\delta^{34}S$ and residual sulphate was present, yielding a theoretical enrichment factor ($^{34}\varepsilon$) of about -5 ‰ (Fig. 4) This very low enrichment factor indicates a mixing of reduction-influenced sulphate and unreduced influent sulphate.

The findings of aqueous phase analyses were supported by pore water and sediment analyses subsequent to the column experiments. Similar microbial counts of autotrophic sulphate reducing bacteria were obtained for column 1 (biotic gcFe) and column 2 (biotic naFe). In column 1, the first third of the flow path showed the highest microbial counts of sulphate reducing bacteria and decrease in sulphate concentrations within the pore water of about 30 mg/L (Fig.6a). Correlat-

Fig. 2.   U and As concentration changes.

Fig. 3. SO_4^{2-} and Fe^{2+} concentration changes.

Active and passive water treatment techniques

ing with this, iron monosulphide and the main part of immobilised U and As were found in sediment samples taken at 5 cm and 15 cm of the flow path of column 1 (biotic gcFe). The pore water analyses and the iron monosulphide contents of column 2 (biotic naFe) prove the occurrence of an effective autotrophic sulphate reduction. U and As were nearly completely immobilised within the first entimeters of the flow path, correlating with the highest biological activity (Fig. 6b). Pore water analyses showed no signifycant sulphate decrease in column 3 (abiotic gcFe). Most uranium and arsenic was retained in the influent area, where an iron hydroxide formation was analysed by sequential sediment extraction.

To verify geochemical and microbial processes within the most effective column 2 (biotic naFe, compare Fig. 2), a phreeqC- transport modelling was carried out. Metallic iron was defined as a new mineral phase according to equation 1. To ensure a complete oxidation, a positive equilibrium constant (log_k 10) was used. Two versions of iron corrosion kinetics were modelled. In version (1), a constant
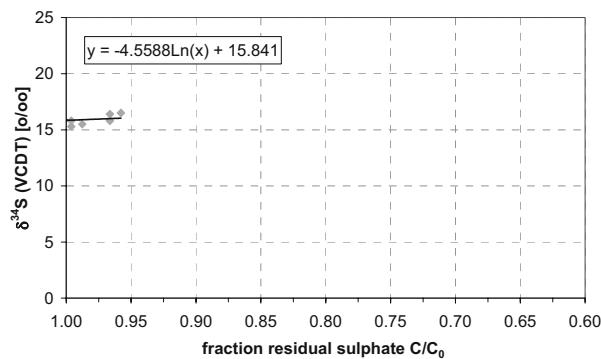
Fig. 4. Column 1: ^{34}S and residual SO_4.
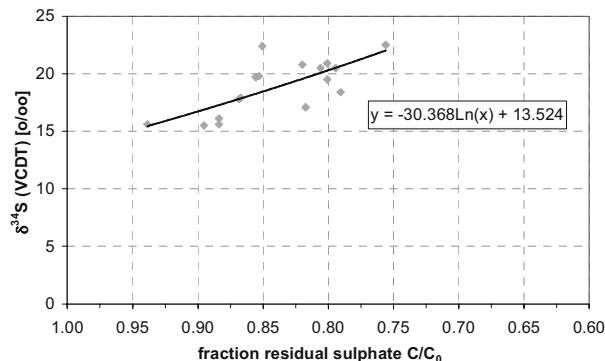
Fig.5. Column 2: 34S and residual SO_4.

Active and passive water treatment techniques

iron corrosion rate ($2.2 * 10^{-8}$ mol/s) was used for the duration of the experiment. To simulate a surface passivation, the corrosion rate was decreased marginally in each time step using the 'Put' and 'Get' functions. In version (2), a short, intensive iron corrosion rate ($5.1 * 10^{-7}$ mol/s) without surface passivation was simulated. The kinetic of autotrophic sulphate reduction was obtained by the measured sulphate concentration decrease. For both versions, the precipitation of siderite and iron monosulphide were the main OH- and Fe(II) consuming processes. Thereby, siderite was dissolved in favour of a biological induced iron monosulphide precipitation accompanied by a HCO_3^- release. The measured concentrations of inorganic carbon could only be fitted with version 2, where significant siderite amounts were precipitated at the initial stage of the test. Hence, an intensive iron corrosion with Fe(II)- storage by precipitation and subsequent sorption of ferrous iron mineral phases (e.g. siderite) on the sediment surface is more probable than a lasting and constant corrosion of nano scale iron. A clear identification of uranium and arsenic immobilisation processes was not possible due to amorphous character of freshly formed mineral phases and the lack of corresponding thermodynamic data. Furthermore, surface complexation sites for FeS are not implicated in phreeqC- databases.
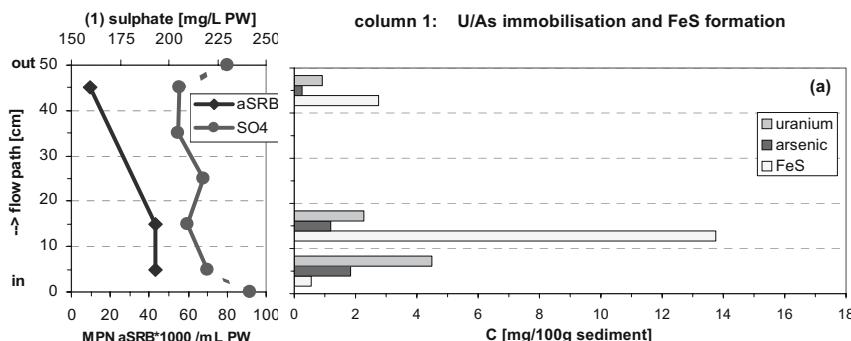
Fig. 6a.   Pore water and sediment analyses analyses in column 1.

Fig. 6b.   Pore water and sediment analyses analyses in column 2.

Active and passive water treatment techniques
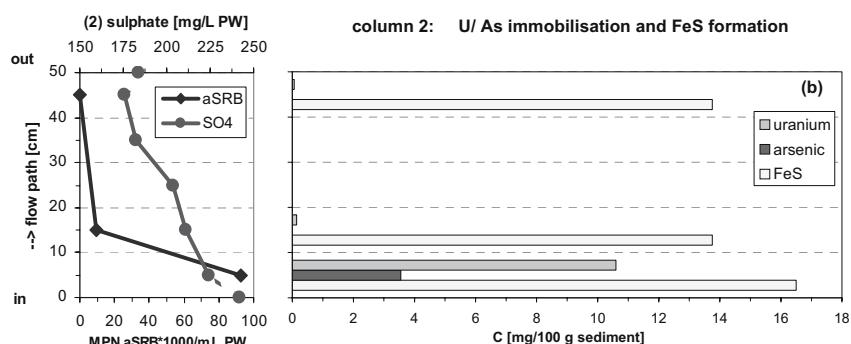
Conclusions

In this study, the long term reactivity of injectible iron particles and the contribution of autotrophic sulphate reduction for uranium and arsenic immobilisation under flow conditions was investigated. In two (biotic and abiotic) columns, 2 g particulate grey cast iron, in a third (biotic) column, 2 g colloidal nano scale iron per kg silica sand were used.

Firstly, we found the combination of anaerobic iron corrosion and autotrophic sulphate reduction have proven most effective for uranium and arsenic immobilisation. While an iron hydroxide formation resulted in a full arsenic and only partial uranium immobilisation in the abiotic grey cast iron column, the highest microbial counts of autotrophic sulphate reducing bacteria and an FeS formation were observed relating to an almost complete pollutant immobilisation in the biotic columns.

Furthermore, we found the particle retention mechanism to be important for an 'reactive zone' formation and their hydraulic conductivity. Due to its particle size (≤ 30 µm), grey cast iron was deposited in the pore space by sedimentation. Thus, a particle displacement caused the formation of cluster like structures in the biotic grey cast iron column. This process resulted in an increase of hydraulic conductivity. Although no sulphate decrease was measured in the effluent of this column, enhanced microbial counts of autotrophic sulphate reducing bacteria as well as iron monosulphide formation were analysed in the cluster like structures. Hence, it was concluded, that most influent water did not react in the iron enriched and reduced clusters. This result indicates the importance of optimised iron particle sizes and injection rates for the formation of homogenous RZ. Nevertheless, grey cast iron shows a lasting and constant corrosion. Due to surface passivation by iron hydroxides, the corrosion was less intensive in the abiotic grey cast iron column.

Because of its adsorptive retention on the sediment surface, the injection of nano scale iron resulted in the formation of a homogenous reactive zone without significant permeability change. A distinct autotrophic sulphate reduction was promoted by direct injection of storable H_2 and CO_2 gas to the pore space of aquifer material. Besides decreasing sulphate concentrations and increasing [34]S-isotope values in the column effluent, enhanced microbial counts of autotrophic sulphate reducing bacteria as well as the abundance of iron monosulphide were observed. It could be shown that autotrophic sulphate reduction was limited by available H_2 amounts. Therefore, enhanced sulphate reduction rates are possible by optimising the in-situ H_2 injection regime. In spite of the temporary and intensive corrosion of nano scale iron, no ferrous iron was detected in the column effluent. By means of a phreeqC- modelling, it was concluded that ferrous iron could be retained in the system by siderite precipitation. In favour of an iron monosulphide precipitation, siderite was dissolved stepwise. Therefore, the combination of nano scale iron corrosion and autotrophic sulphate reduction has proven suitable to achieve effective As und U immobilisation in engineered reactive zones.

Acknowledgments

References

Ehrlich, H.L. (1997) 'Microbes and metals', Appl. Microbiol. Biotechnol. 48, p.687-692

Friedrich, H.J., Knappik, R. (2000) ‚Entwicklung pH-redoxaktiver Sicherungssysteme zur Sanierung von Uran- und Arsenkontaminationen im Bereich von Grundwasserleitern', VKTA Rossendorf e.V.

Gu, B.; Phelps, T.J., Liang, L., Dickey, M.J., Roh, Y., Kinsall, B.L., Palumbo, A.V., Jacobs, G.K. (1999) 'Biochemical dynamics in Zero-valent iron colums: implications for permeable reactive barriers', (Einviron. Sci. Technol. 33, pp. 2170

Knöller,K., Trettin, R.(2003) ‚Isotopenanalytische Bewertung des Sulfathaushaltes in landwirtschaftlich genutzten Wassergewinnungsgebieten', ISSN 0948-9452

LAWA (2000) ‚Geringfügigkeitsschwellen zur Beurteilung von Grundwasserschäden und ihre Begründungen' LAWA Ad-hoc-Arbeitskreis Prüfwerte

Neitzel, P.L., Schneider, P., Hurst, S. (2000) ‚Feldversuche zur in-situ Entfernung von Uran(NAT.) und Ra-226 aus Berge- und Flutungswässern' in Pohl, A., Häfner, F., Schmidt, J., Merkel, B. ‚Wasserwirtschaftliche Sanierung von Bergbaukippen, Halden und Deponien', Freiberger Forschungshefte C 482 Geoingenieurwesen, S. 196-206

Schneider, P., Neitzel, P.L., Osenbrück,K., Noubactep, Ch., Merkel, B., Hurst, S. (2001),In-Situ-treatment of radioactive Mine Water using reactive materials: results of laboratory and field experiments in uranium ore mines in Germany' Acta Hydrochim. Hydrobiol., vol. 29 p.123-138

Simpkin (2003) 'Comparison of ZVI Treatment Zones and Standard PRBs as Groundwater Containment Barriers. AFCEE Technology Transfer Workshop, Texas, USA

SSK (1992) ‚Strahlenschutzgrundsätze für die Verwahrung, Nutzung oder Freigabe von kontaminierten Materialien, Gebäuden, Flächen oder Halden aus dem Uranerzbergbau' Empfehlungen der Strahlenschutzkommission mit Erläuterungen, Veröffentlichung der Strahlenschutzkommission, B. 23, G. Fischer Verlag Stuttgart

US-EPA (1998) "Permeable Reactive Barrier Technologies for Contaminant Remediation." EPA 600-R-98-125

Vance, D.B., 2003: 'Treatment of Chlorinated Hydrocarbon Contamined Groundwater with injectible Nano Scale Reactive Particles', white paper, http://www.2the4.net

Zeien, H. 1995 ‚Chemisch Extraktionen zur Bestimmung der Bindungsformen von Schwermetallen in Böden', Inaugural-Dissertation Institut für Bodenkunde, ISSN 0939-780

The modeling system for finding the optimal mining and wastewater discharge

Jan Novák, Hana Čermáková, Jiřina Královcová

Faculty of Mechatronics and Interdisciplinary Studies, Technical University of Liberec, Hálkova 6, 461 17 Liberec, Czech Republic,
E-mail: cermakova@diamo.cz

Abstract. The paper introduces a tool that enables to improve decision process and specify way and conditions of wastewater disposal. The tool is an information system for water treatment. The system is fully configurable so that user of the system can assign all the relevant ingredients of contamination and kinds of waters. Mixture of waters is confronted to limits allowed for selected checkpoints and to prescripts of contaminant volumes for nature water streams. The overall wastewater disposal admissibility is evaluated. The additional parts of the system are optimizing module and a graphical module. The optimization is performed in accordance to the selected optimization criterion. The system is realized so way that it suits wide aggregate demand for a wastewater treatment on different levels, where the problem is currently solved (economic level, legislative level, ecology institution).

Introduction

The problem of efficient elimination of mining, waste and special waters is an important part of right environment preserving. Such waters originate from previous ecological encumbrance or from currently kept or just eliminated technologies.

Wastewaters (after their eventual purification) are eliminated to a nature stream or they are deposited in slime pits or mixing basins. They can be next discharged from a slime pit under given circumstances. However, the admissibility of discharging and the conditions of inadmissible contamination could come on and have to be solved.

Contamination of wastewaters results from different contaminants. In some cases technological waste comprises single contaminant (for example uranium),

sometimes the waste results from many contaminants (nitrates, organic stuff etc.). There can be many technologies, which produce different wastewaters, just within one company and on the other hand there can be several companies that discharge wastewaters into same nature stream. The problems comprise a wide range of tasks that have to be everyday solved.

The legislative authorities and the economic sphere need an efficient tool, which would support an instant and effective control of the water treatment and should answer the next fundamental questions:

- What is the range of the admissible discharging for a particular economic subject?
- What way should be controlled discharging with respect on technological dispositions of a particular economic subject?
- How to specify the limits for all the economic subjects, which participate in discharging into common natural water stream?

Model description

Water discharging

Method of wastewater disposal fundamental task is present by the mixture problem solution. There is often necessary to deal with big amount of monitored contaminants, withal all off them have to demurely fulfill condition

$$\frac{\sum c_i^l * V_i}{\sum V_i} < c_{Lim}^l \ ,$$

where c_i^l is a concentration of *l-th* component in *i-th* stream [g/l], V_i is a volume of *i-th* stream [m3/min], c_{Lim}^l is a concentration limit of *l-th* component [g/l].

Particular stream represents discharging profiles and river background above the uppermost discharging profile of a concrete part of a watercourse, or different kinds of waters discharged into same profile. Limit can refer to the national norm NV ČR 82/99 (limits for natural streams), or it can be a limit appointed by a competent Civil Service office (limit for particular profiles).

An economic description of the problem comprises evaluation of water-pump and water-purification charges and payments related to the contaminant discharging.

System of the task solution
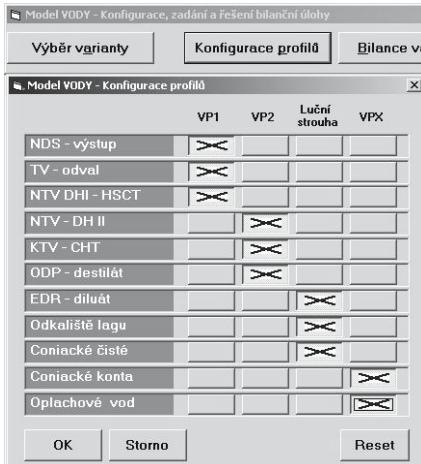
The final system for the solving of the water treatment problem was implemented as a system of computer programs that is executable on common PC under operation systems Microsoft Windows. Solving of the particular problem of water

treatment is accomplished in several steps. An individual program module solves one of four main steps.

1. **Task definition** – The module provides construction of the task structure. It includes an input of all necessary data structures as follows:

   - *List of discharged waters* – All waters, which are an object of the task, are defined in this list.
   - *List of control points and discharging profiles* – The water treatment authority is monitoring a possibility of harming of a watercourse in the last discharging profile and also possible discharging of inadmissible concentrations.
   - *List of monitored contaminants* – It consists of list of contamination components, which are an object of the analysis.
   - *Specification of the control points background* – The control points are specified places in user's administration with given regulation of discharging. Discharging of the contamination in the control point can be realized on background of a water source (channel, gully, creek etc.).
   - *Specification of background of a watercourse* – It is usually a watercourse which ecological quality is an object of the analysis.

As a result of this step, reusable data structures are obtained.

1. **Solving of the discharging balance** – It includes filling of the task with data and following solution of balance of discharged volumes and discharged substances. The easiest balance task is finding whether it is possible to discharge waters, which are an object of analysis, into watercourse without breaking of the legal ecological limits.
2. **Graphical solution of the problem** – Graphical module presents the solution of discharged waters balance in well-arranged graphical form. Primary the module displays results of balance of discharged substances. Besides the module can be used separately without previous calculation of discharging balance. In the second case the module serves for verification of range of acceptable substances discharging under a priori defined conditions. Particularly it solves the problem of acceptable discharging of three waters under premise that discharging of the rest waters in analysis is background of discharging (is assumed to be constant).
3. **Optimizing task** – Result of the optimizing task is the choice of optimal way of water treatment under beforehand-defined criterion. It could be for example a quantity of cleaned (discharged) substances, eventually an economical efficiency of cleaning.

Active and passive water treatment techniques

Fig. 1.   Configuration of profiles. The configuration widow allows assign each discharged water (names of all waters are in the left column) to a particular point (names of available points are in the top row).

Fig. 2. Input parameters of all waters discharged through particular control point.

Managing of the system

Managing of the system is made through set of screens, which serves for input of necessary data and for monitoring of a course of the solved task.

Managing of the system is documented on figures from (Fig. 1) to (Fig. 4). Figure (Fig. 1) shows one of the primary configuration window, which enables to user to define flow of given waters through specified control points.

Active and passive water treatment techniques

Fig. 3. Balance for particular control point.

Figure (Fig. 2) presents a window where the user can set up parameters of all waters discharged through particular point. The parameters are value of water flow rate in m^3/min and concentration of monitored contaminants. Besides the parameters of background for a control point can be set up here.

As a user select "Calculation of profile balance" the window on the figure (Fig. 3) is displayed. Within the upper part of the window the prescriptions of discharging can be set up. As the balance is evaluated is it immediately compared to the setting prescriptions. Lower part of the screen contains information on a discharging balance: total amount of discharged substances without and with the background, an estimation of total discharging for the year.

In the end the balance module calculates balance for the watercourse (Fig. 4). The balance provides summarization within the focused water stream and partial summaries for all defined control points.
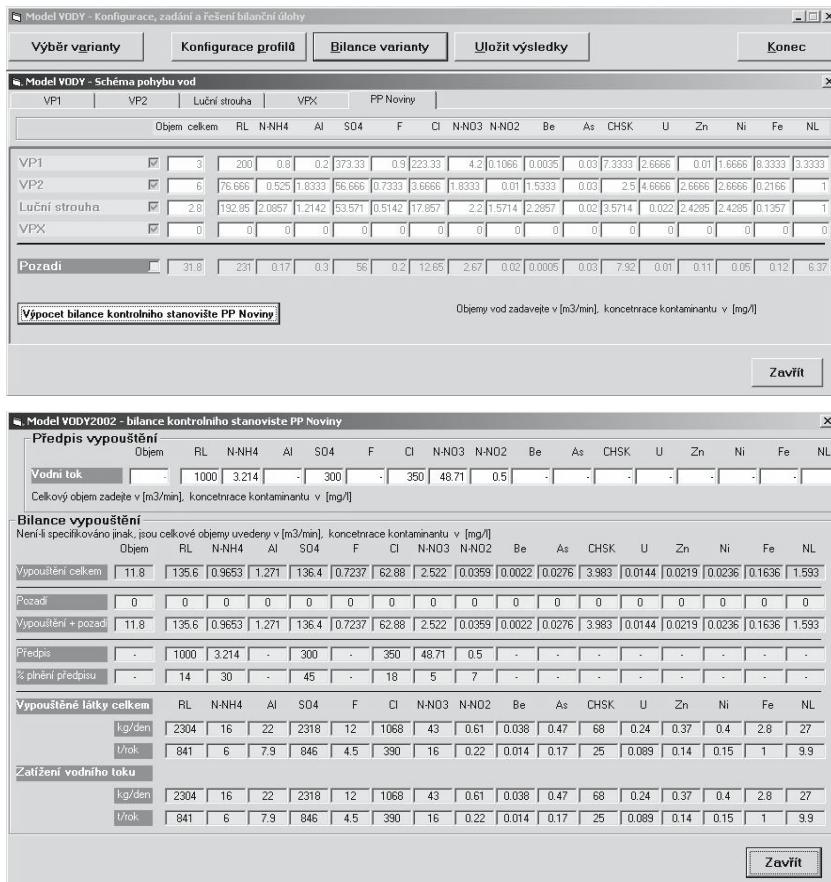
The results stored in output file give an overview of total discharge in solved discharging profiles and in end monitoring profile. The next indicators characterize discharging:

- Discharged volumes,
- Discharged concentration of monitored substances,
- Total amount of discharged monitored substances,
- Total stream flow,
- Total quantity and concentration of monitored substances in watercourse.

View of acceptable discharge conditions

Different combination of discharged waters can comply with the requirements for acceptable discharge in the specific discharging profile or watercourse. If a composition of some water streams is changing in time, a numerical evaluation by input of different combinations of the concentrations is cumbersome and evaluation is not well arranged. For quick orientation the graphical view of results serves.

Changes of volumes and concentrations can be caused by the natural and technological factors. It could be e.g. more intensive leaching and elution of the contaminants from mine dumps or higher volume of drainage waters in rainy season, change of concentration of the substances in waters leaking out from the closed mines or extracted from the contaminated aquifers, or change of technological devices parameters. In many cases the volumes and concentrations of some water streams can be chosen, especially in the case of remediation of large area with extraction of waters of various composition.

Model VODY – Konfigurace, zadání a řešení bilanční úlohy

Výběr varianty | Konfigurace profilů | Bilance varianty | Uložit výsledky | Konec

Model VODY – Schéma pohybu vod

VP1 | VP2 | Luční strouha | VPX | PP Noviny

	Objem celkem	RL	N-NH4	Al	SO4	F	Cl	N-NO3	N-NO2	Be	As	CHSK	U	Zn	Ni	Fe	NL
VP1	3	200	0.8	0.2	373.33	0.9	223.33	4.2	0.1066	0.0035	0.03	7.3333	2.6666	0.01	1.6666	8.3333	3.3333
VP2	6	76.666	0.525	1.8333	56.666	0.7333	3.6666	1.8333	0.01	1.5333	0.03	2.5	4.6666	2.6666	2.6666	0.2166	1
Luční strouha	2.8	192.85	2.0857	1.2142	53.571	0.5142	17.857	2.2	1.5714	2.2857	0.02	3.5714	0.022	2.4285	2.4285	0.1357	1
VPX	0	0	0	0	0	0	0	0	0	0	0	0	0	0	0	0	0
Pozadi	31.8	231	0.17	0.3	56	0.2	12.65	2.67	0.02	0.0005	0.03	7.92	0.01	0.11	0.05	0.12	6.37

Výpocet bilance kontrolního stanovište PP Noviny

Objemy vod zadavejte v [m3/min],   koncetrace kontaminantu v [mg/l]

Zavřít

Model VODY2002 – bilance kontrolniho stanoviste PP Noviny

Předpis vypouštění

	Objem	RL	N-NH4	Al	SO4	F	Cl	N-NO3	N-NO2	Be	As	CHSK	U	Zn	Ni	Fe	NL
Vodní tok	-	1000	3.214	-	300	-	350	48.71	0.5	-	-	-	-	-	-	-	-

Celkový objem zadejte v [m3/min],   koncentrace kontaminantu v [mg/l]

Bilance vypouštění

Není-li specifikováno jinak, jsou celkové objemy uvedeny v [m3/min], koncetnrace kontaminantu v [mg/l]

	Objem	RL	N-NH4	Al	SO4	F	Cl	N-NO3	N-NO2	Be	As	CHSK	U	Zn	Ni	Fe	NL
Vypouštění celkem	11.8	135.6	0.9653	1.271	136.4	0.7237	62.88	2.522	0.0359	0.0022	0.0276	3.983	0.0144	0.0219	0.0236	0.1636	1.593
Pozadi	0	0	0	0	0	0	0	0	0	0	0	0	0	0	0	0	0
Vypouštění + pozadi	11.8	135.6	0.9653	1.271	136.4	0.7237	62.88	2.522	0.0359	0.0022	0.0276	3.983	0.0144	0.0219	0.0236	0.1636	1.593
Předpis	-	1000	3.214	-	300	-	350	48.71	0.5	-	-	-	-	-	-	-	-
% plnění předpisu	-	14	30	-	45	-	18	5	7	-	-	-	-	-	-	-	-

Vypouštěné látky celkem	RL	N-NH4	Al	SO4	F	Cl	N-NO3	N-NO2	Be	As	CHSK	U	Zn	Ni	Fe	NL
kg/den	2304	16	22	2318	12	1068	43	0.61	0.038	0.47	68	0.24	0.37	0.4	2.8	27
t/rok	841	6	7.9	846	4.5	390	16	0.22	0.014	0.17	25	0.089	0.14	0.15	1	9.9

Zatížení vodního toku																
kg/den	2304	16	22	2318	12	1068	43	0.61	0.038	0.47	68	0.24	0.37	0.4	2.8	27
t/rok	841	6	7.9	846	4.5	390	16	0.22	0.014	0.17	25	0.089	0.14	0.15	1	9.9

Zavřít

Fig. 4. Balance for particular profile.

Active and passive water treatment techniques

The graphical analysis can be done for any profile or control point. In appropriate screen form the waters flowing through the profile are split into waters with invariable and with variable concentrations. Further the components of solutions, what the analysis should be done for, are chosen and the combination of concentrations is chosen for three variable waters.

Scheme of choice from the three types of discharged waters can be displayed in triangular graph. The apexes of triangle belong to particular types of solutions and represent discharging of corresponding solution on hundred-per-cent level. The opposite base of triangle represents on the contrary null level of discharging of appropriate solution. The thin network of lines parallel with the sides of triangle represents partial discharging of solutions and is displayed with the step of 10% of the total volume of possible discharge.

On the sides of triangle there are scales of concentrations of all monitored components what can arise by mixing of two types of waters corresponding with the

Fig. 5.   Limits of discharging of cleaned waters into Plouč-nice river. Total volume 6 m^3/min. Comparison for different input concentrations into cleaning technologies.

Active and passive water treatment techniques

adequate apexes of triangle. The area of the triangle is split into areas of satisfactory and unsatisfactory combinations by the lines linking the points of critical values.

The critical concentration c_{krit} is calculated from the total volume of water flowing through the profile, form the limit concentrations of individual substances for the profile and from the composition of invariable waters by the formula

$$c_{crit} = \frac{c_L^l \cdot \sum_{i=1}^{n} V_i - \sum_{i=4}^{n} c_i^l \cdot V_i}{\sum_{i=1}^{3} V_i} \quad ,$$

where $i = 1,2,3$ are indexes of the waters with variable parameters, $i = 4, ..., n$ are indexes of the waters with fixed volumes and concentrations, c_L^l is limit concentrations of l-th substance for given profile [g/l] and c_i^l is limit concentrations of l-th substance in i-th stream [g/l].

The area of acceptable discharge is then an intersection of all acceptable combinations of three waters with variable parameters for all monitored substances.

The methodology is documented on practical example of cleaning and discharge of waters during the remediation of uranium deposit Stráž. Total salinity of discharged waters (TDS) and two substances – NH4 and Cl – are watched. Three streams of cleaned waters are available – the solution after neutralization (S) with high content of TDS and Cl, the dilute from membrane units (D) with medium content of TDS and higher content of HN4 and the condensate from evaporation unit (K) – practically clean water. The triangle is made for volume of 6 m^3/min. Because the maximum production of the condensate is 5 m^3/min, at the appropriate apex there is excluded an area where this value could be exceeded.

Figure (Fig. 5) shows the areas for observed substances and the total acceptable area of discharging. Values of c_{krit} were defined for filling of c_L on 60, 80 and 100 %.

Conclusion

Presented system represents tool that enables to optimize decisions and that can specify way and conditions of wastewater discharging. It is an all-around tool and it is convenient for users in both legislative and economic sphere that have to manage wastewater treatment.

Acknowledgements

Pilot Scale RAPS-System in Gernrode/Harz Mountains

Andrea Hasche–Berger, Christian Wolkersdorfer

TU Bergakademie Freiberg, Lehrstuhl für Hydrogeologie, Gustav-Zeuner-Straße 12, 09596 Freiberg, Germany, E-mail: andrea.hasche@IMWA.info

Abstract. This paper presents experimental studies and first results of a pilot scale RAPS-treatment system to reduce the high iron content of an iron rich mine water. In 1985, economic reasons caused the closure of the fluorspar mine "Hohe Warte" near Gernrode in the German Harz Mountains. Though remediation works were conducted in the preceding years, mine water is currently flowing out freely of the dewatering adit and is impacting the environment and the receiving brook. The mine water is characterised by low pH-values, high conductivities and contains considerable amounts of iron, manganese, and arsenic. Annually, the mine discharges 0.7 Mio m^3 of mine water with 7.8 tons of iron, 3.8 kg of manganese, 13 kg of arsenic, and 2,5 kg of uranium. Therefore, the discharging mine water has a great potential to affect the quality of the receiving streams and resulted in a decrease of biological diversity. Based on hydrogeological and hydrochemical investigations, a passive treatment system would be able to treat the mine water. In February 2003 a pilot system was installed near the dewatering adit consisting of a settlement pond, a RAPS system (reducing and alkalinity producing system) and a constructed wetland. It could be shown that this passive system was able to treat an aliquot of the mine water down to ecologically acceptable standards.
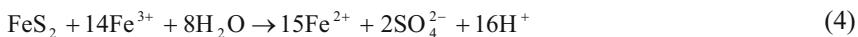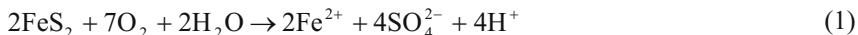
Introduction

Discharges of contaminated mine water from abandoned mine sites associated with ground and surface water pollution are a major environmental problem in many parts of the world. Aggravating factors in association with abandoned un-

derground mines commonly are large open, mined volumes with laterally exten-
sive interconnections being usually flooded (Younger 2000a, Eger and Wagner
2000), access is restricted, and reliable mine maps are often unavailable (Skousen
et al. 2000).

Acid mine drainage (AMD) results from the exposure of sulphides and iron
bearing minerals to erosion and weather. Percolation of water through these mate-
rials results in a discharge water with low pH and high metal concentrations. Al-
though AMD is naturally occurring, mining activities may greatly accelerate its
production since mining exposes new iron and sulphide surfaces (e.g. underground
mine walls, open pit walls, and overburden and mine waste piles) to oxygen. As
such, AMD is one of the primary environmental threats at mining sites (Skousen
et al. 2000; Ziemkiewicz et al. 2003).

The following chemical reactions represent the chemistry of pyrite weathering
upon exposure to air and water (Stumm and Morgan 1996):

$$2FeS_2 + 7O_2 + 2H_2O \rightarrow 2Fe^{2+} + 4SO_4^{2-} + 4H^+ \tag{1}$$

$$4\,Fe^{2+} + O_2 + 4\,H^+ \rightarrow 4\,Fe^{3+} + 2\,H_2O \tag{2}$$

$$4\,Fe^{3+} + 12\,H_2O \rightarrow 4\,Fe(OH)_3 \downarrow + 12\,H^+ \tag{3}$$

$$FeS_2 + 14Fe^{3+} + 8H_2O \rightarrow 15Fe^{2+} + 2SO_4^{2-} + 16H^+ \tag{4}$$

The first reaction in the weathering of pyrite includes the oxidation of pyrite by
oxygen. Sulphur is oxidized to sulphate and soluble ferrous iron and acidity are re-
leased (equation 1).

The second reaction involves the conversion of ferrous iron to ferric iron by
consuming acidity (equation 2). Certain bacteria increase the rate of oxidation
from ferrous to ferric iron. This reaction rate is pH dependent, with the reaction
proceeding slowly under acidic conditions (pH <5) with no bacteria present
(Evangelou 1995; Hedin et al. 1994), at pH values > 8, the abiotic process is fast.
This reaction is known to be the rate limiting step in the abiotic pyrite oxidation
(Sigg and Stumm 1994).

The third reaction is the hydrolysis of iron (equation 3). The formation of ferric
hydroxide precipitate (solid) is pH dependent. Solids form if the pH is above 3.5,
but below pH 3.5, little or no solids will precipitate. Many metals are capable of
undergoing hydrolysis (e.g. aluminium, manganese) and trace metals such as arse-
nic, cadmium, copper, lead, and zinc will coprecipitate with iron to some degree
(Ford 2003).

The fourth reaction is the oxidation of additional pyrite (or other metals) by fer-
ric iron (equation 4). The ferric iron is generated in reaction steps 1 and 2. This is
the cyclic and self-propagating part of the overall reaction and takes place rapidly
and continues until either ferric iron or pyrite (and other metals) is depleted. Note
that in this reaction, iron is the oxidizing agent, not oxygen.

In view of the potential long time-scales over which water pollution from aban-
doned mines may persist (Younger 1997; Wood et al. 1999; Ermite Consortium
2004), there has been an increasing interest in the development of methods for
mine water treatment which can operate over decades or even centuries with little
maintenance and low investment and operational costs (e.g. Eger and Wagner

2002; Ford 2003; Wolkersdorfer and Younger 2002; Younger 2000b). Passive treatment systems are a relatively young technology that involves using sulphate-reducing bacteria or limestone or both to neutralize acidity and precipitate metals.

Advantages are low operating costs and low capital cost, usually no requirement to consume electrical power, and use of non-hazardous materials. Passive systems can often be directly integrated with surrounding ecosystems, and well-constructed passive systems can work for long time periods unattended (Younger et al. 2002).

Disadvantages may be that it is a relatively new technology; hence, experiences are still scarce, precise control of treatment effluent quality is not practicable, relatively high construction costs, and large areas of land are required.

Site description

Situated in the Mid Harz Fault Zone at the northern boundary of the German Harz Mountains, the underground mine "Hohe Warte" is located 1.5 km south-west of the city Gernrode. From 1974 to 1985 the "VEB Harzer Fluß- und Schwerspat Betriebe, Werk Rottleberode" mined there for fluorspar (Fig. 1). Extensive exploration works were conducted in the preceding years and the fluorspar deposit was made accessible through a 1.4 km long dewatering adit (1st level at 300 m above sea level, also referred to as "Hagental adit").

Host rocks of the mineralization are shales with inclusions of calcite and silica, and greywackes of the Blankenburger zone at Devonian and Carboniferous age. During the Variscian phase the Ramberg granite intruded (Upper Carboniferous

Fig. 1. The working Fluorspar Mine "Hohe Warte" in 1983 (Kappe and Scheffer 1990).

Active and passive water treatment techniques

age: 290 Mio ± 10 Mio years; Mohr 1993) into the sediments of the Blankenburg zone, producing cherts by metamorphosis. Trace minerals are sulphide minerals like pyrite, galena, sphalerite, and chalcopyrite; fluorite, haematite, and silica, crystallised in the fractures and fissures of the cherts and granites (Stolle 1984).

During the production phase from 1978 to 1982, three underground levels (2nd and 2½ level at 350 m above sea level, and a 3rd level at 400 m above sea level) above the dewatering adit were mined, by which 200,000 tons of fluorite were extracted. Since 1981 production works above the 3rd level were conducted (Stolle 1984; Bodemann 1987).

On September 31st 1985, economic reasons caused the mine to stop production and in January 1987 the mine was finally closed, after remediation works were conducted in the underground mine (Bodemann 1987). After the cessation of mining, the underground mine "Hohe Warte", especially the 1st level, should have been used as a water reservoir. Based on hydrogeological investigations conducted in April 1984, a poor water quality was predicted and no use of the mine water took place (Stolle 1984). Due to safety-engineering reasons, in 1987 the mine entrance was closed with a brick dam. In the mid 1990's, after local people observed mine water seeping through the dam, a small hole has been broken into the wall to prevent the dam from failure (Fig.s 2 and 3).
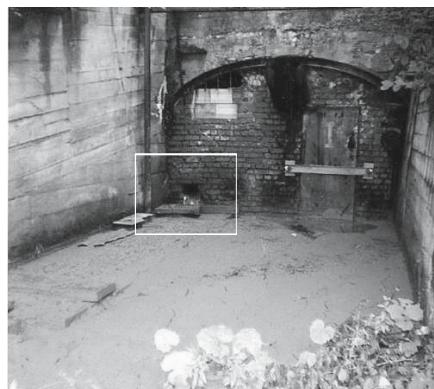
Up to the beginning of 2004 nearly all the mine water was discharged through this hole (Fig. 4) into a 15 m long open channel and from there through a 30 m long pipeline to a natural cascade with a height of about 6 m. Since then construction works are going on but were not finished by the time this report has been written.

After the mine water passes the cascade, the water flows through a lagoon with an area of about 110 m^2, acting as a settlement basin. Thereafter, the mine water drains into the Hagentalbach, a brook with excellent surface water quality up to this confluent and flows into a north-eastern direction to Gernrode and Bad Suderode.

Since 2000 the TU Bergakademie Freiberg has been monitoring the mine water

Fig. 2.   The mine entrance in 2000.

Fig. 3. The mine in 2001 (red colour in front of the dam: ochre precipitates; Tamme 2002).
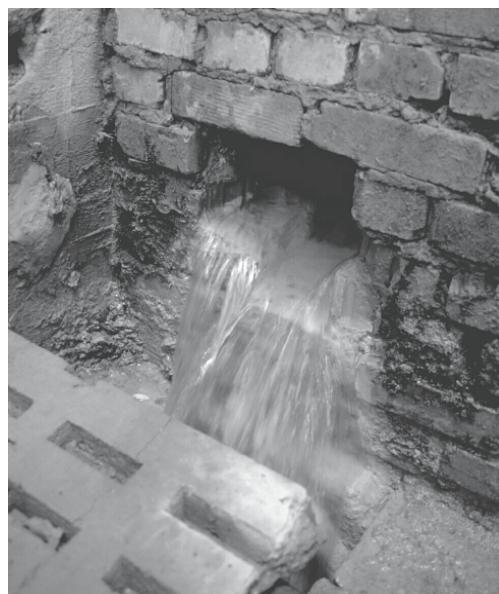
and the brook. Table 1 summarises a comparison of parameters and metal ion concentrations of the mine water at the dewatering adit (MP1, Fig. 4). The mine water is characterised by low pH-values, high conductivities and contains considerable amounts of soluble salts and sulphates, iron, manganese, and arsenic. Annually, the mine discharges 0.7 Mio m^3 of mine water with 7.8 tons of iron, 3.8 kg of manganese, 13 kg of arsenic, and 2,5 kg of uranium.

System Design

General Aspects

Over the last two decades, a variety of passive treatment systems has been developed and deployed for treating polluted mine waters. The primary passive treatment technologies are divided into three main types (Younger et al. 2002):

- Inorganic media passive systems (e.g. anoxic limestone drains, oxic limestone drains, closed systems Zn removal reactors, and siderite-calcite reactors for Cd and As removal)
- Wetland-type passive systems (aerobic wetlands [reed beds], compost wet-

Fig. 4.   Discharge point at the dewatering adit (MP1).

Active and passive water treatment techniques

lands, reducing and alkalinity producing systems [RAPS; originally termed SAPS by their originators (Kepler and McCleary 1994) recently renamed by Watzlaf et al. 2000]).

- Subsurface flow bacterial sulphate reduction systems (in-situ permeable reactive barriers to treat contaminated mine water discharges)

Selection, design, and effectiveness of the passive system used are based on water chemistry, flow rate, local topography, and site characteristics (Hedin et al. 1994; Skousen et al. 2000; Younger 2000b).

Based on the on-site conditions and the water chemistry of the fluorspar mine "Hohe Warte", a passive pilot treatment system (Fig. 6) has been installed at the mine site in February 2003. The pilot system was designed to remove sufficient quantities of iron and manganese from the mine water. It consists of three containers with a length of 1.12 m, width of 0.96 m, and height of 0.95 m. Monitoring points (MP 11 – MP 13) are the inlets of the containers 1 – 3, and the outlet of container 3 (MP 14; Simon 2003).

Because the use of aerobic wetlands (container 3) is limited to the treatment of net alkaline drainage where pH > 6.5 and the total alkalinity > total acidity (Eger and Wagner 2003; Younger et al. 2002; Hedin et al. 1994), the system is used after the alkalinity of the drainage water has been increased in container 2, the successive alkalinity producing system (RAPS). Before flowing into the RAPS-system of the pilot system, a settlement pond (container 1) is arranged to allow iron oxide precipitation.

In the following chapters, the design and construction of the three containers are explained.

Settlement Pond

An aliquot of the mine water flow is drained from the adit entrance (MP1) to the first container by a flexible tube. This container is used as a settlement pond, a preceding aeration cascade increasing the dissolved oxygen concentration and allowing the formation of iron oxide precipitates (Fig.s 5 and 7). The water inflow is $0.5\ L \cdot min^{-1}$ and is controlled by a "technical channel". Due to the container's size, the residence time is about 14 hours.

Table 1. Summary of hydrogeochemical parameters of the Gernrode mine water.

	5.10.99	30.5.00	22.10.02	21.11.02	19.12.02	30.1.03	24.2.03	25.3.03	24.4.03	19.5.03	discharge per year
Flow (L·s⁻¹)	15.0	10.0	–	29.2	26.1	–	25.5	26.5	27.7	–	720,823 m³ a⁻¹
T (°C)	–	–	11.8	11	10.5	10.5	10.9	11.1	11	11.3	–
pH	–	–	5.42	6.13	6	5.67	5.57	5.99	5.65	5.95	–
Lf (µS·cm⁻¹)	–	–	5772	5741	5499	5693	5689	5637	5590	5578	–
Eh (mV)	–	–	338	336	305	400	391	385	380	369	–
O₂ (mg·L⁻¹)	–	–		9.91	9.81	9.11	10.45	10.96	10.42	9.84	–
TDS (ppm)	–	–	4616	4590	4373	4456	4451	4405	4365	4354	–
Fe$_{total}$ (mg·L⁻¹)	9.74		10.98	9.7	12.21	10.67	11.5	9.35	16.17	10.48	7,850 kg a⁻¹
Fe²⁺ (mg·L⁻¹)		8.10	9.21	8.23	9.13	8.97	10.45	6.71	9.76	8.55	6,398 kg a⁻¹
Na⁺ (mg·L⁻¹)	203		253	250	245	248	252	249	243	235	174,439 kg a⁻¹
Ca²⁺ (mg·L⁻¹)	548		801	691	675	690	690	665	653	641	484,874 kg a⁻¹
Cl⁻ (mg·L⁻¹)	1390		1887	1769	1782	1774	1805	1711	1694	1621	1.236 t a⁻¹
SO₄²⁻ (mg·L⁻¹)	76.9		74.7	56	73.1	113	112	89.6	86.1	77	60,741 kg a⁻¹
F⁻ (mg·L⁻¹)			4.24	4.16	4.14	5.88	5.92	6.09	6.64	5.71	3,855 kg a⁻¹
Si (mg·L⁻¹)	–	–	39,5		60.1	43.1	44.9	40.9	44.2	40.1	32,210 kg a⁻¹

Active and passive water treatment techniques

RAPS-System

After the initial settlement pond in the pre-treatment stage, the surface flow is converted to a subsurface flow in container 2 (Fig. 5) with substrate consisting of a 30 cm bottom layer of limestone gravel overlain by a mixture of limestone and horse manure, and an upper layer of horse manure. Total quantities of limestone are 780 kg with a $CaCO_3$-content of 97–98 %, and the horse manure has a volume of 0.5 m^3. The limestone dissolves in the acidic mine water, and because CO_2 cannot escape, conversion of bicarbonate occurs, thus adding alkalinity. The horse manure creates a reducing environment, hence converting ferrous iron to ferric iron and preventing the formation of ferric hydroxide precipitates. The RAPS-System aims to increase the pH value and to create a net alkaline mine water. Because such systems may never fall dry, sufficient water must always flow through the system.

Aerobic wetland

Since March 2003, the aerobic wetland (container 3) operates in the pilot system. The aerobic wetland (Fig. 6) is designed to provide a sufficient residence time to allow metal oxidation and hydrolysis, thereby causing precipitation and physical retention of Fe and Mn hydroxides. These dominant treatment processes make them applicable only to net alkaline mine water.

Fig. 5. View of the RAPS-System.

Fig. 6. View of the Aerobic wetland with *Juncus* and *Typha*.

Active and passive water treatment techniques
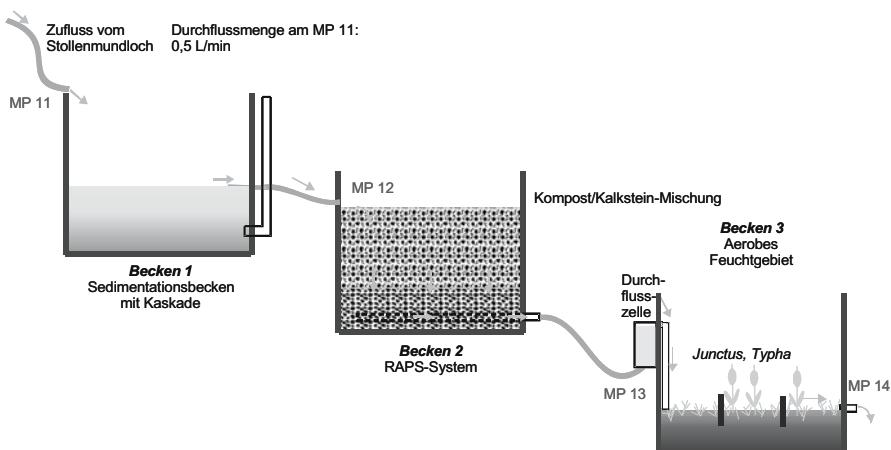
The bottom of the constructed wetland is covered by a 10–30 cm layer consisting of soil and is planted with *Typha* and *Juncus*. The flow of mine water through the constructed wetland was fairly constant and the flow length was in the range of 3–4 m as a result of wooden guides installed, but the main residence time evaluated by tracer tests was only 9 min due to the small area (1 m²) involved.

Results and Discussion

In a first stage, about 10 L of mine water per minute were discharged through the pilot system. Tracer tests using Na-fluorescein and the chemical analyses of the treated water proved that the residence time was too low. Therefore the flow was continuously decreased to about 0.5 L·min^{-1}.

After optimisation of the flow rate, the pilot system was able to lower the Fe_{tot} content from about 20 mg·L^{-1} to 5 mg·L^{-1} and the pH could be raised from about 5.5 to 7. Acid capacity (Alkalinity) was increased from about 0.2 mmol·L^{-1} to 0.7 mmol·L^{-1} while the base capacity (Acidity) was reduced from 1.1 mmol·L^{-1} to 0.6 mmol·L^{-1}. Nitrate concentrations in the discharged water after the RAPS decreased from about 4 mg·L^{-1} in March 2003 to 0.3 mg·L^{-1} in October 2003.

Unfortunately, the system was destroyed by vandalism in mid June 2003 and worked again until winter 2003; in spring 2004 the system had been destroyed again. Nevertheless, our field studies and the laboratory experiments proved that the system configuration chosen can treat the mine water on a long term basis.
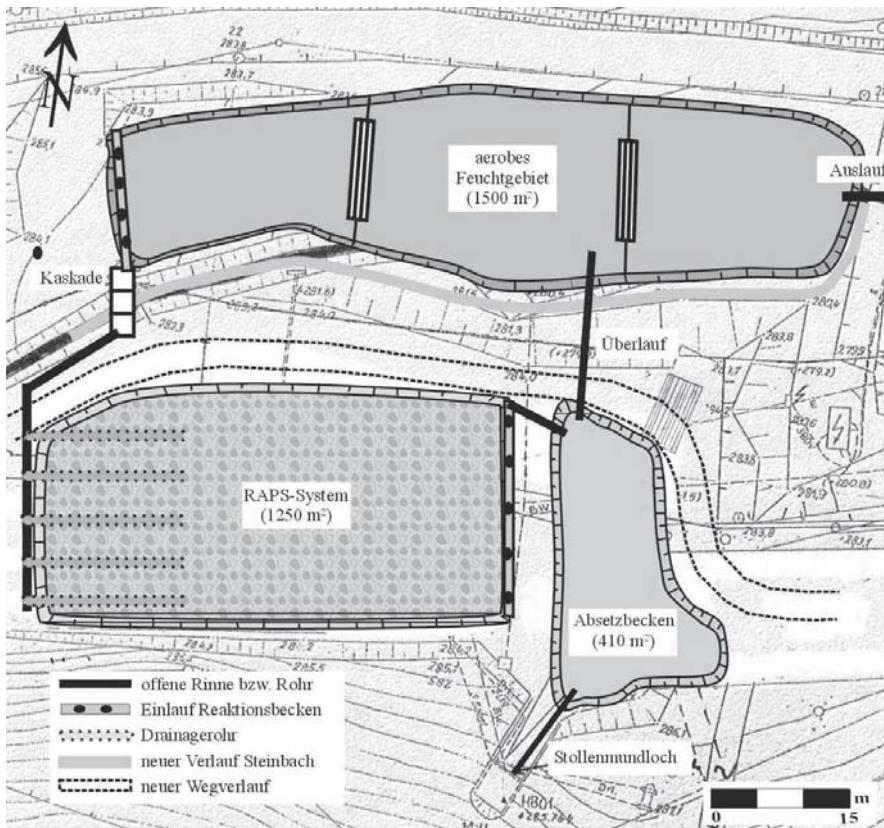
Fig. 7.   Schematically View of the Pilot Scale system with its three treatment processes (Simon 2003).

Active and passive water treatment techniques

Conclusion

It could be shown, that a RAPS system, based on intensive hydrogeological investigations and laboratory studies with the mine water that has to be treated, can be used a the abandoned Gernrode mine. Within the relatively small pilot plant, total iron could be reduced by about 50 %, the alkalinity increased, and the acidity decreased significantly, such resulting in a slightly net alkaline mine water.

We assume that even a comparatively small treatment plant would be able to increase the water quality of the receiving brook, the Hagentalbach, significantly. Based on the experiments we calculated the necessary area for such a treatment system and made a first sketch of the system (Fig. 8). Currently the responsible authorities and consultants are trying to find the best solution for the Gernrode mine site.

Fig. 8.   Recommended passive treatment scheme at the abandoned Gernrode mine.

Active and passive water treatment techniques

Acknowledgements

References

Bodemann, H. (1987): Verwahrungsdokumentation vom Grubenrevier Hohenwarte in der Betriebsabteilung Straßberg, Rottleberode. VEB Fluss- und Schwerspatbetrieb Werk Rottleberode: 12 p. (unpublished).

Eger, P. & Wagner, J. (2002): Wetland Treatment Systems – How long will they really work? – Sudbury 2003 Mining and the Environment: 14 p.

ERMITE Consortium, [eds. Younger, P. & Wolkersdorfer, Ch.] (2004): Mining Impacts on the Fresh Water Environment: Technical and Managerial Guidelines for Catchment Scale Management. – Mine Water and the Environment, **23** (Supplement 1): S2—S80; Berlin.

Evangelou, V. P. (1995): Pyrite oxidation and its control – solution chemistry, surface chemistry, acid mine drainage (AMD), molecular oxidation mechanisms, microbial role, kinetics, control, ameliorites and limitations, microencapsulation. – 293 p.; Boca Raton (CRC Press).

Ford, K.L. (2003): Passive Treatment Systems for Acid mine Drainage – Technical Note 409 April 2003. – Bureau of Land Management; web-based report available online at (http://www.blm.gov/nstc/library/techno2.htm).

Hedin, R. S., Nairn, R. W. & Kleinmann, R. L. P. (1994): Passive Treatment of Coal Mine Drainage. – Bureau of Mines Information Circular, IC-9389: 1—35; Washington.

Kappe, H. & Scheffler, H. (1990): Im Harz, Übertage – Untertage. – 143 p.; Haltern (Bode).

Kepler, D. A. & Mc Cleary, E. C. (1994): Successive Alkalinity-Producing Systems (SAPS) for the Treatment of Acid Mine Drainage **1**. –195-204; Pittsburgh (Proceedings International Land Reclamation and Mine Drainage Conference).

Mohr, K. (1993): Geologie und Minerallagerstätten des Harzes. – 2nd ed., 496 p.; Stuttgart (E. Schweizerbart'sche Verlagsbuchhandlung).

Sigg, l. & Stumm, W. (1994): Aquatische Chemie – Eine Einführung in die Chemie wässriger Lösungen und natürlicher Gewässer. – 498 p.; Zürich Stuttgart (Verlag der Fachvereine & B.G. Teubner Verlag).

Simon, J. (2003): Konzipierung einer passiven Grubenwasserreinigungsanlage im Hagenbachtal bei Gernrode/Harz. – 169 p.; Freiberg (unpubl. Dipl.-Arb. TU Bergakademie Freiberg).

Skousen, J.G., Sexstone, A. & Ziemkiewicz, P.F. (2000): Acid Mine Drainage Control and Treatment. – In: Barnhisel, R. I., Darmody, R. G. & Daniels, W. L.: Reclamation of Drastically Disturbed Lands (6). – 131—168; Madison, Wis. (American Society of Agronomy).

Stolle, P. (1984): Bergschadenkundliche Analyse vom Grubenrevier Hohenwarte (WA Straßberg). VEB Fluss- und Schwerspatbetrieb Werk Rottleberode: 26 p. (unpublished).

Stumm, W. & Morgan, J. J. (1996): Aquatic chemistry – Chemical Equilibria and Rates in Natural Waters. – 3rd ed, 1022 p.; New York (Wiley & Sons).

Watzlaf, G.R., Schroeder, K.T. & Kairies, C.L. (2000): Long-term performances of Anoxic Limestone Drains. – Mine Water and the Environment, **19**: 98—110.

Wolkersdorfer, Ch. & Younger, P.L. (2002): Passive Grubenwasserreinigung als Alternative zu aktiven Systemen. – Grundwasser, 2: 67—77.

Wood, S.C., Younger, P.L. & Robins, N.S. (1999): Long-term changes in the quality of polluted mine water discharges from abandoned underground coal workings in Scotland. – Quarterly Journal of Engineering Geology, 32: 69—79.

Younger, P.L. (1997): The longevity of mine water pollution – a basis for decision-making. – The Science of the Total Environment, 194-195: 457—466.

Younger, P.L. (2000a): Predicting temporal changes in total iron concentrations in groundwater flowing from abandoned deep mines: a first approximation. – Journal of Contaminant Hydrology, 44: 47—69.

Younger, P.L. (2000b): The Adoption and Adaptation of Passive Treatment Technologies for Mine Waters in the United Kingdom. – Mine Water and the Environment, 19: 84—97.

Younger, P.L. (2002a): Deep mine hydrogeology after closure: insights from UK. – In: Merkel, B., Planer-Friedrich, B. & Wolkersdorfer, Ch. (eds): Uranium in the Aquatic Environment: 25—40; Heidelberg (Springer).

Younger, P.L. (2002b): Passive treatment of European mine waters: the European Commission's PIRAMID project. – 1st IMAGE-TRAIN Cluster Meeting "Innovative Groundwater Technologies" held at the Environmental Research Centre, Karlsruhe University – Germany from November 7 — 9, 2001: 14—22; Federal Environment Agency, Austria.

Younger, P.L., Banwart, S.A. & Hedin, R.S. (2002): Mine Water – Hydrology, Pollution, Remediation. – 464 p.; Dordrecht (Kluwer).

Ziemkiewicz, P.F., Skousen, J.G. & Simmons, J. (2003): Long-term Performance of Passive Acid Mine Drainage Treatment Systems. – Mine Water and the Environment, 22(3): 118—129.

Passive Biological Treatment Systems of Mine Waters at WISMUT Sites

Annette Küchler, Gunter Kiessig, Christian Kunze

WISUTEC Wismut Environmental Technologies GmbH, Jagdschänkenstr. 33, D-09117 Chemnitz, Germany, E-mail: info@wisutec.de

Abstract. Water treatment is an important component of WISMUT's remediation activities at uranium mining and milling sites in Eastern Germany, from both an environmental and financial perspective. In most cases, uranium, radium and arsenic are the main contaminants, while at some sites, nickel and other non-radioactive metals are present too. Passive systems are an attractive alternative to conventional treatment facilities. Numerous approaches have been developed that use natural processes to remove metallic contaminants from mine and seepage water. However, implementing biological water treatment systems is still often regarded as "tricky", and scepticism as to their effectiveness and stability is prevalent among practitioners, the public and, perhaps most importantly, regulators. This paper addresses the regulatory and compliance issues, some of the key issues in the development and construction of such systems, and discusses practical examples of passive mine water treatment systems that have been completed and evaluated by WISUTEC already.

Instruction

Passive water treatment technologies, such as wetlands, are an attractive and economically sensible alternative to conventional technologies at abandoned mine sites for long term water treatment and relatively small contaminant loads. Water treatment is an important component of WISMUT's remediation activities at uranium mining and milling sites in Eastern Germany. Apart from water from tailings ponds, which are treated in conventional facilities, seepage waters from waste rock piles, tailings dams, and smaller mines also require treatment before they can be released into streams but do not warrant conventional treatment due to their

low flow rate and the long-term nature of the contamination. In most cases, uranium, radium, and arsenic are the main contaminants, while at some sites, nickel and other non-radioactive metals are present too. For these waters, passive systems are an attractive alternative to conventional treatment facilities. Numerous approaches have been developed and discussed in the literature that use natural processes to remove metallic contaminants from mine and seepage water. Plants and microbes create hydrochemical conditions that lead to a shift of pH or redox potential; in other cases, adsorption or the incorporation of metals in the microbial and/or plant metabolism can be used to reduce the contaminant concentration in the outflow.

WISUTEC, a fully-owned subsidiary of WISMUT, has successfully designed and implemented a number of constructed wetlands for the treatment of waters from WISMUT's mining, industrial, and ore milling sites. Theoretical explanations are available for the chemical and physical processes in constructed wetlands, and the basics seem to be well-understood, in principle. However, implementing biological water treatment systems is still regarded as "tricky" by practitioners, the public and, perhaps most important, regulators. Long-term stability and resilience with respect to external perturbations are a major concern for both wetland operators and regulators. In addition to concerns about potential failure scenarios that lead to a full or partial breakdown of a wetland's function for a certain time, the time a water treatment system needs to restore its function after a breakdown and whether it will fully return to its designed state of operation at all must be considered before approval will be given by regulators.

A necessary precondition for the approval of wetlands by regulators, particularly if radioactive components in the water attract enhanced attention from the public, is that safe operation can be guaranteed over a long time span. Here we are faced with a dilemma: on one side, passive treatment systems derive their attractiveness from the low level of maintenance required, which leads to low costs; on the other side, a certain degree of reliability must be proven before they can be left unattended. This dilemma, combined with the fact that passive treatment systems are not "plug-and-play" technology but need careful adjustment to site conditions and sometimes show seemingly inexplicable fluctuations of performance, is still a barrier to the widespread use of passive systems (Suthersan 2002).

Constructed wetlands as attractive solutions to long-term water treatment at abandoned mining and milling sites

Biological water treatment systems are attractive alternatives for water treatment tasks at abandoned mining and milling sites because of their low operating and maintenance requirements. This general statement will be justified using the experience of WISMUT, the world's largest remediation project for mining and milling liabilities. WISMUT, wholly owned by the German government, is the legal successor to SDAG Wismut, a former Soviet-German company in Eastern Germany, which produced a total of 230,000 tonnes of uranium ore from 1946
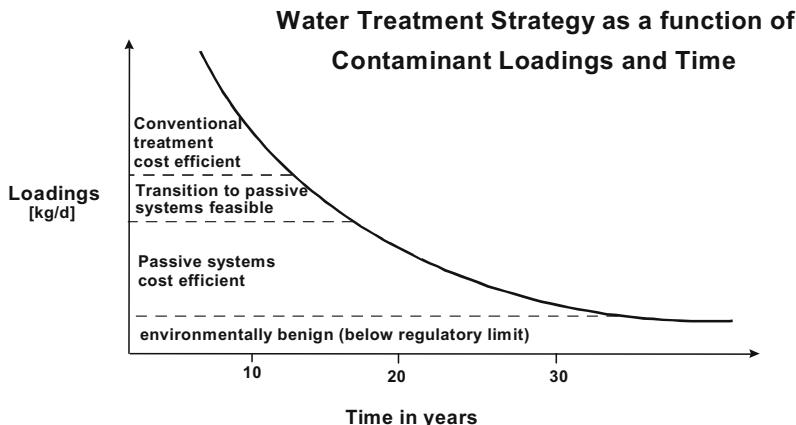
through 1991. WISMUT's mining and milling sites are located in the German Free States of Saxony and Thuringia. The federal government committed a total of 6.6 billion € to the remediation of the environmental liabilities. One of the largest single tasks within the WISMUT project is the treatment of effluents from flooded mines and seepages from tailings and waste rock piles. Water treatment consumes about 15% of the total budget and extends over many decades, while other tasks will be finished much earlier. The typical contaminants at WISMUT sites include uranium, radium, iron, manganese, arsenic, and other heavy metals.

The long term trend of water quality at the WISMUT sites is toward decreasing contamination loads. Because neither the required staff nor the dosage of the chemicals in the plant can be decreased below a certain threshold level, the expected decrease of the contaminant loads in the mine water means that while the plant throughput remains largely constant, the specific costs for removal of a unit of contaminant will continuously increase. Contaminant concentrations decrease relatively quickly several years after complete mine flooding, but then remain at a much lower level for a relatively long time (on the order of decades) which, however, continues to require treatment.

In the schematic diagram (Fig. 1) below, the time-dependent development of the contaminant load and selection of the appropriate treatment technology is shown to relate to the regulatory standards.

The diagram demonstrates that there is a considerable time span over which compliance with regulatory requirements would lead to economically inefficient water treatment if conventional treatment plants were to remain in operation. The conclusion that must be drawn is that over the long term, a technology switch from conventional to alternative treatment methods must be designed.

The development and selection of passive water treatment approaches must fol-

Fig. 1. Typical evolution of contaminant loading and selection of cost efficient water treatment strategy.

Active and passive water treatment techniques

low a number of criteria, apart from that of minimizing total costs:

a) The plant must be laid out to accommodate large fluctuations of throughput and feed water quality. The assessment of the amount of water infiltrating into a mine is subject to major uncertainties at the beginning of and during the flooding process. The same applies to the predictions of quality of mine water and waste pile seepage.

b) Residue generation must be small: Residue minimisation follows from the need for cost and risk minimisation. On-site residue disposal must be ensured for the entire duration of the anticipated operation of the plant and even beyond.

c) Self-regulating systems should be considered. Preference should be given to technologies that operate reliably with minimum input and control, and with a high degree of robustness and resilience. This requirement is based on more than cost; over an anticipated operation time of some decades, loss of institutional control cannot be entirely precluded.

Taking advantage of the international experience, WISMUT/WISUTEC, in cooperation with external partners, have been testing various approaches and design principles for constructing wetlands at many sites. Several passive water treatment systems are presently in the stage of technology development and pilot scale field testing. In October 2004 the first constructed wetland for continuous operation took up the test run.

Constructed wetlands at WISMUT sites: The Poehla case

In this section, we focus on the results obtained from a constructed wetland at the Poehla mine site. The Poehla site comprises a relatively small mine with a flooding volume of 1 million m³. In 1995, contaminated flood water reached the level of natural overflow to the surface, at a flow rate of about 15 m³/h. A conventional chemical/physical water treatment plant was commissioned in 1995 to remove U, Ra, As, Fe, and Mn from the mine effluent. Table 1 shows the development of relevant contaminant concentrations in the water from 1995 through 2001.

It is obvious that only manganese, iron, arsenic, and radium require treatment, while the other components have already reached concentrations below the dis-
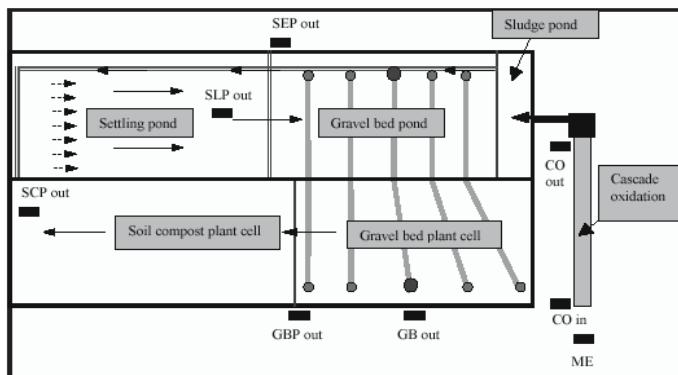
Table 1. Contaminant loading of the Poehla-Tellerhäuser mine water (main components, average values in the 2nd half of 1995 and in 2001) and the permitted discharge concentrations of the water treatment plant.

Component	Unit	Concentration		Discharge limit
		2nd half of 1995	2001	
U_{nat}	mg/l	1.6	0.1	0.2
Ra-226	Bq/l	1.4	4.3	0.3
As	mg/l	0.9	2.2	0.1
Fe	mg/l	17	8.0	2.0
Mn	mg/l	3.7	0.7	2.0

charge limit. However, water treatment must continue for the remaining components in the overflowing mine water, and geochemical modelling predicts that this will continue over approximately 15 years.

In summer 1998, the first constructed wetland of Wismut was put into experimental operation, treating part of the Poehla-Tellerhäuser mine water overflow. Its schematic layout is shown in Fig. 2. Fig. 3 shows the Poehla experimental wetland in 2003. The constructed wetland was placed in a former concrete water retention basin, which was subdivided by concrete walls into five compartments so that various chemical/physical and biological environments could be created at each stage. Upstream was an aeration cascade. The water movement was achieved by an overall gradient across the system, so that no pumping is needed. In the aeration cascade, the ferrous iron dissolved in the flood water was oxidized. In the neutral flood water, iron hydroxide was precipitated to which arsenic and radium are bonded by adsorption. The iron hydroxide flocs sediment in basins 1 and 2 of the constructed wetland. Basin 2 was provided with specific features: planted floating mats, coconut mats und "AQUA-mats[®]". Afterwards, the flood water passed two basins which contain gravel and crushed rock of different granulometry with the water being conducted along the bottom from the first to the second basin. The fill material serves as colonisation area for microorganisms and as filter. The surface of the second gravel basin was planted with helophytes in order to promote the development of biofilms. The final stage of the pilot plant was a planted bottom filter. The reaction space is filled with compost and gravel. The flow is horizontal. In the light of upfront tests, local helophytes were chosen for planting the second gravel basin and the bottom filter area: Typha latifolia, Juncus inflexus, Juncus effusus, Phragmites communis and Iris pseudacorus. Downstream of the constructed wetland are a number of filters filled with reactive material to reduce residual concentrations of arsenic and radium (basin 6 and 7).

Fig. 4. shows the concentration of the relevant contaminants along the sampling points indicated in averaged over a period of 12 months. In the years since installation of the wetland it was demonstrated that it can be successfully used for re-

Fig. 2. Schematic layout of the experimental constructed wetland Poehla site.

Active and passive water treatment techniques
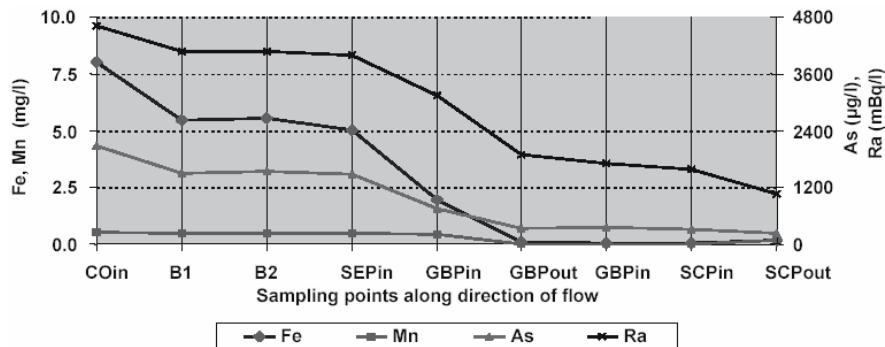
Fig. 3.   Photograph of the pilot-scale wetland at Poehla.

moval of the relevant contaminants at this site. The average removal rates over the last years were: radium, approximately 73%; iron, approximately 97%; manganese, approximately 90%, and arsenic, approximately 83%.

A detailed discussion on the various processes taking place in the system can be found in (Kalin et al. 2002).

The priority task was to intensify both radium and arsenic removal using biological effects. With this objective in mind, investigations were started on the use of macrophyte algae. Accumulation of Ra-226 by various algae species is the subject of intense studies. the continuous black line in the Fig. 5 show in a condensed form the correlation between the specific Ra-226 activity in algae and in feed waters. Investigations conducted by Boojum Research Ltd. demonstrated that some stoneworts species – Characeae – are capable of accumulating considerably higher radium activities. Deviating conditions are indicated in the Fig. 5 by the broken line.

In tests proof was furnished that Characeae are capably of safely removing radium and arsenic from mine water.

Fig. 4.   Contaminant concentration at sampling points along direction of flow through wetland

Active and passive water treatment techniques

However as a rule, it will take several growing seasons for purely biological treatment stages involving areas established with algae or plants to reach their full performance. Also, there may be strong seasonal variations, and in a worst case scenario treatment capability may be completely lost.

Under a WISUTEC research project, reactive materials were developed and tested for the selective removal of radium and arsenic from contaminated mine waters. From these investigations, two reactive materials were selected for further testing at the Pöhla site. One of the materials is "Ferrosorp", a granulated ferric hydroxide. This material is particularly suited for arsenic removal. The second material, called "Hedulat", is also granulated and consists of feldspar in a porous matrix. This product is specifically aimed at radium removal. This radium sorbent has been specifically developed by WISMUT/WISUTEC and partners for passive water treatment purposes; more details can be found in (Kunze et al. 2002b).

In 2001, a separate test section was started to remove residual concentrations of arsenic and Ra-226 from the outflow of the pilot plant. In the scheme of the pilot plant, this unit is represented as treatment basins 6 and 7. The channel is subdivided into two sections, section 1 is filled with "Ferrosorp", section 2 is filled with "Hedulat". During the investigation period of one year, the arsenic level was reduced from an initial average of 452 µg/l down to < 30 µg/l. The activity concentration of radium was also reduced from an average of 1.210 mBq/l down to 16 mBq/l.

The next step at the Poehla site was the construction of a full-scale constructed wetland which will operate according to the same design principles as the pilot system so that the conventional treatment plant at the site can be phased out and replaced with the passive/biological treatment facility. In October 2004 the constructed wetland for the treatment of any mine water at the Pöhla site took up the test run. Fig. 6 shows the layout of the facility. Fig. 7 shows the constructed wetland in 2004. The design of the plant is based on a stand-by system to provide treatment in the case of repair or maintenance. In an initial process stage, the mine water flows through an aeration cascade. Its inclination follows that of the Schildbachhalde mine dump.
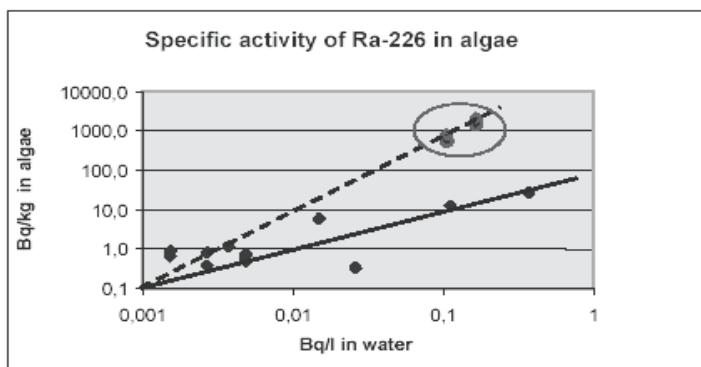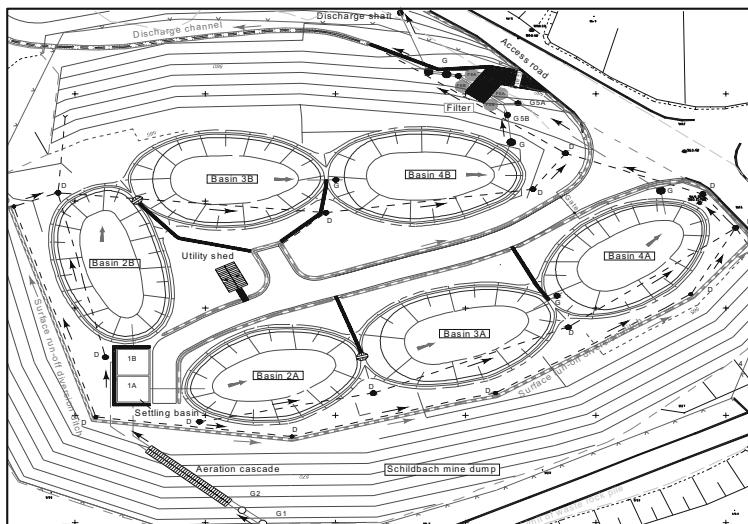
Fig. 5.   Specific activity of Ra-226 in algae.

Active and passive water treatment techniques

Basins 1 A and 1 B are sedimentation basins in which baffle plate thickener are installed. In these basins, iron hydroxide sludges are separated (Sludge volume per basin: ca. 53 m³). Downstream of the sedimentation basins are basins 2 A and 2 B where AQUA-mats® are installed. In basins 3 A and B as well as in 4 A and B Characeae is established to reduce radium and arsenic concentrations down to compliance with applicable discharge standards. The water level in the basins can be controlled over a wide range and hence be adjusted to the growth of the Characeae. The basins 2A/B to 4 A/B are almost identical in their dimensions (water surface between 483 m² and 535 m², maximum volume between 352 m³ and 386 m³). All basins are constructed as plastic lined earth basins. Tightness of the basins is monitored by drainages running below the basins. Filters F 5 A and F 6 A as well as F 5 B and F 6 B are filled with reactive materials. The water is first flowing through the Hedulat filled filter for radium removal and then through the Ferrosorp filled filter for arsenic removal. The treated mine water is discharged to a receiving stream via an outflow channel.

Fig. 6.   Schematic layout of the constructed wetland Poehla site.

Fig. 7.   Photograph of the constructed wetland at Poehla, Autumn 2004.

Active and passive water treatment techniques

The Discharge limits are to be taken from the table 1. The measured average contents of relevant contaminants in input and discharge of the passive biological water treatment facility during the period October 2004 to May 2005 were

- Arsenic: Inflow 2,623 µg/l, Outflow 65 µg/l
- Radium: Inflow 4,430 mBq/l, Outflow 30 mBq/l
- Iron: Inflow 6.6 mg/l, Outflow 0.04 mg/l

In the initial phase where biological processes are not yet involved in contaminant removal, specific costs of mine water treatment are ca. € 1/m^3. As soon as biological processes proven in the bench-scale test will have reached their performance stage, these costs will be down to less than €0.2/m^3.

Robustness of constructed wetlands

As already stated in the introduction, long-term stability and resilience with respect to external perturbations are a major concern for both regulators and wetland operators. There are many approaches to the question of what constitutes a robust system. Definitions and concepts have mainly originated in engineering, biology or sociology, but they are too numerous to be discussed here in detail. With respect to ecosystems, the interested reader is referred to (Jorgensen 2000), which contains a number of interesting concepts. We will confine ourselves to the narrow but practicable terminology of (Gunderson et al. 2000), who uses the terms resistance and resilience as constituents of the broader concept of robustness.

Robustness has to do with the dynamic behaviour of a wetland. Therefore, in order to find a design with high robustness, a dynamic model can be developed based on systems parameters obtained from literature, laboratory tests, or field experiments. Various designs are then simulated under normal operating conditions and external perturbations in order to identify critical design criteria that lead to maximum robustness, i.e. high resilience and resistance, at reasonable cost. This approach has been followed by WISUTEC/WISMUT as part of an R&D project called BioRobust (supported by a grant from the Federal Ministry of Education and Research, operation period 2001 to 2004). A detailed description of the theoretical and experimental work to optimise the robustness of constructed wetlands can be found in (Kunze et al. 2002a).

Apart from laboratory experiments, which produce very valuable parameter sets under controlled conditions, the system's behaviour under real, site-specific climatic conditions must be considered. An experimental wetland has been built at the waste at WISMUT's Schlema mine site for this purpose (see Fig. 8). The objective will be the Uranium separation in waste waters seeping from waste rock dumps. Emission limit values for arsenic, COD and total nitrogen in the discharge of the plant had been established. The pilot plant consists of two parts which can operate independent from each other. The one pilot plant part is based of systems of macrophytes (area ca. 1,400 m², 4 basins). It consists of 4 basins. Two of the basins were planted with Carex and the others with Phragmites.
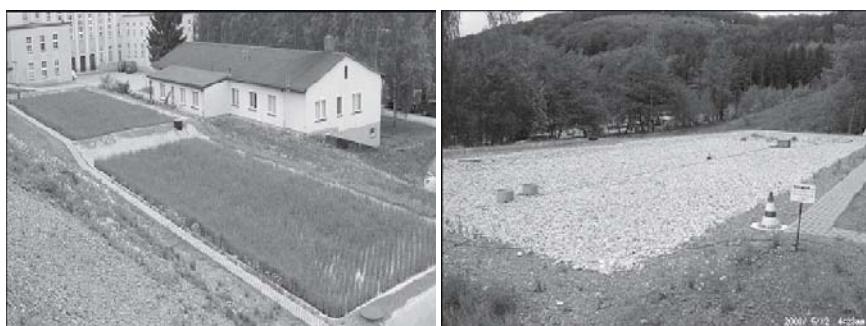
The first and second basin operates in surface flow and the following in subsurface flow. The third basin has a management with changing water levels. The other pilot plant part investigate microbiological induced processes for the treatment of contaminated water (reduction area ca. 360 m², 1 basin, 1 aeration cascade in the outflow of the reduction area). The investigated mechanisms include biosorption, bioaccumulation, reduction processes.

The discharges from the part facilities will be lead to a lagoon and will then discharged to the local receiving stream. For optimized removing of pollutants molasses and methanol is added to the inflow (seepage water).
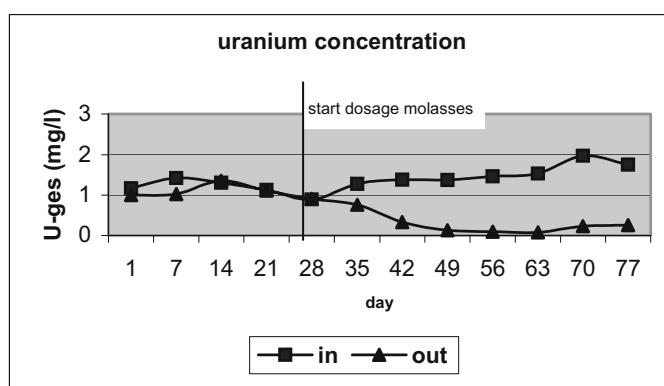
The control of the wetland is very complex because of the different condition needed for removal of arsenic (aerobic) and uranium (anaerobic).

It could be shown, that both parts of the pilot plant are able to reduce the contaminant concentration (see Fig. 9). Considerable divergences from normal operation can lead to intolerable operational state.

The lessons learned from the BioRobust project, as they form part of our design

Fig. 8. Experimental multi-cell wetland at WISMUT's Schlema mine site (left: plant cells, right: microbiological cell with gravel bed).

Fig. 9.   Uranium concentration in the input and discharge of the planted part of the facility.

Active and passive water treatment techniques

principles for constructed wetlands at WISMUT sites and beyond, can be summarized as follows:

- post-treatment filters of adsorption material increase the robustness, especially immediately after inception and/or a temporary breakdown of the biological system
- design-based measures to prevent freezing and to guarantee functionality during winter period
- adjustable overflow level in all ponds/cells
- prevention of surface runoff from flowing into ponds, causing hydraulic problems
- with a minimum of human supervision, small defects can be detected and fixed early, thus preventing larger failure.The pilot plant will be operated after finishing the BioRobust project too. In dependance from the results extension of the constructed wetland area for the treatment of the whole seepage water amount will be planned.

Conclusions and outlook

Since construction of the first experimental wetland at WISMUT's Poehla site in 1998, much has been learned on the behaviour of passive biological systems ("constructed wetlands") for the treatment of mining and mining-related effluents. More solutions using passive biological systems are planned for the WISMUT remediation effort in the near future. These include treatment of seepage of tailings dams and waste rock piles. We believe that from our work to date, highly interesting results and valuable lessons can be distilled and generalised to other sites and other regions of the world. However, each site has its specifics, which means that no plug & play solution exists, in the strict sense exists. Hydraulic and hydrochemical specifics of the site must be carefully analysed before a long-term solution can be devised. This effort is greatly rewarded by a sustainable, robust, low-cost and environmentally appealing solution.

Involved companies in the project

The following companies were involved in the planning and performance of the listed projects: BioPlanta GmbH, Boojum Research Limited, B.P.S. Engineering GmbH and G.E.O.S. Freiberg Ingenieurgesellschaft GmbH.

References

Gunderson L.H. et al. (2000) Resilience in Ecological Systems. Handbook of Ecosystems Theories and Management, ed. by S.E. Jorgensen and F. Müller, Lewis Publishers, Boca Raton, FL, USA, pp.385

Jorgensen, S.E., Müller, F. (2000) Handbook of Ecosystems Theories and Management. Lewis Publishers, Boca Raton, FL, USA

Kalin, M., G. Kießig, A. Küchler (2002) Ecological water treatment processes for underground uranium mine water: Progress after three years of operating a constructed wetland. Uranium in the Aquatic Environment, ed. by Broder J. Merkel, Britta Planer-Friedrich, Christian Wolkersdorfer. Springer Verlag, Heidelberg

Kunze, C., F. Glombitza, A. Gerth, G. Kiessig, A. Küchler (2002a) Long-term Stability and Resilience of Passive Mine Water Treatment Facilities: A Joint Experimental and Simulation Approach. Uranium in the Aquatic Environment, ed. by Broder J. Merkel, Britta Planer-Friedrich, Christian Wolkersdorfer. Springer Verlag, Heidelberg

Kunze, C., E. Hermann, I. Griebel, G. Kiessig, F. Dullies, M. Schreiter (2002b) Entwicklung und Praxiseinsatz eines hocheffizienten selektiven Sorbens für Radium [Development and practical application of a highly selective sorbent for Radium. GWF Wasser Abwasser, 143. Jg., no. 7/8

Suthersan, S.S. (2002) Natural and Enhanced Remediation Systems. Lewis Publishers, Boca Raton, FL, USA

Uranium Fate in Saturated Porous Media under Arsenic, Iron and Bacteria Influence: The Role of Potassium

Clement Mbudi, Broder J. Merkel

Department of Hydrogeology, Technische Universität Bergakademie Freiberg, Gustav-Zeuner Str.12, D-09599, Germany, E-mail:Mbudi@mailstud.tu-freiberg.de

Abstract. Uranium (U) and arsenic (As) of leachates from mine tailing dumps are a notorious cause of environmental concerns. Iron (Fe) oxides and metal reducing bacteria are well known immobilizers of U and/or As in unsaturated and saturated porous media. This paper describes investigations on geochemical controls of U fate under the influence of As, Fe and bacteria. Batch experiments were performed in glass test tubes using natural iron minerals and scrap metallic iron in setups designed to ascertain the kinetics and the influence of arsenic and iron. The effect of the background electrolytes NaCl or KCl and related ionic strengths were also considered. The experiments suggest prevalent role of the scrap iron's corrosion products but also of those of potassium (K) and calcite. Similarly, four glass columns (40 cm height, 2.4 cm diameter) were packed in weight/weight proportion of 90% sand and 10% scrap Fe (0.2-0.8 mm). Two columns without metallic Fe were filled with 50% sand and 50% glass beads and 100% sand respectively. Five columns including a control were leached at 0.12-0.39 ml/min with a 0.01M KCl or NaCl background electrolyte spiked with 0.05mM of U (11.9mg/l) and As (3.7mg/l). Two columns were leached with Schneckenstein (Saxony, Germany) Uranium tailings leachate upgraded to 0.05 mM U and As and a parallel continuous feed of a solution of 1mM glucose. Effluents samples collected regularly for a total of 77 pore water volume (5 litres) show fixation of more than 95% of both U and As in all columns were scrap Fe was present. The control column, however, has shown an unexpected fixation of both U and As between 90-95% suggesting

precipitation/co-precipitation of both U and As through sparingly soluble minerals such as Abernathyite $KUO_2AsO_4 \cdot 4H_2O$ as predicted by PHREEQC (LLNL database). Thus, K may be an efficient and cost effective amendment for immobilizing both U and As in contaminated porous media through precipitation/co-precipitation mechanisms if As and U are present at high concentrations. However, the reduction of both arsenic and uranium is limited by the solubility product of Abernathyite maintaining uranium and arsenic concentrations in the range of tens of µg/L. Potassium as an essential intracellular nutrient might also play a double role of enhancing bacteria mediated biotransformation and immobilization of uranium and arsenic.

Introduction

Uranium is mainly used for nuclear power plants as alternative source for energy production. This trend is primarily subsequent to the steady increase in world population, higher oil and gas demand and hence rapid depletion of fossil fuel reserves and the advances in nuclear power plant operations triggered by the Russian Chernobyl accident and the subsequent radioactive fall out. Thus, current on-going and increasing uranium mining fused with past poor management of uranium mine tailings will remain a major source of uranium and associated metals and metalloids in natural waters. Among numerous metals and metalloids associated with uranium in most geological contexts, arsenic is the most widely known due to the massive poisoning in Bangladesh and India's west Bengal as a result of exposure to arsenic contaminated water. Both uranium and arsenic dissolved in natural fresh waters are of much human health concern due to their notorious chemical toxicity. Therefore, a wealth of studies and knowledge designed to better understand the aquatic chemistry, fate and transport of uranium and arsenic in groundwater systems gathered over the last decades have been published.

Furthermore, studies related to uranium and arsenic competitive fate and transport in saturated porous media are scarce. One of the rare papers within this line is the one Merkel (2003) using PHREEQC geochemical code to simulate uranium mine water dilution taking into account the influence of redox sensitive arsenic, iron and organic matter kinetics on uranium fate. It is worth mentioning, however, that most studies related to uranium and arsenic are linked to their removal efficiency by specific reactive materials primarily zero valent iron (Uhrie et al., 1996; Schneider et al., 2001a, 2001b, Mallans et al. 2002, Morrison et al. 2002, Mbudi and Merkel, 2005). Yet, few studies have reported divergent fate of uranium and arsenic in natural environmental settings where iron and bacteria play a prominent role (Seidel et al. 2002; Wolkersdorfer 1995; Kalin et al. 2002). Iron and bacteria

occur widely in subsurface and control many geochemical processes. Therefore, this study conceived within this framework is a part of ongoing laboratory experiments aimed at contributing to a better understanding of the mechanisms controlling uranium fate in saturated porous media under arsenic, iron and bacteria influence. This laboratory approach is mainly motivated by current limitations of geochemical models related to thermodynamic database uncertainties (Nistche et al. 2000), and lack and/ or reliability of those data particularly for most arsenic species (Zhu and Merkel, 2001; Merkel, 2004).

Experimental setup

The chemicals and reagents used in this study were all of analytical grade and include uranyl nitrate 6-hydrate $UO_2(NO_3)_2.6H_2O$ (Chemapol, Germany), Sodium Arsenate $Na_2HAsO_4.7H_2O$, HCl 37% (Baker, Germany). Arsenazo III (1,8-dihydroxynaphthalene-3,6-disulphonic acid-2,7-bis[(azo2)-phenylarsonic acid)] (Riedel-de-Häen, Germany) used as 0.15% (m/v) aqueous solution, 200 mg of high purity Zn granules (Fluka, Germany), ascorbic acid and oxalic acid both of Chemapol used as 1g each in 100 ml water. All solutions that needed water as solvent were prepared using deionised ultra-pure water throughout. All batch and most column experiments were carried out with input or influent of solution of background electrolyte of either KCl or NaCl in order to avoid potentially competing ions. The selected salts release in water monovalent ions K^+, Na^+, Cl^- generally considered to be conservative, inert and nonsorbing (Dzombak,1990). Also, in all batch and column experiments, mixtures of solid sorbents were made on weight/weight basis.

Batch test tubes

All batch experiments were conducted in 1/10 solid (2g) to solution (20mL) ratio using 25 ml capped glass test tubes in duplicate. The first set of experiments were performed with mixed natural iron minerals of a grain size of 25% (0.25mm-0.5mm) and 75% (0.5mm-0.8mm) with a spike of 0.05 mM of uranium or uranium and arsenic in 0.01M KCl or 0.01 NaCl. XRD characterized the compound referred to as goethite-quartz as 97.89±0.29% goethite and 2.11±0.29% quartz. The second sorbent simply referred to as pyrite-calcite-ankerite was in fact a mixture of calcite (10%) of the grain size (0.2-0.5mm) and a more complex natural mixture XRD characterized as pyrite (74.76±1.23), calcite (10.95±0.72%), ankeriteFe0.54 (5.66±0.81%), sphalerite Fe (4.52±0.33%), chloritellb-2(2.14±0.93%), galena (1.49±0.06%) and quartz (0.48±0.33%).The equilibration time spanned from 168 up to 500 hours. Similarly, raw scrap metallic iron (1-10cm long) obtained from Metallaufbereitung Zwickau (MAZ) known as S69 and containing 92.8%Fe, 3.5%C, 2.1%Si, 0.9%Mn and 0.7%Mn (Noubactep et al. 2003) was crushed and used in the range size 25% (0.25mm-0.5mm) and 75%

(0.5mm-0.8mm) for related sets of experiments without further treatment. A similar set of batch experiments equilibrated scrap metallic iron alone or as a compound of 90% scrap iron (25% 0.25-0.5mm, 75% 0.5-0.8mm) and 10% calcite (1.25-0.25 mm). The background electrolyte of 0.01M was either NaCl or KCl spiked with uranium in the molar range of 0.001 to 0.1 mM or constant uranium (0.05mM) and varying arsenic concentrations so as arsenic/uranium molar ratio range from 0.02 to 2. Also, in order to establish the probable influence of K, further experiments with uranium and/or arsenic concentrations varying from 0.001mM to 0.1mM in a KCl background electrolyte of 0.01mM and 10mM respective ionic strengths were left with scrap metallic iron for one week long to obtain equilibrium conditions.

Column systems
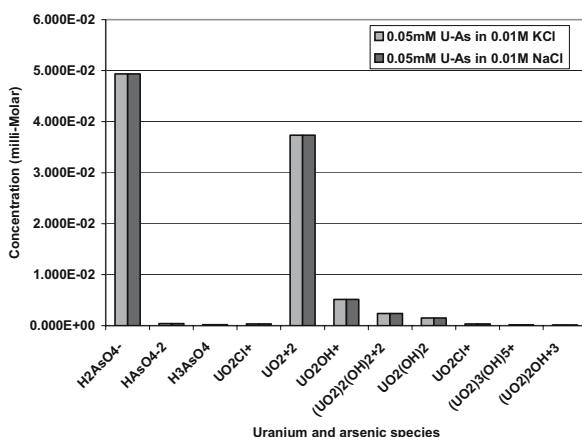
A total of six glass columns of 2.4 cm diameter, 40cm height, glass wool filter within the top cap and about 0.5 cm layer of granule silica beads at bottom and covered with aluminium foil were used. The quartz sand termed F32 (Quarzwerke Frenchen, Germany) with an average grain size of 0,24mm and a specific theoretical surface area of 102cm^2/g was used throughout in all columns. XRD investigations found 98.6$\pm$0.26% quartz and 1.4$\pm$0.26% calcite. The quartz sand contained 99.7% SiO_2, 0.2% Al_2O_3, and 0.03% Fe_2O_3. This sand used in all six columns was washed with diluted (1:10) 65% nitric acid and kept in for 24 hours, rinsed with deionised water and air-dried in the laboratory. One control column was packed with 50% glass beads (0.2-0.8mm) and 50% quartz sand. Four columns were filled with 10% scrap iron of grain size ranges of 25% (0.25mm-0.5mm) and 75% (0.5mm-0.8mm) and 90% quartz sand whilst the last column was filled with washed sand only.

   All six columns were first filled half with deionised water and then respectively filled with sand/mixture resulting in an average porosity of 0.3 and an average pore water volume of 65 mL. The influent solutions were pumped from bottom to top at an average rate of 0.16 mL/min using a high precision tubing pump with planetary drive ISMATEC IPC 24 canals (Ismatec SA, Switzerland). The columns were conditioned by pumping in several pore volumes first of deionised water and of either 0.01M KCl or NaCl. The possible bacteria influence was investigated in two columns. One of the column contained sand only and the other sand and scrap iron. For these columns, however, conditioning and flushing was achieved by pumping of several pore volumes of deionised water first and then by 0.01M glucose. These two columns were thereafter supplied from the top with a 25 mL of a diluted 1:1000 supernatant aliquot in a 0.01M glucose background. This aliquot was derived from 25 g soil of Schneckenstein Uranium tailings (Saxony, Germany) taken from the bottom part of a 5m deep tailing material mixed with 250 ml 0.01 M glucose as $C_6H_{12}O_6.H_2O$ using a 500ml Erlenmeyer placed in a horizontal shaker for 1 hour. A tracer test was performed using Cl. The influent solutions used throughout for all columns were spiked with 0.05mM uranium (11,9mg/L) and arsenic (3.7 mg/L) in 0.01M Nacl or 0.01M KCl background electrolyte, or in

the leachate collected at the Schneckenstein Uranium tailings location coded PNP9. This leachate contained originally in mg/L 1.4F^-, 7.5Cl^-, 3.6 NO_3^-, 210 SO_4^-, 47 Na^+, 2.4 K^+, 45 Ca^{2+}, 13.4 Mg^{2+}, 0.05Fe, 0.035Mn, 0.09Cu, 0.006 As, and 0.691U. The upgraded leachate to 1/1 (Uranium/Arsenic) molar ratio with 0.05mM uranium and 0,05mM arsenic (3.7 mg/l) was pumped in two specified columns in parallel with a 1 mM glucose solution by mixing through a Y connector before entering the column at the average same pumping rate of 0.16 ml/min.

Analytical techniques

Master parameters pH and Eh were measured with combined glass electrodes (WTW GmbH, Germany).All samples collected from batch and columns experiments were filtered with a 0.2μ filter (Schlecher & Schuell, Germany and Sartorius, Germany) and medium pore size filter of the brand FILTRAK (Germany), preserved with 1/1 nitric acid and later cooled at 4 Celsius grad. Uranium was analysed by photometry using arsenazo III method. It involves the sequential addition of two times 2ml concentrated HCl and high purity 200 mg Zn granule to 3mL of water sample aimed at reducing U (VI) to U (IV). At the completion of the resulting reaction, 250 µl of oxalic-ascorbic acid solution, and 250µl of arsenazo III are added to mask major interference and complex uranium. A HACH UV-VIS spectrophotometer with a 1 cm cuvette was used for the absorbance determination at a wavelength adjusted to 665nm. Total arsenic was measured with an Atomic Absorption Spectrometer Zeiss AAS 4 EA. A five points procedure was used to calibrate both spectrometers.
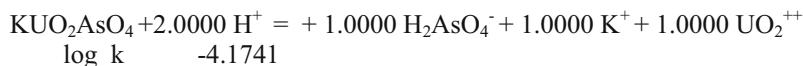
Fig. 1.   PHREEQC simulation output of major uranium and arsenic species content of the synthetic groundwaters used in most experiments (pH = 4.5, Lawrence Livermore National Laboratory thermodynamic database).

Active and passive water treatment techniques

Results and discussion

Comparability of batch and column experiments is not straightforward. Thus, both batch and column experiments are presented separately and the discussion emphasises on the role of potassium on uranium fixation.

In the following graphs uranium or arsenic fixation is expressed normalized with respect to the solution initial concentration C0 and the concentration C at the end of the experiment equilibration time.

Assuming that the Lawrence Livermore National Laboratory thermodynamic database provided and used in Phreeqc (Parkhurst and Appelo, 1999) is reliable in particular for arsenic, Fig. 1 suggests that most reactions at mineral water interface are controlled by $H_2AsO_4^-$ and UO_2^{+2} for both 0.01 M KCL and 0.01 NaCl background electrolytes of synthetic groundwaters. Owing to the slightly equal amount of both major species in either 0.01M KCl and 0.01M NaCl, it is expected that pH dependent protonation/deprotonation reactions and intrinsic behaviour of Na or K make the difference. Potassium is known somewhat to react faster in water than sodium. Thus, in 0.01 M KCl for example, PHREEQC predicts uranium and arsenic fixation through the co-precipitation of the sparingly soluble $KUO_2AsO_{4(s)}$ is likely:

$$KUO_2AsO_4 + 2.0000\ H^+ = +\ 1.0000\ H_2AsO_4^- + 1.0000\ K^+ + 1.0000\ UO_2^{++}$$
$$\log\_k \qquad -4.1741$$

The closest related mineral to the PHREEQC compound KUO_2AsO_4 is the hydrated form known as Abernathyite ($KUO_2AsO_4 \cdot 4H_2O$).

The static batch systems

The role of potassium on the rate of uranium fixation on natural iron minerals under arsenic influence

Due to iron minerals high surface areas, they control the fate and transport of most metals including uranium and arsenic. Fig. 2 portrays the rate of uranium respectively arsenic fixation on natural iron minerals.
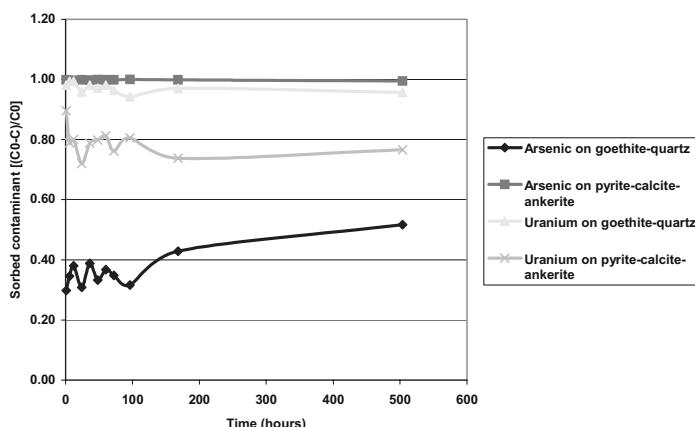
In a mono-component solution of 0.05mM uranium respectively arsenic in 0.01M KCl background electrolyte, both elements behave very differently with respect to the sorbents. This is an illustration of the typical discrepant behaviour of uranium and arsenic reported in the literature.

Almost all arsenic is immobilized by pyrite-calcite-ankerite and the reaction rate seems time independent whereas only more or less 78% of uranium is immobilized in similar conditions and the reaction seems in rather slower and still in metastable state at the end of the 500 hours maximum equilibration. On contrary, uranium is better immobilized by goethite-quartz than arsenic. While the first is in equilibrium after about 200 hours, the latter is not in equilibrium after 500 hours.

By and large, this discrepant behaviour of uranium and arsenic with respect to the studied adsorbents is probably related to both elements intrinsic properties with regard to surface complexation sites and charges. Although common iron oxide in aquifer systems, goethite is reported as a lesser absorbent of arsenic on a per gram basis compared to ferrihydrite for example (Stollenwerk, 2003). This relatively poor adsorption of arsenic on goethite is commonly explained by this mineral better crystallinity. In this particular case there might be lower concentrations of surface-complexation sites that can neutralize the major arsenic species H_2AsO_4- . In contrast, the uranyl hydrolysis complexes adsorption by goethite seems very effective. Gabriel et al. (1998) suggest that uranium sorption in similar case occurs through the creation of inner surface complexes probably in identity coordination with surfaces iron centres. On the contrary, the higher adsorption of arsenic on pyrite-calcite-anchorite (90%) and calcite (10%) is probably due mainly to the well known calcite higher arsenic adsorbing capacity.
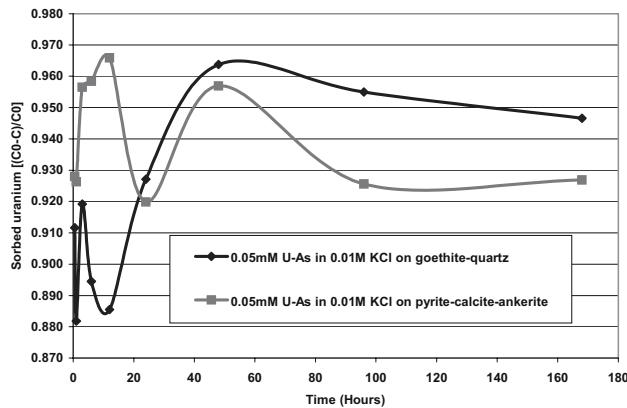
Figs. 3 and 4 show uranium and arsenic fixation rate in similar experimental setting as in Fig. 2 above but in bi-component 0.05mM uranium-arsenic spike in either 0.01M NaCl or 0.01M KCl and shorter equilibration time up to 168 hours.

As noted by Stollenwerk (2003), carbonate minerals are probably the main control of arsenic aqueous concentrations. In fact calcite surface displays positive or negative charge respective above or below its zero-point-of charge that is reported by Foxall et al (1979) to occur at pCa=4.4. This property might explain why calcite can preferably adsorb metal anion species such as $H_2AsO_4^-$ to metal cation species such as uranyl UO_2^{2+}. This reason might explain why uranium shows much lesser adsorption on pyrite-calcite-ankerite (90%) and calcite (10%) that can also be explained by the formation of carbonato uranyl complexes known as very mobile.
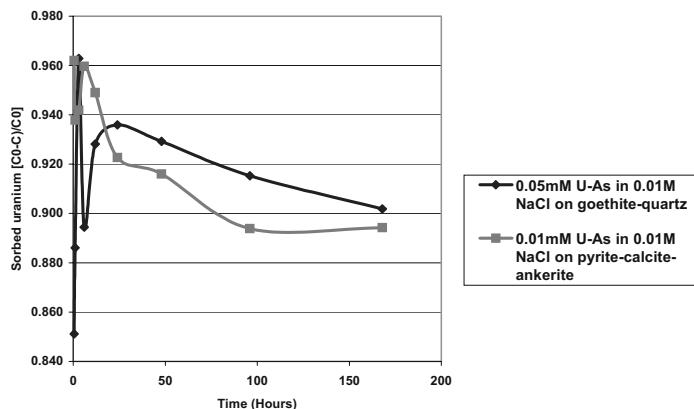
Fig. 2.   The rate of uranium and arsenic fixation on natural iron minerals. Initial mono-component uranium or arsenic solution concentration C0 amounts 0.05mM in 0.01M KCl at pH 4.5.

Active and passive water treatment techniques

Fig. 3 pinpoints two main phases of uranium sorption on goethite-quartz under arsenic influence: a probable fast adsorption phase that goes on up to around 40 hours followed by a plateau that can most likely be precipitation related. Both curves suggest that pyrite-calcite-ankerite remove much more uranium for the first 16 hours than goethite-quartz does. Thus, the addition of arsenic which is better fixed on carbonate surfaces as illustrated in Fig. 2 enhances co-precipitation of uranium with adsorbing arsenate complexes. After 20 hours there is a slight de-
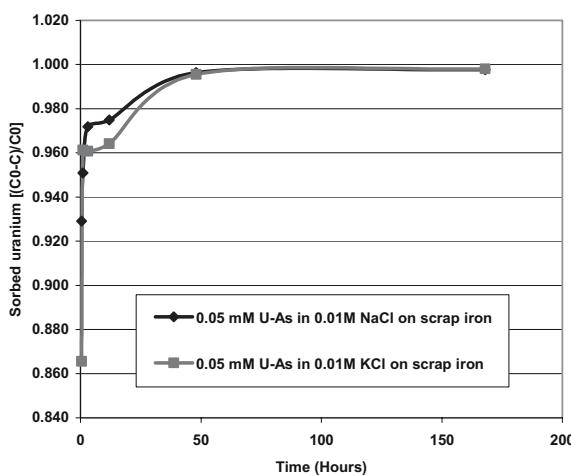
Fig. 3.   Uranium removal by natural goethite-quartz and pyrite-calcite-ankerite (90%) and calcite (10%) from a solution of 0.01M KCl spiked with 0.05mM U-As at overall starting pH of 4.5.

Fig. 4.   Uranium removal rate by natural goethite-quartz and pyrite-calcite-ankerite (90%) and calcite (10%) from a solution of 0.01M NaCl spiked with 0.05mM U under the influence of 0.05mM As at overall starting pH of 4.5.

crease on the amount of uranium removed from solution that can be related to calcite dissolution and subsequent increase in uranium carbonato complexes which are much more mobile. Taken as a whole, Fig. 3 not only indicates that the addition of arsenic promotes uranium removal by both minerals but also in comparison with Fig. 4, the removal is much more efficient in KCl background electrolyte solution than in NaCl background buffer. The reason for better uranium removal from KCl solution might be the faster reactivity of K with water compared to Na. In fact both background electrolytes have in common the same content in major uranium and arsenic species and have the tendency to raise the pH through formation of NaOH and KOH when reacting with water.

The sorption curves in Fig. 4 show a similar trend of uranium sorption in both goethite-quartz and pyrite-calcite-ankerite. It seems, however, that it Fig. 4 the systems have not yet reached equilibrium even at the end of a week long equilibration time. Again as shown in Fig. 1 above, both systems U-As-NaCl and U-As-KCl starting solutions have similar major uranium and arsenic aqueous species. Therefore, differences in uranium fixation rate might only be explained at reactions at the interface water minerals. The Systems control is much more related to sorbent minerals intrinsic properties and partly to the reaction rate of Na versus K related species with water. Hence the likelihood of uranium co-precipitation within sparingly soluble solids such as KUO_2AsO_4 or its hydrated form abernathyite is probable.
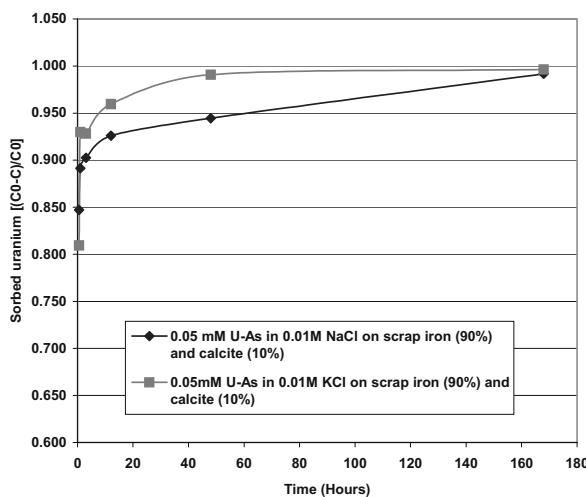
Fig. 5. Uranium removal rate by scrap iron from a 0.01 M NaCl respectively 0.01 M KCl contaminated with 0.05 mM U-As at starting pH of 4.5.

The role of potassium on the rate of uranium fixation on iron corrosion products under arsenic influence

As expected and suggested by Figs. 5 and 6, freshly formed iron corrosion products remove uranium faster and more efficiently than well crystallized and aged iron minerals in similar experimental conditions.

The removal of uranium in either background electrolyte 0.01 M NaCl or 0.01 M KCl of the same ionic strength show similar rate curves pattern as expected. The similarity is particularly expressed by a kinetically controlled fast reaction rate at the beginning of the first 12 hours. This is probably due to the fact that both solutions contains uranyl UO^{2+} as major species which seems at least at the beginning of the curve being reduced and precipitated by newly formed $Fe2^+$ species. The last portion of the curve after more or less 50 hours reactive time show a plateau suggesting the domain of chemical equilibrium and of the prevalence of precipitation/co-precipitation of newly formed iron oxides with either uranium or arsenic. It is also the domain of non iron related minerals such as the solid KUO_2AsO_4 or its hydrated form abernathyite $KUO_2AsO_4. 4H_2O$ is likely to precipitate considering the prevalence of both major species $H_2AsO_4^-$ and UO_2^{+2} in solutions. Both solutions also show in between both curves first and third portions, a transitional or second portion where surface sites seem to show much preference of uranium from the 0.01M NaCl solution than the 0.01 KCl solution. The reason for this preference is unclear except the fact that the portion is probably the domain where both reductive precipitation, adsorption and probably also precipitation/co-precipitation co-exist and control the system.

Fig. 6.   Rate of 0.05 mM uranium removal under 0.05m M arsenic influence as bi-component initial solution of respectively 0.01M KCl and 0.01M NaCl background electrolytes at pH 4.5 to equilibrate with scrap iron (90%) and calcite (10%).

Active and passive water treatment techniques

Furthermore, carbonates are known to be not only ubiquitous but also a major control of most hydrogeochemical reactions as does iron. As for the previous experiments that resulted in results discussed above, it was also important to consider the addition of calcite and how it can affect uranium removal as presented in Fig. 5.
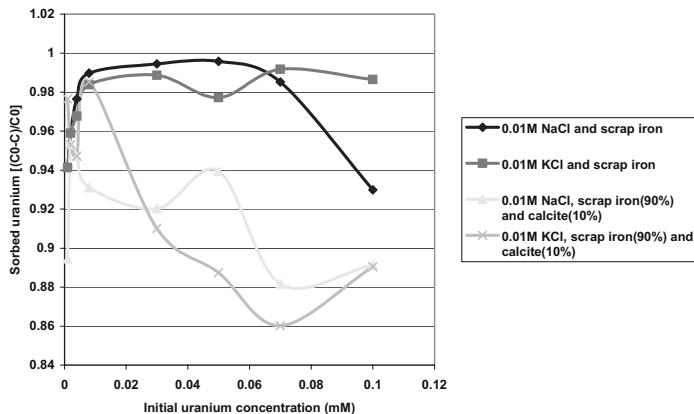
In fact, the addition of 10% calcite to the system presented in Fig. 5 suggests a slightly slow uranium removal rate and efficiency particularly for the 0.01M NaCl solution. Fig. 6 also reveals that the system 0.01M NaCl is less favourable to uranium fixation than its counterpart system 0.01 M KCl. Up to a week after the reactions started; it seems still not have reached chemical equilibrium. On the contrary also, Fig. 6 seems to add in evidence already inferred from Figs. 3 and 4 on the fact that the addition of calcite in the system 0.01M KCl where uranium and arsenic at higher concentration such as 0.05mM U-As promotes uranium removal rather than decreases it. The latter is particularly the case in mono-component uranium system where calcite dissolution rather enhances the formation of carbonated uranium species lesser prone to fixation by iron oxide surfaces. The reason might simply be found on the hypothesis that uranium is not thermodynamically a good electron acceptor in a system where $Ca-UO_2-CO_3$ complexes are prevalent. In fact, the mere presence of Ca has been shown to even inhibit the U(VI) reduction by well known uranium scavenger micro-organisms such as the facultative Shewanella putrefaciens (strain CN32) and the obligate (Desulfovibrio desulfuricans and Geobacter sulfureducens) anaerobic bacteria (Brooks et al 2003).

The enhancement of uranium fixation under the influence of 0.05mM As in 0.01M KCl experimental conditions where $Ca-UO_2-CO_3$ complexes might be induced by calcite dissolution is not fully elucidated. $Ca-CO_3$ system might better promote the reductive precipitation of arsenic and of uranium through sparingly soluble minerals such as abernathyite. In order to ensure whether this apparent greater K promoted uranium better removal also hold at different arsenic concentrations, a new set of experiments resulted in Figs. 7 and 8.
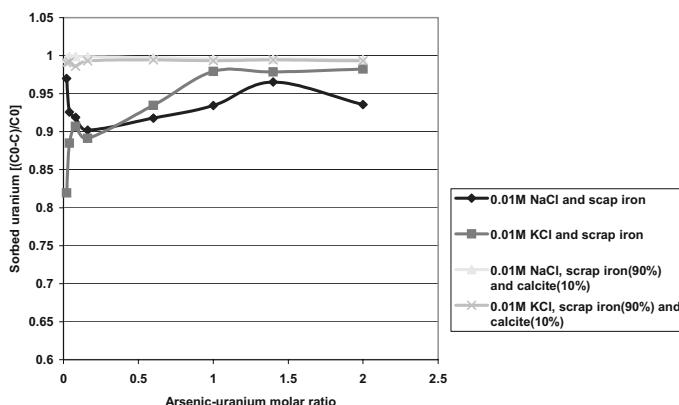
The role of potassium and the influence of arsenic concentration on uranium fixation on iron corrosion products

Fig. 7 clearly shows that calcite addition inhibit the overall uranium fixation from both 0.01 M NaCl and 0.01M KCl with a steady decreasing trend with increasing uranium input concentrations starting around 0.002mM.

Besides the much greater mobility of carbonato uranium species that might be released by calcite dissolution, there is also the calcium itself as competing metal for the same surface sites that might otherwise adsorb uranium.

Fig. 7. Comparative removal of uranium concentrations varying from 0.001mM (0.238 mg/L) to 0.1mM (23.81 mg/L) in 0.01M NaCl and 0.01M KCl background electrolytes in contact with respectively scrap iron alone or mixed with 10% calcite (staring solution pH of 4.5).

Fig. 8. Removal of uranium from solutions of 0.01M NaCl and 0.01M KCl background electrolytes whereby arsenic to uranium molar concentrations ratio varies from 0 to 2. The arsenic concentrations increased within the range of 0.001mM (0.075 mg/L) to 0.1mM (7.5 mg/L) with uranium concentration kept constant at 0.05mM (11.9 mg/L). The solid phase comprised respectively scrap iron alone or mixed with 10% calcite and the solution staring pH equals 4.5.

Active and passive water treatment techniques

The results of the addition of arsenic in molar concentrations ratio to uranium varying from 0 to 2 for arsenic concentrations increased within the range of 0.001mM (0.075 mg/L) to 0.1mM (7.5 mg/L) with uranium concentration kept constant at 0.05mM (11.9 mg/L) is portrayed in Fig. 8. Also, the one week equilibration time under experimental conditions that resulted in Fig. 8 seems to promote uranium removal more efficiently (more than 98%) in the systems that contained calcite under both 0.01 M NaCl and 0.01 KCl buffers. Precipitation or co-precipitation of uranium with arsenic and related carbonated species is probably the main removal mechanism.

On the contrary, the systems with scrap iron alone as solid phase, in particular in the experimental setup where potassium was present as 0.01 M KCl, uranium removal is at its maximum starting at arsenic to uranium molar ratio of one. At arsenic to uranium molar ratio close to or less than 0.08, the system with 0.01M NaCl uranium removal is better. However, this system also shows fixation efficiency with decreasing trend for arsenic to uranium ratio ranging between around 0.001 to 0.008.

Taken as a whole, Fig. 8 suggests that in the systems without calcite under 0.01 M NaCl or 0.01 M KCl, uranium fixation is dependent to arsenic to uranium molar ratio. The probable role of K in enhancing uranium removal is much more prominent in the system without calcite and starting at arsenic to uranium molar ratio of unity.

Overall, from Figs. 1 to 8, experimental results indicate a clear potassium role in promoting uranium fixation in systems where arsenic is present. In order to better ascertain the role of potassium in uranium fate under arsenic influence, the effect of varying the KCl background electrolyte ionic strength has to be investigated in more detail.

The effect of the KCl background electrolyte ionic strength on uranium fixation by scrap iron and iron corrosion products under arsenic influence

Fig. 9 shows that the influence of KCl background electrolyte ionic strength varying from 0.01mM to 0.01 M is more noticeable from uranium concentrations ranging from 0.001mM (0.238 mg/L) to 0.03 mM (7.1 mg/L). This first portion of both three curves seems to be dominated by the prevalence of fixation mechanism other than precipitation/ co-precipitation that is likely the case for the portion beyond 0.03mM uranium.
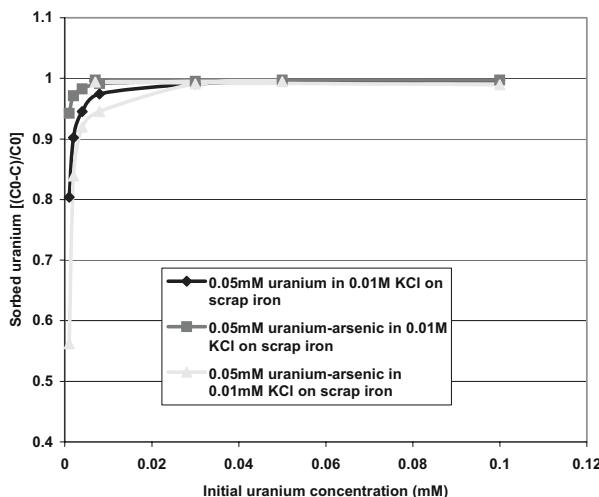
As could be expected based on Fig. 1 through 9 above, at equal 0.01 M KCl ionic strength, the system with 0.05mM arsenic better removes uranium due to the co-existence of both reductive adsorption and precipitation/co-precipitation reaction mechanisms. In contrast, a similar system with 0.05mM uranium and arsenic but with only 0.01 mM KCl shows the lowest uranium removal efficiency.

By and large, batch experiments described above reveals that potassium can play a controlling role in uranium fate under the influence of varying concentrations of arsenic and varying iron sources as natural minerals and scrap.

Experiments designed to verify some of the batch findings in a dynamic system are still needed.

The dynamic column systems
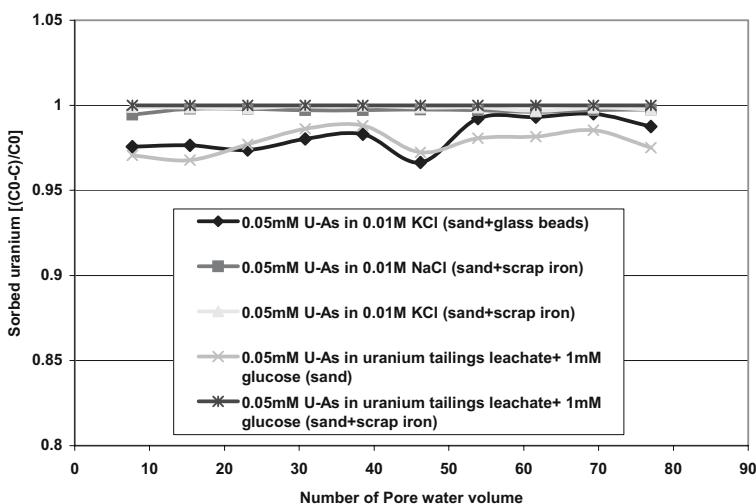
The comparison of batch systems above and the column results illustrated in Fig. 10 is not clear-cut. This is due to the additive effects of the advective, dispersive and diffusive physical mass transport and related chemical transfer processes of uranium under arsenic, iron and micro-organisms influence in 0.01 M NaCl, 0.01KCl, and complex and upgraded Schneckenstein Uranium Tailings leachate PNP9. Thus, comparability reason, column results are presented in the same format of uranium removal efficiency as per batch results rather than the usual breakthrough curves. In all four columns where scrap iron is present, the fixation of uranium is almost total with however a slightly lower position of the 0.01M NaCl related curve with respect to others and to the 0.01 M KCl in particular. Whether potassium has a particular role in the fixation of uranium in columns where scrap iron is present is difficult to establish in a dynamic system considering the similarity of major uranium and arsenic species in both background electrolyte solutions NaCl and KCl. However, in column containing 50% quartz sand and 50 glass beads, the more than 90% average removal of uranium for the total of 77 pore volume (5Litres) elution can not be explained by its retention in glass beads or filters alone. The only plausible explanation is the precipitation of uranium and arse-

Fig. 9.   Uranium fixation under changing ionic strength from 0.01mM KCl to 0.01M KCl spiked with 0.05 mM uranium alone or with 0.05mM arsenic for a one week equilibration time. The solid phase in the reactor vessel was scrap iron alone and the input solution pH was 4.5.

nic through abernathyite as predicted by PREEQC simulation pending on the accuracy of its LLNL data base for this particular solid species.

It is also worth mentioning the similar and unexpected removal effectiveness in another quartz sand column with a liquid biomass seed of natural bacterial consortia from Schneckenstein Uranium Tailings obtained in a procedure described above. The reason for this high removal of uranium might be found in the fact that the column was leached with influent water from the tailings upgraded to 0.05mM uranium-arsenic with a continuous parallel feed of 1mM glucose as the biomass carbon source. This result suggests the likelihood of natural attenuation potential of the uranium tailings. Recent and ongoing studies by Solenska-Pobel (2002) using both direct molecular approaches through Polymerase Chain Reaction (PCR) and the traditional bacteria culture approach in uranium waste piles across the German states of Saxony and Thuringia have come to the conclusion that in all uranium wastes investigated, predominant bacteria groups are mainly those known to biotransform metals. In addition, dilution with the continuous use of 1mM glucose at the average same pumping rate of 0.16 mL/minute is equally important to mention.

Fig. 10. Removal effectiveness of 0.05mM uranium under 0.05mM arsenic, iron and micro-organisms influence in 0.01M NaCl, 0.01M KCl at pH 4.5 and Scheneckenstein Uranium Tailings PNP9 upgraded to 0.05mM uranium-arsenic concentration at near neutral pH.

Active and passive water treatment techniques

Conclusions and environmental implications

This study has shown that even at a laboratory controlled and simplified conditions using mostly synthetic water reduced at minimal composition of either 0.01M NaCl or 0.01M KCl, the fate and transport of uranium under arsenic, iron and bacteria is as complex as the intrinsic hydrogeochemistry of each element involved. Yet, the following conclusions can be drawn from this study experimental conditions and setup.

With respect to iron, uranium fate is different according to the nature of iron sources considered. In general, scrap metallic iron and related freshly formed iron corrosion products better immobilize uranium than natural and old aged iron minerals. In both cases, the presence of calcite which is probably the main control of the much reported discrepant behaviour of uranium and arsenic in aqueous environment also greatly inhibits uranium fixation effectiveness.

The presence of uranium and arsenic particularly at higher concentrations of tens of μg/L can promote uranium and eventually also arsenic precipitation/co-precipitation through sparingly soluble mineral such as abernathyite. Thus, potassium plays an important role in enhancing such uranium and arsenic fixation in systems with or without the presence of calcite. Furthermore, potassium as an essential intracellular nutrient can also play a double role of enhancing bacteria mediated biotransformation and immobilization of uranium and arsenic.

Overall the most important environmental implications is that the addition of potassium can be a valuable alternative option in mitigating both uranium and arsenic contaminants from impacted water bodies where both elements are in higher concentrations. Such aquatic systems with higher uranium and arsenic concentrations are mainly spent mine water or acid mine drainage. In this latter case also, potassium can still play an important remediation role in combination with calcite which is also a pH buffer in order to promote precipitation/co-precipitation of both uranium and arsenic.

References

Brooks S.C., Fredrickson J. K., Carroll S. L., Kennedy D. W., Zachara J.M., Plymale A.E., Kelly S.D., Kemner K.M., Fendorf S. (2003): Inhibition of Bacterial U (VI) Reduction by Calcium. Environ. Sci. Technol., 37, 1850-1858

Foxall T., Peterson G., Rendall H.M., Smith A.L. (1979): Charge Determination at the Calcium Salt/Aqueous Solution Interface. J.Chem.Soc.Faraday Trans.75:1034-1039

Gabriel U., Gaudet J.P., Spadini L., Charlet L. (1998): Reactive Transport of Uranyl in a Goethite Column: An experimental and Modelling Study. Chemical Geology 151, 107-128

Kalin M., Kließig G., Kleichler A. (2002): Ecological Water Treatment Processes for Underground Uranium Mine Water: Progress After 3 Years of Operating a Constructed Wetland. In Merkel B., Planer-Friedrich B., & Wolkersdorfer C. (Eds.) Uranium in the Aquatic Environment. Proc. of the Intern. Conference Uranium Mining and Hydro-

geology III and the Intern. Mine Water Association Symposium Freiberg, Germany, September15-21, Springer, Berlin

Malians D., Diels L., Bastiaens L., Vos J., Moors H., Wang L., Maes N. & Vandenhove H. (2002) Removal of Uranium and Arsenic from Groundwater using six different Reactive Materials: Assessment of Removal Efficiency. In Merkel B., Planer-Friedrich B., & Wolkersdorfer C. (Eds.) Uranium in the Aquatic Environment. Proc. of the Intern. Conference Uranium Mining and Hydrogeology III and the Intern. Mine Water Association Symposium Freiberg, Germany, September15-21, Springer, Berlin

Mbudi C., Merkel B. (2005): A Laboratory Assessment of Uranium and Arsenic Removal Efficiency from Schneckenstein Uranium Tailing Leachates Using Scrap Iron. Wiss.Mitt.Inst. Geol. TU BAF, Vol .28, 43-48 (ISSN 1433-1284)

Merkel B. (2004): Modelling of Arsenic Removal from Water. Means and Limitations. Wiss.Mitt.Inst. Geol. TU BAF, Vol .25, 119-124 (ISSN 1433-1284)

Morrisson S.J.,Metzler,R.D. Dwyer B.P.(2002): Removal of As,Mn,Mo,Se,U,V, and Zn from Groundwater by ZeroValent Iron in a Passive Treatment Cell: Reaction progress Modelling., J. Cont. Hydrol.,56(1/2),99-116

Nietzsche O., Meinrath G., Merkel B. (2000) Database uncertainty as a limiting factor in reactive transport prognosis. Journal of contaminant Hydrology 44: 223-237

Noubactep C., Meinrath G., Dietrich P., Merkel B. (2003): Mitigating Uranium in Groundwater: Prospects and Limitations Environ. Sci. Technol. 37, 4304-4308

Parkhurst D.L., Appelo C.A.J. (1999): User's Guide to PHREEQC (Version 2).-A Computer Program for speciation, Batch-Reaction, One-Dimensional Transport, and Inverse Geochemical Calculations. U.S.G.S., Water Resources Investigation Report 99-4259

Schneider P., Neitzler P.L, Osenbrück K., Noubactep C., Merkel B., Hurst, S. (2001a): In Situ Treatment of Radioactive Mine Waters using Reactive Materials- Results of field Experiments in Uranium Ore Mines in Germany. Acta Hydrochem. Hydrobiol.29, 129-138

Schneider P.,Voerkelius S., Nindel, Forster M., Schreyer (2001b): Release of Contaminants from Uranium Mine waste. Laboratory and Field Experiments. Mine Water and the Environment 20:30-38

Selenska-Pobell S. (2002): Diversity and Activity of Bacteria in Uranium waste Piles. In Keith-Roach M. & Livens F. (eds.). Interactions of Microorganisms with Radionuclides, Elsevier Science Ltd., pp 225- 254

Seidel M. Mannigel., Planer-Friedrich B. Merkel B. (2002): Hydrogeochemical Characterization of Surface water, Sorption of Metals (loids) on Sediments and Exchange Processes within the Wetland Lengenfeld, Germany. In Merkel B., Planer-Friedrich B., Wolkersdorfer C. (Eds.) Uranium in the Aquatic Environment. Proc. of the Intern. Conference Uranium Mining and Hydrogeology III and the Intern. Mine Water Association Symposium Freiberg, Germany, September15-21, Springer, Berlin

Stollenwerk K.G. (2003): Geochemical Processes Controlling Transport of Arsenic in Groundwater: A Review of Adsorption. In Welch A.H., K.G. Stollenwerk (eds.) Arsenic in Ground Water. Kluwer Academic Publishers, Dordrecht

Uhrie J.L., Drever J.I., Colberg P.J.S., Nesbitt C.C.(1996): In Situ Immobilization of Heavy Metals associated with Uranium Leach Mines by Bacterial Sulphate Reduction. Hydrometallurgy 43:231-239

Active and passive water treatment techniques

Wolkersdorfer C. (1995): Flooding of Abandoned Uranium Mine: A Geohydrochemical Case Study in the Saxonian Erzerbirge. In Merkel B., Hurst S., Löhnert E.P., Struckmeier (Eds.) Uranium-Mining and Hydrogeology, Proceedings of the International Conference and Workshop, Freiberg, Germany. Verlag Sven von Loga, Köln

Zhu, Y& Merkel, B. (2001): The Dissolution and Solubility of Scorodite, FeSO4.4H2O-Evaluation and Simulation with PHREEQC. Wiss.Mitt.Inst. Geol. TU BAF, Vol .18, 72-87(ISSN 1433-1284)

Interaction of uranium from seepage water with hydroxyapatite

Jens Mibus, Vinzenz Brendler

1 Forschungszentrum Rossendorf, Institute of Radiochemistry, P.O. Box 51 01 19, D-01314 Dresden, Germany, E-mail: J.Mibus@fz-rossendorf.de

Abstract. Column experiments (in a quartz matrix) assisted by batch experiments helped to quantify and characterize the uranium(VI) retardation by hydroxyapatite, regarded as a highly efficient component of reactive barrier concepts for (radio)toxic contaminants. The sorption of uranyl ions onto phosphate groups is as important as their sorption onto silanol groups, outweighing the low phosphate content. In column experiments retardation factors ranging around 30 were observed. The elution of uranium is governed by two processes of different rate (and probably reversibility) which is consistent with the spectroscopic findings.

Introduction

The protection of the biosphere from hazards due to the release of radionuclides from abandoned uranium mining and processing as well as from final repositories for nuclear waste continues to be a challenge for scientists and engineers. A system of engineered and geological barriers is foreseen to ensure the isolation of pollutants potentially released from the waste.

A number of substances, such as clay minerals, zeolites, or phosphates, have the ability to scavenge metal ions from aqueous solutions. Thus, they are potential materials for the construction of barrier systems or can be used as additional for a retardation or even permanent immobilization of toxic or radiotoxic metals.

Hydroxyapatite HAP ($Ca_{10}(PO_4)_6(OH)_2$) is known for its strong interaction with lanthanides and actinides (Jerden and Sinha 2003). Whereas rare earth elements (REE) are proven to substitute calcium in the crystal lattice of HAP (Jones et al. 1996), actinides are supposed to form surface complexes or surface precipitates. Several uranyl phosphate minerals are stable under weathering conditions.

Well-understood basic processes and a reliable database are essential prerequisites for any assessment modeling of the retardation efficiency of reactive barriers. Here, the major goals are: a) the identification of the species involved in surface

reactions of uranium with HAP under oxidizing conditions, and b) the characterization of these processes and the investigation of their reversibility. Both targets are so far not addressed in the literature. The work described below is embedded into a larger project also involving batch experiments with uranium(VI) and pure mineral phases (HAP, quartz, gibbsite, kaolinite, illite, and montmorillonite) as well as surface complexation modeling of these systems linked to independent spectroscopic proofs of the respective surface species.

Materials and Methods

Materials

A commercially available synthetic hydroxyapatite p.a. (Merck, Germany) was used for all experiments. A mean grain size of 15 µm was certified by the manufacturer. BET measurements (a five-point N_2-BET Coulter SA 3100) yielded a specific surface area of 65.3 m²/g. The chemical composition of the solid was verified by ICP-MS (ELAN 5000-ICP-MS, Perkin Elmer), indicating only very minor amounts of impurities: 510 ppm Si, 200 ppm Al, 180 ppm Fe, 73 ppm Mn, and 26 ppm Ti. A marine quartz sand from Heerlen, Netherlands (supplier Euroquartz, Dorsten, Germany) was applied as matrix material in the column experiments (mean grain size 150 µm, $Fe_2O_3 \leq 0.01$ %, $Al_2O_3 \leq 0.05$ %, $TiO_2 \leq 0.02$ %). The quartz sand was washed with MilliQ water to remove soluble constituents. We used a seepage water synthesized in the laboratory according to original samples from a rock pile of the former uranium mining (shaft 66) in Schlema (Germany) reported in Geipel et al. (1994). The composition is given in Table 1. All experiments were carried out under atmospheric conditions at room temperature.

Table 1. Composition of the synthetic seepage water.

Ion	Concentration [mmol/L]
Ca^{2+}	7.8
Mg^{2+}	17.1
Na^+	0.5
UO_2^{2+}	0.01[a]
SO_4^{2-}	25.6
PO_4^{3-}	< 0.02
HCO_3^-	0.45
Cl^-	0.1
pH	7.82

[a] Solutions for conditioning purposes in the batch and column experiments were prepared without uranium (tracer-free solution).

Batch experiments

A quantity of 0.5 g HAP was placed in a 50 mL polypropylene vial. Subsequently, 40 mL of the tracer-free seepage water were added. After conditioning for four weeks and pH equilibration, 0.4 mL of a 10^{-3} M $UO_2(NO_3)_2$ solution were injected to reach the tracer concentration given in Table 1. After a contact time of 64 hours the samples were centrifuged and the uranium content in the supernatant was measured. Finally, the adsorption to the vial walls was measured and the results were corrected accordingly.

Column experiments

A laboratory column (1.0 m length and 0.1 m diameter) was tightly packed with quartz sand containing 0.1 % by weight HAP. Micro suction probes (Rhizon SMS, Eijkelkamp, Netherlands) were installed at distances of 0.1, 0.3, 0.5, 0.7, and 0.9 m from the inlet.

   The column was percolated with seepage water at a constant Darcy velocity of $(9.5 \pm 0.5) \cdot 10^{-8}$ m/s. The solution was injected at the top and drained at the bottom of the column. Thus, variable water saturated conditions were reached. After conditioning with tracer-free solution for six months (phase 1) seepage water containing 10^{-5} M U(VI) was applied for eight months yielding a long rectangular pulse injection (phase 2). After that the column was rinsed with tracer-free seepage water for twelve months (phase 3). All suction probes and the column outlet were sampled weekly and analyzed for pH, major ions, and uranium. The transport parameters of a conservative tracer were measured by means of tritiated water under the same flow conditions.

   After 610 days (370 days after starting phase 3) solid material was taken from sealable openings at the positions of the suction probes. Aliquots of 2 g were used to determine the volumetric water content. The material was washed with MilliQ water to remove the pore solution probably disturbing spectroscopic measurements.

Spectroscopic investigations

The uranium speciation influenced by various processes such as aqueous complexation, surface complexation, surface precipitation or formation of secondary phases was investigated applying advanced spectroscopic tools. Two series of samples were analyzed. Five solid samples were taken after 610 days from the column and treated as described above. Immediately before that also five aqueous samples were extracted. Time-resolved laser-induced fluorescence spectroscopy (TRLFS) was applied due to its high sensitivity for uranium and the provision of three independent information blocks: the intensity of the fluorescence emission, the spectral shift, and the decay time of the fluorescence signal (describing the time after which the signal has decreased to *1/e* of the start intensity), allowing in
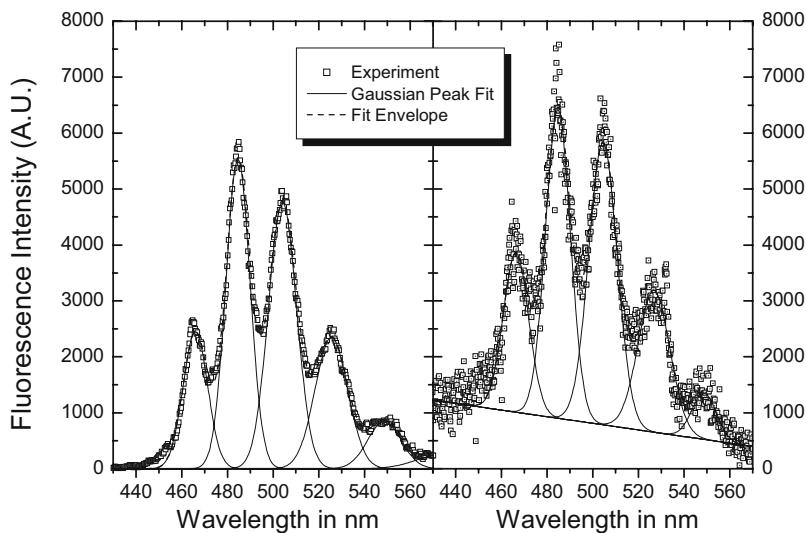
combination a distinction of a variety of uranium surface species and dissolved complexes coupled with semi-quantitative results.

The TRLFS system consists of a Nd:YAG diode laser with subsequent fourth harmonic generation. This wavelength (266 nm) was used for the excitation of the samples, providing an optimal signal-to-noise ratio. The emitted fluorescence radiation was focussed into a spectrograph and the resulting spectra were measured by a diode array (701 intensified diodes). The gate width (exposure time) is variable from 5 ns to 2 ms. Here, 5 µs were used. The delay time after the excitation laser pulse ranges from 0 ns to 6500 ns. For further details concerning the set-up of the TRLFS equipment and operation modes see Geipel et al. (1996). Every spectrum was measured three times, and for each spectrum 100 laser shots were averaged. 31 spectra at steadily increasing delay times were collected totally for one time-resolved spectrum.

Results

Aqueous speciation of uranium(VI)

There are extensive reviews of the aqueous uranium speciation available, the most prominent work was performed under the auspices of the Nuclear Energy Agency (NEA) within the Organisation for Economic Co-operation and Development (OECD). As part of the NEA Thermochemical Database a special volume dedicated to uranium was issued in 1992 (Grenthe et al., 1992), with major revisions published in 2003 (Guillaumont et al., 2003). Based on these data and applying the EQ3/6 geochemical speciation code (Wolery, 1992) the aqueous speciation of uranium in the pH range of interest between 7 and 9 was computed. It turned out that the neutral aqueous complex $Ca_2UO_2(CO_3)_3$ (Bernhard et al., 2001) is the dominating species under the applied experimental conditions, binding around 78 % of all uranium at pH 7 and rising up to nearly 100 % at pH 7.5 and higher. Between pH 7 and 7.5 the contribution from the ternary aqueous complex $(UO_2)_2CO_3(OH)_3^-$ decreases from about 15 % to zero. The calculations furthermore did not indicate any supersaturation with respect to possible secondary uranium phases. Namely, the amount of silica and phosphate released by quartz and HAP dissolution processes, respectively, was too low to precipitate uranyl silicate or uranyl phosphate minerals. Even the formation of respective aqueous uranyl complexes can be neglected.

Fig. 1.   Fluorescence spectra with peak deconvolution of $Ca_2UO_2(CO_3)_3(aq)$ (left side) and pore water from the quartz/HAP column (right side).

These predictions were compared with the spectroscopic findings. A typical spectrum of the aqueous samples is shown on the right side of Fig. 1. The spectrum on the left side was obtained from a solution containing just the neutral $Ca_2UO_2(CO_3)_3$ uranium species. A comparison of the two spectra show a similar blue shift of the major five peaks, of about –5 nm with respect to the uncomplexed uranyl ion in acidic solutions (Bell and Biggers, 1968; Brachmann, 1997). In addi-

Table 2. Fluorescence properties of selected aqueous uranium species.

Spectroscopic Characteristics	Free UO_2^{2+} [a]	$Ca_2UO_2(CO_3)_3$ [b]	This work
1st Peak in nm	472	466	466.4
2nd Peak in nm	488	484	484.9
3rd Peak in nm	510	504	504.5
4th Peak in nm	535	524	526.8
5th Peak in nm	560	-	548.8
Lifetime in ns	1570	43	50

[a] Brachmann, 1997, [b] Bernhard et al., 2001

tion, the fluorescence decay times (43 ns for the $Ca_2UO_2(CO_3)_3$ complex and about 50 ns for the column samples) are very similar. Therefore it is very likely that indeed (as postulated by the geochemical computations) the neutral $Ca_2UO_2(CO_3)_3$ complex is dominating the aqueous uranium speciation. The spectroscopic properties are summarized in Table 2.

Sorption of uranium(VI) onto HAP

In the batch experiments a strong interaction of the uranium contained in the seepage water with HAP was observed. The measured equilibrium concentrations of uranium in the supernatant amounts to $(2.7 \pm 0.3) \cdot 10^{-9}$ M, *i.e.*, four orders of magnitude lower than in the starting solution. Uranium adsorbs nearly quantitatively to the HAP surface. The calculation of the distribution coefficient K_D from this equilibrium concentrations is not meaningful for the steep slope of K_D at adsorption rates approaching 100 %.

The surface speciation of uranium on apatite-like minerals has been investigated in several works: Drot et al., 1998; Fuller et al., 1996 & 2002; Arey et al., 1999; Simon et al., 2004. Unfortunately, no parameter sets for surface complexation models have been derived so far for this system, thus prohibiting predictive modeling.

In addition, the small amount of HAP compared to quartz results in rendering uranyl quartz surface species strong competitors to any uranyl reactions onto phosphate surface groups. This holds despite the much weaker character of the silanol uranyl bond when compared to the phosphate uranyl bond.

Again, the TRLFS investigation proved to be a valuable tool to discriminate between the various possible surface complexes. The measured spectra are rather small and noisy but nevertheless a proper data processing reveals the major spectroscopic properties. The fluorescence decay indicated two distinctive species having lifetimes of (569 ± 53) ns and of (54.6 ± 0.6) µs. However, their major fluorescence peaks did not differ significantly. The peak maxima occur at 482.8, 502.0, 522.1, 547.0, 571.1, and 599.5 nm. This corresponds to an average shift of +11 nm relative to the free uranyl cation. A comparison with typical spectra obtained from uranium sorbed onto pure HAP (average wavelength shift of +12 nm and lifetimes of 570 ns and 3.5 µs) and pure quartz (average wavelength shift of +9 nm and lifetimes of 780 ns and 45 µs) showed that the uranium surface species with the shorter lifetime clearly can be attributed to uranyl sorbed onto HAP. The uranium surface species with the longer lifetime probably is a uranyl unit bond to a silanol surface group from quartz.

Transport behavior of uranium

The interpretation of the tracer transport in the porous medium is based on the one-dimensional transport equation

$$R_f \frac{\partial c}{\partial t} = D \frac{\partial^2 c}{\partial x^2} - v \frac{\partial c}{\partial x} \qquad (1)$$

where c is the tracer concentration, v is the pore-water velocity, D is the hydro-dynamic dispersion coefficient, R_f is the retardation factor, t is the time, and x is the distance. R_f is related to the empirical distribution coefficient K_D by
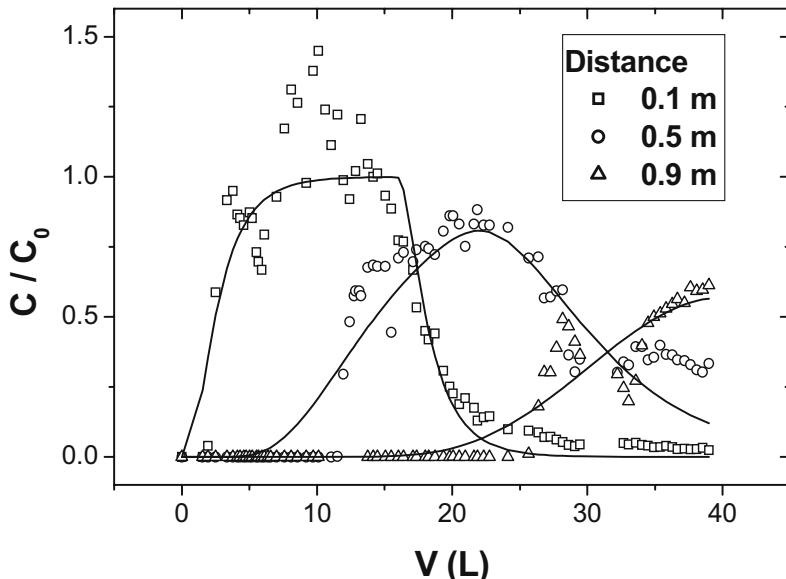
$$R_f = 1 + \frac{\varsigma K_D}{\theta} \qquad (2)$$

where ς represents the dry bulk density and θ the volumetric water content of the porous medium. The connection between pore-water velocity and Darcy velocity v_D is given by

$$v = \frac{v_D}{\theta} \qquad (3).$$

The according parameters were estimated using the CXTFIT code (Toride et al. 1995).

The volumetric water content θ in the column determined gravimetrically at the observed vertical positions is given in Table 3. Water unsaturated conditions occur in the upper three positions whereas the transition zone to water saturated condi-

Fig. 2. Breakthrough curves of uranium normalized to the input concentration C_0 vs. eluted volume at different distances from the inlet (symbols: experimental values, lines: model).

tions is located in the bottom part.

The breakthrough curves (BTC) of uranium normalized to the input concentration C_0 and the corresponding model curves are depicted in Fig. 2. The fitted parameters v, D, and R_f are shown in Table 3. The BTC's exhibit a steeply rising edge. The subsequent expected plateau in phase two is overlaid by concentrations exceeding C_0 in the first monitored position (x = 0.1 m). This could be produced by a temporarily increased input concentration, ion exchange processes displacing uranium, or a mobilization of colloid borne uranium. So far, the reason is not clear. The maximum concentration at the different vertical positions continuously decreases over the column length. The dropping edge of the uranium BTC's exhibits a long tailing at a low concentration level ($0.02 \cdot C_0$ at x = 0.1 m) which was not observed to that degree in the tritium BTC's. Therefore, a double porosity effect in the unsaturated zone might play a role, however, the tailing of the uranium curves is clearly influenced kinetically.

Certainly, the simple model based on the K_D concept is not able to describe the breakthrough behavior perfectly. Above all it fails to model the kinetic processes, *i.e.*, the long tailing. The derived R_f values can only describe the arrival of the contaminant plume, but not its elution. The R_f values over the column length show only minor differences. In the transition zone to the saturated zone it is slightly increased and drops in the saturated zone. In general the observed heterogeneity of the transport properties is small at this scale.

Evaluating the BTC at x = 0.1 m it becomes clear that the elution of uranium is governed by two processes. A fast desorption results in a swift dropdown followed by a slow release over a long period which is not yet completed. This is in concordance with the residual uranium concentration in the solid at the uppermost position where elution is in progress. It still amounts to about 30 % of the solid concentration at the lower positions. Since the elution proceeds at a low level we cannot prove the full irreversibility of the fixation of uranium. The calculation of a recovery makes no sense unless the BTC dropped to zero. Nevertheless, the slow release yields in low uranium concentrations of approximately 10^{-7} mol/L.

Table 3. Transport parameters derived from the column experiment.

Distance	θ^a	$v^{b,c}$	$D^{b,c}$	$R_f{}^b$	$C_{solid}{}^d$
[m]	[mL/mL]	[10^{-6} m/s]	[10^{-8} m^2/s]	[-]	[mg/kg]
0.1	0.09±0.005	1.00±0.05	2.1±0.1	32±3	1.4±0.1
0.3	0.09±0.005	0.97±0.05	0.5±0.03	38±4	3.4±0.3
0.5	0.08±0.005	0.98±0.05	1.0±0.05	37±4	5.3±0.5
0.7	0.13±0.006	0.98±0.05	1.1±0.05	45±4	3.9±0.4
0.9	0.46±0.02	0.53±0.03	0.4±0.02	27±3	3.7±0.4

[a] determined gravimetrically; [b] fitted parameters from CXTFIT; [c] determined from tritium BTC; [d] U concentration in the solid after 610 days

Conclusions

Time-resolved laser-induced fluorescence spectroscopy proved to be a valuable tool in supporting column sorption experiments. We were thus able to identify relevant uranium(VI) species both in solution and on surfaces. Sorption is a significant process and dominated by silanol and phosphate groups stemming from quartz and HAP, respectively. The specific binding (chemisorption) of uranium onto phosphate surface binding sites is much stronger than to silanol groups. This occurrence of two surface species corresponds to the findings from the column experiments. It seems logical to assign the faster sorption / desorption scheme to the uranyl silanol surface species, exhibiting an almost full reversibility. The second observed process creating the long and pronounced tailing in the BTC's can be explained by the much stronger binding of the uranyl moiety to the phosphate sites. There, the significantly lower reversibility may also arise from a beginning surface precipitation or diffusion of UO_2^{2+} into the crystal lattice. This, however, has still to be proven by further spectroscopic investigations. Furthermore, the transport model has to be extended by kinetic terms and appropriate parameters in order to enable a profound prediction of the long-term behavior.

   In general, the addition of phosphate mineral such as HAP even at low concentrations will efficiently increase the retardation. It must, however, be kept in mind that HAP is stable only at pH above 5 (depending on the background concentration of calcium), thus other retarding additives are required for reactive barriers designed to operate also under acidic conditions. The next step is to investigate the influence of the background electrolyte composition, namely with high concentration of other cations competing with the uranyl cation for sorption sites.

Acknowledgement

References

Arey JS, Seaman JC, Bertsch PM (1999) Immobilization of uranium in contaminated sediments by hydroxyapatite addition. Environ. Sci. Technol. 33: 337-342

Bell JT, Biggers RE (1968) Absorption spectrum of the uranyl ion in perchlorate media III. Resolution of the ultraviolet band structure: Some conclusions concerning the excited state of UO_2^{2+}. J. Mol. Spectrosc. 25: 312-329

Bernhard G, Geipel G, Reich T, Brendler V, Amayri S, Nitsche H (2001) Uranyl(VI) carbonate complex formation: Validation of the $Ca_2UO_2(CO_3)_3$(aq.) species. Radiochim. Acta 89: 511-518

Brachmann A (1997) *Zeitaufgelöste laser-induzierte Fluoreszenzspektroskopie zur Charakterisierung der Wechselwirkung des Uranylions mit Huminsäuren und Carboxylatliganden.* Ph.D. Thesis. TU Dresden, 198pp

Drot R, Simoni E, Alnot M, Ehrhardt JJ (1998) Structural environment of uranium(VI) and europium(III) species sorbed onto phosphate surfaces: XPS and optical spectroscopy studies. J. Coll. Interf. Sci. 205: 410-416

Fuller CC, Bargar JR, Davis JA, Piana MJ (2002) Mechanisms of uranium interactions with hydroxyapatite: implications for groundwater remediation. Environ. Sci. Technol. 36: 158-165

Fuller CC, Davis JA, Coston JA, Dixon E (1996) Characterization of metal adsorption variability in a sand gravel aquifer, Cape Cod, Massachusetts, U.S.A. J. Contam. Hydrol. 22: 165-187

Geipel G, Brachmann A, Brendler B, Bernhard G, Nitsche H (1996) Uranium(VI) sulfate complexation studied by time-resolved laser-induced fluorescence spectroscopy (TRLFS). Radiochim. Acta 75: 199-204

Geipel G, Thieme M, Bernhard G, Nitsche H (1994) Distribution of uranium and radionuclides in a uranium-mining rockpile in Schlema, Saxony, Germany. Radiochim. Acta 66/67: 305-308

Grenthe I, Fuger J, Lemire RJ, Muller AB, Nguyen-Trung C, Wanner H (1992) *Chemical Thermodynamics of Uranium.* Elsevier, Amsterdam

Guillaumont R, Fanghänel T, Fuger J, Grenthe I, Neck V, Palmer DA, Rand MH (2003) *Update on the chemical thermodynamics of uranium, neptunium, plutonium, americium and technetium.* Chemical Thermodynamics Vol. 5 (OECD Nuclear Energy Agency, ed.), Elsevier, Amsterdam

Jerden JL jr., Sinha AK (2003) Phosphate based immobilization of uranium in an oxidizing bedrock aquifer. Appl. Geochem. 18: 823-843.

Jones A, Wall F, Williams C (1996) Rare earth minerals: chemistry, origin and ore deposits. Chapman Hall, London, 372p.

Simon FG, Biermann V, Segebade C, Hedrich M (2004) Behaviour of uranium in hydroxyapatite-bearing permeable reactive barriers: investigation using [237]U as a radioindicator. Sci. Total Environ. 326: 249-256

Toride N, Leji FJ, van Genuchten MT (1995) *The CXTFIT Code for Estimating Transport Parameters from Laboratory or Field Tracer Experiments. Version 2.1.* Research Report No. 137. U.S. Salinity Laboratory, Agricultural Research Service, U.S. Department of Agriculture, Riverside, California

Wolery TJ (1992) *EQ3/6, A software package for the geochemical modeling of aqueous systems.* UCRL-MA-110662 Part I, Lawrence Livermore National Laboratory

Active and passive water treatment techniques

Integrated water protection approaches under the WISMUT project: The Ronneburg case

Michael Paul, Manfred Gengnagel, Delf Baacke

WISMUT GmbH, Abteilung Engineering, Jagdschänkenstr. 29, 09117 Chemnitz, Germany, E-mail: m.paul@wismut.de

Abstract. At WISMUT's Ronneburg mine site since 1991 a combined remediation strategy has been realised, which consists of the following central elements: clean-up of operational areas, backfilling of the open pit mine with waste rock from the surrounding piles, flooding of the underground mine and construction/ operation of technical water management systems. This remediation approach can be characterized by a number of environmental benefits which include the termination of water quality problems caused by the waste rock piles which were originally spread over a large area, the immobilization of toxic substances in the area of the underground and the open pit mine and the termination of surface water pollution by the discharge of effluents from the mine drainage system. These effects enabled WISMUT to minimize the additional construction and operational costs for technical water management and treatment systems which are, however indispensable for the successful completion of the closure work.

Introduction

WISMUT GmbH is carrying out the closure of the entire East German uranium mining industry which makes this remediation program to one of the largest mine closure projects in the world. Among WISMUT's former mining sites the Ronneburg mining district which produced from both underground and open pit operations was the most important with a production of approximately 113 kt U between 1951 and 1990. Mineralisation was present as lenses and stockworks within a package of slates, magmatites and limestones, approximately 250 m thick, reaching from upper Ordovician to lower Devonian with an average uranium content of less than 0.1 percent.

By the end of production in 1990 the mining legacy at the Ronneburg site consisted of: (1) a complex underground mine with 40 shafts, about 3000 km of mine workings and an open volume of about 24 million m^3 to be closed, (2) Waste rock material with an overall volume of about 200 Mm^3 to be remediated, (3) Operational areas of 1670 ha to be cleaned up and prepared for reuse, (4) an open pit mine with a total volume of about 160 Mm^3 and a maximum depth of 240 m to be stabilized. Due to partial backfilling during the operational phase the volume of the pit decreased from the original 160 Mm^3 to about 84 Mm^3 before the remediation activities commenced.

The paper gives an overview on the conceptual and remediation activities since 1991 and their specific role concerning the integrated water protection approach which has been realized at the Ronneburg site.

Hydrogeological setting

The Ronneburg uranium mining district in Eastern Thuringia is located on both sides of the water divide between the Weiße Elster and the Pleiße rivers, which are both tributary to the Elbe river basin. The southern part of the district is situated at the so-called Ronneburger Horst, the north-eastern part of the Berga anticline of the Thuringian shale highlands, where the host rocks of the mineralized zones are directly outcropping. In the northern part of the district, which consists of the mine fields of Beerwalde, Drosen and Korbußen, the productive palaeozoic rocks are partly covered by permotriassic platform series.

The mean annual precipitation rate in the district amounts to ca. 680 mm/a according to time series evaluations based on the Gera-Leumnitz station values (German federal weather service) covering the 40-year-period between 1964 and 2003. Groundwater drawdown as a consequence of operating the mine drainage system of the southern mine fields covered an area of about 40 square kilometers. Before flooding the average inflow into the drainage system amounted to about 650 m^3/h with variations from < 500 m^3/h up to 800 m^3/h (based on monthly values, time series between 1991 and 1997). Mine water inflow and area can be used to evaluate the mean groundwater recharge rate of about 140 mm/a or 4,5 l/s*km^2.

In terms of water quality conditions it is characteristic for the Ronneburg district that due to the iron sulfide concentrations of up to 5 % in the palaeozoic rocks the mine waters as well as the seepages from the waste rock dumps were carrying very high concentrations of dissolved iron, sulphate, heavy metals (Mn, Ni, Co, Cu, Zn, Cd) and radionuclides (Table 1). Since the prevailing rock forming carbonate mineral in the deposit is dolomite extreme sulphate concentrations of up to 40 g/L were occuring in waste rock seepage, accompanied by hardnesses of up to 2000 °dH dominated by magnesium.

Prior to remediation the impact on the freshwater reservoirs downstream the mine was dominated by the mine water discharge which was performed both to the Wipse creek (tributary to the Weiße Elster, southern mine fields, see Table 1) and to the Sprotte system (tributary to Pleiße river, northern mine fields). Total

Active and passive water treatment techniques

Table 1. Water quality typical for waste rock dumps in comparison to mine water of the southern mine fields prior to flooding (arithmetic mean, 1992-1997).

	Waste rock seepage, Acid type (Nordhalde, e-443)	Waste rock seepage, Neutral type (H. Paitzdorf, e-508)	Mine water discharge to Wipse creek (e-404)
Flow rate (m^3/h)	0.6	1.6	778
PH	2.9	7.6	6.9
Mg (mg/L)	1390	3443	389
Ca (mg/L)	354	402	339
SO_4 (mg/L)	12,970	14,140	2,354
Total Fe (mg/L)	2,126	1.6	4.3
Total Mn (mg/L)	128	0.8	5.4
Cu ($\mu g/L$)	3,835	14	93
Ni ($\mu g/L$)	30,610	138	1,252
Co ($\mu g/L$)	11,735	14	327
Zn ($\mu g/L$)	23,870	79	625
Cd ($\mu g/L$)	293	2.2	7.5
As ($\mu g/L$)	40	4.0	2.8
U (mg/L)	1.2	1.7	0.3
Diss. ^{226}Ra (mBq/L)	12	32	134

mine water discharge averaged to > 1000 m^3/h for the whole mine district. The only treatment measure consisted of simple aeration/ precipiation in settlement ponds to primarily minimize the iron contents of the discharged mine waters.

Seepage water flow rates from the waste rock dumps amounted to some m^3/h for the smaller objects but up to some tens of m^3/h for the biggest waste rock dumps, such as the former Absetzerhalde with a total area of 225 ha. However, due to the lack of impermeable base liners under the piles and because of the location of most of the piles within the drawdown area of the underground mine most of the seepage water was draining to the underground galleries. So the seepage from the Absetzerhalde and the internal dumps of the open pit became the most important polluters of the mine waters of the Lichtenberg and Schmirchau mine fields.

Basic elements of the remediation strategy

Individual remediation measures at the Ronneburg site are basically grouped into two main complexes:
a) Closure and clean-up of the underground mine including mine flooding,
b) Remediation of the waste rock dumps in combination with the stabilization of the open pit, including area clean-up.

Active and passive water treatment techniques

From the viewpoint of water protection the individual remediation measures can be classified into three groups of approaches: (1) Source control, (2) migration control, (3) water treatment.

Beginning with the first remediation concept in 1991 great importance has been attached on applying a broad variety of source and migration control measures to enhance the sustainability of the whole remediation work but also to minimize the efforts necessary in terms of water treatment which will be the most important and cost intensive long term burden of the entire project. The most important item to be mentioned here is that both the strategies for mine flooding and waste rock dump remediation/ pit backfilling have been developed and implemented in a co-ordinated way to make use of synergetic effects.

The source and migration control concepts applied will be discussed in the following chapters, an overview on the different measures is given in Table 2.

Table 2. Measures applied in terms of water rehabilitation.

category	remediation measures	under-ground mine	open pit	waste rock	conta-minated areas
Source control	flooding	x	x		
	subaquatic deposition	x	x	x	
	alcali addition/ injection	x	x		x
migration control	minimization of the area		x	x	x
	dry covers/ revegetation		x	x	x
	plugging of migration path-ways	x			
	geochemical barriers	x	x		
water treatment		x	x	x	x

Management of AMD-generating waste rock

Dumped mine wastes from the open pit and the underground mines amounted to about 200 million m³ (Weise et al 1996) at 17 single locations. The biggest piles of the district were the Absetzerhalde (65 Mm³) and the Nordhalde (30 Mm³), the smallest were containing some 100,000 m³ only. About 64 Mm³ of mine waste had been deposited in the open pit mine during active mining (Innenkippe, Schmirchau balcony). The wastes comprised for the most part shales, limestones and diabases with a high tendency to AMD (see Table 1).

Extensive investigations were carried out between 1992 and 1996 on waste rock material to determine crucial geochemical and soil physical parameters. The investigations included the review of historical and geological informations, drilling of boreholes, excavation of test pits, static laboratory tests and kinetic column and lime addition tests (Weise et al 1996, Hockley et al 1997).

Based on intensive cost-benefit-analyses of different remediation options the relocation of the waste rock into the Lichtenberg open pit was chosen as the preferred remediation option for more than 90 % of the waste rock. This basic decision makes the controlled backfilling of the Lichtenberg open pit the most important single restoration project of the whole WISMUT program. To minimize the long-term impact of the waste rock material to the ground and surface water bodies waste rock relocation is implementing the following remediation principles:

1) spatial concentration of the waste rock,
2) minimization of the mobility of the contaminants of concern by means of geochemically controlled relocation (separation), alcali and ash addition
3) decrease of the rate of contaminant transport from the backfill to the groundwater due to high compaction of the waste rock and bypassing of the groundwater stream (open drift system in the vicinity of the pit)
4) dry cover construction for infiltration control and minimization of the oxygen ingress including an optimized re-use (predominantly forest)

Since the mobility of radionuclides and heavy metals essentially depends on the degree of acid generation of the waste rock the prediction of long-term geochemical material behaviour was highly significant for remediation planning. The ABA test on drill core samples was chosen for the long-term planning of waste dump relocation, since this test allows rapid assessment of the acid mine drainage risk from sulphide-bearing waste. As the spatial variability of material properties cannot be ascertained in sufficient detail from drilling data (obtained on a 100 m grid) for the purposes of waste pile relocation, long-term planning is supported by a program of short-term excavation control. Under this program, test pit samples are taken on a 25 m grid from the excavation face one to three months ahead of relocation. The material is then classified by a combination of paste pH and NAP pH/conductivity methods (Weise et al. 1996, Hockley et al. 1997). Due to their simplicity, paste and NAP tests, calibrated against ABA data and kinetic test results, are particularly well suited to provide readily available guidance for mining and rehabilitation planning.

Targeted placement in the pit allows the minimization of contaminant release into the groundwater. Acid or acid generating class A material is mixed with quicklime and placed in the deepest zone of the open pit which will be water-satured by rising ground water and hence become anoxic. Class C material placed in the upper zone of the backfilled open pit is to consume incoming oxygen by sulphide oxidation and at the same time impede seepage acidification by neutralisation. Class B material which includes mixtures of A- and C-Material is beeing relocated in between.

Following completion of the backfill that will be up to 60 m above the initial ground level, a dry cover will be placed on top of the backfilled mine wastes. The area to be covered amounts to about 220 ha. As a result of comprehensive studies and investigations, a combined cover of cohesive soil material from on-site excavation (1.6 m) overlain by a 0.4 m thick storage layer to restore natural soil functions for revegetation was derived and submitted for approval (Paul et al. 2003). Together with hydraulic measures, this approach is to meet any requirement in

terms of radiology, water protection, stability, erosion protection, and reuse. Waste rock relocation is planned to be finished in 2007.

Waste rock of the northern mine fields has been concentrated at the location of the Halde Beerwalde waste rock dump with a total volume of 8.8 Mm^3 after aggregation of the former Drosen and Korbußen piles. The pile has been covered with a two layer cover system consisting of a 0.4 m thick compacted sealing layer overlain by 1.5 m of recultivation layer. Seepage water (1-2 m^3/h in average) is being treated together with the contaminated surface and seepage waters of the southern part of the district.

Area clean-up

Operational areas in the Ronneburg region amounted to about 1670 ha from which about 460 ha had been covered by waste rock dumps. Remediation of contaminated areas i.s.s. is being realised basically in two steps: (1) demolition of operational facilities respectively decontamination and (2) reconstruction respectively rehabilitation for future public use or specific needs.

Decontamination includes removal and relocation of mining and production facilities, of organic, inorganic and radioactive contaminated soil and waste rock to stop or minimise the dispersion of toxic agents. Waste disposal activities take place in the Lichtenberg open pit or to a controlled landfill site, respectively.

Remediation measures to be applied have to be conform to the federal mining act as well as to current soil and water regulations, but must also be optimised in terms of costs for both implementation and maintenance.

The footprint areas of the relocated waste rock dumps are represented by often unfertile, sometimes acidic and biological dead raw soil substrates of high compaction and low water storage capacity. Especially the exhumed footprint areas of the Absetzerhalde and the Nordhalde which account for about 80 percent of the waste rock to be relocated and ca. 300 ha of land to be reclaimed, make high demands on the remediation measures. The soils are still carrying substantial amounts of soluble contaminants such as Al, heavy metals, SO_4 and others due to former infiltration of waste rock seepage. As a consequence remediation measures which are strictly beeing adapted to local conditions typically include lime addition to stabilize soil pH and to minimize the mobility of heavy metals. Lime dosage calculated for 4 dm operation depth accounts for clay, gravel and humus content, average lime quantities are 8 t/ha $CaCO_3$. Dispersion of lime is combined with loosening the ground after reshaping of the surface. Depending on the physical characteristics and the state of bedrock up to 0.5 m inert soil will be applied. Thickness of inert soil depends chiefly on future use. Erosion control is guaranteed mainly by sowing a grass-herbage-mixture. In cases of later forestation, which has to be carried out at an area of 200 ha as a compensation measure for clearing of former woodland, good experience has been made with vegetation in strips across to the dip of slopes, keeping soil strips free for tree scions. Fertilizing is adopted to local conditions, fencing against game has been proven to be indis-

pensable. Contaminated run-off from the rehabilitated areas will be treated as long as necessary. Over the medium term the water balance will recover, and pollutant transfer to the receiving streams will drop under a critical limit as a result of the remediation measures performed.

Closure of the underground mine and mine flooding

Prior to mine flooding intensive preparation measures had been realized to remove water contaminants (e.g. oils, lubricants) from the mine, to stabilize/ backfill mine openings and shallow workings and to separate mine fields with different water quality.

Flooding of the underground mine is taking place within two hydraulically isolated areas: (1) Mine fields south of the federal motorway A 4, (2) Mine fields north of the motorway A 4. Both parts of the mine are hydraulically separated. The southern mine fields also include the Lichtenberg open pit mine, which is under backfilling with material from the surrounding waste rock piles since 1991.

Fully fledged flooding of the southern mine fields was initiated at the turn of 1997/1998 after a four-year-permitting and preparation phase. Flooding of the northern mine fields started in 2000 (Paul et al. 2002, Gatzweiler et al. 2002).

Since the mine is completely backfilled in its uppermost 100 meters and no dewatering adits are available the flood waters are expected to eventually discharge as natural exfiltration into local receiving streams. As the mine water quality in the central part of the southern mine fields does not allow untreated discharge, the mine water has to be catched and treated. Due to the orographic and geologic conditions such discharges can arise at the earliest at a flooding level of approx. 240 m above sea level. Thus an extensive water management system had to be designed to avoid an intolerable impact of the mine closure on the environment with special reference to ground and surface waters in the central part of the southern mine fields.

Both model based predictions and monitoring time series from the northern mine fields show much better water quality conditions; so there is no necessity for extensive technical water management facilities as a prerequisite for reaching the final flooding water level.

By May 2005 the water levels in the southern and northern mine fields have reached levels of approx. 220…250 m above sea level. The flooding operation is expected to complete between 2007 and 2009 by reaching a quasi-steady state. First mine water discharge in valley regions could appear in 2006.

In general the Ronneburg mine flooding strategy reflects the philosophy of a rehabilitation process following the extensive impact concerning water balance conditions as a result of active mining operations. Considering this any further technical interferences have to be designed following the specific necessities evaluated from the water quality conditions with their wide variability in the region. From the economic point of view any relevant overcapacities of water catchment, transport and treatment facilities have to be avoided. Extensive moni-

toring activities are an indispensable prerequisite for following that strategic approach.

Water treatment

Despite of all activities of source and migration control water treatment is an indispensable component of the closure plan, at least for the southern mine fields. Due to the expected water volume in the flooded mine and the preferred flooding strategy the water management system for the southern mine fields consists of installations for water collection, transport, treatment and discharge.

Water collection will be mainly realised in the Gessental valley which is expected to be the main water discharge area of the contaminated groundwater after the groundwater rebound has finished. Ascending water consists of mainly mine water bearing groundwater contaminated with typical inorganic pollutants like radionuclides and heavy metals. A basic system of drainage elements installed inside hydraulic conductible quarternary sediments overlaying preferred silurian bedrock is going to collect ascending waters under anaerobic conditions. A pump station downstream will convey the water to the central component of the system, the Ronneburg water treatment plant (WTP). First exfiltrations are predicted for 2006.

The WTP completed in 2001 was the basic precondition for active control of the flooding process and to prevent a hazardous impact to the environment at the end of mine flooding. To meet these requirements, the WTP had been designed for a capacity of 450 m³/h, which is only about 70 % of the mean mine water inflow rate during active mining. This limitation in design capacity could be reached since the inflow rate to the contaminated area has been found to be clearly head-dependent. The decrease of the flow rate has been proven during the initial runs of the WTP in late 2003, where flow rates of ca. 280 m^3/h had been observed.

The plant operates according to the High Density Sludge (HDS) lime precipitation technology, following the principle steps: acidification for decarbonization, neutralisation and aeration for lime precipitation, sedimentation and clear water overflow, thickening of sludge and conditioning for disposal, filtration of clear water for discharge. The main treatment purpose is the separation of heavy metals and radionuclides from the mine water.

The water supply from the mine to the WTP is realized optionally both from the central pumping station of the water drainage system in Gessental valley, and from a well (Well No. 1) which is connected to the underground mine workings in central mine field Schmirchau.

Active and passive water treatment techniques

Table 3. WTP discharge limits for heavy metals, As and Ra-226.

Pollutant		Discharge limit	Pollutant		Discharge limit
As	[μg/l]	20	Ni	[μg/l]	100
Cd	[μg/l]	3	Zn	[μg/l]	200
Co	[μg/l]	100	U	[μg/l]	500
Cu	[μg/l]	50	Ra-226	[mBq/l]	400

Both opportunities of water supply are necessary, since there must be the possibility to influence the flood water rise in the mine directly using the deep well. However, the water level in the mine shall be adjusted over the long term without any water pumping directly from the open mine voids in order to reach a high inundation level, to minimize the catchment area of the mine, to limit the thickness of the unsaturated zone which is subject to further acid generation and finally to lower operational costs for water management, including water treatment and sludge disposal. After reaching the final flooding level the water will be collected in the Gessental water collection system only. At present it is predicted that the water treatment must be carried out over a period of 15 to 25 years without any interruption. The WTP must also treat the remaining contaminated surface seepage in the transition period, as long as the rehabilitation progress does not allow the surface runoff to be directly discharged into the receiving creeks and streams. At present the contaminated surface runoff is highly variable in terms of flow rate and contaminant loads, and options are under investigation to inject these waters into the underground mine to blend them with the mine waters before treatment. Treatment goals for the WTP are given in Table 3. The treated waters from the WTP will be discharged into the Wipse creek flowing to the Weiße Elster river, where additional standards especially concerning sulphate and water hardness must be keeped.

Remediation Effects with respect to ground and surface waters

The active mining and mine remediation activities as a whole can be subdivided with regard to impact on ground and surface waters into the following periods:

1) **Active mining period**, characterized by a steady state groundwater depression cone as a consequence of the mine drainage operation, accompanied by water shortage in receiving streams, water quality deterioration as a consequence of water discharge and diffuse seepage from waste rock piles

2) **Period of mine closure and remediation** with a gradual transformation of the water conditions, groundwater rebound in the wake of the discontinuance of mine water discharge, beginning improvement of the water quality in ground and surface waters

Active and passive water treatment techniques

3) **Post-closure phase** after the completion of entire mine remediation measures, accompanied with final steady state groundwater conditions, operation of water treatment facilities and discharge of the treated waters, ongoing rehabilitation of water balance and quality.

Since the start of the remediation activities the most evident step in terms of improving the water quality of the receiving streams is marked by the start of the fully fledged mine flooding process associated with the cessation of mine water discharge, which happened in early 1998 for the southern mine fields and in June 2000 for the northern mine fields, respectively. Evaluations based on the extensive monitoring activities show load reductions in the recipient streams in an order of > 90 % regarding radionuclide concentrations like uranium and radium.

Further improvement of the water quality in the catchments of the local receiving streams are closely related to the waste rock relocation program which has lead for instance to the removal of the former Gessenhalde and Nordhalde piles from the Gessenbach catchment area. Mine remediation activities concerning these waste rock piles included by early 2003 the complete excavation and transportation to the Lichtenberg open pit mine backfill operations. Meanwhile the pH-values in the Gessenbach have stabilized in a neutral zone between about 6 and 8, also heavy metal concentrations show noticeable improvement but have not yet reached a satisfactory level so far. Similar observations can be reported concerning the groundwater contamination downstream of relocated waste rock piles like the Drosen pile. The removal of the waste rock pile material had been finished in 1999, and meanwhile the groundwater monitoring results show significant decreases regarding sulphate, heavy metal and radionuclide concentrations.

In terms of the future water management at the Ronneburg site WISMUT is going to be committed by the Thuringian permitting authorities within the scope of the licensing procedures for the final design of the open pit backfill, the completion of the flooding process and the operation of the WTP to keep water quality standards for the Wipse, Gessenbach and Sprotte creeks as well as the Weiße Elster river, which are in conjunction with the aims of the EU water framework directive, but account for the specific history of the area, which hosted the biggest European uranium deposit.

References

Gatzweiler R, Jakubick AT, Meyer J, Paul M, Schreyer, J. (2002): Flooding the WISMUT mines - Learning by doing or applying a comprehensive systematic approach?- In: Proc. of the Int. Conf. Uranium Mining and Hydrogeology III, Freiberg, pp. 745-754

Hockley D, Paul M, Chapman J, Jahn S, Weise W (1997): Relocation of waste rock to the Lichtenberg pit near Ronneburg, Germany.- In: Proc. 4th ICARD, Vancouver, B.C. Canada, May 31- June 6, 1997, pp. 1267-1283

Hüttl M, Paul M (2004): WBA Ronneburg – Wasserbehandlung nach dem HDS-Verfahren.- TU Bergakademie Freiberg, Wiss. Mitteilungen 25 (2004), S. 101-106

Paul M, Gengnagel M, Vogel D, Kuhn W (2002): Four years of flooding WISMUT's Ronneburg uranium mine – a status report.- In: Proc. of the Int. Conf. Uranium Mining and Hydrogeology III, Freiberg, pp. 775-784

Paul M, Kahnt R, Baacke D, Jahn S, Eckart M (2003): Cover design of a backfilled open pit based on a systems approach for a uranium mining site.- 6th ICARD, Cairns, Australia 12-18 July 2003, pp. 351-361

Weise W, Paul M, Jahn S, Hoepfner U (1996): Geochemische Aspekte der Haldensanierung am Standort Ronneburg.- Geowissenschaften., 14 (11), 470-475

Active and passive water treatment techniques

The results of the pilot plant study for arsenic removal

Hamidur Rahman[1], Yasumoto Magara[2], Satoshi Miyabayashi[3], Yasuyuki Yagi[3]

[1]University of Rajshahi, Department of Geology and Mining, Rajshahi University Campus, 6205 Rajshahi, Bangladesh, E-mail: mhrahman@librabd.net
[2]Environmental Risk Engineering Lab., Department of Environment Engineering, Hokkdaido University, Japan
[3]Hitachi Plant Engineering & Construction Co Ltd., 456, Alexandra Road, #15-00, NOL Building, Singapore 119962

Introduction

Contamination of potable ground water (well water) with arsenic is a large problem in Bangladesh and India. For removal of arsenic from the well water, various measures are positively examined mainly by UNICEF and WHO. We recently studied, jointly with Hokkaido University and Rajshahi University, a system iron ion and arsenic by sand filtration. This paper reports the results of running of a pilot plant using the well water in Chapi Nawabganj area, which was implemented as a part of this joint study.

Principal arsenic removing methods

Table 1 indicates principal arsenic removing methods. Arsenic removing methods can be roughly classified to coagulation and filtration method, adsorption method and membrane separation method. The adsorption method and membrane separation method are capable of removing the arsenic contained in the water to the order of several mg/l. However, these methods involve problems such as hard operation and high cost. The coagulation and filtration method, on the other hand, provides such merits that the equipment is simple and the cost is low, although the removing effect is rather low, and it is advantageous when well water of a large volume is treated.

Table 1. Principal Arsenic Removing Methods.

Basic principle of coagulation and filtration method

Iron ions are coexistent with arsenic in the well water. When these iron ions are oxidized and insoluble iron hydroxide is formed, arsenic is absorbed in iron hydroxide flocs and is removed from the water. Fig. 1 indicates a model diagram of the arsenic removing principle. Arsenic is located in the water in the forms of As (III) and As (V), and they are caught by the sand filter simultaneously with iron hydroxide flocs.

Pilot plant

Fig. 2 indicates the composition of the pilot plant used for experiments. Two sand filter columns of 200mm in diameter and 2,000mm in height are laid in tandem and each one of them is filled with manganese sand of height 1,000mm. Well water oxidized with air of chemical (NAClO) is continuously supplied to these sand filter columns, and arsenic is removed in the first stage and manganese is removed in the second stage.

Active and passive water treatment techniques
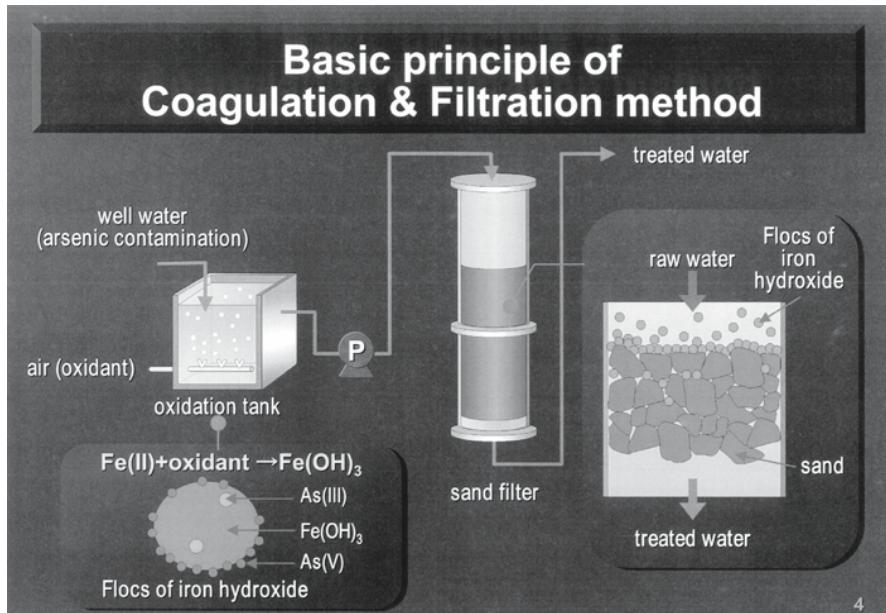
Fig. 1.   Model diagram of the arsenic removing principle.
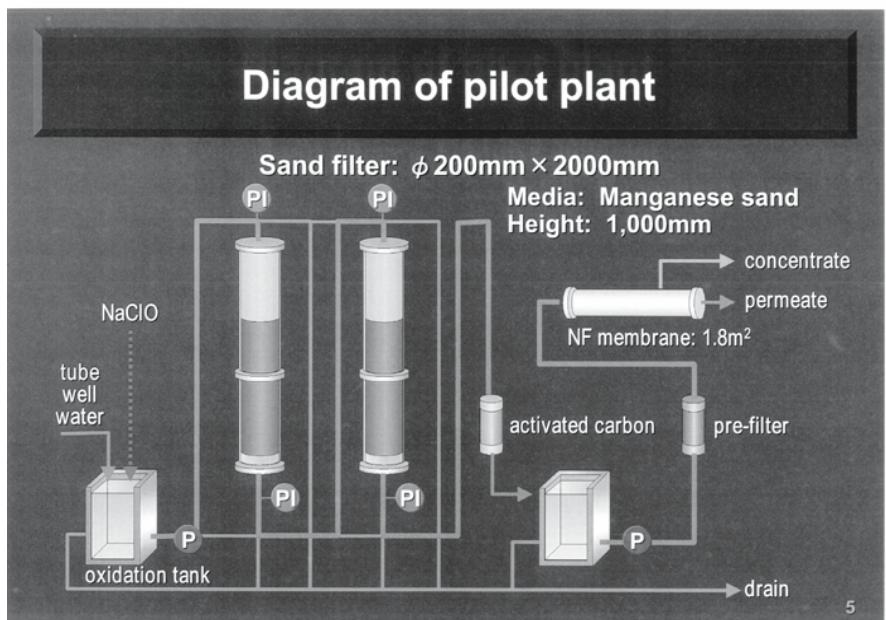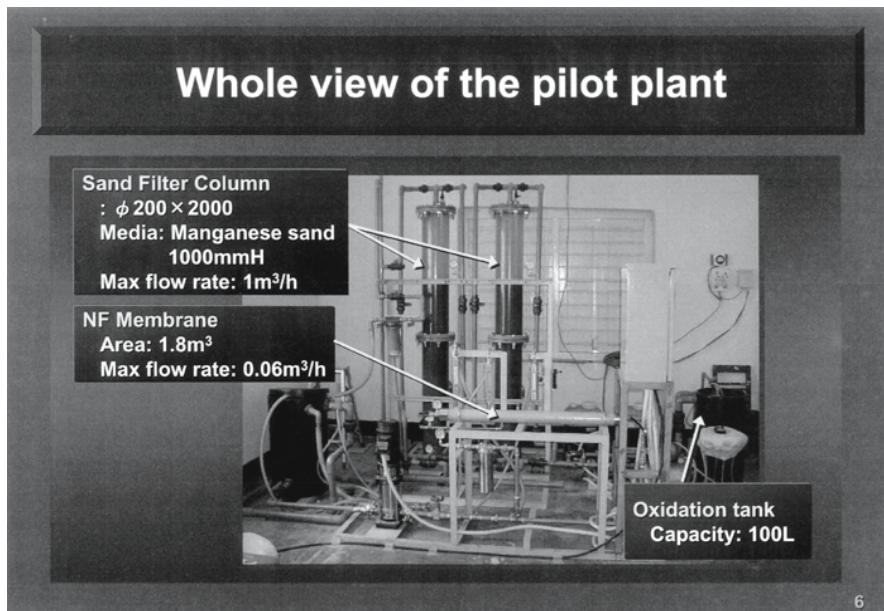
Fig. 2.   Diagram of pilot plant for As removal From tube well water

Active and passive water treatment techniques

Fig. 3.   Whole view of the pilot plant

Furthermore, a nano filtration (NF) membrane was provided for removing to a high degree the trace arsenic that outflows from sand filter columns. Fig. 3 indicates an external appearance of the pilot plant installed in BD Hall located in Chapai Nawabganj area. This pilot plant was installed in April 2001 and field tests at this pilot plant were conducted for about eight (8) months up to December 2001.

Results of experiments

Quality of well water

Fig. 4 indicates daily changes of the quality of the well water. The pH value varied in the range of 6.5 to 7.1 and the water temperature was in the vicinity of 30°C. The arsenic, iron and manganese content are in the range of 98 to 170 mg/l, 2,470 to 9,900 mg/l and 455 to 700mg/l, respectively. The arsenic removing performance of sand filtration is largely affected by the concentration ratio to the coexisting iron. Fig. 5 indicates typical arsenic removal in the cash where Fe/As ratio is varied. As the Fe/As ratio of the well water, which was the object of study of this time, was 20 to 45, we forecasted that the As concentration of the treated water produced by sand filtration is 30 to 40 mg/l (removal rate: 60 to 80%).
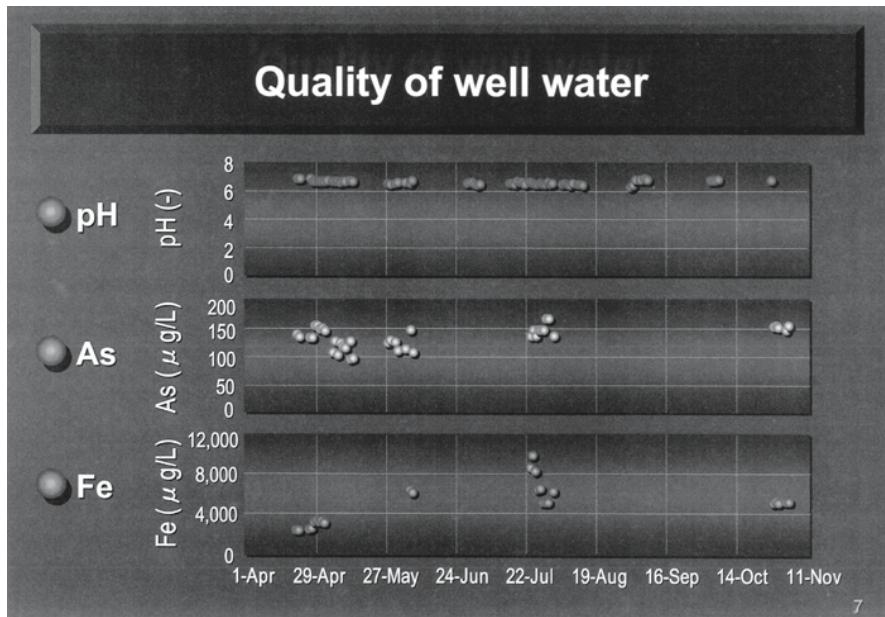
Fig. 4.   Quality of well water.
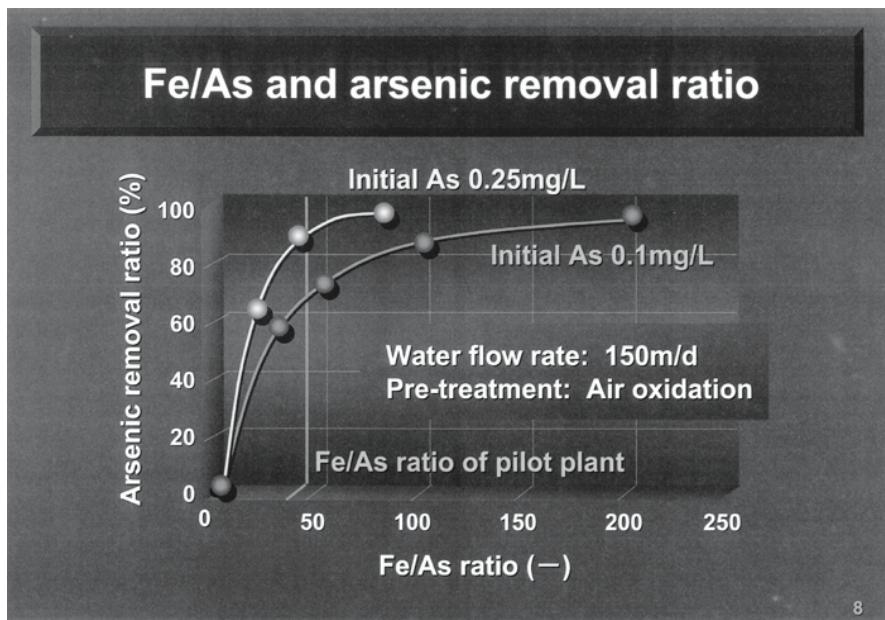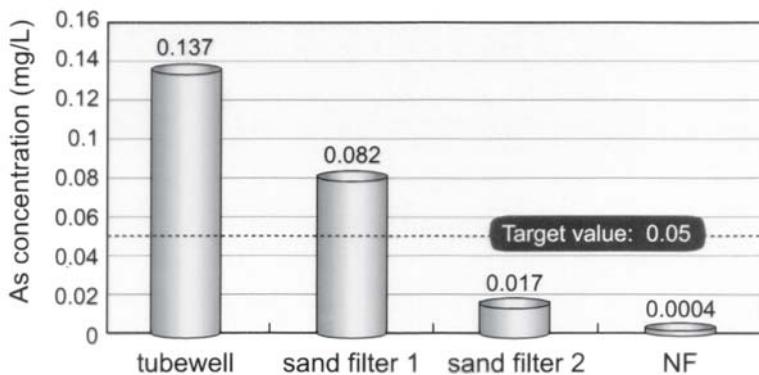
Fig. 5.   Relationship between the Fe/As ratio and As removal rate.

Active and passive water treatment techniques

○ Performance

Fig. 6.   The arsenic removal performance of pilot plant.

Arsenic removing effect of the pilot plant

We examined basic characteristics of each unit during the initial stage of running of the pilot plant. We then evaluated the arsenic removing performance under the optimum running conditions. Fig. 6 indicates the results of this evaluation. The arsenic concentration (0.136 mg/l) of the well water. which is the raw water, was reduced to 0.44mg/l after passage through sand filter column 1. The arsenic removal rate is 68% in this case, and it is less than .05 mg/l, which is the arsenic concentration advocated by WHO. That is, it is possible to remove arsenic and iron simultaneously in the sand filtration process, if the iron contained in the raw water is converted to iron hydroxide flocs by aeration in the oxidizing tank.

The NF equipment was installed with the objective to highly remove the arsenic which is left after sand filter columns. We confirmed that arsenic can be removed stable to 0.4mg/lor less by NF treatment. Although this separation equipment is of excellent arsenic removing performance, it provides the demerit of high cost, we position it as equipment for public facilities such hospitals and schools.

Optimum water feed rate to sand filter columns

The arsenic removing effect of sand filter columns is largely affected by the method for oxidation in the preceding stage and also by the flow rate of water (LV) passing through sand filter columns. Therefore, we examined the arsenic removing performance in the case where aeration is performed in the oxidizing tank and in the case where oxidizing agent (NACIO) is injected to the oxidizing tank. The LV was varied in the range of 150 to 350m/d.
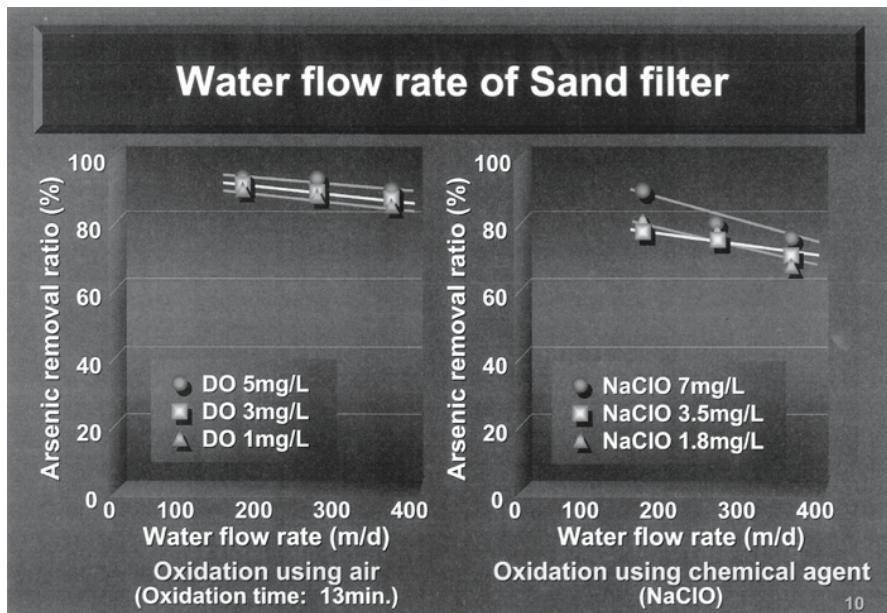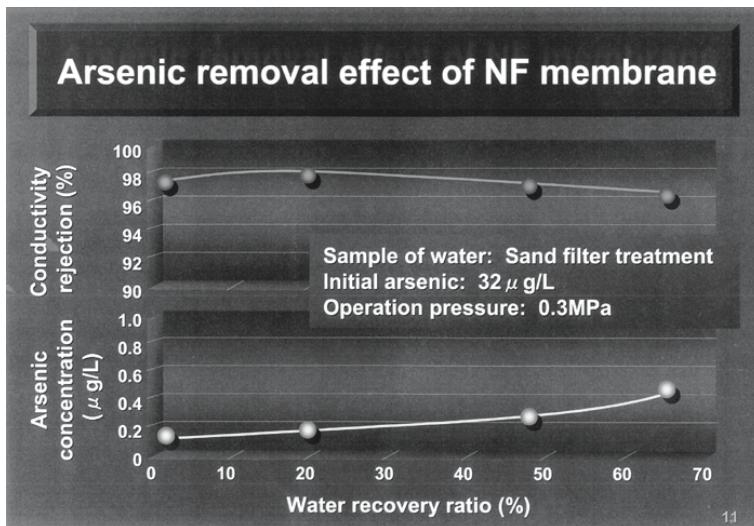
Fig. 7(a). Relationship between water flow rate and as removal ratio under aeration.

Fig. 7(b). Relationship between water flow rare and as removal ratio injection of oxidizing agent (NaCIO)

Fig. 7 (a) indicates the arsenic removing characteristics in case of aeration and Fig. 7(b) indicates the same in case of injection of oxidizing agent. Aeration was implemented with dissolved oxygen concentration used as the index, 1, 3 and 5 mg/l. When filtration was executed under the condition of LV 150 to 350 m/d after aeration (aeration time 13 minutes), although the arsenic removal rate drops to a certain extent as LV increases, arsenic removing effect of 80% or higher was obtained under any condition. On the contrary, the arsenic removing performance was of such a trend that it dropped accompanying increase of LV in case of injection of oxidizing agent. Furthermore, the removal rate was also low compared to the case of aeration.

We estimate that the reasons why the arsenic removing performance is low in case of injection of oxidizing agent are that the oxidizing agent is consumed for carbonate and manganese in the well water and that the oxidizing agent autolyzes in sand filter columns.

From the results stated above, we determined that aeration is more effective for converting iron contained in the water to iron hydroxide and obtained the outlook to be able to secure arsenic removal rate 80% under high speed filtering condition of LV 350 m/d.

Fig. 8.   Relationship between the water recovery rate and As concentration of permeated water.

Arsenic removing characteristics of NF membrane

We examined the arsenic removing performance using NF membrane with sand filtration treated water as the object. Fig 8 indicates typical results. This figure indicates the water recovery rate of the NF membrane and arsenic concentration of the filtered water. The arsenic concentration of the membrane permeated water was 0.05 mg/l or less even at water recovery rate of 60% and we were able to verify excellent arsenic removing performance of the NF equipment.

Conclusion

We installed a pilot plant in BD Hall located in Chapai Nawabganj area and checked the arsenic removing performance using actual well water. As the result to these experiments we were able to clarify the plant running conditions to reduce the arsenic content in the water to 0.05mg/l or less, which is the level advocated by WHO. with a system that combines an oxidizing tank with sand filter columns. Furthermore, we were able to secure potable water with almost on arsenic content as a result of addition of NF Separation equipment in the post stage. We intend to promote putting into practical use of purifying equipment for well water contaminated with arsenic in the future based on the results of these experiments. This type of plant can be installed for community based for getting arsenic free water at a very low cost.

Uranium in natural wetlands: a hydrogeochemical approach to reveal immobilization processes

Angelika Schöner[1], Martin Sauter[2], Georg Büchel[1]

[1]Institut für Geowissenschaften, Friedrich-Schiller-Universität, Burgweg 11; D-07749 Jena, Germany, E-mail: angelika.schoener@uni-jena.de
[2]Angewandte Geologie, Geowissenschaftliches Zentrum der Universität Göttingen, Goldschmidtstraße 3, D-37077 Göttingen, Germany

Abstract. In the former uranium mining area in Eastern Germany small natural wetlands were studied with respect to there removal efficiency for uranium. Within this project we investigated surface water samples, plant material, sediment cores and pore waters to understand hydrogeochemical processes in natural wetlands, which are assumed to be dominant factors for uranium accumulation. Uranium contents of the wetland substrates are enriched up to 3000 times compared to pore water values. Autoradiography and SEM/EDX studies revealed evenly dispersed uranium in the wetland soils. Uranium appears to be mainly sorbed to organic matter, as also shown by sequential extractions. There is no evidence for precipitation of uranium minerals.

Introduction

Historical background

Data from exploration indicate that uranium is frequently accumulated in swamps and peatlands in areas where uranium-rich source rocks occur (e.g. Kochenov et al., 1965; Owen & Otton, 1995). These observations suggest that in environments like wetlands, it might be possible to extract uranium from solutions as well as to immobilize uranium in organic-rich surficial wetland sediments. Hitherto, a limited number of studies dealt with the examination of remediation processes for uranium in natural wetlands (e.g. Idiz et al. 1986; Titayeva 1967) or wetland substrates (e.g. Braithwaite et al. 1997; Finlayson 1994). Beyond it, it was attempted

to reproduce this uranium accumulation in constructed wetlands - partly as pilot plants - in Australia (Klessa 2000; Shinners 1996), USA (Dushenkov 1997), Slovenia (Veselic et al. 2001), Bulgaria (Groudev et al. 1999) and Germany (Gerth et al. 2000), but with ambiguous results. Some dozen of wetland applications described worldwide mostly reveal inadequate efficiency. Most of these treatment wetlands didn't aim primarily at assessing the mechanisms of uranium entrapment and accumulation. However, the long-term stability of uranium species which occur in wetlands is yet unexplored, as well as the dependency of the kinetics of chemical and biological processes on specific environmental conditions (e.g. seasonal climatic changes, variations in pollutant concentrations, varying discharges).

Data from exploration indicate that uranium is frequently accumulated in swamps and peatlands in areas where uranium-rich source rocks occur (e.g. Kochenov et al., 1965; Owen & Otton, 1995). These observations suggest that in environments like wetlands, it might be possible to extract uranium from solutions as well as to immobilize uranium in organic-rich surficial wetland sediments. Hitherto, a limited number of studies dealt with the examination of remediation processes for uranium in natural wetlands (e.g. Idiz et al. 1986; Titayeva 1967) or wetland substrates (e.g. Braithwaite et al. 1997; Finlayson 1994). Beyond it, it was attempted to reproduce this uranium accumulation in constructed wetlands - partly as pilot plants - in Australia (Klessa 2000; Shinners 1996), USA (Dushenkov 1997), Slovenia (Veselic et al. 2001), Bulgaria (Groudev et al. 1999) and Germany (Gerth et al. 2000), but with ambiguous results. Some dozen of wetland applications described worldwide mostly reveal inadequate efficiency. Most of these treatment wetlands didn't aim primarily at assessing the mechanisms of uranium entrapment and accumulation. However, the long-term stability of uranium species which occur in wetlands is yet unexplored, as well as the dependency of the kinetics of chemical and biological processes on specific environmental conditions (e.g. seasonal climatic changes, variations in pollutant concentrations, varying discharges).

Scope and aim of the study

The presented study is part of a doctoral thesis dealing with uranium accumulation mechanisms and their potential use in passive treatment. The objective of the thesis is to investigate the potential for using constructed wetlands as a complementary and/or sustainable method to immobilize uranium from mine waters. What are the mechanisms for uranium entrapping and immobilizing in wetlands? In general, the efficiency of constructed wetlands is examined by collecting and analyzing water samples (e.g. Veselic et al. 2001) or by elucidating uranium fixation under experimental conditions (e.g. Liger et al. 1999). In field scale, a thorough identification of processes rarely occurs, although relevant mechanisms and aspects of longevity can only be assessed by vital case studies. Consequently, the construction of full-scale wetlands for treating mine water cannot be permitted by the authorities in Germany, although observations in natural wetlands indicate the successful wetland application for uranium-bearing discharges.

Active and passive water treatment techniques

The aim of the study was to combine geological examinations and field sampling campaigns with hydrogeochemical laboratory studies to identify mechanisms for uranium fixation in natural wetlands. Therein, predominant redox conditions in the wetland soils were determined via geochemical studies on e.g. the accumulation of iron mono-sulfides, pyrite and elemental sulfur (TRIS-extraction) (Schöner et al. 2004). The association of uranium with different soil fractions was characterized by sequential extractions (Schöner et al. 2005). Thermodynamic calculations including uranium complexes aimed at estimating the effect of potential shifts (EH value) on reductive uranium precipitation. Furthermore, on laboratory scale, uranium adsorption and reduction processes were investigated using artificial wetland substrates (Schöner 2005, in prep.).

Site description

We recorded the uranium concentration in surface water, partly also in sediments and plants from some 20 accessible natural wetlands in the former uranium mining area of Wismut GmbH in eastern Thuringia, Germany (Schöner 2005, in prep.). A specific case, wetlands at the former uranium milling areas near Zwickau (Saxony) and Seelingstädt (Thuringia), has been examined more in detail. There we sampled sediment cores from three wetlands for horizon-wise investigations on pore water and soil.

Two of the three surveyed wetland areas are located adjacent to constructed earth-fill dams which stabilize the tailings ponds of two different milling sites (IAA Crossen and IAA Seelingstädt). Therefore, these wetlands (WLHe and WLCuD) have developed as small ponds (approx. 50-200 m²) as recently as ore milling was started, about 35 years ago. Diffuse seepage from the tailing dams has washed fine-grained organic-rich sediments into the ponds. To date, the wetlands consist of up to 4 decimeters of organic-rich substrates above inorganic sediments. These substrates are water saturated with free water surface almost throughout the whole year. The third surveyed wetland pond has emerged in a forested, half-bog area some kilometers downstream the milling site IAA Crossen (WLZ). After deposition of the tailings, uranium containing seepage fed diffuse springs in the boggy forest. This wetland area contains up to 50 cm of peat, temporary with a low water freeboard.

Distribution of uranium in wetland soils and pore waters

Hydrogeochemistry

Twenty-two samples of three wetland substrate profiles (WLHe, WLZ, WLCuD) were analyzed for their total elemental and organic matter concentrations in pore

water and soil. Pore waters were extracted by centrifugation. Oven dried (60 °C) substrates were digested with a mixture of hydrofluoric, nitric and perchloric acid and analyzed by ICP-OES (Spectro, Germany) and ICP-MS (VG Elemental, USA). The organic carbon concentration was determined by dry combustion using a Vario EL CNS element analyzer (Elementar Analysensysteme GmbH, Germany).

In the pore waters, uranium concentrations from 0,1 to 4,7 mg/L were measured, with a mean concentration of 2,1 mg/L in WLHe, 0,6 mg/L in WLZ and 0,9 mg/L in WLCuD. From wetland pore water and soil analyses, depth profiles of the uranium distribution in three wetlands were determined and enrichment factors were calculated. Uranium contents of the wetland substrates are enriched up to 3000 times compared to pore water values (mg/kg d.w. compared to mg/L). Uranium in 10 soil samples of WLHe has a mean concentration of $509,6 \pm 4,3$ mg/kg d.w. and ranges from 3,5 to 1133,1 mg/kg d.w.; the mean organic carbon content is 12,7 %. Seven samples of WLZ substrate have a mean uranium concentration of $3278,8 \pm 50,7$ mg/kg d.w. and range from 151,5 to 8011,2 mg/kg d.w.; the mean organic carbon content in these samples is 18,0 %. Five WLCuD soil samples have a mean uranium concentration of $217,3 \pm 1,9$ mg/kg d.w. and a range of 62,5 to 442,9 mg/kg d.w.; the organic carbon content in WLCuD samples is very low (mean 2,0 %). There is no clear relation between uranium and organic carbon in all these wetland soil samples. Only WLZ has a poor positive correlation between uranium and organic carbon concentrations (R^2 of 0,53).

For all three wetlands, samples in the uppermost parts (approx. 5 to 25 cm of depth) generally contain more uranium than in the lower parts of the sampled profiles. In the organic-rich moss horizons of the wetlands WLZ and WLHe, uranium is predominantly associated with the organic soil fraction, as shown be sequential extractions (see below). In comparison, sampled plant species growing directly on the wetland soil have an average uranium content less than 12 % of that of the wetland soils (Schöner 2005, in prep.). This suggests that living plant material is not responsible for the uranium accumulation in these wetlands.
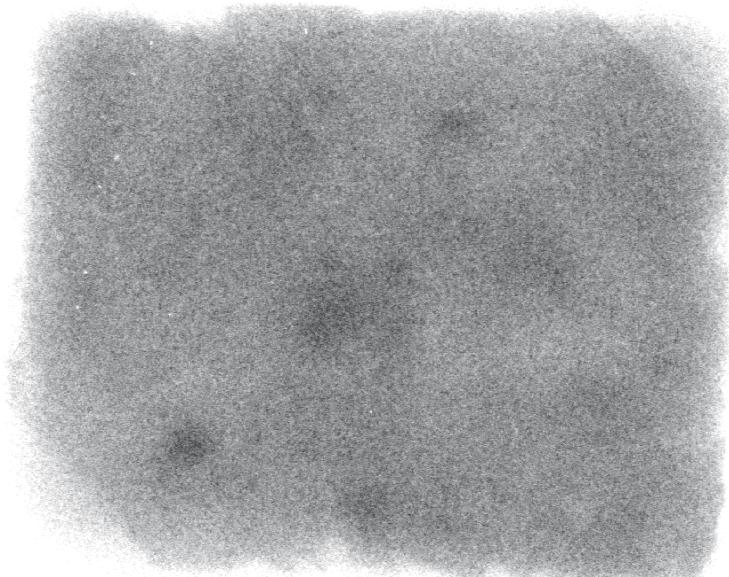
Typical redox potential (E_H) values measured in the investigated wetland sediments range from -200 to +400 mV. Uranium minerals were not detectable with standard techniques like Powder X-ray Diffraction (Seifert-FPM XRD7, Germany) or X-ray photoelectron spectroscopy (XPS), although bulk uranium concentrations in WLZ exceeded the detection limit for XPS (0.05 at-%).

Autoradiography

In order to physically localize uranium containing particles, a screening technique was used. Procedures for autoradiography detection have been applied to soil samples at the Forschungszentrum Karlsruhe, Germany (Dr. J. Römer). The nuclear track detection technique included contact autoradiography with alpha-track detectors in a plastic film. The method is sensible to alpha radiation of uranium. Air dried bulk and sieved wetland samples were used in thin soil section prepara-

tions. The distribution of alpha emitters can be observed and analyzed from the patterns of darkness on the film.

An example of a track created from uranium in an organic-rich layer is shown in Fig. 1. From most of the performed samples autoradiographic images with evenly dispersed darkness patterns were obtained. Sporadic darkness clusters represent higher uranium contents compared to adjacent areas. Distinct particles couldn't be identified. On the autoradiograms, the three wetlands investigated show slight noticeable differences not in the pattern, but in the intensity. This means, that uranium is mainly dispersed evenly in all performed soil sections, but with different contents in the three wetlands as shown by the intensity of the alpha emission from uranium species. Similarly, it could be shown that the sieved soil fractions can be distinguished by means of the emitted alpha radiation of uranium. In the WLZ horizon with maximum uranium concentration, the silt grain size (63-2 µm) contains most of the uranium. As for their chemical characterization the components of this grain size must be investigated by other techniques. We used SEM/EDX to analyze the physical and chemical composition of this soil fraction.
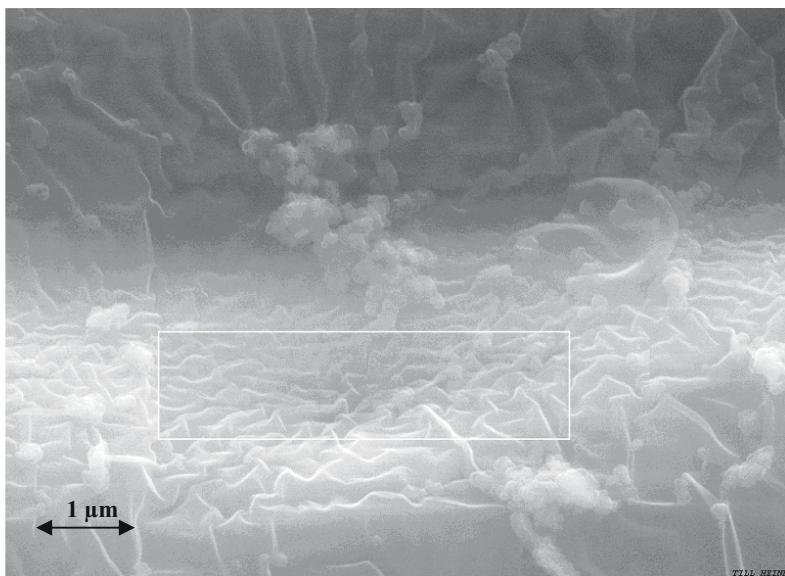
Fig. 1.   Typical autoradiogram from wetland soil sections (area approx. 8 x 10 cm). Sample from WLZ, 40 to 45 cm of depth. Relatively homogenous distribution of alpha emitting uranium is apparent in all autoradiograms, as illustrated by the homogenous darkness pattern. Sporadic darkness clusters represent higher uranium contents compared to adjacent areas. (Performed by Forschungszentrum Karlsruhe, Dr. J. Römer.)

SEM/EDX Analyses

At the field emission scanning electron microscope Gemini SEM Leo1530 (LEO Electron Microscopy Ltd, U,K) equipped for energy dispersive x-ray (EDX) analyses at the GZG, Universität Göttingen, Germany, we performed qualitative and semi-quantitative examinations of selected samples to provide direct information on particle morphology and composition.

Uranium was detectable solely in samples, which were taken from the horizon of WLZ with maximum uranium concentration up to 0,8 %. EDX measurements suggest that uranium is associated mostly with organic carbon and is apparently distributed homogeneously on organic particles. No discrete uranium-bearing phases were observed, and no uranium was detectable by using the back-scattered mode of the electron microscope. However, SEM/EDX clearly showed that also Al rich aggregates contain uranium. These still unidentified Al- and C-rich aggregates occur predominantly in association with organic surfaces, which are supposed to be microbes (fungi like *Ascomycetes* and terrestrial green-algae) and in some cases moss protonema. Future studies should focus on further identifying the microbes by using TEM and by isolating DNA. The findings support the results of the sequential extractions (see below). In no case there was a clear association with identifiable clay minerals or secondary iron minerals as often emphasized in literature (Morris et al. 1994; Hsi & Langmuir 1985). Fig. 2 shows the SEM image of an uranium containing organic surface.

Fig. 2. SEM image from an organic surface (supposedly fungi) in the wetland soil of WLZ. The white box (area approx. 1 x 3,5 µm) indicates the area wherein EDX spectra with homogenous uranium concentrations were obtained. Apparently, in this area no clay minerals are attached to the organic surface.

Mobility of uranium in three natural wetlands

From seven-step sequential extractions of wetland soils (protocol after Miller et al. 1986, modified according to Sowder et al. 2003) it can be concluded that in none of the investigated wetland profiles significant amounts of uranium are immobilized in stable phases, but may rather be available to the aquatic environment under changing conditions (compare Schöner et al. 2005). Uranium is predominantly distributed in labile, moderately labile (acid-extractable) and organically bound ($Na_4P_2O_7$-extractable) fractions. The extraction results also indicate that in the surveyed wetlands uranium is bound to multiple sites, for some horizons in approximately equal quantities, so that any environmental change resulting in pH shifts could release uranium. Regarding the process of uranium accumulation in the negligible residual phase of sequential extraction, particulate transport or in situ precipitation of uranium minerals are to consider. If at all, reductive precipitation of secondary uranium minerals may have occurred to a very small extent, as appropriate redox conditions have not yet been established in the wetlands (Schöner et al. 2004).

Conclusions

Natural wetlands at the former East German mining area were investigated with emphasis on uranium retention processes. The objective was to estimate if constructed wetlands can be used as a sustainable "passive" treatment methodology for uranium bearing mine waters. There is a special interest in uranium, as studies on dominant factors for uranium accumulation in wetlands are still scarce.

Only few of some 20 investigated natural wetlands had major influence on the transport of uranium to areas downstream. Analyses from sediments of three "successful" wetlands show that uranium is predominantly retained in an environment where sulfate reduction is insignificant (Schöner et al. 2004). In the wetland sediments, uranium concentrations are up to 3000 times higher than pore water concentrations. The distribution of uranium could be specified by autoradiography and SEM/EDX. Predominantly, uranium is dispersed evenly in the soils, thereby mainly on organic matter (supposedly microbes), as also shown by sequential extractions. In contrast, there is no clear correlation between uranium and organic carbon concentration. No dominant association of uranium with minerals could be observed. Further studies will focus on identifying the uranium rich organic surfaces.

On the subject of retention processes sorption, mainly on organic matter, is more evident than precipitation of uranium minerals. Regarding sustainability we conclude that external disturbances in wetland systems (e.g. seasonal or hydrological fluctuations, changes in E_H or ph values, or varying microbiological activities) may release labile uranium from wetland sediments. Therefore, if stable conditions can be maintained the use of constructed wetlands may be a promising methodology for primarily removing uranium from mine waters. However, it must

be assumed that in wetlands sustainable geochemical and ecological isolation of uranium from surface and groundwater can't be guaranteed - at least in terms of geological time periods.

Acknowledgements

References

Braithwaite A, Livens FR, Richardson S, Howe MT, Goulding DW (1997) Kinetically controlled release of uranium from soils. Europ J Soil Sci 48: 661-673

Dushenkov S, Vasudev D, Kapulnik Y, Gleba D, Fleisher D, Ting KC, Ensley B (1997) Removal of Uranium from Water Using Terrestrial Plants. Env Sci Techn 31: 3468-3474

Finlayson CM (1994) 13. A metal Budget for a Monsoonal Wetland in Northern Australia. In: Ross SM (ed) Toxic Metals in Soil-Plant Systems. Wiley & Sons, Baffins Lane, Chichester, West Sussex, p 433-452

Gerth A, Böhler A, Kießig G, Küchler A (2000) Passive biologische Behandlung von Bergbauwässern, Poster, WISMUT 2000 – Bergbausanierung, Schlema, Deutschland

Groudev SN, Bratcova SG, Komnitsas K (1999) Treatment of waters polluted with radioactive elements and heavy metals by means of a laboratory passive system. Min Eng 12: 261-270

Hsi C-K, Langmuir D (1985) Adsorption of uranyl onto ferric oxyhydroxides: Application of the surface complexation site-binding model. Geochim Cosmochim Acta 49: 1931-1941

Idiz EF, Carlisle D, Kaplan IR (1986) Interaction Between Organic Matter and Trace Metals in an Uranium Rich Bog, Kern County, California, U.S.A. Appl Geochem 1: 573-590

Klessa DA (2000) Compartmentalisation of uranium and heavy metals into sediment and plant biomass in a constructed wetland filter. In: Rózkowski A, Rogoz M (eds) Mine

Active and passive water treatment techniques

Water and the Environment, 7 th International Mine Water Association Congress, Ustro , Poland, p 407-417

Kochenov AV, Zinevyev VV, Lovaleva SA (1965) Some features of the accumulation of uranium in peat bogs. Geochem Internl 2: 65-70

Liger E, Charlet L, Van Cappellen P (1999) Surface catalysis of uranium(VI) reduction by iron(II). Geochim Cosmochim Acta 63: 2239-2955

Miller WP, Martens DC, Zelazny LW, Kornegay ET (1986) Forms of solid phase copper in copper-enriched swine manure. J Env Qual 15: 69-72

Morris DE, Chrisholm-Brause CJ, Barr ME, Conradson SD, Eller PG (1994) Optical spectroscopic studies of the sorption of UO_2^{2+} species on reference smectite. Geochim Cosmochim Acta 58: 3613-3623

Owen DE, Otton JK (1995) Mountain wetlands: efficient uranium filters - potential impacts. Ecol Engin 5: 77-93

Schöner A (2005 in preparation) Hydrogeochemische Prozesse der Uranfixierung in natürlichen Wetlands und deren Anwendbarkeit in der "passiven" Wasserbehandlung. Dissertation, Friedrich-Schiller-Universität Jena

Schöner A, Sauter M, Büchel G (2004) Untersuchungen zur Rückhaltung von Uran in Wetlands. In: Merkel B, Schaeben H, Wolkersdorfer C (eds) GIS - Geoscience Applications and Developments / Treatment Technologies for Mining Impacted Water, Vol 25. Wissenschaftliche Mitteilungen Institut für Geologie der TU Bergakademie Freiberg, Freiberg, p 141-146

Schöner A, Sauter M, Büchel G (2005) Uranium accumulation mechanisms and their potential use in passive treatment: A hydrogeochemical study of natural wetlands by means of sequential extraction. Securing the Future. International Conference on Mining and the Environment, Skellefteå, Sweden

Shinners S (1996) An overview of the application of constructed wetland filtration at ERA Ranger Mine Engineering Tomorrow Today - The Darwin Summit. The National Conference of the Institution of Engineers, Australia, Darwin, NT

Sowder AG, Bertsch PM, Morris PJ (2003) Partitioning and Availability of Uranium and Nickel in Contaminated Riparian Sediments. J Env Qual 32: 885-889

Titayeva NA (1967) Association of Radium and Uranium with peat. Geochem Inter (translated article from Geokhimiya, No. 12, pp. 1493-1499, 1967) 4: 1168-1174

Veselic M, Gantar I, Karahodzic M, Galicic B (2001) Towards passive Treatment of uranium mine waters. In: Prokop G (ed) 1st Image-Train Cluster-Meeting. Federal Environment Agency Ltd. Austria (Wien), Karlsruhe, p 116-128

Active and passive water treatment techniques

Removal of heavy metals, arsenic and uranium from model solutions and mine drainage waters

Gunnar Horak[1], Christian Lorenz[1], Karsten Steudel[1], Sabine Willscher[1], Wolfgang Pompe[2], Peter Werner[1]

[1]TU Dresden, Faculty of Forest, Geo and Hydro Sciences, Institute of Waste and Site Management, Pratzschwitzer Str. 15, D - 01796 Pirna, Germany,
E-mail: sabine@willschers.de
[2] TU Dresden, Institute of Material Sciences, Hallwachsstr. 3, D-01069 Dresden, Germany

Abstract. The aim of this work was to study the suitability of a new ceramic-based biomass, called Biocer. Different carrier materials were developed to investigate and improve the mechanical and hydrolytical stability of the Biocer material. In this work, the different materials should be compared. The biosorption of the materials was realised in batch equilibrium and first column experiments. First preliminary experiments with the Biocer I material in columns with real mine drainage waters resulted in a good removal of uranium and other heavy metals.

Introduction

Pit waters and seepage from mine tailings or dumps contain a huge potential of harmful substances like arsenic and heavy metals. In the former uranium mining areas in Germany, especially uranium and arsenic are contaminants of enhanced environmental attention. The wastewaters from the flooded pits there as well as seepage waters from the large spoiled piles contain a high future contamination potential.

Many approaches were developed and tested to solve this problem; one of them is the use of biosorption for the treatment of mine drainage waters (Volesky 1990, Allen and Brown 1995, Gadd and White 1993, Tzezos and Volesky 1981, Edgington et al. 1970). In the last years, several sorption experiments with different biomaterials were successfully implemented (Hakajama et al. 1982, Macaskie et al. 1988, 1992, Tsezos and Mac Cready 1989, Naja et al. 1999, Volesky and Tsezos 1983, 2001, Guibal et al. 1992, 1998, Hu et al. 1996, Horikashi et al. 1979, Byerley et al. 1987, Kuyucak and Volesky 1990 Chen and Yiakoumi 1997, Baes et al.

1997, Min and Hering 1998, Rorrer et al. 1993, Dambies et al. 1999, 2000, 2002, Fournel et al. 2001, Vincent and Guibal 2001, Hatzikioseyan et al. 2001, Sasaki et al. 2001, Loukidou et al. 2003, Kratochvil and Volesky 1998, Kefala et al. 2000, Groudev et al. 1999). *Bacillus sphaericus*, the Bacillus strain used here, is known for its excellent sorption capacity of uranium and other heavy metals (Selenska-Pobell et al. 1999, Panak et al. 2000). In this context, a new biosorption material, called Biocer, was developed combining the good sorption properties of the bacteria with mechanical stability by means of the sol-gel technology (Soltmann et al. 2003). The name Biocer means here the combination of a biological component with ceramic material. The vegetative cells are firmly bound in this ceramic material, whereas harmful metal ions can diffuse through the pores of the ceramics and then they become sorbed on the cell walls.

With an optimised grain size, the Biocer material will later be used in column reactors for the treatment of contaminated waters. Such reactors may be applied as small decentral constructions for especially low concentrations of harmful metal ions and arsenic. The Biocer material can also be used for the postprocessing of discharges of conventional treatment units in order to keep the limits of environmental contaminants in the surface water.

The aim of this work was to study the suitability of the new ceramic-based biomass. In first column experiments with the Biocer material and real waste water it was observed that the sorption-active surface and the carrier material were degraded by fouling processes. For this reason different carrier materials were developed to investigate and improve the stability of the Biocer material. In this work, the different materials should be compared in batch equilibrium and kinetic experiments.

Materials and methods

Material

The Biocer materials were supplied by "Kallies Feinchemie AG" Sebnitz (Germany). The Biocer A was a modification of the original Biocer material. It was produced with an ethanolic sol instead of an aqueous sol in the biomass coating. The carrier material used for the Biocer A was the same like for the original Biocer, a SiO_2- based nanosol (Horak et al. 2003).

The Al_2O_3-Biocer contained a composit of Al_2O_3 mixed with nanosol and the biomass. The Al_2O_3 carrier was used to improve the mechanical and hydrolytic stability of the Biocer material against fouling processes.

The Geopolymer material was supplied by the WISUTEC (carrier material) (Kunze et al. 2002) and the Biocer coating by "Kallies Feinchemie AG" Sebnitz (Germany). A problem in working with this material was the coating of the Geopolymer carrier with the biomass nanosol.

Before starting the experiments, the material was conditioned with physiological sodium chloride solution. Therefore, 0.1 g of the material was washed four times for 15 min with 3 ml of the salt solution. After conditioning, the Biocer material was suspended in the metal containing solutions to perform the biosorption experiments.
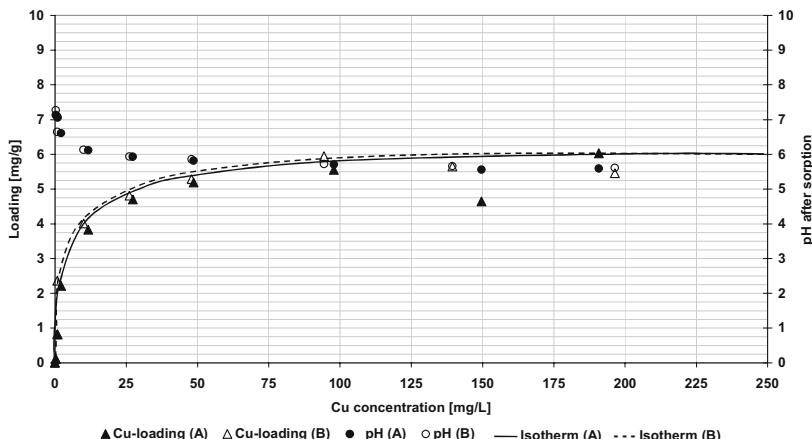
Biosorption experiments

The measurement of the sorption isotherms was carried out in batch experiments in closed test tubings. 1% of the Biocer material (w/v) was added to the metal(loid) solutions, and all was mixed in an overhead shaker for 2 hours. The concentration of the metal(loid) solutions used ranged from 0.1–250 mg/l and they were prepared by dilution of stock solutions in deionised water. The pH of the experimental solutions was adjusted to the appropriate value by adding HNO_3 and NaOH as required. Finally, the metal content of the sample supernatants was analysed by atomic absorption spectroscopy (AAS, Perkin Elmer 4100).

Desorption experiments

The desorption experiments were carried out directly after the end of the sorption experiments. Therefore, the Biocer material was separated from the metal solution, and suspended in a 0.005 M citric acid adjusted to pH 3.2. The desorption experiments were carried out by mixing in an overhead shaker over a time of 20 h.

For a new sorption cycle, the Biocer materials were conditioned again 3-4 times with a physiological sodium chloride solution, as described in point 2.1., and further used as described above.

Fig. 1.   Isotherms of the loading of the Biocer material with Cu^{2+} in tap water (unbuffered, initial pH 4.5).

Active and passive water treatment techniques

Sorption experiments in columns

Sorption experiments were carried out in columns of a length of 25 cm and a diameter of 1.5 cm with real mine drainage waters. The uranium inflow concentration was 2 mg/l, the pumping rate was 30 ml per day.
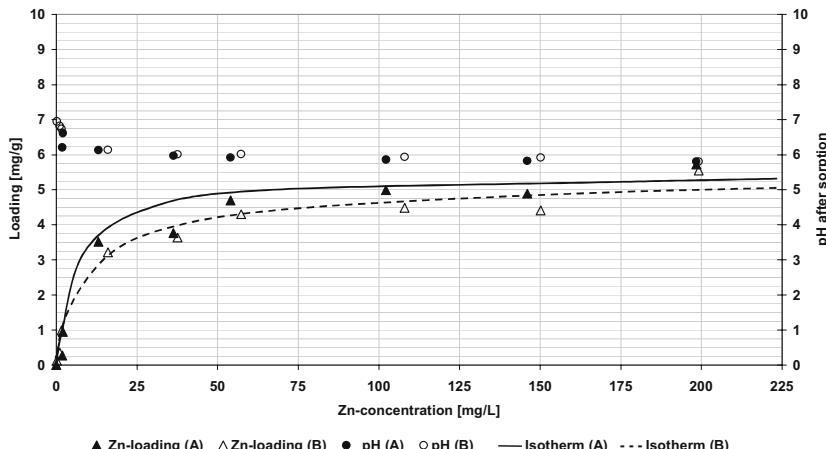
Results and discussion

Biosorption of Cu, Zn and As on the original Biocer material

Biosorption of Cu^{2+}

The first biosorption results for Cu^{2+} on the Biocer material were already reported by Horak et al. (2003). In that research work, a specific sorption capacity up to 6 mg Cu^{2+}/g Biocer was determined at an initial pH of 5 of the solution. In these experiments, a Cu^{2+} sorption was performed again to compare the data for this material charge with the former ones.

The sorption experiments were carried out with tap water as solvent. The influence of additional ions, e.g. in drinking water, should be investigated. In Fig. 1 the sorption isotherms for Cu^{2+} in tap water are shown. A maximum specific sorption capacity of 5.71 mg Cu^{2+}/g Biocer in average was achieved in the experiment.

Fig. 2.   Isotherms of the loading of the Biocer material with Zn^{2+} in deionised water (unbuffered, initial pH 5.5).

Active and passive water treatment techniques

This maximum specific sorption capacity probably includes the precipitation of copper species on the surface of the material, e.g. Antlerite $[Cu_3SO_4(OH)_4]$ and Brochanite $[Cu_4SO_4(OH)_6]$ (Volesky et al. 1999).
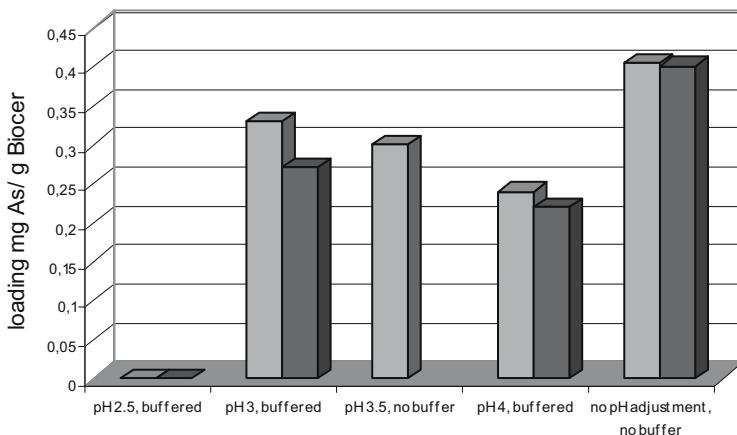
The measurement data correspond extremely well with the sorption data of the former experiments (Horak et al. 2003). According to these experimental results, the Biocer material used here showed a good reproducibility of its sorption characteristics in different production charges.

Biosorption of Zn^{2+}

Zn^{2+} shows a more advantageous speciation characteristic in aqueous solutions compared to Cu^{2+}. It exists up to a pH of 8 as a free cation Zn^{2+} (O'Neill et al. 1998). Thus, no side reactions are expected by precipitation of Zn^{2+} species on the surface of the biosorbens in these sorption experiments. For this reason Zn^{2+} was used in the following biosorption experiments.

A maximum specific sorption capacity of 5,7 mg Zn^{2+}/g Biocer was achieved in the first biosorption cycle (see Fig. 2). The loading of the Biocer with Zn^{2+} is in a compareable range with the Cu^{2+} loading.

In further loading cycles after the desorption of the Zn^{2+} and a regeneration of the material, only up to 3 mg Zn^{2+}/ g Biocer were obtained. The specific sorption capacity demonstrated a strong dependence from the pH of the bulk solution.

Fig. 3. Comparison of the loading of the Biocer material with As(V) at different pH in deionised water.

Active and passive water treatment techniques

Biosorption of As

Besides the sorption experiments with metal cations, also sorption experiments with As(V) were carried out. The sorption of As ions is of high interest for the treatment of contaminated ground-, waste- and seepage waters. The experiments were carried out at different pH values to find out the optimum conditions, because of the speciation characteristics of the As ions and the equilibrium characteristics of the binding-active groups on the surface of the Biocer material (O'Neill et al. 1998, Niu and Volesky 2001). Initial pH values of 4.0, 3.5, 3.0 and 2.5 were adjusted in the sorption solutions. Two experiments were carried out in unbuffered solutions to prove the effect of buffering onto the sorption behaviour (Fig. 3).

The biosorption capacity of As onto the Biocer material is only low compared to the results with the metal cations (Zn^{2+}, Cu^{2+}, see Fig. 1-3). In real groundwaters or seepage waters, As will be sorbed on the Biocer only in low amounts besides the other metal ions, therefore an additional As sorbens will be necessary at enhanced As concentrations. As a result, the Biocer material demonstrated the best sorption characteristics in solutions of dissolved cationic metals compared to the As solutions, in which As exists as an anionic species.

The best sorption results for As(V) were achieved with 0.405 mg As/g Biocer in an unbuffered solution with no pH adjustment (see Fig. 3). In such solutions no competing effects of other anions seem to occur with the As ions for the binding places on the surface of the Biocer material.

In dependency of the initial pH of the sorption solutions, the best results were obtained at an initial pH of 3 with 0.33 mg As/g Biocer (see Fig. 3). The number of binding-active protonated groups on the surface of the Biocer is declining with increasing initial pH of the bulk solution, so that less of the As anions can be sorbed (see Fig. 3). The results of the experiments are corresponding with literature data (Dambies et al. 1999, Niu and Volesky 2001).

Comparison of different Biocer materials

Different carrier materials were coated with the biomass nanosol (see chapter 2.1.) to improve the long-term mechanical and hydrolytic stability of the biosorbens. Sorption experiments for comparison of the different biosorbens were carried out in aqueous Zn^{2+} solutions because the Zn^{2+} sorption showed the least side reactions in the sorption process (see chapter 3.1), so that it was good suited for model investigations. The results of the sorption experiments illustrates Fig. 4. With exception of Biocer A, all desorption data correlated well with the Langmuir model; the correlation coefficients were in average between 98 and 100%.

A modification of the sorption-active surface by processing of the biomass-nanosol coating with ethanol (Biocer A) results in no improvement of the binding capacity (2.48 mg Zn^{2+}/g Biocer) in comparison to the original Biocer material (see Fig. 4).

The use of Al_2O_3 as carrier material improved the mechanical stability of the material, but not its sorption characteristics (3.22 mg Zn^{2+}/g Biocer, see Fig. 4).
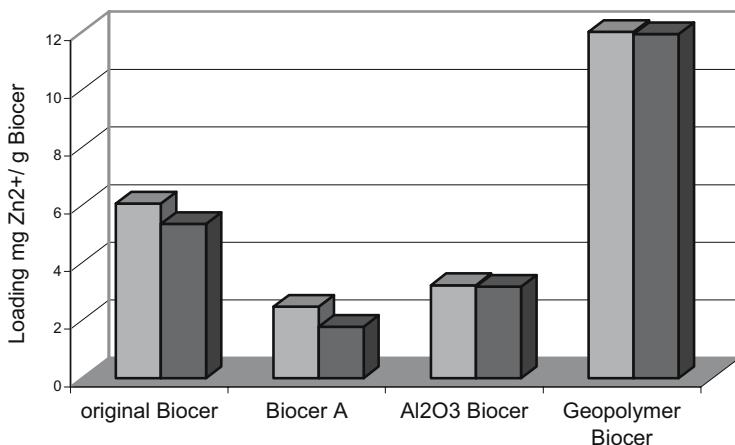
The sorption characteristics after the regeneration of the Al_2O_3 Biocer especially were not satisfactory. The material showed a loss of activity after only a few regeneration cycles. Another problem was the lower pH of the sorption solutions after regeneration which arose lower sorption results compared to the first loading. An explanation for this behaviour might be a lower binding of the biomass-nanosol composite to the Al_2O_3 carrier and thereby a loss of the sorption-active coating after regeneration.

With the Geopolymer Biocer, a high increase of pH was observed in the experiments and for this reason the best elimination results of up to 12.39 mg Zn^{2+}/g Biocer (see Fig. 4). A partial precipitation of Zn^{2+} on the surface additionally to the sorption process is possible at the high solution pH after the sorption experiments (final pH of the bulk solution up to 7.2). The Geopolymer had a good mechanical and chemical stability in addition to the good sorption results; therefore it was chosen for further sorption experiments with the real seepage waters.

Finally, after testing the different biosorption materials, the original Biocer material and the Geopolymer Biocer were chosen for further experiments with the real contaminated waters. The modification of the carrier material resulted in an improved stability of the Biocer, but not necessarily in better sorption results.

Experiments with real mine drainage waters

First preliminary experiments with the Biocer I material resulted in a good removal of uranium and other heavy metals. Fig. 5 presents the breakthrough curve of U in column experiments when the Biocer I material was applied. Due to the degrading stability of the Biocer material after some time of the experiment, a re-

Fig. 4. Specific loading of Zn^{2+} on the different Biocer materials (deionised water, unbuffered; initial pH adjusted).

Active and passive water treatment techniques

markably enhanced outflow concentration of U was observed after 800 – 1100 exchanged bed volumes of the column.
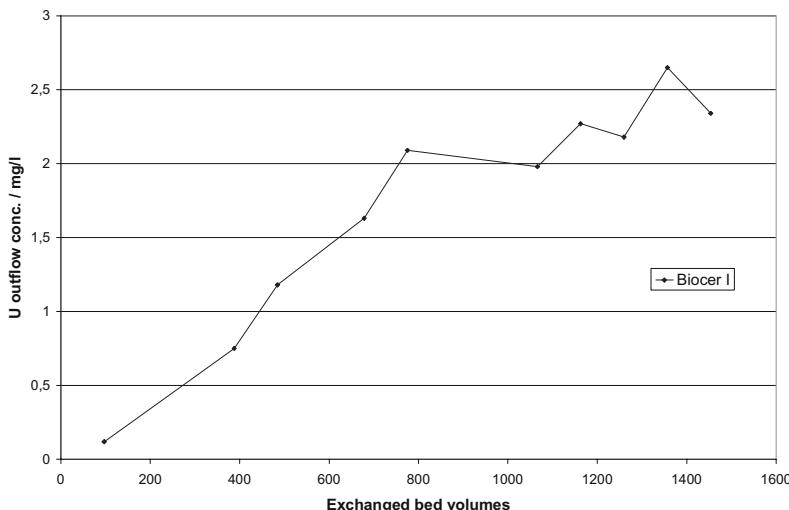
An improvement of the sorption behaviour of the material should be achieved by modification of the material and of the biosorption reaction conditions to enhance the stability of the Biocer.

Conclusions

In the biosorption experiments with Cu^{2+} and Zn^{2+} on the Biocer material good results were obtained. The material seems to be well suited for the removal of such metal ions from contaminated waters. The sorption capacity of the Biocer for As was low; further investigations have to be performed to improve the sorption characteristics or to use an additional sorbens for the complete removal of As from contaminated waters.

The sorption of Zn^{2+} on the Biocer occurs in a fast process, and the desorption is nearly quantitative. These results are good characteristics for a fast regeneration of the Biocer material and the subsequent processing of the metal solutions.

The Biocer material was compared with 3 other modified biosorbents for its sorption characteristics. As a result, the Biocer and a Geopolymer coated with the biomass-nanosol were chosen for further experiments with the real contaminated

Fig. 5.   Breakthrough curve of U in real mine drainage.

Active and passive water treatment techniques

waters due to their good sorption characteristics.

First preliminary experiments with the Biocer I material resulted in a good removal of uranium and other heavy metals. With an improved stability of the Biocer material, better sorption results and particularly an enhanced sorption- and life time of the biosorbens are expected, which shall be reported in a future article.

Acknowledgements

References

Allen, S.J., Brown, P.A. (1995) J. Chem. Tech. Biotechnol. 62: 17

Baes, A.E., Okuda, T., Nishijima, W., Soto, E., Okada, M. (1997) Wat. Sci. Technol. 35: 89

Brookins, D.G. (1988) Eh-pH diagrams for Geochemistry, Springer Berlin, Heidelberg

Byerley, J.J. (1987) Scharer, J.M., Charles, A.M., Chem. Eng. J. 36: B 49

Chen, J., Yiacoumi, S. (1997) Sep. Sci. Technol. 32: 51

Dambies, L.,   Roze, A., Roussy, J., Guibal, E. (1999) Process Metallurgy 9B, Eds. R. Amils, A. Ballester, Elsevier, Amsterdam, NL: 277-287

Dambies, L., Guibal, E., Roze, A. (2000) Colloids Surf. A 170: 19-31

Dambies, L., Vincent, T., Guibal, E. (2002) Water Res.: 3699-3710

Edgington, D.N., Gorden, S.A., Thommes, M.M. Almodovar, L.R. (1970) Limnol. Ocean. 15: 945

Fournel, L., Navarro, R., Saucedo, I., Guibal, E. (2001)   Process Metallurgy 11B, Eds. V.S.T. Ciminelli, O. Garcia Jr., Elsevier, Amsterdam, NL: 109-118

Gadd, G.M., White, C. (1993) Trends Biotechnol. 11: 353

Groudev, S.N., Bratcova, S.G., Komnitsas, K. (1999) Minerals Eng. 12: 261-270

Guibal, E., Milot, C., Tobin, J.M. (1998) Ind. Eng. Chem. Res. 37: 1454

Guibal, E., Roulph, C., Le Cloirec, P. (1992) Water Res. 26: 1139

Hakajama, A., Horikashi, T., Sakaguchi, T. (1982) Eur. J. Appl. Microbiol. Biotechnol. 16: 88

Hatzikioseyan, A., Remoudaki, E., Tsezos, M. (2001) Process Metallurgy 11B, Eds. V.S.T. Ciminelli, O. Garcia Jr., Elsevier, Amsterdam, NL: 265-277

Horak, G., Willscher, S., Werner, P., Pompe, W. (2003) in: Proc. of the Internat. Biohydromet. Symp., IBS- ATHEN: 497-505

Horikoshi, T., Nakajima, A., Sakaguchi, T. (1979) Agric. Biol. Chem. 332: 617

Hu, M.Z.C., Norman, J.M., Faison, N.B., Reeves, M. (1996) Biotechnol. Bioeng. 51: 237

Kefala, M.I., Zouboulis, K.A., Matis, K.A. (2000) Environ. Pollut. 104: 283-293

Kratochvil, D., Volesky, B. (1998) Trends Biotechnol. 16: 291-300

Kunze, C., Hermann, E., Griebel, I., Kiessig, G., Dullies, F., Schreiter, M. (2002) Wasser, Abwasser 143: 7-8

Kuyucak, N., Volesky, B. (1990) Biosorption by algal biomass, CRC Press, Boca Raton, FL

Loukidou, M.X., Matis, K.A., Zouboulis, A.I., Liakopoulou-Kyriadikou, M. (2003) Water Res. 37: 4544-4552

Macaskie, L.E., Blackmore, J.D., Empson, R.M. (1988) FEMS Microbiol. Lett. 55: 157

Macaskie, L.E., Empson, R.M., Cheetham, A.K., Grey, C.P., Skarnulis, A.J. (1992) Science 257: 782

Min, J.H., Hering, J.G. (1998) Wat. Res. 32: 1544

Naja, G., Peiffert, C., Cathelineau, M., Mustin, C. (1999) Process Metallurgy 9B, Eds. R. Amils, A. Ballester, Elsevier, Amsterdam, NL: 343-350

Niu, H., Volesky, B. (2001) Process Metallurgy 11B, Eds. V.S.T. Ciminelli, O. Garcia Jr., Elsevier, Amsterdam, NL: 189-197

Panak, P.J., Raff, J., Selenska-Pobell, S., Geipel, G., Bernhard, G., Nitsche, H. (2000) Radiochim. Acta 88: 71

Rorrer, G.L., Hsien, T.Y. Way, J.D. (1993) Ind. Eng. Chem. Res. 32: 2170

Sasaki, K., Endo, M., Kurosawa, K., Konno, H. (2001) Process Metallurgy 11B, Eds. V.S.T. Ciminelli, O. Garcia Jr., Elsevier, Amsterdam, NL: 279-286

Selenska-Pobell, S., Panak, P., Miteva, V., Boudakov, I., Bernhard, G., Nitsche, H. (1999) FEMS Microbiology Ecology 29: 59

Soltmann, U., Raff, J., Selenska-Pobell, S., Matys, S., Pompe, W., Boettcher, H. (2003) J. Sol-gel Sci. Technol. 26: 1209-1212

Tsezos, M., Mac Cready, R.G.L., Bell, J.P. (1989) Biotechnol. Bioeng. 34: 10

Tsezos, M., Volesky, B. (1981) Biotechnol. Bioeng. 23: 583

Vincent, T., Guibal, E. (2001) Process Metallurgy 11B, Eds. V.S.T. Ciminelli, O. Garcia Jr., Elsevier, Amsterdam, NL: 257-264

Volesky, B., Biosorption of heavy metals, CRC Press, Boca Raton (1990)

Volesky, B., Weber, J., Vieira, R. (1999) Process Metallurgy 9B, R. Amils, A. Ballester (eds.), Elsevier, Amsterdam, NL: 473 – 481

Volesky, B. (2001) Hydrometallurgy 59: 203-216

Volesky, B., Tsezos, M. (1981) Separation of uranium by biosorption, U.S. Pat. No. 4, 320,093, Canad. Pat. No. 1, 143,007 (1983)

Passive Treatment of Minewater at the Schlema-Alberoda Site

André Gerth[1], Anja Hebner[1], Gunter Kiessig[2], Anja Zellmer[2]

[1]BioPlanta GmbH, Deutscher Platz 5, D-04103 Leipzig, Germany,
E-mail: andre.gerth@bioplanta-leipzig.de
[2]WISUTEC GmbH, Jagdschänkenstr. 33, D-09117 Chemnitz, Germany

Abstract. A pilot scale constructed wetland for treatment of seepage water from uranium mining was planned, built and operated. The pilot plant was designed for treatment of 5 m³ per hour. The system consists of 4 basins and 1 lagoon. The objective of the project was the investigation of the long-term stability and robustness of passive water treatment systems. The feasibility of treatment of seepage water from uranium mining in constructed wetlands was proven by the operation of the pilot plant. A series of robustness investigations was conducted; including the operation during long lasting frost periods, under increased hydraulic load and under high carbon load. By using a tracer the hydraulic characteristics of the basins was tested. The control of the wetland is very complex due to different redox condition necessary for removal of arsenic (aerobic) and uranium (anaerobic). Additional information for an increased robustness of the system was derived from the operational results.

Introduction

During and after closing of uranium mining sites in Thuringia and Saxony, contaminated water from mine flooding and seepage occurs. This water usually contains, besides uranium and radium, other metals like arsenic, iron, and manganese. This water is treated by conventional technologies like precipitation, coagulation and ion exchange. The use of passive technologies based on biological, physical and chemical processes could be a cost-saving alternative. Constructed wetlands are such a passive water treatment technology.

BioPlanta and WISUTEC investigated the feasibility of a long-term, stable and reliable treatment of seepage water being contaminated with uranium, arsenic and nitrate in a constructed wetland.

Based on small-scale studies, a pilot plant was built and is operated at the site of mine shaft 371. The constructed wetland system, also referred to as "planted reactor", was designed for the treatment of 5 m³/h. Treatment objective is the removal of uranium, arsenic, radium, nitrate and traces of heavy metals. Defined target concentrations are: uranium 0.3 mg/l, radium 0.2 Bq/l, arsenic 0.1 mg/l and nitrate 10 mg/l. The proof of the long-term stability of the treatment performance and the robustness against external disturbances is a prerequisite for the administrative approval of the technology.

The conduct of the system towards external influences and disturbances was studied by monitoring the reaction to applied targeted failure situations, technical problems and seasonal influences. From these results a statement about the conduct of the system in continuous duty as well as under long-term performance and about measurements to be taken in case of failures to restore the operational state was deducted.

Fundamentals of Metal Removal in Wetlands

Since the 1980s, constructed wetlands have successfully been used for the treatment of acid mine drainage (AMD) and for the removal of iron in Great Britain, USA, Australia and Canada. Studies in natural wetlands showed that in many cases dissolved uranium is removed from the water and accumulated in the wetland sediments. The reproduction of these processes in pilot-scale constructed wetlands has been tested in the USA and in Australia since 1995.

The fundamental process of uranium immobilization is the reduction of the mobile U(VI)-species to insoluble U(IV). The anaerobic wetland sediment has the right conditions for this reaction. Other processes that can lead to an immobilization include: sorption on organic (humic substances) and inorganic (Fe- and Mn-oxides) material, co-precipitation and plant uptake.

Sulphate reducing bacteria (SRB) like *Desulfovibrio* spp. show the effect of enzymatic uranium reduction (Neal et al. 2004). A comprehensive overview of microbial uranium reduction is given by Lutz et al. (2002). The process of reduction and precipitation of uranium is reversible, i.e. under oxidizing condition remobilization can occur.

A removal of arsenic can be achieved by co-precipitation with iron as well with aluminium- and manganese oxides/hydroxides under aerobic conditions. A reducing environment leads to a dissolution of the oxides/hydroxides and thus a mobilization of bound arsenic. Because the water on the investigated site has a low iron content, iron arsenate can only be precipitated to a minor extent.

The conditions in wetlands and the hydraulic, geochemical and biological processes connected with metal removal are extensively reviewed by Younger and Wolkersdorfer (2002). Younger states, that it is yet unknown to which extent tem-

peratures in autumn and winter influence the vitality of sulphate reducing bacteria in wetland sediments.

Bio sorption processes, which also play an important role in the treatment of mining waters, are reviewed by Ondruschka and Bley (2002). The complex formation of U(IV) phosphates and arsenates has been investigated by Geipel et al. (2002). Uranium complexes formed by microbial processes are discussed in Merroun et al. (2002).

Different uranium valences in a nutrient solution and in the biomass of plants cultivated in this solution have been found. Uranium is bound in plants mainly in form of uranyl phosphate groups (Günther et al. 2002).

In column and small scale studies BioPlanta has proven the effective removal of arsenic and uranium by a biological system consisting of a gravel filter, plants, and microorganisms.

The experiments have shown that the carbon supplied by plant roots and detritus is insufficient to reach the required low redox potential in the wetland. So a readily available carbon source was needed for uranium removal. Since the carbon release from compost, straw or other organic solids cannot be controlled, a liquid carbon source was needed, which could be dosed according to the variable demand under changing temperature and hydraulic conditions. Molasses was chosen due to its non-toxicity, low price and content of micro-nutrients, which have shown to have a positive effect on the development of the microflora.

Based on the results of the experiments, the pilot system at the site of shaft 371 was planned and built.

Description of the Pilot System

The pilot system at shaft 371 consists of the following components: storage lagoon, constructed wetland and a polishing lagoon. The wetland system is made up of 4 serially connected cells. The flow in the cells is horizontal. The base area of the cells is 19 m² (cells 1, 2, 4) and 15 m² (cell 3).

The wetland cells are 1.2 m deep earthen basins with PE-lining, filled with washed gravel (2-8 mm) to a layer depth of 0.9 m. The total volume of the planted gravel filter sums to 1,226 m³.

The in- and outflow areas of each cell were constructed of coarse gravel (16-32 mm). Water passes through the cells by gravitational flow. The outflow of each cell connects to shafts for sampling and the control of the water level in the wetland.

The inflow to the wetland system is controlled by a valve and measured by an inductive flowmeter. The cells are planted with reed (*Phargmites australis*) and sedge (*Carex gracilis*).

Fig. 1.   Cells 1 and 2 of the pilot system on the site of shaft 371.

To reach anaerobic conditions in the first two cells, molasses is added to the in-flowing water and the cells 1 and 2 are operated with a constant water level just slightly below the gravel surface. After the passage of the first two cells, the water reaches cell 3, where the water level is periodically changed (fill-and-drain) by means of a time-controlled valve in the outflow of cell 3. During the fill cycle, the water is enriched in oxygen and so aerobic processes for the removal of excess carbon and precipitation of arsenic can take place.

The system started operation in October 2002. Until today investigations of the performance and operation stability were undertaken.

Results of Operation

Problems with administrative permissions and technical problems (clogging of drainage tubes) caused a delay in the start of operation with the configuration as described above. The fully operational state of the system could be established in June 2004. Before that date the system was operated without molasses and without the fill-and-drain system in cell 3.

With the start of the molasses allowance, intentionally planned as an overdose to saturate the first cell with molasses, the outflow concentrations for COD exceeded the permitted level. Reducing conditions were established in all 4 cells, re-
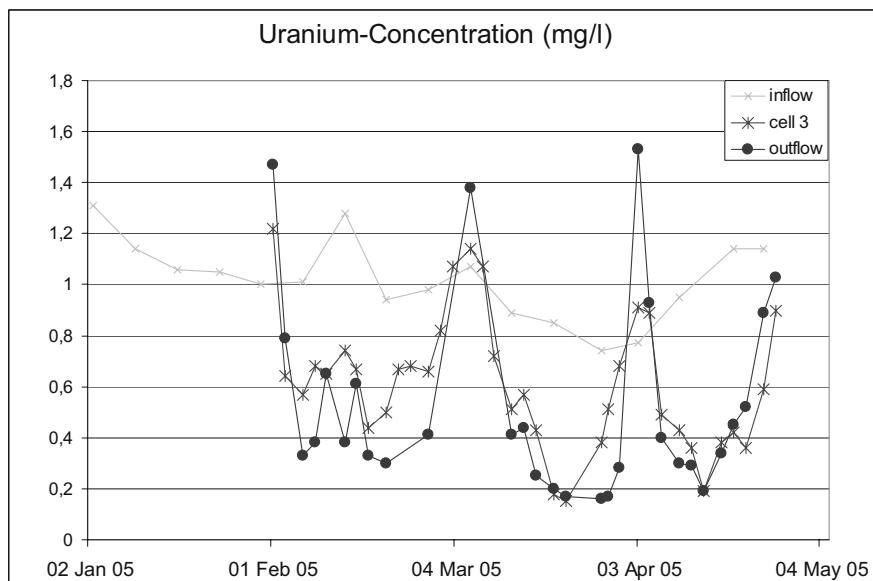
Fig. 2.   Results of operation from 2005, uranium concentrations.

sulting in a good uranium retention and nitrate reduction, but also in an unacceptable mobilization of arsenic. So the system had to be operated in closed circuit. Starting from October 2004, the normal operation was restored and the system was operated with varying hydraulic loads and molasses dosages between 70 l/d and 180 l/d. Uranium retention was low until November 2004, when for the first time sulphate reducing reactions were proven by decreasing sulphate concentrations in the outflow.

The peaks in the outflow uranium concentration, which can be seen in figure 1, occurred during phases of short circuit operation, forced by exceeding permitted COD-concentration in the outflow. Overall it can be seen, that the target value of 0.3 mg/l uranium can be reached under optimal operational conditions. The conditions required for a stable operation have been reached in 2005.

The same holds true for arsenic. In optimal conditions an outflow concentration below 50 µg/l was achieved, but during phases of excess COD input it could reach several times the inflow concentration, which means that arsenic is very easily and fast remobilized.

Conclusions

It could be shown that passive systems as a constructed wetland are a possible solution for treating uranium-contaminated water. The operation under properly controlled redox conditions is essential to reach low arsenic levels at the same time. The design of the pilot-scale system needs to be slightly improved to provide a

better aeration of the basins 3 and 4. With these changes stable removal rates of uranium and arsenic are expected without exceeding permitted COD-levels in the outflow.

References

Neal N, Amonette JE., Peyton BM, Geesey GG (2004) Uranium complexes formed at hematite surfaces colonized by sulphate-reducing bacteria, Environ. Sci. Technol. 38: 3019-3027

Lutze W, Gong W, Nuttall HE (2002) Microbially mediated reduction and immobilization of uranium in groundwater, Uranium in the Aquatic Environment, Springer-Verlag Berlin Heidelberg, 437-446

Younger PL, Wolkersdorfer C (2002) Passive Grubenwasserreinigung als Alternative zu aktiven Systemen, Grundwasser-Zeitschrift der Fachsektion Hydrogeologie 2/2002, 67-77

Ondruschka J, Bley T (2002) Biosoprtion umweltrelevanter Schwermetalle an ausgewählten Biomaterialien als Grundlage für die Reinigung belasteter Abwässer, Chemie Ingenieur Technik 74: 500-504

Geipel G, Bernhard G, Brendler V (2002) Complex Formation of Uranium (IV) with Phosphate and Arsenat, in: Uranium in the Aquatic Environment, Springer-Verlag Berlin Heidelberg, 369-376

Merroun M et al. (2002) Characterization of uranium (VI) complexes formed by different bacteria relevant to uranium mining waste piles, in: Uranium in the Aquatic Environment, Springer-Verlag Berlin Heidelberg, 505-511

Günther et al. (2002) Uranium speciation in plants, in: Uranium in the Aquatic Environment, Springer-Verlag Berlin Heidelberg, 512-520

Decommissioning of Uranium mill tailings ponds at WISMUT (Germany)

Albrecht Neudert, Ulf Barnekow

WISMUT GmbH, Jagdschänkenstr. 29, D-09117 Chemnitz, Germany,
E-mail: a.neudert@wismut.de

Abstract. Approximately 577 ha of Uranium mill tailings ponds containing approx. 154 Mio. m^3 of mill tailings were left as part of the legacy of the uranium mining and milling in Eastern Germany. The decommissioning of these tailings ponds belongs to the most challenging tasks of the entire Wismut remediation project. The remediation activities started in 1990 with defence measures against acute risks, environmental investigations and development of first site specific remediation concepts. Resulting from the site specific remediation concepts WISMUT GmbH decided to prepare for dry decommissioning in situ for all of the mill tailings ponds. Dry decommissioning of tailings ponds consists of the following basic decommissioning steps: expelling of pond water and seepage catchment including water treatment; interim covering of exposed tailings surfaces including dewatering of unconsolidated fine slimes by technical means; re-contouring of dams and ponds and final covering including landscaping and vegetation. This paper presents the development and the principal design of the decommissioning of the large Uranium mill tailings ponds and the progress achieved by WISMUT.

Introduction

From 1951 to 1990 the former Soviet-German Wismut company processed a total of about 216,000 t of uranium in two large mills located near Seelingstädt (Thuringia) and Crossen (Saxony). Tailings dams were erected for separate disposal of uranium mill tailings from soda-alkaline and from acid leaching. The tailings

ponds Culmitzsch A and B, Trünzig A and B near Seelingstädt and the tailings ponds Helmsdorf and Dänkritz 1 near Crossen cover a total area of about 577 ha and contain about 154 Million m^3 of uranium mill tailings. First decommissioning activities started in 1991 including defence measures against acute risks, environmental investigations and development of first site specific remediation concepts. Resulting from the site specific remediation concepts WISMUT GmbH decided to prepare for dry decommissioning in situ for all of the tailings ponds. Decommissioning of tailings ponds consists of the following basic decommissioning steps: expelling of pond water and seepage catchment including water treatment; interim covering of exposed tailings surfaces including dewatering of fine tailings by technical means; re-contouring of dams and ponds and final covering including vegetation. The entire decommissioning of all the uranium mill tailings ponds subject to the WISMUT act, dated Oct. 31, 1991, will cost assumingly EUR 770 Million and is foreseen to be completed by ca. 2015. This paper presents the development and principal design of tailings pond decommissioning and progress achieved by WISMUT GmbH.

Characterization of mill tailings ponds and tailings properties

Most of the uranium mill tailings ponds were erected in old open pits surrounded by either autostable tailings dams or by waste rock dams. Only the Helmsdorf tailings pond is located in a natural valley closed by a dam before. Uranium ore was processed by soda-alkaline leaching or by acid leaching followed by neutralization before tailings disposal. Tailings were usually discharged from the surrounding into the tailings ponds. Due to the historic discharge regimes coarse-grained tailings settled near the discharge spots creating thick sandy tailings beaches. Distant from the discharge spots fines settled below water table forming up to several 10 m thick fine tailings layers. The transition zones in between the tailings beaches and the fine tailings consist of an interlayering of thin fine tailings layers and thin sandy tailings layers.

Fig. 1 shows the tailings ponds Helmsdorf (foreground) and Dänkritz 1 (background) near Crossen in 2003. Fig. 2 shows from the foreground to the background the tailings ponds Trünzig B and A and Culmitzsch A and B in 2004.

Basic technical data of the tailings ponds, data for characterizing contaminants content in the tailings as well as typical geotechnical properties of fine tailings are presented in the following Table 1 to Table 3.

Fig. 1. Tailings ponds Helmsdorf and Dänkritz 1 (background) in 2003.

Fig. 2. Tailings Ponds Trünzig and Culmitzsch in 2004.

Decommissioning Aims

The decommissioning of the uranium mill tailings ponds is to meet the following most relevant decommissioning aims:

a) a maximum over-all radioactive dose of 1 mSv/a to the population enclosing all relevant exposure paths including water path, air path and soil path

b) water released from the sites into the hydrographic net must meet the respective limit values for contaminants to the long term as prescribed by the authorities responsible

c) decommissioning aims met must be granted to the long term (for a period of 200 years up to 1000 years)

Evaluation of the given situation and risk assessment

Extensive environmental, radiological and hydrogeological investigations started in 1991 immediately after the end of the uranium mining and processing period. The investigation results as well as the results of immission measurements on the existing situation were documented in a newly developed environmental data base. The site specific risk assessment proved, that the mill tailings caused unacceptable high radioactive doses to the surrounding environment like:

a) particularly unacceptable radon exhalation rates, direct radiation rates and radioactively contaminated dusting in the air near surface

b) unacceptable contaminant seepage from the tailings ponds into the surrounding aquifers and contaminated runoff to the receiving streams.

Active and passive soil treatment techniques

Tabel 1. Basic technical data of uranium mill tailings ponds.

mill tailings pond	tail. vol. (×10^6 m³)	area (ha)	max. tail. thickness (m)	type of tail. pond	process.
Helmsdorf	45	201	50	valley type	*2)
Dänkritz 1	4,6	27	23	ring dam type	*2)
Culmitzsch A	61,3	158	72	filled open pit	*1)
Culmitzsch B	23,6	76	63	encl. by dams	*2)
Trünzig A	13	67	30	filled open pit	*1)
Trünzig B	6	48	23	encl. by dams	*2)
total	153.5	577			

*1) acid leaching *2) = soda-alkaline leaching + neutralization

Tabel 2. Volumes, masses and average contents of contaminants in uranium mill tailings.

solids		liquids	
total tailings mass (solids+liquids)	ca. 165 Mio t	pond water: volume in 1995 volume in 2005	13 Mill m³ ca. 0.5 Mill m³
mass of U	15340 t	ave. U-content	3.2 mg/l
activity of Ra	15.1* 10^{14}Bq	ave. activity of Ra	1.7 Bq/l
		vol. of pore water	70 Mill m³
ave. U-content	0.009 mass %	ave. U-content	9 mg/l
ave. Ra-activity	9000 Bq/kg	ave. Ra-content	4 Bg/l
mass of As (only TP Helmsdorf)	7.590 t	As-content (only TP Helmsdorf)	30 mg/l

Tabel 3. Geotechnical parameters of uranium fine tailings.

Parameter	TP Helmsdorf	TP Culmitzsch A
processing type	soda-alkaline leaching	acid leaching
Soil group (DIN18196)	TA, UA, TM	UA, TA
water content	0,45 ... > 1,2	0,50 ... > 1,8
liquid limit	0,50 ... 0,60	0,60 ... 0,75
plasticity limit	0,20 ... 0,24	0,22 ... 0,30
void ratio e	1,5 ... > 3,5	2 ... > 5
compression index C_C	0,4 ... 0,55	0,6 ... 0,85
Permeability k_f	1*E-7...1*E-9	2*E-7...5*E-10

Active and passive soil treatment techniques

Based on the site specific risk assessment the measures needed were classified as defence measures against acute risks to the environment/population to be taken in a short term period or as decommissioning measures to grant decommissioning aims after closure to the long term. The defence measures needed were designed immediately and realized in a short term. Defence measures against acute risks enclosed the following activities:

- interim covering of all subaerially exposed tailings surfaces to reduce radon exhalation, direct radiation and radioactively contaminated dusting
- complete reconstruction or new construction of catchment systems to catch the entire seepage and runoff from the the tailings ponds
- Geotechnical investigations on dam stability to prove dam stability to the short term with respect to static and dynamic (seismic) loads.
- Construction of water treatment plants to treat the catched seepage and runoff as well as for expelling pond water with regard to uranium, radium and, if needed, also arsenic.
- Installation of fences surrounding the sites to avoid access to the public
- Installation of extensive monitoring systems in the surrounding to monitor the effects of the tailings ponds to the surrounding before and during further decommissioning activities

Dry decommissioning in situ

While realizing the defence measures needed further extensive investigations were carried out for developing site specific decommissioning concepts. For this different decommissioning options were evaluated. Sophisticated cost-benefit analyses were prepared taking into account the environmental risks after closure, decommissioning costs and time needed for realisation of the different decommissioning options. By the mid 1990´s WISMUT identified the dry decommissioning in situ for to be preferable for all of the mill tailings ponds.
After having received the approval of the permitting authorities on the decision to plan for dry decommissioning in situ decommissioning steps were prepared individually by WISMUT based on further detailed investigations and evaluations. Since then the individual decommissioning measures and constructions have been and are currently designed step-wise. The principal decommissioning steps of the dry decommissioning in situ are presented with the flow sheet in Fig. 3

Interim covering
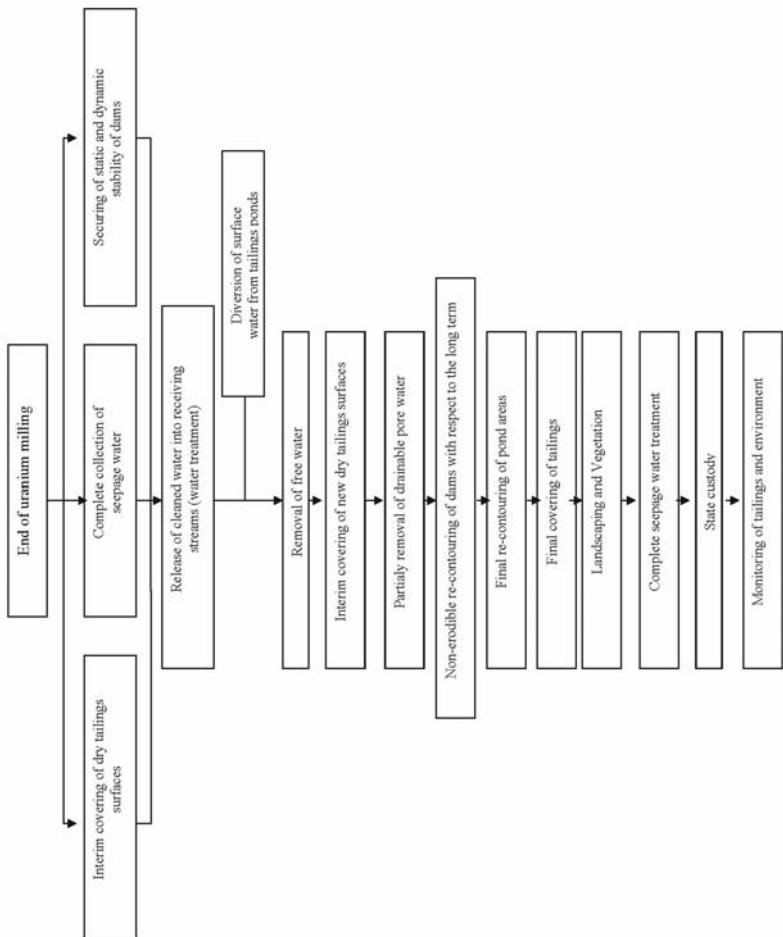
Interim covering of exposed sandy tailings beaches joins both the defence measure to avoid dusting and the decommissioning measure to create a trafficable surface. Interim covering of fine tailings surfaces is needed to create a trafficable surface for any further decommissioning works. Due to expelling the pond water subaerial tailings surfaces dry out during dry seasons thus consolidating the upper tailings

layers near surface and increasing their trafficability. After a while a geotextile and a geogrid are being placed. In the following drainmats or the first thin permeable interim cover layer is placed on top of the geogrids to grant lateral drainage due to further loading. Then the next interim cover layers consisting of thin layers of waste dump material are placed progressively on the entire pond area. The velocity of progressive interim covering on fine tailings depends on the time-dependent consolidation and dewatering of fine tailings thus increasing their shear-strength. The placement of the first interim cover layer on the fine tailings surface is of critical importance for the over-all decommissiong progress. With respect to workers safety a saftey factor eta ≥ 1.3 (acc. to DIN 4084) is to be guaranteed during all stages of ongoing construction works. To speed up the increase of shear strength with time vertical wick drains are stitched in the fine tailings to a depth of ca. 5 m. Before interim covering time-dependent consolidation of fine tailings had been predicted based on geotechnical modeling taking into account the large strain deformations of fine tailings due to loading. Resulting from these models the most critical pond areas were identified. In those pond areas the initial layer of the interim cover was placed under water using swimming barges.

Re-contouring

The dams of the tailings ponds are re-contoured with respect to the long term. For all large tailings ponds of WISMUT dam reshaping has to be designed with respect to seismic stability to the long term. For this the maximum credible earthqake has been taken into account. Reshaped tailings dams are foreseen to be covered. The stability of this cover is to be proven as well. In addition erosion stability of the dams and of any cover placed on the reshaped dam is to be proven. Dam reshaping is currently ongoing by either reshaping the dams inside the pond area or by a combination of dam buttressing of the lower dam slopes and cutting the upper dam slopes inside the pond area.

Re-contouring of the ponds creates a new landscape granting a stable surface runoff to the long term. For designing this new landscape time-dependent settlements and deformations of the underlying tailings during and after decommissioning phase are to be taken into account. A runoff catchment system consisting of ditches and, if needed, runoff retention ponds is to be designed. On certain areas of thick fine tailings layers embankment fills have been placed or will be placed. In order to speed up consolidation of fine tailings along the main ditches for diversion of future runoff deep vertical wick drains were or will be stitched in the weak fine tailings. On Trünzig A tailings pond a 1100 m long and up to 11 m thick embankment fill is currently being placed. Vertical wick drains were stitched in the tailings down to a depth of max. 27 m. The upper part of this embankment fill will be cut after the the fine tailings will have been sufficiently consolidated to place the final cover.

Fig. 3. Flow sheet of dry decommissioning in situ.

The flow chart contains the following boxes:

- End of uranium milling
- Interim covering of dry tailings surfaces
- Securing of static and dynamic stability of dams
- Complete collection of seepage water
- Release of cleaned water into receiving streams (water treatment)
- Diversion of surface water from tailings ponds
- Removal of free water
- Interim covering of new dry tailings surfaces
- Partialy removal of drainable pore water
- Non-erodible re-contouring of dams with respect to the long term
- Final re-contouring of pond areas
- Final covering of tailings
- Landscaping and Vegetation
- Complete seepage water treatment
- State custody
- Monitoring of tailings and environment

Active and passive soil treatment techniques

Final covering

The final cover is the last important construction step of dry decommissioning in situ. Among other functions it shall mainly:
a)   avoid any direct contact of tailings to humans or animals to the long term
b)   guarantee a stable vegetation granting storage and evapotranspiration of water from precipitation
c)   reduce infiltration of precipitation water through the final cover into the tailings

For more than five years WISMUT evaluated the performance of many different final cover types in several test fields of 200 m^2 including the following final cover types: store-and-release cover, capillary barrier cover, cover types including a sealing layer. The evaluation of the daily measurements of runoff, water content and soil suction with depth and percolation through the final cover and of all relevant meteorological parameters showed the advantage of the store-and-release cover system for final covering WISMUT´s tailings ponds with regard to the site specific and regional climate conditions. For example the store-and-release final cover to be constructed on the Helmsdorf tailings pond starting from May 2005 consists of a storage layer of sufficient thickness and plant available water content. The regional climate is characterized by a dry summer/autumn season and by a wet winter/spring season. Cohesive earthen materials are used for constructing the storage layer. The thickness and compaction degree of the placed cohesive earthen storage layer are dimensioned with respect to the climate conditions. During dry summer/autumn season the plant available water content in the storage layer is completely reduced by evapotranspiration. During wet winter/spring season the precipitation is stored in the storage layer. In principle the annual storage capacity of the store-and-release cover can be calculated by the final cover´s plant available water content times its thickness. More than five years of testing showed that the store-and release covers meet the design requirements. They are in particular stable against drying out, frost effects and time-settlements and deformations of the underlying tailings.

State of decommissioning progress

Up to date 90% of seepage and runoff from the tailings ponds is continuously being catched and treated. 95% of the pond water has already been expelled, treated and discharged to the receiving streams. 75% of tailings surfaces have been interim covered. Re-contouring of dams and ponds is currently ongoing on the Trünzig, Helmsdorf and Dänkritz 1 tailings ponds. Large embankment fills were and will be constructed on certain tailings ponds including installation of deep vertical wick drains to speed up settlement of thick fine tailings layers. The final cover is currently being placed on the Trünzig A tailings pond and is going to be placed on the Helmsdorf and Dänkritz 1 tailings ponds starting in May 2005. Fig. 5 shows the state of re-contouring of the Trünzig tailings ponds in autumn 2004. The entire pond is interim covered. Nearly all the dams have been reshaped. Construction of the large embankenment fill is ongoing.

Fig. 4.   Trünzig tailings pond in autumn 2004.

Active and passive soil treatment techniques

Characterizing Uranium Solubilization Under Natural Near Oxic Conditions

Chicgoua Noubactep[1], Dirk Merten[2], Till Heinrichs[1], Jürgen Sonnefeld[3], Martin Sauter[1]

[1]Geowissenschaftliches Zentrum der Universität Göttingen; Goldschmidtstrasse 3, D - 37077 Göttingen, E-mail: cnoubac@gwdg.de
[2]Institut für Geowissenschaften der Friedrich-Schiller-Universität Jena; Burgweg 11, D - 07749 Jena;
[3]Institut für Physikalische Chemie der Friedrich-Schiller-Universität Jena; Lessingstrasse 10; D - 07743 Jena

Abstract. A solubilization study for in total 782 days using not shaken batch experiments with uranium-bearing rock and three natural carbonate minerals was conducted to characterize uranium (U) leaching under oxic conditions. Results showed that aqueous U concentration increased continuously with a solubilization rate of 0.16 □gm-2h-1 for the first 564 d (1.5 y). After 1.5 y, U concentration reached a maximum value (saturation) and decreased afterwards. The saturation concentration of 54 mgL-1 (mean value) was influenced to variable extent by the presence of carbonate minerals. Dissolution/precipitation, adsorption or ion exchange processes appear to control U solubilization.

Introduction

Contamination of soils and groundwater with uranium (U) has been observed at several former mining sites worldwide, posing hazards to human health (e.g. Jerden and Singa 2003, Junghans and Helling 1998). U has a very long half-live (4.5 10^9 years) and can circulate in the environment for millions of years. Therefore, a thourough clean-up of contaminated sites should be performed immediately once pollution occurs. U retention in the soil matrix through processes such as sorption or ion exchange cannot reduce the potential adverse effects of this long-lived radionuclide (e.g. Langmuir 1997, Lee et al. 2005). Therefore, methods have been developed which could enable complete U extraction from soil and groundwater and its eventual subsequent appropriate treatment (e.g. Lee et al. 2005). One of the

most favourite methods consists of immobilizing U in permeable reactive barriers (PRB). U immobilization in PRB can be biotic and/or abiotic (Naftz et al. 2002).

Regardless from the nature of U immobilizing processes in a PRB, the pollutant has to be solubilized (e.g. from tailing materials) and transported to the barrier. U solubilization from soils and mine tailings and its subsequent transport to the PRB is the result of interactions in the system "natural water–geomaterials" (Felmy et al. 2002, Froment et al. 2002). The kinetics of U solubilization at each site will depend on the interactions between local geochemistry and infiltrating natural water. However, available data on U solubilization are mostly gained from leaching experiments performed on synthetic samples with technical solutions; so called lixiviants: $(NH_4)_2CO_3$, Na_2CO_3, $NaHCO_3$, H_2SO_4 (Elles and Lee 1998, Kaplan and Serkiz 2001, Noubactep et al. 2005).

The main reactions taking place between water and mineral phases in the subsurface fall into four main categories: dissolution/precipitation reactions, exchange reactions, acid-base reactions, and redox reactions (Elles and Lee 1998, Wilson 2004). Together with sorption/desorption processes, these interactions control contaminant mobilization/retardation in the environment. Discussions whether sorption/desorption processes or mineral dissolution/precipitation controls the levels of soluble U in nature has been an interesting research area (e.g. Elles and Lee 1998). Natural highly sorptive materials of concern include organic matter and Al/Fe/Mn/Ti oxyhydroxides. In the absence of sorptive materials, dissolution/precipitation reactions, exchange reactions, acid-base reactions, and redox reactions are expected to control U solubilization. The overall kinetics of U(VI) dissolution is relatively rapid compared to U(IV) oxidation. Therefore, it is expected that acid-base and dissolution/precipitation reactions will dominate interactions between water and minerals under oxic conditions.

Short term shaken laboratory batch experiments are commonly performed when investigating U solubilization from environmental samples (Carroll et al. 1998, Eless and Lee 1998, Felmy et al. 2002, Kaplan and Serkiz 2001). Alternatively, long term non stirred batch experiments involving solution replacement are conducted (e.g. Froment et al. 2002). Such experimental conditions are not appropriate for all environmental scenarios. For instance, if groundwater inflow in a subsurface area is faster than the outflow, a quasi-stagnation will be observed. In such regions, groundwater residence time can be long enough to be simulated by not-shaken batch experiments.

The widespread approach to characterize the environmental behaviour of trace metals and radionuclides consists of short-term, well-controlled laboratory experiments with synthetic model substances and transferring the results to more complex natural systems (Carroll et al. 1998, Malmström et al. 2000). Therefore, an important gap exists between laboratory experiments and field observations (Malmström et al. 2000). It is expected that laboratory experiments with natural samples could bridge this gap (Noubactep 2003).

The objective of this study was to characterize U solubilization from a multimineralic rock under quasi-stagnating oxic conditions. For this purpose not shaken batch experiments were conducted with tap water, a defined amount of an U-bearing rock (8 gL^{-1}) and three carbonate bearing additives (Calcite, Dolomite and

Vaterite – 8 to 48 gL^{-1}) for experimental duration of up to two years (782 days). While U-bearing rock was used to mimic tailing materials, the three natural additives of different solubility have been added in order to characterize the effect of CO_3^{2-}-bearing minerals on U solubilization. Carbonate mineral weathering by tap water could provide elevated CO_3^{2-} concentrations as encountered in nature as a result of microbial activity. It is expected that aquo-complexes of U with CO_3^{2-} such as $Ca_2[UO_2(CO_3)_3]\cdot10H_2O$ (Bernhard et al. 2001) will enhance aqueous U solubility and promote rock dissolution.

Experimental Section

Batch experiments were conducted without shaking the suspension. The batches consisted of mixtures of constant amounts of an U-bearing rock (8 gL^{-1}) and a carbonate mineral (Calcite, Dolomite, Vaterite), respectively. Equilibration times varied from 14 to 782 days. A further experiment without carbonate mineral (rock alone) was conducted. Thus, the extent of U solubilization by tap water (proxy for seepage water – Noubactep 2003) as influenced by carbonate minerals was characterized.

Uranium solubilization was initiated by adding 13.0 mL of a tap water to 0.1 g of the U-bearing rock and 0.1 g of each additive in glass essay tubes at laboratory temperature (about 21° C). The used tap water of the city of Jena (Thuringia, Germany) has a composition (in mgL^{-1}) of Cl^-: 15.72; NO_3^-: 10.0; SO_4^{2-}: 72.1; HCO_3^-: 270; Na^+: 8.72; K^+: 5.28; Mg^{2+}: 29.3 and Ca^{2+}: 80.9. Initial pH was 7.4. At selected dates, 0.05 to 0.25 mL of the supernatant solution was retrieved at the top of each tube for U analysis. The aqueous U concentration was recorded as a function of time.

The U-bearing rock was crushed and sieved. The fraction 0.250 to 0.315 mm was used without any further pre-treatment. The rock contains ca. 2.3 % U and is further composed of: 81.25 % SiO_2, 0.14% TiO_2; 7.36 % Al_2O_3, 1 % Fe_2O_3, 0.01% MnO; 0.48 % MgO, 0.67 % CaO, 1.19 % Na_2O, 1.48 % K_2O, 0.36 % P_2O_5 and 0.01% SO_3.

Calcite (pK_{sp} = 8.48; SiO_2: 0.3 %, MgO: 1.02 %, CaO: 55.1 %), Dolomite (pK_{sp} = 17.09; SiO_2: 1.2 %, MgO: 20.3 %, CaO: 31.0 %) and Vaterite (pK_{sp} = 8.34; SiO_2: 0.5 %, MgO: 1.12%, CaO: 55.0 %) minerals were crushed, sieved and the fraction 0.63 to 1.0 mm was used. It is expected that their dissolution will increase kinetic and the extent of U solubilization. Calcite and Dolomite were selected because of their natural abundance (Elfil and Roques 2004, Sherman and Barak 2000). Although Vaterite is very rare in nature, it was used in this study because it has some features such as high specific surface area and high solubility compared to Calcite (Su and Wu 2004).

Dissolved U concentrations were measured with inductively coupled plasma mass spectrometry (ICP-MS, PQ3-S, ThermoElemental) because of its higher sensitivity and fast analytical speed. The quality of the analyses was checked using

synthetic standards. The instrumental precision, determined as ± 1 standard deviation for three runs on the same sample was better than 5%.

The pH value was measured by combination glass electrodes (WTW Co., Germany). All experiments were performed in triplicate. Error bars given in figures represent the standard deviation from the triplicate runs.

In all experiments, dissolved U was normalized to rock surface area (3.53 m^2g^{-1}), solution volume (using 0.013 L for all runs) and rock concentration (7.69 gL^{-1}). Rock dissolution rates ($\mu gUm^{-2}h^{-1}$) were determined from the slopes of linear regressions of normalized U concentration released versus time which also included the origin (0,0). The calculated uncertainty of the slopes ranged from 2.1 to 14.2%.

SEM analyses: Crushed grains of the rock sample were C-coated and examined by scanning electron microscopy (SEM) and mineral phases were identified by semi-quantitative energy dispersive X-ray analysis (EDX) using a LEO1530 Gemini microscope equipped with an OXFORD Inca analytical system. The accelerating voltage was 25 kV, probe current ca 150 pA, counting time 60 sec.

Results and Discussion

SEM Observations

Qualitative SEM–EDX examinations of a rock sample provided direct information on rock composition that complemented information obtained from X-ray fluorescence analyses (experimental section). The EDX analysis revealed that the used U-bearing rock is a multimineralic rock containing among others uraninite (UO_2), arsenopyrite (FeAsS,), and galena (PbS). Associations of U with arsenopyrite was also encountered. The gangue mainly consists of alkali-feldspars and quartz.

Uranium solubilization
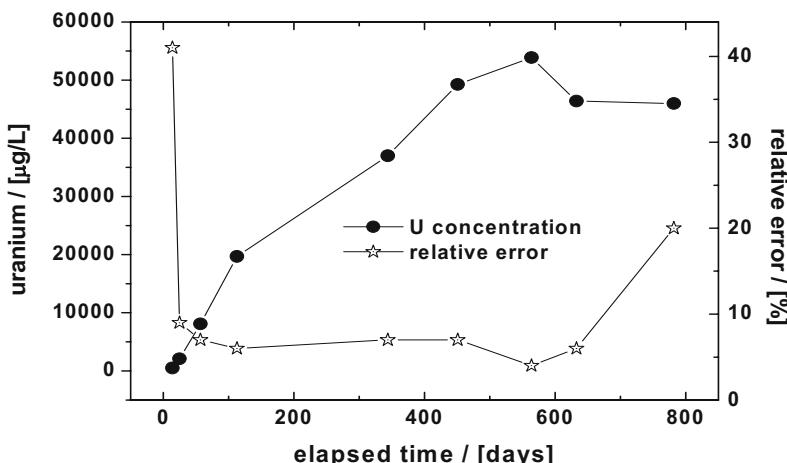
After the determination of the aqueous U concentration (C = mean value of a triplicate) at any time, the corresponding standard deviation ($\square$) was calculated and the relative error (Pr = 100 * $\square$/C; in %) was deduced. At the end of the experiment pH values (7.8 to 8.4 for the eight systems) and aqueous concentrations of selected elements were determined. To characterize U solubilization from the multimineralic rock while taking individual properties of CO3-bearing rocks into account, four different experiments have been performed over a duration of up to 782 d (2.14 y) with 8 gL-1 U rock and 0 or 8 gL-1 additive: I) rock alone, II) rock + Vaterite, III) rock + Calcite, and IV) rock + Dolomite (system I, II, III and IV). Additional experiments were conducted in system III with 16, 32 and 48 gL-1

Calcite [systems IIIa, IIIb and IIIc] and in system IV with 48 gL-1 Dolomite [system IVc] to access the influence of CO32--mineral amount on U solubilization.

Kinetics of U solubilization

Fig. 1 summarizes the variation of the U concentration (C in μgL^{-1}) and the relative error (P_r in %) within the triplicates as a function of time for U-bearing rock in tap water (system I). It can be seen that U concentration increases continually with the time from the start of the experiment (t = 0) to a maximum at t = 564 d, afterwards concentration slowly decreases throughout the end of the experiment (day 782). For t ≤ 564 d, the rate of U solubilization ($\mu gm^{-2}h^{-1}$) was defined as the slope of the straight line, i.e. C = a * t. The rate obtained for U solubilization (a = 0.16 $\mu gm^{-2}h^{-1}$) was comparable to that of amorphous silica reported by Xu and Pruess (2000). This value is by far smaller than 0.78 $\mu gm^{-2}h^{-1}$ obtained under atmospheric conditions in air homogenized batch experiments (Noubactep et al. 2005). The difference is easily explained by the slowness of diffusive processes in the present work.

The plot of the variation of the relative error (P_r) shows a maximum (41%) at the beginning of the experiment (t = 14 d). This value continuously decreases to a minimum of 4 % at t = 564 d, afterwards P_r increases to 20 % at the end of the experiment (t = 782 d). The maximum concentration (C_{max}; U saturation) coincides with the minimum value of P_r suggesting that, after ca. t = 564 d, the system is close to steady state ("pseudo-equilibrium"). The measured maximum concentra-

Fig. 1.   Variation of the uranium concentration (µg/L) and the relative error (%) within the triplicates as a function of time for the reference system (U-bearing rock in tap water).

Active and passive soil treatment techniques

tion C_{max} (54 mgL^{-1}) is comparable to that reported for some contaminated sites (Jerden and Singha 2003, Junghans and Helling 1998), supporting the capability of the experimental procedure (not shaken closed batch systems) to simulate certain field conditions. While performing similar experiments at atmospheric pressure (P_{CO2} = 0.035 %), Noubactep et al. (2005) reported an U concentration of 8.3 mgL^{-1} at pseudo-equilibrium (pH 7.8). This value is obviously larger than that predicted by the solubility of Schoepite (10^{-5} M or 2.4 mgL^{-1}, Noubactep 2003), but thermodynamic equilibria are rare in nature (Meinrath and May 2002). Therefore the present experiments help to explain some observations in nature.

The concentration evolution can be explained by several complex processes: U leaching from rock, U sorption onto rock by-minerals (e.g. Al_2O_3, SiO_2, TiO_2), and U precipitation from the aqueous phase (e.g. $UO_3.2H_2O$). It is emphasized that during the first phase of the experiment ($0 \leq t(d) \leq 564$) U releasing processes dominate. At $t > 564$ d, U precipitation dominates since U concentration decreases. The characterization of individual processes (adsorption, complexation, precipitation…) responsible for the evolution of C under the experimental conditions of this work is not possible. However, the objective of this study is not to accurately define the systems in which the materials (U-bearing rock and CO_3-minerals) are involved, but rather to characterize the effect of the minerals on U solubilization qualitatively. Therefore, the evolution of other systems (system II, III and IV) will be compared to that of the reference system (system I) while characterizing system evolution by the rate of U solubilization and the trend in the variation of both C and P_r.

Effect of the nature of carbonate minerals

Fig. 2 (a and b) summarizes the results of the U solubilization in systems I, II, III and IV and Table 1 gives the variation of the relative error with the experimental duration in all the systems. From figure 2a it is apparent that the best U solubilization rate for the first 250 days is achieved when Vaterite is present (system II), supporting the hypothesis that U solubilization is affected by the presence of CO_3^{2-}-minerals. Apart from Vaterite, all other minerals reveal lower U solubilization during the first 100 days of the experiment (Fig 2a). This observation suggests either that: (1) U solubilization is inhibited by the presence of certain CO_3^{2-}-minerals, (2) solubilized U is adsorbed on rock materials until its sorption capacity is exhausted, or (3) the amount CO_3^{2-}-ions from mineral dissolution is insufficient to solubilize adsorbed U from rock materials.

Table 1. Variation of the relative error (%) in the individual systems as function of the time.

t (days)	I	II	III	IV	IIIa	IIIb	IIIc	IVc
14	41	106	14	21	20	24	26	13
25	9	71	9	43	30	11	45	43
57	7	39	6	23	21	9	9	15
113	6	3	5	8	8	11	5	6
344	7	10	2	13	6	11	2	9
451	7	14	2	12	5	13	2	8
564	4	8	2	8	4	5	7	11
633	6	12	3	11	5	11	3	9
782	21	11	1	11	7	11	1	9

The first hypothesis does not apply since Vaterite and Calcite are almost of the same chemical composition. Therefore, it can be assumed that once U is leached from the rock, it is adsorbed to rock by-materials until sufficient CO_3^{2-}-ions are generated to form soluble U complexes. Thus Vaterite with the highest solubility could enhance U solubilization already at the early stage of the experiment. For other minerals this enhancing effect was delayed due to their lower solubility.
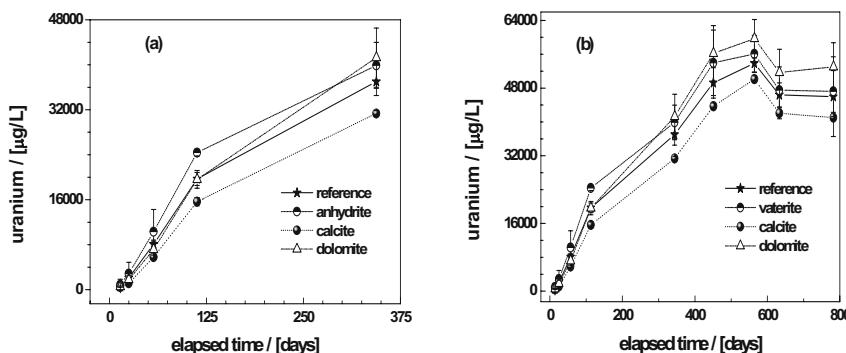
The solubilization efficiency is lowest when Calcite is present (system III); this observation is confirmed by the values of the rate of U solubilization (Table 2). For longer experimental durations (up to 564 days, Fig. 2b), system III still exhibits the smallest U solubilization rate whereas system II and IV (Vaterite and Dolomite) significantly increase U solubilization compared to the reference system. The solubilization enhancement was highest in the presence of Dolomite (system IV). These observations cannot be explained by the relative solubility of the mineral, since Dolomite is by far less soluble than Calcite and Vaterite. It should be kept in mind that solubility products are defined for pure phases. The evolution of the relative error (P_r, Table 1) shows that the mineral dissolution is a complex process. In fact, system II exhibits the largest variation of P_r-values in the initial phase (up to 105 %) which then rapidly decreases to 3 % after 113 days. Apart from system IV (Dolomite) for which the P_r-value was not maximal at the beginning of the experiment (14 days) all other additives showed the same evolution of P_r as the reference system with the only difference that no minimum was attained but rather a relative constant value at the end of the experiment ($t > 300$ d). The fact that the curve of P_r-value did not reach a minimum as for system I illustrates the complexity of the processes determining C under experimental conditions. Since CO_3^{2-}-mineral dissolution was not at equilibrium it can be emphasized that the concentration decrease results from precipitation (e.g. $UO_2.2H_2O$, UO_2CO_3), co-precipitation (e.g. $CaUO_2(CO_3)_2$) and U incorporation into the structure of CO_3^{2-} minerals.

Effect of the amount of carbonate minerals

To further investigate the impact of CO_3^{2-}-minerals on U solubilization and in particular the possibility of U incorporation into the structure of CO_3^{2-}-minerals (e.g. Reeder et al. 2000) larger amounts of Calcite and Dolomite were tested in systems III (IIIa, IIIb, IIIc) and IV (IVc). If the impact of U incorporation into the structure of Calcite and Dolomite is important, then U concentration in systems IIIc and IVc (48 g.L^{-1} additive) will be significantly lower than in system III and IV (8 g.L^{-1} additive) at any time. The results for system III showed that during the whole experiment, system III (8 g.L^{-1} Calcite) exhibits the lowest U solubilization whereas the evolution of systems with other Calcite amounts (16, 32 and 48 g.L^{-1}) was very close to that of the reference system. Therefore, for higher Calcite mineral amounts U solubilization is enhanced. For Dolomite (system IV), U solubilization was higher in system IV (8 g.L^{-1}) than in system IVc (48 g.L^{-1}) from the beginning of the experiment to t = 400 d. Later on the inverse applies. These observations suggest that U incorporation into mineral structure is more likely to occur in Dolomite that in Calcite. In both cases, P_r-value variation was minimal in the system with the highest mineral amount (IIIc and IVc).

Solubilization of other elements

In order to gain insight into the solubilization behaviour of other components of the multi-mineralic rock, the concentration of nine (9) elements was determined at the end of the experiment (t = 782 d), i.e. Co, Ni, Cu, Zn, Rb, Sr, Sb, Ba and Pb.

Fig. 2.   Comparison of U(VI) solubilization as influenced by carbonate minerals for 344 days (a) and 782 days (b). For clarity, only the plots for the reference system (system I) and the systems with 8 g/L additives (system II, III & IV, see text) are presented. The experiments were conducted in triplicates. Error bars give standard deviations. The lines are represented to

Table 2. Co, Ni, Pb, Sb, Sr and U concentrations as measured in different systems at the end of the experiment (782 d). a ($\mu gm^{-2}h^{-1}$) is the rate of U solubilization. The absolute element concentration ([X] in $\mu g/L$) of system I is given in the first line and serves as reference for the definition of the relative concentration. The elements are ranged in the order of increasing relative concentration for system II from the left to the right.

System	a $\mu gm^{-2}h^{-1}$	^{121}Sb	^{238}U	^{208}Pb	^{88}Sr	^{60}Ni	^{60}Co
[X](μgL^{-1})		28	55.000	116	360	0.55	0.09
I	0.16	100	100	100	100	100	100
II	0.17	52	105	172	215	565	980
III	0.14	59	92	128	99	105	138
IV	0.18	69	114	131	107	108	77
IIIa	0.16	57	103	129	101	161	187
IIIb	0.17	61	105	183	108	186	552
IIIc	0.17	59	106	114	103	111	192
IVc	0.17	46	110	132	107	187	220

Table 2 presents the results for five selected elements together with Uranium. The absolute concentration (C - mean value of triplicates) of each element in the reference system is given. For other systems the relative concentrations are given. The relative concentration (P_r' in %) is defined as $100 * C/C_{ref}$, such that for system I (reference) $P_r' = 100$ %; $P_r' > 100$ % when a CO_3^{2-}-mineral enhances element solubilization and $P_r' < 100$ % when a mineral inhibits element solubilization.

From Table 2 it can be seen that, apart from Sb, CO_3^{2-}-minerals enhance solubilization of all other elements. The extent of the solubilization modification varies from 46 % for Sb in system IVc to 980 % for Co in system II (Calcite). It would have been interesting to follow the evolution of several of these elements with time. To characterize target mixed contamination scenarios, one or more metal-bearing rocks can be mixed similar to the present study for solubilization studies.

Conclusions

The mixture of U- and CO_3^{2-}-bearing minerals has revealed that adsorption, solution/precipitation and U incorporation in mineral structures are essential in discussing U solubilization. In nature, the situation will be complicated by organic ligands derived from decomposing organic matter or from the direct activities of soil microbes or plant roots (e.g. Wilson 2004). In closed areas of the natural environment U concentrations can reach very high values. The extent of U transport from such areas into the environment for instance after for example a rainfall event depends on site specific geochemical conditions. When sufficient amounts of organic matter and/or Al/Fe/Mn/Ti oxyhydroxides are present, U transport can

be significantly retarded, if groundwater flow is slow enough to allow adsorption equilibrium. Otherwise U can be transported to distances of up to hundreds of kilometers within relatively short time periods (Lee et al. 2005). Field and laboratory studies suggest that both dissolution/precipitation of U-bearing minerals and adsorption/desorption reactions are the most important processes in the attenuation or release of U (e.g. Elless and Lee 1998). However, attempts have been made to deduce the nature of mineral phases from U concentrations via thermodynamic arguments. This work has shown that under stagnant conditions metastable states can persist over months. Therefore any attempt to determine solubility limiting phases from field U concentration is uncertain (Fanghänel & Neck 2002).

The results of the present study indicate that investigating the dissolution from multi-mineralic rocks can be a powerful tool to characterize multi-contaminant systems. Further testing of mineral-water systems under various experimental conditions is asked for, to verify capacity of such systems to describe natural processes.

Acknowledgments

References

Bernhard G, Geipel G, Reich T, Brendler V, Amayri S, Nitsche H (2001) Uranyl(VI) carbonate complex formation. Radiochim Acta 89: 511-518.

Carroll SA, O'Day PA, Piechowski M (1998) Rock-Water Interactions Controlling Zinc, Cadmium, and Lead Concentrations in Surface Waters and Sediments, U.S. Tri-State Mining District. Environ Sci Technol 32: 956-965.

Elfil H, Roques H (2004) Prediction of the limit of the metastable zone in the "$CaCO_3$–CO_2–H_2O" system. AIChE Journal 50**:** 1908-1916.

Elless MP, Lee SY (1998) Uranium solubility of carbonate-rich Uranium-contaminated Soils. Water Air Soil Pollut. 107: 147-162.

Fanghänel Th., Neck V. (2002) Aquatic chemistry and solubility phenomena of actinide oxides/hydroxides. Pure Appl. Chem. 74: 1895-1907.

Felmy AR, Rai D, Hartley SA, LeGore VL (2002) Solubility and Leaching of Radionuclides in Site Decommissioning Management Plan (SDMP) Slags. Report NUREG/CR-6632. 60pp.

Froment P, Cara J, Ronneau C (2002) The solubilisation of Ru and U from condensation particles released b overheated nuclear fuel and maturated in air and in argon. Radiochim. Acta 90: 395-398.

Jerden Jr JL, Singha AK (2003) Phosphate based immobilization of uranium in an oxidizing bedrock aquifer. Appl Geochem 18: 823-843.

Active and passive soil treatment techniques

Junghans M, Helling C (1998) Historical Mining, uranium tailings and waste disposal at one site: Can it be managed? A hydrogeological analysis. In Tailings and Mine Waste '98, Balkema, Rotterdam, 117-126.

Kaplan DI, Serkiz SM (2001) Quantification of thorium and uranium sorption to contaminated sediments. J Radioanal Nucl Chem 248: 529-535.

Langmuir D (1997) Aqueous Environmental Geochemistry. Prentice Hall, 600 pp.

Lee J-U, Kim S-M, Kim K-W, Kim IS (2005) Microbial removal of uranium in uranium-bearing black shale. Chemosphere 59: 147-154.

Malmström ME, Destouni G, Banwart SA, Strömberg BHE (2000) Resolving the scale-dependence of mineral weathering rates. Environ Sci Technol 34: 1375-1378.

Meinrath G, May P (2002) Thermodynamic prediction in the mine water environment. Mine Water Environ 21: 24-35.

Naftz D, Morrison SJ, Fuller CC, Davis JA (eds) (2002) Handbook of groundwater remediation using permeable reactive barriers-Applications to radionuclides, trace metals, and nutrients. Academic Press, San Diego, Calif., 539 pp.

Noubactep C (2003) Dissertation, TU Bergakademie Freiberg, Wiss. Mitt. Institut für Geologie der TU Bergakademie Freiberg, Band 21, 140 pp, ISSN1433-1284.

Noubactep C, Sonnefeld J, Sauter M (2005) Laboruntersuchungen zur Freisetzung von U_{nat} aus einem Gestein unter oxischen Bedingungen. Grundwasser 10: 35-42.

Reeder RJ, Nugent M, Lamble G M, Tait CD, Morris DE (2000) Uranyl Incorporation into calcite and argonite. Environ Sci Technol 34: 638-644.

Sherman LA, Barak P (2000) Solubility and Dissolution Kinetics of Dolomite in Ca–Mg–HCO_3/CO_3 Solutions at 25°C and 0.1 MPa CO_2. Soil Sci Soc Am J 64: 1959-1968.

Sun D-M, Wu Q-S (2004) Assembly synthesis of sheet-like calcite array and stable-vaterite by supported liquid membrane. Chin J Chem 22: 1067-1069.

Wilson M.J. (2004) Weathering of the primary rock-forming minerals: processes, products and rates. Clay Miner. 39: 233-266.

Xu T., Pruess K. (2000) in Proceedings World Geothermal Congress 2000 (Kyushu - Tohoku, Japan), 2983–2988

Active and passive soil treatment techniques

The optimal strategy of cleaning of fucoid sandstone

Michal Balatka[1], Hana Čermáková[1], Jan Novák[1], Jiří Mužák[2]
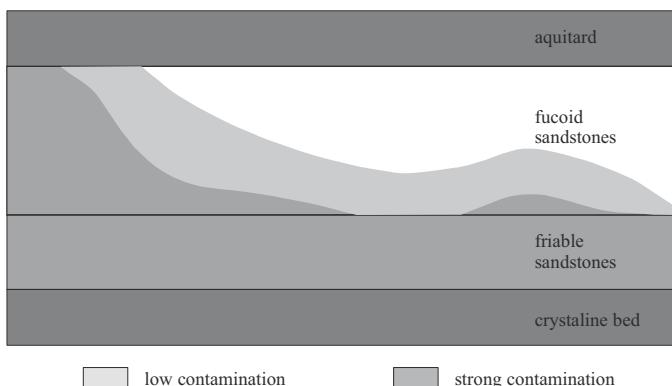
[1]Technical University in Liberec, Dept. of Modelling of Processes, Hálkova 6, 461 17 Liberec 1, Czech Republic, E-mail: jan.novak.lbc@volny.cz
[2]DIAMO, s. p., o. z. TÚU, Math. Modelling Centre, Máchova 201, 471 27 Stráž pod Ralskem, Czech Republic

Introduction

Uranium ore was exploited in the Stráž deposit of north-bohemian cretaceous sediments. There was also used in-situ leaching. Now there is running an extensive remediation process of rock environment. In Cenomanian aquifer there are 4.5 millions tons of dissolved substances. Two strata form the aquifer: friable and fucoid sandstones stratum. Lower friable sandstone stratum is 15 - 25 m thick and it is well permeable. Fucoid sandstone roof is about 40 metres. It is not wholly homogenous strata. The sub layer permeability ranges from centimetres to decimetres per day and it is almost twice lower then friable sandstone.

The contamination's scale of the fucoid sandstone is very changeable. In some places the contamination permeates the whole strata in the concentration reaching 50 g/l TDS. In general, the concentration is not so strong and declines in upper sub layers. Sometimes the contamination doesn't touch the top of the strata. The

Fig.1. Distribution of contamination in Cenomanian aquifer.

amount of the contamination of fucoid sandstone is about 35 %. The situation of contamination in the Cenomanian aquifer is at Fig. 1.

All computer models result in a necessity of at least partial cleaning of the fucoid sandstone strata. At this time the cleaning is rating to well permeable friable sandstone places of high contamination. At present time there are used the original exploitation pumping wells which were opened at the cenomanian base. At this method of pumping solids off, the contamination's scale in fucoid sandstone will lower only a little at the time of achievement required rank.

The purpose of this work is to find the optimal and effective method of cleaning the worse permeable layers. According to the results of this work, there are chosen the places of fucoid sandstone needing to be clean and which method will be used.
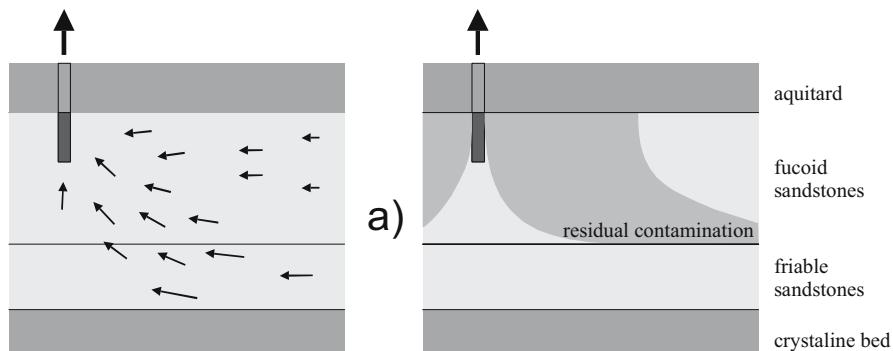
Methodology

To reach the effective cleaning of the fucoid sandstone there is three possibilities:
- Drawing solutions from the layers under the top of the strata
- Forcing out the contamination by injection the water or slightly alkaline lotion into these layers accordingly with drawing from the permeable friable sandstone sub base
- And to combine both preceding steps - to inject to the fucoid sandstone and to draw from this one
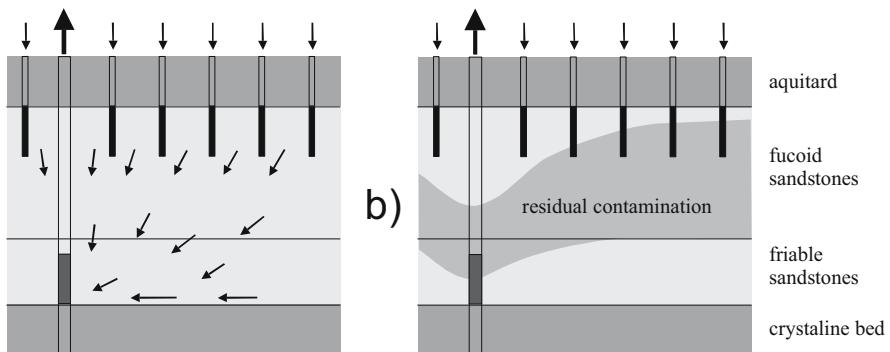
There is scheme of these processes at the Fig. 2a,b,c. There is demonstrated the flow on the left of figure. On the right there is the allocation of residual contamination that characterize proceeding of cleaning after the time.
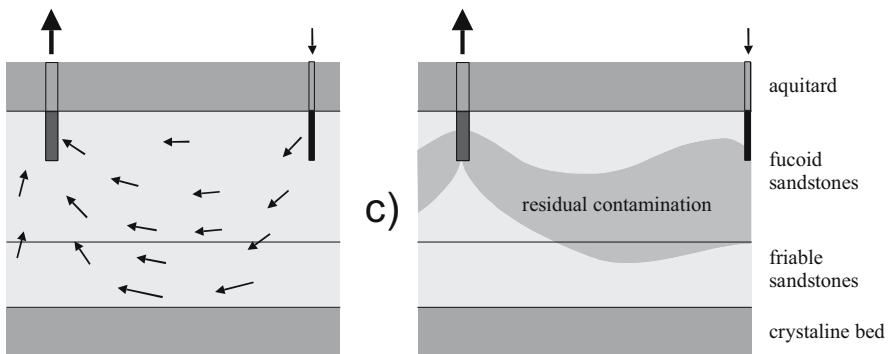
Several modelling tools were developed to find the effective method of remediation. They can monitor the amount of the withdrawn solids and the evaluation of situation in the underground. Technological and economical extensions serve for comparison of particular cleaning scenarios.

Fig. 2a.   Drawing solutions from the layers under the top of the strata.

Active and passive soil treatment techniques

Fig. 2b. Forcing out the contamination by injection the water or slightly alkaline lotion into these layers accordingly with drawing from the permeable friable sandstone sub base.

Fig. 2c.   Injection to the fucoid sandstone and drawing from this one.

Ranking of the technological effect

The first step in our solution is the simulation of underground processes (flow and transport) in dependence on well pattern configuration. The amount of removed solids out from the fucoid sandstone stratum expresses the technological effect of remediation process. The pattern of well spacing agrees with actual situation in Straz deposit. The capacity of pumping wells is 300 l/min default. This well is possible to clean various measure of deposit area. There can be used the current wells to pump the contamination solids out from lower friable sandstone stratum. For direct pumping from fucoid sandstone stratum there is necessary to drill new wells.

At places with the highest scale of contamination there are used the square modules 28x28 m of well nets. Those wells have small boring diameter and they

can't be used for pumping the solids out but for injection to fucoid sandstone stratum.

DIAMO cooperated with Technical University in Liberec to develop the mix-hybrid model of the finite element method. This model was used for the computer simulation of remediation. In the first stage of project there were simulated variant calculations on the schematic model mesh. The model mesh was divided into 18 layers with 3 m thickness. The physical parameters of each layer are shown at the Fig. 3.

In the first, second and third column (k_x, k_y, k_z) there are the coefficients of hydraulic conductivity in direction of particular axis. The coefficients are in m/day. Then there follow dates about active (n_a) and total porosity (n_Σ). The parameter α indicates the rate exchange of solutions between active and inactive pores. This time in days is needed to reduce the concentration differences scale down to the half.

There was the square mesh at the ground plan. This mesh covers a quarter of the area where is one pumping well. The module of inner dividing came up to the mesh of present used wells that is 28 x 28 meters.
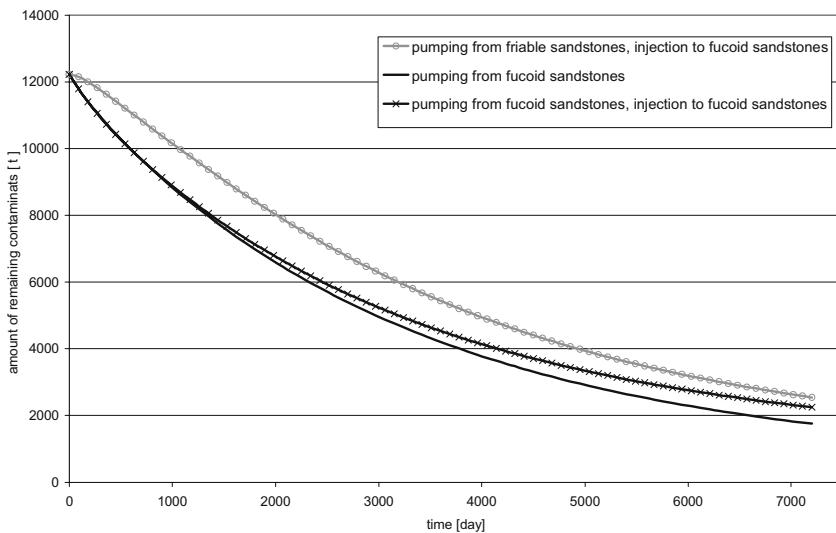
	model layer	k_x	k_y	k_z	n_a	n_Σ	α
fucoid sandstone	F13						
	F12	0.6	0.6	0.3	0.08	0.32	180
	F11						
	F10						
	F9	0.3	0.3	0.15	0.08	0.32	180
	F8						
	F7						
	F6	0.5	0.5	0.25	0.08	0.32	180
	F5						
	F4	0.05	0.05	0.02	0.04	0.32	720
	F3						
	F2	0.5	0.5	0.25	0.08	0.32	180
	F1						
friable sandstone	R5						
	R4	4	4	2	0.1	0.25	120
	R3						
	R2	2	2	1	0.1	0.25	120
	R1						

Fig. 3. The physical parameters of idealized rock environment of Cenomanian collector.

Active and passive soil treatment techniques
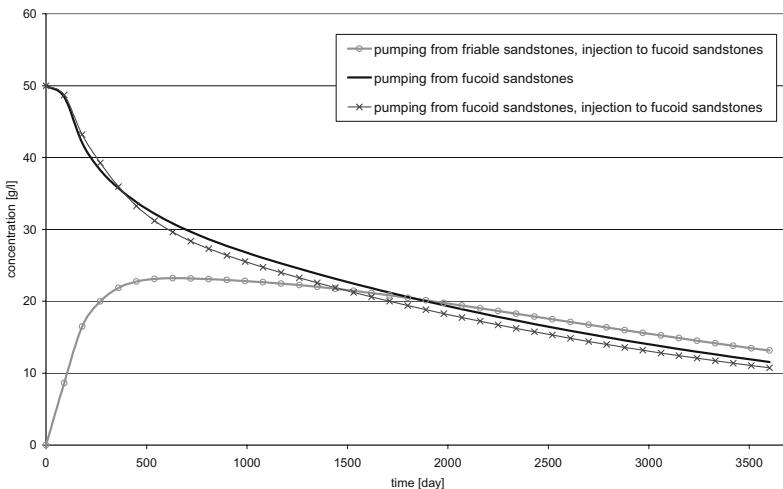
The Fig. 2a shows the pumping from fucoid sandstone stratum. In case of pumping from underground friable sandstone stratum, (Fig. 2b) the injecting wells were staggered with various densities (4 - 15 wells/ha) at the whole area. In case of pumping from fucoid sandstone stratum, (Fig. 2c), they were staggered around periphery of area. The extent of area belongs to one pumping well were changed in several variant (from 3 - 30 ha). As well the started contamination's range were various to correspond to the mostly occurred types at the Stráž deposit.

At the Fig. 4, there is comparison of technological effect of different cleaning methods. The concentration curves of contamination in pumped solutions are plotted at the Fig. 4a, residual contamination proceeding is at the Fig. 4b.

The strongly contaminated area, which is cleaning by one pumping well, is 8 ha large. Only the pumping of solids from fucoid sandstone stratum leads to the fastest cleaning. With area enlargement it is more effectively both to pump out from fucoid sandstone stratum and to inject to this one.

Fig. 4a. The comparing of technological effect of different cleaning methods - concentration curves of contamination in pumped solutions.

Active and passive soil treatment techniques
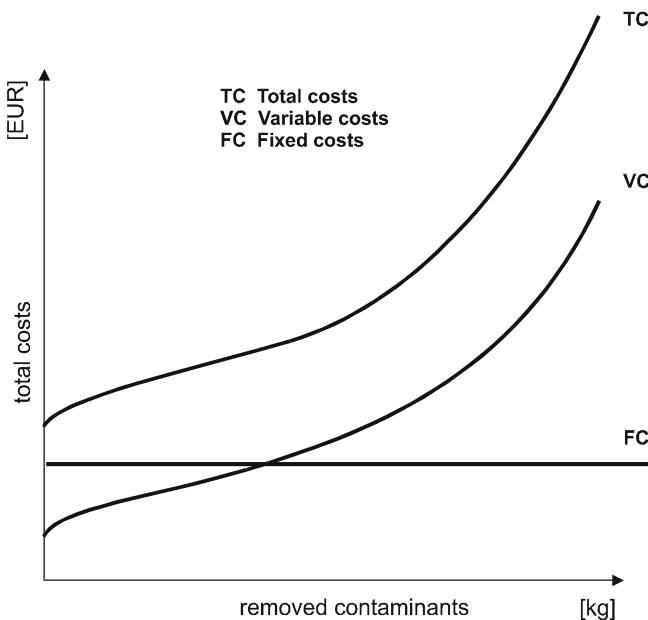
Fig. 4b. The comparing of technological effect of different cleaning methods - curves of concentration of residual contamination.

The optimizing problem
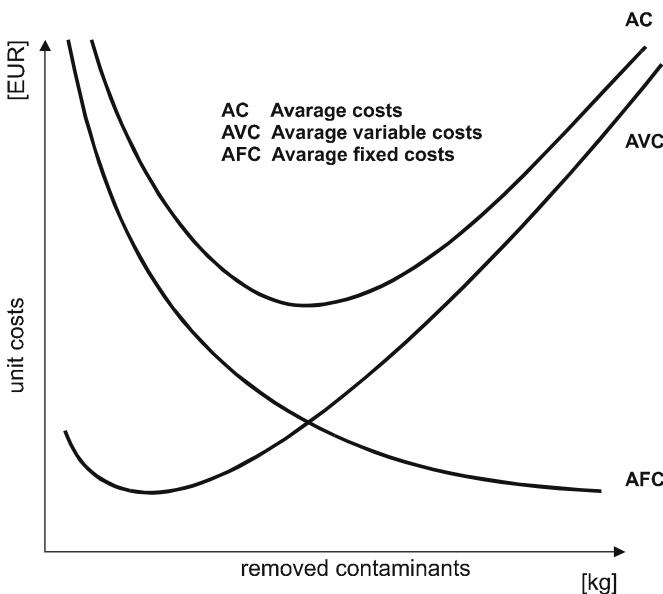
The efficiency of variant cleaning method depends on started contamination's range at a concrete place of Stráž deposit and on required target of residual contamination. The residual contamination at the monitored place can differ from required target to whole Cenomanian aquifer. The efficiency can be evaluated by economic criteria.

At first, it is necessary to build the cost model. The costs are divided into the fix costs and variable costs. The fix costs are considered as costs for preparing the particular cleaning site (drilling, pipe lines, etc.). The variable costs represent the volumes of injected and abstracted solutions (the unit costs were calculated per 1 m^3), salaries, maintenance and monitoring (unit costs were calculated per 1 ha per year).

The target of the cleaning is to remove a certain amount of contaminants so that the needed level of remaining contamination is achieved. So, the costs for removing of 1 kg of contaminants were chosen as the decision criterion. At the Fig. 5 there are shown the dependences of the total and unit costs on the amount of removed contaminants.

Active and passive soil treatment techniques

Fig. 5a. The dependence of total costs on amount of contaminants removed.

Fig. 5b. The dependence of unit costs on amount of contaminants removed.

Active and passive soil treatment techniques
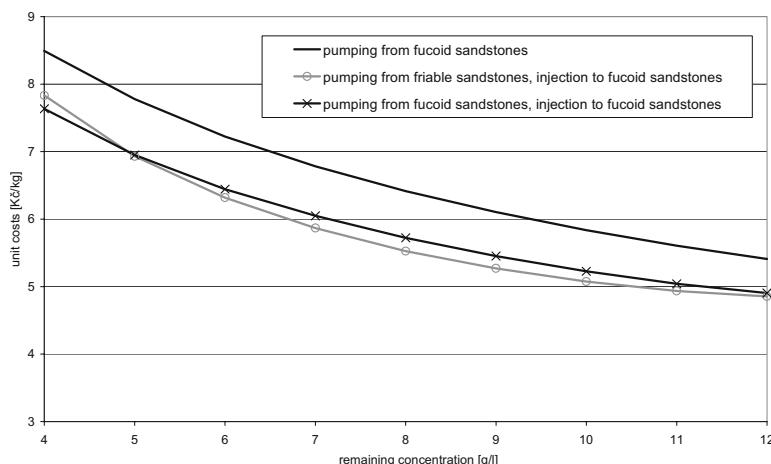
To find out the effective method of cleaning the modelling tool were developed. The models enable us to observe the amount of contaminants removed and to evaluate the situation in the underground. The technological and economical models serve for comparison of efficiency of individual cleaning scenarios. The obtained results we use for decision making in the whole remediation process.

Obtained results

The contaminated sites up to ca 30 ha can be effectively cleaned by one abstraction well. If the area is up to 12 ha, the most efficient method of cleaning is to use single well opened under the ceiling of the fucoid sandstone strata, see the Fig. 2a. Such method is more efficient than displacing of contamination (see Fig. 6). For areas between 12 and 30 ha is good to complete the single abstraction well by injection of water into the strata. It causes the displacing of the contamination.

The large continuously contaminated areas they are necessary to clean by contamination displacement by area injecting (Fig. 2b). The wells should be opened in friable sandstone strata. The density of the abstracting well pattern is more considerable than the density of the injecting well pattern. In the case of strong contamination, (see Fig. 8), it is suitable to use quite dense well pattern (224 x 224 m).

In the case of weak contamination, (see Fig. 8), it is suitable to use quite sparse well pattern (336 x 336 m), when demands on the target level of cleaning are not so strong. On the other hand, when demands on the target level of cleaning are too strong, it is suitable to use quite dense well pattern (224 x 224 m).

Fig. 6.   The efficiency of cleaning methods – contaminated area – 8 ha.

Active and passive soil treatment techniques
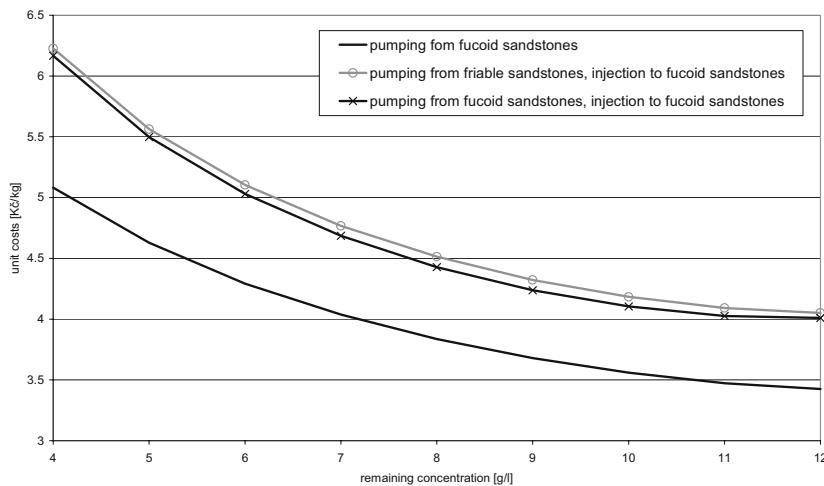
Fig.7.   The efficiency of cleaning methods – contaminated area – 16 ha.
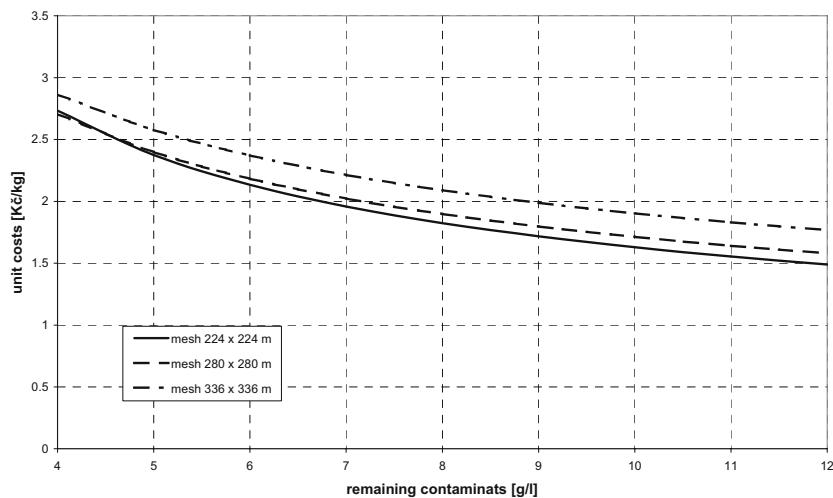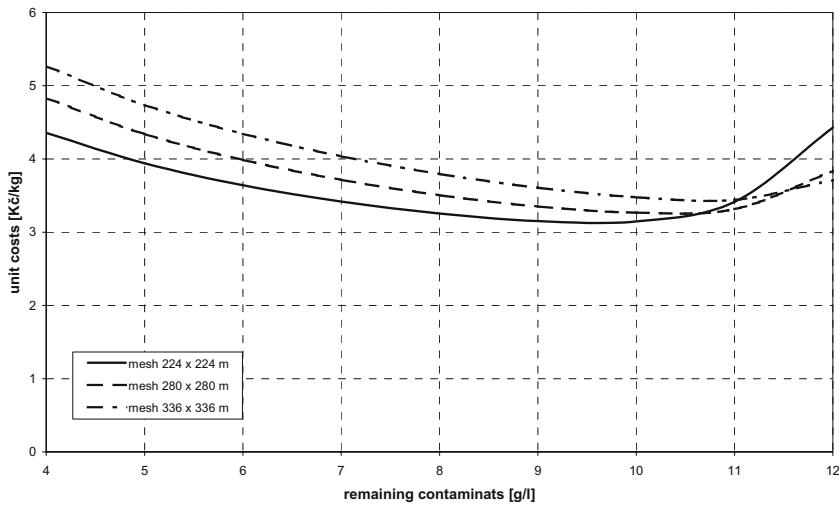
Fig. 8.   The efficiency of density of well pattern – strong continuous contamination.

Active and passive soil treatment techniques

Fig. 9.   The efficiency of density of well pattern – weak continuous contamination.

Conclusion

The removing of contamination from low permeable geological layers neighbouring high permeable layers is specific task in the frame of remediation of rock environment in the former uranium deposit Stráž. For the solution of the task the modelling system was developed. Using the system, we can evaluate technologic and economic effect of various cleaning approaches. The calculation results indicated the main principles of effective cleaning strategies. The system developed is suitable for planning and decision making during the remediation process. It is also suitable for specification of methods of cleaning of contaminated areas with the view to physical, geological, geochemical and other parameters.

References

Čermáková H.: Optimizing the remediation of the subsurface environment in the Stráž deposit. In B. Merkel, B. Planer-Friedrich, Ch. Wolkersdorfer eds. Uranium in the Aquatic Environment, Proceedings of the International Conference Uranium Mining and Hydrogeology III and the International Mine Water Association Symposium, Freiberg, Germany, 15 – 21 September 2002, pp. 793 – 802, Springer – Verlag Berlin Heidelberg 2002, ISBN 3 – 540 – 43927 – 7.

Čermáková H., Mužák J., Novák J.: Application of Numerical Simulation System on Turonian Aquifer Remediation Control. In B. Merkel, B. Planer-Friedrich, Ch. Wolkersdorfer eds. Uranium in the Aquatic Environment, Proceedings of the International Conference Uranium Mining and Hydrogeology III and the International Mine Water Association Symposium, Freiberg, Germany, 15 – 21 September 2002, pp. 319 – 326, Springer – Verlag Berlin Heidelberg 2002, ISBN 3 – 540 – 43927 – 7.

Mužák J., Novák J., Pisková E.: The Mathematical Modelling of the natural and the technological processes on the uranium deposit Stráž the models and the application. In Proceedings of the Conference ECMS 99, Liberec

Novák J.: Groundwater Remediation in the Straz Leaching. In Tagungsband Internationale Konferenz Wismut 2000, Bergbausanierung. in Schlema, Germany

Novák J., Mareček P., Smetana R.: Modellind of the ISL process in the Stráž deposit. In IAEA Technical Committee Meeting on Computer Application in Uranium Exploration and Production – Case History and Current Status, Vienna, 15 - 18 November 1994.

Novák J., Mareček P., Smetana R.: System of the model solutions of the physical-chemical processes in the Stráž deposit used for rock environment restoration. In Merkel, B., Hurst, S., Lőhnert, E. P. & Struckmeier, W., editors, Proceedings of the International Conference and Workshop on Uranium-Mining and Hydrogeology, Freiberg, Germany, October 1995. Verlag Sven von Loga.

Novák J., Smetana R., Šlosar J.: Remediation of sandstone's aquifer following chemical mining of uranium in the Stráž deposit, Czech Republic. In Arehart G. B. and Hulston J. R. Editors, Proceedings of the 9th International Symposium on Water-Rock Interaction, pages 989-992, Taupo, New Zealand

Smetana R., Mužák J., Novák J.: Environmental Impact of Uranium ISL in Northern Bohemia. In B. Merkel, B. Planer-Friedrich, Ch. Wolkersdorfer eds. Uranium in the Aquatic Environment, Proceedings of the International Conference Uranium Mining and Hydrogeology III and the International Mine Water Association Symposium, Freiberg, Germany, 15 – 21 September 2002, pp. 699 – 708, Springer – Verlag Berlin Heidelberg 2002, ISBN 3 – 540 – 43927 – 7

Active and passive soil treatment techniques

A novel technology for sealing and immobilization – the use of precipitation processes from supersaturated solutions

Gerald Ziegenbalg

TU Bergakademie Freiberg, Institute of Technical Chemistry, Leipziger Str. 29, 09599 Freiberg, Germany, E-mail: gerald.ziegenbalg@chemie.tu-freiberg.de

Abstract. Mineral forming solutions can be prepared by using of special precipitation inhibitors. These are compounds allowing the mixing of solutions which are incompatible under normal conditions, for example $BaCl_2$ and Na_2SO_4 solutions or lime suspensions and diluted sulfuric acid. Clear, temporary stable solutions are obtained. If these are used as grout, directed precipitation takes place in the flow paths. The paper summarizes the fundamentals of the technology and gives an overview about the characteristics of gypsum and $BaSO_4$ forming solutions. Their immobilization effect was proven by column tests, which are discussed in detail.

Introduction

Precipitation processes play an important rule in nature. For example, the generation of acid rock drainage is stopped when formation of hard and insoluble crusts of hydroxides or sulfates takes place. The precipitated minerals protect deeper zones against the infiltration of water and oxygen and prevent the oxidation of sulfidic ores. Such "self healing" processes leading to the closure of flow paths are widely known. They base mainly on coupled dissolution and precipitation processes and need long times because only small amounts of mass are transported (Chermark 1996, Ettner 1999). The aim of this paper is to present the fundamentals of a novel technology for sealing and remediation of porous or fractured formations by using directed precipitation processes. Solutions are prepared and used as grout which are highly supersaturated in respect to slightly soluble minerals. The preparation of these solutions bases on the use of special precipitation inhibitors. These allow mixing of components which are normally incompatible. The resulting solutions are stable for a limited period of time only, depending on the degree of supersaturation, the used inhibitor and its concentration.

Experimental

Preparation of supersaturated, mineral forming solutions

$BaSO_4$ as well as gypsum supersaturated solutions were prepared step by step by mixing solutions containing $BaCl_2/CaCl_2$ or $Ba(OH)_2/Ca(OH)_2$ with Na_2SO_4 or $MgSO_4$ containing solutions/diluted sulfuric acid, respectively, in the presence of various types of precipitation inhibitors. Barium sulfate forming solutions characterized by reducing properties were obtained by using Na_2SO_3 as source for sulfate generation. The stability of the obtained supersaturated solutions was determined by stirring experiments at room temperature. The temporal change of the barium or calcium concentrations served as a measure for the course of $BaSO_4$ or gypsum crystallization.

Column tests

The columns used to determine the immobilization capacity of $BaSO_4$ producing solutions had a height of 1000 mm and a diameter of 300 mm. They were filled with approximately 60 kg of broken sandstone (from the Koenigstein mine of Wismut GmbH) with an average diameter of 2 cm. To assess the effectiveness of $BaSO_4$ producing solutions, a second column was flushed with water. The solution or water, respectively, was pumped from bottom to top at an average rate of 1.2 l/d. A volume of approximately 23 l was required to fill the columns right up. The immobilization tests were carried out with a solution resulting in the formation of 300 mg/l $BaSO_4$. At an inhibitor concentration of 50 mg/l the stability was in excess of 96 hours. In order to increase the immobilization capacity small amounts of sodium silicate were added. Technical grade $Ba(OH)_2*8H_2O$, Na_2SO_3 and sodium silicate solution were used. The feed solution was discontinuously prepared step by step by mixing solutions of the separate constituents.
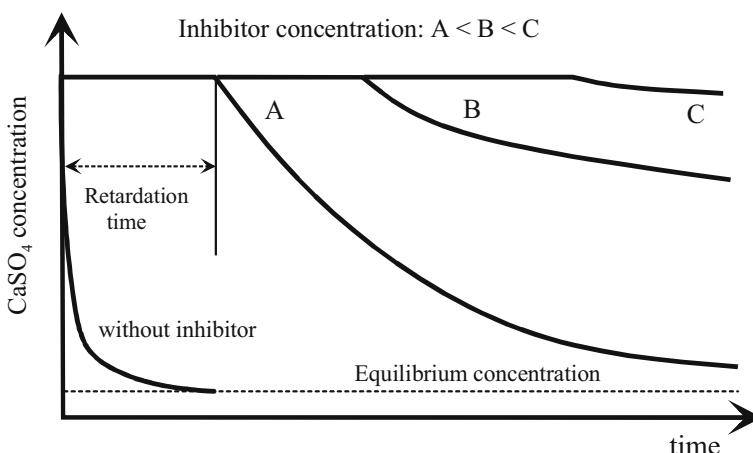
Results and Discussion

Preparation and properties of gypsum forming solutions
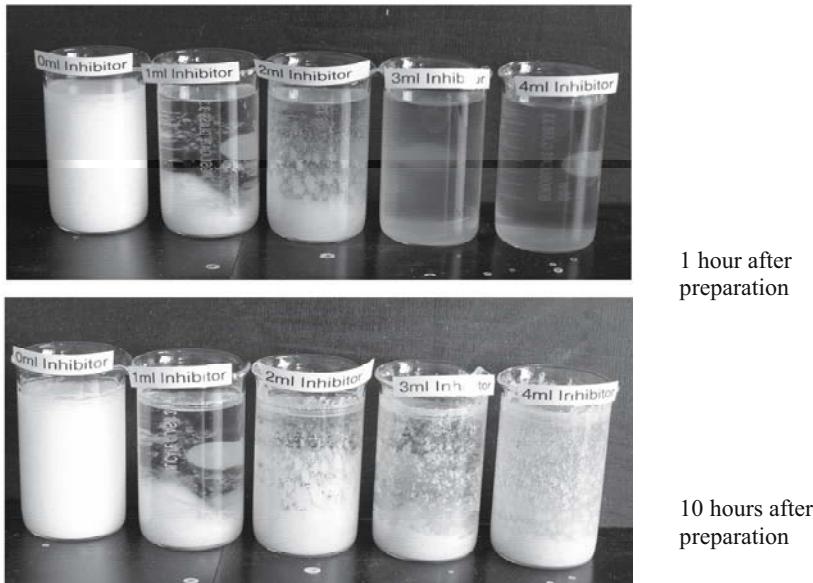
Gypsum has at 25 °C a solubility of approximately 2.5 g/l in water. It has been found, however, that gypsum is able to produce long time stable layers in waste rock dumps and tailings. Gypsum forming processes can be enhanced if solutions are applied which transport higher amounts of dissolved $CaSO_4$ than natural waters. Such solutions can be prepared by mixing of $Ca(OH)_2$ suspensions with di-

luted sulfuric acid. The presence of a suitable precipitation inhibitor is essential, otherwise fast and almost quantitative precipitation takes place. Precipitation inhibitors are compounds which are able to interrupt the crystallization process temporarily. This effect bases on the adsorption of the inhibitor on formed gypsum nuclei. The growth of the nuclei is temporarily blocked and the solution remains supersaturated for a limited period of time.

Fig. 1 explains the action of precipitation inhibitors. Fast crystallization takes place in the absence of an inhibitor. In the most cases, already few ppm are enough to prevent spontaneous gypsum crystallization. Increasing inhibitor concentrations result in solutions with raising stability. The extent of crystallization in a 0.5 molar $CaSO_4$ solution depending on the inhibitor content is visible in Fig. 2. The amounts of formed gypsum decrease with increasing volumes of added inhibitor solution. High inhibitor concentrations allow complete stabilization of the solution for a limited period of time. After that, crystallization starts as well. Factors influencing the stability of supersaturated solutions are temperature, pH and mechanical agitation as well as the presence of solids. Due to adsorption of the inhibitor on the surface of many solids, faster crystallization takes place in suspensions than in pure solutions. NMR investigations on gypsum formed in supersaturated solutions have proven that the inhibitor is incorporated into the growing crystals. If $CaCl_2$ and sodium or magnesium sulfate solutions are mixed together in the presence of a suitable inhibitor, final $CaSO_4$ concentrations up to 100 g/l are possible. Concentrations up to 45 to g/l $CaSO_4$ can be achieved in the case of using lime milk and diluted sulfuric acid. All solutions are completely clear; their stability depends on the type and the concentration of the used inhibitor. Gypsum forming solutions have a high sealing capacity. If they are used as grout in porous or fractured soil or rock formations, gypsum crystallization takes place in the treated flow paths and leads to a step by step reduction of the permeability.

Fig. 1.   Course of crystallization from supersaturated solutions in the presence of precipitation inhibitors.

Active and passive soil treatment techniques

1 hour after preparation

10 hours after preparation
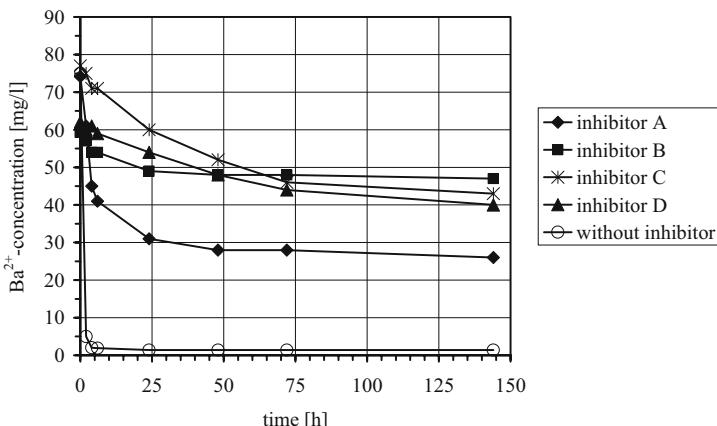
Fig. 2. Gypsum crystallization depending on the amount of added inhibitor solution

Preparation and properties of BaSO$_4$ solutions
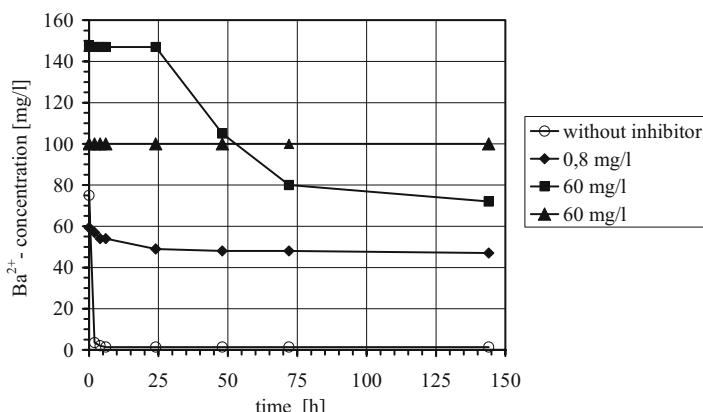
Barite (BaSO$_4$) is a mineral with an extremely low solubility. It normally precipitates immediately upon mixing of solutions of barium ions with sulfate containing solutions. The resulting precipitates are capable of binding many ions, mainly Fe^{3+}, Al^{3+}, Cl$^-$ and PO$_4^{3-}$. In principle, three different options are possible:

- Mixing of BaCl$_2$ and Na$_2$SO$_4$ or MgSO$_4$ solutions;
- Mixing of Ba(OH)$_2$ solutions and diluted H$_2$SO$_4$;
- Mixing of Ba(OH)$_2$ and sodium sulfite solutions.

In all cases it is necessary to add a suitable inhibitor. While the first option produces a solution containing dissolved NaCl as a by-product, the second results in a solution containing, apart from the inhibitor, only dissolved barite. The third solution has reducing properties. $BaSO_4$ is formed as a result of sulfite oxidation. The solution has an alkaline character and it is possible to add sodium silicate solutions to enhance the immobilization capacity. Temporal stability of $BaSO_4$ supersaturated solutions depends on the overall solution composition, the used precipitation inhibitors (Fig. 3) and the latter's concentration. Fig. 4 shows the course of $BaSO_4$ precipitation as a function of inhibitor concentration. While an inhibitor concentration of 0.8 mg/l suffices to stabilize a solution containing 50 mg/l of Ba^{2+}, 60
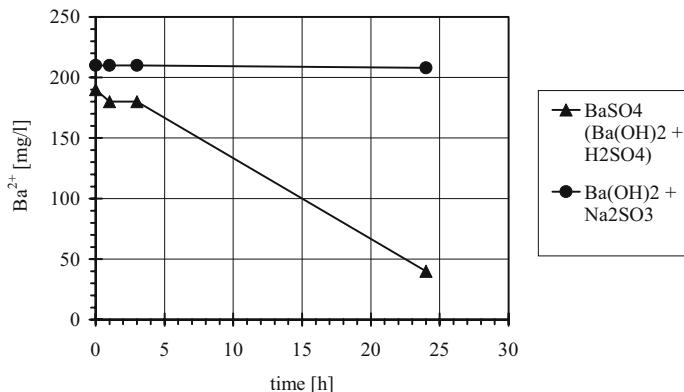
Fig. 3.   Stability of $BaSO_4$ solutions depending on the used inhibitor.

Fig. 4.   Course of $BaSO_4$ precipitation from supersaturated solutions depending on the inhibitor concentration.

Active and passive soil treatment techniques

mg/l of inhibitor are capable of stabilizing 100 mg/l of Ba^{2+} for a period of more than 140 hours. In general, higher supersaturations require higher inhibitor contents. $BaSO_4$ concentrations up to 800 mg/l can be stabilized temporarily. This is approximately 350 times higher than the equilibrium concentration of $BaSO_4$ in water. It is possible to prepare solutions having acidic as well as alkaline character. In general, a higher inhibitor concentration does not only allow the stabilization of higher $BaSO_4$ concentrations, but also leads to a slower crystallization process. While "pure" $BaSO_4$ solutions have an extremely high stability, interactions with reactive mineral surfaces can provoke fast crystallization.

At the same inhibitor level, alkaline solutions prepared on the basis of $Ba(OH)_2$-, Na_2SO_3 solutions are characterized by a higher stability than neutral solutions composed by mixing of $Ba(OH)_2$ and diluted sulfuric acid (Fig. 5).

Fig. 5.   Course of $BaSO_4$ precipitation depending on the used sulfate source (80 mg inhibitor/l).

Active and passive soil treatment techniques

Results of column experiments

The first column was treated with water for a period of 56 days. After that period, the water was drained off completely. The sandstone remained in the column for a period of 25 weeks, then followed a second flushing with water. The course of concentrations in the solutions collected after passing the column is summarized in Fig. 6. The first solutions were characterized by high concentrations. They de-
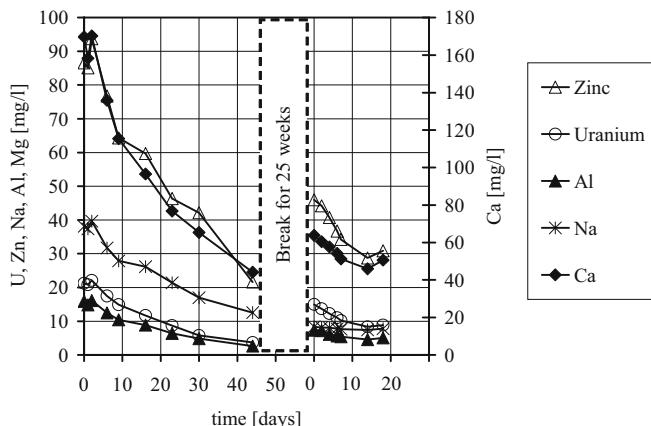
Fig. 6.   Change of effluent concentrations during flushing the column with water.
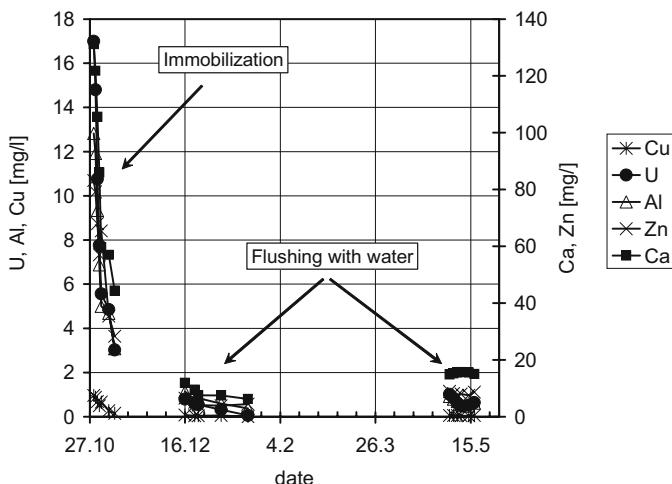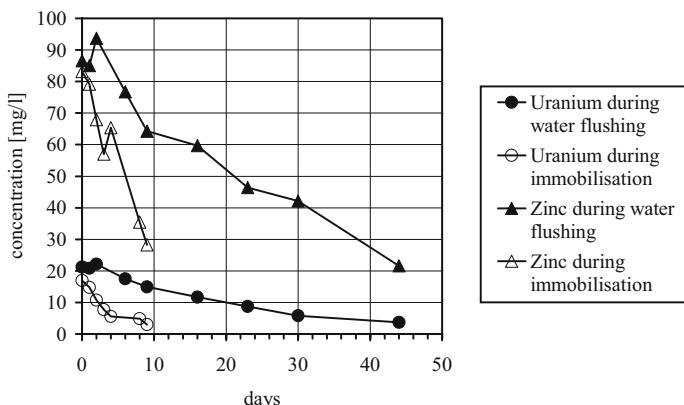
Fig. 7.   Change of effluent concentrations during and after immobilization of the column with BaSO$_4$ solutions.

Active and passive soil treatment techniques

crease over time; however, this is a slow process. The replacement of more than 23 l of solution was necessary to reduce the concentrations by half. As a consequence, pH shifted only slowly. After the outflow of 44 l the solution was characterized by uranium concentrations of 3.8 mg/l while zinc concentration was 21 mg/l. The second treatment with water produced solutions with concentrations similar to the first flushing process. This indicates that oxidation processes have led to the mobilization of further contaminants. In other words, flushing with water results in large amounts of contaminated solutions characterized by only slowly dropping concentrations. No immobilization takes place; and contact with oxygen causes the mobilization of leachable heavy metals.

In contrast, solutions resulting from the treatment with $BaSO_4$ were characterized by rapidly decreasing concentrations (Fig. 7). The used solution had the following composition: 176 mg/l Ba^{2+}, 150 mg/l SiO_2, 102 mg/l SO_3^{2-}, 50 mg/l inhibitor. Fast and almost complete reduction of all main components was observed in the effluents during the $BaSO_4$ treatment of the column. It becomes apparent that $BaSO_4$ forming solutions lead to rapid immobilization. $BaSO_4$ concentrations were detected below the natural solubility of barite. This is an indication of complete $BaSO_4$ precipitation. It was also of great importance to see complete inhibitor ad-

sorption on the sandstone. After 22 l of $BaSO_4$ forming solution had passed through the column the flow was stopped. The column was emptied completely, and treatment with water started a week later. The low concentrations in the output solutions demonstrated the formed precipitates' resistance to water. Flushing with water was stopped after the outflow of approximately 20 l of water. Again, the water was drained off completely. A second flushing with water was carried out 17 weeks later. In contrast to the column treated with water only, the contact with air did not lead to significant oxidation processes. The amounts of discharged contaminants were low in comparison to the flushing process. Stable immobilization was achieved with $BaSO_4$ forming solutions.

As visible from Fig. 8, the treatment with $BaSO_4$ forming solutions produces effluents in which the contaminant concentrations decrease faster than during flushing with water. This means, the use of $BaSO_4$ solutions results in reduced total amounts of discharged contaminants and produces a long time protection against oxidation and leaching.

Active and passive soil treatment techniques

Fig. 8.   Comparison of effluent concentrations during water flushing and immobilization.

Conclusions

Solutions supersaturated in respect to gypsum or barite can be prepared by the use of precipitation inhibitors. Systems are obtained characterized by concentrations high above the normal solubility of the minerals. The solutions are temporary stable. If they are used as grout, directed crystallization takes place in the penetrated flow paths. Due to the high amounts of mass that can be transported gypsum forming solutions are favored for sealing purposes. The application of $BaSO_4$ oversaturated solutions is seen as a favorable way to in-situ immobilize heavy metals within porous rock or soil formations. $BaSO_4$ layers covering reactive mineral surfaces as well as secondary precipitates such as hydroxides or hydroxysulfates are formed. Due to the extremely low solubility of barite a long time stable immobilization is achieved.

The described laboratory investigations were the basis for large scale field tests in the Koenigstein mine of Wismut GmbH. These have resulted in the decision to use $BaSO_4$ forming solutions for the immobilization of selected parts of the mine (Ziegenbalg, 1003A, Ziegenbalg 2003B, Jenk 2005).

Further applications of the technology are seen in the remediation of rock formations treated by acidic as well as alkaline is-situ leaching techniques and to stop or reduce the formation of acid rock or mine drainage.

Acknowledgements

References

Chermark, J. A.,Runnels, D.D.(1996). Self-sealing hardpan barriers to minimize infiltration of water into sulfide-bearing overburden, ore and tailing piles, in: Tailings and Mine Waste, 199`96 (Proc. Internat. Conf. Tailings and Mine Waste), pp. (1996) 265–73.

Ettner, D.C., Braastad, G.(1999). Induced hardpan formation in a historic tailings impoundment, Roros, Norway, in : Tailings and Mine Waste, (Proc. 6th Internat. Conf. Tailings and Mine Waste, 1999) pp.265–73.

Jenk, U., Ziegenbalg, G. (2005), The use of $BaSO_4$ supersaturated solutions for in-situ immobilization of heavy metals in the abandoned Wismut GmbH uranium mine at Koenigstein. This book

Ziegenbalg, G., Schreyer, J., Jenk, U., Pätzold, C., Müller, E. (2003A). In-situ Schadstoffimmobilisierung in der Grube Königstein der Wismut GmbH, Glückauf Forschungshefte 64 (2), 53- 59.

Ziegenbalg, G., Schreyer, J., Jenk, U. (2003B). Feldversuche zur Schadstoffimmobilisierung in gelaugtem Quadersandstein, Glückauf Forschungshefte 64(1), 18-23

Active and passive soil treatment techniques

Variation in heavy metal uptake by crop plants

Hans Bergmann, Klaus-Dieter Voigt, Bernd Machelett, Gerhard Gramss

Friedrich-Schiller-University, Institute of Nutrition, Dornburger Strasse 25, D-07743 Jena, Germany

Abstract. Relative to heavy metal (HM) excluder plants (French bean, lupin, maize, cereals), HM sequestering crops (buckwheat, beet root species) accumulate up to the 18-fold concentrations of As, Cd, Cr, Cu, Ni, Pb, and Zn as a sum in their shoot tissue. Soil amendment with nitrogen increased HM uptake further. This is a novel treatment to make continuous phytoextraction technologies more efficient without increasing the soil's leaching rate.

Introduction

Uranium mining in East Germany left numerous rocky mine tailings and heavy metal (HM) containing overburden and ore processing deposits. Their restricted use in agriculture or their re-vegetation with the goal to stabilize and reduce the pool of HM implies the selection of plant species and a careful substrate management. Phytostabilization may be facilitated when plant covers of perennial herbs or woody plants are able to form arbuscular or ectomycorrhizal associations, respectively, or foster a root-associated bacterial flora. Microorganisms bind HM to their surfaces and extramatrical polysaccharides and proteins, or form intracellular metal complexes with proteins, peptides, and oxalates which are no longer accessible or toxic to the plant (Berthelsen et al. 2001; Van der Lelie 1998). This will less apply to annual crops whose element concentrations in root and shoot correlate frequently with those in the soil solution (Schönbuchner et al. 2002; Tyler and Olsson 2001). Its composition in a given soil is determined by variables such as pH (Sumner et al. 1991), microbial activity, the presence of complexing agents (Cotton et al. 1987; Hayes 1991), and high concentrations of Ca, K, and Mg cations which precipitate HM and metal-humic complexes from solution, and reduce the metal content in the plant (Gramss et al. 2003a).

Table 1. Organic U soil amendments and their acronyms.

Amendment	Applied at seeding	6 wk prior to seeding	2 wk prior to harvesting
Molasses 42 % (0.42 % W/DW)	M1	M2	M3
Casein (0.44 %)	C1	C2	
Sucrose (1 %)		S1	
Sucrose (0.5 %)			S2
Rape shoot homogenate (6.2 %)	R		
Aminoethanol (0.03 %)			AE

All of these soil parameters can be controlled by application of organic-C- or N-rich compounds. Amendment with sucrose initiated the microbial production of metal-chelating carboxylic acids under low pH conditions. Their mineralization turned pH then to alkalinity and solubilized humic substances. Soil amendment with casein increased pH in the phase of NH_3 release to end in soil acidification and the precipitation of humic substances in the nitrification stage (Gramss et al. 2003b; Voigt et al. 2004). With the temporary formation of the exchange cation NH_4^+, Ca^{2+} was released from the soil matrix. Its coagulating effect removed humic and fulvic acids, the dominant ligands of HM, from the soil solution to give rise to the formation of metal complexes with Cl^- and oxoanions of C, S, and P (Cotton et al. 1987; Gramss et al. 2005), which may be more plant-available. Beside the preferred free cation, sound roots seem also to take up complete sulphate and chloro complexes of Cd (McLaughlin et al. 1998) as well as ligands such as citrate, histidine, EDTA (Bell et al. 2003), and humic molecules < 3500 Da (Nardi et al. 2002). It has not yet been shown whether these compounds enter sound root cells as complete metal chelates.

In this study, seventeen crop plants were grown on uranium mine dump soil with the goal to monitor their excluder or sequestrator properties by determining the degree of HM accumulation in shoot and root, and to stimulate HM uptake by soil treatments with N, organic C, or the biocatalyst, 2-aminoethanol. With the estimation of the natural or manipulable HM accumulation potential, technologically controllable plants for a restricted crop production on moderately contaminated soils, for phytoextraction, and for phytostabilization (immobilization) treatments shall be recommended.

Materials and Methods

The common crops, Avena sativa (cv. Flämingstern); Beta vulgaris (Rote Kugel); B. vulgaris rapaceae (Eckdorot); Brassica chinensis (Granaat); B. napus (Liratop); B. rapa (Goldball); Cannabis sativa (Lipko); Fagopyrum esculentum (Sobano); Helianthus annuus (Capital); Hypericum perforatum; Lupinus albus (Ares); Nicotiana tabacum; Phacelia tanacetifolia; Phaseolus vulgaris (Juvina); Sinapis alba

(Asta); Triticum aestivum (Monopol); and Zea mays (Mentor) were exposed to uranium mine dump soil (U soil) from Settendorf (Germany) of pH (KCl), 7.20 ± 0.02; C_{org}, 2.50 ± 0.01 % (w/w); and organic N, 1972 ± 104 mg kg^{-1}. The soil contained (mg kg^{-1} ± SD) Al, 10025 ± 225; As, 278.2 ± 23.2; Ba, 53.0 ± 9.0; Ca, 8998 ± 598; Cd, 11.2 ± 1.2; Co, 55.4 ± 4.4; Cr, 22.0 ± 0; Cu, 564.5 ± 44.5; Fe, 19982 ± 218; K, 3503 ± 17; Li, 27.7 ± 1.7; Mg, 6349 ± 281; Mn, 1139 ± 8.9; Mo, 2.3 ± 1.3; Na, 131.1 ± 4.0; Ni, 102.1 ± 1.9; P, 866.7 ± 16.7; Pb, 114.3 ± 11.7; Sr, 78.1 ± 10.1; Ti, 86.6 ± 0.4; U, 105.8 ± 4.2; V, 30.2 ± 3.2; and Zn, 1113 ± 53. Pot cultures (10 cm in diameter, 0.5 L) of U soil (sieve 5 mm) were seeded to 3-6 plants each and incubated, after seedling emergence, for 28 to 42 d in growth chambers at a 22° C / 16 h and 16° C / 8 h day-night regime and a light intensity of 550 µmoles m^{-2} s^{-1}. Plants were also grown on soils organically amended at different stages of the experiment (Table 1). For the determination of metal contents in root and shoot (ICP-AES and ICP-MS after pressurized microwave digestion), and the concentrations of soluble elements in soils (aqueous extracts 10 mL g^{-1} soil) compare Gramss et al. (2004).

Results and Discussion

Variability in heavy metal uptake by common crops

Concentrations of HM in shoots of 17 common crops from U soil varied extremely (Table 2). Of the most critical elements, shoot concentrations of As and Cd, but not of Pb, exceeded the tolerable limits. The commonly accepted concentrations in Cr, Cu, Ni, and Zn (Table 2) were observed at least by some of the crops. Agriculture on HM contaminated soil includes therefore the *in-situ* selection of crop plants with excluder properties, which are denoted by a restricted HM transfer to the target biomass and in particular to grain and oil seed. Cereals with a common Cd load around 0.035 mg kg^{-1} fresh wt (Schachtschabel et al. 1998 p. 318) came to 0.08 to 0.29 mg kg^{-1} in 15 spring barley, and to 0.13 to 0.39 mg kg^{-1} in 20 winter wheat cultivars (decreed limits 0.1 and 0.2 mg kg^{-1} fresh wt, respectively) on soils with a natural Cd contamination in the Saxonian Mulde district (Klose 2004, 2005). Similarly, Cd concentrations in radish could be halved by the selection of the optimum excluder cultivar to indicate the importance of plant breeding (Table 3). But also sparing nitrogen fertilization reduced the transfer of HM from root to shoot (Gramss et al. 2005).

Table 2. Concentrations (mg kg^{-1} DW ± SD) of HM in shoots of seedlings potted for 28 to 42 d on U soil in quadruplicate cultures. Adapted from Voigt et al. (2004).

Plant	As	Ba	Cd	Co	Cr	Cu	Mn	Ni	Pb	U	Zn	Sum[a]
Cannabis Sativa	4.58 ±1.61	16.1 ±2.61	0.73 ±0.8	0.33 ±0.17	2.93 ±0.6	7.45 ±1.34	66.3 ±5.58	3.70 ±0.1	1.13 ±0.87	0.35 ±0.09	34.7 ±8.58	55.2 ±8.93
Phaseolus vulgaris	5.03 ±1	11.3 ±2.2	1.00 ±0.61	0.50 ±0.31	1.30 ±0.38	5.93 ±0.98	48.1 ±3.4	6.93 ±2.04	1.08 ±0.36	1.03 ±0.46	48.7 ±16.4	69.9 ±16.6
Triticum aestivum	8.58 ±1.72	16.0 ±2.95	1.13 ±0.26	0.40 ±0.2	6.37 ±0.66	7.53 ±2.75	37.4 ±9.65	3.78 ±1.4	1.48 ±0.78	1.03 ±0.45	47.3 ±18.4	76.2 ±18.8
Lupinus albus	2.45 ±0.62	5.13 ±1.76	0.38 ±0.09	0.73 ±0.22	1.28 ±0.82	8.58 ±1.76	567 ±164	8.30 ±3.68	1.20 ±0.68	1.87 ±1.25	81.3 ±9	104 ±9.95
Zea mays	1.83 ±1.01	3.98 ±0.8	2.03 ±0.71	0.20 ±0.18	0.80 ±0.38	9.13 ±2.94	42.0 ±13.2	1.60 ±1.16	0.70 ±0.42	0.10 ±0	96.0 ±20.5	112 ±20.8
Avena sativa	6.45 ±0.92	2.18 ±0.67	2.40 ±0.85	0.20 ±0.07	1.50 ±0.14	11.1 ±0.95	42.0 ±14.4	8.53 ±0.98	0.83 ±0.65	0.40 ±0.23	86.0 ±28.6	117 ±28.7
Hypericum perforatum	7.03 ±2.13	4.03 ±1.06	22.6 ±3.40	0.50 ±0.22	0.57 ±0.13	13.8 ±4.14	39.7 ±6.79	1.90 ±0.66	0.77 ±0.48	1.37 ±0.88	74.0 ±34.3	121 ±34.7
Nicotiana tabacum	12.1 ±0.73	15.6 ±3.59	22.3 ±5.51	0.53 ±0.13	0.60 ±0.17	14.3 ±4.46	37.6 ±6.06	2.93 ±0.34	0.97 ±0.48	1.20 ±0.70	95.0 ±13.1	148 ±15.0
Phacelia tanacetif.	31.6 ±9.79	93.3 ±22	3.70 ±0.67	0.50 ±0.08	4.37 ±2	8.40 ±3.21	47.7 ±4.18	7.77 ±1.8	0.60 ±0.22	0.67 ±0.21	121 ±25.3	178 ±27.5
Brassica chinensis	3.60 ±0.51	12.9 ±4.71	4.87 ±0.62	0.57 ±0.24	2.97 ±0.66	15.6 ±1.8	22.6 ±3.75	4.50 ±0.45	0.40 ±0.08	0.20 ±0	177 ±23.8	209 ±23.9
Brassica napus	1.90 ±0.59	10.2 ±3.15	4.93 ±1.4	0.78 ±0.46	0.80 ±0.47	13.8 ±4.42	62.0 ±14.3	3.23 ±0.17	0.95 ±0.68	0.53 ±0.46	184 ±55.3	209 ±55.5
Helianthus annuus	8.27 ±2.87	13.1 ±3.29	5.27 ±0.69	0.50 ±0.18	1.68 ±0.21	8.08 ±0.89	74.7 ±11	5.37 ±0.74	0.63 ±0.18	0.40 ±0.21	221 ±24	250 ±24.2
Brassica rapa	6.35 ±3.6	27.6 ±5.59	7.80 ±2.21	1.43 ±0.61	1.53 ±1.01	31.1 ±11.1	92.2 ±29.5	6.05 ±2.35	2.63 ±2.18	2.73 ±1.64	257 ±88.9	312 ±89.7
Sinapis alba	2.18 ±0.05	11.9 ±3.26	3.90 ±1.34	0.38 ±0.13	1.65 ±0.48	11.6 ±4.6	22.6 ±2.58	2.93 ±0.29	1.28 ±1.18	0.60 ±0.41	294 ±128	318 ±128
Fagopyrum esculentum	4.23 ±1.09	18.8 ±2.93	15.2 ±3.17	0.78 ±0.19	6.30 ±1.13	35.3 ±5.19	81.4 ±6.09	11.7 ±1.68	1.20 ±0.33	0.43 ±0.46	318 ±57	392 ±57.4
Beta vulgaris	7.17 ±2.45	70.5 ±5.08	25.5 ±2.04	1.48 ±0.39	1.40 ±0.81	29.0 ±4.57	199 ±18.5	7.47 ±3.12	1.68 ±0.8	1.00 ±0.33	841 ±77.5	913 ±77.7
B. vulgaris rapaceae	4.90 ±0.97	50.3 ±10.7	26.5 ±1.62	0.83 ±0.25	1.90 ±1.31	25.5 ±7.05	237 ±28.1	6.93 ±1.02	1.98 ±0.9	0.75 ±0.35	926 ±106	994 ±106
Mean shoot conc.	6.96	22.5	8.84	0.63	2.23	15.1	101	5.51	1.15	0.86	230	269
Mean root conc.[b]	159	36.4	30.6	7.38	4.78	174	60.8	32.0	12.2	62.0	663	1075

[a] Sum of As, Cd, Cr, Cu, Ni, Pb, and Zn concentrations. [b] Individual data not shown.
Shaded type, outstanding natural HM accumulation potential.
Tolerable concentrations of HM (Schachtschabel et al. 1998 p. 318): As, 0.01-1; Cd, 0.05-0.4; Cr, 0.1-1; Cu, 2-20; Ni, 0.1-3; Pb, 0.1-6; Zn, 10-100 mg kg^{-1} DW.
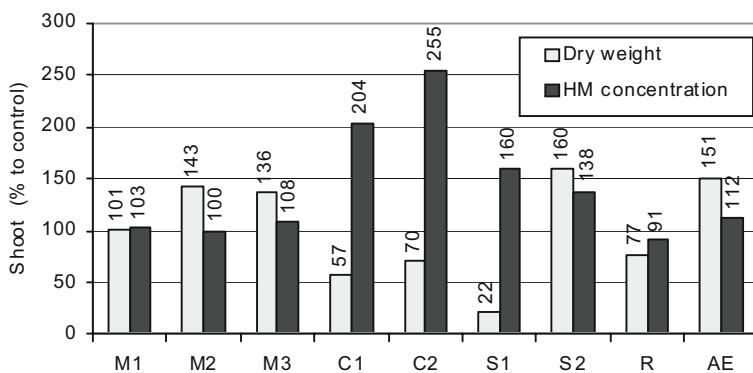
Table 3. Uptake of Cd from soil (10 mg kg^{-1} Cd) by radish cultivars.
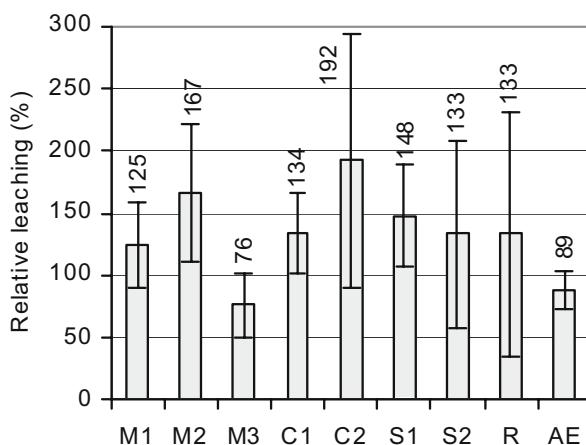
Cultivar	Cd content mg kg^{-1} biomass
Eiszapfen	23.1
Flamboyant	26.7
Mean	41.1
Cherry B	43.3
Rudi	49.5
Rodos	50
Isabell	54.3

None of the 17 crop plants examined in Table 2 displayed natural hyperaccumulation potential to the HM considered. Nevertheless, As concentrations in *Phacelia*, and Cd, Cu, and Zn levels in beet root species deserve attention when the exchangeable soil HM fractions shall be controlled by phytoextractive crops. It is the cations of Cd, Co, Cu, (Mn), Ni, and Zn, whose uptake to, and transport across the root symplasm was promoted by affinities of the CPx-ATPase transmembrane transport proteins (Williams et al. 2000), and whose translocation from root to shoot was stimulated by repeated soil treatment with nitrogen (Gramss et al. 2005). Application of the exchange cation NH_4^+ desorbed Ca^{2+} (and Mg^{2+}) from the soil matrix which, in turn, precipitated several HM and most of the dissolved humic substances, the dominant ligands of metal cations, from the soil solution to give rise to the formation of more plant-available metal complexes (e.g., McLaughlin et al. 1998). Moreover, soil application of the model substances, casein and sucrose altered greatly pH value and solubility of elements during nitrification and the formation of carboxylic acids, respectively (Gramss et al. 2003b; Voigt et al. 2004).

Fig 1.   Influence of different soil treatments on dry wt of, and HM concentrations in, shoots of a mean of 17 crop plants, expressed in % to the water-treated controls (= 100%). Percentage values of HM comprise those of As, Cd, Cr, Cu, Ni, Pb, and Zn.

Phytoremediation

In pot trials, treatments with casein (15.6 % N, w/w), the carbohydrate-dominated molasses, sucrose, and rape shoot homogenate, and the biocatalyst, 2-aminoethanol interfered therefore with biomass production and uptake of several HM (Table 4). Elevated shoot HM concentrations were predominantly linked with NH_4/NO_3 formation from mineralizing casein applied 0 or 6 wk prior to seeding (treatments C1; C2), with microbial carboxylic-acid production from sucrose applied 6 wk prior to seeding (S1), and with the application of aminoethanol (AE) applied 2 wk prior to harvesting (individual data not shown). As a mean across all 17 crop plant species with their wide interspecific variations (data not shown), soil treatments with molasses (M2; M3), late applied sucrose (S2), and aminoethanol (AE) promoted dry wt production of aboveground biomass (Fig. 1), whereas casein (C1; C2) and early sucrose (S1) applications inhibited growth by a temporary fatty-acid toxicity (Armstrong and Armstrong 1999; Gramss et al. 2003b). Nevertheless, it were these detrimental treatments (C1; C2; S1) which promoted HM accumulation in shoots (Fig. 1). The biocatalyst, aminoethanol, stimulated HM accumulation in shoots of higher biomass although this compound is commonly applied in near-homeopathic doses (Bergmann et al. 1999). Contrary to the conditions in chelator-induced phytoextraction technologies (Salt 2000), soil treatments with N and organic C did not significantly increase water-solubility and leaching of hazardous elements in U soil (Fig. 2).

Fig.2.   Influence of different soil treatments on water-solubility (potential leaching) of As, Cd, Cr, Cu, Ni, Pb, and Zn, expressed in % to the conditions in water-treated soil (= 100 %).

Table 4. Maximum concentrations (mg kg^{-1} DW) of HM in shoots of seedlings grown for 28 to 42 d on U soil, stimulated by soil treatment with N, organic C, or aminoethanol.. Blanks, moderate metal concentrations not given. Adapted from Voigt et al. (2004).

Plant	As	Ba	Cd	Co	Cr	Cu	Mn	Ni	Pb	U	Zn
Cannabis sativa					33.0 S2						
Nicotiana tabacum	50.9 C2	57.5 C2	53.5 C2			43.0 C2	2453 C2	25.9 C2	29.3 C2	13.5 C2	535 C2
Phacelia tanacetif.		191 S1				42.0 S1					
Brassica napus			23.7 C1			43.0 C2	2273 C2				954 C1
Helianthus annuus					15.5 M3		2999 C2				833 C1
Brassica rapa			20.9 C1	24.5 C2		61.0 S1	2328 C2	28.1 C2			994 C1
Sinapis alba			17.0 C1	22.1 C2		56.0 C2		41.1 C2			1733 C1
Fagopyrum esculentum				44.9 C2			3922 C2	53.2 C2			806 M1
Beta vulgaris		173 S1	37.9 S1	33.8 C2			3536 C2	47.0 C2			1395 AE
B. vulgaris rapaceae		75.9 S1	36.8 AE	62.5 C2			4709 C2	70.2 C2			1324 AE

Soil treated with AE, aminoethanol; M, melasses; C, casein; S, sucrose (see Materials). Water controls see Table 2.

Trapping dissolved heavy metal fractions by catch crops?

Several authors accept that it is impossible to quantify the plant-available (heavy) metal fraction by extracting a given soil with any chemical solution (Finck 1992). In the present study, the supernatants of U soil-water suspensions (1:10) shaken for 3 h at 25° C were partially centrifuged until the remaining clay, clay-humic, and humic particles were no longer self-depositing. A high surface area to mass ratio conferred colloidal properties (Schachtschabel et al. 1998 p. 149) to the particles up to 2 µm in size. Whereas these supernatants with their considerable metal content (HM fraction ([a]), Table 5) could gain access to surface waters, only portions with particles < 0.45 µm and a restricted metal content (HM fraction ([b]), Table 5) passed through soil columns.

Upon the re-vegetation of uranium mine tailings, overburden soils, and ore processing deposits, plants may serve as a water-depleting mechanical barrier to the flow of contaminated surface water and a temporary sink for toxic soil solution constituents (Table 5). Both the possible 20 t ha^{-1} of aboveground biomass and 4 t ha^{-1} root tissue with the mean uptake potential of Table 2 were able to trap 3 times the Cd load of a static soil solution such as HM fraction ([b]). In comparison to the

soil's total HM content, the portion of the temporarily trapped elements remained low (Table 5). A vegetation cover reduced nevertheless percolation in fallow land with 600 mm annual rainfall from 250 to < 50 mm (unpublished).

Re-vegetation comprises the formation of sparingly soluble HM phosphates in plant tissue (e.g., Günther et al. 2002) and the slow and repeated release of the soluble HM species from decaying biomass which may facilitate their gradual and time-consuming incorporation into soil minerals and the quantitatively increasing soil organic substance (Schachtschabel et al. 1998). Fungi and bacteria of living and decaying plant material bind HM to cell surfaces, exopolysaccharides, proteins, peptides, and oxalates and reduce their plant-availability (Berthelsen et al. 2001; Van der Lelie 1998). This is counteracted by metal-chelating carboxylic and amino acids of root and microbial origin (Hayes 1991) and may be one of the reasons that planting increased the soluble HM fraction in U soil, which must not necessarily result in higher shoot HM concentrations (Gramss et al. 2004).

Table 5. Temporary accumulation (%) of the water-soluble HM fraction[b] of U soil by a vegetation cover of 20/4 metric tons ha^{-1} of dry aboveground/root biomass with the mean shoot/root uptake potential indicated in Table 2.

	As	Ba	Cd	Co	Cr	Cu	Mn	Ni	Pb	U	Zn
HM fraction[a]	5.59	0.61	0.08	0.32	0.53	5.80	4.17	1.49	0.66	0.88	13.1
mg kg^{-1} ± SD	±0.36	±0.01	±0.01	±0.02	±0.08	±0.16	±0.12	±0.04	±0.05	±0.15	±0.30
HM fraction[b]	2.76	0.17	0.04	0.14	0.09	4.70	2.59	0.91	0.27	0.13	4.63
mg kg^{-1} ± SD	±0.57	±0.01	±0.01	±0.05	±0.03	±0.81	±0.21	±0.06	±0.09	±0.06	±0.74
HM fraction in shoots[c] %	2.52	134	315	4.44	25.6	3.21	39.1	6.07	4.26	6.67	49.6
HM fraction in roots[d] %	23.0	86.6	279	20.8	22.0	14.8	9.40	14.1	18.0	192	57.3
Uptake of total HM[e] %	0.25	0.70	2.33	0.06	0.19	0.15	0.11	0.18	0.05	0.24	0.44

Water-soluble HM fraction carried off by surface water ([a]), and migrating through soil columns ([b]). Binding (%) of HM fraction ([b]) by aboveground biomass ([c]), and by roots ([d]). Accumulation of the soil's total HM concentration (see Materials) by whole biomass ([e]).

Conclusions

The sum of As, Cd, Cr, Cu, Ni, Pb, and Zn concentrations in shoot tissue of 17 common crop plants varied by factor 18 when grown on a moderately HM contaminated uranium mine dump soil (Table 1). Excluder plants such as French bean, lupin, maize, and several cereals confined HM transfer to shoot tissue and potentially to the grain fruit. Sequestrator plants such as buckwheat and beet root species accumulated with Cd, Cu, (Mn), Ni, and Zn those elements to which the plant's proteinogenic amino acids showed highest affinities (Gramss et al. 2005). This mechanism did not apply to the low-concentrated Cr, Pb, and U. Soils with a specific HM contamination can be admitted to the production of excluder crops

whose HM load can be further reduced by the selection of appropriate cultivars and by a restricted N fertilization. For the remediation of seriously HM contaminated soils, the phytoextractive potential of *Phacelia* (As) and *Beta* sp. (Cd, Cu, Zn) is negligible but manipulable by soil treatment with N and organic C compounds in an upcoming field of research. The phytostabilisatory effect of plant covers with their root zone microflora is multicomponent and indispensable to soil forming processes. Increases in the water-solubility of HM in planted soils do not immediately result in their increased plant-availability.

References

Armstrong J, Armstrong W (1999) *Phragmites* die-back: toxic effects of propionic, butyric and capronic acids in relation to soil pH. New Phytol 142: 201-217

Bell PF, McLaughlin MJ, Cozens G, Stevens DP, Owens G, South H (2003) Plant uptake of ^{14}C-EDTA, ^{14}C-citrate, and ^{14}C-histidine from chelator-buffered and conventional hydroponic solutions. Plant Soil 253: 311-319

Bergmann H, Lippmann B, Leinhos V, Tiroke S, Machelett B (1999) Activation of stress resistance in plants and consequences for product quality. J Appl Bot 73: 153-161

Cotton FA, Wilkinson G, Gaus PL (1987) Basic inorganic chemistry. 2nd edn. New York, USA: J. Wiley & Sons, Inc.

Berthelsen BO, Lamble GM, MacDowell AA, Nicholson DG (2001) Analysis of metal speciation and distribution in symbiotic fungi (Ectomycorrhiza) studied by micro X-ray absorption spectroscopy and X-ray fluorescence microscopy. In: Gobran GR, Wenzel WW, Lombi E, eds. Trace elements in the rhizosphere. Boca Raton, USA: CRC Press, 149-164

Finck A (1992) Dünger und Düngung. Grundlagen und Anleitung zur Düngung der Kulturpflanzen. 2nd edn. Weinheim, Germany: VCH Verlagsgesellschaft

Gramss G, Voigt K-D, Bergmann H (2003a) Irrigation with plant extracts in ecofarming increases biomass production and mineral and organic nitrogen content of crop plants. J Plant Nutr Soil Sci 166: 612-620

Gramss G, Voigt K-D, Bublitz F, Bergmann H (2003b) Increased solubility of (heavy) metals in soil during microbial transformations of sucrose and casein amendments. J Basic Microbiol 43: 483-498

Gramss G, Voigt K-D, Bergmann H (2004) Plant availability and leaching of (heavy) metals from ammonium-, calcium-, carbohydrate-, and citric-acid-treated uranium-mine-dump soil. J Plant Nutr Soil Sci 167: 417-427

Gramss G, Büchel H, Bergmann H (2005) Soil treatment with nitrogen facilitates continuous phytoextraction of heavy metals. This symposium.

Günther A, Bernhard G, Geipel G, Rossberg A, Reich T (2002) Uranium speciation in plants. In: Merkel BJ, Planer-Friedrich B, Wolkendorfer C, eds. Uranium in the aquatic environment. Proc. Int. Conf. Uranium Mining and Hydrology III and Int. Mine Water Assoc. Symp., Freiberg, Germany, 15-21 Sept. 2002. Berlin, Germany: Springer, 513-519

Hayes MHB (1991) Influence of the acid / base status on the formation and interactions of acids and bases in soils. In: Ulrich B, Sumner ME, eds. Soil acidity. Berlin, Germany: Springer, 80-96

Klose R (2004) Empfängliche Sorten. Bauernzeitung (Sachsen Regional) 9. Woche

Klose R (2005) Ursa will kein Kadmium. Bauernzeitung (Sachsen Regional) 4. Woche

McLaughlin MJ, Andrew SJ, Smart MK, Smolders E (1998) Effects of sulfate on cadmium uptake by Swiss chard: I. Effects of complexation and calcium competition in nutrient solutions. Plant Soil 202: 211-216

Nardi S, Pizzeghello D, Muscolo A, Vianello A (2002) Physiological effects of humic substances on higher plants. Soil Biol Biochem 34: 1527-1536

Salt DE (2000) Phytoextraction: present applications and future promise. In: Wise DL, Trantolo DJ, Cichon EJ, Inyang HI, Stottmeister U, eds. Bioremediation of contaminated soils. New York, USA: Marcel Dekker, Inc., 729-743

Schachtschabel P, Blume H-P, Brümmer G, Hartge KH, Schwertmann U (1998) Lehrbuch der Bodenkunde, 14th edn. Stuttgart, Germany: Enke

Schönbuchner H, Leiterer M, Machelett B, Bergmann H (2002) Mobility and plant availability of heavy metals in soils of uranium mining dumps. In: Merkel BJ, Planer-Friedrich B, Wolkendorfer C, eds. Uranium in the aquatic environment. Proc. Int. Conf. Uranium Mining and Hydrology III and Int. Mine Water Assoc. Symp., Freiberg, Germany, 15-21 Sept. 2002. Berlin, Germany: Springer, 529-536

Sumner ME, Fey MV, Noble AD (1991) Nutrient status and toxicity problems in acid soils. In: Ulrich B, Sumner ME, eds. Soil acidity. Berlin, Germany: Springer, 149-182

Tyler G, Olsson T (2001) Plant uptake of major and minor mineral elements as influenced by soil acidity and liming. Plant Soil 230: 307-321

Van der Lelie D (1998) Biological interactions: The role of soil bacteria in the bioremediation of heavy metal-polluted soils. In: Vangronsveld J, Cunningham SD, eds. Metal-contaminated soils: in situ inactivation and phytorestoration. Berlin, Germany: Springer, 31-50

Voigt K-D, Martin M-L, Bergmann H, Gramss G (2004) Entwicklung von Grundlagen zu Sanierungstechniken für schwermetall- bzw. radionuklidkontaminierte Böden durch Nutzung des Transfers der Kontaminanten in Pflanzenbiomassen. Abschlussbericht Institut für Ernährungswissenschaften, Lehrbereich Lebensmittelkunde, Friedrich-Schiller-Universität Jena, 132 pp

Williams LE, Pittman JK, Hall JL (2000) Emerging mechanisms for heavy metal transport in plants. Biochim Biophys Acta 1465: 104-126

Phytoavailability of uranium: influence of plant species and soil characteristics

Lise Duquène[1], Hildegarde Vandenhove[1], Filip Tack[2], Ellen van der Avoort[1], Jean Wannijn[1], May van Hees[1]

[1]SCK•CEN, Radioecology Section, Boeretang 200, B-2400 Mol, Belgium
E-mail : lduquene@sckcen.be
[2] Ghent University, Laboratory for Analytical Chemistry and Applied Ecochemistry, Coupure Links 653, B-9000 Gent, Belgium

Abstract. Five plants (Maize, Indian mustard, Wheat, Pea and Ryegrass) with reported differences in uranium uptake were screened in a greenhouse experiment for their uranium soil-to-plant transfer from two soils. Soils were spiked with ^{238}U and were distinct in uranium availability characteristics. It was investigated if variability in uptake could be traced back to a different interaction of plants with the soil matrix or to different organic acid concentrations in the soils after plant growth. Clearly distinct transfer factors were obtained between soil groups which could be traced back to a difference in uranium availability between soils. However, within a soil group, there was no relation between (plant-induced changes in) soil characteristics and the transfer factors observed. The mechanisms by which the plants inhibit or promote root-shoot transfer seemed more important than soil characteristics to explain the difference in uranium transfer factor observed.

Introduction

Uranium is reported to be the most frequent radionuclide contaminant in groundwater and surface soils (Riley et al. 1992). In Europe, the major sources of soil contamination are the residues of uranium mining and milling and the residues of industries extracting or processing material containing naturally occurring radionuclides like the phosphate processing industry and the power production stations from coal.

Improper remediation of uranium contaminated areas and/or soil allocation (cattle grazing, agriculture...) may induce potential toxicological risks via the food

web. Because plants represent the first step of the food web, it is essential to understand the main factors playing a role in the soil-to-plant uranium transfer. A good knowledge of parameters influencing U migration in soil and uranium uptake by plants is also important for an efficient management of contaminated areas.

Uranium uptake by plants can be expressed as a transfer factor ratio (TF: ratio Bq per g dry weight plant to Bq per g dry weight soil). The transfer factor is a global parameter; its value depends on soil characteristics like pH, carbonate content, content of phosphates, iron oxides and hydroxides, organic matter... Soil-to-plant uranium transfer is also influenced by plant physiological characteristics, such as nutrient uptake strategies and organic acid exudation. Plants have been screened for [238]U uptake in different plant compartments and under various experimental conditions like hydroponics (Dushenkov et al. 1995, Ramaswami et al. 2001), pot experiments (Huang et al. 1998, Ramaswami et al. 2001), and field conditions. Citric acid has been identified as the most powerful organic acid to enhance U phytoextraction (Huang et al. 1998, Ebbs et al. 1998).

In the present study, we screened the transfer factor of five plant species different in their reported uranium uptake characteristics, phylogeny and nutrient uptake strategy for two soils distinct in uranium availability characteristics. Observed transfer factors will be linked with soil characteristics and plant-induced changes of the soil environment.

Material and Methods

Two soils were used in this experiment: an acid soil with provenance the Belgian Campine Region (Plaggept) and an alkaline soil from the Belgian Loam Region (typic Hapludalf). The acid soil was characterized by a low CEC (3.77 ± 0.66 $cmol_{+}.kg^{-1}$), a field capacity of 123 ± 1 $ml.kg^{-1}$, an organic matter content of 2.74 ± 0.07 % and a clay content of 5.5 ± 0.1 %. For the alkaline soil a high CEC (34.98 ± 3.77 $cmol_{+}.kg^{-1}$), a field capacity of 182 ± 1 $ml.kg^{-1}$, an organic matter content of 4.07 ± 0.04 % and a clay content of 17.7 ± 0.4 % were observed.

About 45-kg soil batches soils were brough to field capacity, fertilized, contaminated with 330 $Bq.kg^{-1}$ [238]U added as uranyl nitrate hexahydrate and incubated for 3 weeks. After incubation, soils were analysed for pH and major cations (Ca^{2+}, Mg^{2+} and K^{+}), phosphates and total inorganic carbon (TIC) in the soil solution extracted from the soil through centrifugation. Uranium was also measured in the soil solution and in the exchangeable fraction (extraction with 1 M ammonium acetate pH 7).

A greenhouse experiment was realised with 5 plant species: Maize var. *Anjou 230*, Indian mustard var. *Vitasso*, Wheat var. *Baldus*, Pea var. *Kalife* and Ryegrass var. *Melvina*. Three pots were prepared per soil type per plant. Plants were harvested after 7 weeks, except for ryegrass which was harvested after 5 and 10 weeks. Plant shoots and roots (only for the acid soil) were weighed and dried.

Uranium content was measured in the dried shoot and root (acid soil only) samples.

Soils were analysed again at the end of the experiment after pot-dismantling for before-mentioned soil characteristics.

For the acid soil, the concentration of 4 organic acids (malate+succinate, oxalate and citrate) was measured in the soil solution following Ström et al. (2001). Malate and succinate could not be separated and are given as one common peak. Organic acid concentrations in the soil solution were expressed per gram of root.

Results

Soils

Soil characteristics before and after plant growth are listed in Table 1. A five-fold higher uranium concentration was observed for the alkaline soil (0.61 Bq L^{-1}) than for the acid soil (0.12 Bq L^{-1}). Exchangeable uranium was a factor eight higher for the alkaline soil. Comparing the soil characteristics of the acid and the alkaline soil, one would expect a higher uranium availability for the acid soil, given its low pH (4.6) and expected presence of the soluble uranyl cation (Ebbs et al., 1998) and its lower CEC, organic matter and clay content than the alkaline soil. The pH of the alkaline soil was 7.2, at which highly mobile, anionic uranyl-carbonate complexes are formed (Shahandeh and Hossner 2002). This increased solubility at higher pH must hence overrule the prevalent uranium binding properties of the soil. Total inorganic carbon and Ca content were also higher in the alkaline soil.

Uranium in the soil solution before plant growth was statistically correlated with the uranium exchangeable fraction, soil solution phosphate concentration and total inorganic carbon content.

After plant growth, uranium in the soil solution increased significantly in all treatments. Uranium enhancement was higher in acid soil (factor 18-123) than in alkaline soil (factor 9-52) for all plants. The highest soil solution uranium concentration increase was observed for wheat, with a factor 123 and 52 for the acid and alkaline soils respectively. The smallest increase was observed after growth of maize (only about ten-fold increase). Exchangeable uranium decreased slightly (~10 %) in alkaline soil but did not change in acid soil.

Soil pH tended to increase slightly (0.1-0.3 pH units) on the acid soil and decreased slightly on the alkaline soil. Soil solution phosphates content increased in the acid soil but decreased in the alkaline soil. The total inorganic carbon content (TIC) was higher in all treatments. Soil solution cation content decreased, especially in the acid soil.

Table 1. Comparison of soil characteristics following incubation, before and after plant growth. Acid = acid soil, Alk = alkaline soil. M = Maize, I = Indian mustard, W = Wheat, P = Pea and R2 = Ryegrass at second harvest. SS = soil solution, exch. = exchangeable fraction. All analyses realized in 3 replicates. SD are presented in grey below values.

Parameter	Unit	Soil	Before	After				
				M	I	W	P	R2
U SS	Bq.L^{-1}	Acid	0.12	2.20	5.63	14.81	8.45	4.94
			0.01	0.11	0.71	1.76	4.17	0.47
		Alk.	0.61	6.87	5.48	31.66	6.54	13.59
			0.09	1.76	0.36	3.34	3.99	1.56
U exch.	Bq.kg^{-1}	Acid	21	26	22	23	25	27
			1	1	1	1	1	2
		Alk.	174	155	151	150	149	140
			2	15	2	2	2	3
pH H$_2$O	-	Acid	4.6	4.7	4.8	4.9	4.7	4.9
			0.1	0.1	0.1	0.1	0.1	0.1
		Alk.	7.2	6.9	6.9	7.0	6.9	7.0
			0.0	0.0	0.1	0.1	0.0	0.0
HPO$_4^{3-}$	μM	Acid	95	153	168	164	126	169
			4	13	12	34	41	35
		Alk.	20	d.l^a	14	d.l^a	d.l^a	d.l^a
			2		1			
TIC†	mg C.$^{-1}$	Acid	1.1	4.0	2.0	24.7	2.8	1.9
			0.3	1.6	0.9	9.1	2.2	0.5
		Alk.	7.9	14.5	18.6	30.3	15.3	31.6
			0.5	2.6	1.9	0.8	4.4	1.4
Ca^{2+} SS	mM	Acid	15.8	0.7	0.6	0.5	0.8	0.5
			1.5	0.1	0.1	0.1	0.0	0.1
		Alk.	23.3	8.7	4.3	4.0	6.4	1.6
			0.7	0.3	0.9	0.4	1.9	0.0
Mg^{2+} SS	mM	Acid	5.4	0.2	0.2	0.2	0.3	0.1
			0.4	0.0	0.0	0.0	0.1	0.0
		Alk.	1.8	0.7	0.3	0.3	0.5	0.1
			0.0	0.0	0.1	0.0	0.1	0.0
K$^+$ SS	mM	Acid	12.6	0.2	0.8	1.0	1.0	0.4
			0.3	0.1	0.2	0.1	0.1	0.0
		Alk.	2.0	0.3	0.4	0.3	0.4	0.1
			0.1	0.0	0.1	0.0	0.0	0.0

^{a} d.l = at least two replicates under detection limit (5.26 μM)
† total inorganic carbon
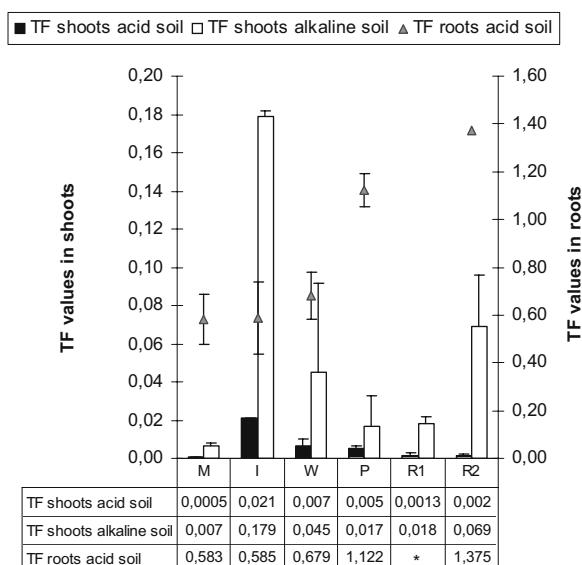
Uranium soil-to-plant transfer factors

Uranium transfer factors (TF) to roots (acid soil only) and shoots are shown in Fig.1. Three (for pea) to 35-fold (ryegrass) higher soil-to-shoot transfer factors were obtained for the alkaline soil than for the acid soil. The observed difference in shoot TFs between soils were higher than the difference in soil solution uranium concentration.

The lowest shoot-TFs on the alkaline soil were observed for maize (0.007 ± 0.003) and the highest for Indian mustard (0.179 ± 0.047). Paradoxically, the lowest soil solution uranium concentration was observed for Indian mustard. Wheat, with the highest soil solution uranium concentration after plant growth, showed the third highest uranium soil-to-shoot transfer factor. For the alkaline soil, no significant correlation was observed between the soil-to-plant transfer and any soil parameter screened.

The shoot-TFs recorded on the acid soil were also lowest for maize (0.0005 ± 0.0001) and highest for Indian mustard (0.021 ± 0.003). As for the alkaline soil, there was no agreement between the soil solution or exchangeable uranium concentration and the transfer factor observed. The soil-to-root transfer factors recorded on the acid soil only differed about two-fold between plants. The highest root TFs were observed for ryegrass (1.375 ± 0.104) and pea (1.122 ± 0.071) and the lowest for maize (0.583 ± 0.010) and Indian mustard (0.585 ± 0.151). The recorded root TFs were a factor 28 (Indian mustard) to a factor 1166 (maize) higher than the soil-to-shoot transfer factors observed.

The potential of ryegrass to transfer uranium to its shoots was very variable. No increase in uranium shoot TF was observed for the acid soil between the two harvests, whereas a nearly four-fold increase was observed at the second harvest for

	M	I	W	P	R1	R2
TF shoots acid soil	0,0005	0,021	0,007	0,005	0,0013	0,002
TF shoots alkaline soil	0,007	0,179	0,045	0,017	0,018	0,069
TF roots acid soil	0,583	0,585	0,679	1,122	*	1,375
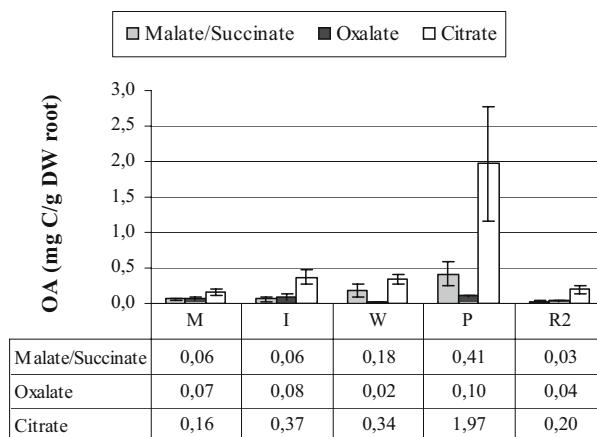
Fig. 1.   U soil-to-plant transfer factors in shoots and roots (acid soil only) after greenhouse experiment on acid and alkaline soil contaminated with 330 Bq.kg^{-1} ^{238}U added as uranyl nitrate. M = Maize, I = Indian mustard, W = Wheat, P = Pea, R1 = Ryegrass at first harvest, R2 = Ryegrass at second harvest. n = 3 replicates. * = no data available.

Phytoremediation

the alkaline soil, despite a 41 and 22-fold increase in soil solution uranium concentration for both soils. Possibly the bioavailability of uranium in the soil solution was more enhanced on the alkaline soil as could be inferred from the four-fold increase in total inorganic carbon content following plant growth (not observed for the acid soil) and the consequent increased presence of soluble and bioavailable uranyl carbonates uranium.

Organic acids

Fig.2. presents the concentration of organic acids in the soil solution of the acid soil at the end of the greenhouse experiment. The recorded organic acid concentrations were highly variable within treatment. The highest soil solution organic acid concentrations were observed for pea, especially for citrate. For pea we obtained important uranium concentrations in the soil solution and in the roots. Overall, however, the organic acid concentrations (total and single acid) in the soil solution were not correlated with the uranium concentration in the soil solution or the uranium uptake by roots and shoots. For example, for wheat we observed a relatively low production of citrate and other organic acids compared to pea yet a higher uranium concentration in the soil solution than pea and a medium root-TF. Ryegrass showed low organic acid concentrations in the soil solution, a low uranium concentration in the soil solution but the highest root-TF.

It should be mentioned, however, that the concentration of organic acids is highly influenced by microbial activity.

	M	I	W	P	R2
Malate/Succinate	0,06	0,06	0,18	0,41	0,03
Oxalate	0,07	0,08	0,02	0,10	0,04
Citrate	0,16	0,37	0,34	1,97	0,20

Fig. 2.   Concentration of organic acids (OA) in the soil solution of acid soil after experiment expressed as mg C per g of root (dry weight). M = Maize, I = Indian mustard, W = Wheat, P = Pea, R2 = Ryegrass at second harvest. All analyses realized with HPIC. n = 6 replicates.

Discussion

The most important result concerning the evolution of soil characteristics before and after plant growth was the enhancement of the uranium concentration in the soil solution through the action of the plant roots.

In agreement with previous studies (Shahandeh and Hossner 2002), the transfer factors observed were higher for the alkaline soil than for the acid soil. This result is explained by the solubility of uranyl carbonates in alkaline soils.

Indian mustard showed the highest uranium shoot-TF on both soils and maize the lowest. However, considering all plants, the order in which they were able to transfer uranium differed between soil groups indicating that plant species react differently if the soil properties change.

Considering both soils or within each soil group, no relation was found between the (plant-induced) uranium concentrations in the soil solution and the observed transfer factors to roots and shoots. Neither the exchangeable uranium fraction, nor the organic acids recorded in the soil solution or any other soil parameter could explain the differences in transfer factors observed between plants. Prediction of the uranium phytoavailability from soil characteristics seems at this stage impossible.

The results obtained for the acid soil also point to the important influence of plant properties on the observed shoot transfer factors. The reported uranium soil solution concentration after plant growth varied about seven-fold, the root TF only about 2-fold and the shoot transfer factor fourty-fold. This means that the difference in the observed shoot concentrations or shoot TF is more influenced by plant factors than by plant-induced differences in soil characteristics. Looking at the results for Indian mustard, for example, clearly shows this. Soil solution uranium concentration was among the lowest for Indian mustard as was the observed root TF whereas the shoot TF was the highest. The ability of plants to inhibit or promote root-to-shoot transfer of uranium can be expressed by the root-shoot ratio which varied 41-fold: from 28 for Indian mustard to 1166 for maize. The mechanism by which plants can inhibit or promote root-to-shoot transfer of uranium are however not known.

Conclusions

Clearly distinct transfer factors were observed between soil groups for all plants tested which could be traced back to a difference in uranium availability and explained by soil properties, for the two distinct soils studied here.

It was, however, impossible to predict the observed transfer factors between plants from soil properties. Plants species interact differently when soil properties change. For a given soil, there was no agreement between plant-induced changes in soil characteristics and observed uptake. Not at the level of the roots but even less so at the level of the shoots since the ability of the plants to inhibit or allow

root-to-shoot transfer is a more important source of variability in observed shoot TFs than is any soil characteristic.

Efforts to predict uranium transfer factors, required for the assessment of food web transfers and phytomanagement approaches, should be directed to unravel both the role of soil characteristics in affecting transfer and the mechanisms by which plants regulate internal transfer of uranium.

References

Dushenkov V, Nanda Kumar PBA, Motto H, Raskin I (1995) Rhizofiltration: the use of plants to remove heavy metals from aqueous streams. Environ Sci Technol 29: 1239

Ebbs SD, Norvell WA, Kochian LV (1998) The Effect of Acidification and Chelating Agents on the Solubilization of Uranium from Contaminated Soil. J Environ Qual 27: 1486-1494

Huang JW, Blaylock MJ, Kapulnik Y, Ensley BD (1998) Phytoremediation of Uranium-Contaminated Soils: Role of Organic Acids in Triggering Uranium Hyperaccumulation in Plants. Environ Sci Technol 32: 2004-2008

Ramaswami A, Carr P, Burkhardt M (2001) Plant-Uptake of Uranium: Hydroponic and Soil System Studies. International Journal of Phytoremediation 3: 189-201

Riley RJ, Zachara JM, Wobber FJ (1992) Chemical contaminants on DOE lands and selection of contaminant mixtures for subsurface science research DOE/ER-0547T. DOE Office of Energy Research Report

Shahandeh H, Hossner LR (2002) Role of soil properties in phytoaccumulation of uranium. Water, Air and Soil Pollution 141: 165-180

Ström L, Owen AG, Godbold DL, Jones DL (2001) Organic acids behaviour in a calcareous soil: sorption reactions and biodegradation rates. Soil Biology and Biochemistry 33: 2125-2133

Uranium accumulator plants from the centre of Portugal – their potential to phytoremediation

João Pratas, Nelson Rodrigues, Carlos Paulo

Earth Sciences Department, Faculty of Sciences and Technology of the University of Coimbra, Portugal, carlos.januario@gmail.com

Abstract. The strategies of metal tolerance developed by several plants that enable them to survive in contaminated and polluted sites allow that some of them may accumulate significant concentration of a specific element. The work presented here is part of a larger on going study about the uraniferous geochemical province of Central Portugal, and it focus only in a preliminary description of results obtained with aquatic plants that show potential for phytoremediation. We have observed that *Apium nodiflorum*, *Callitriche stagnalis*, *Lemna minor* and *Fontinalis antipyretica* accumulate significant amounts of uranium, whereas *Oenanthe crocata* inhibit the uranium uptake.

Introduction

The use of plant species as indicators of metal contamination is based on their response to elements present in the substrate (Kabata-Pendias, 2001). Plants growing near abandoned mine sites, usually indicate the mineral composition of the soil and waters. These plant species are tolerant to metals and they are able to accumulate or exclude toxic metals and this ability can be used in mineral prospecting or, if the biomass and bioproductivity are high, in phytoremediation (Hooper and Vitousek, 1997, Brooks, 1998).

The work presented here is part of a larger on going study about the uraniferous geochemical province of Central Portugal. It is oriented for the use of aquatic plants as indicators of metal contaminated waters and their potential use in phytoremediation. Even though we have observed very low concentration of U in the fresh waters of the studied sites we found a set of vegetable species with the ability to accumulate uranium in concentrations which are orders of magnitude higher than the surrounding environment. We have also seen one species that was inhibiting the uptake of this metal.
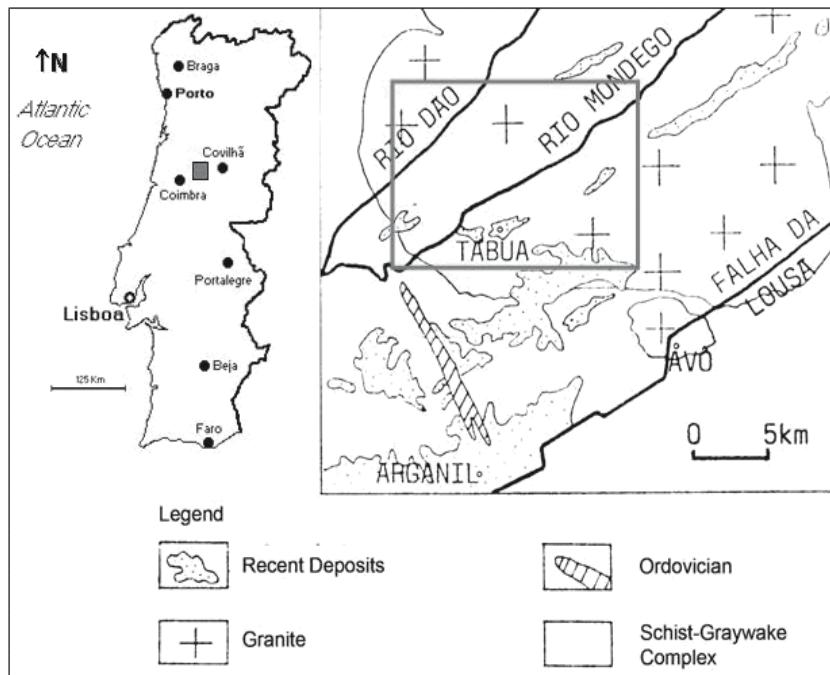
Location and Geology

The studied area is located in the counties of Tábua, Nelas and Oliveira do Hospital of the Centre of Portugal (Fig.1). This area is in the south-west part of the uraniferous region of Beiras (Centre of Portugal). The uraniferous area occupies about 10000 km^2 and it belongs to the geotectonical Central-Iberian Zone. In this region there are large occurrences of several phases of hercynian granites which intrude the formations of the Ante-Ordovician Schist-Graywake Complex. Above this Complex sits discordingly Ordovician formations. In the region there are also occurrences of Terciary deposits.

    The uraniferous deposits are located on the hercynian granites, on the metasediments enclaves and in the metamorphism contact haloes. The occurrences of uranium define an arch which is located on the NE border of the Serra da Estrela horst.

    The principal uranium minerals present in these deposits are pechblende, autonite, thorbernite, uranocircite and sabugalite within quartziferous gang or argyles (Ferreira, 1971).

    Several of these deposits were exploited either by underground or surface mining methods. The main mineral processing method used was lixiviation, specially during the last working activity phase (the last mine closed in 2001). Many of the places were left in different stages of degradation.

Fig. 1.   General location and geology of the study area (Ponte and Pereira, 1991).

Phytoremediation

Materials and Methods

Field sampling

The samples for this work were collected in running and in standing waters, in the places were it was possible to observe aquatic species. In these sites, samples of the waters and of the vegetable species were taken. The vegetable species collected represented the free floating and the rooted emergent plants in running waters. In the ponds, the collection focused mainly in the free floating plants.

Sampling treatment

All samples were processed in the Chemistry Laboratory of the Earth Science Department of University of Coimbra.

The waters were filtered and acidified. The plants were cleaned in running water in order to withdraw all the residues. Afterwards they were dried in an oven at 60 ºC. After drying, they were ground and crushed for later chemical analysis.

Analytical procedures: uranium determination

For determination of the mass concentration of uranium in samples of natural water and plants it was used the "Fluorat-02-2M" analyzer (made by Lumex, Russia).

In this device the concentration of uranium in solution is deducted from the measurement of the intensity of the delayed fluorescence of the uranyl-ions (λ=530 nm).

The water samples were analysed by standard fluorimetric analysis. For the control of the results it has been used a certified reference water produced by the National Water Research Institute of Canada (reference TMDA-62).

The methodology adopted for the determination of the uranium content in the plants was fluorometry, as described in the work of Huffman, Jr. and Riley, 1970, and Van Loon and Barefoot, 1989). In order to assure the quality of the analytical results certified Virginia tobacco leaves (reference CTA-VTL-2, Polish certified reference material) have also been analysed.

Results

For this preliminary work, we have selected *Apium nodiflorum(L.)Lag.* , *Callitriche stagnalis Scop.*, *Lemna minor L.*, *Fontinalis antipyretica L.* and *Oenanthe crocata L.* among all the collected species because they were the most representative species. A summary of the chemical analysis results is presented in Table 1.

Discussion

The results show a strong accumulation of uranium in the plants in comparison to the uranium present in the water. From these observations we can advocate their use both in biogeochemical prospecting for the location of natural occurrences of uranium or anthropogenic pollution and as an indication of their possible use for phytoremediation of polluted sites.

From the observed species the ones that appear to be more appropriate for phytoremediation are *Callitriche stagnalis* and *Apium nodiflorum*. The first species allows a good rooting in all kinds of running and standing waters and the other species seems to be more appropriate for marginal waters. Their biomass and bioproductivity are relatively high. Both species are also excellent indicators of pollution because they show a large range of values and the results correlate positively with those present in the waters.

The species *Oenanthe crocata,* in spite of its high biomass and bioproductivity, does not reflect, in its aerial organs, a significant accumulation and the values are not correlated with those found in the waters.

The bryophyte *Fontinalis antipyretica* which grows normally on top of the rocks within the waters reveals a strong ability to monitor the contamination present in the running waters.

The free floating *Lemna minor* shows good ability to accumulate uranium in a similar way as it has been observed in *Lemna gibba L.* (Mkandawire and Dudel, 2005). However it was observed a discrepancy when the results from running waters were compared with those from standing waters (Table 2).

Table 1. Uranium Concentration in plant species (expressed in mg/kg DW) and in fresh waters (expressed in ng/mL).

Species	No.of samples	Min	Max	Background	T/t
Apium nodiflorum	10	0,20	31,61	0,31	102
Waters		0,5	18,6		
Callitriche stagnalis	19	0,53	112,16	0,66	170
Waters		0,4	18,6		
Lemna minor	22	0,28	52,98	0,43	123
Waters		0,5	18,6		
Oenanthe crocata	10	0,03	1,68	0,12	14
Waters		0,4	18,6		
Fontinalis antipyretica	10	3,37	32,78	3,83	9
Waters		0,4	18,6		

[a] T/t – relation between the maximum and background level

Table 2 shows that the values of the maximum accumulation, the ratio T/t and the Biological Accumulation Coefficient are much higher in the standing waters compared with those of the running waters. This indicates a positive correlation between concentration in the plant and the residence time for this accumulation. If this is proved to be the case then there is a good opportunity for its use in phytoremediation in closed tanks where it would be grown. This obviously depends on further studies regarding its biomass and bio-productivity.

Table 2. Uranium Concentration in *Lemna Minor* (expressed in mg/kg DW) and in standing and running waters (expressed in ng/mL).

	Samples	Min	Max	Background	T/t	BAC
Plant concentration in running waters	8	0,41	8,54	0,40	21	$1,56 \times 10^3$
Waters		0,5	18,6			
Plant concentration in standing waters	14	0,28	52,98	0,45	118	$2,87 \times 10^3$
Waters		0,6	4,16			

[a] BAC – Biological Absorption Coefficient

Conclusions

This is a preliminary work envisaging the use of aquatic plants as indicators of metal accumulation and their potential use in phytoremediation. This work focus on waters contaminated by uranium and on the selection of plants which might be candidates for futures phytoremediation studies.

Pursuing these purposes we analysed several representative species of areas we expected to be contaminated with this metal. These areas were old uranium mines where there had been no obvious restoration programs.

This preliminary work opened good perspectives for the use of the selected species in prospecting and in their use phytoremediation.

The species *Fontinalis antipyretica* proved to be a good candidate for biomonitoring. This species accumulates large quantities of uranium in its tissues. It is known that, in general, the bryophytes have a great potential for rapid accumulation and also good recorders of seasonal fluctuations of the contaminations (Cenci, 2000). Also and due to the fact that this species does not have a root system but only rhizoids the uptake occurs as an ionic exchange between the environment and the leaves with no root intervention. The biological accumulation coefficient for this species is high, of the order of $1,4 \times 10^4$, and this means it can be considered an hyperaccumulator plant following the definition of Brooks (1998).

The species *Apium nodiflorum*, *Callitriche stagnalis* and *Lemna minor,* part of the analysed species, also accumulate significant amount of uranium. The species *L. minor* is a floating aquatic plant so the uranium accumulation is only related

with the surrounding water concentration. It showed an average biological accumulation coefficient of $1,56 \times 10^3$ in running waters and of $2,87 \times 10^3$ in standing waters. In both cases there is a great capacity for bioaccumulation and, as before, it can also be considered an hyperaccumulator plant.

These species show great potential for phytoremediation because they are endemic and easy to grow in natural conditions. In addition *A. nodiflorum* and *C. stagnalis* show a good bioproductivity. However it must be stressed that these results are preliminary and further studies are required to properly assess the true potential of these plants for phytoremediation.

Acknowledgements

References

Brooks, R.R. (1998), Plants that Hyperaccumulate Heavy Metals, CAB International, 380 p.

Cenci, R.M., (2000) The use of aquatic moss (Fontinalis antipyretica) as monitor of contaminationin standing and running waters: limits and advantages, J. Limnol., 60 (Suppl.1) 53-61.

Ferreira, M. R. P. V., 1971, Jazigos Uraníferos Portugueses Jazigos de Au-Ag-Sulfuretos do Norte de Portugal, I Cong. Hispano-Luso-Americano de Geologia Económica, Lisboa, 81p.

Hooper, D.V., Vitousek, P.M. (1997) The effects of plants composition and diversity on ecosystem processes, Science 277, 1302-1305.

Huffman, Jr. C., Riley, L.B. (1970) The Fluorimetric Method – Its use and precision for determination of uranium in the ash of plants, U.S. Geol. Survey Prof. Paper, 700-B, p 181-183.

Kabata-Pendias, A. (2001) Trace Elements in Soils and Plants, CRC Press, Florida, p. 432

Mkandawire, M.; Dudel, E.G. (2005) Accumulation of arsenic in *Lemna gibba* L. (duckweed) in tailing waters of two abandoned uranium mining sites in Saxony, Germany, Science of the Total Environment, 336, (1-3), 81-89.

Ponte, M.J.B., Pereira, L.C.G. (1991) Aspectos Litológicos e estruturais do complexo xistograuváquico no bordo sudoeste da faixa Ordovícica da região de S.Paio-Ázere, Memórias e Notícias, Publ. do Museu e Laboratório Mineralógico e Geológico da Universidade de Coimbra, 12 (A), 135-146.

Van Loon, J.C., Barefoot, R.R. (1989) Analytical Methods for Geochemical Exploration, Academic Press, 344 p.

Soil treatment with nitrogen facilitates continuous phytoextraction of heavy metals

Gerhard Gramss[1], Georg Büchel[2], Hans Bergmann[1]

[1]Friedrich-Schiller-University, Institute of Nutrition, Dornburger Strasse 25, D-07743 Jena, Germany
[2]Friedrich-Schiller-University, Institute of Geological Sciences, Burgweg 11, D-07743 Jena, Germany

Abstract. NH_4Cl was the optimum N compound to make soil heavy metals more plant-available but less leachable, and to increase biomass production, root uptake, and translocation to the shoot of Cd, Co, Cu, Mn, Ni, and Zn in Chinese cabbage. Their total weight in the shoots of higher biomass increased to 765 %.

Introduction

Uptake of heavy metals (HM) by plants increases frequently with their concentration in the soil solution and their adequate speciation. Free metal cations and metal-mineral acid complexes were taken up by *Beta vulgaris* to the same extent (McLaughlin et al. 1998). Concentrations of dissolved elements increase in the presence of neutral (NH_3, H_2O, CH_3OH) or anionic ligands (H^-, Cl^-, CN^-, OH^-, oxoanions of C, P, S) (Cotton et al. 1987), of chelators such as humic, low-*MW* carboxylic, and amino acids (AA, Hayes 1991), and under acidifying conditions (Sumner et al. 1991) resulting from CO_2 release, nitrification, and organic acid production. Involvement of organic bases such as amines with biocatalytic properties (Bergmann et al. 1999) has not been studied. Humic substances and HM precipitate from a soil solution saturated with $Ca^{2+}>Mg^{2+}>>K^+$ (Gramss et al. 2004).

Treating HM contaminated soils with synthetic (EDTA) and phytochelators (citrate, malate) increased total plant uptake and translocation to the harvestable shoot of Pb-EDTA and U by 100- to 1000-fold (Salt 2000). Chelators damaged root cell plasma membranes whose proteinaceous channels control uptake of elements (Williams et al. 2000) and allowed for the immediate access of metal chelates to the plant's transpirational flow. Daily applications of NH_4 and casein to Chinese cabbage for 36 d increased accumulation of Cd, Cu, Mn, Ni, and Zn in shoots 1.1 to 2.8 times more than in roots (Gramss et al. 2004). These elements chelate with those AA which could result from the microbial transformation of NH_4 and casein. Root uptake of metal-AA complexes was shown for gramina-

ceous plants (Uren 2001). Metals present in the soil solution as free cations and mineral-, humic-, and fulvic-acid complexes may be released into the xylem as free cations, oxoanions, and chelates of carbocylic acids, histidine, cysteine, nicotinamine (Pich and Scholz 1996; Salt 2000), metallothioneins and phytochelatins (Shahandeh et al. 2001). Complexation of HM cations may thus repeatedly change on their way via CPx-ATPase transport proteins of root cell plasma membranes (Williams et al. 2000), symplasm, and during their release into the xylem.

In this study, Chinese cabbage potted on HM contaminated soil received daily doses of NH_4Cl, the biocatalyst 2-aminoethanol, and HM chelating cysteine and histidine, whose residues dominate the transmembrane domains of CPx-ATPase transport proteins (Williams et al. 2000). It was the goal to determine (uptake and) *in planta* formation of free AA as potential long-distance transporters of HM, the influence of AA, amines, and their mineralization products on the solubility of soil HM in competition with humic acid ligands, long-term changes in the solubility of elements in soils treated with (chelating) nitrogen compounds, and the influence of the treatments on uptake and translocation of HM to the harvestable shoot to improve phytoextraction of HM under controlled leaching conditions.

Materials and Methods

Uranium mine dump soil (U soil) from Settendorf (Germany) of pH (KCl), 7.20 ± 0.02; C_{org}, 2.50 ± 0.01 % (w/w); and organic N, 1972 ± 104 mg kg^{-1} contained (mg kg^{-1} ± SD) Al, 10025 ± 225; As, 278.2 ± 23.2; Ba, 53.0 ± 9.0; Ca, 8998 ± 598; Cd, 11.2 ± 1.2; Co, 55.4 ± 4.4; Cr, 22.0 ± 0; Cu, 564.5 ± 44.5; Fe, 19982 ± 218; K, 3503 ± 17; Li, 27.7 ± 1.7; Mg, 6349 ± 281; Mn, 1139 ± 8.9; Mo, 2.3 ± 1.3; Na, 131.1 ± 4.0; Ni, 102.1 ± 1.9; P, 866.7 ± 16.7; Pb, 114.3 ± 11.7; Sr, 78.1 ± 10.1; Ti, 86.6 ± 0.4; U, 105.8 ± 4.2; V, 30.2 ± 3.2; and Zn, 1113 ± 53.

Triplicate pot cultures (8 cm) of Chinese cabbage (*Brassica chinensis* L., cultivar Chico F1) were daily irrigated with solutions of NH_4Cl, histidine, cysteine, 2-aminoethanol (AE, all at 20 mM N), and sunflower seed oil suspension (10 g L^{-1}) from day 7 to 33 in a total quantity of 1.3 L kg^{-1} soil. Daily N doses amounted 1.3 mM referred to suspended soil. Unplanted control soils were treated in the same way. For more details and the determination of free AA in fresh shoot tissue (Amino acid analyzer LC 3000, Eppendorf, Maintal), the metal content in root and shoot (ICP-AES after pressurized microwave digestion), and the concentrations of soluble elements, humic substances (HS), and N compounds in soils (aqueous extracts 10 mL g^{-1} soil) compare Gramss et al. (2004).
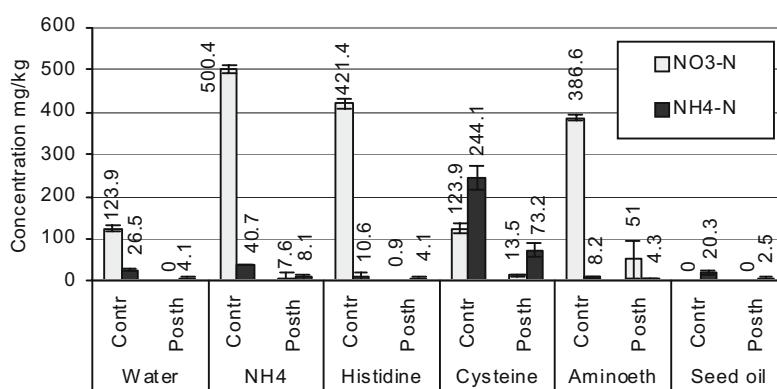
Results

Mineralization products of the daily applied doses of NH_4Cl, His, Cys, and AE (14 mg N g^{-1} soil) accumulated in control soil and retained a minimum of NO_3-N in

planted soil. Microbial consume of seed oil depleted N even in the control (Fig. 1).

Accordingly, shoots of Chinese cabbage attained dry weights of (g ± SD kg^{-1} soil) 7.54 ± 0.56 (control); 15.45 ± 1.25 (NH$_4$Cl); 12.5 ± 1.59 (His); 9.33 ± 0.65 (Cys); 10.18 ± 2.28 (AE); and 5.41 ± 0.4 (seed oil). Respective organic-N concentrations amounted (mg g^{-1} DW) 3.4 ± 0.6; 13.5 ± 0.8; 19.4 ± 2; 12.9 ± 0.8; 21.4 ± 3.4; and 7.3 ± 0.2, and corresponded with the concentrations of free AA (Fig. 2). N supply raised Arg, Gly, His, Leu, Pro, and Thr, lagging in control plants, above the detection limit of 4 µg g^{-1}. Increases were recorded for Ala (3.6 x); γ-Aba (4.2 x); Asp (7.5 x); Gln (51.6 x); Glu (4 x); and Ser (7.4 x). Concentrations of free AA in the His>Cys treatment lagged partially behind those of the NH$_4$ treatment.

Inorganic NH$_4$Cl, KNO$_3$, NaNO$_3$, NH$_4$NO$_3$, and CaCl$_2$ salts, sixteen of the AA found free in shoot tissue, and several organic bases in extracting fluids (20 mM N) showed different effects on the solubility of 22 elements and HS in U soil which compete for solution at a comparable pH (Table 1). The monovalent extractant cations NH$_4^+$=K$^+$>Na$^+$ desorbed Ca and Mg which, in turn, precipitated metal-containing HS and altered the solubility of the same cations as CaCl$_2$ extractants did. Solubilities of Al, Cr, Fe, Li, Pb, Ti, U, and V diminished to 0-28 %, whereas Ba, K, Na (76-151 %), Sr (365-1218 %), and Cd, Mn (Table 1) gained mobility. Amino, imino acids, amides and only 2 of 9 organic bases solubilized, in contrast to NH$_4^+$, Cu>>Co Ni>Zn>Cd>Ca Mg Mn but no other elements (Table 1). Solubility increases in the range those of metal containing HS (1 to 1.61 x) were certainly caused by HS rather than AA complexation. AA such as Arg, Lys, Ala, and β-Ala as well as most aliphatic and aromatic bases showed therefore no outstanding metal-complexing abilities in a multi-component soil solution. Hydroxy and acid AA at the respective pH value were more active and reached, apart from Co, Mn, and U, 25-100 % the solubilizing efficacy of citric acid. The level of U solubilization by citrate was only reached by the alkalinizing AE.

Fig. 1.   Concentrations (mg kg^{-1} DW) of N in control and postharvest soils of Chinese cabbage pot cultures from different treatments. Error bars indicate confidence interval of 95%.

Phytoremediation

With the wide mineralization of the daily applied N compounds in control soil (Fig. 1), their long-term effects on the desorption of Ca and Mg and the resulting precipitation of HM and HS were widely uniform (Table 2). Uptake of Ca and Mg in planted soil ameliorated these effects. Elevated solubilizations of Cu, Ni, and Zn in the His, and Co, Mn, and Ni in the Cys treatment beyond the limits given by the levels of dissolved HS point to complexations by the corresponding AA. Means of the solubilities of Al, As, Ba, Cd, <u>Co</u>, <u>Cr</u>, Cu, <u>Fe</u>, <u>Li</u>, Mn, <u>Mo</u>, Ni, P, <u>Pb</u>, Sr, <u>Ti</u>, U, <u>V</u>, and Zn in the NH$_4$Cl treatment divided by those in the water control amounted 70 % for control soils and 73.5 % for postharvest soils. The concentrations of dissolved HS diminished to 16 and 65 %, respectively, to indicate a reduced hazard of leaching. Immobilization was highest in the underlined elements. Solubility conditions in soils of the seed oil treatment were identical to those in the water control (data not shown).

Table 1. Quotients of the solubility of U soil elements and humic substances (HS) in N (20 mM) and citric acid (13.3 mM) containing extractants divided by the solubility in water extractant (compare Table 2 for absolute values). pH, acidity of the aqueous soil extract.

Extractant	pH	Ca	Cd	Co	Cu	Mg	Mn	Ni	U	Zn	HS
NH$_4$Cl	6.85	4.76[a]	1.38[a]	0.41[a]	0.62[a]	1.66[a]	2.17[a]	0.77[a]	0[a]	0.46[a]	0.48[a]
KNO$_3$	6.67	4.70[a]	0.47[a]	0.32[a]	0.49[a]	1.72[a]	1.26[a]	0.42[a]	0[a]	0.33[a]	0.41[a]
CaCl$_2$ 10mM	6.52	41.9[a]	3.24[a]	0.80[a]	0.40[a]	3.33[a]	4.96[a]	0.88	0[a]	0.60[a]	0.14[a]
Alanine[b]	6.75	1.13[a]	1.27	0.97	1.50[a]	1.10[a]	1.11[a]	1.12[a]	1.69[a]	1.05	1.01
Leucine[c]	6.99	1.21	1.00	2.84[a]	19.7[a]	1.11	2.19[a]	2.33[a]	1.60[a]	1.39[a]	1.08
Serine[d]	6.95	1.33[a]	1.29[a]	4.99[a]	22.2[a]	1.11	1.53[a]	4.67[a]	1.03	2.06[a]	1.14
Aminoethanol	10.0	1..57[a]	2.23[a]	3.17[a]	7.16[a]	1.24[a]	1.08	2.04[a]	24.5[a]	1.64[a]	2.47[a]
o-Phospho-aminoethanol	6.10	5.61[a]	4.61[a]	1.42[a]	1.36[a]	1.92[a]	6.05[a]	1.78[a]	1.94[a]	2.05[a]	0.59[a]
Cysteine	7.26	2.22[a]	1.68[a]	69.0[a]	4.85[a]	1.31[a]	8.38[a]	7.72[a]	1.40[a]	1.67[a]	1.61[a]
Histidine	7.41	1.32	6.72[a]	4.15[a]	18.5[a]	1.17[a]	1.41[a]	12.0[a]	0.32[a]	11.5[a]	1.36[a]
Aspartic acid	4.94	17.2[a]	20.2[a]	5.58[a]	12.3[a]	4.53[a]	19.7[a]	8.69[a]	0.64	12.2[a]	0.30[a]
Glutamic acid	5.18	15.0[a]	13.1[a]	3.88[a]	7.03[a]	4.09[a]	15.7[a]	4.52[a]	0.57	8.36[a]	0.33[a]
Citric acid[e f]	5.16	17.1[a]	38.7[a]	89.4[a]	20.1[a]	4.34[a]	76.7[a]	25.4[a]	50.8[a]	33.2[a]	2.24[a]
Aspartic acid[f]	7.04	3.81[a]	2.43[a]	4.64[a]	22.6[a]	1.67[a]	1.60[a]	10.4[a]	0.82	4.83[a]	0.98[a]
Glutam. acid[f]	6.74	3.30[a]	1.37	1.09	18.2[a]	1.50[a]	1.42[a]	2.81[a]	0.57[a]	1.08	0.86[a]
Citric acid[e f]	7.35	14.8[a]	2.77[a]	33.6[a]	12.7[a]	5.60[a]	59.1[a]	14.9[a]	25.1[a]	13.9[a]	4.66[a]

[a] Deviations from quotient 1.00 with its internal tolerance field significant at $p \leq 0.05$.
[b] Similar solubility quotients in the amino acids: Arg, Lys, β-Ala; aliphatic amines: cholinechloride, hydroxylamine, triethanolamine, urea; aromatic compounds: 2-benzylaminoethanol, salicylamide, sulfanilamide. [c] Similar solubility quotients in the amino acids: Gln, Gly, Pro, Val. [d] Similar solubility quotients in the amino acids: Asn, Thr.
[e] Reference chelator for Asp and Glu, all at 40 mM COOH and a comparable pH.
[f] Extractants of Asp, Glu, and citric acid neutralized with NaOH.
Amino compounds, amines and amides, with the exception of acid AA (Asp, Glu), did not increase the solubility quotients of Al, As, Ba, Cr, Fe, K, Li, Na, P, Pb, Sr, Ti, U, and V more than those of humic substances with which these U soil elements were widely linked.
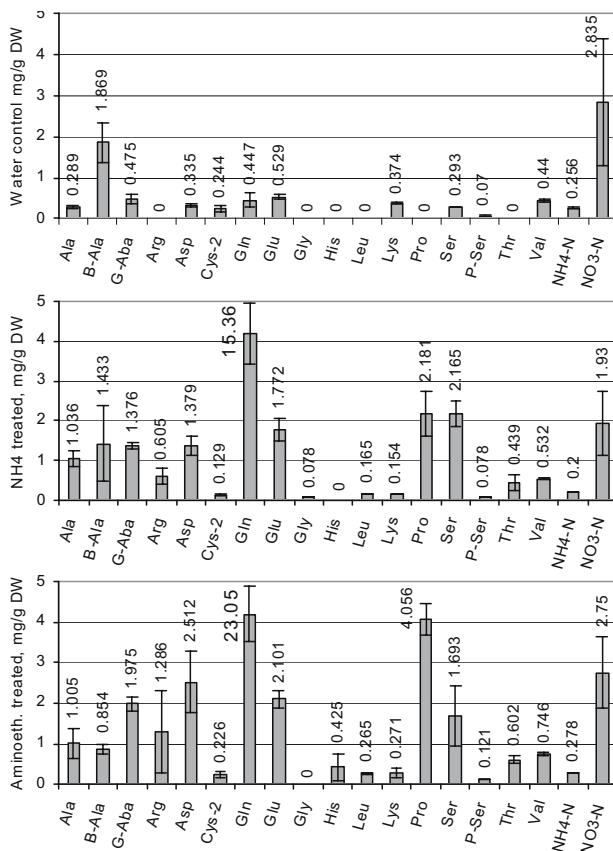
Table 2. Solubility (mg kg^{-1}) of elements and humic substances (HS) in control (C) and postharvest soils (P) from Chinese cabbage cultures. pH, acidity of aqueous soil extract.

Treatment		pH	Ca	Cd	Co	Cu	Mg	Mn	Ni	U	Zn	HS
Water	C	7.06	158	0.06	0.21	3.99	113	2.42	0.91	0.41	9.88	2981
	P	7.54	124[a]	0.09	0.32[a]	3.28	114	4.79[a]	1.12	0.90	13.1	5365[a]
NH$_4$Cl	C	5.29	841[b]	0.16[b]	0.03[b]	3.58	346[b]	1.82[b]	0.93	0.26	9.50	473[b]
	P	6.80	229[b]	0.09	0.19	3.04	158	2.08[b]	1.15	0.46	11.7	3460[b]
	[c]C	7.00	225	0.05	0.01	4.90	228	0.43	0.45	0.27	2.68	ND
Histid-ine	C	6.85	446[b]	0.04[b]	0.05[b]	1.51[b]	190[b]	0.24[b]	0.31[b]	0.46	2.74[b]	1603[b]
	P	7.24	127	0.14	0.41	5.02[b]	152	5.35	1.62[b]	1.01	21.7[b]	5367
Cyst-eine	C	6.41	896[b]	0.29[b]	1.55[b]	4.47	325[b]	75.1[b]	2.40[b]	0.60	15.8[b]	1333[b]
	P	6.31	684[b]	0.19[b]	1.05[b]	3.79	282[b]	45.4[b]	2.21[b]	0.13	9.32	1628[b]
	[c]C	7.00	606	0.24	1.35	4.93	269	45.1	2.06	0.60	10.6	ND
Amino-ethanol	C	6.87	410[b]	0.05	0.08[b]	1.96[b]	181[b]	0.74[b]	0.58[b]	0.58	4.50[b]	1918[b]
	P	7.20	120	0.11	0.39	4.07	136	4.05	1.50	1.33	18.6	5111

[a] Values of water-treated postharvest soil significantly ($p \leq 0.05$) different from those of water-treated control soil. [b] Values significantly ($p \leq 0.05$) different from corresponding values of water-treated control and postharvest soil, respectively. [c] Control soil values recalculated for pH 7.0 to exclude metal solubilizing effects of low pH. ND, not determined.

Relative to water-treated cultures of Chinese cabbage, soil treatment with NH4Cl or AE resulted in equal or lower solubilities of Cd, Co, Cu, Mn, Ni, and Zn but predominantly in higher root acquisition and higher translocation rates (S/R) of these elements to the shoots (Table 3). In the His and Cys treatments, root and shoot concentrations increased with the solubilities of HM in postharvest soils. Root concentrations in the N-starved plants of the seed oil treatment were as high as those of water treated plants, whereas HM translocation to shoots was significantly inhibited. The range of root-to-shoot translocation quotients (S/R) varied thus with the N supply to, and the resulting AA formation in, Chinese cabbage. With the mineralization of AE in control and planted soils (Fig. 1) and the resulting loss in alkalinity (Table 1), the amine was no longer able to solubilize U in potted soil (Table 2) and promote its uptake by the plant. Nevertheless, in NH$_4$Cl-treated plants grown for 48 d the concentrations of organic N (1.9 x), Co (2.7 x), Mn (3 x), Ni (1.8 x), and U (7.85 mg g^{-1} DW) were higher than in 34-d-old plants.

Fig. 2. Concentrations (mg g^{-1} DW) of free AA, NH$_4$-N, and NO$_3$-N in shoots of 34-d-old Chinese cabbage, irrigated daily with water, NH$_4$Cl, or 2-aminoethanol.

Error bars indicate confidence intervals of 95 %.

Ala, alanine; B-Ala, β-alanine; G-Aba, γ-amino-n-butyric acid; Arg, arginine; Asp, aspartic acid; Cys-2, cystine; Gln, glutamine; Glu, glutamic acid; Gly, glycine; His, histidine; Leu, leucine; Lys, lysine; Pro, proline; Ser, serine; P-Ser, phosphoserine; Thr, threonine; Val, valine. Not depicted: Isoleucine; β-aminoisobutyric acid.

Not detected: Asparagine; phenylalanine; tyrosine; taurine; hydroxyproline; α-aminoadipic acid; citrulline; α-aminobutyric acid; cystathionine; methionine; 3-methylhistidine; 1-methylhistidine; tryptophane; carnosine; ornithine. Cysteine (Cys) concentration may be twice the measured cystine value.

Total N (mg g^{-1} DW) bound to free AA: 0.767 (control); 4.780 (NH$_4$Cl); 7.125 (AE); 3.418 (His); 1.943 (Cys treated).

Phytoremediation

Discussion

Microbial consume of AA with their half life of 1-3 h in soil is saturated at concentrations of 1 mM (Jones et al. 2005). With daily applications of 1.3 mM, their mineralization products did not accumulate in planted soil (Fig. 1) and created no leaching problems. Traces of applied organic N should nevertheless rhythmically persist in soil and expose the plant to metal-AA complexes. Nitrogen supplements introduced not only metal-desorbing $Cl^->NO_3^-$ ligands (Shuman 1991) into the soil solution. The NH_4^+/Ca^{2+} Mg^{2+} couple gave rise to extensive HM precipitations and the wide neutralization of the dominating HS ligands (Table 1). With uptake of Ca and Mg, the plant ameliorated these effects which were expressed, e.g., in control soil of the NH_4Cl treatment (Table 2). In this case, the sum of solubilized cations amounted 6685 mg g^{-1} of dissolved C (Fig. 3). In the wide absence of the dominating HS ligand, cations should be complexed with Cl^- and oxoanions of C, S, and P many of which are as easily taken up by the plant as the free cation itself (McLaughlin et al. 1998). In the postharvest soil, the sum of solubilized elements (580 mg g^{-1}) was as low as those in most other treatments (Fig. 3). The surmised changes in complexation could be causal for the increased uptake and shoot trans-

Table 3. Mineral content (mg kg^{-1}) in shoot (S) and root (R) of Chinese cabbage grown on treated U soil for 34 d. S/R, quotient of shoot to root concentration divided by the corresponding quotient in the water control.

Treatment		Ca	Cd	Co	Cu	Mg	Mn	Ni	U	Zn
Water	S	12764	3.37	0.72	11.4	3117	38.7	6.29	0.94	137
control	R	9678	9.15	8.70	185	6627	132	32.1	155	466
	S/R	1.00	1.00	1.00	1.00	1.00	1.00	1.00	1.00	1.00
NH$_4$Cl	S	25128[a]	12.5[a]	1.93	21.2[a]	6052[a]	155[a]	11.6[a]	0.89	535[a]
	R	21978[a]	26.7[a]	16.7[a]	184	6283	242[a]	56.0[a]	40.9[a]	998[a]
	S/R	0.87[b]	1.28	1.39	1.86[c]	2.05[c]	2.19[b]	1.05	3.67	1.80[c]
Histidine	S	18727[a]	6.01[a]	1.10	15.9	5081[a]	122[a]	4.59[a]	0.15	284[a]
	R	23415[a]	16.4[a]	15.6[a]	175	5898[a]	188	60.4[a]	77.4[a]	835[a]
	S/R	0.61[c]	0.99	0.85	1.46[c]	1.83[c]	2.21[b]	0.39[c]	0.33	1.16
Cysteine	S	27523[a]	12.7[a]	8.85[a]	14.9	5182[a]	838[a]	12.4	0.62	531[a]
	R	8801	26.0[a]	53.8[a]	744[a]	5840	707[a]	74.4[a]	74.0[a]	121[a]
	S/R	2.37[c]	1.33	1.98	0.32[c]	1.89[c]	4.05[c]	0.85	1.33	1.50[c]
Amino-	S	21302[a]	7.41[a]	1.35	21.9[a]	5010[a]	161[a]	6.93	0.27	377[a]
ethanol	R	21127[a]	14.3[a]	24.6[a]	274[a]	6155	514[a]	114[a]	91.7[a]	896[a]
	S/R	0.76[b]	1.41	0.66[c]	1.29	1.73[c]	1.07	0.31[c]	0.50	1.43
Sunflower	S	19406[a]	2.19[a]	0[a]	9.06	3237	12.4[a]	1.76[a]	0	116[a]
seed	R	20212[a]	12.0	9.77	197	6895	140	35.0	168	702[a]
oil	S/R	0.73[c]	0.50[b]	0[c]	0.75[c]	1.00	0.30[c]	0.26[c]	0[c]	0.56[c]
Variability of S/R quotient		3.89	2.86	∞	5.81	2.05	13.3	4.04	∞	3.21

[a] Values S and R significantly ($p \leq 0.05$) different from the corresponding shoot or root values of the water control. S/R quotients significantly different [b] at $p \leq 0.33$; [c] at $p \leq 0.05$ from those of the water control of 1.00 with their internal tolerance fields. Variability of S/R factor for further elements without/with the data of the seed oil treatment: As, 11.5/∞; Ba, 2.48/2.54; Cr, 11.4/∞; Li, 1.66/∞; Mo, 6.64/7.78; Na, 1.85/1.85; P, 1.59/1.59; Pb, 2.38/∞; Sr, 2.65/2.71; Ti, 2.77/2.77; U, 11.0/∞; V, 3.6/∞.

location of metals although treatments with NH$_4$Cl had reduced their concentration in the soil solution to a mean of 70 %. The influence of most AA and amines on solubilization and complexation of elements as well as on the physiological state of the plant should be restricted to their N content set free during nitrification, although His in the present treatment, and AA in general (Jones et al. 2005) were taken up by the plant.
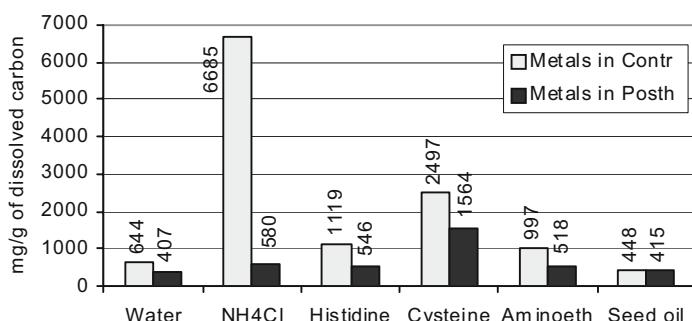
The N content of free AA in shoots of Chinese cabbage correlated with the potential NO$_3^-$ resources indicated by the control soils ($r = 0.750$; Figs. 1 and 2). Inorganic N stimulated AA formation more than did His and Cys supplements to the soil, but stimulation was surpassed by the biocatalyst AE. Although free AA are associated with long-distance transports of N and the local degradation and resynthesis of proteins in plant tissue (Ortiz-Lopez et al. 2000), their abundance could facilitate the transport of metals they preferentially complex. Plants treated with NH$_4$Cl showed predominantly higher concentrations of free Asp (preferring Co, Cu, Ni, Zn), Ser (Co, Cu, Ni), Thr (Cu, Ni), and Pro, Gln, and Glu (Cu) than plants from His>Cys treatments (data not shown). Total uptake and shoot translocation of heavy metals were higher, too (Table 3), although the plants lagged free His and notable Cys concentrations. This means that other high-affinity AA such as Asp, Ser, and Thr could play a role in the *in-planta* metal transport. In transmembrane domains of CPx-ATPase transport proteins presumed to carry heavy metals across plasma membranes of (root) cells, residues of Cys, His, Pro, Ser, and Met dominate whereby Leu, Phe, and Tyr residues contribute to specific affinities for Cd, Cu, Hg, and Zn (Williams et al. 2000).

The negligible translocation quotients for Ni in the His, and for Cu in the Cys treatment (Table 3) suggest a re-complexation of these elements on their way from soil solution to shoot rather than an unimpaired passage of the original metal-AA complex. Translocation of Ni to the xylem of *Alyssum montanum* L. was increased by 40-fold when Ni^{2+} was replaced by Ni-His complex (Krämer et al. 1996). On U soil, translocation of Ni to shoots of His and AE treated plants remained inhibited (Table 3) although these plants were the only to express free His in their tissue (Fig. 2). In several Ni hyperaccumulating plants, Ni was associated with citrate, malate, and malonate rather than with His (Salt 2000). The background of the dramatic uptake and translocation rates in the Cys-preferred elements, Co, and Mn (Table 3) should be re-examined in this context, as they are readily solubilized by carboxylic acids, too (Table 1), which could be formed upon the degradation of the carbon skeleton of AA (Hayes 1991).

Continuous treatment with organic C such as seed oil inhibited metal translocation to shoots of the small and N-starved plants. Tyler and McBride (1982) reported inhibited translocation of Cd to shoots of French bean as a result of ion competition with Ca. Table-3 data document that neither the translocation of Cd nor of most other elements correlated negatively with Ca concentrations in root or shoot of plants from the different treatments. Factors such as plant nutritional status and soil metal speciation should therefore be involved.

Summary and Conclusions

Chinese cabbage plants potted for 34 d on U soil were daily irrigated with deionized water and metabolizable N doses applied as NH_4Cl, His, Cys, and AE, or with seed oil to create the conditions of N starvation with the goal to make soil heavy metals more plant-available but less leachable. Owing to the rapid mineralization of N supplements to NO_3^-, N-treated plants increased shoot DW up to 204 % and free-AA nitrogen to 623-929 % relative to the water control. Whereas NH_4^+ as an intermediate mineralization product liberated Ca and Mg from the soil matrix which repressed the solubility of HS and a mean of 21 elements to 70 %, the AA found free in shoot tissue solubilized mainly Cd (1-6.7x); Co (1-69x); Cu (1.5-22.6x); Mn (1.1-8.4x); Ni (1.1-12x); and Zn (1.1-11.5x) at a comparable pH by complexation, and had no effects on others of the 23 elements examined. Surprisingly, plants from NH_4Cl, His, Cys, and AE treatments showed the same uptake preferences although the solubility of these elements in NH_4Cl treated soil had been reduced and lagged AA ligands. In addition, NH_4Cl-treated plants with access to the highest soil nitrate resources combined highest root concentration and shoot translocation rates of these elements with highest concentrations of free AA. The metals taken up were apparently determined by the affinity of the AA residues in the transmembrane domain of the CPx-ATPase transport proteins of cell membranes (Williams et al. 2000). Resulting shoot concentrations of Cd, Co, Cu, Mn, Ni, and Zn for which AA were selective showed maximum increases to 377, 1229, 192, 2165, 197, and 391 %, respectively across all treatments, promoted by higher translocation rates from roots to shoots (1.05 to 4.04-fold). Uptake of U was not promoted. Hence, application of NH_4Cl increased the total accumulation of these elements in the shoots of higher biomass to 765 %. A root uptake of unsplit metal-AA complexes could not be postulated. It is therefore concluded that accumulation of AA-preferred heavy metals in shoots is best stimulated by NH_4 rather than by undegraded AA, or by biocatalytic amine compounds. NH_4 did not only trigger the formation of more plant-available metal species via

Fig. 3.   Sum of the dissolved 20 cationic elements examined (without As, Mo, P, in mg g^{-1} of dissolved C) in the solution of control (Contr) and postharvest (Posth) soils of Chinese cabbage pot cultures from different treatments.

interaction with Ca^{2+}. It promoted the development of large, vigorous plants with a high content in protein and free AA, a need for trace metals in the shoot, and with the energy to re-complex soil metals for their transport through plasma membranes, symplasm, and xylem. As these advantages did not apply to the small and N-starved plants of the seed oil treatment, differences in the extent of metal translocation from the root to the shoot were inevitable. Repeated mineral-N supply at the limit of metabolizable doses was therefore a key to the improvement of continuous phytoextraction technologies.

References

Bergmann H, Lippmann B, Leinhos V, Tiroke S, Machelett B (1999) Activation of stress resistance in plants and consequences for product quality. J Appl Bot 73: 153-161

Cotton FA, Wilkinson G, Gaus PL (1987) Basic inorganic chemistry. 2nd edn. New York, USA: J. Wiley & Sons, Inc.

Gramss G, Voigt K-D, Bergmann H (2004) Plant availability and leaching of (heavy) metals from ammonium-, calcium-, carbohydrate-, and citric-acid-treated uranium-mine-dump soil. J Plant Nutr Soil Sci 167: 417-427

Hayes MHB (1991) Influence of the acid / base status on the formation and interactions of acids and bases in soils. In: Ulrich B, Sumner ME, eds. Soil acidity. Berlin, Germany: Springer, 80-96

Jones DL, Shannon D, Junvee-Fortune T, Farrar JF (2005) Plant capture of free amino acids is maximized under high soil amino acid concentrations. Soil Biol Biochem 37: 179-181

Krämer U, Cotter-Howells JD, Charnock JM, Baker AJM, Smith JAC (1996) Free histidine as a metal chelator in plants that accumulate nickel. Nature 379: 635-638

McLaughlin MJ, Andrew SJ, Smart MK, Smolders E (1998) Effects of sulfate on cadmium uptake by Swiss chard: I. Effects of complexation and calcium competition in nutrient solutions. Plant Soil 202: 211-216

Ortiz-Lopez A, Chang H-C, Bush DR (2000) Amino acid transporters in plants. Biochim Biophys Acta 1465: 275-280

Pich A, Scholz G (1996) Translocation of copper and other micronutrients in tomato plants (*Lycopersicon esculentum* Mill.): nicotinamine-stimulated copper transport in the xylem. J Exp Bot 47: 41-47

Salt DE (2000) Phytoextraction: present applications and future promise. In: Wise DL, Trantolo DJ, Cichon EJ, Inyang HI, Stottmeister U, eds. Bioremediation of contaminated soils. New York, USA: Marcel Dekker, Inc., 729-743

Shahandeh H, Lee J-H, Hossner LR, Loeppert RH (2001) Bioavailability of uranium and plutonium to plants in soil-water systems and the potential of phytoremediation. In: Gobran GR, Wenzel WW, Lombi E, eds. Trace elements in the rhizosphere. Boca Raton, USA: CRC Press, 93-124

Shuman LM (1991) Chemical forms of micronutrients in soil. In: Mortvedt JJ, Cox FR, Shuman LM, Welch RM, eds. Micronutrients in agriculture, 2nd edn. Madison, Wisconsin, USA: Soil Science Soc. of America, Inc., 113-144

Sumner ME, Fey MV, Noble AD (1991) Nutrient status and toxicity problems in acid soils. In: Ulrich B, Sumner ME, eds. Soil acidity. Berlin, Germany: Springer, 149-182

Tyler LD, McBride MB (1982) Influence of Ca, pH and humic acid on Cd uptake. Plant Soil 64: 259-262

Uren NC (2001) Types, amounts, and possible functions of compounds released into the rhizosphere by soil-grown plants. In: Pinton R, Varanini Z, Nannipieri P, eds. The rhizosphere. New York, USA: Marcel Dekker, Inc., 19-40

Williams LE, Pittman JK, Hall JL (2000) Emerging mechanisms for heavy metal transport in plants. Biochim Biophys Acta 1465: 104-126

Possible biomineralisation of uranium in *Lemna gibba* G3

Martin Mkandawire[1, 2], E. Gert Dudel[1], Carsten Müller[1]

[1] Dresden University of Technology, Institute of General Ecology and Environmental Protection, Pienner Straße 8, D-01737 Tharandt. Germany,
E-mail: mkanda@forst.tu-dresden.de
[2] Dresden University of Technology, Institute of Material Sciences and Nanotechnology, Hallwachsstrasse 3, D-01069 Dresden. Germany.

Abstract. We investigate biomineralisation of U(VI) accumulated in *Lemna gibba* G3 under laboratory conditions. Almost 50.3 ± 11.2 % of uranium was eluted from biomass resulting into 243.5 ± 111.7 mg Kg^{-1}, and 308.9 ± 189.3 µg L-1 in eluates in a 30 minutes deportation experiment. No further uranium losses or concentration increase in aliquot were observed in weekly analysis of soaked biomass for 5 weeks. Phase Contrast and Scanning Electron Microscope shows crystal formation in and on the fronds. Energy dispersion X-ray showed that the crystals contain uranium and elements that support the phenomenon of metal oxalate formation in Lemna sp. Uranium was likely fixed culture as uranyl oxalates species in *Lemna gibba*. Hence, further studies are required to determination uranyl oxalates species structures and ascertain the biomineralisation.

Introduction

Acceptance of phytoremediation as an alternative restoration technology of contaminated surface waters in abandoned uranium mining sites depends on ability to manipulate the uranium immobilisation capacity and durability. To engineer the phytoremediation capacity requires insight knowledge of the process involved. One of the processes that result into long term fixation of metals in plants is biomineralisation of metals. The term biomineralisation characterizes the formation of inorganic solids by living organisms (Mann et al. 1989). Processes of biomineralisation are either under strict biological control or induced by biological activities leading to adventitious precipitation (Mann et al. 1989). Hence, biomin-

eralisation in remediation of metals in the aquatic system would present one of the most durable fixations of uranium in an ecological way.

In view of this, we investigated uranium immobilisation by *Lemna gibba* G3 through possible biomineralisation processes in synthetic mine water in the laboratory. The investigation were aimed at proving the hypothesis that durability of uranium fixation in *Lemna gibba* and other aquatic macrophyte is partially a result of biomineralisation processes which start with precipitation of uranium-organic complexes e.g. oxalate ligands in the plant and in the milieu media, followed by sedimentation (digenesis). The current hypothesis was reached following our earlier studies, in which we found that *Lemna gibba* exuded low molecular weight organic acids most likely oxalic acids into the media under phosphate deficiency, and also under uranium loading (Mkandawire; Dudel 2005: Mkandawire et al. 2004). Chemical speciation modelling with PhreeqC predicts that complexes of uranyl oxalates are likely to form and precipitated the medium.

There are also publications that document production of calcium oxalates in the fronds of most *Lemna* sp (Kostman et al. 2001: Mazen et al. 2004: Volk et al. 2002). Recent studies have also shown that oxalate production by plants and fungi can result into precipitation of metals inform of insoluble metal oxalates (Ganesh et al. 1999: Lytle et al. 1998: Mazen; El-Maghraby 1998). Oxalates are listed among the low molecular weight organic compounds that are involved in the initial stages of metal biomineralisation by plants (Table 1) (Mann et al. 1989).Thus, the precipitation of uranyl oxalates and actual bioaccumulation of uranium in fronds were assumed to be prime responsible for uranium immobilisation in *Lemna gibba* culture. Other well-known biomineralisation processes of uranium include biological reduction of U(VI) to insoluble U(IV) by microbes (bacteria) involved in sulphate and iron reduction (Benders et al. 2000: Liu et al. 2002: Robinson et al. 1998).

Therefore, it is expected that uranium-oxalate in *Lemna gibba* or particulate-bound uranium should lead to formation of secondary uranium minerals in the sediments of the aquatic system. Once this is achieved, phytoremediation would

Table 1. The type of the inorganic solids (biominerals) found in macrophytes and algae as reported in literature (after Mann et al 1989) relevant for uranium complexation (Hence, Si is not considered.).

Mineral	Formula
Calcium carbonate	
Calcite	$CaCO_3$*
Amorphous	$CaCO_3 \bullet nH_2O$
Metal oxalates	
Whewellite	$CaC_2O_4 \bullet H_2O$
Weddelite	$CaC_2O_4 \bullet 2H_2O$
Group IIA metal sulphates	
Barite	$BaSO_4$
Iron oxide	
Ferrihydrite	$5Fe2O3 \bullet 9H2O$

*a range of Mg-substituted calcites are also formed

provide a permanent fate of mobile uranium in aquatic systems. Hence, the current study was to confirm the formation of uranyl oxalate complexes in both *Lemna gibba* and it culture media.

Material and Methods

The hydroponic culture and experimental conditions

A strain of *Lemna gibba* G3 was obtained from LemnaTech GmbH (Würselen, Germany – see acknowledgements) and used in the experiment. The strain was cultured in synthetic mine water in semicontinuous mode in ecotron (Plant-growth chamber NEMA GmbH, Netzschkau, Germany) for 21 days (Mkandawire; Dudel 2005: Mkandawire et al. 2004). The synthetic mine water was composed of 5× diluted Hutner media, and other relevant values of water quality of surface mine water in abandoned uranium mines at Lengenfeld and Mechelgrün in the Free State of Saxon, Germany (Mkandawire; Dudel 2005: Mkandawire et al. 2004). These water quality values included 1000 μg l^{-1} uranium prepared from $UO_2(NO_3)_2 \cdot 6H_2O$, pH r6.5±1.5, Eh range 350 – 550 mV, conductivity of 600, alkalinity or hardness (8.2±2.0 mg L^{-1} dissolved HCO_3^-).The pH was adjusted by drop-wise addition of either 50 mg l^{-1} $NaHCO_3$ or with 65% HNO_3, while water hardness was adjusted with addition of $CaCO_3$. All reagents were of analytical grade.

The ecotron was also programmed to summer conditions of the two abandoned uranium mining sites as follows: 16 h daylight and 10 h dark; 85–125 μE m^{-2} s^{-1} light intensity (PAR) range; and 24±2°C and 16±2°C day and night temperatures, respectively. Chemical speciation was calculated regularly using the PhreeqC geochemical modelling program (Version 2.8, USGS, USA) to ensure optimal solubility and bioavailability of uranium at all time during the culture period. All *Lemna gibba* biomass was harvested after the 21 day of culturing. A few fronds were selected at random for analysis with Scanning Electron while the rest of the biomass was freeze-dried (Christ freeze dryer ALPHA 1-2/LD, Osterode am Harz, Germany) in preparation for the leaching experiment.

Leaching experiment

Approximately 5 g of the freeze-dried biomass were put into Erlenmeyer glass flask containing 500 ml of distilled water. After 10 minutes of stirring with a magnetic stir, 1 ml of water sample and 1 g of biomass were collected, and centrifuged before analysis with ICP-MS (PQ2+ Thermo, Cheshire, England, UK). The procedure was repeated every week for four consecutive weeks. All experiments were replicated four times in factorial arrangement. All biomass samples were

dried in a vacuum drier at 49°C until constant weight was reached. Then, the dry biomass were digested using HNO_3–H_2O_2 mixture in a microwave digester (MW-Digestion, CEM MARS 5, Matthews, North Carolina, USA) in preparation for uranium determination with ICP-MS.

Microscopic analysis

The fronds selected randomly soon after harvesting were divided into samples to be analysed under Phase Contrast Microscope (PCM) (Interference Microscope Peraval Interphako, Carl Zeiss, Jena. Germany), and Scanning Electron Microscope (SEM, JEOL JSM-T330A, JEOL Ltd., Tokyo, Japan),). The samples for PCM were first separated into root-like structures. Then, the root-like structure and leaflets were grounds using separately before being mounted on microscope glass slides. A litre of the medium was also collected at the end of the cultures period and re-concentrated by dewatered in freeze drier i.e. the 1 L of medium was sublimated until the volume was reduced to 20 ml. A drop of the concentrated medium was also mounted on the microscope slides for analysis.
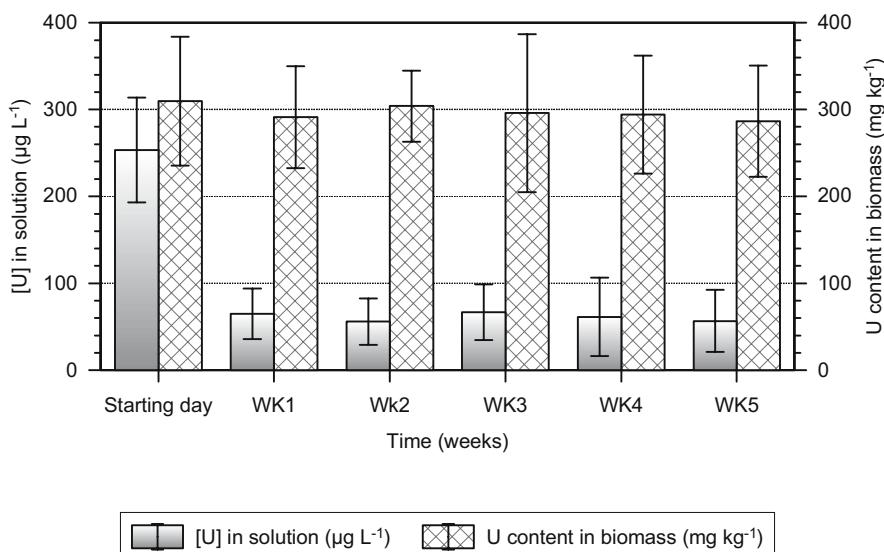
Frond sample for SEM analysis were deep in liquid nitrogen for rapid freezing to avoid ice development during slow freezing, which damages the cells and cell components. The samples were held on copper holder, and freeze-dried (EMITECH K1250, Ashford, Kent, UK). Then, the samples were broken before being exposed to carbon steam (EMITECH K-450X Carbon Evaporator, Ashford, Kent, UK). After carbon steaming, the samples were investigated for any crystal formation on Scanning Electron Microscope. An Energy Dispersive X-ray (EDX) spectrograph coupled to the Scanning Electron Microscope set at 15 kV was used to determine micro-chemical composition of the crystals.

Results

The leaching and decay experiment was conducted to determine the amount bio-accumulated uranium which readily re-mobilised once dry matter get into contact with water, and when the biomass degrades. The remobilised uranium was collected in the aliquot, and the durably fixed uranium remained in the *Lemna gibba* biomass. The results of analysing the aliquot and biomass samples collected weekly for a period o five weeks (figure 1). It was observed that uranium biomass initially lost about 50.3±11.2 % or the accumulated uranium before stabilising within the first week. In the following weeks, loss of uranium from the biomass was negligible. Likewise, after dissolution of uranium into the aliquot in the initial stage, there were no significant observable increases in uranium concentration in the aliquot until the end of the experiment. Thus, uranium fixation in the biomass remained the same by the time of termination of the experiment. *Lemna gibba* biomass has not degraded by the end of the experiment.

The PCM was used to identify crystal-like structures in *Lemna gibba* in relation to uranium in the media. The results of PCM analysis showed that there is formation of crystals more in the leaflets, followed by root-like structure and little in the solution (Figure 2). In the leaflets, crystals were observed in both control and uranium containing experiments. The only difference between the experiments was that the crystal formations as observed in uranium experiment were bigger and more than in the control experiment (Figure 2 (a) and (b)). Crystals were also observed in the root-like structure of *Lemna gibba*. However, it was distinctly more crystal formation in the roots of Lemna gibba exposed to uranium (Figure 2 (c) and (d)). No crystals were observed in the media of the control experiment, while some crystals were observed in the uranium experiment. There may be a number of reason for low formation of the crystals in the media like the ration between the biomass and the media, and also dissolution of crystals in the media, just to mention a few.
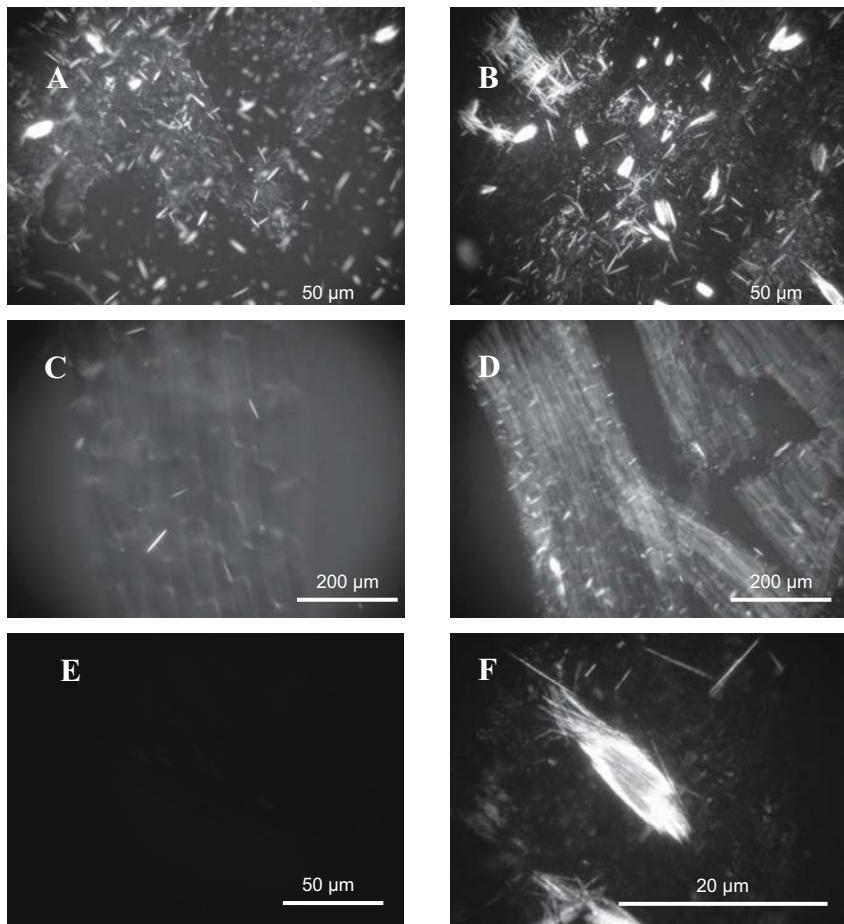
The purpose was of SEM examination to substantiate presumed uranyl oxalate complexes based on crystal identification with PCM, and to determine localisation of uranium in *Lemna gibba* fronds. Using the SEM-EDX facility, the analysis was expected to ascertain that the crystals observed contained the uranium. The pictures of the observation and localisation of the crystals presumed to be the uranyl oxalate in and on the surface of *Lemna gibba* are presented in Figure 3. Figure 3 (a) indicates that the formations of the crystals are in the proximity of the *Lemna gibba* cell wall.

Fig.1. Fractions of uranium in fronds and concentration of elutes and leachates after elutions and leaching of *Lemna gibba* dead biomass. The analyses on the starting day were done on the after eluted biomass and the resulting eluent. The values are mean of four replications and the error bar is standard deviation.
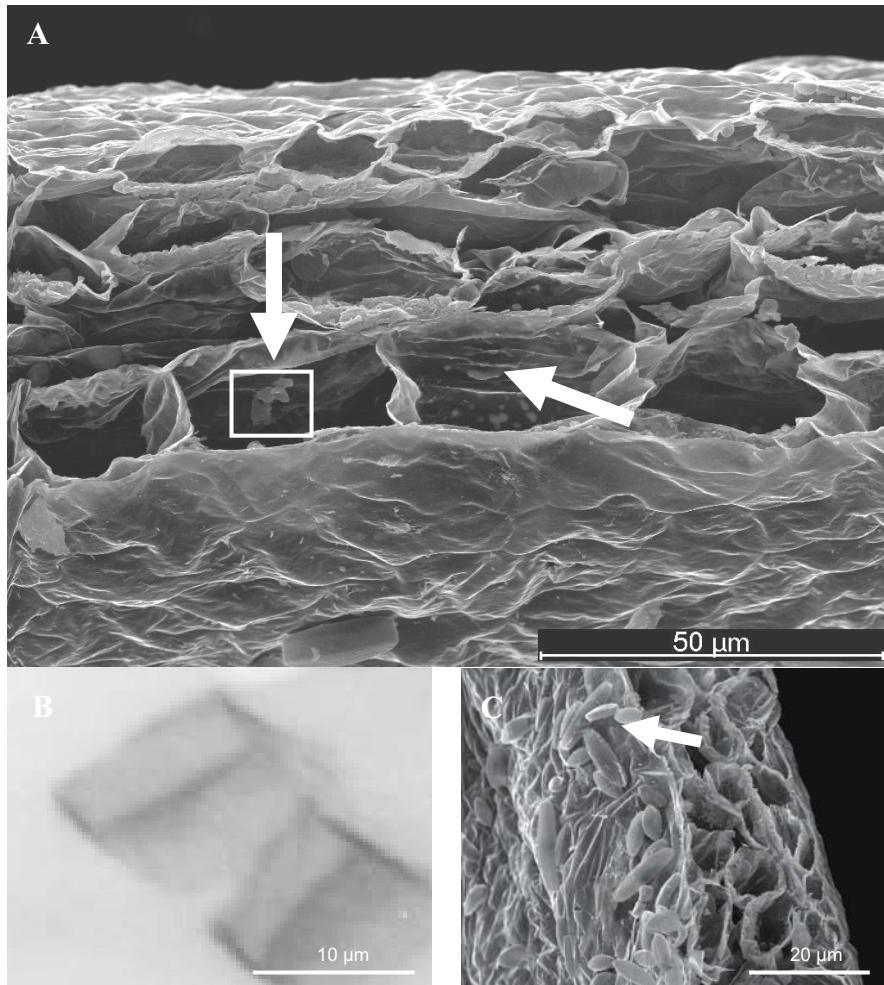
The mean size of the crystals in the cells is 40±20 µm (Figure 3(b)). On the surface of *Lemna gibba*, the crystals are also observed. Figure 4 presents the analysis of the element composition of the crystals using the EDX coupled to SEM. The results show that the crystals contain carbon, hydrogen and oxygen, which are components of oxalates. Further, the crystal contained large amount of uranium and calcium. Some of Fe was observed. Other components like K, S and Cl are expected in the plant material because they are essential elements.

The mean size of the crystals in the cells is 40±20 µm (Figure 3(b)). On the sur-

Fig. 2. Crystals in and on the surface of *Lemna gibba* and its media under Phase Contrast Microscope. (A) and (B) are crystal in the frond leaflet under control and 1 mg L^{-1} initial uranium in the media, respectively; (C) and (D) are crystal in the frond root under control and 1 mg L^{-1} initial uranium in the media, respectively; and finally (E) and (F) are crystal in the media under control and 1 mg L^{-1} initial uranium in the media, respectively.

face of *Lemna gibba*, the crystals are also observed. Figure 4 presents the analysis of the element composition of the crystals using the EDX coupled to SEM. The results show that the crystals contain carbon, hydrogen and oxygen, which are components of oxalates. Further, the crystal contained large amount of uranium and calcium. Some of Fe was observed. Other components like K, S and Cl are expected in the plant material because they are essential elements.
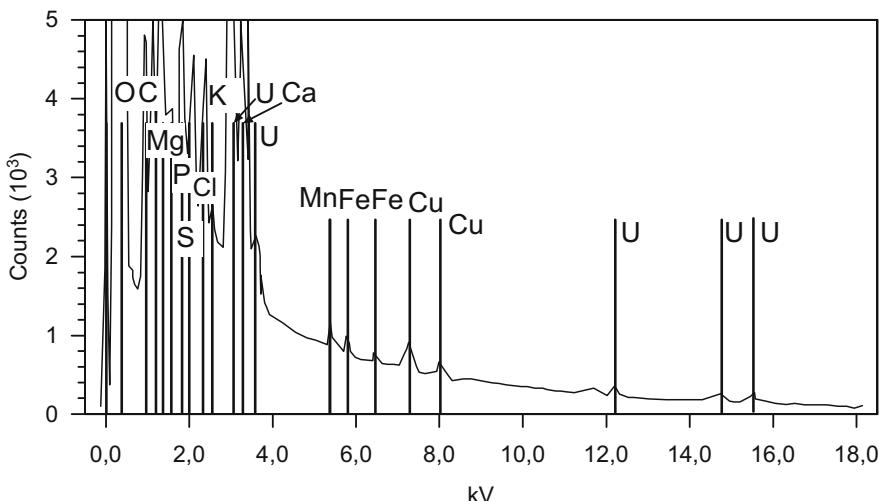
Fig. 3. Scanning electron microscope pictures of *Lemna gibba* fronds. (A) shows crystal development in the cells; (b) is the higher magnification of the crystals and the part analysed by Energy Dispersive X-ray (EDX); and (C) shows some crystal formation on the surface of *Lemna gibba* leaflet.

Phytoremediation

Discussion

There are a few documentations of saccharides, proteins, peptide, and oxalate formation in response to toxic stress in *Lemna* sp. in literature (Amado et al. 1980: Farooq et al. 2000: Horner et al. 2000: Kostman et al. 2001: Mazen; El-Maghraby 1998: Mazen et al. 2004: Ovodova et al. 2000: Sauter 1988). One of the recent and detailed work come from Mazen et al (2004), who described the formation of ox-alate crystal are in crystal-forming cells (crystal idioblasts). In the current study, we have found the crystal similar to the structure described by Mazen et al (2004) (figure 3). Additionally, the structures are also found in the submerse root-like structures and even in the media (figure 2). Some studies have attribute formation of calcium oxalate in *Lemna* sp. as sinks for bulk regulation of calcium, and de-toxification of oxalic acid. The association of the crystals with uranium found in our study may indicate that the crystal formation may be general compartmentali-sation or intracellular sequestration of toxic substances in the plants.

Immobilization of metals can result from sorption to cell components or exopolymers, transport and intracellular sequestration or precipitation as organic and inorganic compounds, e.g. oxalates, and sulphides. Oxalate forms complexes with a wide variety of metallic ions including transition metals (e.g., Fe^{3+} and Al^{3+}) and actinides (e.g., UO_2^{2+} and PuO_2^{2+}) (Ganesh et al. 1999: Mazen; El-Maghraby 1998). However, uranium observed in oxalate crystal idioblast, in this study, has never been described before (figure 2 and figure 3). Similarly, forma-tion of uranyl oxalate crystal (figure 2) confirms modelling results in our previous study (Mkandawire and Dudel, 2002). The durability of fixation demonstrated by the leaching experiment confirms also that uranium might be tightly fixed in the biomass (figure 1). In atomic energy industries, precipitations of uranyl oxalates

Fig. 4.   Energy Dispersive X-ray (EDX) spectrograph of crystal shown in Figure 3 (a).

Phytoremediation

are used to separate and purify uranium in fuel reprocessing flow sheets. Oxalates are also used to concentrate uranium in alkaline waste solutions by forming insoluble uranyl oxalate precipitates (El-Nadi et al. 2003: Robinson et al. 1998). Hence, if oxalate form naturally in *Lemna gibba* as shown in this study, biomineralisation of uranium in surface mine waters is possible.

A number of synthetic polycrystalline uranyl oxalate complexes have also been investigated (Havel et al.: Szabó; Fischer 2002: Tel 1999). Based on the empirical formula of the compounds and analytical results, structures of the complexes have been identified as linear uranyl cations connected by tetradentate bridging oxalate groups yielding a two-dimensional network. These nets are stacked to form the crystal structure. Such structures includes $UO_2C_2O_4 \cdot 3H_2O$, $(UO2)_2C_2O_4(OH)_2 \cdot 2H_2O$, $K_2(UO_2)_2(C_2O_4)_3 \cdot 4H_2O$ or $Ca(UO_2)_2(C_2O_4)_3 \cdot 4H_2O$ which form at room temperature as determined by the research group of Dr Burns at University of Notre Dame in USA (personal communication with Paul Giesting). Comparison of these synthetic crystals with those produced natural have a number of similarities such as the colour (yellow), size and shape. Nonetheless, the crystals from *Lemna gibba* need to be further investigated to ascertain if they are really uranyl oxalate species, and identify the real chemical structure.

Conclusion

The current results from our experiments indicate that uranium is probably immobilised *Lemna gibba* in aquatic system as crystal-like complexes most likely uranyl oxalates species (e.g. $UO_2C_2O_4 \cdot 3H_2O$, $(UO2)_2C_2O_4(OH)_2 \cdot 2H_2O$, $K_2(UO_2)_2(C_2O_4)_3 \cdot 4H_2O$ or $Ca(UO_2)_2(C_2O_4)_3 \cdot 4H_2O$) in and on fronds, and in the media through exudation. With the knowledge that metal oxalate end into biomineralisation, and the results obtained in this study on stability of uranium in decaying organic matter, *Lemna gibba* facilitate significantly the biomineralisation of uranium. If this happens, then uranium immobilisation using macrophytes like *Lemna gibba* would present a durable and clean technology of phytoremediation of contaminated surface water in abandoned uranium mines. Further investigations are required to determine of the structure degree of order of the crystals other possible minerals U complexes and qualification per volume biomass unit inside and outside of the cells and in the medium in relation to the environmental conditions of the uranyl oxalate crystals in *Lemna gibba*. It would therefore imperative to identify the structure using X-Ray Diffraction or similar technology.

Acknowledgement

MS analyses. Dr. Joachim Rotsche assisted in mineral crystal identification with Phase Contrast Microscope. The strain of *Lemna gibba* G3 was kindly provided by Matthias Eberius of LemnaTech GmbH. Paul Giesting of Environmental Molecular Science Institute at the University of Notre Dame in USA kindly provided structures of synthetic uranyl oxalate species for comparison with those found in *Lemna* culture.

References

Amado, R., R. Muller-Riemeyer, and U. Morti, 1980: Protein, neutral sugar content and amino acid composition of Lemnaceae. *Biosystematic investigations in the family of duckweeds (Lemnaceae)*, E. Landolt, Ed., B .Veröff. Geobotanisches Institut ETH, 102-117.

Benders, J., M. C. Duff, P. Phillips, and M. Hill, 2000: Bioremediation and bioreduction of dissolved U(VI) by microbial mat consprtium supported on silica gel particles. *Environ. Sci. Technol.*, 34, 3235-3241.

El-Nadi, Y. A., N. E. El-Hefny, and J. A. Daoud, 2003: Mechanism of Extraction of Hexavalent Uranium from Alkaline Medium by Aliquat-336/Kerosene Solution. *Journal of Nuclear and Radiochemical Sciences*, 4, 19-22.

Farooq, M., G. S. Babu, R. S. Ray, R. B. Misra, U. Shankar, and R. K. Hans, 2000: Sensitivity of duckweed (Lemna major) to ultraviolet-B radiation. *Biochemical and Biophysical Research Communications*, 276, 970-973.

Ganesh, R., K. G. Robinson, L. L. Chu, D. Kucsmas, and G. D. Reed, 1999: Reductive precipitation of uranium by Desulfovibrio desulfuricans: Evaluation of cocontaminant effects and selective removal. *Water Research*, 33, 3447-3458.

Havel, J., J. A. Soto-Guerrero, and P. Lubal, 2003: Spectrophtometric Study of Uranyl-oxalate Complexation in Solution. *Polyhedron, Velká Británie*, 21, 1411-1420.

Horner, H. T., A. P. Kausch, and B. L. Wagner, 2000: Ascorbic acid: A precursor of oxalate in crystal idioblasts of *Yucca torreyi* in liquid root culture. *International Journal of Plant Sciences*, 161, 861-868.

Kostman, T. A., N. M. Tarlyn, F. A. Loewus, and V. R. Franceschi, 2001: Biosynthesis of L-ascorbic acid and conversion of carbons 1 and 2 of L-ascorbic acid to oxalic acid occurs within individual calcium oxalate crystal idioblasts. *Plant Physiology*, 125, 634-640.

Liu, C. X., J. M. Zachara, J. K. Fredrickson, D. W. Kennedy, and A. Dohnalkova, 2002: Modeling the inhibition of the bacterial reduction of U(VI) by beta-MnO2(S)(g). *Environmental Science & Technology*, 36, 1452-1459.

Lytle, C. M., F. W. Lytle, N. Yang, J. H. Qian, D. Hansen, A. Zayed, and N. Terry, 1998: Reduction of Cr(VI) to Cr(III) by wetland plants: Potential for in situ heavy metal detoxification. *Environmental Science and Technology*, 32, 3087-3093.

Mann, S., J. Webb, and R. J. P. Williams, 1989: *Biomineralisation - Chemical and Biological pespectives.* VCH Verlagsgesellschaft, 541 pp.

Mazen, A. M. A. and O. M. O. El-Maghraby, 1998: Accumulation of cadmium, lead and strontium, and a role of calcium oxalate in water hyacinth tolerance. *Biologia Plantarum*, 40, 411-417.

Mazen, A. M. A., D. Zhang, and V. R. Franceschi, 2004: Calcium oxalate formation in *Lemna minor* physiological and ultrastructural aspects of high capacity calcium sequestration. *New Phytologist*, 161, 435-448.

Mkandawire, M. and E. G. Dudel, 2005: Accumulation of arsenic in Lemna gibba L. (duckweed) in tailing waters of two abandoned uranium mines in Saxony, Germany. *Science of the Total Environment*, 336, 81-89.

Mkandawire, M., E. G. Dudel, and B. Taubert, 2004: Accumulation of uranium in *Lemna gibba* L. in relation to milieu conditions of tailing waters in abandoned uranium mines in Germany. *Mine Water - Process, Policy and Progress*, A. P. Jarvis, Dudgeon B. A., and Younger P. L., Eds., Springer, 9-18.

Ovodova, R. G., V. V. Golovchenko, A. S. Shashkov, S. V. Popov, and Y. S. Ovodov, 2000: Structural studies and physiological activity of lemnan, a pectin from Lemna minor L. *Bioorganicheskaya Khimiya*, 26, 743-751.

Robinson, K. G., R. Ganesh, and G. D. Reed, 1998: Impact of organic ligands on uranium removal during anaerobic biological treatment. *Water Science and Technology*, 37, 73-80.

Sauter, J. J., 1988: Temperature-induced Changes in Starch and Sugars in the Stem of *Populus* X *canadensis `robusta´*. *Journal of Plant Physiology*, 132, 608-612.

Szabó, Z. and A. Fischer, 2002: Redetermination of dipotassium diuranyl tris(oxalate) tetrahydrate. *Acta Cryst.*, E58, i56-i58.

Tel, H., 1999: Preparation and characterization of uranyl oxalate powders. *Journal of Nuclear Materials*, 275, 146-150.

Volk, G. M., V. J. Lynch-Holm, T. A. Kostman, L. J. Goss, and V. R. Franceschi, 2002: The role of druse and raphide calcium oxalate crystals in tissue calcium regulation in Pistia stratiotes leaves. *Plant Biology*, 4, 34-45.

Accumulation of natural radionuclides in wooden and grass vegetation from abandoned uranium mines. Opportunities for phytoremediation

Rossitsa Petrova

Department "Soil science" – University of Forestry, Kl. Ochridsky str.10, 1756 Sofia, Bulgaria, E-mail: rpetrova_fri@yahoo.com

Abstract. The survey is focused on accumulation of uranium, radium and the concomitant heavy metals in forest and grass vegetation growing upon uranium waste rock dumps.

In the report are presented the final results from long-term investigations of factors on which depends the accumulation of natural radionuclides and heavy metals in vegetation.

Shown are the results of greenhouse vegetational experience with grasses and sorbents. Tracked are main growth indexes (increase in height and thickness and increase in volume) in the species of black pine-tree (Pinus nigra Arn.) and white pine-tree (Pinus sylvestris L.).

Introduction

Mining rock dumps from an abandoned uranium mines, after weathering, are sources of environmental pollution with natural radionuclides as uranium and radium, and heavy metals - iron, zinc, cadmium, lead, copper, arsenic. Frequently are observed acid rock drainage waters containing radioactive elements and sulphates as main pollutants.

Contamination of soils, groundwater, sediments, surface water and air with radionuclides and heavy metals is one of the major problems in the uranium mining areas. Different methods of remediation are known. Most of them are based on excavation of rock dumps, re-grading and stabilization the slopes, leveling the horizontal part and engineered dry covers – clay and soil masses. Traditional engineering technologies may be too expensive for remediation of most sites. Re-

moval of metals from these soils using accumulating plants is the goal of phytoremediation (Baker et al., 1994; Brown et al., 1994; Brown et al., 1995a; Brown et al., 1995b; Blaylock et al., 1997; Carey, 1996; Chaney et al., 1997; Cunningham and Ow, 1996; Cunningham et al., 1996; Dushenkov et al., 1995; Moffat, 1995; Nanda Kumar et al., 1995; Raskin et al., 1994; Rouhi, 1997; Salt et al., 1995). Baker et al. (1991) concluded that phytoremediation, using certain species, could offer a low cost, low technology alternative to current clean up technologies.

Phytostabilization is the use of certain plant species to immobilize contaminants in the soil and groundwater through absorption and accumulation by roots, adsorption onto roots or precipitation within the root zone of plants (rhizosphere). This process reduces the mobility of the contaminant and prevents migration to the ground water or air, and thus reduces bioavailability for entrance into the food chain. This technique can be used to re-establish a vegetative cover at sites where natural vegetation is lacking due to high metals concentrations in surface soils or physical disturbances to surface materials. Metal-tolerant species can be used for restoration of vegetation in the sites, thereby decreasing the potential migration of contamination through wind erosion and transport of exposed surface soils and leaching of soil contamination to groundwater.

Though U and its daughter elements have not been shown to be essential or beneficial to either plants or animals, many plant species will absorb U and incorporate it into their biomass along with other heavy metals (Mortvedt, 1994; Sims and Kline, 1991; Sheppard et al., 1989; Singh and Narwal, 1984; Narwal et al., 1983; Moffet and Tellier, 1977). This observation suggests the possibility for remediation of U-contaminated soils through plant uptake.

The purpose of this study was the comprehensive survey of the ability of selected tree and grass vegetation to accumulate radionuclides and toxic metals from contaminated media. Assessment of growth of tree species – Pinus sylvestris L. and P. nigra Arn. in the conditions of uranium rock dumps.

The objects of this investigation were rock damps and natural vegetation of some uranium mines, situated in mountains "Stara planina" and "Rhodopa" in Bulgaria.

The Buhovo Mining Area (BMA) was the most important uranium ore region in Bulgaria. The total uranium production of BMA was 26% of the Bulgarian production. Mining activities in BMA were started in 1936 and continued until 1990. At that time mining activities developed in Goten, Chamilov kamak, Borche, Chora and in the main ore deposits – Seslavzi 1, 2 and 3, mainly as underground mines.

Buhovo ore field is located in the south slopes of "Stara planina" mountain (Kremikovci region of the Sofia Municipality). The total sum affected land from development of BMA is 2867 dca and formation of 141 dumps. Waste rock substrates of 19589.5 thousands m3 were deposited. Main rocks around the ore are clayshists, clayshists with high coal content, sandclayshistes, sandstones, granosienites, quartzsienites and pegmatites.

Table 1. ^{238}U concentration and concentration ratios (CRs) in plants and rock substrates.

Uranium mine	Sampling location	Plant species	Number of samples	Weight basis	Plant concentration, Bq/kg	Rock substrates/soil concentration, Bq/kg	CR
						„Stara planina" mountain	
BMA	Rock dumps	Robinia pseudoacacia – leaves	15	A	ND		
		Pinus nigra – 1age needles	15	A	0.886		0.0002
		Pinus nigra – 2age needles	12	A	1.291		0.0004
		Pinus sylvestris – 1age needles	12	A	1.472		0.0004
		Pinus sylvestris – 2age needles		A	2.772	160 – 27940	0.0008
		Corilus avellana – leaves	2	A	2.947		0.0008
		Populus tremula – leaves	5	A	2.089		0.0006
		Carpinus betulus – leaves	5	A	2		0.0006
		Juniperus communis	3	A	61		0.0170
		Tussilago farfara – leaves	19	A	2.425		0.0007
	Background – Hromic Luvisols/Dystric Cambisols	Pinus nigra – 1age needles	7	A	0.866	304/1955.8	0.0008
		Pinus nigra – 2age needles	7	A	4.74	304/1955.8	0.0042
		Pinus sylvestris – 1age needles	5	A	3.09	304/1955.8	0.0027
		Pinus sylvestris – 2age needles	5	A	1.894	304/1955.8	0.0017
						„Rodopa" mountain	
Kalach borun	Rock dumps	Pinus sylvestris – 1age needles	15	A'	1.38	958 – 1336	0.0014
		Salix caprea – leaves	5	A	3.11		0.0031
	Open pit	Pinus sylvestris – 1age needles	15	A	2.59	508 – 32938	0.0004
		Picea excelsa – 1age needles	10	A	2.18		0.0003
Kara tepe	Rock dumps	Pinus sylvestris – 1age needles	15	A	3.6	227 – 230	0.0159
		Salix caprea – leaves	5	A	2.25	228 – 230	0.0099
Sufan dere	Background – Dystric Cambisols	Pinus sylvestris – 1age needles	3	A	1.9	227	0.0084
		Picea excelsa – 1age needles	3	A	1.73		0.0076
		Salix caprea – leaves	3	A	3.03		0.0133
Sdravez	Rock dumps	Pinus sylvestris – 1age needles	5	A	2.94	50 – 1462	0.0039
		Tussilago farfara – leaves	10	A	2.59		0.0034
Narechen	Rock dumps	Mix grasses	8	A	29 – 40		0.0040
		Carpinus betulus – leaves	5	A	43	254 – 39514	0.0049
		Tussilago farfara – leaves	5	A	29		0.0033
		Pinus nigra – 1age needles	5	A	28		0.0032
		Fraxinus ornus – leaves	5	A	105		0.0120

Comments: A - ash

Phytoremediation

The uranium mines "Sdravez", "Kalach borun", "Kara tepe' and "Narechen" are situated in central part of "Rhodopa" mountain. Main rocks around the ore are eruptive (granites) and metamorphic (shistses, gneisses, clayshistes, marbles).

All dumps are located on the slopes of existing gullies and often dam them. The slopes are very steep, which is a reason for transport of materials together with the surface water run-off.

Materials and methods

Samples were taken by standard ANSI-C998-83.

Experiment with 7 variants for studying of the accumulation of radionuclides and toxic metals from waste substrates with different sorbents was carried out.

The results from green mass and contents of radionuclides were worked out statistically.

Results

Many studies have been conducted on the relationships between plants and soils relevant to radionuclide accumulation by plants. In these studies it was generally observed that plant species differ in U accumulation. Uranium accumulates mainly in the roots and depth of U placement and substrate properties influence absorption by plants. There is contradictory information on the phytotoxicity of soil U to plants (Sheppard et al., 1992). Levels as low as 1 mg kg -1 in soil, well within the normal background range, have been cited as toxic.

Measurements of uranium and radium concentrations in rock substrates and plants from the objects are presented in Tables 1and 2.

It was established that:

1. In the dumps of BMA - "Stara planina" mountain, that mainly consists of clayshists, granosienities and quartz, the contents of:
   - Radium in the excavated rock substrates vary from 60 to 3600 Bq/kg and in the vegetation – from 0.1 to 50.6 Bq/kg. The background contents of 226Ra in the soils of the region (Hromic Luvisols – 304.8 Bq/kg и Dystric Cambisols - 123 Bq/kg) significantly differs from the world's characteristic - 0,03 Bq/g and from the soils in Bulgaria – 0,1 x 10-10 – 2,1 x 10-10% (Raikov, 1969; Raikov at all, 1971).
   - Uranium in the excavated rock substrates vary from 160 to 27940 Bq/kg and in the vegetation – from 0.8 to 61 Bq/kg. The background contents of 238U in the soils of the region (Hromic Luvisols – 80 Bq/kg and Dystric Cambisols – 482.5 Bq/kg) significantly differs from the world's characteristic - 0,03 Bq/g and from the soils in Bulgaria – n x 10-5– n x 10-4% (Raikov, 1978).

Phytoremediation

2. In the dumps from objects in "Rhodopa" mountain, that mainly consists of granites crystalline shists and gneisses, the contents of:

- Radium in the excavated rock substrates vary from 39 to 29945 Bq/kg, and in the vegetation - from 1.55 to 201.33 Bq/kg. The background contents of 226Ra in the soils of the region - Dystric Eutryc Cambisols is 37 Bq/kg.
- Uranium in the excavated rock substrates vary from 50 to 32938 Bq/kg, and in the vegetation – from 1.38 to 105 Bq/kg. The background contents of 238U in the soils of the region (Hromic Luvisols – 80 Bq/kg and Dystric Cambisols – 482.5 Bq/kg) significantly differs from the world's characteristic - 0,03 Bq/g and from the soils in Bulgaria – n x 10-5– n x 10-4% (Raikov, 1978).

Radium has slow mobility and the concentrations in the substrate are in direct connection with these in the main rock. This determines its high accumulation fron vegetation. Radium is accumulating more intensively compared to uranium. Relatively higher bioaccumulation of radium in the vegetation can be found in the objects from "Rhodopa mountain" compared to "Stara planina" mountain (CR from 0.006 to 0.12). This is result mainly from differences in: intensity of weathering of the rock substrates, soil texture, different sorption capacity of the formed during the weathering minerals, etc. For the BMA region the soil texture of fraction lower than 2 mm alters from heavy sandy clay to sandy clay, cation exchange adsorption capacity (T8.2) is represented mainly from clayish minerals of the kaolinite-illite and for the objects from "Rodopa mountain" the soil texture is from loamy sand to sandy loam and cation exchange adsorption capacity (T8.2) is represented by clay minerals muskovit and illit.

Stem analysis of model trees of Pinus sylvestris L. and P. nigra Arn.

It was established that: the white and the black pine trees can be characterized with strongly decreased values of indexes height and diameter, compared to the same from growth tables for the same species:

- Height of the modeled stem shows strongly decreased values in comparison with growth tables. The percent of such deviation has high values as it lessen with aging. This regularity can be seen in both surveyed species.
- d1,3 (DBH) – shows deviation from growth table as until 15 years of age in the white pine tree and until 20 years of age in the black pine tree has lower values and after that they increase and are greater values than the index in growth table.
- Growth in volume shows greatly decreased values compared to growth table. The percent of deviation lessens with aging which is representative for the adaptation of coniferous vegetation in aggravates growing conditions.
- Accumulation of radionuclides is in inverse proportion to the soil texture, the contents of organic substance and cation exchange adsorption capacity.

The results are presented in Tables 3 and 4.

Phytoremediation

Table 2. ^{226}Ra concentration and concentration ratios (CRs) in plants and rock substrates.

Uranium mine	Sampling location	Plant species	Number of samples	Weight basis	Plant concentration, Bq/kg	Rock substrates/soil concentration, Bq/kg	CR
		„Stara planina" mountain					
		Robinia pseudoacacia – leaves	15	A	22		0.0288
		Pinus nigra – lage needles	15	A	0.211		0.0003
		Pinus nigra – 2age needles	12	A	0.166		0.0002
		Pinus sylvestris – lage needles	12	A	0.962		0.0013
	Rock dumps	Pinus sylvestris – 2age needles	2	A	1.026		0.0013
		Corilus avellana – leaves	2	A	7.952	764.6	0.0104
		Populus tremula – leaves	5	A	0.45		0.0006
BOF		Carpinus betulus – leaves	5	A	1.96		0.0026
		Juniperus communis	3	A	14.2		0.0186
		Tussilago farfara – leaves	19	A	0.9		0.0012
		Лопен	3	A	50.6		0.0662
	Background – Hromic Luvisols/Dystric	Pinus nigra – lage needles	7	A	0.516	123	0.0042
		Pinus nigra – 2age needles	7	A	0.415	123	0.0034
		Pinus sylvestris – lage needles	5	A	0.495	123	0.0040
		Pinus sylvestris – 2age needles	5	A	4.355	123	0.0354
		„Rodopi" mountain					
Kalach borun	Rock dumps	Pinus sylvestris – lage needles	15	A*	15.635	199	0.0786
		Salix caprea – leaves	5	A	10.974		0.0551
	Open pit	Pinus sylvestris – lage needles	15	A	45.708	374-29945	0.0064
		Picea excelsa – lage needles	10	A	201.333		0.0280
Kara tepe	Rock dumps	Pinus sylvestris – lage needles	15	A	1.554	39	0.0398
		Salix caprea – leaves	5	A	2.385		0.0612
Sufian dere	Background – Dystric Cambisols	Pinus sylvestris – lage needles	3	A	4	37	0.1081
		Picea excelsa – lage needles	3	A	2.877		0.0778
		Salix caprea – leaves	3	A	2.338		0.0632
Sdravez	Rock dumps	Pinus sylvestris – lage needles	5	A	1.287	255-2235	0.0015
		Tussilago farfara – leaves	10	A	9.872		0.0116
		Mix grasses	8	A	36.8		0.0376
Narechen	Rock dumps	Carpinus betulus – leaves	5	A	45		0.0460
		Tussilago farfara – leaves	5	A	41	648 - 1313	0.0419
		Pinus nigra – lage needles	5	A	2		0.0020
		Fraxinus ornus – leaves	5	A	117		0.1195

Comments: A - ash

Uranium and radium uptake in grass, cultivation in greenhouse

Made is single factor disperse analysis using computer code STATGRAPHICS PLUS7.0 of the data (contents of radioactive elements in the vegetation mass) from separate treatment with corresponding repetitions.

The results for bioaccumulation of radionuclides in the comparative vegetation (Lolium perenne L.) are presented in Table 5.

The single factor disperse analysis shows good results depending on the contents of radioactive elements Ra and 236U in vegetation samples from the treatment option as the corresponding levels of significance are 0.0066 and 0.0074. With this two radioactive elements there is statistically reliable difference in control option from the other conducted options with ninety five percent "Duncan" and in it (control option) is observed the maximum accumulation. For the Th and K are not obtained statistically reliable differences in the used test between the separate options. Their contents in the overviewed experiment with Lolium perenne L. Do not directly depends on the way of treatment of the substrates.

By their effect on phytoremediation, sorbents could be divided into three groups: (i) highly reducing (a) – corresponding variants 05 for 226Ra and 06 for 238U; reducing (ab) – corresponding variants 01, 03, 04 and 06 for 226Ra and variants 01, 03 and 04 for 238U, (ii) no effect (bc, b) - corresponding variants 02 for 226Ra and variants 02 and 05 for 238U.

Conclusion

1. Bioaccumulation of radionuclides in tree and grass vegetation from dumps of uranium mining ores depends mainly on contents of radionuclides in the substrates, intensity of volatization and soil texture. Accumulation of 226Ra in leaf mass is more intensive than the 238U.
2. In the first years the growth of species of white and black pine trees is significantly oppressed. Later the tree vegetation is adapting to the harder conditions and shows sufficient growth.
3. Treating of the substrates with sorbents, containing organic substance and clay leads to strong reduction of bioaccumulation of 226Ra и 238U.

Table 3. Comparison of values of model stem with indexes for height (H), diameter (d1,3) and volume (V) with growth table.

Type	A(r)	H		d1,3 (DBH)		V	
		Growth table	Model stem	Growt h table	Model stem	Growth table	Model stem
White pine tree	5	1.3	0.4	2.2	-	0.00304	0.00005
(Pinus sylvestris L.)	10	3.3	1.4	4.3	1.9	0.00897	0.00098
	15	5.6	3.0	5.7	5.8	0.01760	0.00444
	18	6.8	5.3	6.8	7.6	0.02509	0.00807
Black pine tree	5	1.1	0.3	1.4	-	0.00038	0.00007
	10	2.2	1.3	3.4	0.6	0.00421	0.00054
	15	3.7	1.5	5.2	4.0	0.01208	0.00130
(Pinus nigra Am.)	20	5.2	2.8	7.0	8.7	0.02407	0.00680
	25	6.8	5.2	9.0	12.0	0.04327	0.02046
	28	7.8	7.3	10.0	14.4	0.05570	0.04850

Table 4. Percent of deviation of indexes H, d1,3 and V from growth table.

Type	A(r)	H	d1,3	V
White pine tree	5	-69.2	-	-98.4
	10	-57.6	-55.8	-89.1
(Pinus sylvestris L.)	15	-46.4	1.75	-74.8
	18	-22.1	11.8	-67.8
Black pine tree	5	-72.7	-	-81.6
	10	-40.9	-82.4	-87.2
(Pinus nigra Am.)	15	-59.5	-23.1	-89.2
	20	-46.1	24.3	-71.7
	25	-23.5	33.3	-52.7
	28	-6.4	44.0	-12.9

Table 5. Average values of radioactive elements in the leaf mass of the species Lolium perenne by options of treating of substrate and homogenic groups.

Treating option	^{226}Ra	^{238}U	^{232}Th	^{40}K
01	76.67 ab	676.77 ab	53.33 a	2069.33 a
02	90.00 bc	715.00 b	62.50 a	2484 a
03	67.67 ab	543.33 ab	60.50 a	2201.67 a
04	78.00 ab	656.67 ab	68.33 a	1320.33 a
05	54.00 a	703,89 b	65.00 a	4252 a
06	62.00 ab	515.00 a	43.00 a	3104 a
07	115.67 c	916.67 c	75.67 a	3041.33 a

Comments: The variants tick off with Latin letter formed one homogeneous group for given indicator. 01 – substrate + zeolit sorbent; 02 – substrate + modified zeolit (rhodopin); 03 – substrate + zeolit:rhodopin – (2:3); 04 – substrate + zeolite: coal ash – (5:1); 05 – substrate + vermiculite; 06 – substrate + hydrolyzed lignin + CaO + NPK fertilizer.

Acknowledgements

References

Adriano, D.C., K.W. McLeod and T.G. Ciravolo. 1981. Plutonium, curium, and other radionuclide uptake by the rice plant from a naturally weathered contaminated soil. Soil Sci. 132(1):83-88.

Baker, A.J.M. 1981. Accumulators and excluders: strategies in the response of plants to heavy metals. J. Plant Nutr. 3:643-654.

Baker, A.J.M. and R.R. Brooks. 1989. Terrestrial higher plants which hyperaccumulate metallic elements -- a review of their distribution, ecology and phytochemistry. Biorecovery 1:81- 126.

Baker, A.J.M., R.D. Reeves and A.S.M. Hajar. 1994. Heavy metal accumulation and tolerance in British populations of the metallophyte Thlaspi careulescens J.& C. Presl (Brasssicaceae). New Phytol. 127:61-68.

Baker, A.J.M., R.D. Reeves and S.P. McGrath. 1991. In situ decontamination of heavy metal polluted soils using crops of metal accumulating plants? A feasibility study. In situ Bioreclamation; Hinchee, R.L., Olfenbuttel, R.F., Eds.; Butterworth-Heinemann: Boston.

Blaylock, M.J., D.E. Salt, D. Slavik, O. Zakharova, C. Gussman, Y. Kaoulnik, B.D. Ensley and I. Raskin. 1997. Enhanced accumulation of Pb in Indian mustard by soil-applied chelating agents. Environ. Sci. Technol. 31:860-865.

Boileau, L.J.R., E. Nieboer and D.H.S. Richardson. 1985. Uranium accumulation in the lichen Cladonia rangiferina. II. Toxic effects of cationic, neutral, and anionic forms of the uranyl ion. Can. J. Bot. 63:390-397.

Brooks, R.R., J. Lee, R.D. Reeves and T. Jaffre. 1977. Detection of nickelferrous rocks by analysis of herbarium specimens of indicator plants. J. Geochem. Explor.. 7:49-57.

Brown, S.L., R.L. Chaney, J.S. Angle and A.J.M. Baker. 1994. Zinc and cadmium uptake by Thlaspi caerulescens and Silene cucubalis in relation to soil metals and soil pH. J. Environ. Qual. 23:1151-1157.

Brown, S.L., R.L. Chaney, J.S. Angle and A.J.M. Baker. 1995a. Zinc and cadmium uptake of Thlaspi caerulescens grown in nutrient solution. Soil Sci. Soc. Am. J. 59:125-133.

Brown, S.L., R.L. Chaney, J.S. Angle and A.J.M. Baker. 1995b. Zinc and cadmium uptake by hyperaccumulator Thlaspi caerulescens and metal tolerant Silene vulgaris grown on sludge-amended soils. Environ. Sci. Technol. 29:1581-1585.

Bunzl, K., R. Kretner, P. Schramel, M. Szeles and R. Winkler. 1995. Speciation of 238 U, 226 Ra, 210 Pb, 228 Ra, and Stable Pb in the soil near an exhaust ventilating shaft of a uranium mine. Geoderma 67:45-53.

Campbell, M.D. and K.T. Biddle. 1977. Frontier areas and exploration techniques. Frontier uranium exploration in the south-central United States. p. 3-44. In M.D. Campbell

(ed,) Geology of Alternate Energy Resources. Houston Geological Society, Houston, Texas.

Campbell, W.F. and E.A. Rechel. 1979. Tradescantia a "super-snooper" of radioactivity from uranium mill wastes. Utah Science. p.101-103.

Carey, J. 1996. Can flowers cleanse the earth? Business Week, Feb. 19, p. 54.

Chaney, R.L., M. Malik, Y.M. Li, S.L. Brown, J.S. Angle and A.J.M. Baker. 1997. Phytoremediation of soil metals. Current Opinions in Biotechnology. In press.

Chaney, R.L., Y.M. Li, S.L. Brown, J.S. Angle and A.J.M. Baker. 1995. Hyperaccumulator based phytoremediation of metal-rich soils. Fourteenth Annual Symposium. Current topics in plant biochemistry, physiology and molecular biology. Will plants have a role in bioremediation? April 10-22, 1995. Columbia, Missouri. p. 33-34.

Ciavatta, L., D. Ferri, I. Grenthe and F. Salvatore. 1981. The first acidification step of the tris(carbonato)dioxourantantate(VI) ion, UO 2 (CO 3) 3 4- . J. Inorg. Chem. 20:463467.

Cunningham, S.D., T.A. Anderson, A.P. Schwab and F.C. Hsu. 1996. Phytoremediation of soils   contaminated with organic pollutants. Adv. Agron. 56:55-114.

Cunningham, S.D. and D.W. Ow. 1996 Promises and prospects of phytoremediation. Plant Physiol. 110:715-719

Department of Energy. 1988. Health physics manual of good practices for uranium facilities.DOE88-013620. U.S. Dept. of Energy, Washington, D.C.

Duff, M.C. and C. Amrhein. 1996. Uranium(VI) Adsorption on geothite and soil in soil carbonate solutions. Soil Sci. Soc. Am. J. 60:1393-1400.

Dushenkov, V., P.B.A. Nanda Kumar, H. Motto and I. Raskin. 1995. Rhizofiltration-the use of plants to remove heavy metals from aqueous streams. Environ. Sci. Technol. 29:1239- 1245.

Entry, J.A., N.C. Vance, M.A. Hamilton, D. Zabowski, L.S. Watrud and D.C. Adriano. 1996. Phytoremediation of soil contaminated with low concentrations of radionuclides. Water, Air, and Soil Poll. 88:167-176.

Ernst, W.H.O. 1988. Decontamination of mine sites by plants: An analysis of the efficiency. p. 305-310. In Proceedings of the Conference on Environmental Contamination, Venice; CEP Consultants: Edinburgh, 1988.

Grenthe, I., J. Fuger, R. Konings, R.J. Lemire, A.B. Muller, C. Nguyen-Trung and J. Wanner. 1992. The chemical thermodynamics of uranium. Elsevier. New York

Gulati, K.L., M.C. Oswal and K.K. Nagpaul. 1980. Assimilation of uranium by wheat and tomato plants. Plants and Soil. 55:55-59

Huang, J.W., M.J. Blaylock, B.D. Ensley and Y.K. Kapulnik. 1997. Phytoremediation of uranium contaminated soils. Agronomy Abstracts ASA Meeting Anaheim, CA. Oct. 26-31.

Johnson, R., C.M. Wai, B. McVeety, H. Lee and H. Willmes. 1980. Uranium in soil around phosphate processing plants in Pocatello, Idaho. Bull. Environm. Contam. Toxicoll. 24:735-738.

Langmuir, D. 1978. Uranium solution-mineral equilibrium at low temperatures with applications to sedimentary ore deposits. Geochim. Cosmochim. Acta 42:547-569.

McGrath, P.S., C.M.D. Sidoli, A.J.M. Baker and R.D. Reeves. 1993. The potential for the use of metal-accumulating plants for the in situ decontamination of metal-polluted soils. p. 673-676 In Integrated Soil and Sediment Research: A Basis for Proper Protection. H.J.P. Eijsackers and T. Hamers (eds.). Kluwer Academic Publishers, Dordrecht.

Meinrath, G., Y. Kato, T. Kimura and Z. Yoshida. 1996. Solid-aqueous phase equilibria of uranium(VI) under ambient conditions. Radiochemica Acta. 75:159-167.

Moffat, A.S. 1995. Plants proving their worth in toxic metal cleanup. Sci. 269:302-303.

Moffett, D. and M. Tellier. 1977. Uptake of radioisotopes by vegetation growing on uranium tailings. Can. J. Soil Sci. 57:417-424.

Mortvedt, J. J. 1994. Plant and soil relationships of uranium and thorium decay series radionuclides - a review. J. Environ. Qual. 23:643-650.

Nanda Kumar, P.B.A., V. Dushenkov, H. Motto and I. Raskin. 1995. Phytoremediation: the use of plants to remove heavy metals from soils. Environ. Sci. Technol. 29:1232-1238.

Narwal, R.P., B.R. Singh and A.R. Panhwar. 1983. Plant availability of heavy metals in a sludge treated soil: I. effect of sewage sludge and soil pH on the yield and chemical composition of rape. J. Environ. Qual. 12(3):358-365.

Raskin, I., P.B.A. Nanda Kumar, S. Dushenkov and D.E. Salt. 1994. Bioconcentration of heavy metals by plants. Current Opinions in Biotechnology. 5:285-290.

Rouhi, A.M., 1997. Plants to the rescue. C&EN Washington pp. 21-23.

Salt, D.E., M. Blaylock, N.P.B.A. Kumar, V. Dushenkov, B.D. Ensley, I. Chet and I. Raskin. 1995. Phytoremediation: a novel strategy for the removal of toxic metals from the environment using plants. Biotechnology. 13:468-474.

Saric, M.R., M. Stojanovic and M. Babic. 1995. Uranium in plant species grown on natural barren soil. J. Plant Nutr. 18(7):1509-1518.

Sheard, J.W. 1986a. Distribution of uranium series radionuclides in upland vegetation of northern Saskatchewan. I. Plant and soil concentrations. Can. J. Bot. 64:2446-2452.

Sheard, J.W. 1986b. Distribution of uranium series radionuclides in upland vegetation of northern Saskatchewan. II. Patterns of accumulation among species and localities. Can. J. Bot. 64:2453-2463.

Sheppard, M.I. and D.H. Thibault. 1984. Natural uranium concentrations of native plants over a low-grade ore body. Can. J. Bot. 62:1069-1075.

Sheppard, M.I. and D.H. Thibault. 1992. Desorption and extraction of selected heavy metals from soils. Soil Sci. Soc. Am. J. 56:415-423.

Sheppard, M.I., S.C. Sheppard and D.H. Thibault. 1984. Uptake by plants and migration of uranium and chromium in field lysimeters. J. Environ. Qual. 13:357-361.

Sheppard, S.C., W.G. Evenden and R. J. Pollock. 1989. Uptake of natural radionuclides by field and garden crops. Can. J. Soil Sci. 69:751-767.

Sheppard, S.C., W.G. Evenden and A.J. Anderson. 1992. Multiple assays of uranium in soil. Environ. Toxicol. Wat. Qual. 7:275-294.

Sims, J.T. and J.S. Kline. 1991. Chemical fractionation and plant uptake of heavy metals in soils amended with co-composted sewage sludge. J. Environ. Qual. 20:387-395.

Singh, B.R. and R.P. Narwal. 1984. Plant availability of heavy metals in a sludge-treated soil II. metal extractability compared with plant metal uptake. J. Environ. Qual. 13(3):344-349.

Titaeva, N.A., A.I. Taskaev, V. Y. Ovchenkov, R.M. Aleksakhin and I.I. Shuktomova. 1979. Content and characteristics of U, Th, Ra, and Rn uptake in plants growing under different radioecological conditions. Institute of Biology. Komi Branch of the Academy of Sciences of the USSR. Translated from Ekologiya, No. 4, pp. 37-44, July-August, 1978.Revision submitted November 17, 1977. 1979 Plenum Publishing Corporation pp. 328-334.

Phytoremediation

Tsivoglou, E. and R.L. O'Connell. 1964. Nature, volume and activity of uranium mine wastes. Radiological health and safety in mining and milling of nuclear materials. 2:101-105.

Willet, I.R. and W.J. Bond, (1995). Sorption of maganese, uranium and radium by highly weathered soils. J. Environ. Qual. 24:834-845.

Zafrir, H., Y. Waisel, M. Agami, J. Kronfeld and E. Mazor. 1992. Uranium in plants of southern Sinai. J. Arid Environ. 22:363-368.

Study of radiophytoremediation on heavily polluted area in South Bohemia

Petr Soudek, Sarka Valenova, Tomas Vanek

Institute of Organic Chemistry and Biochemistry, Academy of Sciences of the Czech Republic, Prague, Czech Republic, E-mail: domingo@uochb.cas.cz

Abstract. A phytoremediation study was performed on the area of the old uranium mill tailings waste depot of a former uranium ore reprocessing factory in South Bohemia. The distribution of ^{226}Ra in contaminated soil was found to be extremely variable (from 7 to 32 Bq ^{226}Ra/g of DW). No direct relation was proved between plant species characteristics and their radioactivity content. The results showed a great range of variation in the accumulation of ^{226}Ra by the plant species found. The highest activity of ^{226}Ra was found in *Potentilla reptans* (4.09 Bq ^{226}Ra/g of DW), *Mentha arvensis* (4.00 Bq ^{226}Ra/g of DW), and *Daucus carota* (3.70 Bq ^{226}Ra/g of DW). The greenhouse and small scale field experiments show *Cannabis sativa* "Beniko" as a good potential accumulator of activity ^{226}Ra.

Introduction

Soil contaminated with radionuclides poses a long-term radiation hazard to human health through exposure *via* the food-chain and other pathways. Phytoremediation of radionuclide-contaminated soils has become increasingly important. The understanding of the mechanism of radionuclide uptake and accumulation is necessary prerequisite for the application of radiophytoremediation in "real" scale.

The objectives of our work were to: (i) perform a geobotanical study of the wild plants growing in the area of uranium mill tailings; (ii) determine the distribution of ^{226}Ra among selected plant species; (iii) carry out the biomonitoring of recultivated areas; (iv) test the low contaminated sited for production of non-food plants and (v) propose the mechanism of clean-up of water contained uranium and ^{226}Ra. The goal of this work was also to select appropriate plant candidates for potential utilization in radiophytoremediation processes.

Material and Methods

Collection and preparation of substrate samples for measurement

To determine the basic chemical properties of the mill tailings substrate, the samples (three duplications) were collected at five sampling points on the top of dump K1. The samples were dried at 80 °C for 72 h. and afterwards weighed and measured in Marinelli beakers. The average characteristics of mill tailings deposited in waste dump K1 are presented in Table 1.

Table 1. Substrate properties of mill tailings deposited in waste dump K1.

soil characteristic	
SiO_2	600 g/kg
gypsum	100 - 200 g/kg
Fe, Al hydroxide	20 - 100 g/kg
grain size	< 0.5 mm
soluble compounds	30 - 53 g/kg
^{226}Ra	5 - 32 kBq/kg
Mn	1050 mg/kg
NH_4^+	750 - 1050 mg/kg
U	< 1.5 mg/kg
SO_4^{2-}	18 - 30 mg/kg
heavy metals (Zn,Ni,Co,Cd)	≈ 3 mg/kg
pH	5.0 - 7.0

Greenhouse experiment

The technical crops, food crops, and fodder crops were cultivated in control conditions in mixture of uranium mill mine tailings (32 Bq ^{226}Ra/g DW) and soil in ratio 1:3. The total activity of soil mixture was about 13 Bq ^{226}Ra/g DW.

Small scale field experiment

The technical crops, food crops, medicinal plants, grasses and fodder crops were cultivated from June to October 2004 on field with the activity about 9 Bq ^{226}Ra/g DW.

Collection and preparation of plant samples for measurement

Plant samples were collected in the autumn of 2004. The whole plants were rinsed in a high pressure water stream, dried at 80 °C for 72 h., homogenized and then weighed and measured in Marinelli beakers. Only one sample was prepared from each plant species which represented an average of many whole plants, because the Marinelli beaker used for the measurement of radioactivity had to contain about 100 g of dry material.

Sample measurement

The [226]Ra radioactivity in the sample was determined after reaching the decay equilibrium in sealed Marinelli beakers by means of a gamma scintillation spectrometer (Canberra – Packard, model PCAP-Nal 2007, channel width 4.986 keV, energy resolution 9% at 662 keV) relatively to [226]Ra standard of 3.000 kBq (Czech Institute of Metrology, type MBSS 5). Using PC programme Genie 2000 (Canberra – Packard), the comparison of a sample and standard peaks of [214]Bi (609.3 keV) was applied for the evaluation of [226]Ra activity. For Quality Assurance and Control two standards were also used: [60]Co (Czech Institute of Metrology, type MBSS 7) for checking of spectrometer stability and [137]Cs (Czech Institute of Metrology, type MBSS 4) for energy resolution measurement. All three standards were used for energy calibration of the spectrometer (Soudek et al. 2004a).

Table 2. The plant species with the most high and lowest activity, which was collected on the top of dump K1.

Plant species	Activity ± S.D. [Bq [226]Ra/g DW]
Potentilla reptans	4.09 ± 0.043
Mentha arvensis	4.00 ± 0.077
Calamagrostis epigeios	3.40 ± 0.033
Daucus carota	3.70 ± 0.035
Rubus caesius	2.65 ± 0.025
Silene vulgaris	2.60 ± 0.028
Cirsium arvense	2.46 ± 0.013
Hypericum perforatum	2.13 ± 0.033
Echinum vulgare	1.79 ± 0.047
Sphagnum fallax	1.76 ± 0.042
Artemisia vulgaris	0.19 ± 0.006
Urtica dioica	0.11 ± 0.008
Sisymbrium loesselli	0.10 ± 0.003
Tanacetum vulgare	0.08 ± 0.006
Melilotus officinalis	0.06 ± 0.004
Melilotus alba	0.02 ± 0.003
Amanita phalloides	0.00 ± 0.000
Trifolium repens	0.00 ± 0.000
Polygonum amfibium	0.00 ± 0.000

Results and Discussion

Concentrations of radionuclides in plant samples collected in the surrounding areas of the uranium ore processing factory were studied. Radionuclides detected both in soil and plants were ^{226}Ra, ^{214}Pb and ^{214}Bi. We found the best accumulation ability (cca. 4 Bq ^{226}Ra/g of dry weight (DW) to 1.8 Bq/g DW) in *Calamagrostis epigeios*, *Hypericum perforatum*, *Silene vulgaris*, *Cirsium arvense* and *Rubus caesius* etc. All this plants was collected on sampling point with activity 32 Bq/g of dry soil.

The greenhouse experiments were in progress from March to July 2004. The first results show differences between crops plant species, which was cultivated in flowerpots. The counting rate of soil was about 13 Bq ^{226}Ra/g DW. The best accumulation we detected for *Amaranthus tricolor* „Early Splendor" and *Lupinus polyphyllus* (2.16 or 2.20 Bq ^{226}Ra/g DW). The significant differences between cultivars of same plant species were not found. But we found differences in accumulation of ^{226}Ra between plants from the same genus (*Lupinus* sp.).

The small field experiments were done on experimental are which was situated on lakeside of sludge bed IV/R (activity 9 Bq ^{226}Ra/g DW). The best activity accumulation was determined for *Mentha pipericum* (about 3.05 Bq ^{226}Ra/g DW). We not found again differences in accumulation of ^{226}Ra for different cultivars of all tested plant species and between plants from same genus, except *Lupinus* sp. The high activity was determined also in grasses *Bromus lanceolatus* and *Festuca glauca* (2.17 or 1.70 Bq ^{226}Ra/g DW).

Table 3. The activity of plants cultivated in greenhouse on soil mixture with activity 13 Bq ^{226}Ra/g DW and on small field on the lakeside of sludge bed IV/R on soil with activity 9 Bq ^{226}Ra/g DW. (n/g = not growth).

Plant species	Activity ± S.D. [Bq ^{226}Ra/g DW]	
	greenhouse	small field
Linum usitatissimum „Atalante"	0.45 ± 0.013	0.15 ± 0.006
Linum usitatissimum „Jitka"	0.35 ± 0.018	0.26 ± 0.012
Cannabis sativa "Beniko"	0.42 ± 0.008	0.28 ± 0.006
Cannabis sativa „Juso-11"	0.40 ± 0.016	0.41 ± 0.010
Cannabis sativa „Silesia"	0.52 ± 0.010	0.38 ± 0.024
Amaranthus hypochondriacus „Pygmy Torch"	0.74 ± 0.020	0.18 ± 0.004
Amaranthus tricolor „Early Splendor"	2.16 ± 0.071	n/g
Amaranthus tricolor	0.59 ± 0.022	0.27 ± 0.005
Amaranthus caudatus „Atropurpureus"	0.76 ± 0.020	0.44 ± 0.006
Phaseolus vulgare „Bobis Nano"	0.95 ± 0.039	0.30 ± 0.006
Phaseolus vulgare „Aida Gold"	0.55 ± 0.031	0.57 ± 0.013
Pisum sativum „Ambrosia"	0.32 ± 0.030	n/g
Pisum sativum „Gloriosa"	0.43 ± 0.019	n/g
Capsicum annuum „Berta"	0.40 ± 0.026	0.20 ± 0.020
Capsicum annuum „Drákula"	0.46 ± 0.025	0.94 ± 0.081
Capsicum annuum „Maryša"	0.56 ± 0.021	0.20 ± 0.035
Lycopersicon lycopersicum „Albertovské"	0.86 ± 0.027	0.47 ± 0.008
Lycopersicon lycopersicum „Stupické"	0.57 ± 0.023	0.28 ±0.005
Lycopersicon lycopersicum „Start F1"	0.32 ± 0.021	0.26 ± 0.010
Lupinus albus	0.72 ± 0.039	0.89 ± 0.042
Lupinus luteolus	1.24 ± 0.093	0.66 ± 0.014
Lupinus polyphyllus	2.20 ± 0.097	1.29 ± 0.031
Daucus carota	1.10 ± 0.016	-
Sinapis alba	0.55 ± 0.012	0.31 ± 0.008
Helianthus annuus	0.41 ± 0.016	n/g
Brassica oleracea	0.75 ± 0.030	0.61 ± 0.008
Zea mays	n/g	n/g
Panicum miliaceum	-	0.38 ± 0.005
Achillea millefolium	-	0.55 ± 0.008
Achillea filipendulina	-	0.78 ± 0.051
Sorghum bicolor	-	1.03 ± 0.014
Sorghum nigrum	-	1.55 ± 0.020
Euphorbia marginata	-	0.08 ± 0.005
Hypericum perforatum	-	1.02 ± 0.062
Lepidium sativa	-	0.14 ± 0.006
Festuca glauca	-	1.70 ± 0.041
Agrostis nebulosa	-	0.67 ± 0.017
Bromus lanceolatus	-	2.17 ± 0.021
Iberis umbellata	-	0.25 ± 0.011
Solidago canadiensis	-	1.60 ± 0.025
Mentha pipericum	-	3.05 ± 0.032

Conclusion

The obtained results prove the possibility of utilization of radiophytoremediation for practical application, at least in the case of wastewater treatment, where the conditions of contaminants uptake can be similar to hydroponic arrangement. Of course, for the soil-cleaning purposes, the solubility of contaminant and its mobility in soil will be the most limiting factor as well as extend of root-zone of selected plant species.

The second problem of practical application is after-harvest treatment of contaminated plant material. Its storage and composting (as radioactive waste), or its incineration under strictly controlled conditions, respectively, can be considered.

Acknowledgement

Reference

Clulow F.V.. Davé N.K.. Lim T.P.. Cloutier N.R. (1996) U- and Th-series radionuclides in snowshoe hare (*Lepus americanus*) taken near U mill tailings close to Elliot lake. Ontario. Canada. *Environmental Pollution* **94**. 273-281.

Mortvedt J.J. (1994) Plant and soil relationships of uranium and thorium decay series radionuclides – *A review. Journal of the Environmental Quality* **23**. 643-650.

Soudek P.. Podracká E.. Vágner M.. Vaněk T.. Petřík P.. Tykva R. (2004a) [226]Ra uptake from soils into different plant species. *Journal of Radioanalytical and Nuclear Chemistry* **262**. 187-189.

Soudek P., Tykva R., Vaněk T. (2004b) laboratory analyses of 137Cs uptake by sunflower, reed and poplar. *Chemosphere* **55**, 1081-1087.

Localisation of uranium in roots by chemical extractions and by a short term uptake study. Influence of phosphate.

Anne Straczek, Jasmine Dams, Hildegarde Vandenhove

Radioécologie, Bât.GKD, SCK CEN, Boeretang 200, 2400 Mol, Belgium,
E-mail: astracze@sckcen.be

Abstract. Pea roots were exposed to nutrient solution containing 25 µmol L^{-1} of uranium in presence or absence of phosphate. The uptake of U was followed during the first 90 minutes of exposure. Fifty percent of the uranium was removed after 45 minutes and after between 60-90 minutes in absence and in presence of phosphate respectively. After 24 hours exposure, root were extracted, to remove uranium from the root apoplasm. Copper extracted similar amounts of uranium than EDTA for root exposed to a solution with phospate while copper extracted only 18% of uranium extracted by EDTA for root exposed to a solution devoid of phosphate. Phosphate decreased the availability of uranium to roots of pea. The presence of phosphate decreased also the amounts of uranium extracted.

Introduction

The transfer of uranium from soil to plants depends on uranium speciation in soil and in soil solution, and on the capacity of plants to take up and detoxify uranium. One mechanism to detoxify a toxic metal in plants consists in the storage of the considered metal in the roots of plants and more precisely in the apoplasm of roots. The apoplasm consists of the plasma membrane, the cell wall (specific structure of the cells of plants), and the inter-cell wall and intercellular free spaces. Carboxylic and peptic compounds present in the cell walls create negative charges onto which cations can adsorb (Dufey et al. 2001). These negative charges confer to the root cation exchange capacity which is between 20 and 50 cmol$_{(+)}$ kg^{-1} for the dicotyledons and between 10 and 20 cmol$_{(+)}$ kg^{-1} for the monocotyledons.

Two methods are usually applied to determine the importance of the adsorption of a metal onto the cell wall. The first one consists in following the uptake kinetics

of the metal by the plant: the adsorption of the metal onto the cell wall is a rapid process; the entrance of the metal in the cell is slower. The second approach consists in chemical extractions with other cations (Rengel and Robison 1989). Some authors used copper which has a high affinity for root cell walls and which is present as trace elements in plants (Dufey et al. 2001). Adsorption of uranium onto cell wall of algae was also quantified performing extraction with EDTA (Fortin et al. 2004).

Roots of plants can rapidly remove high amounts of uranium from contaminated solution: Ramaswami et al. (2001) showed that different plant species (Sunflower, Vetch, Juniper, Mustard, and Bean) can remove between 60 and 90% of uranium from a solution containing 210 µmol L^{-1} of uranium in demineralized water within 48 hours. Significant uranium retention by root was also observed for smaller exposure time: Eapen et al. (2003) obtained a 50% reduction in uranium solution concentration (initial concentration up to 500µmol L^{-1}) after 2-3 hours of exposure for hairy roots of *Brassica juncea* and after 2 to 8 hours for roots of *Chenopodium armanticolor*. Bhainsa and D'Souza (2001) observed 54% retention after 4 minutes contact time between dried roots of water hyacinth and a solution containing 840 µmol L^{-1} uranium. The rapid uptake of uranium from the solution could indicate an important adsorption of uranium onto the cell wall of plants.

Phosphate could play a role in uranium retention by roots of plants at two levels. First, metals could also precipitate with phosphate in the apoplasm or around the root (Sarret et al. 2002; Straczek 2003) and uranium has been shown to be associated with phosphate in lupine (Gunther et al. 2002). However phosphate could also decrease the bioavailability of uranium for plants (Ebbs et al. 1998).

The main objectif of this work was to compare uranium uptake of pea in presence or absence of phosphate. Two methods were applied: short term uptake studies and chemical extractions on the roots with copper and EDTA. Here preliminary results are shown.

Material and Methods

Pre-culture

Plants were grown in a growth chamber (16 / 8 h light / dark cycle, 65% humidity 24°C). Seed of pea were disinfected with H_2O_2 10% during 30 minutes. After one week of germination, pea was grown on Hoagland nutrient solution during 2 weeks.

Exposure to uranium

Following the pre-culture, plants were grown for a additional day on a nutrient so-lution containing as much iron and oligoelements as the Hoagland solution and the concentrations of the major elements were at fourth strength (diluted Hoagland nutrient solution). The roots were then briefly rinsed with desionised water. Plants were exposed during 24 h to the diluted Hoagland nutrient solution containing 23 μmol L^{-1} of 238 uranium and 2 μmol L^{-1} of 233 uranium, and 0 or 5 μmol L^{-1} of phosphate.

Uptake of uranium as a function of time

A sample of the nutrient solution was taken at different time intervals (0,3,5, 10, 15,20, 30,45, 60, 90 minutes) to determine the kinetic of the uptake of uranium by roots.

Chemical extractions

After 24 h of exposure to uranium, roots were harvested and divided in two parts. The first part was extracted with EDTA 250μmol L^{-1} during 90 minutes. The sec-ond part was extracted with $CuSO_4$ 10 mmol L^{-1} during 30 minutes.

Analyses

The concentration of uranium was assayed by a scintillation counter.

Results and discussion
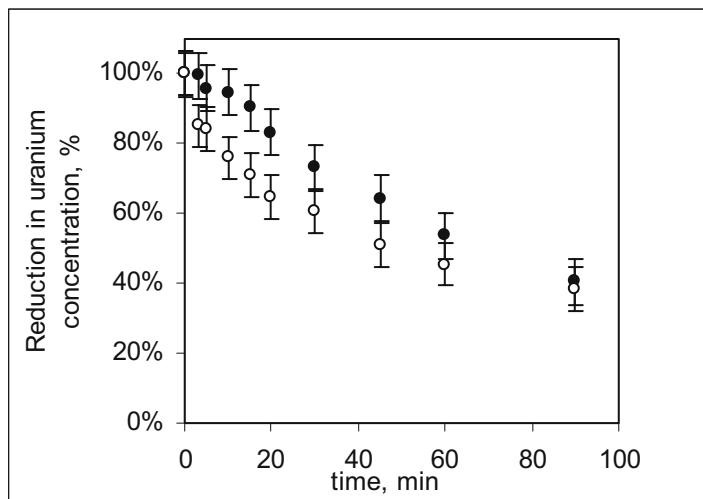
Short term uptake study

Roots of pea rapidly removed uranium from solution (Fig. 1). In presence of phosphate, 50% of uranium was removed after between 60 and 90 minutes. The removal of uranium was faster in the solution devoid of phosphate; in this case, 50% of uranium was removed after 45 minutes of contact between the solution and the roots of pea. This result indicate that phosphate decreases the bioavailabil-ity of uranium for the roots of pea. The removal of uranium by roots of pea was faster than that observed by Eapen et al. (2003) for *B juncea* and *C. amaranticolor* and lower than that observed by Bhainsa and D'Souza (2001) for dried root of hyacinth. However the biomass volume ratio (1g dried biomass by one liter) used

by these authors was higher than our biomass volume ratio (0.3 g dried biomass by one liter)

EDTA and copper extraction

Copper is supposed to desorb uranium adsorbed onto the cell wall while EDTA could remove metal adsorbed and complexed by the roots. Copper and EDTA extracted similar amounts of uranium from roots exposed to solution containing phosphate (Table 1). In opposite, copper was less efficient than EDTA in remaining uranium from the roots in absence of phosphate: only 18% with EDTA was removed with copper. This indicates that without phosphate in solution, uranium was rather precipitated or complexed in the apoplasm than adsorbed onto the cell wall. EDTA and copper extracted more uranium in absence of phosphate than in presence of phosphate (respectively 10 and 35 times). These results indicate that after 24 hours, like following the short exposure time, less uranium was removed by root from the solution containing phosphate than from the solution devoid of phosphate. This result could also indicate that in the case of phosphate in solution, uranium was precipitated in root with phosphate and that this precipitated was not extractable by copper or EDTA.

Fig. 1.   Reduction in uptake concentration in solution as a function of the exposure time . Roots of pea were exposed to a diluted Hoagland solution containing 25 μmol L^{-1} of uranium and 0 (white symbols) or 5 (black symbols) μmol L^{-1} of phosphate.

Table 1. Uranium extracted by copper or EDTA from pea roots (μmol g^{-1} fresh weight) exposed during 24 hours to a diluted Hoagland solution containing 50μmol L^{-1} of uranium and 0 or 5μmol L^{-1} of phosphate.

Phosphate	Copper extraction	EDTA extraction
0 μmol L^{-1}	18,8 $\pm$ 10,7 nmol L^{-1}	105.1 $\pm$ 58.7 nmol L^{-1}
5 μmol L^{-1}	1,8 $\pm$ 0,8nmol L^{-1}	2.9 $\pm$ 0.5 nmol L^{-1}

Conclusion and perspectives

This study showed that roots of pea could remove uranium from contaminated solution in a short time. In absence of phosphate, EDTA extracted more uranium than copper, indicating that other mechanisms than adsorption onto the cell walls occurred. Phosphate decreased the uranium bioavailability for the plants. But on other hand, phosphate could increase the precipitation of uranium in the apoplasm. Roots after extraction will be analysed for the remaining uranium content to determine total uranium uptake after 24 hours exposure and to quantify the proportion of total uranium removed from the nutrient solution which was extracted by copper and EDTA.

These experiments were performed with pea which is a dicotyledon species. A similar experiment will be performed with maize, a mocotyledon species.

References.

Bhainsa KC and D'Souza SF (2001). Uranium(VI) biosorption by dried roots of Eichhornia crassipes (water hyacinth). Journal of environmental science and health A36: 1621-1631.

Dufey JE, Genon JG, Jaillard B, Calba H, Rufyikiri G, Delvaux B (2001). Cation exchange on plant roots involving aluminium: experimental data and modeling. In: Gobran, GR, Wenzel, WW , Lombi, E (Eds.), Trace Elements in the Rhizosphere, CRC Press LCC, Boca Raton, Florida, USA, 2 pp. 228-252.

Eapen S, Suseelan KN, Tivarekar S, Kotwal SA, Mitra R (2003). Potential for rhizofiltration of uranium using hairy root cultures of Brassaica juncea and Chenopodium amaranticolor. Environmental research 91: 127-133.

Ebbs SD, Brady DJ, Kochian LV (1998). Role of uranium speciation in the uptake and translocation of uranium by plants. Journal of experimental botany 49: 1183-1190.

Fortin C, Dutel L, Granier-Laplace (2004). Uranium complexayion and uptake by a green alga in relation to chemical speciation: the importance of the free uranyl ion. Environmental Toxicology and Chemistry 23: 974-981.

Gunther A, Bernhard G, Geipel G, Reich T, Rossberg A, Nitsche H 2002. Uranium speciaiton in plants. Radiochemical Acta 91 319-328.

Ramaswami A, Carr P, Burkhardy M (2001): Plant-uptake of uranium: hydroponics and soil system studies. International journal of phytoremediaition 3: 189-201.

Rengel Z, Robinson DL (1989). Determination of cation exchange capacity of ryegrassroots by summing exchangeable cations. Plant & Soil 116:217-222.

Sarret G, Saumitou-Laprade P, Bert V, Proux O, Hazeman JL, Traverse An Marcus MA, Manceau A (2002). Forms of zinc accumulated in the hyperaccumulator Arabidopsis halleri. Plant Physiology 130: 1815-1826.

Straczek A 2003. Mobilisation accumulation et distribution de Zn par et dans des tabacs modifiés pour leur capacité d'excrétion de protons et d'accumulation des métaux. PhD, University of Montpellier France, 130pp

Study of the chemical leaching of uranium from several mineralogical layers

Marian Raileanu[1], Rodica Calmoi[1], Catinca Simion[1], Gabriel Barbir[2], Alexandru Cecal[1]

[1]"Al.I. Cuza" University, Department of Inorganic Chemistry, 11–Carol I, 700506 Iasi, Romania, E-mail: cecal@uaic.ro
[2]Uranium National Company, Suceava Branch, Crucea - Romania

Abstract. The purpose of the present work was to study the oxidation of uranium species coming from different samples of some Romanian uranium ores at U(VI), in the presence of the following oxidizing agents: $KMnO_4/H_2SO_4$, H_2O_2 and royal water. It was established that the highest capacity of leaching is shown by $KMnO_4/H_2SO_4$ that achieved values of ca. 100% in about seven days. This chemical reaction was explained through the chemical and mineralogical composition of the studied samples.

Introduction

Uranium, a naturally occurring radioactive element, is a primordial constituent of the earth crust (Chopin et al, 1995, Plant at al, 1999). Even though, until the beginning of the XX century, its concentration was extremely low in the biosphere; after 1945, uranium started to be mined and milled and enriched in its fissile isotope ^{235}U. Therefore, in the areas of uranium plants, its concentration increased to values exceeding the maximum accepted limits (Tykva and Berg, 2004). The same happened in the areas where are activities connected to the reprocessing of spent nuclear fuel elements.

If speaking about lower oxidation states (III, IV and V) it should be mentioned that uranium is insoluble in water. In the presence of the oxidant agents and water, solubility change rapidly when U(VI), as uranyl ion, UO_2^{2+} appeared. Therefore, the following aspects must be considered:
- performance of activities connected to the cycle of the nuclear fuel elements without environmental release of U(VI)

- the quantitative extraction of uranium from the ore; therefore the risk of oxidation by the pluvial waters of the traces of U(IV) to UO_2^{2+}, when the latest passes to the surface waters must be eliminated (Blackman, 2001).

Taking into account the above-mentioned aspects, the aim of the present study is to test (at laboratory scale) some oxidizing agents that may perform the quantitative leaching of UO_2^{2+} ions from different uranium ores. The study has in view the correlation of the leaching capacity with the chemical and mineralogical composition of the studied samples.

Materials and methods

Six uranium ore samples (marked from "1" to "6") obtained from some Romanian uranium mining areas were subjected to the chemical leaching. They had different contents of uranium and their chemical and mineralogical composition ranged between various values.

The uranium ores were broken by grinding in agate ball mill. The grains size distribution determined by sieving is: 0.10 mm $< \phi <$ 0.125 mm (3.9 %), 0.09 mm $< \phi <$ 0.10 mm (6.4 %), 0.08 mm $< \phi <$ 0.09 mm (14.6 %), 0.071 mm $< \phi <$ 0.08 mm (56.2 %), 0.063 mm $< \phi <$ 0.071 mm (13.8 %), 0.056 mm $< \phi <$ 0.063 mm (5.1 %) (Cecal et al, 2000).

The content of the heavy metals in the studied samples was determined after the dissolution in 1 M HNO_3 or 1 M HCl with a UV-VIS Carry 210 spectrophotometer. To establish the mineralogical association of the uranium, the powder sample was analyzed by X-ray diffraction. For the purpose, a Dron 2.0 diffractometer with $CoK_{\alpha(1+2)}$ $\left(\overline{\lambda} = 1.79019 \right)$ radiation filtered with iron was used.

The following liquid reagents were used: (a) arsenazo III: 0.0352 g in 50 ml buffer solution (Keil 1979). (b) buffer solution: 75 ml acetic acid solution 0.2 M in 925 ml sodium acetate solution 0.2 M. (c) solution 0.1 M potassium permanganate – concentrate sulfuric acid 1:3 (v:v).

In order to perform the leaching experiments, 1 g from each ore sample was contacted with 50 ml of oxidizing mixture. In order to determine the amount of dissolved uranium (as UO_2^{2+} ions), from each sample, 1 ml clear solution was extracted at different moments (24, 48, 72, 168 and 336 hours). The pH was corrected to 3.0, using small volumes of 1 M NaOH or 1 M HCl solution. The correction of pH is done because the cation, as acceptor of electrons, may be considered a poli-alkaline acid able to react with many other alkaline substances, with several coordination's number. After the correction of pH, 1 ml arsenazo III solution was added, and afterwards it was completed with 50 ml buffer solution. The absorbance at the wavelength of 665 mm was read, using as standard the solvent with which the extraction was made. Taking into account this absorbance, there was calculated the extracted amount of uranium as UO_2^{2+} ions.

The concentration of the other elements in the uranium ores composition was established by means of atomic absorption spectrometry.

Table 1. The chemical composition of the analyzed samples.

Sample	Zn	Cu	Fe	Mn	Pb	Ni	Co	Cr	Cd	U
					ppm					
1	3.28	7.3	84	6.5	7.1	114	56	17.8	0.65	560
2	3.28	5.1	70	5.5	-[1]	54	32	17.8	0.70	430
3	0.30	5.5	56	4.5	-[1]	60	32	12.7	1.20	380
4	5.66	8.0	61	6.5	7.1	84	60	12.7	8.00	140
5	0.89	4.7	75	6.5	7.1	48	36	12.7	0.50	480
6	5.66	6.2	65	10.5	53.4	84	44	22.9	8.30	2450

[1] no data

Table 2. The mineralogical composition of the uranium sample number "1".

Mineral	Chemical formula	Abundance, %
Quartz	SiO_2	55.00
Ankerite	$CaMg_{0.77}Fe_{0.23}(CO_3)_2$	11.20
Sanidine	$K(AlSi_3O_8)$	8.30
Muscovite	$[SiAlO_{10}Al_2(OH)_2]K_2$	4.70
Thucolite	$(U,Th,Pb)(CO_3)_x$	3.75
Biotite	$K_2(Fe_{2.76}Mg_{2.32}Ti_{0.55})(Al_{2.41}Si_{5.58}O_{20})(OH)_2$	3.00
Hematite	Fe_2O_3	2.60
Blende + Pyrite	$ZnS+FeS_2$	1.10
Pyrochlore	$(Na,Ca,U)_2(Nb,Ta)_2O_6(OH,F)$	0.35
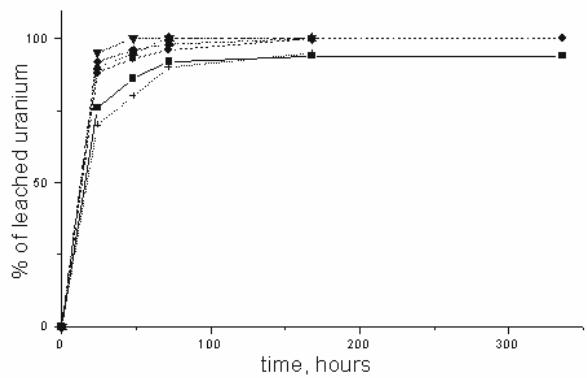
Results and discussion

The heavy metals' content of the studied uranium ores samples used in the leaching experiment is presented in Table 1.
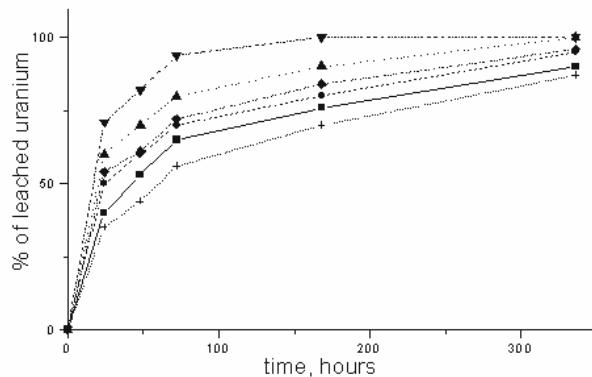
For illustration, the mineralogical composition of the sample labeled with "1" is presented (Table 2). This uranium ore sample has a molar mass M = 344.8 and is crystallized in the cubic system (a = 10.42 Å, crystallographic group Fd3m). (Ianovici et al., 1979).

For the samples 2-5, the concentration of the quartz is higher as 55% and those of the other minerals are lower, but the relative abundance is almost the same. The "sample 6" has a concentration in thucolite and pyrochlore higher as presented in Table 2.
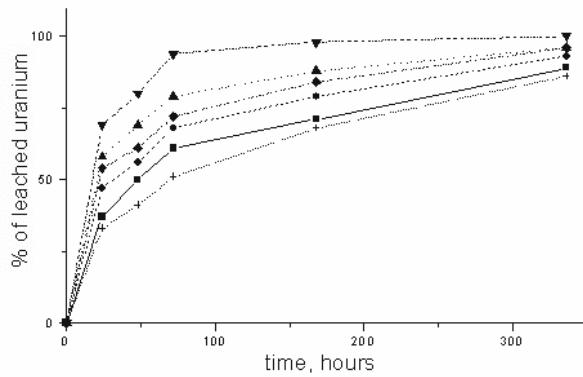
It can be observed that uranium exists in two distinct mineralogical associations, thucolite and pyrochlore. Both of them are extremely hard because uranium is part of the crystal lattice. At the same time, the high content of quartz (55 %) suggested a leaching method based on the acid treatment type.

(a)

(b)

(c)

Fig. 1. The time dependence of the uranium leaching using: $KMnO_4/H_2SO_4$ (a), H_2O_2 (b) and $HCl+HNO_3$ 1:3, *v:v* (c) (■: ore "1", ●: ore "2", ▲: ore "3", ▼: ore "4", ♦: ore "5", +: ore "6").

In-situ leaching of uranium ores

The leaching phenomenon has its origin in the *"in situ"* oxidizing action of the atomic or molecular oxygen on the species of uranium in intermediate oxidation level, according to the most probable chemical reaction:

$$UO_2 + [O] + 2H^+ = UO_2^{2+} + H_2O$$

The results of the leaching experiments are summarized in the Figures 1.

It can be noticed the oxidizing/leaching capacity of the intermediate species of uranium to U(VI), in the case of all the studied oxidizing agents. The efficiency of the process reaches values of approximately 100 % after seven days of contact in the oxidizing system; in case of $KMnO_4/H_2SO_4$ system, the process is taking place faster. The higher concentrations of uranium (sample number "6") involve higher extraction efficiency, the process being limited by the time factor.

From the Figs. 1, a good efficiency of the leaching process can be noticed. This efficiency is related to the solution of $KMnO_4/H_2SO_4$ where the effect of the interferences is manifested at the end of the experiment only (Komersova et al, 2001). In case of royal water, a constant increase of the absorbance along with the whole experiment can be noticed, thus meaning a high efficiency of this acids mixture in the way that the whole extraction was made during a 24 hours time interval, until the first reading of the absorbance was performed.

For all experiments, higher the concentration of quartz and lower concentrations of thucholite and pyrochlore, lower the extraction degree of uranium as UO_2^{2+} ions.

A part of the microelements: Fe, Ca, Ni, Cr in the sludge, which remains after the uranium leaching, should be considered for the further chemical treatments with the view to be separated.

Conclusions and perspectives

The dissolution of six uranium ore samples and the leaching of the reduced species of uranium to U(VI) were studied in the presence of $KMnO_4/H_2SO_4$, H_2O_2, and royal water. All the oxidizing agents led to remarkable results that could not be achieved in case of the alkaline or the microbiological leaching. It can find an explanation in the property of the strong acids to destroy the mineralogical matrix that includes uranium.

In the given conditions, the waste contains just traces of uranium that are not leading to the radioactivity increase of the environment. In addition, these micro quantities must be retained, if it considers the large volume of depleted uranium that gathers in the areas of the mining exploitations. Due to the fact that for small concentrations the chemical methods are not presenting any interest from the costs point of view, the using of microbiological methods of leaching/ storage have to be considered.

Acknowledgement

References

Al-Jundi J, Werner E, Roth P, Hollriegl V, Wendler I, Schramel P (2004) Thorium and uranium contents in human urine: influence of age and residential area. J. Environm. Radioactivity 71: 61-70.

Blackman Jr, WC (2001), Basic hazardous waste management, 3rd edition, Lewis Publishers, Boca Raton, pp. 211.

Cecal A, Humelnicu D, Popa K, Rudic V, Gulea A, Palamaru I, Nemtoi Gh (2000) Bioleaching of uranium (VI) from poor uranium ores by means of cyanobacteria. J. Radioanal. Nucl. Chem. 245 (2): 427–429.

Cecal A, Popa K, Craus ML, Patachia S, Moraru TR (2002), On the bioleaching of UO22+ ions from a Romanian poor uranium ore. J. Radioanal. Nucl. Chem. 254 (1): 81–84.

Chopin GR, Rydberg J, Liljenzin JO (1995) Radiochemistry and Nuclear Chemistry. Butterwoth - Heinemann, New York, pp. 110.

Ianovici V, Stiopol V, Constantinescu E (1979) Mineralogy, EDP, Bucharest, pp. 239.

Keil R (1979) Hochselektive spektralphotometrische Spurenbestimmung von Uran (VI) mit Arsenazo III nach Extraktionstrennung. Fresenius Z. Anal. Chem., 279: 384-387.

Komersova A, Bartos M, Kalcher K, Vytras K (2001) Some new methods of indirect determination of metals based on adsorption and complexation properties of arsenazo III azo dye. Coll. Czech. Chem. Comm., 66: 456-464.

Tykva R, Berg D (2004) Man-made and natural radioactivity in environmental pollution and radiochronology. Kluwer, Dordrecht, p. 114.

Environmental Management and Optimization of In-situ-Leaching at Beverley

Horst Märten

Heathgate Resources Pty. Ltd., Australia, and
Umwelt- und Ingenieurtechnik GmbH Dresden, Germany,
E-mail: h.maerten@uit-gmbh.de

Abstract. Heathgate Resources Pty. Ltd. operates the Beverley Uranium Mine in South Australia (SA) by utilizing a moderately acidic In-situ leaching (ISL) technology, which is best in terms of minimizing surface disturbance. The paper describes the optimization of ISL operation with regard to both leaching efficiency and minimization of environmental impacts in the framework of relevant approvals and regulations.

Introduction: Beverley ISL Mine

Heathgate Resources (Heathgate 2005) operates the Beverley Uranium Mine located on the arid plane between the Flinders Rangers and Lake Frome (Fig. 1), approximately 550 km North of Adelaide in South Australia (SA). After purchasing the mineral lease in 1990, Heathgate developed the mine utilizing a moderately acidic in-situ leach (ISL) technology including oxidant dosage to the mining solution (lixiviant) to increase uranium dissolution in the underground ore body. Initial field leach trials were performed in 1998. After obtaining all required permits, commercial mining commenced in November 2000. The Beverley project is licensed to produce 1,500 t of uranium oxide equivalent (U_3O_8) per annum. The 2004 production was 1,100 t U_3O_8.
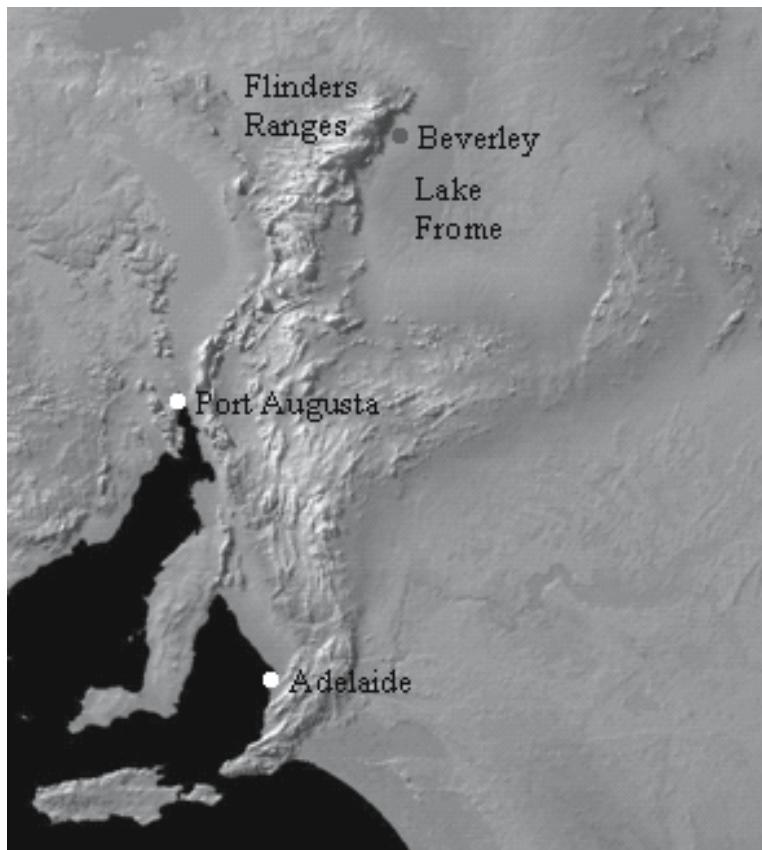
Approvals and Regulation

The mine has been subjected to the scrutiny of a vigorous regulatory approval process and many subsequent inquiries; all have shown the Beverley mine to have no adverse impacts on the environment and by most considered to be world's best practice.

The major approvals required prior to commencing a commercial uranium mine in SA include:

a) Environmental Impact Statement - Commonwealth, SA (Heathgate 1998)
b) Mining Lease (Primary Industry and Resources SA - PIRSA)
c) Mining and milling license (SA EPA)
d) Uranium export permit (Commonwealth)
e) Permit to posses nuclear material (Commonwealth, Nuclear Non-proliferation Act)
f) License to store and handle dangerous goods (SA Workplace Services)

Heathgate reports to federal and state regulators quarterly and holds 6-months meetings with regulators. The Annual Environment Report to PIRSA is accessible on the website (Heathgate 2005).


Fig. 1.   Geographic map of part of South Australia showing the location of Beverley between Flinders Ranges (West) and Lake Frome (East).

In-situ leaching of uranium ores

ISL technology and environment

Of all the mining processes, ISL is the best technique in terms of minimizing surface disturbance and of all the ISL projects in the world, the Beverley Uranium Mine is the most technologically advanced. The ISL process requires minimal surface infrastructure in the form of a processing plant, more like a water treatment plant and has small wellfield areas that involve only the installation of water wells, some pipes and other utilities and a few small pumping huts called wellhouses. These wellfields are a rolling development that move along the (mineralized) paleochannels and can be progressively rehabilitated as completed. This ability to rehabilitate prior to the completion of mining at the area associated with a processing plant significantly reduces the observed surface impact for each mine.

An independent review of environmental impacts of acid ISL uranium mining has been published by CSIRO Land and Water (Taylor et al., 2004) for EPA SA, concluding that Beverley "has initiated and implemented world best practice methods" and that ISL mining of uranium is "more cost effective and environmentally responsible than any suggested alternative techniques".

Due to the Beverley deposit's location in the Frome Basin many of the wellfields are surrounded by environmentally sensitive areas and areas of cultural significance to the local Aboriginal people. With this in mind the Beverley wellfields have been designed in a way which minimizes the surface disturbance and minimizes the risk of other environmental impacts (Fig. 2). The installation of a state of the art digital control system has allowed total control of all wellfield operations from a central control room.

Continuous monitoring includes monitoring wells around the active ISL mining area, vegetation, fauna, soil and surface hydrology, meteorology, waste management, and environmental radiation.

Fig. 2.   Wellfield within an environmentally sensitive area (creek), where environmental impacts (surface disturbance) were minimized to preserve vegetation.

In-situ leaching of uranium ores

Beverley hydrogeology and mineralogy

The Beverley deposit is located in Tertiary Age paleochannel sediments of the Eyre Basin in the Lake Frome region. The ore-bearing paleochannel sands (Beverley aquifer) are completely confined by clays above (Beverley clay) and below (Alpha Mudstone). The impermeable Poontana Fault Zone is an effective boundary of the Beverley aquifer to the West of the mineralized area. The Beverley sands grade into silts at the northern, southern and eastern boundaries. The undisturbed groundwater in the Beverley aquifer is quasi stagnant. The Great Artesian Basin (GAB) aquifer underlying the Alpha Mudstone has pressurized groundwater (Cadna-owie formation). Any contact of the Beverley aquifer to the GAB sediments is absolutely impossible because of the massive mudstone aquitard in between and due to the GAB pressurization. The Beverley uranium ore bodies are approximately 100-120 m below surface and about 10 m thick. The granite rocks of the Flinders Ranges probably served as the source for the uranium deposits.

The quartzose paleochannel sands of the Namba Formation (host rock) are fine to coarse grained. Uranium mineralization appears as extremely fine grained coffinite $U(SiO_4)_{1-x}(OH)_{4x}$ in voids and coatings of grains (Fig. 4). Kaolinite $Al_2Si_2O_5(OH)_4$ is the dominant clay phase. The underlying Alpha Mudstone consists of Smectite clays (Montmorillonite $(Na,Ca)(Al,Mg)_6(Si_4O_{10})_3(OH)_6 \cdot nH_2O$ mainly). Pyrite and other sulfides are less abundant. The U ore typically contains 0.1 to 0.5 % U_3O_8.

The initial Beverley resources in the North, Central, and South deposits were 3,900 t, 6,200 t, 3,900 t U_3O_8, respectively (14,000 t in total). Exploration activities around Beverley are in progress. Present exploration data are promising to increase the reserves considerably in the near future.
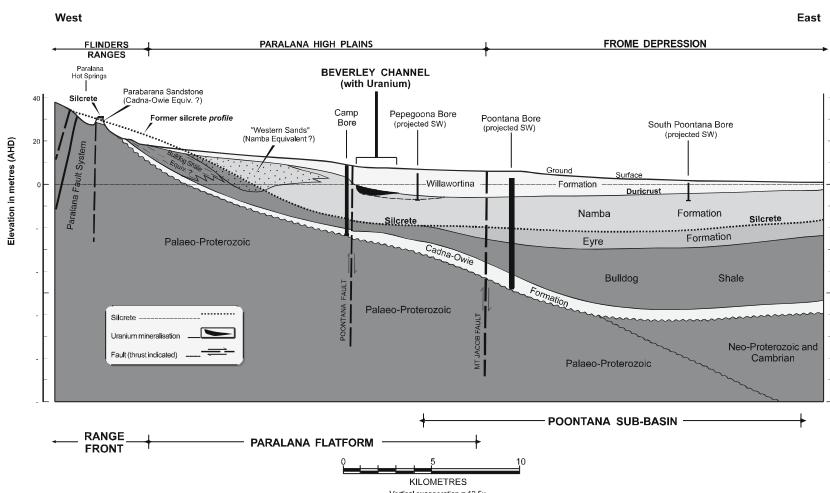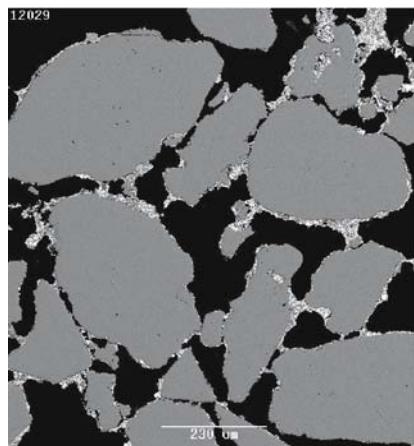
Fig. 3.   Stratigraphic profile of the Willawortina-Namba-Cadna-Owie formations

In-situ leaching of uranium ores

Uranium ISL and processing (overview)

ISL mining and U processing include the following major operational areas (cf. Fig. 5): (i) lixiviant (closed-loop) cycle through several wellfields in parallel, each consisting of about 14 extraction wells and about twice as much of injection wells, (ii) barren lixiviant acidification and oxidant dosage point, (iii) U capture from the pregnant lixiviant by applying an anionic ion exchange (IX) resin in sequences of two columns (head and tail), (iv) in-place elution in a two-stage operation, (v) uranium precipitation with hydrogen peroxide, (vi) thickening and washing (for removal of dissolved impurities), de-watering, drying, packaging.

Fig. 4.   Backscattered electron micrograph of the mineralized sand: quartz grains (grey) with cof-finite+kaolinite minerals against open porosity (black).

Optimizing leaching hydrology

Efficient leaching requires a water exchange rate within the ore body fast enough for optimum contact between the oxidizing lixiviant and the uranium mineral, whereas dissolution rates were found to be remarkably higher. The design of well-fields (pattern and spacing) varies greatly depending on the local conditions such as permeability, sand thickness, grade and distribution. In order to obtain more than 70 % recovery within 1 year or less (economic criterion), a minimum pore volume exchange rate (PVE) of more than 70 is generally required. .The optimum drilling density for production bores can then be balanced against surface limitations, grade distribution and budgetary considerations to give a final design.

The types of patterns (cf. Fig. 6) employed at Beverley so far include (i) 5-Spot pattern (usually 20 to 25 m spacing), (ii) 7-Spot pattern with distances between wells varying between 13.5 and 20 m, (iii) "line drive" generally only used if the ore is confined to skinny channels where no other pattern design is possible, (iv) "wall", i.e. a sequence of rows each consisting of extractors and injectors (concept for low grade, average thickness zones). Real (optimized) patterns are usually more sophisticated as shown in Fig. 6 (bottom).
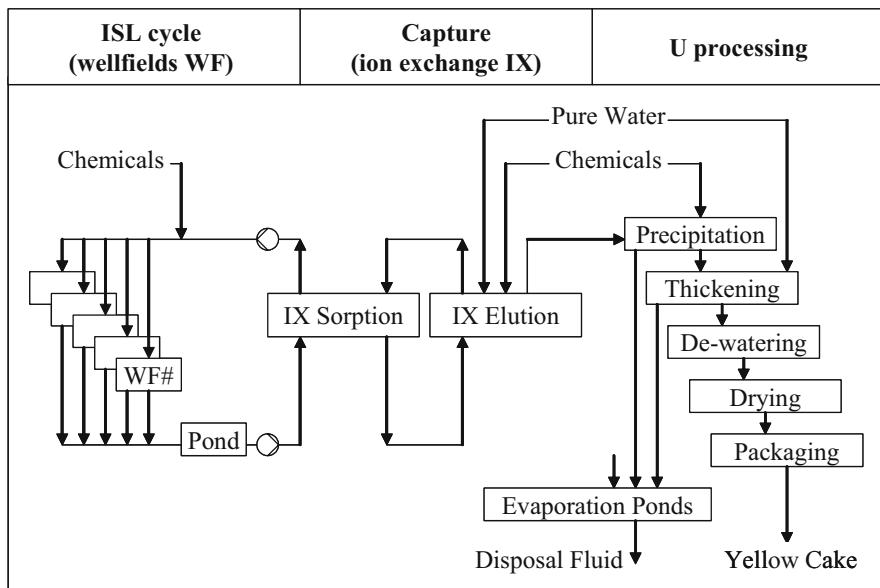
The primary wellfield design is based on a standard delineation drilling program. Usually, wellfield design and performance is adjusted (optimized) during operation for maximizing recovery rates.

The sequence of a wellfield operation is roughly as follows:

- Phase 1: leaching according to primary wellfield design
- Phase 2: additional measures to increase recovery (infill wells, role reversals) based on the evaluation of wellfield performance in phase 1
- Phase 3: wellfield flushing (combined with U capture) and restoration

Optimizing leaching geochemistry

Barren lixiviant pH and ORP have been adjusted for optimum leaching of the ore. The pH is kept at moderately acidic conditions (injection pH in the range from 1.6
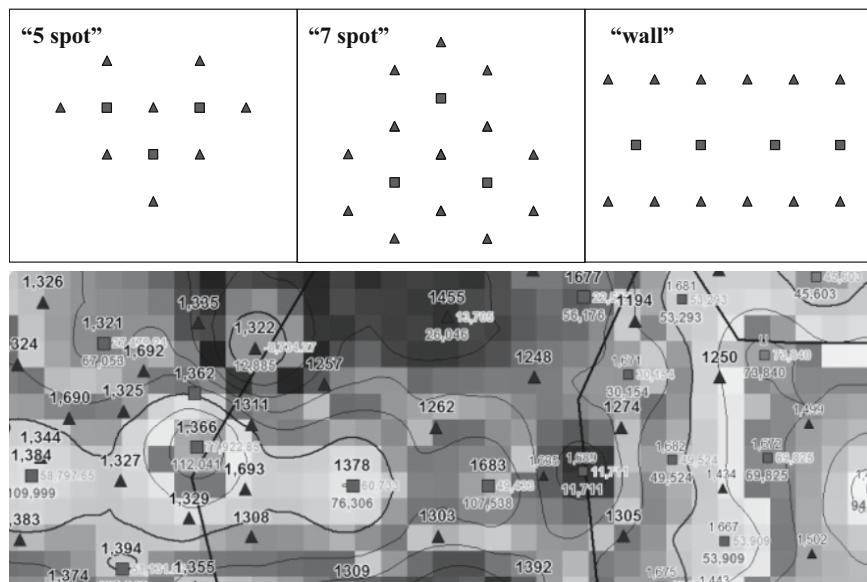
Fig. 5.   Schematic of ISL cycle, capture and uranium processing.

In-situ leaching of uranium ores

to 2.3). It must be controlled such that it is low enough to ensure a stable lixiviant (both in ensuring uranium stays mobile and limiting the precipitation of secondary phases such as gypsum and iron phases) and high enough to limit the dissolution of host minerals (such as silicates). The ORP of the barren lixiviant is adjusted by the dosage of oxidant so that most of the majority of the iron is oxidized to ferric (conditional dosage).

Uranium recovery and processing

The typical average head grade at Beverley is about 180 ppm (2004 average). The uranium species formed in the acidic lixiviant, $UO_2(SO_4)_2^{2-}$ and higher order complexes, are captured via anionic ion exchange (IX) resins. The efficiency of resin loading is heavily dependant on the concentrations of competing anions and total dissolved solids (TDS). The Beverley ore bodies are located in highly saline aquifers with TDS between 6 and 14 g/L naturally with interfering leaching effects, the TDS in the lixiviant is even higher. In particular the presence of chlorides in the lixiviant, up to 5.5 g/L, limits the capture efficiency considerably. However, IX operation has been optimized to enable an economic U production under these chemical constraints. The ion exchange process consists of three "trains" each with five IX columns, capable of treating in excess of 300 L/s. Four of the columns are used for capture usually configured as two lead columns and two tail


Fig. 6.   Wellfield pattern types (top, triangles – injectors, squares – extractors) and cut of a real wellfield pattern with an underlying map showing the spatial distribution of left uranium reserves (tool for leaching performance control).

In-situ leaching of uranium ores

columns. The fifth column is either being eluted or is idle. The IX columns can be configured in any arrangement of lead, tails, elution or idle which allows for continuous loading and elution of ion exchange resin.

Loaded resin is eluted in-place using a two stage process: (i) main elution by 1.5 bed volumes (BV) of ~1M NaCl eluant followed by (ii) conversion by 1.5 BV of ~0.1M H_2SO_4). This elution regime is a balance between elution efficiency, time and reagent consumption to produce a pregnant solution in excess of 10 g/L U_3O_8. Uranyl peroxide is precipitated by the addition of hydrogen peroxide combined with caustic soda dosage for pH adjustment, followed by thickening, washing, de-watering and finally drying of the precipitate to produce a final pure Yellow Cake product.

Water balance and control

The lack of available water at suitable quality makes water balance one of the major challenges in operating the Beverley Mine. Beverley is located in an arid region, where the temperature from November to March regularly exceeds 40oC, with an average mean maximum temperature of over 30°C in the summer months and 15oC in the winter. The average annual evaporation rate is around 3,000 mm against an average yearly rainfall of only 192 mm. Consequently, there is no access to surface water for the mining operation. The water used for mining operation and uranium processing is drawn from two main sources: the Namba aquifer (outside of the mining zone) and the GAB.
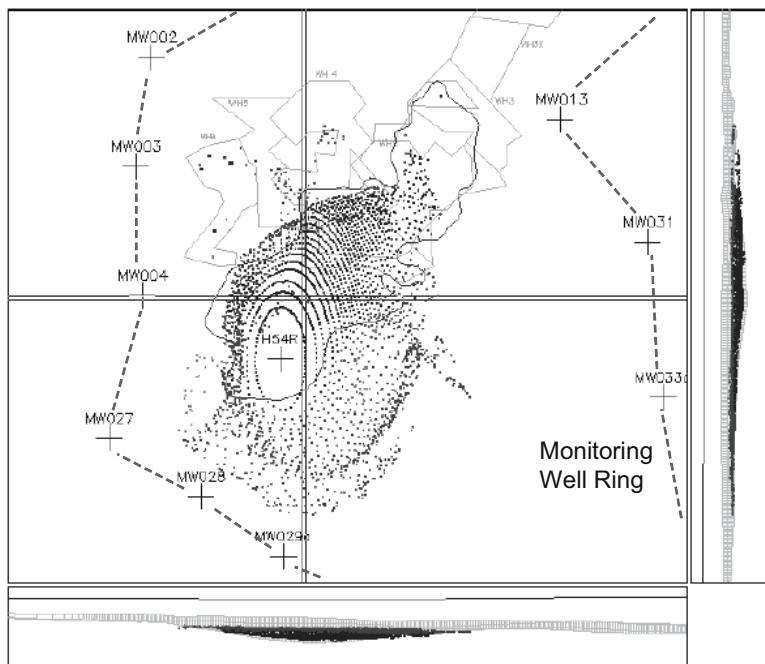
Fig.7.   View of the U processing plant showing part of the IX columns for U capture.

In-situ leaching of uranium ores

Despite the poor quality of water form the Namba aquifer (annual usage around 200 ML) it is still acceptable for (i) make-up of eluant solutions, (ii) plant wash down water, and (iii) first wash of the precipitated product. The use of the better-quality GAB water is highly regulated (limited to 57 ML/y). GAB water is used for (i) final washing of the product, (ii) feed to the potable water RO plants, (ii) dust suppression on roads, (iii) periodic dilution of the lixiviant, and (iv) drilling mud make-up water.

To meet a total neutral water balance as a precondition for avoiding pollutants migration in the underground, the disposal fluid volume is considerably reduced by evaporation in ponds. The mining aquifer at the Beverley Mine was proven to be confined during the EIS (Environmental Impact Statement) process. Control must be maintained of mining fluids within the Beverley mining aquifer to ensure no excursions occur laterally outside of the mining area. Flows in and out of the wellfield are constantly recorded and regularly analyzed to ensure a neutral water balance is maintained. To monitor the effectiveness of the flow control program, monitor wells have been installed surrounding the mining zones.

A rigorous monitoring program demonstrates that the mining and disposal fluids remain under control. To better enable the tracking of fluid movements Heathgate has developed a hydro-geological model of the Beverley sands. This is the latest in advanced technology and provides a diagrammatic map of the current


Fig. 8.   Disposal flow pattern (hydrological model forecast based on a model calibration by monitoring data) within the monitoring well ring.

In-situ leaching of uranium ores

flow paths and in addition serves as a prediction tool. This tool assists Heathgate in demonstrating the sustainability of current and future operations at Beverley.

Summary and Outlook

Heathgate Resources Pty. Ltd. continues to operate and develop the Beverley mine to meet both conditions: technological and economic optimization based on world's best practice on the one side and minimization of environmental impacts on the other side.

An extensive exploration program in the area is continued to increase the potential uranium reserves.

Further initiatives for developing and improving ISL operation, uranium processing, overall water management, and rehabilitation include:

- Introduction of a water recycling program to treat disposal fluid by membrane technology to minimize water consumption
- Desalination technology to remove unwanted ions, specifically chloride ions, in the lixiviant and to limit TDS in long term for better leaching and improved capture efficiency
- Implementation of a wellfield restoration program after the abundance of first wellfields, i.e. phase 3 operation by flushing the leached ore bodies in conjunction with uranium capture and conditioning of rest groundwater for enhanced natural attenuation

Acknowledgement

References

Heathgate Resources Pty. Ltd. (2005) Website: www.heathgateresources.com.au

Heathgate Resources Pty. Ltd. (1998) Beverley Uranium Mine Environmental Impact Statement, ACN 011 018 232

Taylor G, Farrington V, Woods P, Ring R, Molloy R (2004) Review of Environmental Impacts of the Acid In-situ Leach Uranium Mining Process, CSIRO Land and Water Client Report

Favourable Factors for Uranium Mineralization in District Surguja, India

S. K. Sharma

24 National Road, Dehradun 248001, India, E-mail: SKS105@rediffmail.com

Abstract. In view of world analogy for the favorable sites of Uranium mineralization in the sedimentary Proterozoic rocks, the ENE-WSW trending Narmada-Son Lienament/ fractured basement of Proterozoic Arachean age overlain unconformably by the Gondwana Super Group sandstones of Mesozoic to Lower Permian age in District Surguja offers an ideal site for the Uranium mineralization. Some of the favourable factors, namely, the nature of basement rocks present in the area, surrounding rocks, type of environment which favours the mineralization and tectonic features etc have been discussed.

Introduction
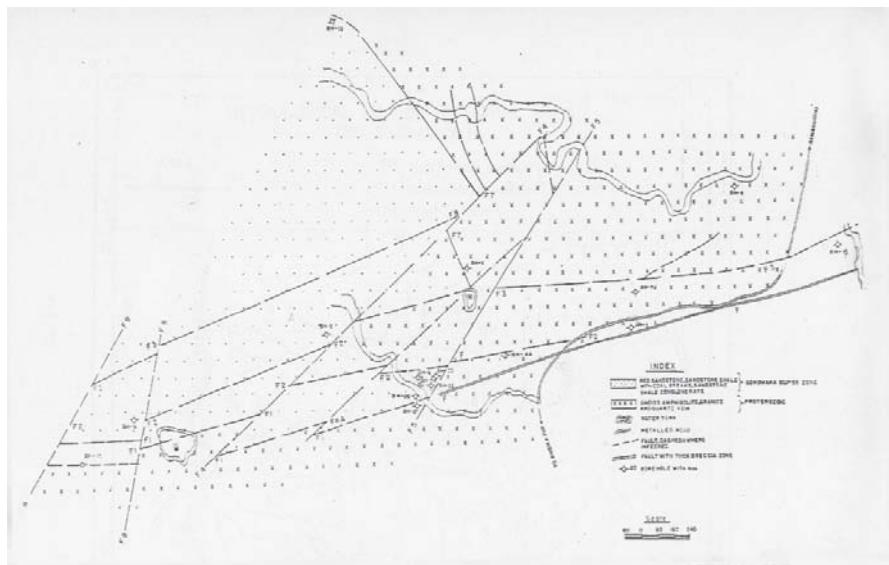
Despite India's extensive development achievements in the last more than five decades since independence, the fact remains that it is still remains on the poorest nations in the world in terms of per capita income and energy consumption. The per capita energy consumption which indicates the economic status of a nation, is only 0.25 tons of oil equivalent (toe) as against nearly 8.5 toe of developed nations. If the economic standard of the country is to be raised, an accelerated growth of economy becomes imperative which can greatly be facilitated through increased availability of energy, be it a conventional or non conventional source of energy. Fortunately, India has vast unexploited resources of power estimated at about 84000 MW, the harnessing of which is expected to meet the domestic demand of ever growing population on one hand and relieve the country from heavy burden of foreign exchange outflow and dependence on imported fuel for generating electricity on the other hand. Any new find of uranium obviously plays a significant role in country's development.

Area under study

The study area is located near the border of the Chattisgarh and Bihar states and falls close to the regional Balarampur fault zone and spread over an area of about 400 m x 600 m and perhaps, the ENE-WSW trending Narmada-Son Lienament (NSL) zone is one of the most significant lineament in the Indian shield. Tattapani fault is a major fault in the region forming a boundary between Archean formation towards the south and the Gondwana formation towards the north (Fig. 1) in the western part of the study area.

Geology of the Area

Detailed geological studies have been carried out by Geological Survey of India (G.S.I.; Thussu et al. 1987). The surface geology presents different rock types, which include quartzite, schist, gneisses and phyllite of Proterozoic Arachean age. These are generally folded and cross-folded. The Archean rocks show foliation in the direction $N70^0E$—$S70^0W$ and $N80^0W$—$S80^0E$ with dips of 75^0 to 85^0 towards north. Granites, granodionites, pegmatites, amphibolites and quartz veins represent the intrusive rocks of the region. The phyllites are mainly carbonaceous and graphites are associated with Pyrite mineralisation. The granites and granodiorites occur as plutons while the amphibolites occur as dykes and sills and the pegmatite as intrusive. Quartz veins ate associated with magnetic mineralisation. Table 1 presents the stratigraphic sequence of the formations.

Fig. 1.   Geology of the study area forming part of District Surguja.

In-situ leaching of uranium ores

Gondwna sequence of formations in this area, lying unconformably over the Proterozoics, consists of conglomerates, sand stones, shale and minor coal beds. These show low dips (15^0) with a general strike direction of N80^{0}W—S80^{0}E.
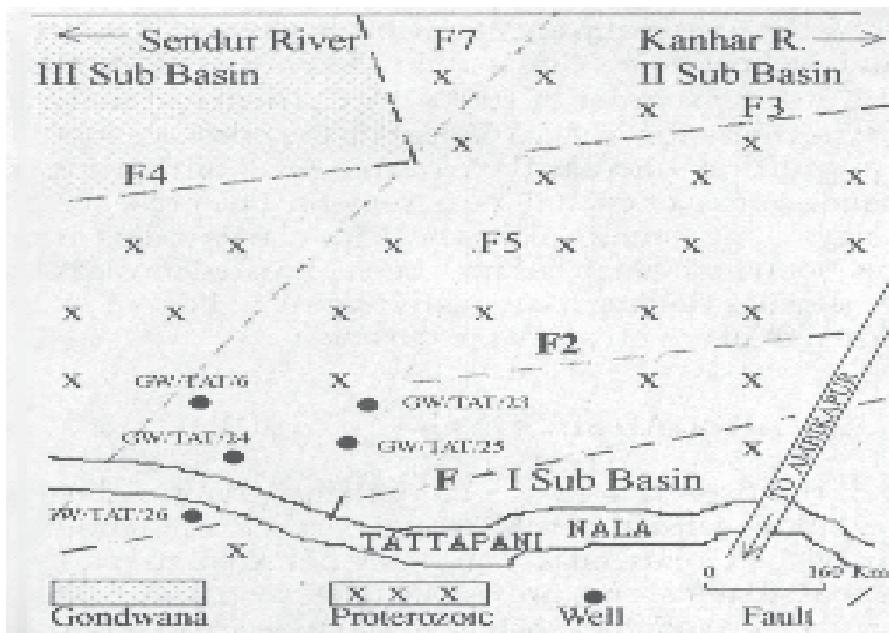
Fig. 1 above presents the geological and structural map. In general, as can be seen from the figure, the major geological formations are separated by ENE-WSW regional faults, which in turn are affected by a number of cross faults striking in NNW—SSE and NE—SW direction. Several faults are also observed towards south of hot spring near Balarampur and Lurgutta and are located within the Proterozoic sequence in the area (Ravishanker et al. 1987).

Table 1. Stratigraphic sequence of Tattapani area, Chattisgarh Basin, District Surguja (After Thussu et al, 1987).

Age	Formation	Rock Type
Recent		Soil/river alluvium
Quarternary		Hydrothermally altered clay
--------------------------- Unconformity --------------------------------		
Lower Tertiary to Upper Cretaceous	Deccan Trap	Dolerite sills and dykes intruding Gondwana sediments (near Jajawal)
Mesozoic to Lower Permian	Gondwana Super Group (possibly Mahadeva)	Post Barakar brown to reddish brown sandstone showing current bedding and ripple marks and subordinate conglomerate, no coal seems
	Barakar Formation	Sandstone and shale with grit bands, grey shale with plant fossils and coal seems
	Talchir Formation	Green splintery shale, sandstone with minor grit bands and conglomerates
--------------------------- Unconformity --------------------------------		
Proterozoic		Phyllite, graphitic at some places, Quarzite, Grey gneiss, Biotite schist, Actinolite, Remolite schist kyanite-sillimanite schist, Garnet gneiss, hornblende gneiss, granulite, Amphibolite, augen gneiss, diorite, Calcgranulite and pink gneiss.

In-situ leaching of uranium ores

Hydrology of the area

Geohydrological studies of the area clearly demarcate three sub basins (Fig. 2). Basin I and II showing flow of groundwater towards Kanhar river in easterly direction. The gradients of Basin III are towards west feeding Sedur river. Both the rivers flowing towards north ultimately feed the Son river. The thermal groundwater in Gondwana occurs in confined conditions while in Proterozoic rocks, under water table conditions. The meteoric water due to deep circulation collects heat and rises to the surface through conduits provided by highly fractured deep seated fault zones.

Discussions and conclusions

In view of the geological characters, geohydrological parameters and world analogy especially similarity to the Franceville Basin , Gabon, the District Surguja in India has become one of the favourable sites for the uranium mineralization due to the following favourable factors:
- Nature of basement rocks: The basement rocks mainly comprising mainly of Quarzite, Grey gneiss, Biotite schist, Garnet gneiss, hornblende gneiss, granulite, Amphibolite, augen gneiss, diorite, Calcgranulite and pink gneiss of Pro-

terozoic age contains traces of uranium. The basement rocks of Bengpal granite gneisses in the nearby area are known to have anomalous concentration of Uranium (2 to 102 ppm) which is available for mobilization (Cahaturvedi 1998).

- Surrounding rocks: The Post Barakar Brown to reddish brown sandstone showing current bedding and ripple marks and subordinate conglomerate of Gondwana Super Group, Mesozoic to Lower Permian age are separated by an unconformity from the basement.
- Type of environment: The phyllites are mainly carbonaceous and graphites are associated with pyrite mineralization. The presence and arial extent of pyrite in the fractures as the hydrothermal alteration mineral in an area of about 2 km^2 , indicating a reducing environment demarcates the limit of uranium mineralization in the area.
- Volcanic activity: Deccan Trap (Lower Tertiary to Upper Cretaceous) consisting of the Dolerite sills and dykes found intruding the Gondwana sediments.

The beds are also gently dipping (maximum 15^0) and the groundwater movement is slow enough to deposit the uranium from water in the surrounding sandstone deposits of mainly the fluviatile origin from the Gondwana Super Group. A higher concentration of uranium is yet to be traced which is expected in the area due to very favourable mineralization conditions. The area thus, represents a high potential and an ideal site for sandstone type uranium mineralization. The further work is in progress.

Acknowledgement

References

Chaturvedi S N, Saha A, Saxena V.P. (1998) Uranium potential for sandstone type deposits around NE part of the Proterozoic Abujhman Basin, Bastar District, Madhya Pradesh, India. Proc. Nat. Symp : Recent Researchers in Sedimentary Basin : 139-149

Ravisankar, Thussu J.L, Prasad J M (1987) Geothermal studies at Tattapani hot sprint area, Surguja District, Central India. Geothermics : 61-76

Thussu J L, Prasad J M, Saxena R K, Prakash G, Muthuraman K (1987) Geothermal energy potential of Tattapani hot spring belt, Surguja, M.P. Rec. of GSI : 115, 30-35.

In-situ leaching of uranium ores

Long-term aspects of waste rock piles and tailing in Kyrgyzstan

Yuriy Aleshin, Isakbek Torgoev
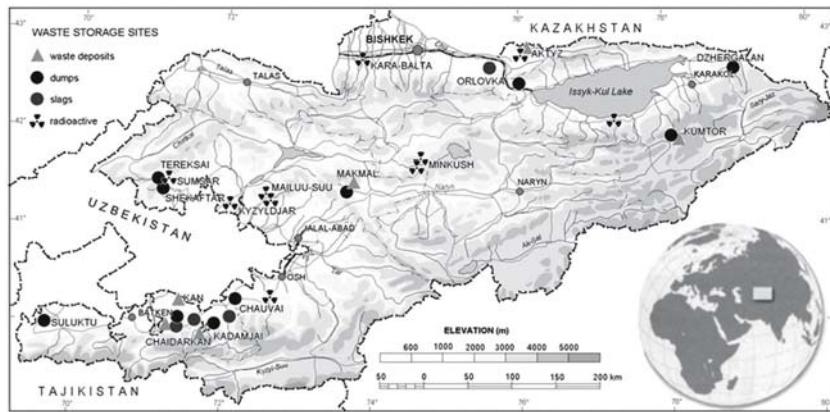
SEC "Geopribor", Mederova Str. 98, 720035 Bishkek, Kyrgyzstan,
E-mail: geopribor@mail.ru

Abstract. The complex of man-caused and natural factors, determining a high risk of long-term storage of radioactive waste on the territory of Tien-Shan is analysed. This complex involves the large-scale levels: regional geodynamical position; local tectono-geophysical, hydro-geological conditions; petrophysical rock properties on the sites of construction of tailings. The effective control of both lithosphere and tailing condition is possible by using geophysical methods.

Indroduction

The necessary condition to guarantee safety functioning of long-term storage objects of both mining and uranium ore processing radioactive waste is the reliable isolation of radionuclids from ecosphere during the whole period of their potential radiobiological hazard, which is aggregating in thousands of years, that is comparable to geologic time school of Upper-quaternary period. Required safety level can be ensured by multibarrier protection system, in which both natural and engineering barriers are involved, also including retaining constructions and guard shields. The most compound and ill-studied element of this system is rock massif containing disposal object, since during geological evolution period its structure, state and component rock characteristic are subjected to repeated alterations including man-caused ones. Consequently, the following mountain massive distinctive features are formed, such as discreteness, heterogeneity, anisotropy of properties, stressed state and others demonstrating at various hierarchies – from regional to local ones. Besides, tectonophysical processes occurring in the earth's crust (vertical and horizontal movements, earthquakes) lead to geological structure transformation, while reforming their main characteristics, as: tectonic fault level, mineral-chemical composition, petrophysical rock characteristics, hydrodynamical and hydrochemical groundwater parameters.

    The location areas of uranium mining waste in Kyrgyzstan (Fig. 1) are characterized by deep partition of topography, while having absolute levels: from 900 to
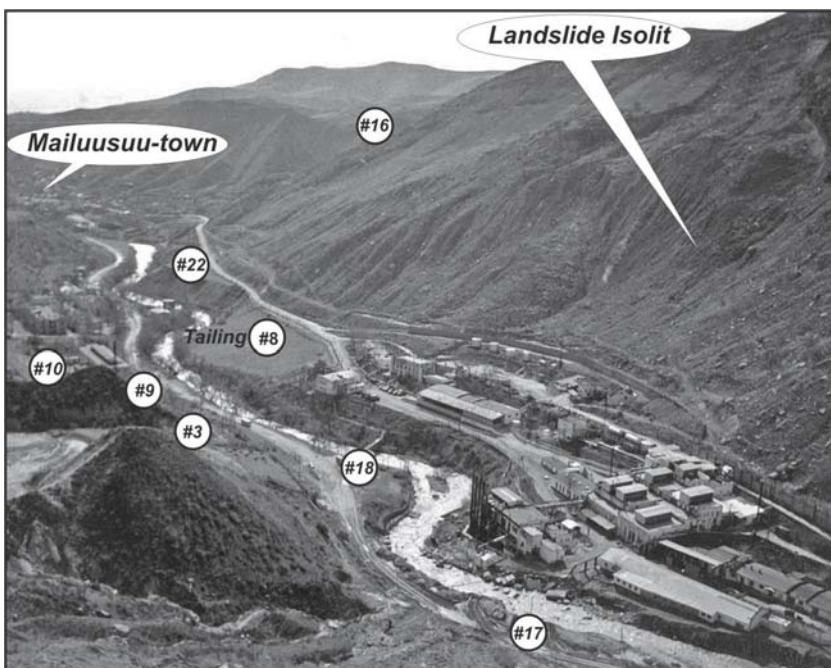
Fig. 1.   Most large-sized waste storage sites in Kyrgyzstan.

1100 m within the areas of radioactive waste disposal (over-floodplain river ter-races) in Mailuu-Suu, and from 1400—1500 m at the crests of local watersheds along river valley edges (zones of fifth and sixth river terraces); respectively from 1800—2100 m and 2500 m in Ak-Tuiz and Minkush and more higher. With re-spect to tailings undercurrent river valleys are occupied and built-up with indus-trial and civic buildings, engineering services; flood-lands and over-floodplain ter-races are exploited for farm production of rice, corn and other vegetables. All the rivers are either transboundary or tributaries of transboundary rivers: Naryn (Syr-Darya) and Chu. Thus, all reservoirs are directly adjoining to residential areas, their surface area is being exploited by local people as foot-paths or for livestock pasture territory.

The distinctive features of orographic site location of radioactive waste disposal in Kyrgyzstan are narrow valleys, which are deeply cut into rock massive, and they are characterized by slightly stable edges, where present exogenous geologi-cal processes are developing. Numerous sites show themselves in a form of an-cient landslide slopes and loose massifs of mudflow hard component generation. Complex of orographic, geologic-tectonic and climatic factors predetermine the following problems:

- along valley concentration of people separation, apartment houses, industrial objects, engineering communications, agricultural lands, rock piles and tailings, inasmuch as the latter ones have been located in flood-lands and over-floodplains of mountain river terraces due to a lack of unconfined spaces (Fig. 2);
- prevailing wind direction, while relating to valley orientation, is adverse by rea-son of its radon hazard for population of upper- and downstream villages (summer lower phenes are the most hazardous for the latter ones);
- extensive hydrographic network of major river with short tributaries of mixed spring-snow feeding with violent floods during April-July period each year; also water discharge 5—10 times beyond the average with discharge intensifi-

Fig. 2.   Former factory for uranium enrichment in Mailuu-Suu in surrounding tailings, located along river banks.

cation rising up to 4—5 m^3/s a day; maximum recorded water discharge during flood process is exceeding the average annual level in 10—20 times; waterflow speed up to 2—5 m/s in terms of longitudinal slopes from 0.01 to 0.1, with bulk average annual concentration of bottom sediment runoff of 2.5—500.0 mm in average diameter, including also from 0.01 to 0.1% of suspended solids of 0.05—0.4 mm in average diameter, and from 0.05 to 0.2%; river water is being used for rural irrigation, animal ponds, rural and often drinking water supply of local population; all tailings fall into catchments of major river valleys situated in 10—200 m from a coastline, some of them are located practically in river-beds and in river floodplains; high level of riverbed meandering and high speed of flow can determine severe scouring of quaternary clay-detrital rocks of coastline from 0.2 to 0.6 m^3/hour per 1 m of stream length;
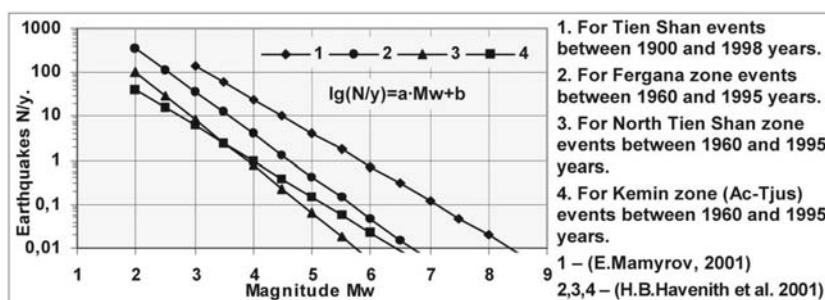
- high degree of mudflow hazard, that is under effect of non-central inflow valleys, easy-washout rocks, deep partition of topography (300-500 m) with steep (15-30°) and very steep (30-45°) slopes – right up to abrupt ones; scattered steppe and mountain-meadow vegetation; temporal coincidence of intensive snow-melting period with a time of spring rain showers; for instance, inside Mailuu-Suu river basin there are more than 90 mudflow tributaries with sup-posed mudflow volume from 27 thousand m^3 to 1.13 mln. m^3 , and bulk concentration of solid phase is in average from 10 to 40%; here mudflow frequency

Risk assessment studies

is 1-1.5 years; 33% of mudflows are occurred in May; riverbed location is considerably modified in the zones of mud composition breakdown;

- low coefficients of geomechanical stability of mountain slope overlying covers along valley edges, wide development of various-aged landslide movements: from ancient Quaternary ones 0.1 to 4 km^2 in the area to the present movements from 0.01 to 0.5 km^2 in the area; in addition, it is characterized by the present activation of stabilized both ancient and old landslides, secondary large-sized landslides are being developed in their bodies at present time; for instance in Mailuu-Suu areal affection coefficient ~ 100 km^2 by ancient landslides is 17%; about 50 present landslides have been developed and partly unloaded in old landslide bodies during the last 50 years. Active stage of multiple shearings of landslide bodies is spreading up to ten years or more; approximately about 40 landslides and local areas of mountain slopes with tensile cracks and subsidence of surface, sometimes to 5 mln. m^3 are enduring the stage of major displacement and preparation phase to this major displacement in Mailuu-Suu. The unloading basis of practically all the landslides is developed by riverbeds of major river valleys and lateral tributaries under the hazard of their blocking by goaf dams, barrier lakes formation and their subsequent inrush resulting to mudflow creation. So, landslide generation is occurred at the altitude of 50-400 m relatively to unloading basis, and on the slope within 50 to 1000 m away from a coastline. Weathering, sloughing, avalanches, and landslide are widespread phenomena in all rock complexes. Usually Mesozoic-Cainozoic rocks are met in a form of full, discontinuous sections. Stability of slopes layered by them is explained by the least strong clays and gypsum characterized by abrupt strength retrogression under severe weathering, leaching and watering. It is especially typical for upper-Cretaceous and Paleogene clays. When longitudinal wave speed is from 2.0 to 3.5 km/s the resistance to uniaxial compression R_{kmp} is 0.3-10.0 MPa, cohesion C = 0.02-0.05 MPa, angle of internal friction φ = 8-20°. Quaternary sediments lying on landslide slopes are usually introduced by loess-like loamy soils from 2 to 25 m thickness, also by prolluvial- dealluvial ones of least strength indexes severely relying on humidity W: where W ≈ 10% cohesion C ≈ 0.08-0.06 MPa, φ = 25-30°; where W ≈ 20% cohesion C ≈ 0.04-0.01 MPa, φ = 18-22°, longitudinal wave speed V_P ≈ 0.4-0.8 km/s. Frequently on a contact area between various-aged loamy soils sliding motion surfaces are occurred, since yearly-Quaternary ones involve more clay fractions, and upper-Quaternary ones involve macroporous fractions;

- closer to surface ground water level in over-floodplain terraces and bottom of ravines and gullies, where tailings are located, since under-riverbed flow appears as the basis of groundwater pinching-out of hydrogeological horizon. Generally this horizon is deposited at 8-30 m depth often pinching into original ground near socles of over-floodplain terraces, its thickness can be up to 10-20 m; water-bearing horizons in Neogene sediments are generally of lens-type; the huge role in watering process of Quaternary covering of valley edges play seasonal perched waters, which food areas are located in eluvial-dealluvial deposits near local watersheds. These water are usually local, discontinuously spread

Risk assessment studies

with no hydraulical connection between specific horizons with 0.1 to 1.5 thickness rate, and with flow rate from 0.3 to 1.8 m³/hour; additionally on the slopes with several fracture systems created by tectonic faults and thrust zones involving low-permeable units of tectonic clays, shielding groundwaters, where unloading of the latter ones occurs on the slopes located much higher than valley thalwegs. Thus, inthrust zones of increased fissuring characterized by more capacity, during the most watered years contribute to accumulation near unloading zones of large volumes of groundwaters, which may have local excess forcing under subface of low-permeable clay covering deposits.

To the number of leading regional characteristics of radioactive waste tailing areas in Kyrgyzstan it is necessary to consider the special features of present block movements of Earth crust in Tien-Shan, complicated stressedly-deformed state and increased seismicity conditioned by meridional compression of the earth crust in Tien-Shan due to continued collision of Hindustan and Eurasian plates and pressure intaking from the side of Pamir and Tarim. South-western part of Tien-Shan and specifically the eastern part of Fergana depression are affected by frontal activity of Hindustan wedge and Pamir peak moving in the northern direction. Meridional direction of indenter pressure (Pamir), which peal is confined to the eastern part of Fergana depression coupled with strong tectonically fractured lithosphere in the study area, are calling for the most strong compression of the earth crust within this area, also various intensity (from 3 to 20 mm a year), and directivity of subvertical and horizontal movements of earth crust blocks including opposing and rotary motions of single blocks and microplates.
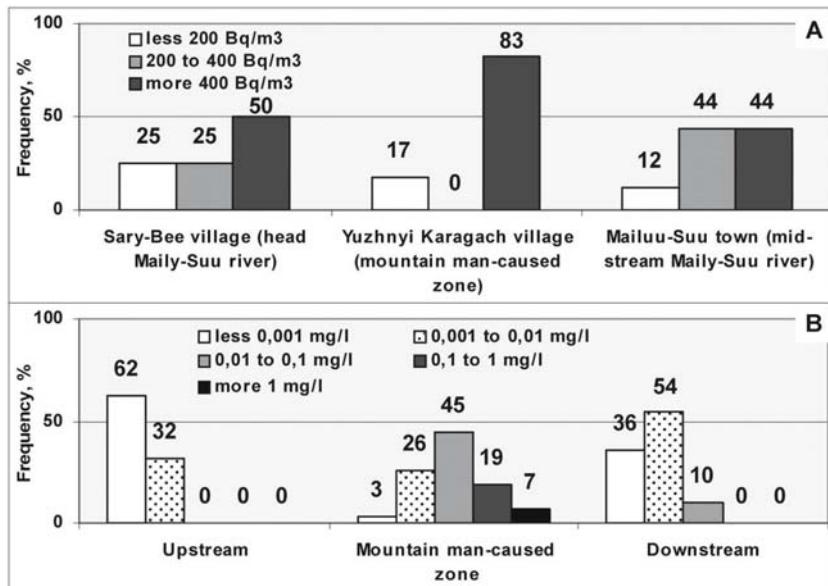
   Taking into consideration the abovementioned findings Tien-Shan is the most seismo-tectonically active region of Central Asia. Practically the whole territory of Kyrgyzstan is characterized by earthquake intensity with more than 8 points, while in the Northern and North-Western Tien-Shan seismic effect is more than 9 points (20% of the territory). Areas of the most concentrated number of earthquakes are accounted for border zones of Tien-Shan and Pamir. That is the Southern Tien-Shan seismically active zone with a series of large-sized faults delimiting Tien-Shan from Pamir and from Tarim microplate. Second zone is the area located round Fergana depression or Western Tien-Shan seismically active zone with the
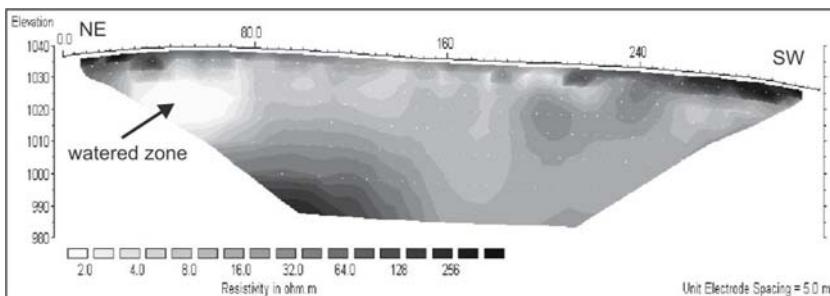

Fig. 3.   The Gutenberg-Richter's law for certain of the Tien-Shan areas.

Risk assessment studies

largest Talas-Fergana and Southern-Fergana faults. Third one is the Northern Tien-Shan seismically active zone with a series of analogous faults overlapping near-boundary areas in the north part of Kyrgyzstan and Kazakhstan. According to data collected during the last hundred years (Havenith et al. 2001, Mamyrov 2001) frequency diagram of large-sized earthquakes is given in the Fig. 3.

Geographical location of Kyrgyzstan in the center of Eurasia, vicinity of deserts and high elevation of territory above sea level can predetermine a climate formation with sharp continentality and aridity, altitude-zonal features of climatic zones, considerable variation of meteorological indexes either in within-year, or long-


Fig. 4.   The concentration distribution: A – the radon in the apartment houses, B – the uranium in the superficial water of the Mailuu-Suu river.
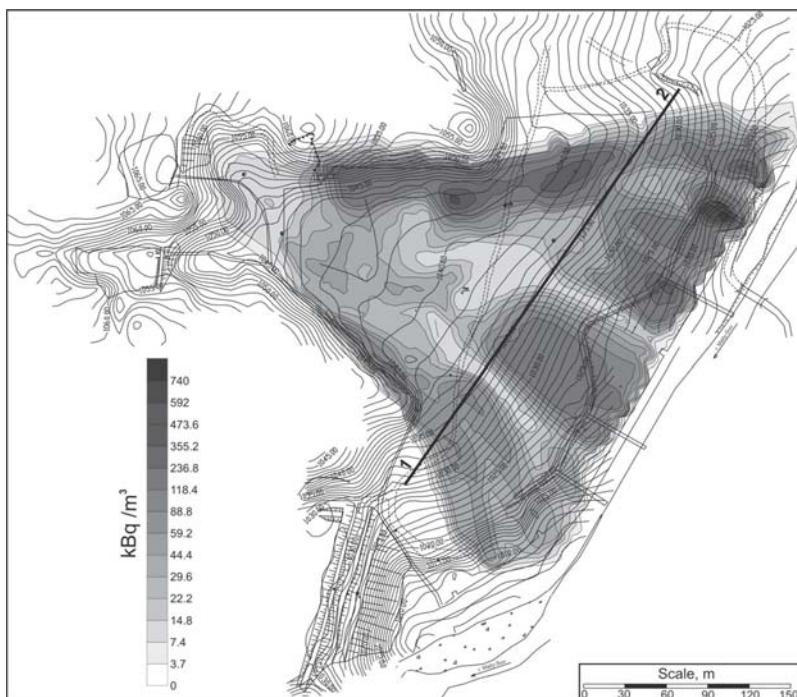

Fig. 5.   Geoelectrotomogram of No7 tailing (section along 1-2 line, see Fig.6. for location).

Risk assessment studies

term sections. Total solar radiation at horizontal surface level in terms of average cloudiness conditions in Tien-Shan is 6700±300 MJ/m^2 per annum, where monthly average maximum temperatures during summer season is more than 30°, and monthly average minimum during winter time is lower than minus 20°C in low-mountain and middle-mountain zone, where the objects of radioactive waste disposal are placed. During summer period monthly average soil temperature is (25±2.5)°C, minimum temperature during winter season is (-10±4.2)°C, while absolute maximum temperature may reach to 70°C, and absolute minimum is -50°C within the same area. If low values of monthly average precipitation during spring season come to 60-90 mm the coefficient of variation is 0.5-0.7, and average-maximum daily precipitation may be up to 30 mm. At the same time during summer and autumn time from June to October months the duration of periods with no precipitation may be more than a month, and precipitation total within this period generally is less than 30% of annual rate, and 10-15% in some other years.

Against abovementioned natural peculiarities it is worth noting the man-caused distinctive features of tailings and rock piles. They all have been formed at the yearly stages of nuclear power engineering elaboration within the period from 1947 to 1967 as temporary sections for radioactive waste distribution, while aiming to their further processing and repeated disposal when the technology of hydrometallurgical cycle of Uranium extraction (acid or carbonate ones) from ore mineral was only in progress. Those factors, together with social-economic, geologic-morphologic conditions and underestimation of radiation hazard predetermine the following:

- close arrangement of numerous little-sized tailings and rock piles to mining sites, hydrometallurgical factories and apartment block (in Mailuu-Suu) ~ 3·10^6 m^3 of waste are placed in 23 tailings and 13 rock piles with a volume of 10^3 to 10^6 m^3 each, distributed along the river and its tributaries on the area ~ 15 km^2) – factor of decentralization and primary dispersion of radioactive components; impeding quality monitoring and population access restriction, insulation of disposal materials, determination of their leakage system and synergetic series of radioactive risk for the population;

- increased content of Uranium in waste products, especially distinctive in Mailuu-Suu, where some attempts were made to process heterogeneous ores including the ones delivered from ore-deposits in the Eastern Germany and Czechoslovakia (probably, also from other countries); here the average coefficient of Uranium extraction from local ores during initial period scarcely exceeded 90% that conditioned rather high α-activity of tailing materials – from 12 to 60 Bq/g and Uranium concentration from 0.01 to 0.02 (during ore processing from other ore-deposits coefficient of Uranium extraction was substantially lower and its content in disposal sites (sections of tailings No 3, 5, 7) run up to 0.5% with total α-activity exceeding 200Bq/g; average content of Radium in some tailings varied in the wide range: from 10^{-8} % to $n \cdot 10^{-7}$ %, Thorium concentration – up to 10^{-4} %, Lead –up to 0.8 · 10^{-2} %, Chromium –more than 2 · 10^{-3} %, Arsenic – more than 0.6 · 10^{-2} %, Selenium – more than 0.2 · 10^{-2} % (Aleshin et al. 2000);

Risk assessment studies

- poor quality of both the engineering-geological survey and projects of tailing building, and consequently, these objects were not equipped with engineering barrier system (impervious screens), and pulp was given onto soil surface, dams were built mainly by hydraulic fill method with following covering by loamy soil (0.2-0.7 thickness rate) and by ballast materials – rock debris and pebble-stone with ~ 0.5-0.8 m thickness. Zone of suspended water in disposal areas of tailings and rock piles is represented by inequigranular sands, loamy soils, sandy loams, pebblestone, coarse rock debris, i.e. traditional materials of alluvial terraces and prolluvial-dealluvial cones which are not specified by high sorbent characteristics. In the areas of placing of tailings there are no geochemical barriers (biogeochemical, sorption, gley, acid ones etc.) - either natural or man caused. Taking into account rather a high filtration coefficient of disposal materials, making in average from 0.1 to 0.2 m/day, and in some places – to 1 m/day, under average porosity from 30 to 35%, it must be expected that on the all objects there will be an active migration of radionuclids beyond the tailing bounds along with groundwaters recharged by bedded low-Cretaceous waters of anticlines, at the foot of which those tailings have been placed, or by underflow of alluvial terraces including atmospheric precipitation flow from catchment area of surrounding slopes (Fig.4). It can be confirmed by sampling analysis of groundwaters pinched out from bottom of tailings: U-238 and U-234 concentration $n \cdot (10^{-3} – 10^{-2})$ g/l, that corresponds to ~600 Bq/l, in
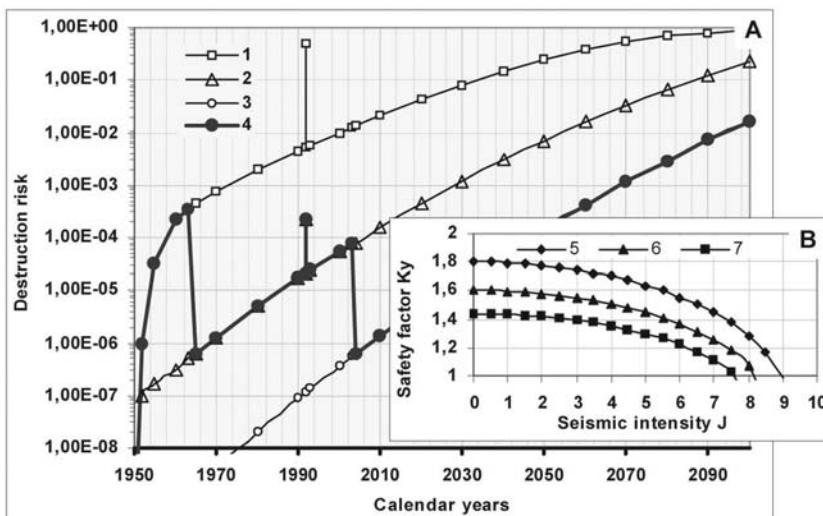

Fig. 6.   Radon field on the surface of No7 tailing in Mailuu-Suu.

Risk assessment studies

this connection background content of Uranium in groundwaters is $n \cdot (10^{-7} - 10^{-6})$ g/l. Thus, Uranium concentration makes up $n \cdot 10^{-4}$ g/l in stream waters washing the bottom of rock piles with no coating.

In terms of high seismotectonical activity of the region gas- and dampproofing of beds, sides, dams and surfaces of tailings loose their screening properties. This can be confirmed by geophysical and atmogeochemical investigations held in tailings of Mailuu-Suu. 40 years after conservation some of these objects contained disposal material in fluid-plastic consistency with a watered bed (Fig.5). Radon field on No 7 tailing surface (Fig. 6) is virtually everywhere exceeded the geochemical background level ($\sim 3 \cdot 10^3$ Bq/m^3) coming to $7 \cdot 10^5$ Bq/m^3. Radon diffuse halations were revealed also beyond tailings in the direction of Maily-Su river. Profile of emanation survey drawn in 20-30 m distance from tailing dam showed that Radon concentration in soil air in diffuse halations, particularly in the northern part, is also high, and these halations are ribbon-formed and stretching to riverbed side. Additionally, these halations register essential leakage of Radon beyond the bound of tailings.

In terms of average slopes of tailing beds from 0.1 to 0.15, disposal material washing, cup cantledge by surrounding slope denudation products, and seismic effects problems of geomechanical stability of objects are facing. This can have a fine demonstration referring to example of No3 tailing in Mailuu-Suu, which had a double rehabilitation: from 1963 to 1965 when $\sim 35 \cdot 10^3$ m^3 of waste has been


Fig. 7.   Prognosis of: (A) – the destruction risk, (B) – the factor of seismic safety of the tailing dump No 3 (Mailuu-Suu town). Notation conventions: (1),(5),(6) – according to initial project; (2) – after 1st rehabilitation in 1963-1965; (3),(7) – after rehabilitation by Tacis project (2003); (4) – the resultant risk dynamics; (9), (10) – after recession of level subterranean waters to 2,5 meters.

Risk assessment studies

moved away from it, and in 2003, when according to Tacis Project dam base of downstream side was cantledged. Both of the arrangements contributed to tailing stability increase and reduction of its failure risk. Nevertheless, constant cup cantledge by denudation products is lasting with increasing risk of this object failure (Fig.7). Catastrophical effects of tailing destruction were considered by us in (Aleshin, Torgoev, 2002) publication. It is worth noting that we still have no available information about behavior of loam materials under long-term radioactive irradiation. During recent years some publications (Dashko, 2005) proved that after the following dose $\sim 10^5$-10^7 Gr clay materials decrease their strength characteristics in 2-4 times. The similar doses can be derived in high-active tailings during ~ 1000 years.

According to experience gained during study of tailings of mining enterprises in Kyrgyzstan, and also based on researches conducted in their placing areas, it is evident that the methodology of environmental risk assessment of long-term radioactive waste must be founded on probability analysis of lithospheric space change of properties in their location areas at least at three scaled levels: regional geodynamical environment, local tectonic-physical, exogeodynamic and hydrogeological conditions, petrostructural characteristics and petrophysical parameters of rocks under influence of hydromechanical. physical-chemical processes in nearby and distant disposal fields. In Kyrgyzstan all system elements of multibarrier environmental protection from radioactive pollutants of tailings is remained under complex influence of mentioned scaled levels and, consequently, cannot guarantee high level of safety for long-term periods of time.

References

Aleshin Y.G., Torgoev I.A., Losev V.A. (2002) Radiation ecology of Mailuu-Suu. – Bishkek; Ilim. – 96 p

Aleshin Y.G., Torgoev I.A., Shmidt G. (2002) Environmental risk management at Uranium tailing ponds in Mailuu-Suu, Kyrgyzstan / B.I. Merkel, B. Planer – Fridrich, C. Wolkersdors: Uranium in the Aquatic Environment. – Springer – Verlag, 2002 – pp. 881-888

Dashko R.E. (2005) Specific features of engineering-geological and geoecological study and assessment of clay materials appeared as a technique of radioactive waste disposal / Sergeev readings. M: GEOS, - pp. 233-240

Havenith H. – B., Trefois P., Jongmans D., Abdrakhmatov K., Delvaux D. Probabilistic seismic hazard map of Kyrgyzstan: Application to the regional hazard of seismically induced landslides / Problems of geomechanics of mining area geotechnical development. Bishkek: Ilim, - pp. 183-191

Mamyrov E / (2001) Earthquakes / Mountains of Kyrgyzstan. - under the editorship of A.A. Aidaraliev. – Bishkek: Technology – pp. 177-188

Risk assessment of emergency situation initiation in the uranium tailings of Kyrgyzstan

Isakbek Torgoev, Yuriy Aleshin, Dmitriy Kovalenko, Pavel Chervontsev

Scientific Engineering Center "GEOPRIBOR" of the Institute of physics and rock mechanics, Bishkek, Kyrgyz Republic, E-mail: geopribor@mail.ru

Abstract. The present report represents the results of works done for risk evaluation, which was made by analysis of potentially hazardous phenomena and conditions in the Alpine Uranium tailing Tuyuk-Su in Min-Kush village in Kyrgyzstan. Short description of this tailing environmental influence is also provided. The most ecologically hazardous is the real scenario of Tuyuk-Su tailing collapse as a result of this narrow river valley blockage, where the tailing is located, by landslide masses. Some recommendations for risk mitigation of catastrophic situation initiation are given.

Introduction

The Tura-Kavak Uranium and Coal deposit No 248 (Guide book IAEA, 1996) is related to the number of Kyrgyz Uranium deposits actively developed during a "cold war" period.

During 1953-1968 on the base of this deposit in the Min-Kush village located in the center of Tien-Shan mountain system the Kavak Uranium mine was functioning and uranium-containing coals and sandstone were processed at the local concentrating mill.

Uranium ore was mined at the Kavak mine located in the mountain slopes adjacent to Min-Kush. The mineralization consisted of pitchblende veins in Jurassic coal and conglomeratic rocks, both situated near by Proterozoic gneisses. Average grade was approximately 0.14%U.

The tailings from the Uranium mill were deposited at four sites, all located within a range of approximately ten kilometers from Min-Kush: Tuyuk-Su, Taldy-Bulak, "K" and "D". The total amount of tailings generated at the Kavak mine was in order of 1,500,000 tons.

According to the classification of Environmental House, all tailing sites belong to the first generation of tailing disposal sites. They are characterized by the ab-

sence of engineered protective structures (Bottom seals and drainage layers) and of radium treatment facilities.

The analysis of the present geoecological situation in the Alpine areas of Kyrgyzstan, where Uranium mining and processing waste is located, shows that its negative influence on environment and population can be expressed in two major forms:

- In high risk of physical destruction of a number of tailings and rock piles with catastrophic effects of regional and transboundary types under possible natural hazards or disasters, which are typical for mountain regions (earthquakes, landslides, mudflows, floods or inundations);
- In contamination of environment, first of all, surface and ground waters, by radionuclids and other toxic elements (heavy metals) keeping for a long time in various forms and concentrations in radioactive waste tailings, and penetrating into the environment due to unequal gas- and hydro isolation of tailings and rock piles, gradual degradation of their protective (drainage) constructions and/or systems (Torgoev et al.,2002).

Based on results of hazard identification and risk analysis of tailing areas in the Min-Kush village it is evident that the Tuyuk-Su tailing is the most dangerous and threatening object.

Major characteristics of the Tuyuk-Su tailing

The tailing site is located in a narrow south-southwest trending V-shaped valley of the Tuyuk-Su river (Fig. 1), approximately one kilometer upstream from its mouth at the Min-Kush river. The gradient of the valley bottom is 5.3% inclined towards north-northeast. The valley is asymmetric with the western left-bank slope extending to a height of 150 m and the eastern slope to a height of up to 500 m above the valley bottom and tailing bowl.

Mountain peaks in the area run up to about 3,500 m. The sites of tailings have been constructed in the valleys at elevation ranging from 2,020 to 2.060 m above sea level (Fig. 2).

The Tuyuk-Su river while flowing into Min-Kush river is pertaining to the basin of the largest water-way of Kyrgyzstan and Central-Asian Naryn (Syrdaria) river.

The Tuyuk-Su tailing site covers an area of approximately five hectares. Approximately 766,000 tons of solid were deposited. The tailing volume was verbally specified as 450,000 m^3. Coal ash from a power station, demolition rubble from mine buildings, and municipal waste also have been stored there. The total volume of the tailings is rather in the order of 640,000 m^3. Waste total activity is about 2,000 Ku.

Three structures retain the Tuyuk-Su tailing mass: an upstream dam at the south end of the facility, an intermediate structure located about two thirds of the total length downstream from the south dam and a dam at the north end of the facility

(Fig. 2). The dams are built of loamy sands and loam mixed with gravel. The bulk density is in the order of 1.6 to 2 tons per m^3.

The crown of the north end dam is approximately 80 m long and 14 m high. At the bottom of the dam there are the openings of two parallel concrete pipes with a parabolic cross section. Three pairs of man holes were constructed to provide access to the concrete pipes from cleaning from fluvial debris. The pipes originally channeled the Tuyuk-Su river underneath the tailing mass, however, they were frequently clogged by river sediments, thus, resulting to an increased risk of erosion of the tailing mass (Fig. 1).

In order to reduce the risk of erosion of tailings due to overflow of the underground bypass system, the river was diverted into an open channel along the eastern edge of the facility of tailings. This channel has been constructed out of concrete slabs and has a near-rectangular cross section with a depth of 1.9 m and a maximum width of 6 m. Raffles were constructed near the north end to break the energy of the flow.

At the western edge of the facility, a smaller concrete channel with a width varying from 0.85 to 1.5 m and a depth ranging from 0.8 to 1.0 m was constructed to intercept runoff from the steep slope adjacent to the tailing site. At the northern end of the facility the small channel is routed across the dam to direct runoff into the eastern channel carrying the Tuyuk-Su river water.

The tailings are overlain by 0.2 to 0.7 m thick cover consisting mostly of gravel, and, to a minor extent, loamy soil. The vegetation on the cover material consists of grass and small shrubs that are continuously reduced by foraging cattle and sheep.
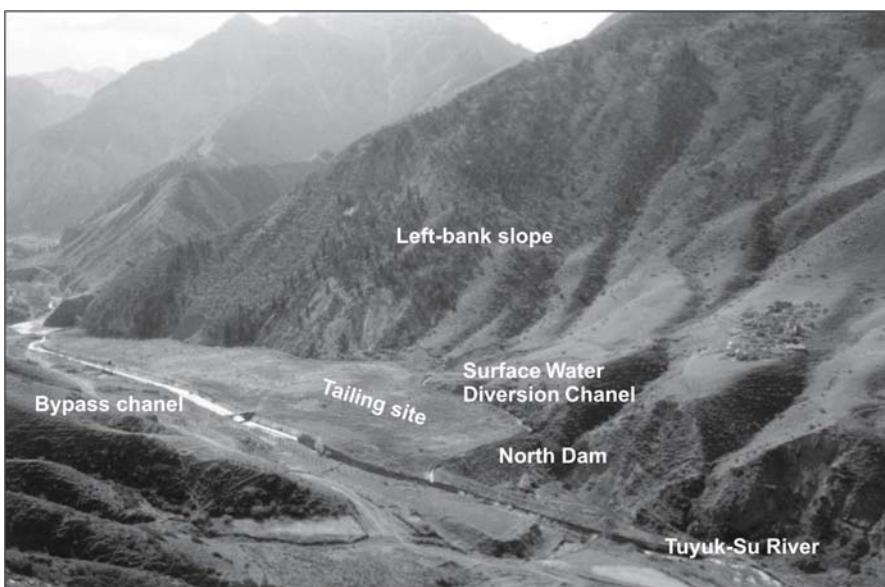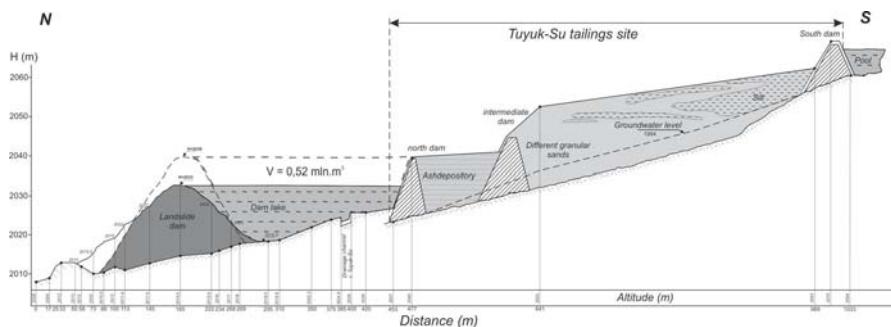

Fig. 1.   The common view of the tailing in valley of river Tuyuk-Su.

Risk assessment studies

Fig. 2. The modeling results of landslide blockage of river in lower part of tailing Tuyuk-Su.

As a result of stability assessment of the northern dam retaining the tailing body the following facts have been discovered:

- At high ground water levels occurring mainly during spring the dam stability may be at risk
- Under dynamic conditions, i.e. during an earthquake, the dam may be stable, provided the phreatic surface is at low levels. However, the Tuyuk-Su tailing storage facility is located in the river valley, which is the expression of a zone of structural weakness. This zone may be activated during an earthquake of a magnitude (M=7.2) of the Susamyr event in 1992. In case of activation of this zone the north dam is likely to fail (Final Report TACIS, 1995).

The tailings represent the leached ore residues, i.e. minerals that have resisted the leaching and products generated by neutralization or ore treatment solutions as well as residues from water treatment. In addition, reagents like flocculants may have been added. Depending on the efficiency of the mill, residual Uranium may be present at varying concentrations.

Chemical composition of waste and its radiobiological characteristics is the following:

Tailings: 128 ppm U; Ra^{226} = 4,0 Bq/g; alpha activity 74,2 Bq/g; Pb (av. 37 ppm); organic carbon C = 0,5-3,0%. The maximum ion radiation dose rate on the top cover of tailings is 0,72 µSv/h

Environmental Impact

Environmental impact of the Tuyuk-Su tailing with regard to inadequate state of its major and protective constructions, as well as specialities of its distribution in the riverbed first of all is shown in contamination of surface waters.

Slightly elevated uranium concentrations in water up to 500 m downstream from the Tuyuk-Su site indicate that uranium is being released from the tailings. Lead content in the stream water exceed the low Kyrgyz limits for fish waters up-

Risk assessment studies

stream and downstream from the Tuyuk-Su site. Therefore, it is assumed that the higher lead concentrations are of geogeny origin.

Leaching of radionuclids may take place by infiltrating water (at all sites) or flow-through ground water (at the Tuyuk-Su site). The release of Ra^{226} appears to be small. However, radionuclids like Pb^{210} and Tn^{230} may be released at Tuyuk-Su site via the water path due to ground water entering the tailings in the upstream portion of the tailing mass and most likely by water infiltrating from the river by-pass channel.

Radiological survey of soil and vegetation growing on the territory of the Tuyuk-Su tailing showed the following:

The uranium concentration within the upper soil layer (0 – 25 cm), the grass and the tree leaves ranges from 0.5 to 4.5 ppm U. These values are comparable to concentrations found in other natural materials. For instance, the uranium concentration in igneous rocks and soil is typically 48 Bq/kg (approximately 2 ppm) and 24 Bq/kg (0.9 ppm), respectively (Final Report TACIS /91/EKY 03, 1995).

The average Ra^{226} concentration in the upper soil layer is 0.047 Bq/g, in the grass samples is 0.087 Bq/g, and in tree leaves is 0.063 Bq/g. The soil typically contains 0.07 Bq/g. The total average alpha activity of 3.1 Bq/g in the upper soil layer exceeds the typical value of 0.06 Bq/g for soil. Grass contains 2.7 Bq/g and tree leaves contain 1.7 Bq/g.

Assessment of hazard and risks

In the case of the Min-Kush area tailings the data base is insufficient to undertake a quantitative risk safety assessment. Therefore, a qualitative risk assessment of potentially hazardous phenomena was conducted in the area of Tuyuk-Su tailing.

Due to abovementioned specialities of present state of the Tuyuk-Su tailing with regard to physical-geographical, climatic, geological conditions of studied area the following types of hazard were determined:
- radiation exposure due to human and bio-intrusion,
- chemical instability, i.e. release of radionuclids and chemicals into air and water,
- structural failure due to flooding, liquefaction of tailings related to seismic activity and others
- long-term erosion due to avalanches and landslides, bio-intrusion by burrowing animals, and anthropogenic borrowing for use as construction material.

The results of comparative risk assessment of listed hazards are given in Table1.

Based on results of qualitative analysis of risks related to the Tuyuk-Su tailing area is evident that the most hazardous process at present time is the risk of northern dam and channel failure, which may happen as a result of earthquakes, landslides, mudflow initiation, flooding in the Tuyuk-Su river. It is also possible to assume joint synchronous activity of these hazardous processes and phenomena.

Table 1. Assessment of risk related to tailings in the Min-Kush area if not taking into account the mitigative measures and continuous maintenance.

RISK	Tuyuk-Su site	"K" site	"D" site
Human and Bio-intrusion	high	high	high
Leaching	medium	low	low
River Bypass Failure	high	not applicable	not applicable
Runoff Collection Failure	high	medium	not applicable
Dam Failure	high	low	low
Long-term Erosion	high	medium	medium

In summer 2004 at the site of right-bank (eastern) slope of Tuyuk-Su valley 200 m beneath the tailing cracking processes have occurred with a large-sized landslide initiation (more than 0.5 mln. m^3 in the volume). Series of earthquakes with (M = 3.9 - 4.8) magnitude, which epicenters were in up to 80 km from the Min-Kush village, as well as large amount of precipitation during spring and summer 2004 appeared as the key natural factors of landslide formation. Some anthropogenic effects, particularly slope foot trimming during laying of motor road and pipelines towards the Tuyuk-Su tailing also stimulated this hazardous landslide origination.
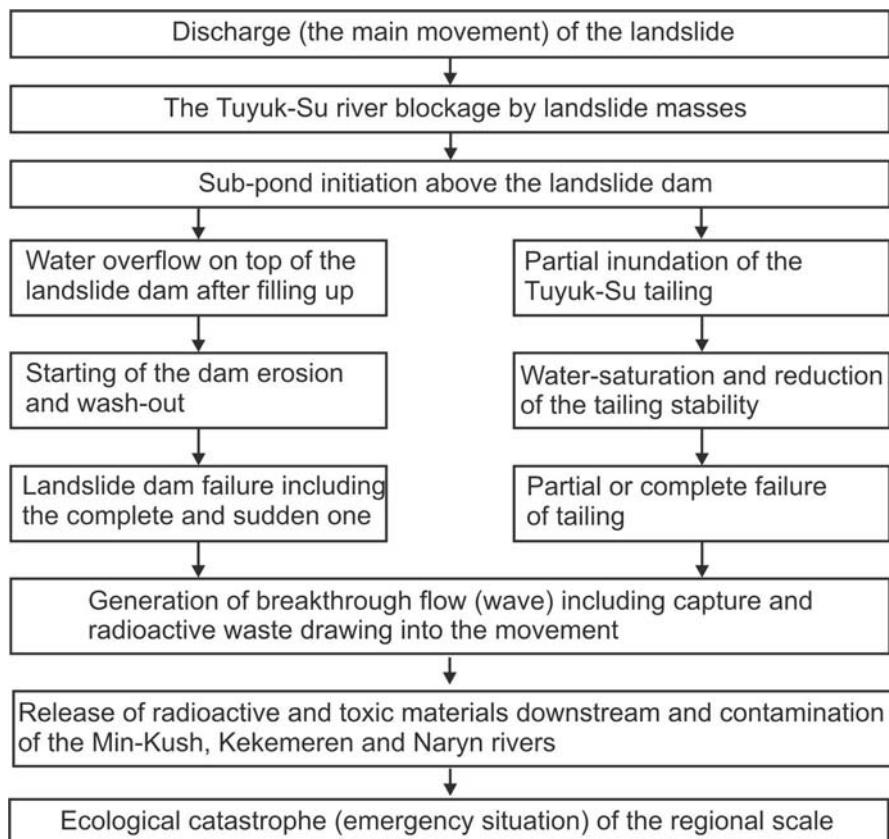
The stage of the general movement of landslide masses predicted for spring-summer 2005 is fraught with river bed blockage downstream the tailing with possible catastrophic effects.

Fig. 2 represents the results of modelling of river blockage by a landslide dam, which elevation in case of the worst scenario may reach 25 m above the river bottom. Fig. 3 provides the schematic model of possible sequence of developing hazardous events, which may lead to a destruction of both the dam and the tailing resulting in catastrophic environmental effects of regional scale.

The most disastrous effects for areas located downstream the tailing and the landslide dam may come in case of a sudden and complete destruction of landslide dam that is fraught with breakthrough flow initiation. The special hazard and risk of such a catastrophic scenario realization are related to a possible partial or complete capture and drawing into breakthrough flow the radioactive waste stored in the Tuyuk-Su tailing. According to the calculations the maximum initial discharge of breakthrough flow of "tails" may be more than 3,000 m^3/c. This will entail destruction of dwellings located in the mouth part of the Tuyuk-Su river, and also radioactive contamination of beds and floodplains or the Min-Kush, Kokomeren and Naryn rivers.

Evidently, that in terms of any situation arisen and in case of any developing events (Fig. 3) it is impossible to allow either partial or total inundation of the Tuyuk-Su tailing, as well as both sudden and complete failure of the landslide dam. This can be achieved if providing controlled and guided water discharge accumulated above the landslide dam.

The recommended cardinal step is to relocate the Tuyuk-Su tailing to the more safety sites, where will be no risks related to possible hazardous effects of earthquakes, landslides, mudflows and floods. According to the proposals of the

Fig. 3. Schematic sequence of events including initiation of the catastrophic situation during landslide movement beneath the Tuyuk-Su tailing.

TACIS project (Final Report TACIS, 1995) even in 1995 it was recommended to relocate the Tuyuk-Su tailing to the sites of "K" and "D" tailings, which seem to be rather suitable for placing of waste on their territories. Thus, the most economical method of waste relocation was recommended as transportation of "tails" by use of tracks.

Conclusion

The analysis of the risks associated with the tailing sites in the Min-Kush area shows that the radiological and stability hazards are associated with all tailing sites, particularly with the Tuyuk-Su tailing sites. According to the international standards, e.g. to guidelines issued by the International Atomic Energy Agency, the conditions at the site call for remediation measures. The objective of any remediation activities at the tailing sites is to reduce the radiation exposure at the

tailing sites, the release of radionuclids and chemicals, the risk of structural failure and the long-term erosion.

The high risk of failure of the man-made structures by earthquake, landslide, mudflow effects and by the continuing ground water flow through the tailing mass at Tuyuk-Su poses a stability hazard that cannot be substantially reduced by institutional control (maintenance of bypass and runoff collection channels) as practiced to date. Therefore, the conditions at the Tuyuk-Su site call for relocation of the Tuyuk-Su tailings to a site that implies lesser risks. Both "K" and "D" sites appear suitable for receiving the tailings.

After relocation and decommissioning of the sites a monitoring program needs to be implemented that would cover the air and water pathways for a certain time period yet to be determined.

References

Guidebook to accompany IAEA Map (1996): World Distribution of Uranium Deposit. IAEA, Vienna.

Torgoev I., Aleshin Y. and Havenith H-B. (2002). Impact of Uranium Mining and Processing on the Environment of Mountainous Areas of Kyrgyzstan. In: Uranium in the Aquatic Environment. B.E. Merkel et al. (eds) Springer-Verlag Berlin Heidelberg 2002 – pp 93-98

Final Reports of Project TACIS /91/ EKY 03 (1995). Development and Training Activities for the Environmental Improvement of the Former Kavak Uranium Mill of Tuyuk-Su

Environmental regulation of uranium mining in Australia

Peter Waggitt

Waste Safety Section, Division of Radiation, Transport & Waste Safety, Interrnational Atomic Energy Agency, PO Box 200, Wagramerstrasse 5 A-1400 Vienna, Austria, E-mail: P.Waggitt@iaea.org

Abstract. Uranium mining has been taking place in Australia more or less continuously since the late 1930s but it really only came to the fore after 1945. Environmental protection legislation did not become established until 1976. As a consequence the environmental management of many early uranium mines was virtually non-existent and a number of adverse environmental impacts were recorded. The development of modern uranium mines, essentially since 1970, has been associated with two major issues: a growing understanding by industry and regulators of the need for environmental management and pollution control, and increasing community pressure for minimisation of adverse environmental impacts from all mines. Under these conditions Australia has developed regulatory regimes for uranium mines which incorporate some of the highest environmental standards in the world. This paper sets out to describe how the current uranium mines in Australia are regulated from an environmental viewpoint. The discussion deals with the regulation of underground, open cut and in-situ leach uranium operations in climatic zones varying from the wet-dry tropics to arid deserts.

The regulatory regimes involve a complex mix of federal and state governments as well as traditional Aboriginal Landowners and other significant stakeholders. The paper sets out how these different agencies and organisations work together to ensure that uranium mines are operated in accordance with the expectations of the community in terms of their environmental, health and safety expectations whilst maintaining economic viability and operational efficiency.

Introduction

The generation of electricity using the nuclear cycle was first achieved on a commercial scale at the Calder Hall power plant in the United Kingdom in 1956. This new form of power generation had been hailed as the future for cheap electricity worldwide. As a consequence the search for supplies of uranium, the fuel used in the nuclear fuel cycle was increased. In Australia the Government offered a substantial reward to the discoverer of a major new deposit. At the same time uranium was also in demand for use in nuclear weapons and so the issue of regulation came under consideration to ensure that this strategic material would only be exploited in a controlled manner.

Australia was a major supplier of uranium in the 1950s and 60s and is still considered to be the repository for the world's largest reserves of low-recovery-cost uranium. Australia has been estimated to have 28% of the world's supply of uranium recoverable at a cost of less than $US80/kg Uranium (OECD, 2003). Australia is a significant player in the world uranium mining industry and the Australian Government has the responsibility of managing the nation's nuclear activities in both the national and international arenas.

However, regulation of mining and the protection of the environment are activities that are generally the responsibility of State and Territory governments. But as the Australian Government has undertaken a deepening involvement in environmental protection involving matters of national importance so a system of shared responsibilities has developed. A similar situation has evolved specifically in relation to uranium mining. Hence the environmental management oversight of uranium mining is undertaken by the Australian Government with day-to-day operational regulation undertaken by the Governments of South Australia and the Northern Territory in their own jurisdictions. The Australian Government maintains control through the granting of export permits for the uranium. This is an effective control as there is no domestic market for the output from Australia's uranium mines.

This process of regulation may appear complex but it has been developed to minimise duplication of effort, especially in respect of administrative processes.

Mining Background

The history of modern uranium mining in Australia can be considered to begin with the operation at Rum Jungle (Waggitt, 2004). The discovery of the deposit in 1949 was followed by the decision for the Australian Government to assume ownership of the minerals and to have the site operated on its behalf by a commercial mining company. Australia has a federated system of government. When the 7 colonial states came together to form the Commonwealth of Australia in 1901 the constitution set out which activities would be controlled by the Australian Government and which would be regulated by the State Governments. Mining was deemed to be an activity that was to be controlled by the States although the min-

erals remain the property of the Government with the miners paying an appropriate *pro-rata* royalty for the right to develop the mineral resources.

In the case of uranium the Australian Government decided that it would control the commodity through a number of statutes, including the requirement for an export licence prior to the product being allowed to leave the Australian continent. However the day to day regulation of mining is under the direction of State level authorities. Thus none of the actual mining activities could be regulated directly as this would represent an infringement of the rights of the States. Within each state there is an agency or department charged with the responsibility for regulation of the exploitation of mineral resources, including their environmental management.

The exception was for the uranium deposits of the Northern Territory. As the Northern Territory is a self-governing territory, and not a state, the Australian Government is able to impose an element of direct rule in the regulation of mining. In practice this represents more of an oversight role as the Australian Government does not have the necessary detailed legislation to regulate all the wide range of activities in mines. Hence, for the Northern Territory there is a regulatory regime which is different from that found in South Australia, the only other Australian state where uranium mining is currently active. This paper describes the development of the various regulatory regimes and operations in place in the Australian uranium mining industry in 2004, with specific reference to environmental management.

Historical Operations

Early mining operations were not subject to any environmental regulation and many operations were simply abandoned at the end of their economic life. This was especially true in Australia as exemplified by the uranium mining and milling operations at Rum Jungle (1950-63), Moline (1959-64) and in the South Alligator valley (1953-64), all in the Northern Territory, Radium Hill in South Australia (1954-62) and after the first "life" of the uranium mining at Mary Kathleen in Queensland (1958-63). Rehabilitation was not mandatory anywhere; there was no legal requirement for mining companies to deposit securities against the costs of rehabilitation; little, if any, environment protection legislation was in place at any level, and there was little outcry from the community in most locations. Under these circumstances the lack of rehabilitation was not surprising.

Then the situation changed. Rum Jungle became notorious as the site had become a source of pollution resulting in extensive adverse environmental impacts in parts of the Finniss River catchment. For up to 14 km downstream of the former mine site there were greatly reduced populations of aquatic flora and fauna, both in the watercourse and on the banks. The problem was caused by acid drainage developing from the effects of the tropical temperatures and an annual rainfall of about 1400 mm on the highly sulphidic mining wastes left on the surface. This effluent leached heavy metals, primarily copper, from the waste rock which in turn polluted the watercourses downstream of the site.

Risk assessment studies

This situation remained unchecked apart from a limited program of works in 1977-78 when there was some clean up carried out at the treatment plant area (Verhoeven, 1988). At the same time the Northern Territory achieved self-government, which included assumption of the regulation of mining. In 1982 planning for a program of rehabilitation was begun. The program was to be funded by the Australian Government and it was agreed that the work would be implemented by the Northern Territory Government. The works program was completed in 1986 on the main site, and in 1990 at Rum Jungle Creek South (an outlying ore body developed at the same time as the main site).

The decision to undertake rehabilitation had been brought about because society's expectations were changing. As the community's general awareness of issues such as pollution and environmental protection grew in intensity from the early 1970s onwards, legislators began to put suitable controls in place, including in relation to mining operations. The Australian Government introduced the *Environment Protection (Impact of Proposals) Act* in 1974. This legislation required, *inter alia*, that major development projects, such as new mines, would be required to publish Environmental Impact Statements which would in turn be subjected to a rigorous program of assessment before any development approvals could be given. Uranium mining received special attention in this legislation. The immediate consequence was the instigation in 1975, under this new legislation, of an inquiry into the proposals for development of uranium deposits in the Alligator Rivers Region of the Northern Territory.

The Ranger Uranium Environmental Inquiry (RUEI) was chaired by Mr Justice Fox and was the first inquiry of its type held in Australia. There were two reports produced by the "Fox Inquiry", as the inquiry was more familiarly known. The first report (RUEI, 1977a) dealt with major policy issues in respect of the continuation of Australia in nuclear fuel cycle activities and had 15 recommendations. These included that there was no justification for "a decision not to develop Australian uranium mines", another recommendation stated that "development of Australian uranium mines should be strictly regulated and controlled"; and a third recommendation deferred a decision into development of the "new" Northern Territory mines "until the second Report of this Commission is presented". The Inquiry made no comments in relation to the continuation of the Mary Kathleen operation in Queensland.

The second report (RUEI, 1977b) contained eleven pages of recommendations, all related to the proposed development of the Ranger uranium mine. Amongst the list were recommendations that the Australian Government appoint a Supervising Scientist to exercise a supervisory and integrating role over the environmental research and monitoring programs that would be agreed upon by a Co-ordinating Committee that would also be established. The day to day regulation of the mining operation would remain a responsibility of the Northern Territory Government. The initial authority to mine was issued by the Australian Government under the Atomic Energy Act, despite a recommendation from RUEI that this should not be done. The Authority, issued under s.41 of the Act, also included 44 Environmental Requirements (ERs) which covered environmental aspects of the operation including appointment of suitably qualified staff, use of Best Practicable Technology

(BPT) which was itself defined in the ERs, water management issues and the mandatory return of tailings to mined-out pits at the cessation of mining. The Authority also required the mining company (ERA) to submit annually a costed plan of rehabilitation for assessment by the NT and Australian Governments. Once this plan had been approved by the governments ERA were required to deposit to a trust fund a cash amount at least equal to the approved rehabilitation estimate.

Current Operations

At present (in 2004) there are three active uranium mining operations in Australia.

There are two operations in South Australia, both regulated primarily by the South Australian State Government and located in the arid desert environment in the northern part of the state.

The more established is the Olympic Dam underground mine owned and operated by WMC Resources Limited, which has been in production since 1988. This site is located about 560 km north-north-west of Adelaide and contains the largest known uranium ore body in the world. The ore body is polymetallic with copper as the main source of revenue (75%), followed by uranium (20%) and silver and gold (5%). Uranium production for 2002 was announced as 2867 tonnes U_3O_8.

A more recent operation is the Beverley uranium mine located about 520 km to the north of Adelaide. This is an in-situ leach (ISL) operation that has been in production since November 2000. The production for 2002 was announced to have been 746 tonnes of U_3O_8.

In addition there is a second in-situ leach project under development at the Honeymoon project in South Australia which is still to enter full production after a number of years of trials.

The third site is located in the Northern Territory about 250 km east of Darwin, in the wet/dry tropics. The open cut Ranger mine is owned and operated by Energy Resources of Australia, which in turn is majority owned by Rio Tinto Australia. Ranger production for 2002 was reported as 4470 tonnes U_3O_8, representing about 12% of world production. This is the longest running uranium mine of the three having commenced operations in 1980.

The regulatory regime at Ranger is perhaps one of the most complicated in the world involving both the Northern Territory and Australian Governments at the site level and on almost a day-to-day basis. In the cases of the other two mines the Australian Government's involvement is much more at arm's length.

Also in the Northern Territory is the Jabiluka Project. This is an underground prospect owned by ERA and located some 22 km to the north of their existing Ranger mine. Initial development of the Jabiluka project commenced in 1996 and some 2000 metres of underground workings were created. However, issues over final EIA approval for ERA's preferred development option, the permission of Aboriginal Traditional landowners and an undertaking by ERA not to run two mines concurrently resulted in the site being placed on long term care and mainte-

Risk assessment studies

nance in late 2003. This program included the backfilling of the underground workings and removal of virtually all the above ground infrastructure.

Regulatory Regimes

In Australia, as previously stated, the regulation of mining activities lies within the jurisdiction of the States and Territories, particularly with reference to the issues of health and safety for the workforce. Environmental management issues are similarly regulated except in the Northern Territory where the Australian Government has an additional specialist group to oversee environmental matters for uranium mining. The Supervising Scientist Division of the Department of the Environment & Heritage comprises two branches with the common aim of ensuring that the environmental management of uranium mines within the Alligator Rivers Region (ARR) is of the highest standards and the environment remains protected from any adverse impacts as a consequence of mining. The two branches are the Office of the Supervising Scientist (OSS), which deals with matters of policy, supervision and audit in relation to environmental management at uranium mines within the ARR; and the Environmental Research Institute of the Supervising Scientist (*eriss*) which carries out research the areas of environmental radioactivity, ecosystem protection, hydrological and ecological processes and ecological risk assessment all in relation to uranium mining in the ARR.

Australian Government Legislation

The Australian Government has the power to regulate uranium mining through a number of instruments. The most significant seven are briefly described below:

- *Atomic Energy Act 1953*
  This Act established that ownership of all uranium minerals found in Australian territories is vested in the Australian Government. An authority established under s.41 of this Act provides for the Ranger uranium mine to operate. The prime importance of this Act is that attached to the s.41. Authority are the Environmental Requirements (ERs) which place environmental management obligations on the operators of the Ranger uranium mine. This act is administered by the Department of Industry, Tourism and Resources (DITR).
- *Environment Protection and Biodiversity Conservation Act 1999*
  This Act replaced the previous *Environment Protection (Impact of Proposals) Act 1974*. All authorities and approvals granted under the previous legislation are still valid. The former Act was the instrument under which all present uranium mines were originally approved and so the new Act is not retrospectively applied to those operations. Should there be any major changes to existing operations requiring a change in a current approval then the new Act would be triggered. The new Act (EPBC Act) is the source of the Australian Govern-

ment's legislation in respect of the mining, use and disposal of uranium. A list of six environmental issues of national importance includes "nuclear actions" amongst which are listed:

> *"(d) mining and milling of uranium ore*
>
> *(f) de-commissioning or rehabilitating any facility or area in which an activity described in paragraph (a), (b), (c), (d), or (e) has been undertaken."*

Clearly the mining of uranium is covered here. The main interest is that under the EPBC Act such activities may only proceed after approval has been given by the Minister. Such approval may only be granted after an environmental assessment has been made of the proposed action using an approved process and a satisfactory outcome obtained. This act is administered by the Department of the Environment & Heritage (DEH)

- *Nuclear Non-Proliferation (Safeguards) Act 1987.(DITR)*
  This legislation is to ensure the security of nuclear materials within Australia

- *Environment Protection (Alligator Rivers Region) Act 1978 (DEH)*
  This Act arose from the recommendations of the Ranger Uranium Environmental Inquiry held in 1976-1977. This Act provides for the administrative arrangements between the Australian and Northern Territory Governments which enable the Australian Government's oversight of uranium mining operations in the region. Also this Act establishes the Supervising Scientist and associated facilities. The Act also establishes two committees relevant to uranium mining activities within the region:
    - The Alligator Rivers Region Technical Committee (ARRTC) which is to review monitoring and research programs carried out in the region that are related to uranium mining; and
    - The Alligator Rivers Region Advisory Committee (ARRAC) which serves as a forum for information exchange on environmental issues in relation to uranium mining in the region; ARRAC also facilitates communication between all the major stakeholders including mine operators, Aboriginal Traditional Landowners, representatives from various elements of the community and the two governments.

- *Australian Radiation Protection and Nuclear Safety Act 1998*
  This Act established the Australian Radiation Protection and Nuclear Safety Agency (ARPANSA), the statutory body responsible for the protection of the health and safety of people and protection of the environment from the harmful effects of radiation. In the main this Act deals with the transportation and storage of uranium and associated products as well as general issues of radiation protection.

- *Aboriginal Land Rights (Northern Territory) Act 1976*
  This Act establishes the Northern Land Council as a statutory body to represent the interests of the Aboriginal traditional landowners. This is of significance as the uranium mines in the ARR are all on land that has been acknowledge as being traditionally owned by various Aboriginal groups.

- *Customs (Prohibited Exports) Regulations 1958 under the Customs Act 1901*

Risk assessment studies

Export of radioactive materials, including uranium concentrates, requires an export licence. As there is no domestic market for these products this is a very robust control mechanism over uranium mining. In 2000 these regulations were modified such that the Australian Government was enabled to attach conditions to export licences, including environmental conditions. The export of uranium products for all mines presently operating are subject to the Environmental Requirements issued under the previous *Environment Protection (Impact of Proposals) Act 1974*.

In addition to the laws there are also three Codes of Practice issued by ARPANSA which deal with various aspects of radiation protection for human health and the environment. All three have relevance to the uranium mining industry. These codes were originally introduced through the Environment Protection (Nuclear Codes) Act 1978 but have been revised from time to time and the current versions are:

- Code of Practice on the Management of Radioactive Wastes from the Mining and Milling of Radioactive Ores (1982) ["waste code"]
- Code of Practice on Radiation Protection in the Mining and Milling of Radioactive Ores (1987) ["health code']
- Code of Practice for the Safe Transport of Radioactive Substances (1982) ["transport code"]

The "waste code" and the "health code" are currently under revision. The two codes are being combined into one document. The working title is *Code of Practice and Safety Guide for Radiation Protection and Radioactive Waste Management in Mining and Mineral Processing*" and it is anticipated that the final draft will be available for public consultation early in 2004 with final publication anticipated before the end of 2004.

ARPANSA also publishes a set of recommendations : "Recommendations for limiting exposure to ionising radiation (1995)" which in effect replaces the previous "transport code".

All these ARPANSA publications have a regulatory function as compliance with their provisions, in whole or in part, is required as conditions of Authorisations and licences issued by the Northern Territory and South Australian Governments respectively in relation to the mining of uranium.

All of the foregoing regulatory apparatus applies to uranium mines wherever they are located in Australia. In the following sections the additional legislation applicable in each of the two jurisdictions will be described.

The relationship between the Governments of Australia and the Northern Territory is defined by a set of Working Arrangements (WA) which clearly set down the areas of responsibility for each participant in the arrangement. Whilst the Northern territory Government is the regulator on a day-to-day basis the WA provide for the Australian Government to have the power to direct the NT Minister to a course of action if his proposed action is not in agreement with advice from the Supervising Scientist. The WA are currently in the process of being revised at the time of writing in 2004.

Risk assessment studies

Northern Territory

Legislation and regulation

The Northern Territory government has the overall responsibility for the regulation of uranium mining within its jurisdiction, at the operational level. The activities are regulated primarily by the Department of Business, Industry and Resource Development (DBIRD) through administration of the *Mining Management Act 2001 (NT)*. This act deal with all the operational issues related to mining, apart from the issue of title to the site which is regulated through the *Mining Act 1982 (NT)*. The Act requires the mining company to produce a Mining Management Plan, at least annually, which contains the schedule of activities for the next 12 months. This schedule must include, *inter alia*, the monitoring programs proposed by the operator, reporting regimes, future development plans, details of management systems for health and safety issues and for environmental management and interpretation of previous environmental data.

In order to operate a uranium mine in the Northern Territory the mining company must have four valid authorisations:

1. An Authorisation to mine which has been granted in recognition of the operator having a Mine Management Plan (MMP) approved in accordance with the requirements of the Mining Management Act and any additional conditions specified by the NT Minister. In the specific case of uranium mining, the NT Minister must also consult with the Australian Government Minister and act in accordance with any advice provided by that Minister before issuing the Authorisation.
2. The operator must have either:
    - At Ranger -an Authority to mine issued under s.41 of the Atomic Energy Act (1953)
    - At Jabiluka – a Mineral lease issued under the *Mining Act (1982).*
3. The operator must hold an export licence for radioactive material issued under the *Customs Act 1901* by the Minister for Industry, Tourism and Resources..
4. The operator must also have approval to export uranium from the relevant Australian Government Minister. At present this is the Minister for Resources, but in the future, for any new developments, it would be the Minister for the Environment.

Environmental management

The fact that both the Ranger mine and the Jabiluka prospect are located in "windows" surrounded by the World Heritage listed Kakadu National Park provides an explanation for the intense interest in environmental management at both sites. The close proximity of the Magela wetlands and the floodplains of the Alligator

River systems has led to the development of an intense regime of environmental monitoring and supervision for the mining operations. From the beginning the s.41 authority at Ranger was issued with 44 Environmental requirements (ERs) attached. A similar set of ERs was also found as attachments to the relevant NT legislation and an agreement to mine issued under s.44 of the *Aboriginal Land Rights Act (NT) 1976.* The ERs were in place for 26 years until the original s.41 Authority expired. The process of renewing that Authority provided an opportunity to change the ERs and the stakeholders took advantage of the situation to modify them in the light of advances in technology and more than 20 years operational experience. The revised list of 19 ERs cover the same range of issues but are less prescriptive and thus allow for "best practice" to be continuously improved rather than remain as a static prescription, as in some of the original ERs.

At Jabiluka the ERs are still the original set of 38 as the opportunity to update them has not yet arisen. However, should the project go ahead the expectation is that there would be an opportunity to revise the Jabiluka ERs to mirror the improved set in use at Ranger.

Monitoring

At the ERA sites there is an environmental monitoring program undertaken by the company, and approved by the regulator in consultation with major stakeholders. In addition there is a comprehensive check monitoring undertaken by the regulator and a basic independent monitoring program undertaken by the Supervising Scientist. Monitoring data are reported to the authorities monthly, or more frequently if required, for example in the event of any authorised water release. The whole monitoring program is discussed and interpreted, including analysis of trends, in a major report submitted annually. This report is required to be submitted within 6 weeks of the main creeks ceasing to flow during the dry season. This usually means reporting around 1 August each year, which is in time for the document to be discussed at the August meeting of the Alligator Rivers Region Advisory Committee (ARRAC), the prime forum for data exchange and discussion between stakeholders. ARRAC meets twice a year in August and December to discuss the data from the previous wet season and the preparations for the following wet season respectively.

Check monitoring data from the NTDBIRD are interpreted and reported every six months and are also discussed at the ARRAC meetings.

The data from the Supervising Scientist's monitoring program are published to a site on the internet each week, whilst the creeks are flowing. In addition the data are interpreted and discussed at the regular ARRAC meetings.

Risk assessment studies

South Australia

Legislation and regulation

In South Australia the application of Australian Government regulation is broadly similar to that in the Northern Territory with the marked exceptions of the absence of the Supervising Scientist and any reference to the *Aboriginal Land Rights (NT) Act 1976.* There are two operating uranium mines. The in-situ leach mine at Beverley and the underground mine at Olympic dam. In both cases the mine operator is still required to possess two approvals from the Australian Government, as follows :

- An export licence for uranium issued under the *Customs Act 1901*
- An approval from the relevant Australian Government Minister to export uranium

Remaining legislative requirements arise from South Australian legislation and include :

- A licence to mine and mill radioactive ores issued under the *Radiation Protection and Control Act 1982 (SA)*
- A mining lease issued under the *Mining Act 1971 (SA)*
- Permits for all water wells drilled, issued through the *Water Resources Act 1997 (SA)*

The mine operator must also comply with requirements of other legislation which can have environmental implications including:

- Mines Works Inspection Act 1920 (SA)
- Radiation Protection and Control Act 1982 (SA)
- Environment Protection Act 1993 (SA)
- Dangerous Substances Act 1979 (SA)
- Occupational Health Safety & Welfare Act 1995 (SA)

In addition, for the Olympic Dam mine there is an over-arching piece of specific legislation, the *Roxby Downs (Indenture Ratification) Act 1982 (SA)* which governs many aspects of the operation. The indenture is primarily in place to provide security of tenure for the operator as well as protecting the interests of stakeholders including the State, the workers, the environment, the public at large and the local community. The indenture also protects financial interests of relevant parties through the setting of royalty rates for the various outputs from the mine. The indenture has the effect of modifying several state laws. In particular the operator has to apply to only one source for any permit, authorisation, licence etc related to the project - the Minister for Mines and Energy. There are special exemptions and conditions for the project issued under the *Noise Control Act 1977,* the *Aboriginal Heritage Act 1979* and the W*ater Resources Act 1981*, all SA legisla-

tion. These special conditions have also been applied to legislation which came later, including specifically *the Environment Protection Act 1993 (SA).*

The absence of any role for the Supervising Scientist means that the level of environmental supervision by the Australian Government is considered in some quarters to be less than at the mines in the Alligator Rivers Region. Under clause 11 of the Indenture the mine operator is required to obtain state government approval for an environmental management program, including an associated reporting regime, and the plan must be reviewed every three years. In addition the operator must provide an annual environmental interpretive report describing the outcomes of the pervious year's monitoring program as well as quarterly monitoring reports for submission to the quarterly meetings of the Environmental Radiation Review.

The formal involvement of the Australian Government at both the Beverley and Olympic dam mines is through membership of the stakeholder Consultative Committees. These are known as the Beverley Environment Consultative Committee (BECC) and the Olympic dam Environment Consultative Committee(ODECC). Both committees are required to meet very six months to review the environmental performance of the respective operations. The committees have no regulatory power but function primarily as review bodies.

As mentioned earlier, although there is an Environmental Protection Act in South Australia it is preceded by the Indenture in the case of operations at Olympic Dam. The EP Act is applicable to the Beverley operation and prescribes a general duty of care to the operator not to carry out activities that could result in pollution of the environment, all reasonable care and precautions having been taken. The Environment Protection Agency (EPA) is the authority for the issuing of licences in respect of discharges from mines including all gaseous discharges.

Conclusions

The environmental regulation of uranium mining in Australia is comprehensive at all three active minesites. The regulation involves both the Australian and State governments at differing levels depending on the locations. The most intensive regulation may be seen in the Alligator Rivers Region of the Northern Territory where the Australian Government has an oversight role but is also involved in routine environmental monitoring. The outcomes obtained in terms of environmental performance at all Australia's uranium mines is arguably as good as can be achieved through the implementation of best practice environmental management. The systems may be complex but the successful results speak for themselves.

Risk assessment studies

Acknowledgements

The author would like to thank his colleagues in the various government agencies and mining companies who have contributed data and comments to the preparation of this paper.

References

OECD (2003) Uranium 2003: Resources, Production and Demand. A Joint report by the OECD Nuclear Energy Agency and the International Atomic Energy Agency. Organisation for Economic Cooperation and Development (OECD), OECD, Paris.

RUEI (1977a). The Ranger Uranium Environmental Inquiry First Report. Australian Government Publishing Service, Canberra.

RUEI (1977b). The Ranger Uranium Environmental Inquiry Second Report. Australian Government Publishing Service, Canberra.

Verhoeven, T.J. (1988). Rum Jungle Rehabilitation Project. A report prepared for the Austrlian Mineral Council International Environmental Workshop, Darwin, September 1988. Power and Water Authority of the Northern Territory, Darwin.

Waggitt, P.W. (2004) A history of Uranium mill tailings management in northern Australia. Proceedings, WM'04 Conference, February 29 - March 4, 2004, Tucson, AZ. Waste Management, Tucson.

Former mining activities influence Uranium concentrations in the Elbe river near Magdeburg

Martina Baborowski[1], Margarete Mages[1], Carola Hiltscher[2], Jörg Matschullat[2], Helmut Guhr[1]

[1] UFZ Centre for Environmental Research Leipzig-Halle, Department River Ecology, Brückstraße 3a, 39114 Magdeburg, Germany,
E-mail: martina.baborowski@ufz.de
[2] Technical University Bergakademie Freiberg, Interdisciplinary Environmental Research Centre, Department for Geochemistry and Earth System Science, Brennhausgasse 14, 09599 Freiberg, Germany

Abstract. This paper presents data of dissolved and total uranium concentrations after the 2002 flood event, at a flood in spring 2003, and during an extreme low water period 2003 in the river Elbe. In addition, data from several Saale river tributaries are evaluated. The results reveal the remaining pollution potential in the Mansfelder Land catchment that requires the development of remediation strategies.

Introduction
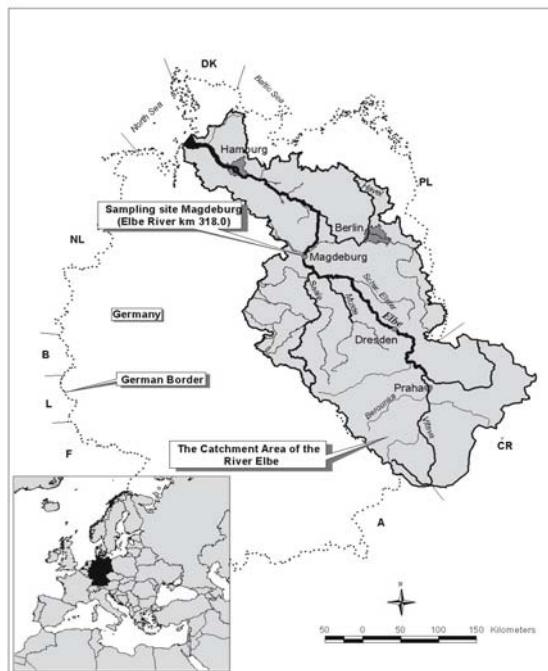
Transport and fate of uranium (U) in the Elbe river are not integrated in the current water quality monitoring programs. As a result of the 2002 flood event in the Elbe and Mulde rivers – that triggered flooding and destruction of former mining areas – U concentrations in the Elbe river are now in the scientific focus.

Samplings were carried out in the Elbe river at different hydrological conditions at Magdeburg monitoring station. This sampling site is also part of the measurement programme of the International Commission for the Protection of the Elbe (IKSE/MKOL) and situated on the left bank at river km 318 (Fig. 1). The water quality here depends on inputs of upper Elbe stretches from the Czech Republic and the Dresden industrial region as well as of the polluted tributaries Mulde and Saale. The confluences of the rivers Mulde and Saale are 59 km and 27 km upstream of the sampling site on the left bank. Both tributaries were affected

by former mining activities. However, under normal discharge conditions, data of the sampling station represent the pollution situation of the middle Elbe.

At low water flow the input of the Saale river to the water quality at this site is increasing, due to the high salt load of the Saale which is detectable at the left side of a long stretch of the river Elbe (about 100 km).

To assess the origin of the Saale U pollution, several of its tributaries were investigated (Fig. 2).

Fig. 1.   Sampling site Magdeburg with main tributaries of the river Elbe (Map: O. Büttner, UFZ Centre for Environmental Research Leipzig-Halle).

Fig. 2.   Lower Saale river stretch with main tributaries.

Risk assessment studies

Methods

The monitoring of the water quality of the Elbe at river-km 318, left side was based on a daily sampling during the extreme events 2002 and 2003 as well as a weekly sampling in the remaining time. From June to August 2004, a screening of the Saale tributaries Weiße Elster, Salza, Schlenze, Wipper, Fuhne, Bode was carried out above their mouths (seven samplings) into the river. Due to the importance of the input of the drainage gallery Schlüsselstollen into the Schlenze a diurnal investigation was performed (September 2004) in the outlet of the gallery as well as above and below the mouth of the gallery into the river.

The content of suspended particulate matter (SPM) was measured according to German Industrial Standards (DIN 38409 part H2). Dry weight (dried for two hours at 105°C) and loss on ignition (ignited for four hours at 500°C) were determined from sample water filtered onto Whatman GF/F glass fibre filter (vacuum filtration method, -200 mbar).
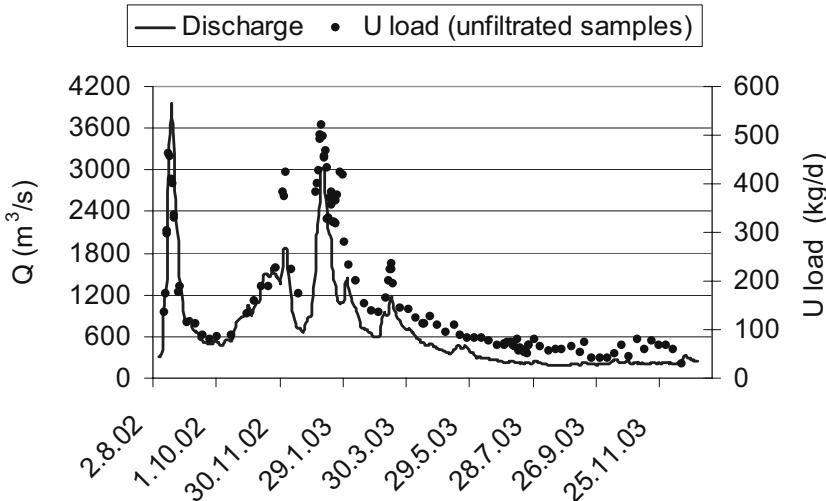
Physico-chemical parameters (pH, water temperature, conductivity, dissolved oxygen, redox potential) were measured in situ.

U was analysed in non-filtered as well as filtered (0.45 µm syringe filters, Minisart, non-pyrogenic) water samples. After microwave assisted digestion with HNO_3/H_2O_2 of the non-filtered samples and acidification of the filtered samples with HNO_3, these were analysed by ICP-MS (Agilent instrument). The detection limit was 0.5 µg/l.
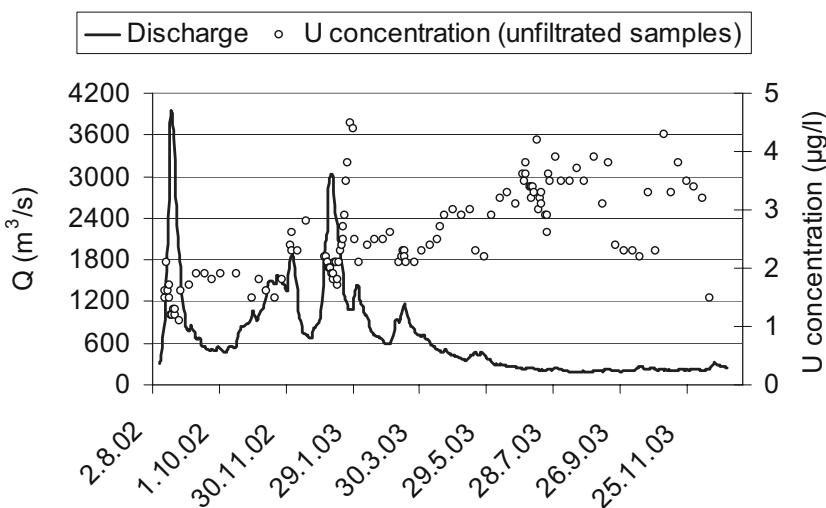
In this paper, U concentrations in non-filtered samples are referred to as "totals", while element contents from filtered samples are referred to as "dissolved". "Particulate" concentrations are calculated from the difference between "total" and "dissolved".

Results and discussion

After a "centennial" flood in August 2002 (originated in upper Elbe and Mulde catchment) and a flood in January 2003 (originated in Saale catchment), the river Elbe saw an extremely low runoff period from June/July until December 2003. The changes of uranium loads with varying discharge in the river Elbe at Magdeburg monitoring station are shown in Fig. 3. The flood of 2002 destroyed built-up and former mining areas and caused a widespread erosion and the relocation of soils and river sediments. Unlike the ore and companion elements arsenic, lead and copper, the concentrations and loads of which were significantly increased in August 2002 (Baborowski et al. 2004), and the uranium load was higher during floods that originated in the Saale catchment (November 2002, January 2003). The data reveal some remaining uranium pollution sources from former mining areas in the Saale catchment (Gera-Ronneburg ore mining area, Mansfelder Land copper schist area). This assumption is supported by increasing U concentrations at low discharge, as shown in Fig. 4.

Fig. 3. Uranium load and discharge between August 2002 and December 2003 in the river Elbe at river-km 318, left bank (discharge values: daily averages, water level gauge river km 326.6)


Fig. 4. Total uranium concentrations and discharge between August 2002 and December 2003 in the river Elbe at river-km 318, left bank (discharge values: daily averages, water level gauge river km 326.6)

Risk assessment studies

Results of water quality measurements during low water periods present higher impact of tributaries to the main stream due to changes in mixing processes. Increasing U-concentrations developped with conductivity (Fig. 5). This clearly reflects inputs of the river Saale especially of the former mining areas in the Saale catchment whose rocks are characterised by high salt content. Increased concentrations of trace elements during long time low water periods were less important to the annual load but to the ecosystem.
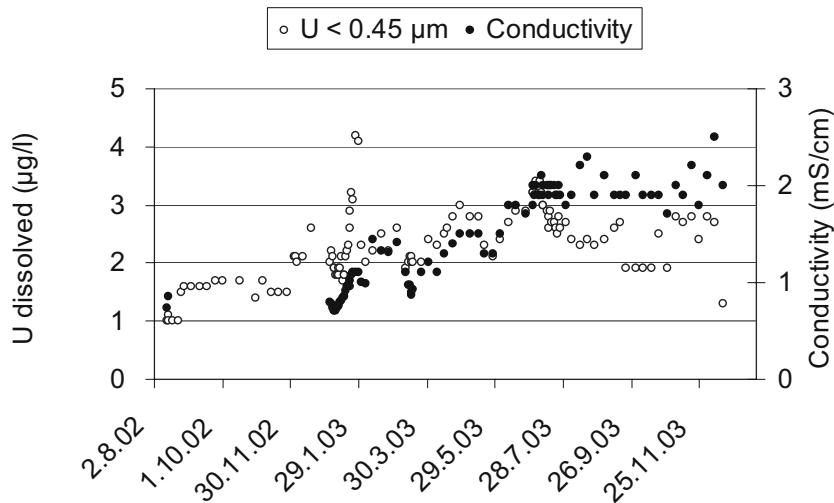
In contrast to the correlation of the dissolved U concentrations and conductivity, particulate uranium showed no evident relation to particulate matter, especially to the organic content as demonstrated by loss on ignition (Fig. 6). Relating to the temporal variability of particulate concentrations, the expected increase in the vegetation period, due to the incorporation or attachment of dissolved uranium to phytoplankton, could not be shown.

However, the results of the measurements at Magdeburg monitoring station raise the question of the participation of the tributaries in the lower Saale catchment on their U pollution. An overview of the variation of U concentrations as well as the mean values of conductivity and SPM is given in Table 1. The results varied strongly between the tributaries. Due to difficulties to obtain actual discharge values representing the sampling locations, the table contains daily averages of discharge near the mouth of the tributaries. The discharge values are data of water level gauges provided by the Saxony-Anhalt State Company for Flood Control and Water Management of the stations Oberthau (W. Elster), Baalberge (Fuhne), Zappendorf (Salza), Friedeburg (Schlenze), Großschierstedt (Wipper) and Hadmersleben (Bode). The value of the Schlenze covered a fixed estimated value of 0.3 m^3/s (based on http://www1.mw.sachsen-anhalt.de/gla/infos/inggeo/seekonferenz.htm) for the outlet of the gallery water.
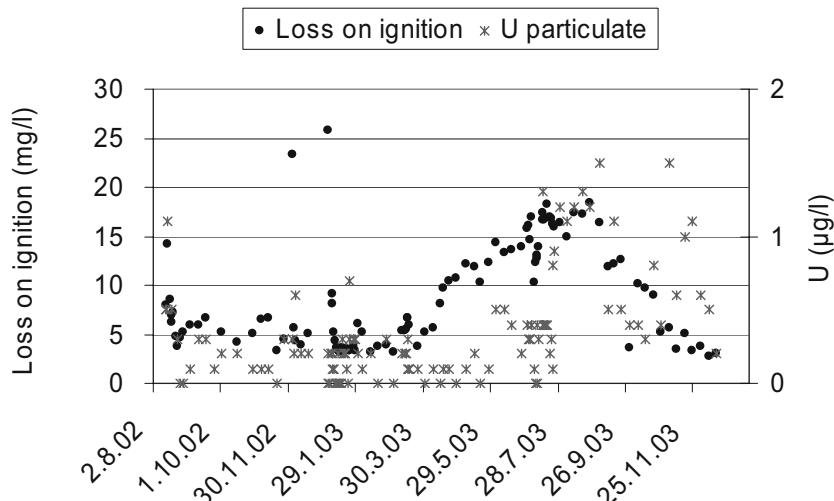
Table 1. U concentrations in tributaries of the lower part of the river Saale (n=7, June to August 2004).

Concentration (µg/l)	Weiße Elster	Fuhne	Salza	Schlenze	Wipper	Bode
Minimum	3.0	11.0	9.7	54.0	2.6	1.4
Maximum	5.0	15.0	17.0	66.0	5.6	3.2
Mean	4.1	12.4	14.5	58.1	4.3	2.4
Median	4.7	13.0	14.0	56.6	4.8	2.5
Conductivity (mS/cm)	2.3	1.9	3.2	36.4	1.2	6.4
SPM (mg/l), mean	16.0	5.9	18.4	19.4	13.9	5.0
Q (m^3/s) Minimum …	9.13 …	0.472 …	0.592 …	~ 0.39 …	0.482 …	6.36 …
maximum	22.4	1.1	0.918	~ 0.44	1.5	7.95

Risk assessment studies

The lowest total U-concentrations were found in the Bode river, the highest ones in the river Schlenze. Beside uranium the highest salt concentrations in the Schlenze were measured, too. The dissolved fraction of the total uranium (data not shown) varied from 80 to 100%.
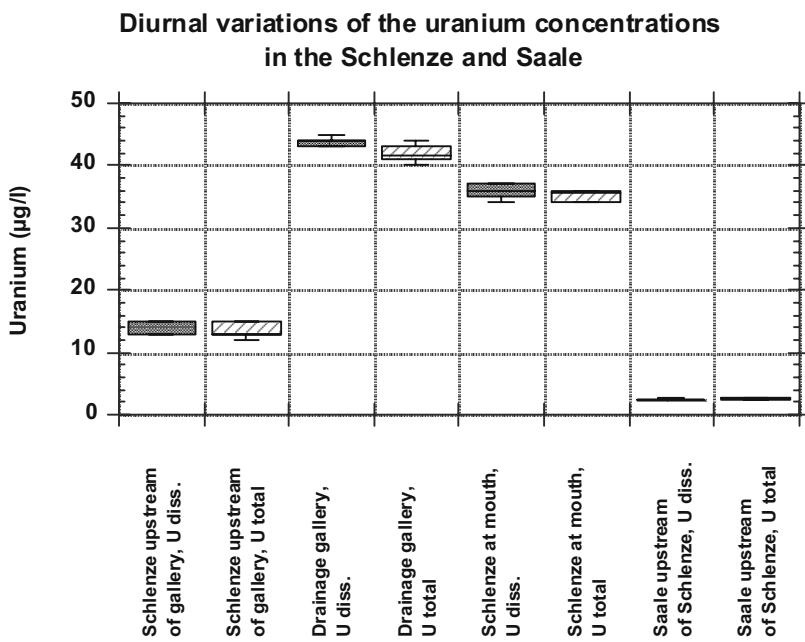

Fig. 5.   Dissolved U concentrations and conductivity in the river Elbe at river-km 318, left bank (August until December 2002 no conductivity values available).


Fig. 6.   Particulate U concentrations and loss on ignition of SPM in the river Elbe at river-km 318, left bank.

Risk assessment studies

Results of diurnal investigations of the Schlenze river are given in Fig. 7. It could be shown that the water quality of the Schlenze depends on the input of the drainage gallery Schlüsselstollen that drains part of the Mansfeld copper schist area. The diurnal investigations at the outlet of the gallery showed low fluctuating, mainly dissolved transported U concentrations related to stable physico-chemical conditions. This indicates groundwater influence on the gallery waters.

The discharge of the gallery water is approximately 3 times higher and accompanied by 3 to 4 times higher U concentrations as compared with the discharge and U concentration of the Schlenze above the gallery outlet. Due to the short distance (about 3 km) between the outlet and the mouth of the Schlenze into the river Saale the quality of the outlet water has a decisive influence on the input of the Schlenze into the Saale.


Fig. 7. Diurnal variation of the dissolved and total U concentration (9./10. September 2004, n=12) at the sampling locations Schlenze, above and below the mouth of the drainage gallery into the river Schlenze, as well as in the gallery outlet, and in comparison in the river Saale above the mouth of the Schlenze.

Risk assessment studies

Conclusions

Using uranium as a tracer, the assessment of flood and low discharge conditions revealed a higher influence of the Saale input to the Elbe river below Magdeburg monitoring station, left side as compared with the Mulde river. The screening of the Saale tributaries indicated a remaining pollution potential in the Saale catchment. The U-concentrations in the tributaries, originating from the Mansfelder Land catchment (Salza, Schlenze), exceeded those from the Weiße Elster river, which is influenced by former mining activities in the Gera-Ronneburg ore mining area. The Schlenze acts as point source for uranium in the Saale due to the relatively constant input of the drainage gallery Schlüsselstollen. Although the load is low compared to the Weiße Elster, and the concentrations will be diluted by mixing with the Saale water, the concentrations considerably exceed existing thresholds. The protection aim for surface water is 3 µg/l (Report BRD 2003). WHO guidelines for drinking water propose an U limit of 2 µg/l (Reimann and Banks 2004). For the aquatic ecosystem it is of importance that the dissolved fraction dominated the total content of uranium. Therefore, the remaining pollution potential from former mining activities in the Mansfelder Land requires the development of remediation strategies.

Acknowledgements

References

Baborowski M, v Tümpling W, Friese, K (2004) Behaviour of suspended particulate matter (SPM) and selected trace metals during the 2002 summer flood in the River Elbe (Germany) at Magdeburg monitoring station. Hydrology and Earth System Sciences, 8 (2): 135-150.
Reimann C, Banks D (2004) Setting action levels for drinking water: Are we protecting our health or our economy (or our backs!)? Science of the Total Environment 332: 13-21.

Risk assessment studies

Modelling Underground Ventilation Networks and Radon Flow for Radiological Protection Using VUMA

Guido Bracke, Hakan Alkan, Wolfgang Müller

Institute for Safety Technology, Schwertnergasse 1, 50667 Cologne, Germany, E-mail: bgu@grs.de

Abstract. In uranium mines radon (^{222}Rn) is of major concern for occupational health and the concentration has to be maintained within allowable limits. It is necessary to ensure safe working conditions and occupational health in advance by predicting the expected radon concentrations throughout the underground network and to provide evidence of this in licensing procedures (SSK 1997; IAEA 2004).

This can be achieved by numerical modelling of the ventilation network as well as the contaminant transport. All flow modelling efforts require the geometrical setup of an underground network and validation. The resulting model of the network can then be used for the development of ventilation strategies with regard to contaminant transport.

This study presents the modelling of radon flow in a ventilation network of a hypothetical uranium mine using VUMA. The ventilation is modelled using the "fixed flow" option. The radon concentrations are computed using non-site-specific but realistic radon sources. Sensitivity is studied by varying the locations and exhalation rates of radon. The results are evaluated in terms of radon concentrations and compared to allowable limits.

The results of this study using VUMA show its applicability for modelling radon flows. VUMA may be used to assess the requirements for ventilation strategies to comply with regulations for occupational radiation protection. Additional conclu-

sions can also be drawn for effective energy management as well as safe working conditions in mines.

Description of VUMA

VUMA is a Windows-based software package for simulating atmospheric and environmental conditions in underground mines (Marx et al. 2001).

VUMA allows a mine network to be built up by linking underground elements such as tunnels, shafts, fans, control elements including air coolers and regulators. In such a network the fluid and heat flow, temperature, humidity as well as dust and contaminant/gas concentration distribution can be numerically modelled. The "steady-state" simulation of the flow allows evaluating the aerodynamic, thermodynamic and contaminant dynamics effects for all network components simultaneously accounting for natural ventilation effects and density changes.
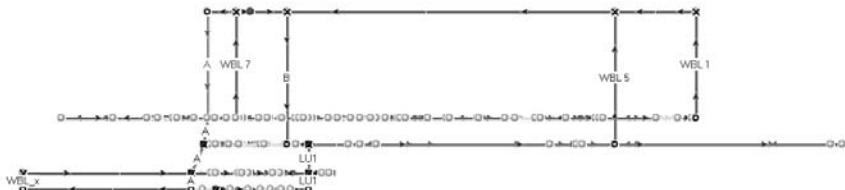
The set-up of a geometrical model of an underground mine and its verification by using actual ventilation data permits the use of this "calibrated" network to monitor the details of the ventilation operation and to plan the necessary changes for new ventilation strategies. The contaminant transport is modelled in VUMA as tracer in the air flow throughout the network. Gas or dust sources can be introduced in each network component and the transport can be monitored for selected/expected flow conditions. In addition radon exhalation as well as its transport taking the decay into account is allowed to be simulated. The radon exhalation rate should be entered into the network components and the steady-state radon concentration distribution can be calculated as function of the aerodynamic conditions.

The big advantage of VUMA is that the geometric view in 3-D is based on real co-ordinates. A diagrammatic view introduces an artificial level spacing to enhance visibility of levels.

When networks are viewed, results are displayed graphically by colouring nodes and/or branches in correspondence with a colour bar graph. The colour bar graph indicates the full range of values from minimum to maximum of the parameter being displayed at that stage.

The network model

A ventilation network is created for a hypothetical uranium mine. The network consists of approx. 225 ventilation components, mainly tunnels and two main shafts in four horizons, at 165 m depth, 206 m depth, 250 m depth and 275 m depth. The north-south extension of the network reaches approximately 2000 m, and east-west extension up to 1000 m (see Fig. 1). The geometry of the tunnels is

Risk assessment studies
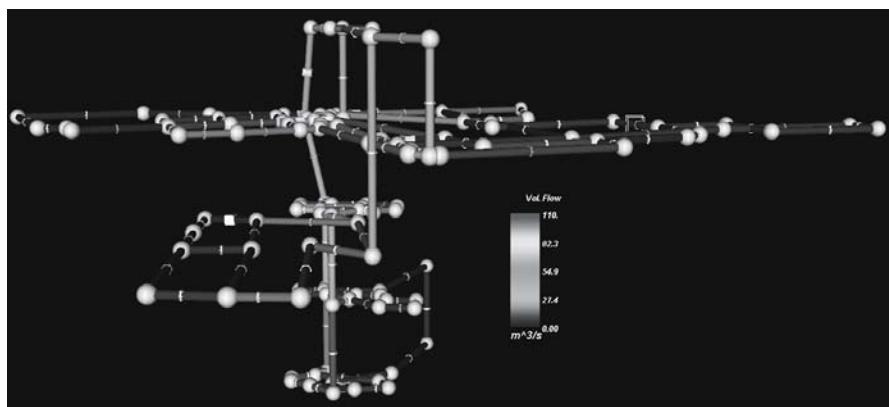
Fig. 1.   Strike view of the network model.

held constant namely as regular quadratic in shape with dimensions of 3x3 m. The shafts are introduced as regular circular in shape with a diameter of 4 m.

Ventilation of the network

Realistic ventilation parameters of real mines are used. The distribution of the incoming fresh air throughout the network is performed by using the "fixed-flow" option for some main tunnels and shafts to allow a simple and a robust ventilation design. The main modelling purpose is modelling of the radon concentration. The friction factor is constant for all tunnels. The flow rate in the tunnels of the network is shown in Fig. 2.

Fresh air is provided from two shafts with a total flow rate of approximately 110 m³/s. The air is discharged from the four venting shafts from the upper two levels at 165 m and 206 m depth. As can be concluded from Fig. 2 most tunnels are ventilated with air flow smaller than 10 m³/s. A linear color scale ranging from zero (dark blue) to maximum value (red) is applied to all figures in the following.

**Fig. 2.**   Flow rates in the network.

Risk assessment studies

Calculation of Radon concentration

Basic scenario

The radon exhalation is set at a uniform rate of 2 Bq/(m^2.s) in all tunnels. This is within an expected range for uranium mines. The result is depicted in Fig. 3.
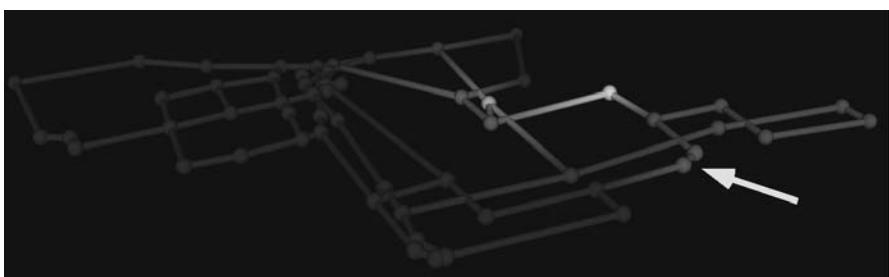
The total ^{222}Rn discharge is 348 kBq/s rsp. 11 TBq/a. The highest radon concentration at a venting shaft is 8 kBq/m^3, whereas a high radon concentration of 2600 kBq/m^3 is observed in a tunnel at the level 165 m. Most radon concentration are below 250 kBq/m^3 (blue).

Additional scenarios

Some demonstrative changes to the basic parameters are made in order to study the effects on the radon concentration.
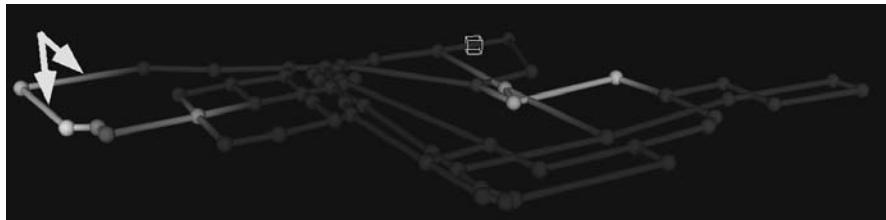
**Fig. 3.**   Radon concentration using a uniform exhalation rate.
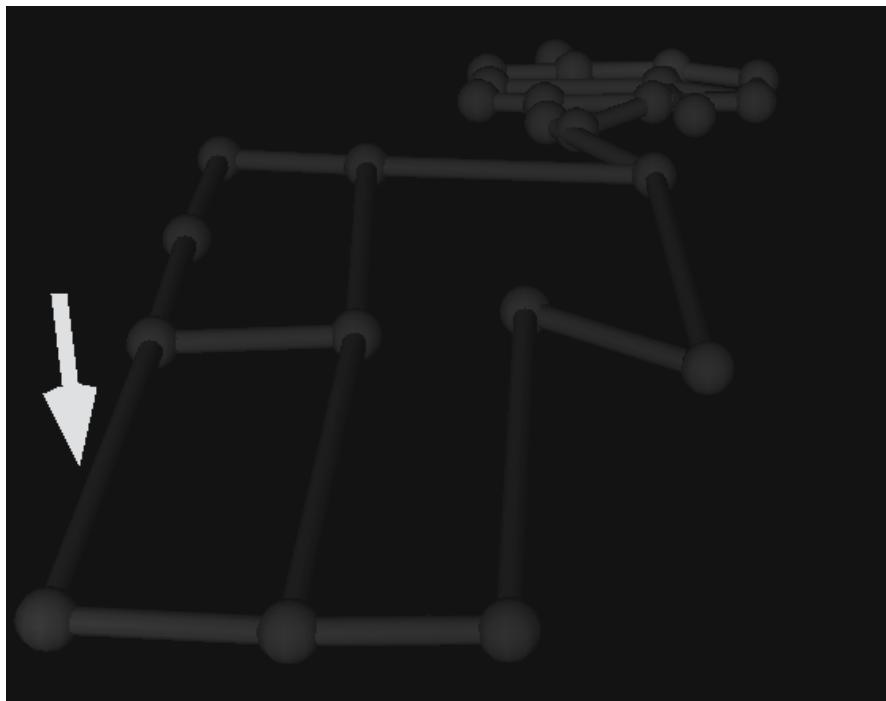
Fig. 4.   Radon concentration of level 165 m after redirection of flow.

Risk assessment studies

Redirected or increased ventilation rates

Redirecting the air flow can lower high radon concentrations. The low flow rate of the tunnel with a high radon concentration in Fig. 3 was increased to 8 m^3/s using the fixed flow option (yellow arrow, Fig. 4.). The resulting distribution of ^{222}Rn concentrations is shown in Fig. 4. The maximum radon concentration is relocated and reduced to 1400 kBq/m^3. Subsequent testing will improve the ventilation network to comply with occupational radiation protections limits.


**Fig. 5.**   Radon sources and concentration at level 165 m.

Fig. 6.   Radon source and concentration at level 206 m.

Risk assessment studies

Increased local radon sources

Localised radon sources are defined with increased exhalation rates of 2000 Bq/(m2.s) in two tunnels on level 165 m and one tunnel on level 206 m. The sources are indicated (yellow arrows) in Fig. 5 (level 165 m) and Fig. 6 (206 m) and the resulting radon concentration is shown. Increased 222Rn concentrations are observed for level 165 m (up to 3320 kBq/m3). Most radon concentration are below 330 kBq/m3. The tunnel at level 206 m has 132 kBq/m3 222Rn. The total 222Rn discharge is increased only slightly by 14 kBq/s to 362 kBq/s rsp. 11.4 TBq/a.

Discussion and Summary

ISTec has introduced VUMA as a new tool for modelling ventilation of underground networks with respect to radon. Setting up a network is time consuming since a large amount of network information is required for a detailed evaluation.

A comparison with other software for modelling of underground mine ventilation shows superior graphical display capabilities which allow an easy understanding of contamination pathways.

Testing on a hypothetical uranium mine network yielded reasonable results. The values calculated for radon concentration in this example have been relatively high since 1 kBq/m^3 ^{222}Rn is already close to the working limit of 40 MeV/cm^3 (depending on equilibrium factor). The average radon discharge of approx. 3 kBq/m^3 (radon discharge of 348 kBq/s, air flow 110 m^3/s) clearly shows that not all locations can comply with this limit.

VUMA also allows adjusting additional parameters such as temperature, pressure and humidity. These options are not discussed with the work presented here.

If a reasonable database (underground network, validated set of parameters and flows) is provided this tool is able to model the radon concentration and to assess the compliance with occupational radiation protection limits. In addition it would allow to assess further details, such as energy costs, and to figure out an efficient ventilation strategy.

Conclusion

The results of our study show the applicability of VUMA for modelling radon concentration in underground networks of uranium mines. VUMA may be used to assess the requirements for ventilation strategies to comply with regulations for occupational radiation protection. Additional conclusions can also be drawn for effective energy management as well as safe working conditions in mines.

References

Marx WM, von Glehn FH, Bluhm SJ, Biffi M (2001) VUMA (Ventilation of Underground Mine Atmospheres) - A Mine Ventilation and Cooling Network Simulation Tool. Proceedings of the 7th International Mine Ventilation Congress, Krakow, Poland, June 2001, Chapter 49, pp 317-323, ISBN 83-913109-1-4.

SSK Strahlensschutzkommission (1997) Richtlinie zur Emissions- und Immissionsüberwachung bei bergbaulichen Tätigkeiten (REI-Bergbau).

IAEA, International Atomic Energy Agency (2004) Occupational radiation protection in the mining and processing of raw materials. Safety Guide No RS-G-1.6: ISBN 92-0-115003-2.

Bigu J (1991) Practical Difficulties in Determining ^{222}Rn Flux Density in Underground Uranium Mines. Health Physics 61 (6): 763-773

Integration of Life Cycle Assessments in the decision-making process for environmental protection measures and remedial action at active and abandoned mining sites

Stefan Wörlen, Stephan Kistinger, Guido Deissmann

Brenk Systemplanung GmbH, Heider-Hof-Weg 23, 52080 Aachen, Germany,
E-mail: g.deissmann@brenk.com

Abstract. Life-Cycle Assessments (LCA) have increasingly been used to evaluate the environmental performance of industrial processes and products and have been employed as a basis in decision making processes in the public and industrial sector. In contrast, assessment methodologies for environmental protection measures and remediation measures with respect to their consumption of natural resources are generally poorly developed. In this paper a methodology for LCA of environmental protection measures and remedial actions is suggested, using the remediation/reclamation of mining sites as an example.

Introduction

During the United Nations UNECD conference in Rio de Janeiro, Brasil, in 1992, the protocol "Agenda 21" (UN 1992) was ratified by more than 170 countries. Since then, in the frame of "sustainable development" environmental Life-Cycle Assessments (LCA), which provide a framework for identifying and evaluating environmental burdens associated with the life cycles of materials and services in a "cradle-to-grave" approach, have been increasingly employed as a basis for decision making processes in the public and industrial sector. In contrast to industrial processes, assessment methodologies for environmental protection measures and reclamation/remediation measures with respect to their consumption of natural resources are generally poorly developed.

In the presentation a methodology for LCA of environmental protection measures and remedial actions is outlined. In this context, the term environmental protection measures encompasses

- end-of-pipe technologies (e.g. water-treatment, exhaust-gas purification, waste management and recycling),
- reclamation/remediation measures at contaminated sites, and
- radiation protection measures.

In general terms, environmental protection measures aim at issues such as (i) reduction/prevention of existing contamination of air, soil, ground and surface water bodies, etc. and/or (ii) prevention of contemporary and future emissions, via air, soil and water pathways, and thus to minimise present and future exposition of natural species and humans to hazardous substances or radiation.

In contrast to their environmental benefits, environmental protection measures themselves usually utilise and consume natural resources such as energy, raw materials, soil/land and are also accompanied by emission of gases (e.g. CO_2 and greenhouse gases, or ozone), waste water and/or noise and odorous substances, which in our opinion suggests the use of LCA for such measures, too.

General approach to LCA

As environmental awareness increases, the environmental performance of products and processes has become a key issue in the industrial and public sector. One tool for the assessment of the environmental compliance and the improvement of the environmental performance of products or industrial systems is the LCA. LCA as defined by ISO 14040 (ISO 1997) comprises a compilation of input and output flows of materials, energy, wastes etc. and associated potential environmental detriments of a product or a service throughout its life cycle.

In general, a four-part approach to LCA – in compliance with ISO 14040ff. (ISO 1997, 1998, 2000a,b) – is widely accepted today (cf. Fig. 1):
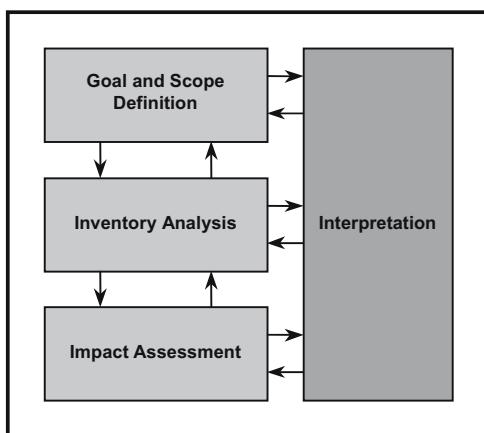
1. Goal and scope definition (i.e. description of the product, process, or activity; definition of boundaries and environmental effects that have to be considered)
2. Life Cycle Inventory (LCI), i.e. quantification of energy/material inputs and environmental releases (e.g. solid wastes, waste water discharge, air emissions) associated with each stage of the life cycle (cf. Fig. 2);
3. Life Cycle Impact Assessment (LCIA), i.e. assessment of the impacts of the material, energy and waste streams identified in the LCI on human health and the environment (cf. Fig. 3); and
4. Interpretation of the results of LCI and LCIA and evaluation of opportunities to reduce energy/material inputs and/or environmental impacts.

One of the key aspects of the LCA is the valuation step in which the results from LCI and LCIA are compiled and weights or relative values are assigned to the different impact categories to make them comparable and to allow a transparent ranking of the options considered. For this purpose, various qualitative and quantitative assessment methodologies have been developed (e.g. verbal argumentation, outranking, monetarization, Ecopoints, UBA/ifeu, CML, SETAC, Eco-indicator,

Risk assessment studies
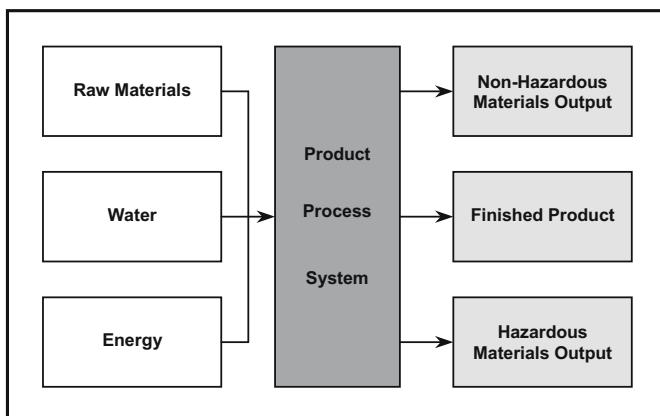
CAU, e.g. IFEU 1995; Barnthouse et al. 1998; Bengtsson 2000; US EPA 2001; MVROM 2001; Ciroth et al. 2003).

Application of LCA to environmental protection measures in the mining industry

The extraction of metallic ores, lignite, coal or other natural resources and the associated milling processes may have environmental impacts on various scales, ranging from local to global. Potential effects to be considered in LCA of mining activities comprise e.g. the consumption of natural resources (including the extracted ore or energy resource), land use, emission of greenhouse gases, dispersion


Fig. 1.   Phases of an LCA.

Fig. 2.   Generic flow diagram of input and outputs for a process or system.

Risk assessment studies

Resource Depletion	**Acidification**
Land Use	**Eutrophication**
Global Warming	**Salinisation**
Ozone Depletion	**Hazardous Wastes**
Photochemical Smog	**Odorous Substances**
Human Toxicity	**Noise**
Terrestrial Toxicity	**Detriments on Ecosystems**
Aquatic Toxicity	**Detriments on Landscapes**
Radioactivity	**Letality/Human Health**

Fig. 3.   Commonly used life cycle impact categories.

of dust, disposal of tailings and waste rock, generation of acid mine drainage, waste water discharges, etc. Environmental protection measures at active mining at milling sites like end-of-pipe-technologies (water treatment plants, tailings management technologies), measures for reduction of energy consumption and air emissions, or recycling techniques (e.g. of lubricating oils) can be addressed as part of the whole production process, i.e. their environmental performance can be evaluated during environmental LCA of the whole process as in other industrial sectors.

However, remedial actions at contaminated and abandoned industrial sites in general are usually not addressed by LCA. Therefore the following part of the presentation focuses on the application of LCA to reclamation measures during the close-out of mining activities and the remediation of abandoned mining sites.

In general, the clean-up of contaminated sites requires appropriate and efficient methodologies for the decision-making about priorities and extent of remedial measures that aim at two usually conflicting goals to (i) protect people and the environment by reducing detrimental impacts to the extent feasible, and (ii) to minimize the expenditure of money and other resources. Extensive mining of polymetallic sulfide ores, uranium ores, or coal/lignite often requires considerable clean-up efforts to protect the environment and the public. This can be seen e.g. from various projects in the context of the UMTRA (Uranium Mill Tailings Remedial Action) and CERCLA (Comprehensive Environmental Response, Compensation, and Liability Act; commonly known as 'Superfund') programmes in the United States (e.g. King 1995) or the estimated financial liabilities associated with mine tailings and waste rock in Canada (e.g. BCMEM 1998).

Abandoned mining and milling sites can represent complex environmental situations, where health risks and environmental detriments may result from various sources, such as the discharge of contaminated mine waters into ground and

Risk assessment studies

surface water bodies as well as mining-related hazards like slope failure of waste dumps, failure of tailings dams, collapse of underground workings, etc.. Furthermore, at uranium mining and milling sites, or at sites, where former mining activities were associated with naturally occurring radioactive materials (e.g. extraction of heavy minerals, zircon, REE, tin, etc.), radiological risks (e.g. from radon exhalation, dispersion of radioactive dust from mine wastes, contaminated surface and ground waters) may have to be taken into account.

The clean-up of contaminated mining and milling sites must therefore take into consideration a variety of different contaminants and risks to humans and the environment arising for various exposure pathways. In general, the following factors have to be included in the site assessment and the evaluation of remediation options:

- health damage for humans due to carcinogenic and/or toxic substances (e.g. arsenic, heavy metals) and in some cases radiological risks (external irradiation; incorporation of radioactive substances);
- environmental detriments like damage to ecosystems, such as lakes and rivers, due to the discharge of contaminated mine waters;
- damage to resources due to contamination of groundwater and surface water bodies;
- direct physical risks (e.g. the danger of dam failures) and risks ensuing from the clean-up activities themselves (e.g. working or traffic accidents).

The decision making on appropriate remediation measures at contaminated (mining) sites is generally based on the legal framework and the existing regulatory guidelines (e.g. with respect to surface water contamination, radiation doses for the public, etc.), the reasonably achievable reduction of environmental contamination and remaining risks, and the financial efforts associated with the remediation options/measures in the short- and long-term, taking into account the potential land use and the socio-economic environment. Usually costs and benefits of the remediation measures are focal points in the decision making process and the selection of concrete (technical) measures. In some cases (e.g. if radiation protection is an issue) the risks to workers may be included in the assessment. However, to the authors knowledge, the overall environmental performance of remediation alternatives is mostly not included in the decision-making process, although their consumption of natural resources and the associated emissions and wastes may be rather different. This aspect will be illustrated in the following examples.

One of the major environmental problem at mining sites is the generation of contaminated acid or neutral mine drainage, which may require long term efforts for water treatment. In many cases various active and passive water treatment technologies are available to achieve the required treatment goals. Usually the treatment alternative with the lowest costs is chosen, omitting an assessment of the overall environmental compliance with respect to materials/energy inputs and waste/emission outputs. Active treatment technologies show large differences e.g. with respect to their energy consumption (e.g. membrane vs. neutralisation/precipitation processes), the amount of treatment chemicals required, and/or the amount, toxicity and emission behaviour of the residues (e.g. High density

sludge vs. conventional lime neutralisation). Passive treatment methods ("wetlands", SAPS) are characterised by low energy and material consumption but often utilise large areas and can be associated with gaseous (CO_2, CH_4) or odorous emissions.

The remediation of waste rock dumps and tailings ponds may require the reshaping/recontouring of dumps, the relocation of waste material, and/or the construction of engineered covers e.g. to avoid/reduce acid mine drainage generation and the amount of seepage water, to minimise emission of dusts/radon, or to allow further land use. Potential environmental burdens associated with such measures are fuel consumption of and emission from trucks/loaders used for transport of mine wastes or cover material, consumption of land used as disposal areas for mine waste, or the excavation of soils and clay for cover construction at other locations.

The consumption of natural resources by remediation measures including those during the close-out or at abandoned (large scale) mining sites and their associated emissions as illustrated above should in our opinion be integrated in the decision making process. In this context the use and inclusion of LCA for remediation measures is suggested to derive optimized concepts for the reclamation of abandoned sites. Based on experience with risk based cost-benefit analyses for the decision-making on remediation measures at large scale uranium mining and milling sites (cf. Goldammer et al. 1999, Deissmann and Kistinger 2004), a monetarization approach in the valuation step is suggested to make the different risks and impacts resulting from the site before/after remediation as well as from the remedial action comparable. Furthermore this approach allows the comparison to the financial expenditures for the measures in the short- (e.g. application of engineered covers on waste rock or tailings; backfilling of mine waste in open pits) and long-term (e.g. costs for monitoring, maintenance, seepage collection and – if required – water treatment). This monetarization approach utilises different methodologies for the various impact categories. E.g. the risks for human life and health during, before and after remediation are expressed as a 'mean effective loss of life expectancy' (MEL), which is converted into an equivalent monetary value according to ICRP (ICRP 1991). The monetary equivalent of emissions can be derived by applying the ExternE methodology (EC 1995). Damage to ecosystems, in particular surface water systems, and resources can be expressed in monetary terms, based on the societal willingness and ability to pay for the prevention or mitigation of ecological damage. Uncertainties in the basic data and assumptions made can be taken into account, e.g. by using probabilistic simulation techniques (Monte Carlo simulations).

Concluding Remarks

Reclamation measures at contaminated (mining) sites aim at issues such as (i) reduction of existing environmental contamination and/or (ii) prevention of contemporary and future emissions, to minimise present and future exposition of natural species and humans to hazardous substances or radiation. In contrast to their environmental benefits, these measures themselves usually utilise and consume natural resources (e.g. energy, raw materials, water, soil/land) and are accompanied by emissions (e.g. greenhouse gases, waste water, dust, noise, etc.). In our opinion this aspects suggest the use of LCA for such measures, too, to evaluate not only regulatory compliance (e.g. with respect to ground and surface water quality, air quality, radiation protection guidelines etc.) and costs but also the environmental performance of the remediation measures and their sustainability. In this context, the use of a monetarization approach of risks and impacts in the valuation step of the LCIA is suggested, to make the different impact indicators comparable. The proposed methodology should serve as a basis for rational and transparent decisions about clean-up measures in order to implement optimized remediation concepts, based on a holistic approach that considers aspects of costs, benefits, risks, and consumption of natural resources, including the effects resulting from the remedial action itself.

References

Barnthouse L, Fava J, Humphreys K, Hunt R, Laibson L, Noesen S, Norris G, Owens J, Todd J, Vigon B, Weitz K, Young J (1998) Life cycle impact assessment: the state-of-the-art. SETAC, 145 p

Bengtsson M (2000) Environmental valuation and Life Cycle Assessment. Chalmers University, Göteborg

BCMEM - British Columbia Ministry of Energy and Mines (1998) Policy for metal leaching and acid rock drainage at mine sites in British Columbia.

Ciroth A., Fleischer G, Gerner K, Kunst H (2003) A new approach for a modular valuation of LCAs. Int. J. LCA 8: 273-282

Deissmann G, Kistinger S (2004) Application of risk-based cost-benefit analyses for decision-making in environmental restoration of uranium mining and milling sites. Proceedings International Workshop on Environmental Contamination from Uranium Production Facilities and Remediation Measures. ITN Portugal

EC - European Commission (1995) ExternE, Externalities of Energy. Vol. 2: Methodology.

Goldammer W, Nüsser A, Bütow E, Lühr, HP (1999) Integrated assessment of radiological and non-radiological risks at contaminated sites. Mathematische Geologie 3: 53-72

ICRP International Commission on Radiological Protection (1991): 1990 Recommendations of the International Commission on Radiological Protection. Annals of the ICRP, 21

IFEU - Institut für Energie und Umweltforschung (1995) Bilanzbewertung in produktbezogenen Ökobilanzen. Evaluation von Bewertungsmethoden, Perspektiven. UBA Texte 23/95

Risk assessment studies

ISO International Organization of Standardization (1997) Environmental Management - Life Cycle Assessment - Principles and Framework (ISO 14040)

ISO International Organization of Standardization (1998) Environmental Management - Life Cycle Assessment - Goal and Scope Definition (ISO 14041)

ISO International Organization of Standardization (2000a) Environmental Management - Life Cycle Assessment - Life Cycle Impact Assessment (ISO 14042)

ISO International Organization of Standardization (2000b) Environmental Management - Life Cycle Assessment - Life Cycle Interpretation (ISO 14043)

King VV (1995) Environmental considerations of active and abandoned mine lands – Lessons learned from Summitville, Colorado. U.S. Geological Survey Bulletin 2220: 1-38

MVROM - Ministerie van Volkshuisvesting, Ruimtelijke Ordening en Milieubeheer (2001) The Eco-indicator 99. A damage orientated method for Life Cycle Impact Assessment - Methodology Report

UN- United Nations (1992) United Nations Conference on Environment and Development (Rio de Janeiro, 3-14 June 1992) - Documents - Agenda 21

U.S. Environmental Protection Agency (2001) LCAccess - LCA 101: 1-41

Risk assessment studies

Simulation of Liberation and Transport of Radium from Uranium Tailings

Maria de Lurdes Dinis, António Fiúza

Department of Mining Engineering, Research Center in Environment and Resources – CIGAR. Engineering Faculty of Oporto University. Rua Dr. Roberto Frias, s/n, 4200-465 Oporto, Portugal. mldinis@fe.up.pt;afiuza@e.up.pt.

Abstract. The uranium tailings contain a large amount of radium, besides other radionuclides like uranium, thorium, polonium and lead. The transport and fate of radionuclides in groundwater are assumed to follow the theoretical approach represented by the basic diffusion/dispersion – advection equation. Our algorithm uses the analytical solution for the one dimensional steady-state transport problem of a reactive substance with simultaneous retardation and radioactive decay. The final output is the radionuclides concentration in a hypothetical well location as function of the elapsed time.

Introduction

The environmental effects resulting from uranium mining activities are mainly derived from the wastes generated by the ore processing.

Uranium mill tailings are the solid residues resulting from the leaching of the ores. The tailings possess, in their composition, hazardous radioactive and toxic by-products and are generally disposed in open air piles. Since only the first four isotopes in the uranium 238 decay series are extracted, all other member of the family remain in the tailings at their original activities. In addition, small residual amounts of uranium are left in the tailings, depending on the efficiency of the extraction process used. Although the activity in most uranium tailings is relatively low, some radiological hazard will last virtually forever because of the long half-life of the radionuclides involved.

The uranium tailings disposal represents the highest potential source of environmental contamination for the great majority of uranium mining activities. Approximately 70% of the original activity from uranium ore remains in the tailings and it is essentially due to the ^{230}Th and its descendents, in particular ^{226}Ra. The radionuclides in the tailings are more mobile and chemically reactive than in

original ore. They are now potentially more able to enter in the environment by seepage, leaching and as dust, becoming a contamination source to the air, soil, superficial water and groundwater.

Radium is often considered to be the most important radiotoxic decay product in the uranium decay series not only by its high radioactivity but because it also produces radon (^{222}Rn), an inert gas whose decay products can cause lung cancer. Airborne radon degrades into a series of short half-life decay products that are hazardous if inhaled. However, ^{210}Pb is also an important decay product, both because of its radiotoxicity and because of the mobility of ^{210}Po, a subsequent daughter.

Uranium mill tailings also contain potentially dangerous materials such as arsenic and selenium. These toxic and other radioactive materials like radium and uranium may get into the human body mainly through the food chain if they are not properly disposed off.

The transport of radionuclides from a site may occur by the infiltrated precipitation. As water percolates through the pores, some radionuclides are released from the pile where they are exposed, adsorbed to sediments or dissolved in water. This contaminated water may migrate downward to the subsoil and contaminate the groundwater. Once in the groundwater the radionuclides may become accessible to humans or other forms of life when they reach a hypothetical well. The radionuclides present in the water pumped from a well will represent a potential hazard to the nearby population resulting either from a possible ingestion or from its use for irrigation.

This work proposes a two-direction model for simulating the radionuclides release from a uranium tailings pile and its migration process through the soil to the groundwater. The final result is the radionuclide concentration in the groundwater as function of the elapsed time, at a defined distance from the pile, where is considered to be located the well.

Methods and Results

The Release Mechanism

The model is divided into three sub-models describing each one different processes: (i) the release mechanism which accounts for the infiltrating water through the cover and the radionuclides leaching out from the contaminated material, (ii) the transport either in the vertical direction, downwards into the soil through the unsaturated zone until an aquifer is reached, either in the horizontal direction, through the saturated zone to the well, and finally (iii) the radionuclides concentration in the well water after the elapsed time.

The algorithm may incorporate four zones with different properties for the vertical transport: the cover, the contaminated zone, the unsaturated zone and the

saturated zone. The source is considered homogenous, without taking in account the spatial distribution of the radionuclides activity, and is modelled as an infiltration point where the vertical transport starts.

A simple water balance concept is used to estimate the amount of infiltrating water into the soil which will leach the radionuclides from the contaminated matrix (IAEA 1992). The annual infiltrating water rate can be estimated as a function of the cover failure. It may be necessary to consider both components: the intact portion and the failed portion. For the failed portion, the inflow rate will increase as a consequence of the cover cracking or erosion effects.

The infiltrated water will leach some radionuclides adsorbed in soil being contaminated after the contact with the waste material. A simplified model is adopted in our work considering a single-region flow transport where the water flow is assumed to be uniform through relatively homogeneous layers of soil profile (EPA 1996). The simplified model assumes an idealized steady-state and uniform leaching process to estimate the radionuclides concentration in the infiltrated water based on a chemical exchange process.

The leaching model is characterized by a sorption-desorption process where the radionuclide concentration is estimated as a function of the equilibrium partioning between the solid material and the solution. The degree of sorption between the two phases is described by a distribution or partitioning coefficient, K_d. The following equation is used to estimate the leachate concentration under equilibrium partitioning conditions (EPA 1996; Hung 2000):

$$C_{wt} = I_t / \left[A \left(D\theta + D\rho K_d \right) \right] \qquad (1)$$

From the above equation, it is known that leachate concentration, C_{wt} (Bq/m^3) is determined by (1) its K_d (cm^3/g) value, which decides the relative transport speed of the radionuclide to that of water in the pore space; (2) soil properties such as bulk density, ρ (g/cm^3), the volumetric water content, θ (dimensionless); and (3) the extent of contamination, which is described by the contaminated zone thickness, D (m), area, A (m^2) and the amount of radionuclide activity in the source, I_t (Bq).

Another important mechanism of release is uncontrolled seepage of contaminated liquids contained in the tailings pile. Seepage may initially occur due to the tailings liquids associated with the solids when placed. However, in a longer term, seepage is provoked by water seeping into the tailings moving the radionuclides as water moves through and out of the tailings (IAEA 1992).

The Radionuclides transport

The Vertical Transport

The radionuclides are considered to be mobilized sequentially in two directions: vertically downwards into the soil until it reaches an aquifer and then horizontally through the aquifer to a hypothetical well.

Risk assessment studies

The flow in the vertical direction is simulated for different degrees of saturation depending on the properties of the geologic strata involved. It is also assumed that there is retardation during the vertical transport. The retardation factor (R_v) is the ratio of the average pore water velocity to the radionuclide transport velocity and is calculated assuming that adsorption-desorption process can be represented by a linear isotherm. Following the simplest mathematical approach derived from the Freudlich isotherm equation, the retardation factor can be estimated with the following formula (EPA 1996; Hung 2000):

$$R_v = 1 + \frac{\rho K_d}{\varepsilon R_s} \tag{2}$$

Concentrations of radionuclides in the well water are time-dependent and are function of two transport times – the breakthrough time (vertical transport time to reach the aquifer) and the rise time (horizontal transport time to reach the well). These parameters are combined to estimate the time necessary to transport vertically the radionuclides to the aquifer and also the water velocity in the vertical direction.

The Horizontal Transport

Among the great variety of hydrologic models available in the literature describing the contaminants transport in groundwater, most of them fail in considering the process of radionuclide decay and its sorption and in this way these models are not adjusted for the exposure assessment purpose.

Radionuclides transport and fate in groundwater follow the theoretical approach of the transport processes represented by the basic diffusion/dispersion-advection equation. The model uses the analytical solution for the one dimensional steady-state transport problem of a reactive substance with radioactive decay. The general equation describing the mass conservation law applied to a reactive solute can be represented by:

$$D \frac{\partial^2 C}{\partial x^2} - V \frac{\partial C}{\partial x} \pm \frac{r}{\theta} = \frac{\partial C}{\partial t} \tag{3}$$

In this equation, D represents the molecular diffusion coefficient ($L^2.T^{-1}$), C represents the solute concentration ($M.L^{-3}$), V represents the interstitial velocity ($L.T^{-1}$), θ represents the moisture content (dimensionless) and the r represents the mass produced or consumed. The term $\pm r/\theta$ may have different forms depending on the kind of reactions involved. The component dispersive and diffusive is represented by $\partial^2 C/\partial x^2$, the advection is represented by $V.\partial C/\partial x$ and the concentration gradient is represented by $\partial C/\partial x$.

For the radioactive substances, having a first order kinetic, the parameter r, describes the radioactive decay in the mass conservation law:

$$r = \frac{d(\theta C)}{dt} = -\lambda \theta C \tag{4}$$

Radionuclides that finally reach the aquifer will generally be transported at velocities lower or equal than the flow velocity of the aquifer due to retardation by

the sorption phenomena. The retardation factor, R, is used to estimate the time that it takes to transport the radionuclides to the well located at a defined distance and can be estimated by the equation (2) assuming that all hydro-geologic parameters refers to the aquifer material, namely, the aquifer material density, the aquifer porosity (dimensionless) and the distribution coefficient between the radionuclide and the aquifer material.

The following expression describes the basic equation for the advective and dispersive transport with radioactive decay and retardation for the radionuclide transport in the groundwater:

$$D\frac{\partial^2 C}{\partial x^2} - V\frac{\partial C}{\partial x} - R\frac{\partial C}{\partial t} - \lambda RC = 0 \tag{5}$$

Using this equation implies that the flow of the fluid carrying the radionuclides is steady, uniform and one-dimensional, that the dissolved radionuclides are in equilibrium with those adsorved by the solids in the aquifer formation and that the radioactive decay occurs for both dissolved and adsorved radionuclides. The analytical solution was obtained assuming the mathematical simplification as presented by Hung (Hung 1986) in his optimum groundwater transport model. The term for the contaminant concentration, C, was replaced by the rate of radionuclide transport, Q, in the previous equation (Hung 1986):

$$Q'(t) = Q_0\left(t - \frac{RL}{V}\right)e^{[-(\lambda_d R L)/V]} \tag{6}$$

One of the simplifications assumed is neglecting the dispersion term ($\partial^2 Q/\partial x^2$) and in this way Q'(t) (Bq/yr) represents the rate of radionuclide transport with the dispersion effects neglected. The others parameters represents the rate of radionuclides transport at x = 0, Q_0 (Bq/yr), the elapsed time, t (yr), the retardation factor, R (dimensionless), the distance from the disposal site to the well point, L (m), the interstitial groundwater velocity, V (m/yr), and the radioactive decay constant, λ_d (yr^{-1}).

Neglecting the dispersion in the basic transport equation will generate an inherent error that should be compensated. In this way, a correction factor is used to compensate the effects of longitudinal dispersion (Hung 1986).

The correction factor, η, is defined as a function of the Peclet number and the parameter expressed by $\lambda_d.R.L/V$. This parameter represents the ratio of the radioactive decay constant, λ_d, and the transport number V/(R.L). The Peclet number is a dimensionless parameter which expresses the diffusion process and the convective transport. The transport number can be estimated by the hydrologic system parameters (Hung 1986).

$$\eta = \frac{e^{\left[(P_e/2)-(P_e/2)\left(\sqrt{1+(4\lambda_d RL)/(P_e V)}\right)\right]}}{e^{[-(\lambda_d R L)/V]}} \tag{7}$$

The final analytical solution for the radionuclides transport with the dispersion effects considered, $Q_p(t)$ (Hung 1986):

$$Q_p(t) = \eta Q_0\left(t - \frac{RL}{V}\right)e^{[-(\lambda_d R L)/V]} \tag{8}$$

Risk assessment studies

The Radionuclides Concentration in the Well Water

The processes that control the radionuclides fate as they are transported from the source to the receptor may be divided into the radioactive decay and the transport - destiny. These last processes (sorption, ion exchange and precipitation) can facilitate or retard the movement of groundwater contaminants but radioactive decay always result in loss of the initial activity of the radionuclide. However, radioactive decay also result in an increase of radioactive or chemically toxic daughter products as the parent radionuclides disintegrates.

The leachate concentrations will be diluted by mixing with the ambient water along the travel path. As a first approximation, the degree of mixing may be estimated by the aquifer volumetric flow rate which means the total rate of flow available for dilution, W_A (m³/yr).

The concentration of a radionuclide in a downgradient receptor may subsequently be adjusted for dilution using the $Q_p(t)$ obtained from the previous expression in conjunction with the aquifer volumetric flow rate. As a result, a simple algebraic equation (9) can be used to estimate the radionuclides concentration in the well water, C_{wp} (Bq/m³), corrected for dilution, using the radionuclide transport through the section of the well, Q_p (Bq/yr) and the rate of contaminated water flow available for dilution, W_A (m³/yr). This term, W_A, is calculated considering the lateral dispersion of the flow, the depth of the well penetrating into the aquifer, the groundwater velocity, the porosity of the aquifer material, the site width and the distance from the center of the contaminated site to the well. The final output is the radionuclides concentration in a hypothetical well location as function of the elapsed time (Hung 2000).

$$C_{wp} = \frac{Q_p}{W_A} \tag{9}$$

A Case Study
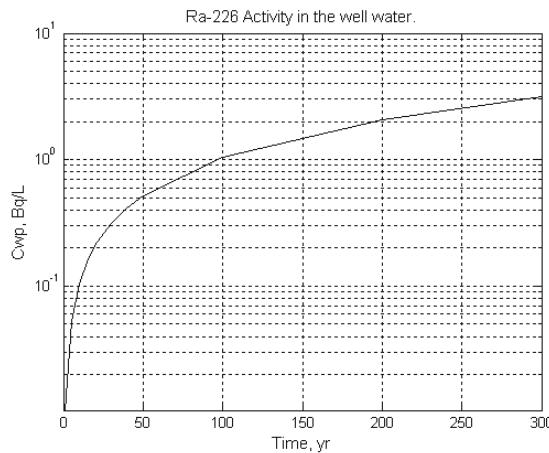
The model was applied to a specific contaminate site, the Urgeiriça uranium tailings. The Urgeiriça uranium mine is located in the north of Portugal, near Nelas (Viseu). The mine is surrounded by small farms and country houses, with most of the local population living in a village within about 2-km of the mine.

The mine's exploitation began in 1913 for radium extraction. The activity of the Urgeiriça mine was maintained until 1944 then exclusively dedicated to the radium production. In 1951, a chemical treatment unit for the production of low-grade U_3O_8 concentrates was built, and in 1967 was transformed into a modern unit with the capacity to treat about 150 t of ore per day (Bettencourt et al. 1990). In 1991, local mining stopped but the facilities were still being used for the treatment of ores from other mines in the same region until 2000.
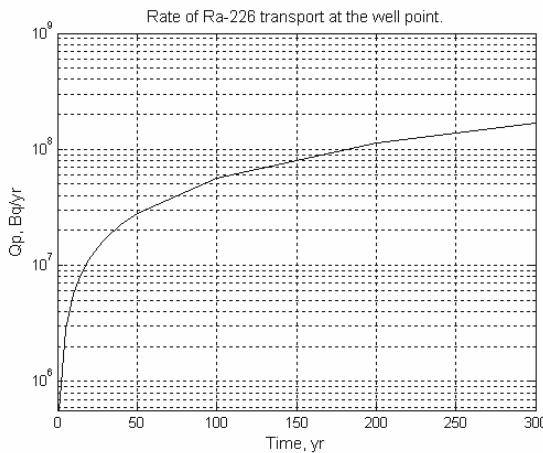
The exhausted exploitation and treatment of the uranium ore in the Urgeiriça mine, has led to an accumulation of large amounts of solid wastes (tailings).

About 4×10^9 kg of rock material was routed into natural depressions confined by dams that cover an area of about 0,13 km^2. A tailings pile is located near the mine and in addition, liquid effluents after neutralization and decantation were used to be discharged into a small streamlet. The solid wastes are composed mainly of sand and silt particles, transported as a pulp to the site from the counter-current decantation, that were previously submitted to grinding and acid leaching.

The model was tested in different situations varying some of the parameters involved. Some parameters were adopted from published data referring to the Urgeiriça site (Bettencourt et al. 1990; Reis et al. 2000; Pereira et al. 2004). The unknown parameters were estimated from available data.
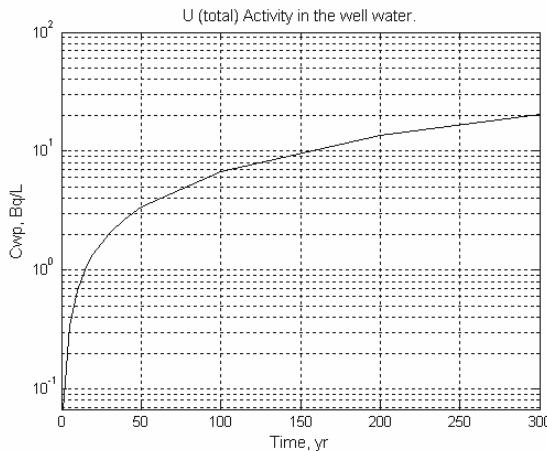
**Fig. 1.** Radium activity concentration in the well water, Bq/L.
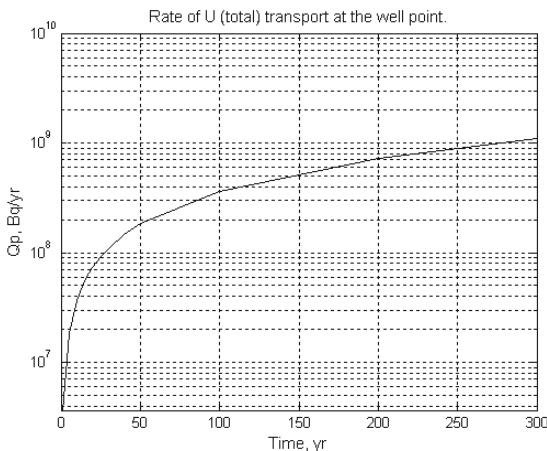
Fig. 2. Cumulative rate of radium release, Bq/yr.

Risk assessment studies

   Data concerning meteorological parameters, namely precipitation and evaporation were used for estimate the infiltrating water rate into the contaminated zone. The precipitation and evaporation data refers to the Nelas meteorological station. It was considered that there is no irrigation in the local so the only inflow rate to the water balance is due to precipitation rate.

   The calculating procedure uses the following steps: i) estimative of infiltrating water rate, ii) estimative of the radionuclide concentration in the leachate, iii) the transport in the vertical direction through the unsaturated zone, vi) estimative of the radionuclide release rate to groundwater, v) the transport in the horizontal through the saturated zone and vi) the radionuclide concentration in the well.


**Fig. 3.**   Uranium activity concentration in the well water, Bq/L.

Fig. 4.   Cumulative rate of uranium release, Bq/yr.

Risk assessment studies

The contaminated site is considered to be a total area of approximately 133 000 m^2. We considered, for this case, the inexistence of a covering system in this area and that surface is homogeneous without cracking. The radionuclide concentration was also considered homogenous and equal in all the contaminated area: an average value for each radionuclide concentration was used.

Local hydro-geological conditions were considered for each zone where the radionuclides transport occurs (Pereira et al. 2004), namely for the contaminated zone, for the unsaturated zone and for the saturated zone, different density, porosity, hydraulic conductivity, radionuclide distribution coefficient and thickness, were used. The well is located at the downgradient edge of the contaminated zone.

We considered as initial conditions that for t = 0 the well water is not contaminated and the simulation is done from 0 year until 300 years after the groundwater contamination starts. For the breakthrough time no radionuclides can reach the aquifer until the model simulation exceeds the travel time. As final output we obtain the radionuclide concentration in the well water and also the cumulative rate of radionuclides transported to the well, after the time considered.

The nuclides initially considered were uranium, radium, thorium, polonium and lead. The concentration in the well water was calculated for each radionuclide.

The results presented were obtained for the same case study applied for uranium and radium. Other radionuclides were considered and the results were in accordance with the expected. Due to the slow rates of contamination migration, only radionuclides with relatively long half-life are of importance in the transport process. This is what happened with polonium: a nil concentration was obtained in the well water and it can be explained by the fact that polonium half-life is three minutes for the isotope ^{218}Po and $1,6 \times 10^{-4}$ seconds for the isotope ^{214}Po which means that their half-life is not enough to be mobilized by the groundwater flow and they will decay before they can reach the exposition point, the well water.

The radionuclides ^{230}Th and ^{210}Pb are generally not transported to significant distances due to the particle reactive nature of thorium, which will tend to react slowly in-situ with water, oxygen and other compounds; by in-situ decay forms a wide variety of compounds; the lead has a great tendency to be adsorbed by the aquifer sediments (although such transport may occur under acid conditions). Consequently, the radionuclides of primary concern are ^{238}U, ^{234}U and ^{226}Ra. The Figs. 1-4 show the results obtained for radium and total uranium (combined ^{234}U and ^{238}U).

Conclusions

The work presented may be considered a first approach in modeling the radionuclide release and transport in the groundwater to the purpose of exposure assessment to contaminated water from wells located close to a uranium tailings pile. It predicts the cumulative amount of radionuclides flowing through a section and also the amount of radionuclides reaching the well point.

We should be aware that the application of an analytical solution is limited by its specific form of boundary conditions which can result from some approximation even before the analytical solution can be applied. This will generate some error due to the approximation of the boundary conditions. However, the magnitude of this error depends largely on the conformity between the local conditions and those of the theoretical model.

The model is idealized for a situation in which the hydrological strata can reasonably be approximated by a sequence of uniform, horizontal data.

Many soil specific parameters can affect the amount of time that it takes for a radionuclide to travel to groundwater. We should refer the difficulties that may be found when trying to obtain the data needed to characterize the soil specific parameters for the contaminated soil, the unsaturated zone and the saturated zone for a particular contaminated site. Also the water transporting the radionuclides depends on detailed variations of the hydraulic properties of the media through which the water passes and even during the site characterization phase these data are rarely available. The accuracy of the results predicted is determined by the accuracy of the effective input parameters used.

References

Bettencourt A. O., Teixeira M. M., Elias M. D., Madruga M. J. (1990), Environmental Monitoring in Uranium Areas. In: Environmental Behaviour of Radium, Vol. 2. Technical Reports Series N.º 310, pp. 281-294, IAEA, Vienna.

EPA (1996), Documenting Ground-Water Modeling at Sites with Radioactive Substances. U.S. Environmental Protection Agency, 9355.0-60, EPA 402-R-96-003, PB96-963302, Washington, D.C.

Hung C. Y. (1986), An Optimum Groundwater Transport Model for Application to the Assessment of Health Effects Due to Land Disposal of Radioactive Wastes. Proceedings of Nuclear and Chemical Wastes Management, Vol. 6, pp. 41-50.

Hung C. Y. (2000), User's Guide for PRESTO-EPA-CPG/POP Operation System. U.S. Environmental Protection Agency, Version 4.2, EPA 402-R-00-007, Washington, D.C.

IAEA (1992), Current Practices for the Management and Confinement of Uranium Mill Tailings. International Atomic Energy Agency, Technical Reports Series N. º335, IAEA, Vienna.

Pereira A.J.S.C., Dias J.M.M., Neves L.J.P.F. & Nero J.M.G. (2004), Modelling Efficiency of a Rehabilitation Plan for a Uranium Mill Tailing Deposit (Urgeiriça, Central Portugal). XI International Congress of the Radiation Protection Association, Madrid, Spain, 23-28 May.

Reis M., Faísca C., Brogueira A., Teixeira M. (2000), Avaliação da Exalação de ^{222}Rn para a Atmosfera em Barragens de Estéreis das Minas da Urgeiriça. Report DPRSN Serie A, N.º 2, Sacavém, Portugal.

Risk assessment studies

Preliminary Hydrogeologic Investigations of Nubia Sandstone and fractured Basement Aquifers in the Area between El Shalateen and Halayeb, Eastern Desert, Egypt

Yehia L. Ismail[1], Esam El Sayed[2], Mohammed A. A.Gomaa[1]

[1]Desert Research Center, Mataria, Cairo, Egypt
[2]El Minia Univeristy, Faculty of Science, 61519 Minia, Egypt,
E-mail: esamelsayed@yahoo.com

Abstract. El Shalateen-Halayeb triangle is a promising district for tourism and agricultural development. Pre-Miocene rocks (fractured basement and Nubia sandstone) represent the main water-bearing formations in the investigated area. Rainfall and occasionally flash floods represent the main sources of recharge. Groundwater occurrence and movement in basement aquifer is mainly controlled by the structural elements, where interaction between fractures and intrusive dykes reflect a good environment for groundwater entrapment. In fractured basement aquifer, the transmissivity ranges from 2.75 m^2/day to 784 m^2/day. Such wide variation could be attributed to the lateral facies changes as well as the impact of the complicated structural setting. Nubia sandstone is detected as a water-bearing in Abraq, Abu Saafa and EL Dif localities, its transmissivity varies from 2.72 m^2/day to 72.4 m^2/day. Poor potentiality of aquifers is mainly due to high channel gradient, which gives no chance for groundwater replenishment. Regionally, the direction of groundwater flow is mainly restricted by the variable hydraulic gradients from locality to another.
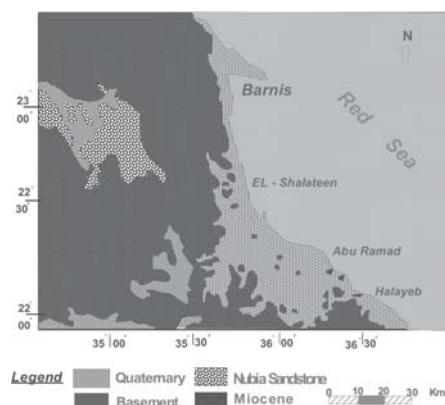
Twenty-three groundwater samples were collected and chemically analysed. Groundwater salinity of basement aquifer varies from 438 mg/l to 10409 mg/l, reflecting a wide variation in groundwater quality from fresh to saline. The groundwater quality of Nubia sandstone aquifer varies from fresh to brackish, where the

salinity ranges from 459 mg/l to 1292 mg/l. In basement aquifer, the type Cl–Na is dominant, while in Nubia sandstone aquifer, HCO_3-Na and Cl-Na water types are recognized. In basement aquifer, the groundwater is mostly characterized by permanent hardness (except Nos. 1, 6 & 13 have a perfect temperary hardness). In Nubia sandstone aquifer, the groundwater is mainly characterized by temporary hardness. In basement groundwater, Cl is the most correlated anion with salinity (R^2 = 0.9615), and Na is the most correlated cation with salinity (R^2=0.9153). In Nubia sandstone groundwater, SO_4 is the most correlated anion with salinity (R^2 = 0.7573) and Na is the most correlated cation with salinity (R^2 = 0.8578). Groundwater quality was evaluated for different uses and some recommendations were given.
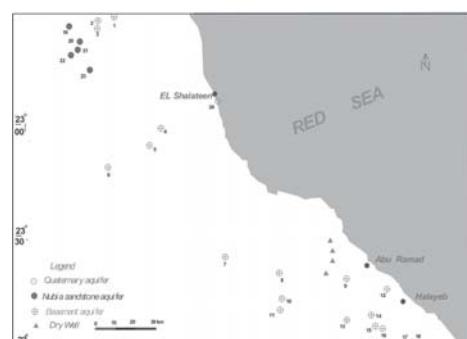
Introduction

Rising populations in Egypt are putting increased pressure on existing fresh Nile water supply. Arid and semi–arid regions are subjected to sustainable development, so they are vulnerable to drought and rapidly rising water demands. Groundwater management in such regions needs an implemented policy emphasizing optimal utilization of water resources. The main objective of this study is to evaluate groundwater resources quantitavely and qualitatively.

Meteorologically, Eastern Desert lies within the Egyptian arid belt. The investigated area is characterized by scarce rainfall and occasional flash floods, so, floodwater control should be taken into consideration.


**Fig. 1.** Geological map of Barnis – Halayeb district.

Fig. 2. Water points distribution withinthe investigated area.

Risk assessment studies

Hydrographically, the investigated area is distinguished into three great basins facing Red Sea to the east. The first is Barnis basin (3000 km^2), the second is EL Shalateen – Abu Ramad Basin (2300 km^2) and the third is Halayeb Basin (2500 km^2). Geologically (Fig. 1), the investigated area is occupied from the western side by basement rocks. Nubia sandstone outcrops close to water divide. Tertiary volcanic rocks are extruded at the foot slope of Red Sea mountainous shield. Isolated patches of Miocene sediments outcrops due west of Abu Ramad and Halayeb area, (alternating limestone and marl of Gebel EL Rusas Formation). Quaternary deposits form deltas of Wadis as well as Wadi fill of main channels.

Groundwater Occurrences

Twenty-three water points were selected to evaluate groundwater resources in the study area (Fig.2, and Table 1). Eighteen of them are tapping fractured basement aquifer and five get their water from Nubia sandstone aquifer in the upreaches of Wadi Hodein.

Hydrogeologic conditions of the basement aquifer

Fractured basement aquifer is composed of older granitoids, younger granites, gneisses, migmatites, schists, metasediments, gabbro, diorites and quartazites. These rocks are highly weathered and strongly fractured, jointed as well as faulted, giving a great chance for accumulation and movement of groundwater. Depth to water varies from 1 m at Mahareka well (No. 10) to 27 m at Gomidlum well (No. 8). Water level ranges between + 40 m at Meisah well (No.7) and + 326.5 m at Salalat Osar well (No.13). Groundwater occurrence and movement in fractured basement are mainly controlled by the orientation, size and density of the intrusive dykes, which act as a doming factors for percolated water as in EL Gahelia well (No.1). Interaction between fractures and intrusive dykes reflects a good environment for groundwater entrapment (Aggour and Sadek, 2001).

Risk assessment studies

Table 1. Hydrogeological data of the investigated aquifers   (Jan, 2004).
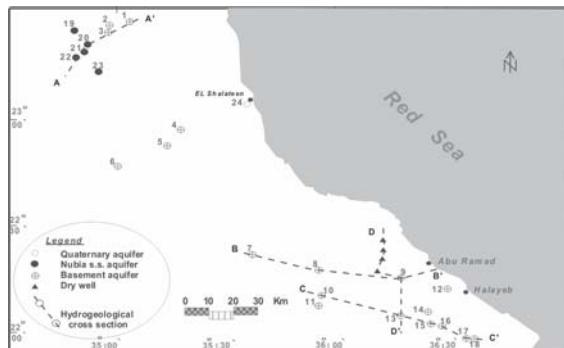
Well No.	Water Point	Basin	Aquifer Facies	Well Type	Well Diameter (m)	Depth to Water (m)	Total Depth (m)	Ground Elevation (m)	Water Level (m)
1	EL Gahelia well	Wadi Hodein		Dug Well	3.30	3.30	9.50	+400	—
2	Eiqat-a well	Wadi Hodein		Dug Well	2.00	7.00	—	+134	+127
3	Eiqat-b well	Wadi Hodein		Dug Well	1.90	8.50	10.25	+134	+125.5
4	EL Beida-a well	Wadi EL Beida		Dug Well	2.00	4.2	4.4	—	—
5	EL Beida-b well	Wadi EL Beida		Dug Well	1.80	3.00	3.8	—	—
6	Madi well	Wadi Madi		Dug Well	1.90	6.7	7.85	—	—
7	Meisah well	Wadi Meisah		Dug Well	2.10	5.90	—	+45.9	+40
8	Gomidlum well	Wadi EL Deib	Basement	Dug Well	2.00	27	28	+83	+56
9	Aquamatra well	Wadi Audeib		Dug Well	2.10	4.5	—	+285	+280.5
10	Mahareka well	Wadi EL Deib		Dug Well	1.35	1.00	2.00	+85	+84
11	Shoshab well	Wadi EL Deib		Dug Well	1.50	18.16	19.00	+94	+75.84
12	Sararah well	Wadi Sermatay		Dug Well	1.00	17.00	22.38	+112	+95
13	Salalat Osar well	Wadi Sermatay		Dug Well	1.80	13.50	—	+340	+326.5
14	Sararat well	Wadi Sermatay		Dug Well	1.00	21.2	23.00	+220	+198.8
15	Okak well	Wadi Shandodi		Dug Well	1.20	5.40	—	+320	+314.6
16	Eremit well	Wadi Shandodi		Dug Well	2.15	11.80	—	+300	+288.2
17	Frukit-a well	Wadi Shalal		Dug Well	2.00	17.0	—	+300	+283
18	Frukit-b well	Wadi Shalal		Dug Well	3.15	15.5	17.7	+300	+284.5
19	Ain Abraq	Wadi Abraq		Spring	—	Flowing	—	—	—
20	Abu Saafa-a well	Wadi Hodein	N. Sandstone	Drilled	—	22	310	+270	+248
21	Abu Saafa-b well	Wadi Hodein		Drilled	—	8.17	90	+315	+307
22	Abu Saafa-c well	Wadi Hodein		Drilled	—	13.30	87	+294	+281
23	EL Dif well	Wadi EL Dif		Drilled	—	21.75	134	+241	+219

Risk assessment studies
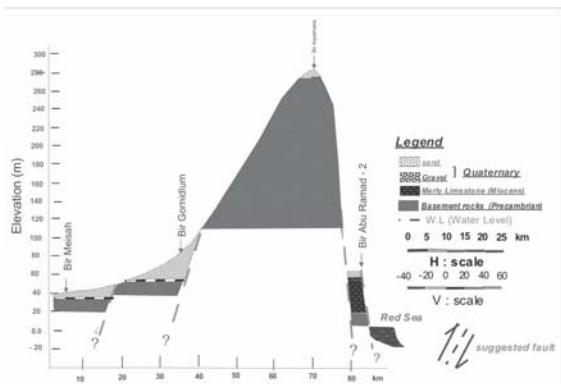
Abu Ramad area

To understand the hydrogeological setting of the basement aquifer at Abu Ramad area, a hydrogeological cross-section A–A' was constructed (Fig. 3a and 3b). The section crosses Meisah well, Gomidlum well, Aquamatra well and Miocene rocks (marly limestone). All these water points are tapping fractured basement aquifer.
   The section reflects the following:
- Faults are dominant in the study area.
- Two geological units are recognized, as a thin layer of Quaternary wadi fill, and the fractured basement rocks.
- It hosts four separate local and limited water-bearing rock units. The first body is located at Meisah well. The second one is located at Gomidlum well. The third one lies at Aquamatra well, while, the fourth water body is located at the eastern side of this section.
- The water level varies from + 40 m at Meisah well to + 280.5 m at Aquamatra well. It is attributed to geographic irregularities.

**Fig. 3a.**   Direction of hydrogeological cross sections.
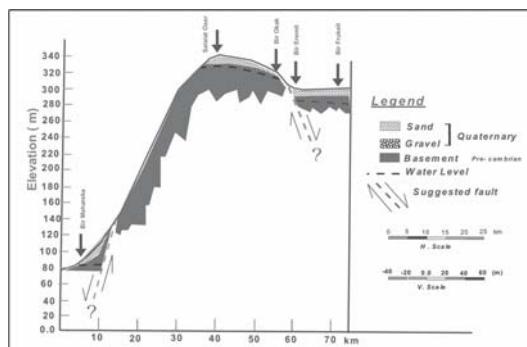
Fig. 3b.   Hydrogeological crossection B–B' from west to east (Abu Ramad region).

Risk assessment studies
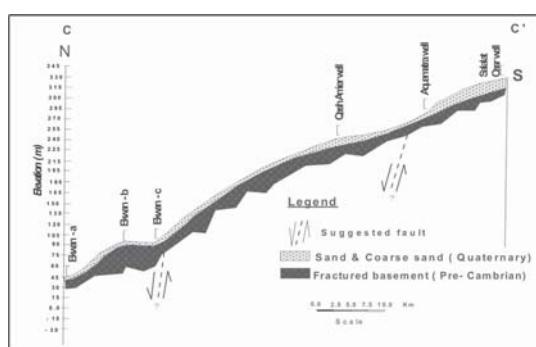
Halayeb area

To throw the light on the hydrogeologic setting at Halayeb area, a hydrogeological cross-section B-B' was constructed (Fig.4). It traverses Mahareka well, Salalat Osar well, Okak well, Eremit well and Frukit–a well. Two horizons could be recognized from top to bottom as following:

- The upper one is represented by a thin layer of Quaternary wadi fill deposits, while the lower reflects the water-bearing formation composed of fractured basement rocks.
- Water level varies from + 84 m at Mahareka well (No. 10) to 326.5 m at Salalat Osar well (No. 13) due to topographic irregularities.

Moreover, the areal extension of the hydrogeological setting encountered in this region was illustrated through the cross section C – C' (Fig. 5). The section revealed the extensions and characteristics of geological boundaries, barriers or structural faults that have a direct impact on the groundwater occurrence and its movement. It is clear, that the structural dykes act as barriers against the groundwater movement towards the north. So, the recent bore holes tests are dry.


**Fig. 4.**   Hydrogeologic cross section B-B' from west to east (Halayeb region).

Fig. 5.   Hydrogeological crossection (C–C') from north to south (Abu Ramad – Halayeb district).

Risk assessment studies

Hydraulic parameters

Seven pumping tests were carried out on selected seven dug wells using the following methods:

$T = Q / 4JI \, sw * F(Uw, B)$ $S = 4 \, Tt / (rw)^2 * (Uw)$ (Papadopolus   and Cooper, 1967)

$T = (rc)^2 / t * 1$ $S = (rc)^2 / (rs)^2 * \alpha$ (Papadopolus et al., 1973)

Where,

T: is the transmissivity (m^2 /day)

Q: is the rate of discharge (m^3 / hour)

rw: is the well radius (m)

sw: is the well drawdown (m)

rs: is the radius of open hole (m)
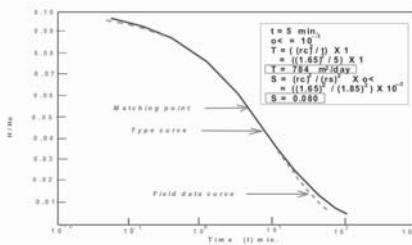
rc: is the radius of casing in interval over which water level fluctuates (m)

F (μw, B): is the well function.
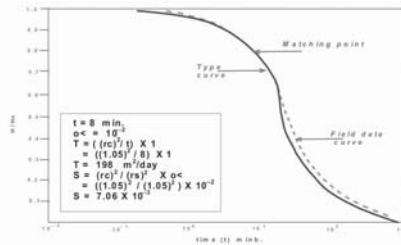
The obtained results (Figs. 6-12, inclusive Table 2), revealed a wide variation in transmissivity due to the strong impact of the structural and lithological setting on the groundwater occurrences. The fractured basement aquifer at Sararat area displays very low transmissivity due to less deformed younger granites. Poor groundwater potentiality is due to weak chance for surface runoff to replenish or feed the concerned aquifer (high velocity of surface runoff as a result of high channel gradient).

Table 2. The calculated hydraulic parameters of the basement aquifer.
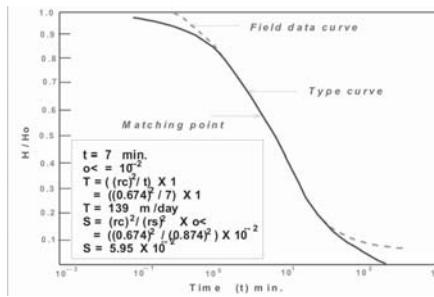
| Well No.	Water Point	T (Transmissivity) m^2/day	S (Storativity) dimensionless
1	EL Gahelia well	784	0.08
7	Meisah well	198	7.06×10^{-3}
10	Mahareka well	139	5.95×10^{-3}
17	Forkit–a well	19.23	1.52×10^{-4}
2	Eqat well	12	2.22×10^{-5}
11	Shoshab well	4.58	$1.13 * 10^{-6}$
12	Sararat well	2.75	$1.27 * 10^{-6}$
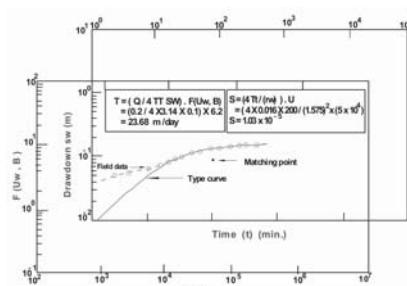
Fig. 6. Analysis of pumping test data of El Gahelia dug well using slug test (Papadopulos et al. 1997).
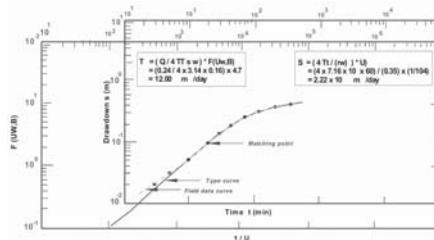

Fig. 7. Analysis of pumping test data of Bir Meisah dug well using slug test (Papadopulos et al. 1997).
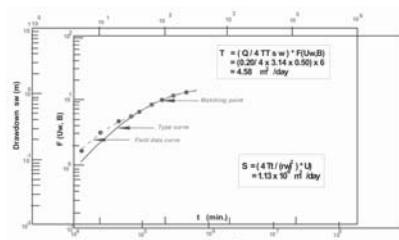

Fig. 8. Analysis of pumping test data of Bir Maharika dug well using slug test (Papadopulos et al. 1997).
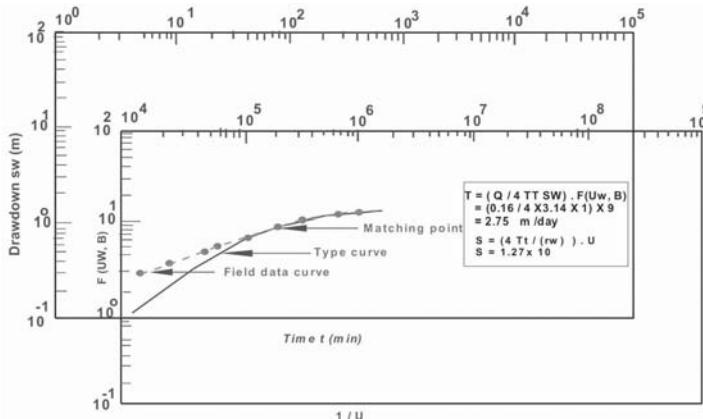

Fig. 9. Analysis of pumping test data of Frokeit well (Papadopulos' method).


Fig. 10. Analysis of pumping test data of Eqat dug well (Papadopulos et al. 1997).


Fig. 11. Analysis of pumping test data of Shoshab dug well using Papadopulos method.

Risk assessment studies

Fig. 12. Analysis of pumping test data of Sararat Sermatay by using Papadopulos method.
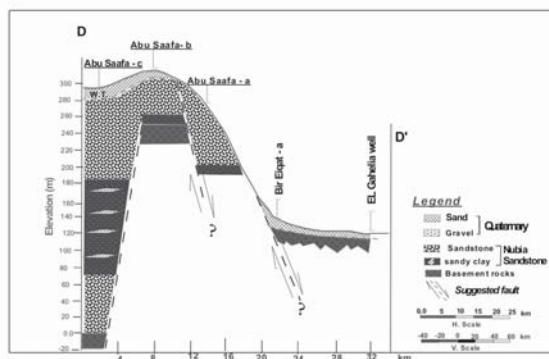
Hydrogeologic conditions of Nubia sandstone aquifer

Nubia sandstone aquifer has a tremendous importance in the area. It covers the northwestern part of the investigated area. Nubia sandstone rests directly on basement rocks. It is composed of fine to coarse sandstone intercalated with clay. The thickness ranges between 100 m up to 500 m (Aglan, 2001). It is detected as a water- bearing in Wadi Abraq, Abu Saafa and Wadi EL Dif. Five representative water points were selected in the study area. The groundwater occurs under confined conditions (Abraq spring) and semi- confined conditions (drilled wells). Rainfall and flash floods on the sandstone plateau and the surrounding fractured basement rocks are considered to be the main sources of groundwater replenishment. Depth to water varies from 8.17 m at (Abu Saafa-b well) to 21.75 m (El Dif well) from the ground surface. On the other hand, the water level ranges between + 248 m at Abu Saafa-a well and + 281 m at Abu Saafa–c well (Table 1).

Abu Saafa area

Abu Saafa area is considered one of the most important Wadis that run in the sandstone territory at the northwest of wadi Hodein. It runs almost E–W at its upstream, then merges to run S 30 o E to join Wadi EL Dif that lies south to it. To investigate the hydrogeological setting in this area, a hydrogeological cross section D–D' was constructed (Fig. 13). This section passes through Abu Saafa - b well, Abu Saafa-a well, Eqat–a well and EL Gahelia well. The section displays the succession of layers from to top to bottom as follows:

Risk assessment studies
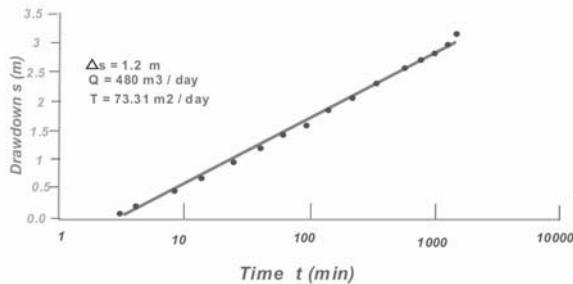
- The first layer extends through the whole section and represents Quaternary wadi fill deposits. Its thickness varies from 4 m at EL Gahelia well to 9 m at Abu Saafa-c well.
- The second layer extends through Abu Saafa's wells only. The thickness of this layer ranges between 15 m at Abu Saafa-a well and 20 m at Abu Saafa-c well. This layer reflects a part of Upper Cretaceous Umm Barmil Formation, which consists of fluviatile sandstone, and is considerable water- bearing formation.
- The third layer is composed of sequences of grained sandstone with thick shale intercalation of Upper Cretaceous Timsah Formation. The total thickness of this layer varies from 8 m at Abu Saafa well-b to 130 m at Abu Saafa-c well. Obviously, this layer is mainly affected by a predicated fault, which acts as a barrier for groundwater flow. So, Abu Saafa springs issues beside Abu Saafa well-b through such fault plain.
- The fourth layer represents the fractured basement rocks. The top surface of this layer is located at shallow depth (46 m from the ground surface at Abu Saafa–b well and deeper (210 m from the ground surface) at Abu Saafa-c well. ON the other hand, the top of this layer is not reached at Abu Saafa–a well.


Fig. 13. Hydrogeological crossection (D–D') from southwest to northeast (Abu Saafa – El Gahelia area).

The hydraulic parameters of Nubian sandstone aquifer

Elewa (2000) mentioned that, the aquifer sediments reflect a wide range of transmissivity (from 2.72 m2/day to 72.4 m2/day)). This could be attributed to the lateral facies change as well as the impact of the structural setting. To confirm the obtained results, a trial was carried out by the author using raw data of pumping tests of EL Dif well (GARPAD, 1996), using Jacob straight line method (1963). The obtained value of the transmissivity is comparable to the previous data (Fig.14).

Risk assessment studies

Fig. 14.   Analysis of pumping test data of Bir El Dif.
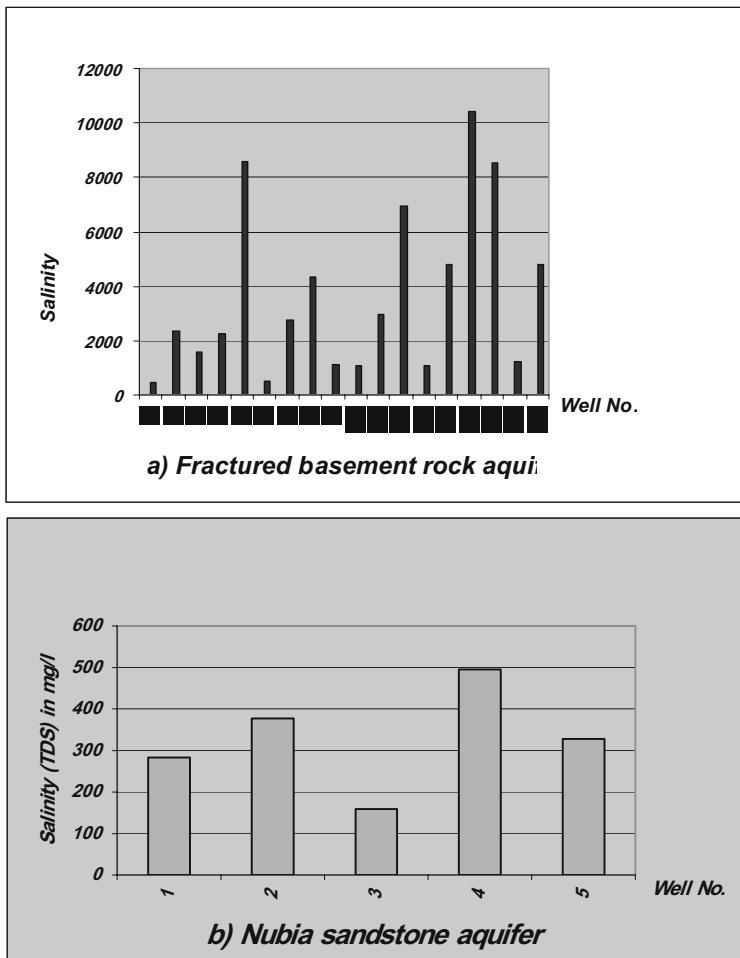
Hydrogeochemical aspects

Hydrogeochemical aspects of parts of the concerned aquifers are discussed through the hydrochemical analyses of twenty three groundwater samples as well as two samples representing rainwater and Red Sea water (Table 3). They reflect the following results.

Groundwater salinity

The groundwater salinity ranges from 438 mg/l at Wadi Madi (No. 6) to 10409 mg/l at Wadi Shandodi (No. 15) indicating a wide variation in quality from fresh to saline in the fractured basement rock aquifer (Hem, 1989). On the other hand, the groundwater salinity varies from 459 mg/l at Abraq spring (No. 19) to 1292 mg/l at Abu Saafa wells (Nos. 20 and 21), reflecting fresh to brackish water in the Nubia Sandstone aquifer (as they are closer to the watershed area).

The presence of more than one peak or more than high frequency intervals for the investigated groundwater samples (Fig. 15) confirms the existence of different water types. This could be attributed to the presence of separate local parts of each aquifer and the great variation of facies.


Fig. 15.   Irrigular distribution of groundwater salinities.

Risk assessment studies

Table 3. The hydrochemical analyses data (2004).

No	Water point	pH	TDS	Ca	Mg	Na	K	CO_3	HCO_3	SO_4	Cl
1	EL Gahelia well	8.10	438	9.80	45.24	95	12	7.62	312.5	15	98
2	Eqat–a well	8.35	2368	58.80	107.20	660	27	72.39	418.30	590	644
3	Eqat–b well	7.87	1600	47.04	111.90	385	21	22.90	511.30	370	386.40
4	EL Beida–a well	7.18	2244	135.20	69.54	600	10	Nil	230.12	200	1115
5	EL Beida–b well	7.13	8586	594.10	290.10	2100	13	Nil	275	1100	4352
6	Madi well	7.95	511	46.20	18.10	120	9	Nil	335	50	100.50
7	Meisah well	7.83	2750	219.50	19.05	680	19	11.43	352.5	600	1024.80
8	Gomidlum well	7.12	4330	712.10	160	550	15	Nil	49.70	950	1918
9	Aquamatra well	7.30	1111	58.20	40.10	290	15	Nil	296	180	380.11
10	Mahareka well	7.87	1080	113.68	38.10	220	10	3.81	143.30	135	448
11	Shoshab well	8.39	2980	58.80	71.44	1000	7	15.24	267.30	140	1554
12	Sararah well	7.85	6967	529.20	202.40	1700	23	15.24	286.60	1750	2604
13	Salalat Osar well	8.00	1096	54.9	38.10	310	12	19.05	367.90	100	378
14	Sararat well	8.00	4776	548.8	202.4	975	8	26.67	197.5	495	2422
15	Okak well	7.75	10409	901.6	476.30	2400	7	11.43	205.30	800	5712
16	Eremit well	7.85	8537	352.8	261.95	2500	6	15.24	344.70	100	5129.40
17	Frokeit–a well	7.30	1246	40.50	63.17	350	11	Nil	288.14	150	488.14
18	Frokeit–b well	7.12	4786	812.40	200	610	19	Nil	69.80	1100	2010
19	Ain Abraq	8.10	459	54.88	35.72	75	8	3.81	351.40	15	91.10
20	Abu Saafa– a	7.10	1223	44.10	65.12	310	12	Nil	310	100	537.10
21	Abu Saafa–b	7.30	1292	27.25	22.40	430	11	Nil	599.10	230	272.10
22	Abu Saafa–c	7.11	1219	88.15	67.14	250	14	Nil	265.10	230	438.10
23	EL Dif well	7.10	591	59.20	44.12	100	17	Nil	365	40	148.50
-	Rain water	7.86	155	10	9	21	2	Nil	63	14	31
-	Sea water	7.96	38120	439	1343	12000	380	18	137	2300	21568
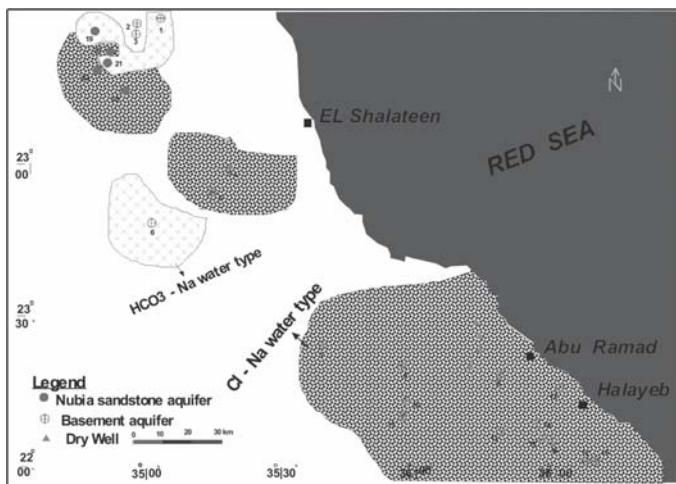
Note : TDS in mg/l; Ca, Mg, Na, K, CO_3, HCO_3, SO_4, Cl in ppm

Risk assessment studies

Groundwater chemical types

The groundwater in the fractured basement aquifer is characterized by Na > Ca(Mg) > Mg(Ca) / Cl > SO4(HCO3) > HCO3(SO4) ionic proportion. So, the groundwater chemical type is mainly Cl–Na (Fig. 16), reflecting the final (mature) stage of groundwater evolution (except Nos. 1 and 6 are characterized by HCO3–Na water type, showing the initial phase of groundwater evolution as they are mainly closed to the watershed area). On the other hand, the ionic proportion; Na > Mg > Ca / HCO3 (Cl) > Cl (HCO3) > SO4 characterises the Nubia sandstone aquifer. Consequently, two chemical water types are recognized. The first type HCO3–Na is recorded at Abraq and Abu Saafa areas (Nos. 19 & 21), reflecting the first stage of groundwater evolution, while the second type Cl–Na is detected at Abu Saafa area (Nos. 20 and 22), indicating the final phase of groundwater metasomatism.

Groundwater hardness
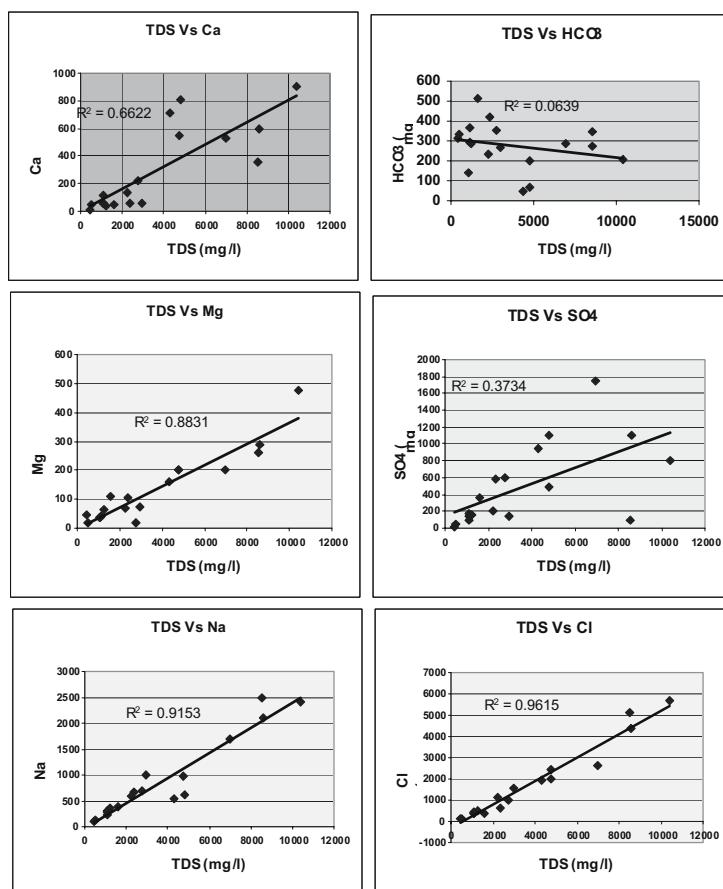
The investigated groundwater is very hard (Table 4). In basement aquifer, it is mostly characterized by permanent hardness (except Nos. 1, 6, 13 have a perfect temporary hardness). This type of hardness can't be removed by boiling. On the other hand, in Nubia sandstone aquifer, the groundwater is mainly characterized by temporary hardness. Such type of hardness can be virtually removed by boiling water, where calcium and magnesium carbonates precipitate.


Fig. 16.   Distributionof different chemical water types.

Risk assessment studies

Salinity-major components relationships

The relation between salinity (TDS) and major components were statistically illustrated (Figs. 17 and 18). According to these diagrams, a positive correlation between salinity and concentration of ions is evident, since the increasing of major constituents leads to the increasing of total salinity. The more significant correlation coefficient, the more correlated with salinity. In the fractured basement aquifer, Cl, Na, Ca & Mg are significant, SO_4 is little significant, while HCO_3 is not significant with total salinity (Fig. 17). On the other hand, in Nubia sandstone aquifer, Na, SO_4 and Cl are significant, while Ca, Mg and HCO_3 are not significant (Fig. 18).


Fig. 17.   Salinity–major components relationship in fractured basement groundwater.

Note: Ca, Mg, Na, Cl vs TDS are significant
SO_4 vs TDS is little significant
HCO_3 vs TDS is not significant

Risk assessment studies

Groundwater classification

The investigated groundwater samples were plotted on semilogarithmic paper suggested by Schoeller (1962). They reflect a general resemblance and similarity among each other (Fig. 19). In the fractured basement aquifers, two ionic patterns are recognized, due to the presence of separate local parts of aquifers characterized by the great facies changes. The first is $Ca > Mg < Na\&K < Cl > SO_4 > HCO_3$ (Nos 4, 5,6,7,8,10,12,14,15 and 18). The second is $Ca < Mg < Na\&K < Cl > SO_4 < HCO_3$ (Nos 1,2,3,9,11,13,16 and 17). On the other hand, in Nubia sandstone aquifer, the groundwater samples follows the pattern; $Ca < Mg < Na\&K > Cl > SO_4 < HCO_3$, exhibiting fresh water characters except the slightly increase of Mg over Ca due to the presence of sediments rich in Mg in Nubia sandstone aquifer.
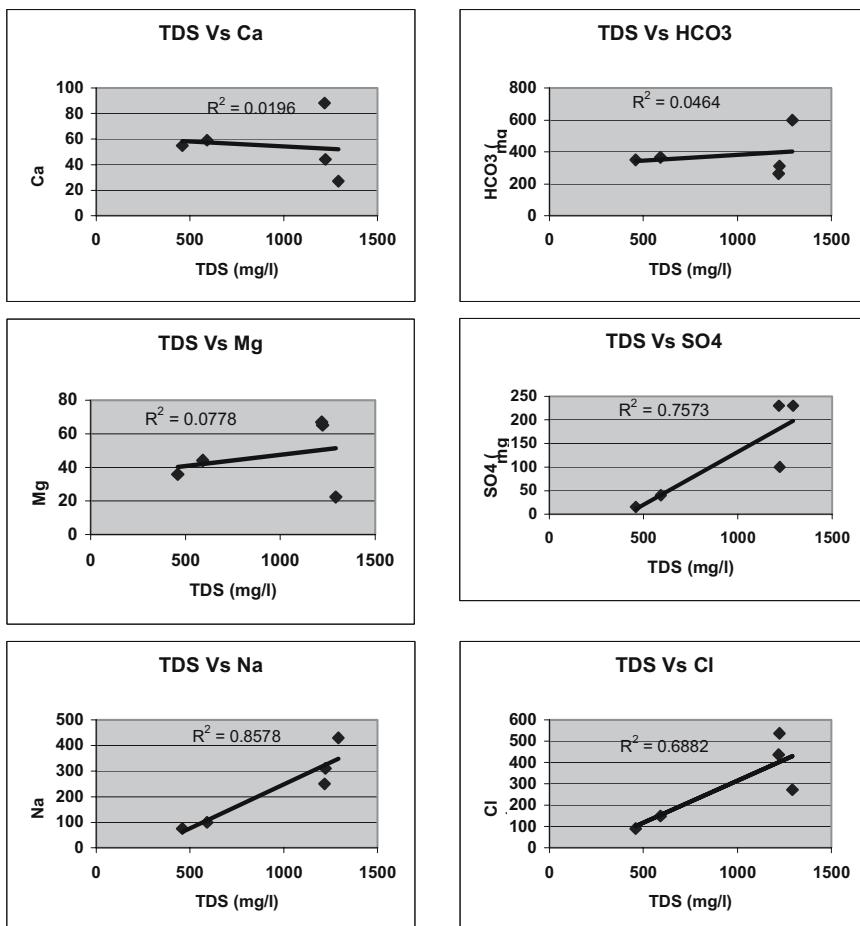

Fig. 18.   Salinity–major components relationship in Nubian sandstone groundwater.

Note: Na, SO_4, Cl vs TDS are significant
         Ca, Mg, HCO_3 vs TDS are not significant

Table 4. Some hydrochemical parameters (2004).

Well No.	Total Hardness*	Alkalinity*	Temporary hardness*	Permanent hardness*	Specific Electrical Conductivity**	Sodium Adsorption Ratio
1	210	275	275	-65	684	2.77
2	560	463	463	97	3700	12.15
3	577	457	457	120	2500	6.97
4	623	188	188	434	3506	10.47
5	2677	225	225	2451	13415	17.65
6	189	274	274	-85	798	3.80
7	981	307	307	673	4296	9.45
8	2436	40	40	2396	6765	4.84
9	341	292	292	48	1735	6.84
10	438	123	123	315	1687	4.57
11	440	244	244	196	4656	20.80
12	2154	259	259	1894	10885	15.87
13	293	333	333	-40	1712	7.87
14	2203	206	206	1997	7462	9.04
15	4211	187	187	4024	16264	16.10
16	1958	307	307	1651	13339	24.59
17	360	236	236	124	1946	8.04
18	2850	57	57	2793	7478	4.97
19	283	294	294	-11	717	1.94
20	377	254	254	123	1910	6.94
21	159	490	490	331	2018	14.83
22	495	217	217	278	1904	4.89
23	328	299-	299-	29	923	2.39
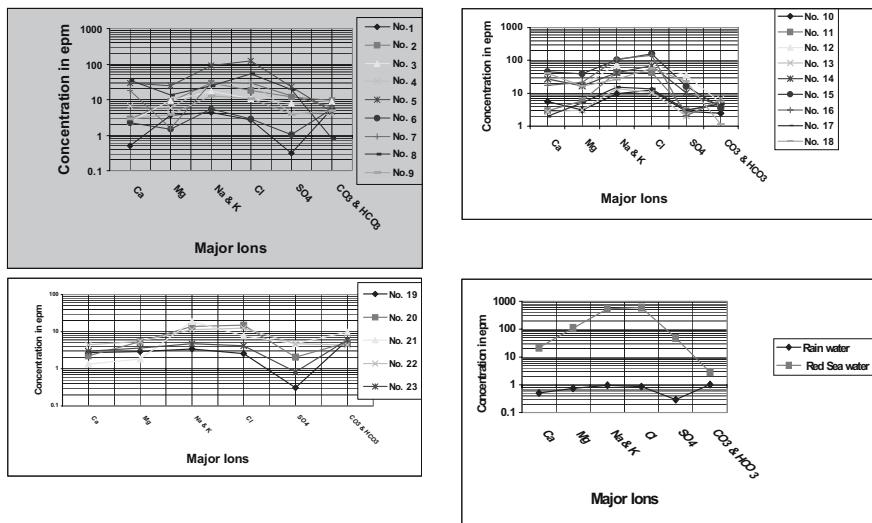
* mg/l as $CaCO_3$ **micromhos/cm

Table 5. Drinking water standards (WHO, 1984).

Items	Acceptable (mg/l)	Permissible (mg/l)
PH	7-8.5	6.5-9.5
TDS	500	1500
Ca	75	200
Mg	50	150
SO_4	200	400
Cl	200	600

Suitability of groundwater quality for uses

Comparing the results of the hydrochemical analyses (see Table 3) with World Health Organization standards (WHO,1984), (Table 5), it is clear that, the groundwater quality of fractured basement aquifer is suitable for drinking at El-Gahlia and Madi areas, where the salinity lies within the range 438 to 511 mg/l (Nos. 1 and 6). In Nubia sandstone aquifer, the groundwater quality is suitable for drinking at Abraq and El-Dif areas, where the groundwater salinity lies within the range 459 to 591 mg/l (Nos. 19 and 23). On the other hand, the proposed approach by the United States Salinity Laboratory staff of agriculture (USSLs, 1954) is applied for determining the suitability of groundwater for irrigation. In this method a nomogram based on specific electrical conductivity as a function of salinity

Fig. 19. Logarithmic representation of the investigated groundwater (Following Schoeller diagram, 1962)

against sodium adsorption ration as a function of sodium hazard is used. Distribution of the groundwater samples within the nomogram (Table 4 and Fig. 20), revealed that, groundwater of El-Gahlia, Madi, Abraq and El-Dif is suitable for irrigation. On the other hand, groundwater quality of El-Beida-b, Gomidlum, Sararah, Sararat, Okak, Eremit and Frokeit-b is not suitable for irrigation due to high salinity as well as high sodium hazard (only can be used to irrigate tolerant crops as palm trees). The rest of groundwater samples are of intermediate scale and suitable to irrigate certain kinds of crops as alfalfa, tomato, lettuce and cucumber.

Conclusions and Recommendations

The aquifers of fractured basement and Nubia sandstone rocks represent the available groundwater resources in the investigated area. The main sources of recharge are the local rainfall and sometimes flash floods after occasional showers. Groundwater occurrence and movement in basement aquifer are mainly controlled by the structural features, where the interaction between fractures and intrusive dykes reflect a good environment for groundwater entrapment. The hydraulic parameters of the fractured basement aquifer revealed wide variation in the transmissivity due to the strong impact of the structural and lithological setting on the groundwater occurrences. The poor groundwater potentiality of the fractured basement aquifer is attributed to the weak chance of infiltration of water during surface runoff to replenish the concerned aquifer.

Risk assessment studies

On the other hand, Nubia sandstone aquifer is detected as a water-bearing formation in Wadi Abraq, Abu Saafa and Wadi EL Dif. It rests unconformably directly above the fractured basement rocks. The groundwater occurs under confined conditions (Abraq spring) and semi–confined conditions (drilled wells). It is worth to mention that, the aquifer reflects a wide range of transmissivity (2.72 m^2/day to 72.4 m^2/day). It can be attributed to the lateral facies changes of the water–bearing rocks as well as the impact of the structural setting.

From the hydrochemical point of view, the groundwater quality of the fractured basement aquifer varies from fresh to saline, while in Nubia sandstone aquifer, it varies from fresh to brackish. In basement aquifer, the type Cl–Na is dominant, while in Nubia sandstone aquifer,

HCO_3-Na and Cl-Na water types are recognized. In basement aquifer, the groundwater is mostly characterized by permanent hardness (except Nos. 1, 6 & 13 have a perfect temporary hardness). In Nubia sandstone aquifer, the groundwater is mainly characterized by temporary hardness. In basement groundwater, Cl is the most significant correlated anion with salinity (R^2 = 0.9615), and Na is the most significant correlated cation with salinity (R^2=0.9153). In Nubia sandstone groundwater, SO_4 is the most significant correlated anion with salinity (R^2 = 0.7573) and Na is the most significant correlated cation with salinity (R^2 = 0.8578).

In view of the present conclusions, aiming to the safety use and development of groundwater resources, the following are recommended:

- A detailed study of the structural setting should be done to find out the relation betwwen Nubia sandstone aquifer and the underlying fractured basement one.
- More attention should be focused on flood insurance through the construction of earth and concrete dykes on the upstream portions, specially of Red Sea wadis, which have high gradients to prevent the risk of flash floods and also to increase groundwater recharge.
- Large diameter wells are recommended to be drilled in the fractured basement rocks.
- Advanced irrigation system must be applied (drip and sprinkle irrigation).
- Chemical analyses should be carried out periodically for groundwater samples to ensure that water is valid for different uses (as a long term monitoring program).

References

Aggour, T. A. and Sadek, M. A. (2001) : "The recharge mechanism of some cases of the different groundwater aquifers, Eastern Desert, Egypt". Bull. Fac. Sci. Mansura Univ., Vol. 28 (1), pp. 34-78.

Aglan, O. Sh., (2001): " Geology of water resources in Wadi Hodein Basin, Southeast of the Eastern Desert. Ph. D. Thesis, Fac. Sci., Ain Shams Univ., 211p.

Risk assessment studies

Elewa, H. H. (2000): " Hydrogeology and hydrological studies in Halaib – Shalateen Area, Egypt, using remote sensing technology and other techniques. Ph. D. Thesis, Fac. Sci. Ain Shams Univ., 105p.

General Authority for Rehailitation Project and Agricultural Development (GARPAD), (1996) :"Lithological and raw data of pumping test of El Dif well". Internal report.

Hem, J. D. (1989):"Study the interpretation of the chemical characteristics of natural water", USGS, Water Supply paper 1473.

Jacob, C. E. (1963) : " Correction of drawdowns caused by a pumped well tapping less than the full thickness of an aquifer". In Bentall, R. (Editor) : Methods of determinig permeability, transmissivity and drawdown. U.S.Geol. Survey, Water-Supplly paper 1536 – I : pp. 272-282.

Papadopulos, I. S., Bredehoeft, J. D. and Cooper H. H. (1973): " On the analysis of slug test data". Water Resources Res. pp. 1087 – 1089.

Papadopulos, I. S. and Cooper, H. H. (1967): " Drawdown in a well of large diameter" .Water Resources Research Division First Quarter, U. S. G. S. Vol. 3 No. 1.

Schoeller, H. (1962):" Les Eaux souterraines " 642 pp. Paris, Massion"

U. S. Salinity Lab. Staff (1954): " Diagnosis and improvement of saline and alkaline soils " U. S. Depart. Agric., Hand – Book No. 60.

World Health Organization, WHO (1984) : "International standards for drinking water". Third edition, Vol. 1, Geneva, Switzerland, 70 p.

Risk assessment studies

Development of water-borne radioactive discharges at WISMUT and resulting radiation exposures

Peter Schmidt, Thomas Lindner

Wismut GmbH, Jagdschänkenstrasse 29, D-09117 Chemnitz, Germany,
E-mail: p.schmidt@wismut.de

Abstract. Since 1989, collected discharges of uranium loads via the water pathway have dropped from a total of 27.5 tonnes to less than 3 tonnes in 2004. Commissioning of modern water treatment plants has greatly contributed to this achievement. Resulting site-specific effective doses to the population are significantly below 1 mSv/a. However, diffuse discharges of contaminated seepage or percolation waters from tailings ponds may cause doses in the order of 1 mSv/a. Capping operations are instrumental in reducing the diffuse discharge of radioactive effluents via the water pathway to a reasonably low level.

Introduction

The radiological situation prevailing in 1991, immediately after the termination of uranium ore mining and uranium processing in East Germany, was marked by the discharge of radioactive substances carried by water both into receiving streams and underground. Such discharges contributed significantly to public exposure. Ever since the state-owned company Wismut GmbH initiated remediation procedures, the volume of discharges was continuously reduced. Furthermore, the changing of nature of discharge and its comprehensive monitoring helped to systematically bring down public radiation exposure at former mining sites in Thuringia and Saxony.

The development of discharges, of radiation exposure due to radioactively contaminated waters, as well as avenues of reducing this exposure further are discussed below.

Classification of water-borne emissions
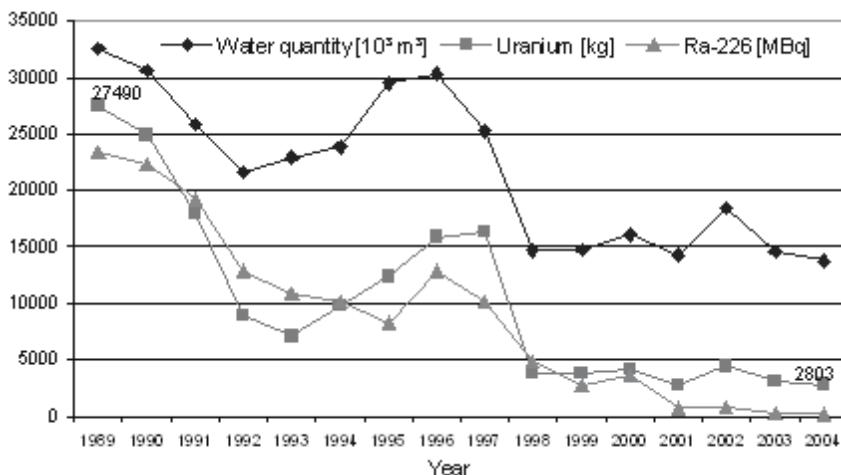
In the following, a clear distinction is made between:
1. Controlled discharge into receiving streams or underground: Typically, such waters are collected and monitored for volume and quality. Discharge is from specific hydraulic structures (drainage structures) or from water treatment plants.
2. Diffuse leakage of seepage and percolating waters into ground and running waters: Quantity and to some extent the quality of such waters can only be evaluated by modelling. Their sources are infiltration waters percolating through mine dumps, tailings ponds, and mine workings.

Development of controlled water discharges and of resulting radiation exposures

The development of controlled radioactive discharges in terms of the radiological main components uranium and Ra-226 together with the quantities of discharged waters is illustrated by Fig. 1.

The development of pumped mine waters discharged from the Ronneburg, Aue, Gittersee, and Königstein mine fields (flooding of mines involving treatment of pumped flood waters) has a decisive impact on waste water quantities. The drop in concentration levels in water discharges is reflected by a more significant drop in the loads released or the activities discharged, respectively, in comparison with the decrease in water quantity. This is the result of powerful water treatment plants


Fig. 1.   Development of radioactive discharges from 1989 to 2004.

Risk assessment studies

(WTP) coming on line. Table 1 provides a picture of water treatment plants operated by WISMUT, their performance parameters, as well as permitted discharge standards.

In addition to treated waters, controlled discharge also includes untreated waters. In the majority of cases, feed waters are made up of collected seepage from mine dumps for which no conditioning in terms of (some local) treatment is yet available and which therefore have to be discharged into receiving streams of appropriate size. Peak concentration levels are up to 5 mg/l for U_{nat} and 0.2 mBq/l for Ra-226. Compared to the quantities of water discharged from WTPs, the amount of untreated but controlled discharges is negligible (order of 5 %). As average concentrations of radio-nuclides in these waters are normally of the same order of magnitude as in the case of WTP-treated waters, the same applies for discharged activities.

Discharge-induced radiation exposures are insignificant. The following section exemplifies the order of magnitude of effective doses to the public which may attain in case where 100 % use is made of discharged waters showing concentration levels equal to permitted discharge standards (conservative assumption). As a rule, however, straightforward use of discharged waters is improbable or ruled out when properly collected. Upon discharge into receiving streams, the collected waters are by majority of cases diluted. The magnitude of the mixing ratio ranges from 1 : 20 (discharge from the Aue WTP into the Zwickauer Mulde river) up to 1 : 2000 (Königstein WTP into the Elbe river). Only at the Seelingstädt site, during periods of low water flux of the receiving Culmitsch creek the ratio comes close to one.

Table 1. Survey of water treatment plants operated by WISMUT and of discharge waters.

Site	Capacity [m³/h]	Type of feed water	Main radio-logical component [a]	Permitted discharge standard		
				U_{nat} [mg/l]	Ra-226 [Bq/l]	U_{nat} loads [t/a]
Aue	1000	Mine water	5 mg/l U_{nat}	0.5	0.4	4,4
Pöhla	130	Mine water	2.5Bq/l ^{226}Ra	0.2	0.3	0,175
Helmsdorf	250	Supernatant w.	10 mg/l U_{nat}	0.5	0.2	0,88
Königstein	650	Mine water	100 mg/l U_{nat}	0.3	0.4	1,7
Seelingstädt	300	Supernatant w. Seepage	2 mg/l U_{nat}	0.3	0.2	0,63

[a] Level order of magnitude

Risk assessment studies

Diffuse release of radioactive substances and related radiation exposures
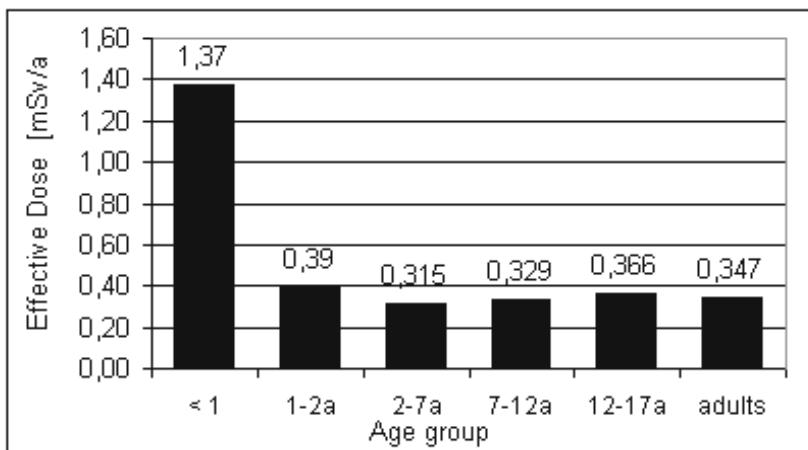
The uncontrolled, i. e. diffuse release of radioactive substances and the related radiation exposures are exemplified by the situation at the Trünzig Tailings Management Area (TMA). With its content of radioactive and chemico-conventional uranium processing residues (volume of 19 million m³, area of 120 ha to be covered), the Trünzig TMA is one of the large-size facilities of the Seelingstädt site. The environmental assessment performed in 2000 to evaluate the status of the site at that time (in 2000 the facility was partly regraded and provided with an interim cover) concluded that, in addition to 114.000 m³ of seepage emerging near the surface and being collected and fed to the Seelingstädt WTP, some 69.000 m³ of percolating water would propagate either to the ground water or disperse in the receiving streams (Lerchenbach, Finkenbach creeks) (Wismut, 2000). Uranium levels observed in groundwater flowing downstream from the tailings deposit were up to 1 mg/l close to the facility. This allows a rough estimate of an annual uranium load of about 100 kg being released from the Trünzig TMA.

Diffuse groundwater flow to the receiving streams is reflected in increased nuclide levels in surface waters. Table 2 shows findings of water samples taken from the Lerchenbach creek north of the Trünzig TMA and analysed for nuclide levels. Nuclide levels as well as the nuclide vector where uranium nuclides are dominant are in the range of levels measured near tailings management areas elsewhere.
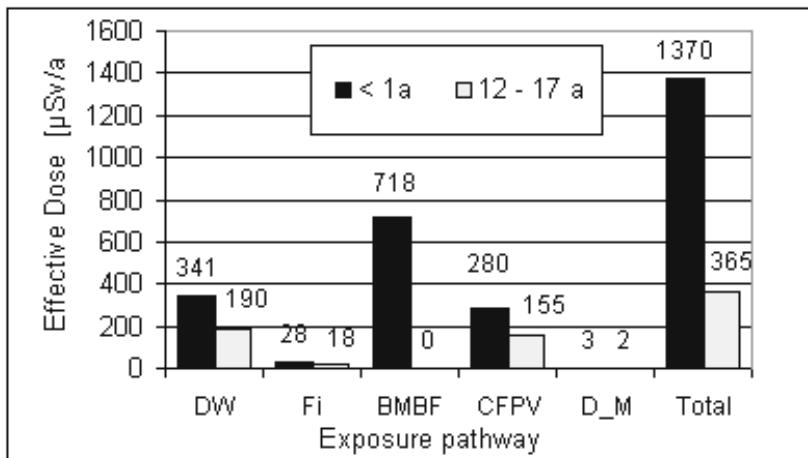
Fig. 2 and 3 below illustrate the resulting radiation exposures likely to follow the use of water of such quality. While the exposure scenarios are conservative, they cannot be fully ruled out. All computations are based on Berechnungsgrundlagen Bergbau, the German guidelines for calculation of effective doses at mining sites (BMU,1999). Water use assumptions made included 100 % consumption as drinking water as well as 100 % use for food production (consumption of fish taken from the Lerchenbach creek, cattle watering, irrigation of field and garden crops; amounting to 25 % satisfaction of annual consumption rate). Fig. 4 exemplifies for two exposure pathways the contribution of the various nuclides from the uranium-radium decay chain to the effective dose of the local public.

Table 2. Radionuclide levels [in Bq/l] established for water in the Lerchenbach creek north of the Trünzig TMA.
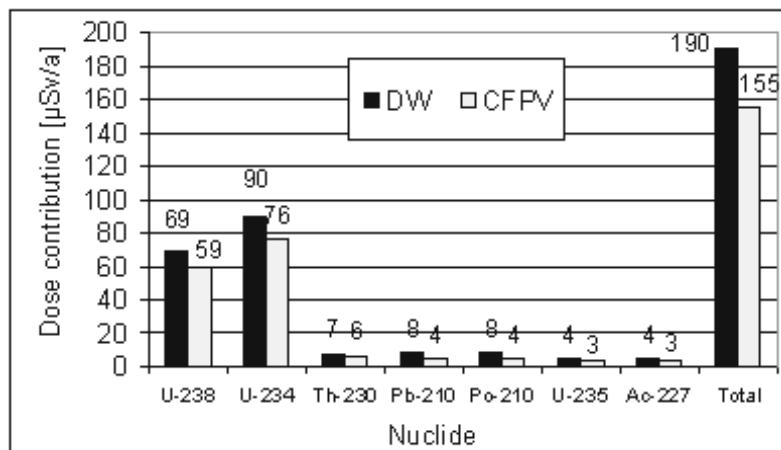
| U-238	U-234	Th-230	Ra-226	Pb-210	Po-210	U-235	Pa-231	Ac-227
5.2	6.1	0.17	0.02	0.025	0.025	0.24	0.015	0.015

Risk assessment studies

Fig. 2. Annual effective dose resulting from consumption and use of water taken from the Lerchenbach creek for all age groups to be considered; contribution from all exposure pathways taken into account (see Fig. 3 in detail).


Fig. 3. Effective annual dose resulting from consumption and use of water taken from the Lerchenbach creek; contributions from the exposure pathways taken into account for age groups [< 1 a] and [12 -17 a]; (DW – drinking water; Fi- fish consumption; BMBF– consumption of breast milk / baby food prepared with the water; CFPV – consumption of locally produced cereals, fruit, potatoes, vegetables).

Risk assessment studies

Fig. 4.   Effective annual dose resulting from consumption and use of water taken from the Lerchenbach creek; contributions from nuclides for age group [12 - 17 a], consideration of the exposure pathways DW- drinking water and CFPV – consumption of locally produced cereals, fruits, potatoes, and vegetables, respectively.

Some general conclusions may be drawn beyond the example considered:
1. Given the characteristics of waters encountered in the vicinity of abandoned WISMUT sites (with mostly neutral or acidic pH), the nuclide vector is typically determined by the nuclides U-238, U-234, and U-235. Predominance of these nuclides is that great that they account for the major part of the effective dose, notwithstanding relatively low dose coefficients as compared to Po-210 or Ac-227.
2. When applying standard scenarios of Berechnungsgrundlagen Bergbau (BMU, 1999), giving in particular full consideration to the drinking water path, the highest individual doses will be to the small child up to one year of age. Thereby, the pathways DW - drinking water, and BMBF - consumption of breast milk and baby food prepared with the water, respectively, are dominating the level of effective dose in this age group.
3. Overrun of the guidance value of 1 mSv/a is most likely for age group [< 1 a] when applying standard scenarios. However, exposure pathway analyses performed as part of environmental assessments show that effective doses due to the aquatic pathway are as a rule less than 1 mSv/a.
4. Consideration of site-specific exposure scenarios instead of standard scenarios and consumption rates of a reference man according to (BMU, 1999) when performing exposure pathway analyses almost exclusively leads to effective doses due to the aquatic pathway of significantly less than 1 mSv/a.

Risk assessment studies

Evaluation of and possibilities to reduce discharges and releases of radioactive substances from abandoned WISMUT sites

With the continuation of water treatment, radiation exposure due to discharges will also be kept low in the future. According to model predictions, water treatment plants will have to be operated for another decade, in some cases even for up to 20 years. It is anticipated that concentration levels in feed waters to WTPs will have sufficiently faded away by then to allow alternative treatment methods (passive procedures) or to discontinue water treatment altogether.

Uncontrolled leakage of contaminated waters from TMAs and mine dumps as well as from mine workings is being reduced as rehabilitation advances. Mines are flooded in a controlled manner, involving treatment of pumped mine waters. Tailings management areas and mine dumps left in place are being capped. Capping of the tailings areas is done with the primary objective of denying access and assuring their long-term stabilisation and providing long-term geochemical stability of their inventory. In the case of mine dumps, capping is done in a manner to minimise radon exhalation in addition to reduce the leakage of contaminated waters.

By their levels in the order of 1 mSv/a, individual doses as a result of water discharges as outlined in the above section do not suffice to constitute the sole basis for the optimisation of rehabilitation measures. The immense costs involved in the rehabilitation of TMAs in particular can only be justified by a multitude of factors considered in an optimisation process (long-term enclosure, geostability, geochemistry, impact by conventional contaminants). The radiological impact on the environment via the aquatic pathway constitutes an essential aspect in that effort, but is one among others.

References

Wismut (2000)   Environmental impact assessment for the remedial measure „Final Covering of the Trünzig Tailings Pond" (Umweltbewertung für die Sanierungsmaßnahme „Endabdeckung der IAA Trünzig"); WISMUT GmbH, Department of Engineering; WIS-S178/6, Chemnitz, November 2000 (in German)

BMU (1999)   Guidelines on How to Calculate Effective Doses Caused by Natural Radioactivity at Mining Sites" (Berechnungsgrundlagen zur Ermittlung der Strahlenexposition infolge bergbaubedingter Umweltradioaktivität - Berechnungsgrundlagen Bergbau), Federal Ministry for Environment, Nature Protection and Reactor Safety, Bonn, July 1999 (in German)

Radionuclide Data for Geothermal Prospection – A Contribution to the Geothermal Resources Map of Saxony

Petra Schneider[1], Helmut-Juri Boeck[2], Thomas Lange[2]

[1]C&E Consulting und Engineering Chemnitz, Jagdschänkenstr. 52, D-09117 Chemnitz, Germany, E-mail: p.schneider@cue-chemnitz.de
[2]C&E Analytik- und Umweltdienstleistungs GmbH Chemnitz, Jagdschänkenstr. 52, D-09117 Chemnitz, Germany.

Abstract. Geothermal energy is one of the long term perspectives in the field of renewable energy. A research and development project was started to evaluate the deep geothermal potential in Saxony, East Germany. The investigation is a contribution to the geothermal resources map of Saxony. The geological setting of Saxony is characterised by a variety of solid rocks. A lot of them are containing remarkable radionuclide concentrations, so they are source of radioactive heat generation due to radioactive decay. This source was investigated quantitativly.

Introduction

Geothermal energy comes in two forms: One form is the thermochemical energy (heat released from chemical reactions), the other the radiogenic energy (produced by radioactive decay). The source of the geothermal gradients is coming from conductive heat flow from the deep crust and mantle and from radioactive decay of uranium, thorium, and potassium isotopes on the other side. Some granitic rocks in the upper crust contain abnormally high concentrations of radioactive elements causing an enhanced heat flow towards the earth's surface.

Different authors (e.g. Paschen et al 2003) come to the conclusion that only 5% of available geothermal resources in Germany are stored in form of thermal water resources in heated aquifers. On the other hand 95% of the geothermal resources in Germany are stored in form of "dry heat" in crystalline rocks. Under this conditions Saxonia with a large portion of crystalline rocks offers good conditions for the use of geothermal energy.

The use of geothermal resources has an interesting potential considering the important part of surface-near solid rock units in Saxony. Due to the intensive ex-

ploration and mining activities in the region a remarkable number of information is known about the temperature distribution in the underground. Especially the variscic granites of the Ore Mountains are characterised by increased heat flow values, while in other regions only small heat flow rates are found. Within the well investigated Ore Mountains can be assumed, that a majority of the heat flow in this area is of radiogenic origin.

Geophysical techniques have a variety of applications to environmental problems. So geophysical techniques, especially radiometrics, can be an important tool in the field of geothermal exploration. Radiometrics, commonly referred to as gamma ray spectrometry, is prepared from airborne platforms, hand held instruments, or downhole logging to measure the radioactivity of the ground. Airborne surveys have been used to estimate abundances of potassium, thorium, and uranium for a variety of activities including regional lithologic discrimination, mineral exploration, and environmental background studies (Nielsen and others, 1990; Darnley and Ford,1989). Maps of terrestrial gamma radiation aided the geothermal mapping in this project. Data of gamma spectroscopy, which were collected on gamma spectroscopy flights by airplane, were be used for the spacial assessment of the radioactive heat generation potential in Saxony.

Investigations on Radioactive Heat Production

Fundamentals in Radioactive Heat Production

Radioactive Heat Generation RHG means the heat which is set free due to radioactive decay of natural radionuclides in the earth's crust and absorbed in the rock. The potential of RHG is depending on the concentration C of these nuclides in the rocks. Usually only the concentration of the most important and most frequent radionuclides are considered because in case of radioactive equilibrium the importance of short-lived isotopes arising within the radionuclide decay chains isn't remarkable. The concentration of the decay products depends on the concentration of the natural mother nuclide and the decay rate of the daughter nuclide. Isotopes with short half-live times cause usually no substantial enrichment of heat within the rock. Therefore radioactive heat generation data in the literature are documented on the basis of the concentrations of the isotopes K-40, Th-232 and U-238. Generally the relation of the radioactive heat generation is indicated in the form:

$$RHG = A_1 \cdot d \ \cdot (A_2 \cdot c_U + A_3 \cdot c_{Th} + A_4 \cdot c_K)$$

with d... density and ci... concentrations of the radionuclides. On the basis of the priority of the rock density the amount of absorption of the gamma and/or particle radiation is expressed. The emitted radiation is absorbed the faster, the more largely the density is. Following values for the coefficients Ki are indicated in SCHÖN (1996):

Risk assessment studies

$$RHG = 10^{-5} \cdot d \cdot (95.200 \cdot c_U + 25.600 \cdot c_{Th} + 3,48 \cdot c_K)$$

On the basis of the absorption potential is shown that the main part of the energy develops from the decay of the elements thorium and uranium. Potassium supplies on the average over all rocks an additional contribution of approximately 15 % of the total energy quantity. Depending on the kind and composition of the rock this portion can vary within larger ranges (see Table 1).

Table 1. Radiogenic heat production of rocks (after literature data).
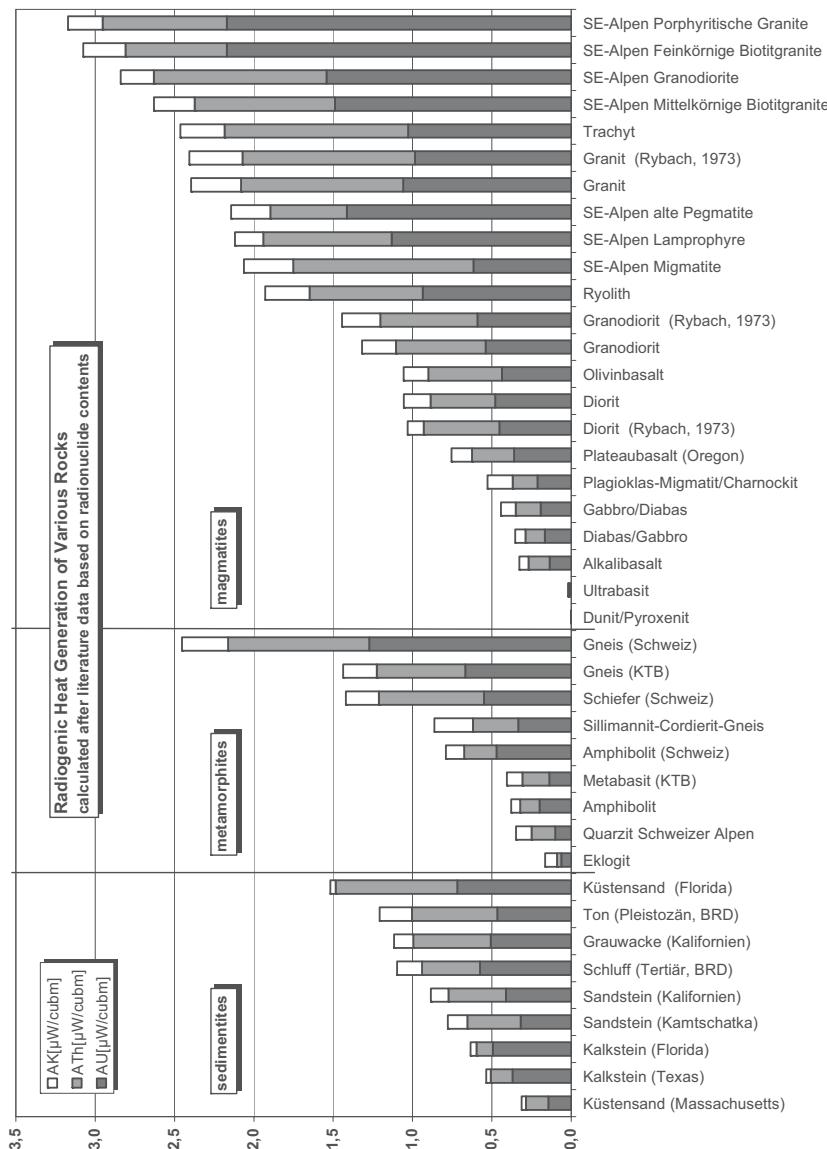
Day	A in [μW/m³] after Buntebrath (1980)	A in [μW/m³] after Oelsner (1982)	A in [μW/m³] after Schön (1983)
granite	3.000	5.500	5.280
schiefer	-	2.100	1.550
diorite	1.100		1.300
ultrabasite	-	0,010	0,013
peridodite	0,010	-	0,010
gneiss	2.400	4.200	

Correlations between Gamma Radiation and RHG

After Bücker and Rybach (1996) correlations between the gamma radiation and the radioactive heat generation exist in the following way (where GR is gamma ray and API the investigation standard coming from petrol industries):

$$RHG\ [\mu W/m^3] = 0.0158\ (GR\ [API] - 0.8)$$

Ranges of radioactive heat generation of the most important rock classes are documented in the literature. Detailed geological and gammaspectrometric investigations of different magmatites were made in the 1970th by the former SDAG Wismut. In Fig. 1 is shown a comparison of the ranges of radioactive heat generation of the most important rock classes in Saxony. Considering the radiogenic energy it can be concluded that special attention has to be dedicated to sour intrusive rocks in the geothermal basis model. Sour intrusive rocks are especially granites and granitoide rocks. Due to their elevated radionuclide contents this rocks can be dedicated by airborne gamma ray spectrometry.

Fig. 1.   Comparison of the ranges of radioactive heat generation of the most important rock classes (after Schön 1996, Just 1977, and Wismut, 1972).

Risk assessment studies
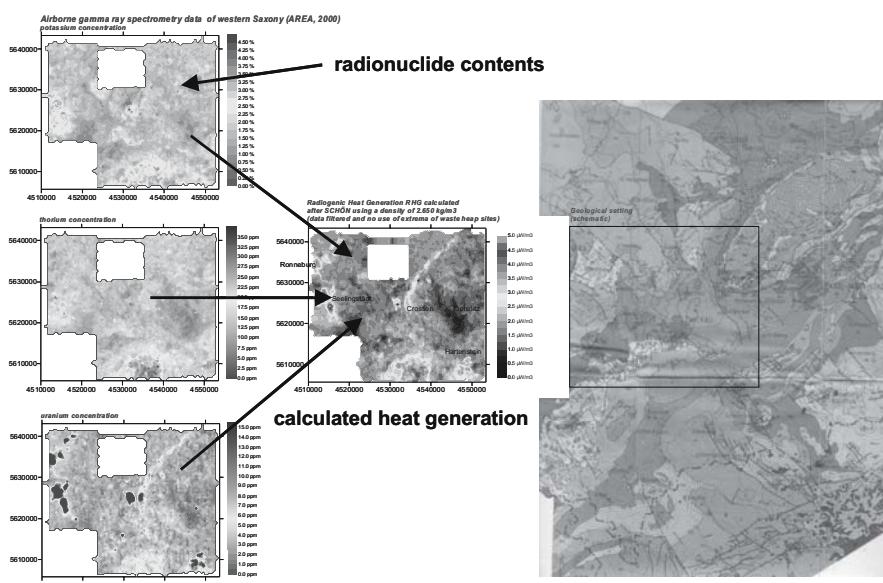
Investigation Concept

The investigation concept is shown in Fig. 2. Using the airborne gamma ray spectrometry data which represent the spacial radionuclide contents the calculation of the radioactive heat generation was prepared for Saxony. The airborne gamma ray spectrometry data were of two sources: data of the EU project AREA and data of the Environmental authorities. The airborne measurements were calibrated using a combination of in situ and soil/rock sample data. The surficial radioactive heat generation data allow also a geothermal modeling into the deep geological layers.

Results

Spacious Calculation of the Radioactive Heat Generation of Saxony
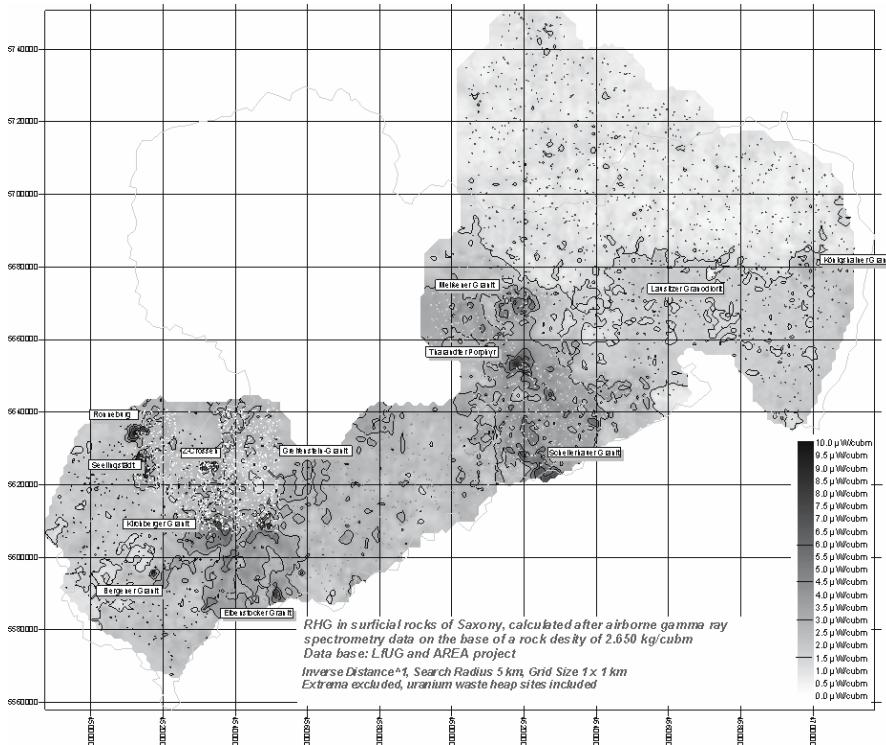
In Fig. 3. are shown the results of the spacious calculation of the radioactive heat generation. Due to the geological structure of Saxony the areas relevant for radioactive heat generation are in the western and middle part of Saxony. The geological structure indicates granites and gneisses in these parts of Saxony. The values of radioactive heat generation in these areas cover 2 to 10 µW/m³. The eastern part is covered by sedimentary rocks. The radioactive heat generation in these areas is


Fig.2.   Method of the calculation of the radioactive heat generation due to radioactive decay based on spacial gamma spectroscopy data.

Risk assessment studies

very low due to values between 0 to 2 µW/m³.

Values up to 15 µW/m³ are calculated in parts of the areas of former uranium mining in Saxony. These sites will be mitigated in the next few years.

**Fig. 3**.   Results of the spacial calculation of the RHG for Saxony.

Risk assessment studies

Conclusions

The geological setting of Saxony is characterised by a variety of solid rocks. Some of them are containing remarkable radionuclide concentrations, so they are source of radioactive heat generation due to radioactive decay. The spacious calculation of the radioactive heat generation based on airborne gamma ray spectrometry data is a suitable tool for the investigation of the radioactive heat generation. But one has to consider that this geothermal source is small in comparision to thermo-chemical energy.

Acknowledgements

References

AREA 2000

Boeck, H-J.; Lange, T.; Grafe, F.; Schneider, P.; Tunger, B.; Wilsnack, T. (2004): Bestandsaufnahme und nutzungsorientierte Analyse des tiefengeothermischen Potentials des Freistaats Sachsen und seiner unmittelbaren Randgebiete, Zwischenbericht zum Forschungsvorhaben AZ 40410229, i. A. des Landesamtes für Umwelt und Geologie.

Bücker Ch., Rybach L., (1996): A simple method to determine heat production from gamma-ray logs. Marine Geology 13, 373-377

Buntebrath, G. (1980), Geothermie, Springer Verlag, Berlin - Heidelberg - New York.

Darnley, A.G.; Ford, K.L. (1989): Regional airborne gamma-ray surveys: A review, p.229-240, in: Proc. of Exploration 87: Third Decennial International Conference on Geophysical and Geochemical exploration for mineral and groundwater, Special Volume 3.

Nielson, D.L., Linpei, C.; Ward, S.H. (1990): Gamma-ray spectrometry and radon emanometry in environmental geophysics, in Ward, S.H., ed., Geotechnical and Environmental Geophysics,Society of Exploration Geophysicists,p.219-250.

Just, G. (1977): Spezielle Untersuchungen der Radioaktivität von Gesteinen, Wässern, Bodenproben und Aerosolen durch Messung der natürlichen Gammastrahlung, Externe Diplomarbeit, Universität Leipzig, Sektion Physik

Oelsner, C. (1982), Grundlagen der Geothermie, Sektion Geowissenschaften der TU BAF.

Paschen, H., Oertel, D.; Grünwald, R. (2003): Möglichkeiten der geothermischen Stromerzeugung in Deutschland. - Sachstandsbericht, Büro für Technikfolgen-Abschätzung beim Deutschen Bundestag, Arbeitsbericht 84: 129 S.; Berlin (TAB).

Pfenner, I. (2005): Ansätze zur Modellierung der Temperaturverteilung im Hot Dry Rock-System am Beispiel des Eibenstocker Granits mit der Software ANSYS-FLOTRAN, Diplomarbeit, TU BA Freiberg.

Rybach L., (1973): Wärmeproduktionsbestimmungen an Gesteinen der Schweizer Alpen. Beitr. Geol. Schweiz, Geotechn. Serie Nr. 51, 43 p.

Schön, J. (1983), Petrophysik, Akademie Verlag, Berlin.

Schön, J. (1996): Physical Properties of rocks: Fundamentals and Principles of petrophysics, in Handbook of geophysical exploration, Vol.18, Pergamon-Verlag, Leoben.

SDAG WISMUT (1972): Otschet po teme „Ozenka radiogeochimitscheskich ossobenostej magmatitscheskich porod juschnoj tschasti GDR na osnowe primenenija metoda polewoj gamma-spektrometrij" (russ.), Grüna, unveröffentlicht, ZGA, Inv.-Nr. LGA 290/88

Risk assessment studies

Contaminated Sediments in the Elbe Basin and its Tributary Mulde

Petra Schneider[1], Heinrich Reincke [2]

[1]C&E Consulting und Engineering Chemnitz, Jagdschänkenstr. 52, D-09117 Chemnitz, Germany, E-mail: p.schneider@cue-chemnitz.de
[2]Senatskanzlei der Stadt Hamburg, Senatskanzlei-Planungsstab, Poststr.11 D-20354 Hamburg, Germany, E-mail: heinrich.reincke@sk.hamburg.de

Abstract. Data from the Elbe River and its tributaries indicate, despite extensive improvement in water quality since reunification, that the sediment situation of many priority pollutants has not reached an acceptable level. The risks for downstream sites, especially the port of Hamburg, the lower part of the tidal river Elbe and the North Sea will persist in future. In practice, the catchment-wide assessment of contaminated soil and sediment should be identified and valued for acquiring a management plan for the EC Water Framework. The focus will be the on the tributary Mulde.

Introduction

The pollution of the Elbe River and especially the catchment area of the tributary Mulde with rising groundwater-level in the mining areas and tailings of the old mining in the Ore Mountains is one of the great environmental problems of the Elbe catchment. In Saxony, the draining water from nearly all of the uranium mining sites flow into the Mulde River. In July 1998 the conference of the Elbe River responsible ministers decided to develop a strategy concept to improve the Elbe water quality, reducing the impacts of uranium mining on the Elbe River. Main objective is to get a good ecological condition of the Elbe catchment according to the EC Water Framework Directive (EC-WFD). Important steps in the improvement of the water quality of the Elbe river were done since 1998.

Nevertheless the sediments are sinks for ongoing releases from many contaminant sources; these include wet and dry fallout from air emissions, runoff from farms, solid and dissolved inputs from mines, discharges from landfills, industrial plants, and sewage-treatment plants. Even if water quality improves, sediment and floodplain soil contamination will remain a 'legacy of the past'.

Risk due to erosion of contaminated sediments and their potential impacts downstream is not covered by existing regulations. Existing regulations focus on local impacts of the relocation of contaminated sediments and do not take the whole catchment into account. On the other hand, the EC-WFD, which focuses on the catchment scale, does not explicitly mention sediments nor sediment quality and quantity. However, the strategies against chemical pollution of surface waters (EC-WFD article 16), i.e. implementation of monitoring programs until 2006 and establishment of the program of measures until 2009, have to consider sediment quality at the catchment scale.

The Elbe River is one of the major rivers in the western Europe. From its spring in the Giant Mountains (Czech Republic) to its mouth at the North Sea near Cuxhaven (Germany) it covers a distance of 1091 kilometres and a catchment area of 148.268 km^2 (see Fig. 1).

Within this region of interest, the Mulde rivers (Zwickauer Mulde, Freiberger Mulde, and United Mulde) form an important contribution to the contamination of the Elbe river (Beuge et al. 1999). The river basin of Mulde with encloses 7400 km^2 including the heavily populated industrial region Chemnitz, Zwickau and the former chemical industry centre Bitterfeld as well as the mining and metallurgy centre around Freiberg (see Fig. 2). In some of the former mining areas the recharge of groundwater in the groundwater depression cones are still not completed (Schneider et al 2003b).
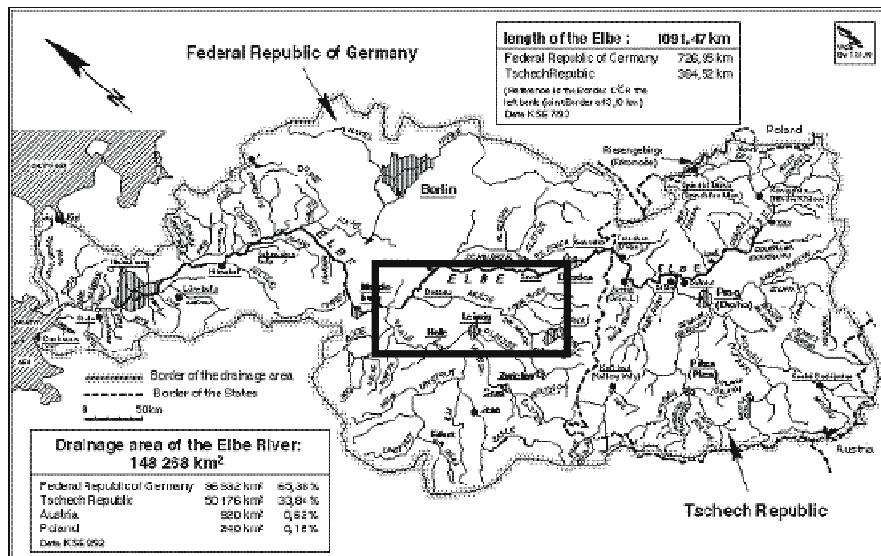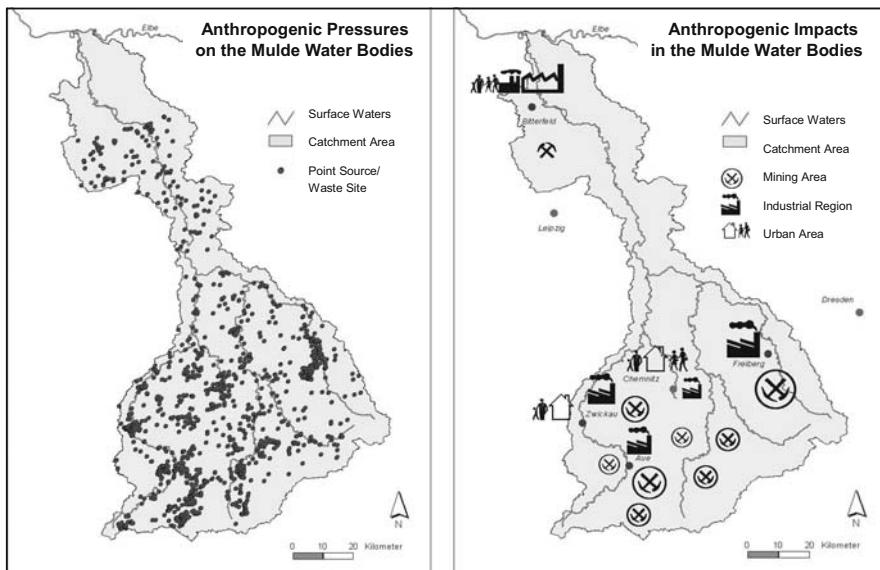

Fig. 1.   Drainage area of the Elbe river and its Tributary Mulde (black marked).

Risk assessment studies

Fig. 2. Significant pressures on the Mulde river basin water bodies (after Beuge et al. 1999, Zweig et al. 2003).

Historically Contaminated Sediments and Soils in the Elbe River Catchment Area

Data from the Elbe River and its tributaries indicate, despite extensive improvement in water quality during the last 15 years, that the respective sediment situation of many priority pollutants has not reached an acceptable level. Historical pollution from sediments and soils becomes a significant source of contamination in Hamburg harbor, in the Elbe estuary, and in the coastal areas. Again, major deficiencies are in the assessment and prognosis of resuspension processes, and potential approaches to fill this gap are described from examples of the Elbe River.

The mines, tailings and sedimentation ponds of hard coal, metal and uranium mining along the Mulde River(s) present long-term pollutant sources. Both river basins show metal burdens above average. The elevated metal burden includes the typical ore metals Cd, Pb, Zn and U, mainly. The industrial areas provide essentially halogenated hydrocarbons, polycyclic aromatic hydrocarbons, phenols, cyanides and, to a lesser extent, metallic pollutants. Effluent seepage from tailings and mines show high metal and sulfate concentrations, which contribute to the contaminant transport in the nearby rivers. So, the united Mulde Rivers form the main path of metals into the Elbe River. Besides, one has to take in consideration, that an important part of the Mulde catchment covers landscapes with metallogenic origin, as the Ore Mountains (Schneider et. al. 2003a). The sediment contamination of the Mulde river was characterised by Beuge et al. 1999, see Table 1.

Risk assessment studies

Table 2 compares several metals in the sediments (quarterly mean values from 1992 to 2003) of the Mulde catchment with averages in the earth crust and clay minerals (Beuge et al. 1989).

The highest sediment concentrations were investigated

- Freiberger Mulde: in the area of the mining and processing region Freiberg: As, Cd, Pb, Zn, Cu,
- Zwickauer Mulde: in the area of uranium mining and processing (Aue, Niederschlema, Hartenstein, Crossen): U, As
- United Mulde: in the area of the former industrial centre of Bitterfeld: Hg and organic compounds.

Hydraulic processes form the primary input factors for the large-scale dispersion of historical contaminated sediments. Unlike problems related to conventional polluted sites, the risks are primarily connected with the depositing of contaminated solids on soils in downstream regions. Therefore, sediment physical parameters and techniques form the basis for any risk assessment in this field. As floods frequently occur in the main river and its tributaries one has to take into account the impact of increasing discharge levels. Considering these facts sediment transport represents an important contaminant potential especially during floods. For example, table 3 shows the contaminant transport in flood sediments during the millenium flood 2002 in Saxony in the Elbe and the Mulde tributaries.

The importance of sediments as sinks for releases from many contaminant sources can be shown by data of reservoirs and other sediment sinks (e.g. see table 4). The owners of large sediment sinks, such as the big ports, mostly at the end

Table 1. Metals and arsenic in sediments of the Mulde tributaries (after Beuge et al. 1999).

I$_{geo}$-class (Müller 1979)	Heavily contaminated	Heavily to excessively contaminated	Excessively contaminated	Extremely contaminated
Freiberger Mulde	Cu			As, Pb, Zn, Cd
Zwickauer Mulde	Pb, Cu	As, Zn	U	Cd
United Mulde	U	Pb	As, Hg, Zn	Cd

Table 2. Comparison of metal pollutants in the sediments of the Mulde catchment (quarterly mean values 1992 to 2003) with average values of the earth crust [mg kg-1].

element	clark value	clay rock	Freiberger Mulde				Zwickauer Mulde				United Mulde
[mg/kg]	(Vinoradow)	(Turekian, Wedepohl)	Holzau	Muldenhütten	Obergruna	Mdg. Erlln	Schönheide	Niederschlema	Remse	Mdg. Sermuth	Bad Düben
As	2,0	7,0	260,0	285,3	1592,2	353,3	195,0	377,0	83,1	74,0	200,0
Cd	0,13	0,3	22,5	43,0	115,9	28,7	4,6	17,2	22,3	20,3	17,0
Co	18,0	19,0						100,0	57,0		
Cr	83,0	90,0	72,5	79,2	132,5	82,3	48,2	113,9	143,3	55,5	86,0
Cu	47,0	45,0	95,5	354,1	886,0	166,7	94,7	401,0	171,7	133,3	150,0
Ni	58,0	68,0	112,5	45,8	57,9	56,0	36,9	298,0	156,7	79,4	76,0
U	3,0	4,0					76,0	168,7	58,0		
Zn	200,0	95,0	1120,0	1990,0	5667,6	1533,3	339,8	1347,0	1633,3	1020,0	1000,0

Risk assessment studies

of navigable rivers, are put at a disadvantage as they have to pay the expenses of all former, actual and future shortcomings in emission control within their entire catchment areas. Table 4 shows sediment data of the Glauchau reservoir, the Zwickauer Mulde upstream the Glauchau reservoir and the Freiberger Mulde.

In the Mulde catchment one has to consider, that radioactive compounds are drained off the mining waste heap sites in the catchment too and deposited in the sediment sinks. Considering the live time of radioactive compounds it becomes quite clear that the management of contaminated sediments will be a long term task. Table 5 shows sediment data of radioactive compounds in the Glauchau reservoir and the river upstream and downstream the reservoir.

Table 3. Contaminant transport in flood sediments of the millenium flood 2002 in Saxony in the Elbe and the Mulde tributaries, after Rank 2004 (S = sediments, R = riverside soils).

element	Elbe			Freiberger Mulde			Zwickauer Mulde		
[mg/kg]	samples S / R	median S	median R	samples S / R	median S	median R	samples S / R	median S	median R
As	40 / 605	22	20	59 / 105	480	118	27 / 27	95	92
Cd	26 / 568	2,0	0,74	57 / 98	9,3	1,7	26 / 21	3,6	3,2
Pb	26 / 568	96	54	57 / 98	803	300	26 / 21	89	96

Table 4. Metals and arsenic sediment data of the Glauchau reservoir, the Zwickauer Mulde upstream the Glauchau reservoir and the Freiberger Mulde (after Hoppe et al. 1994).

element	KLOKE natural background (mg/kg)	sediment data reservoir Glauchau (mg/kg), n = 18	sediment data Zwickauer Mulde upstream the Glauchau reservoir, (mg/kg), n = 21	sediment data Freiberger Mulde, (mg/kg), n = 27
Cd	3	6,9	4	100 – 1.600
Pb	100	105	2	812 – 18.000
Cu	100	181	10	150 – 4.500
Zn	300	445	50	1.360 – 34.000
Ni	50	53,8	10	40 - 350
As	100	55	154	50 – 1.600
Co	50	17	35	10 - 100

Table 5. Uranium and radium-226 data of the Glauchau reservoir and the river upstream and downstream the reservoir (after Ruhl, 1995).

	number of samples	uranium in dry residues			radium-226-activity		
		min	mean	max	min	mean	max
reservoir sediment (upper soil)	16	8 mg/kg	29 mg/kg	87 mg/kg	0,15 Bq/g	0,35 Bq/g	0,55 Bq/g
reservoir sediment (lower soil)	3	40 mg/kg	55 mg/kg	63 mg/kg	0,42 Bq/g	0,56 Bq/g	0,80 Bq/g
river upstream the reservoir	2	0,004 mg/l		0,005 mg/l	< 10 mBq/l		14 mBq/l
Zwickauer Mulde downstream the reservoir	12	0,007 mg/l		0,06 mg/l	40 mBq/l		160 mBq/l

Risk assessment studies

Therefore, it is a matter of 'hydro solidarity' to achieve a full upstream/downstream integration of monitoring, stakeholder consultation, models and expert systems that can link basin pressures to transfers, across various administrative and/or political boundaries, and between the various land users, water users and other stakeholders. This could be practiced in a river basin-wide sediment assessment and management is needed.

Conclusions

A river basin-wide sediment assessment should, at first, perform inventories of interim depots with the catchment area, i.e. underground and surficial mining residues, river-dams, lock reservoirs and flood plain and groyne field sediments. Within a typical river section of 1 km length in the lower middle Elbe, the estimated nutrient and pollutant loads, deposited on the floodplains and in the river course, clearly demonstrate the specific sink function of both sites. At the same time, however, the results suggest, in contrast to the deposits in the floodplains, that sediments within the river course may partly be remobilized.

Detailed measurements for critical sites can apply the wider spectrum of laboratory and in-situ erosion stability tests. The study of erosion stability on sediment core profiles can be combined with analyses of the acid neutralizing capacity, providing a first indication on the heavy metal mobility in the grain matrix relative to the (bio-)chemical processes, which can form acidity. The flood plain profile from the Middle Elbe river exhibits a relatively high acid neutralizing capacity, and it can be expected that relocation processes involving oxidation of sulfide minerals will not induce long-term problems with respect to the mobility of heavy metals.

With respect to the latter date, already the first step – screening of all generic sources that can result in releases of priority substances and priority hazardous substances – will include the specific source/pathway 'historical pollution from sediment'. In practice, a catchment-wide assessment of historical contaminated soil and sediment should apply a three-step approach:

- Identification of substances of concern (s.o.c.) and their classification into 'hazard classes of compounds';
- identification of areas of concern (a.o.c.) and their classification into 'hazard classes of sites';
- identification of areas of risk (a.o.r.) and their assessment relative to each other with regard to the probability of polluting the sediments in the downstream reaches.

Risk assessment studies

Outlook

Limited financial resources require a direction of investments to those sites with the highest efficiencies in risk reduction. Establishing a rough sediment dynamic model, building on tributary/main river dilution factors, sedimentation data, suspended particulate matter monitoring data as well as calculations of long-term costs and benefits, could be essential steps in a basin wide river management. This could include the use of 'soft' (geochemical and biological) techniques on contaminated soils and sediments, such as sub-aqueous depots, active capping, and application of natural attenuation processes (Beuge et al. 2002; Reincke et al. 2004). The problems discussed here are relevant also to other European countries. So the approach of a sediment management system considering seepage and disposal of waste from uranium tailings should be included in practical guidelines for the realisation of the WFD.

References

Beuge, P.; Greif, A.; Hoppe, T.; Kluge, A.; Klemm, W.; Martin, M.; Mosler, U.; Starke, R.; Alfaro, J.; Anders, B., Behrens, K.; Grundwald, N.; Haurand, M.; Knöchel, A.; Meyer, A.; Poteger, H.; Staub, S.; Stocker, M. (1999): Die Schwermetallsituation im Muldesystem, Bd. 1 – 3, TU Bergakademie Freiberg, TU Hamburg Harburg und Universität Hamburg, Im Auftrag des Bundesministerium für Bildung und Forschung.

Beuge, P.; Klemm, W.; Degner, T.; Scheel, M.; Baake, D.; Calmano, W.; Zoumis, T.; De Arevalo, A.; Knöchel, A.; Chinon, M.; Eifler, D.; Feuerborn, J.; Kinzel, T.; Meyer, A.-K.; Miller, F.; Staub, S. (2002): Abschlußbericht zu den Projekten 02-WT 9640/4, 02-WT 9641/7, 02-WT 9642/0, 02-WT 0038 „Entwicklung geochemischer Methoden zur naturnahen Schadstoffdemobilisierung im Muldesystem", TU Bergakademie Freiberg, TU Hamburg Harburg und Universität Hamburg, Im Auftrag des Bundesministerium für Bildung und Forschung.

European Community/ Europäische Komission (2000): Richtlinie 2000/60/EG des Europäischen Parlaments und des Rates vom 23.10.2000 zur Schaffung eines Ordnungsrahmens für Maßnahmen der Gemeinschaft im Bereich der Wasserpolitik. in: Amtsblatt der Europäischen Gemeinschaften, L 327 vom 22.12.2000, Luxemburg.

Hoppe, T.; Kluge, A.; Beuge, P.; Schach, H.G. (1994): Untersuchungsergebnisse von Wasser- und Sedimentproben des Stausees Glauchau.- LfUG Bericht - Schriftenreihe des Landesamtes für Umwelt und Geologie Sachsen.- Heft 1.- 1994.- S. 50-55.

Meinrath, A., Schneider, P., Meinrath, G. (2003) Uranium ores and depleted uranium in the environment, with a reference to uranium in the biosphere from the Erzgebirge/Sachsen, Germany; In: Journal of Environmental Radioactivity 64 (2003) 175–193.

Müller, G. (1979) Schwermetalle in den Sedimenten des Rheins - Veränderungen seit 1971, in: Umschau, 24, S. 778 - 773.

Rank, G. (2004): Arsen- und Schwermetallbelastung im Mulde- und Elbe-Einzugsgebiet nach dem Augusthochwasser in Sachsen, Wasser und Abfall 3/2004, pp34-39.

Reincke, H.; Schneider, P. (2004): Strategy Concept Elbe - Passive Water Treatment Methods for the Minimisation of Impacts on Water Bodies by Ore Mining Activities; In: Geller, W. et al: Proceedings of the 11th Magdeburg Seminar on Waters in Central and Eastern Europe: Assessment, Protection, Management; ISSN 0948-9452.

Ruhl, A. (1995): Radiologische Untersuchungen der Sedimente des Stausee Glauchau.- LfUG Bericht - Schriftenreihe des Landesamtes für Umwelt und Geologie Sachsen.- Heft 5.- 1995.- S. 14-17.

Schneider, P., Neitzel, P., Schaffrath, M., Schlumprecht, H. (2003a): Physico-chemical Assessment of the Reference Status in German Surface Waters: A Contribution to the Establishment of the EC Water Framework Directive 2000/60/EG in Germany, In: Hydrochimica et hydrobiologica Acta. 31 (1), pp. 49-63.

Schneider, P.; Neitzel, P.; Frenzel, M.; Schaffrath, M.; Sittner, H: (2003b): Umsetzung der EU-Wasserrahmenrichtlinie: Erarbeitung fachlicher Grundlagen zur Erstellung eines Bewirtschaftungskonzeptes für Grundwasser im Locker- und Festgestein am Beispiel der Steinkohlebergbau-Folgelandschaft Zwickau-Oelsnitz; Forschungsbericht AZ 13.8802.3522/68-1 im Auftrag des Sächsischen Landesamtes für Umwelt und Geologie, März 2003.

Zweig, M.; Schneider, P.; Frenzel, M. (2003): Flussgebietsbezogene Altlastenbehandlung am Beispiel der altbergbaubeeinflussten Zwickauer Grundwasserkörper, In: Wasser, Luft und Boden, Vol. 11-12, Supplement TerraTech pp. TT12-TT16.

Risk assessment studies

Lead isotope ratios as a tracer for contaminated waters from uranium mining and milling

Henk Coetzee, Mari Rademeyer
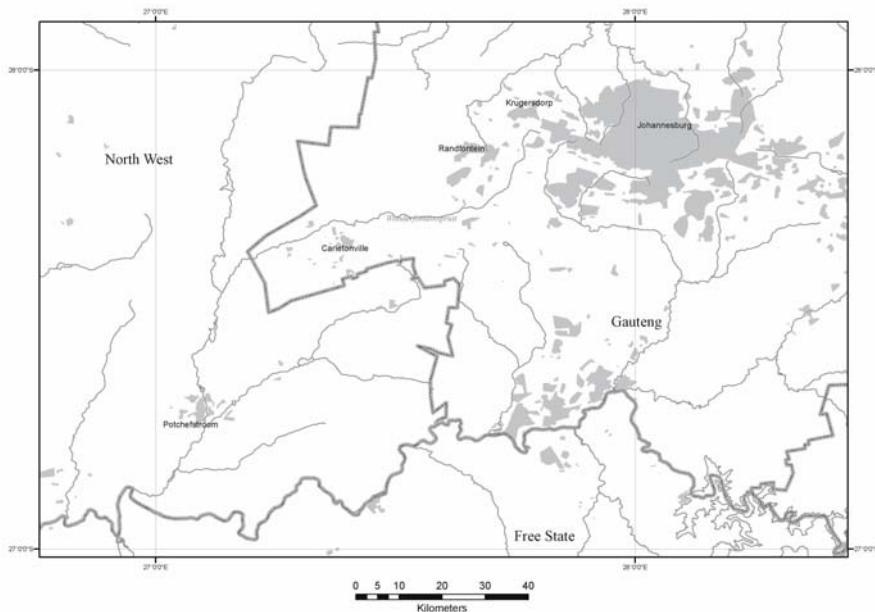
Council for Geoscience, Private Bag X112, Pretoria, 0001, South Africa,
E-mail: henkc@geoscience.org.za

Abstract. The elevated uranium concentrations of the ores of the Witwatersrand and the great age of the deposits have resulted in the development of extremely radiogenic lead isotope ratios. These ratios are reflected in the wastes and effluents generated by mining activities and may be used for the identification and tracing of Witwatersrand-sourced contamination. Fine sediments act as accumulators of heavy metals in the streams and rivers downstream of mining activities. Analysis of the lead isotopic compositions of these sediments can be used to identify and apportion the sources of this contamination.

Introduction

Gold has been mined in the Witwatersrand of South Africa since the late 19th Century. The gold ores contain appreciable (up to 5.8%) concentrations of uranium, which was economically extracted starting in the early 1950s. This production made South Africa the world's 4th largest producer of uranium (Cole, 1988).

This study looks at lead isotope ratios in the Wonderfonteinspruit catchment (see Fig. 1), which has its source in the mining areas of the West Rand, west of Johannesburg and flows south-west through the Far West Rand mines, finally discharging into the Mooi River, where it becomes a significant source of domestic water for the city of Potchefstroom (population ~300 000). The upper portion of the catchment (around Krugersdorp and Randfontein) is referred to as the upper Wonderfonteinspruit, while the lower portion (downstream of Carletonville) is referred to as the lower Wonderfonteinspruit. Between these two sections of the river it flows in a pipeline, which has been constructed to prevent water entering the mine workings below the stream bed. The work formed part of a larger study of the contamination of this catchment by mining activities, which found that uranium contamination posed a significant risk to water users, while uranium and

Fig. 1. Location of the Wonderfonteinspruit in the Gauteng and North West Provinces of South Africa.

other heavy metal contamination of stream sediments constitute a potential long term risk to downstream communities (Coetzee 2005).

Isotope ratio measurements may be applied for the tracing and, in some cases, apportionment of water and contaminant sources in mining areas. Eglington et al. (2001) present an approach to the use of different stable isotope systems for the tracing of acid mine drainage. In uranium mining districts, the radiogenic isotopes of lead (the daughter isotopes of uranium and thorium) provide a powerful tool for the tracing of waters and contaminant streams, as their evolution over geological time in a uranium rich orebody produces isotopic signatures which are distinct from normal environmental lead.

Radiogenic and common lead

Environmental lead is known to vary significantly in isotopic composition. Naturally occurring lead comprises four stable isotopes, with mass numbers 204, 206, 207 and 208. These have different origins, ^{204}Pb having been produced only during cosmogenesis, and ^{206}Pb, ^{207}Pb and ^{208}Pb being formed in the radioactive decay of ^{238}U, ^{235}U and ^{232}Th respectively. These three isotopes produced during radioactive decay are referred to as radiogenic isotopes, while ^{204}Pb is referred to as common lead.

Case studies: active and abandoned Uranium mines

These decays are governed by the decay law, which can be written for each isotopic system as:

$$\frac{^{206}\text{Pb}}{^{204}\text{Pb}} = \left(\frac{^{206}\text{Pb}}{^{204}\text{Pb}}\right)_i + \frac{^{238}\text{U}}{^{204}\text{Pb}}(e^{\lambda_{238_U} t} - 1)$$

$$\frac{^{207}\text{Pb}}{^{204}\text{Pb}} = \left(\frac{^{207}\text{Pb}}{^{204}\text{Pb}}\right)_i + \frac{^{235}\text{U}}{^{204}\text{Pb}}(e^{\lambda_{235_U} t} - 1)$$

$$\frac{^{208}\text{Pb}}{^{204}\text{Pb}} = \left(\frac{^{208}\text{Pb}}{^{204}\text{Pb}}\right)_i + \frac{^{232}\text{Th}}{^{204}\text{Pb}}(e^{\lambda_{232_{Th}} t} - 1)$$

Where t is the period elapsed since the system became closed w.r.t. uranium, thorium and lead, the R_i's represent the initial isotopic ratio (*i.e.* the ratio at the time of formation) and λ_X is the decay constant of the respective parent nuclide. In the case of rocks, these relationships can be used to determine the age of formation of a mineral grain or rock.
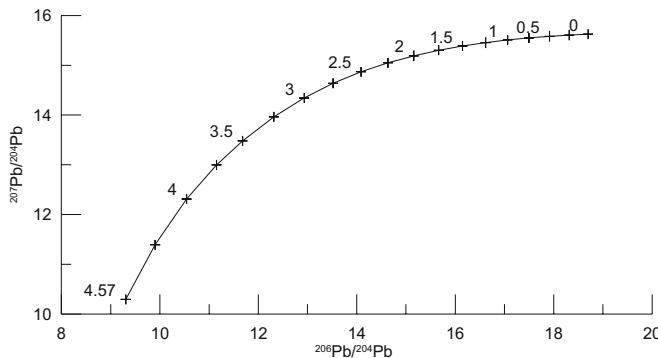
These relationships show that lead isotopic ratios will change over time depending on the uranium and thorium concentrations of the material and time. The half lives of all three of the parent nuclides is sufficiently long (10^8-10^{10} years) that no significant change will take place during the historical scale time periods generally investigated during environmental studies, while the small relative mass differences between isotopes (At mass ~206, a 1 a.m.u. mass difference amounts to less than one half of a percent of the atomic mass, compared to differences of several percent seen in the light stable isotopes) result in no significant fractionation by normal environmental processes. Thus, while lead, and many other metal, concentrations may change significantly due to different environmental processes, the isotope ratios of lead remain constant, being influenced only by mixing of lead from different sources.

Isotopic evolution of lead in the Earth's crust
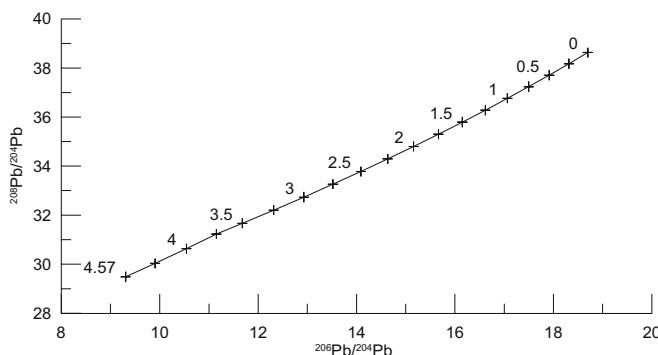
A number of models of the isotopic evolution of lead in the crust have been proposed. These will be discussed in detail in any text on isotope geochemistry. One commonly used is that of Stacey and Kramers (1975). In this model, it is assumed that the isotopic composition of lead in the earth's crust has evolved over time in response to the decay of uranium and thorium. The values calculated by the model for ^{206}Pb, ^{207}Pb and ^{208}Pb, all normalised to ^{204}Pb are presented on Fig. 2 and Fig. 3.

For environmental fingerprinting, it is not always practical to use these ratios, which are commonly used for geochronology, due to the difficulty in analysing ^{204}Pb at low levels of lead and the uncertainty introduced by the measurement of large ratios. For this reason, ^{207}Pb is used as a normalising isotope. The Stacey-Kramers curve is shown using this convention on Fig. 4.

Case studies: active and abandoned Uranium mines
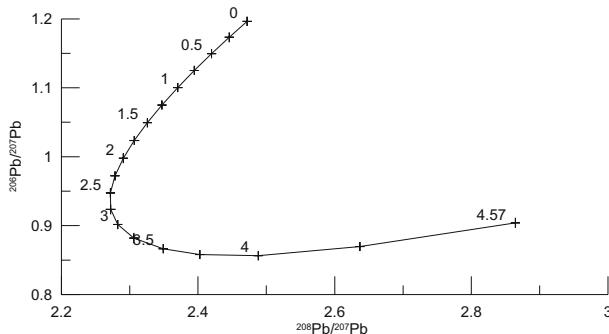
In isotope geochemistry, this model is used as a dating tool, with lead being extracted from the crustal reservoir at a certain time and then describing a new trajectory on the curves depending on the new $^{238}U/^{204}Pb$ and $^{232}Th/^{204}Pb$ ratios (μ and ω). In the case of sulphides in mineral deposits, particularly galena in lead deposits, a negligibly small concentration of uranium and thorium will be included in the sulphides, meaning that μ and ω are very small. Isotope ratios from mineral deposits will therefore plot on or close to the crustal evolution curve, at a position relating to the age of the deposit. Uranium and/or thorium rich deposits will however have much higher values of μ and ω, and will therefore grow to a point significantly removed from the crustal evolution curve.

Fig. 2.   Stacey-Kramers crustal isotopic evolution curve for lead $^{206}Pb/^{204}Pb$ and $^{207}Pb/^{204}Pb$, showing the evolution of these ratios over time (tick marks indicate different times in the earth's history in billions of years).

**Fig. 3.**   Stacey Stacey-Kramers crustal isotopic evolution curve for lead $^{206}Pb/^{204}Pb$ and $^{208}Pb/^{204}Pb$, showing the evolution of these ratios over time (tick marks indicate different times in the earth's history in billions of years).

Case studies: active and abandoned Uranium mines

Fig. 4.   Stacey Stacey-Kramers crustal isotopic evolution curve for lead ^{208}Pb/^{207}Pb and ^{206}Pb/^{207}Pb, showing the evolution of these ratios over time (tick marks indicate different times in the earth's history in billions of years).

Sampling and analysis

Sampling

Samples of mine tailings were collected from two source areas where active discharge of mine water is taking place. These were selected to represent the orebodies mined in the West Rand and Far West Rand gold fields. At the time of sampling, no method for the direct analysis of lead isotope ratios in water, which often contains a very low lead concentration, was available in the laboratory used. River sediments downstream of the relevant mines were therefore used for the analyses, these having been shown to concentrate heavy metals dissolved in the water column by precipitation and adsorption (Wade et al. 2002; Coetzee et al. 2002). Samples were collected in uncontaminated areas to provide background isotopic compositions (Unfortunately, it is not possible to sample the Wonderfonteinspruit upstream of mining activities, as these have been developed in the source area of the river). Since leaded petrol is still extensively used in South Africa, the isotopic composition of South African leaded petrol has also been included.

Analysis
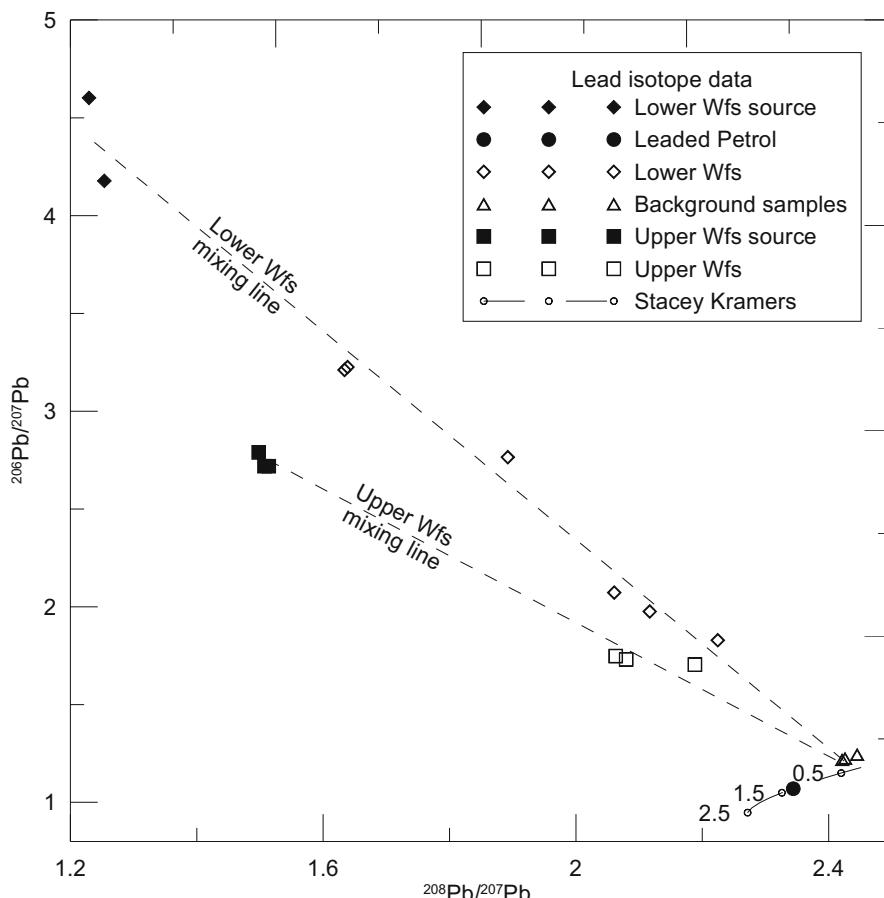
Samples were dissolved in a mixture of concentrated HF and HNO$_3$, the resulting solution dried down and redissolved in 0.6N HBr. Lead was separated from this solution by passing it through quartz glass columns using an anion exchange resin. The samples were loaded in a silica gel bed on rhenium filaments and analysed by

thermal ionisation mass spectrometry on a Finnigan MAT261 mass spectrometer. Chemical separations were undertaken in clean air, using double distilled reagents.

Results and discussion

Lead isotope data determined on river sediments from the Wonderfonteinspruit are presented on Table 1 and Fig. 5.

Two distinct mixing trends can be seen in these data. These are defined by the source and background end-members. Data from the two sections of the river plot along these trends, indicating that the lead in these samples constitutes a mixture between lead from these end-members, that the source of lead contamination in the samples can be determined from the individual sample and that the contribu-


Fig. 5.   Lead isotope data determined on river sediments from the Wonderfonteinspruit (Wfs).

Case studies: active and abandoned Uranium mines

tion of the source, relative to the background lead can be determined.

The data show that there is little downstream transport of lead from the upper to the lower catchment, as the data collected from sediments in the lower part of the catchment plot along a distinct mixing line and do not appear to contain a significant component of "Upper Wfs source" lead. This can be attributed to the relatively low solubility of lead and may not apply to the more soluble components of the waste stream.

Another notable feature of the data is the extremely uranogenic lead isotope ratios determined on samples from the vicinity of the gold/uranium mines. These ratios result from the extremely high initial uranium/lead ratios and the great age of the deposits.

Table 1. Lead isotope data determined on river sediments from the Wonderfonteinspruit.

Sample Number	Sample source	$^{206}Pb/^{204}Pb$	$^{207}Pb/^{204}Pb$	$^{208}Pb/^{204}Pb$	$^{208}Pb/^{207}Pb$	$^{206}Pb/^{207}Pb$
1-12	Background (mean of 12 analyses)	19.088	15.792	38.495	2.438	1.209
13	Lower Wfs	76.144	23.716	38.748	1.634	3.211
14	Lower Wfs	76.025	23.571	38.621	1.639	3.225
15	Lower Wfs	57.300	20.726	39.217	1.892	2.765
16	Lower Wfs	31.030	17.852	36.961	2.070	1.738
17	Lower Wfs	38.296	18.477	38.074	2.061	2.073
18	Lower Wfs	35.716	18.078	38.267	2.117	1.976
19	Lower Wfs	31.946	17.469	38.857	2.224	1.829
20	Lower Wfs source	137.595	31.804	39.872	1.254	4.178
21	Lower Wfs source	155.115	33.709	41.442	1.229	4.602
22	Upper Wfs	30.882	17.843	37.103	2.079	1.731
23	Upper Wfs	31.226	17.862	36.848	2.063	1.748
24	Upper Wfs	29.551	17.339	37.943	2.188	1.704
25	Upper Wfs source	66.810	24.071	36.441	1.514	2.718
26	Upper Wfs source	65.489	24.091	36.311	1.507	2.718
27	Upper Wfs source	67.860	24.328	36.441	1.498	2.789
	S.A. Leaded Petrol (mean of 5 analyses)	16.547	15.467	36.255	1.070	2.344

Conclusions

Lead isotope ratios may be used to "fingerprint" the lead contained in a variety of environmental samples. Where more than one lead source, for example lead from a mine discharge and background environmental lead, is present, mixing relationships, such as binary mixing lines may be used to apportion the contribution of the different sources.

In the case of uranium mines or mines exploiting ores with significantly elevated uranium concentrations, particularly where the deposits are geologically old, the highly radiogenic lead isotope ratios provide an excellent fingerprinting tool. This has been successfully applied in a case study of a river draining two Witwatersrand mining districts. Using lead isotope ratios, it is possible to identify and separate waste streams from the two districts.

References

Coetzee H, Wade P, Winde F (2002) Reliance on existing wetlands for pollution control around the Witwatersrand gold/uranium mines of South Africa – are they sufficient? In: Merkel BJ, Planer-Friedrich B, Wolkersdorfer C [eds] (2002): Uranium in the Aquatic Environment. Springer, Berlin, Heidelberg, 59-65.

Coetzee, H (compiler) (2005) An assessment of current and future water pollution risk with application to the Mooirivierloop (Wonderfonteinspruit). WRC report no K5/1214, Pretoria, 908pp, in press.

Coetzee H, Rademeyer M (2005) Lead Isotope characterisation of Gauteng Environments – Preliminary Report, Council for Geoscience Report, 26pp.

Eglington BM, Meyer R, Talma AS (2001) Assessment of the effectiveness of isotope chemistry for quantifying acid rock drainage contributions from different sources to ground and surface water. WRC Report 647/1/01, Water Research Commission, Pretoria, 72pp.

Stacey J S & Kramers J D (1975) Approximation of terrestrial lead isotope evolution by a two-stage model. Earth and Planetary Science Letters 26: 207-221.

Moab, Utah, UMTRA Site: The last large uranium mill tailings pile to be cleaned up in the United States

Kenneth E. Karp[1], Donald R. Metzler[2]

[1]S.M. Stoller Corporation, 2597 B¾ Road, Grand Junction, Colorado 81503 USA
[2]U.S. Department of Energy Office of Environmental Management,
2597 B¾ Road, Grand Junction, Colorado 81503 USA,
E-mail: donald.metzler@gjo.doe.gov

Abstract. The U.S. Department of Energy (DOE) is tasked with cleaning up surface contamination and developing and implementing a ground water compliance strategy to address contamination resulting from historical uranium-ore processing at the Moab, Utah, remedial action site. During the years of operations, the facility accumulated approximately 10.5 million tons of tailings and contaminated soils in an unlined pile about 750 feet from the Colorado River. The DOE preferred alternatives are to relocate the tailings to an alternate site away from the river and to implement long-term ground water remediation. An interim action ground water extraction/injection system is currently in operation to reduce the contaminant mass in ground water discharging to the river.
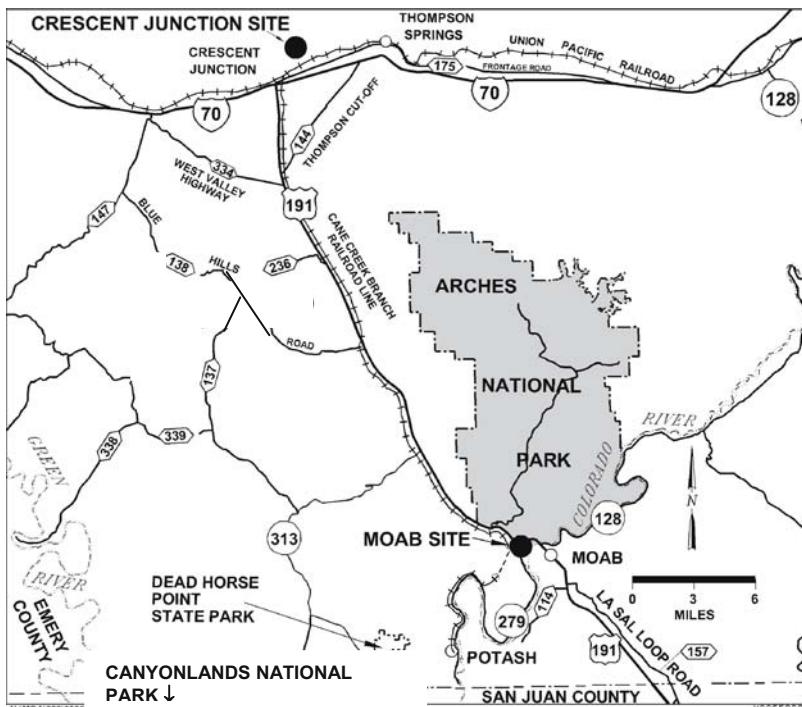
Introduction

The Moab, Utah, site is a former uranium-ore processing facility located about 3 miles northwest of the city of Moab in Grand County, Utah, (Fig. 1) and lies on the west bank of the Colorado River at the confluence with Moab Wash. Arches National Park has a common property boundary with the Moab site on the north side of U.S. Highway 191, and the park entrance is located less than 1 mile northwest of the site. Canyonlands National Park is located about 12 miles to the southwest.

During the years of operation, the facility accumulated approximately 10.5 million tons of tailings and contaminated soils. The tailings are located in a 130-acre unlined pile that occupies much of the western portion of the site. The top of the tailings pile averages 94 feet (ft) above the Colorado River floodplain (4,076 ft above mean sea level) and is about 750 ft from the Colorado River. The pile was constructed with five terraces and consists of an outer compact embankment of coarse tailings, an inner impoundment of both coarse and fine tailings, and an interim cover of soils taken from the site outside the pile area. Debris from dismantling the mill buildings and associated structures was placed in an area at the south end of the pile and covered with contaminated soils and fill.

Radiation survey results indicate that some soils outside the pile also contain radioactive contaminants at concentrations above the U.S. Environmental Protection Agency (EPA) standards in Title 40 Code of Federal Regulations (CFR) Part 192.

Besides tailings, contaminated soils, and debris, other contaminated materials requiring cleanup include ponds used during ore-processing activities, disposal trenches, other locations used for waste management during mill operation, and buried septic tanks that are assumed to be contaminated. The U.S. Department of Energy (DOE) estimates the total contaminated material at the Moab site and vicinity properties has a total mass of approximately 11.9 million tons and a volume of approximately 8.9 million cubic yards (yd³). Evidence indicates that historical


Fig. 1. Location map of the Moab site and surrounding area.

Case studies: active and abandoned Uranium mines

building materials may contain asbestos.

Ground water in the shallow alluvium at the site was contaminated by ore-processing operations. The Colorado River adjacent to the site has been affected by site-related contamination, mostly because of ground water discharge. The primary contaminant of concern in ground water and surface water is ammonia. DOE has identified two ammonia plumes associated with the site – a deep plume beneath the tailings pile and a shallower plume emanating from the toe of the tailings pile to the Colorado River. Ground water from the shallow plume has been demonstrated to discharge to the Colorado River and to have a localized impact on surface water quality. Degradation of surface water quality is of concern because of potential effects on aquatic species in the area, particularly endangered fish.

To minimize potential adverse effects to human health and the environment in the short term, DOE instituted environmental controls and interim actions at the site. Controls include storm water management, dust suppression, pile dewatering activities, and placement of an interim cover on the tailings. Interim actions include restricting site access and monitoring ground water and surface water. An interim action ground water extraction/injection system was implemented to reduce the contaminant mass in ground water discharging to the Colorado River.

Regulatory Framework

The title of the Moab site was transferred to DOE in 2001 along with the responsibility for site cleanup in accordance with Title I of the Uranium Mill Tailings Radiation Control Act (UMTRCA). The act further requires that remediation of the site include ground water restoration. Ground water compliance standards applicable to the Moab site are the EPA standards established in 40 CFR 192. Subparts A and B of 40 CFR 192 provide standards for cleanup and final disposal of contaminated materials for Title I Uranium Mill Tailings Remedial Action (UMTRA) Ground Water Project sites. Subpart A standards apply to protection of ground water from future contamination released from the disposal system after cleanup is complete. Subpart B standards pertain to cleanup of residual radioactive materials, including ground water, at the site. The Subpart B cleanup standards are the same as the Subpart A protection standards except that Subpart B allows for an extended time frame to attain compliance with the standards and allows the use of a natural flushing compliance strategy, providing certain other criteria are met.
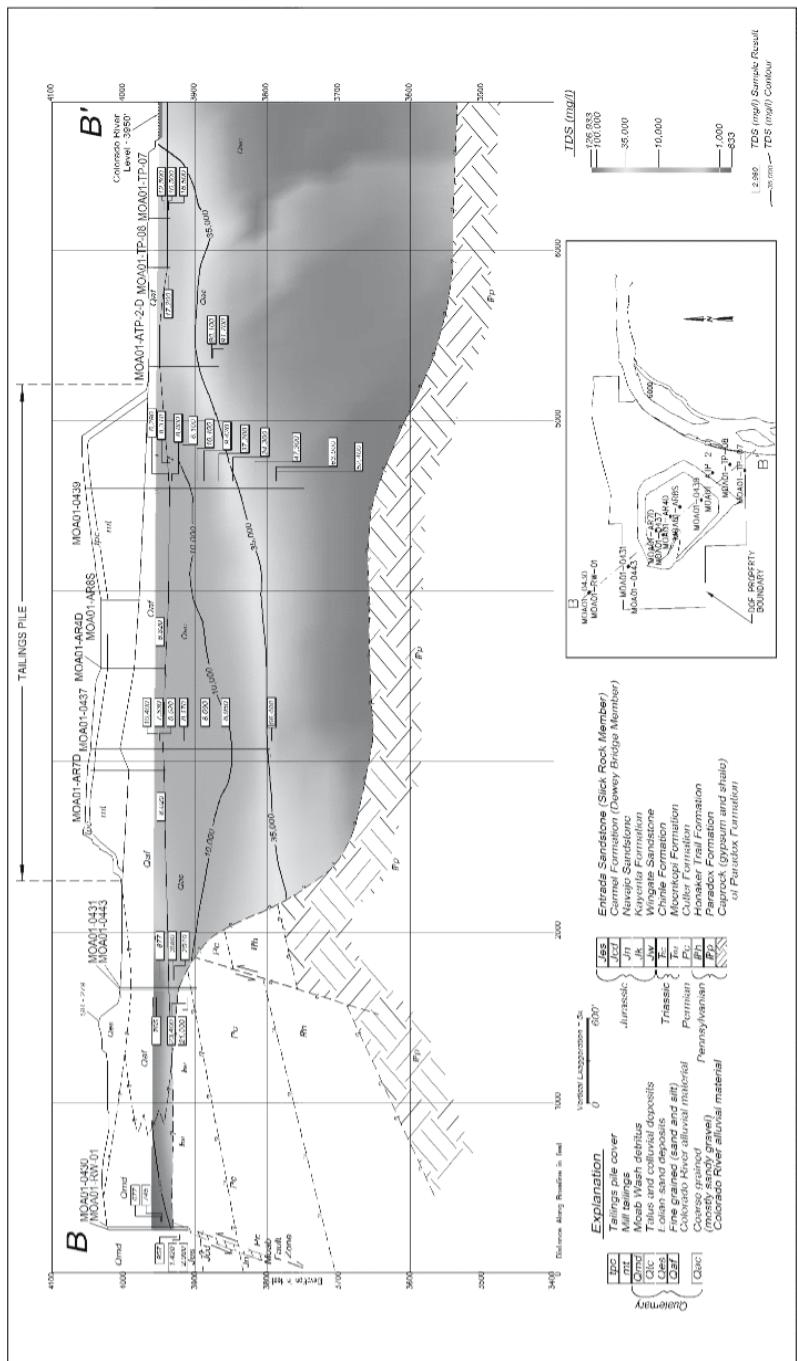
Pursuant to the National Environmental Policy Act (NEPA), title 42 *United States Code* (U.S.C.) section 4321 *et seq.*, DOE prepared an Environmental Impact Statement (EIS) to assess the potential environmental impacts of remediating the Moab site. DOE analyzed the potential environmental impacts of both on-site and off-site remediation and disposal alternatives involving both surface water and ground water contamination. DOE also analyzed the no action alternative as required by NEPA implementing regulations promulgated by the Council on Environmental Quality. Some government agencies and the public expressed concern about the potential effects of capping the contaminated materials at the site, one of

the proposed alternatives, because of engineering uncertainty of river migration and the long-term effects of contaminated ground water entering the Colorado River. For these reasons and other factors, the DOE preferred alternative is to relocate the tailings to an alternate site away from the Colorado River and to implement long-term ground water remediation to address contamination that resulted from historical uranium-ore processing at the former millsite.

Conceptual Hydrogeologic Model

Ground water at the site occurs mostly in alluvial sediments that may be as deep as 120 meters (m) or more. Total dissolved solids (TDS) concentrations in the alluvial ground water vary naturally from slightly saline water (TDS = 1 to 3 kilograms per cubic meter [kg/m^3]; 1000 to 3000 milligrams per liter [mg/L]), to those categorized as moderately saline (TDS = 3 to 10 kg/m^3), very saline (TDS =10 to 35 kg/m^3), and briny (TDS > 35 kg/m^3). The primary source of the slightly saline water, which is found only in the shallowest parts of the saturated zone, appears to be ground water discharge from bedrock aquifers that subcrop both near the northwest border of the site and north of the tailings pile. Brine waters dominate the deepest parts of the alluvium and are attributed to chemical dissolution of the underlying Paradox Formation, a large and relatively deep evaporite unit that has been deformed to create a salt-cored anticline aligned with and underlying the Moab Valley .

A cross section of the subsurface hydrogeology through the site showing the interface between the deeper brine and the overlying brackish-to-freshwater system is illustrated on Fig. 2. The interface is assumed to exist where the TDS concentration equals 35,000 mg/L. The transition from brine to freshwater sometimes occurs over a short vertical distance; by convention, the line demarcating the boundary between brine and freshwater in such cases is typically referred to as a "sharp" interface. TDS concentrations above the interface decrease gradually before reaching an elevation where relatively freshwater is observed. This diffuse zone is brought about by mixing of more saline water with fresher water through the process of hydrodynamic dispersion. For convenience, the term saltwater interface is used to describe the depth at which a TDS concentration of 35,000 mg/L is observed.
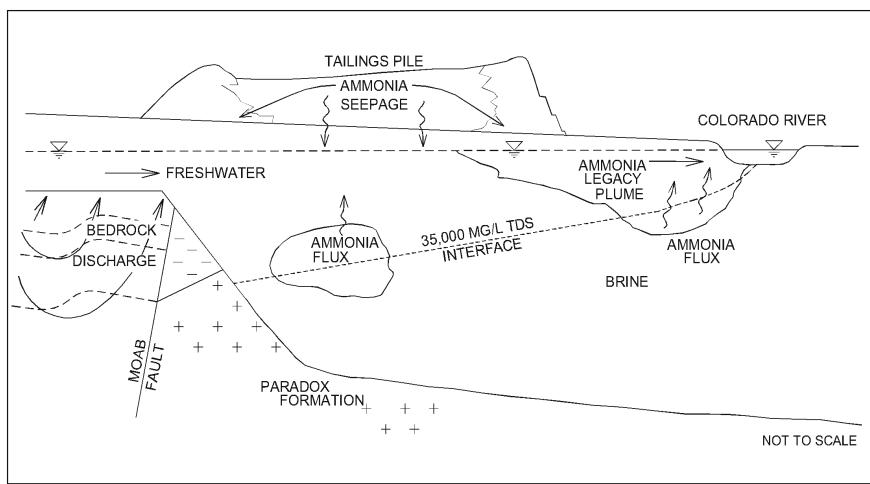
Fig. 2. Cross section through the site of the subsurface hydrogeology and the salt water interface at 35,00 mg/L TDS.

Case studies: active and abandoned Uranium mines

During milling operations, the tailings pond contained fluids with TDS concentrations ranging from 50,000 to 150,000 mg/L. Because these salinities exceed 35,000 mg/L, they had sufficient density to migrate vertically downward through the freshwater system and into the brine. This downward migration of the tailings pond fluids into the saltwater system is believed to have created a reservoir of ammonia that now resides below the saltwater interface. This ammonia plume below the interface probably came to rest at an elevation where it was buoyed by brine having a similar density.

Under present conditions, the ammonia plume beneath the saltwater interface represents a potential long-term source of ammonia to the freshwater system. The conceptual model presented in Fig. 3 illustrates the ammonia source at the saltwater interface (basal flux), the legacy plume, and seepage of ammonia from tailings pore fluids.

Nature and Extent of Ground Water Contamination

Site-related constituents including ammonia, nitrate, sulfate, molybdenum, uranium, gross alpha, and gross beta have contaminated the basin-fill aquifer beneath the tailings pile and beneath the former millsite. DOE identified two ammonia plumes associated with the site – a deep plume beneath the tailings pile and a shallower plume emanating from the toe of the pile to the Colorado River (Fig. 4). Although ammonia has no EPA standard in 40 CFR 192, it occurs at concentrations significantly greater than natural background, is the most prevalent contaminant in the ground water, and is the constituent of greatest ecological concern that is discharging to the Colorado River.


N:\MOA\999\0005\02\014\X00534\X0053400.DWG 10/11/04 10:01am J50191   X0053400

Fig. 3.   Conceptual model of seepage of ammonia concentrations from the tailings pile.

Case studies: active and abandoned Uranium mines

The highest ammonia concentrations in surface water samples are detected in samples collected in backwater areas adjacent to the site. Ammonia levels have been of concern since ammonia was first detected river samples, largely because of the designation of this segment of the Colorado River as critical habitat for the
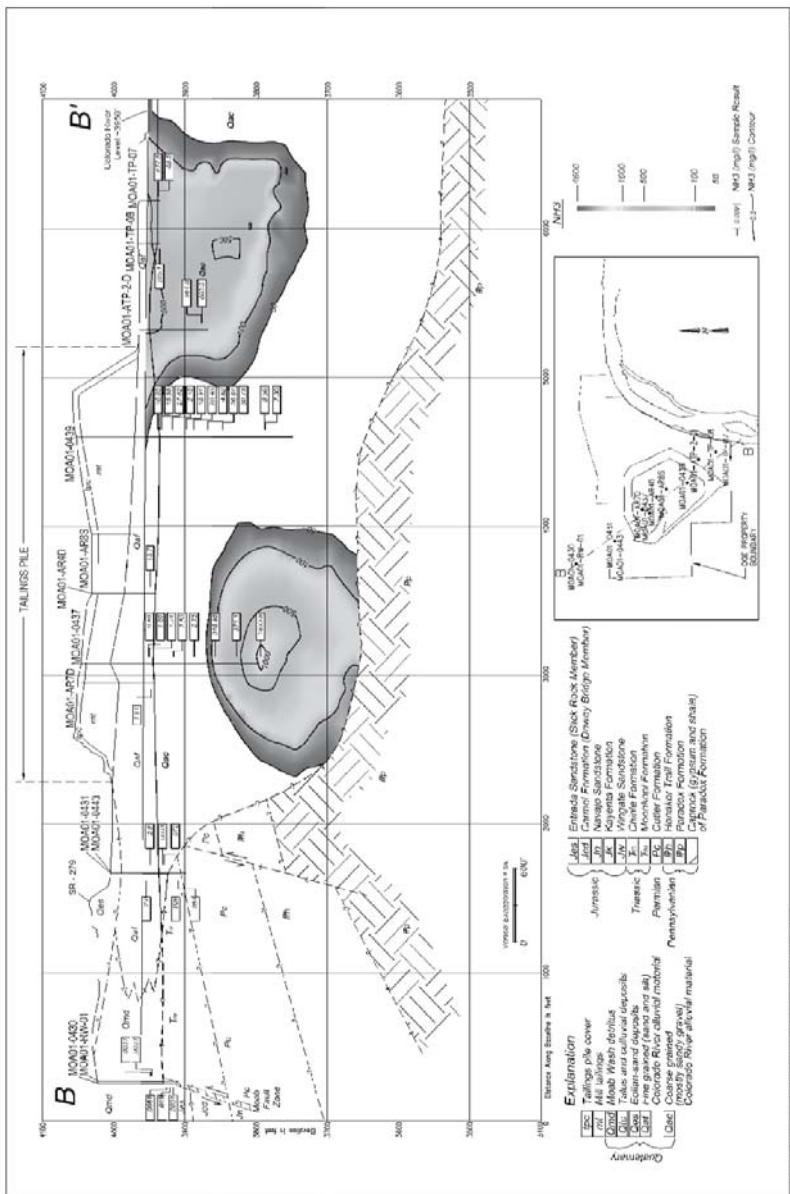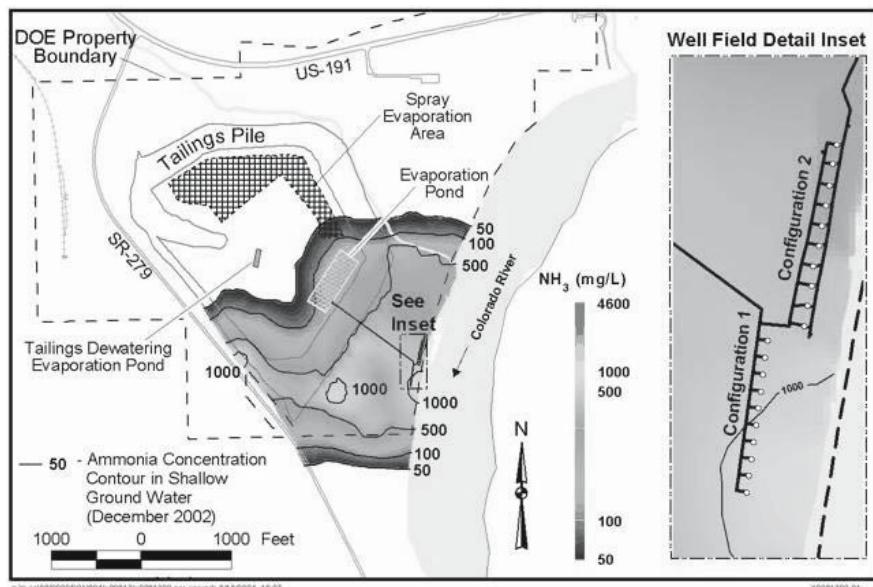
Fig. 4.   Cross sectional view of ammonia concentrations in ground water beneath the tailings pile area.

Case studies: active and abandoned Uranium mines

Colorado pikeminnow (previously referred to as Colorado squawfish) and three other endangered fish species (razorback sucker, bonytail chub, and humpback chub). Pikeminnow favor slow-moving backwater areas of the river as nursery habitat for young-of-year fish.

Tailings Fluid Dewatering

As the mill tailings were slurried to the disposal area and formed the pile, pore fluids in the tailings naturally accumulated within the pile. To dewater the tailings pile, the former site trustee installed a system of 17,000 "wicks" (vertical band drains) in the pile prior to DOE site ownership. The vertical band drains provide a pathway for the pore fluids to more quickly travel out of the pile. Overburden material was added to the top of the pile to provide additional weight that helps "squeeze" or force some of the fluids up to the top of the pile through the vertical band drains. A lined evaporation pond was constructed on top of the tailings pile to collect the fluids being collected from the vertical band drains (Fig. 5).

DOE continues to dewater the Moab tailings pile. As of April 30, 2005, approximately 1,054,797 gallons of pore fluids (Fig. 6), 59,893 kg of ammonia, and 60 kg of uranium have been pumped from the pile and evaporated from the lined evaporation pond. Dewatering the pile allows consolidation of the pile to occur prior to relocation and will minimize the amount of wet material that has to be
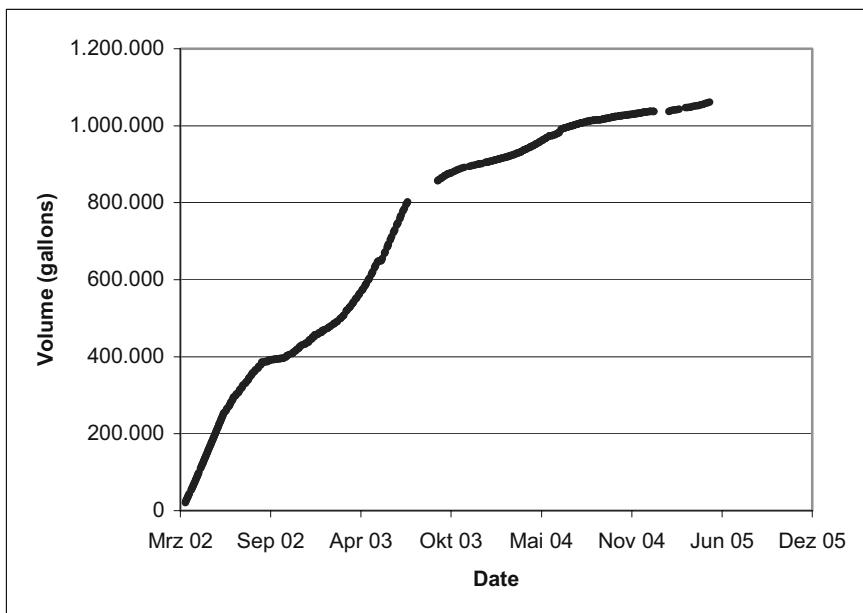

Fig. 5. Locations of the interim action systems and ammonia concentrations in the shallow ground water beneath the tailings pile.

Case studies: active and abandoned Uranium mines

handled. Dewatering also reduces the amount of contamination from the pile that can leach into the ground water or to the Colorado River. The effectiveness of the dewatering system is decreasing as excess pore pressure from the additional soils of the overburden material is dissipated.

Extraction and Freshwater Injection Well Fields

In 2003, DOE implemented the first phase of the ground water interim action at the site while a decision for the long-term solution to site contamination was being developed. Referred to as Configuration 1 (Fig. 5), the first phase consisted of 10 closely spaced extraction wells designed to remove contaminant mass (ammonia) from the ground water system before it discharges to critical habitat areas of the Colorado River. The expected hydraulic result of operating Configuration 1 extraction wells is to manipulate the ground water flow gradients near the river as shown conceptually on Fig. 7.

   Operation of the Configuration 1 system at relatively high pumping rates results in a growth of the cone of depression that extends to the river. The pumping rates are operated to minimize upconing of the saltwater interface to the backwater areas and increasing ammonia and TDS loading in those areas and to maximize a reversal of the ground water flow gradients near the west bank of the river to in-
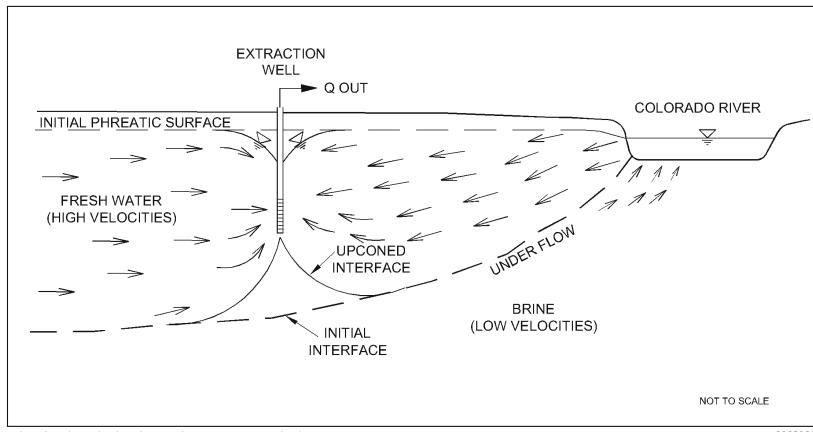

Fig. 6. Cumulative volume of tailings pore fluids extracted by the dewatering system.

troduce clean river water into the near-bank backwater areas and reduce ammonia concentrations by dilution. Dilution only occurs in the shallow ground water because underflow of the pumped zone would continue transporting ammonia toward the riverbed.
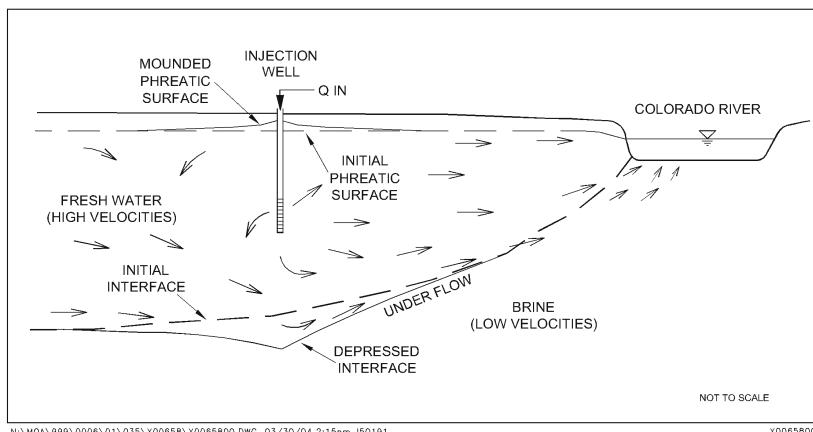
Configuration 2 of the interim action was completed in 2004 with the addition of a series of 10 dual-purpose extraction and freshwater injection wells to the north of Configuration 1 (Fig. 7). The objective of freshwater injection is to create a freshwater mound that would provide a hydraulic barrier between the ammonia plume and the river. A conceptual model of the effect of operating the Configuration 2 system with freshwater injection is shown on Fig. 8. Mounding of clean water at the injection well provides a hydraulic barrier between the ammonia plume and the river. Freshwater discharging to the near-shore backwater areas provides dilution of ammonia concentrations and thereby improves the quality of the surface water. It is possible that freshwater injection occurring near the bank of the Colorado River, advection and dispersion of the freshwater, depresses the saltwater interface and moves the ground water discharge of the ammonia plume farther east and beneath the Colorado River.

Treatment by Evaporation

Ground water extracted from the shallow aquifer from Configurations 1 and 2 is pumped via pipeline to a solar evaporation pond for treatment (Fig. 5). The evaporation pond covers approximately 4 acres and was constructed outside the 100-year floodplain on top of the tailings pile. In addition to the evaporation pond, a 17-acre land-applied spray evaporation system was installed in 2004 to enhance evaporation of ground water pumped from the interim action extraction wells by using a sprinkler system installed on top of the tailings pile next to the evaporation pond. The sprinkler system consists of micro-spray nozzles on 25-ft centers. The system was expanded to include an additional 11 acres in 2005. The combined 28 acres of sprinklers operate in conjunction with the existing evaporation pond, which has more than doubled the capacity of the existing interim action. The system is designed to evaporate the water before it infiltrates the tailings pile and to provide dust suppression.

**Fig. 7.**   Conceptual model of the Configuration 1 extraction system.

Fig. 8.   Conceptual model of the hydraulic barrier by the Configuration 2 freshwater injection system.

Conclusions

In October 2001, DOE was tasked with the requirements to clean up surface contamination and develop and implement a ground water compliance strategy to address contamination that resulted from historical uranium-ore processing at the abandoned Moab millsite. The Moab site is the last large uranium mill tailings pile to be cleaned up in the United States.

DOE instituted environmental controls and interim actions at the site to minimize potential adverse effects to human health and the environment in the short term while a draft EIS was being prepared to evaluate long-term remediation alternatives. Comments received from some government agencies and the public on the draft EIS, released for public comment in November 2004, expressed concern about the potential effects of capping the contaminated materials at the site because of engineering uncertainty of river migration and the long-term effects of contaminated ground water entering the Colorado River. For these reasons and other factors, the DOE preferred alternative is to relocate the tailings to an alternate site away from the Colorado River and to implement long-term ground water remediation.

The final EIS, incorporating public comments and summaries, will be distributed to the public in summer 2005. A final Record of Decision is expected to be issued in fall 2005. The interim action system will continue to operate and may eventually become part of the final ground water remedy. Monitoring data are currently being collected to demonstrate the effectiveness of the system prior to design and construction of the long-term ground water strategy.

Acknowledgment

Case studies: active and abandoned Uranium mines

U isotopic fractionation – a process characterising groundwater systems

Juhani Suksi[1], Kari Rasilainen[2], Nuria Marcos[3]

[1]University of Helsinki, Laboratory of Radiochemistry, 00014 HY, Finland,
E-mail: juhani.suksi@helsinki.fi
[2]VTT Processes, 02044 VTT, Finland
[3]Helsinki University of Technology, 02015 Espoo, Finland

Abstract. The activity of ^{234}U relative to ^{238}U (AR) in groundwaters is controlled by isotope fractionation in water-rock interface. The fractionation is controlled by redox-conditions and rock-groundwater contact time. The measured ARs form thus an important source of information and offer an effective tool to characterise groundwater systems along with other hydrochemical data. The purpose of this paper is to elucidate the link between ARs and groundwater conditions. The paper considers the formation of AR in groundwaters and examines measured data from several study sites in the Fennoscandian Shield.

Introduction

Present groundwater conditions in glaciated terrain represent a snapshot in the long-term groundwater evolution. A characteristic feature of the present ground-waters in the Fennoscandian Shield is stratified hydrochemistry which appears to reflect slowly changing or stable conditions. This means that current groundwater circulation cannot reach very deep. Evidence of the generally shallow circulation depth of waters is further supported by the reducing groundwater conditions deeper down (Puigdomenech et al. 2001).

Investigations of U concentrations and ^{234}U/^{238}U isotope activity ratios (AR) in groundwaters form a part in site characterization for nuclear waste repositories. Uranium isotopes can enter groundwater via physical and chemical processes. In this context we are interested in ^{234}U because it is the isotope adjusting AR. The physical process is direct α-recoil of ^{234}U and the respective chemical process promoting the release of ^{234}U is related to the different origin of uranium isotopes.
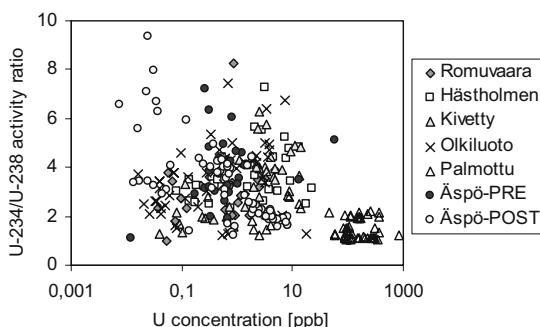
It could be called indirect α-recoil as it is expressly α-recoil that has caused the increased susceptibility for [234]U to be released preferentially.

It is well-known that [234]U release is controlled by the redox-conditions and water-rock contact time (Osmond and Cowart 1976). It is also well-known that rocks display [234]U depletion (AR<1). We have measured ARs in rocks which are clearly below the theoretical minimum of 0.5 that α-recoil can generate, indicating [234]U release mechanism other than direct α-recoil (Suksi and Rasilainen, 2002).

In this paper we discuss the use U isotope fractionation and resulting AR as a hydrogeologic characterisation tool. Fig. 1 shows plotted U-AR data sets from several study sites in Finland and Sweden. The plot shows how the data are usually presented for interpretation. We show how they can be utilised in an other way. To do this we pose first some questions. Why do groundwaters show such large AR variations? Why variations are seen in the shallow bedrock depths as well as deeper far beyond the range of present-day circulation. What do very high ARs mean? It is evident that large AR values in the depths of several hundreds of meters cannot be explained by present-day waters. Because variations in Fig. 1 occur independently of depth, does this mean that all ARs could be explained by the same mechanisms?
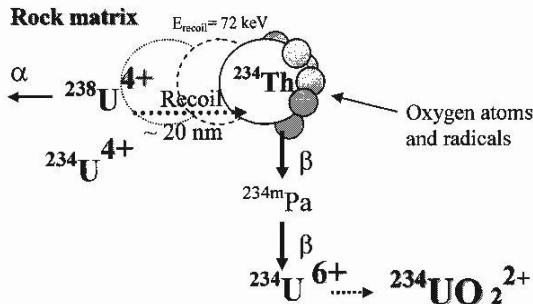
Release of U isotopes from rocks and isotopic fractionation

Uranium isotopes can enter groundwater through physical and chemical processes. The physical process is the direct α-recoil but it concerns only [234]U isotope. It is completely independent of geochemical conditions maintaining thus continuous [234]U flux into groundwater everywhere where uranium is present. The chemical
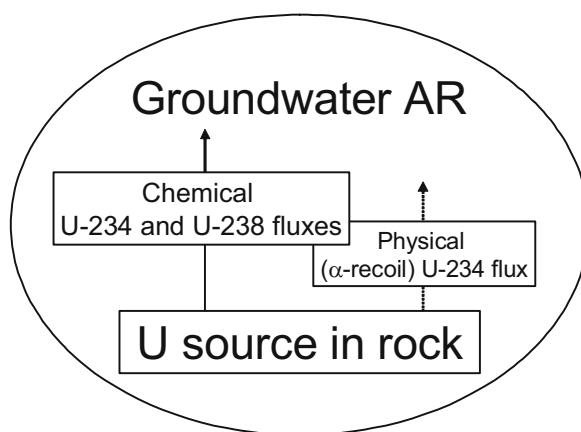

Fig.1.   Uranium concentrations and ARs in Finnish and Swedish groundwaters. Typical to all groundwaters are large concentration and AR variations. Äspö-PRE and ÄSPÖ-POST refer to data taken before and after the excavations of Hard Rock Laboratory.

Case studies: active and abandoned Uranium mines

process is groundwater dissolving, naturally, all uranium isotopes, but ^{234}U dissolution is always more probable. Decay series ^{238}U $\rightarrow$ ^{234}Th $\rightarrow$ ^{234}Pa $\rightarrow$ ^{234}U and related recoil chemistry increases the susceptibility of ^{234}U for groundwater leaching. Fig. 2 shows how the process is believed to proceed (modified from Ordonez Regil et al., 1989 and Adloff & Roessler, 1991). As a difference to direct α-recoil chemical release of ^{234}U when dominating over ^{238}U requires favourable groundwater conditions.

Fig. 2.   A model of successive physical and chemical events during decay of ^{238}U to ^{234}U. The oxygen atoms pushed the ^{234}Th atom along its trajectory creates a locally oxic environment that oxidises the ^{234}U which in turn creates valence contrast between the isotopes, thus contributing selective dissolution of ^{234}U.


Fig. 3.   U flux from rock into water. The flux consists of chemical and physical component.

Case studies: active and abandoned Uranium mines

^{234}U mass flux and groundwater conditions

Groundwater conditions control chemical U flux from rock into water. The flux contains all U isotopes, including physical ^{234}U flux (Fig. 3). In oxidising conditions the flux consists of U isotopes roughly in the ratio they occur in U source (congruent release) because prerequisites for isotopic fractionation have been eliminated. In anoxic conditions dissolution of U is reduced and flowing water tends to be enriched with the more mobile ^{234}U.

In stagnant anoxic waters chemical U flux is in minimum when the physical ^{234}U flux may become important. However, the recoil-induced increase of AR to notable values above unity will take hundreds to thousands of years, depending on the U source. Groundwater flow at already moderate rates is sufficient to eliminate the influence of the physical ^{234}U flux (Rasilainen et al. 2005a, b). Therefore, it seems that in most cases it is the chemical ^{234}U flux that controls AR in groundwater.

The ARs greater than the equilibrium value of unity observed in the shallow bedrock most probably relate to changes in redox-conditions as in oxidising conditions isotope fractionation is suppressed. In deep groundwaters ARs exceeding unity are possible for the same reason but other process than present-day recharge, possibly glacial melt water intrusion, must have produced them. High ARs can be generated in water if it has flowed (or flow) through rocks rich in U (U mineralization) because strong U source contributes physical ^{234}U flux.

Examination of site specific U data

Groundwater obtains its U concentration and AR from the bedrock through which it percolates. ARs can be considered a sort of indicator of groundwater conditions. To see the relevant "signal" various data presentation techniques have been used (Osmond and Cowart, 1976). The oft-used technique is to plot AR versus U concentration (Fig. 1). The weakness of this technique is that it shows weighted averages and is not necessarily applicable for all groundwater systems. We present here another technique, which allows consideration of U isotope mass flows and thus more quantitative interpretation of ARs.

Treatment of the U data

The U concentration in groundwaters is usually expressed in mass units (µg/l or ppb) and it always represents ^{238}U isotope because the mass of ^{234}U is four orders of magnitude less. The concentration can be alternatively expressed in radioactivity units (Bq/l or dpm/l), which is needed for presenting AR. In radioactive equilibrium (AR equals unity), the corresponding ^{234}U/^{238}U mass ratio is 0.000055.

Case studies: active and abandoned Uranium mines

Radioactivity is derived from

$$A_i = \lambda_i N_i \tag{1}$$

where A_i = activity of nuclide i (Bq)

λ_i = radioactive decay constant of nuclide i (1/s)

N_i = number of atoms of nuclide i (atoms)

Estimating the number of atoms of nuclide i for a unit mass of water one obtains

$$N'_i = \frac{C_i}{M_i} N_A \tag{2}$$

where M_i = molecular weight of nuclide i (g/mol)
N_A = Avogadro's constant = number of atoms /mole ($6 \cdot 10^{23}$ atoms/mol)
C_i = concentration of nuclide i in water (g /g water)

Here N'_i is expressed as (atoms / g water). Thus for ^{238}U and ^{234}U one obtains

$$A'_{U-238} = \lambda_{U-238} N'_{U-238} = \lambda_{U-238} \frac{C_{U-238}}{M_{U-238}} \cdot N_A \tag{3}$$

$$A'_{U-234} = \lambda_{U-234} N'_{U-234} = \lambda_{U-234} \frac{C_{U-234}}{M_{U-234}} \cdot N_A \tag{4}$$

where A'_i = activity per g water (Bq/g).
Activity ratio AR is consequently:

$$AR = \frac{A'_{U-234}}{A'_{U-238}} = \frac{\lambda_{U-234} \dfrac{C_{U-234}}{M_{U-234}} \cdot N_A}{\lambda_{U-238} \dfrac{C_{U-238}}{M_{U-238}} \cdot N_A} \approx \frac{\lambda_{U-234}}{\lambda_{U-238}} \cdot \frac{C_{U-234}}{C_{U-238}} \tag{5}$$

For the convenience of presenting U data we want to express the concentration of ^{234}U as a function of ^{238}U concentration:
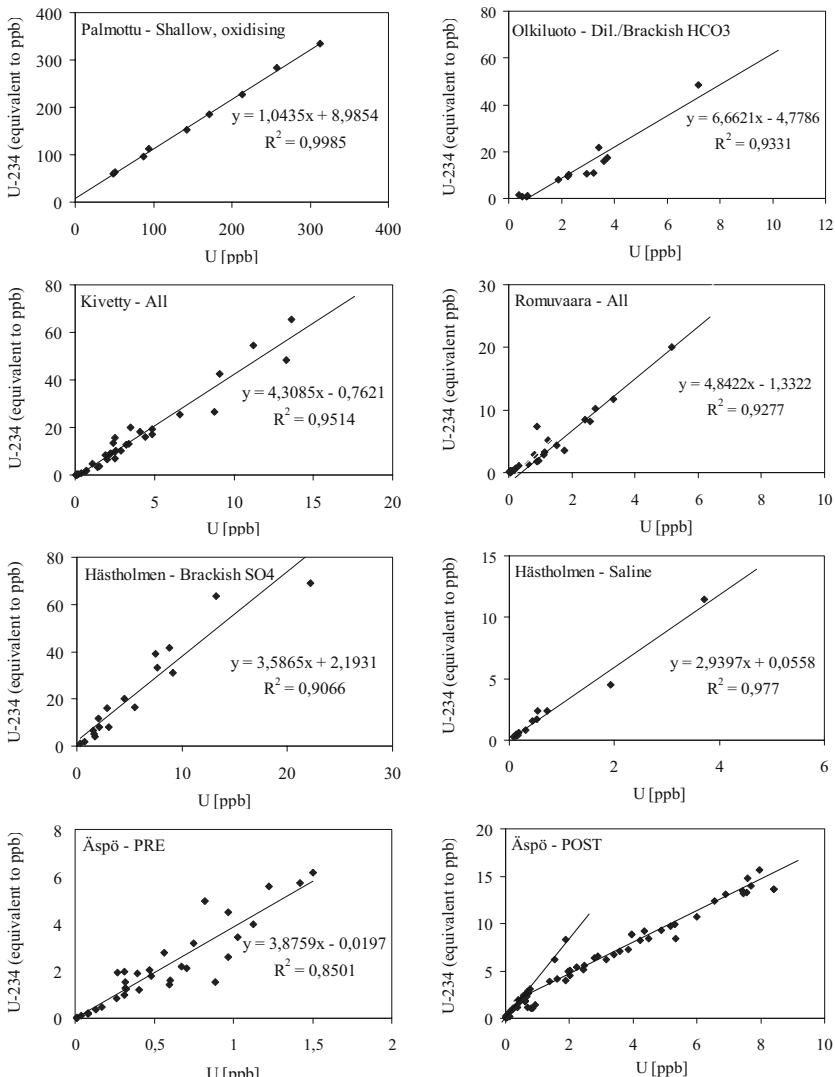
$$C_{U-234} \approx AR \cdot \frac{\lambda_{U-238}}{\lambda_{U-234}} C_{U-238} \tag{6}$$

For graphical presentation we neglect the constant $\lambda_{U-238}/\lambda_{U-234}$ in Eq. (6) and the concentration so obtained is referred to as equivalent ^{234}U concentration.

Observations

The data sets in Fig. 1 were modified and equivalent ^{234}U concentrations against U concentration were plotted (Fig. 4). Good correlation was obtained irrespective of the site and depth, which is in agreement with the general view of stable groundwater conditions. The correlation offers an interesting opportunity to use line fitting for interpretation. The slope of the line (multiplier of x) gives in reality the ^{234}U/^{238}U leaching ratio in terms of mass, cf. Eq (6).

The meaning of the line slope seems to be clear. The meaning of the other line parameter that is the constant in the line equation shown in the pictures (intercept) is not so clear. Because leaching is considered the main mechanism to feed U in water one would expect to see the lines intercept ordinate in the origin (constant in the line equation is zero). The intercepts seem however to deviate from the origin,


Fig. 4.   Presentation and examination U data from Finnish (Blomqvist et al. 2000, Pit-känen et al. 1996, 1998, 1999, 2001, 2004) and Swedish (Tullborg et al. 2004) study sites. Graphs have been chosen to show the typical range of leaching ratio (multiplier of x) and line constant (intercept). There are data sets available for different water types.

Case studies: active and abandoned Uranium mines

obtaining both positive and negative values. In physical sense positive values would mean another mechanism to introduce ^{234}U in water, i.e. direct α-recoil. Whether the positive values of the intercept are real and show the recoil addition of ^{234}U remains to be solved in further studies.

Leaching ratio values vary between 1 (Palmottu) and 6.6 (Olkiluoto), indicating the influence of chemical conditions. In oxidising conditions at Palmottu isotope fractionation cannot be seen in the leaching ratio value, whereas at Olkiluoto where rapid change from oxidising to anoxic conditions in recharging water is known to occur (Pitkänen et al. 1999, 2004) strong fractionation is evident.

Negative intercepts are interesting because intercepts were thought to be placed in origin or have positive values. Exceptionally large negative value was obtained for the dil./brackish HCO$_3$-system at Olkiluoto (Fig. 4). One plausible explanation for negative values is U removal from water as a consequence of geochemical changes because the process, whatever it is, does not change AR. Independent hydrochemical data support significant changes in redox-conditions (Pitkänen et al.2004)

Hydrological implications

Although ARs in a site seem to vary considerably they can still reflect the same hydrological event. Large ARs can be thought to reflect steep changes in redox-conditions. Good correlation of the data plots is notable because the data represent relatively large geographical area. Correlation seems to be independent on the U source too. This suggests that respective groundwaters have undergone similar process and that this process has affected U release in a similar manner, i.e. both U isotopes have been leached in the same ratio within relatively large bedrock units. This can be interpreted a signal of a process which is much more pervasive than present-day recharge and which has occurred at all sites.

The large AR values in groundwater represent a relatively unique signature and may indicate geochemical conditions changing from oxic to anoxic. The good correlation obtained could be used to identify groundwater samples representing different groundwater system.

Acknowledgements

References

Adloff, J.P. and Rössler, K., 1991. Recoil and transmutation effects in the migration behaviour of actinides. Radiochim. Acta 52/53, 269-274.

Blomqvist, R., Ruskeeniemi, T., Kaija, J., Ahonen, L., Paananen, M., Smellie, J., Grundfelt, B., Pedersen, K., Bruno, J., Pérez del Villar, L., Cera, E., Rasilainen, K., Pitkänen, P., Suksi, J., Casanova, J., Read, D. & Frape, S. 2000. The Palmottu natural analogue project – Phase II: Transport of radionuclides in a natural flow system at Palmottu. Luxembourg: European Commission, 192 s. (Nuclear Science and Technology Series EUR 19611 EN.).

Ordonez-Regil, E., Schleiffer, J.J., and Adloff, J. P., 1989. Chemical effects of α-decay in uranium minerals. Radiochim. Acta 47, 177-185.

Osmond J.K. and Cowart J.B., 1976. The theory and uses of natural uranium isotopic variations in hydrology. Atomic Energy Review 14(4), 621-679.

Pitkänen, P., Snellman, M., Vuorinen, U. and Leino-Forsman, H., 1996. Geochemical modelling study on the age and evolution of the groundwater at the Romuvaara site. Posiva 96-06, 120 p.

Pitkänen, P., Luukkonen, A., Ruotsalainen, P., Leino-Forsman, H. and Vuorinen, U., 1998. Geochemical modeling of groundwater evolution and residence time at the Kivetty site. Posiva 98-07, 139 p.

Pitkänen, P., Luukkonen, A., Ruotsalainen, P., Leino-Forsman, H. and Vuorinen, U., 1999. Geochemical modeling of groundwater evolution and residence time at the Olkiluoto site. Posiva 98-10, 184 p.Pitkänen, P., Luukkonen, A., Ruotsalainen, P., Leino-Forsman, H. and Vuorinen, U., 2001. Geochemical modeling of groundwater evolution and residence time at the Hästholmen site. Posiva 2001-01, 175 p.

Pitkänen, P., Partamies, S. and Luukkonen, A., 2004. Hydrogeochemical interpretation of Baseline groundwater conditions at the Olkiluoto site. Posiva 2003-07, 159 p.

Rasilainen, K., Suksi, J., Marcos, N., & Nordman, H. 2005a. 234U/238U activity ratio in groundwater – an indicator of past hydrogeological processes?, Helsinki University of Technology, Report TKK-GT-A-1, 41 p.

Rasilainen, K., Nordman, H., Suksi, J. & Marcos, N. 2005b. Direct alpha-recoil as a process to generate U-234/U-238 disequilibrium in groundwater. MRS2005, Ghent, Belgium 12-16 September 2005, Scientific Basis for Nuclear Waste Management XXIX

Suksi, J. & Rasilainen, K. 2002. Isotopic fractionation of U reflecting redox conditions around a groundwater flow route. Pp. 961– 969 (Mat. Res. Soc. Symp. Proc. Vol. 663).

Puigdomenech, I. (ed.), 2001. Hydrochemical stability of groundwaters surrounding a spent nuclear fuel repository in a 100000 year perspective. SKB Technical Report TR-01-28, 83 p.

Tullborg, E-L., Smellie, J. and MacKenzie, A.B., 2004. The use of natural uranium decay series in support of understanding redox conditions at potential radioactive waste disposal sites. Mat. Res. Soc. Symp. Proc. Vol. 607, 571-576.

Case studies: active and abandoned Uranium mines

Contamination of Hydrographic Bassins in Uranium Mining Areas of Portugal

Fernando P. Carvalho, João M. Oliveira, Maria J. Madruga, Irene Lopes, Albertina Libânio, Lubélia Machado

Instituto Tecnológico e Nuclear, Departamento de Protecção Radiológica e Segurança Nuclear, Estrada Nacional 10, 2686-953 Sacavém, Portugal,
E-mail: carvalho@itn.pt

Abstract. The uranium-radium mining industry generated about six million tons of radioactive by-products composed mainly by the tailings of uranium milling facilities and by fine mud deposits resulting from treatment of acid mine waters. Most of these radioactive materials are deposited on the ground in the village of Urgeiriça, near Viseu, and are currently exposed to weathering. Following rains, leaching and surface runoff of these tailings drain into a stream, Ribeira da Pantanha that joins the river Mondego. In this river a wide artificial lake, Barragem da Aguieira, is the main water reservoir for the centre region of the country. Other rivers flowing through the mining region, namely the rivers Dão, Vouga and Távora, may also receive drainage from the areas of old uranium mines. The radioactive contamination that uranium mining and milling wastes may have originated in rivers and water reservoirs is assessed.

Introduction
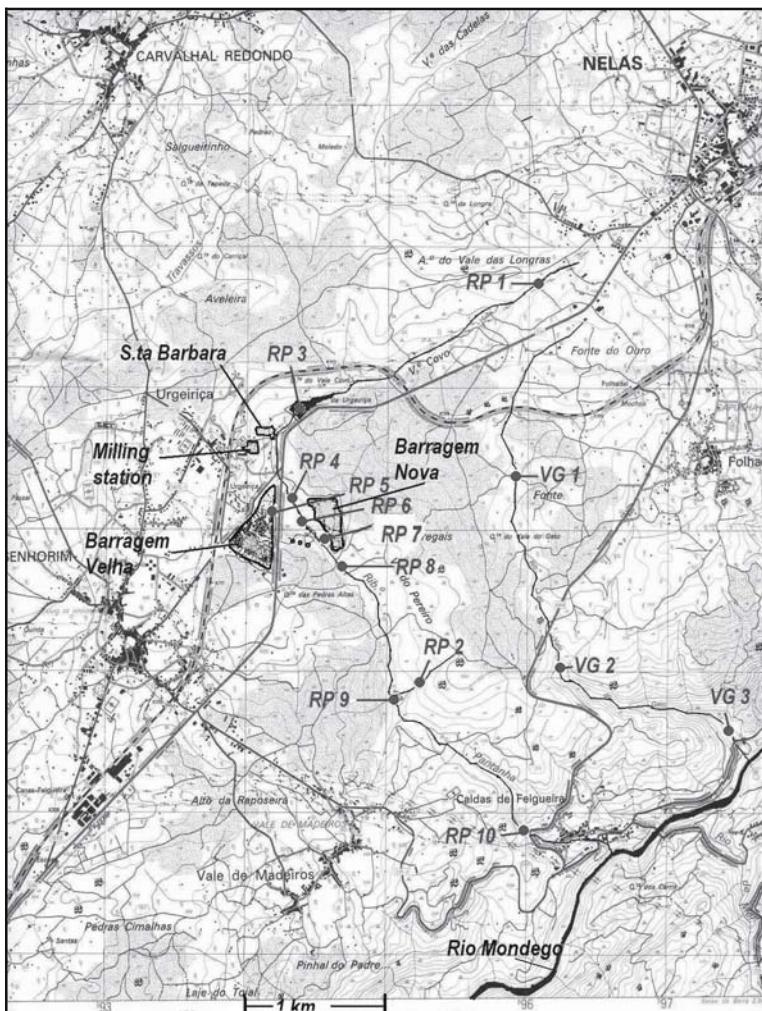
The mining of radioactive ores in Portugal begun in 1909 for the production of radium salts exported to France. At that time no recuperation of uranium was made. After 1945, the production of uranium was profitable and became the main aim of radioactive ores mining industry while the production of radium was abandoned. The exploitation of uranium mines and production of U_3O_8 concentrates continued until 2001. During the entire radium-uranium mining cycle that lasted 90 years, about 60 sites with deposits of uraniferous mineralisations were exploited in Hercynian granites. These sites are located in the uranium bearing region of the North-centre of the country in the departments of Guarda, Viseu and Coimbra

(JEN, 1964). The mines were of different size, ranging from vary small to relatively large exploitations, and in total the production of U_3O_8 amounted to about 4×10^6 tons. Most of the mines were exploited as open pits, and only a few as underground works. In most of the mine sites only barren rocks were left as mining waste. The ore from small mines was transported to one of the main facilities of the mining company and it was milled and extracted there. The main facilities for chemical treatment of radioactive ores were installed at Urgeiriça/Canas de Senhorim, Quinta do Bispo, Senhora dos Remédios and Bica. In a few other places, sulphuric acid was used for *in situ* leaching of uranium and did originate acid mine waters (JEN, 1964; Carvalho et al. 2005).

In the ore processing facilities with milling and chemical treatment plants, there are tailings with solid waste disposed off on the ground. In Urgeiriça there are two main tailing areas: one, known as Barragem Velha (BV), received the sand like materials remaining after the ore milling and uranium extraction, and another, known as Barragem Nova (BN), receiving since years ago the precipitate (radioactive mud) from neutralization of acid mine waters with barium chloride and calcium hydroxide. Two other spoil heaps containing radioactive materials are the "tailings" of Santa Bárbara, actually a heap of low grade ore disposed near the administration buildings of Urgeiriça mine, and the spoil heap at the milling station in the site of the former discharge of uranium ore transported by lorries. The amount of solid mining and milling waste in Urgeiriça is estimated at about 3 million tons.

In the past, seepage and surface runoff from these tailings may have drained directly into the streams. In the present, those are barely collected into a pond for acid neutralization and, after co precipitation of radionuclides and pH adjustment, the supernatant water is released into the Ribeira da Pantanha, a stream tributary to the River Mondego. During the last few years, acid water from the galleries of the underground mine of Urgeiriça, was pumped into this pond for pH neutralization also. In the past, process water from the uranium extraction procedure was released into the Ribeira da Pantanha at this same point. This area of Urgeiriça was selected as a case study (Fig. 1).

The three administrative Departments where the 60 old mining sites are located encompass the catchments areas of several main rivers. These rivers might have received the discharges of mine wastes and, today, may still receive surface runoff and discharges of small tributary creeks flowing across the mine sites. As dispersal of radionuclides from radioactive ores might have occurred in these hydrographical systems, the basins of the rivers Mondego, Dão, Vouga and Távora were selected to investigate enhanced levels of natural radioactivity (Fig. 2).

Case studies: active and abandoned Uranium mines

Fig. 1. Map of the region Urgeiriça/Canas de Senhorim/Nelas. The mining and milling facilities and radioactive tailings in Urgeiriça are indicated. Tagged points show sampling sites.
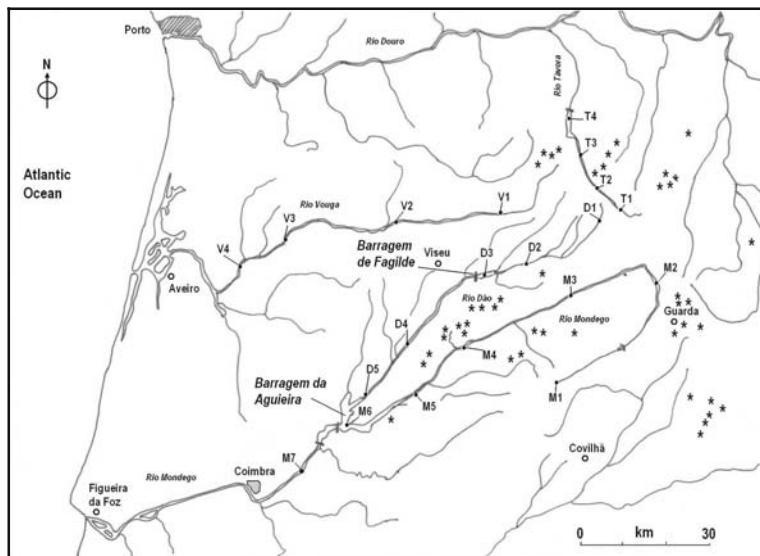
Materials and Methods

Samples of the top layer from soils and tailings were collected with a metal tube sampler. Several samples of the tailings materials were combined for analysis in order to obtain results better representing radionuclide concentrations in these wastes.

Case studies: active and abandoned Uranium mines

Samples of river bed sediments and river water were collected in four to seven stations in each river, from the source in the mountains to the river section in the coastal plain (Fig. 2). The water samples were filtered in the same day, near the collection site, using large diameter (142 mm) 0.45 μm pore size Millipore membrane filters. Sediments and folded filters were transported in plastic bags. In the laboratory, sediments were sieved through a stainless steel metallic screen of 63 μm pore size and only the fraction <63 μm was analysed to allow for inter sample comparisons (Carvalho, 1995). Sediment samples and filters with the suspended matter were dried in the oven, at 60º C, before analysis.

The filtered waters were acidified with HNO_3 to pH<2 and known activities of isotopic tracers ^{232}U, ^{229}Th, ^{209}Po and stable lead were added, to be used as internal tracers for the yield of the radiochemical procedure. Dissolved radionuclides were co precipitated with MnO_2. Solid samples were weighted with analytical precision and tracers added to the sample in a beaker along with mineral acids for complete dissolution of the sample (Carvalho 1997).

Radionuclides were separated and purified through ion chromatography columns UTeVa following a procedure described in detail elsewhere (Carvalho, 1997; Oliveira and Carvalho, 2005). Purified radioelements were electroplated on stainless steel discs using a power supply source and a platinum wire as anode. Polonium isotopes were plated on a silver disc from HCl 0.5 M solution in the presence of ascorbic acid. Lead carrier was precipitated to remove ^{210}Pb from solution as lead chromate. After several months of storage, this precipitate was dissolved to determine the ^{210}Po formed from the radioactive decay of ^{210}Pb. All these alpha emitting radionuclides were measured using silicium surface barrier detec-


Fig. 2.   The Centre-north of Portugal and hydrographical basins investigated. Stars indicate old uranium mines and tagged points indicate sampling stations.

Case studies: active and abandoned Uranium mines

tors connected to an Octete system from Ortec Eg&G and spectra analyzed with the software Maestro.

Radon in water was measured in samples directly collected into glass vials containing scintillation cocktail, tightly closed and measured in the laboratory in a Tri Carb liquid scintillation spectrometer (Lopes et al. 2004). In the field, the main physical-chemical parameters of waters were determined with a portable multi-parameter probe, Horiba Instruments. Ions in solution were determined in separate samples, collected in glass vials and kept in the refrigerator until analysis performed with a liquid chromatograph Dionex DX-500.

Results and Discussion

Solid residues from mining operations

The concentrations of radionuclides measured in samples from the uranium mining and milling facilities at Urgeiriça, are shown in Table 1. Concentrations of alpha emitting radionuclides in the heap of low grade ore in the tailings of Santa Barbara (SB), can be compared with concentrations in sand like materials from the tailings of rejected materials (BV) and with the concentrations of radionuclides in the top soil layer of the spoil heap near the ore milling station (MS). Concentrations of radionuclides differ widely amongst sites. Results of the analysis of agriculture soils from the region, collected several km apart of Urgeiriça are shown in Table 1 to provide a comparative near background value. One may observe that the soil at the milling station (MS) is highly contaminated, with concentrations similar to uranium ore, and much higher than those in the pile of untreated low grade ore (SB). In both materials there is no radioactive secular equilibrium of radionuclides belonging to uranium series. The weathering and, likely, the leaching by rain water did nearly halve the radioactivity concentration of ^{226}Ra relative to ^{230}Th and ^{238}U concentrations, and did remove also a fraction of ^{210}Pb that might have existed in the original ore.

In the tailings of Barragem Velha (BV), there is an obvious reduction of uranium concentration, with ^{238}U accounting for about 6% of the ^{238}U concentration measured in the spoil heap at the milling station (MS). However, ^{226}Ra, ^{230}Th and ^{210}Pb concentrations are high in the mill tailings and, clearly, these radionuclides have not been co-extracted with uranium in the chemical treatment plant but, instead, followed the rejected solid waste disposed of in Barragem Velha (Table 1).

The solid wastes disposed of in Barragem Nova (BN) originate from the neutralization of acid mine water and acid runoff from the BV tailings. These wastes are the mud from co precipitation of radionuclides with $BaCl_2$ and $Ca(OH)_2$ in a pond. It is interesting to compare radionuclide concentrations in this mud (BN) with concentrations in mill tailings (BV; Table 1).

Table 1. Residues from mining operations in Urgeiriça. Radionuclide concentrations (Bq.kg^{-1} ± 1σ) in solid materials from mining and milling wastes, in soils, in mine water and surface runoff from tailings.

	^{238}U	^{235}U	^{234}U	^{230}Th	^{226}Ra	^{210}Po	^{232}Th
Tailings and soils							
BV-Tailings Bar. Velha	2530± 94	118 ± 12	2876 ± 105	10337 ± 598	24717 ± 2039	20354±681	412 ±32
BN-Tailings Bar.Nova	41598 ±1228	1959 ± 67	40182 ± 1187	13390 ± 613	1690 ±150	1176±43	386 ± 22
SB-Tailings Sta Barbara	6108 ± 173	276 ± 14	6175 ± 175	8052 ± 282	3608 ± 133	3501±112	112 ± 7
MS- Tailings Milling station	38316 ± 1154	1717 ± 67	38247 ± 1152	30115 ± 1123	15569 ± 707	30824±1147	426 ± 21
Soil - Póvoa Espinho #13	230±10	10±2	236±10	301±24	619±96	287±11	226±19
Soil - Espinho #37	386±18	13±2	412±19	301±48	1242±365	321±12	301±48
Urgeiriça mine water							
Filtered water (-20 m)	2.17±0.07	0.106±0.005	2.18±0.07	0.015±0.003	1.48±0.06	0.146±0.004	0.0007±0.0006
Filtered water (-70 m)	2.24±0.07	0.105±0.005	2.24±0.07	0.010±0.005	1.44±0.06	0.129±0.004	0.0006±0.0005
Suspended matter(-20 m)	(35.1±1.7)x10^3	(1.6±0.1)x10^3	(35.0±1.7)x10^3	(1.8±0.1)x10^3	(12.1±0.5)x10^3	(52.5±2.8)xx10^3	(0.69±0.05)x10^3
Suspended matter(-70 m)	(61.1±2.0)x10^3	(2.7±0.1)x10^3	(60.4±0.2)x10^3	(5.4±0.2)x10^3	(14.4±0.5)x10^3	(92.2±4.7)x10^3	(0.034±0.004)x10^3
Runoff from tailings							
BV1(solution)-surface runoff	13.2±0.6	0.66±0.06	12.7±0.6	1.17±0.08	0.672±0.06	0.69±0.03	0.024±0.010
BV2(solution)-percolation water	35.7±1.1	1.64±0.07	34.8±1.1	1.06±0.06	1.84±0.03	0.70±0.04	0.044±0.009
BV4(solution)- pond discharge	5.8±0.2	0.28±0.01	5.4±0.2	nd	0.035±0.003	0.020±0.001	nd
BV1(susp.mat)	(1.96±0.08)x10^3	(0.10±0.02)x10^3	(2.08±0.08)x10^3	(4.8±0.3)x10^3	(3.6±0.2)x10^3	(7.2±0.3)x10^3	<(0.006)x10^3
BV2(susp.mat)	(5.0±0.2)x10^3	(0.28±0.04)x10^3	(5.4±0.2)x10^3	(2.8±0.3)x10^3	(0.92±0.18)x10^3	(9.2±0.5)x10^3	(0.57±0.12)x10^3
BV4(susp.mat)	(10.6±0.3)x10^3	(0.50±0.03)x10^3	(10.7±0.3)x10^3	(1.4±0.3)x10^3	(4.0±0.3)x10^3	(4.4±0.2)x10^3	(0.20±0.11)x10^3

The mud in BN display high concentrations of uranium and very low concentrations of ^{226}Ra and ^{210}Po (= ^{210}Pb), indicating that the precipitation method used to remove radionuclides from liquid wastes may has been effective with uranium but was not very effective with radium and lead.

Mine water and liquid waste
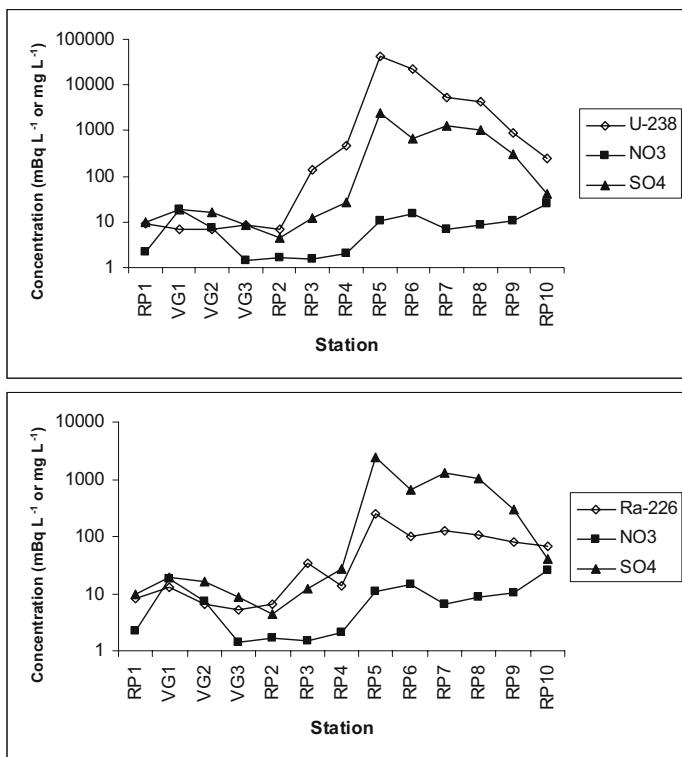
From the sulphuric acid used in the Urgeiriça mine and partial flooding of the underground works, resulted a large volume of acid mine water. During several years after cessing the exploitation of the Urgeiriça mine in 1991, the acid mine water was pumped and neutralized at an external facility near the ponds of BN. In 2003, the pumping of mine water was stopped and the mine was rapidly flooded. The acid mine water, now at pH near 5, contains dissolved uranium series radionuclides (Table 1). This water may come up in surface wells of the region. The mine water was sampled through the main vertical well of the Urgeiriça mine at two different depths, -20m and -70 m below the water surface, and analyzed. The radionuclides in solution and in the particulate phase display very high concentrations (Table 2). This water, after treatment at the neutralization pond and pH adjustment to near neutrality, is released into the Ribeira da Pantanha.

The seepage of rain water and surface runoff from the tailings, loaded with radionuclides leached from the rejected waste materials, drain into the Ribeira da Pantanha (Table 2). These waters are acid and contain also elevated sulphate ion concentrations that are residues of the chemical treatment of uranium ore. Supernatant water released from the neutralisation pond (sample BV4) still contains 5.8 Bq L^{-1} of ^{238}U, *i.e.,* more uranium than water from the Urgeiriça mine, 2.2 BqL^{-1}, although much less ^{238}U than percolation water from BV tailings, 35.7 Bq L^{-1}.

Radionuclides in the percolation water and surface runoff from the mill tailings, currently displaying a pH<3, are mostly in the dissolved phase. Therefore, an effective precipitation would have been important for their removal from waste water before release into the Ribeira da Pantanha.

Ribeira da Pantanha

The water of Ribeira da Pantanha near the source of this stream and upstream the tailings, contains relatively low concentrations of naturally occurring radionuclides. These concentrations are similar to those measured in Ribeira de Vale do Gato, a small stream nearby, and in a tributary to the Ribeira da Pantanha, ranging from 7 to 9 mBq L^{-1}, and can be considered as the non-modified radioactive background (Table 2, RP1 through to RP2). However, drainage from the tailings, containing 42x10^3 mBq L^{-1} of ^{238}U, and water discharges from the pH neutralization pond containing 5.5x10^3 mBq L^{-1} of ^{238}U, increase the uranium (^{238}U) concentration in the stream to 4.4x10^3 mBq L^{-1}. The same happens with ^{226}Ra. With increased distance from the tailings area, this small river contains decreasing con-

Fig. 3. Concentration of dissolved radionuclides (mBq L^{-1}) and sulphate and nitrate ions (mg L^{-1}) in the streams Ribeira da Pantanha and Vale do Gato.

centrations of radionuclides because of dilution with water from other sources and sorption of dissolved radionuclides onto sediments (Fig. 1 and Table 1). Near the discharge into the river Mondego, ^{238}U in the water of Ribeira da Pantanha decreases to 253 mBq L^{-1}. The radionuclide discharges of Pantanha into the river Mondego are still noticed a few km downstream but are rapidly diluted in the much higher volume of Mondego waters.

In this set of water samples (Table 2), the concentrations of dissolved uranium (^{238}U) and radium (^{226}Ra) display statistically significant positive correlations with concentrations of sulphate ion, R^2= 0.72 and R^2=0.92 respectively (Fig. 3). This correlation reflects the common origin of the dissolved radionuclides and sulphate in the BV tailings. No significant correlations exist between the same radionuclides and the nitrate ion in the water, R^2= 0.04 and R^2=0.09 respectively, revealing that nitrate does not come from the same source (Fig. 3). Instead, nitrate likely comes from agricultural fields mainly located after the tailings. ^{210}Po in the filtered water does not show concentration peaks after the tailings due to its very low water solubility and high distribution coefficient (Kd).

Case studies: active and abandoned Uranium mines

Radioactivity concentrations in the suspended matter of Ribeira da Pantanha were analyzed also. Upstream the tailings, ^{238}U in suspended matter varies between 0.6 and 1.5 kBq kg^{-1}. After the discharge of contaminated water, ^{238}U concentration raises to about 23 kBq kg^{-1} and it is traceable downstream to the discharge into the river Mondego. The signal of the uranium waste discharges from facilities at Urgeiriça is detected also in the bottom sediments of the Ribeira da Pantanha (not shown) with maximum concentrations, about 18 kBq kg^{-1}, at the stations RP8 and RP9 (Fig. 1).

Still today, in the water of Pantanha there is a clear signal of the radioactive wastes from past mining operations. The current levels are likely lower than during the years of ore processing in Urgeiriça, where at the station RP10 ^{238}U concentrations around 6.5 Bq L^{-1} have been reported (Severo at al. 1995). Nevertheless, current levels of radionuclides could still enhance levels in soils and plants if the water from this stream is used for irrigation purposes.

Rivers of the region

The ranges of radionuclide concentrations dissolved in the water of the four rivers are shown in Table 3. Sampling stations were selected, as much as possible, upstream and downstream the uranium mining areas (Fig. 2). The results show that the River Mondego displays at the source, in the granite mountain of Serra da Estrela, very high concentration of radon but negligible concentrations of uranium and uranium daughters in the soluble phase. Down river concentrations are slightly increased in the mining region (M4 and M5) near the discharge of Ribeira da Pantanha at Caldas da Felgueira, with a maximum of 11 mBq L^{-1} of ^{238}U measured there. Nevertheless, radionuclide concentrations decrease again with distance and in the artificial lake of Aguieira (M6), the radioactivity concentrations are reasonably low. Also in the reservoir of Fagilde in the river Dão (D3), radionuclide concentrations in the water are reasonably low.

Concentrations of radionuclides in the waters of rivers Dão, Távora and Vouga can be compared with those of Mondego (Table 3). One could notice that near the source, the water of river Dão contains comparatively high concentrations of radionuclides including uranium, radium and dissolved radon. This is likely due to the mineralogy composition of the surface soils and rocks in the respective river basin. Due to the existence of several unexploited and exploited uranium deposits near the source of Dão, these elevated concentrations are not entirely surprising.

The range of concentrations measured in these rivers is much lower than in the water of Ribeira da Pantanha subject to discharges from the mill tailings, nevertheless, they are comparable to the background values in Ribeira da Pantanha e Ribeira de Vale do Gato.

Table 2. Concentration of dissolved radionuclides (mBq L^{-1}± 1σ) in water of Ribeira da Pantanha (RP) and Ribeira de Vale do Gato (VG) in the area of Urgeiriça.

	^{238}U	^{235}U	^{234}U	^{230}Th	^{226}Ra	^{222}Rn	^{210}Po	^{232}Th
RP1	8.9 ± 0.3	0.43 ± 0.05	9.4 ± 0.3	0.78 ± 0.08	8.0 ± 0.7	(16.1±1.1)x10^3	9.2 ± 0.2	0.36 ± 0.05
VG1	6.7 ± 0.3	0.31 ± 0.05	6.8 ± 0.3	0.74 ± 0.09	12.9 ± 1.2	(9.9±0.8)x10^3	7.8 ± 0.2	0.74 ± 0.09
VG2	7.0 ± 0.2	0.34 ± 0.04	7.7 ± 0.2	0.91 ± 0.18	6.7 ± 0.4	—	9.5 ± 0.3	0.39 ± 0.15
VG3	8.6 ± 0.3	0.38 ± 0.03	9.0 ± 0.3	1.5 ± 0.1	5.2 ± 0.3	(2.5±0.3)x10^3	10.9 ± 0.3	0.35 ± 0.07
RP2	7.1 ± 0.4	0.37 ± 0.08	7.8 ± 0.4	0.42 ± 0.11	6.7 ± 0.9	(72.8± 3.0)x10^3	22.6 ± 0.9	0.13 ± 0.09
RP3	135 ± 5	6.2 ± 0.3	129 ± 4	2.6 ± 0.2	33.4 ± 1.8	(11.0± 0.7)x10^3	11.7 ± 0.3	0.10 ± 0.06
RP4	464 ± 15	22.0 ± 0.9	472 ± 15	4.7 ± 0.3	13.8 ± 0.9	(3.8± 0.3)x10^3	6.6 ± 0.2	0.30 ± 0.08
RP5	(42±1)x10^3	(1.84±0.09)x10^3	(41±1)x10^3	(1.3±0.1)x10^3	247 ± 16	(73.6±12.9)x10^3	134 ± 7	44.8 ± 6.3
RP6	(22.6±0.8)x10^3	992 ± 39	(22.2±0.8)x10^3	691 ± 31	99.8 ± 3.5	(116.8±4.0)x10^3	176 ± 9	14.3 ± 1.7
RP7	(5.5±0.6)x10^3	235 ± 30	(5.3±0.6)x10^3	2.7 ± 0.3	125 ± 14	(1.9±0.4)x10^3	19.0 ± 0.8	0.46 ± 0.14
RP8	(4.4±0.2)x10^3	202 ± 13	(4.4±0.2)x10^3	2.5 ± 0.4	103 ± 6	(1.9±0.4)x10^3	20.6 ± 0.8	0.51 ± 0.30
RP9	874 ± 48	38.0 ± 3.5	873 ± 48	5.6 ± 0.6	78.5 ± 3.4	—	21.5 ± 0.9	0.63 ± 0.27
RP10	253 ± 8	11.2 ± 0.7	262 ± 8	4.6 ± 0.5	66.2 ± 3.5	—	22.7 ± 0.9	0.41 ± 0.21

Table 3. Range of radionuclide concentrations (mBq L^{-1}) in filtered water of the rivers Dão, Vouga, Távora, and Mondego.

	^{238}U	^{235}U	^{234}U	^{230}Th	^{226}Ra	^{222}Rn	^{210}Po	^{232}Th
River Dão (D1-D5)	8.0 - 23	0.36 - 1.2	8.4 -25.6	1.9 -13.1	5.3 - 23.5	(1.1 - 81) x10^3	7.6 - 26.5	0.10 - 0.60
River Vouga (V1-V4)	3.7 - 6.6	0.14 - 0.30	3.8 - 6.6	0.86 - 1.4	4.4 - 7.5	(1.7 - 2.5)x10^3	6.9 - 13.0	0.19 - 0.30
River Távora (T1-T4)	3.6 - 7.6	0.14 - 0.36	3.7 - 7.8	0.88 - 1.6	1.3 - 5.2	(0.9 - 15.1)x10^3	9.0 - 17.7	0.14 - 0.21
River Mondego (M1-M7)	3.4 - 11.0	0.17 - 0.60	3.8 - 11.5	0.52 - 2.1	2.5 - 8.9	(<LLD - 103)x10^3	5.3 - 12.2	0.15 - 0.30

Case studies: active and abandoned Uranium mines

Conclusions

The concentrations of radionuclides of the uranium series in the mill tailings and mud from neutralization of acid mine waters in Urgeiriça, are 10 to 180 times higher than agriculture soils of the region. The disposal of those spoil materials in the open air, without coverage and confinement, facilitates the dispersal of radioactive waste in the environment. Such dispersal may cause an unacceptable exposure of the population to external radiation doses and may lead to internal contamination. Therefore, would be advisable to take appropriate measures to prevent such a radiation exposure (IAEA, 2002). Furthermore, the drainage from mill tailings and liquid discharges from acid water treatment ponds, increase the concentrations of radionuclides in the Ribeira da Pantanha. These radionuclide levels are above the recommended limits and, if water is used for irrigation or to feed cattle, may transfer contamination to the plants and to livestock.

The analysis of waters and sediments in the main rivers of this region indicate that the dispersal of radionuclides did not spread far from the mine sites and mill tailings. Although Ribeira da Pantanha displays a strong enhacement of radioactivity levels, no significant enhancement of radioactivity levels were detected in the main river basins of the region. In particular, the two main water reservoirs in the region, Aguieira and Fagilde dams, in the rivers Mondego and Dão, respectively, do not show enhanced radioactivity levels. Furthermore, radionuclide concentrations in water are currently below the legal limits applicable to water for human consumption. Nevertheless, measures should be implemented to keep that milling waste properly confined near the mines and avoid waste dispersal and transport to the hydrographical basins and to agriculture soils.

The proper management of the radioactive mining and milling waste would advise to confine the uranium mining wastes, especially those in the mill tailings, and monitor the environmental contamination (IAEA, 2002). Furthermore, this would go along with precaution measures to prevent consequences of natural catastrophes that may turn into radiological emergences. Actually, the total amount of radioactive mining and milling waste is meaningful and it is exposed to weathering. Exceptional storms or even average rainy weather conditions may flush these solid wastes from the tailings to the river basins, and eventually this would cause a meaningful radiological impact in water reservoirs of the region.

Acknowledgements

References

Carvalho,F.P. (1995). 210Pb and 210Po in sediments and suspended matter in the Tagus estuary, Portugal. Local enhancement of natural levels by wastes from phosphate ore processing industry. The Science of the Total Environment 159: 201-214.

Carvalho, F. P. (1997). Distribution, cycling and mean residence time of 226Ra, 210Pb and 210Po in the Tagus estuary. The Science of the Total Environment 196: 151-161.

Carvalho, F.P., Madruga, M.J., Reis, M.C., Alves, J.G., Oliveira, J.M., Gouveia. J., Silva, L. (2005). Radioactive survey in former uranium mining areas in Portugal. In: Proceedings of an Intern. Workshop on Environ Contamination from Uranium Production Facilities and Remediation Measures, organized by the ITN/DPRSN and the IAEA, Sacavém, 11-13 Feb 2004 (in press).

IAEA (2002). Monitoring and Surveillance of Residues from the Mining and Milling of Uranium and Thorium. Safety Reports Series Nº 27.International Atomic Energy Agency, Vienna.

JEN (1964). Uranium and Nuclear Raw Materials in Portugal. Junta de Energia Nuclear, Lisbon.

Lopes I., Madruga, M.J., Carvalho, F.P. (2004). Application of Liquid Scintillation Counting Techniques to Gross Alpha, Gross Beta, Radon and Radium Measurements in Portuguese Waters. In: Proceed. "NORM IV Conference, Naturally Occurring Radioactive Materials", Szczyrk, Poland, May 2004 (In press).

Oliveira, J. M., Carvalho, F.P. (2005). A sequential extraction procedure for determination of uranium, thorium, radium, lead and polonium radionuclides in environmental samples. 15th International Conference on Radionuclide Metrology and its Applications, ICRM 2005. September 5-9, 2005, Oxford, England. (accepted).

Severo A., Ferrador, G., Oliveira, J.M. (1995). Características de algumas águas junto de explorações mineiras abandonadas. In: Proceed. of the "1995 National Conference on the Environment", pp. 1623-1628 (In Portuguese). Publ. Universidade Nova de Lisboa.

Case studies: active and abandoned Uranium mines

Environmental impact evaluation of uranifer waste dumps from mining explorations – Barzava mine

Dragos Curelea, Dan Georgescu, Florian Aurelian, Camelia Popescu

Research and Development National Institute for Metals and Radioactives Resources, Blvd. Carol I, no. 70, Bucharest, Romania. E-mail: icpmrr@icpmrr.ro.

Abstract. The Barzava Uranium Mine is located in the west of Romania, in Arad District, in the south of the Zarand Mountains. The exploitation of the Uranium Ore started in 1963. This procedure was achieved by 2 shafts and 2 galleries located in the Poc Stream Valley, an affluent of the Barzava River. In 40 years, the waste rocks suffered erosion and migration activities of the Uranium. It contaminated the soil nearby. The waste rock from the Central Shaft 3 is located in the Barzava City, extremely close to the Barzava River and lengths on a 3,600 sqm surface. It has a 20,000 m^3 volume and the gamma debit values are within 0, 3 μSv/h and 4.5 μSv/h as maximum values and the Radon have a concentration of 1,250 Bq/ m^3.

Introduction

The old Barzava exploitation is located in the south of the Highis-Drocea Mountains, in the north of the Barzava Village, Arad district, in the west of Romania.

Between 1963—1964 there had been executed some exploitation in the Barzava area, that is mining and drilling exploitation. In 1966 starts the Uranium exploitation. It lasted 3 years and stopped in April 1969, as a result of the low profitableness and the decreased resources.
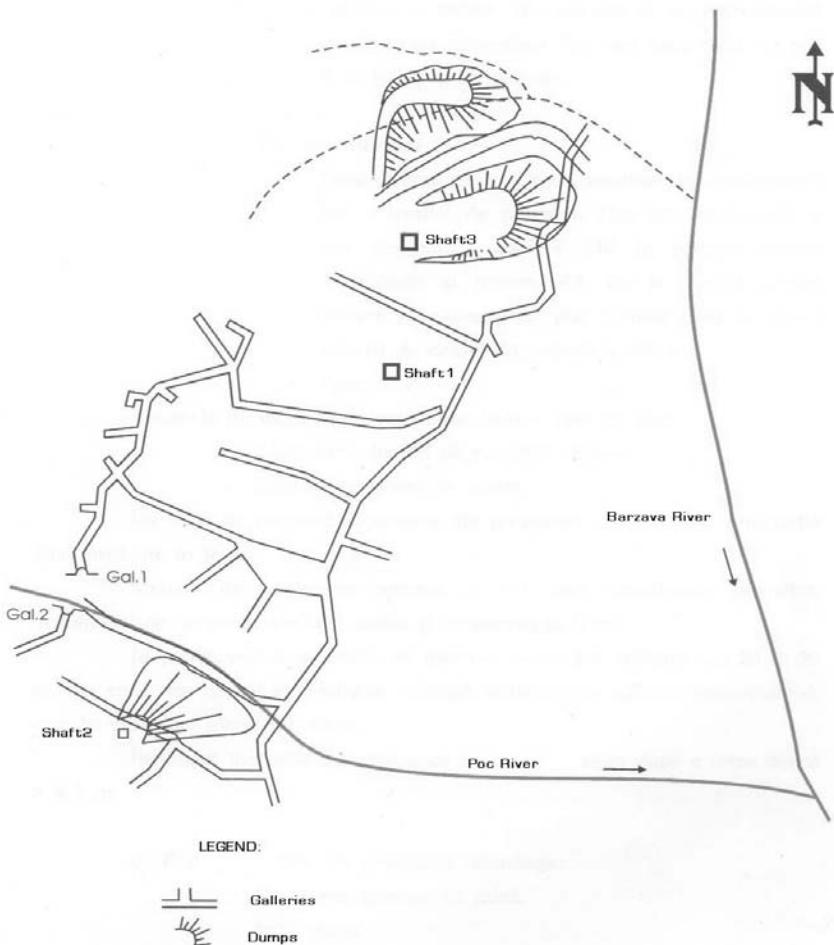
The utilities and the appending buildings were set out of order after the suspension of the activities, but it wasn't made any ecology of the area and there wasn't any mine closing project, because, in that time, the environmental protection was not a priority, but more, it was the last to consider.

Three shafts and two galleries were the result of the exploitation. Their location is the following: the Main Shaft and the Shaft no.1 are located near the Barzava

Brook, an affluent of the Mures River, at about 70 meters from it. Shaft no.2 and Galleries no.1 and 2 are located on the Poc Brook Valley, a temporary affluent of the Barzava Brook.

The Main Shaft Dump is located at 50 meters from the first houses of the Barzava Village and it is very important because of its impact over the environment and over the people (Fig.1).
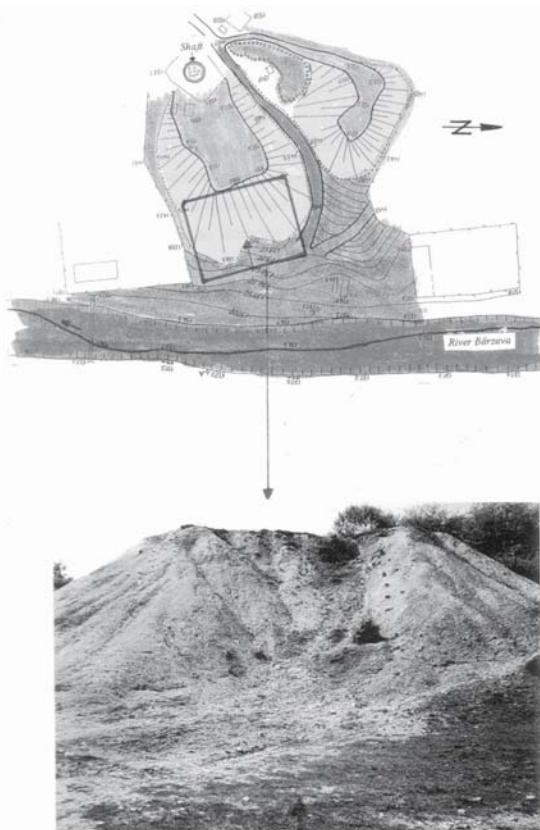
The exploitation area is located in the Drocea Mountain, at the junction with Mures Corridor. It is characterized by simple forms: hills with an altitude of about

Fig. 1. The location of the old Barzava mine.

Case studies: active and abandoned Uranium mines

500 meters, crossed by deep valleys with small water volumes, affluent of the Mures River.

The waste-dump with the low ore and sterile was drilled at the shaft entrance and has the following characteristics: it has a surface of 3,600 m^2 and has a volume of 20,000 m^3; it is located on a land with a rate of 6-12°; the ore material is made of gray sandstone; micro-conglomerates; clay with organic substances and adulterated crystalline schistose, with a grain size between 10 – 100 mm; it is not covered with vegetation (Fig. 2)

Fig. 2.   Picture of Barzava dumps from shaft 3.

Case studies: active and abandoned Uranium mines

Table 1. Radioactives elements concentrations.

No.	Sampling place	U_{nat}(mg/Kg)	Ra226 (Bq/g)
1	Near shaft 3	53	0.15
2	4 m from the base of the dump	55	0.32
3	10 m east from the dump	85	0.50
4	On the road near the dump	175	0.90

Environmental Impact

In order to observe the impact of the sterile waste dump the environment during the 40 years of exploitation, there were gathered samples from all directions, especially from the flowing direction of the spouting waters towards the Barzava Brook.

The laboratory analyses proved that there are outruns of the Legal Standard only for radioactive elements U_{nat} (up to 25 times bigger) and Ra ^{226} .

There is a concentration process of the radioactive elements in the soils nearby the Main Shaft Dump. The argillaceous materials in the soil acted like an absorption barrier, especially for Uranium.

The vegetation samples

The radioactive elements analyzed for these samples are saturated Uranium and Radium. The Romanian Legislation does not provide references values for chemical and radioactive elements in vegetation. The interpretation of the concentrations will be done comparing the background values from the mineralized area: U = 4 ppm/mg/kg of ash; Ra = 0, 03 Bq/g of ash.

It has been noticed that the vegetation that grew on the contaminated soil from the bottom of the waste dump concentrated values of Uranium up to 20 ppm and Ra up to 0, 4 Bq/g.
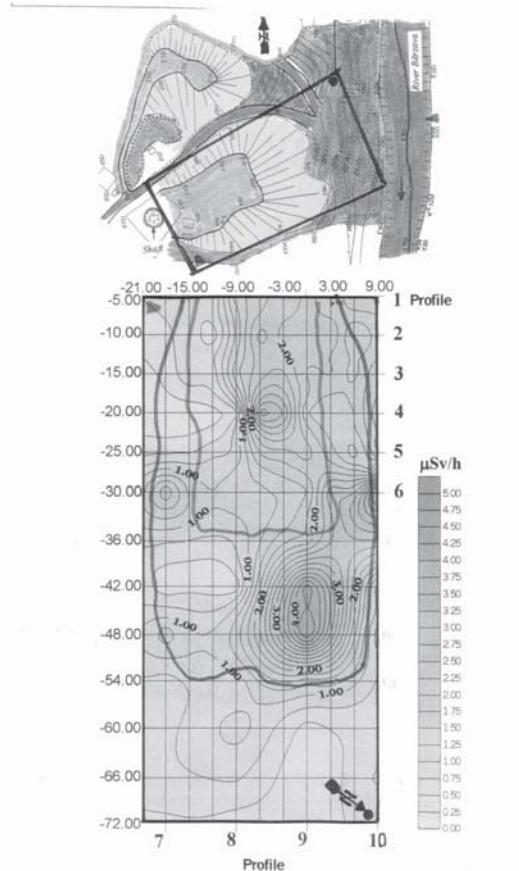
Through assimilation processes the vegetation can lead to the limitation of the migration of the elements and, this way, reduces the pollution of the hydrographic network nearby.

The analysis of the water samples and sediments from the Barzava Brook and the fountains nearby does not revealed pollution with radioactive elements or hard metals.

The external Gamma irradiation level

In order to distinguish the areas found over the influence of the sterile waste dump and the irradiation potential of the persons who stay or travel around the dumps, there had been made measurements of the Gamma rate dose in the following ways: on all the waste-sump surface, both horizontal and inclined surfaces; around the waste dump – on the access road, the farming lands; in the inhabited area (the nearest to the waste dump); in the middle of the Barzava Village.

The external gamma irradiation measurements had been done in a grind (Fig.3) that covers both the dump and the land between the waste-dump and the Barzava Brook.

Fig. 3.   The external gamma irradiation measurements

The Radon Measurements

Outruns of the Radon concentration for the population had been observed on the dump, especially on the horizontal area and on in eastern side of the inclined surface. This can signify a danger for the people who travel through the waste dump, mostly for children who can choose the dump as a playground as a result of its location near the houses and because the wastes dump is not surrounded by a fence or guarded.

Scenario

The source is the surface of the 3rd shaft and the Barzava Brook.
Location: on the right side of the Barzava Brook. The nearest houses are located at 50m from the waste-dump.
Contaminants: U, Ra, Rn; gamma radiation
Exposure ways to gamma radiation: water and food ingestion, Rn and its short-life descendants, long-life radionuclid dust ingestion.
Receivers: people who lives near the dump, animals that eats near the dump, vegetation.
Altitude – 300 meters, wind direction – S and SV, annual rainfalls media - 623mm.

The calculation for a dose received by a person through ingestion (internal irradiation)

Aquatic way

We suppose that an adult person, from the critical group, uses for drinking and irrigation of the crops, in a period of one year, the water from the Barzava brook from the waste dump area.

We also assume that the same water is used for watering the cattle and the food of the cattle is the grass contaminated by the same water, which has the following concentrations: U = 0,014mg/l; Ra = 0,043Bq/l.

The calculation for the dose received by a person in the previous conditions through water ingestion, vegetal, meat, milk, fish is 0,051mSv/year, from which the additional dose obtained through ingestion is :

$E^a_{additional\ i}$ = 0,033mSv/year

Terestrial way

We suppose that a person who stays near the dump ingests daily, as a result of un-predicted causes, a certain quantity of radioactive material. This quantity is presumed to be 0,1g/day for an adult person and 0,5g/day for children.

In this case:

$E^t_{additional\ i} = 0,023mSv/year$ (for adults)

$E^t_{additional\ i} = 0,450mSv/year$ (for children)

The total additional dose obtained through ingestion for a period of one year is:

$E^t_{total\ i} = 0,033 + 0,023 = 0,056mSv/year$ (for adults)

$E^t_{total\ i} = 0,033 + 0,450 = 0,483mSv/year$ (for children)

The calculation for a dose received by a person through external irradiation

The data used for the calculation is:

- the gamma dose rate is 4,5 µSv/hour
- the maximum Uranium concentration is U = 0,0175%
- the stationing time – 5 months x 180hours/month = 900hours

In the previous conditions, the total dose caused by gamma irradiation is:

$$E_\gamma = 4,050mSv/year$$

To this value we should add 0,943mSv/year for the rest of 7860 hours spent in the normal conditions, with the background value of 0, 15µSv/year.

So, the total annual gamma irradiation dose is:

$$E_{\gamma T} = 4,993mSv/year$$

from which the additional dose received by a person is:

$$E_{\gamma\ supl} = 3,942mSv/year$$

The calculation for a dose received by a person through Rn and short life descendants ingestion (internal irradiation) – air way

The data used for the calculation is:

- CRn = 1250 Bq/m3
- the stationing time – 5 months x 180hours/month = 900hours

In case of staying/passing near the high Rn concentration area, the total dose is:

$$E_{h\ Rn\ l} = 2,835mSv/year$$

to which should be added $E_{h\ Rn\ 2} = 0,185mSv/year$ for the rest of the time spent in the background conditions $C_{Rn} = 12\ Bq/m^3$

Case studies: active and abandoned Uranium mines

The total annual dose received through ingestion is:

$$E_{h\,Rn\,T} = 3{,}020 mSv/year$$

from which the annual additional dose is

$$E_{h\,Rn\,additional} = 2{,}808 mSv/year$$

The calculation for a dose received by a person through long-life radionuclids dust ingestion (internal irradiation) – air way

The data used for the calculation is:
- the dust quantity in air = $0{,}01 g/m^3$
- the Uranium quantity in the waste-dump U = $0{,}0175\%$
- the Uranium quantity in the air U = $0{,}00175\,\mu g/m^3$
- A = $0{,}444 Bq/m^3$
- period of exposure – 900 hours
- respiratory volume - $1\,m^3/hour$
  $$E_{h\,i\,additional} = 0{,}0008 mSv/year$$

The total dose obtained from all the doses obtained by all the ways by a person, in all the scenario conditions is:

$$E_T = 8{,}086 mSv/year\ (adults)$$
$$E_T = 8{,}512 mSv/year\ (children)$$

The total additional dose for a year is:
$$E_{T\,additional} = 6{,}807 mSv/year\ (adults)$$
$$E_{T\,additional} = 7{,}234 mSv/year\ (children)$$

Attention: The total additional dose for a period of a year outruns 7 times the admitted value for the population, in accordance to the Romanian Legislation.

Conclusions

The sterile and low Uranium ore dumps from Barzava Valley are the sources and pollution potential of the soil and vegetation from the Barzava Brook area. During the 40 years since the exploitation had been stopped, there had been a migration of the Uranium and Radium radioactive elements and they concentrated in the soil area from the bottom of the dump. The samples showed values of Unat – 175mg/kg; Ra^{226} – 0,9Bq/g. It can be said that the argillaceous soil from the bottom of the waste dump worked as a frontier that stopped the pollution with radioactive elements of the Barzava Brook.

In case of some pouring summer rains the flowing waters from the dump will surely discharge in the Barzava Brook, along with the easily elutriating Uranium element.

I hope that in a nearby future the Barzava waste-dump will be encapsulated and integrated in the natural landscape of the surrounding area.

References

Popescu M,Georgescu D. (1998) Comparative studies regarding the impact on environmental factors of uranium minim activity in some areas from Romania; International Symposium on Environmental, Swempankara, may 1998

Hydrochemical Aspects of the Flooding of the Mine Königstein – A Water Mixing Model for Recognizing the Influence of Groundwater by Contaminated Water

Karl-Otto Zeißler[1], Kerstin Nindel[2], Thomas Hertwig[1]

[1]Beak Consultants GmbH, Am St. Niclas Schacht 13, 09599 Freiberg, Germany,
E-mail: zeissler@beak.de
[2]Wismut GmbH, Jagdschänkenstraße 29, 09117 Chemnitz, Germany

Abstract. A water mixing model has been developed which supports the decision for evaluating the influence of groundwater by contaminated water. Given the main statistical parameters of the water classes (mean and standard deviation), for each concrete value vector a probable water mixture is determined. If the value vector is close to the probable water mixture, an influence by the contaminated water can be assumed. The model has been implemented in a software program and tested on the basis of the flooding data of the mine Königstein.

The Uranium Mine Königstein

The uranium mine Königstein is situated in the sandstones of the Elbsandstein mountains near the famous castle Königstein. The mine has a depth of about 300 m at a territory of over 6 km². From 1967 to 1990 about 18000 t uranim were produced. Since 1984 the uranium was produced by leaching with sulphuric acid.

Since 2001 the mine has been flooded. A complex water monitoring program investigates the influence of the groundwater aquifers by contaminated water during the flooding process. 330 measuring points and 12 km service tunnels are part of this monitoring program. The aquifer GWL3 is of special importance (Fig. 1).

In 2005 based on the monitoring data the Beak Consultants GmbH had to evaluate the externalities of the flooding process. One special task was the development of a decision support for determining the source of influence of the groundwater by flooding water/stockpile seepage water. The paper shows the results of this work.

The water mixing model

Basic model ideas

Due to the evaluation of an influence of contaminated water on the groundwater we developed a model, which will be referred to as "water mixing model". The basic ideas of the model are:

- Each class of measuring points is represented by a set of points (point cloud) in the value space. Each point consists of the analysis value of one sample. Up to the 3rd dimension this characteristic can be visualized by means of special software (for example STATGRAPHICS).
- This point cloud is described by an average value vector and a vector of the standard deviations. In the graph the standard deviations are drawn parallel to the axes of coordinates in both directions - beginning with the average value vector as center of the cloud - (Fig. 2).
- The influence of a measuring point of the groundwater class by flooding water and/or stockpile seepage water is expressed by the fact that the measured value vectors move away from the point cloud of the groundwater class. From elementary physical considerations it is postulated that this "moving away" takes place along the connecting line of the two centers of the point clouds.
- The decision, which class causes the influence, depends on to which connecting line the measuring vectors will lie closer.
- Since the added quantities of wasted water are generally small, also the meas-
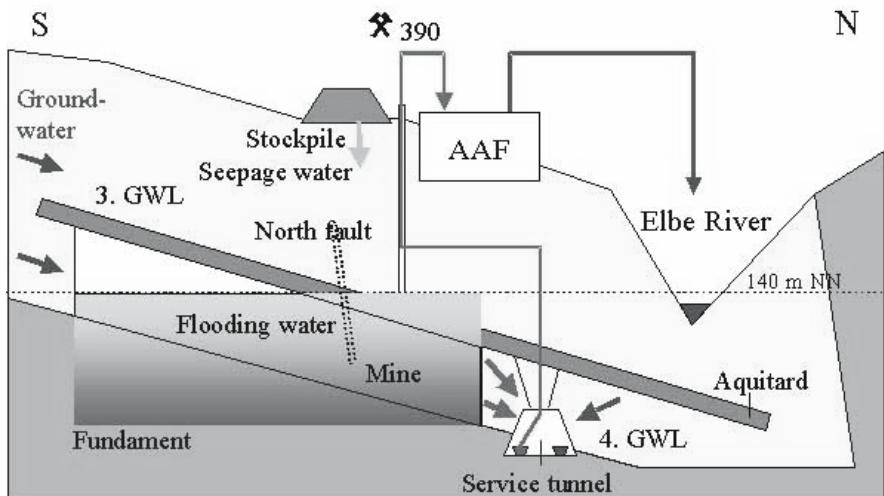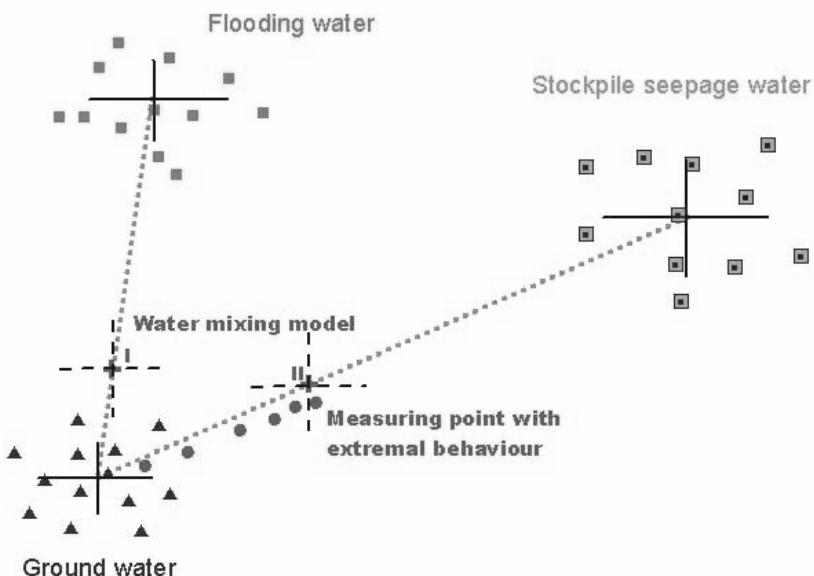
Fig. 1.   Schematic profile of the uranium mine Königstein.

Case studies: active and abandoned Uranium mines

ured value vectors do not change significantly despite substantially larger pollutant contents. Due to the reinforcement of this effect all values have been logarithmized. This logarithmizing has an inflating effect on the range of the small values. Furthermore the logarithmizing leads to normal distributed populations.

Concerning the water mixing model we had to solve the following problems:
- choose the relevant water classes,
- choose the analysis values for modeling,
- define the water mixture of 2 water classes depending on the rate parameter t,
- define the distance measure between a value vector and a water mixture,
- determine the fitted rate parameter t_0 realizing the minimum distance for a given value vector,
- determine the threshold separating a real water mixture from a random varability of values of pure water classes,
- make a decision support for the most likely influence class in case of real water mixture.

Fig. 2.   Scheme of the water mixing model including groundwater, 2 possible influence water classes (flooding water and stockpile seepage water), value vectors with extreme behaviour and 2 water mixing models for the most extremly value vector.

Case studies: active and abandoned Uranium mines

Water classes for mixing

The available monitoring data of the flooding of the mine Königstein were divided into 9 water classes. Concerning the influence on the groundwater by contaminated water, four classes became important: the ground water classes GWL3 and GWL4, the flooding water and the stockpile seepage water. The aim was to determine whether the flooding water or the stockpile seepage water are influencing the groundwater at measuring points with extremal behaviour.

Choosed analytical data

If one wants to recognize mixing from other water classes as early as possible, it is obvious to select analytical parameters whose average class values related to the associated standard deviations for groundwater and contaminated water have an explicit difference. It is also preferable to have analytical parameters that show differences between the flooding water and the stockpile seepage water classes. Under these criteria the following analysis parameters were selected: chlorid, sulfat, electrical conductivity, zinc, uranium total.

Formal Description of the Model

Model parameter

Suppose C_1 is the groundwater class and C_2 is the contaminated water class. C_1 is described by the parameter set $P_1(Q_1,S_1)$ where Q_1 is the vector of all averages and S_1 is the vector of all standard deviations. $Q_1(i)$, $S_1(i)$; $i = 1…n$. C_2 has the same description $P_2(Q_2,S_2)$.

   A water mixture C_t with t parts from C_2 and (1-t) parts C_1 will be described by $P_t(Q_t,S_t)$ as a linear function.

   $P_t = P_1 + t*(P_2 − P_1)$

   $Q_t(i) = Q_1(i) + t*(Q_2(i) − Q_1(i))$; $S_t(i) = S_1(i) + t*(S_2(i) − S_1(i))$

This linear function is plausible from physical considerations.

   Remark. The case of logarithmized data. In this case the standard deviations of the logarithmized data will remain the same. $S_f(i) = S_1(i) + f*(S_2(i) − S_1(i))$. Considering the averages every i has his own f_i. That means that the line between Q_1 an Q_2 is not longer a straight line.

   Suppose $y=Q(i)$, average of the $\log(m_i)$; $y'=Q(j)$, average of the $\log(m_j)$, $i<>j$. $y=\log(x)$; $y'=\log(x')$.

For $y_f = y_1 + f*(y_2 - y_1)$ the real mixing rate t of x_1 and x_2 has to be found.

$$\log(x_t) = \log(x_1) + f*(\log(x_2) - \log(x_1)) =$$
$$= (1-f)*\log(x_1) + f*\log(x_2) =$$
$$= \log(x_1^{(1-f)} * x_2^{f})$$

$$x_t = x_1^{(1-f)} * x_2^{f}$$

On the other side $x_t = x_1 + t*(x_2 - x_1)$. That's why

$$t = \frac{x_1^{(1-f)} * x_2^{f} - x_1}{x_2 - x_1}.$$

This mixing rate t has to be used for the calculation of y_f'.

$$y_{f'} = \log(x_t') = \log(x_1' + t*(x_2' - x_1')).$$

Defining the Distance

M describes a vector of measured values. $M = M(i)$, $i = 1\ldots n$. The distance from M to P_t is defined as

$$b(M,t) = \frac{1}{n} * \sqrt{\sum_{i=1}^{n} a_i^2}, \text{ where}$$

$$a_i = \frac{\left|M(i) - Q_t(i)\right|}{S_t(i)}$$ (normalized differences by standard deviation)
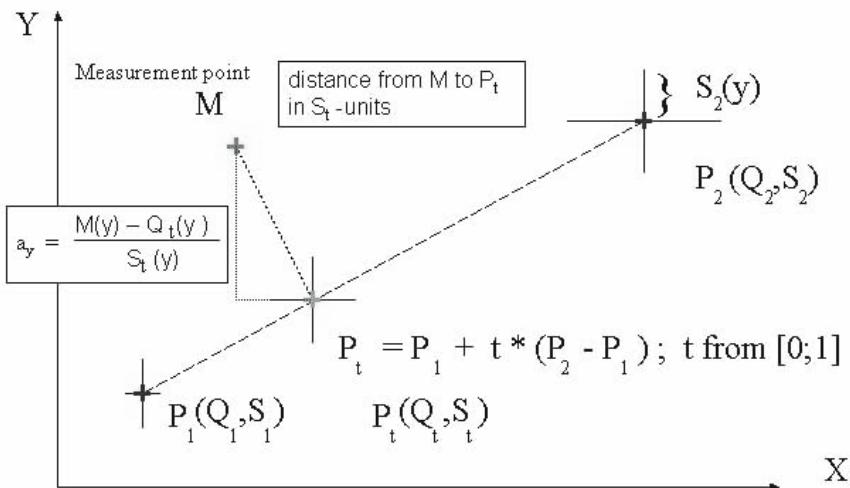
Fig. 3.   Scheme of model parameters and distance measure.

Case studies: active and abandoned Uranium mines

The probable water mixture

The measurement vector M will be assigned to the water mixture class C_τ which realizes the minimum distance.

$$\tau : b(M,\tau) = \min_{t \in [0;1]}(b(M,t))$$

$$B(M) = b(M,\tau)$$

Suppose B(M) is normally distributed N(0,1) for representants M of C_τ then all B(M)<1 indicate a good fit to the water mixing model P_τ. B(M)<2 shows an acceptable fit. If B(M)>2.5, then the model P_τ is unsuitable for describing M.

Threshold for a possible influence

If τ is near 0 we can assume a random fluctuation inside groundwater and no influence by contaminated water. Thus a threshold t_s is needed that indicates an influence when $\tau \geq t_s$. For this purpose Qt can be seen as a vector of measurement values and analyse the distance from the center of groundwater values Q0 to Qt: $b(Q_t,0)$. Supposing b as normally distributed N(0,1) for groundwater vectors Qt , t>0 84% of all values are smaller then 1 and 95% of all values are smaller then 1.645. In this case the 84% value was used for defining the threshold.

$$t_s : b(Q_{t_s},0) = 1$$
.
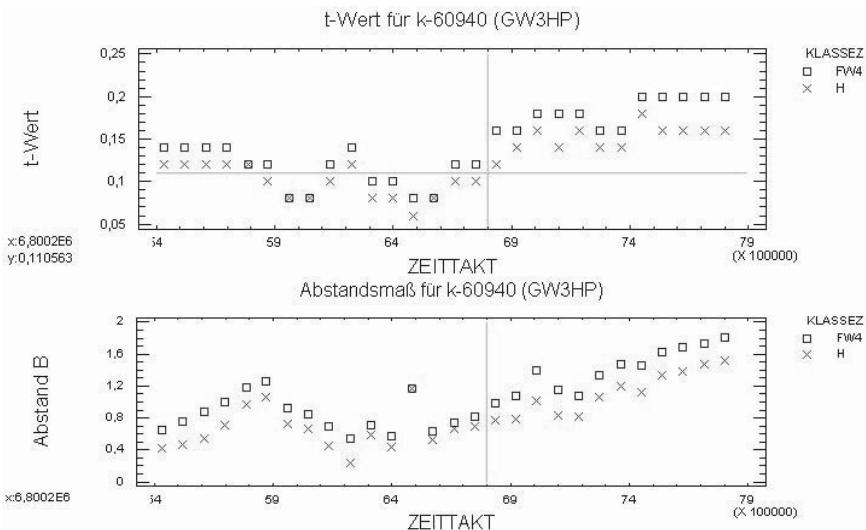
Remark. If the assumptions of normal distribution of b and B are not true, we still will have thresholds, but without statistically confirmed coefficients.

The most likely source of influence

Suppose X is a groundwater measurement point and M_j are vectors of measurement values at time j. The potential influence water classes are flooding water (F) and stockpile seepage water (H). For each water mixing model a threshold $t_s^{(F)}$ exists and $t_s^{(H)}$. $\tau_j^{(F)}$ and $\tau_j^{(H)}$ are the mixing parameters for the water mixing models.

(1) If $\tau_j^{(F)} > t_s^{(F)}$ and $\tau_j^{(H)} > t_s^{(H)}$ for all j>j$_0$, then the measuring point X has an extremal behaviour (individual random events are not of interest). The point X is influenced.

(2) If $B^{(F)}(M_j) < B^{(H)}(M_j)$ and $B^{(F)}(M_j) < 2$

Case studies: active and abandoned Uranium mines

Fig. 4.   Measuring point k-60940. t-Wert - τ; ZEITTAKT – time j; Abstand B – distance.

for all j>j1, then the measurement point X is assumed to be influenced by flooding water (analogous influence by stockpile sepage water).

(3) If $\min\left(B^{(F)}\left(M_j\right), B^{(H)}\left(M_j\right)\right) > 2.5$ then the extremal behaviour of point X cannot be explained by the water mixing model.

Example

The behaviour of the example measuring point k-60940 is shown below (Fig. 4). Beginning with time $j_0=68$, the τ („t-Wert") are greater than 0.11 (=t_s). At all succeeding times the measurement vectors are closer ("Abstand B") to the stockpile seepage water model (H) than to the flooding water model (FW4). As the distance is smaller than 2, the influence of stockpile seepage water is preferred.

References

Hertwig Th., Zeissler, K.-O., Schynschetzky H., Neumann V. (2005) Auswertung der Monitoringergebnisse der Überwachung des Wasserpfades während der Flutung der Grube Königstein bis zum Flutungsstand von 110 m NN - Abschlussbericht (unveröff.) 187 S.

Case studies: active and abandoned Uranium mines

The use of BaSO$_4$ supersaturated solutions for in-situ immobilization of heavy metals in the abandoned Wismut GmbH uranium mine at Königstein

Ulf Jenk[1], Udo Zimmermann[2], Gerald Ziegenbalg[3]

[1]Wismut GmbH, Jagdschaenkenstraße 29, 09117 Chemnitz, Germany,
E-mail: u.jenk@wismut.de
[2]Wismut GmbH, Jagdschaenkenstraße 29, 09117 Chemnitz, Germany, Niederlassung Königstein, Germany
[3]TU Bergakademie Freiberg, Institute of Technical Chemistry, Leipziger Str. 29, 09599 Freiberg, Germany

Abstract. The former uranium ISL-mine at Königstein (Germany) is presently being flooded. To support the flooding process, a new technology to reduce contaminant potential in the source was developed and applied. The application based on the injection of supersaturated BaSO4-solutions to precipitate solved contaminants and to cover reactive mineral surfaces. Since 2002 the technology is applied in the southern part of the mine in order to immobilize contaminants in highly polluted areas before flooding. The article describes the fundamentals of the technology and the full-scale application.

Introduction
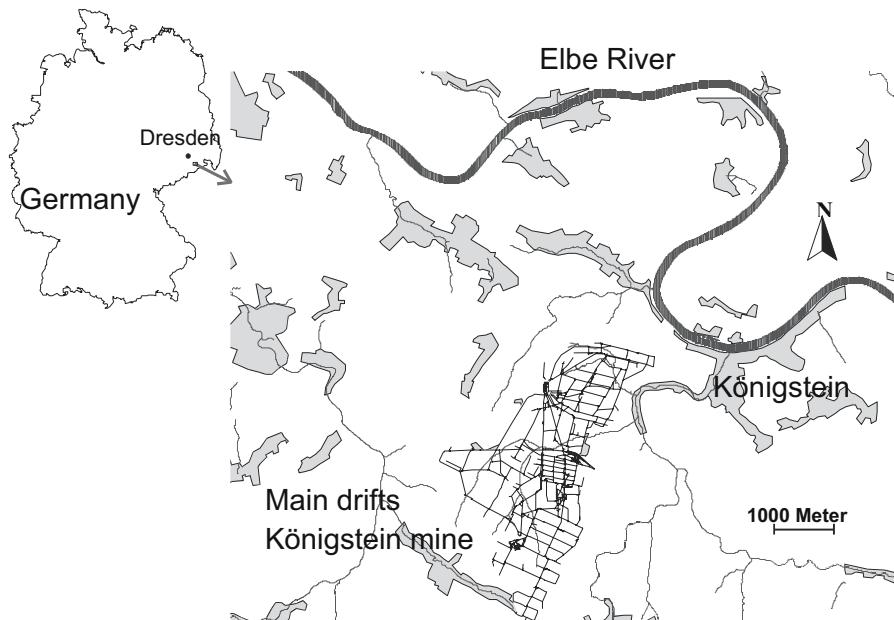
Closure of several underground uranium mines is a central issue of the WISMUT project in Germany. A special case is the remediation of the Königstein mine near Dresden. The mine is situated in an ecologically sensitive and densely populated area (Fig.1). Conventional mining started in the sixties and approximately 19,000 t of uranium were produced till 1990.

The ore body is located in the 4th sandstone aquifer, the deepest of four hydraulically isolated aquifers in a Cretaceous basin. The 3rd aquifer is an important water reservoir for the Dresden region and is environmentally and economically very significant.

The uranium was extracted from the 4th sandstone aquifer initially using conventional mining methods, but later an underground in situ leaching method using sulphuric acid was implemented. In situ leaching was performed on sandstone blocks with volumes of 100,000 to 1,000,000 m³. 104 blocks were leached with solutions of 2 to 3 g/l H_2SO_4. During the in situ leaching period, about 130,000 t of sulphuric acid were applied within the deposit. Additionally, an unknown amount of sulphuric acid produced by pyrite oxidation was released within the mine. Especially due to the reactions of the oxidizing sulphuric acid, the geochemical nature of the deposit was substantially changed, with a high level of pollution remaining within the deposit, mainly sulphate, heavy metals and natural radionuclides. Remaining pore water in the sandstone water is characterized by pH 2.0, EC 700 mV, 10 g/l SO_4, 2 - 3 mg/l Fe, 200 mg/l Zn, 200 mg/l U 300 mg/l Al.

Flooding of the Königstein Mine

Final mine remediation can only be achieved by flooding the mine. In the case of uncontrolled flooding (walk-away option) it was expected that highly polluted groundwater would rise up into the overlying aquifer through natural or technical hydraulic connections. Thus a concept of controlled flooding was developed. The major element of this approach is a control drift system which allows collection of draining flooding water down-gradient of the deepest part of the mine. The flood-


Fig. 1.   Location of the Königstein mine.

Case studies: active and abandoned Uranium mines

ing water collected in this control drift system can be treated and discharged to the Elbe river.

To reduce the long term costs of conventional water treatment, two alternative in-situ technologies were developed for full-scale application: (1) direct source immobilization and (2) use of reactive material deposited in open mine cavities as a reactive barrier. Construction of a reactive barrier in open drifts proved not to be feasible due to problems with air ventilation and mine safety. The immobilization technology (direct source immobilization by a special solution) was applied in the southern part of the mine as part of the closure plan.

Fig.2.   Column tests with white precipitation products on the sandstone surfaces.

Case studies: active and abandoned Uranium mines

Development of the immobilization technology
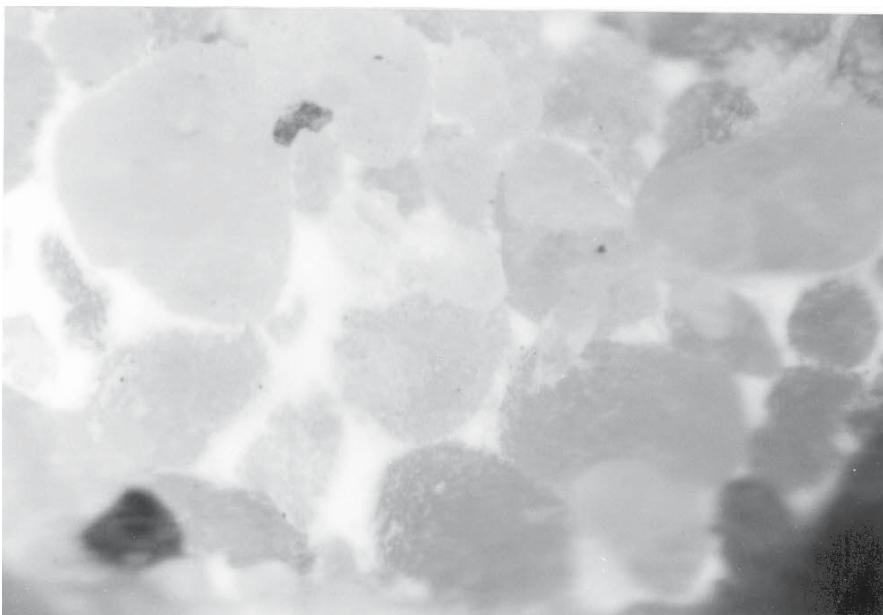
In-situ immobilization is based on using mineral precipitation or crystallization processes similar to those occurring in nature. First, laboratory experiments ware carried out to create suitable solutions (Ziegenbalg 2003a, Ziegenbalg 2005). $BaSO_4$ supersaturated solutions were prepared by mixing solutions containing $Ba(OH)_2$ with sulphate-containing solutions in the presence of various types of precipitation inhibitors. Solutions characterized by reducing properties were obtained using Na_2SO_3 as a source for sulphate generation.

In a second step column tests were used to determine the immobilization capacity of $BaSO_4$ producing solutions and to investigate crystallisation products inside the sandstone (Fig.2).

In order to increase the immobilization capacity, small amounts of sodium silicate were added. After immobilization, the sandstone was investigated by chemical and mineralogical methods.

$BaSO_4$ layers filled pores and covered reactive mineral surfaces and secondary precipitates, such as hydroxides or hydroxysulfates, were found as reaction products (Fig. 3). Because of the extremely low solubility of barite, long-term stable immobilization was achieved.

Field tests were carried out on blocks in the southern part of the Königstein mine (Ziegenbalg 2003a). The average mineral composition as well as the geological and mineralogical situation was similar to the average conditions of the deposit.


Fig. 3. $BaSO_4$ crystals formed in sandstone pores.

Case studies: active and abandoned Uranium mines

A solution containing Ba(OH)$_2$*8H$_2$O, Na$_2$SO$_3$, sodium silicate and a precipitation inhibitor was prepared in a small-size grout plant (Fig. 4). The grout preparation was based on the simultaneous addition of a Ba(OH)$_2$ solution and an inhibitory-Na$_2$SO$_3$-sodium silicate solution into a water-bearing pipe.

The field test was characterized by different stages during which a block was alternately treated with immobilization solutions and small amounts of water. At the end, the block was flushed with water in order to determine the stability of the achieved immobilization. The amounts of contaminants discharged were between 50 and 70 % lower than would be expected when flushing the block with water.

Full-scale application

In the light of the results of the laboratory, column and field tests, the decision was made to apply the newly developed technology to selected areas of the Königstein mine.

In a first step, approximately 100,000 m^3 of immobilization solutions were prepared and injected into three different blocks in the southern mine field between December 2001 and May 2002 (Ziegenbalg 2003b, Ziegenbalg 2005).

The blocks had been prepared for uranium leaching, but the operation had to be suspended when uranium mining was terminated. As the rock had been in contact with air and moisture for more than 10 years, flooding of the mine would have caused the formation of highly concentrated acidic solutions. Treatment with im-
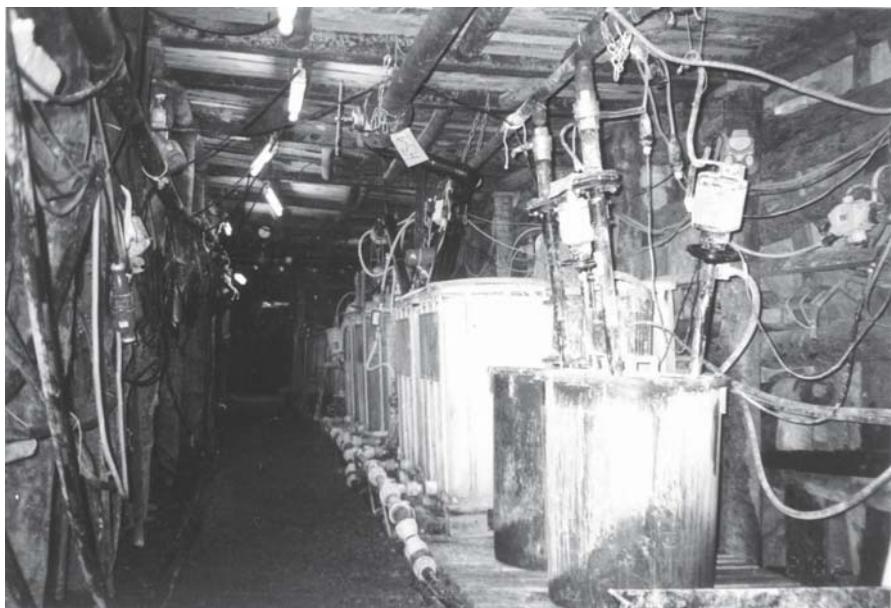
Fig. 4.   View of the grout plant used for field tests and first full scale application.

Case studies: active and abandoned Uranium mines

mobilization solutions was aimed at precipitating contaminants, inhibiting oxidation processes, and reducing contaminant discharge during the flooding process at a later stage.
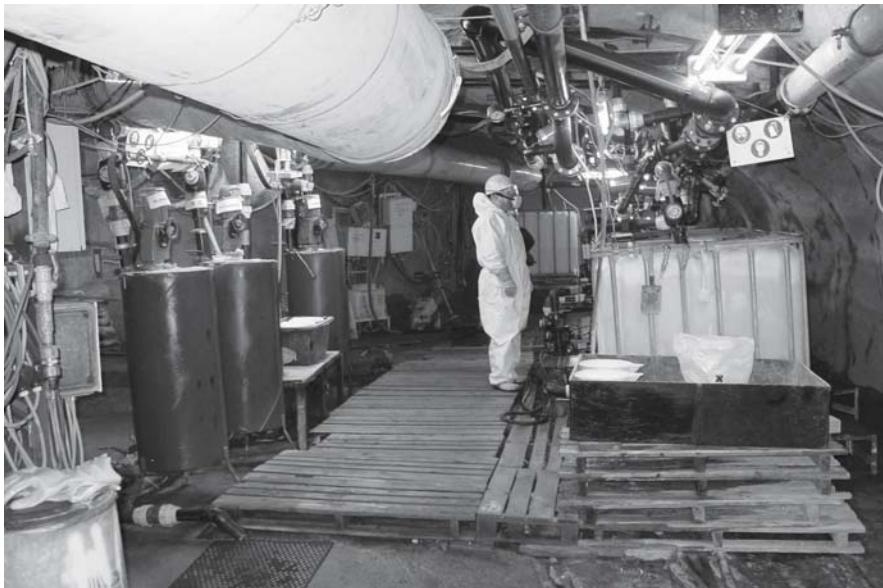
As in the test fields, the solution was based on $Ba(OH)_2*8H_2O$, Na_2SO_3, water glass, and a precipitation inhibitor. Preparation of the solution was carried out in a grout plant similar to that used in the field tests (Fig. 4).

Solutions were mixed within a pipe with water and an inhibitor-sodium-sulphite-sodium-silicate solution; up to 50 m^3/h of supersaturated solution could be prepared. About 500,000 m^3 of sandstone were treated. Samples taken from different locations demonstrated the successful use of $BaSO_4$ forming solutions.

In a second step, between November 2003 and May 2005 about 1.1 million m^3 of sandstone have been treated in the southern part of the mine with about 225,000 m^3 solution. For this, a improved grout plant was installed in the southern mine field. To avoid long pipelines, the plant was disassembled and moved to 2 other positions. There were no technical problems to reuse the components (Fig. 5).

Field preparation of the immobilization solutions was trouble-free. Chemical cost of the immobilization solution is about €1/m^3. A grout plant to produce immobilization solution for underground conditions with a capacity of about 200,000 to 300,000 m^3/a year would cost between 100,000 and 200,000 € and can be run by 2 employees.

The immobilization technology (direct source immobilization) has been applied in the southern part of the mine as part of the closure plan. It is expected that this approach will minimize the source in the final flooding process which will signifi-


Fig. 5. Immobilization grout plant 2005, capacity up to 50 m³/h, solution vessels on the left site, mixing facilities on the right site, storage vessels in the background.

cantly reduce the costs for conventional water treatment over the long term after ground water rebound has been completed.

In addition, the immobilization technology has other potential applications beyond remediation of acid-contaminated rocks; it could also be used for other contaminated rock formations or for inhibition of acid rock drainage generation. The technology is environmentally friendly, stable, and can be easily adapted to local site and field conditions.

Acknowledgement

References

Ziegenbalg G, Schreyer J, Jenk U (2003a) Feldversuche zur Schadstoffimmobilisierung in gelaugtem Quadersandstein. Glückauf-Forschungshefte 64 (2003) Nr.1

Ziegenbalg G, Schreyer J, Jenk U, Pätzold C, Müller E (2003b) In-situ-Schadstoffimmobilisierung in der Grube Königstein der Wismut GmbH. Glückauf-Forschungshefte 64 (2003) Nr.2

Ziegenbalg G (2005) A novel technology for sealing and immobilization – the use of precipitation processes from supersaturated solutions. This book

Case studies: active and abandoned Uranium mines

Management of uranium mill tailings and associated environmental monitoring in India

Amir Hasan Khan, V.N. Jha, R. Kumar, S.K. Sahoo, A.K. Shukla, R.M. Tripathi, V. D. Puranik

Environmental assessment Division, Bhabha Atomic Research Centre, Trombay, 400085 Mumbai, India, E-mail: khan@magnum.barc.ernet.in

Abstract. Mining of low grade uranium ore commenced at Jaduguda in eastern India in the mid 1960s. Presently, the uranium ore from four underground mines located within a distance of 22 km is processed by the Uranium Corporation of India Ltd. (UCIL). A few more mines are envisaged to meet the nuclear fuel requirements. Management of mine water, mill tailings and the effluents from the tailings containment facility is given due importance. Liquid effluents are treated with BaCl2 and lime slurry to remove 226Ra, Mn and other pollutants. A large portion of the treated effluents is re-used, the rest being disposed to the aquatic system after ensuring that they meet the regulatory standards of discharge. Surface and ground water monitoring results are presented in the paper.

Introduction

The first uranium ore deposit of economic importance in India was discovered at Jaduguda in eastern India where mining and ore processing operations commenced in mid 1960s. Subsequently, three other deposits at Bhatin, Narwapahar and Turamdih, all within a distance of about 22 km, were taken up for underground mining.

The ore from these mines is processed in the mill at Jaduguda. Opening of a few new mines in other parts of the country is envisaged.

Mining and ore processing

Underground mining

The Jaduguda mine was developed in three stages to reach the deepest ore deposit, currently at a depth of about 900 m. A central shaft serves as entry for men, material and as main ventilation intake. The ore excavated from different stopes is brought to a central location and hoisted to surface and discharged on to a conveyor system leading to the mill. Ventilation is provided through two exhaust fans of total capacity of 120 $m^3.s^{-1}$.

Bhatin is a relatively small mine, developed through adits and winzes to reach the ore body. It has entry through an adit, which also serves as intake route for ventilation air and transport of the excavated ore to surface. An exhaust fan provides ventilation of 30 $m^3.s^{-1}$.

Narwapahar mine is one of the most modern mines in the country with a combination of trackless mining through decline and a vertical shaft to reach the deeper ores. Three large fans provide a ventilation of 225 $m^3.s^{-1}$.

The Turamdih mine combining a system of trackless mining through a decline and a vertical shaft is in the advance stage of development (Bhasin 1998, 2001).

An underground mine at Bagjata and an open cast mine at Banduhurang are being developed in the same region. Another large ore processing mill is also under construction.

A few more underground and opencast mines with ore processing mill are envisaged in southern and north-eastern parts of the country.

Ore processing

The low grade uranium ore (<0.1 % U_3O_8) from all the mines are presently processed in the mill at Jaduguda. The initial ore processing operations comprise of crushing, screening, wet grinding to a size of -200 mesh and de-watering to control pulp density. This is followed by leaching with sulphuric acid in presence of pyrolusite (MnO_2) in air agitated vessels.

Depending on the ore, a temperature of 40 - 50 ^{o}C is maintained by using steam. The leachate is filtered, purified and concentrated using ion-exchange process. After precipitating sulphate and ferric iron by addition of lime slurry, magnesia slurry (MgO) is added to the pure liquor to precipitate uranium as magnesium diuranate (MDU; Beri 1998).

Treatment of mine water and mill tailings

Mine water

Large quantities of water are pumped out of the mines. This comprises of the ground water seepage in to mine galleries containing dissolved radionuclides and that sent to the mine for drilling, dust suppression and stowing or backfilling operations.

As it contains dissolved uranium and radium the mine water is collected, clarified and reused in the mill process after ion-exchange step since it also contains chlorides.

Mine water from Bhatin and Narwapahar mines is brought through pipe lines to the effluent treatment plant (ETP) at Jaduguda. About 4000 m^3 of mine water is reused per day as industrial water after clarification (Beri 1998).

Separate treatment schemes are in place for mine water from Turamdih and Bagjata mines which are in advance stage of development and located about 22 km west and east of Jaduguda, respectively.

Mill effluents

Water sprayed on the ore pile for suppression of dust as well as any runoff water from ore yard is collected and used as a part of the process water in mill after clarification. Overflow from the magnetite (a byproduct recovered from the tailings) settling pits is sent to the ETP for treatment. Water from storm water drains is also treated for use as industrial water.

Tailings treatment and containment

In view of the low grade of the ore processed, the bulk of the ore processed in mill emerges as waste or 'tailings'. It comprises of the barren cake from the drum filters containing all the un-dissolved radionuclides and the barren liquor from ion exchange columns having some dissolved activity. Disposal of tailings in a permanent containment system is, therefore, an important aspect of uranium mining and ore processing operations.

The barren liquor from the ion exchange columns is treated with lime stone slurry initially to a pH of 4.2 - 4.3 followed by addition of lime slurry to raise the pH to 10 - 10.5. It is then mixed with the barren cake slurry from the drum filters and a final pH of 9.5 - 10 is maintained. At this pH the residual uranium, radium, other radionuclides and chemical pollutants including Mn get precipitated. The treated slurry is classified into coarse and fine fractions using hydro-cyclones. The coarse material forming nearly 50% of the tailings is sent to mines for back-filling. The fine tailings or 'slimes' are pumped to an engineered tailings pond for perma-

nent containment. The slimes along with the precipitates settle down and clear liquid is decanted. A series of decantation wells with Hume pipes connected at bottom and side channels are provided to lead the decanted liquid to the ETP through an engineered concrete pipe line.

There are three valley-dam types of tailings ponds at Jaduguda. The first and second stages of the tailings pond of about 33 and 14 hectare (ha) surface area, respectively, are located adjacent to each other in a valley with hills on three sides and engineered embankments on downstream side of natural drainage (Fig.1). The 1st and 2nd tailings embankments were constructed by upstream method in which an initial dam was constructed at the downstream toe. The central line of the embankment was shifted towards the pond area as the height of the dam was increased from an initial elevation of 107 m (RL) to the final height of 130 m in stages. The second stage tailings dam was constructed upstream of the 1st dam at the far upper end from an initial elevation of 126 m to a height of 150 m. To provide additional stability the 1st stage embankment was strengthened (Prasad and Beri 1989; Gupta and Siddique 2003). These two tailings containment ponds are nearly filled up and ready for closure. Experiments are underway to decide the thickness of the cover material to reduce gamma radiation and radon emanation to an acceptable level for the long-term. The third stage of the tailings pond (Fig.2) having a surface area of about 30 ha, which is currently in use, is also located nearby in a similar setting. The third stage tailings pond embankment has been constructed by central line method in which the central line of the top of the embankment remains the same and downstream toe of each subsequent dike rests over the firm ground for better stability (Gupta and Siddique 2003. The height of


Fig. 1.   1st and 2nd Tailings Containment Ponds.

Fig. 2.   3rd Tailings Containment Ponds.

the 3rd tailings pond embankment starts from an initial elevation of 125 m and is expected to reach a final elevation of 160 m. The underlying soil and the bedrock of these tailings ponds have very low permeability. The tailings ponds are fenced.

Effluent Treatment
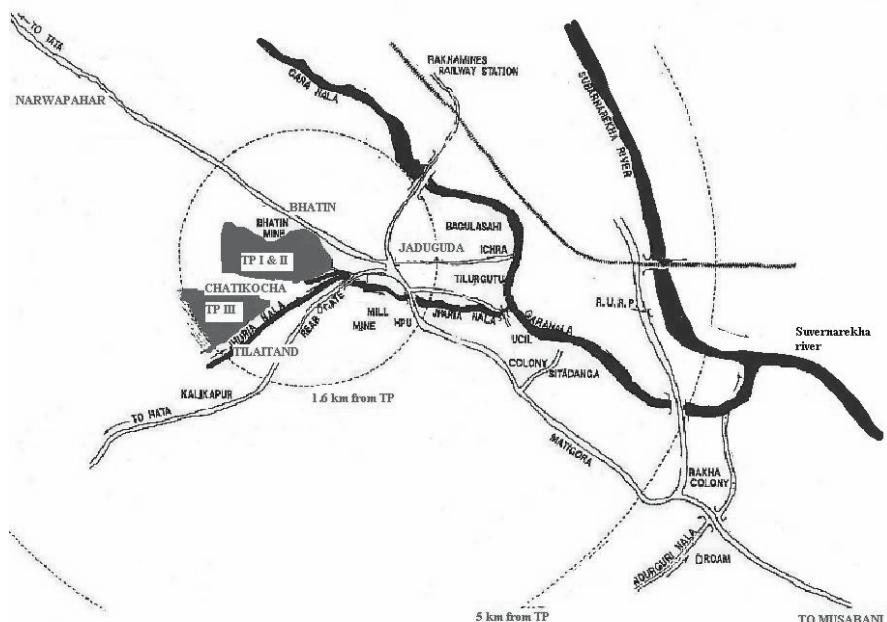
The treatment of tailings with lime in the tailings treatment plant of the mill helps in precipitating the dissolved radionuclides and other pollutants from the process effluents. After depositing the tailings in the containment pond reduction of pH in the tailings pond due to oxidation of sulphide radicals may occur over a period of time. This increases the concentrations of some radionuclides and chemical constituents in the effluents decanted from the tailings containment system. Hence the effluents requires further treatment to meet the regulatory discharge limits. The effluents coming from the tailings pond to the ETP are, therefore, first clarified and a large portion of this is reused in the milling process. The rest is treated first with $BaCl_2$ and then with lime slurry to precipitate the radioactive and chemical pollutants, especially ^{226}Ra and Mn. It is then clarified and the settled sludge carrying the $Ba(Ra)SO_4$ and $Mn(OH)_2$ precipitates is pumped to the tailings pond with the main tailings and the clear effluent is discharged to environment after monitoring (Beri, 1998).

Environmental surveillance

A Health Physics Unit with Environmental Survey Laboratory established at site maintains a comprehensive surveillance on the environment around the mines, mill and the tailings pond to evaluate the effectiveness of control measures, assess the environmental impacts and ensure regulatory compliance.

Radiation levels

Uranium tailings are low specific activity material and hence a source of low levels of gamma radiation and environmental radon. Gamma radiation and radon levels over the tailings pile, on the embankment and nearby areas are monitored. The ^{226}Ra content of the tailings is in the range of about 4 to 8 Bq.g^{-1}. The gamma radiation levels directly 1 m above the tailings pile range from about 0.8 to 3.3 μGy.h^{-1}, depending on thickness of the pile. This reduces to about 0.3 to 0.5 μGy.h^{-1} on the embankment and attains the local background levels of 0.10 to 0.15

Fig. 3.   Environmental Map of Jaduguda Showing Jaduguda, Bhatin, Narwapahar and TPs.

Case studies: active and abandoned Uranium mines

μGy.h^{-1}within a short distance from the embankment. The average radon emanation rate from the tailings pile is of the order of 1.5 Bq.m^{-2}.s^{-1}and the atmospheric radon concentration directly above the tailings averages around 35 Bq.m^{-3}compared to the natural background level of about 10 – 15 Bq.m^{-3}in the region (Khan et al, 2004).
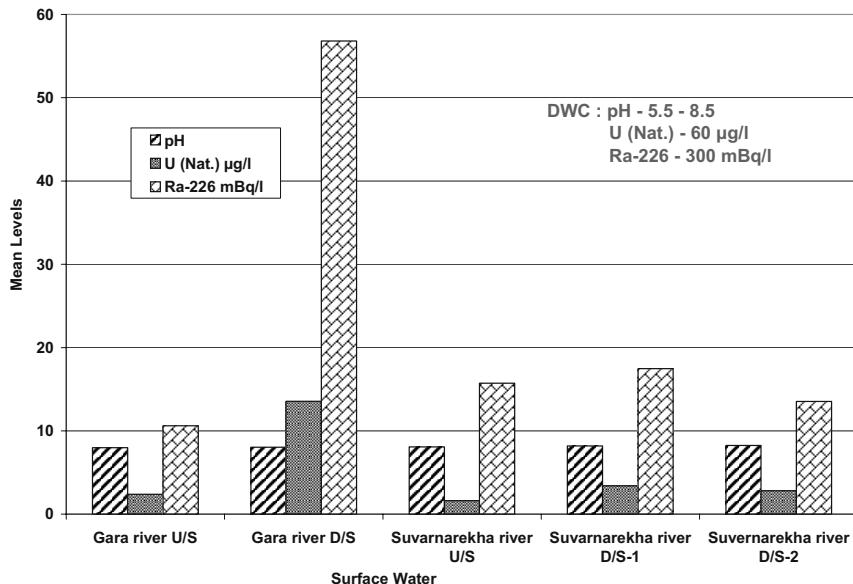
Surface and ground water

The liquid effluents released after treatment and monitoring have a small potential to contribute to the radioactivity level of the recipient surface water system in the immediate vicinity. In view of the clayey soil and hard rock at the bottom of the tailings containment system, the hydraulic conductivity is low. However, any underground migration of radionuclides from the tailings pond may show up in the local ground water. The environmental surveillance, therefore, also includes monitoring of uranium (nat.) and ^{226}Ra in surface and ground waters in the vicinity of uranium mining and tailings containment. The surface and ground waters are monitored regularly in the environment around the facility (Fig. 3).
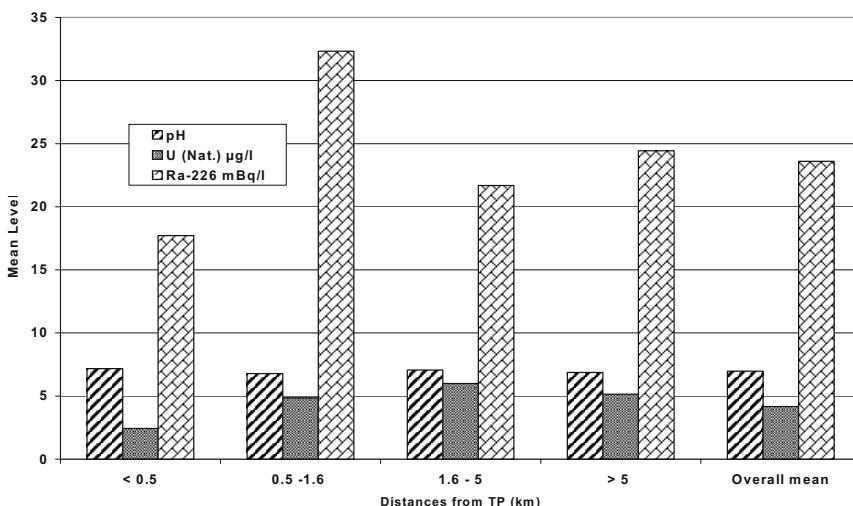
The Gara, a relatively small river and tributary of the Subarnarekha River, receives the treated effluents from the uranium mining and milling industry. The mean of pH, U(nat) and ^{226}Ra concentrations observed in the surface waters for the last 9 years are summarized in Fig. 4. It may be noted that uranium and radium concentrations in water from the Gara and Subarnarekha rivers downstream of UCIL operations are nearly of the same order as the respective background levels observed upstream. Slightly elevated levels of uranium and radium in the immediate recipient Gara River are well within the respective derived water concentration limits. The levels in Subarnarekha River reduce further and approach the regional background values.

The ground water sources comprising of dug wells, hand pumps (tube wells) and some deep holes drilled for geological prospecting in the past are monitored for uranium (nat.) and radium-226. The results obtained during the last 9 years are summarised with respect to distance from the tailings containment system and presented in Fig. 5.

Uranium and radium levels in the ground water sources in the region vary over a wide range of <0.5 – 55 μg.l^{-1} averaging around 4 μg.l^{-1} for uranium and in the range of <3.5 – 455 mBq.l^{-1} averaging around 23 mBq.l^{-1}for radium. The higher values are observed in water flowing out of some deep drill holes made for geological prospecting in the past, over 3 – 5 km away from the uranium mining and tailings pond sites. The lower values of about 2.5 μg.l^{-1} for uranium and about 18 mBq.l^{-1} for radium observed within 0.5 km from the tailings pond are comparable to the regional average of 4.2 μg.l^{-1} for uranium and about 23.5 mBq.l^{-1} for radium. This also indicates that tailings containment facility does not have any discernible impact on the ground water in its vicinity.

DWC : pH - 5.5 - 8.5
U (Nat.) - 60 µg/l
Ra-226 - 300 mBq/l

Fig. 4. pH, Uranium (nat.) and Ra-226 Levels in Surface Water around Uranium Mining Complex.

Fig. 5. pH, Uranium (nat.) and Ra-226 Levels in Ground Water around Tailings Pond.

Case studies: active and abandoned Uranium mines

Conclusions

In view of the importance given to the safe management of mine and mill effluents including uranium tailings   from the very beginning, uranium mining and ore processing operations have not resulted in any discernible impact on the environment. The continuous environmental surveillance   has been effective in controlling the environmental releases of radioactivity. Treatment and reclamation of waste water for reuse in the plant is another positive feature as it helps in conserving fresh water.

Acknowledgement

References

Beri, K.K., (1998), Uranium ore processing and environmental implications; Metal, Materials and Processes, Vol.10, No.1,pp. 99-108.

Bhasin, J.L., (2001), Mining and milling of uranium ore: Indian scenario; Impact of new environmental and safety regulations on uranium exploration, mining and management of its waste, IAEA-TECDOC-244 (2001), pp189-200.

Bhasin, J.L., (1998), Uranium exploration and mining; Nu-Power, vol.12, No.1.

Prasad, S.N. and Beri, K.K. (1989), Impounding of Tailings at Jaduguda - Planning, Design and Management, Proceedings of the National Symposium on Uranium Technology, BARC, Bombay, Dec. 13-15.

Gupta, R. and Siddique, S., (2003), Management of the tailings and liquid effluents in uranium mining and milling operations; Radiation Protection and Environment, vol.26, No.3 & 4, 2003, pp.506 -515.

A.H. Khan, Fabby Sunny, S.K. Sahoo and V.D. Puranik (2004), Long-term management of uranium mill waste: proposal for stewardship after decommissioning of the tailings pond, Presented at the IAEA Technical Meeting on Long-term Radiological Liabilities: Stewardship Challenges, Vienna, October 11-15, 2004 (Version 3.1 -2005-02-14).

Cover and final landform design for the B-zone waste rock pile at Rabbit Lake Mine

Brian Ayres[1], Pat Landine[2], Les Adrian[2], Dave Christensen[1], Mike O'Kane[1]

[1]O'Kane Consultants Inc., Saskatoon, Saskatchewan, Canada
[2]Cameco Corporation, Saskatoon, Saskatchewan, Canada,
E-mail: Pat_Landine@cameco.com

Abstract. A detailed study was undertaken to evaluate various cover system and final landform designs for the B-zone waste rock pile at Rabbit Lake Mine in Canada. Several tasks were completed including physical and hydraulic characterization of the waste and potential cover materials and numerical modelling to examine erosion and slope stability. Soil-atmosphere numeric simulations were conducted to predict net infiltration and oxygen ingress rates through several cover system alternatives. A seepage numerical modelling programme was completed to predict current and future seepage rates from the base of the pile for alternate cover system designs. Several final landform alternatives were developed for the pile along with a preliminary design for a surface water management system. The potential impact of various physical, chemical, and biological processes on the sustainable performance of the final landform was also considered. This paper provides an overview of the investigations completed towards the development of a cover system and final landform design for the B-zone waste rock pile.

Introduction

Rabbit Lake Mine, owned and operated by Cameco Corporation, began operation in 1975, and is the longest operating uranium production facility in Saskatchewan, Canada. The operation is located 700 km north of Saskatoon (Fig. 1). Historic and current operations at this site include four open pits, one underground mine, several mine waste storage facilities, and a mill.

Cameco is developing a decommissioning plan for the B-zone area at Rabbit Lake Mine, which includes a flooded open pit, a waste rock pile, and an ore stor-

age pad. Proper closure of the B-zone waste rock pile (BZWRP) will be important to minimize the impacts of seepage emanating from the stockpile on the long-term water quality of the flooded open pit and other nearby surface water receptors. The BZWRP will be decommissioned in-place meaning that an engineered cover system is required for closure.

A multi-phase study is underway to determine the optimum landform and cover system design for the BZWRP. Several field investigations have been completed to evaluate the geochemical, physical and hydraulic characteristics of the waste rock and locally available cover materials, as well as the hydrogeological setting of the stockpile. Various numerical modelling programmes have been initiated to predict net infiltration, oxygen ingress, and erosion rates for various cover system

Fig. 1.   Map of northern Saskatchewan showing the location of Rabbit Lake Mine.

Case studies: active and abandoned Uranium mines

alternatives, source terms for contaminants of concern in the stockpile, and environmental loadings to the receiving environment. All of these studies are linked, with the ultimate goal being to develop cover performance criteria based on minimizing impacts to surface water and groundwater receptors. Another key aspect for closure of the BZWRP is design of the final landform; poor surface water management and landform instability are common factors leading to failure of cover systems around the world (MEND 2004).

The key investigations completed towards developing a cover system and final landform design for the BZWRP are reviewed in this paper.

Background

Rabbit Lake Mine is surrounded by lakes and wetlands as well as low relief glaciated landforms comprised mainly of sand and gravel. The climate in the area is semi-humid, sub-arctic, characterized by generally wetter conditions in the fall, winter and spring, and drier conditions during the hot summer months. The mean annual precipitation and potential evaporation for the site is approximately 540 mm and 400 mm, respectively. About 33% of the annual precipitation occurs as snow.

The current BZWRP landform is between 18 and 30 m high with 37° side-slopes, covers a surface area of approximately 22 ha, and has a volume of about $4.6 \times 10^6 \, m^3$. The water quality of seepage emanating from the pile is characterized by elevated levels of several metals and radionuclides, notably As, Ni, Mn, ^{226}Ra and U, and a pH typically between 3.3 and 5.5. Metal leaching, as opposed to acid rock drainage, is the primary catalyst for the production of contaminated seepage. Therefore, the primary function of the pile cover system is to reduce the net infiltration of meteoric water, as opposed to limiting the ingress of atmospheric oxygen. Limiting surface erosion and providing a medium for sustainable vegetation are also important functions.

Mine waste covers can be simple or complex, ranging from a single layer of earthen material to several layers of different material types, including native soils, non-reactive tailings and/or waste rock, geosynthetic materials, and oxygen consuming organic materials (MEND 2004). Factors that control the economic and technical feasibility of a particular cover system include site climate conditions, availability of cover material(s) and distance to borrow source(s), cover and waste material properties and conditions, and vegetation conditions. Cover material(s) and therefore cover performance will evolve over time due to the impacts of site-specific physical, chemical, and biological processes, which should be considered in the design process (INAP 2003). Cover system alternatives evaluated for the BZWRP include varying thicknesses of non-compacted local soils and/or compacted waste rock on the stockpile surface.

Waste rock and cover material characteristics

Field sampling / testing and laboratory testing was conducted to determine the physical and hydraulic characteristics of the near surface material in the BZWRP and potential cover materials at the site. Field testing examined the *in situ* moisture content, density and permeability of the materials. The laboratory programme included tests for particle size distribution (PSD), specific gravity, compaction characteristics, saturated hydraulic conductivity (K_{sat}), and moisture retention characteristics. Fig. 2 shows typical PSD curves for the near surface waste rock and sandy-gravel till borrow (cover) material.

The near surface material across the top of the BZWRP is relatively heterogeneous, indicative of weathered sandstone and basement rock materials. Geochemical studies conducted by Cameco suggest that, at a minimum, a thin till cover will be required for the BZWRP to prevent post-closure contamination of surface water in the vicinity of the waste rock pile. The matrix of the surface material is relatively well-graded from cobble down to silt and clay size particles with a median diameter on a mass basis of approximately 4 mm. The K_{sat} of the waste rock material ranges from 5.0×10^{-5} cm/s for a lower density condition to 6.0×10^{-6} cm/s for a higher density condition.

An ideal material for a "simple" cover system, in terms of moisture store-and-release and long-term stability, has a well-graded PSD (i.e. an equal representation by mass for all particle sizes). Based on the results of the PSD test programme and field observations, the most promising borrow source for cover material is a drumlin located six kilometers from the BZWRP (material sample TP14-1). The matrix of the till borrow material is relatively well-graded from cobble down to silt and clay size particles with a median diameter on a mass basis of approximately 0.4 mm. The K_{sat} of the till borrow material ranges from 6.0×10^{-3} cm/s for a lower density condition to 3.0×10^{-5} cm/s for a higher density condition.
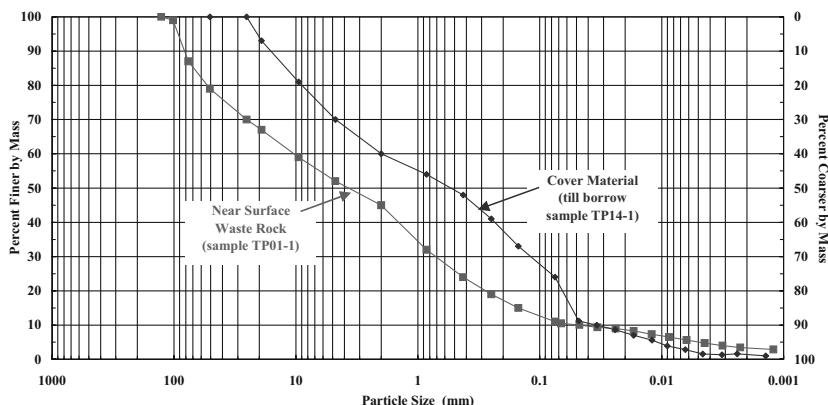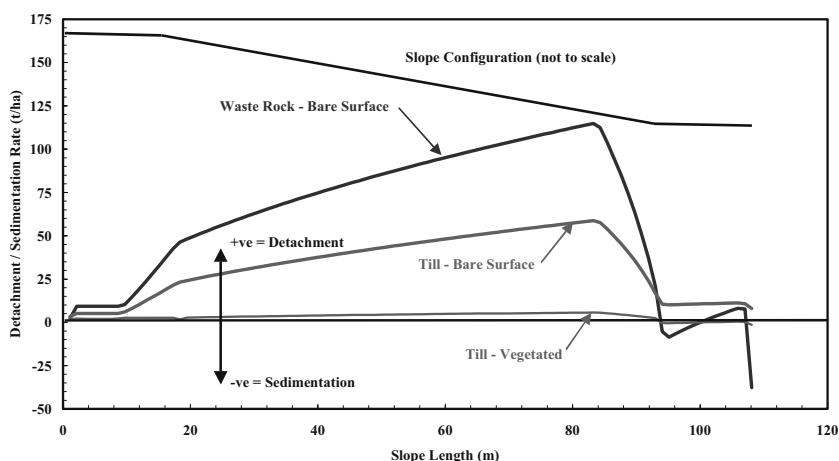

Fig. 2.   Typical PSD curves for the near surface waste rock and till cover materials.

Case studies: active and abandoned Uranium mines

Surface erosion numeric analyses

Erosion numerical modelling was completed to estimate the distribution and magnitude of erosion from various cover surfaces and final landform alternatives for the BZWRP under historical precipitation conditions and significant storm events. The Water Erosion Prediction Project (WEPP) model (Flanagan et al. 1995), a two-dimensional, process-based computer program, was used in this study. WEPP models erosion from interrill areas, and detachment and transport from overland flow and channel flow in rill areas. The following three material and surface types were examined in the modelling programme: 1) waste rock with a bare surface, 2) till with a bare surface, and 3) till with a "poor" stand of grass vegetation. The modelling programme included 3H:1V and 4H:1V linear slope configurations and one concave slope, featuring a steep upper segment (2H:1V) and a gentler lower segment (5H:1V).

The erosion modelling programme predicted the bare till surface is more erodible than the bare waste rock surface under historical precipitation conditions, but less erodible under significant storm events. The addition of a "poor" stand of grass vegetation to the till surface greatly reduces the predicted erosion to rates well below the simulated bare surfaces (Fig. 3). Minimal difference in the erosion rate was predicted between each of the simulated side-slope configurations for a given climate year or storm event. This is attributed to the relatively small difference in the surface gradients between all three alternatives, as well as the relatively small height of the pile and corresponding short slope lengths. A sensitivity analysis showed that the climate year (i.e. precipitation) has the largest influence on the predicted erosion rates.


Fig. 3.   Predicted soil loss rate by position on the 4H:1V linear slope for the waste rock and till materials during the 100-year, 24-hour storm event.

Soil-atmosphere cover design numerical modelling

Soil-atmosphere modelling was completed with the two-dimensional finite element model VADOSE/W (Geo-Slope International Ltd. 2004a), to evaluate the performance of alternate cover system designs for the top (or plateau) and various re-contoured side-slope configurations for the BZWRP. A key feature of VADOSE/W is the ability of the model to predict actual evaporation and transpiration based on potential evaporation and predicted soil suction, as opposed to the user being required to input these surface flux boundary conditions. Predicted net infiltration rates were used as the primary indicator of cover system performance; however, oxygen ingress to the underlying waste material was also evaluated.

Each simulation was run for 365 days, with the simulation period beginning November 1st and ending October 31st of the following year. This simulation period best suits a cold northern climate by allowing the formation of snowpack during the winter season, occurrence of snow melt in the spring, and extending through the frost-free period at the site. The entire snowpack was applied for each simulation assuming no drifting or sublimation of the snowpack. Runoff water produced from the spring freshet and storm events for simulations involving a cover system was removed from the model, which is deemed to be representative of the 2-3% slope planned for the top of the final BZWRP landform. The bare waste rock simulations considered two options for spring freshet and storm runoff: restricting flow causing a pool of water to be formed on the surface and allowing runoff water to drain. Vegetated-surface simulations assumed a "poor" grass vegetation cover, which has a leaf area index of 1.0 during the growing season.

Table 1 summarizes the key predictions from VADOSE/W for the bare waste rock surface condition and four cover system alternatives for the top of the pile. The net percolation prediction for the bare surface condition is indicative of the waste rock matrix (i.e. this does not account for large macropores or "drains" in the pile that would act as preferential flow paths for infiltration during significant storm events). Net percolation and oxygen ingress rates decrease as the quality of

Table 1. Net percolation and oxygen ingress model predictions for the bare waste rock surface condition and four cover system alternatives for the top of the pile.

Cover System Alternative	Net Perc. (mm)	Net Perc. (% of AP*)	O_2 Ingress (mol/m^2)
Bare waste rock (WR) – no runoff	200	37.3	-
Bare WR – runoff	150	28.1	-
0.3 m till cover	85	15.9	208
1.0 m till cover	55	10.3	39
Compacted WR with 0.5 m till cover	54	10.1	35
Compacted WR with 1.0 m till cover	34	6.6	14

* AP = annual precipitation

Case studies: active and abandoned Uranium mines

the cover system increases, as expected. However, there is not a significant difference between the predicted net percolation through the 1.0 m till cover system and that predicted through the 0.2 m compacted waste rock with 1.0 m till cover system. This is attributed to the relatively high K_{sat} of the non-compacted till and *in situ* waste rock material, and the assumption that field compaction of the near surface waste rock will only reduce its permeability by one order of magnitude. The highest quality cover system evaluated for the BZWRP is expected to reduce the net percolation of meteoric water to the underlying waste material by 83% compared to the current or bare waste rock surface condition (no runoff).

A sensitivity analysis found the presence of vegetation and the K_{sat} of the compacted waste rock have the largest influence on the predicted net percolation through the cover systems. Although not shown, the compacted waste rock with 1.0 m till cover system is predicted to have the best performance on the re-contoured stockpile side-slopes, followed by the thick till cover system and the compacted waste rock with 0.5 m till cover system.

Waste rock pile seepage numerical modelling

Numerical seepage modelling was completed for this study to evaluate current and post-closure seepage rates from the base and toe of the BZWRP. SEEP/W (Geo-Slope International Ltd. 2004b), a two-dimensional seepage model, was used for this purpose. A representative two-dimensional cross-section of the pile was modelled to examine groundwater flow immediately surrounding the BZWRP, as well as the mounding characteristics of groundwater within the pile itself. The material properties within the model were estimated by calibrating predicted heads to measured piezometric heads in the BZWRP and immediate surrounding area.

The simulation of future conditions found that there is a significant reduction in the elevation of the phreatic surface, as well as seepage from the base and toe of the BZWRP for the first 10 to 20 years following placement of an engineered cover system. These values continue to slowly decrease with time until they tend to approach an equilibrium condition 60 to 65 years following closure. Long-term equilibrium total flux rates from the waste rock pile for a "higher" quality cover were approximately one order of magnitude less as compared to that predicted for a "moderate" quality cover system.

Evaluation of BZWRP final landform alternatives

The following guidelines were used to develop final landform alternatives for the BZWRP:
- Landform / surface materials must be able to withstand flow velocities associated with the 1:100 year, 24-hour design storm event (88 mm);

- Results of erosion numeric simulations and slope stability analysis should be considered in developing the final landform;
- Minimize expansion of the current pile footprint and as much as possible, remain inside the footprint defined by the perimeter collection ditch;
- Minimize picking up waste rock (i.e. more economical to re-contour with a large dozer provided the material pushing distances are not significant);
- Minimize ponding of water on the landform (i.e. promote runoff);
- Balance the cut/fill earthmoving material volumes; and
- Incorporate features of local glaciated landforms into the final pile landform design where possible for aesthetic purposes.

The software packages Eagle Point 2001 and AutoCAD 2004 were used to create a digital terrain model (DTM) of the existing landform, and then create several new landform designs based on the existing DTM and specified design constraints and criteria. The model selected for estimating the peak flow and total runoff volume from the design storm event is the one described by the United States Department of Agriculture Technical Release 55 (TR-55) – Urban Hydrology for Small Watersheds (USDA 1986).

Preferred cover system and final landform design

The preferred cover system design for the BZWRP is a 0.2 m thick layer of compacted *in situ* waste rock overlain by 1.0 m of non-compacted sandy till. This cover system is predicted to perform the best on the plateau and side-slopes of the final BZWRP landform in terms of reducing the net percolation of meteoric water and remaining stable against erosive forces. The preferred cover system design is based primarily on the available borrow materials at the site and the results of surface erosion and soil-atmosphere cover design numeric simulations, but also takes into consideration the potential impacts of various processes on sustainable performance as discussed below.
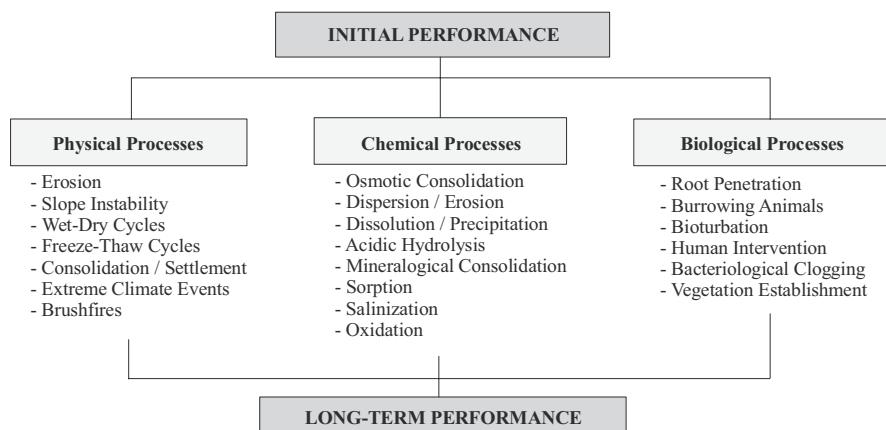
Based on the landform criteria described above and the results of numeric simulations of surface erosion and analyses of slope stability, the preferred final landform design for the BZWRP is shown in Fig. 4.

The landform consists of:

- Two catchments on the landform each approximately 4.4 ha that are "dished" to channel runoff water to a central light armoured drainage channel and subsequently to the north or south heavily armoured slope drainage channels (plateau slope ranges between 2 and 5%);
- Linear 20% (5H:1V) slopes on both the north and south slope of the landform to manage runoff volumes / flow velocities for the design storm event using 75 mm median stone size for riprap armouring; and
- Concave east and west slopes comprised of a 50% (2H:1V) sloped segment for the upper quarter and a 20% (5H:1V) sloped segment for the lower three-quarters of the slope.

Addressing potential impacts on sustainable performance

INAP (2003) conducted an examination of the processes shown in Fig. 5, and discovered that their effects could be related to the change in three key cover performance properties; namely, the K_{sat} and moisture retention characteristics of the cover materials and the physical integrity of the cover system. The K_{sat} and moisture retention curve are key hydraulic properties of a cover system layer. A sensitivity analysis should be conducted as part of the soil-atmosphere modelling programme to examine the potential impact on cover performance due to changes in the material hydraulic properties. Consideration of the effects of long-term changes in biological and chemical processes on performance has been generally dealt with in a qualitative manner, if addressed at all (MEND 2004). The key processes that could impact on sustainable performance of the BZWRP cover system and final landform are erosion, freeze-thaw and wet-dry cycling, root penetration, and bioturbation.


Fig. 4.   Processes that could impact the sustainable performance of soil cover systems (from INAP 2003).

Case studies: active and abandoned Uranium mines

The design of the preferred final landform directs runoff water from the plateau to heavily armoured drainage channels sloping to the north and south ends of the pile. This reduces the amount of runoff water reaching the concave east and west side-slopes resulting in decreased overall erosion for the landform. The proposed final landform design reduces the average slope gradient and slope length for runoff waters as compared to a conventional "domed" landform design.

It is proposed that the compacted waste rock layer be covered with 1.0 m of non-compacted till for protection and the establishment of vegetation. The 1.0 m thick layer of non-compacted till is required to ensure long-term performance of the cover system as a whole, because of the inevitable presence of woody species. The coniferous and deciduous woody species native to the site are prone to lateral and shallow root development, as they anchor themselves to the surface. The 1.0 m of non-compacted till does not guarantee that woody species roots will not develop in the compacted layer, but it is likely that more than 85% of the woody species root development would be contained in the upper non-compacted layer.

The proposed cover system design for the BZWRP comprises a layer of compacted waste rock material, which has little to no clay content and thus should possess resistance to cracking during drying. The compacted waste rock layer will undergo freeze-thaw cycles. There has been minimal research on the effects of freeze-thaw cycles on compacted granular material. However, it is anticipated that the change in material properties will be minimal. In addition, there is no supply of water (i.e. a saturated underlying material) to support large-scale frost heave of the compacted waste rock material, and in general, alterations in the void ratio due to freezing.

Concluding remarks

A detailed study has been completed to evaluate several cover system and final landform alternatives for the B-zone waste rock pile at Rabbit Lake Mine. The ultimate cover system and final landform design have not been finalized yet because other studies are in progress that are evaluating potential impacts on the receiving environment based on the predicted performance of varying cover and landform designs.

It is common for numerical modelling to be dismissed as being "useless" due to a lack of predictive accuracy. However, the key advantage to the numerical modelling results obtained for this study is the ability to enhance judgement. Hence, rather than a focus on the absolute results predicted, it is recommended that the modelling results be viewed as a tool to understand key processes and characteristics that will influence performance of the BZWRP cover system, and develop engineering decisions based on this understanding.

References

Flanagan D, Ascough J, Nicks A, Nearing M, and Laflen J (1995) Technical documentation – USDA Water Erosion Prediction Project. NSERL report no 10, West Lafayette, IN

Geo-Slope International Ltd. (2004a) GeoStudio 2004 VADOSE/W on-line help v6.12

Geo-Slope International Ltd. (2004b) GeoStudio 2004 SEEP/W on-line help v6.12

International Network for Acid Prevention (INAP) (2003) Evaluation of the long-term performance of dry cover systems, final report. Prepared by O'Kane Consultants Inc., report no. 684-02, March

Mine Environment Neutral Drainage (MEND) (2004) Design, construction and performance monitoring of cover systems for waste rock and tailings. Canadian Mine Environment Neutral Drainage Program, Project 2.21.4, July

United States Department of Agriculture (USDA) (1986) Urban hydrology for small watersheds. Technical release 55 (TR-55), Natural Resources Conservation Service, June

A GPS-Based System for Radium/Uranium Contamination Gamma Scanning

Robert Meyer, Michael Shields, Scott Green, Janet Johnson

MFG Inc., Suite 100, 3801 Automation Way, 80525 Fort Collins, Colorado, USA, E-mail: Robert.Meyer@mfgenv.com

Abstract. MFG Inc. in 2001 developed a Global Positioning System (GPS)-based gamma scanning technique for use during site surveys at a large (16 km2) in-situ-leach uranium mine being developed in Kazakhstan. Since that time, the system has been improved and used at a total of eight radium/uranium-contaminated sites in the western U.S. At one former uranium mill site in Texas, data acquisition occurred at a rate of seven acres/hour on the 600 acre site. High-speed scanning allows 100% coverage of a site in a short period, providing color-coded output defining gamma exposure rates over the entire site.

The GPS/Gamma Scan System

With the deployment of the Global Positioning System (GPS) satellite constellation, a number of new data collection methods became possible. Development of handheld GPS receivers has made such approaches feasible and cost-efficient. MFG staff have been involved in radiation measurements work for years. We decided in the late 1990's to link gamma detection units with GPS and computer systems to allow the development of very high density mapped data sets. Such data are useful to identify contamination at sites including uranium mills and mines, other metal mine facilities (for example, copper, vanadium and rare earth) with secondary radioactive contamination, and facilities with other contamination, including accidental. The GPS-based detection systems may also be used to direct remedial action at such sites, and become especially valuable when providing a record of the final radiation status of a remediated site.

Each system used to collect gamma exposure rate data includes the following:
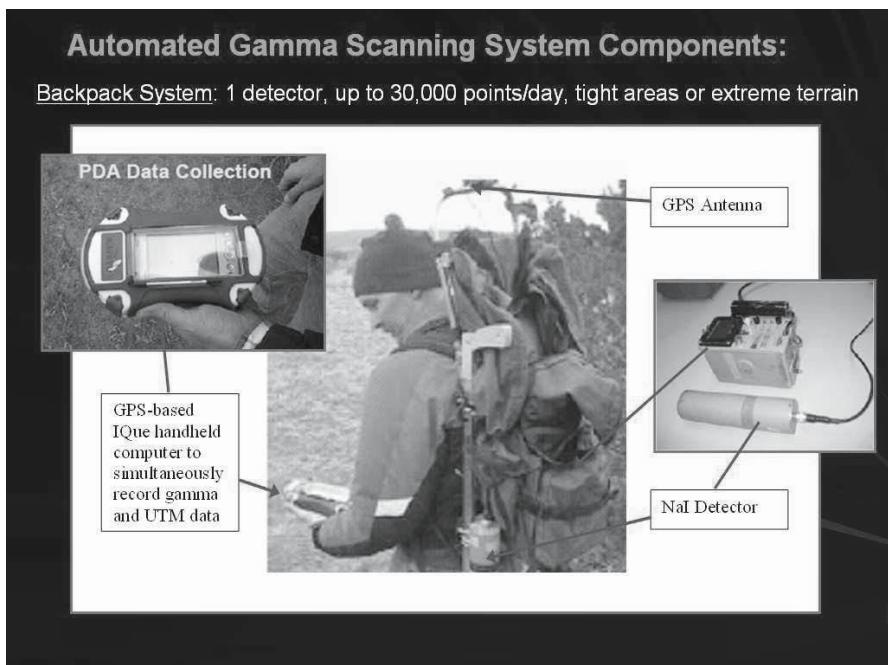
- Ludlum 2350-1 radiation detection datalogger
- Ludlum 44-10 2x2 inch NaI gamma detector
- Garmin iQue 3600 GPS/Personal Digital Assistant (PDA)

- MFG code to capture data on iQue memory, and to sort and view data.

The Ludlum 2350-1 datalogger includes a bidirectional RS-232 port, allowing communication with PC and PDA devices. The iQue GPS data can be captured internally with appropriate programming, and an RS-232-capable port on the iQue allows communication with the 2350-1 for data transfer initialization and capture. Fig. 1 presents views of the system in use in a "backpack" configuration.

The system may be deployed in a single-detector configuration, with the gamma detector carried 1 meter above the ground, either lead-shielded or unshielded. The single detector system scans an effective width of two meters. It may also be deployed, using a portable computer, a USB hub, and individual WAAS-enabled GPS units to replace the iQue 3600, with multiple detectors carried on a truck or all-terrain vehicle. The latter configuration increases data collection speed, with two or more gamma detectors each providing data once per second to the PC. Fig. 2 provides a view of a three detector system, with detectors spaced on 2 meter centers at 1 meter height. The three detector system scans an effective width of 6 meters.

Developing a correlation between soil radionuclide concentrations and gamma exposure rates requires careful attention to sample and gamma data collection. Relatively uniform areas of contamination (typically 10 m squares) must be selected prior to sampling. Ten to twenty aliquots of soil, taken to 15 cm depth, are composited from each square, and sent to a qualified laboratory for Ra-226 con-
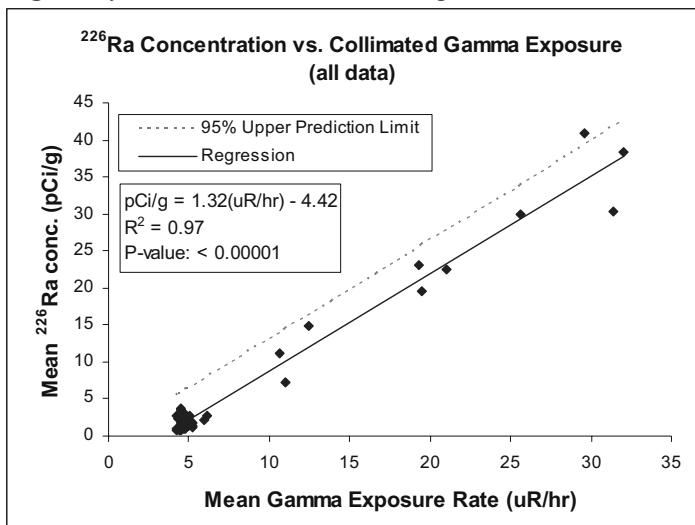

Fig. 1.   System in Backpack Configuration.

Case studies: active and abandoned Uranium mines

centration analysis (after drying, grinding and homogenization). The sampled area is carefully scanned using either a backpack or truck-mounted GPS/gamma scan setup, to develop a useful correlation. Fig. 3 presents the results of such a correlation analysis, utilizing data collected at another client site in the western U.S.
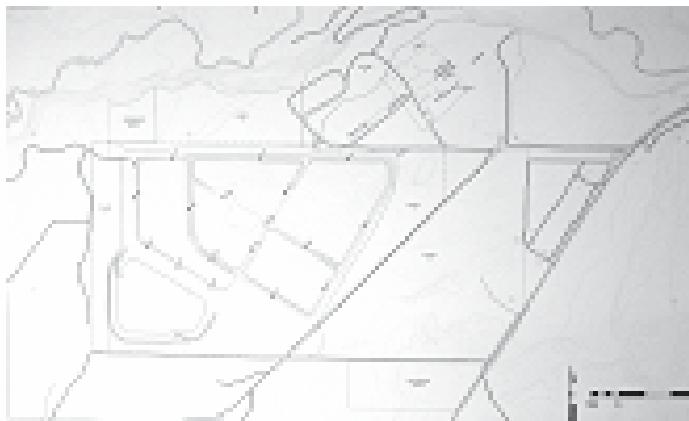
**Fig. 2.**   System in Three Detector Configuration.

Fig. 3.   Soil Analysis vs. GPS/Gamma Scan Exposure Data.

Case studies: active and abandoned Uranium mines

Using the GPS/Gamma Scan System

Figs. 4 and 5 show characterization data developed at a client facility currently being remediated Initially, a base drawing of the plant was evaluated using computer automated design (CAD) systems. Such a drawing, developed earlier using available information, may not accurately present the locations of the site's features. The base map for this site was therefore "ground-truthed" by collecting GPS data at several dozen points throughout the site. This information was used to "warp" the original CAD drawing to fit the GPS findings. Fig. 4 presents such a corrected drawing, ready for gamma data display.

**Fig. 4.**   Initial base map of a facility, corrected using on-site GPS data.
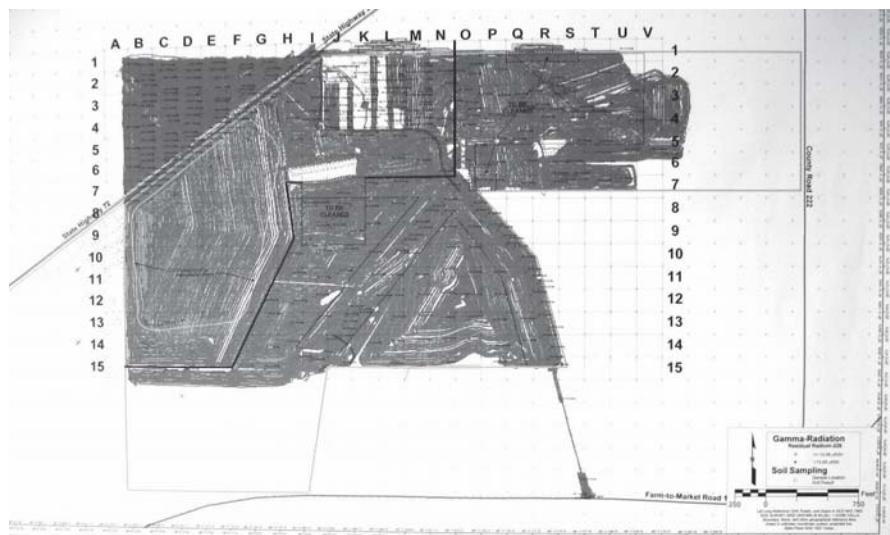
Fig. 5.   Full Data Set Prior to Initiation of Remedial Action

Case studies: active and abandoned Uranium mines
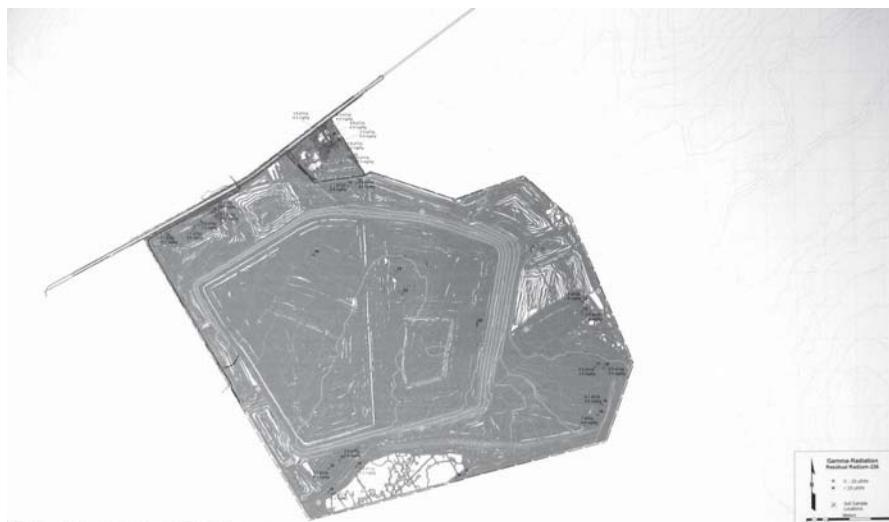
Fig. 5 displays gamma exposure rate data collected using the MFG systems detailed above. The figure displays the facility's gamma status, as it exists prior to remedial action. Initial data were used to characterize site exposure rates, to identify areas from which soil samples could be taken to establish a site-specific correlation between gamma levels and actual soil Ra-226 concentrations. Note that such correlations are approximate only. Remedial action (cleanup) criteria, specified as allowable residual soil concentrations, may then be compared to color-coded data as shown, to allow quick identification of areas in which remedial action will be required. As excavation of contaminated soil proceeds during cleanup, new will be layered over this plot, providing a nearly real-time display of site remedial action status. Hand-held gamma detectors, of the same type used to develop the plot data, are used for excavation control.

Fig. 6 presents the status of another client site in the western U.S. This project is currently moving toward completion of remedial action. Given that a large number of soil samples have established a good correlation with gamma exposure rate for this site, the Geographical Information System (GIS) display has been modified to show green areas highly likely to meet the soil standard (6 pCi/g Ra-226 at this facility), or red areas requiring additional soil removal. Modification of the data presentation to this two-color format allows for quick identification of areas requiring additional work. All plots that we produce using the GPS/gamma system display high-resolution latitude/longitude (lat/lon) coordinates, allowing re-location of such contaminated areas easily, using "walk-back" features common to hand-held GPS units.

Fig. 7 presents the results of a "current status" check of another client's site in the southwestern U.S. The purpose of the survey was to check for potential con-


Fig. 6.   Data Filtered to View Areas of Potential Remediation.

Case studies: active and abandoned Uranium mines

Fig. 7.   Contamination Status Check Using GPS/Gamma Scan Data

taminated material left behind after completion of earlier remedial actions. Earlier survey techniques were unable to provide data at this resolution (the plot displays some two million data locations). Detailed soil sampling was used to establish a correlation between the GPS/gamma exposure rate and actual soil Ra-226 concentrations. Areas exceeding the allowable residual concentration, based on gamma levels, will be easy to find if additional remediation is determined by the client to be appropriate.

Summary

The MFG GPS/Gamma Scan system has been refined since 2001 for use on a variety of radioactive contamination sites. The current configuration allows for very rapid data collection, development of useful correlations between soil concentration and gamma exposure rate, and display of very large data sets in a flexible and easily reviewed format. The system is currently in use at several U.S. remedial action sites.

Use of underground excavated space for disposal of low radioactive mining waste resulted from uranium ore exploitation. Study case

Dan Bujor Nica, Dan Georgescu, Traian Boboiceanu, Stefan Petrescu

Research and Development National Institute for Metals and Radioactive Resources.68 – 70, Bd. Carol I, Sector 2, 020917 Bucuresti, Romania,
E-mail: icpmrr@icpmrr.ro

Abstract . The article presents the actual situation of the Avram Iancu uranium mine, located in Romania; where important quantities of radioactive waste rock from the uranium mining industry accumulated and become a major risk for the environment. The result of the analysis of the particular conditions of this mining perimeter was that the relocation of the contaminated material in the abandoned mines pits is the most advantageous solution regarding the long term protection against radiation and the costs.

Introduction

The increasing quantities of radioactive waste resulted from the geological research and extraction of the uranium ore raises serious ecological and economical problems. The past development of the uranium extraction industry in a manner insufficiently controlled regarding the environmental problems seriously affects the ecological balance in the area of the uranium ore extraction. The radioactive waste resulted from the uranium mining industry was deposited in waste rock piles with surfaces of thousands or tens of thousands hectares. The management of these waste rock piles, mainly formed out of radioactive waste with low uranium content, is actually a serious problem regarding the contamination of the environment.

Under these circumstances, the main objective of the long term treatment of the low radioactive uranium waste rock is to eliminate the risk of contamination by storing it in secured underground locations, preferably in abandoned mine pits resulted from the exploration or exploitation of the uranium resources.

The most favorable solution for the application of this procedure is in the case of the mines still operated but scheduled for closure, where the technical situation and the layout of the pits and adits is known and the machinery to be used for the relocation of the waste is available.

Even in the situation of a non-radioactive mining waste, that does not raises the radioactive contamination risk, the relocation of the waste rock in the abandoned mining pits and adits is in most cases the only suitable solution, technically and economically, for the ecological rehabilitation of the abandoned mining areas.

The case study presented here is an example of the use of the abandoned mining pits for the disposal of the radioactive waste rock generated within the perimeter of Avram Iancu uranium mining facility, which is actually under a program of closure and ecological rehabilitation.

The solution decided after the feasibility study prepared for the Avram Iancu mining   facility, taking into consideration the complex geological and geomorphological conditions of the area was the relocation of the radioactive waste into the abandoned mining pits.

The mining facility Avram Iancu

The Avram Iancu uranium delf was developed as one of the most important production centers for uranium ore, exploited for a long period of time. The place is situated in the southern part of the Bihor mountains, in a region that is the cutwater between the hydrographic basin of Ariesul Mic and Crisul Negru rivers

The region is a high mountain area with altitudes between 720m and 1840m, where the geological structure is formed of crystalline slates belonging to the Unit of Biharia. The geological complex is formed out chlorite slates with albite porphyryblasts, quartzy-chlorite-albite slates, chlorite mica-schist, crystalline limestone and magma products metamorphosed with granodiorite intrusions.

The hydro-thermal activity led to the establishment of some economical areas in the region, some of these being based on the uranium extraction - one at the Avram Iancu mine and another one at the Baita open pit.

The uranium mine was exploited through the horizontal adits.

The economy in the region of Avram Iancu mine is based on forestry, lumber industry, farming, exploitation of polymetalic sulphides and molybdenum and tourism in the nearby areas, which generated the demand for programs of environmental protection.

The risk assessments made in the area revealed as main sources of surface and underground pollution the waste water of the mines and the waste rock piles where the low-radioactive uranium waste rock was deposited.

The production center Avram Iancu was closed due to the exhaust of the ore reserves and due to the reorganization of the mining activity at national scale.

Starting with 1952, the year when the mine was opened, important quantities of uranium waste rock with low radioactivity were generated and deposited in differ-

Case studies: active and abandoned Uranium mines

ent dump-sites, positioned on the valleys of Ariesul Mic, Crisul Negru and Dedes rivers, on terrains with slopes of more than 20^0.

All this waste rock piles must be ecologically rehabilitated in such a way that the limits of the maximum admissible concentration of the pollutants, established through the national and European legislation are not exceeded.

The characteristics of the waste rock piles

The waste resulted from the mining activity was generally disposed in waste rock piles placed nearby the mine entrances and represent the major risk regarding the quantities, the radioactivity and the radius of impact - high due to the transport agent - the water.

The waste rock piles in the area of the Avram Iancu mine have many similarities:

- they are placed in woody areas
- they are placed on terrains with inclinations of more than 20^0
- they are situated in the immediate vicinity of water courses
- they have only one level of up to 30 meters
- the slopes of the waste rock piles have inclinations between 30 and 45^0

The analysis of the radiological risk revealed areas of the waste rock piles with external gamma radiation of more than 0,3μSv/h (table 1).

The closure procedure decided for the ecological rehabilitation of the Avram Iancu mine, was the relocation of the waste rock and contaminated material in the abandoned pits.

This option was taken because it was the most advantageous for the specific conditions of the mining area Avram Iancu, easy to realize and with the lowest costs compared with other solutions.

Table 1. Characteristics of the waste rock piles.

Dump site	Contaminated area (m^2)	Volume (m^3)	Level of external radiation (μSv/h)	
			0.3-0.45	over 0.45
Gal. XIV – XVI	2000	4400	x	-
Gal. X – X bis 2	1600 / 350	3400 / 700	x	x
Gal. 1, 2, 4	80	100	x	-
Gal. XII	10	20	x	-
Gal. 6	100	75	x	-
Gal. XI vechi şi XI nou	75	100	x	-
Gal. XVI bis	2100	2000	x	-
"A", "B","C","D"	500	250	x	-

The identification and evaluation of the underground location for the relocation of the waste rock

The following aspects were examined before the relocation of the waste rock in abandoned pits was started:

- The actual state of the mining works
- The geological suitability of the relocation area
- The conformity with the requirements concerning the Environment, health and safety compliance

The actual state of the mining works

Along the conservation period, the horizontal mining works were preserved in good shape. Best conserved were those located on the transport and circulation track (adits XXIII, Noroc Bun, XVI bis and blind pit no. 2)

The blind pit no. 1 is no more operational and the connections with the mining works network were closed, so its actual state is no more known.

The ventilation stations Dibarz, gal. XVI Vest, Izvorul Bihorului and Valea Vacii-Valea Leucii are out of order; the only one remained functional being at gallery XVI bis (eastern area).

It is necessary to execute remedy works on the underground access to west and south-west areas, on the galleries XIV, XVI west, and Dibarz 902, as the access to these areas is only possible from underground, till the surface access is re-established.

The Geology and the Hydrogeology of the underground environment
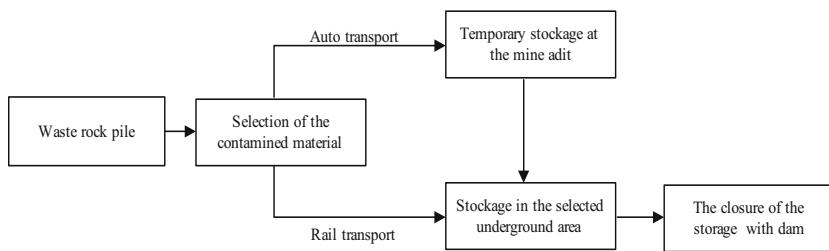
The decision to relocate the waste rock in the abandoned pits was decided after a complex geological, geochemical, geotechnical and hydrological evaluation.

From the geological point of view, there are no incompatibilities between the host rocks and the waste rock, as both are part of the same delf an equilibrium was established during the geological evolution. There are low chances of chemical interaction between the mineral components of the two systems, which can create new pollutants.

The geological environment is characterized by a natural fissuration of the rocks, but the mining activity generated supplementary breakdowns in the rock massive.

The fissuration according to the actual state of the mining works does not significantly influence the stability, as the excavations were made in hard rock that did not necessitate support of mines.

The role of the fissuration is also not important regarding the water infiltrations in underground. The hidrogeological research and the long history of the Avram

Fig. 1.   The main steps in disposal of radioactive waste from the pile to the storage places

Iancu mine demonstrated that the underground water penetrated into the mining works only when the fissures communicated through major active faults.

The relocation places were chosen out of the areas affected by fissures and active faults.

The chemical analysis of the underground waters underlines two critical aspects for establishment of the relocation places:

- the determinations for carbon bioxide indicate the absence of the aggressiveness against concrete.
- the pH between 6.2 and 7.6 show a slight acid tendency but insignificant regarding a high chemical aggressiveness.

The conclusion was that the infiltrations of water in the relocation areas will not create chemical disequilibrium that can generate supplementary pollutants.

The Environment, health and safety compliance

The relocation of the radioactive mining waste in the abandoned pits must be made in respect of the regulations concerning the protection of the environment and human health.

The radiological security norms established for the management of the radioactive waste from the mining and preparation of the uranium and thorium ore (NMR - 02/2002) explicitly recommends that the solid waste represented by mineralized rocks and waste rocks generated by the opening and operation of the mines "can be and must be used as filling material for resloping of the pits and other mining works, starting from the operational age of the mine"

The same national regulation recommends that when the solutions for the mine closures are analyzed, of a great importance is to check the possibility to use the waste rock as filling material for resloping and other mining works, situated in the deep area of the mine.

Other recommendations and regulations are given through the following documents:

- the law of the environmental protection
- the law of the waters

Case studies: active and abandoned Uranium mines

- the law of the mines
- the law concerning the safety of the nuclear activities

The planning and the execution of the mining works

The relocation of the radioactive waste rock from the surface to underground areas of the mine pits took place following a simple planning chart (Fig.1), based on the technical possibilities available at the Avram Iancu mine.

The selection of the radioactive material was made by radiological measurements on the waste rock piles and at the mine entrance.

After selection, the waste rock was transported to the underground relocation area either directly from the waste rock pile or from temporary piles containing material brought from other piles, according to the different conditions existing in the western and eastern sectors of the mine.

The load of the material and the transport to the mine adits were made with a front loader and trucks. The transport of waste rock within the mine, in the transverse galleries and the reshaping were made mechanized, where possible, and manual.

Table 2. The underground locations of repository and its characteristics.

Mine work	Level of external gamma irradiation μSv/h	Resloped length (m)	Cover thickness (m)	Distance to the gallery entrance (m)
Gal. 25.1.16	0.30-0.45	150	325 – 330	1000
Gal. 21.1.16	0.30-0.45	150	290 – 300	900
Gal. 8.1.16	0.30-0.45	50	290 – 310	840
Gal. 6.1.16	0.30-0.45	150	290 – 310	800
Gal. 4.1.16	0.30-0.45	150	240	960
Gal. Tr. 3	0.30-0.45	50	240	640
Gal. 4.a	0.30-0.45	150	240 – 260	620
Gal. 5.a	0.30-0.45	50	220	580
Gal. 4.c	0.30-0.45	150	230	460 – 560
Gal. 4.b	0.30-0.45	150	220 – 230	460 – 560
Gal. 3.1.16	0.30-0.45	150	260 – 270	540
Gal. 2.3.1.16	0.30-0.45	150	180 – 190	580
Gal. 2.1.16	0.30-0.45	50	180 – 190	580
Gal. 1.c	0.30-0.45	150	170	520 – 540
Gal. 14.1.16	>0.45	300	320 – 330	900 – 1200
Gal. 12.1.14	0.30-0.45	150	330	1060
Gal. 2.18.1.14	0.30-0.45	50	260	1100
Gal. 20.1.16	0.30-0.45	50	270 – 280	1100
Gal. 9.1.16	0.30-0.45	150	270	800
Gal. 17.1.16	0.30-0.45	150	270 – 280	1150
Gal. Dir. 1.14	0.30-0.45	150	over 100	1000

After the reshaping of the material, at the mine adits were closed with dikes. The waste rock with a gamma activity of more than 0.45 µSv/h (approximately 900 m³) was relocated in one separate gallery with supplementary security measures.

The volume of radioactive contaminated material was of approximately 3 m³/m of gallery. The relapsed length and the characteristics of storage places are presented in Table 2.

Types of disturbances and potential dangers

The evaluation of the disturbances that can appear in time must take into consideration that the relocation and the storage of the radioactive waste rock in the abandoned pits is definitive, as it is connected to the mine closure.

In the case of the Avram Iancu mine, the solution that was chosen for closure guarantees the long term safety.

The future possible potential dangers, concerning the stability and the security of the relocation areas may be considered as unforeseen events generated by the following causes:
- subsidence phenomena
- topographical modifications
- modification of the hydrogeologycal configuration
- landslides
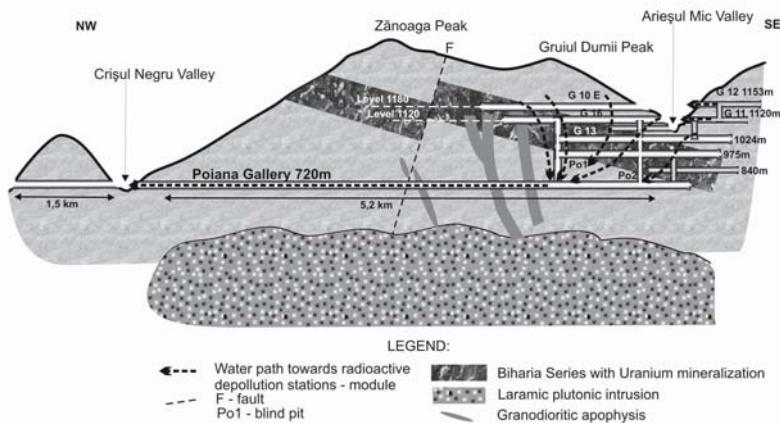
Analyzing the factors that lead the transmission of the underground fallings towards the surface, on the basis of calculations that take into consideration the physical and mechanical properties of the rocks, the thickness of the cover and the void size left after the settlement of the embankment, it resulted that only a small part of the upper part of the cover is affected. There are not expected subsidence phenomena that may lead to the creation of natural water reservoirs with infiltration potential.

On the other side, the locations selected for definitive storage of the waste rock are placed outside the area of influence of the exploited space and not in the vicinity of profound active faults.

The stability of the surface guarantees the geo-dynamical long-term external geo-dynamical equilibrium, without topographical modifications or important landslides.

From the hydrogeologycal point of view, as long as the underground fallings are not transmitted towards the surface, there are not expected any important infiltrations in the relocation areas, this way the waste rock remaining in a dry state.

The risk of environment contamination with radionuclides is minimum, except the waters infiltration due to the   unexpected events. In this case the danger is eliminated by free flowing of the waters up to the radioactive depollution stations – module following the route of mining works (Fig. 2)

Case studies: active and abandoned Uranium mines

Fig. 2.   Schematic cross – section of Avram Iancu uranium mine.

Conclusions

The paper presented here is an example of using the underground excavated space for disposal of the radioactive mining waste resulted from uranium ore exploitation in the case of a mine which is under a program of closure. The preservation of horizontal mining works in a good shape and the favourable geologycal – mining conditions, were the reason that decided upon the procedure of contaminated material relocation in the abandoned pits.

The deep disposal of the radioactive mining waste, the stability of the covering rocks and the favorable hydrogeologycal conditions guarantee the long term safety in respect of the regulations concerning the protection of environment and human health.

This option is the most advantageous for the specific conditions of the mining area Avram Iancu, easy to realize and with the lowest costs compared with other solutions, because a lot of activities are included in the mine closure programme.

References

Popescu M,Georgescu D. (1998) Comparative studies regarding the impact on environmental factors of uranium minim activity in some areas from Romania; International Symposium on Environmetal, Swempankara, may 1998

Stefan O.(1998) International experience in use of underground space. Scientific Bulletin of Baia Mare University

Changes in discharged water quality from abandoned uranium mines near Kalna

Zoran Nikić[1], Jovan Kovačević[2], Branislav Radošević[3]

[1]Forestry Faculty University of Belgrade, 11030 Belgrade, Kneza Višeslava1, Serbia and Montenegro, e-mail: znikic@yubc.net
[2]''Geoinstitut'', 11000 Belgrade, Rovinjska 12, Serbia and Montenegro
[3]''Advanced Systems'', 11000 Belgrade, Vojislava Ilića 12, Serbia and Montenegro

Abstract. Various genetic types of uranium minerals (infiltrated, hydrothermal, etc.) have been found in the region of Stara Planina. Uranium minerals in granitic rocks that build up the area of Kalna in central Stara Planina are selected for their importance and the degree of exploration. The analyzed levels of the natural radioactive and trace elements in water and fluvial deposits from a general area of the closed mines are presented in this paper. Relatively wide ranges of the obtained uranium concentrations in ground and surface waters are explained in this work by the presence of various geochemical barriers and by the variations in the quantity and velocity of ground water flow over the year.

Introduction

This paper is concerned with the area of abandoned mines at Kalna on Stara Planina, which was explored, where uranium ore was extracted and where water and soil are radioactive. The concentration levels of the natural radioactive uranium, radium and radon elements were measured in water bodies, fluvial deposits, humus, and spoils of the old mines. Our purpose in writing this contribution is to present the state of the natural radioactivity in the abandoned mines, where nuclear mineral ore was extracted, and in the surrounding area that could be contaminated from mine workings. The research data are used to indicate the water and soil contamination in the given area.
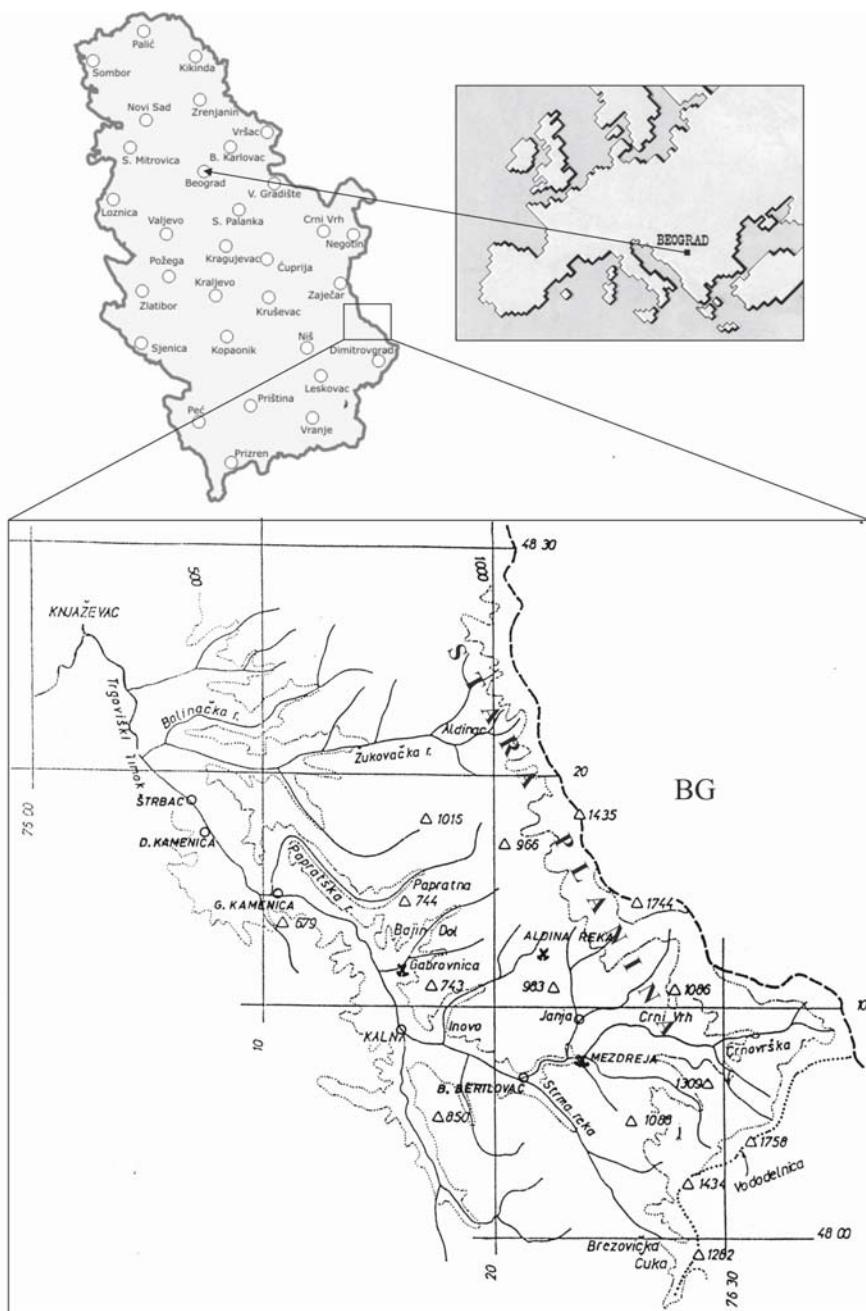
Fig. 1.   Geographical location of Stara Planina and the exploration area.

Case studies: active and abandoned Uranium mines

Geological prospecting and exploration in the area of the old uranium mines at Kalna on Stara Planina were carried out from 1992 to 1998. The methods used in the exploration were radiometry, geochemical, hydrogeochemical, and laboratory analyses.

The geological exploration for nuclear mineral (uranium) ores near Kalna was started in 1949 when the mineral was found at Mezdreja, Gabrovnica, Srneći Do and Aldina Reka. Mine workings and ore extraction began in 1960 and discontinued in 1966. A separation plant was erected at Mezdreja. Field exploration for uranium at Kalna was discontinued in 1998. Since then, only the collected information and records have been studied.

The exploration area

The mountain of Stara Planina, situated in the extreme SE of Serbia, its ridge bounding on Bulgaria, covers a surface area of about 1100 km^2 and altitudes from 400 m to 2169 m. The Trgoviški Timok and Visočica and their many tributaries drain the mountain. Major towns in the region are Zaječar in the north, Knjaževac in the central area, and Pirot in SE, all connected by asphalted roads. There are small mountain villages that can be reached by narrow dirt roads. After the mines were closed, local population live and work on the land.

The Kalna mines are centrally situated on Stara Planina. The Trgoviški Timok and its tributaries drain the area.
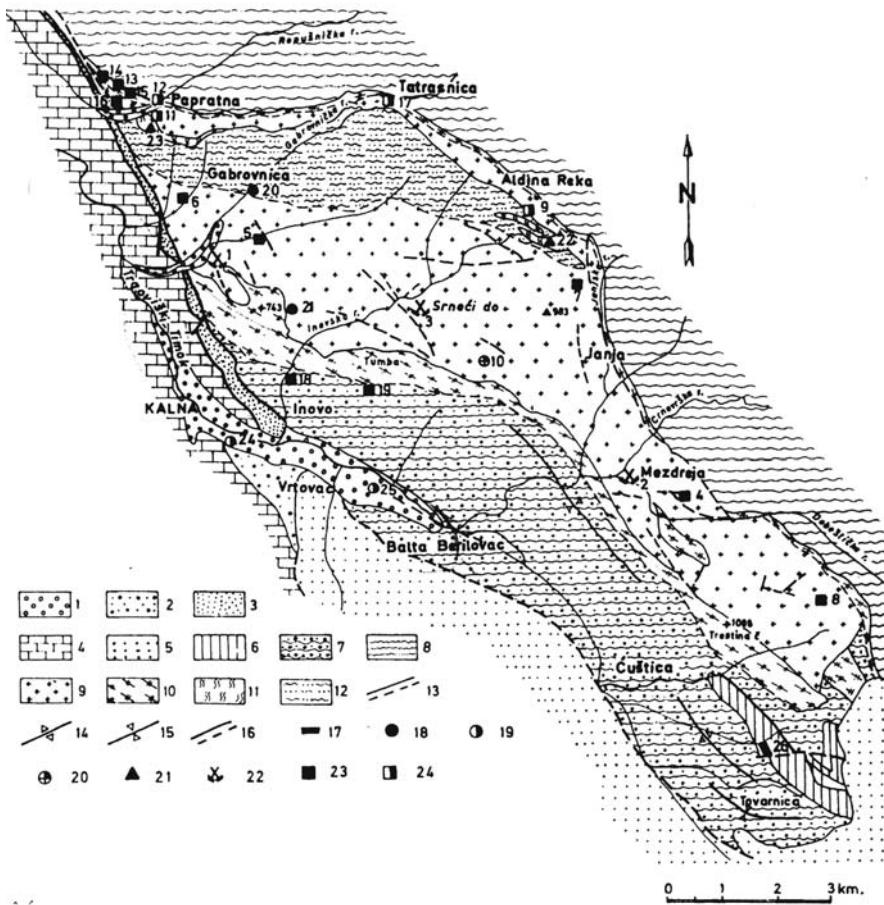
Geology and metallogeny of Kalna area

The area is made up of varied lithological complexes that differ in age, origin, mineral and petrographic compositions (Fig.2). The oldest rocks are amphibolite, gneiss and greenstone of Riphean/Cambrian age (diabase phyllite formation). During the Ordovician, these rocks were intruded by basic (gabbroid) and acidic (granitic) magmatic rocks, and during the Silurian and Devonian molasse and other sediments were deposited. Carboniferous lake sediments and volcanogenic-sedimentary products deposited later. The Mesozoic is represented by sandstone, marlstone and limestone, and the Quaternary by alluvial deposits of the Trgoviški Timok in a maximum thickness of 30 m and width about 1 km (Kovačević and Gertik 1995).
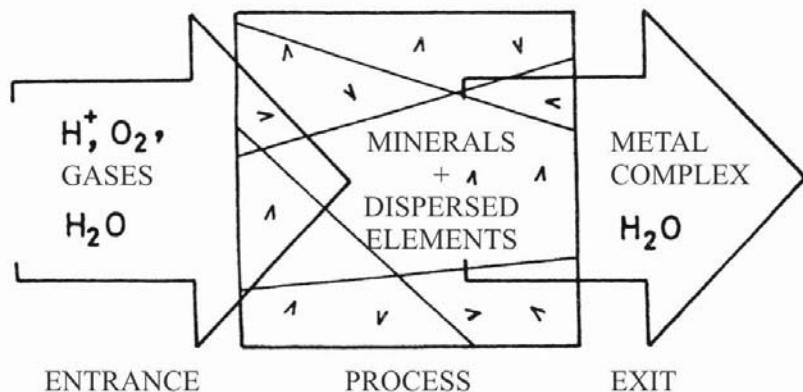
Stara Planina is characterized by a complex tectonic pattern of many regional and local fault zones. Major uranium ore occurrences and deposits are spatially associated with the granite massif of Janja, or the ore field of the same name on the western slopes of central Stara Planina. High-temperature uranium-thorium minerals and hydrothermal vein/lens uranium minerals are located in Kalna ore field. The high-temperature uranium-thorium minerals at Aldina Reka are associated with the products of serpentinite granitization in zones either in the serpentinite it-

self or at its contact with granite. The hydrothermal vein/lens deposits and occurrences of uranium ore (Mezdreja, Gabrovnica and Srneći Do) are associated with repeatedly activated fault zones. Minerals occur in lenticular ore bodies that build columns and complex ore veins. These are minor deposits of the estimated reserve of a few hundred tons U_3O_8 (Gertik et al. 1990).

The Gabrovnica deposit in Janja granite is an example how abundant uranium accumulations are formed by its redistribution and deposition in clayey and friable

Fig. 2.   Geological map of Kalna region. 1. Alluvium; 2. Sand and clay (Pl); 3. Miocene deposits; 4. Cretaceous deposits; 5. Permian deposits; 6. Carboniferous volcanogenic-sedimentary rocks; 7. Metasediment of the Inovo Series; 8. Crni Vrh Formation rocks; 9. Granitic rock; 10. Gabbroid rocks; 11. Serpentinized peridotite; 12. Gneiss; 13. Boundary; 14. Anticline axis; 15. Syncline axis; 16. Fault; 17. Black coal occurrence; 18. Au (primary) occurrence; 19. Au (alluvial) occurrence; 20. Cu and Mo occurrence; 21. Cr occurrence; 22. Uranium deposit; 23. Uranium occurrence; 24. Uranium and thorium occurrence.

Case studies: active and abandoned Uranium mines

Fig. 3.   Mineralized fluid formational proces.

surficial rocks of the fault zone. This process has evolved from the formation of faults to the present day (Fig.3).

One of the principal factors of uranium mobilization from granite rocks is the supply of mildly acidic aqueous solutions that altered and leached the rocks. The solutions were also oxidizing, because they contained oxygen that intensified U^{+4} oxidation and the formation of uranium ions that built complexes mainly of $Ca_2(UO_2(CO_3/_2(N_2O)$ type and a smaller amount of $Ca(UO_2(SO_4)_2(H_2O)$. These complexes are relatively easily transported by solutions (Romberger 1984). The highly migratory uranium also indicates its relatively slow deposition. For the uranium deposition in the given instance, the minerals of clays, iron oxides and organic matter in rivers are important (Gržetić and Jelenković 1995).

Generally, the mean uranium content in granites of Janja is about 6 ppm, locally up to 20 ppm, whereas the mean proportion of dissolved uranium in the granites is 3.82 ppm.

Research results

Comprehensive explorations and annual observation of uranium and characteristic elements in the area of the abandoned uranium mines of Mezdreja and Gabrovnica were carried out from 1992 to 1998 (Kovačević 1997). The collected data are given in Tales 1,2,3. Radiometric analysis of the samples from spoil dumps is not presented in this paper. The analytical results are given only for subsurface and surface waters and fluvial deposits of the Trgoviški Timok.

Table 1 shows chemical analysis of water from Mezdreja and Gabrovnica mines. The table above shows increased uranium, strontium and iron in mine water. The relatively wide ranges of some contained elements can be explained by the sampling indifferent seasons, thereby different ground water flow rates through fractures in the ore bodies and adjacent rocks (Nikić et al. 2002).

Table 1. Ranges of measured elements in pit water of Mezdreja and Gabrovnica mines.

Location	Range of measured quantities							
	U (µg/l)	Ra (Bq/l)	Fe (mg/l)	Sr (mg/l)	Pb (mg/l)	Mineral. (mg/l)	pH	Ep (µS/cm)
Mezdraja	93,8-420	0,07-0,32	0,37-1,08	4,40-12,38	0,005-0,01	470-860	7,4-7,5	460-580
Gabrovnica	27,2-50,0	1,50-4,42	0,13-0,56	0,48-0,48	0,01-0,02	622-720	6,8-6,9	380-570

Table 2. Ranges of measured elements in well water of Balta Berilovac, Vrtovac, Inovo, Gornja Kamenica, Donja Kamenica, Štrbac, Baranica villages.

Location	Range of measured quantities						
	U (mg/l)	Sr (mg/l)	Cu (mg/l)	Ra (Bq/l)	Mineral. (mg/l)	pH	Ep (µS/cm)
Balta Berilovac	0,005-0,009	0,01-0,06	0,01-0,03	0,05-0,07	750-920	7,3-7,4	660-680
Vrtovci	0,001-0,002	0,01-0,03	0,01-0,02	0,09-0,20	790-938	7,0-7,1	700-740
Inovo	0,002-0,008	0,01-0,02	0,01-0,02	0,05-0,06	485-560	7,4-7,7	460-510
Gornja Kamenica	0,001-0,002	0,09-0,15	0,01-0,02	0,20-0,60	828-1020	7,3-7,5	695-870
Donja Kamenica	0,001-0,003	0,11-0,20	0,01-0,03	0,10-0,19	395-570	7,5-7,8	420-495
Štrbac	0,001-0,003	0,01-0,03	0,01-0,03	0,05-0,07	687-900	7,1-7,3	605-680
Baranica	0,001-0,003	0,01-0,02	0,01-0,02	0,11-0,20	272-360	7,4-7,6	440-460

Table 3. Radiometric data of the Trgoviški Timok alluvial deposit.

Semple	Kind of analysis: from to			
	U (ppm)	Th (ppm)	K (%)	Th/U
Fluvial deposit	1,3778-4,32672	3,38058-13,3282	0,68497-2,11951	1,63218-4,46154

Case studies: active and abandoned Uranium mines

Table 2 gives chemical composition of water from dug wells used for local water supply. The well water contains relatively low uranium, but increased iron. The wells are dug in the Trgoviški Timok alluvium, which is in direct hydraulic communication with the river. The alluvium consists of several alternating layers of gravel, sand and clay. Clay minerals and the organic material contained in them rapidly precipitate uranium in the marginal part of the alluvial plain. This is probably the reason for the relatively low uranium concentration in well water (Protić 1994). The sampled village wells are located in the middle of the Trgoviški Timok broad alluvial plain.

Table 3 gives radiometric data for the Trgoviški Timok alluvial deposit downstream of the mines, sampled (16 samples) at every 1000 m over a length of 16 km. The geomorphologic and hydrogeological characters of the area control the gravity flow of both surface and subsurface waters to the Trgoviški Timok. These waters carry dissolved uranium and its products to chemical barriers (clay minerals, organic material, etc.) where it is deposited. In view of the geological relationships and the hydrogeological conditions in the drainage area and the contained uranium minerals, the concentrations of radioactive elements in river deposits are not much anomalous.

Conclusion

The natural radioactive elements (uranium, thorium, radium, radon) concentration levels were measured in samples of pit water, well water and fluvial deposits. All the obtained data for the area of the old uranium mines at Kalna (Stara Planina) lead to the following conclusions. The primary source of uranium in the area is the much-fragmented granitic rocks. Fault zones are the environments of uranium deposition. Systems of fractures in granitic rocks are the flow paths of ground water that carries out uranium from the pre-formed ore bodies and the adjacent rocks. As a result, uranium and trace elements are increased in pit water. Geochemical barriers of clays and organic materials (alluvium) and the greater amounts and faster filtration of ground water control the dissolution of uranium and trace elements in ground water downstream of the mines.

References

Gertik S, Ilić B, Kovačević J (1990) Uranium Minerals of Eastern Serbia. 12th Geological Congress of Yugoslavia, Ohrid, Vol.III: 589-598

Gržetić J, Jelenković R (1995) Natural Radioactive Elements, Geological Origin, Forms of Occurrence and Migration-Ionizing Radiation from Nature. Institute "Vinča", Belgrade: 3-39

Kovačević J, Gertik S, (1995) Uranium Minerals of the Poreč-Stara Planina Metallogenic Zone. "Geoinstitut", Belgrade: 83-96

Kovačević J, (1997) Geological Exploration of the Natural Radioactive Element Concentration Levels in the Area of the Old Uranium Mines near Kalna. Fondovska dokumentacija "Geoinstituta", Belgrade: 5-21

Nikić Z, Kovačević J, Radošević B, (2002) Uranium Content in Ground Water in Stara Planina Triassic Sediments. Proceedings of the International Conference on Uranium Mining and Hydrogeology III and the International Mine Water Association Symposium, Freiberg: 99-106

Protić D, (1994) Indicative Hydrochemical Radioactivity Anomalies in Search of Uranium Ore Deposits. "Geoinstitut", Vol. 30, Belgrade: 287-298

Romberger S, (1984) Transport and Deposition of Uranium in Hydrothermal Systems at Temperatures up to 300ºC: Geological Implications. Institution of Mining and Metallurgy, London: 12-17

Environmental impact evaluation of a pilot installation for „in situ" processing for uranium ore

Stefan Petrescu, Dan Georgescu, Simona Ciuciu, Dragos Curelea

Research and Development National Institute for Metals and Radioactive Resources, 70, Bd. Carol I, Sector 2, 020917 Bucharest, Romania,
E-mail: icpmrr@icpmrr.ro

Abstract. As a result of the Gamma Geological Research during the 1955-1956 period in the south-west of Romania, there were identified some radioactive anomalies organized in 16 areas. These are placed near Danube River and some of its confluent rivers (Streneac, Ilişova). The exploitation of the Ilisova Uranium Ore started in 1962 and it was partially suspended in 1972. The exploration and exploitation activities restarted in 1976. In the same time it was also started the pilot project consisting in the acid leaching "in situ" of the Uranium Ore extracted from the Ilişova Mines. After 1990 the activity was stopped and all activity abandoned. In 2002, the closing and rehabilitation procedures of the perimeter affected by the exploitation and exploration of the Uranium Ore was started, especially because this perimeter is in the National Park "Portile de Fier" land.

Introduction

The Ilisova Uranium exploitation is located in south-west of Romania, in Banat region at about 50 m from Danube River, on the left side.

The pilot plant for "in situ" leaching of Uranium ore is located inside of Ilisova Exploitation at about 100 meters from G3, G6 and G7 Galleries (Fig. 1).

In order to identify pollution sources that generates by means of their radio elements content and also by different ways, additional effective doses to critical groups, it was need to perform the following investigations:

- Field measurement of gamma rate dose in matrix
- Rock sampling and analyses for U, Ra, Cu, Pb, Zn, Ni, Co.
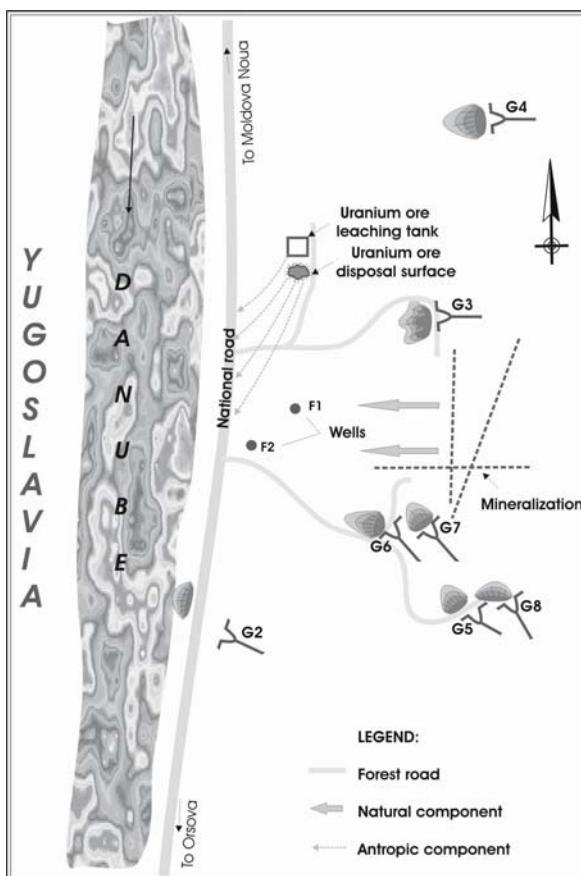
- Water sampling
- Determination of Radon level
- Preservation of water, soil, sediments and vegetation samples from area around the pilot

Pilot plant for in situ leaching of U ore

In the region of DN 57, at +83 m altitude, a pilot plant for U leaching was built.

This plant consists in an ore deposit having a 6200 sqm surface, a concrete tank for leaching, having a 1000 sqm surface and an U recovery module formed by two columns having 6x3 meters each.

After 1990 year the pilot was set out of order after the suspension of the activities, without developing any closing or ecology project of the area.

Fig. 1.   Ilisova exploitation.

Case studies: active and abandoned Uranium mines
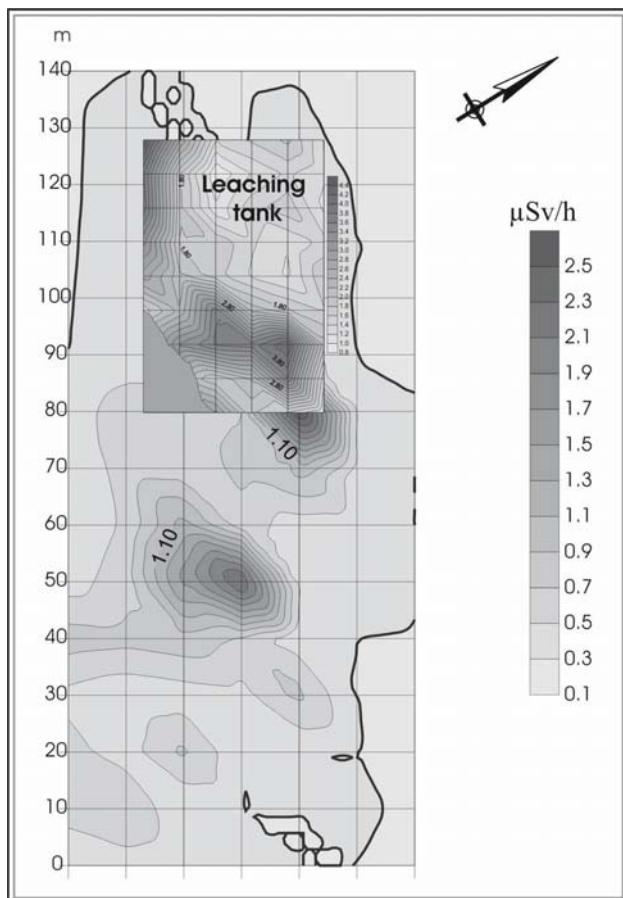
In the concrete tank remained small amounts of materials, in the preserved samples finding the contents: U = 100 ppm, Ra = 2 Bq/g, As = 100 ppm, Cu = 55 ppm, Pb = 60 ppm, Mo = 325 ppm, V = 17 ppm, Ni = 25 ppm, Zn = 36 ppm.

By proceeding measurements in a 5/5 meters matrix in order to determine gamma rate dose on entire tank surface, levels between 0.8 μSv/h – 4.4μSv/h were found.

Close to concrete tank exists a storage surface for U ore used in experiment here, measurements for gamma rate dose performed in a 10/10 meters matrix and about 4.800 sqm surface revealed maximal levels of 2.5μSv/h (Fig.2).

In the preserved samples from this area were found the following maximal element contents: U = 351 ppm; Ra = 2.8 Bq/g; As = 370 ppm; Cu = 310 ppm; Pb = 242 ppm ; Mo = 10 ppm; V = 17 ppm; Ni = 120 ppm; Ag = 250 ppm; Zn = 120 ppm.

Fig. 2.   Gamma debit dose distribution in ore leaching tank and around.

Case studies: active and abandoned Uranium mines

About 80% from surface of ex- ore deposit is now naturally vegetative covered and integrated in the natural landscape of the area. Rn^{222} content inside the concrete tank is 350 Bq/ m^3 on the ex- deposit surface, Rn^{222} content being130 Bq/m^3. Two wells, F1 and F2 are located close to ex- ore deposit and from this water samples were preserved. The levels for radioactive elements were slowly higher than background level: in F1

 U = 0.036 mg/ l; in F2, U= 0.09mg/l and Ra = 0.11 Bq/ l.

Higher U levels, mainly in F2 could have the following explanation: groundwater washes the upper size of some uphill mineralization or it is contaminated by waste-waters which run off from leaching tank and from ex- deposit surface (Fig.1).

The annual effective dose evaluation

A main objective regarding radioprotection in exploration and exploitation of nuclear raw materials is to assess the supplemental permissible doses due to internal and external irradiation that could accidentally or permanently exist.

The International and also Romanian Legal Standards (August 2000) provide for each individual person supplemental effective dose by 1 mSv/ year. This level involves all different ways resulting sources from industrial activity in area that person lives.

This supplemental dose (E_{Supl}) by 1 mSv/year overlay background supplemental effective dose ($E_{T\ back}$). Thus, the local effective dose (E_T)   is a sum of those two:

$E_T = E_{supl} + E_{T\ back}$

So,

$E_{Supl} = E_T - E_{T\ back}$

where: E_T- totally effective dose in presence of background;

E_{Tback}- background effective dose;

E_{Supl} – supplemental effective dose caused by all sources from area;

The annual effective dose (E_T), named also effective dose equivalent (EDE) is:

$E_{T =} E_\gamma + E_i^c + E_i^a + E_{hi} + E_{hRn}$, where

E_γ = external effective dose;

$E_i^c + E_i^a$ = ingestion effective dose;

$E_{hi} + E_{hRn}$ = inhalation effective dose;

$E_{T\ supl} =$ $E_T - E_{T\ back}$

where:

$E_{T\ back}$ = local background dose;

Case studies: active and abandoned Uranium mines

Supplemental effective dose estimation for a person who lives nearby Ilisova exploitation (ex-ore deposit surface and G6 gallery)

Supplemental effective dose estimation will be performed for all the exposure path ways: aquatic way (ingestion), by air (inhalation), ground way (gamma irradiation).

Dose estimation due to ingestion for one person (aquatic way)

We assumed that person uses mine water from G6 gallery and from F2 well, this water having the following contents: U = 0.028 mg/ l, Ra = 0.006 Bq/l for mine water and U= 0.090 mg/l, Ra = 0, 11 Bq/l for F2 water.

   In this case supplemental effective dose received by a person is:
   $E_{i\,sup}{}^{a}$ = 0.207 mSv/year

Effective dose estimation due to external irradiation

The highest levels of gamma debit dose were registered on ex- ore deposit surface and inside of leaching tank. It was found a value of 4.4 µSv/year of gamma debit dose which comply with a U content by 419 ppm and Ra content by 10 Bq/g. We assumed that person stays in the area five months, 6 hours/day each (900 hours). There were taken into account only five months, because the nearby houses are not permanent, being used only in summer season.

   Thus, annual effective dose due to gamma irradiation is $E_{\gamma T}$= 4.7 mSv/year, $E_{\gamma back}$ being 0.981 mSv/ year. The resulting supplemental effective dose is $E_{\gamma supl}$ =4.7 – 0.981 = 3.710 mSv/year.

Dose estimation due to Radon inhalation and to short lifetime radionuclide

Based on very high Radon content at the gallery entrance, G6 (17.300 Bq/m^3) and on 5 months interval of 6 hours/day each (900 hours), the effective dose will be:
   $E_{hRn\,1}$ = 39.236 mSv.

At this value is added the time spent by person in normal condition (6100 hours).
   $E_{hRn\,2}$ = 0.384 mSv for Rn^{222}= 25 Bq/m^3.

Note: Gallery entrance G6 is extremely close to a house, at about 30 meters.
   Thus, the annual effective dose due to inhalation is $E_{hRn\,T}$ = 39,62 mSv/year.
   Taking into account the background Rn content $E_{hRn\,back}$ = 0.441mSv/year , the resulting supplemental effective dose will be $E_{hRn\,back}$ = 39.179 mSv/year.

Evaluation of dose due to inhalation of dust containing long time radionuclides

In order to evaluate this dose the following preliminary data were using:

- Stationary time 900 hours
- dust content in atmosphere = 0.0001 g/m^3
- U content = 0.035%
- Ra content = 2.8Bq/g
- U activity level in aerial dust = 0.00087 Bq/m^3
- Ra activity level in the aerial dust = 0.00028Bq/m^3.

$E_{hi\,sup}$ = 0.025mSv/year
The supplemental effective dose is the sum of the entire doses:
$E_{T\,sup} = E_{i\,sup}{}^a + E_{\gamma\,sup} + E_{hRn\,sup} + E_{hi\,sup}$
$E_{T\,sup}$ = 43.130 mSv/year.

The most influence in supplemental effective dose is given by Radon content from gallery entrance G6. Although conditions and data from this scenario are almost impossible to accomplish, over 43 mS/year level represents a very high risk for people around the area.

Conclusions

As a result of pilot plant for "in situ" U leaching processing, about 7000 sqm surface was contaminated and a part of ground water of the ex-ore deposit also. At present the highest risk for population is concrete tank, which still contains amounts of ore and the ex- ore deposit surface that could be any time used for a picnic by the tourists came to visit the"Portile de Fier" National Park.

References

M. Popescu, Risk assessment of population from critical groups by evaluation of supplementary doses resulting after Ilisova mine closing project

PHARE PROJECT PH 4.02.1994 "Guidelines on how to measure Radioactivity and its Dispersion at Uranium Milling and Mining sites"

IAEA – International Basic Safety Standards for Protection against ionizing Radiation and for Safety of Radiation Sources, Vienna, 1996

Low no. 111/1996 (modified in 1998) regarding safety development of nuclear activities Basic Standards of Radiation Safety. The Official Monitor No. 404 bis, August 29, 2000

D. Georgescu, M. Popescu, F. Aurelian, Camelia Popescu (2001) "Analyses of the population risks belonging to an uranium mine by the pathways determination of the radionuclides and supplemental effective doses estimation" IRPA Regional Congress on Radiation Protection in Central Europe. Radiation Protection and Health. Croatia Dubrovnik, may 20 – 25,

D. Georgescu, M. Popescu, (2000)"Environmental Impact Evaluation and contamination effects to uranium mining and exploitation areas", NUC Info 2000, 5 – 8 sept., Baita, Bihor.

Concept of a Surface Water Monitoring at the Former Uranium Mining Site Schlema-Alberoda

Petra Schneider[1], Ralf Löser[1], Jürgen Meyer[2], Elke Kreyßig[2], Andrea Schramm[2]

[1]C&E Consulting und Engineering Chemnitz, Jagdschänkenstr. 52, D-09117 Chemnitz, Germany, E-mail: p.schneider@cue-chemnitz.de
[2]WISMUT GmbH Chemnitz, Jagdschänkenstr. 29, D-09117 Chemnitz, Germany

Abstract. After the remediation works at the Schlema-Alberoda Mining Site the existing water monitoring has to be modified. The monitoring has to focus on the main contaminated streams. The separation of contaminated and not contaminated streams an their distribution in surface respectively underground portions allows the determination of the real transported load of radioactive and toxic compounds. The principle of load determination is the more suitable concept in the assessment of discharges like in industry and waste water treatment (EU) .

Introduction

The Schlema-Alberoda Mine in Saxony, East Germany, was closed in 1990 due to the end of uranium production in the former GDR (Meyer et al 1998). As a result of the exploitation of the mine about 40 dumps were left in the Schlema-Alberoda area. After the remediation works at Mining Site in the last decade the existing water monitoring has to be modified. Due to the geochemical situation of the explorated deposit the main contaminants are uranium and arsenic. The current water monitoring is characterised by sampling points in surface water, groundwater and flooding water serving during the remediation as:

- surface water: observation of the quantity and quality mainly at the drainage systems of the dumps and the rivers nearby
- ground water: oberservation of the ground water quantity and quality in the weathered rock zone underlaying the dumps and the unweathered rock zone of the former uranium deposit
- flooding water: observation of the water level, water quality and temperature in the flooded Schlema-Alberoda Mine and oberservation of the quantity and composition of the sludge in the water treatment plant.

Due to the end of the flooding of the mine and the remediation works of the dumps (covering with mineral soil and recultivation by planting) there will be three types of water in future:

- Mine water of the shafts reaching the surface. This type is treated.
- Seapage water of the dumps. This type is partly collected in drainage systems. The other part is reaching the bottom of the dumps and flowing into the unweathered rock zone causing regional diffuse contaminant transport into the nearby rivers.
- Surface water, which will not be influenced by contaminants, because the path is interrupted (water, which flow on top of the mineral soil cover of the dumps and are collected in surface water drainage systems).

Considering the contaminant transport only mine and dump water (flooding and seapage water) will be of relevance for the subsequent monitoring in future.

Site Characterisation
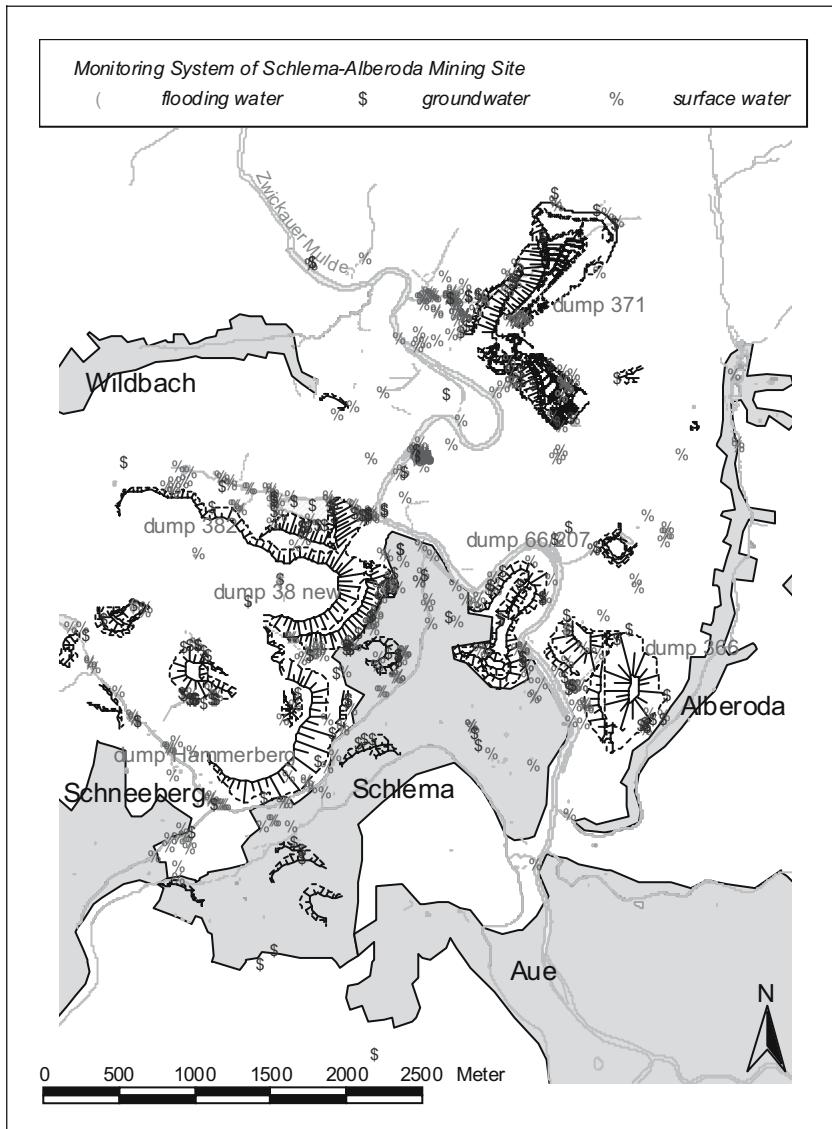
Hydro(geo)logical Setting and Contaminant Transport

The Schlema-Alberoda area is characterised by paleozoic micas and phyllites, which were formed during the variscic orogenesis. The rock is fractured and clayey weathered from the surface into a depth of 2 to 30 m. The shaft 371 reaches down to about 1800 m. In the end of 2004 about 94 % of Schlema-Alberoda Mine were flooded. The dumps containing the mining waste are situated around the shafts in the Schlema-Alberoda area. Upstream and downstream of the dumps monitoring points (wells and surface water sampling points) were installed. These monitoring points describe the water flowing in the dumps, the rock aquifer and the weathering zone of the phyllites. Based on the measured data the contaminant impact on ground and surface water can is monitored.

The dumps are partly situated in former river valleys. The regional drainage river system is the Zwickauer Mulde. In most parts of the dumps, an impermeable basement is missing. Percolating dump water can directly enter the phyllite. Referring to pumping tests, the mean hydraulic conductivities of the underlaying unweathered rock zone range from 10^{-7} to 10^{-8} m/s, with elevated values of 10^{-5} m/s in tectonic structures. The weathered loamy zone has a permeability of $10^{-7}…10^{-6}$ m/s. The dump material reaches an average permeability between $10^{-4}…10^{-3}$ m/s. The phyllite can be described as fracture aquifer. Recharge takes place throughout the study area by infiltration of precipitation and vertical leakage. An artesic ground water table has formed in the loamy weathering zone, locally. So the hydrogeological setting of the area is characterised by absence of a regional natural groundwater body. Due to this situation there is no regular use of natural groundwater in the Schlema-Alberoda area.

Overview on the Current Monitoring

Fig. 1 shows the hydrological setting including monitoring points at the former Uranium Mining Site Schlema-Alberoda.


Fig. 1.   Hydrological setting including monitoring points at the former Uranium Mining Site Schlema-Alberoda.

Case studies: active and abandoned Uranium mines

Relevant Streams and Contaminant Transport

Fig. 2 shows the mine flooding scheme of the Schlema-Alberoda site. This water is influenced by mining components, uranium and arsenic mainly. The flooding water is not causing an environmental impact because it is treated.

After covering and the development of various plants on the surface of the dumps the main path of contaminated water is the interflow in the underground.
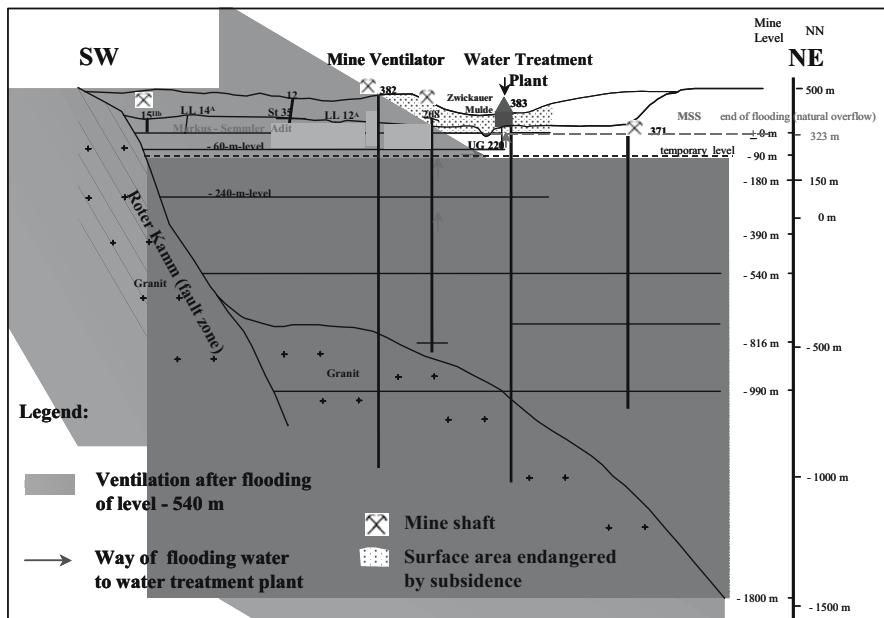
Proportion of Mining and Dump Water

Considering the actual water management in the Schlema-Alberoda area the proportion of mining and dump water can be described as follows:

- treated flooding water of the Schlema-Alberoda Mine:
- surface water mixed with seepage water of dump 371:
- drainage water of Borbach Valley:
- drainage water of dump 366:
- mining water of flooded historical mining of the Schneeberg Mine:

The proportion of these streams is determined by uranium and arsenic loads.

There has to be considered, that the flooding water of the bordering historical mining site Schneeberg (explored in the Middle Ages), has an own hydraulic transfer off the mine (defined level), which is not in the responsibility of Wismut GmbH. As the measured water volumes show the main water amount is caused by


Fig. 2.   Mine flooding scheme of the Schlema-Alberoda site.

Case studies: active and abandoned Uranium mines
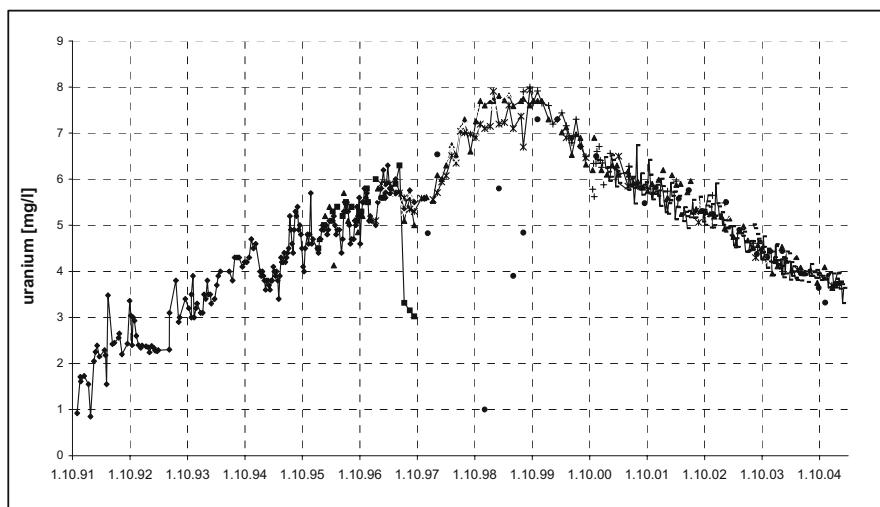
the flooding water. So the amount of controlled water is much higher than the amount of diffuse migrating water. It is expected, that this situation will last in future, because the cavities in the geological underground force the regional groundwater recharge. Since the start of the water treatment in the end of 1999 the loads of substances are decreasing. On basis of experiences of former mine floodings it is expected that the contaminant transport will reach background values after decades, naturally.

Prognosis of the Water Quality

The prognosis of the water quality of flooding and dump water was prepared by geochemical modeling on the base of the measured monitoring data. The concentrations of uranium and arsenic in the flooding water have decreased since august 2000 (see Figs. 3 and 4).

A halving of the concentrations took place since start of the flooding. It was calculated that the water treatment will last up to 25 years. The contaminant transport of the dumps has decreased in correlation to the covering of the dumps. After interruption of the water path way the concentrations of uranium and arsenic have reduced down to 4,3 mgU/l and 230 µgAs/l (see figure 5). These loads are calculated for the water, which is drained off the dump 366 (largest dump in remediation).

**Fig. 3.**   Development of the uranium concentrations in the flooding water of Schlema-Alberoda-Mine.

Case studies: active and abandoned Uranium mines

Consequences for the Subsequent Monitoring

Assessment of Contamination
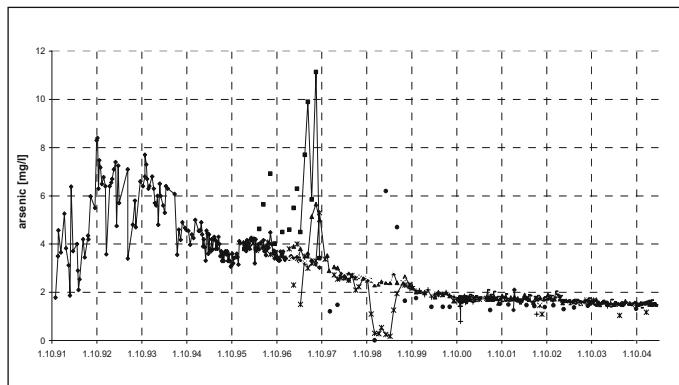
The results of the current monitoring show, that emissions of the mining site cause impacts on the Zwickauer Mulde, primary. The emission of contaminants is focused on selected streams and cause metal and arsenic loads leaving the catchment. These loads are decreasing due to remediation works.

Main task of the subsequent monitoring will be an adjustment to the main load streams of contaminants. The separation of contaminated and not contaminated streams and their distribution in surface respectively underground portions allows the determination of the real transported load of radioactive and toxic compounds. The structure of the subsequent monitoring depends also on the catchment characteristics, the mean residence time of ground and surface waters and the chemical changes in the waters during passage of the catchment. Assessing these concentrations one has to consider the elevated natural background in the Ore Mountains (Neitzel et al. 2002).
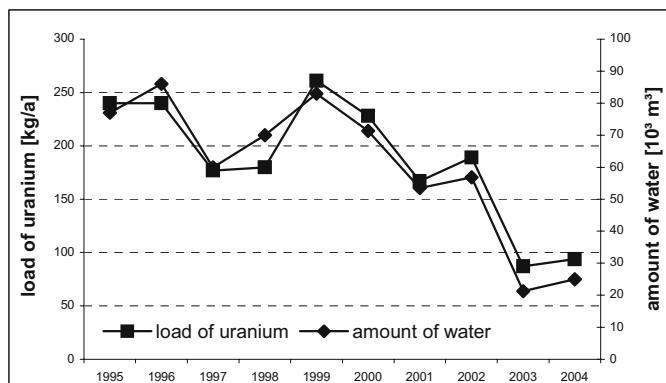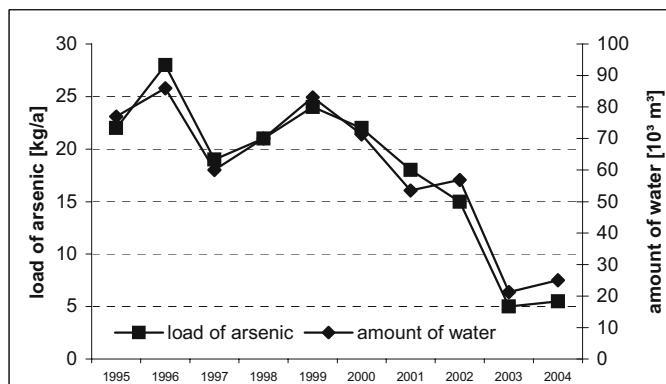
Relevance of the EC Water Framework Directive

The remediated areas will be administrated by the freestate Saxony in future. So the subsequent water monitoring has to consider the demands of the EC Water Framework Directive (Schneider et al. 2003). Of special meaning is the objective of attaining, or maintaining the good status in the European water bodies. A subsequence monitoring has to focus on these tasks. The resulting demand for the subsequent monitoring is to control the emission trends considering the dominating load streams. That means in case of the Schlema-Alberoda site the monitoring of uranium and arsenic in the dump interflow.

In consideration of the EC Water Framework Directive the main aims are the improvement of the surface water quality of the Zwickauer Mulde and the protection of the ground water under notice of the natural background.

Fig. 4.   Development of the arsenic concentrations in the flooding water of Schlema-Alberoda-Mine.


Fig. 5.   Decrease of the contaminant transport of the dump 366.

Case studies: active and abandoned Uranium mines

Critical Levels and Critical Loads Concept

The current monitoring (especially in case of emission control) is mainly focused on the assessment of critical levels (concentrations), also in case of small emission streams. This view is one-sided, because it doesn't consider the often observed trend of decreasing loads of radioactive and toxical compounds by simultaneously increasing or stagnant concentrations due to remediation work (for instance covering of dumps). This effects will be strengthened after the end of remediation. The load determination is the basic concept for an objective assessment in the EU (see IPPC) in industry and waste water treatment. This procedure is continued in the European Water Framework Directive by the demand of management plans for water bodies. In case of the critical loads concept (e.g. Juggings et al 1995) the critical load of a compound will be focused on sensitive aquatic biota. In the EU the discharging industries and waste water treatment plants are registered in the European Pollutant Emission Register EPER register currently. So the emissions in a water body can be assessed as sum of all emitters in the catchment. That means a splitting of the contribution of the emissions due to the portion of the total emission. In practice that means, that a emitter based stream flow analysis is needed.

Conclusions

In future a subsequent monitoring at the Schlema-Alberoda Mining Site has to be modified into a reduced long term monitoring. On this way the subsequent monitoring has to adjust to the known main stream flows and the mainly transported loads of radioactive and toxic compounds. For future decisions in connection with remediation strategies a discussion to the loads concept (instead of levels/concentrations) especially with the public authority is inevitable.

References

EUROPEAN COMMUTNITY (2000): Richtlinie 2000/60/EG des Europäischen Parlaments und des Rates vom 23.10.2000 zur Schaffung eines Ordnungsrahmens für Maßnahmen der Gemeinschaft im Bereich der Wasserpolitik. in: Amtsblatt der Europäischen Gemeinschaften, L 327 vom 22.12.2000, Luxemburg.

IPPC - Council Directive 96/61/EC of 24.09.1996 concerning integrated pollution prevention and control, Official Journal L 257, 10/10/1996 p. 0026 – 0040.

Juggins, S., Ormerod, S.J. and Harriman, R. (1995) Relating critical loads to aquatic biota. In: Critical Loads of Acid Deposition for UK Freshwaters. Chapter 4, p. 9-13. Department of the Environment.

Meyer J, Jenk U, Schuppan W, Knappik R (1998) Hydrogeochemical Aspects of the Aue pit Flooding. In: Merkel B, Helling C (eds.): Uranium-Mining and Hydrogeology, GeoCongress II, S. 124-129, Verlag Sven von Loga, Köln.

Neitzel, P.L., Schneider, P., Schlumprecht, H. (2002): Physico-chemical Surface Water Conditions of Catchments with Metallogenic Origin: A Contribution to the Establishment of the EC Water Framework Directive 2000/60/EG in Germany, in: Merkel B.J.; Planer-Friedrich, B.; Wolkersdorfer, C: Uranium in the Aquatic Environment, pp. 77-84, Springer Verlag ISBN 3-540-43927-7.

Potential environmental impact resulting from inadequate remediation of uranium mining in the Karoo Uranium Province, South Africa

Nico Scholtz[1], O.F. Scholtz[2], Gerhard P. Potgieter[2]

[1]Department Geology, University of the Free State, Bloemfontein, South Africa, E-mail: scholtzn.sci@mail.uovs.ac.za
[2]Department of Plant Sciences, University of the Free State, Bloemfontein, South Africa, E-mail: scholtzof.sci@mail.uovs.ac.za

Abstract. Inadequate remediation of uranium mining in the Karoo Uranium Province, South Africa led to a disused open pit and inclined shaft, uranium ore in stockpiles and barrels, as well as other mining related equipment.

Land owners were unaware of the potential threat of uranium and coherent heavy metals resulting in livestock grazing amongst ore stockpiles and drinking from contaminated water supplies. Land owners consequently used stockpiled uranium ore for gravel road maintenance and construction of farmhouse foundations. The concentration of the radioactive gas radon (^{222}Rn) was monitored in the aforementioned farmhouse and reached 835 Bq.m^{-3}, thus exceeding the concentration limitations (150 Bq.m^{-3}) for radon gas in dwellings set by the United States Environmental Protection Agency.

Lycium cinereum, Fingerhuthia africana, *Aristida congesta congesta* and *Phragmites australis* growing within these mining locations revealed high concentrations of uranium and molybdenum in leaves and roots. *Lycium cinereum* were found to accumulate molybdenum up to 650 ppm in some leaves. Uranium readily accumulates in the roots of some of the species, whilst only a fraction is translocated to the leaves. Plants were also subjected to protein profile studies revealing a general tendency that with an increase in uranium and molybdenum concentrations, protein concentrations in the leaves tend to decrease. These fauna serve not

only as a toxicological hazard for grazing livestock, but also as potential phytore-mediators of polluted soils.

Xenopus laevis were found to reside within a water filled open pit where uranium and molybdenum concentrations reach 20 mg/l and 4 mg/l respectively. These aquatic organisms contain high hepatic, renal and bone concentrations of uranium and molybdenum. Histological sections of liver and kidney revealed anomalous levels of lymphocytes, indicative of infection or neoplasia, possibly as a result of heavy metal uptake.

Introduction

Traces of uranium mineralisation occur throughout the Karoo Supergroup, South Africa (Fig. 1). During the late 1970's the spot uranium price reached its zenith ($40 to $44/pound U) and the largest deposits became economically extractable (Wilson and Anhaeusser 1998). This report briefly describes the uranium trial mining operations within the Karoo Uranium Province, namely Ryst Kuil (on the farm Ryst Kuil 351) and Rietkuil (on the farm Rietkuil 307) as well as coherent inadequate rehabilitation and potential environmental impact.
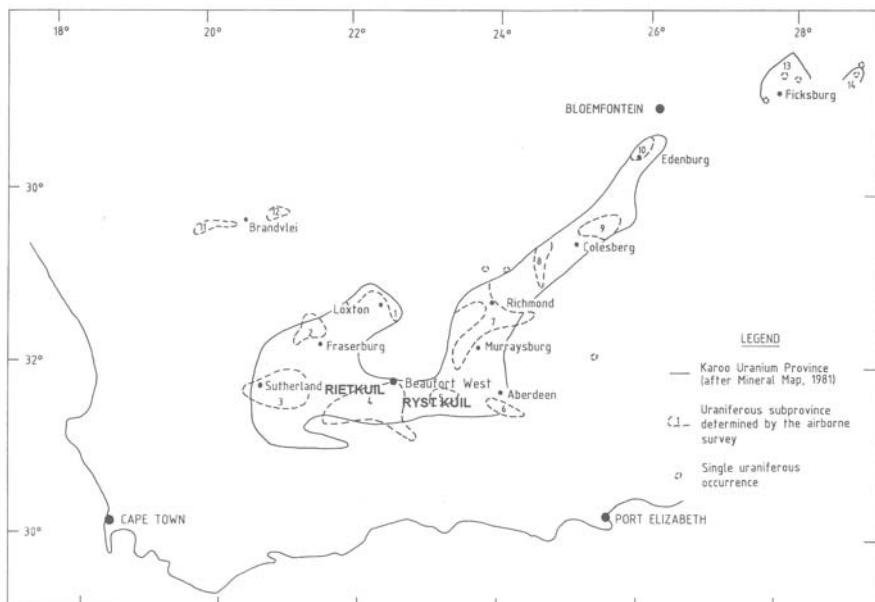

Fig. 1.   Karoo Uranium Province showing mining locations (After Cole et al. 1991).

Case studies: active and abandoned Uranium mines

Uranium is harmful to living organisms if the metal or its decay products enter the body (Ragnarsdottir and Charlet 2000). Deliberate overdose of uranium in mammals and fish resulted in, amongst other symptoms, acute renal failure, liver disfunction and paralytic ileum (Cooley et al. 2000).

Radiation exposure in the natural and urban environment is focused upon radon, the only radioactive gas that is formed by the decay of uranium and thorium. The gas is ingested respiratoraly where it can cause damage as severe as lung cancer (United States Department of Health 1990). In the open air, the concentration of radon is generally very low. Radon becomes a hazard in unventilated uranium mines or in homes, built in areas with a high natural uranium occurrence in the soil or bedrock.

Molybdenum is an essential micronutrient for life, but can be toxic when received in high doses. High levels of molybdenum can account for molybdenosis in livestock, a secondary copper deficiency (Ammerman et al. 1980).

Materials and methods

Environmental assessment included sampling and analysis of stockpiled ore and ore containing barrels, soil, surface water, water logged sediment, foliage, aquatic organisms and radon gas monitoring.

Sampling

Ore stockpiles were randomly sampled by removing the top layer of rock and sampling qualitatively from the top to the bottom of the stockpile. Equipment used included a stainless steel scoop and plastic sample bags.

The following techniques were used in sampling, storage and treatment of soils and water logged sediment as described by Djingova and Kuleff (2000) and Boulding (1994):

- Stainless steel scoop and plastic sample bags used.
- Sample taken on 30 cm depth and cooled to 4°C.
- Samples dried in laboratory at 110°C after removal of stones, roots and living organisms.
- Screening of samples through a 2 mm stainless steel mesh.

Water sample preparation and storage, as described by Djingova and Kuleff (2000) and Greenberg et al. (1985), were as follows:

- Use of 500 ml plastic water containers.
- Cleansing of water containers with Hydrochloric Acid (30% HCl) before sampling.
- Rinsing with sample medium before sampling.
- Filtering through ALBET low ash filter paper.

- Lowering pH to 2 with Nitric Acid (55% HNO_3) after sampling and storage at 4°C.

Radon gas was monitored within a farmhouse using etched track radon gas monitors over a period of two months in November and December 2003 as well as May and June 2004. This technique allows for potential ventilation fluctuations between summer and winter months, which may affect radon gas concentrations.

Xenopus Laevis samples were collected using a baited trap set in the water filled open pit. Samples were transported alive to the laboratory where dissection and removal of tissue took place.

Analysis

Whole rock, soil and sediment geochemical analysis were processed on a PHILLIPS PW 1404 X-ray spectrometer. Major element analyses were executed on fused glass discs, using the technique of Norrish and Hutton (1969). Trace elements were analysed for on pressed powder briquettes.

Water samples were analysed by Inductively Coupled Plasma Optical Emission Spectroscopy (ICP-OES). This technique is used for qualitative and quantitative determination of metals in solution.

Fig. 2.   Un-rehabilitated uranium ore in stockpiles and barrels on Ryst Kuil.

Case studies: active and abandoned Uranium mines

Uranium and molybdenum concentrations in the roots and shoots of plants were extracted by acid digestion (Lamas et al. 2002) and the concentration thereof determined by ICP-OES.

Tissue from Xenopus Laevis were analysed using Inductively Coupled Mass Spectrometry (ICP-MS) after acid digestion.

Results

Ryst Kuil

Numerous mining related structures and equipment are located within the mining area, including the easily accessible, sub-horizontal Cameron Shaft, ore stockpiles (Fig. 2) and barrels, ore crushing - and ventilation structures as well as collapsed core storage (Scholtz 2003).

The Ryst Kuil landowner's lack of knowledge regarding the potential toxicity of uranium and coherent metals (Table 1), led to the usage of water from the Cameron Shaft for crop irrigation. Stockpiled uranium ore was also used for gravel road maintenance and construction, including tennis court and concrete in housing foundations. Uranium ore used for the latter, led to possible accumulation of radon gas in the homestead.

The United States Environmental Protection Agency (EPA) has set an acceptable level of 150 Bq.m^{-3} and 4 pCi/L for indoor radon in the domestic environment. Above these concentrations an action must be taken to reduce the radon levels (Table 2).

The uranium and molybdenum concentration in *L. cinereum* leaves from the mining area on Ryst Kuil were greater than the control leaf sample measurements (Fig. 3). The concentration of these metals in *L. cinereum* roots was not only greater than the control roots but also greater than the concentrations measured in the soil, indicating bioaccumulation and active uptake of uranium and molybdenum from the soil.

Uranium and molybdenum concentrations in leaves and roots from *A. congesta congesta* within the mining area are greater than those in the soil. These values were considerably higher than background leaf and root concentrations (Scholtz et al. 2005).

Table 1. Uranium and molybdenum in stockpiled ore and soil on Ryst Kuil. Normal concentratrions for soil from Alloway (1993).

		Stockpiled ore and barrels (ppm)	Soil (ppm)
Uranium	On site	4000	20
	Normal	N/A	1[a]
Molybdenum	On site	1500	3
	Normal	N/A	2[a]

N/A Not applicable
[a]Normal concentrations for metals in soils.

Table 2. Radon gas concentrations in farmhouse built with stockpiled uranium ore.

Monitor Location	NOV / DEC 2003			MAY / JUNE 2004		
	[Rn] (Bq m^{-3})	[Rn] (pCi/L)	Annual dose (mSv/a)	[Rn] (Bq m^{-3})	[Rn] (pCi/L)	Annual dose (mSv/a)
BEDROOM 1	835	22.57	14.19	797	21.00	13.55
BEDROOM 2	533	14.41	9.05	722	19.57	12.27
BEDROOM 3	502	13.57	8.54	610	16.53	10.37
KITCHEN	351	9.49	5.97	528	14.31	8.98
MOTOR GARAGE	N/A	N/A	N/A	108	2.93	1.84
STORE ROOM 1	N/A	N/A	N/A	207	5.61	3.52
STORE ROOM 2	N/A	N/A	N/A	269	7.29	4.57

Rietkuil

A test mining pit was excavated in 1977, covers an area of 5600m^2 and is approximately 15m deep (Scholtz 2003). A high concentration of uranium and molybdenum is present within the surface water and water logged sediment in the open pit (Table 3).

Soil uranium and molybdenum concentration from the mining area was less than concentrations in the leaves and roots of *L. cinereum* and *F. africana*, indicating possible bioaccumulation of these metals. The values for *L. cinereum* and *F. africana* roots and leaves, obtained from the mining area, were also greater than those from the control area (Fig. 4; Scholtz et al. 2005).
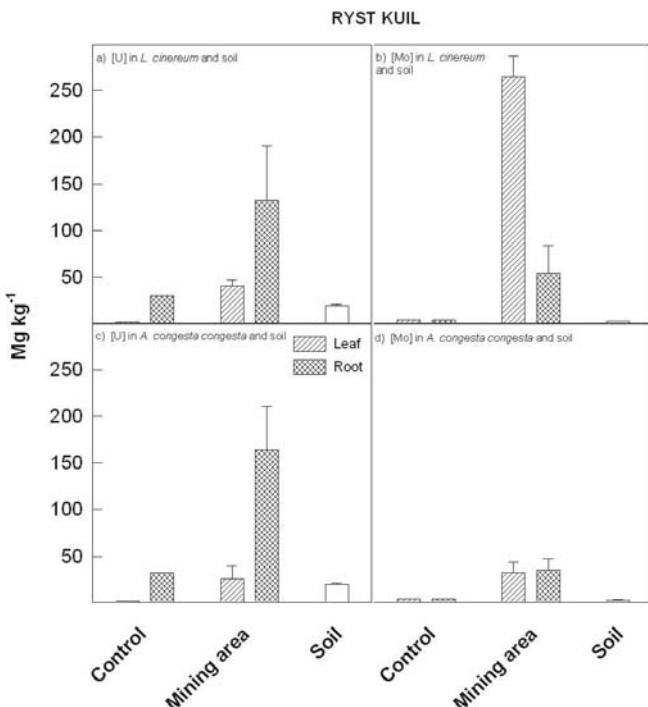
Phragmites australis, a reed growing in uranium-contaminated water (20 mg l^{-1}), accumulated uranium mostly in the roots (258 mg kg^{-1}) and to levels higher than its control counterparts (results not shown graphically).

Xenopus Laevis resides within the water filled open pit on Rietkuil, which contains high uranium and molybdenum concentrations. These organisms were analysed for uranium and molybdenum in various bodily tissues (Fig. 5) and revealed elevated values in comparison to control samples.

Discussion

A matter of concern is the fact that the farm owners were unaware of the possible toxic effects associated with uranium and molybdenum. The owner of Ryst Kuil consequently used the uranium ore for concrete in farmhouse foundations leading to accumulation of radon gas to above maximum allowed levels. The residents have been living in the aforementioned home without any knowledge of high levels of radon gas and its potential influence on health (Personal communication with Mr H.G. Scheün, owner of Ryst Kuil).

The water within the Rietkuil open pit yields molybdenum and uranium concentrations of up to 4 and 20 mg/l respectively. The concentrations of these metals

Fig. 3.   Uranium and molybdenum concentrations in Ryst Kuil foliage and soil.

Case studies: active and abandoned Uranium mines

Table 3. Uranium and molybdenum in Rietkuil soil, sediment, water and stockpiled ore. Normal concentrations for soil from Alloway (1993).

		Stockpiled ore and barrels (ppm)	Soil (ppm)	Sediment (open pit) (ppm)	Surface water (open pit) (mg/L)
Uranium	On site	3500	15	700	20
	Normal / Max. allowed	N/A	1[a]	N/A	0.5[b]
Molybdenum	On site	1000	2	600	4
	Normal / Max. allowed	N/A	2[a]	N/A	0.2[b]
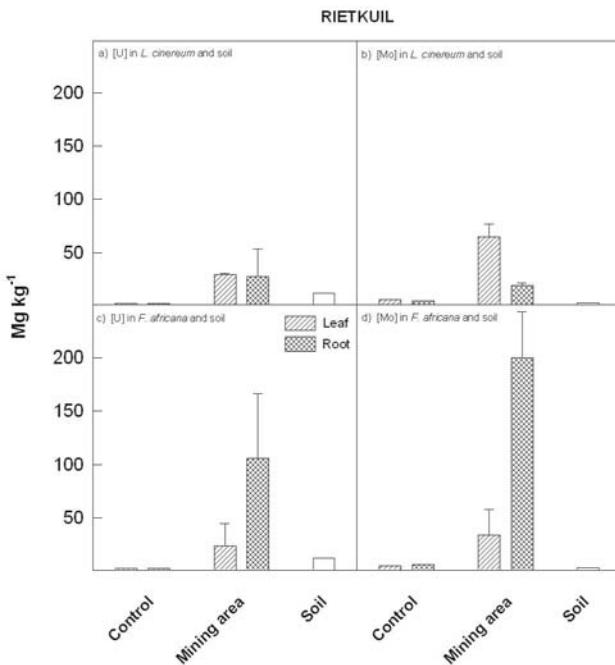
N/A Not applicable

[a]Normal concentrations for metals in soils

[b]Canadian Environmental Quality Guidelines (CEQG) for livestock watering. Maximum allowed concentrations (derived from CEQG) for aquatic ecosystems are 0.07 mg/L for molybdenum; no concentrations are available for uranium.
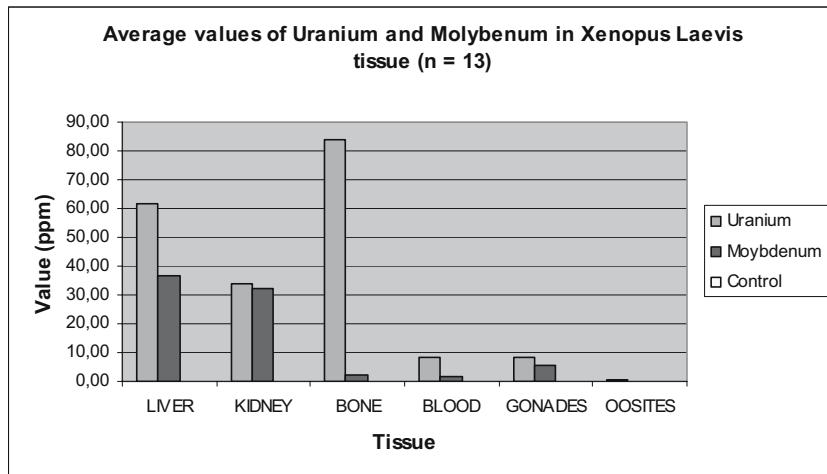
exceeds the maximum allowed levels suitable for aquatic life (Canadian Environmental Quality Guidelines 1999). *Xenopus Laevis*, an amphibian species, resides within this water, concentrating the metals into various bodily tissues. Although histological sections through *X. Laevis* organs revealed anomalous concentrations of lymphosytes, possibly indicative of neoplasia, no other deformities of any kind were visible, indicating a possible tolerance of the organism towards the specific metals and associated radiation.

On all four trial mining locations livestock are allowed to graze amongst the ore stockpiles and drink from the water filled open pit. Certain foliage types were also identified as uranium and molybdenum accumulators. The potential effects on livestock drinking from the Rietkuil open pit and grazing on metal accumulating foliage needs urgent investigation..

This research suggests that, *L. cinereum*, *F. africana*, *A. congesta congesta* and *Phragmites australis* can serve as bio-indicators for uranium and molybdenum pollution in contaminated soil and water. Differences between heavy metal concentrations in soil and plants collected within the mining area, indicate that the above mentioned plants bio-accumulate uranium and molybdenum. These plants also exhibit phytoextraction and rhizofiltration (*P. australis*) possibilities of these elements from contaminated soils and water. Harvested plants can be incinerated to reduce volume and the heavy metals either extracted from the ash or stored as hazardous waste.

**Fig. 4.**   Uranium and molybdenum concentrations in Rietkuil foliage and soil.

Fig. 5.   Uranium and molybdenum concentrations in *Xenopus Laevis*.

Case studies: active and abandoned Uranium mines

Molybdenum transport mechanisms are evident in *L. cinereum*. The molybdenum concentrations are greater in the leaves than in the roots. The latter, together with *L. cinereum*'s high biomass productivity, makes it a strong candidate for the phytoextraction of molybdenum from contaminated soils.

Uranium accumulation in *L. cinereum* was generally higher in the roots compared to the leaves, but uranium still accumulates in reasonably high concentrations in the leaves. This suggests that fractions of the uranium in the roots are translocated to the above-soil biomass, making *L. cinereum* a possible phytoextractor of uranium as well.

Uranium and molybdenum accumulation in the grasses *F. africana* and *A. congesta congesta* appear to be greater in the roots than in the leaves. Comparing the uranium and molybdenum concentrations in the soil to those in the leaves indicate the translocation of uranium and molybdenum from roots to shoots. The low biomass yield of these grass species does not, however, allow them to be successful phytoremediators of heavy metal contaminated areas.

Conclusions

The failure to properly remediate the uranium trial mining areas in the Karoo, through removing ore stockpiles, waste rock and mining structures as well as preventing entry into open pits and shafts leads to the existence of a largely overlooked and potentially very serious environmental hazard.

The results obtained from the present investigation are of a disturbing nature, revealing previously underestimated and overlooked sources of localised pollution of hazardous substances in soil, surface water, foliage and aquatic organisms as well as anthropogenic sources of radiation.

Acknowledgements

References

Alloway B.J. 1993. Heavy metals in soils. Blackie. Glasgow and London, 339pp.

Ammerman C.B., Fontenot J.P., Rae Spivey Fox M., Hutchinson H.D., Lepore P., Stowe H.D., Thompson J.D. and Ullrey D.E. 1980. Mineral tolerance of domestic animals. National Academy of Sciences. Washington D.C. 578 p.

Boulding J.R. 1994. Description and sampling of contaminated soils. 2nd Edition, Lewis Publishers.

Canadian Environmental Quality Guidelines. 1999. Canadian Council of Ministers of the Environment.

Cole D.I., Labuschagne L.S. and Söhnge A.P.G. 1991. Aeroradiometric survey for uranium and groundwater follow up in the main Karoo Basin. Memoir 76 of the Geological Survey. Department of mineral and energy affairs, 145pp.

Cooley H.M., Evans R.E. and Klaverkamp J.F. 2000. Toxicology of dietary uranium in lake whitefish (*Cerogonus clupeaformis*). Aquatic Toxicology 48, 495 – 515.

Djingova R. and Kuleff I. 2000. Instrumental techniques for trace analysis. 137-185. In: Trace Elements – Their distribution and effects in environment (Eds: Markert B. and Friese K.). 582pp.

Greenberg A.E., Trussel R.R. and Clessceri L.S. 1985. Standard methods for the examination of water and wastewater, 16th edition. American Public Health Association, Washington D.C. 1268pp.

Lamas M, Fleckenstein J, Schroeter S, Sparovek RM, Schnug E (2002) Determination of uranium by means of ICP-QMS. Communications in Soil Science and Plant Analysis 33: 3469-3479

Norish K. and Hutton J.T. (1969) An accurate X-ray spectrographic method for the analysis of a wide range of geological samples. Geochim. Et Cosmochim Acta, 33, 431-453.

Ragnarsdottir K.V. and Charlet L. 2000. Uranium behaviour in natural environments, 245-289. In: Environmental Mineralogy: Microbial Interactions, Anthropogenic Influences, Contaminated Land and Waste Management. (Eds: Cotter Howells J.D., Campbell L.S., Valsami Jones E. and Batchelder M.). Mineralogical Society Series, 9, Mineralogical Society, London.

Scholtz N. 2003. Assessment of potential toxic influence of uranium trial mining in the Karoo Uranium Province. M.Sc thesis. Univ. of the Free State. Bloemfontein, 143pp.

Scholtz O.F., Potgieter G.P. and Scholtz N. 2005. Uranium (U) and molybdenum (Mo) accumulation in *Lycium cinereum, Fingerhuithia africana* and *Aristida congesta congesta* and its possible role as bio-indicators and phytoremediators of heavy metal contaminated soils in the central Karoo, South Africa. *(Unpublished results)*

United States Department of Health. 1990. Toxicological profile for radon. Public Health Service. Agency for Toxic Substances and Disease Registry, 172pp.

Wilson M.G.C. and Anhaeusser C.R. 1998. The mineral resources of South Africa. 6th edition. Council for Geoscience, 740pp.

Regulating Idle Uranium Mines In Canada

Ron Stenson

Canadian Nuclear Safety Commission, P.O. Box 1046, Station B, Ottawa, Canada K1P 5S9, E-mail: stensonr@cnsc-ccsn.gc.ca

Abstract. On May 31, 2000 the *Nuclear Safety and Control Act (NSCA)* came into force in Canada. As a result of changes introduced in this new legislation new attention was brought to the assessment and regulation of these legacy properties. Most were abandoned and their safety and long-term management is the responsibility of various levels of government. Canadian Nuclear Safety Commission (CNSC) staff initiated the Contaminated Lands Evaluation and Assessment Network (CLEAN) program to determine what regulatory activities were required at these and other sites in Canada. The idle mine portion of the CLEAN program began as an outreach program to inform various stakeholders of their responsibilities under the *NSCA* and to catalog the available information for each of these mines. This resulted in two separate initiatives, one to licence high-risk sites and one to exempt radiologically low-risk sites from CNSC licensing.

Introduction/Background

Radium mining in Canada began in the early 1930's. In the early 1940's uranium mining replaced radium mining and continued through two periods, the first of which ended in 1963 with the end of foreign sales guarantees. The second phase started in the 1970's, and is still ongoing, with significantly more increased interest starting in 2004.

The majority of early uranium mines in Canada operated with little or no regulation from the Atomic Energy Control Board (AECB). Those still operating in the 1970's to date were licensed and inspected by the AECB with worker safety being the initial concern, before progressing to include environmental and international obligations on security. The AECB regulated these sites as the lead in a Joint Regulatory Group. This meant that both Provincial and other Federal agen-

cies with a mandate that applied to the sites were involved with the AEBC in regulatory reviews and inspections.

Prior to the 1970's, the AECB issued various types of permits under the Atomic Energy Control Act (AECA) which allowed the mine and mill to operate. Usually, the only condition attached to these permits was that the mine/mill needed to be operated in compliance with Provincial health and safety standards. One other stipulation included in the permits was that the operator had to have a contract with Eldorado Nuclear, a federal Crown corporation, to sell all products to them. Eldorado was responsible for meeting all international sales contracts.

In 1963 when guaranteed sales of uranium in support of international contracts disappeared, so did many of the mines and mills in operation at the time. Many owners literally sent their employees home and walked away from the now nonprofitable mines.

The legacy that this left was social, economic and environmental. Unconfined tailings and waste rock drainage were left unchecked until the 1980's. Control of most of these sites fell to the Provincial/Territorial governments. Since the AECA did not bind these governments the AECB could not require that these sites be remediated. It should be understood that until the mid-1970's there was little public or political concern for the potential hazards at any mine sites, including uranium mine sites. Unless there was an obvious problem, little was done at these sites.

During the 1970's both the Provincial governments and the AECB began to require any idle uranium mine/mill sites under private ownership to begin remediation. These existed primarily in Bancroft and Elliot Lake, Ontario. Any operating mine/mill sites were licensed and at the end of their operations were required to undergo decommissioning. This resulted in Beaverlodge (northern Saskatchewan) and Madawaska (Bancroft, Ontario) being decommissioned in the early 1980's. Various sites in Elliot Lake, Ontario were decommissioned in the 1990's. Currently Cluff Lake (northern Saskatchewan) a modern mine that was assessed and built in the early 1980's, is undergoing decommissioning.

Any remediation at other sites was not done under AECB license and although it met the general standards of the day, the AECB only provided advice, not guidance. During the 1990's the AECB had approached those they believed to be in control of the idle uranium mine/mill sites to apply for AECB licenses. However, the AECA could not compel a government agency to apply for a license and the private sector companies that controlled other sites resisted. This was primarily because the current companies were not the original operators of the mines and resented having to assume the long-term liabilities associated with remediation under a perpetual license. To address the long-term liabilities associated with monitoring and maintenance of these facilities discussions were begun with the Provinces that, it was hoped, might lead to the Provinces taking over management of these sites in the future.
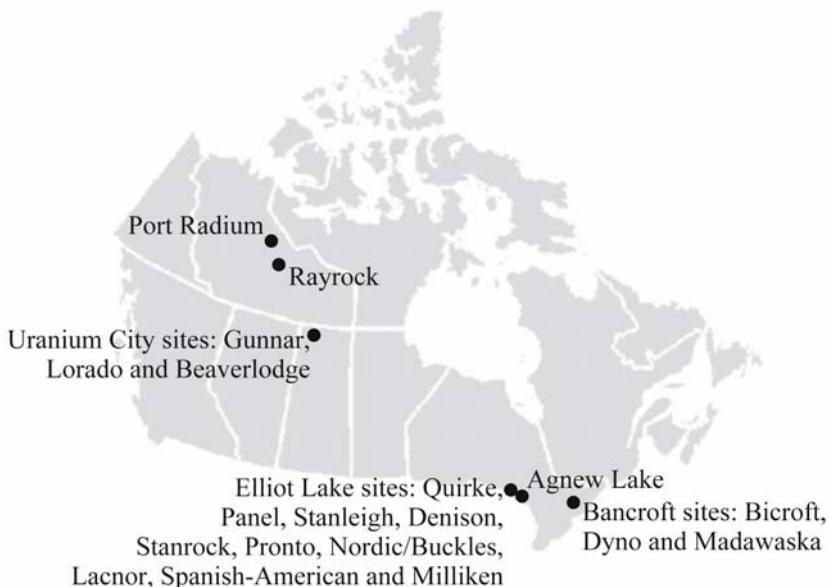
Since the NSCA was imminent, it was decided by the AECB not to pursue licensing under the AECA, since it was not yet clear what the requirements would be under the new Act.

Case studies: active and abandoned Uranium mines

The CLEAN Program

The idle mine portion of the CLEAN program began as an outreach program to inform various stakeholders of their responsibilities under the *NSCA* and to catalog the available information for each of these mines. After the initial, and somewhat crude, cataloging of the numerous mine sites (only 19 had mills), it was decided that there were two separate groups to consider. A risk-informed approach quickly identified the sites with tailings as the higher-risk sites (Fig. 1). The others, mostly small mines that shipped the ore off site for milling, shared very few concerns with the tailings sites. Somewhere in the middle were sites with large waste rock inventories. These coincidentally tended to be associated with sites with mills and tailings. Two initiatives sprung from this assessment. The first was to license the so-called higher-risk sites. The second was to characterize the idle mines without tailings and determine the appropriate regulatory approach to be taken.

Contact was made directly with the person last known to have responsibility for managing the higher-risk sites. In retrospect it was lucky that many of these people were still in place. Since the CLEAN program began retirements have resulted in the loss of knowledge and of personal "ownership" of the sites.

Three workshops were held over three years. The first of these was to bring together the prospective proponents for the sites and provide them with information on the requirements of the NSCA and the process that needed to be followed to bring all of the sites under CNSC licenses. It was also an opportunity to create a

Fig. 1.   Location of tailings management sites from now idle uranium mines in Canada.

Case studies: active and abandoned Uranium mines

community of proponents who could communicate with each other and take advantage of each other's experiences and expertise. The workshop was well attended and provided the basis for the next workshop about a year later. The second workshop brought together not only the proponents, but also CSNC specialist staff was available to help coach the group on our expectations for various studies required to characterize and assess the sites. Specialists from the CNSC environmental protection group, geosciences group, and the licensing group all attended. The third and last workshop brought together the proponents and various other regulatory agencies from the Provincial and the Federal government. These agencies provided information on their various requirements for long-term site monitoring and maintenance.

Between each workshop CNSC staff stayed in communication with the various proponents and provided guidance and support to move the proponents through the licensing process. CNSC staff was also in contact with the various regulatory agencies that had an interest in these sites, the JRG. This gave rise to an awkward hurdle. Some of the JRG members were also proponents for other sites. Since the NSCA now bound other government agencies the CSNC was now required to regulate other regulators. This was the case in Ontario where two sites (one mine, one contaminated land site) required licenses, in Saskatchewan where two sites required licenses, and in the Northwest Territories (NWT) where numerous sites (one mine) required licenses. Although every attempt to treat all proponents the same has been our standard operating procedure, there were very good arguments to stray from this policy.

The CNSC had to be sensitive to the mandates of other regulatory agencies. These agencies have their own, often different, political priorities and imperatives. Although everyone recognized that the law applied to him or her, delivering his or her own mandate took precedence. Some agencies resented the CNSC involvement in their affairs, while others had rigid decision-making structures that hampered communication. In the end, familiarity and visible respect were seen as the paths forward. Extra time was built into the CNSC's normal processes to allow agencies to adjust to their new roles and to encourage constructive dialog.

Two things were done specifically to deal with the immediate problems of regulating other government agencies. The first was that staff requested temporary exemptions from the requirement to license the possession, management and storage of nuclear substances at these sites. This allowed sufficient time for the agencies to meet licensing requirements without radical internal changes. The second was a complicated exemption from cost recovery fees for government agencies associated with these sites. Both of these required a lot of staff time and were unprecedented decisions under the new Act.

It should be noted that all of the same safety and long-term management requirements at these sites apply equally to private and public sector licensees. Only time and cost recovery considerations have been made.

Two examples of how the CLEAN program has made adjustments to allow other government agencies to maintain control of their own mandates are the licensing of the Port Radium idle mine in the NWT, and the licensing of the Gunnar idle mine in Saskatchewan. Indian and Northern Affairs Canada (INAC) had al-

ready begun a community-based process to identify concerns at the Port Radium site. This process saw the native community at Deline working as a partner with INAC and other federal departments to both assess the site and to determine the best possible remedial options for the site. The CSNC began sitting as an observer at the table in 2000. Rather than push for licensing commitments and potentially complicating an already complicated social and cultural situation, CNSC staff requested a series of exemptions from the requirements to license the possession, management and storage of nuclear substances at the site until the end of 2007. This has allowed the INAC/Deline process sufficient time to evolve into a solution and a license application is anticipated from INAC by the end of 2005.

In Saskatchewan, where the Provincial government controls the Gunnar idle mine site, the CNSC has granted a similar exemption to allow the Province to implement an Institutional Control Policy for the long-term management of idle mine sites. This is the first such policy in Canada and will help to address industry concerns that long-term management (perhaps thousands of years) under a CNSC license is an impractical requirement both legally and financially.

A new approach has recently grown out of the CLEAN program project to license higher-risk mine/mill sites. It was the formation of a network of stakeholders called the Canadian Uranium Regulatory Examination (CURE) Team. CURE is composed of representatives of government (Federal, Provincial, and Municipal) and the private sector. It is looking at the long-term disposition of higher-risk uranium mine and mills sites. Some areas being followed are potential changes to current regulations, public perception and institutional controls.

The second initiative was the characterization of idle mines without tailings. This program involved the identification through provincial/territorial records of almost 80 idle mines across Canada. The majority of these are in northern Saskatchewan and central Ontario. These mines shipped the ore they recovered to local mills for processing. Once a primary list was made CNSC staff gathered as much information as possible about each mine. This was aided in Saskatchewan by a very recent survey of all of their idle mines and the publication of two volumes detailing the 40 uranium mines in the Province.

Based on the information available a basic risk assessment was applied to the sites. This was difficult to do in Ontario and the NWT since no radiological information was available in provincial records. CNSC staff then selected about 20 of the most likely higher-risk sites and field-proofed the available data during two campaigns. Radiological data was gathered for some sites that previously did not have any.

In the end it was determined that none of the idle mines without tails posed a radiological hazard. The Provinces already regulated the mines for conventional and environmental hazards. In the absence of a radiological hazard, it was seen as duplication and overlap for the Federal government to regulate them.

CNSC staff recommended that the Commission grant a permanent exemption from the requirements to license the possession, management and storage of nuclear substances at these mines (as specifically listed in an appendix to the exemption). It was granted in December 2004.

Case studies: active and abandoned Uranium mines

Conclusion

Although the uranium mines portion of the CLEAN program was only one of ten concerns, it has accounted for about half of the resources and time expended. It has shared a common philosophy with the rest of the program, but has had unique and important challenges particular to it. Through patience and flexibility the CLEAN program has dispositioned 75 idle mines without tailings and has licensed 16 of the 19 idle mines with tailings across Canada. The remaining three are at various stages of licensing and immediate safety precautions have been taken at the sites.

The program has taken a soft rather than a hard approach to regulating. If hazards existed they have been, or are being, dealt with. Time was the most important and available concession used to enable those in control of the sites to comply with the NSCA. Although the primary aim of the CLEAN program was to bring sites under the appropriate regulatory control, a secondary aim was to develop good licensees. This approach was an investment in the future as we continue to work with the network to fulfill the CNSC's safety mandate

Long-term Impacts of Gold and Uranium Mining on Water Quality in Dolomitic Regions – examples from the Wonderfonteinspruit catchment in South Africa

Frank Winde

North West University, School of Environmental Sciences and Development, Private Bag X6001, Potchefstroom, 2520, Republic of South Africa,
E-mail: ggffw@puk.ac.za

Abstract. A number of gold and uranium mines in South Africa are located in areas where compartmentalised dolomitic rock forms extensive karst aquifers overlaying mined reefs. Apart from dewatering of such aquifers triggering widespread sinkhole formation and impacting on water availability by drying up of springs and boreholes, mining activities also impact on the quality of local water resources. Of particular concern to downstream users is uranium pollution of ground- and surface water often associated with gold in the mined reefs. This paper estimates potential U-fluxes associated with different types of mining-sources assessing their varying significance in past, present and future.

Introduction

Large scale gold mining in South Africa commenced more than a century ago at outcrops of gold-rich Witwatersrand sediments marking the shoreline of an ancient lake. With mined auriferous reefs dipping deeper towards the centre of this lake, mining depth steadily increased reaching maxima of up to 4000m below surface.

In large parts of the Witwatersrand basin gold mining developed below extensive, compartmentalized karst aquifers in dolomitic bedrock hosting large volumes of groundwater, a much needed resource in a water-stressed country such as South Africa.

As a consequence of increasing ingress of dolomitic groundwater into underlying mine workings, it was decided in the early 1960's to dewater affected dolo-

mitic compartments as a matter of policy for economical and safety reasons. The associated lowering of the groundwater table by up to several hundreds of meters in some compartments, however, unexpectedly triggered massive ground movements in near-surface karst areas in the form of sinkholes and dolines, frequently with disastrous consequences for residents and infrastructure (Jennings et al. 1965).
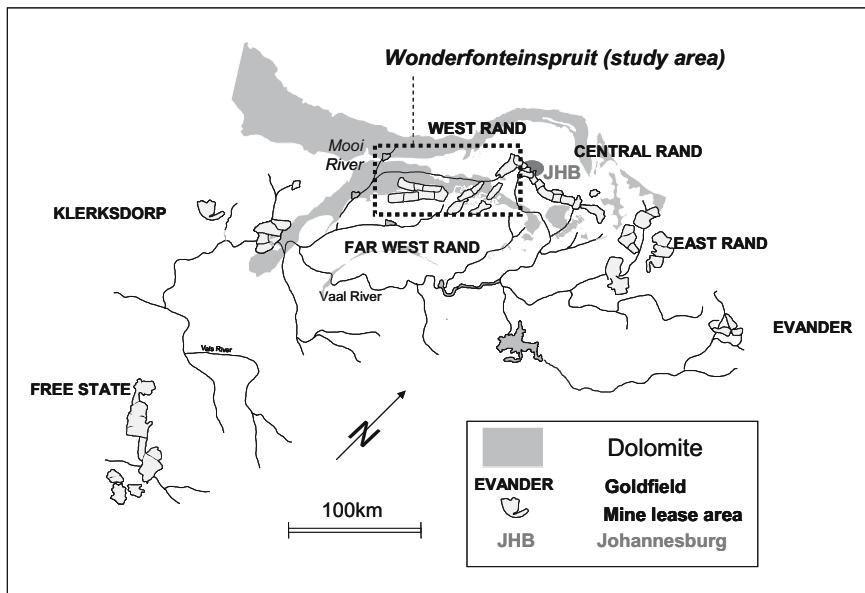
Apart from the associated land degradation and negative impacts on water availability (drying up of irrigation boreholes and dolomitic springs feeding into the otherwise non-perennial stream), mining also caused pollution of the remaining ground- and surface water resources in the area. Originating from a wide variety of point- and non-point sources, most problems are associated with excessive sulphate (Sulphate mainly originates from oxidized sulphides and sulphuric acid used by many gold mines in the past to leach U from auriferous ore. Although not toxic, high sulphate concentrations severely limit the fitness of water for many usages and contribute to water stress in semi-aid South Africa, where dilution to acceptable limits as practiced in many humid mining countries is not a feasible option due to the lack of water) and nitrate (High nitrate concentrations are mainly linked to the use of explosives for underground blasting. The use of cyanide as leaching agent in gold recovery may also contribute to elevated concentration of N-compounds since the extremely toxic cyanide is believed to soon decay into harmless C/ N-components once exposed to UV radiation (sunlight)) concentrations in mine effluents, acidic mine drainage and a variety of toxic heavy metals including radioactive elements such as uranium.

This paper focuses on sources of mining-related U-pollution in the Far West Rand goldfield 70km south west of Johannesburg where U is found associated with gold in many of the mined reefs. Owing to potential risks for human health, the radioactive heavy metal is of particular concern to downstream users such as local residents and riparian land owners as well as the Potchefstroom municipality depending directly on water from the WFS. Identifying and characterizing all potential sources of U pollution is a first step contributing to current efforts by the government to comprehensively assess the extent of historic, current and possible future water pollution. It forms part of a knowledge base needed to develop appropriate water management strategies for the period during and after successive mine closures in the area.

Mining history and natural conditions of the study area

Gold- and uranium mining

Apart from the FWR goldfield, the catchment of the WFS also includes parts of the much older West Rand (WR) goldfield, which developed soon after the discovery of gold in 1886, mostly located in the non-dolomitic head water region of

Fig. 1. Location of the study area (Wonderfonteinspruit catchment) within the Witwatersrand basin in relation to the goldfields as defined by lease areas of gold mines, the surface hydrology and outcropping dolomitic limestone.

the catchment (also known as the upper WFS; Fig. 1). Many gold mines in this area are abandoned and associated mining residues such as sand dumps and slimes dams are often several decades old and heavily eroded.

Gold mines in the lower, dolomitic part of the catchment were only developed in the late 1930's after a newly invented cementation technology allowed for sealing of sunken shafts against flooding by dolomitic groundwater.

As part of the global search for uranium resources for atomic weapons initiated by the 'Manhattan Project', the uranium-rich gold reefs of the WR and FWR were used by many gold mines in the area to produce U as a by-product of gold from the early 1950's on. At one stage 9 out of 22 gold mines produced U for a total of 7 metallurgical U recovery plants in the area. The importance of the area for South African U production is illustrated by establishing the Nuclear Fuels Corporation of South Africa (NUFCOR), as one of the world's largest continuous producer of uranium oxide, in the area (upper part of the catchment). After peaking in 1980, U production in South Africa declined steadily, leaving only one gold mine in the area currently (2005) still producing U. At all other mines U is no longer extracted from the milled ore and discarded onto slimes dams together with the leached ore.

Climate and Geology

The study area is part of a semiarid to arid interior plateau ('Highveld') ranging in elevation from 1700 – 1400 m a.m.s.l., where potential evaporation exceeds mean annual precipitation (MAP) of 600-750mm by a factor of 2-3. Rainfall occurs mainly as part of convectional thunderstorms in summer (Nov-April), while the winters months are normally dry.

The surface geology is dominated by two 10-15km wide E-W running bands of carbonate limestone (dolomite) covering large parts of the lower catchment. Within the upper 100-150m of the 1-1.5km thick dolomite chemical weathering developed extensive karst systems. The total volume of groundwater stored in the karst aquifers exceeds the storage volume of the Vaal Dam at full capacity by far. Later intrusions of syenite and diabas dykes associated with volcanism hydraulically separated the dolomitic blocks into several sub-units ('compartments'). Four of the nine compartments within the catchment are dewatered by mining, which also mined through some of the dykes, effectively linking adjacent compartments hydraulically. Since the northern band of the dolomite is not affected by mining it is not discussed further.

Hydrology

The WFS originates just south of the sub-continental divide separating the watersheds of the Indian Ocean (to the north) and the Atlantic (to the south). After passing the quartzite-dominated head water region the WFS traverses seven dolomitic compartments forming the stream bed for more than 80% of its total length of about 90km. Prior to mining the WFS was fed by a succession of springs at the downstream dykes of each compartment where naturally dammed up dolomitic groundwater decanted into the stream.

Since inception of dewatering, however, all springs in the four dewatered compartments dried up, significantly reducing stream flow in affected reaches. Instead, the stream now receives groundwater pumped from underground mine workings and discharged into the WFS downstream of the dewatered compartments via an extensive network of pipelines and canals. Furthermore, dewatering also caused massive losses of stream water to the underground through the many sinkholes that occurred in the stream channel due to dewatering. In order to reduce these losses and the increased costs for pumping this water from the mine void back to the surface, a 30km-long stretch of the WFS where its crosses the three (lower) dewatered compartments was diverted into a pipeline of 1m diameter.

After its confluence with the upper Mooi River the WFS provides a significant proportion of the drinking water supply for approximately 250,000 residents of the Potchefstroom municipality 20km downstream of the confluence.

Sources of uranium contamination

Types of sources

U pollution in the WFS catchment is mainly caused by sources associated with gold mining activities. However, possible contributions of not directly mining-related sources cannot be excluded. These include the production of uraniferous fertilizer (phosphates) and its application on agricultural land, impacts from the U concentrate refinery NUFCOR via several possible pathways including air- and waterborne migration and road transport as well as natural ore bodies in contact with free moving water. However, in view of the contribution of mining operations to U-pollution in the area these sources are of marginal significance.

Mining-related sources of U pollution can further be divided into 'on-site sources', comprising all possible pollution originating from the actual mine property (lease area) and 'off-site sources' comprising mining-related pollution sources outside the mine boundaries e.g. eroded tailings particles transported into the adjacent environment, tailings material used to fill sinkholes of karst aquifers, contaminated mining material used for construction purpose in nearby communities, etc. From a water management point of view a division of sources according to their spatial extent into point and non-point (diffuse) is often useful. Typically, point-sources relate to a somehow controlled release of U (e.g. discharging mine effluents via pipelines) and commonly affect surface water bodies. In contrast, U release from non-point sources often cannot be controlled and mainly affects subjacent aquifers.

Point sources of U pollution

A comprehensive overview of potential point sources of U contamination associated with gold and uranium mining in the WFS catchment is given in Winde (2004). In this paper the focus is on three major types of point sources namely:

- Mining effluents (consisting of process water from metallurgical plants, fissure and service water from underground, surplus water from tailings storage systems, outflow of settlings ponds, etc.)
- Domestic waste water from mining-related sewage works and
- Polluted run off from storm water drainage systems of mines and adjacent municipalities.

Mining effluents

For the period of active U-production between the early 1950's and the mid 1980's it is likely that point sources contributed significantly to water pollution since U was leached from the ore and therefore present at much higher concentra-

tions in water circuits of metallurgical plants. Low recovery efficiency in the early days of the newly introduced U leaching technology and frequent process failures allowed for much of the leached U to leave the metallurgical plant along with the waste water stream (Mc Lean 1994). However, increasing recycling and reuse of process water later on caused increased U concentration in process water that finally needs to be discharged. In the early 1990's, after U production in many gold mines had ceased, Pulles (1991) reported an average U-concentration of 0.74mg/l for mining effluents across the Witwatersrand basin. Based on associated discharge volumes it is conservatively estimated that point sources of gold mines in the study area discharge about 12t U/a mostly into the WFS (Winde 2004).

To be added to this are contributions of point sources that are not controlled, including spillages, leakages from pipeline and water treatment systems and surface run-off from contaminated areas such as ore piles, slimes dams etc. draining into storm water systems. Leakages from damaged reticulation systems in the area are likely to be above average due to increased seismic activity repeatedly damaging even surface buildings, and due to karst-related ground movements (sinkholes and subsidences) still occurring in the area several decades after dewatering commenced.

Apart from process water and contaminated surface run off, groundwater seeping into underground mine workings (usually referred to as 'fissure water' since it migrates into the mine void via cracks and fissures connected to he dolomitic aquifer several hundreds to thousands of meters above), also must be considered. Being in contact with oxidized ore bodies and other possible U-sources such water was found to contain up to 11mg/l U_{nat} (Deelkraal Gold Mine 1991). However, the vast majority of fissure water, pumped by mines into the WFS, is of good quality frequently diluting waste loads from upstream in the WFS.

Domestic waste water from mining-related sewage works

Workforces of gold mines in the order of tens of thousands of people cause sewage volumes comparable to those of many medium-sized towns in the area. The treated wastewater mainly originates from imported tap water bought from a water service provider ('Rand Water'), although some mines also use treated fissure water. Higher U-concentrations in domestic wastewater from mines were linked, amongst others, to miners drinking U-contaminated water, such as chilled cooling water in underground mine workings, resulting in elevated U-levels in urine (Deelkraal Gold Mine post-1990). Samples from toilet drains of changing rooms at shafts taken at several gold mines displayed U-concentrations of 0.4 - >13 mg/l (Pulles 1991).

Surface run off from storm water drainage systems

Although being a natural non-point source by nature, rain water run-off becomes a point source of water pollution once it enters storm water drainage systems discharging the water collected from a much larger area spatially concentrated via several outlets into receiving water courses. Storm water drainage systems collect

mainly rainwater run-off from sealed surfaces such as tarred roads, concrete covered areas and roofs. Due to much higher run-off coefficients this can result in almost 100% of the rainwater from such areas flushing untreated into nearby streams. Containing a wide range of heavy metals such as Pb (originates in petrol), Cd (abrasion of tyres), Zn and Cr (corrosion of cars, gutters, roof material) run-off from roads and other sealed surfaces constitutes a significant source of stream contamination (Winde 1996). In addition, frequently windblown dust from adjacent slimes dams is also washed off from sealed surfaces nearby. Based on measured dust concentration, the size and mean annual run-off volumes of affected areas, a sediment load of approximately 100,000t/a was estimated to be discharged from storm water drainage systems into receiving water courses. With wind blown tailings material containing on average U concentration >100mg/kg, storm water-drainage systems discharge >10t particle bound U per year mainly into the WFS (Winde 2004). Other sources likely to contribute to the U contamination of storm water include run-off from ore piles, rock and sand dumps as well as from U-plants where possible spillages of process water, dust and U-concentrate may occur. In addition, tailings particles eroded from nearby slimes dams are also transported into storm water drainage canals. Rainstorms exceeding an intensity of a 1:50a event will in most cases result in additional spills of run-off from slimes dams overflowing the prescribed 0.8m high free board of storm water retention dams. In some cases storm water-drainage channels are also illegally used to dispose of highly contaminated process water from gold mines (Parker 1982).

Non-point sources of U-pollution

Seepage from slimes dams

Owing to their large surface area and content of contaminants slimes dams are likely to be the single largest source of diffuse water pollution by mining.

Along with some 1.1 billion t of gold ore that was milled by mines in the West Rand and Far West Rand up to 1998 more than 150,000t of uranium were brought to the surface. With only a quarter of it being extracted and sold the majority of the mined U remains in tailings. The slimes dams of the West Rand and Far West Rand contain a total of well above 100,000t of uranium (1998), reaching average concentrations in some mines of up to 300ppm. The mass-weighted mean U_{nat}-concentration in all tailings of about 100ppm is about two orders of magnitude above the natural background in soils and surface rocks of the area rendering slimes dams a potential source of U-contamination (Winde 2004).

Seepage from slimes dams frequently displays significantly elevated concentrations of uranium and other toxic heavy metals as well as dissolved salts such as sulphates. In tailings where sulphide oxidation leads to acid mine drainage (AMD) the leaching rate for uranium and other heavy metals can increase by orders of magnitude. This results in concentrations of dissolved U reaching maxima of several hundred mg/l (Mrost & Loyd, 1970) compared to a discharge-unweighted

Case studies: active and abandoned Uranium mines

mean of global background concentration for uranium in freshwater of 0.0003mg/l (DWAF 1995). Based on surface area covered by slimes dams, average U concentration in tailings and seepage and rainfall, flow rates of seepage from slimes dams only in the WFS catchment are estimated to be in the order of 12 million m³/a (Winde 2004). Assuming an average U-concentration in tailings seepage of 1mg/l about 12t/a of dissolved U are transported from slimes dams into ground- and surface water of the WFS system (up to 30mg Unat/l were found; Winde & de Villiers 2002). With many gold mines having abandoned U-production in the mid 1980's, the associated increase of U-concentration in tailings by a factor of ten is likely to be reflected in the long-term increases of U concentrations in seepage from such slimes dams (U-leaching by sulphuric acid on average had an extraction efficiency of some 90%).

Associated groundwater contamination is exacerbated by the fact that most slimes dams in the area are not lined and deliberately placed - in the FWR area - on top of (permeable) karstic dolomite in order to enhance natural drainage of tailings porewater und reducing the risk of dam failure. However, this practice allows for highly contaminated seepage to enter directly into underlying groundwater.

Different problems are found in the non-dolomitic head water region of the WFS where large parts of the (small) catchment are covered by heavily oxidized old sand dumps and slimes dams. Here much of the baseflow feeding into the WFS actually consist of acidic seepage from slimes dams migrating along shallow aquifers into the stream, as indicated by low pH values (3-4) and high electrical conductivity of the stream water. In dry winter months when no uncontaminated rain water dilutes such seepage, particular high U levels in stream water of the WFS are likely. This even more so since the very source of the WFS is buried under tailings deposits.

Sinkholes filled with tailings material

Soon after dewatering commenced a large number of sinkholes occurred within and near the stream bed of the WFS where it crossed the dewatered compartments. By 1987 some 271 sinkholes with a total volume of 2.45 million m³ had occurred within a narrow band alongside the 30km-long stretch of the stream channel of the WFS where it flows over the three lower dewatered dolomitic compartments (Swart et al. 2003).

In order to reduce the infiltration of stream water and associated cost for pumping it from the mine void back to the surface, affected gold mines attempted to close these conduits by filling some of the larger sinkholes with tailings produced from nearby metallurgical plants. However, in several instances large volumes of slimes pumped into the sinkhole for several months, suddenly disappeared into underlying karst receptacles (cavities). In one particular sinkhole at Venterpost compartment a total volume of 77 000m³ of tailings and waste rock was dumped , of which 35 000m³ of tailings disappeared into the underlying karst aquifer. However, waterborne erosion associated with intense rain fall and flood events in many cases reactivated sinkholes filled in that manner (Swart et al. 2003).

Tailings also entered the underlying karst aquifer via sinkholes occurring in slimes dams placed on dolomite. Slimes directly injected into the dewatered aquifer may act as potential source of U pollution once mining ceases and groundwater tables recover. Using geochemical modelling Dill & James (2003) estimate that seepage from tailings material filled into sinkholes may contain U concentrations between 60mg/l and 310mg/l.

Summary and conclusions

Hosting large volumes of scarce groundwater close to the extremely water-stressed metropolitan areas of Johannesburg and Pretoria, dolomitic karst aquifers in the Far West Rand are of increasing significance as future sources of water supply. However, impacts of deep level gold mining on water availability and quality currently restrict the utilization of these resources. While the cessation of mining and rewatering of dolomitic compartments might cause water availability in the Far West Rand to improve, water quality is likely to remain poor.

The presented analyses of potential U-sources associated with mining suggest that, over time, the significance of different sources for the overall pollution changed. While many contributions to pollution from point sources of U-contamination ceased or will cease, those from many non-point sources will remain significant in the medium to long-term future. This is especially true for seepage from extensive deposits of uraniferous tailings often impacting directly on groundwater. This is of particular concern since high flow rates and low adsorption capacity typical for karst systems allow for far-reaching downstream transport of contaminants. Owing to close interactions between groundwater and surface in dolomitic regions this is also associated with the pollution of surface water systems currently used for drinking water supply (Winde 2005).

In addition, groundwater decanting from the flooded underground mine may in future contribute considerably to U-pollution of surface water. In the head water region of the WFS acidic groundwater currently decants from a flooded mine void with considerably elevated U-levels. Assuming that pre-mining spring flow at all dewatered dolomitic compartments will be re-established after all mining in the area ceased, approximately two thirds of the future dolomitic spring flow into the WFS (some 133Ml/d) will consist of contaminated groundwater decanting from mine voids of the four rewatered compartments. With current pumping rates in these compartments significantly exceeding rates of pre-mining spring flow, considerably higher decant volumes (some 230Ml/d) are possible (Winde 2005).

In view of the different spatial and temporal characteristics of mining-related sources contributing to U-pollution in dolomitic aquifers, further research into transport mechanisms in karst aquifers with very complex surface and groundwater interactions and into associated health risks for downstream user is needed. Based on this strategies on how to manage these important water resources after mining have ceased can be developed.

References

Deelkraal Gold Mine (post 1990): Pilot study to determine uranium levels in urine of un-derground mine workers at Deelkraal Gold Mine.pp.2, unpublished.

Deelkraal Gold Mine (post 1991): Analytical results of fissure water sampling. Unpub-lished. pp. 11).

Dill S, James AR (2003): The assessment of the impact on groundwater quality associated with the backfilling of dolomitic cavities with gold mine tailings. Final report to the WRC, project no. 115-002, January 2003, 93pp.

DWAF (Department for Water Affairs and Forestry) (1996): South African Water Guide-lines. Volume 1: Domestic Water Use. Pretoria

Jennings JE, Brink ABA, Louw A, Gowan GD (1965): Sinkholes and subsidences in the Transvaal dolomite of South Africa. 6th. Int. conf. on soil mechanics and foundation engineering, Montreal.

Mc Lean CS (1994): The uranium industry of South Africa. The Journal of The South Afri-can Institute of Mining and Metallurgy. March, 113-122.

Mrost MJ, Lloyd PJ (1977): Bacterial oxidation of Witwatersrand slimes. Proceed Symp on the recovery of uranium from its ores, Sao Paulo, Aug. 1970, p 223-239

Parker NFE (1982): Survey of the upper Wonderfonteinspruit below Krugersdorp. Report no. E 0323, pp. 25, unpublished.

Pulles W (1991): Radionuclids in South African gold mining water circuits: an assessment of licensing, health hazards, water and waste water regulations and impact on the envi-ronment and workforce. Restricted Report no. 17/91. Chamber of Mine of South Af-rica Research Organisation (COMRO), Johannesburg.

Swart CJU, Stoch EJ, van Jaarsveld, Brink ABA (2003): The lower Wonderfontein Spruit: an expose'. Environmental Geology, 43, 635-653.

Winde F (1996): Untersuchungen zur Herkunft und Schwermetallkontamination von Schlämmen in Nebenvorflutern der Halleschen Saaleaue. In: Raumentwicklung und Umweltverträglichkeit. 50. Deutscher Geographentag. Potsdam 1995. Bd. 1. 206-216.

Winde F, de Villiers AB (2002): The nature and extent of uranium contamination from tai-lings dams in the Witwatersrand gold mining area (South Africa). In: Merkel BJ, Planer-Friedrich B, Wolkersdorfer C [Eds]: Uranium in the Aquatic Environment. Pro-ceedings of the International Conference Uranium Mining and Hydrogeology III and the International Mine Water Association Symposium, Freiberg, Germany, 15-21 Sep-tember 2002, Springer, Berlin, Heidelberg, New York, 889-897.

Winde F (2004): Inventory of uranium sources and transport pathways in the Wonderfon-teinspruit catchment. In: Council for Geoscience (compiler): An assessment of current and future water pollution risk with application to the Mooirivierloop (Wonderfontein-spruit), WRC report project no. 1214, Pretoria, chapter 2, 41pp.

Winde F (2005): Interactions between groundwater and surface water in dolomitic areas af-fected by deep level gold mining – Examples from the Far West Rand goldfield (South Africa). Proceedings of the Biennial Ground Water Conference, 7-9 March 2005, CSIR International Conference Centre, Pretoria, CD-ROM, ISBN 0-620-33659-5, pp.4.

Tracer Tests as a Mean of Remediation Procedures in Mines

Christian Wolkersdorfer

TU Bergakademie Freiberg, Lehrstuhl für Hydrogeologie, Gustav-Zeuner-Str. 12, 09596 Freiberg/Sachsen, Germany, E-mail: c.wolke@tu-freiberg.de

Abstract. Mining usually causes severe anthropogenic changes by which the ground- or surface water might be significantly polluted. One of the main problems in the mining industry are acid mine drainage, the drainage of heavy metals, and the prediction of mine water rebound after mine closure. Consequently, the knowledge about the hydraulic behaviour of the mine water within a flooded mine might significantly reduce the costs of mine closure and remediation. In the literature, the difficulties in evaluating the hydrodynamics of flooded mines are well described, although only few tracer tests in flooded mines have been published so far. Most tracer tests linked to mine water problems were related to either pollution of the aquifer or radioactive waste disposal and not the mine water itself.

Applying the results of the test provides possibilities for optimising the outcome of the source-path-target methodology and therefore diminishes the costs of remediation strategies. Consequently, prior to planning of remediation strategies or numerical simulations, relatively cheap and reliable results for decision making can be obtained by the use of tracer tests.

Introduction

During the last decades hundreds of underground mines were closed and in most of the cases no preliminary investigations of the potential hydrodynamic regime within the flooded mine were conducted. Usually, the operator's interest is to close down the mine as quick as possible and to flood the open underground space in the shortest possible time. Though this can be understood from an economic

point of view, the ecologic consequences of such a procedure are seldom understood in detail.

Several tracer tests in flooded underground mines that were conducted since the early 1990ies, proved that two different types of mines must be distinguished from a hydrodynamic point of view. The first type, exemplified by the Nieder-schlema/Alberoda or Straßberg/Harz tracer tests have a complicated layout of shafts and galleries, whereas the second type, as the Brixlegg/Tyrol and the Ra-benstein/Saxony tracer tests showed, have a simple mine layout.

A basic rule of the source-path-target methodology is to treat pollutants as close at the source as possible (Loxam 1988). Transferred to a flooded underground mine, the source would be the mine workings, the path could either be the drainage gallery or the shaft, whereas the target can be a receiving stream, an industrial plant, or a drinking water supply. For all three cases, solutions have been described in the literature, most of them focussing on either the path or the target.

All the tracer tests conducted by the TU Bergakademie Freiberg research team were multi-tracer tests with 2—6 injection points and up to three different types of tracers, thereunder *Lycopodium* spores, microspheres, Na-fluorescein, and rock salt brine. It could be shown that all those tracer types are suitable for acidic and circum-neutral mine waters and that the recovery rates are high enough to gain evaluable results (Wolkersdorfer 2002).
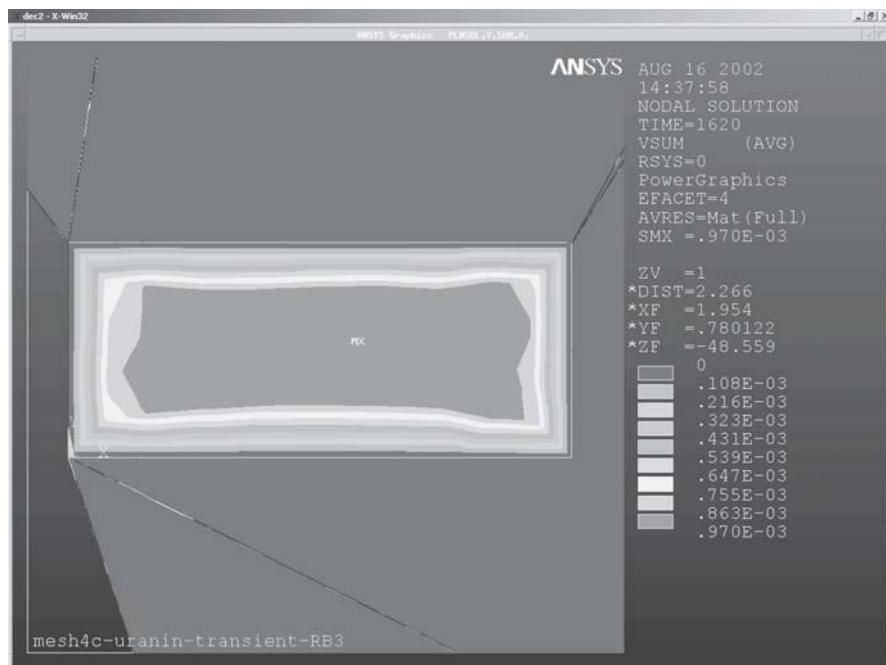
Investigations and Discussion

A total of nine mine water tracer tests were conducted by the Bergakademie Freiberg research team and nearly 30 different flow paths investigated. They have already been described in the literature (see table 1 and Wolkersdorfer 2002) and shall not be further discussed here. Instead, two interesting results from all those tests will be described and explained. At the end a final conclusion will be given.

Before a tracer test is conducted, several months of preliminary hydrogeological and hydrochemical investigations have to be spend. In all those investigations, conducted by Bergakademie Freiberg, flow measurements were a crucial point, as the flow determines the amount of tracer to be used and the possible duration of the tracer test. From that flow usually a simplified analytical piston flow model was applied for the calculation of the tracer amounts to be used and the expected test duration. Certainly, the flow in a conduit network is either laminar or turbulent and the velocity distribution in the conduits definitely does not meet a piston flow distribution, but simplified piston flow is commonly used to interpret tracer investigations (Maloszewski and Zuber 1996). Yet, in all – but one – cases it could be shown that the potential velocities were underestimated and the test's duration overestimated by a factor of 2 … 5. Unfortunately, no general rule for finding a reliable correction factor could be deduced from the current results. Therefore, it must be concluded that simplified piston flow models do not sufficiently enough describe the conduit flow in a flooded underground mine.

Due to the fact that the wall roughness in the adits and galleries is comparably high, a lower effective velocity compared to the velocity calculated by the piston flow model would have been expected. For the Brixlegg/Tyrol tracer test a numerical FEM model with ANSYS-FLOTRAN was set up to further investigate the results obtained (Unger 2002). Though it was possible to calibrate the model and understand some of the results, it became not clear what the reasons for the discrepancy between the two models were (Fig. 1). Similar experiences have been described by Ren et al. (1996) who investigated flow in soil cores and got 0.2 … 3 times higher effective velocities than those compared to a piston flow model.

Another result is more obvious and refers to the ratio of horizontal to vertical lengths of the mine workings. The longer the water flows through horizontal mine workings, the bigger is the effective velocity, because horizontal mine workings, compared to vertical workings (especially shafts) commonly have smaller diameters. This fact was first described in Wolkersdorfer et al. (1997) and since than has been observed in other mines as well. From a practical point of view this behaviour can be used to control the duration of the first flush or the maximum concentration of the pollutants after the mine has been flooded. If the vertical mine workings are dammed and a preferential flow at the horizontal mine workings is obtained, the maximum pollutant concentrations might be expected earlier than

Fig. 1.   Results of the numerical simulation in the Brixlegg Georgi-Unterbau mine. The velocity distribution indicates that the flow in the shaft, though very low, seems to be turbulent (from Unger 2002).

Case studies: active and abandoned Uranium mines

without any technical installations. On the other hand, dams on the horizontal mine workings would minimize the annual pollutant load (indeed not the total load).

One of the main results of the tracer test has been indicated in one of the first paragraphs of this paper. It is connected to the mine geometry and, simplified, means that complicated mine geometries with many shafts and levels have higher effective velocities than mines with a simple geometry. When Uerpmann (1980) investigated potential scenarios for radioactive waste disposal, he assumed that a mine with only one shaft would be optimal to reduce the radio nuclide transport from the source to the anthroposphere. An extreme situation occurred in the Rabenstein/Saxony underground limestone mine, where the tracer needed nearly 2 years to come back to background values (first two rows in tab. 1). This flooded mine has only two shafts and 2 levels and therefore is an extreme simplified type of mine. The other extreme is the Niederschlema/Alberoda mine with extreme quick response times and distances of nearly 3 km (tab. 1, Wolkersdorfer et al. 1997).

In the view of the mentioned source-path-target methodology (Loxam 1988) and the results obtained form the tracer tests it is recommended to install technical installations to separate mine parts with height contamination or acid producing potentials from the other parts of the mine. As fast ground water transport is usually restricted to the upper parts of the mine the dams should be constructed in such a way that the upper parts are separated from the lower parts, where – based on the investigations of the Bergakademie Freiberg – higher pollutant concentrations are usually expected. Using the means of technical installations can reduce both the annual pollutant load and the maximum concentration of the first flush. Yet, the total load over the lifetime of the mine water discharge can not be affected by such means.

By controlling the pollutant source of a flooded underground mine and reducing the pollutants' concentrations, passive treatment technologies can substitute active techniques at an earlier time than without such control measures.

Acknowledgements

Case studies: active and abandoned Uranium mines

Table 1. Distances and mean velocities of worldwide tracer tests in underground mines. Table is given for comparisons only, details concerning geological setting and hydraulic parameters are given in the literature cited. Mean of all 40 tracer tests: 0.3—1.7 m min^{-1} (95% confidence interval of 40 tracer tests); [x] result propably wrong.

Distance, km	v_{eff}, m min^{-1}	v_{eff}, m d^{-1}	Reference
0.015	0.0001	0.1	Wolkersdorfer (unpublished)
0.17	0.0003	0.4	Wolkersdorfer (unpublished)
0.2	0.001[x]	1.4	Aljoe and Hawkins (1993)
0.044	0.004	5.8	Aljoe and Hawkins (1993)
0.093	0.004	5.8	Wolkersdorfer (unpublished)
0.093	0.006	8.6	Wolkersdorfer and Hasche (2004)
0.13	0.01	14.4	Aljoe and Hawkins (1994)
0.077	0.01	14.4	Canty and Everett (1998)
0.78	0.01	14.4	Wolkersdorfer (1996)
0.238	0.014	20.2	Wolkersdorfer (unpublished)
0.048	0.02	28.8	Wolkersdorfer et al. (2002)
0.01	0.03	43.2	Wolkersdorfer et al. (2002)
1.182	0.07	101	Wolkersdorfer (unpublished)
0.35	0.1	144	Mather et al. (1969)
1.181	0.1	144	Wolkersdorfer (unpublished)
3.539	0.1	144	Wolkersdorfer (unpublished)
0.077	0.12	173	Canty and Everett (1998)
0.077	0.14	202	Canty and Everett (1998)
0.283	0.15	216	Wolkersdorfer and Hasche (2004)
1.773	0.15	216	Wolkersdorfer and Hasche (2004)
0.171	0.17	245	Canty and Everett (1998)
6.564	0.17	245	Wolkersdorfer (unpublished)
1.7	0.2	288	Parsons and Hunter (1972)
0.229	0.23	331	Canty and Everett (1998)
3.6	0.3	432	Aldous and Smart (1987)
4.798	0.3	432	Wolkersdorfer and Hasche (2004)
0.15	0.4	576	Mather et al. (1969)
0.172	0.4	576	Wolkersdorfer et al. (1997)
0.216	0.5	720	Wolkersdorfer et al. (1997)
0.22	0.5	720	Wolkersdorfer et al. (1997)
0.2	0.6	864	Mather et al. (1969)
3.18	0.7	1008	Wolkersdorfer and Hasche (2004)
0.5	1.3	1872	Aldous and Smart (1987)
2.25	1.5	2160	Wolkersdorfer and Hasche (2004)
0.776	1.6	2304	Wolkersdorfer et al. (1997)
0.736	1.8	2592	Wolkersdorfer et al. (1997)
0.78	2	2880	Wolkersdorfer et al. (1997)
2.159	5.7	8208	Wolkersdorfer et al. (1997)
2.723	7.9	11376	Wolkersdorfer et al. (1997)
0.5	11.1	15984	Aldous and Smart (1987)

Case studies: active and abandoned Uranium mines

References

Aldous P J, Smart P L (1987) Tracing Ground-Water Movement in Abandoned Coal Mined Aquifers Using Fluorescent Dyes. Ground Water 26(2):172–178.

Aljoe W W, Hawkins J W (1993) Neutralization of Acidic Discharges from Abandoned Underground Coal Mines by Alkaline Injection. Report of Investigations – US Bureau of Mines 9468:1–37.

Aljoe W W, Hawkins J W (1994) Application of aquifer testing in surface and underground coal mines. Proceedings, 5th International Mine Water Congress, Nottingham, UK 1:3–21.

Canty G A, Everett J W (1998) Using tracers to understand the hydrology of an abandoned underground coal mine, vol. 15. Princeton: Proceedings, 15th Annual National Meeting – American Society for Surface Mining and Reclamation: 62–72.

Loxam M (1988) The predictive assessment of the migration of leachate in the subsoils surrounding mine tailings and dredged spill sites. In: Salomons W, Förstner U. Environmental management of solid waste – Dredged materials and mine tailings. Berlin u.a.: Springer: 3–23.

Maloszewski P, Zuber A (1996) Lumped Parameter Model for the Interpretation of Environmental Tracer Data. IAEA-TECDOC – Manual on mathematical models in isotope hydrogeology 910:1–58.

Mather J D, Gray D A, Jenkins D G (1969) The use of tracers to investigate the relationship between mining subsidence and groundwater occurrence at Aberfan, South Wales. J Hydrol 9(2):136–154.

Parsons A S, Hunter M D (1972) Investigation into the movement of groundwater from Bryn Pit above Ebbw Vale, Monmouthshire. Water Pollut Control 71:568–572.

Ren G-L, Izadi B, King B, Dowding E (1996) Preferential Transport of Bromide in undisturbed Cores under different Irrigation Methods. Soil Sci 161(4):214–225.

Uerpmann E-P (1980) Hydrogeologische Fragen bei der Endlagerung radioaktiver Abfälle. Clausthal: Unveröff. Diss. TU Clausthal: 128.

Unger K (2002) Hydrodynamische Verhältnisse im gefluteten Unterbau des Bergkwerks Großkogel/Tirol – Numerische Modellierung mit ANSYS-FLOTRAN. Freiberg: Unveröff. Dipl.-Arb. TU Bergakademie Freiberg: 117.

Wolkersdorfer C (1996) Hydrogeochemische Verhältnisse im Flutungswasser eines Uranbergwerks – Die Lagerstätte Niederschlema/Alberoda. Clausthaler Geowissenschaftliche Dissertationen 50:1–216.

Wolkersdorfer C (2002) Mine water tracing. Geological Society Special Publication 198:47–61.

Wolkersdorfer C, Hasche A (2004) Tracer Investigations in flooded mines – The Straßberg/Harz Multitracer Test. Conference Papers, vol. 35. Wien: Umweltbundesamt: 45–56.

Wolkersdorfer C, Trebušak I, Feldtner N (1997) Development of a Tracer Test in a flooded Uranium Mine using Lycopodium clavatum. In: Kranjc A. Tracer Hydrology 97, vol. 7. Rotterdam: Balkema: 377–385.

Wolkersdorfer C, Hasche A, Unger K, Wackwitz T (2002) Tracer Techniken im Bergbau – Georgi-Unterbau bei Brixlegg/Tirol. Wissenschaftliche Mitteilungen 19:37–43.

Case studies: active and abandoned Uranium mines

Typification of Radioactive Contamination Conditions in Ground Water at the Semipalatinsk Test Site.

Ella Gorbunova

Institute for Dynamics of Geospheres, Russian Academy of Sciences, 38-1 Leninsky prosp., Moscow, Russia, E-mail: emgorbunova@mtu-net.ru

Abstract. For the first time the complex investigations on study of radioactive contamination in ground water at the underground nuclear explosion sites were carried out at the Semipalatinsk Test Site. Definition of the radioactive contamination aureoles of the basic water-bearing horizon located within the exogenous rocks fracturing area is based on the proper analysis of the experimental data on the biologically hazardous radionuclides content. Data on the current radionuclide activity in water-bearing horizon can be used for the retrospective analysis of the radioactive contamination of geological environment.

Introduction

One of the most important scientific and technical problems is the radiation environment monitoring on the areas of higher risk including the former test sites.

Complex scientific research on radioactive contamination study of water-bearing horizon referred to weathered fracturing zone of Paleozoic rocks occurring at the depth of 10 to 30 m within the radius of 0.2 to 2.3 km away from epicenter of underground nuclear explosion (UNE) at 1003 and 1388 sites were carried out in the framework of the project K-810 International Science and Technology Center at the Semipalatinsk Test Site (STS). The area selection depended on the level of site knowledge and type of UNEs. Findings of activities were used as the base data for typification of radioactive contamination conditions in ground water at the STS area.

17 years later after the camouflet UNE conduction in well 1388 the basic contamination in ground water was localized within cone of depression which has limited distribution in the central structural tectonic block (Fig.1). Piezometric surface within the radius of 0.5 km and far from UNE epicenter reached the initial

points. Basic ground water discharge carries out in the north-eastward in accordance with major flow direction (Fig.2).
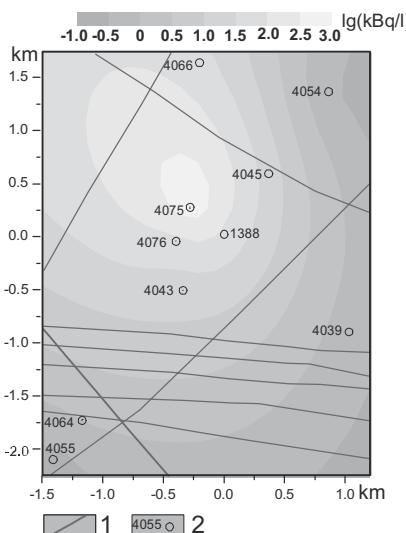
Gamma-activity of bedrocks (Paleozoic) is changed in the near zone at the distance of up to 0.3 km (Fig.3). In the well 4075 which was drilled after the UNE conduction the displacement of the gamma-activity main peak was determined upwell by 10 m. Probably, that was connected with piezometric surface recovery. According to condition in 10/21/88 – the depth of occurrence is 40.7 m, according to condition in 03/01/04 – 16.1m.

Main source of radionuclide transfer into ground water is focused in fractured zone of fault occurrences, adjacent with zones of fracturing, related to chimney of UNE. The structural boundary reduction which is the partition between weathered, fractured and comparatively solid Paleozoic rocks runs up to 20 m, at the distance of 0.3 km away from UNE epicenter was traced (Fig.4).
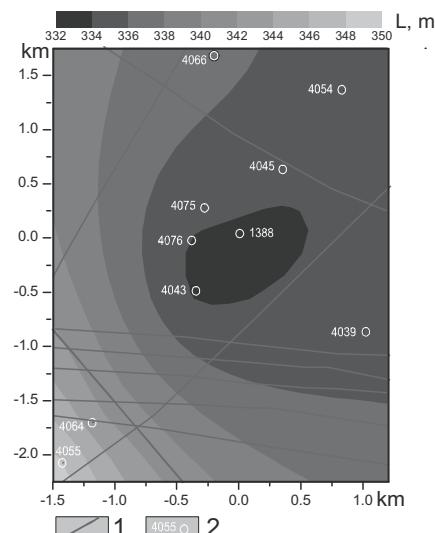
Contour asymmetric stretched in the north-eastward is conditioned by massif anisotropy, general north-west spread, and occurrence of structural forms (folds) with well-defined dip plane of the rocks in the north-eastward.

Formation of additional source of radionuclide transfer into ground water was presumably caused by man-caused renovation of south fault system which served as a south boundary of the central structural tectonic block. Formation of zones of some fraction development at the level of UNE conduction contributed to radioactive inert gases distribution in tectonically weak zones.

Possibility of radionuclide transfer into ground water from surface is impossible. Data of gamma spectrometric measurements conducted at the height of 0.3 m

Fig. 1. Scheme of ^{3}H distribution (max.values, lg(kBq/l; 1 – fault; 2 – well and its number).

Fig. 2. Piezometric Surface (absolute point, m; as of 11/01/03; 1 – fault; 2 – well and its number).

Case studies: elevated uranium in groundwater without uranium mining impact
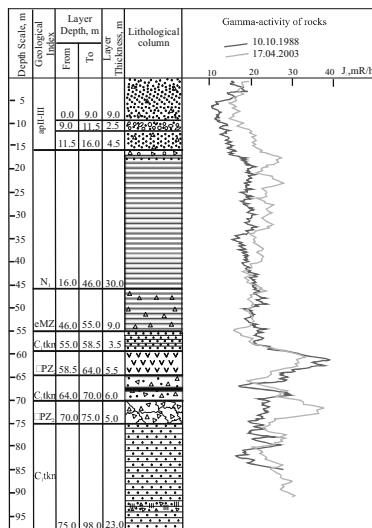
and 1 m, and the results of soil sampling in the near-mouth area of the well 1388 indicate radioactive background within limits of allowable standards.

According to prediction modeling data of radionuclide migration in ground water conducted at the site 1388 the aureole of radioactive contamination in ground water along the radioactive tracer which extends in accordance with filtration characteristics of underground flow can be determined at the site border 3 km away from epicenter, only 150 years later after UNE conduction.
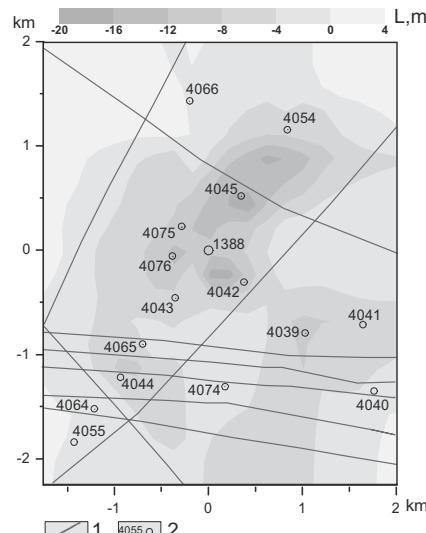
On October 1965, conduction of UN excavating explosion for civil purposes at the well 1003 was accompanied with base wave formation extending in the zone of 600 m in diameter and dust column of 120 m in diameter (Izrayl et al. 1970). Ground radioactive contamination within the radius of 75 m away from epicenter is determined by initial ground ejection out of crater. Primary trace of radioactive contamination of day surface stretched in the north-eastward formed due to fall-out.

Presence of spots of ground radioactive contamination within the studied area determined at the bulk zone of ejected grounds along axis of radioactive trace and at the distance of 0.2 – 0.4 km in south-east of the explosion epicenter was confirmed in accordance with radiometric observations in 1999.

Nonuniform tectonic structure of the Site is shown in variability of paleorelief observed on upper part of rocks. The allocation of experimental and observant wells to buried slope of paleovalley determines the nature of water-bearing horizon developed in zone of jointing of Paleozoic rocks as confined-unconfined one. The general unloading of the ground water carried out in the north-east direction (Fig.5).



Fig. 3.   Results of well 4075 radiometry.
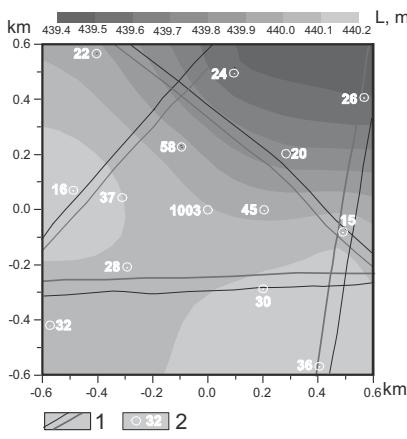
Fig. 4.   Change in Depth of Occurrence of Structural Boundary (m; 1 – fault; 2 – well and its number).

Case studies: elevated uranium in groundwater without uranium mining impact

Within the site of the well 1003 location the irregular radioactive contamination in ground water was revealed 40 years late after UNE conduction. Main aureole of ³H maximal concentration was referred to the effected zone of sub latitudinal fault, probably, man-made renewed during UNE (Fig.6). Hence, conduction UN excavating explosion resulted in not only formation of radioactive spot traced on the surface, but in massif radioactive contamination at the level of UNE conduction.
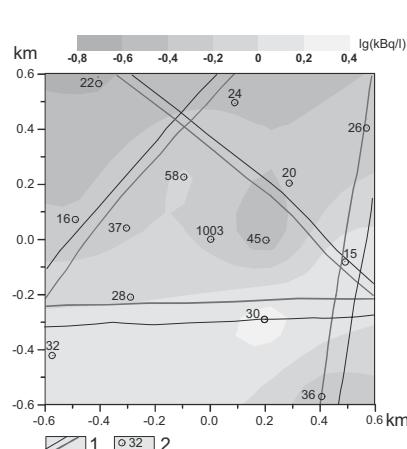
Revealed regularities of current radioactive contamination distribution in ground water within the selected studied areas were used for method elaboration of radiation probing of the STS area. During the period of 1965-1989, 131 UNEs of camouflet type with range of yields from 0.001 to 150 kt and 2 UN excavating explosions at 1003 and 1004 wells were carried out at STS (Table 1). These explosions resulted in radioactive products release into the atmosphere in aerosol and gas phases with formation of craters on the surface.

The part of UNEs of incomplete camouflet type was accompanied by insignificant outflow of radioactive inert gases (RIG). There were determined 7 incidents of with non-standard situations which are characterized by early head outflow of RIG in the atmosphere (Adushkin 2000).

The fulfilled research activities on radiation monitoring of the STS area allowed to determine and delineate the radiation contamination traces which are due to low atmospheric and aboveground explosions (Shkol'nik et al. 2003). Formation of local radioactive spots is due to UNEs of excavating type and with non-standard situations. Increased dose rates of gamma radiation were traced at the sites of experimental wells they are characterized by early RIG outflow.


Fig. 5. Piezometric Surface (absolute point, m; as of 02/01/03; 1 – zone of dynamic effect of the fault; 2 – well and its number).

Fig. 6. Scheme of ³H distribution (max.values, lg (kBq/l; 1 - zone of dynamic effect of the fault; 2 – well and its number).

Case studies: elevated uranium in groundwater without uranium mining impact

Specific of radionuclide distribution in natural landscapes within the area of radioactive trace and their accumulation at higher areas of small hills determines the conditions of possible local contamination of surface and ground water due to initial primary fallout of aerosols and as the result of following washing-off, transfer and infiltration of radioactive particles from soil surface.

Areas of ground water discharge into surface watercourses at the places of steadfast confining layer absence stand as the second contamination centers of primary water-bearing horizon from the surface. Therefore, when typification of conditions of radioactive contamination in ground water it is necessary to provide scheme-mapping of regional confining layer spread at the STS area.

Besides radionuclide migration from "surface", there is risk of radioactive contamination from "low parts" at the areas of UNE conduction. The breaking-down moment of the cavity determined in many respects the nature of radioactive contamination in all zones of man-made fracturing. A number of radionuclides (volatile, having gas predecessors, and tritium) which were not fixed in melt in full released out of cavity and dispersed within zone of man-made fracturing (Izrayl and Stukin 2000). Formation of aureole of radioactive contamination in ground water is due to gradual impoverishment of the center that contains long-living radionuclides.

The local zones with man-made disturbed regime in ground water associated with general change in geological environment were determined for the areas of UNE conduction (Gorbunova 2003). Formation of cones of depression within the radius of 0.3 - 0.5 km away from epicenter was evidence of establishment of hydraulical connections between water-bearing horizon referred to weathered roof of host rocks and to zones of man-made fracturing which are enriched with RIG.

Accordingly, definition of the sites with man-made disturbed regime of ground water in accordance with archival and current data will allow to determine existence of potential sources of concealed radionuclide migration from zones of man-made fracturing. The tracing of counter spread of post explosive deformations on the day surface by different methods (reconnaissance observation of UNE epicenters, results of remote probing) serves as indirect corroboration of massif irreversible deformation at depth.

During UNE conduction of incomplete camouflet type and with non-standard

Table 1.

Group №	Quantity of UNEs	Time of RNG discharge	UNE depth m/kt$^{1/3}$	Complete gas content in rocks, %	Remark
1	30	10 sec - 20min	70 - 960	4.5 - 18	RIG discharge outside pipe of well
2	40	25 - 60min	88 - 236	2.6 - 14.4	Late discharge of RIG in the epicenter
	30	1 - 5h			
	10	5 - 25h			
3	23	-	96 - 225	4 - 12	RIG discharge was absent

Case studies: elevated uranium in groundwater without uranium mining impact

situations associated with head inflow of RNG the possibility of radioactively contaminated in ground water of the epicenter zone is high. The sites of well flowing during UNE conduction was special hazard since during the first seconds and hours of pressure excessive outbreak the transfer of active radioactive product into water-bearing bed was possible, accordingly.

The special activities on radionuclide migration study at the determined areas were not carried out. But results of sampling of the nearest wells determine the high radionuclide content. Particularly, in the unused well 1419 located at the distance of 1.5 km south-east of well 1069 where was ejection of casing pips and driving complex, the tritium concentration was more than 1000 kBk/l (Logachev et al. 2002).

Probably, the ground water exposed to radioactive contamination as well as site of well location where coal-bed fire was determined. So, 15 years later after the UNE conduction the epicentral zone failure with formation of explosion crater 115 m in diameter and depth of 30 m occurred in the well "Glubokaya" in April, 1992 (Logachev et al. 2002). Consequently, the sites of UNE conduction of incomplete camouflet type and with non-standard situations should be referred to the objects of higher risk.

Special emphasis should be given to assessment of man-made activation on effected zones of faults connected with UNE. Tracing of fault main systems of defined in accordance with archival geologic-geophysical data should be confirmed by the results of remote probing. It is recommended to use computer-aided system of satellite images LESSA allowing to specify the structure and nature of effected zones of faults as well as to contour the allocation area of post explosive deformations on the day surface connected with UNE (Gorbunova and Ivanchenko 2004).

Any man-made load onto man-made changed massif especially at the level of depths which correspond to hypsometric position of UNE hypocenter is peculiar trigger for massif "simplification" (topology) due to formation of additional fracturing and renew of present. Particularly, conduction of whole series of non-nuclear experimental and calibration explosions to destruct 13 unused wells up to depth of 10 m and over the range of 50 – 580 m with charge of yield up to 50 – 100 kg, 2 t and 25 t were recorded by all seismic stations in 1997 - 1998 (Shkol'nik et al. 2003). Then, formed craters were covered up with earth and leveled to initial state.

The openworking coal field Karazhir in the central part of STS is connected with treat of possible contaminated ground water involving into areas of cone of depression developing due to drainage activities as well as with probable accidents – failure of pit wall by blowout of hydrocarbon gases. It should be noted UNEs were conducted to the south and south-east of the pit. Dominant direction of regional fault is the north-west.

During radioecological assessment of the STS condition it is necessary to provide area cadastre making up with criterion elaboration on vulnerability of ground water upon the following gradations: unprotected, weakly protected and conditionally protected. The protectability of ground water radioactive contamination from "surface" means the interception of water-bearing horizon by low-penetrating (waterproof) sediments which impede penetration of radionuclides

Case studies: elevated uranium in groundwater without uranium mining impact

from surface into ground water. Reliability of radionuclide preservation out of "bottom" guarantees hydraulical connection absence between water-bearing horizon and zones of man-made fracturing. For the mapping of natural protectability of STS area it is necessary to counter the zones of mechanical effect of UNE. The block massif structure should be taken into account during the engineering-geological characteristic of the area.

The hydrogeological analysis of the situation should be carried out in accordance with condition study of distribution and filtration features of water-bearing filtration. The special emphasis should be given to the sites of natural and man-made discharge of ground water. To the last ones relate the areas of established hydraulic connection between artificial reservoirs formed during the UN excavating explosions and non-standard situations as well as the zones of split-off effects are characterized by alteration of watered rock parameters (increase, reduction of thickness, penetrability) under the UNE impact. The zones of massif irreversible deformations which include bands of man-made fracturing enriched by RNG are potential radionuclide sources.

Further elaboration of general conception of typification of radioactive contamination conditions in ground water will serve as base of radioecological assessment of situation at the STS area.

References

Adushkin VV (2000) Effect of geological factors on radioactive product distribution during underground nuclear explosions - Radioactivity during nuclear explosions and accidents. Proceedings of the International Conference. Moscow April, 24-26 2000. St. Petersburg: Hydrometeoizdat Volume 1: 585—593

Gorbunova EM (2003) Formation peculiarities of man-caused disturbed regime in ground water. The third All-Russian Scientific Conference "Physical problems in ecology" (Ecological physics). Reports, №11 M, MSU: 70—78

Gorbunova EM, Ivanchenko GN (2004) Study of Geological Structure Around Boreholes at the Semipalatinsk Test Site Using Computer-Aided Interpretation of Satellite Images. International Conference on Monitoring of Nuclear Tests and Their Consequences. NNC Bulletin. Kurchatov, NNC: 76—81

Izrayl YuA et al. (1970) Radioactive contamination of natural environment during underground nuclear explosions and prediction methods. Leningrad, Hydrometeoizdat: 68

Izrayl YuA, Stukin ED (2000) Phenomenology of ground water contamination after underground nuclear explosion - Radioactivity during nuclear explosions and accidents. Proceedings of the International Conference. Moscow April, 24-26 2000. St. Petersburg: Hydrometeoizdat, Volume 1: 616—623

Logachev VA (2002) Nuclear tests in USSR: Current radioecological condition of the sites. M, IzdAt: 652

Shkol'nik VS et al. (2003) The Semipalatinsk Test Site (creation, activity, conversion). Almaty: 344

Case studies: elevated uranium in groundwater without uranium mining impact

Spatial and temporal variations in the uranium series background in Alpine groundwater

Heinz Surbeck[1], Otmar Deflorin[2], Olivier Kloos[1]

[1]Center of Hydrogeology (CHYN), University of Neuchatel, Emile-Argand 11, CH-2007 Neuchatel, Switzerland, E-mail: heinz.surbeck@unine.ch
[2]Cantonal Laboratory and Food Inspectorate, Planaterrastr. 11, CH-7000 Chur, Switzerland

Abstract. In areas with uranium mining it is hard if not impossible to decide if increased uranium, radium or radon levels are due to these industrial activities or if they are just natural variations. There are rarely reliable data available taken prior to mining. Therefore our data from the Swiss Alps, a region with known uranium mineralizations but no uranium mining may help to get an idea about the range of spatial and temporal variations of the natural background. They may also serve as a baseline against which possible influences of climate change or future industrial activities in the Alps can be compared.

Introduction

A search for uranium mineralizations in Switzerland started around 1950 (Payot 1953) with the measurement of ^{222}Rn and ^{226}Ra in numerous Swiss springs, neglecting the already then known fact that temporal variations can mask spatial ^{222}Rn variations (Perret 1918) and that radium is a bad proxy for uranium because of it's very different geochemical behavior. The study thus did not give any useful hint where to look for uranium. More successful have been dose rate measurements above ground and in tunnels excavated for the then fast developing Alpine hydroelectric plants (Gilliéron 1988). However, as is the case for most minerals in the Swiss Alps, ore deposits turned out to be frequent but too small to be mined commercially. Some tons of uranium rich ore from the only exploration tunnel ever dug were sold to France and some hundred kg finished in university collections.
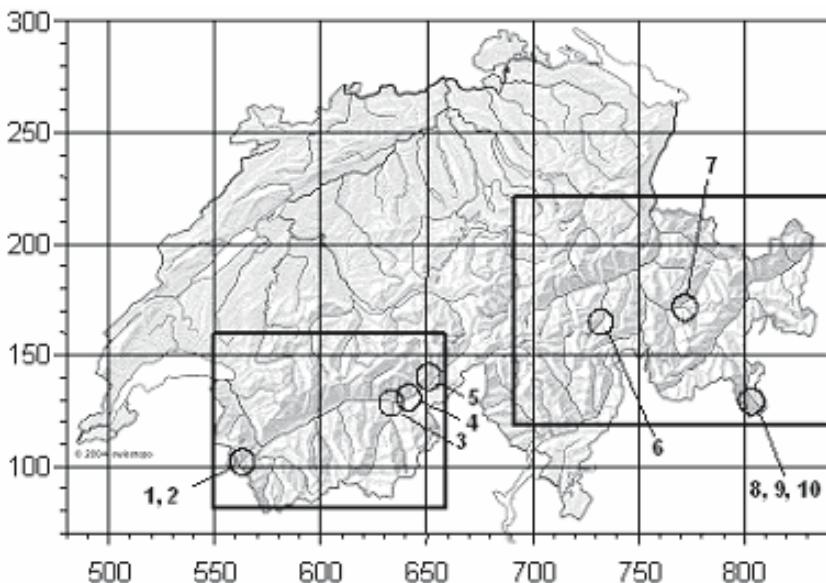
There have been small coal, lead, copper, gold and iron mines in the Swiss Alps, some with increased uranium concentrations (Woodtli et al. 1987), but none

has been a lasting commercial success. They have never been productive enough to lead to important tailings.

The largest tailings ever seen in the Swiss Alps are currently building up. They are the result of the ongoing excavation of two large railway tunnels, both together more than 80 km long. Systematic and at some places continuous dose rate measurements of the extracted material showed that no important uranium ore deposit has been hit so far .

To summarize, there are numerous small uranium anomalies in the Swiss Alps, but there has been no important mining activity that could have led to considerable groundwater contamination. We thus consider the Swiss Alps as a favorable area to study natural variations in the uranium series concentrations in groundwater.

The work presented is the result of several studies carried out between 1995 and 2005 (Deflorin and Surbeck 2002, Deflorin 2004, Gainon 2003, Kloos 2004 and unpublished internal reports of the Swiss Federal Office of Public Health) in the Cantons of Grisons (eastern part of the Swiss Alps) and Valais (western part of the Swiss Alps). The two areas covered are shown in Fig.1. We consider the large spatial and temporal variations observed for uranium, radium and radon concentrations in groundwater as being representative for a young mountain range with complex geologic and tectonic features. We have no intention to propose our data as beeping representative for mature old ranges like the Erzgebirge, but they show

Fig. 1. Swiss map with the study areas outlined. Circles show the sites of the springs (Nr. 6 to Nr. 10) and public fountains (Nr. 1 to Nr. 5) where time series have been taken. 1: Châtelard Frontière, 2 : Finhaut, 3 : Visp, 4 : Brigerbad-Dorf, 5 : Lax, 6 : Vals Leis, 7 : Bergün, 8 : Poschiavo Pedecosta, 9 : Poschiavo Al Bait, 10 : Poschiavo Sass da Li Rondolli. Coordinates given are the Swiss National N-S/W-E km coordinates.

Case studies: elevated uranium in groundwater without uranium mining impact

clearly how large variations can be, even without industrial impact. Our data may also serve as a baseline against which possible impacts of climate change or future industrial activities in the Alps can be compared.
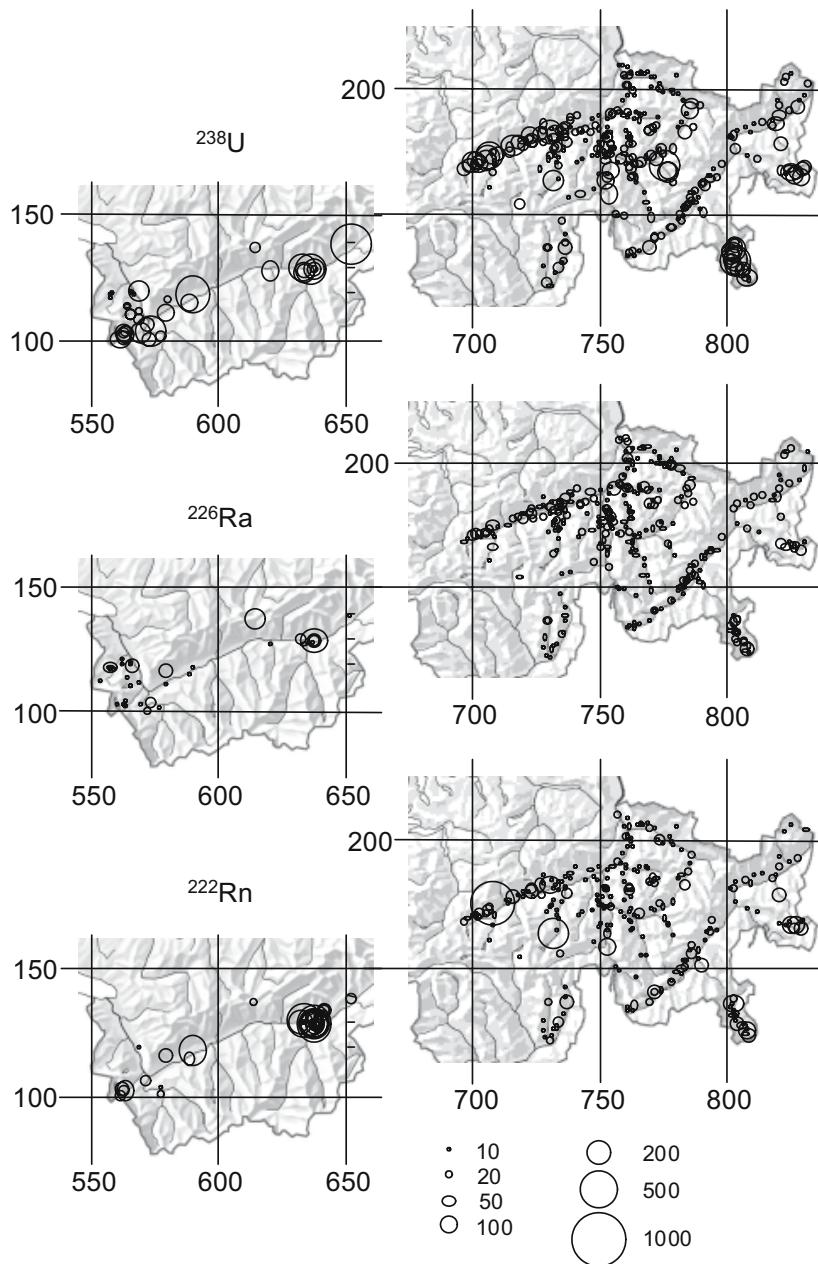
We are well aware of the fact that even dense spatial and temporal sampling will never cover all possible variations. We thus also present what we think we have learned from these data about processes leading to these large variations.

Only uranium series data are shown here, although [228]Ra has also been measured for all Canton of Grisons samples (for these additional data see Deflorin 2004, for the analytical method used Eikenberg et al. 2001).

Experimental

All samples have been taken either by cantonal drinking water inspectors, by hydrogeologists or by scientific personnel with a good knowledge in water sampling. Depending on the measurement technique used, 10 to 250 ml samples were taken in glass bottles for the radon determination and approx. 250 ml (unfiltered, not acidified, PE- or PET-bottles) for uranium and radium determination. Samples have been taken as close as possible to the springs or in the case of pumped groundwater as close as possible to the pumps, after sufficient pumping time to have a representative sample. A total of approx. 400 different springs and groundwaters have been sampled in the Canton of Grisons and approx. 50 in the Canton of Valais. Samples in the Canton of Grisons cover all public drinking water supplies and all known mineral water springs. Sampling in the Canton of Valais has been more biased towards springs that seemed to be interesting from a geological point of view. For 5 springs and 5 public fountains (locations see Fig.1) time series where taken over periods from months to several years, in general a sample a month.

Uranium has either been determined by ICP-MS or by alpha spectrometry (Surbeck 2000). ICP-MS data have been converted to ^{238}U activity by applying a factor of 12.4 mBq/l per ppb U. All ^{226}Ra determinations have been made by alpha spectrometry (Surbeck 2000). For ^{222}Rn either bubbling in a closed circuit (measurement in the gas phase with a RAD7 (Niton)) or liquid scintillation counting after liquid-liquid extraction (extraction with MaxiLight (Hidex), measurement with Tricarb (Canberra Packard) or Triathler (Hidex)) has been used. For measurement uncertainties see error bars in Fig. 4.

Case studies: elevated uranium in groundwater without uranium mining impact
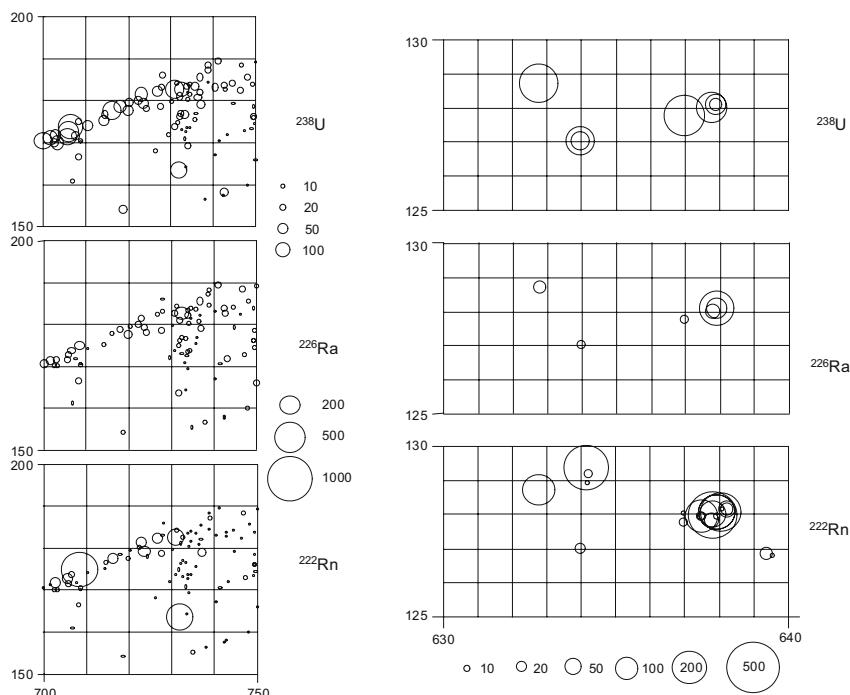
Fig. 2.   Spatial distribution for ^{238}U, ^{226}Ra and ^{222}Rn. Units for ^{238}U and ^{226}Ra are in mBq/l, for ^{222}Rn in Bq/l. For measuring uncertainities see Fig.4. Coordinates given are the Swiss National N-S/W-E km coordinates.

Case studies: elevated uranium in groundwater without uranium mining impact

Results and Discussion

Fig. 2 shows the spatial distributions for ^{238}U, ^{226}Ra and ^{222}Rn on a 50 km grid and Fig. 3 zoomed parts at 10 km and 1 km grid sizes. They show how large spatial frequencies can be. Cumulative frequencies for the Canton of Grisons data can be seen in Fig. 4. At low concentrations not all the points are drawn. Up to a cumulative frequency of 80 % every 10th value is drawn, from 80 % to 90 % every 5th, from 90 % to 95 % every second. All values are drawn above a cumulative frequency of 95 %. Data for drinking water and data for mineral water springs are drawn separately.

No cumulative frequencies for the Canton of Valais data are presented because of the potential sampling bias mentioned above.
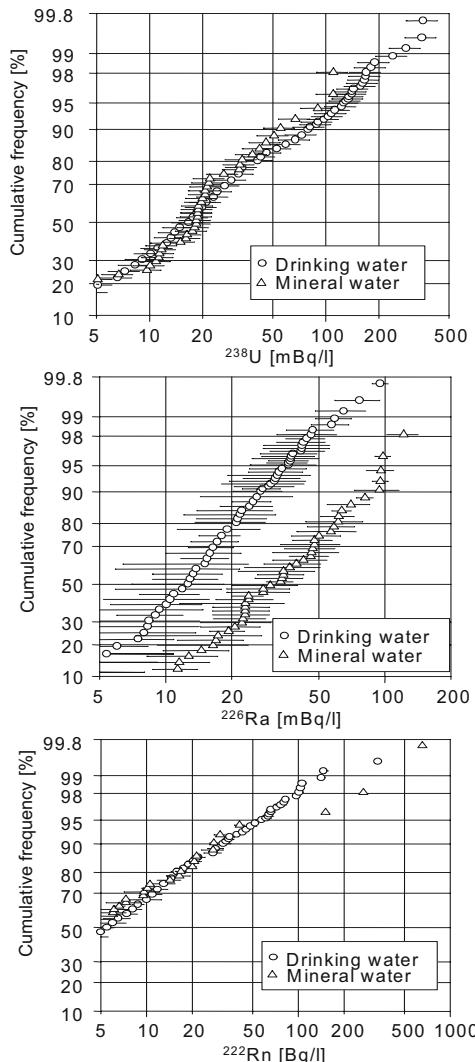
Cumulative frequencies clearly show lognormal distributions. Uranium and radon frequency distribution are very similar for drinking water samples and mineral water samples respectively. However for ^{226}Ra the two distributions are clearly different. This behavior may be due to the fact that waters with low oxygen concentrations are not used as drinking water whereas mineral waters in general are anoxic. In anoxic groundwater there is no iron-hydroxide precipitation and thus dissolved radium is not adsorbed. Large sampling campaigns like the one we

Fig. 3.   Zoomed parts of Fig.2, showing high spatial frequencies. Units for ^{238}U and ^{226}Ra are in mBq/l, for ^{222}Rn in Bq/l. For measuring uncertainties see Fig.4.

Case studies: elevated uranium in groundwater without uranium mining impact

did in the Canton of Grisons, with a total of more than 400 samples, take some time. In our case three months from March 2002 until May 2002. During this period precipitations have been frequent but irregular and snowmelt at higher altitudes had just started.

We thus can't be sure that we did not mix up spatial and temporal variations. To get an idea how large temporal variations can be we sampled 5 springs in the Can-
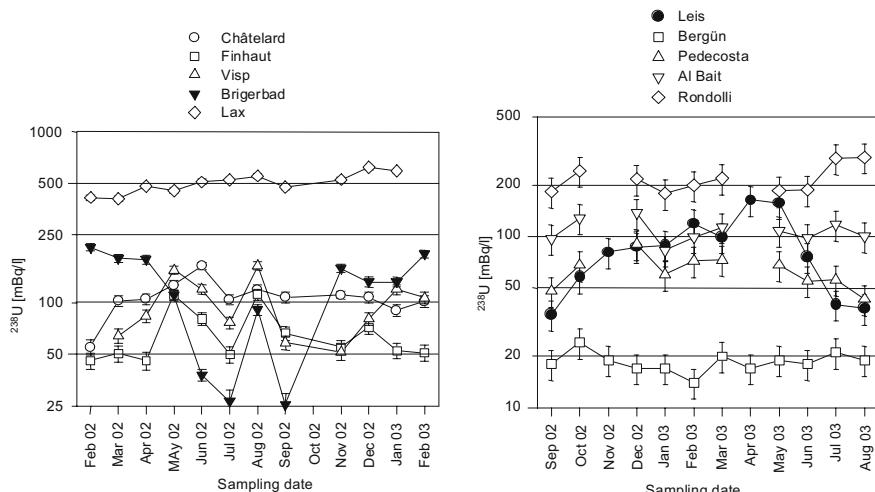
Fig. 4.   Frequency distributions for the Canton of Grisons data. Drinking water : 360 samples, mineral waters : 42 samples. Error bars correspond to 1 sigma counting statistics for ^{226}Ra and ^{222}Rn and to a total uncertainity of 20 % for the ICP-MS uranium data.

Case studies: elevated uranium in groundwater without uranium mining impact

ton of Grisons and 5 public fountains in the Canton of Valais monthly for a whole year. Fig. 5 shows the uranium data for these samples. Variations are considerable even for the 5 Grisons springs where anthropogenic influences can be excluded. The extreme variations for one of the the public fountains (Brigerbad-Dorf) turned out to be an intentional mixing, due to a drought, with water from a nearby village. Claimed origins of fountain waters may sometimes just be wishful thinking.

We assume that monthly sampling has been adequate for the type of springs considered. However we are well aware of the fact that a better temporal resolution may bring to light even larger variations, for example in Karst springs (Eisenlohr and Surbeck 1995, Savoy and Surbeck 2003, Bossy and Surbeck 2004).

Sampling in the Canton of Grisons has been very dense, but it is impossible to sample every spring or well in the whole Swiss Alps. As the time series show it would even be necessary to take samples at least once a month.

Therefore some ideas about the geochemical processes behind are needed for a more targeted search. First steps to a conceptual model are the following trends we have seen in our data : 1) radon concentrations above 50 Bq/l are very local phenomena, connected to radium adsorptions on iron hydroxides produced by the mixing of oxygen rich young waters with old anoxic waters (Gainon 2003), 2) anoxic waters from limestone formations generally show increased ^{226}Ra concentrations (up to 200 mBq/l). The higher the temperature the higher the ^{226}Ra concentration (Kloos 2004), 3) increased uranium concentrations (> 100 mBq/l ^{238}U) are found in a) cold, oxygen rich, low mineralized waters from crystalline rocks with at least part of the uranium present as UO_2^{2+} and b) cold, highly mineralized (mainly sulfate) waters with no significant sign of UO_2^{2+}, but strong evidence for complexation with CO_2.

Fig. 5.   Uranium time series for the 5 springs and 5 public fountains marked in Fig.1.

Case studies: elevated uranium in groundwater without uranium mining impact

Conclusions

Large spatial and temporal variations in the uranium series concentrations have been observed in groundwaters in an area rich in poor uranium ore deposits, but without any important mining activity. Our data are for a young mountain range, but may also be of some help to assess claims about the impact of mining activities elsewhere. In addition these data can be used as a baseline against which impacts of climate change or future industrial activities in the Alps can be compared. Temporal variations turned out to be important, masking or simulating at least some spatial variations. First trends observed in our monitoring data open the way to a conceptual model for a more targeted sampling.

Acknowledgments

References

Bossy F., Surbeck, H. (2004), La sursaturation gazeuse dans les sources karstiques; exemple de la source de la Neirivue (Gruyère, Préalpes fribourgeoises), In : Proc. 2nd Swiss Geoscience Meeting, Nov. 19-20, 2004, Lausanne, Switzerland

Deflorin, O. , Surbeck, H. (2003), Natürliche Radionuklide im Trinkwasser am Beispiel des Kantons Graubünden. GWA (Gas, Wasser, Abwasser), 1, 2003, 40 – 45.

Deflorin, O. (2004) Natürliche Radionuklide in Grundwässern des Kantons Graubünden, PhD thesis, University of Neuchâtel, Switzerland

Eikenberg, J., Tricca, A., Vezzu, G., Bajo, S., Ruethi, M. and Surbeck, H.,(2001), Determination of Ra-228, Ra-226 and Ra-224 in natural water via adsorption on MnO2-coated discs, J. Environmental Radioactivity 54 (2001), 109-131

Eisenlohr L., Surbeck, H. (1995), Radon as a natural tracer to study transport processes in a karst system; an example from the Swiss Jura, C.R. Acad. Sci. Paris, t.321, série IIa, 761-767

Gainon F. (2003), Etude hydrogéologique de la source radioactive de St-Placidus, Disentis, canton des Grisons, Diploma thesis, University of Neuchâtel, Switzerland

Gilliéron, F. (1988), Zur Geologie der Uranmineralisation in den Schweizer Alpen, Beitr. Geol. Schweiz, geotechn. Ser. ,77

Kloos, O. (2004), Hydrochimie et hydrogéologie des sources thermales de Brigerbad (Valais), Diploma thesis, University of Neuchâtel, Switzerland

Payot, R. (1953), Distribution de la radioactivité en Suisse, PhD thesis, Univ. of Neuchâtel, Switzerland

Perret, H. (1918), Radioactivité des eaux neuchâteloises et Seelandaises, PhD thesis, Univ. of Neuchâtel, Switzerland

Savoy ,L., Surbeck, H. (2003), Radon and CO2 as natural tracers in a karst system, In : Proc. 7th Int. Conf. on Gas Geochemistry, ICGG-7, Sept. 22-26, 2003, Freiberg, Germany

Surbeck, H. (2000), Alpha spectrometry sample preparation using selectively adsorbing thin films, Applied Radiation and Isotopes 53 (2000) 97-100

Woodtli, R., Jaffé, F., von Raumer, J.(1987) Prospection minière en Valais : le projet Uromine, Beitr. Geol. Schweiz, geotechn. Ser., 72

Case studies: elevated uranium in groundwater without uranium mining impact

Distribution Pattern Uranium Isotopes in Lake Sediments

Ashraf Khater

National Center for Nuclear Safety and Radiation Control, Atomic Energy Authority P.O. Box 7551 Nasr City, Cairo11762, Egypt.
Email: khater_ashraf@yahoo.com

Abstract. Sediment samples from three Egyptian Lakes' (Qarun, Bardawill and Edku) were collected to study the environmental behavior of naturally occurring radionuclides in these lakes. The three lakes have different hydro-geological, physical and chemical features, which could affect the concentrations and the distribution pattern of uranium isotopes in the lakes' sediments. In this study, the specific activity of uranium isotopes (U-238, U-235 and U-234) were measured using alpha spectrometers after radiochemical separation and uranium alpha source electroplating on stainless steel disk. The distribution patter of uranium and the affects of sediment texture, organic matter contents, and other ecological parameters were investigated.

Introduction

Radioactivity substances occur naturally in the environment, but can also result from human activity. It is now more than half a century since the discovery of nuclear fission, and uranium. Uranium is the fuel for about 1000 nuclear reactors of various kinds that exist in the world. These reactors produce electricity, produce plutonium for nuclear and thermonuclear weapons, and serve the search need of physical and biological scientists (Eisenbud and Paschoa 1989). Natural uranium can be detected in low concentrations in nearly all environmental samples. In radiochemical equilibrium, it consists of the isotopes ^{234}U, ^{235}U and ^{238}U with the activity ratio of 1: 0.0462: 1, corresponding to a mass ratio of 0.0054: 0.711: 99.2836 percent. All of these three nuclides are alpha-emitters, which have a high biological effectiveness. From nuclear facilities, additional amounts of uranium are discharged into the environment. In effluents from nuclear facilities, the ratios of uranium isotopes differ very much. To be able to compare them with that from

natural background, it is necessary to determine not only the concentration of total uranium but also the ratio of the different uranium isotopes (Pimpl et al. 1992). This study is aimed at investigating the distribution pattern of uranium in three Egyptian lakes.

Experimental work

Sampling and samples preparation

Total of 47 bottom sediment samples were collected from Qarun, Bardawill, and Edku lakes, Fig. 1. The bottom sediment samples were collected using a grab sediment sampler according to lenz (Ekman-Birge). The collected samples were dried at 115 ^{o}C, mechanically crushed, mixed and sieved through 2 mm mesh sieve. The organic content percentage, igination percentage, in sediment samples was determined as weight loss after ashing the samples at 450 ^{o}C for about 8 hours (USDOE 1992; Khater et al. 2001).
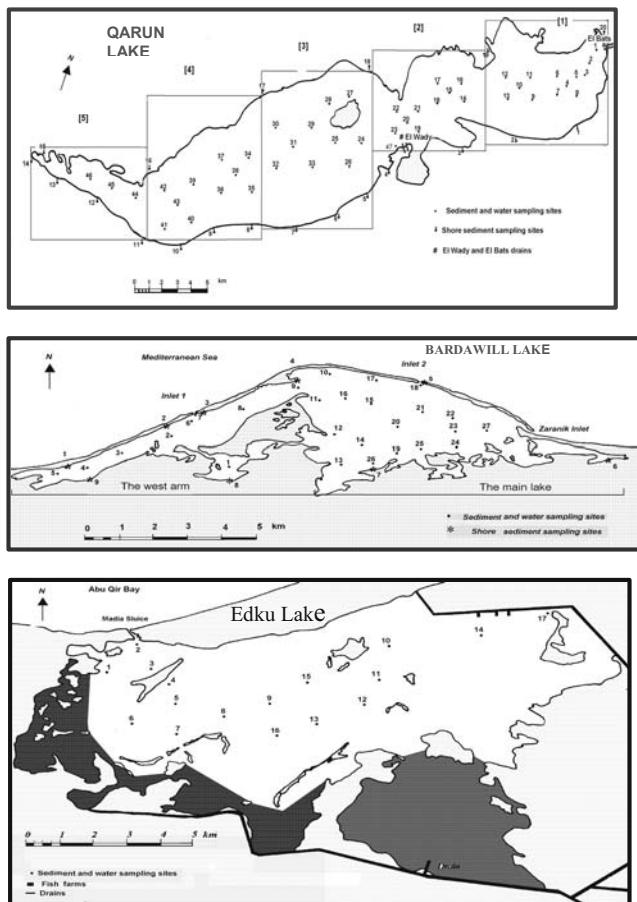
Analytical methods

Radium-226 analysis

^{226}Ra specific activity (Bq/kg dry weight) was measured using a well calibrated gamma ray spectrometers based on Hyper-Pure Germanium detectors. The details of ^{226}Ra analysis are given in our previous work (Khater et al. 2001).

Uranium isotopes analysis

Uranium isotopes analysis, 1-5 g of the ashed samples were spiked, for chemical recovery and activity calculations, with ^{232}U tracer and dissolved using mineral acids (HNO$_3$, HF and HCl). The uranium was extracted with Tri-octylphosphine oxide in cyclohexan, back-extracted with NH$_4$F/HCl solution, then co-precipitated with La(NO$_3$)$_3$ and purified by passing through an anion exchange column. Uranium then was electroplated on a stainless steel disk from oxalate-chloride solution. The prepared samples were measured using alpha spectrometry based on surface barrier detectors with 450 mm^2 surface area, about 17% efficiency and about 20 keV resolution. The chemical recovery was in the rang of 45-70 %. The lower detection limit of the procedure is in the range of 1 mBq/ sample, for a 1000 min. measuring time (Pimpl et al. 1992).

Case studies: elevated uranium in groundwater without uranium mining impact

Fig. 1.   Bottom sediment sampling locations from Qarun, Bardawill and Edku Lakes- Egypt.

Results and discussion

The average specific activities of ^{238}U, ^{235}U, ^{234}U and total uranium (Bq/kg dry weight), and $^{234}U/^{238}U$ and $^{226}Ra/^{238}U$ ratios in Qarun, Bardawill and Edku lakes bottom sediment are represented in Table 1. Sediment texture (clay, silt and sand percentages), organic matter content, electric conductivity- EC and pH) are represented in Table 2.

The specific activities of ^{238}U and ^{234}U in Qarun and Bardawill lakes are two fold higher than that of Edku Lake. That may be explained because of water salinity and hydrological features of these lakes. Qarun and Bardawill lakes are closed lakes. They are nearly without any water's outflow except by evaporation and may

Case studies: elevated uranium in groundwater without uranium mining impact

be by underground water. So, the uranium contents of inflow water (drain water in Qarun and sea water in Bardawill) are accumulating in lakes' environment. Edku lake water's is derived mainly from three drains (as Qarun Lake) and the sea (as Bardawill Lake). So, there is in and outflow water through the lake. Exchange of water between the lake and the sea occurs through a narrow inlet and most of the time in the direction of the sea. The water outflow in Edku Lake (through the inlet to the sea) is higher than that of Qarun and Bardawill lakes. The uranium contents increase greatly where the flow of water is low. It noticed that the range of uranium concentrations in Qarun Lake is larger than that of Bardawill Lake. That may be explained due to mineralogical properties of bottom sediments and the water resources of these lakes; drain water for Qarun Lake and sea water for Bardawill Lake. Although, the amount of uranium supplied to surface waters by rock and soil weathering is more or less constant. The continuous accumulation of uranium input from the drain water over many years and other parameters such as sediment texture, calcium carbonate percentage and the organic matter content could be a reason for such a big range of uranium concentration (Ivanovich and Harmon 1992).

The concentration of uranium varies widely in natural waters over four orders of magnitude. This is in part due to its varied chemical behavior in response to redox condition, from insoluble 4^+ valence in reducing conditions to soluble 6+ valence in oxidation conditions. Most surface waters are oxidizing. The concentration of uranium in surface water is correlated with bicarbonate ion concentration or total dissolved solids (TDS) or both. The uranium concentrations increase with increasing TDS (Ivanovich and Harmon 1992; Coal and Bruland 1987; TDS: there is an empirical relationship between uranium concentration and water salinity, U-238 (dpm/l) = 0.07081 x salinity, Coal and O'Hara 1987). The average water salinity of Qarun, Bardawill and Edku lakes are 32.4, 60.5 and 2.86 g/l respectively.

The average $^{234}U/^{238}U$ activity ratios in lakes sediment are close to the equilibrium value of unity. Where leaching is less dominant, as in arid regions, these activity ratios become quit high. The reason is the relative importance of recoil fractionation over gross leaching in the less intensely weathered soils. The key factors in the development of $^{234}U/^{238}U$ activity ratios out of equilibrium are the relative rates of leaching, mechanical erosion, and daughter half-life. If uranium remains a considerable time relative to the ^{234}U lifetime, then the process of recoil will cause fractionation. Although the range of these activity ratios vary greatly in surface waters, often by a factor of 2 or 3, the global average value is closely constrained at 1.2–1.3 (Ivanovich and Harmon 1992).

Case studies: elevated uranium in groundwater without uranium mining impact

Table 1. Specific activity of U-238, U-235, U-234 and total uranium (Bq/kg dry weight) and U-234/U-238 and Ra-226/U-238 ratio in Qarun, Bardawill and Edku lakes bottom sediment.

	U-238 ± E	U-235 ± E	U-234 ± E	Uranium ± E	U234/ U-238 ± E	Ra226/ U-238 ± E
	48.0 ± 3.66	1.41 ± 0.20	53.4 ± 4.09	102.9 ± 7.69	1.13 ± 0.04	0.37 ± 0.03
Qarun	(21.5 - 81.7)	(0.19 - 4.25)	(22.4 - 97.7)	(45.1 - 182.5)	(0.72 - 1.59)	(0.19 - 0.79
	[25]	[25]	[25]	[25]	[25]	[25]
	45.4 ± 7.48	1.84 ± 0.68	46.6 ± 8.33	93.6 ± 16.0	0.99 ± 0.07	0.34 ± 0.21
Bardawill	(9.8 - 61.6)	(0.34 – 4.9)	(7.74 - 63.3)	(17.9 - 128.8)	(0.79 - 1.27)	(0.11 - 1.16)
	[6]	[6]	[6]	[6]	[6]	[6]
	25.5 ± 3.16	1.00 ± 0.20	29.3 ± 4.57	57.9 ± 8.65	1.11 ± 0.40	0.67 ± 0.1
Edku	(11.6 - 55.7)	(0..25 - 3.25)	(12.8 - 84.7)	(27.0 - 142.3)	(0.9 - 1.52)	(0.17 - 1.34)
	[16]	[16]	[16]	[16]	[16]	[16]

* Mean ± standard error of the mean, (Range), and [Sample number].

Table 2. Mechanical analysis parameters, Igination factor %, EC and pH of Qarun, Bardawill and Edku lakes.

	Depth (m)	Organic matter %	Silt %	Clay %	Sand %	CaCO$_3$ %	E.C.	pH
Qarun	3.4	12.4	15.8	21.0	53.4	22.7	14.3	8.1
Bardawill	1.5	10.4	10.2	12.3	68.2	21.8	18.4	8.2
Edku	0.8	12.2	23.0	25.4	47.1	18.1	2.1	7.6

The average ^{226}Ra/^{238}U activity ratios in Qarun, Bardawill and Edku lakes sediment are very low, 0.37, 0.32 (with excluding one figure corresponding to the maximum ratio, it becomes 0.16) and 0.67. That may be because of the amount of radium in surface waters is more variable than the amount of uranium. There are many chemical and physical circumstances in which radium is adsorbed on to or desorbed from associated sediments. The general condition is that sediment arrives at drain's mouth with radium adsorbed to the particulate surface, and then radium is desorbed in the more saline environment. That is clear in Qarun Lake where the activity ratio is less and the salinity is higher than that of Edku Lake. For Bardawill lake, the lowest ratio activity may be because of the low ^{226}Ra concentration (0.002 Bq/l) in sea water comparing to ^{238}U concentration (0.04 Bq/l) (Ivanovich and Harmon 1992; Maul and O'Hara 1989).

Case studies: elevated uranium in groundwater without uranium mining impact

Acknowledgements

References

Eisenbud M, Paschoa A (1989) Environmental radioactivity. Nuclear Methods in physics Research A 280: 470-482.

Pimpl M, Yoo B, Yordanova I (1992) Optimization of radiochemical procedure for the determination of uranium isotopes in environmental samples. J. Radioanalytical and Nuclear Chemistry 161: 437-441.

US department Of Energy (1992) EML procedures manual. Report HASL-300.

Khater A, Higgy R, Pimpl M (2001) Radiological impacts of natural radioactivity in Abu-Tartor phosphate deposits Egypt. J. Environmental Radioactivity 55: 255–267.

Ivanovich M, Harmon R (1992) Uranium series disequilibrium. Second edition, Clarendon press, Oxford.

Coal K, Bruland K (1987) Oceanic stratified euphotic zone as elucidated by Th-234: U-238 disequilibrium. Limnol. Oceanogr. 32: 189-200.

Mual P, O'Hara P (1989) Background radioactivity in environmental materials. J. Environmental Radioactivity 9: 265-280.

Case studies: elevated uranium in groundwater without uranium mining impact

Origin of high ^{234}U/^{238}U ratio in post-permafrost aquifers

Igor Tokarev[1], A.A. Zubkov[2], Vyacheslav G. Rumynin[1], V.A. Polyakov[3], V.Yu. Kuznetsov[4], F.E. Maksimov [4]

[1]IGE RAS, SPb Div., VO, 14 lin., 29, 199178 Sankt-Petersburg, Russia,
E-mail: tokarev@hydra.nw.ru
[2] SCC, LGTM, ul. Kurchatova 1,636000 ZATO Sewersk, Tomsk reg.,Russia,
[3] VSEGINGEO, pos. Zelenyi, 142452 Moscow reg., Russia,
[4] SPSU, VO, Srednii pr., 41, 199178 Sankt-Petersburg, Russia,

Abstract. Isotope composition and concentration (δ^2H, δ^{18}O, ^{234}U/^{238}U, Ar, ^{40}Ar/^{36}Ar, ^{3}He/^{4}He and ^{20}Ne/^{4}He) were measured in the groundwaters (Tomsk-7). Water has a distinct cold climate isotope signature δ^2H = -127..-140, δ^{18}O = -17.0.. -18.2 in contrast of modern meteoric water δ^2H = -117, δ^{18}O = -15.9. Stable isotopes are in concord with noble gas temperature t_{NGT} = 0..+4 ^{o}C and helium model ages t = 7-14 ka. Disequilibrium uranium ^{234}U/^{238}U up to 16 (activity ratio) obtained and explained of ^{234}U leaching by the melt water during the permafrost degradation.

Introduction

During the last decades, the Earth sciences have become increasingly focused on U-series isotope geochemistry and its application in global climate exchange. In closed systems older than 10^6 yrs uranium-238 decay chain should be at equilibrium that is rightly applied to general volume of Earth's crust. Secular equilibrium is ^{234}U/^{238}U =$\gamma \approx 1$ in activity ratio or ^{234}U/^{238}U $\approx 5.47*10^{-5}$ in atom ratio (Holden 1990; Ludwig et al. 1992; Cheng et al., 2000).

Uranium mass distribution between solid and liquid phases in water-saturated rocks is about $U_{SOLID}/U_{AQUA} \approx 1000:1$ as a rule, therefore it was to be expected $\gamma \approx 1$ in deluted uranium. However depletion of ^{238}U in natural objects is a well known phenomenon after (Chalov 1954, 1964, 1975), (Cherdyntsev 1955, 1971), (Rosholt 1959), (Thurber 1962), (Rosholt and Ferreira 1965), etc. They and follow workers demonstrated very wide scale of ^{234}U/^{238}U ratios in natural environmental

which present in Table 1. The application of U-series geochemistry to the Earth Sciences was thoroughly summarized by (Ivanovich and Harmon 1982, 1992).

More significant result from Table 1 is $^{234}U/^{238}U$ ratio in ocean (big averaging reservoir on Earth's surface) which is $\gamma \approx 1.15$ that points to preferred transport of ^{234}U from continents in comparison with ^{238}U. Excluded very high γ in bones, the greatest depletions of ^{238}U are observed in groundwaters. For example (Yamamoto et al. 2003) showed $^{234}U/^{238}U$ activity ratios a wide range from 2.7 to 51 in Tatsunokuchi hot spring waters and (Polyakov 1991) obtained $^{234}U/^{238}U \approx 54$ in cold water on island Saaremaa (Estonia).

The range of $^{234}U/^{238}U$ is affected by combination of recoil and leaching processes which discussed in large quantity of works. Initially the recoil atom is displaced from the site where parent one was located. The displacement distance is approximately n*10 nm depending on the substrate (Harvey 1962). It can thus be ejected directly into an adjacent phase, for example in water or other mineral. On the other hand, the daughter ^{234}U (free radical) is more likely to be oxidized to hexavalent state (U^{6+}) and forming the more soluble $(^{234}UO_2)^{2+}$ ions or complex with carbonates $^{234}UO_2(CO_3)_2^{2-}$ than parent species ($^{238}U^{4+}$) included in mineral lattice (Chalov 1975, Sun and Semkow 1998, Cui and Eriksen 2000, Marcos et al. 2000). Lastly, the tracks are damaged by the α-particles, which sizes are about 2 μm (Fleisher et al. 1975, Farley et al. 1996). These three reasons make the daughter species more prone to subsequent mobilization from solid phase to water than parent one.

This article is an attempt to bring the advances in the explanation of high $^{234}U/^{238}U$ ratio in some groundwaters and examining the time scale of any dynamic processes induce fractionation.

Table 1. Ranges of $^{234}U/^{238}U$ activity ratio found in natural environments after (Chenery et al. 2002, data recalculated into activity ratio).

Object	$^{234}U/^{238}U$		Object	$^{234}U/^{238}U$	
	min	max		min	max
Uderground waters	0.59	11.7	Igneous rocks	0.59	2.05
Terrestrial surface waters	0.78	2.44	Volcanic tuffs	0.49	1.56
Open-ocean water	1.07	1.15	Minerals and extract of minerals	0.78	7.80
Waters of uranium mineralisation	1.17	8.58	Sandstones	0.78	1.95
Various surfacial carbonates	0.88	2.93	Peat deposit	0.88	1.95
Fossil shells and bones	0.98	243.8			

Case studies: elevated uranium in groundwater without uranium mining impact
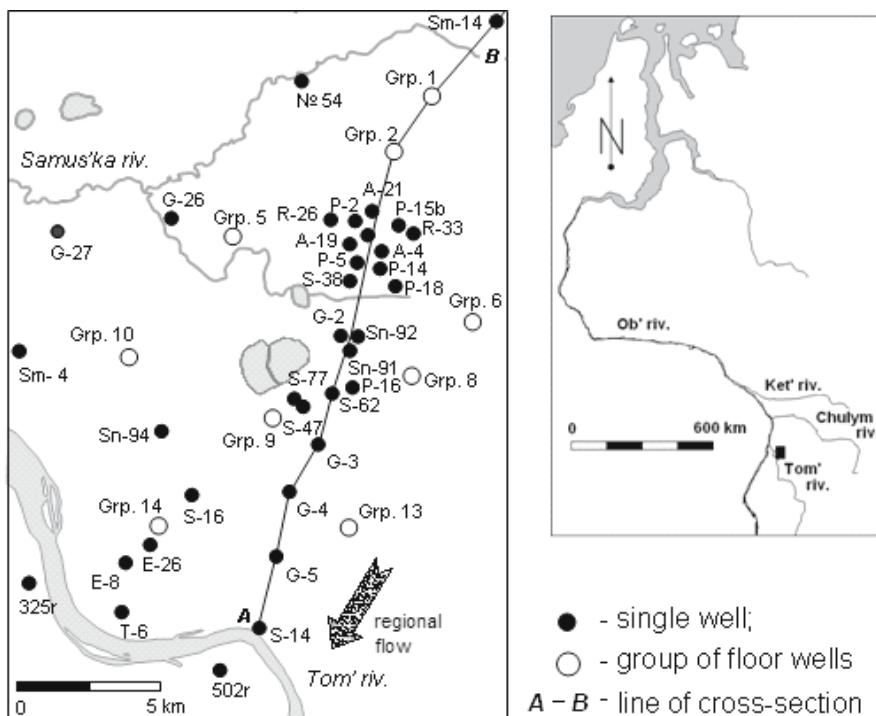
Geological settings

Studied area is located to the north of Sewersk (Tomsk-7), when radioactive wastes of Siberian Chemical Combine (SCC) have been injected since 1963 in the deep terrigenous aquifers. Region is situated on south-east flank of Western Siberian artesian basin and on the north-west slope of Tomsk ledge of crystalline basement (see Figs. 1, 2 and Rybalchenko et al. 1998).

The geological groups of terrigenous marine and coastal sediments are distinguishes due to hydrogeological measurements and geological attributes. More sandy layers are identified as I, II, III, IVa, IVb, V and VI aquifers (bottom-up) and more clayey sediments are A-E aquitards. There are no carbonates in geological cross-section.
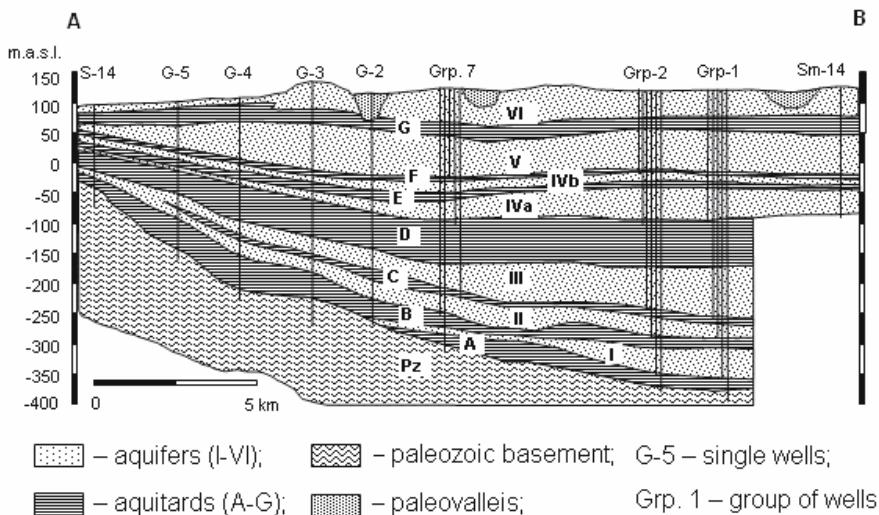
The groundwater recharge area is located to the north-east from the studied area on a watershed between rivers Tom' and Chulym at a distance about 40 km. The total regional water flow trends from the north-east to south-west towards the Tom' river valley. Groundwaters are fresh M = 0.2-0.4 g/l and sodium-calcium hydrocarbonate by chemistry.

Radioactive wastes are injected into I and II aquifers at the depth of about 270-390 m below surface. Filtration front of radioactive wastes is perfectly marked by

Fig. 1.   Field plan of Sewersk region.

Case studies: elevated uranium in groundwater without uranium mining impact

tritium, so its concentration in natural waters of IV aquifer and below is zero. In contrary the tritium contents in wastes are ranged up to n*10^4 Bq/l. Here will be analysed only data for natural water without considerable tritium to avoid of artificial effects.

Fig. 2.   Geological cross-section of Sewersk region.

Results and discussion

Isotope measurements were performed in period from 1995 to 2003 (δ^2H, δ^{18}O, ^{3}H, ^{234}U/^{238}U, Ar, ^{40}Ar/^{36}Ar, ^{3}He/^{4}He and ^{20}Ne/^{4}He). Stable isotopes were measured by standard procedure on pair of two-inlet MI-1201 mass-spectrometers, with accuracy 0.5 and 0.1 ‰ for hydrogen and oxygen respectively (Poljakov et al. 1988). Uranium isotope composition was measured on self-reconstructed alpha-spectrometer (Kuznetsov et al. 2000). Low tritium concentrations were measured after electrolytic concentration on TRICARB and MARC-2 apparatus by scintillation techinque with lower limit about 2 Bq/l (Poljakov et al. 1988). Extraction, purification and mass-spectrometric measurements of noble gases were carried out after (Kamensky et al. 1991). Standard deviations of reproducibility of volumertic argon analysis were 3-5 %, and isotope compositions 1, 1.5 and 3 % for ^{40}Ar/^{36}Ar, ^{20}Ne/^{4}He and ^{3}He/^{4}He, respectively.
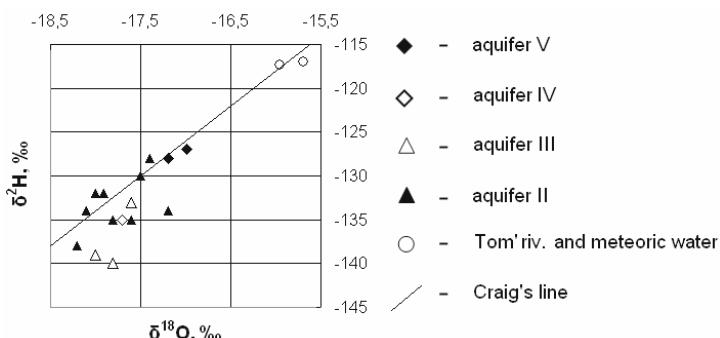
Stable isotope composition of water taken from II-V aquifers is shown in Fig. 3 and Table 2. Majority of samples are shifted to the right of world meteoric water line (W.M.W.L., Craig's line on Fig. 3) and they have strong more negative delta values than the modern waters (Tom' river and meteoric water).

Table 2. Stable isotope data for groundwater of Sewersk region.

Borehole	Aquifer	$\delta^{18}O$, ‰ SMOW	δ^2H, ‰ SMOW
E-8	V	-17.2	-128
Sn-92	V	-17.0	-127
Sn-91	IV	-17.7	-135
A-21	III	-17.6	-133
G-2	III	-18.0	-139
P-2	III	-17.8	-140
A-4	II	-17.4	-128
A-19	II	-17.8	-135
P-5	II	-17.6	-135
P15b	II	-18.2	-138
P-16	II	-18.1	-134
P-18	II	-17.2	-134
S-38	II	-17.5	-130
S-47	II	-18.0	-132
S-77	II	-17.9	-132
Tom' river		-15.7	-117
Meteoric water [a]		-15.96	-117.4

[a]Novosibirsk is the nearest point (Vienna, ISOHIS-GNIP http://isohis.iaea.org/).

It seems heaving of isotope values caused by frozen of water after recharging (Polyakov 1995). There are no permafrost in this region now, but isle permafrost obtained on about 250 km to north in Ket' river valley, maximum of ice cement is located on the deep 120-280 m (Evseeva 1998). This interval approximately likes to the average altitude of II-IV aquifers, in addition III aquifer contains water with the lightest isotope composition and more shifts from W.M.W.L. If the shift was produced by the frozen mechanism then initial delta was below then $\delta^2H = -$

Fig. 3. Stable isotope composition. The isotope data shifts to the right of Craig's line (W.M.W.L.) and possibly to heavier values are caused by frozen of water after recharging.

Case studies: elevated uranium in groundwater without uranium mining impact

140 ‰ and $\delta^{18}O = -18$ ‰ and consequently temperature of the recharging water was closed to zero.

Radiogenic argon was subtracted by using $^{40}Ar/^{36}Ar$ ratio and the concentrations of atmospheric argon were interpreted as under controlled conditions of the atmospheric noble gases dissolution in the recharge water. It is possible to neglect altitude of the Earth' surface, because of it is varied in the narrow range 40-200 m above sea level (m.a.s.l.), so a temperature is a main parameter (Aeschbach-Hertig et al. 1999). The temperatures of the argon dissolution were calculated and listed in Table 4 as NGT, a precision of this estimation is not better 1 °C. Minimum of the temperature is in III aquifer that is adjusted with the stable isotope data.

Using $^{3}He/^{4}He$ vs $^{20}Ne/^{4}He$ systematics (Kamensky et al. 1991) we calculated an amount of the radiogenic helium in waters (see Table 3). Concentration of uranium and thorium in the water-bearing rocks was analysed by ICP MS and was compared with the large quantity of the gamma-logging data. Limits of [U] and [Th] variation are not wide (see Table 4).

For (U-Th)/4He age calculation is used mathematical model, which based on the follow equations (Rumynin and Karachevtsev 1992, scheme see on Fig. 4):

$$v_i m_i \frac{\partial C_i}{\partial x} - m_i n_i P_i' - J_{i-1} + J_i = 0 \text{ , where } J_i = \frac{D_M}{m_{0i}} (C_i - C_{i+1})$$

Table 3. Calculated data for groundwater of Sewersk region.

Aquifer	$\delta^{18}O$, ‰	$\delta^{2}H$, ‰	NGT , °C	Radiogenic helium, [^{4}He], cm^{3}SPT/cm^{3}H$_2$O
V	-17.1 (2) [a]	-128 (2)	+4.2 (8)	$6.81 \cdot 10^{-8}$ (8)
IV	-17.7 (1)	-135 (1)	+2.6 (8)	$3.92 \cdot 10^{-7}$ (8)
III	-17.8 (3)	-137 (3)	–0.2 (8)	$3.34 \cdot 10^{-6}$ (8)
II	-17.7 (9)	-133 (9)	+1.4 (8)	$5.28 \cdot 10^{-6}$ (8)
I			+2.0 (4)	$4.78 \cdot 10^{-6}$ (4)
Pz basement				$1.37 \cdot 10^{-5}$ (1)

[a] here and after number of measurements is in the brackets.

Table 4. Uranium and thorium in rocks of Sewersk region.

Horizon	U, ppm	Th, ppm	Th/U
V, *F*, **IVb**, *E*, **IVa**	2.27 (14)	7.42 (14)	3.3
D, **III**, *C*, **II**, *B*	1.26 (29)	5.34 (29)	4.2

Case studies: elevated uranium in groundwater without uranium mining impact

Table 5. Uranium isotope data for groundwater of Sewersk region.

Borehole	Aquifer	^{234}U/^{238}U ±2σ	Borehole	Aquifer	^{234}U/^{238}U ±2σ
325r	V	1.74 ±0.63	G-26	III	1.94 ±0.63
502r	V	1.74 ±0.63	R-33	III	4.73 ±0.31
S-14	IV	6.47 ±0.79	Sn-94	III	14.7 ±2.6
Sm-4	IV	3.9 ±1.1	R-26	II	16.1 ±3.9
T-10	IV	9.9 ±1.2	S-16	II	2.46 ±0.22

and v_i –filtering velocity, LT^{-1}; m_i, m_{0i} – thickness of aquifer and aquitard, respectively, L; n_i – porosity; D_M – molecular diffusion, L^2T^{-1} , C_i – helium concentration, $molL^{-3}$; P'_i – production rate of ^{4}He in solid, $molL^{-3}T^{-1}$; x – lateral coordinate, L.

Combined equations for $i = 4$ (A+I+B+II), (C+III), (D+IVa+E+IVb), (F+V) (see Fig. 2); [U], [Th], x_i from this work; D_M, n, and m_i from (Alexandrova et al. 2003) were calculated numerically by fit on C_i, due to iteration of v_i. Constant boundary conditions were on upper limit $C_{UPP} = 0$ and lower one C_{LOW} equal to the helium concentration in water of Paleozoic basement. Obtained v_i and measured x_i were used for the age calculations, results of simulation are listed on Fig. 5.
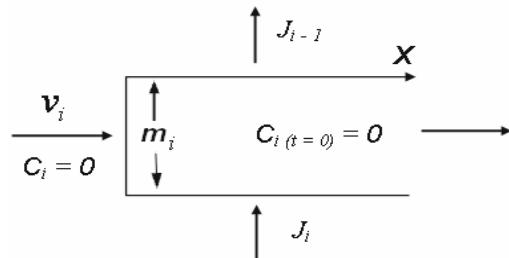
The isotope ages for I, II, III aquifers lie in the range of 7-14 ka and look like to the end of the last glacial period in this region (see Fig.6). The measured uranium contents in groundwater are low or about ICP MS limit (0.01 μg/l) only in S-14 is [U] ~ 0.02 μg/l, so 1300 l samples were collected and prepared by co-precipitation with charcoal on the isotope analysis. The measured isotope composition of uranium varies from 1.74 to 16.1 (Table 5) and show very disequilibrium uranium in the deep interval 150-300 m below Earth' surface, which likes on the isle permafrost location in Ket' river valley.

What is a reason(s) of the soluted uranium disequilibrium? The hydrothermal activity is absent in region at least after start of Cretaceous, the dilution of rocks in water can be ignore completely take into consideration the chemistry of water is fresh and the concentration of uranium is very low. The distinct cold climate isotope signature (δ^2H, δ^{18}O) of water is adjusted with NGT of groundwater (t_{NGT} =0..4 °C) and with isotope ages about t ≈ 10 ka for I, II and III aquifers, therefore the disequilibrium is most likely stimulated by the permafrost degradation.
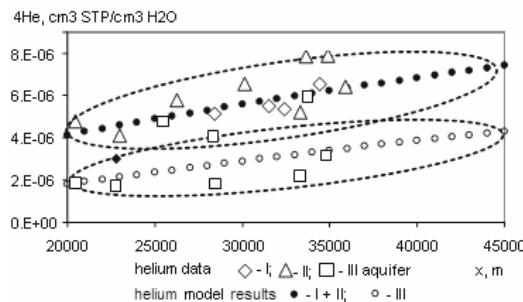
Possibly follow process led to forming of isotope effect on the soluted uranium. During the Pleistocene ice cycle ^{234}U is accumulated in the rock, but could not leave the lattice, because the water was frozen. After start of the ultimate deglaciation the melt water extracted whole of ^{234}U which was born in 120 ka time interval. Excess of ^{234}U is very low in that part of II aquifer (see S-16 in Table 5) which was located below the permafrost bottom, i.e. deeper 350 m from the Earth' surface. In addition excess of ^{234}U absents in the upper aquifers (V and VI) where the old melt water replaced to modern meteoric water due to high rate of the water cycle.

Conclusion
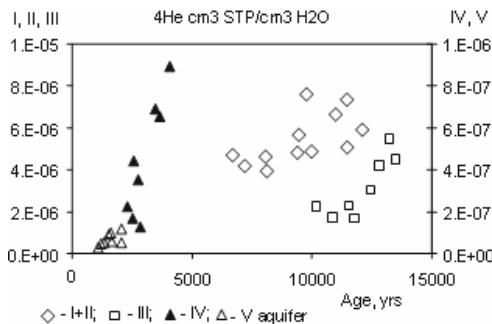
Isotope data ($\delta 2H$, $\delta 18O$, $234U/238U$, Ar, $40Ar/36Ar$, $3He/4He$ and $20Ne/4He$) were measured in the groundwaters (Tomsk-7). Water has a distinct cold climate isotope signature $\delta 2H = -127..-140$, $\delta 18O = -17.0.. -18.2$ in contrast of modern meteoric water $\delta 2H = -117$, $\delta 18O = -15.9$. Stale isotope data are in concord with


**Fig. 4.**   Mathematical model of radiogenic helium migration.

Fig. 5.   Comparison of measured helium data and model one for I, II, III aquifers.

Fig. 6.   The helium model ages of groundwater.

Case studies: elevated uranium in groundwater without uranium mining impact

noble gas temperature tNGT = 0..+4 oC and the model helium ages 7-14 ka. Disequilibrium in the uranium serie (234U/238U up to 16) is explained of 234U leaching by the melt water during the last permafrost degradation.

Acknowledgments

References

Aeschbach-Hertig W, Peeters F, Beyerly U and Kipfer R (1999) Interpretation of dissolved atmospheric noble gases in natural warets. Water Res Res 35 (9): 2779-2792

Alexandrova LN, Glinsky ML, Danilov VV, Zinin AI, Zinina GA, Zubkov AA and Samsonova LM (2003) Prediction of radioactive liquid waste migration at the Siberian Chemical Combine underground injection site based on mathematical modeling. Abstr in "Underground Injection Science and Technology, Berkeley, California October 22-25, 2003": 46-53

Chalov PI (1954) Investigation of 234U/238U ratio in some natural objects. Academic Diss, Alma-Ata

Chalov PI, Tuzova TV, Musin YA (1964) The 234U/238U ratio in natural water and its use in nuclear geochronology. Geoch Int v 3: 402-408

Chalov PI Isotope fractionation of natural uranium. Ilim Press, Frunze, 1975

Chenery SRN, Ander EL, Perkins KM, Smith B (2002) Uranium anomalies identified using G-BASE data – Natural or anthropogenic? A uranium isotope pilot study. British Geo. Surv, Internal Report IR/02/001

Cheng H, Edwards RL, Hoff J, Gallup CD, Richards DA, Asmerom Y (2000) The half lives of uranium-234 and thorium-230. Chem Geol 169: 17-33

Cherdyntsev VV (1955) Isotope composition of radioelements in natural objects in connection with geochronology. Tudy III sessii Komisii po opredeleniju absolutnogo vosrasta geologicheskikh formazii

Cherdyntsev VV (1971) Uranium-234. Israel Program for Scientific Translations, Jerusalem

Cui B and Eriksen T (2000) Fracture-filling minerals as uranium sinks and sources, a natural analogue study at Palmottu, Finland. Radiochim Acta 88: 751-755

Evseeva NS (1998) Atlas of Tomsk region, Tomsk State University Press, Tomsk

Farley KA, Wolf RA and Silver LT (1996) The effects of long alpha-stopping distance on (U-Th)/He ages. Geoch et Cosmoch Acta, 60 (21): 4223-4229

Fleisher RL, PB Price, Walker RM (1975) Nuclear tracks in solids. University of California Press

Harvey BG (1962) Introduction to Nuclear Physics and Chemistry. Prentice Hall Inc, New Jersey

Holden NE (1990) Total half-lives for selected nuclides. Pure Appl Chem 62(5): 941-958

Ivanovich M and Harmon RS (eds) (1982, 1992) Uranium series disequilibrium: Applications to problems in earth sciences (1st and 2nd editions) Clarendon Press, Oxford

Case studies: elevated uranium in groundwater without uranium mining impact

Kamensky IL, Tokarev IV, Tolstokhin IN (1991) 3H-3He dating: a case for mixing of young and old qroundwaters. Geoch et Cosmoch Acta, 55 (10): 2895-2900

Kuznetsov VYu, Arslanov KhA, Shilov VV, Cherkashev GA, Maksimov FE (2000) Uranium and thorium distribution in metallogenic sediments from the hydrothermal zone of the North Atlantic. Radiochimia, 6: 565-568

Ludwig KR, Simmons KR, Szabo BJ, Winograd IJ, Landwehr JM, Riggs AC, Hoffman RJ (1992) Mass-spectrometric 230Th-234U-238U dating of the Devils Hole calcite vein. Science 258: 284-287

Marcos N, Suksy J, Ervanne H, Rasilainen K (2000) Fracture smectite as a long-term sink for natural radionuclides – indications from unusual U-series disequilibria. Radiochim Acta 88: 763-766

Polyakov VA, Tkachenko AE and Krishtal NN (1988) Investigation of hydrogeological and engineering-geological objects by geophysical and isotope methods. Moscow, VSEGINGEO Press

Polyakov VA (1991) The causes of groundwater chemistry and resources changing on Estonia coastal water-supply systems by isotope data. Thes of "Vsesojusnaja konferecija, Zvenigorod" Academik Press: 60-62

Polyakov VA (1995) Cryogenic metamorphism of groudrwater isotope composition on the permafrost area. Thes of "XIV symposium po geochimii isotopov 19-21 oktjabrja 1995" Moscow: 168-169

Reyss JL, Lemaitre N, Bonté P and Franck D (2002) Anomalous 234U/238U ratios in deep-sea hydrothermal deposits. Nature 325: 798-800

Rosholt JN (1959) Natural radioactive disequilibrium of the Uran serie. US Geol. Surv Bull. 1084-A. Washington,

Rosholt JN and Ferreira CP (1965) Fractionation of uranium isotopes and daughter products in uranium-bearing sandstone, Gas Hills, Wyoming. Geological Surv Res Chap-C, N 525-C

Rumynin VG and Karachevtsev NF (1992) Estimation of groundwater chemistry in case of surface fallout of non-stable species (theoretical models). Vodnye Resursy 3: 50-72

Rybalchenko AI, Pimenov MK, Kostin PP, Balukova V/D, Nosukhin AV, Mirekin EI, Egorov NN, Kaimin EP, Kosareva IM, Kurochkin VM (1998) Scientific and practical results of deep-injection disposal of liquid radioactive waste in Russia. Battele Press, Columbus Richland, Washington

Sun H and Semkow TM (1998) Mobilization of thorium, radium and radon radionuclides in ground water by successive alpha-recoils. J of Hydrol 205: 126-136

Thurber DL (1962) Anomalous U234/U238 in nature. J Geoph Res, v 67, N 11: 2381-2395

Yamamoto M, Sato T, Sasaki K, Hama K, Nakamura T. and Komura K. (2003) Anomalously high 234U/238U activity ratios of Tatsunokuchi hot spring waters, Ishikawa Prefecture, Japan. J of Radioanalyt and Nucl Chem 255 (2): 369-373

Case studies: elevated uranium in groundwater without uranium mining impact

Uranium in phosphate fertilizer production

W. Eberhard Falck, Denis Wymer

International Atomic Energy Agency, PO Box 100, A-1400 Vienna, Austria,
E-mail: W.E.Falck@iaea.org

Abstract. The production of fertilizers from natural phosphate ore can lead to the redistribution of uranium and other radionuclides in products, by-products and residues and, hence, to environmental impacts and increased radiation exposures.

Uranium and other radionuclides are mainly found in the process residue phosphogypsum and to a lesser degree in the final fertilizer products. The input of radionuclides of natural origin into the food chain via phosphate fertilizers appears to be of lesser concern. Because the radionuclide activity concentrations in most of the process materials are only slightly above levels in soil, the need for specific measures to control radiological hazards to individuals and the environment is very limited. In most cases, normal occupational health and environmental protection measures designed for non-radiological hazards will be sufficient to protect against radiological hazards as well.

Introduction

This paper summarizes the findings of recent reviews concerning radionuclides of natural origin in phosphate fertilizer production and associated radiation exposures. Uranium series and other radionuclides are ubiquitous in geological materials. The mining and processing of phosphate rock (phosphorite) to produce phosphate fertilizers, detergents, animal feeds, food additives, pharmaceuticals and other phosphorus-containing chemicals redistributes the uranium and other radionuclides (IAEA 2003).

The principal constituent of phosphate rock (or phosphorite) is the mineral apatite. The typical phosphate (P_2O_5) concentration of the rock is about 15-40%, with clay, sand, carbonate and other impurities present in varying quantities. Phosphate in mineable quantities is concentrated by sedimentary, igneous, weathering and biological processes (e.g. guano). Approximately 30 countries around the world

produce significant quantities of phosphate rock. The principal suppliers of phosphate rock are the USA, Morocco, China and the Russian Federation, which together are responsible for about two thirds of total world production. Almost all phosphate rock is mined in open pit mines (IAEA 2003).

Uranium may be incorporated in sedimentary phosphorite ores through ionic substitution into the carbonate-fluoroapatitic crystals or by adsorption. Igneous phosphorite contains less uranium, but more thorium. Radionuclide concentrations in ores are given in Table 1.

Beneficiation

Generally, the starting material in production is beneficiated phosphate ore, referred to as marketable phosphate rock. During beneficiation, phosphate particles (mainly apatite and phosphorite) are separated out. Beneficiation can be simple, just screening or sieving the material and the overburden can be piled or returned to the mine; or more elaborate, including washing and flotation steps, producing phosphatic clay and sand tailings. Clay tailings are stored in large settling areas. Sand tailings are either returned to the mine and used as a backfill, used in the construction of clay-tailings retention dams or mixed with clay tailings to increase clay-tailings solids content and reduce settling times. In general, the beneficiation does not reduce the radionuclide concentration in the ore.

The phosphate ore is processed either by acid leaching, resulting in phosphoric acid, or by heat treatment in furnaces, leading to elemental phosphorus.

Table 1. Concentration of major radionuclides for different phosphate rocks (Roessler et al. 1979, Osmond et al. 1985, van Straaten 2002, Chernoff 2002, Makweba 1993, Banzi 2002, Othman 1992, CEC 2000, van der Westhuizen 2002).

Country	Activity concentration [Bq/kg]					
	^{238}U	^{230}Th	^{226}Ra	^{232}Th	^{228}Ra	^{228}Th
Sedimentary						
Central Florida	750–3100	1300	700–3100	20		
Northern Florida	60–100		200–500			
North Carolina	600					
China, Guangxhi	600–1100					
Morocco	1000					
Tanzania	20–11 000	30–4500	5800	7–1100	500	150–1100
Egypt, Nile Valley	700					
Syria	750–1500					
Igneous						
Russian Federation, Kola	70			100		
South Africa	200		200	400		400

Case studies: mining activities with uranium as side product / problem

Wet processing for phosphoric acid

The commercial production of phosphoric acid and of phosphatic application products proceeds by 'acidulation' with strong acids (H_2SO_4, HCl, HNO_3). The phosphoric acid is separated and further processed. Acidulation with sulphuric acid predominates world production (95%) and leads to the formation of 'phosphogypsum'. The gypsum precipitate can be easily separated from the raw phosphoric acid by filtration followed by washing. A neutralization step may be included. Unless the phosphoric acid is used for fertilizer production, it is further purified according to product requirements, e.g. by solvent extraction. The production of 1 t of phosphate (P_2O_5) results in the generation of approximately 4–5 t of phosphogypsum. A number of variations of the basic process (Fig. 1) are in use, mainly to reach higher yields and cleaner and more concentrated phosphoric acid.

Thermal processing for elemental phosphorus

Phosphate rock can be melted in a furnace (1400°C) with sand, iron oxide and coal for the reductive production of elemental phosphorus. Phosphorus and carbon monoxide are driven off as gases. The off-gases pass through dust collectors and then through water spray condensers, where the phosphorus is condensed and trapped in water. The residual solids in the furnace contain ferrophosphorus and calcium silicate, the slag. Slag is the principal residue while ferrophosphorus is considered to be a by-product.
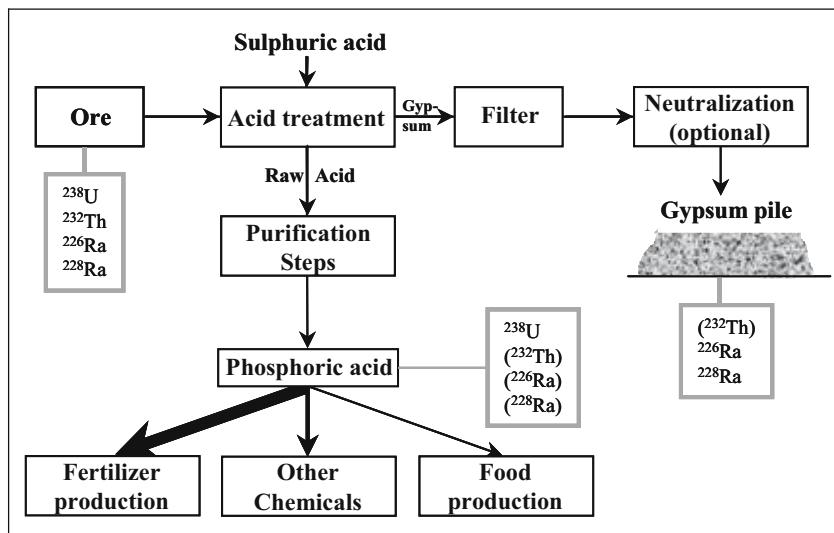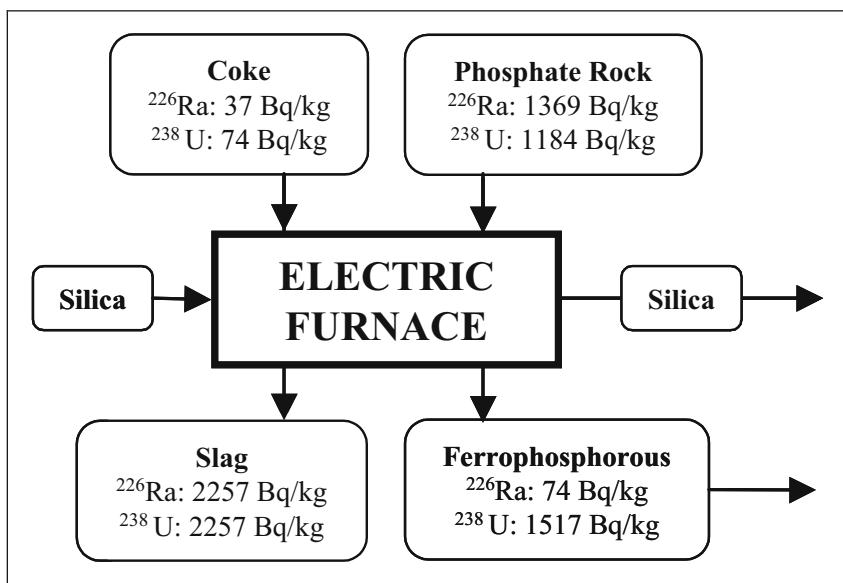
Fig. 1.   Flow diagram of the sulphuric acid P-extraction process (IAEA 2003).

Case studies: mining activities with uranium as side product / problem

Radioactivity in products, by-products and residues

Phosphogypsum is the principal waste product generated by the wet process and arises as a slurry that is typically either deposited in piles (stacks) or discharged into rivers or the sea (Schmidt et al. 1995, World Bank 1998). Stacks may be covered with water to prevent radon emanation. In general, about 80% of the ^{226}Ra, 30% of the ^{232}Th and 14% of the ^{238}U is left in the phosphogypsum. Uranium and thorium become enriched in the fertilizer to about 150% of their original value (70% of the total U and Th budget) (Hull & Burnett 1969, Vandenhove et al. 2000). However, the amounts of radioactivity that are fractionated into gypsum vary significantly. The disposal of these wastes does not contribute significantly to the resulting radiation exposure. In the long term, radiological problems may arise, due to an unauthorized removal of wastes. Some countries have elaborate systems to manage these wastes. Management systems are likely to be dictated more by the non-radiological impacts (e.g. heavy metals) than by the radiological impacts.

The quantity of the slag from the thermal process amounts to 85% of the raw phosphate ore and contains the major fraction (93%) of ^{238}U and ^{226}Ra (Hull & Burnett 1969, Vandenhove et al. 2000). while part of the lead and polonium isotopes leave the oven with the gas stream due to their volatility. The electrostatic dust filter separates part of the radionuclide content from the gas stream, while polonium leaves the process mainly with the off-gas. The quantity of dust produced is about 1% of the raw phosphate ore. This may be recycled back into the process,

Fig. 2.   Flow diagram and radioactivity balances for elemental phosphorous production (Hull and Burnett 1969).

Case studies: mining activities with uranium as side product / problem

but small amounts have to be purged from the system periodically to limit the build-up of high concentrations of organic matter and metals, which cause instability in the operation of the furnace. This recycling also causes a build-up of radionuclide concentrations. The dust purged from the system contains ^{210}Pb and ^{210}Po at activity concentrations of up to 1 000 000 Bq/kg (Erkens 1997), which can be immobilized with cement. A flow diagram for radioactivity balances in an American plant is given in Fig. 2.

Table 2 gives an overview of the radionuclide concentrations in residues from various process and of different origin.

The radioactivity content of fertilizers depends on the radionuclide content of the phosphate ore and on the method of production. Table 3 shows some values reported by Baetslé (1991) and extracted from a number of references. Fertilizers are generally depleted in ^{226}Ra content and display a U concentration pattern that is the result of either the dilution or the concentration effects of the fertilizer production process on the initial phosphate concentration in the ore. Although most of the U and Th remain in the fertilizer, fertilizer application does not significantly contribute to the general dose. Commercial calcium phosphates from furnace grade phosphoric acid do not contain any of the radionuclides present in natural phosphate.

Work carried out in Finland has shown that the annual contribution of ^{238}U contained in NPK fertilizers was about 0.25% of the total uranium naturally occurring in the top 10 cm of the soil. Similar results have been reported from Belgium. The long-term effects of phosphate fertilization on radioactivity have been studied in the United States. Triple superphosphate produced from Florida phosphate rock

Table 2. Radionuclide concentration in residues [Bq/kg], based on IAEA (2003) and references therein.

Country (Source)	^{226}Ra	^{238}U	^{210}Pb	^{210}Po	^{232}Th
Phosphogypsum					
USA S & C Florida	507-1358	41-366	577-1853	437-1765	11
N. Florida	270-599	22-451	348-551	355-566	
Europe	15-1700	500	1300	900	10
South Africa					
Local rock	45-48	64-73	76-132		205-284
Togo rock		17			61
Australia	280-350	10-24	320-440	150-360	4-7
Furnace slag					
USA	407-1517	444-2072	56	31	9-41
Europe	1000	1000-1500			
Ferrophosphorus					
USA	7-44	359-407	27-144	37	3
Calcined dust					
Europe			1 000 000		

and applied at the rate of 30 kg/ha of P during more than 50 years did not change the concentrations of U, Th, and Ra in corn leaves and grain, wheat grain and straw, or soybean leaves and bean, compared to non-fertilized plots (IFDC/ UNIDO 1998).

Utilization of byproducts and residues

Since there are large quantities of phosphogypsum, the industry encourages its reuse in order to minimize the disposal problem; it is used as a fertilizer and soil conditioner, in road construction, and as building material (plasterboard and aggregate in concrete). In the USA, the primary use of phosphogypsum is in agriculture (1-2% of the generation), while the use in construction/building materials is now banned (USEPA 1990) due to the radon emanation. Other applications being considered include sulphur recovery from the gypsum, its introduction into municipal landfills to increase biological decomposition, construction of artificial reefs, and its conversion to calcium carbonate and ammonium sulphate (Florida 1996).

Phosphate slags find use as substitutes for valuable raw materials such as aggregate in asphalt manufacturing and as aggregate in concrete for making construction blocks etc. Slag has been incorporated in roofing shingles and, in the past, in the manufacture of 'rockwool' insulation. Phosphate slag is also used as railroad ballast and as stabilization material for stockyards (USEPA 1990). Forty percent of the phosphate slag produced in the USA is utilized in construction materials.

Environmental impacts of residues

The environmental impacts from (phosphate) fertilizer production has been summarized in a recent report (UNEP/UNIDO 1998). The release of radium into leachate and surface run-off from phosphogypsum piles is mainly determined by the solubility of the gypsum, which is generally very low. The dose resulting from ingestion of contaminated drinking water or food products is generally of no concern even for a member of a critical group living close to the pile. Exposure due to dust inhalation and radon are generally low due to the predominantly liquid stage of the gypsum stack. Furthermore, gypsum hardens when dry.

River dumping of gypsum may result in the contamination of the river embankments and increased exposure to the people living close by, mainly due to external exposure and exposure to radon (World Bank 1998).

Furnace slag is a glassy material containing the radioactivity in a vitrified matrix, resulting in limited leaching of radionuclides. In addition, the slag has a high carbonate content, which also reduces radionuclide solubility. However, USEPA's

Report to Congress on Special Wastes (USEPA 1990) documents groundwater contamination at several phosphate slag waste management sites.

Application of international radiation protection standards

The International Basic Safety Standards for Protection against Ionizing Radiation and for the Safety of Radiation Sources (the BSS), jointly sponsored by six international organizations and published by the International Atomic Energy Agency (IAEA) in 1996, provide the basic requirements for the control of exposure to both artificial and natural sources of radiation (IAEA 1996). The BSS are supplemented by a number of IAEA Safety Guides. Although all raw materials contain radionuclides of natural origin, most do not warrant any form of regulation to control exposure to radiation, and the BSS apply only to those materials in which the radionuclide concentrations exceed the upper end of the worldwide distribution of activity concentrations in soil. This upper bound is deemed to be 1000 Bq/kg for uranium and thorium series radionuclides and 10 000 Bq/kg for potassium-40 (IAEA 2004a). It is usually unnecessary to regulate raw materials with activity concentrations below these values, and such materials can therefore be regarded as excluded from the scope of application of the BSS. For raw materials in which these levels are exceeded, regulatory control needs to be considered, but the regulatory body may still decide that the optimum regulatory option is not to apply regulatory requirements to the legal person responsible for the material, especially

Table 3. Radioactivity levels [Bq/kg] in phosphate products (Baetslé 1991, Vandenhove et al. 2000).

Products	^{238}U	^{226}Ra	^{232}Th
Phosphoric acid	1200-1500	300	
Normal superphosphate	520-1100	110[*]-960	15-44
Triple superphosphate	800-2160	230[*]-800	44-48
Mono ammonium phosphate	2000	20	63
Di-ammonium phosphate	2300	210	<15
Di-calcium phosphate		740	<37
PK	410	370	<15
NP	920	310	<30
NPK	440-470	210-270	<15

* low value for Former Soviet Union countries.

Case studies: mining activities with uranium as side product / problem

when the levels are exceeded by only a few times. In many cases, such a decision will be made by the regulatory body on a case by case basis and will take the form of an exemption. In several countries, regulatory requirements are applied only if the material is expected to give rise to doses to individuals exceeding 1 mSv in a year.

It can be seen from Tables 1–3 that most materials encountered in the phosphate industry either will qualify for exclusion or can be considered as candidates for exemption. Often, it is the presence of non-radiological hazards that will determine the need for occupational health or environmental protection measures, and such measures will usually have a beneficial effect on any radiological impacts. For instance, in the thermal processing of phosphate rock, normal industrial hygiene measures to control exposure to airborne dust will usually be sufficient to protect workers against the inhalation of radionuclides contained in the dust. Similarly, measures to limit the non-radiological impacts of phosphogypsum piles (e.g. leaching of heavy metals) will usually be sufficient to control any radiological impacts.

Measures for improvement and remediation

Three possible hazards from phosphogypsum waste have to be considered:
- the potential for releasing radium and non-radioactive contaminants into the environment;
- radon exhalation into the atmosphere, particularly in enclosed structures;
- the potential reuse of materials due to the loss of institutional control.

Options for remedial action on phosphogypsum piles can be guided by the technological state of the art in remediation of wastes from uranium mining and milling (IAEA 2002a,b, 2004b, in press), because the various hazards and requirements are quite similar. However, the radionuclide activity concentrations in phosphogypsum are typically one or two orders of magnitude lower, and this needs to taken into account when deciding upon the most appropriate course of action. In particular, the focus is likely to shift away from the radiological hazards more towards the non-radiological hazards.

There are processes, involving the concentration of the phosphoric acid and sedimentation, for the production of uranium in the form of 'yellow cake'. However, the process is not economically viable at the present price of uranium (OECD/IAEA 2002).

Possible environmental benefits from efforts to reduce uranium and other radionuclide concentrations in fertilizer products would have to be weighed against environmental costs, such as increased concentrations in residues and higher energy consumption.

Conclusions

The main residue of concern from the production of phosphate fertilizers is the phosphogypsum, since uranium and other radionuclides are mainly found there and only to a lesser degree in the fertilizer products. Long-term stable solutions for the safe use or disposal of phosphogypsum will have to be designed in order to prevent environmental impacts (including non-radiological impacts such as those from heavy metals). The radionuclide input into the food chain via phosphate fertilizers appears to be of lesser concern. Most process materials in the production of phosphate fertilizers are borderline in terms of the applicability of international radiation protection standards, as the concentrations of radionuclides of natural origin are not very far above those found in soils worldwide. Radiological impacts on workers, members of the public and the environment will in most cases be adequately controlled by the application of normal industrial hygiene and environmental protection measures designed to protect against non-radiological hazards.

References

Baetslé LH (1991) Study of Radionuclides Contained in Waste Produced by the Phosphate Industry and their Impacts of the Environment, CEC-Report EUR 13262, Luxembourg.

Banzi FP, Msaki P, Makundi IN (2002) A Survey of Background Radiation Dose Rates and Radioactivity in Tanzania, Health Phys. 82(1): 80-86.

Chernoff CB, Orris GJ (2002) Data Set of World Phosphate Mines, Deposits, and Occurrences — Part A: Geologic Data, Open-File Report 02-156-A, United States Geological Survey, Reston VA.

Hofmann J, Leicht R, Wingender R., Wörner J. (2000) Natural Radionuclide Concentrations in Materials Processed in the Chemical Industry and the Related Radiological Impact, CEC Report EUR 19264, Luxembourg.

Erkens WHH (1997) Electrothermal Phosphorus Production, Radioactivity in the Environment and Workplace, Proc. Internatl. Symp. on Radiological Problems with Natural Radioactivity in the Non-Nuclear Industry, European Commission/KEMA, Amsterdam, 8-10 September, 1997.

Florida Institute of Phosphate Research (1996) Proceedings of the Phosphogypsum Fact-Finding Forum, Dec. 7, 1995, Tallahassee, FL, FIPR Publ. No. 01-132-117, Bartow, FL.

Hull CD, Burnett WC (1969) Radiochemistry of Florida Phosphogypsum, J. Environ. Radioactivity 32(3): 213-238.

International Atomic Energy Agency (1996) International Basic Safety Standards for Protection against Ionizing Radiation and for the Safety of Radiation Sources, IAEA Safety Series No. 115, IAEA, Vienna.

International Atomic Energy Agency (2002) Management of Radioactive Waste from the Mining and Milling of Uranium and Thorium Ores, IAEA Safety Guide No. WS-G-1.2.

International Atomic Energy Agency (2002) Monitoring and Surveillance of Residues from the Mining and Milling of Uranium and Thorium, IAEA Safety Report Series No. 27, IAEA, Vienna.

International Atomic Energy Agency (2003) Extent of Environmental Contamination by Naturally Occurring Radioactive Material (NORM) and Technological Options for Mitigation, Technical Reports Series No. 419, IAEA, Vienna.

International Atomic Energy Agency (2004a) Application of the Concepts of Exclusion, Exemption and Clearance, IAEA Safety Guide No. RS-G-1.7, IAEA, Vienna.

International Atomic Energy Agency (2004b) Remediation of Sites with Dispersed Radioactive Contamination, IAEA TRS-424, IAEA, Vienna (2004).

International Atomic Energy Agency (in press) Remediation of Sites with Mixed Contamination of Radioactive and Other Hazardous Substances, IAEA-TRS-4XX, IAEA, Vienna.

International Fertilizer Development Center/United Nations Industrial Development Organisation (1998) Fertilizer Manual', Kluwer Academic Publishers, Dordrecht, The Netherlands.

Makweba MM, Holm E (1993) The Natural Radioactivity of the Rock Phosphates, Phosphatic Products and Their Environmental Implications, Sci. Total Environ. 133: 99-110.

OECD-Nuclear Energy Agency/International Atomic Energy Agency (2002) Uranium 2001, Resources, Production and Demand, OECD, Paris.

Osmond JK, Cowart JB, Humphreys CL, Wagner BE (1985) Radioelement Migration of Natural and Mined Phosphate Terrains, Report 05-002-027, FIPR, Bartow, FL.

Othman I, Al-Husari M, Raja G (1992) Radiation Exposure Levels in Phosphate Mining Activities, Radiat. Prot. Dosim. 45(1-4): 197-201

Roessler CE, Smith ZA, Bolch WE, Prince RJ (1979) Uranium and Radium-226 in Florida Phosphate Materials, Health Phys. 37: 269-277.

Schmidt G, Kuppens C, Robinson P (1995) Handling of Radium and Uranium Contaminated Waste Piles and Other Wastes from Phosphate Ore Processing, CEC Report EUR 15448EN, Luxembourg.

United Nations Environment Programme/United Nations Industrial Development Organisation (1998) Mineral Fertilizer Production and the Environment. Part 1. The Fertilizer Industry's Manufacturing Processes And Environmental Issues, IFA/UNEP/UNIDO, Technical Report No.26 Part 1: 66 p.

US Environmental Protection Agency (1990) Report to Congress on Special Wastes from Mineral Processing, Office of Solid Waste and Emergency Response, Report EPA/530-SW-90-070C, Washington, DC.

Vandenhove H, Bousher A, Hedemann Jensen P, Jackson D, Lambers B, Zeevaert T (2000) Investigation of a Possible Basis for a Common Approach with Regard to the Restoration of Areas Affected by Lasting Radiation Exposure as a Result of Past or Old Practice or Work Activity - CARE, Final Report to the European Commission, Contract 96-ET-006, Radiation Protection 115: 285 p.

Van der Westhuizen R, Foskor Limited, Phalaborwa, South Africa (2002) Personal communication.

Van Straaten P (2002) Rocks for Crops: Agrominerals of Sub-Saharan Africa, International Centre for Research in Agroforestry, Nairobi, Kenya.

World Bank Group (1998) Pollution Prevention and Abatement Handbook – Phosphate Fertilizer Plants, New York

Case studies: mining activities with uranium as side product / problem

Uranium contents in acidic lakes and groundwater of Lower Lusatia (Germany)

Elke Bozau[1], Hans-Joachim Stärk[2]

[1]Umweltforschungszentrum Leipzig-Halle, Department Gewässerforschung, Magdeburg, Brückstraße 3a, D-39114 Magdeburg, Germany, E-mail: elke.bozau@ufz.de
[2]Umweltforschungszentrum Leipzig-Halle, Department Analytische Chemie, Leipzig, Permoserstraße 15, D-04318 Leipzig

Abstract. Acidic pit lakes are typical for the landscape of Lower Lusatia. The lakes of a former lignite mine were investigated to find remediation strategies. Hydrogeology and geochemistry of the drainage basin were characterized by collecting numerous data. This study is focussed on the geochemistry of uranium. The investigated waters have low U concentrations (≤ 2 µg/l). There is no definite correlation between pH and U concentration.
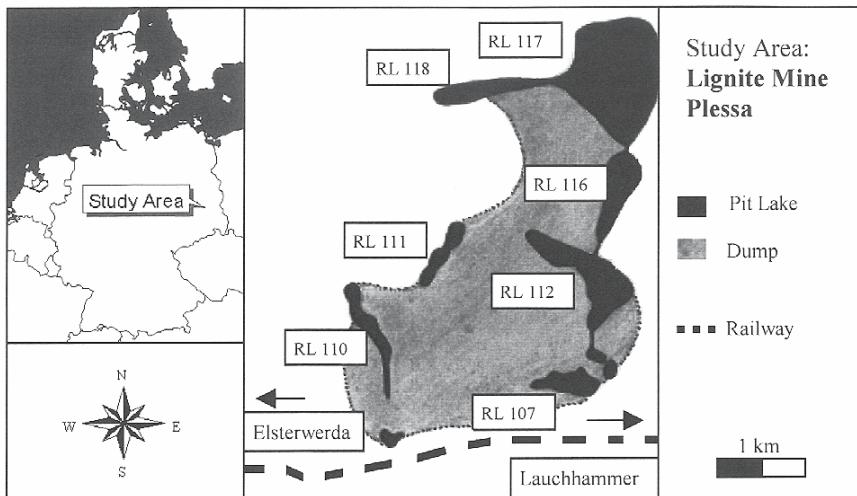
Introduction

There are more than 100 acidic pit lakes in Lower Lusatia (Germany) caused by pyrite oxidation in the surrounding dump sediments (Geller et al. 1998). A sequence of such pit lakes developed in the former lignite mine Plessa-Koyne.

The pH-values of these lakes lie between 2.4 and 3.0. Therefore, the biological diversity is limited due to the unfavourable living conditions. The lakes can be used neither as a drinking water reservoir nor as recreation sites. The geochemistry including the uranium contents of three acidic pit lakes ("RL 107", "RL 111", "RL 117") was investigated (Fig. 1). Mining periods and morphological data of the investigated lakes are given in Table 1.

Table 1. Description of the investigated pit lakes (LENAB 1998).

	RL 107	RL 111	RL 117
Mining period	1897 - 1928	1929 - 1958	1956 -1966
Water level (m a.m.s.l.)	92.3	94.1	92.3
Area (m^2)	122,000	107,000	950,000
Max. depth (m)	4.0	10.2	14.0
Average depth (m)	1.9	4.6	11.0

Fig. 1. The former lignite mine with the acidic pit lakes (Bozau and Strauch 2002).

Methods

The geochemistry including U and Th contents of three acidic pit lakes, as well as in pore water of the lake sediments, surrounding groundwater and dump sediments of the lake "RL 111" were investigated.

Lake water of several depths was taken by a water sampler. Groundwater was sampled by pumping, sediments by digging and drilling. The sediments were digested with acid (HNO_3/HCl) by microwave extraction to analyse trace elements, and also used for leaching experiments according to DIN 38414/4 (water-extractable contents). Chemical analyses were performed by ionic chromatography (SO_4^{2-}, NO_3^-, Cl^-), photometry (NH_4^+), and ICP-OES (Ca, Mg, K, Na, Fe_{tot}, Al) on 0.2 µm filtered water samples.

U and Th analysis was carried out on the 0.2 µm filtered and acidified water samples, as well as the sediment digests by ICP-MS using a Perkin Elmer ELAN 5000a instrument. The detection limit was 0.007 µg/l. The isotopes chosen for the measurement were ^{238}U and ^{232}Th.

Results and discussion

The lake water of all investigated lakes has low pH-values (≤ 3.0) as well as high iron and sulphate concentrations (Table 2). Lake "RL 107" has the lowest pH (2.4) and the highest iron and sulphate concentrations, whereas the lake "RL 117" with a pH-value of 3.0 shows lower iron and sulphate concentrations. These differences can be explained by the amount of inflowing acidic groundwater, which is correlated to the extent of the bordering dump area. Erosion processes from the dump sediments on the lake shore also contribute to the lake acidification.

K, Na, and Cl are not increasing with lower pH-values. The lowest values of these elements are found in pit lake "RL 107". It is possible that the precipitation of minerals from the lake water is responsible for this. K and Na are precipitating within jarosite $[(H,K,Na)Fe_3(OH)_6(SO_4)_2]$ as investigated in the lake "RL 111" (Göttlicher et al. 2001). U concentrations of the lake water lie between 0.04 and 2.1 µg/l (Fig. 2). WHO guidelines for drinking water give a provisional limit of 2 µg U/l (Reimann and Banks 2004).

The highest U concentration is found in the lake "RL 111". The differences within the water column of lake "RL 111" can be explained by an increased groundwater inflow to the deepest part of the lake (Knöller 2000). The chemical differences within the water column of the lake "RL 107" are caused by the melting of the ice cover. The ice cover prevents the wind from mixing the water column, while its melting leads to lower concentrations in the upper water layer. After the mixing of the whole water column in spring, no chemical differences will occur. The shallow depth (max. 4 m) and the meteorological conditions do not allow a stable stratification of the lake "RL 107" (Schimmele 2000). Due to its wide

Table 2. Chemical characteristics of the lakes (SHE = Standard Hydrogen Electrode).
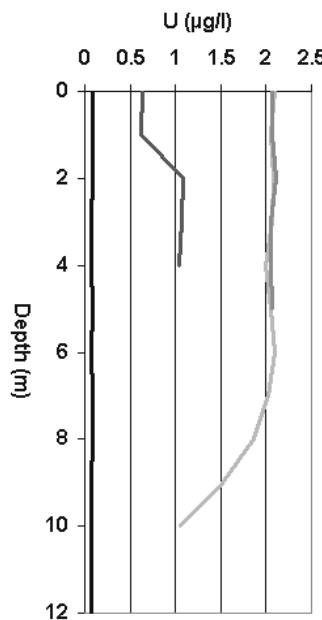
	RL 107 March 2003		RL 111 August 2003		RL 117 June 2003	
Water depth	0 m	4 m	0 m	10 m	0 m	12 m
pH	2.6	2.5	2.6	2.8	3.0	2.8
Eh (mV, SHE)	770	680	760	590	670	690
Cond. (mS/cm)	1.6	3.0	2.6	1.8	0.9	0.9
Ca (mg/l)	151	356	196	254	85	74
K	0.9	1.7	2.7	5.8	4.2	3.6
Mg	18	44	25	32	13	11
Na	3.0	6.4	5.9	8.0	8.3	7.8
SO_4 (mg/l)	1360	3260	1220	1700	387	385
Cl	6.0	10	8.3	8.1	13	13
Fe (mg/l)	265	730	134	341	10	10
Al	29	64	33	36	1.2	1.0
DOC (mg/l)	2.3	4.5	0.5	5.7	0.5	0.5
U (µg/l)	0.6	1.0	2.1	1.1	0.05	0.04
Th	0.5	0.7	1.3	0.6	0.08	0.07

surface and wind stress, lake "RL 117" is relatively well mixed during all seasons. Therefore, no significant chemical differences within the water column can be measured.Speciation calculations for the lake waters were performed using the code PHREEQC (Parkhurst and Appelo 1999). According to Gammons et al. (2003), the sulfate complexes UO_2SO_4 and $UO_2(SO_4)_2^{2-}$, as well as UO_2^{2+} are dominant in all waters.

The groundwater of the drainage basin of lake "RL 111" is characterised by lower concentrations (0.01-0.6 µg/l) than the lake, whereas the water-soluble fraction of dump sediments shows maximum uranium concentrations up to 50 µg/l (Fig. 3).

Uranium concentrations from 3 to 6 mg/kg in lignite (4 samples from boreholes near lake "RL 111") and from 2 to 4 mg/kg in dump sediment (3 samples of the shore of lake "RL 111") were analysed. These concentrations are slightly higher than the U contents of the upper crust (0.91 mg/kg, Taylor and McLennan 1985; 1.8 mg/kg, Mason and Moore 1985).

There is a good correlation between the pH-value, the sulphate and iron concentrations in the water of the three investigated lakes. But the uranium contents
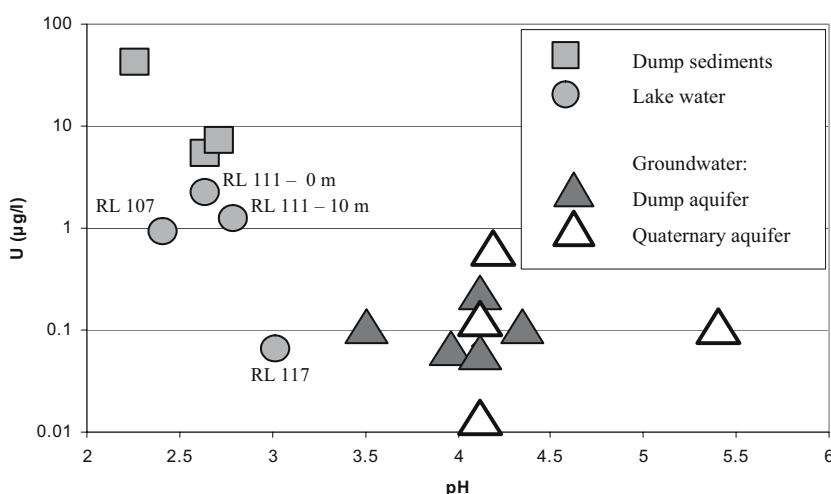
Fig. 2.   U in the water column of the investigated lakes RL 107 – March 2003 (after melting of the ice cover), middle of the lake (4 m) RL 111 – August 2003, north (6 m) and middle basin (10 m) RL 117 – June 2003, middle of the lake (12 m).

Case studies: mining activities with uranium as side product / problem

of the lake water do not really correlate with the pH-values (Fig. 3 and Table 2). The anoxic groundwater has lower contents than the water of the lakes "RL 107" and "RL 111".

The conventional geochemical behaviour that Fe(II) of anoxic water is more soluble and the oxidized Fe(III) tends to precipitate, whereas U(IV) is almost insoluble and the oxidized U(VI) is well soluble (e.g. Kronfeld et al. 2004) cannot be easily applied to the drainage basin of the acidic lake "RL 111".
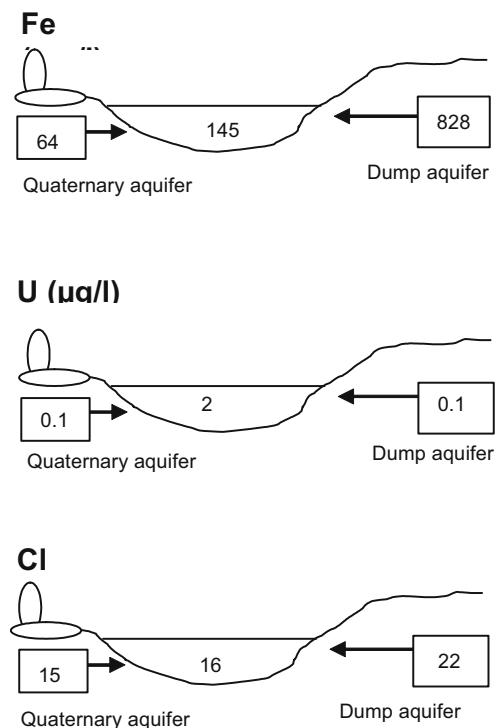
According to the mixing model of lake "RL 111" (Fig. 4; Bozau et al. 2004), chloride can be considered as a conservative tracer. Iron precipitates during the groundwater inflow to the lake. The water mixing model of lake "RL 111" does not explain the uranium distribution. There is more U in the lake than in the inflowing groundwater. One possible explanation might be that during the groundwater inflow into the lake sediments, geochemical changes (e.g. oxidation of Fe(II) to Fe(III), precipitation of hydrous ferric oxides and the pH-decrease) lead to a release of uranium. But pore water profiles of lake "RL 111" indicate that higher U concentrations in the pore waters are correlated to the higher contents of Fe minerals (as goethite and jarosite) in the sediments (data not shown). These different observations for the lake water, the pore water of the lake sediments and the inflowing groundwater at the same lake are in contrast.

It could be that the weathered sediments dumped on the lake shores and reaching the lake water by erosion processes are also an important source of uranium (Fig. 3). Gammons et al. (2003) also consider this hypothesis for their investigated lake: "An alternative hypothesis is that UO_2^{2+} behaves conservatively, and that its concentration is simply a function of the rate of input from weathering and wall-rock leaching compared to the total water flux."

Fig. 3. U concentration against pH-value (Lakes "RL 107", "RL 111" "RL 117", groundwater and leached dump sediments).

Case studies: mining activities with uranium as side product / problem

The Th concentrations of lake "RL 107" and "RL 111" are lower than the U concentrations, whereas lake "RL 117" shows an opposite concentration ratio (Table 2). The data measured for Th indicate the same geochemical behaviour as already discussed for U. In the drainage basin of the lake "RL 111" groundwater has Th concentration from 0.01 to 0.1 µg/l. The surface water of the lake shows Th concentrations of 1.3 µg/l. According to the higher groundwater inflow (with lower Th concentrations) to the deepest part of the lake, a Th concentration of 0.6 µg/l was analysed for the water sampled at 10 m.

Fe

| 64 | 145 | 828 |

Quaternary aquifer   Dump aquifer

U (µa/l)

| 0.1 | 2 | 0.1 |

Quaternary aquifer   Dump aquifer

Cl

| 15 | 16 | 22 |

Quaternary aquifer   Dump aquifer

Fig. 4.   Interaction of lake and groundwater as a mixing model of lake "RL 111". The lake water concentration can be analysed (data shown above) or calculated according to the amount of inflowing groundwater (Bozau et al. 2004). The differences between the analysed and calculated concentrations lead to conclusions about the geochemical behaviour of the elements. Behaviour of Fe (precipitation of hydrous ferric oxides, analysed < calculated concentration), Cl (non reactive tracer, analysed = calculated con-centration) and U (unknown source, analysed > calculated concentration).

Case studies: mining activities with uranium as side product / problem

Conclusions

Compared to acidic waters which resulted from ore mining (Elbaz-Poulichet et al. 1999, Gammons et al. 2003), or neutral waters from bedrock wells in granitic/gneissic formations (Frengstad et al. 2000), the U concentrations of the investigated acidic pit lakes are low.

To explain the higher U and Th concentrations in the lake "RL 111" compared to the inflowing groundwater, further investigations considering erosion processes and particle transport are necessary. According to the investigation of Reiller et al. (2002), the interaction between U, Th and natural organic matter (escpecially the complexation with humic/fulvic acids, as well as their sorption on hydrous ferric oxides) in acidic waters should be involved in these investigations.

Furthermore, the geochemical behavior of U and Th is quite different from the geochemistry of rare earth elements (REE) studied in the drainage basin of lake "RL 111" by Bozau et al. (2003 and 2004). The REE concentrations and patterns allow the distinction between the two aquifers filling that lake, whereas U does not follow this trend. Therefore, results of REE studies of acidic waters should not be simply transmitted to the behavior of actinides.

Acknowledgements

References

Bozau E, Friese K, Stärk H-J (2003) Geochemistry and REE pattern of acidic mining lakes in Lower Lusatia (Germany). Technische Universität Bergakademie Freiberg, Institut für Geologie, Wissenschaftliche Mitteilungen 24: 15-18.

Bozau E, Leblanc M, Seidel J L, Stärk H-J (2004) Light rare earth elements enrichment in an acidic mine lake (Lusatia, Germany). Applied Geochemistry 19: 261-271.

Bozau E, Strauch G (2002) Hydrogeological aspects on biotechnological remediation of the acidic mining lake 111, Lusatia (Germany). Water, Air, and Soil Pollution: Focus 2 (3): 15-25.

DIN 38414/4 (1984) Schlamm und Sediment (Gruppe S), Bestimmung der Eluierbarkeit mit Wasser. Beuth Verlag, Berlin.

Elbaz-Poulichet F, Morley N H, Cruzado A, Velasquez Z, Achterberg E P, Braungardt C B (1999) Trace metal and nutrient distribution in an extremely low pH (2.5) river-estuarine system, the Ria of Huelva (South-West Spain). The Science of the Total Environment 227: 73-83.

Frengstad B, Midtgård A K, Banks D, Krog J R, Siewers U (2000) The geochemistry of Norwegian groundwaters. III. The distribution of trace elements in 476 crystalline bed-

rock groundwaters, as analysed by ICP-MS techniques. The Science of the Total Environment 246: 21-40.

Gammons C H, Wood S A, Jonas J P, Madison J P (2003) Geochemistry of the rare-earth elements and uranium in the acidic Berkeley Pit Lake, Butte, Montana. Chemical Geology 198: 269-288.

Geller W, Klapper H, Salomons W (1998) Acidic Mining Lakes. Springer, Berlin - Heidelberg - New York.

Göttlicher J, Pohlmann M, Bozau E, Gasharova B (2001) Mineralbildungen aus eisen- und sulfathaltigen Wässern. Beih. z. Eur. J. Mineral. 13, 1: 67.

Knöller K (2000) Anwendung stabiler Umweltisotope zur Bewertung hydrochemischer Zustände und Prozesse in Folgelandschaften des Braunkohlebergbaus. PhD thesis, Universität Leipzig.

Kronfeld J, Godfrey-Smith D I, Johannessen D, Zentilli M (2004) Uranium series isotopes in the Avon Valley, Nova Scotia. Journal of Environmental Radioactivity 73: 335-352.

LENAB-Abschlußbericht (1998) Niederlausitzer Bergbaufolgelandschaft: Erarbeitung von Leitbildern und Handlungskonzepten für die verantwortliche Gestaltung nachhaltige Entwicklung ihrer naturnahen Bereiche. BMBF-Förderkennzeichen: 0339648.

Mason B, Moore C B (1985) Grundzüge der Geochemie. Enke, Stuttgart.

Parkhurst D L, Appelo C A (1999) PHREEQC-2.4 - A computer program for speciation, batch reaction, one dimensional transport, and inverse geochemical calculations. U.S. Geological Survey, Water Resources Report 99-4259, Lakewood, Colorado.

Reiller P, Moulin V, Casanova F, Dautel C (2002) Retention behaviour of humic substances onto mineral surfaces and consequences upon thorium (IV) mobility: case of iron oxides. Applied Geochemistry 17: 1551-1562.

Reimann C, Banks D (2004) Setting action levels for drinking water: Are we protecting our health or our economy (or our backs!)? The Science of the Total Environment 332: 13-21.

Schimmele M (2000) Limnophysikalische Untersuchungen an Tagebaurestseen des Lausitzer Braunkohlenreviers. In: Friese K, von Tümpling W (Hrsg.), Biologische und chemische Entwicklung von Bergbaurestseen. UFZ-Bericht 26/2000: 41-57.

Taylor S R, McLennan S M (1985) The continental crust: its composition and evolution. Blackwell, Oxford.

Case studies: mining activities with uranium as side product / problem

Changes in Uranium concentration in the Weisse Elster River as a mirror of the Remediation in the former WISMUT mining area

Wolfgang Czegka[1], Christiane Hanisch[1], Frank Junge[1], Lutz Zerling[2], Martina Baborowski[3]

[1]Saxon Academy of Sciences at Leipzig, Dept. Pollutant Dynamics, K.-Tauchnitz-Str. 1, D-04107 Leipzig, Germany, E-mail: czegka@saw-leipzig.de
[2]Saxon Academy of Sciences at Leipzig, Commission of Environmental Problems, K.-Tauchnitz-Str. 1, D-04107 Leipzig, Germany
[3]UFZ - Centre for Environmental Research, Dept. Lake Research, Brueckstr. 3°, D-39114 Magdeburg, Germany

Abstract. Since 1990 the research group „Pollutant Dynamics" at the Saxon Academy has been investigating the process of self-purification of the former highly anthropogenically affected river Weisse Elster. This long term study, focusing on uranium, includes the components water (< 0.45 µm), suspended matter (SPM), sediment and floodplain soil (grain-size < 20µm,) from 1990 up to 2004.

Introduction

Eastern Germany was once one of the world's biggest uranium producers, mining 220,000 tonnes between 1945 and 1990 (see Tondorf 1994, Kämpf et al. 1995). The repercussions of uranium mining in eastern Thuringia and western Saxony continue to have a severe impact on the local environment (cf. Schultze and Knappe 2001 and Beleites 1992). For example, uranium still persists in the Weisse Elster and its tributary Pleisse, the receiving water of the Ronneburg mines near Gera, as well as in the Göltzsch, a tributary whose catchment area contained the uranium processing plants.

Since 1990 the research group „Pollutant Dynamics" from the Saxon Academy of Sciences has been investigating the process of self-purification of a former highly anthropogenically affected river initiated by remediation on the example of the Weisse Elster river system. This study, focusing on heavy metals, includes the components water, suspended matter (SPM), sediment and floodplain soil (regional background) as well as using sequential speciation on selected sediments. This paper reports about a long-term decrease of uranium in the river downstream

the uranium mining discharges at the Gera-Ronneburg-Area. These will be shown from data of river longitudinal profiles as well as monthly collected samples upstream the confluence with the Saale river at Halle/Saale.
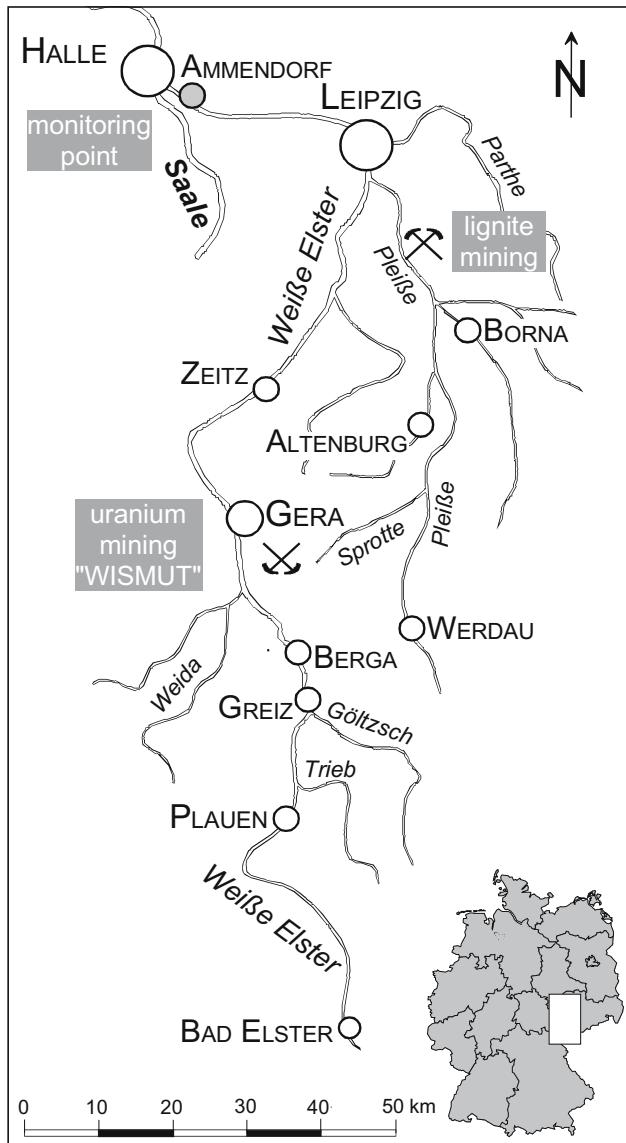
Fig. 1.   Sketch of the Weisse Elster catchment area.

Case studies: mining activities with uranium as side product / problem

Methods

Sampling

In order to determine the complete quantities of metals currently contaminating the Weisse Elster, mixed samples were taken from recent surface sediment. The suspended matter was separated from the water at the sampling site by filtration (celluloseacetate filter < 0.45 μm).

The recent sediment was pressed into bottles under water without being allowed to come into contact with the air. The idea was to enable the samples to be processed under both oxidizing and anoxic conditions. Pre-industrial, if possible layered and datable Holocene alluvial loam profiles were used to determine the geogenic background values. Dense vertical sampling enabled anthropogenically contaminated samples and samples which had been altered by chemical processes in the soil and water in the range of the ground-water level to be excluded. For more information on sampling and sample preparation, as well as the analytical methods used, see the detailed description in Müller et al. (2000).

Analyses

Wet sieving was used to obtain the <20 μm fraction from the mixed samples of recent sediment and soil samples. The fraction was then treated with aqua regia in accordance with DIN 38 414-S7. The small quantities of metals in the suspended matter obtained with the celluloseacetate filter and the residual fraction of sequential speciation were treated using a standardized aqua regia extraction technique developed together with the University of Leipzig's Institute of Analytical Chemistry in the microwave field. The results of this method correlate with the digestion process specified in DIN 38414-S7; cf. Dittrich et al. (1995).

ICP-MS (inductively coupled plasma mass spectroscopy), a reliable method for determining several different elements at once known as was applied detecting uranium. The ICP-MS measurements were used to determine the rare elements in all the analysis samples, as well as to determine the other metals owing to their low concentrations in the water, suspended matter and sequential extracts. Appropriate analysis techniques were developed for the task at hand and their reliability was tested. According to the results from inter-laboratory tests and AAS reference measurements, ICP-MS provided accurate results when used for the determination of metals in sediment samples and suspended matter with no significant differences from those obtained pursuant to DIN 38 414 (Lohse 1997). The accuracy of all the measurements was checked using standard reference materials.

Regional Frame – Regional Background of Uranium

The Weisse Ester river (mean anual waterflow 25 m^3/s) draining the saxo-thuringian industrial region was one of the most badly polluted tributaries in the Elbe river system (Fig. 1). In terms of its uranium content, the catchment area of the Weisse Elster can be divided into three sections: the mainly geogenic upper course; the upper middle course dominated by the aureole of granite in the western Erzgebirge and the anthropogenically contaminated tributaries coming from the east; and the lower middle course together with the lower course influenced by uranium mining in Ronneburg. The samples used for the analyses of all metals in sediment, water and suspended matter were taken from a dense network (cf. Müller et al. 1998).
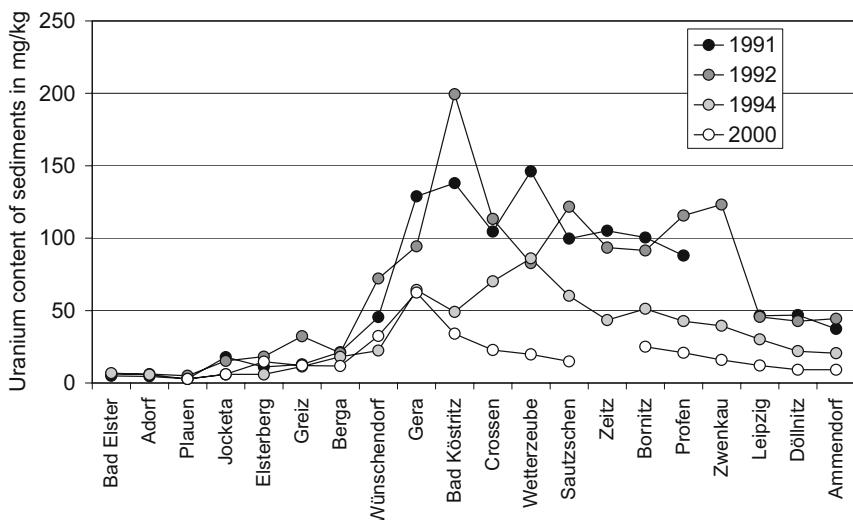
According to Müller, Zerling and Hanisch (2003), the catchment area of the Weisse Elster and the Pleisse can be divided in terms of geogenic background values into eight sub-regional areas (Table 1). The background values listed are means calculated from 12–20 samples containing background levels. Uranium's mean geogenic background in the Weisse Elster catchment is 3.3 mg/kg. This is below the generally accepted argillaceous rock standard according to Turekian and Wedepohl (1961) of 3.7 mg/kg, but which is based on the total extract. The background value for uranium in the upper course is far lower at just 2.0 mg/kg. However, it rises to 4.2 mg/kg in the area of Berga downstream of the inflow of tributaries (especially Göltzsch and Trieb) whose courses touch the west Erzgebirge granite complexes (Bergen and Kirchberg granite; cf. Förster and Tischendorf 1994). In the Gera region the mean background value drops back to 3.6 mg/kg. All other sub-regions – with the exception of the Leipzig district – have values which are around or below the argillaceous rock standard.

Table 1. The local geogenic background values of uranium (in mg/kg) in fine-grained river sediment of the Weisse Elster catchment area.

River	Sampling area	Geogenic background for uranium	No. of samples
Weisse El-ster	Pirk-Geilsdorf downstream of Oels-nitz	2.0	20
	Eula upstream of Berga	4.2	12
	Ahlendorf between Gera and Zeitz	3.6	16
	Großstorkwitz (near Pegau)	2.9	17
	Cospuden and Leipzig-Süd	4.6	18
	Rassnitz and Zöschen, SE of Halle	3.9	15
Pleisse	Münsa and Kraschwitz (near Alten-burg)	2.5	12
	Markkleeberg-Ost	3.1	14
Mean for the area of the Weisse Elster		3.3	124

Case studies: mining activities with uranium as side product / problem

Characterization of Uranium in recent Sediment

The uranium levels in the sediment of the upper course of the Weisse Elster in 1991, 1992 and 1994 were between 2.8 and 6.9 mg/kg, approximately tallying with the geogenic background (Table 1, Fig. 2). The tributaries Trieb and Göltzsch, whose upper courses from the aureole of the west Erzgebirge granite already contained higher geogenic background levels (6-18 mg/kg), were enriched with uranium levels up to 30 mg/kg (and as much as 60 mg/kg in 1992) by the legacy of ore-mining and processing operations. This was caused in particular by the Plohnbach creek near Lengenfeld, and even prompted slight uranium contamination (6–18 mg/kg) in the Weisse Elster in the area of Greiz. The sudden uranium contamination of the sediment in the Weisse Elster, starting downstream of Berga, resulted from the influx of water from the Ronneburg uranium-mining district operated by the East German-Soviet Wismut AG, especially from the Gessenbach creek, which contained levels of dissolved uranium of as much as 268 mg/kg in the sediment and 76 µg/l in the water (see Müller et al. 1998). Other small creeks contained up to 400 mg/kg uranium in suspended matter (SPM) and up to 300 µg/l dissolved uranium. The high concentrations in the sediment of the Weisse Elster downstream of Gera gradually declined owing to dilution down to 30–50 mg/kg (in 1994 15-25 mg/kg) until it flowed into the Saale. Part of the water from uranium processing was at times discharged eastwards, reaching the Pleisse via the Sprotte. As a result, the uranium contamination in the Pleisse downstream of the influx of the Sprotte creek more than doubled despite the high dilution. In 2000 clearly a tremendous decrease of uranium in the recent sediments can be seen in

Fig. 2. Uranium content of recent sediments in 1991, 1992, 1994, and 2000 from upstream (Bad Elster) to downstream (Halle-Ammendorf).

Case studies: mining activities with uranium as side product / problem

fig 2. Never the less the uranium content in the sediment sampled in 2000 ist enriched to factor 3-6 compared to the regional geogenic uranium background.

Comparison over time (Fig. 2) shows, that until 1994 the uranium levels in the Weisse Elster upstream of Berga remained almost constant, but greatly declined in the contaminated area till 2000. Even more striking is the decline in the Pleisse (cf. Müller et al. 1998).

Examination of the ratio between dissolved and particulate uranium in the course of the river revealed that dissolved uranium was enriched upstream relative to particulate uranium by a factor of 2.5. The concentration of dissolved uranium also declined upstream, albeit not as rapidly as that of the particulate phase (Fig. 3). Uranium is one of the elements with a low tendency to bind to particulate substances (Fig. 4). One reason for this is the high volatility of uranium in acidic milieus and under reducing conditions in sediment (where it forms highly soluble complexes). Since the sulphate and chloride concentration is important for the solubility of uranium, let us turn our attention to the sources of the two main anions present in the water of the Weisse Elster: sulphate and chloride. In 1992 and 1994 the sulphate levels increased considerably from the upper course until the point where the Weisse Elster flows into the Saale. A sharp increase in the sulphur input is to be observed in the Berga area. Furthermore, the level of the sulphate load was found to be higher in 1994 than in 1992. Due to the reduction of mining water input caused on the remedion of lignite mines south of Leipzig there was a strong decrease of sulphate rich mining water up to 2000 (Czegka et al 2003).
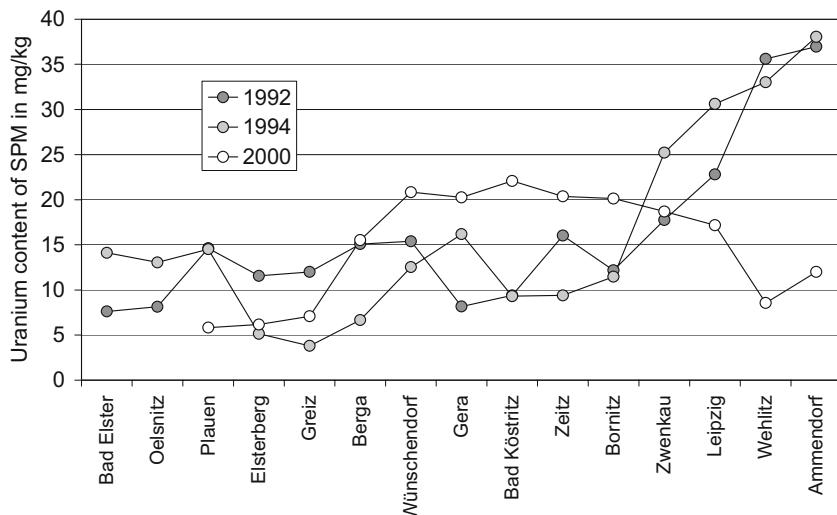
Uranium in Suspended Matter (SPM)

We use three graphics to present the development of uranium in suspended matter (SPM) and dissolved uranium in the Weisse Elster river.
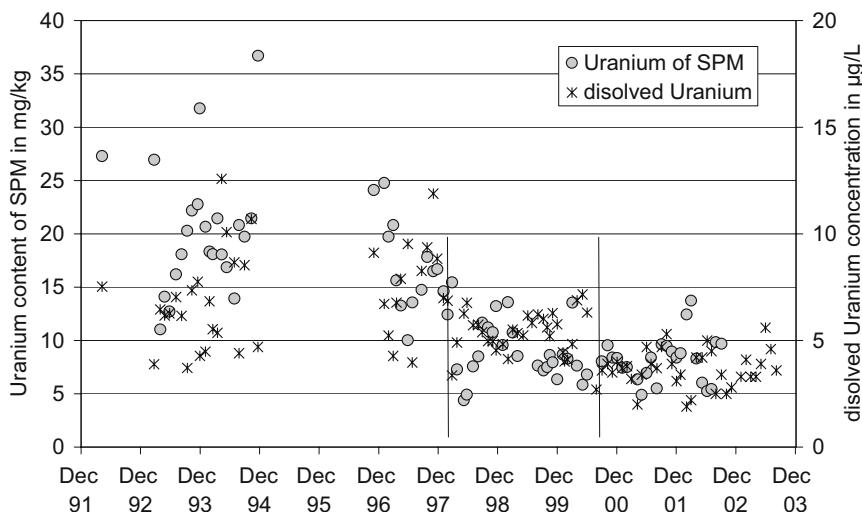
The spot check samples data from our sampling sites from 1992, 1994 and 2000 are presented in a longitudinal river section (from source to mouth) can be seen in Fig. 3. Sampling during the years 1992 and 1994 took part at a normal water level, in 2000 during a decaying flood event.

The uranium content lay in the longitudinal section in the upper courses of the Weisse Elster (till Berga) in the SPM within the years 1992, 1994 and 2000 between 3.5 and 14 mg/kg uranium. In the middle course the content of uranium in SPM increases on 12-22 mg/kg. Here the results from 2000 lie clearly over those of the years 1992 and 1994, caussed by the different water levels during sampling. In the lower course the values in 2000 are decreasing, in 1992 and 1994 they were increasing. This effect can primarily connected the change of water chemistry (e.g. pH, SO_4^{2-} content) in the late 1990ies by reducing the input of sour lignite open pit waste-waters. (see above).

The second illustration (Fig. 3) shows the development of the uranium in SPM
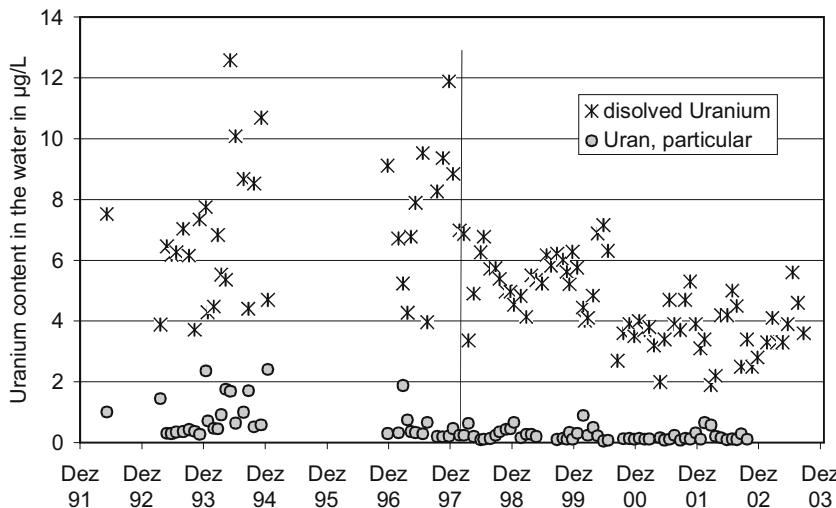
Fig. 3.   Uranium contend in SPM 1992,1994 and 2000.

Fig. 4.   Uranium content of suspended matter (SPM) and dissolved uranium concentration at the Weisse Elster at Halle Ammendorf between 1991 and 2004.

Case studies: mining activities with uranium as side product / problem

as well as the dissolved uranium at our monitoring sampling site at the confluence of the Weisse Elster with the Saale at Halle. The graphics resulted from monthly sampling between 1991 and 2004. It is very obvious that the uranium contents, both in SPM and solution, decrease rapidly after 1996. Additionally a stepwise reduction can be seen especially in the data of uranium in solution. (comp. Geletneky, J., Büchel, 1999; Geletneky, J.: 2002). Nevertheless as shown in Fig. 4 the total amount of transported uranium in the Weisse Elster is realted to the soluted phase but not to SPM. Generally the content of disolved uranium is up to 3-6 times more than in SPM.

Fig. 5.   Uranium content in water (dissolved and particular) at Halle Ammendorf between 1991 and 2004.

Case studies: mining activities with uranium as side product / problem

Conclusions

Caused by the appearance of different uranium ore leading rocks in the catchment area of the Weisse Elster river, the regional geogenic uranium background is increased compared to the clay standard of Turekian and Wedepohl (1961). This fact is particularly defining the uranium content in the upper course of the Weisse Elster.

On the other hand the middle and lower course of the Weisse Elster are dominated by the anthropogenic uranium input caused by the uranium ore dressing of the former Wismut AG.

Long time examinations at recent sediment, SPM and water documents altogether a decrease in the anthropogenic uranium supply in the time period from 1991 to 2004.

This is justified as a result of the remedial actions which were carried out in the Wismut abandoned hazardous sites in the Gera-Ronneburg area during this time period. The decrease in the uranium contents was carried out gradually, according to the way, effectiveness and time of the remedial actions. This fact is extremely obvious with the putting into service of the water conditioning plant at the Ronneburg/ Culmitzsch uranium site in spring 1998. As of this time no more uranium loaded leachate reached into the Weisse Elster, which is documented by the erratic decrease of uranium in the different uranium-compartments (SPM, dissolved uranium, sediment). On reason of the low particular binding ability of uranium the gradual decrease shows themselves amplified at the dissolved uranium fraction in the water of the Weisse Elster. In site of the remedial actions the uranium load of the sediments of the middle und lower course are up 3-6 times over the regional geogenic background.

Acknowledgements

References

Beleites, M. (1992): Altlast Wismut.-Ausnahmezustand, Umweltkatastrophe und das Sanierungsproblem im deutschen Uranbergbau. Brandes&Appel, Dresden.

Czegka, W. Hanisch, C., Zerling, L. Müller, A, Kunert, M. (2003): The cehmical bonding of uranium in recent sediments of the Weisse Elster river: results of sequential extration in comparison with local backgrounds. In Köhne, S. , Wycisk, P. [Eds.]Geowissenschaften und Umwelt, UZU Schriftenreihe Band7: 83- 94

Dittrich, K., Lohse, M., Hanisch, C., Walter, A.(1995): Determination of heavy metals in suspended matter in the storage lake "Bitterfelder Muldestausee". Fresen. J. Anal. Chem. 353: 16–20

Förster, H. J., Tischendorf, G.(1994): The Western Erzgebirge–Vogtland Granites: Implications to the hercynian magmatism in the Erzgebirge–Fichtelgebirge Anticlinorium. In: Seltmann, R.; Kämpf, H., Möller, P. [Eds.]: Metallogeny of collisional Orogens. – Czech Geological survey, Prague: 35–48

Geletneky, J., Büchel, G.(1999): Hydrogeological case study of the Gessental Valley: a pre-flooding scenario at the Ronneburg uranium mining site (Thuringia, Germany). J. Conf. Abstr., 4: 510.

Geletneky, J.(2002): Hydrogeologische/Hydrologische Untersuchung einer Prä-Flutungssituation am Beispiel des Gessentals im ehemaligen ostthüringischen Uranbergbaugebiet. http://www.db-thueringen.de/servlets/DerivateServlet/Derivate-1303/DissertationGeletneky.txt (date accessed: 02.05.2005)

Kämpf, H., Bankwitz, P., Schauer, M., Lange, G. (1995) [Eds.]: Uranlagerstätten der Gera-Jachymov-Störungszone. Z. geol. Wiss. 23: 516–808

Lohse, M.(1997): Methodische und applikative Untersuchungen zur Spurenelementbestimmung in aquatischen Proben mittels Massenspektrometrie mit induktiv gekoppeltem Plasma. Diss. Univ. Leipzig

Müller, A., Hanisch, C., Zerling, L., Lohse, M., Walter, A.(1998): Schwermetalle im Gewässersystem der Weissen Elster. Natürliche und anthropogene Elementverteilung im Sediment, im Schwebstoff und in der gelösten Phase. Abh. Sächs. Akad. Wiss. Leipzig, Math.-nat. Kl., 58 (6), Leipzig, Weimar, Halle

Müller, A.; Hanisch, C.; Zerling, L.(2000): Geogene Standard-Elementgehalte in Auensedimenten der Saale und ihre Anwendung zur Bewertung rezenter Sedimentbelastungen. In Friese, K.; Witter, B.; Miehlich, G.; Rode, M. [Eds.]: Stoffhaushalt von Auenökosystemen. Springer, Berlin-Heidelberg-New York: 247-256

Müller, A. Zerling, L., Hanisch, C.(2003): Geogene Schwermetallgehalte in Auensedimenten und –böden des Einzugsgebietes der Saale. Ein Beitrag zur ökologischen Bewertung von Schwermetallbelastungen in Gewässersystemen.- Abh. d. Sächs. Akad. d. Wiss. zu Leipzig, Math.-nat. Kl. 59 (6), Leipzig, Weimar, Halle

Schultze, M.; Knappe, S. (2001): Auswirkungen der Bergbautätigkeit im Einzugsgebiet auf die Wasserbeschaffenheit der Saale und ihrer Nebenflüsse. Nova Acta Leopoldina, 84 (319): 45-64

Tonndorf, H.(1994): Metallogenie des Urans im ostdeutschen Zechstein. – Abh. Sächs. Akad. Wiss. Leipzig, Math.-nat. Kl., 58 (3), Leipzig, Weimar, Halle

Turekian, K., Wedepohl, K. H.(1961): Distribution of the elements in some major units of the earth´s crust. – Bull. Geol. Soc. Am. 72: 175–192

Factors affecting the plant availability of uranium in soils

Susanne Schroetter[1], Maria Rivas[1], Maria Lamas[2], Jürgen Fleckenstein[1], Ewald Schnug[1]

[1] Institute of Plant Nutrition and Soil Science, Federal Agricultural Research Centre Braunschweig – Völkenrode, Germany, E-mail: susanne.schroetter@fal.de
[2] Department of Soil Science, University of Buenos Aires, Argentina

Abstract. Uranium (U) is a toxic heavy metal. The background values of natural soils differ between 0.79-11 mg kg^{-1} U. U is accumulated in the A horizons and its plant availability is influenced by both natural soil properties and anthropogenic activities. Recently, the use of phosphorus fertilizers in agriculture will be reported as a longer-term risk for the soil-plant-system. An alien source of environmental pollution results from military operations. Soil fertility, pH value and nutrient supply can effect the U content of crops growing on U contaminated soils.

Introduction

Uranium (U) is a natural constituent of the rocks in the earth's crust. Typical natural soil background values differ between 0.79-11 µg g^{-1} U, in relation to the parent material (Kabata-Pendias and Pendias 2001). U is generally accumulated in the A horizons and its plant availability is influenced by both natural soil properties and anthropogenic activities. Soil contaminations with U are a severe problem in mining areas and in the surrounding of processing plants.

Recently, new threats for the soil-plant-system have been reported. Phosphorus fertilizers commonly used in agriculture originate from rock phosphates. Besides the essential nutrient P this mineral fertilizers contain various amounts of U. Thus, it might be possible that critical contamination levels in soils result from common fertilization practices.

An alien source of environmental pollution results from military operations, in which ammunition with penetrators manufactured from depleted uranium (DU) is used. During military conflicts, e.g. in Kosovo, over 30,000 rounds of such DU containing projectiles were fired from aircraft. DU is a by-product remaining after the U enrichment process. Though its content of ^{235}U is depleted to about 0.2-

0.3 %, DU keeps an unstable, radioactive heavy metal with toxic properties influencing life processes. The majority of these above-named penetrators missed the targets (around 90%). They are still in the soil with nearly no chance of detection within the ordinary scope of search. Plant available U will be released by permanent conversion processes of DU in the active soil horizon. Concentrations of up to 400 µg g^{-1} U in the soil close to the metal projectiles were reported (UNEP 2001).

Hazardous effects on health originate if humans and animals will be contaminated by U compounds through inhalation, ingestion or skin contacts. Whereas skin contact is particularly a threat for those working in the U industry, inhalation and ingestion are probable contamination pathways for broader levels of population living in U polluted regions. Ingestion of U occurs by drinking water, and through the food chain via crop plants, animal feed, and animal products.

Uranyl (UO_2^{2+}) is the soluble form transported within the body by the blood stream and it forms complexes with protein and anions. U tends to accumulate in the body, preferentially in the liver and the kidneys. U is damaging the organism either by radioactivity, or by its biochemical toxicity as a heavy metal. The dangers arising from the biochemical toxicity of uranium are generally considered to predominate the risks from its radioactivity. The U ingestion cannot be completely avoided. It varies according to the humans' local diets: daily, up to 4 µg U will be incorporated with the solid food. In addition, the U intake via drinking water, especially mineral waters, is to consider. Even at low concentration levels drinking water accounts to more than 80% of the total U ingestion (Schnug et al. 2005; Milvy and Cothern 1990; Cothern and Lappenbusch 1983).

Heavy metals mobility is affected by the soil redox potential and thus subjected to nearly all changes in soil conditions. The conversion of the metal ionic valences leads to changes of the binding conditions within the soil minerals, resulting in more unstable and soluble forms of metal ions. Under reducing situations, many heavy metal ions form insoluble sulfide compounds, abating the risk of absorption by roots. Alterations of the soil reaction involve a changing solubility of metal cations (McLaughlin 2002). Plant available UO_2^{2+} ions will be released from the surface of soil colloids by ion exchange. After lime fertilization the UO_2^{2+} ions will be replaced by Ca^{2+} ions. In consequence of soil acidity the UO_2^{2+} ions will be substituted by H^+ ions. Microorganisms and plant roots themselves release organic compounds, e.g. phenolic acids and amino acids, which acidify the surrounding soil. Afterwards, the free metal ions will be bound within natural chelate complexes, which have a high affinity to heavy metal ions.
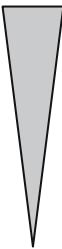
In such a way bounded U ions can diffuse directly through the epidermis of plant roots as well as will easily dissolve from these organic complexes by plant originated enzymes and taken up by the roots as cations.

Case studies: mining activities with uranium as side product / problem

The distribution within the stems, leaves, flowers, and storage organs occurs via the xylem. The U will be incorporated in cell membranes and vacuoles, predominantly.

Material and methods

The influence of soil fertility and fertilization on the plant availability of U in contaminated soil substrates was investigated. The effect of phosphorus (P) fertilization, liming, nitrogen (N), and sulfur (S) nutrition on growth and U uptake of different crops was tested in two multi-factorial, fully randomized pot experiments

Table 1. Set of the treatments for pot experiment 1, (detailed description see Lamas, 2005).

Experiment 1:	*Lolium perenne*; duration 2 years	U contamination [mg kg⁻¹ U]	P fertilization [mg kg⁻¹ P]	Liming [mg kg⁻¹ CaCO₃]
High	Grassland topsoil (GT) [a,c]	0	0	0
	Grassland subsoil (GS) [b,c]	250		
	Forest topsoil (FT) [a,d]	500	1,500	5,000
	Forest subsoil (FS) [b,d]	1,000		
Low				

Soil fertility (High → Low)

[a] topsoil: soil depth 0…25 cm;   [c] Dystric Cambisol/ Orthic Luvisol
[b] subsoil: soil depth 25…30 cm;   [d] Leptic Podzol

Table 2. Set of the treatments for pot experiment 2, (detailed description see Rivas, 2005).

P_t in the soil [mg kg⁻¹ P]	U contamination [mg kg⁻¹ U]		N fertilization [mg kg⁻¹]	S fertilization [mg kg⁻¹]
Experiment 2:	*Zea mays L., Helianthus annuus L., Vicia faba L.*; duration 6 weeks			
334	at low P_t level	at high P_t level	250	0
	non-contaminated	non-contaminated		
	166	173	500	50
1,558	329	385		
	660	644		

Case studies: mining activities with uranium as side product / problem

(Table 1, Table 2). The differences in soil fertility arose from the sites where the substrates derived from: a natural grassland site and a forest site. At both sites, soil from different depths (0-25 cm and 25-50 cm) was removed, representing topsoil and subsoil quality.

The soil substrate used in the 2nd experiment originated from the 1st pot experiment and mixed again considering the different U contamination levels and the P fertilization treatments.

The soil substrates were contaminated before the beginning of the first experiment with the green modification of U_3O_8. This substance was gained from uranylnitrate according to the procedure reported by Fleckenstein (1972). The contamination occurs separately for each pot by mixing the corresponding portion of the oxide powder with the substrate. The plants grew in a vegetation hall under controlled water conditions. The grass yielded 6 cuts. Maize, sunflowers, and faba beans were harvested during the elongation stage (BBCH stage 32; BBCH Scale: adapted from Meier 2001). After the determination of the total dry matter yield the plant material was digested by microwave.

Before the pot experiment started the original soil substrates were analyzed for pH (soil suspension by $CaCl_2$); total C (C_t: by LECO carbon analyzer); total N (N_t: by Kjeldahl); P_{CAL}, K_{CAL} (extractable by calcium acetic lactat according to Schüller 1969).

The soil samples were digested with

- Aqua Regia (nitrohydrochloric acid) to extract the total U and P contents (U_t, P_t), and with
- AAAcEDTA (acid-ammonium-acetate-EDTA) (Lamas et al. 2002) to extract the plant available fraction ($U_{available}$, $P_{available}$).

The amount of U and P containing in the extracts of the soil and plant samples, were measured by Inductively Coupled Plasma-Quadrupole Mass Spectrometry (ICP-QMS). The lowest limit of detection was estimated to 5 ng L^{-1} (Sparovek et al. 2001).

Results and Discussion

Effect of soil fertility, P fertilization and liming on the plant available U in soils

The investigated soil substrates varied in the quality-determinant properties depending on their derivation (Table 3).

Both topsoil substrates featured higher total carbon and nitrogen content. The grassland topsoil contained considerably more P_{CAL} than the other substrates. Both grassland topsoil and subsoil were higher supplied with K_{CAL} than the forest substrates. The differences between the background values of plant available U were only small.

Table 3. Characterization of the original soil substrates.

Origin	Soil type	German classification	Soil depth		pH	C_t	N_t	P_{CAL}	K_{CAL}	$U_{available}$
			[cm]			[%]	[mg g^{-1}]	[mg kg^{-1}]		
Grassland	Silty-loamy sand	Podzolic Brownearth	GT	0-25	5.9	1.2	1.0	108	261	0.02
			GS	25-30	4.8	0.5	0.4	20	246	0.03
Forest	Sandy	Podzol	FT	0-25	3.5	2.0	1.1	48	25	0.04
			FS	25-50	3.8	0.6	0.4	20	5	0.04

The artificial U contamination resulted in significantly increased $U_{available}$ contents of the untreated substrates corresponding to the U contamination levels. In GT, the substrate with the highest fertility, the lowest amounts of plant available U were determined (Table 4).

Notably higher $U_{available}$ contents were detected in the lower fertile substrates (GS, FT, FS). The deficient P contents as well as the lower pH values compared to those of GT could be the reason for the differences (Table 3).

The P fertilization in form of $CaHPO_4$ at the beginning of the experiment resulted in considerably decreased $U_{available}$ contents in the soil substrates (Table 5). Whereas in the GT substrate the U contents of all contaminated treatments decreased approx. to the half, the decreasing effect in the lower fertile substrates was extreme: up to 89 % lower contents of plant available U were measured.

The addition of $CaCO_3$ simulating lime fertilization caused only in the GT a 20 % decrease of the $U_{available}$ content (Table 5). There was a minor effect in GS and FT at the 250 mg kg^{-1} U contamination level only. In the most cases the lime addition even resulted increased values of plant available U. This is attributed

Table 4. Content of plant available U [mg kg^{-1} U] in different fertile, unfertilized soil substrates contaminated with U_3O_8; experiment 1; *Lolium perenne*, 58 weeks after the contamination, cut 7.

Soil substrate **unfertilized**	U contamination rate [mg kg^{-1} U]			
	0 (control)	250	500	1,000
	$U_{available}$ [mg kg^{-1}]			
GT	0.02	25	54	117
GS	0.03	79	130	309
FT	0.04	78	160	297
FS	0.04	86	148	317
Mean	0.03	67	123	260
LSD$_{0.05}$:		32.2		

Case studies: mining activities with uranium as side product / problem

to the raised amount of Ca^{2+} ions in these treatments. Metal ions bounded at the soil colloids were replaced by Ca^{2+} ions and released (Schroeder 1992). The portion of free UO^{2+} ions in the soil substrates was raised.
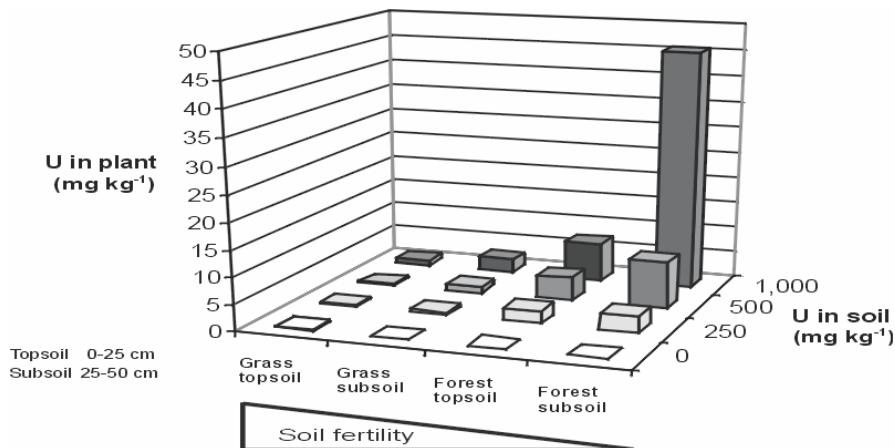
Table 5. Effect of P fertilization and liming on the content of plant available U [mg kg^{-1} U] in different fertile soil substrates contaminated with U_3O_8; experiment 1; *Lolium perenne*, 58 weeks after the contamination, cut 7.

Soil substrate fertilized	U contamination rate [mg kg^{-1} U]							
	control	250	500	1,000	control	250	500	1,000
	P fertilization				Liming			
	$U_{available}$ [mg kg^{-1}]							
GT	0.01	12	27	55	0.01	21	42	92
GS	0.01	15	27	77	0.03	69	145	260
FT	0.02	29	18	78	0.02	70	159	307
FS	0.03	13	33	61	0.03	87	172	313
Mean	0.02	18	26	68	0.03	62	130	243
LSD$_{0.05}$:		9.7				13.0		

Effect of soil fertility, P fertilization, and liming on the U content in plants

The U content of *Lolium perenne* increased corresponding to the increased U content of the soil substrates. This effect was even more pronounced for the plants growing in the lower fertile soil substrates (Fig.1). The highest U content was determined in grass growing at the 1,000 mg kg^{-1} U contamination level, averaged over all other treatments.

In Table 6 the U contents of *Lolium perenne* shows the main effects of the investigated treatments, calculated as mean values of all U contamination levels. The higher the natural soil fertility the lower was the detectible U content of the grass leaves. The effect of a sufficient P nutrition appeared in a significantly lower U concentration in the plants.

Fig. 1. Uranium concentrations in *Lolium perenne* (4th cut, 40 weeks after contamination) grown on top and subsoil material derived from grassland and forest sites with different U contamination, experiment 1.

Table 6. Effect of soil fertility, P fertilization, liming, and changing pH values on the U content in *Lolium perenne* [mg kg^{-1}], experiment 1, 50 weeks after contamination, cut 6.

U content in *Lolium perenne*, treatment averages [mg kg^{-1} U]					Soil pH
Soil substrate		P fertilization		Liming	
GT	0.27	-[a]	0.35	-	0.44	6.3
				+	0.25	6.9
		+[b]	0.18	-	0.20	6.5
				+	0.16	6.8
GS	0.90	-	1.63	-	1.72	5.0
				+	1.55	6.7
		+	0.18	-	0.14	5.6
				+	0.21	6.6
FT	1.19	-	2.22	-	3.72	3.6
				+	0.71	5.6
		+	0.16	-	0.17	4.4
				+	0.15	6.1
FS	1.64	-	3.17	-	4.89	4.2
				+	1.45	5.6
		+	0.11	-	0.11	4.9
				+	0.11	6.3

[a] -...no fertilization [b] with fertilization

The addition of lime had a comparable impact on the $U_{available}$ content in the soil. In combination with P fertilizing the decreasing effects were still enhanced. The plants growing in the corresponding treatments continuously developed more biomass due to the sufficient nutrient supply, the higher pH values of the soil substrates, and the subsequent better growing conditions. Hence, the alleviated U contents in the plant tissue are to interpret as a dilution effect. The U content of aboveground plant tissues was reduced to values given as tolerable (< 0.4 mg kg^{-1}; following Dreesen and Marple 1979).

The investigations of juvenile crops in the 2nd pot experiment documented that differences exist between several plant species in terms of their capability to absorb U from the soil (Table 7). Although, at the end of the experiment the $U_{available}$ content of the pot's soil substrates differed non significantly, the dicotyledonous species, sunflower and faba bean, showed a higher uptake ratio than the monocotyledonous maize. The amount of detectable U in the aboveground plant parts increased depending on the U contamination level, except for the legume faba bean.

In the plant species a highly raised U content was measured at the strongest U contamination level, the both lower contaminated substrates resulted in nearly unspecific differing U concentrations.

Sufficient N nutrition tested for maize and sunflowers increased the U content of in the plants. S fertilization decreased the U content of all crops, whereas the effect was clearly marked for maize.

Table 7. Effect of P, N and S nutrition on the U content in *Zea mays*, *Helianthus annuus*, and *Vicia faba* growing on soil substrates contaminated with various rates of U_3O_8, experiment 2.

Treatment levels		$U_{available}$ in soil substrate [mg kg^{-1} U]			U content in plant [mg kg^{-1} U]		
[mg kg^{-1}]		Maize	Sunflower	Faba bean	Maize	Sunflower	Faba bean
U rate effect	166/173	39.1	37.6	33.5	1.21	0.95	1.82
	329/385	78.1	76.6	74.6	1.66	2.31	1.60
	660/664	180	176	178	3.72	4.34	5.28
P effect	334	156	154	154	2.27	3.02	2.92
	1,558	41.6	39.2	37	2.00	2.04	2.89
N effect	250	101	98.1	95.3	1.71	2.01	2.90
	500	97.3	95.6		2.59	3.05	
S effect	0	99.6	98.2	92.8	3.10	3.02	3.31
	50	98.5	95.4	97.9	1.25	2.04	2.50
Crop specific effect		99.1	96.8	95.3	2.13	2.53	2.90

Case studies: mining activities with uranium as side product / problem

The investigation revealed that U incorporated in soils could be easily mobilized and absorbed by plant roots. High Ca concentrations in the soil solution can lead to a raising release of mobile uranyl ions, which are plant available. A factor limiting the soil/plant transfer is a high concentration of phosphates in the soil.

A fertilization management combining P addition with liming improves the conditions of poor soils for growing plants. The soil content of plant available U will simultaneously reduced by binding in stable phosphate complexes. A sufficient S nutrition of the growing plants seems to be another measure to minimize the U uptake by plants, and thus to avoid that the toxic heavy metal U enters the food chain via soil/plant transfer.

References

Cothern CR, Lappenbusch WL (1983) Occurrence of Uranium in Drinking Water in the U.S. Health Physics 45: 89-99

Dreesen DR, Marple ML (1979) Uptake of trace elements and radionuclides from uranium mill tailings by four-wing saltbrush (Altriplex canescens) and alkali sacaton (Sporobolus airoides). Symposium on uranium mill tailings management. Colorado State University, Fort Collins, Colorado: 127-143

Fleckenstein J (1972) Untersuchungen an Alkalioxofluorouronaten. Dissertation. Universität Tübingen

Kabata-Pendias A, Pendias H (2001) Trace Elements in Soils and Plants. CRC Press: Boca Raton, London, New York: 413 p

Lamas M (2005) Factors affecting the availability of uranium in soils. Landbauforschung Völkenrode Special Issue 278: 102 p

Lamas M, Fleckenstein J, Schroetter S, Sparovek RM, Schnug E (2002) Determination of Uranium by Means of ICP-QMS. Comm Soil Sci Plant Anal 15-18(33): 3469-3479

McLaughlin MJ (2002) Heavy Metals. In Lal, R. (ed) Encyclopedia of Soil Science. Marcel Dekker, New York, Basel: 650-653

Meier U. (2001) Entwicklungsstadien mono- und dykotyler Pflanzen, BBCH Monografie, 2. Auflage, Biologische Bundesanstalt für Land- und Forstwirtschaft.

Milvy P, Cothern CR (1990) Scientific Background for the Development of Regulations for Radionuclides in Drinking Water. In Cothern CR, Rebers P (eds) Radon, Radium and Uranium in Drinking Water. Lewis Publishers, Chelsea, Michigan: 1-16

Rivas M (2005) Interaction between Uranium Contamination and Fertilization on Uranium Content and Uptake of plants and Soil Microbial Parameters. Landbauforschung Völkenrode Special Issue: in preparation

Schnug E, Sparovek, RBM, Lamas M, Kratz S, Fleckenstein J, Schroetter S (2005) Uranium Contamination. In Lal, R. (ed) Encyclopedia of Soil Science. Marcel Dekker, New York, Basel: (in print)

Schroeder D (1992) Bodenkunde in Stichworten. Verlag Ferdinand Hirth, Berlin, Stuttgart 5th rev. ed.: 175 p

Schüller H (1969) Die CAL-Methode zur Bestimmung des pflanzenverfügbaren Phosphates in Böden. Z. Pflanzener. Bodenk. 123(1): 48-63

Sparovek RBM, Fleckenstein J, Schnug E (2001) Issues of Uranium and Radioactivity in natural waters. Landbauforschung Völkenrode 4(51): 149-157

UNEP (2001) Depleted Uranium in Kosovo. Post-Conflict Environmental Assessment; United Nations Environmental Programme: Nairobi, Kenya: 186 p

Case studies: mining activities with uranium as side product / problem

Index